年報 Annual Report 2016

近畿大学医学部消化器内科学教室

医局員集合写真

目　　次

2016年Annual Reportの発刊にあたって

近畿大学消化器内科学教室主任教授　工藤正俊

1.はじめに

2016年の教育、研究、診療の実績をお届けします。近畿大学医学部に消化器内科学教室が新設されたのは平成11年4月であります。従って平成27年3月で区切りの16年が経過したことになります。開設当初は医局のスペースも2部屋のみでスタッフ8名、研修医6名、計14名での出発でありました。現在では狭山の本院に籍を置くスタッフは約40名、また堺病院や奈良病院もそれなりに人材・設備共に整いつつあります。

しかしながら、私立医大の宿命かもしれませんが、2004年より始まった新臨床研修医制度の余波をまともに受けて消化器内科も毎年5～6人から12～13人入局していた入局者数が最近では激減し、また次第に開業あるいは結婚退職、郷里へのUターンなどの退職者も増え、現在なお厳しい状況に置かれているというのが現状です。ただし、ここ数年は2-4人の入局がコンスタントに続いており、良い傾向が見え始めました。今後の更なる消化器内科学教室の発展のために医局員一同が一致団結して診療、研究、教育活動に専念していかなければならない重要な時期であると考えております。

2.診療活動

別添えの資料をご覧頂ければ一目瞭然でありますが、消化器内科の年間の入院及び外来収入、及びそれを合計した総収入は平成11年の開設初年度は約8億程度でありましたが、平成27年には45億円を超える収入となっており、病院経営にも多大の貢献をしております。また一日平均入院患者数も年間を通して80人前後、平均在院日数も7日前後であり極めて多忙な診療活動を行っていることがおわかり頂けると思います。腹部超音波検査の件数も確実に右肩上がりであり、内視鏡の件数も総件数が平成27年度は19,275例と着実に上昇を示しております。また、肝癌に対するラジオ波治療（RFA）の総件数も多く、日経新聞や朝日新聞、読売新聞、週刊朝日等にも度々取り上げられ、総件数としては連続9年以上、日本国内の2位もしくは3位（内科と外科の件数、及び転移性肝癌を含めて）に位置づけられるという実績を残しております。ラジオ波は平成11年6月より開始し、平成25年12月末の時点で総件数4,500例に達しており、5年生存率は70%強と、手術とほぼ同等の治療成績が得られております。現在、C型肝炎治療を積極的に行っており、大阪南部からC型肝炎・肝癌を根絶したいと願っています。平成26年からはいよいよIFN freeの経口剤（DAA）のみによる治療が開始されました。難治性のIb型高ウイルス検査のSRV率もほぼ100%となることが見込まれています。B型肝炎も核酸アナログで制御されるようになって

いる現在益々、肝癌の治療が重要になってくるものと思われます。

平成 15 年度に導入した早期胃癌に対する内視鏡的粘膜下層切開剥離術（ESD）も確実に症例数が増え、今後も益々増え続けていくものと考えております。もちろん、ESD 関連の研究論文も少しずつ増えていっております。また、大腸 ESD も平成 22 年より開始され、症例も増加しています。また従来より行っていた胆膵グループによる超音波内視鏡検査の件数も増加しています。平成 23 年度には内視鏡室が光学治療センターに格上げとなり、スペースも拡充されました。平成 23 年 11 月 27 日に第 1 回目を行った関西消化器内視鏡ライブコースも第 2 回目を平成 24 年 11 月 25 日に行われ、第 3 回目は平成 26 年 2 月 9 日に行い、約 300 人の参加者を得て成功裏に終わりました。

御承知のように大和川以南は一般に「南大阪」と呼ばれておりますが、その南大阪の人口は約 240 万にも達しております。その 240 万人の医療圏の中で特定機能病院大学医学部は近畿大学のみであります。その意味でこの 240 万人の方々の健康を守るのが我々に課せられた使命であります。さらには、平成 35 年には医学部・病院が泉ヶ丘の駅の隣接した地に新築移転する計画が発表されました。消化器内科も含めた近畿大学医学部の発展がさらに期待されます。

3. 教育活動

教育は当然のことながら大学医学部の役割の極めて根幹を占める重要な部分であります。消化器内科学は消化器コースの内の肝臓の責任科であり、肝臓のユニットを 1 週間担当している他、上部消化管、下部消化管、胆膵のユニットや臨床腫瘍コースならびに画像診断のコースでも講義を担当しております。更には病因・病態のコースの 3 週間のうち 1 週間の責任科として大変多忙な教育活動を行っております。5 年生 6 年生のクリニカルクラークシップも例年 6 年生を常時 6 人程度受け入れており、講義や総括など充実した bed side 教育となるよう全力を尽くしております。国家試験の成績も是非とも向上させなければなりません。

平成 20 年 10 月から病院長に任ぜられ、3 期目となりましたが無事平成 26 年 9 月には任期満了により退任いたしました。その間は公務のために教育活動の多くの部分を北野准教授、松井講師はじめ多くの先生方にご負担をおかけすることになってしまい、申し訳なく思っております。消化器コース及び病因・病態コースあるいは日々のクリニカルクラークシップ等の教育活動では決して手を抜かず積極的に行っていくつもりですので何卒ご容赦下さい。この紙面をお借りして感謝とお詫びを申し上げたいと思います。

1. 研究活動

(1) 論文業績

英文論文の発表は 1999 年消化器内科の設立当初は一桁台でありましたが、年と共に確実に増

加し、3 年目からは平均 20 編以上の英文論文がコンスタントに出るようになりました。2010 年の英文論文数は 51 編に達しました。残念ながら 2011 年は 48 編、2012 年は 44 編にとどまりました。しかし、2014 年からは再び 57 編と 50 編の大台に回復しました。また 17 年間の総インパクトファクターは 1838.372 点であり英文総論文数は 530 編ですので、近畿大学消化器内科のような小さな所帯の教室としてはまずまずの結果を残せているのではないかと思っております。来年以降は最低、英文原著論文は 60 編以上を目標に頑張っていきたいと考えておりますので教室員の皆様の自覚と更なる奮闘を期待致しております。

(2) 厚生労働省科学研究費補助金事業研究班の活動

平成 22 年度に採択された厚労科研（がん臨床部門）**「進行・再発肝細胞癌に対する動注化学療法と分子標的薬併用による新規治療法の確立を目指した臨床試験（Phase III）ならびに効果を予測する biomarker の探索研究」**（工藤班）の主任研究者として日本発のエビデンスを創出すべく、努力していまいりました（平成 22－24 年)。また平成 23 年度には厚労科研（難病･がん等の疾患分野の医療の実用化部門）**「慢性ウイルス性肝疾患の非侵襲的線化評価法の開発と臨床的有用性の確立」**（工藤班）の主任研究者としても採択され、多くの大学との協同研究を行いました（平成 23－25 年)。平成 26 年度には厚生労働科学研究委託費（肝炎等克服実用化研究事業（肝炎等克服緊急対策研究事業))「慢性ウイルス性肝炎の病態把握（重症度・治療介入時期・治療効果判定・予後予測）のための非侵襲的病態診断アルゴリズムの確立」という課題が採択となり、更に 3 年間新しいエビデンスを創出すべく頑張りたいと思っております。平成 26 年度には平成 27 年度日本医療研究開発機構（AMED）の委託費となり現在研究が進行中です。またその他にも下記の厚労科研の分担研究者として教室の先生方に実務を担当して頂いております。この場をお借りして感謝申し上げます。

① 「抗悪性腫瘍薬による肝炎ウイルス再活性化の調査とその対応に関する研究」(池田班)（国立がん研究センターがん研究補助金）
② 「初発肝細胞癌に対する肝切除とラジオ波焼灼両方の有効性に関する多施設共同研究」(國土班)（厚労科研）
③ 「進行肝胆膵がんの治療法の開発に関する研究」(奥坂班)（国立がん研究センターがん研究補助金）

(3) 今後の研究の方向性

今年の消化器内科の論文も一覧するとやはりまだまだ Impact factor の高い雑誌に掲載されているのは少ないようです。やはり Impact factor 15 点以上の雑誌を目指すには prospective な

比較試験など中・長期的な視野に立った研究計画を組んで質の高い臨床研究を進めて行くことが現時点での我々に課せられた最も大きな課題と考えております。臨床試験については2008年9月11日に大阪府より認証を受けたNPO法人「日本肝がん臨床研究機構（JLOG)」を中心に現在7つのprospective studyが走っております。なかでもSELECTED studyはH24年10月に終了し、ポジティブな結果が得られたため平成25年のAASLDでoral発表すると共に、NEJMにも投稿予定です。来年中にはSILIUS試験の結果も出る予定です。これからも世界へ向けて発信できるような成果を出して行くつもりでおります。もちろん、retrospectiveな解析研究で新しいデータをpublishしていくという努力も今後も続けていかなければなりません。

また基礎研究の分野でも西田直生志准教授、櫻井俊治講師、萩原智講師を中心に積極的に研究を進めて頂いており、今後のpublicationを期待しております。

もう一つの重要な点は私が常日頃申し上げておりますように症例観察の重要性であります。臨床においては一例一例がたとえ同じ病名であったとしても一例として同じ症例はありません。同じ病気でも一つとして全く同一であるということはなく、何か異なるメッセージを発信しているのです。そのことを的確にキャッチすることにこそ意味があるという目で一例一例の患者さんを注意深く診療し観察していくことこそが最も大事であると考えています。そのような注意深い観察から新しい臨床的な発見も生まれてきますし、また逆にそのような観察眼が生まれる素地としては臨床家として真面目に臨床と向き合って最高のlevelに到達している必要があります。そのような点で日々の臨床の現場には”clinical pearl”とでも言うべきものがあちこちに転がっている、まさに宝の山であります。そのような理由で症例観察に基づいたケースレポートを書くということも極めて、その本人の勉強になることはもちろんのこと、今後の新しい疾患概念の確立、新しい治療法の着想などに結びつき得る重要な姿勢であると思われます。残念ながら、ケースレポートは最近のImpact factor重視主義の多くのJournalから採用されない傾向にはありますが、それでもshort reportやLetter to the Editorなどとしては採用されますので業績をあげるという目的ではなく、症例をキチンと観察・整理してdocumentしていくという姿勢に立つことは重要であります。すなわち症例の観察研究を報告することは我々、アカデミアに籍を置く者に課せられた使命であると自覚すべきと考えております。

大規模な前向きな比較試験を行うべきということと症例の観察研究とでは全く正反対の次元の違うことを述べているように思われるかもしれません。しかしこの2つは臨床を知り尽くし、かつ、臨床をじっくり真面目にやっている医師にしかできないことであるという点で共通していることであります。基礎研究あるいは臨床に結びつくかもしれない基礎研究まではMDではなくともPhDでも実行可能なことであり、そのfieldではしばしばPhDの方がqualityの高い研究成果を上げ得るかも知れません。しかしながら、臨床の疑問点にもとづいた基礎研究もしくは本当に臨床に直結するような基礎研究や症例の観察研究、および大規模臨床試験などはその価値を知

り得るMDにしかできないことであることは間違いありませんし、それらを遂行し得るのは患者さんと日々正面から向き合っている最高水準の医師にしかできない研究であります。そのような点でこの二つは決して矛盾するものではありませんし、両方ともに臨床家こそがやるべき研究であります。

以上、述べた2つの異なったアプローチは、我々の教室の研究の方向性として今後も積極的に実行して行きたいと思っております。繰り返しになりますが、臨床的な発想に基づく、あるいは臨床に本当に必要な基礎的データを抑えるという研究は、大変重要ですのでそれらは引き続き継続していかなくてはなりません。

2009年に私が立ち上げた日本肝がん分子標的治療研究会（第1回研究会：2010年1月16日、参加者450人）は年2回開かれております。これからはC型肝炎もB型肝炎も、ほとんどが経口剤だけで容易に治癒して行く時代になりますので、相対的に肝癌治療の重要性が増してゆきます。また肝癌はこれからは分子標的治療が大変重要な治療のひとつとなる時代ですのでゲノム生物学教室（西尾和人教授）との共同研究は今後も継続していきたいと思っています。特許も出願することが出来ましたし、Impact Factorが7以上の雑誌にもこの分野で2-3編通りました。臨床的ニーズに基づいた基礎研究で成果を上げることほどエキサイティングなことはありません。是非とも近畿大学から肝癌に関して臨床に貢献できる基礎的エビデンスを次々と発信して行きたいと心から願っています。

(3) Research Conference

現在消化器内科では定期の各グループの臨床カンファレンスに加え、毎週火曜日の早朝の1時間みっちりとResearch Conferenceを行っております。このカンファレンスでは全て英語でPresentationからDiscussionまでを行っております。ほとんど1年を通じて海外からの留学生がおりますし、特筆すべき点としてこれまではアジアの留学生が中心でしたが平成22年はイタリア人のDr. Lorenzoがapplyしてできたことです。これも日本における肝細胞癌研究のleading centerとしてヨーロッパの国からも認知され始めている証拠であると思いますので大変喜ばしいと思っております。平成23年には世界で最も古い歴史のあるイタリアボローニャ大学のProf. Bolondiの教室からDr. Albertoがやってきて3か月の研修を終えて帰りました。そのような留学生にも配慮してResearch Conferenceは英語で行っておりますが、やはりこのEnglish Research Conferenceというのが消化器内科が行っているカンファレンスの中でも最も重要であると考えております。もちろん、このカンファレンスへの出席は本人の自発的意欲に基づくものではありますが、毎週多くの教室員に参加して頂いております。以下にこの数年の出席率を示しますが、出席率の高い医局員ほどやはり研究に対するactivityが高い傾向にあると感じておりますので今後も引き続き積極的に参加して頂きたいと思っております。

副次的な効果としてこのカンファレンスを通じて海外で英語でDiscussionできる英語力や自信も自然と磨かれるものと確信しております。

English Reseach Conference 出席状況

	2010		2011		2012		2013		2014		2015		2016	
	出席数	出席率	出席数	出席率	出席数	出席率	出席数	出席率	出席数	出席率	出席数	出席率	出席数	出席率
工藤	29/29	100%	23/23	100%	32/32	100%	25/25	100%	22/22	100%	21/21	100%	28/28	100%
樫田	12/19	63%	20/23	87%	27/32	84%	19/25	76%	20/22	91%	16/21	76%	20/28	71%
西田			5/5	100%	24/32	75%	10/25	40%	4/22	18%	13/21	62%	9/28	32%
北野	21/29	72%	21/23	91%	25/32	78%	21/25	84%	12/22	55%	9/21	43%	2/28	7%
松井	23/29	79%	23/23	100%	30/32	94%	23/25	92%	20/22	91%	21/21	100%	25/28	89%
上嶋	12/29	41%	7/23	30%	9/32	28%	6/25	24%	5/22	23%	9/21	43%	15/28	43%
櫻井	17/19	89%	20/23	87%	25/32	78%	15/25	60%	15/22	68%	14/21	67%	20/28	71%
南	-	-	13/14	93%	31/32	97%	22/25	88%	19/22	86%	20/21	95%	15/28	54%
萩原	9/29	31%	11/23	48%	10/32	31%	9/25	36%	4/22	18%	12/21	57%	8/28	29%
井上	25/29	86%	21/23	91%	23/32	72%	17/25	68%	5/22	23%	-	-	-	-
矢田	26/29	90%	14/23	61%	9/32	28%	15/25	60%	3/22	14%	19/21	90%	9/28	32%
竹中													20/28	71%
坂本	12/19	63%	11/23	48%	20/32	63%	15/25	60%	5/22	23%	-	-	-	-
北井	15/29	52%	13/23	57%	20/32	63%	16/25	64%	13/22	59%	11/21	52%		
朝隈	11/29	38%	15/23	65%	15/32	47%	15/25	60%	15/22	68%	12/21	57%	15/28	54%
米田	-	-	-	-	-	-	-	-	22/22	100%	17/21	81%	23/28	82%
永井	14/29	48%	12.5/23	54%	23/32	72%	14/25	56%	-	-	14/21	67%	16/28	57%
川崎	4/29	14%	6/23	26%	4/32	13%	2/25	8%	-	-	-	-	-	-
田北	15/29	52%	7/23	30%	9/23	39%	12/25	48%	4/22	18%	8/21	38%	13/28	46%
早石	5/29	17%	8/23	35%	9/23	39%	-	-	-	-	-	-	-	-
田中	-	-	-	-	24/27	89%	18/25	72%	5/22	23%	17/21	81%		
山田	-	-	-	-	23/25	92%	15/25	60%	6/22	27%	8/21	38%		
山雄	-	-	-	-	-	-	14/25	56%	19/22	86%	16/21	76%	22/28	79%
永田	16/29	55%	12/23	52%	11/32	34%	2/25	8%	-	-	-	-	-	-
今井	18/29	62%	10/23	43%	13/32	41%	7/25	28%	8/22	36%	16/21	76%		
岡崎	-	-	-	-	-	-	-	-	15/22	68%	6/21	29%		

有住	15/29	52%	17/23	74%	26/32	81%	18/25	72%	19/22	86%	10/21	48%	24/28	86%
鎌田	15/29	52%	10/23	43%	16/32	50%	9/25	36%	6/22	27%	15/21	71%	27/27	96%
高山	-	-	13/14	93%	16/32	50%	16/25	64%	4/22	18%	-	-	-	-
宮田	16/29	55%	14.5/23	63%	22/32	69%	15/25	60%	17/22	77%	11/21	52%	18/28	64%
岡元	-	-	-	-	-	-	12/25	48%	18/22	82%	14/21	67%	19/28	68%
河野	-	-	-	-	-	-	-	-	20/22	91%	8/21	38%	12/28	43%
峯	17/29	59%	17/23	74%	19/32	59%	19/25	76%	4/22	18%	7/21	33%	2/28	7%
足立	-	-	8/14	57%	22/32	69%	17/25	68%	16/22	73%	8/21	38%	9/28	32%
大本	-	-	12/14	86%	29/32	91%	19/25	76%	18/22	82%	15/21	71%	13/28	46%
門阪	-	-	12/14	86%	22/32	69%	16/25	64%	9/22	41%	15/21	71%		
千品	-	-	-	-	29/32	91%	22/25	88%	17/22	77%	10/21	48%	10/28	48%
南(知)	-	-	-	-	-	-	21/25	84%	19/22	86%	16/21	76%	18/28	64%
松田											9/21	43%		
三長											11/21	52%	19/28	68%
岩西											17/21	81%	3/28	11%
岡本													15/28	54%

4. 学会活動および海外における活動

2016 年における国内の学会発表については 38 演題、国際学会の発表については 45 演題、海外特別講演は 19、国内特別講演は 34 でありました。私自身の海外出張は 2016 年は 12 回となりました。

1. 4 月 13 日 - 18 日
   ヨーロッパ肝臓学会にて発表（ILC）(Barcelona, Spain)

2. 6 月 2 日 - 9 日
   米国臨床腫瘍学会にて共著として発表（ASCO）(Chicago, USA)

2. 7 月 6 日 - 10 日
   第 7 回アジア太平洋肝癌専門家会議に参加（APPLE）(Hong Kong, China)

3. 8月22日 - 25日
第33回世界内科学会会議に参加（WCIM）（Bali, Indonesia）

4. 8月25日 - 8月27日
アジア太平洋肝臓癌研究グループ会議に参加（AHCC）（Singapore）

5. 8月31日 - 9月1日
TACEコンセンサスアップデート会議に参加（Seoul, Korea）

6. 9月7日 - 12日
第10回国際肝癌学会議にて発表（ILCA）（Vancouver, Canada）

7. 10月20日 - 21日
アジア太平洋肝臓イメージ研究会にて講演（APLIS）（Beijing, China）

8. 10月22日 - 23日
中華民国医用超音波医学会にて講演(Taipei, Taiwan)

9. 10月27日 - 28日
第3回アジア腫瘍局所治療学会にて講演（Seoul, Korea）

10. 11月11日 - 15日
第67回米国肝臓学会議に出席（AASL）（Boston, USA）

11. 11月23日 - 25日
ソウル国際消化器病シンポジウムにて講演（Seoul, Korea）

12. 12月15日 - 18日
第57回インド消化器病学会にて講演（ISGCON）（Delhi, India）

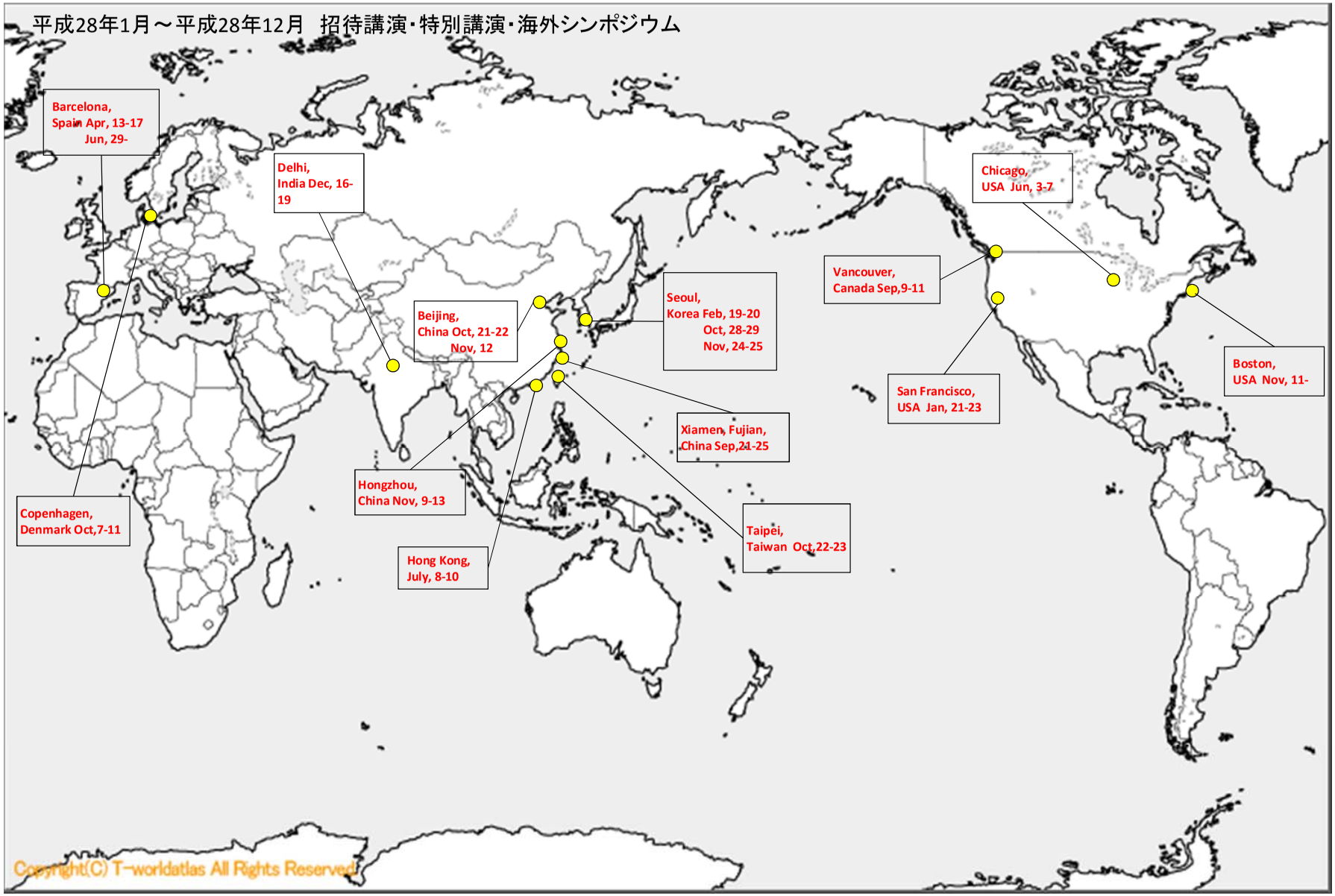
平成28年1月～平成28年12月　招待講演・特別講演・海外シンポジウム
Barcelona, Spain Apr, 13-17 Jun, 29-
Delhi, India Dec, 16-19
Beijing, China Oct, 21-22 Nov, 12
Seoul, Korea Feb, 19-20 Oct, 28-29 Nov, 24-25
Chicago, USA Jun, 3-7
Vancouver, Canada Sep,9-11
San Francisco, USA Jan, 21-23
Boston, USA Nov, 11-
Xiamen, Fujian, China Sep,21-25
Hongzhou, China Nov, 9-13
Taipei, Taiwan Oct,22-23
Hong Kong, July, 8-10
Copenhagen, Denmark Oct,7-11
Copyright(C) T-worldatlas All Rights Reserved

平成28年1月～平成28年12月　招待講演・特別講演

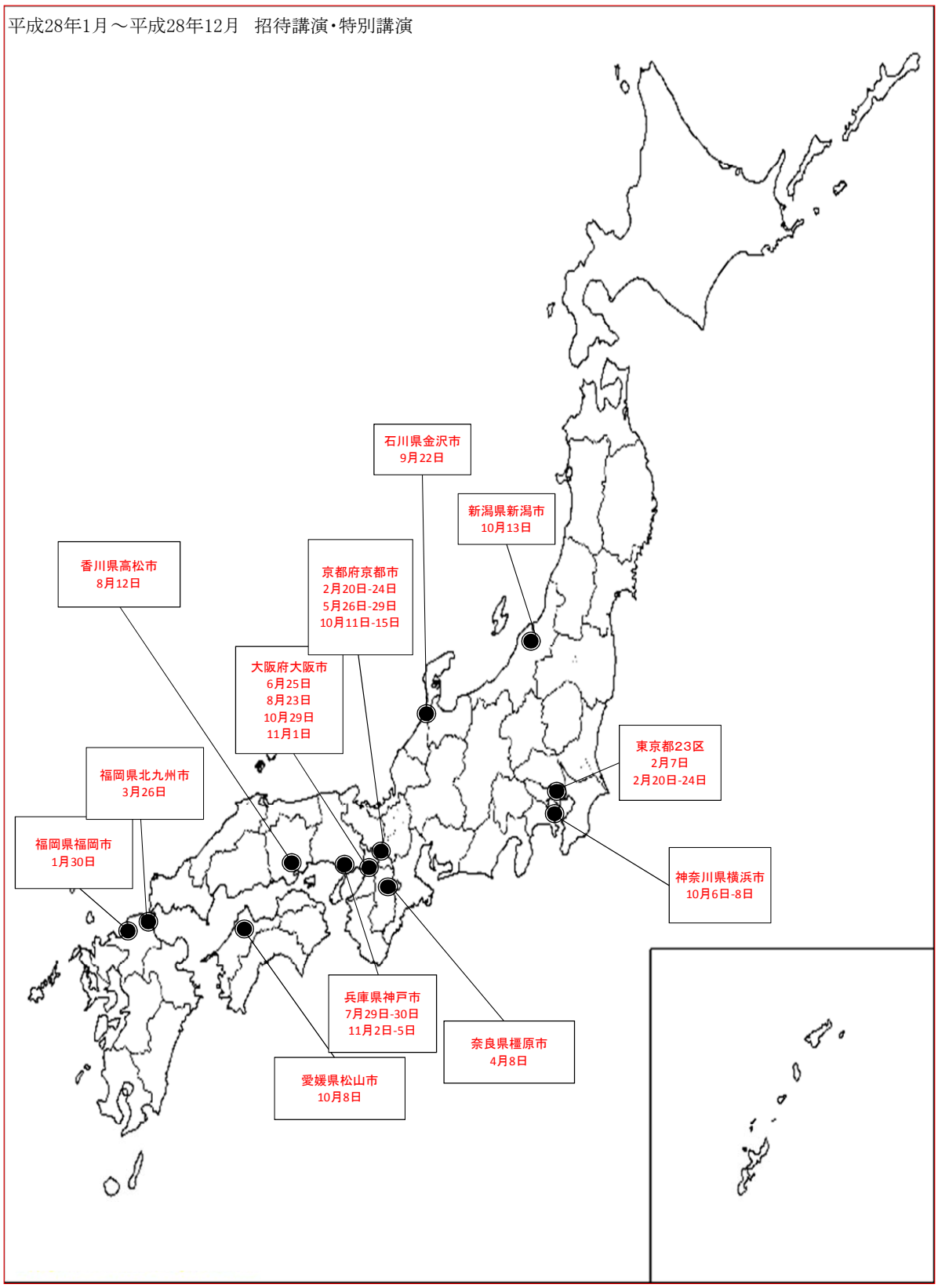

5. 留学生受け入れ

留学生の受け入れですが、1999年から2000年にかけて中国上海からDing Hong先生（丁紅）（上海医科大学)、2001年には中国広州からWen YL先生（文　艶玲）（中山医科大学)、2002年には中国広州からZheng RQ先生（鄭　栄琴）（中山医科大学)、2003年には中国重慶よりZhou Pei先生(周　佩)(人民解放軍重慶病院)、2004年にはカンボジアよりLy Sokhey先生、2005年にはタイからWorawan Chinamnan先生、同じく2005年に若干時期を違えてインドからKaushal Madan先生（All India Institute of Medical Science: AIIMS)、2007年Kunal Das先生を受け入れました。2008年 Yu Xia先生（北京、中国)、2009年　Md. Nadiruzzaman先生（バングラディシュ)、2010年Lorenzo Andreana先生（イタリア）が来ていました。またエジプトからAlshimaa先生も来られました。2011年にはマレーシアからHadzri先生が来られましたし、またイタリア　ボローニャ大学からもAlberto先生が来られました。2012年7月 - 9月には中国からZhang Shuo先生も受け入れました。2013年10月にはマレーシアからChai Soon Ngiu先生が来られました。2014年9月にはインドから。2015年には、インドからHarwani Yogesh Purshottam先生、Sanjay Rajput先生、韓国からHyun-Jong Choi先生、Yun Nah Lee先生、LEE Sung Chan先生が来られました。2016年は台湾からKwok Wing Yee Doris先生が、2017年はバングラディッシュからShahinur Haque先生と台湾からSz-Iuan Shiu先生が来られました。このように毎年、留学生が日中友好協会、笹川財団や日本消化器病学会、日本超音波医学会のフェローシップ留学生あるいは自国でのfundをもって私どもの教室を希望して頂き、受け入れてきました。また来年度以降も先生方にはご迷惑をお掛けするかと思いますが、これも国際交流、アジアや世界への日本の貢献、各々の英語力に磨きをかけるという意味で有益と思いますので何卒御理解・御協力のほどお願い申し上げます。

6. 人事について

冒頭でも述べましたが、2003年までの入局者は毎年5、6名～12、13名と大学内でも最も多くの入局者がおりましたが、2004年に新臨床研修医制度が開始されてからの入局者、すなわち2006年の入局者は2名に留まり、2007年の入局者も1名に留まりました。2008年には8名もの入局者が入って来られました。2011年は3名の研修医が入局し、2012年にも3名が入局しました。反面、2-3人の方が医局を離れました。2015年は4名、2016年も4名の先生が入局されました。2017年は9名の入局となりました。

多くの人に入局して頂き、教育・研究・診療を円滑に行っていきたいと考えております。

7. NPO 法人「日本肝がん臨床研究機構（Japan Liver Oncology Group)」の活動

1. **JLOG 0801 trial**「肝癌早期診断のための多施設共同無作為化比較試験（Sonazoid-Enhanced LivEr Cancer Trial for Early Detection (SELECTED Study))」

→2012 年 10 月終了、現在データ解析中、論文発表予定

2. **JLOG 0901 trial** 「進行・再発肝細胞癌に対する動注化学療法と分子標的薬併用による新規治療法の確立を目指した臨床試験（Phase III）ならびに効果を予測する biomarker の探索研究（Randomized Controlled Trial Comparing Efficacy of Sorafenib versus Sorafenib In combination with Low dose cisplatin/fluorouracil hepatic arterial InfUSion chemotherapy in Patients with Advanced Hepatocellular Carcinoma And Explolatory Study of Biomarker Predicting Its Efficacy (SILIUS Phase III trial))」

→2010 年より厚労科研に移行（厚生労働省科学研究費補助金　厚生労働省科学研究費補助金事業研究班（がん臨床部門）平成 23 年度「進行・再発肝細胞癌に対する動注化学療法と分子標的薬併用による新規治療法の確立を目指した臨床試験（Phase III）ならびに効果を予測する biomarker の探索研究」（工藤班)）→2013 年で終了、試験自体は 2015 年 6 月終了予定。

3. **JLOG 0902 trial**「早期肝癌診断における EOB-MRI の有用性に関する多施設共同研究（Diagnosis of Early LIver Cancer Through EOB-MRI(DELICATE Study))」

4. **JLOG 1001 trial** 「切除不能肝細胞癌に対する肝動脈化学塞栓療法（TACE）とソラフェニブの併用療法第 II 相臨床試験（Phase II study: Transcatheter Arterial Chemoembolization Therapy In Combination with Sorafenib (TACTICS Study))」

5. **JLOG 1002 trial**「慢性肝疾患における非侵襲的弾性検査法を用いた肝線維化評価予測に関する研究(Assessment of Liver FIBROsis by Real-time Tissue ELASTography in Chronic Liver Disease (FIBROELAST Study))」

→2011 年より厚労科研に移行（厚生労働省科学研究費補助金事業研究班（難病･がん等の疾患分野の医療の実用化部門）平成 23 年度「慢性ウイルス性肝疾患の非侵襲的線化評価法の開発と臨床的有用性の確立」（工藤班))

6. **JLOG 1003 trial**「非侵襲的弾性検査法を用いた肝線維化度評価によるウイルス性肝炎患者における肝発癌・門脈圧亢進症の発現予測（Prediction of Incidence of Liver Cancer or porTal Hypertension in Patients with Viral Hepatitis by Use of Real-time Tissue Elastography (PICTURE Study))」

→2011 年より厚労科研に移行（厚生労働省科学研究費補助金事業研究班（難病･がん等の疾患分野の医療の実用化部門）平成 23 年度「慢性ウイルス性肝疾患の非侵襲的線化評価法の開発と臨床的有用性の確立」（工藤班))

7. JLOG 1004 trial「インスリン抵抗性を合併するC型代償性肝硬変患者を対象としたBCAA顆粒製剤の肝細胞癌抑制効果に関する第III相臨床試験（BCAA Granule for patients with Hepatitis C-related Liver Cirrhosis and Insulin Resistance On the Effect of Reduction of Carcinogenic RisK in the Liver(Phase III study)(BLOCK Study))」

8. おわりに

この年報を作成にあたりましては例年の如く、教授秘書、医局秘書の秘書連合軍の皆様に全面的に編集をして頂き大変感謝を致しております。また、医局員の皆様にも大変この一年お世話になりました。この一年間も大変なハードワークではありましたが、無事皆様の頑張りにより乗り切ることができました。この場をお借りして深く感謝申し上げます。2010年には念願の一病棟まるまる消化器内科が占めるという状態が実現しましたし、腹部超音波室も拡充されました。2014年12月には救急災害棟も完成いたしました。光学治療センターの拡充も終了しましたので何卒昨年以上にモチベーションを上げて頂いて日本一、あるいは世界一の消化器内科学教室へ育つようにご尽力頂きたいと思います。2018年も教育・診療・研究において、特に英文論文、新しい研究の立ち上げということについては2018年以上に積極的に取り組んでいきたいと考えておりますので医局員全員が共通の価値観と消化器内科の将来の方向性に対するベクトルを共有し、心を一つにして邁進して頂きたいと祈念・期待しております。

2018年3月　大阪狭山にて

工藤正俊（くどうまさとし）

（平成 28 年 12 月 13 日更新）



昭和 29 年	愛媛県西条市生まれ
昭和 53 年	京都大学医学部 卒業
同	京都大学医学部附属病院 勤務（研修医）
昭和 54 年	神戸市立中央市民病院内科　勤務（研修医）
昭和 55 年	同　消化器内科　医員
昭和 60 年	同　消化器内科　副医長
昭和 62 年	カリフォルニア大学留学（デービスメディカルセンター）
平成元年	神戸市立中央市民病院消化器内科　副医長　復職
平成 4 年	同　消化器内科　医長
平成 9 年	近畿大学医学部第２内科学　助教授
平成 11 年	近畿大学医学部消化器内科学 主任教授　現在に至る

（その他大学内役職）

平成 19 年-20 年	近畿大学医学部附属病院副病院長
平成 20 年-26 年	近畿大学医学部附属病院病院長
平成 27 年-現在	学校法人近畿大学理事（医学部・附属病院担当理事）

（現在の併任）

近畿大学ライフサイエンス研究所所長（平成 26 年 10 月 1 日-現在）
近畿大学医学部奈良病院消化器内科　教授（兼務）
近畿大学医学部堺病院消化器科　教授（兼務）
神戸市立中央市民病院消化器内科　顧問（兼務）

主な所属学会

日本消化器関連学会機構（JDDW）（理事)、日本消化器病学会（財団評議員・指導医・専門医)、日本肝臓学会（理事・指導医・専門医・国際委員会委員長)、日本消化器内視鏡学会（社団評議員・指導医・専門医)、日本超音波医学会（理事長・指導医・専門医・国際交流委員会委員長)、日本内科学会(評議員・認定内科医)、日本高齢消化器病学会（理事)、日本癌学会（評議員)、日本臨床腫瘍学会（協議員)、日本核医学会(評議員・専門医)、日本肝癌研究会（常任幹事・追跡調査委員長・事務局代表)、日本肝移植研究会（世話人)、肝血流動態イメージ研究会（世話人)、日本腹部造影エコー・ドプラ診断研究会（事務局・代表世話人)、肝癌治療シミュレーション研究会（副代表幹事)、超音波治療研究会（常任世話人)、日本肝がん分子標的治療研究会（代表世話人・事務局代表)、日本消化器内視鏡財団（評議員)、米国肝臓学会（AASLD）（肝癌部門企画運営委員: Steering Committee of hepatobiliary malignancy)、米国消化器病学会（AGA)、米国消化器内視鏡学会（ASGE)、世界肝臓学会 （IASL)、欧州肝臓学会（EASL）、など

委員・資格など

- 世界超音波医学会（WFUMB）Immediate Past President（前理事長）
- アジア超音波医学会（AFSUMB）President-elect（理事長）
- アジア太平洋肝癌学会(APPLE) President（理事長）
- 国際肝癌学会（ILCA）理事（Founding Board Member, Governing Board Council Member）
- 米国肝臓学会（AASLD）肝癌部門運営委員会委員（Steering Committee Member）
- 日本肝がん臨床研究機構（JLOG）（理事長）
- 世界保健機構（WHO）Blue Book「Classification of the Tumor」改訂委員（平成21年5月1日）
- ウイルス肝炎研究財団　日米医学協力研究会肝炎専門部会研究員
- International Liver Thought Leadership Study (ILCS), Council member
- 全国医学部長病院長会議　理事（平成26年5月17日-平成28年）
- IASGO 癌分子標的治療国際委員長 （Executive Board President of International IASGO Molecular Targeting Therapy Section）（平成26年12月6日-現在）
- ILCA School of Liver Cancer Committee Member（平成27年4月30日-現在）
- Editor-in-Chief「Liver Cancer」(Karger, Basel)（2012年-現在）

受賞

- 米国核医学会 Berson-Yalow Award 受賞（平成元年6月）
- 日本対がん協会がん研究助成奨励賞 受賞（平成4年3月）
- 日本消化器病学会奨励賞 受賞（平成4年4月）
- 日本核医学会賞 受賞（平成5年10月）
- 米国超音波医学会（AIUM）学会賞受賞（平成15年6月4日）
- ボローニャ大学医学部医学会名誉会員賞（平成18年9月15日）

- フィリピン超音波医学会名誉会員（Honorary Member of PSUCMI）（平成 20 年 3 月 19 日）
- アジア太平洋消化器病学会（APDW）OKUDA Award 受賞（平成 20 年 9 月 13 日）
- 北米放射線学会 Certificate of Merit 受賞（平成 20 年）
- インド肝臓学会 Madangopalan Award 受賞（平成 21 年 3 月 28 日）
- 北米放射線学会 Cum Laude 賞受賞（平成 21 年 12 月）（7000 編の論文中上位 10 編に採択）
- 日本肝臓学会「日本肝臓学会機関誌 Highest Citation 賞」受賞（平成 22 年 6 月）
- JISAN Lecture Award Presented by Korean Society of Ultrasound in Medicine（平成 22 年 5 月）
- 米国超音波医学会名誉会員賞（AIUM Honorary Member Award）受賞（平成 23 年 4 月）
- 韓国超音波医学会名誉会員賞（KSUM honorary Award）受賞（平成 23 年 5 月）
- 日本肝臓学会「日本肝臓学会機関誌 Highest Citation 賞」受賞（平成 23 年 6 月）（2 回目）
- Romanian Society of Ultrasound in Medicine and Biology（SRUMB）Honorary Award 受賞（平成 23 年 6 月）
- 北米放射線学会 Certificate of Merit 受賞（平成 23 年 11 月）（2 回目）
- USE 論文賞（応用物理学会論文賞）」受賞（平成 24 年 11 月）
- Lorenzo Capussotti Award 受賞（from IASGO）（平成 26 年 12 月）

著書（単著）

- Contrast Harmonic Imaging in the Diagnosis and Treatment of Liver Tumors（Springer-Verlag 2003）
- 肝腫瘍における造影ハーモニックイメージング（医学書院 2001）

編集

- 松井 修，**工藤正俊**,編集：消化器疾患の造影エコーUp Date. 南江堂，東京，2003.
- **工藤正俊**，編集：肝細胞癌治療の最近の進歩，消化器病セミナー97，へるす出版，東京，2004.
- 河田純男，白鳥康史，**工藤正俊**，榎本信幸，編集，小俣政男，監修：肝疾患 Review 2004，日本メディカルセンター，東京，2004.
- 河田純男，白鳥康史，**工藤正俊**，榎本信幸，編集，小俣政男，監修：肝疾患 Review 2006-2007,日本メディカルセンター，東京，2006.
- 河田純男，横須賀收，**工藤正俊**，榎本信幸，編集，小俣政男，監修：肝疾患 Review 2008-2009，日本メディカルセンター，東京，2008.
- 河田純男，横須賀收，**工藤正俊**，榎本信幸，編集，小俣政男，監修：肝疾患 Review 2010-2011，日本メディカルセンター，東京，2010.
- 幕内雅敏，菅野健太郎，**工藤正俊**，編集：今日の消化器疾患治療指針 第 3 版，医学書院，東京，2010.
- **工藤正俊**，泉 並木，編集：症例から学ぶ ウイルス肝炎の治療戦略. （株）診断と治療社，

東京, 2010.

- **工藤正俊**, 編集: 肝細胞癌の分子標的治療, アークメディア, 東京, 2010.
- 山雄健次, **工藤正俊**, 編集: 見逃し､誤りを防ぐ!肝･胆･膵癌画像診断アトラス, 羊土社, 東京, 2010.
- **工藤正俊**, 編集: 医学のあゆみ「肝癌の分子標的治療」, 医歯薬出版株式会社, 東京, 2011.
- **工藤正俊**, 編集:「肝細胞がん診療の進歩: Up-To-Data」,最新医学社, 大阪, 2011.
- **工藤正俊**, 編集: 朝倉内科学, 矢崎義雄,「総編集」, 朝倉書店, 東京, 2013.
- **工藤正俊**, 國分茂博, 編集 : EOB-MRI/ソナゾイド造影超音波による肝癌の診断と治療, 医学書院, 東京, 2013

Editor-in-Chief:

- Liver Cancer (Karger, Basel)

EDITORIAL BOARD:

国際学術雑誌: J Gastroenterol Hepatol (Sydney), Hepatology International (Tokyo), Liver International (New York), Ultrasound Med Biol (New York), J Oncology (New York), Oncology (Germany)

国内学術雑誌: 5

論文査読委員

Lancet Oncol(24.725), J Clin Oncol(17.879), Gastroenterology(13.926), Hepatology(11.190), J Hepatol(10.401), Am J Gastroenterol(9.213), Endoscopy(5.196), Oncologist(4.540), Expert Rev Mol Diagn(4.270), Clin Exp Metastas(3.725), Cancer Sci(3.534), Eur Radiol(4.338), Liver Int(4.412), J Gastroenterol(4.020), Eur J Clin Invest(2.834), J Nucl Med(5.563), J Gastroen Hepatol(3.627), Oncology-Basel (International Journal of Cancer Research and Treatment)(2.613), Ultrasound Med Biol(2.099), Acta Paediatr(1.842), Hepatol Int(2.468), Eur J Gastroen Hepat (2.152), J Hepato-Bil-Pan Sci (2.313), Hepatol Res(2.218), Int J Clin Oncol(2.170), Jpn J Clin Oncol(1.747), Internal Med(0.967), J Clin Ultrasound(0.801), Biomark Med(2.858), Hepato-Gastroenterol(0.907), Ann Nucl Med(1.507), Expert Review of Anticancer Treatment(0), J Cancer Res Ther (0.949), CSR National Registry(0), J Gastrointest Liver (1.849), Cancer Informatics(0), Expert Review of Proteomics and Future Oncology(0)

SIENTIFIC PAPER PUBLICATION:

学術論文 英文論文: 657 (IF: 2422.640)

和文論文: 845

特別講演・招待講演・教育講演:

国際学会: 348

教科書（単著）　英文：2　和文：6　**国内学会**：649
分担執筆　英文：21　和文：264

科学研究費等外部資金の獲得状況

・ 文部科学省科学研究費補助金　基盤研究(A)　2 件（総額 1,100 万円）
基盤研究(B)　6 件（総額 2,311 万円）
基盤研究(C)　12 件（総額 1,240 万円）
挑戦的萌芽研究　3 件（総額　310 万円）
（主任研究者）　（　260 万円）
「肝細胞癌の発癌･進展の分子機序：造影超音波クッパー相と遺伝子発現を用いた融合解析」
（分担研究者）　（　50 万円）
「肝細胞癌のソラフェニブ著効例における感受性規定遺伝子変異の探索」(主任研究者　西尾和人)

・ 知的クラスター創生事業（がんペプチドワクチン）　1 件（総額　10 万円）

・ 車両財団がん研究助成金　1 件（総額　100 万円）

・ 学会奨励研究補助金　6 件（総額　530 万円）

・ 医師会・民間医学振興財団等研究補助金　32 件（総額 2,089 万 5 千円）

・ 国立がん研究センターがん研究開発費（分担研究者）　（　245 万円）
「抗悪性腫瘍薬による肝炎ウイルス再活性化の調査とその対応に関する研究」(班長　池田公史)

・ 国立がん研究センターがん研究開発費（分担研究者）　（　12 万円）
「進行肝胆膵がんの治療法の開発に関する研究」(班長　奥坂拓志)

・ **厚生労働省科学研究費**　**主任研究者**　3 件（総額 3 億 825 万円）

1. （がん臨床研究事業）
「進行・再発肝細胞癌に対する動注化学療法と分子標的薬併用による新規治療法の確立を目指した臨床試験（Phase III）ならびに効果を予測する biomarker の探索研究」（平成 22 年 - 24 年度）
2. （難病・がん等の疾患分野の医療の実用化研究事業）
「慢性ウイルス性肝疾患の非侵襲的線化評価法の開発と臨床的有用性の確立」(23 年-25 年度)
3. 平成 27 年度日本医療研究開発機構委託研究開発費(AMED)
（肝炎等克服実用化研究事業（肝炎等克服緊急対策研究事業））「慢性ウイルス性肝炎の病態把握（重症度・治療介入時期・治療効果判定・予後予測）のための非侵襲的病態診断アルゴリズムの確立」(26 年-現在)

厚生労働省科学研究費　**分担研究者**　29 件（総額 3,325 万円）

1. （肝炎等克服緊急対策研究事業）
「血小板低値例へのインターフェロン治療法の確立を目指した基礎および臨床的研究」（班長　西口修平）
2. （がん臨床研究事業）
「初発肝細胞癌に対する肝切除とラジオ波焼灼両方の有効性に関する多施設共同研究」（班長　國土典宏）
3. （肝炎等克服緊急対策研究事業）
「肝がんの新規治療法に関する研究」（班長　本多政夫）
4. （難治性疾患克服研究事業）
「多発肝のう胞症に対する治療ガイドライン作成と試料バンクの構築」（班長　大河内信弘）
5. （難病・がん等の疾患分野の医療の実用化研究事業）
「慢性ウイルス性肝疾患患者の情報収集の在り方等に関する研究」（班長　相崎英樹）

ガイドライン策定委員会委員

- 「科学的根拠に基づく肝癌診療ガイドライン」（日本肝臓学会編），金原出版
- 「「慢性肝炎の治療ガイドライン」（日本肝臓学会編），文光堂
- 「肝癌診療マニュアル」（日本肝臓学会編），医学書院
- 「肝癌治療効果判定基準」（日本肝癌研究会取扱い規約委員会編），肝臓
- 臨床病理「肝癌取り扱い規約」（日本肝癌研究会編）
- Clinical Practice Guidelines for Hepatocellular Carcinoma, Japan Society of Hepatology, Hepatology Research
- General Rules for the Clinical and Pathological Study of Primary Liver Cancer, 3rd English Version, Liver Cancer Study Group of Japan, Kanehara, Tokyo, 2010
- Response Evaluation criteria in the Cancer of the Liver (RECICL), Liver Cancer Study Group of Japan, Hepatology Research
- 「多発肝のう胞症に対する治療ガイドライン」
- RECICL 2014 update 版, Hepatology Research

ガイドライン策定

- 日本肝臓学会　肝癌診療ガイドライン作成委員会委員
- 日本肝臓学会　肝癌診療マニュアル作成委員会委員
- 日本肝臓学会　慢性肝炎治療ガイドライン作成委員会委員
- 日本肝臓学会　多発性肝嚢胞治療ガイドライン作成委員会委員
- 日本超音波医学会　肝臓のエラストグラフィ作成委員会委員長
- 世界超音波医学会　エラストグラフィガイドライン作成委員会委員長

特許取得

発明の名称：　ソラフェニブの効果予測方法
出願番号：　特願 2011-104275
出願日：　2011 年 5 月 9 日
発明者：　荒尾徳三、松本和子、西尾和人、工藤正俊
出願人：　学校法人近畿大学

発明の名称：　N 型糖鎖を利用した膵臓癌の診断方法
公開番号：　特許公開 2009-270996
公開日：　2009 年 11 月 19 日
発明者：　荒尾徳三、松本和子、西尾和人、坂本洋城、北野雅之、工藤正俊
出願人：　住友ベークライト株式会社

全国規模の学会・研究会事務局

・日本肝癌研究会（事務局・追跡調査委員長）
・日本腹部造影エコー・ドプラ診断研究会（代表世話人）
・NPO 法人日本肝がん臨床研究機構（理事長・事務局）
・日本肝がん分子標的治療研究会（代表世話人・事務局）

全国規模の研究会世話人・役員

平成 6 年 4 月–8 年 3 月　　日本超音波医学会腹部造影エコー研究部会幹事
平成 7 年 11 月–現在　肝血流動態イメージ研究会世話人
平成 8 年 4 月–現在　日本腹部造影エコー・ドプラ造影研究会世話人（事務局兼務）
平成 9 年 7 月–現在　肝動脈塞栓療法研究会世話人
平成 10 年-現在　　国際造影超音波研究会世話人
平成 11 年 10 月–現在　臨床消化器病研究会世話人
平成 11 年 7 月–現在　西日本肝臓研究会世話人
平成 13 年 5 月–現在　肝疾患フォーラム世話人
平成 14 年 4 月—現在　犬山シンポジウム会員
平成 14 年 9 月–現在　日本消化器画像診断研究会世話人
平成 16 年-現在　　Liver Forum in Kyoto 世話人
平成 18 年-現在　　肝癌治療シミュレーション研究会副代表世話人
平成 19 年 11 月-現在　日本超音波治療研究会常任世話人
平成 20 年-現在　　日本肝がん分子標的治療研究会（代表世話人）

関西地区研究会代表世話人

・平成 11 年　　関西超音波造影剤研究会代表世話人（日本シェーリング（株））

・平成 13 年　関西 B 型肝炎研究会代表世話人(グラクソ･スミスクライン(株))
・平成 14 年　肝癌局所治療研究会代表世話人（持田製薬）
・平成 14 年　大阪消化器化学療法懇話会代表世話人（大鵬薬品）
・平成 15 年　臨床消化器病フォーラム代表世話人（エーザイ）
・平成 18 年-平成 22 年　Bay Area Gut Club 代表世話人（エーザイ）
・平成 18 年-平成 22 年　South Osaka Liver Club 代表世話人（シェリングプラウ）
・平成 19 年　関西肝血流動態イメージ研究会代表世話人（エーザイ）
・平成 20 年　Kinki Liver Club（代表世話人）
・平成 21 年　南大阪肝疾患研究会代表世話人
・平成 21 年　南大阪肝胆膵疾患研究会代表世話人

関西地区研究会世話人

・平成 2 年　大阪肝穿刺生検治療研究会世話人（大鵬薬品、山之内製薬）
・平成 6 年　兵庫インターベンショナルラディオロジー研究会世話人（山之内製薬）
・平成 8 年　肝胆膵治療フォーラム・神戸世話人（第一製薬）
・平成 9 年　京都肝疾患懇話会世話人（山之内製薬）
・平成 9 年　肝臓分子生物学研究会（大塚製薬）
・平成 11 年　肝代謝コロキウム世話人（興和株式会社）
・平成 11 年　南大阪肝胆膵懇話会世話人（大塚製薬）
・平成 11 年　南大阪肝胆膵疾患懇話会世話人（第一製薬）
・平成 11 年　南大阪消化器病懇話会世話人（ゼリア新薬）
・平成 11 年　南大阪肝疾患研究会世話人（味の素ファルマ）
・平成 11 年　泉州消化器ラウンドテーブルディスカッション世話人（大塚製薬）
・平成 11 年　泉州肝臓病研究会世話人（シェリングプラウ（株））
・平成 11 年　大阪肝炎ミーティング世話人（住友製薬）
・平成 12 年　大阪肝臓病談話会世話人（科研製薬）
・平成 12 年　関西経皮内視鏡的胃瘻造設術研究会世話人（ダイナボット（株））
・平成 12 年　肝疾患座談会世話人 in Kyoto（住友製薬）（京大関係）
・平成 12 年　近畿肝癌談話会常任幹事（協和発酵工業）
・平成 13 年　関西肝血流動態イメージ研究会世話人（エーザイ株式会社）
・平成 16 年　あおい肝臓研究会世話人（住友製薬）
・平成 18 年　大阪肝臓ミーティング世話人（大日本住友）
・平成 19 年　近畿・超音波内視鏡研究会世話人顧問

全国規模の国内研究会主催（会長）

・　1997 年 2 月　第 3 回肝血流動態イメージ研究会（神戸）
・　1996 年 10 月　第 1 回日本造影エコー・ドプラ診断研究会（神戸）

・ 2005 年 2 月　　第 11 回肝血流動態イメージ研究会（横浜）
・ 2007 年 9 月　　第 2 回肝癌治療シミュレーション研究会（大阪）
・ 2008 年 9 月　　第 49 回日本消化器画像診断研究会（大阪）
・ 2010 年 1 月　　第 1 回日本肝癌分子標的治療研究会（神戸）
・ 2014 年 2 月　　第 20 回肝血流動態・機能イメージ研究会（大阪）

国内学会主催（会長）

・ 第 45 回日本肝臓学会総会（2009 年 6 月）,神戸
・ 第 83 回日本超音波医学会学術集会（2010 年 5 月）,京都
・ 第 50 回日本肝癌研究会（2014 年 6 月）,京都
・ 第 89 回日本超音波医学会学術集会（2 回目：AFSUMB との併催のため）（2016 年 5 月）,京都

近畿地区学会主催（会長）

・ 第 82 回日本消化器内視鏡学会近畿支部例会（2009 年 8 月）
・ 第 95 回日本消化器病学会近畿支部例会（2011 年 8 月）

国際学会主催（会長）

・ JSH Single Topic Conference on HCC (2005 年), Awaji-shima
・ The 3rd International Kobe Liver Cancer Symposium on HCC (IKLS) (2009 年 6 月), Kobe
・ The 2nd Asia Pacific Primary Liver Cancer Expert Meeting (APPLE) (2011 年 7 月), Osaka
・ The 14th WFUMB 2013(世界超音波医学会)(2013 年 5 月), Sao Paulo(Co-President with Leandro Fernandez and Giovanni Guido Cerri)
・ The 4th International Kyoto Liver Cancer Symposium (IKLS) (2014 年 6 月), Kyoto
・ The 8th International Liver Cancer Association（国際肝癌学会）(2014 年 9 月 5 日-7 日）, Kyoto (Co-President with Peter Galle)
・ The 6th Asia Pacific Primary Liver Cancer Expert Meeting (APPLE) (2015 年 7 月), Osaka
・ AFSUMB 2016（アジア超音波医学会）(2016 年 5 月), Kyoto

2016 年度表彰式一覧

- Highest Impact Factor Award 2016（最高インパクトファクター賞）

1 位　萩原　智　　11.711（Hepatology）
2 位　松井繁長　　10.383（Am J Gastroenterol）
2 位　三長孝輔　　10.383（Am J Gastroenterol）

※　工藤正俊　4.47（Liver Int）

- Most Numbers of Paper Award 2016（最多英文論文発表賞）

1 位　三長孝輔　8 本（Gastrointest Endosc×1, Ther Adv Gastroenter×1, World J Gastroenterol×3, Endoscopy×2, Am J Gastroenterol×1）
2 位　萩原　智　4 本（Digest Dis×1 , Hepatology×2, Internal Med×1）

※　3 位　西田直志　3 本（Digest Dis×2 , J Gastroen Hepatol×1）
　　3 位　鎌田　研　3 本（Endoscopy×2 , Ultrasonography×1）
※　工藤正俊　14 本

- Total Highest Impact Factor Award 2016（累積最高インパクトファクター賞）

1 位　三長孝輔　40.1127（8 本）
2 位　萩原　智　26.031（4 本）

※　3 位 鎌田　研　11.268（3 本）
※　工藤正俊　17.413（14 本）

- 最多入院受持患者賞

1 位　河野匡志　271 人
2 位　大本俊介　231 人

※　3 位　岡元寿樹　221 人

- 最多緊急内視鏡賞

1 位　大本俊介　86 件
2 位　河野匡志　66 件

※　3 位　三長孝輔　46 件

- 最多外来患者診療賞

1 位　萩原　智　3,209 人
2 位　松井繁長　2,746 人

※ 3 位　上嶋一臣　2,681 人
※ 工藤正俊　1,541 人

消化器内科学教室業績抜粋

	1999	2000	2001	2002	2003	2004	2005	2006	2007
英文論文 (Impact Factor)	7 50.641	11 46.062	23 70.709	13 23.244	21 59.851	20 82.744	24 69.706	15 47.563	31 103.707
和文論文 (著書・分担執筆を含む)	37	41	43	34	31	54	45	39	45
海外学会発表	2	9	4	6	24	23	14	14	17
国内学会発表	46	56	71	113	105	79	69	52	79
海外特別講演	0	11	4	11	8	18	16	25	18
国内特別講演	37	40	40	52	37	38	39	27	36
単著教科書			1		1 (英文)				

平成29年12月現在

2008	2009	2010	2011	2012	2013	2014	2015	2016	2017	計
43 165.623	26 110.193	51 134.922	48 163.558	44 213.479	56 265.114	57 290.949	68 382.878	73 396.685	132 655.216	763 3332.844
74	81	126	59	54	17	21	55	15	35	906
26	20	34	64	52	35	37	32	47	34	494
87	65	96	100	118	117	105	98	69	91	1616
36	34	42	28	34	33	16	19	16	14	383
39	62	94	75	59	43	28	40	34	35	818
										2

近畿大学医学部消化器内科　英文論文総数（763編）

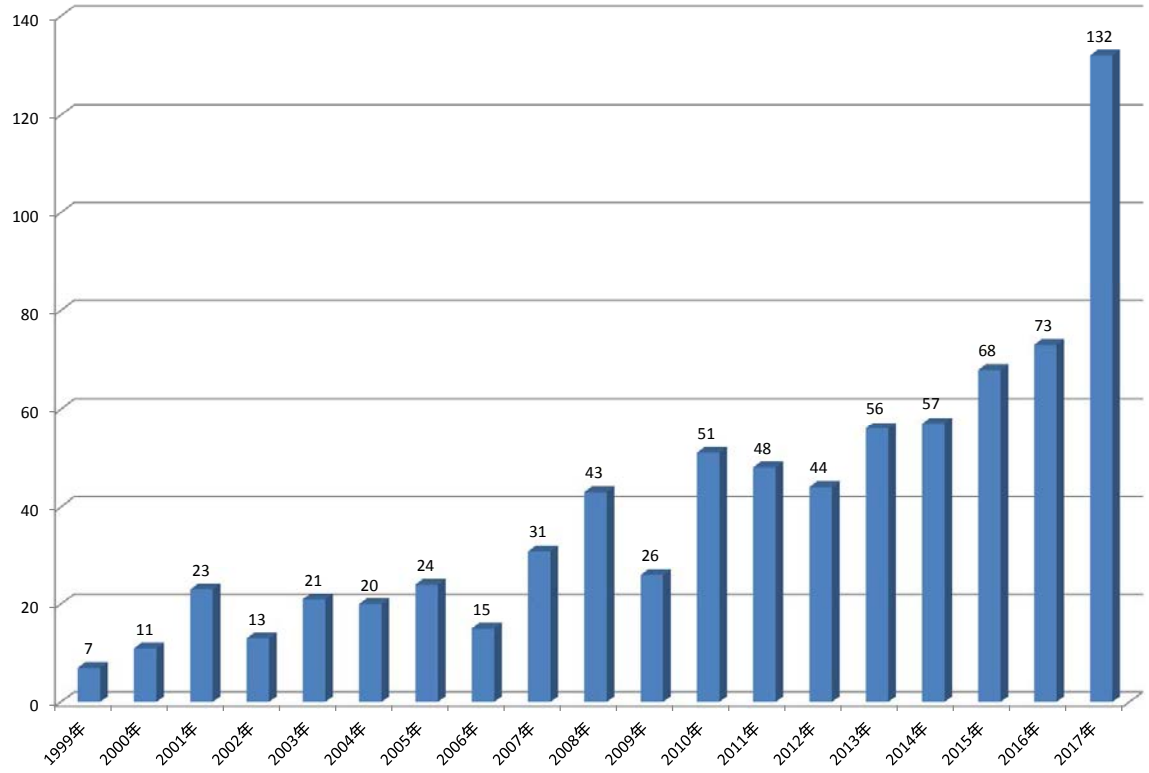

近畿大学医学部消化器内科　英文論文　Impact Factor総数
（IF=3332.844）

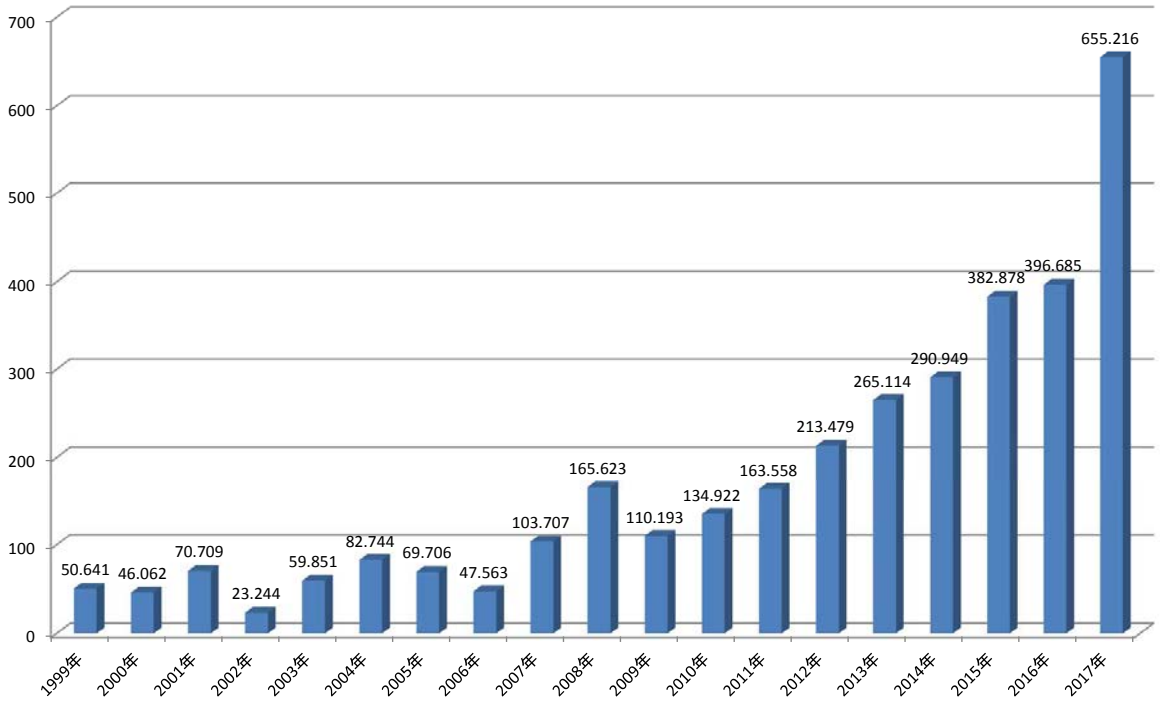

消化器内科年度別診療実績

	H11	H12	H13	H14	H15	H16	H17	H18	H19	H20
稼働床	40	44	44	44	60	78	78	77	76	73
稼働率	107.2%	98.5%	126.7%	148.2%	121.0%	89.5%	95.3%	89.2%	94.7%	96.3%
日平均入院患者数	40.0	43.3	55.8	65.2	72.6	69.8	74.4	68.7	72.0	70.3
平均在院日数	31.1	25.6	21.4	18.6	15.4	14.7	12.8	10.7	10.5	9.6
年間入院収入	501,570,188	570,616,464	801,199,124	923,171,333	1,065,481,449	1,023,271,279	1,152,778,111	1,106,484,453	1,224,122,968	1,244,806,271
年間外来収入	314,641,639	334,517,979	386,084,329	530,035,297	635,562,806	649,876,475	818,049,485	966,247,389	1,013,910,559	1,257,804,553
消化器内科年間収入	816,211,827	905,134,443	1,187,283,453	1,453,206,630	1,701,044,255	1,673,147,754	1,970,827,596	2,072,731,842	2,238,033,527	2,502,610,824

	H21	H22	H23	H24	H25	H26	H27	H28	H29(1-11)
稼働床	85	84	84	84	80	80	80	95	100
稼働率	91.8%	89.9%	85.8%	89.0%	91.0%	93.9%	98.7%	96.8%	91.9%
日平均入院患者数	70.3	76.1	72.0	74.7	77.0	75.1	78.9	84.7	90.7
平均在院日数	9	8.6	7.9	7.2	7.2	6.7	7.0	7.6	6.9
年間入院収入	1,312,812,506	1,516,925,835	1,417,104,402	1,535,069,456	1,575,321,748	1,621,531,082	1,700,694,167	1,816,140,190	1,303,798,857
年間外来収入	1,432,350,698	1,464,645,183	1,529,385,181	1,610,826,432	1,586,645,573	1,771,578,798	2,914,910,768	2,027,534,890	1,280,028,970
消化器内科年間収入	2,745,163,204	2,981,571,018	2,946,489,583	3,145,895,888	3,161,967,321	3,393,109,880	4,615,604,935	3,843,675,080	2,583,827,827

平成29年11月現在

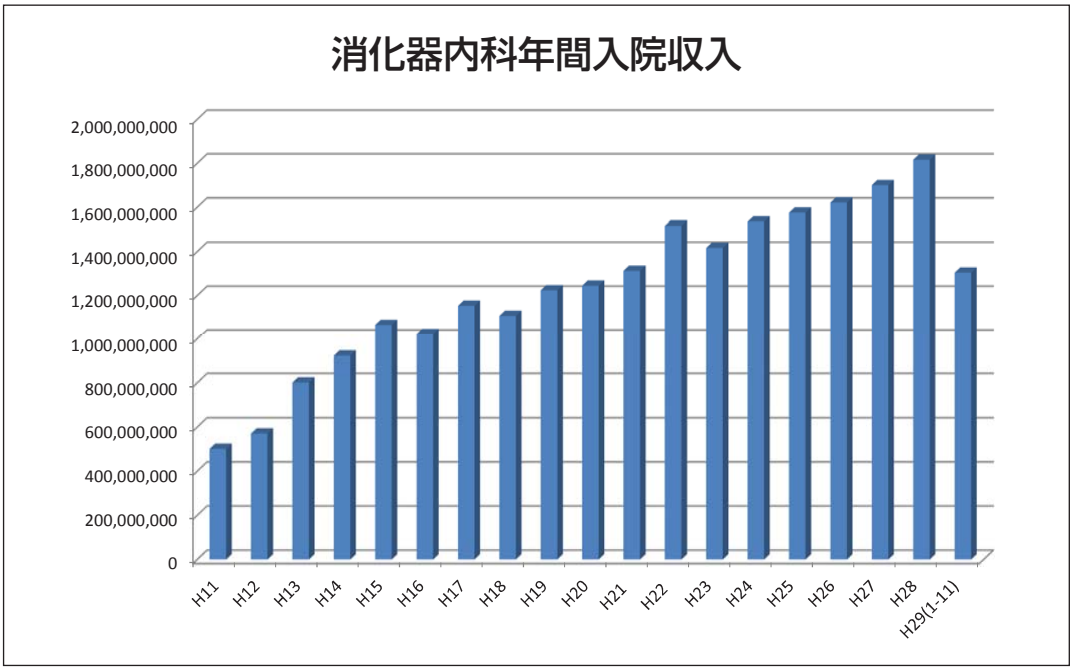

平成29年11月現在

平成29年11月現在

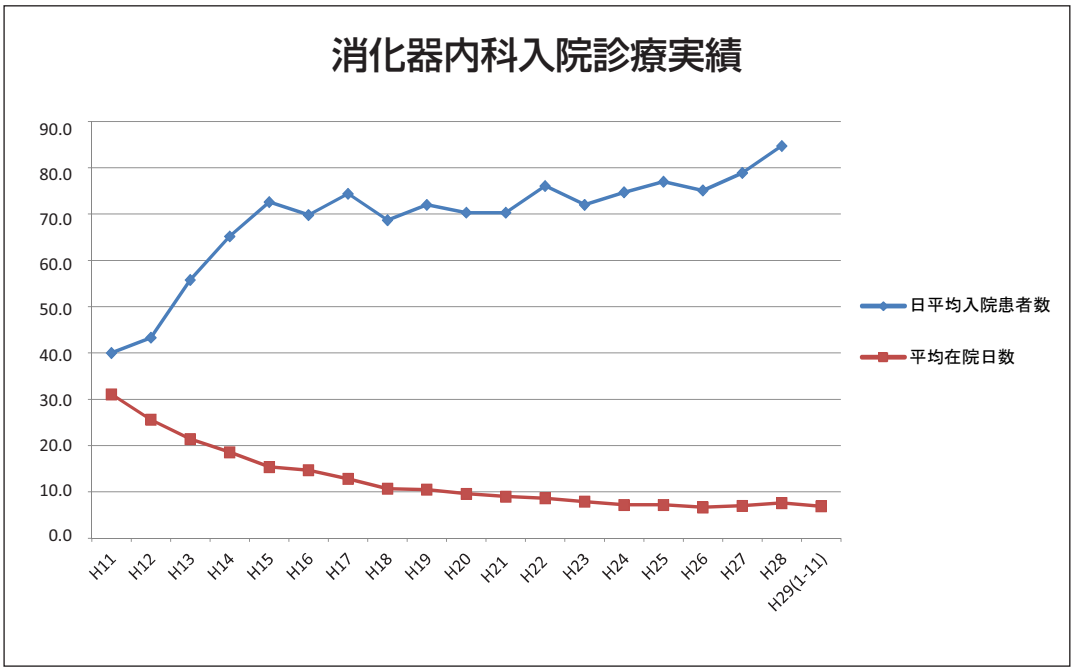

平成29年11月現在

エコー室件数

1月-12月	H11	H12	H13	H14	H15	H16	H17	H18	H19	H20	H21	H22	H23	H24	H25	H26	H27	H28	H29
肝生検		54	89	145	117	110	110	104	135	125	200	191	214	264	225	200	133	183	117
RFA		205	214	224	340	291	310	353	340	291	343	239	270	272	235	249	216	211	163
PEIT		24	0	7	0	2	3	0	0	1	4	2	0	0	0	0	0	0	0
レボビスト	21	381	362	489	367	345	339	258	18	0	0	0	0	0	0	0	0	0	0
ソナゾイド	0	0	0	0	0	0	0	0	529	628	645	617	602	580	562	599	529	590	565

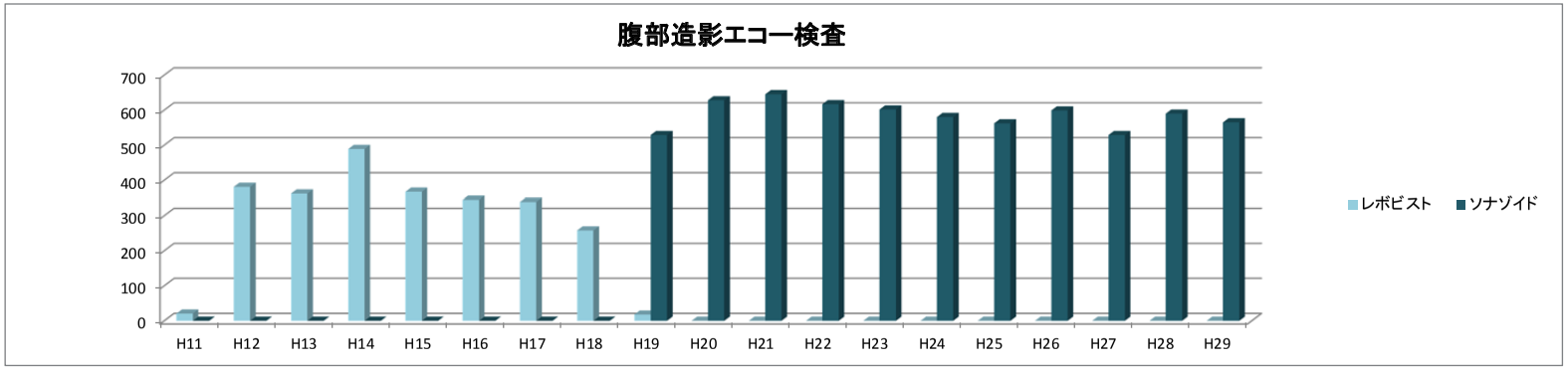

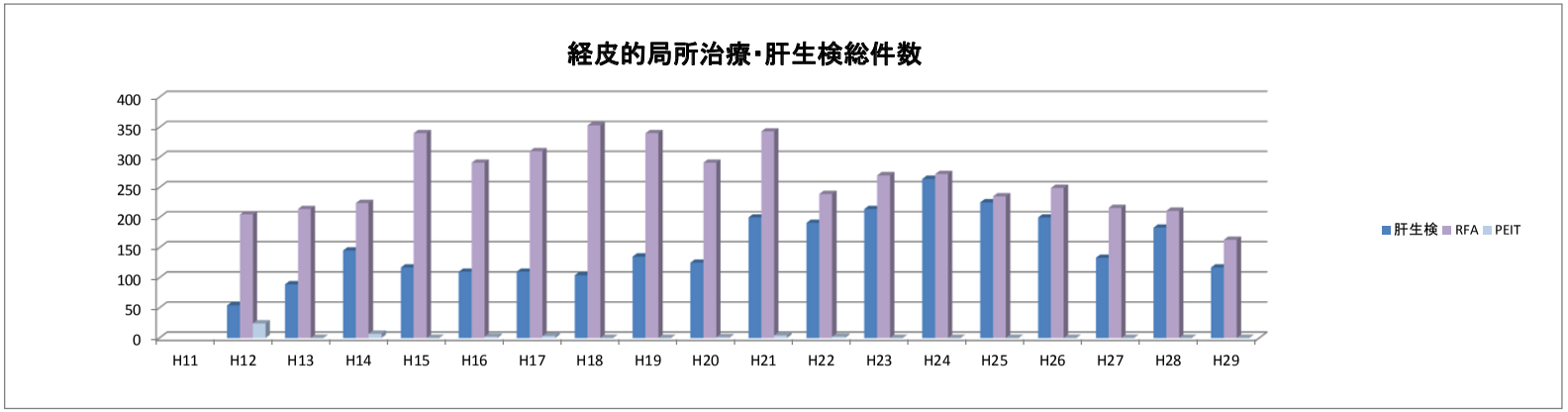

平成29年11月現在

内視鏡部年報

年（1～12月）

検　　査	H26	H27	H28	H29（1～11月）
食道・胃・十二指腸　球部（EUS含む）	9003	8993	8487	8011
超音波内視鏡（胃）	42	53	72	71
超音波内視鏡（胆膵）	1603	1817	1609	1455
胃・十二指腸　ポリペク	4	40	3	6
胃・十二指腸　EMR	206	236	224	209
止血・上部	125	158	165	130
食道静脈瘤結紮術（EVL）	51	63	56	61
硬化療法（EIS）	0	7	9	10
EISL	29	25	28	35
食道ブジー	163	153	69	73
経皮内視鏡的胃瘻造設術（PEG）	73	68	59	60
ステント留置（食道）	10	11	16	13
ステント留置（胃・十二指腸）	33	38	24	38
イレウス管（経口）	45	54	64	61
トロビン撒布	30	25	24	19
異物除去	371	405	415	200
大腸ファイバースコピー（EUS含む）	3903	3928	3813	3701
超音波内視鏡（大腸）	12	10	14	17
大腸　ポリペク・EMR（大腸ESD含む）	769	729	760	777
止血　大腸	50	42	40	34
異物除去	30	25	24	0
大腸ブジー	6	8	7	7
（経肛門）イレウス管	45	54	64	2
小腸ファイバースコピーのみ	97	125	95	98
小腸　ポリペク	0	0	1	0
小腸EMR	4	1	4	4
止血　小腸	5	5	3	5
小腸ブジー	0	0	7	0
小腸カプセル内視鏡	34	17	34	43
胆道ドレナージ	278	349	382	281
乳頭切開	120	127	127	123
乳頭バルーン拡張術	2	1	1	1
結石除去	125	106	129	121
気管支ファイバースコピー	495	542	544	481
胸腔鏡	—	—	17	17
予約外内視鏡検査	1117	1101	846	672

平成 29 年 2 月　部門別医師構成

近畿大学医学部　消化器内科

主任教授

工藤正俊

〇消化管グループ

樫田博史、松井繁長、渡邊智裕、櫻井俊治、朝隈　豊、米田賴晃、永井知行、足立哲平、河野匡志、岡元寿樹、岡本彩那

〇肝グループ

西田直生志、上嶋一臣、依田　広、南　康範、萩原　智、矢田典久、田北雅弘、有住忠晃、千品寛和、南　知宏、岩西美奈、橋本有人

〇胆膵グループ

竹中　完、今井　元（留学中)、山雄健太郎、鎌田　研、宮田　剛、三長孝輔

近大堺病院

辻　直子、川崎正憲、松本　望、尾﨑信人

近大奈良病院

川崎俊彦、水野成人、高山政樹、奥田英之、木下大介、泰　康倫、岡崎能久

関空クリニック

汐見幹夫

富田林病院

小牧孝充、由谷逸朗、山田光成

串本病院

大本俊介

教授秘書

田中真紀、本廣佳香、正野江梨

肝癌研究会秘書

田村利恵、前原なつみ、上妻智子

臨床研究補助秘書

弓削公子、児玉美由紀

医局秘書

胡桃由佳、朝隈　智、浦田亜樹

実験助手

鏡　郁子、矢川沙知

近畿大学　消化器内科学教室医局員

（平成 28 年 7 月現在）

役職		氏名	卒年	
主任教授		工藤正俊	S53	肝臓・消化器・肝癌の診断と治療
教授（内視鏡部）		樫田博史	S58	下部消化管
准教授		汐見幹夫	S55	上部・胆膵内視鏡（関空クリニック所長・教授兼務）
		西田直生志	S60	肝臓病学・肝癌の分子生物学
		渡邉智裕	H5	消化管全般
講師	医局長	松井繁長	H3	食道静脈瘤止血・上部消化管
医学部講師	病棟医長	上嶋一臣	H7	慢性肝炎・肝癌の治療
	外来医長	櫻井俊治	H7	上部消化管・分子生物学
		依田　広	H8	肝疾患・消化器一般
		南　康範	H9	肝疾患・消化器一般
		萩原　智	H10	肝疾患・消化器一般
		矢田典久	H11	肝疾患・消化器一般
		竹中　完	H13	胆膵疾患・消化器一般
		朝隈　豊	H14	上部消化管・消化器一般
		田北雅弘	H15	肝疾患・消化器一般
医学部助教		永井知行	H16	消化器一般
		今井　元	H17	消化器一般
		山田光成	H18	胆膵疾患・消化器一般
		有住忠晃	H19	胆膵疾患・消化器一般
		鎌田　研	H19	消化器一般
		宮田　剛	H19	肝疾患・消化器一般
		足立哲平	H21	胆膵疾患・消化器一般
		大本俊介	H21	胆膵疾患・消化器一般
		岡本彩那	H23	胆膵疾患・消化器一般
		橋本有人	H26	消化器一般
大学院生	4 年	千品寛和	H22	消化器一般
		南　知宏	H23	消化器一般
	3 年	山雄健太郎	H18	消化器一般
		河野匡志	H22	消化器一般
	2 年	米田頼晃	H13	消化器一般
		三長孝輔	H19	胆膵疾患・消化器一般
		岡元寿樹	H23	消化器一般
	1 年	岩西美奈	H25	消化器一般

2017 年 12 月

消化器内科学教室業績一覧

(2016 年)

論文発表（英文）

1. Minaga K, Kitano M, Imai H, Miyata T, Kudo M: Acute spinal cord infarction after EUS-guided celiac plexus neurolysis. Gastrointest Endosc 83:1039-1040, 2016.
2. Kudo M*: Defect reperfusion imaging with sonazoid®: a breakthrough in hepatocellular carcinoma. Liver Cancer 5:1-7, 2016.
3. Kudo M*: Breakthrough imaging in hepatocellular carcinoma. Liver Cancer 5:47-54, 2016.
4. Kamata K, Kitano M, Omoto S, Kadosaka K, Miyata T, Yamao K, Imai H, Sakamoto H, Harwani Y, Chikugo T, Chiba Y, Matsumoto I, Takeyama Y, Kudo M: Contrast-enhanced harmonic endoscopic ultrasonography for differential diagnosis of pancreatic cysts. Endoscopy 48:35-41, 2016.
5. Kudo M*, Ueshima K, Kubo S, Sakamoto M, Tanaka M, Ikai I, Furuse J, Murakami T, Kadoya M, Kokudo N, Liver Cancer Study Group of Japan: Response evaluation criteria in cancer of the liver (RECICL)(2015 revised version). Hepatol Res 46:3-9, 2016.
6. Inoue T, Hyodo T, Korenaga K, Murakami T, Imai Y, Higaki A, Suda T, Takano T, Miyoshi K, Koda M, Tanaka H, Iijima H, Ochi H, Hirooka M, Numata K,Kudo M*: Kupffer phase image of Sonazoiod-enhanced US is useful in predicting a hypervascularization of non-hypervascular hypointense hepatic lesions detected on Gd-EOB-DTPA-enhanced MRI: A multicenter retrospective study. J Gastroenterol 51:144-152, 2016.
7. Kudo M*: Heterogeneity and subclassification of Barcelona Clinic Liver Cancer Stage B. Liver Cancer 5:91-96, 2016.
8. Miyata T, Kitano M, Omoto S, Kadosaka K, Kamata K, Imai H, Sakamoto H, Nishida N, Harwani Y, Murakami T, Takeyamas Y, Chiba Y, Kudo M: Contrast-enhanced harmonic endoscopic ultrasonography for assessment of lymph node metastases in pancreatobiliary carcinoma. World J Gastroenterol 22:3381-3391, 2016.
9. Kudo M*, Kanai H: Inclusion of Journal of Medical Ultrasonics in MEDLINE. J Med Ultrason 43:163, 2016.
10. Kamata K, Kitano M, Yasukawa S, Kudo M, Chiba Y, Ogura T, Higuchi K, Fukutake N, Ashida R, Yamasaki T, Nebiki H, Hirose S, Hoki N, Asada M, Yazumi S, Takaoka M, Okazaki K, Matsuda F, Okabe Y, Yanagisawa A: Histologic diagnosis of pancreatic masses using 25-gauge endoscopic ultrasound needles with and without a core trap: a multicenter randomized trial. Endoscopy 48:632-638, 2016.
11. Hagiwara S, Nishida N, Kudo M: Reply. Hepatology 63:1744-1745, 2016.
12. Geschwind JF, Kudo M, Marrero JA, Venook AP, Chen XP, Bronowicki JP, Dagher L, Furuse J, de Guevara LL, Papandreou C, Sanyal AJ, Takayama T, Ye SL, Yoon SK, Nakajima K, Lehr R, Heldner S, Lencioni R: TACE treatment in patients with sorafenib-treated unresectable hepatocellular carcinoma in clinical practice: final analysis of GIDEON (Global Investigation of therapeutic DEcisions in hepatocellular carcinoma and Of its treatment with sorafeNib). Radiology 279:630-640, 2016.
13. Matsui S, Kashida H, Kudo M: Gastric perineurioma. Am J Gastroenterol 111:453, 2016.
14. Minaga K, Kitano M, Imai H, Yamao K, Kamata K, Miyata T, Matsuda T, Omoto S, Kadosaka K, Yoshikawa T, Kudo M: Modified single transluminal gateway transcystic multiple drainage technique for a huge infected walled-off pancreatic necrosis: A case report. World J Gastroenterol 22(21):5132-5136, 2016.
15. Kitano M, Imai H, Kamata K, Kudo M: Response. Gastrointest Endosc 83(6):1303, 2016.
16. Kitai S, Kudo M*, Nishida N, Izumi N, Sakamoto M, Matsuyama Y, Ichida T, Nakashima O, Matsui O, Ku Y, Kokudo N, Makuuchi M, for the Liver Cancer Study Group of Japan: Survival benefit of locoregional treatment for hepatocellular carcinoma with advanced liver cirrhosis. Liver Cancer 5:175-189, 2016.
17. Minaga K, Kitano M, Sakamoto H, Miyata T, Imai H, Yamao K, Kamata K, Omoto S, Kadosaka K, Sakurai T, Nishida N, Chiba Y, Kudo M: Predictors of pain response in patients undergoing EUS -

guided neurolysis for abdominal pain caused by pancreatic cancer. Ther Adv Gastroenterol 9:483-494, 2016.
18. Kamata K, Kitano M, Omoto S, Kadosaka K, Miyata T, Minaga K, Yamao K, Imai H, Kudo M: New endoscopic ultrasonography techniques for pancreaticobiliary diseases. Ultrasonography 35:169-179, 2016.
19. Minaga K, Kitano M, Imai H, Yamao K, Kamata K, Miyata T, Omoto S, Kadosaka K, Yoshikawa T, Kudo M: Urgent endoscopic ultrasound-guided choledochoduodenostomy for acute obstructive suppurative cholangitis-induced sepsis. World J Gastroenterol 22:4264-4269, 2016.
20. Abou-Alfa GK, Puig O, Daniele B, Kudo M, Merle P, Park JW, Ross P, Peron JM, Ebert O, Chan S, Poon TP, Colombo M, Okusaka T, Ryoo BY, Minguez B, Tanaka T, Ohtomo T, Ukrainskyi S, Boisserie F, Rutman O, Chen YC, Xu C, Shochat E, Jukofsky L, Reis B, Chen G, Di Laurenzio L, Lee R, Yen CJ: Randomized Phase II placebo controlled study of codrituzumab in previously treated patients with advanced hepatocellular carcinoma. J Hepatol 65:289-295, 2016.
21. Kudo M*, Izumi N, Ichida T, Ku Y, Kokudo N, Sakamoto M, Takayama T, Nakashima O, Matsui O, Matsuyama Y, and the Liver Cancer Study Group of Japan: Report of the 19th follow-up survey of primary liver cancer in Japan. Hepatol Res 46:372-390, 2016.
22. Kudo M*, Lencioni R, Marrero JA, Venook AP, Bronowicki JP, Chen XP, Dagher L, Furuse J, Geschwind JFH, Ladron de Guevara L, Papandreou C, Sanyal AJ, Takayama T, Yoon SK, Nakajima K, Lehr R, Heldner S, Ye SL: Regional differences in sorafenib-treated patients with hepatocellular carcinoma: GIDEON observational study. Liver Int 36:1196-1205, 2016.
23. Imai H, Kitano M, Omoto S, Kadosaka K, Kamata K, Miyata T, Yamao K, Sakamoto H, Harwani Y, Kudo M: EUS-guided gallbladder drainage for rescue treatment of malignant distal biliary obstruction after unsuccessful ERCP. Gastrointest Endosc 84:147-151, 2016.
24. Kudo M*: Chronic Liver diseases and liver cancer: state-of-the art progress in 2016. Digest Dis, 34:617-619, 2016.
25. Hagiwara S, Nishida N, Watanabe T, Sakurai T, Ida H, Minami Y, Takita M, Minami T, Iwanishi M, Chishina H, Ueshima K, Komeda Y, Arizumi T, Kudo M: Outcome of asunaprevir/daclatasvir combination therapy for chronic liver disease type C. Digest Dis 34:620-626, 2016.
26. Nishida N, Kono M, Minami T, Chishina H, Arizumi T, Takita M, Yada N, Ida H, Hagiwara S, Minami Y, Ueshima K, Sakurai T, Kudo M: Safety, tolerability, and efficacy of sofosbuvir plus rivavirin in elderly patients infected with hepatitis C virus genotype 2. Digest Dis 34:632-639, 2016.
27. Takita M, Iwanishi M, Minami T, Kono M, Chishina K, Arizumi T, Yada N, Hagiwara S, Minami Y, Ida H, Ueshima K, Nishida N, Kudo M*: Monoethanolamine oleate sclerotherapy for polycystic liver disease. Digest Dis 34:654-658, 2016.
28. Chishina H, Hagiwara S, Nishida N, Ueshima K, Sakurai T, Ida H, Minami Y, Takita M, Kono M, Minami T, Iwanishi M, Umehara Y, Watanabe T, Komeda Y, Arizumi T, Kudo M*: Clinical factors predicting the effect of tolvaptan for refractory ascites in patients with decompensated liver cirrhosis. Digest Dis 34:659-664, 2016.
29. Nishida N, Kudo M: Clinical significance of epigenetic alterations in human hepatocellular carcinoma and its association with genetic mutations. Digest Dis 34:708-713, 2016.
30. Minami Y, Minami T, Chishina H, Kono M, Arizumi T, Takita M, Yada N, Hagiwara S, Ida H, Ueshima K, Nishida N, Kudo M: US-US fusion imaging in radiofrequency ablation for liver metastases. Digest Dis 34:687-691, 2016.
31. Ogawa C, Minami Y, Morita M, Noda A, Arasawa S, Izuta M, Kubo A, Matsunaka T, Tamaki N, Shibatouge M, Kudo M*: Prediction of embolization area after conventional transcatheter arterial chemoembolization for hepatocellular carcinoma using SYNAPSE VINCENT. Digest Dis 34:696-701, 2016.
32. Kudo M*: Recent trends in the management of hepatocellular carcinoma with special emphasis on treatment with regorafenib and immune checkpoint inhibitors. Digest Dis 34:714-730, 2016.
33. Kim SK, Shin MH, Sugimoto K, Kim SR, Imoto S, Kim KI, Taniguchi M, Oh HK, Yano Y, Hayashi

T, Kudo M: Coffee intake and liver enzyme association in Korean immigrants and Japanese: a comprehensive cross-sectional study. Digest Dis 34:665-670, 2016.
34. Yada N, Sakurai T, Minami T, Arizumi T, Takita M, Hagiwara S, Ida H, Ueshima K, Nishida N, Kudo M*: Prospective risk analysis of hepatocellular carcinoma in patients with chronic hepatitis C by ultrasound strain elastography. Digest Dis 34:650-653, 2016.
35. Sugimoto K, Kim SK, Kim SR, Kobayashi M, Kato A, Morimoto E, Imoto S, Kim CW, Tanaka Y, Kudo M, Yano Y, Hayashi Y: Efficacy and safety of sofosbuvir plus ribavirin treatment for patients with chronic hepatitis C genotype 2. Digest Dis 34:627-631, 2016.
36. Kawasaki T, Hata K, Kinoshita D, Takayama M, Okuda H, Mizuno S, Kudo M*: Radiofrequency ablation guided by contrast-enhanced sonography versus B-mode sonography for hepatocellular carcinoma after transcatheter arterial chemoembolization. Digest Dis 34:692-695, 2016.
37. Iwamoto T, Imai Y, Kogita S, Igura T, Sawai Y, Fukuda K, Yamaguchi Y, Matsumoto Y, Nakahara M, Morimoto O, Seki Y, Ohashi H, Fujita N, Kudo M, Takehara T: Comparison of contrast-enhanced ultrasound and Gadolinium-Ethoxybenzyl-Diethylenetriamine Pentaacetic Acid-enhanced MRI for the diagnosis of macroscopic type of hepatocellular carcinoma. Digest Dis 34:679-686, 2016.
38. Arizumi T, Ueshima K, Iwanishi M, Minami T, Chishina H, Kono M, Takita M, Kitai S, Inoue T, Yada N, Hagiwara S, Minami Y, Ida H, Sakurai T, Kitano M, Nishida N, Kudo M*: Validation of Kinki criteria, a modified substaging system, in patients with intermediate stage hepatocellular carcinoma. Digest Dis 34:671-678, 2016.
39. Wu T, Wang P, Zhang T, Zheng J, Li JZ, Zeng J, Kudo M, Zheng R: Comparison of two-dimensional shear wave elastography and real-time tissue elastography for assessing liver fibrosis in chronic hepatitis B. Digest Dis 34:640-649, 2016.
40. Nagai T, Arao T, Nishio K, Matsumoto K, Hagiwara S, Sakurai T, Minami Y, Ida H, Ueshima K, Nishida N, Sakai K, Saijo N, Kudo K, Kaneda H, Tamura D, Aomatsu K, Kimura H, Fujita Y, Haji S, Kudo M*: Impact of tight junction protein ZO-1 and TWIST expression on post-operative survival of patients with hepatocellular carcinoma. Digest Dis 34:702-707, 2016.
41. Ramaswami R, Pinato DJ, Kubota K, Ishizuka M, Arizumi T, Kudo M, Jang JW, Kim YW, Pirisi M, Allara E, Sharma R: Prognostic sub-classification of intermediate-stage hepatocellular carcinoma: a multicenter cohort study with propensity score analysis. Med Oncol 33:114-121, 2016.
42. Minaga K, Kitano M, Imai H, Harwani Y, Yamao K, Kamata K, Miyata T, Omoto S, Kadosaka K, Sakurai T, Nishida N, Kudo M: Evaluation of anti-migration properties of biliary covered self-expandable metal stents. World J Gastroenterol 22:6917-6924, 2016.
43. Kudo M*, Izumi N, Sakamoto M, Matsuyama Y, Ichida T, Nakashima O, Matsui O, Ku Y, Kokudo N, Makuuchi M, for the Liver Cancer Study Group of Japan: Survival analysis over 28 years of 173,378 patients with hepatocellular carcinoma in Japan. Liver Cancer 5:190-197, 2016.
44. Kudo M*: Risk of Hepatocellular carcinoma in patients with hepatitis C virus who achieved sustained virological response. Liver Cancer 5:155-161, 2016.
45. Cheng AL, Thongprasert S, Lim HY, Sukeepaisarnjaroen W, Yang TS, Wu CC, Chao Y, Chan SL, Kudo M, Ikeda M, Kang YK, Pan H, Numata K, Han G, Balsara B, Zhang Y, Rodriguez AM, Zhang Y, Wang Y, Poon RT: Randomized, open-label phase 2 study comparing frontline dovitinib versus sorafenib in patients with advanced hepatocellular carcinoma. Hepatology 64:774-784, 2016.
46. Watanabe T, Sadakane Y, Yagama N, Sakurai T, Ezoe H, Kudo M, Chiba T, Strober W: Nucleotide-binding oligomerization domain 1 acts in concert with the cholecystokinin receptor agonist, cerulein, to induce IL-33-dependent chronic pancreatitis. Mucosal Immunol 9:1234-1249, 2016.
47. Nishida N, Yada N, Hagiwara S, Sakurai T, Kitano M, Kudo M: Unique features associated with hepatic oxidative DNA damage and DNA methylation in non-alcoholic fatty liver disease. J Gastroen Hepatol 31:1646-1653, 2016.
48. Makino Y, Imai Y, Igura T, Kogita S, Sawai Y, Fukuda K, Iwamoto T, Okabe J, Takamura M, Fujita N, Hori M, Takehara T, Kudo M, Murakami T: Feasibility of extracted-overlay fusion imaging for intraoperative treatment evaluation of radiofrequency ablation for hepatocellular carcinoma. Liver

Cancer 5:269-279, 2016.
49. Ikeda M, Shimizu S, Sato T, Morimoto M, Kojima Y, Inaba Y, Hagihara A, Kudo M, Nakamori S, Kaneko S, Sugimoto R, Tahara T, Ohmura T, Yasui K, Sato K, Ishii H, Furuse J, Okusaka T: Sorafenib plus hepatic arterial infusion chemotherapy with cisplatin versus sorafenib for advanced hepatocellular carcinoma: Randomized phase II trial. Ann Oncol 27: 2090-2096, 2016.
50. Kudo M*: Regorafenib as second-line systemic therapy may change the treatment strategy and management paradigm for hepatocellular carcinoma. Liver Cancer 5:235-244, 2016.
51. Hagiwara S, Nishida N, Kudo M: Reply: Hepatocyte damage due to protoporphyrin deposition. Hepatology 64:306, 2016.
52. Minaga K, Kitano M, Enoki E, Kashida H, Kudo M: Needle-tract seeding on the proximal gastric wall after EUS-guided fine-needle aspiration of a pancreatic mass. Am J Gastroenterol 111:1515, 2016.
53. Kim SK, Kim SR, Imoto S, Kim CW, Matsuoka T, Nakashima O, Sasaki M, Kumabe T, Kudo M, Fukusato T, Kondo F: Bile duct adenoma in patient with chronic hepatitis C: As a benign neoplasm by pathological and imaging studies. Pathol Int 66:640-642, 2016.
54. Kokudo T, Hasegawa K, Matsuyama Y, Takayama T, Izumi N, Kadoya M, Kudo M, Ku Y, Sakamoto M, Nakashima O, Kaneko S, Kokudo N: Survival benefit of liver resection for hepatocellular carcinoma associated with portal vein invasion. J Hepatol 65:938-943, 2016.
55. Hagiwara S, Nishida N, Chishina H, Ida H, Sakurai T, Komeda Y, Kitano M, Kudo M: Cases with refractory ascites and a delayed response to tolvaptan. Intern Med 55:3273-3277, 2016.
56. Minaga K, Takenaka M, Miyata T, Ueda Y, Kitano M, Kudo M: Through-the-mesh technique after endoscopic ultrasonography-guided hepaticogastrostomy: a novel re-intervention method. Endoscopy 48: E369-E370, 2016.
57. Minaga K, Kitano M, Yoshikawa T, Omoto S, Kamata K, Yamao K, Kudo M: Hepaticogastrostomy guided by real-time contrast-enhanced harmonic EUS: a novel technique. Endoscopy 48:E228-229, 2016.
58. Kudo M*, Ikeda M, Takayama T, Numata K, Izumi N, Furuse J, Okusaka T, Kadoya M, Yamashita S, Ito Y, Kokudo N: Safety and efficacy of sorafenib in Japanese patients with hepatocellular carcinoma in clinical practice: a subgroup analysis of GIDEON. J Gastroenterol 51:1150-1160, 2016.
59. Marrero JA, Kudo M, Venook AP, Ye SL, Bronowicki JP, Chen XP, Dagher L, Furuse J, Geschwind JH, de Guevara LL, Papandreou C, Takayama T, Sanyal AJ, Yoon SK, Nakajima K, Lehr R, Heldner S, Lencioni R: Observational registry of sorafenib use in clinical practice across Child-Pugh subgroups: the GIDEON study. J Hepatol 65:1140-1147, 2016.
60. Pinato DJ, Arizumi T, Jang JW, Allara E, Suppiah P, Smirne C, Tait P, Pai M, Grossi G, Kim YW, Pirisi M, Kudo M, Sharma R: Combined sequential use of HAP and ART scores to predict survival outcome and treatment failure following chemoembolization in hepatocellular carcinoma: a multi-center comparative study. Oncotarget 7:44705-44718, 2016.
61. Yamao K, Kitano M, Kayahara T, Ishida E, Yamamoto H, Minaga K, Yamashita Y, Nakajima J, Asada M, Okabe Y, Osaki Y, Chiba Y, Imai H, Kudo M: Factors predicting through-the-scope gastroduodenal stenting outcomes in patients with gastric outlet obstruction: a large multicenter retrospective study in West Japan. Gastrointest Endosc 84:757-763, 2016.
62. Kudo M*, Trevisani F, Abou-Alfa GK, Rimassa L: Hepatocellular carcinoma: therapeutic guidelines and medical treatment. Liver Cancer 6:16-26, 2016.
63. Sakurai T, Kashida H, Komeda Y, Nagai T, Hagiwara S, Watanabe T, Kitano M, Nishida N, Fujita J, Kudo M: Stress response protein RBM3 promotes the development of colitis-associated cancer. Inflamm Bowel Dis 23:66-74, 2016.
64. Ikeda K, Kudo M, Kawazoe S, Osaki Y, Ikeda M, Okusaka T, Tamai T, Suzuki T, Hisai T, Hayato S, Okita K, Kumada H: Phase 2 Study of Lenvatinib in patients with advanced hepatocellular carcinoma. J Gastroenterol, 2016 (epub ahead of print).

65. Kudo M*, Hatano E, Ohkawa S, Fujii H, Masumoto A, Furuse J, Wada Y, Ishii H, Obi S, Kaneko S, Kawazoe S, Yokosuka O, Ikeda M, Ukai K, Morita S, Tsuji A, Kudo T, Shimada M, Osaki Y, Tateishi R, Sugiyama G, Abada PB, Yang L, Okusaka T, Zhu AX: Ramucirumab as second-line treatment in patients with advanced hepatocellular carcinoma: Japanese subgroup analysis of the REACH trial. J Gastroenterol, 2016 (epub ahead of print).
66. Minami Y, Takita M, Tsurusaki M, Yagyu Y, Ueshima K, Murakami T, Kudo M: Semi-quantitative Prediction of Early Response of Conventional Transcatheter Arterial Chemoembolization for Hepatocellular Carcinoma using Postprocedural Plain Cone-beam CT. Hepatol Res, 2016 (epub ahead of print).
67. Kono M, Minami Y, Iwanishi M, Minami T, Chishina H, Arizumi T, Komeda Y, Sakurai T, Takita M, Yada N, Ida H, Hagiwara S, Ueshima K, Nishida N, Kudo M*: Contrast-enhanced tissue harmonic imaging versus phase inversion harmonic sonographic imaging for the delineation of hepatocellular carcinomas. Oncology, 2016 (epub ahead of print).
68. Kwok WY, Hagiwara S, Nishida N, Watanabe T, Sakurai T, Ida H, Minami Y, Takita M, Minami T, Iwanishi M, Chishina H, Kono M, Ueshima K, Komeda Y, Arizumi T, Enoki E, Nakai T, Kumabe T, Nakashima O, Kondo F, Kudo M: Malignant transformation of hepatocellular adenoma. Oncology, 2016 (epub ahead of print).
69. Hagiwara S, Nishida N, Watanabe T, Sakurai T, Ida H, Minami Y, Takita M, Minami T, Iwanishi M, Chishina H, Ueshima K, Komeda Y, Arizumi T, Kudo M: Outcome of combination therapy with sofosbuvir and ledipasvir for chronic type C liver disease. Oncology, 2016 (epub ahead of print).
70. Zhu AX, Baron AD, Malfertheiner P, Kudo M, Kawazoe S, Pezet D, Weissinger F, Brandi G, Barone CA, Okusaka T, Wada Y, Park JO, Ryoo BY, Cho JY, Chung HC, Li CP, Yen CJ, Lee KD, Yang L, Abada PB, Chang SC, Chau I: Ramucirumab as second-line treatment in patients with advanced hepatocellular carcinoma: Analysis of REACH Trial results by Child-Pugh score. JAMA Oncol, 2016 (epub ahead of print).
71. Park JO, Ryoo BY, Yen CJ, Kudo M, Yang L, Abada PB, Cheng R, Orlando M, Zhu AX, Okusaka T: Second-line ramucirumab therapy for advanced hepatocellular carcinoma (REACH): an East Asian and non-East Asian subgroup analysis. Oncotarget, 2016 (epub ahead of print).
72. Watanabe T, Yamashita K, Kudo M: IgG4-related disease and innate immunity. Curr Top Microbiol, 2016 (epub ahead of print).
73. Minaga K, Kitano M, Gon C, Yamao K, Imai H, Miyata T, Kamata K, Omoto S, Takenaka M, Kudo M: Endoscopic ultrasonography-guided choledochoduodenostomy using a newly designed laser-cut metal stent: feasibility study in a porcine model. Digest Endosc, 2016 (epub ahead of print).
74. Watanabe T, Kudo M, Strober W: Immunopathogenesis of pancreatitis. Mucosal Immunol, 2016 (epub ahead of print).
75. Pinato DJ, Sharma R, Allara E, Yen C, Arizumi T, Kubota K, Bettinger D, Jang JW, Smirne C, Kim YW, Kudo M, Howell J, Ramaswami R, Burlone ME, Guerra V, Thimme R, Ishizuka M, Stebbing J, Pirisi M, Carr BI: The ALBI grade provides objective hepatic reserve estimation across each BCLC stage of hepatocellular carcinoma. J Hepatol, 2016 (epub ahead of print).
76. Bruix J, Qin S, Merle P, Granito A, Huang YH, Bodoky G, Pracht M, Yokosuka O, Rosmorduc O, Breder V, Gerolami, Masi G, Ross P, Song T, Bronowicki JP, Ollivier-Hourmand I, Kudo M, Cheng AL, Llovet JM, Finn RS, LeBerre MA, Baumhauer A, Meinhardt G, Han G, on behalf of the RESORCE Investigators: Regorafenib for patients with hepatocellular carcinoma who progressed on sorafenib treatment (RESORCE): a randomised, double-blind, placebo-controlled, phase 3 trial. Lancet, 2016 (epub ahead of print).
77. Lencioni R, Kudo M, Venook A, Ye SL, Bronowicki JP, Chen XP, Dagher L, Furuse J, Geschwind JF, Guevara LL, Papandreou C, Sanyal AJ, Takayama T, Yoon SK, Nakajima K, Lehr R, Heldner S, Marrero JA: Second IA of the GIDEON (Global Investigation of therapeutic DEcisions in HCC and Of its treatment with sorafeNib) non-interventional study. Liver Int, 2016 (in press).
78. Nishikawa H, Enomoto H, Saito M, Aizawa N, Tsuda Y, Higuchi K, Okazaki K, Seki K, Seki T,

Kim SR, Hongo Y, Jyomura H, Nishida N, Kudo M, Osaki Y, Nishiguchi S: Treatment response and tolerability in elderly patients with chronic hepatitis C: subgroup analysis in ReGIT-J study. Acta Gastro-Ent Belg, 2016 (in press).
79. Hagiwara S, Nishida N, Sakurai T, Park AM, Komeda Y, Kitano M, Kudo M: Identification of a HBx mutation that enhances human hepatocarcinogenesis through the activation of the JNK and Wnt pathways. BMC Cancer, 2016 (in press).
80. Nishida N, Kudo M, et al: Serum microRNA profile that predict initial effect of sorafenib in patients with advanced hepatocellular carcinoma. Liver Cancer, 2016 (in press).
81. Kudo M*: A new horizon in liver disease. Oncology, 2016 (in press).
82. Yada N, Sakurai T, Minami T, Arizumi T, Takita M, Hagiwara S, Ida H, Ueshima K, Nishida N, Kudo M*: Influence of liver inflammation on liver stiffness measurement in patients with autoimmune hepatitis evaluation by combinational elastography. Oncology, 2016 (in press).
83. Nishida N, Kudo M: Immunological microenvironment of hepatocellular carcinoma and its clinical implication. Oncology, 2016 (in press).
84. Tochio H, Tamaki E, Imai Y,Iwasaki N, Minowa K, Chung H, Suginoshita Y, Inokuma T, Kudo M*: CD68-positive cells in hepatic angiomyolipoma. Oncology, 2016 (in press).
85. Kudo M*: Hepatocellular carcinoma treatment with immune checkpoint inhibitors. Oncology, 2016 (in press).
86. Kudo M: Molecular targeted agents for hepatocellular carcinoma: current status and future perspectives. Liver Cancer, 2016 (in press).
87. Hiraoka A, Kumada T, Kudo M, Hirooka M, Tsuji K, Itobayashi E, Kariyama K, Ishikawa T, Tajiri K, Ochi H, Tada T, Toyoda H, Nouso K, Kawasaki H, Hiasa Y, Michitaka K: Albumin-bilirubin (ALBI) grade as part of treatment algorithm of Liver Cancer Study Group of Japan: Comparison with liver damage and Child-Pugh classifications. Liver Cancer, 2016 (in press).
88. Komeda Y, Kashida H, Sakurai T, Tribonias G, Okamoto K, Kono M, Yamada M, Adachi T, Mine H, Nagai T, Asakuma Y, Hagiwara S, Matsui S, Watanabe T, Kitano M, Chikugo T, Chiba Y, Kudo M: Removal of diminutive colorectal polyps: a prospective randomized clinical trial between cold snare polypectomy and hot forceps biopsy. World J Gastroenterol, 2016 (in press).
89. Komeda Y, Kashida H, Sakurai T, Kono M, Nagai T, Asakuma Y, Hagiwara S, Matsui S, Watanabe T, Chikugo T, Kudo M: A case of type II enteropathy-associated T-cell lymphoma (EATL) in a patient with ulcerative colitis. Am J Gastroenterol, 2016 (in press).
90. Pinato DJ, Ramaswami R, Arizumi T, Ferrari C, Gibbin A, Burlone M, Guaschino G, Tonuitto P, Black J, Sellers L, Kudo M, Pirisi M, Sharma R: Integration of the cancer-related inflammatory response as a stratifying biomarker of survival in hepatocellular carcinoma treated with sorafenib. Oncotarget, 2016 (in press).
91. Kamata K, Kitano M, Omoto S, Miyata T, Minaga K, Yamao K, Imai H, Takenaka M, Kudo M: Endoscopic ultrasound-guided gallbladder drainage for acute cholecystitis: long-term outcomes after removal of a self-expandable metal stent. World J Gastroenterol, 2016(in press).
92. Ogura T, Masuda D, Saori O, Wataru T, Sano T, Okuda A, Miyano A, Kitano M, Abdel-Aal UM, Takeuchi T, Fukunishi S, Higuchi K: Clinical outcome of endoscopic ultrasound-guided liver abscess drainage using self-expandable covered metallic stent (with Video). Dig Dis Sci 61(1):303-308, 2016.
93. Ogura T, Chiba Y, Masuda D, Kitano M, Sano T, Saori O, Yamamoto K, Imaoka H, Imoto A, Takeuchi T, Fukunishi S, Higuchi K: Comparison of the clinical impact of endoscopic ultrasound-guided choledochoduodenostomy and hepaticogastrostomy for bile duct obstruction with duodenal obstruction. Endoscopy 48(2):156-163, 2016.
94. Shiokawa M, Kodama Y, Kuriyama K, Yoshimura K, Tomono T, Morita T, Kakiuchi N, Matsumori T, Mima A, Nishikawa Y, Ueda T, Tsuda M, Yamauchi Y, Minami R, Sakuma Y, Ota Y, Maruno T, Kurita A, Sawai Y, Tsuji Y, Uza N, Matsumura K, Watanabe T, Notohara K, Tsuruyama T, Seno H, Chiba T: Pathogenicity of IgG in patients with IgG4-related disease. Gut 65(8): 1322-1332, 2016.
95. Asano N, Imatani A, Watanabe T, Fushiya J, Kondo Y, Jin X, Ara N, Uno K, Iijima K, Koike T,

Strober W, Shimosegawa T: Cdx2 Expression and Intestinal Metaplasia Induced by H. pylori Infection of Gastric Cells Is Regulated by NOD1-Mediated Innate Immune Responses. Cancer Res 76(5):1135-1145, 2016.

96. Minaga K, Kitano M, Takenaka M: Through-the-scope enteral metal stent placement using a short-type single-ballon enteroscope for malignant surgically reconstructed jejunal stenosis (with video). Digest Endosc 28(7):758, 2016.
97. Kanno A, Masamune A, Fujishima F, Iwashita T, Kodama Y, Katanuma A, Ohara H, Kitano M, Inoue H, Itoi T, Mizuno N, Miyakawa H, Mikata R, Irisawa A, Sato S, Notohara K, Shimosegawa T. Diagnosis of autoimmune pancreatitis by EUS-guided FNA using a 22-gauge needle: a prospective multicenter study. Gastrointest Endosc, 2016 (in press).
98. Ogura T, Onda S, Takagi W, Sano T, Okuda A, Masuda D, Yamamoto K, Miyano A, Kitano M, Takeuchi T, Fukunishi S, Higuchi K. Clinical utility of Endoscopic ultrasound-guided biliary drainage as a rescue of re-intervention procedure for high-grade hilar stricture. J Gastroenterol Hepatol, 2016 (in press).
99. Isayama H, Nakai Y, Rerknimitr R, Khor C, Lau J, Wang HP, Seo DW, Ratanachu-Ek T, Lakhtakia S, Ang TL, Ryozawa S, Hayashi T, Kawakami H, Yamamoto N, Iwashita T, Itokawa F, Kuwatani M, Kitano M, Hanada K, Ponnudurai R, Moon JH, Itoi T, Yasuda I, Irisawa A, Maetani I: The Asian consensus statements on endoscopic management of walled-off necrosis Part1: Epidemiology, diagnosis and treatment. J Gastroenterol Hepatol, 2016 (in press)
100. Isayama H, Nakai Y, Rerknimitr R, Khor C, Lau J, Wang HP, Seo DW, Ratanachu-Ek T, Lakhtakia S, Ang TL, Ryozawa S, Hayashi T, Kawakami H, Yamamoto N, Iwashita T, Itokawa F, Kuwatani M, Kitano M, Hanada K, Ponnudurai R, Moon JH, Itoi T, Yasuda I, Irisawa A, Maetani I: The Asian consensus statements on endoscopic management of walled-off necrosis Part2: Endoscopic management. J Gastroenterol Hepatol, 2016 (in press).
101. Fusaroli P, Napoleon B, Gincul R, Lefort C, Palazzo L, Palazzo M, Kitano M, Minaga K, Caletti G, Lisotti A: The clinical impact of ultrasound contrast agents in EUS: a systematic review according to the levels of evidence. Gastrointest Endosc, 2016 (in press).

論文発表（和文）

1．松井繁長，樫田博史，工藤正俊：生検で胃癌が疑われたinflammatory fibroid polyp. 特集「粘膜下腫瘍のすべて」，消化器内視鏡 28;302-303，2016.
2．工藤正俊：医用画像における超音波画像の今日的座標を説く-最新技術がもたらす新しい展開. 月刊新医療 8:80-82，2016.
3．西田直生志，工藤正俊：肝細胞癌の発生とエピゲノム制御. 日本消化器病学会誌 113：775-784，2016.
4．工藤正俊：肝細胞癌における免疫チェックポイント阻害剤の開発. 特集「がん治療が変わる-免疫チェックポイント阻害剤の与えるインパクト-」，肝胆膵 73:401-412，2016.
5．工藤正俊：免疫チェックポイント阻害剤の限界と課題. 特集「がん治療が変わる-免疫チェックポイント阻害剤の与えるインパクト-」，肝胆膵 73:423-427，2016.
6．工藤正俊，石田靖雅，池田公史，田中真二：座談会「“免疫チェックポイント阻害剤“の基礎から臨床成績および開発動向」．肝胆膵 73：429-443，2016.
7．工藤正俊：肝細胞癌に対する分子標的治療薬開発の現状と将来展望. 医学あゆみ 258:537-543，2016.
8．大本俊介，北野雅之，工藤正俊，松本逸平，竹山宜典：急性膵炎診療における地域連携モデルの構築. 肝胆膵72:1003-1007，2016.
9．北野雅之，三長孝輔，今井　元，工藤正俊：超音波内視鏡下胆管ドレナージ-最近の展開-. 胆道 30:689-698，2016.
10．三長孝輔，北野雅之，竹山宜典，大本俊介，宮田　剛，鎌田　研，山雄健太郎，工藤正俊：WONに対する内視鏡的ドレナージ.肝胆膵 73:41-51，2016.
11．竹中　完，北野雅之，鎌田　研，三長孝輔，大本俊介，宮田　剛，山雄健太郎，今井　元，工藤正俊：EUSガイド下胆嚢ドレナージ術. 消化器内視鏡 28:1669-1678，2016.

12. 青山真吾，足立哲平，松井繁長，樫田博史，工藤正俊 : 抗血栓薬服用患者における検査･治療について. 近畿大学医学雑誌 41:129-134，2016.
13. 工藤正俊 : 切除不能肝がん、regorafenib投与でOS延長. Medical Tribune Web，2016（印刷中）
14. 高山政樹，大原裕士郎，秦　康倫，木下大輔，奥田英之，川崎俊彦，水野成人，若狭朋子，太田善夫，工藤正俊 : 悪性黒色腫に対しニボルマブ投与中に潰瘍性大腸炎類似の大腸炎を認めた1例. 日本消化器内視鏡学会雑誌，2016（印刷中）.
15. 鎌田　研，竹中　完，北野雅之，大本俊介，三長孝輔，宮田　剛，山雄健太郎，今井　元，工藤正俊 : 膵癌早期診断におけるEUSの実際. 膵臓，2016 (印刷中)
16. 上嶋一臣 : 肝細胞がんの薬物療法―分子標的治療と肝動注のエビデンス. 特集「肝胆膵がん治療2016」，Mebio 33:2-9，2016.
17. 三長孝輔，北野雅之，竹中　完，今井　元，山雄健太郎，鎌田　研，宮田　剛，松田友彦，大本俊介 : EUSガイド下胆道ドレナージにおけるBILERUSH Selectiveの使用経験. BILERUSH SELECTIVE Case Report vol. 2，2016.
18. 北野雅之，鎌田　研 : 膵癌を疑った場合、EUSは診断に有用か？膵癌診療ガイドライン2016，pp70-72，2016.
19. 北野雅之，鎌田　研 : 膵癌を診断するための次のステップとしてERCPは有用か？膵癌診療ガイドライン2016，pp73-74，2016.
20. 河野匡志，松井繁長，樫田博史 : 胃底腺ポリープ（FAPに伴うもの）. 特集「胃疾患アトラス」，消化器内視鏡 28:1170-1171，2016.
21. 石井達也，三長孝輔，小川　智，多木未央，籔内洋平，松本久和，赤松拓司，瀬田剛史，上野山義人，山下幸孝 : 閉塞性大腸癌に対する術前ステント留置術における18mm径ステント使用経験. Gastroenterol Endosc 58:121-129，2016.
22. 三長孝輔，北野雅之，山下幸孝，樫田博史 : 膵体部癌に対するEUS-FNA後8カ月目に発見された胃壁内へのneedle tract seeding. 消化器内視鏡 28:868-869，2016.

招待講演・特別講演（海外）

1. Kudo M: Invited Lecture “Immuno-oncology for HCC: Beyond the target therapy”, the 1st Anniversary International Symposium of Yonsei Liver Center, Newilhan Memorial Hall, Avision BioMedical Research Center, Korea, February 19-20, 2016.
2. Kudo M: Invited Lecture “Non-Curative Treatment (TACE/Sorafenib) of HCC”, APASL HCC Guideline, 25th Conference of the Asian Pacific Association for the Study of the Liver (APASL), International Convention Center Pamir, Tokyo, Japan, February 20-24, 2016.
3. Kudo M: Invited Lecture “Hepatocellular cancer drug development”, 8th Annual Asian Oncology Summit (AOS 2016), Kyoto International Community House, Kyoto, Japan, March 3-6, 2016.
4. Kudo M: Invited Lecture “Proposal of new BCLC stage B subclassification”, Symposium 1 “Improvement of outcome beyond TACE in intermediate stage HCC”, 52nd Annual Meeting of Liver Cancer Study Group of Japan, Toranomon Hills Forum, Tokyo, July 1, 2016.
5. Kudo M: State-of-the Art Lecture “Recent Advancement in HCC Treatment”, 7th Asia-Pacific Primary Liver Cancer Expert Meeting (APPLE), Crowne Plaza Hong Kong Kowloon East, Hong Kong, July 8, 2016.
6. Kudo M: Special Lecture “Role of EOB-MRI in the management of HCC”, Bayer Sponsored Meeting From Diagnosis to Treatment, 7th Asia-Pacific Primary Liver Cancer Expert Meeting (APPLE), Crowne Plaza Hong Kong Kowloon East, Hong Kong, July 10, 2016.
7. Kudo M: Invited Lecture “Efficacy and safety of regorafenib versus placebo in patients with hepatocellular carcinoma (HCC) progressing on sorafenib: results of the international, randomized phase 3 RESORCE trial”, 14th Annual Meeting of the Japanese Society of Medical Oncology, Kobe International Exhibition Hall/Kobe International Conference Center, Kobe, Japan, July 29, 2016.
8. Kudo M: Invited Lecture “Global GIDEON data: subgroup analysis of sorafenib dosing pattern in patients with unresectable hepatocellular carcinoma”, 14th Annual Meeting of the Japanese Society

of Medical Oncology, Kobe International Exhibition Hall/Kobe International Conference Center, Kobe, Japan, July 30, 2016.

9. Kudo M: Invited Lecture “New subclassification and treatment strategy for intermediate stage HCC”, the 12th JSH Single Topic Conference, Hotel Nikko Kanazawa, Kanazawa, September 22, 2016.
10. Kudo M: Invited Lecture “Value of EOB in clinical perspective: Japan”, Asia Pacific Liver Imaging Symposium (APLIS 2016), Conrad Beijing, China, October 21-22, 2016.
11. Kudo M: Invited Lecture “CEUS in the evaluation of RFA treatment efficacy”, 2016 Annual Convention of Taiwan Society of Ultrasound in Medicine (TSUM), Taipei International Convention Center, Taiwan, October 22-23, 2016.
12. Kudo M: Invited Lecture “CE-US guided RFA for HCC”, Luncheon Symposium I, the 3rd Asian Conference on Tumor Ablation (ACTA), Asan Medical Center, Seoul, Korea, October 28-29, 2016.
13. Kudo M: Invited Lecture “HCC clinical practice and ongoing trials in Japan”, Asia Advisory Board Meeting on GI Tumors, Beijing, China, November 12, 2016.
14. Kudo M: Invited Lecture “Fusion imaging for the treatment of liver cancer”. The Westlake International Forum on Ultrasound in Medicine and Biology (WIFUMB 2016) in conjunction with the International Contrast Ultrasound Society (ICUS) meeting, Hongzhou, China, November 9-13, 2016.
15. Kudo M: Invited Lecture “Contrast-enhanced EUS for pancreatobiliary disease”. The Westlake International Forum on Ultrasound in Medicine and Biology (WIFUMB 2016) in conjunction with the International Contrast Ultrasound Society (ICUS) meeting, Hongzhou, China, November 9-13, 2016.
16. Kudo M: Invited Lecture “Immune checkpoint blockade in hepatocellular carcinoma”, Symposium 3 “Emerging Issues in the Management of Advanced Liver Disease”, Seoul International Digestive Disease Symposium (SIDDS 2016), Grand Hilton Seoul Hotel, Seoul, Korea, November 24-25, 2016.
17. Kudo M: Invited Lecture “Detection of early HCC-advance in diagnosis”, 57th Annual Conference of Indian Soceity of Gastroenterology (ISGCON 2016), New Delhi, India, December 16-19, 2016.
18. Kudo M: Invited Lecture “Classification and management algorithm of HCC”, 57th Annual Conference of Indian Soceity of Gastroenterology (ISGCON 2016), New Delhi, India, December 16-19, 2016.
19. Kudo M: Invited Lecture “Recent trends of TACE”, 57th Annual Conference of Indian Soceity of Gastroenterology (ISGCON 2016), New Delhi, India, December 16-19, 2016.

招待講演・特別講演（国内）

1．工藤正俊：特別講演「Intermediate肝癌の細分類と新しい分子標的薬への期待」，第12回九州C型肝炎研究会，平成28年1月30日，ホテル日航福岡，九州.
2．工藤正俊：特別講演「Intermediate Stageの細分類」，第4回ディーシービーズ検討会～DEB-TACEの可能性を探る～，平成28年2月7日，東京ビッグサイト，東京.
3．工藤正俊：特別講演「肝細胞癌に対する新規分子標的薬の開発動向と免疫チェックポイント阻害薬への期待」，第18回北九州肝癌治療研究会，平成28年3月26日，リーガロイヤルホテル小倉，北九州.
4．工藤正俊：特別講演「Intermediate Stage肝癌の細分類と免疫チェックポイント阻害剤への期待」，第4回奈良消化器病セミナー，平成28年4月8日，橿原ロイヤルホテル，奈良.
5．工藤正俊：教育講演「免疫チェックポイント阻害剤による肝細胞癌治療への期待」，第16回関西肝血流動態・機能イメージ研究会，平成28年6月25日，オーバルホール，大阪.
6．工藤正俊：特別講演「Intermediate Stage 肝癌の多様性と治療戦略」，TACE Refractory Focus Expert Meeting，平成28年8月12日，JRクレメントホテル高松，香川.
7．工藤正俊：ラジオ出演「C型肝炎について」(番組名：高岡美樹のべっぴんラジオ),ラジオ大阪，大阪，平成28年8月23日.
8．工藤正俊：特別講演「肝胆膵領域の超音波診療：最近の動向」，日本超音波医学会第26回四国地方会

学術集会，愛媛大学医学部40周年記念講堂，愛媛，平成28年10月8日.

9．工藤正俊：特別講演「肝細胞癌診療の最近のtopics」，第2回肝疾患Up to Date研究会，ANAクラウンプラザホテル新潟，新潟，平成28年10月13日.

10. 工藤正俊：理事長特別講演「超音波がもたらすイノベーション」, 第43回日本超音波医学会関西地方会，平成28年10月29日，大阪国際会議場，大阪.

11. 工藤正俊：特別講演「Intermediate/Advanced stage HCCの治療戦略」，Nexavar® HCC Web Conference，平成28年11月1日，大阪.

12. 萩原　智：特別講演「当院におけるウイルス性肝炎診療」，第20回奈良肝臓ミーティング，平成28年2月5日，橿原ロイヤルホテル，奈良.

13. 有住忠晃：肝臓病の血液データの読み方と画像診断．平成27年度「肝がん撲滅運動」, 平成28年2月7日，堺商工会議所，大阪.

14. 萩原　智：B型肝炎の最先端．平成27年度「肝がん撲滅運動」，平成28年2月7日，堺商工会議所，大阪.

15. 依田　広：C型肝炎とインターフェロン・フリー治療．平成27年度「肝がん撲滅運動」，平成28年2月7日，堺商工会議所，大阪.

16. 南　康範：肝硬変の診断と治療．平成27年度「肝がん撲滅運動」, 平成28年2月7日, 堺商工会議所, 大阪.

17. 田北雅弘：内科治療～ラジオ波焼灼術と肝動脈塞栓術～．平成27年度「肝がん撲滅運動」，平成28年2月7日，堺商工会議所，大阪.

18. 上嶋一臣：肝癌治療薬の最新動向．平成27年度「肝がん撲滅運動」, 平成28年2月7日, 堺商工会議所, 大阪.

19. 北野雅之：特別講演「インターベンショナルEUS」．第6回大分胆膵スキルアップセミナー, ホルトホール大分，大分.

20. 上嶋一臣：講演「肝細胞癌に対する新規分子標的薬の開発動向と免疫チェックポイント阻害剤を用いた新しい治療戦略」，アッヴィ肝炎フォーラム，平成28年3月5日，スイスホテル南海大阪，大阪.

21. 萩原　智：特別講演「C型慢性肝炎の最新治療」，CHC Expert Meeting，平成28年3月24日，ホテル・アゴーラリージェンシー堺，大阪.

22. 萩原　智：特別講演「肝細胞癌治療の最新知見」，CHC Expert Meeting，平成28年3月24日，ホテル・アゴーラリージェンシー堺，大阪.

23. 北野雅之：特別講演「Convex EUSによる診断の基本とコツ」. 第5回岡山EUS研究会, アークホテル岡山，岡山.

24. 萩原　智：特別講演「当院における肝疾患診療 - トルバプタン治療成績も含めて - 」．第2回北・中河内患者のQOLを考える会，平成28年6月9日，ザ・リッツカールトン大阪，大阪.

25. 萩原　智：特別講演「化学療法施行時のB型肝炎の再活性化-対策と現状-」．第3回阪奈血液疾患治療セミナー，平成28年6月24日，スイスホテル南海大阪，大阪.

26. 南　康範：教育講演「RFA治療におけるUS-US image fusionでの治療効果判定」，第16回関西肝血流動態・機能イメージ研究会，平成28年6月25日，オーバルホール，大阪.

27. 萩原　智：特別講演「当院における肝疾患診療」．Liver Disease Meeting，平成28年7月28日，ホテル・アゴーラリージェンシー堺，大阪.

28. 萩原　智：特別講演「B型肝炎と言われたら」．近畿大学医学部附属病院肝疾患診療連携拠点病院事業肝臓病教室，平成28年8月9日，近畿大学医学部附属病院PET棟3階大会議室，大阪.

29. 萩原　智：特別講演「HCV感染透析患者の最新治療」. 阪南HCV連携セミナー, 平成28年9月8日, ホテル・アゴーラリージェンシー堺，大阪.

30. 上嶋一臣：特別講演「肝細胞癌治療の最新動向～分子標的薬・免疫チェックポイント阻害薬による腫瘍抑制～」，南大阪肝疾患診療連携セミナー，平成28年9月15日，スイスホテル南海大阪，大阪.

31. 萩原　智：特別講演「当院におけるウイルス性肝疾患診療」．伊都医師会学術講演会, 平成28年10月8日，ラポール橋本商工会館，和歌山.

32. 上嶋一臣：特別講演「ここまできた肝細胞癌治療～薬物療法の進歩を中心に～」．伊都医師会学術講演会，平成28年10月8日，ラポール橋本商工会館，和歌山.

33. 萩原　智：特別講演「整形外科医が知っておくべきB型・C型肝炎最新治療」,Joint operation seminar ～整形外科・消化器疾患について～，平成28年12月1日，ホテル・アゴーラリージェンシー堺，大阪.

34. 萩原　智：特別講演「新しい肝炎治療時代の臨床検査―肝炎ウイルスマーカーの意義を再検討する―」，大阪府医師会医学会臨床検査シリーズ，平成28年12月15日，大阪府医師会館，大阪.

シンポジウム・パネル発表（海外）

1．Kudo M: Biomarker and Imaging Diagnosis of HCC. Symposium 11 “Update of HCC Treatment”, 25th Conference of the Asian Pacific Association for the Study of the Liver (APASL), International Convention Center Pamir, Tokyo, Japan, February 20-24, 2016.
2．Kudo M: Regional differences in practice patterns among countries. Luncheon Symposium “New light on the integration of evidence into practice”, 25th Conference of the Asian Pacific Association for the Study of the Liver (APASL), International Convention Center Pamir, Tokyo, Japan, February 20-24, 2016
3．Kamata K, Kitano M, Kudo M: Utility of endoscopic ultrasonography for follow-up of IPMN. シンポジウム 消化器Joint「Role of EUS in diagnosis and treatment of digestive diseases」, 日本超音波医学会第89回学術集会, 第36回日本乳腺甲状腺超音波医学会学術集会, アジア超音波医学生物学会第12回学術集会（AFSUMB）, アジア造影超音波会議第8回学術集会（ACUCI）(Ultrasonic Week 2016), 平成28年5月26-29日, 国際京都国際会館, 京都.
4．Minaga K, Kitano M, Imai H, Yamao K, Kamata K, Miyata T, Matsuda T, Omoto S, Kadosaka K, Kudo M: EUS-guided interventions for walled-off pancreatic necrosis: clinical outcomes of a step-up approach and risk factors for failed endoscopic treatment. シンポジウム 消化器Joint「Role of EUS in diagnosis and treatment of digestive diseases」, 日本超音波医学会第89回学術集会, 第36回日本乳腺甲状腺超音波医学会学術集会, アジア超音波医学生物学会第12回学術集会（AFSUMB）, アジア造影超音波会議第8回学術集会（ACUCI）(Ultrasonic Week 2016), 平成28年5月26-29日, 国際京都国際会館, 京都.
5．Nishida N, Kudo M: Identification of fetal liver-type hepatocellular carcinoma based on a methylome analysis and its associations with genetic alterations. International Session (Symposium) 1 “Genomics of hepatocellular carcinoma: hepatitis virus infection and hepatocarcinogenesis”, 第20回日本肝臓学会大会, 第58回日本消化器病学会大会, 第92回日本消化器内視鏡学会総会, 第14回日本消化器外科学会大会, 第54回日本消化器がん検診学会大会(JDDW 2016), November 3, 2016, ポートピアホテル, 兵庫.
6．Takenaka M, Kitano M, Kudo M: Estimation of EUS findings of early chronic pancreatitis in comparison with clinical symptoms. International Session (Workshop) 1“Recent progress in chronic pancreatitis”, 第20回日本肝臓学会大会, 第58回日本消化器病学会大会, 第92回日本消化器内視鏡学会総会, 第14回日本消化器外科学会大会, 第54回日本消化器がん検診学会大会(JDDW 2016), November 3, 2016, ポートピアホテル, 兵庫.

シンポジウム・パネル発表（国内）

1．山田光成，樫田博史，米田頼晃，工藤正俊：直腸NETの内視鏡治療．シンポジウム1「神経内分泌腫瘍の診断と治療」，日本消化器病学会近畿支部第104回例会，平成28年2月6日，大阪国際交流センター，大阪.
2．大本俊介，北野雅之，工藤正俊：膵神経内分泌腫瘍診断におけるEUSの有用性．シンポジウム1「神経内分泌腫瘍の診断と治療」，日本消化器病学会近畿支部第104回例会，平成28年2月6日，大阪国際交流センター，大阪.
3．朝隈　豊，松井繁長，樫田博史，工藤正俊：周在性の大きな食材表在癌に対する内視鏡治療の有用性．ワークショップ1「消化器腫瘍に対する低侵襲治療」，日本消化器病学会近畿支部第104回例会，平成28年2月6日，大阪国際交流センター，大阪.
4．峯　宏昌，松井繁長，樫田博史，工藤正俊：潰瘍性大腸炎症例における重症度別の栄養指標と術後経過の検討．ワークショップ2「消化器疾患の栄養療法」，日本消化器病学会近畿支部第104回例会，平成28年2月6日，大阪国際交流センター，大阪.
5．米田頼晃，樫田博史，工藤正俊：大腸腫瘍診断・治療におけるJNET分類の試用結果．パネルディスカッション8「大腸腫瘍の治療法選択としての画像強調観察の意義」，第102回日本消化器病学会総会，平成28年4月21-23日，京王プラザホテル，東京.
6．有住忠晃，上嶋一臣，工藤正俊：BCLC Bの細分類と治療選択．パネルディスカッション9：

Intermediateから進行肝細胞癌治療の最前線」，第102回日本消化器病学会総会，平成28年4月21-23日，京王プラザホテル，東京.

7．南　康範，南　知宏，工藤正俊：US-US fusionを用いた肝細胞癌へのラジオ波焼灼術と治療効果判定，ワークショップ9「新規技術を用いた肝疾患診療の未来～診断から治療へ」，第102回日本消化器病学会総会，平成28年4月21-23日，京王プラザホテル，東京.

8．櫻井俊治，樫田博史，工藤正俊：既存治療の効果予測の可能性，プレナリーセッション「IBD　臨床」，第102回日本消化器病学会総会，平成28年4月21-23日，京王プラザホテル，東京.

9．小川　力，荒澤壮一，芝峠光成，西田知紗，村上佳子，河合直之，丸山哲夫，木太秀行，大西宏明，工藤正俊：シミュレーション機能を用いた超音波検査の教育体制．シンポジウム 領域横断2「Image Fusionは診断能・治療成績をどの様に向上させたか？」，日本超音波医学会第89回学術集会，第36回日本乳腺甲状腺超音波医学会学術集会，アジア超音波医学生物学会第12回学術集会（AFSUMB），アジア造影超音波会議第8回学術集会（ACUCI）(Ultrasonic Week 2016)，平成28年5月26-29日，国際京都国際会館，京都.

10. 南　知宏，南　康範，工藤正俊：転移性肝癌に対するUS-US fusionを用いたラジオ波焼灼術．シンポジウム 領域横断2「Image Fusionは診断能・治療成績をどの様に向上させたか？」，日本超音波医学会第89回学術集会，第36回日本乳腺甲状腺超音波医学会学術集会，アジア超音波医学生物学会第12回学術集会（AFSUMB），アジア造影超音波会議第8回学術集会（ACUCI）(Ultrasonic Week 2016)，平成28年5月26-29日，国際京都国際会館，京都.

11. 赤坂和美，工藤正俊，飯島尋子，上原麻理子，斎藤明子，椎名　毅，高野真澄，谷口信行，畠　二郎，平井都始子，古川まどか，山口　匡：日本超音波医学会男女共同参画委員会　アンケート調査報告．パネルディスカッション 領域横断3「日本超音波医学会が取り組むキャリア支援（JSUM男女共同参画委員会共同企画）」，日本超音波医学会第89回学術集会，第36回日本乳腺甲状腺超音波医学会学術集会，アジア超音波医学生物学会第12回学術集会（AFSUMB），アジア造影超音波会議第8回学術集会（ACUCI）(Ultrasonic Week 2016)，平成28年5月26-29日，国際京都国際会館，京都.

12. 工藤正俊:日本超音波医学会理事長としてキャリア支援を考える．医師の立場から，パネルディスカッション 領域横断3「日本超音波医学会が取り組むキャリア支援（JSUM男女共同参画委員会共同企画）」，日本超音波医学会第89回学術集会，第36回日本乳腺甲状腺超音波医学会学術集会，アジア超音波医学生物学会第12回学術集会（AFSUMB），アジア造影超音波会議第8回学術集会（ACUCI）(Ultrasonic Week 2016)，平成28年5月26-29日，国際京都国際会館，京都.

13. 矢田典久，工藤正俊:Shear wave imagingによる非アルコール性脂肪性肝疾患の病態診断，シンポジウム 消化器2「消化器領域におけるエラストグラフィーの最先端」，日本超音波医学会第89回学術集会，第36回日本乳腺甲状腺超音波医学会学術集会，アジア超音波医学生物学会第12回学術集会（AFSUMB），アジア造影超音波会議第8回学術集会（ACUCI）(Ultrasonic Week 2016)，平成28年5月26-29日，国際京都国際会館，京都.

14. 大本俊介，北野雅之，工藤正俊:造影ハーモニックEUSの定量的血流評価による膵腫瘍診断，シンポジウム 消化器3「胆膵疾患の造影エコー診断up-to-date」，日本超音波医学会第89回学術集会，第36回日本乳腺甲状腺超音波医学会学術集会，アジア超音波医学生物学会第12回学術集会（AFSUMB），アジア造影超音波会議第8回学術集会（ACUCI）(Ultrasonic Week 2016)，平成28年5月26-29日，国際京都国際会館，京都.

15. 角谷眞澄，池田公史，高山忠利，沼田和司，泉　並木，國土典宏，古瀬純司，奥坂拓志，山下哲史，奥村正文，工藤正俊：ソラフェニブ国際共同非介入試験GIDEON最終解析～日本における肝癌治療の実際～，シンポジウム2「進行肝癌に対するカテーテル治療」，第14回日本肝がん分子標的治療研究会，平成28年6月11日，スペース36，大阪

16. 西田直生志，海道利実，工藤正俊：ゲノム・エピゲノム・染色体情報に基づいた肝癌の亜分類と転移再発予測．パネルディスカッション2「肝細胞癌の新たなサブクラス分類と治療ストラテジー」，第52回日本肝癌研究会，平成28年7月1日，虎ノ門ヒルズフォーラム，東京.

17. 小川　力，野田晃世，荒澤壮一，出田雅子，久保敦司，石川哲朗，松中寿浩，玉置敬之，芝峠光成，工藤正俊：予測塞栓領域を考慮したTACE治療の試み．ビデオセッション3「肝癌・背景肝の画像評」，第52回日本肝癌研究会，平成28年7月1日，虎ノ門ヒルズフォーラム，東京.

18. 國土貴嗣，長谷川　潔，松山　裕，高山忠利，泉　並木，角谷眞澄，工藤正俊，具　英成，坂元亨宇，

中島　収，金子周一，國土典宏：門脈腫瘍栓合併肝細胞癌に対する外科的切除の意義の検討-肝癌研究会追跡調査より．パネルディスカッション3「進行肝細胞癌の治療：切除、動注、放射線科、分子標的治療薬の役割」，第52回日本肝癌研究会，平成28年7月2日，虎ノ門ヒルズフォーラム，東京.

19. 萩原　智，西田直生志，工藤正俊：NASH関連肝発癌における線維化進展と遺伝子変化．ワークショップ2「非ウイルス性肝細胞癌の病態と分類」，第52回日本肝癌研究会，平成28年7月2日，虎ノ門ヒルズフォーラム，東京.
20. 米田頼晃，樫田博史，工藤正俊：大腸潰瘍の治療法選択におけるJNET分類の診断能に関する検討．シンポジウム2「大腸腫瘍の診断･治療における戦略と展望」，日本消化器病学会近畿支部第105回例会，平成28年9月17日，大阪国際交流センター，大阪.
21. 有住忠晃，上嶋一臣，西田直生志，工藤正俊：肝細胞癌治療アルゴリズムの検討．パネルディスカッション「肝細胞癌の治療アルゴリズムをめぐる諸問題」，日本消化器病学会近畿支部第105回例会，平成28年9月17日，大阪国際交流センター，大阪.
22. 鎌田　研，竹中　完，北野雅之，工藤正俊：急性胆嚢炎に対する超音波内視鏡下胆嚢ドレナージ術～Self-expandable metal stent抜去後の長期成績～，ワークショップ2「胆道疾患疾患診断および治療の最近の進歩」，日本消化器病学会近畿支部第105回例会，平成28年9月17日，大阪国際交流センター，大阪.
23. 鎌田　研，北野雅之，工藤正俊：急性胆嚢炎に対するEUSガイド下胆嚢ドレナージの長期成績～長期成績からみたSEMS早期抜去の有用性～，ワークショップ2「胆道疾患に対する超音波内視鏡の有用性」．第52回日本胆道学会学術集会，平成28年9月29-30日，新横浜プリンスホテル，神奈川.
24. 竹中　完，北野雅之，工藤正俊：経乳頭的、経皮的治療抵抗性の切除不能肝門部悪性胆道狭窄に対するEUS-guided biliary drainage (EUS-BD)の有用性，ビデオワークショップ「胆道内視鏡のトラブルシューティング」．第52回日本胆道学会学術集会，平成28年9月29-30日，新横浜プリンスホテル，神奈川.
25. 矢田典久，工藤正俊：肝病態診断におけるエラストグラフィの有用性．シンポジウム1「腹部超音波検査の進歩と新たな展開」，第43回日本超音波医学会関西地方会，平成28年10月29日，大阪国際会議場，大阪.
26. 小川　力，盛田真弘，野田晃世，出田雅子，久保敦司，石川哲朗，松中寿浩，玉置敬之，芝峠光成，工藤正俊：画像解析ソフトを用いた超音波診療の教育システム．シンポジウム1「腹部超音波検査の進歩と新たな展開」，第43回日本超音波医学会関西地方会，平成28年10月29日，大阪国際会議場，大阪.
27. 萩原　智，西田直生志，工藤正俊：エンテカビルとPEG-IFNα2a/2b 48週併用療法の効果および治療効果予測因子の検討．ワークショップ9「B型肝炎治療のアップデート」，第20回日本肝臓学会大会，第58回日本消化器病学会大会，第92回日本消化器内視鏡学会総会，第14回日本消化器外科学会大会，第54回日本消化器がん検診学会大会(JDDW 2016)，平成28年11月3-6日，神戸コンベンションセンター，兵庫.
28. 渡邉智裕，工藤正俊：形質細胞様樹状細胞が産生するIL-33がIgG4関連疾患の状態に果たす役割．ワークショップ16「消化器領域におけるIgG4関連疾患の病態」，第20回日本肝臓学会大会，第58回日本消化器病学会大会，第92回日本消化器内視鏡学会総会，第14回日本消化器外科学会大会，第54回日本消化器がん検診学会大会(JDDW 2016)，平成28年11月3-6日，神戸コンベンションセンター，兵庫.
29. 山雄健太郎，北野雅之，工藤正俊：pTis/pT1a膵癌の診断における内視鏡の役割．パネルディスカッション5「膵・胆道癌の早期発見における内視鏡の役割」，第20回日本肝臓学会大会，第58回日本消化器病学会大会，第92回日本消化器内視鏡学会総会，第14回日本消化器外科学会大会，第54回日本消化器がん検診学会大会(JDDW 2016)，平成28年11月3-6日，神戸コンベンションセンター，兵庫.
30. 鎌田　研，北野雅之，工藤正俊：IPMN併存膵癌の臨床像と早期発見におけるEUSの有用性．ワークショップ10「IPMN併存膵癌における諸問題と対策」，第20回日本肝臓学会大会，第58回日本消化器病学会大会，第92回日本消化器内視鏡学会総会，第14回日本消化器外科学会大会，第54回日本消化器がん検診学会大会(JDDW 2016)，平成28年11月3-6日，神戸コンベンションセンター，兵庫.
31. 米田頼晃，樫田博史，櫻井俊治，朝隈　豊，工藤正俊：大腸腫瘍内視鏡治療後の局所再発に対するサーベイランスについて．パネルディスカッション2「大腸腫瘍内視鏡治療後のfollow upの課題」，日本消化器内視鏡学会近畿支部第97回支部例会，平成28年11月26日，京都テルサ，京都.
32. 竹中　完，三長孝輔，山雄健太郎，工藤正俊：膵頭十二指腸切除術胃膵部吻合部狭窄に対するEUS-PDの検討．ワークショップ1「膵がんにおけるEUS-FNA関連手技の現状と問題点」，日本消化器内視鏡学会近畿支部第97回支部例会，平成28年11月26日，京都テルサ，京都.

学会発表・抄録（米国及び国際学会）

1. Kudo M, Okusaka T, Kaneko S, Furuse J, Takeuchi M, Fang X, Date Y, Takeuchi M: Identification of a high-response patient population to S-1 via predictive enrichment strategy analysis of the S-CUBE phase III trial. American Society of Clinical Oncology, 2016 Gastrointestinal Cancers Symposium (ASCO GI 2016), San Francisco, USA, January 21-23, 2016.
2. Kudo M: Regional differences in efficacy/safety/biomarkers in a randomised study of axitinib in 2nd line patients (pts) with advanced hepatocellular carcinoma (HCC). American Society of Clinical Oncology, 2016 Gastrointestinal Cancers Symposium (ASCO GI 2016), San Francisco, USA, January 21-23, 2016.
3. Zhu A, Galle PR, Kudo M, Finn RS, Yang L, Abada P, Chang SC, Llovet JM: A randomized, double-blind, placebo-controlled phase III study of ramucirumab versus placebo as second-line treatment in patients with hepatocellular carcinoma and elevated baseline alpha-fetoprotein following first-line sorafenib (REACH-2). American Society of Clinical Oncology, 2016 Gastrointestinal Cancers Symposium (ASCO GI 2016), San Francisco, USA, January 21-23, 2016.
4. Lee HC, Cheng AL, Raoul JL, Peck-Radosavljevic M, Nakajima K, Kudo M, on behalf of the OPTIMIS Investigators: Regional Differences in the Use of Transarterial Chemoembolization (TACE) in HCC: Interim Analysis of OPTIMIS, an International Observational Study Assessing the Use of Sorafenib After TACE. 25th Conference of the Asian Pacific Association for the Study of the Liver (APASL), International Convention Center Pamir, Tokyo, Japan, February 20-24, 2016.
5. Kudo M, Venook A, Lencioni R, Ye SL, Nakajima K, Marrero J: Practice patterns, sorafenib dosing and safety in Asian hepatocellular carcinoma patients in GIDEON. 25th Conference of the Asian Pacific Association for the Study of the Liver (APASL), International Convention Center Pamir, Tokyo, Japan, February 20-24, 2016.
6. Blanc JF, Chan SL, Park JO, Ryoo BY, Yen CJ, Kudo M, Poon R, Pastorelli D, Baran A, Pfiffer T, Okusaka T, Kubackova K, Trojan J, Sastre J, Chau I, Abada P, Chang SC, Yang L, Zhu A: Ramucirumab as second-line treatment in patients with advanced hepatocellular carcinoma: Analysis of REACH patients by albumin-bilirubin (ALBI) grade. The International Liver Congress 2016 (EASL 2016), Barcelona, Spain, April 13-17, 2016.
7. Pinato DJ, Yen C, Arizumi T, Giarda P, Howell J, Ramaswami R, Burlone ME, Kudo M, Pirisi M, Sharma R: An objective model to optimize treatment decisions in advanced hepatocellular carcinoma after sorafenib failure: the SORFA score. The International Liver Congress 2016 (EASL 2016), Barcelona, Spain, April 13-17, 2016.
8. Kudo M, Ueshima K, Yokosuka O, Obi S, Izumi N, Aikata H, Nagano H, Hatano E, Sasaki Y, Hino K, Kumada T, Yamamoto K, Imai Y, Iwadou S, Ogawa C, Okusaka T, Arai Y, Kanai F, Akazawa K, and SILIUS Study Group: Prospective randomized controlled phase III trial comparing the efficacy of sorafenib versus sorafenib in combination with low-dose cisplatine/fluorouracil hepatic arterial infusion chemotherapy in patients with advanced hepatocellular carcinoma. The International Liver Congress 2016 (EASL 2016), Barcelona, Spain, April 13-17, 2016.
9. Kitano M, Kamata K, Omoto S, Minaga K, Yamao K, Imai H, Takenaka M, Kudo M: Contrast-enhanced harmonic EUS for pancreatic diseases. 8th Asian Conference on Ultrasound Contrast Imaging (ACUCI), 12th Congress of the Asian Federation of Societies for Ultrasound in Medicine and Biology (AFSUMB), 89th annual meeting of the Japan Society of Ultrasonics in Medicine (JSUM) (Ultrasonic Week 2016), Kyoto International Conference Center, Kyoto, Japan, May 27-29, 2016.
10. Ogawa C, Minami Y, Kudo M: New US technology using 3D volume analyzer synapse VINCENT. 8th Asian Conference on Ultrasound Contrast Imaging (ACUCI), 12th Congress of the Asian Federation of Societies for Ultrasound in Medicine and Biology (AFSUMB), 89th annual meeting of the Japan Society of Ultrasonics in Medicine (JSUM)(Ultrasonic Week 2016), Kyoto International Conference Center, Kyoto, Japan, May 27-29, 2016.
11. Ogawa C, Minami Y, Kudo M: Usefulness of contrast-ehnaced ultrasonography with sonazoid in the

preperative evaluation of histological differentiation and gross types of hepatocellular carcinoma. 8th Asian Conference on Ultrasound Contrast Imaging (ACUCI), 12th Congress of the Asian Federation of Societies for Ultrasound in Medicine and Biology (AFSUMB), 89th annual meeting of the Japan Society of Ultrasonics in Medicine (JSUM)(Ultrasonic Week 2016), Kyoto International Conference Center, Kyoto, Japan, May 27-29, 2016.

12. Minami Y, Minami T, Kudo M: US-US image fusion in radiofrequency ablation therapy for hepatocellular carcinoma. 8th Asian Conference on Ultrasound Contrast Imaging (ACUCI), 12th Congress of the Asian Federation of Societies for Ultrasound in Medicine and Biology (AFSUMB), 89th annual meeting of the Japan Society of Ultrasonics in Medicine (JSUM)(Ultrasonic Week 2016), Kyoto International Conference Center, Kyoto, Japan, May 27-29, 2016.
13. Sangro B, Melero I, Yau TC, Hsu C, Kudo M, Crocenzi TS, Kim TY, Choo SP, Trojan J, Meyer T, Kang YK, Anderson J、Dela Cruz C, Lang L, Neely J, El-Khoueiry AB: Safety and antitumor activity of Nivolumab (nivo) in patients (pts) with advanced hepatocellular carcinoma (HCC): interim analysis of dose-expansion cohorts from the phase 1/2 checkmate 040 study. 52nd American Society of Clinical Oncologys Annual Meeting 2016 (ASCO 2016), Chicago, Illinois, June 3-7, 2016.
14. Abou-Alfa GK, Sangro B, Morse M, Zhu AX, Kim RD, Cheng AL, Kudo M, Kang YK, Chan SL, Antal J, Boice J, Xiao F, Morris SR, Bendell J, 022 Study Group: Phase 1/2 study of durvalumab and tremelimumab as monotherapy and in combination in patients with unresectable hepatocellular carcinoma (HCC). 52nd American Society of Clinical Oncologys Annual Meeting 2016 (ASCO 2016), Chicago, Illinois, June 3-7, 2016.
15. Zhu AX, Galle PR, Kudo M, Finn RS, Yang L, Abada P, Llovet JM: A randomized, double-blind, placebo-controlled phase III study of ramucirumab versus placebo as second-line treatment in patients with hepatocellular carcinoma and elevated baseline alpha-fetoprotein following first-line sorafenib (REACH-2). 52nd American Society of Clinical Oncologys Annual Meeting 2016 (ASCO 2016), Chicago, Illinois, June 3-7, 2016.
16. Kokudo T, Hasegawa K, Matsuyama Y, Takayama T, Izumi N, Kadoya M, Kudo M, Ku Y, Sakamoto M, Nakashima O, Kaneko S, Kokudo N: Survival benefit of liver resection for hepatocellular carcinoma associated with portal vein invasion: A Japanese nationwide survey. 52nd American Society of Clinical Oncologys Annual Meeting 2016 (ASCO 2016), Chicago, Illinois, June 3-7, 2016.
17. Haruna Y, Hasegawa N, Imanaka K, Inoue A, Kudo M: Impact of vitamin K dosing during sorafenib treatment for hepatocellular carcinoma: Effect on ischemic tumor cell damage caused by sorafenib. 52nd American Society of Clinical Oncologys Annual Meeting 2016 (ASCO 2016), Chicago, Illinois, June 3-7, 2016.
18. Zhu A, Galle PR, Kudo M, Finn RS, Abada P, Llovet JM: A randomized, double-blind, placebo-controlled phase III study of ramucirumab versus placebo as second-line treatment in patients with hepatocellular carcinoma and elevated baseline alpha-fetoprotein following first-line sorafenib (REACH-2). ESMO 18th World Congress on Gastrointestinal Cancer 2016, Barcelona, Spain, June 29-July 2, 2016.
19. Bruix J, Merle P, Granito A, Huang YH, Bodoky G, Boucher E, Yokosuka O, Rosmorduc O, Breder V, Gerolami R, Masi G, Ross P, Qin S, Song T, Bronowicki JP, Ollivier-Hourmand I, Kudo M, LeBerre MA, Baumhauer A, Meinhardt G, Han G, on behalf of the RESORCE investigators: Efficacy and safety of regorafenib versus placebo in patients with hepatocellular carcinoma (HCC) progressing on sorafenib: Results of the international, randomized phase 3 RESORCE trial. ESMO 18th World Congress on Gastrointestinal Cancer 2016, Barcelona, Spain, June 29-July 2, 2016.
20. Sangro B, Melero I, Yau T, Hsu C, Kudo M, Crocenzi TS, Kim TY, Choo SP, Trojan J, Meyer T, Kang YK, Anderson J, dela Cruz C, Lang L, Neely J, El-Khoueiry AB: Safety and antitumor activity of Nivolumab (Nivo) in patients (pts) with advanced hepatocellular carcinoma (HCC): Interim analysis of dose-expansion cohorts from the Phase 1/2 CheckMate-040 study. 7th Asia-Pacific Primary Liver Cancer Expert Meeting (APPLE), Crowne Plaza Hong Kong Kowloon East, Hong Kong, July 8-10, 2016.

21. Ogawa C, Shibatoge M, Kudo M: Easy detection of tumor-feeding branches of hepatocellular carcinoma with SYNAPSE VINCENT during transcatheter arterial chemoembolization. 7th Asia-Pacific Primary Liver Cancer Expert Meeting (APPLE), Crowne Plaza Hong Kong Kowloon East, Hong Kong, July 8-10, 2016.
22. Zhu AX, Galle PR, Kudo M, Finn RS, Yang L, Abada PB, Llovet JM: A randomized, double-blind, placebo-controlled phase III study of ramucirumab versus placebo as second-line treatment in patients with hepatocellular carcinoma and elevated baseline alpha-fetoprotein following first-line Sorafenib (REACH-2). 7th Asia-Pacific Primary Liver Cancer Expert Meeting (APPLE), Crowne Plaza Hong Kong Kowloon East, Hong Kong, July 8-10, 2016.
23. Ueshima K, Kudo M, Izumi N, Kadoya M, Kaneko S, Ku Y, Kokudo N, Takayama T, Sakamoto M, Nakashima O, Matsuyama Y: New subclassification of intermediate stage HCC: Analysis of 46,997 Japanese HCC patients from a nationwide survey of the Liver Cancer Study Group of Japan. 10th Annual Conference International Liver Cancer Association (ILCA), Vancouver, Canada, September 9-11, 2016.
24. Sangro B, Melero I, Yau T, Hsu C, Kudo M, Crocenzi T, Kim TY, Choo SP, Trojan J, Meyer T, Kang YK, Anderson J, dela Cruz C, Lang L, Neely J, El-Khoueiry A: Safety and antitumour activity of Nivolumab (Nivo) in patients with advanced hepatocellular carcinoma (HCC): Interim analysis of dose-expansion cohorts from the phase 1/2 checkmate-040 study. 10th Annual Conference International Liver Cancer Association (ILCA), Vancouver, Canada, September 9-11, 2016.
25. Kokudo N, Kokudo T, Hasegawa K, Matsuyama Y, Takayama T, Kadoya M, Kudo M, Ku Y, Sakamoto M, Nakashima O, Kaneko S, Izumi N: A propensity score analysis on survival benefit of liver resection for hepatocellular carcinoma associated with portal vein invasion using nationwide survey data in Japan. 10th Annual Conference International Liver Cancer Association (ILCA), Vancouver, Canada, September 9-11, 2016.
26. Kudo M, Ueshima K, Yokosuka O, Obi S, Izumi N, Aikata H, Nagano H, Hatano E, Sasaki Y, Hino K, Kumada T, Yamamoto K, Imai Y, Iwadou S, Ogawa C, Okusaka T, Arai Y, Kanai F, Akazawa K: Prospective randomized controlled phase III trial comparing the efficacy of sorafenib versus sorafenib in combination with low-dose cisplatin/fluorouracil hepatic arterial infusion chemotherapy in patients with advanced hepatocellular carcinoma. 10th Annual Conference International Liver Cancer Association (ILCA), Vancouver, Canada, September 9-11, 2016.
27. Cheng AL, Raoul JL, Lee HC, Kudo M, Nakajima K, Peck-Radosavljevic M on behalf of the OPTIMIS Investigators: An international observational study to assess the use of sorafenib after transarterial chemoembolization (TACE) in patients with hepatocellular carcinoma (HCC): OPTIMIS interim analysis. 10th Annual Conference International Liver Cancer Association (ILCA), Vancouver, Canada, September 9-11, 2016.
28. Zhu AX, Galle PR, Kudo M, Finn RF, Yang L, Abada PB, Llovet JM: A randomized, double-blind, placebo-controlled phase III study of ramucirumab versus placebo as second-line treatment in patients with hepatocellular carcinoma and elevated baseline alpha-fetoprotein following first-line sorafenib (REACH-2). 10th Annual Conference International Liver Cancer Association (ILCA), Vancouver, Canada, September 9-11, 2016.
29. Ogawa C, Shibatoge M, Kudo M: New technology to detect of tumor-feeding branches and simulate embolization area of hepatocellular carcinoma with SYNAPSE VINCENT durint transcatheter arterial chemoembolization. 10th Annual Conference International Liver Cancer Association (ILCA), Vancouver, Canada, September 9-11, 2016.
30. Arizumi T, Ueshima K, Kudo M: Validation of a proposed substaging system for patients with intermediate hepatocellular carcinoma. 10th Annual Conference International Liver Cancer Association (ILCA), Vancouver, Canada, September 9-11, 2016.
31. Ye SL, Lencioni R, Nakajima K, Kudo M: Patients benefit from treatment with sorafenib for more than 28 weeks: analysis from the GIDEON study according to duration of treatment. 10th Annual Conference International Liver Cancer Association (ILCA), Vancouver, Canada, September 9-11,

2016.

32. Ye SL, Lencioni R, Marrero JA, Venook AP, Nakajima K, Kudo M: Treatment patterns in >3000 sorafenib-treated patients: final analysis of GIDEON (Global Investigation of therapeutic DEcisions in hepatocellular carcinoma and Of its treatment with sorafeNib). The 19th Annual Meeting of Chinese Society of Clinical Oncology (CSCO), Xiamen International Conference and Exhibition Center, China, September 21-25, 2016.
33. Minami Y, Nishida N, Kudo M: US-US fusion imaging in radiofrequency ablation therapy for hepatocellular carcinoma. The 12th JSH Single Topic Conference, Hotel Nikko Kanazawa, Kanazawa, September 22, 2016.
34. Sakurai T, Nagai T, Kashida H, Kudo M: The oncoprotein gankyrin promotes the development of colitis-associated cancer by mediating STAT3 and ERK activation. The 75th Annual Meeting of the Japanese Cancer Association, Pacifico Yokohama, Kanagawa, October 6-8, 2016.
35. Bruix J, Merle P, Granito A, Huang YH, Bodoky G, Yokosuka O, Rosmorduc O, Breder V, Gerolami R, Masi G, Ross PJ, Qin S, Song T, Bronowicki JP, Isabelle Ollivier-Hourmang, Kudo M, LeBerre MA, Baumhauer A, Meinhardt G, Han G: Efficacy, safety, and health-related quality of life (HRQoL) of regorafenib in patients with hepatocellular carcinoma (HCC) progressing on sorafenib: Results of the international, double-blind phase 3 RESORCE trial. ESMO 2016, Copenhagen, Denmark, October 7-11, 2016.
36. Zhu A, Galle P, Kudo M, Finn R, Yang L, Abada P, Llovet J: A randomized, double-blind, placebo-controlled phase III study of ramucirumab versus placebo as second-line treatment in patients with hepatocellular carcinoma and elevated baseline alpha-fetoprotein following first-line sorafenib (REACH-2). ESMO 2016, Copenhagen, Denmark, October 7-11, 2016.
37. Finn R, Chan S, Zhu A, Knox J, Cheng AL, Siegel A, Bautista O, Watson P, Kudo M: Pembrolizumab vs best supportive care for second-line advanced hepatocellular carcinoma: Randomized, phase 3 KEYNOTE-240 study. ESMO 2016, Copenhagen, Denmark, October 7-11, 2016.
38. Zhu A, Knox J, Kudo M, Chan S, Finn R, Siegel A, Ma J, Watson P, Cheng AL: Pembrolizumab in patients with previously treated advanced hepatocellular carcinoma: Phase 2 KEYNOTE-224 study. ESMO 2016, Copenhagen, Denmark, October 7-11, 2016.
39. Melero I, Sangro B, Yau T, Hsu C, Kudo M, Crocenzi T, Kim TY, Choo SP, Trojan J, Meyer T, Willing T, Yeo W, Chopra A, Anderson J, dela Cruz CX, Lang L, Neely J, El-Khoueiry A: Safety and preliminary efficacy of nivolumab (nivo) in patients (pts) with advanced hepatocellular carcinoma (aHCC): Interim analysis of the phase 1/2 CheckMate-040 study. ESMO 2016, Copenhagen, Denmark, October 7-11, 2016.
40. Hagiwara S, Nishida N, Kudo M: Combination therapy with peginterferon and entecavir for persistent viral suppression in patients with chronic hepatitis B. 23rd International Symposium on Hepatitis C Virus and Related Viruses (HCV2016), Kyoto International Conference Center, Kyoto, Japan, October 11-15, 2016.
41. Minami Y, Kudo M: US-US fusion imaging in radiofrequency ablation therapy for hepatocellular carcinoma. the 3rd Asian Conference on Tumor Ablation (ACTA), Asan Medical Center, Seoul, Korea, October 28-29, 2016.
42. Kamata K, Takenaka M, Kudo M: Endoscopic ultrasound-guided gallbladder drainage for acute cholecystitis: long-term outcomes after removal of a self-expandable metal stent. Asian Pacific Digestive Week (APDW 2016), Kobe Convention Center, Hyogo, November 2-5, 2016.
43. Melero I, Sangro B, Yau T, Hsu C, Kudo M, Crocenzi TS, Kim TY, Choo SP, Trojan J, Meyer T, Welling TH, Yeo W, Chopra A, Anderson J, dela Cruz C, Lang L, Neely J, Tang H, El-Khoueiry AB: Nivolumab (Nivo) in patients (Pts) with advanced hepatocellular carcinoma (HCC): the CheckMate 040 study. American Association for the Study of Liver Diseases (AASLD 2016), Boston, USA, November 11-15, 2016. (Researchmap未)
44. Melero I, Sangro B, Yau T, Hsu C, Kudo M, Crocenzi TS, Kim TY, Choo SP, Trojan J, Meyer T, Welling TH, Yeo W, Chopra A, Anderson J, dela Cruz C, Lang L, Neely J, Tang H, El-Khoueiry AB:

Nivolumab dose escalation and expansion in patients with advanced hepatocellular carcinoma (HCC): the CheckMate 040 study. American Association for the Study of Liver Diseases (AASLD 2016), Boston, USA, November 11-15, 2016.（acceptされたかチェック、Researchmap未）

45. Chung HC, Chao Y, Lee KW, Kudo M, Yen CJ, Kim TW, Yamazaki K, Shih JY, Kim SW, Sohn JH, ChengR, Zhang Y, Binder P, Mi G, Orlando M, Muro K: Ramucirumab safety in East Asian (EA) compared to non-EA patients: A meta analysis of adverse events (AEs) across 6 global, randomized, double-blind, phase 3 clinical trials. ESMO Asia 2016, Singapore, December 16-19, 2016.（acceptされたかチェック、Researchmap未）

学会発表（国内）

1．南　知宏，萩原　智，岩西美奈，千品寛和，有住忠晃，田北雅弘，北井　聡，矢田典久，南　康範，依田　広，上嶋一臣，西田直生志，工藤正俊：若年男性に発症した肝細胞腺腫の悪性転化の一例．日本消化器病学会近畿支部第104回例会，平成28年2月6日，大阪国際交流センター，大阪.

2．岩西美奈，依田　広，高島耕太，南　知宏，千品寛和，有住忠晃，田北雅弘，北井　聡，矢田典久，萩原　智，南　康範，上嶋一臣，西田直生志，工藤正俊，平瀬主税，前西　修，筑後孝章：自己免疫性溶血性貧血を合併した自己免疫性肝炎の一例．日本消化器病学会近畿支部第104回例会，平成28年2月6日，大阪国際交流センター，大阪.

3．岡元寿樹，樫田博史，米田頼晃，河野匡志，田中梨絵，山田光成，足立哲平，峯　宏昌，永井知行，岡崎能久，朝隈　豊，櫻井俊治，松井繁長，工藤正俊：漢方薬服用者に見られた突発性腸間膜静脈硬化症の2例．日本消化器病学会近畿支部第104回例会，平成28年2月6日，大阪国際交流センター，大阪.

4．秦　康倫，木下大輔，奥田英之，高山政樹，末吉功治，岸谷　譲，川崎俊彦，水野成人，辻江正徳，井上雅智，若狭朋子，太田善夫，工藤正俊：術前診断が困難であった腸間膜悪性リンパ腫の一例．日本消化器病学会近畿支部第104回例会，平成28年2月6日，大阪国際交流センター，大阪.

5．吉川智恵，鎌田　研，北野雅之，大本俊介，門阪薫平，松田友彦，三長孝輔，宮田　剛，山雄健太郎，今井　元, 工藤正俊, 榎木英介, 木村雅友：造影ハーモニックEUS画像と病理組織像の対比･検討を行った胆嚢癌の一例．日本消化器病学会近畿支部第104回例会，平成28年2月6日，大阪国際交流センター，大阪.

6．千品寛和，萩原　智，岩西美奈，南　知宏，有住忠晃，田北雅弘，北井　聡，矢田典久，依田　広，南　康範，上嶋一臣，西田直生志，工藤正俊：当院でのダクラタスビル/アスナプレビル併用療法の検討．日本消化器病学会近畿支部第104回例会，平成28年2月6日，大阪国際交流センター，大阪.

7．小川　力，野田晃世，荒澤壮一，出田雅子，久保敦司，石川哲朗，松中寿浩，玉置敬之，柴峠光成，工藤正俊：Color RVSを用いたRFAの治療効果判定．第22回肝血流動態・機能イメージ研究会，平成28年2月6-7日，東京ビッグサイト「国際会議場」，東京.

8．渡口真史，鶴崎正勝，兵頭朋子，沼本勲男，熊野正士，松木　充，村上卓道，矢田典久,工藤正俊：肝線維化診断におけるMR elastographyの有用性の検討：生検検体を用いたTransient elastographyとの比較．第22回肝血流動態･機能イメージ研究会，平成28年2月6-7日，東京ビッグサイト「国際会議場」，東京.

9．矢田典久,工藤正俊：次世代型Shear wave imaging測定値の信憑性を表す指標VsNの有用性について．第22回肝血流動態･機能イメージ研究会，平成28年2月6-7日，東京ビッグサイト「国際会議場」，東京.

10. 出田雅子，小川　力，三野　智，野田晃世，荒澤壮一，久保敦司，石川哲朗，松中寿浩，玉置敬之，柴峠光成，隈部　力，中島　収，工藤正俊：USが肝細胞癌との鑑別に有用と思われたリンパ増殖性疾患が疑われた肝腫瘍の一例．第22回肝血流動態･機能イメージ研究会，平成28年2月6-7日，東京ビッグサイト「国際会議場」，東京.

11. 南　康範，岩西美奈，南　知宏，千品寛和，河野匡志，有住忠晃，田北雅弘，矢田典久，萩原　智，上嶋一臣，西田直生志，工藤正俊：ラジオ波焼灼術後のバブルによる高エコー域を壊死部とみなして良いか？第29回日本腹部造影エコー･ドプラ診断研究会, 平成28年4月2日, 宮崎市エムアールティ･ミック，北九州.

12. 河野匡志，南　康範，工藤正俊：病変の視認性に着目した肝腫瘍に対する低音圧造影tissue harmonic imaging (low MI CE-THI)の検討．第29回日本腹部造影エコー・ドプラ診断研究会，平成28年4月2日，

宮崎市エムアールティ・ミック，北九州.

13. 大本俊介，北野雅之，工藤正俊：膵神経内分泌腫瘍診断における造影ハーモニックEUSの有用性．第29回日本腹部造影エコー・ドプラ診断研究会，平成28年4月2日，宮崎市エムアールティ・ミック，北九州.
14. 萩原　智，千品寛和，工藤正俊：トルバプタンにおける初期、および遅発性効果予測因子の検討．第102回日本消化器病学会総会，平成28年4月21-23日，京王プラザホテル，東京.
15. 小川　力，野田晃世，荒澤壮一，出田雅子，久保敦司，石川哲朗，松中寿浩，玉置敬之，柴峠光成，工藤正俊：カラー表示RVSを用いた小HCCの診断、およびRFAの治療効果判定．第102回日本消化器病学会総会，平成28年4月21-23日，京王プラザホテル，東京.
16. 岡元寿樹，松井繁長，田中梨絵，山田光成，足立哲平，高山政樹，峯　宏昌，永井知行，岡崎能久，米田頼晃，朝隈　豊，櫻井俊治，樫田博史，工藤正俊：術後胃に発生した胃石症の特徴と治療．第102回日本消化器病学会総会，平成28年4月21-23日，京王プラザホテル，東京.
17. 横川美加，前野知子，塩見香織，前川　清，矢田典久，依田　広，南　康範，樫田博史，工藤正俊:低音圧Tissue Harmonic Imagingによる造影超音波の検討．日本超音波医学会第89回学術集会，第36回日本乳腺甲状腺超音波医学会学術集会，アジア超音波医学生物学会第12回学術集会（AFSUMB），アジア造影超音波会議第8回学術集会（ACUCI）(Ultrasonic Week 2016)，平成28年5月26-29日，国際京都国際会館，京都.
18. 前野知子，横川美加，市島真由美，塩見香織，前川　清,南　康範，樫田博史，工藤正俊，八木　誠:超音波で観察し得た小児における腸重責症の検討．日本超音波医学会第89回学術集会，第36回日本乳腺甲状腺超音波医学会学術集会，アジア超音波医学生物学会第12回学術集会（AFSUMB），アジア造影超音波会議第8回学術集会（ACUCI）(Ultrasonic Week 2016)，平成28年5月26-29日，国際京都国際会館，京都.
19. 小川　力，野田晃世，出田雅子，久保敦司，石川哲郎，松中寿浩，玉置敬之，芝峠光成，工藤正俊：ネクサバールでCRが5年間持続後にSOF+RBVを行いSVR12が得られている症例．第14回日本肝がん分子標的治療研究会，平成28年6月11日，スペース36，大阪.
20. 田北雅弘，南　知宏，千品寛和，有住忠晃，矢田典久，萩原　智，南　康範，依田　広，上嶋一臣，西田直生志，任　誠雲，柳生行伸，松木　充，鶴崎正勝，村上卓道，工藤正俊：当院におけるDrug eluting bead (DEB)-TACEの現況.第16回関西肝血流動態･機能イメージ研究会, 平成28年6月25日, オーバルホール，大阪.
21. 小川　力，野田晃世，盛田真弘，出田雅子，久保敦司，松中寿浩，玉置敬之，芝峠光成，工藤正俊：予測塞栓領域を考慮したTACE治療の試み.第16回関西肝血流動態・機能イメージ研究会，平成28年6月25日，オーバルホール，大阪.
22. 橋本有人，松井繁長，岡本寿樹，河野匡志，田中梨絵，山田光成，足立哲平，峯　宏昌，永井知行，米田頼晃，朝隈　豊，櫻井俊治，渡邉智裕，樫田博史，工藤正俊，榎木英介，木村雅友：透析患者の胃粘膜組織から炭酸ランタン沈着を証明できた一例.日本消化器病学会近畿支部第105回例会，平成28年9月17日，大阪国際交流センター，大阪.
23. 森本真衣，高山政樹，岡崎能久，秦　康倫，木下大輔，奥田英之，川崎俊彦，水野成人，古形修平，辻江正徳，井上雅智，若狭朋子，太田善夫，工藤正俊：主膵管の著名な拡張を呈したIPMNの一例.日本消化器病学会近畿支部第105回例会，平成28年9月17日，大阪国際交流センター，大阪.
24. 鎌田　研，北野雅之，工藤正俊：胆嚢病変の治療方針決定における造影ハーモニックEUSの有用性．第52回日本胆道学会学術集会，平成28年9月29-30日，新横浜プリンスホテル，神奈川.
25. 竹中　完，北野雅之，工藤正俊:慢性膵炎合併良性胆道狭窄に対するfully covered metallic stentの有用性．第52回日本胆道学会学術集会，平成28年9月29-30日，新横浜プリンスホテル，神奈川.
26. 横川美加，前野知子，市島真由美，塩見香織，前川　清，矢田典久，依田　広，南　康範，工藤正俊：造影超音波を施行した膵NET肝転移の一例．第43回日本超音波医学会関西地方会，平成28年10月29日，大阪国際会議場，大阪.
27. 宮田　剛，北野雅之，工藤正俊：膵癌の癌性疼痛に対するEUSガイド下神経叢融解術の治療効果予測因子の検討．第20回日本肝臓学会大会，第58回日本消化器病学会大会，第92回日本消化器内視鏡学会総会，第14回日本消化器外科学会大会，第54回日本消化器がん検診学会大会(JDDW 2016)，平成28年11月3-6日，神戸コンベンションセンター，兵庫.

28. 南　康範，工藤正俊：US-US image fusionを用いた肝細胞癌へのラジオ波焼灼術と治療効果判定．第20回日本肝臓学会大会，第58回日本消化器病学会大会，第92回日本消化器内視鏡学会総会，第14回日本消化器外科学会大会，第54回日本消化器がん検診学会大会(JDDW 2016)，平成28年11月3-6日，神戸コンベンションセンター，兵庫.
29. 三長孝輔，北野雅之，工藤正俊：EUSガイド下胆道ドレナージ困難例に対する治療ルート変更の有用性．第20回日本肝臓学会大会，第58回日本消化器病学会大会，第92回日本消化器内視鏡学会総会，第14回日本消化器外科学会大会，第54回日本消化器がん検診学会大会(JDDW 2016)，平成28年11月3-6日，神戸コンベンションセンター，兵庫.
30. 石村香織，朝隈　豊，岡元寿樹，河野匡志，足立哲平，峯　宏昌，永井知行，米田頼晃，櫻井俊治，松井繁長，樫田博史，工藤正俊：PTP誤嚥による食道気管支瘻に対しOTSCによる閉鎖が奏功した一例.日本消化器内視鏡学会近畿支部第97回支部例会，平成28年11月26日，京都テルサ，京都.
31. 國田裕貴，三長孝輔，竹中　完，大本俊介，松田友彦，宮田　剛，鎌田　研，山雄健太郎，樫田博史，工藤正俊：ショートシングルバルーン内視鏡を用いた金属ステント留意が有用であった十二指腸癌術後再発による挙上空腸狭窄の1例.日本消化器内視鏡学会近畿支部第97回支部例会，平成28年11月26日，京都テルサ，京都.
32. 橋本有人，山雄健太郎，竹中　完，大本俊介，鎌田　研，宮田　剛，三長孝輔，樫田博史，工藤正俊，松本逸平，竹山宜典，筑後孝章：主膵管狭窄を2年間経過観察し得た膵上皮内癌の1例.日本消化器内視鏡学会近畿支部第97回支部例会，平成28年11月26日，京都テルサ，京都.
33. 岩津友大，鎌田　研，竹中　完，大本俊介，三長孝輔，宮田　剛，山雄健太郎，今井　元，工藤正俊：自己免疫性膵炎に対するステロイド投与の影響を造影ハーモニックEUSで評価しえた症例.日本消化器内視鏡学会近畿支部第97回支部例会，平成28年11月26日，京都テルサ，京都.
34. 吉川和也，大本俊介，竹中　完，宮田　剛，鎌田　研，三長孝輔，山雄健太郎，工藤正俊，松本逸平，竹山宜典，筑後孝章：胆管合流異常症に合併した拡張胆管内隆起病への1例.日本消化器内視鏡学会近畿支部第97回支部例会，平成28年11月26日，京都テルサ，京都.
35. 上田泰大，宮田　剛，竹中　完,三長孝輔，大本俊介，松田友彦，鎌田　研，山雄健太郎，樫田博史，工藤正俊：EUS-HGSステント閉塞に対しtrough the mesh法でreinterventionしえた1例.日本消化器内視鏡学会近畿支部第97回支部例会，平成28年11月26日，京都テルサ，京都.
36. 水野成人，奥田英之，高山政樹，木下大輔，秦　康倫，岡崎能久，川崎俊彦，工藤正俊，一木美穂，近藤宏樹，虫明総太朗，若狭朋子，太田善夫：当院における小児上部消化管内視鏡検査の状況.日本消化器内視鏡学会近畿支部第97回支部例会，平成28年11月26日，京都テルサ，京都.
37. 奥田英之，秦　康倫，木下大輔，高山政樹，岡崎能久，川崎俊彦，辻江正徳，石川　原，水野成人，若狭朋子，太田善夫，工藤正俊：胆道出血を契機に発見された胆嚢管癌の1例.日本消化器内視鏡学会近畿支部第97回支部例会，平成28年11月26日，京都テルサ，京都.
38. 櫻井俊治，工藤正俊，渡邊智裕，樫田博史，西田直生志，米田頼晃，永井知行，萩原　智：癌遺伝子ガンキリンは炎症細胞でのSTAT3を活性化することで大腸発癌を促進する．第2回G-PLUS，平成28年12月17日，ホテルイースト21東京，東京.

写真で綴る消化器内科

2016年

2016年度特別講義








2016 年 9 月北野先生

教授就任を祝う会

2016 年峯先生送別会

2016 年 Doris 先生送別会

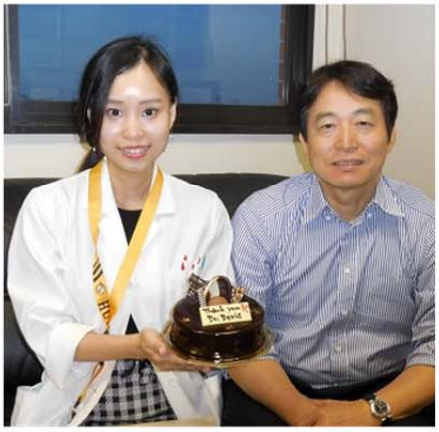

別刷
新聞・雑誌・報道等


INSAL
ISGCON
2016 New Delhi
57th Annual Conference of
Indian Society of Gastroenterology
This is to certify that
Masatoshi Kudo
has participated in ISGCON 2016 as an
Invited Faculty
Dr. S.P. Misra
President ISG
Dr. Randhir Sud
Chairman ISGCON

Massimo Raimondo, MD, *Associate Editor for Focal Points*

Acute spinal cord infarction after EUS-guided celiac plexus neurolysis

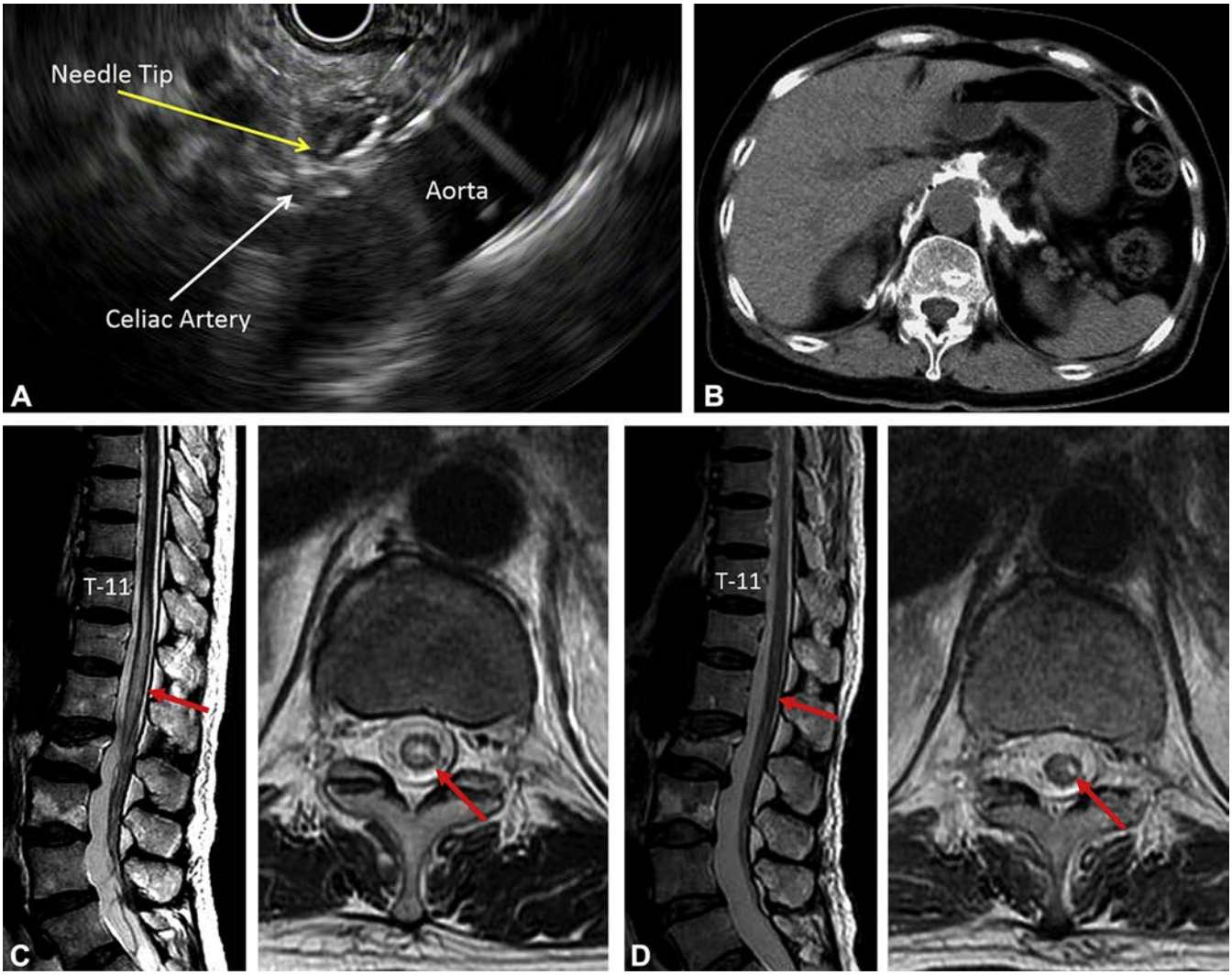

A 73-year-old woman underwent EUS-guided celiac plexus neurolysis to treat severe pancreatic cancer–associated pain. The procedure was performed after administration of intravenous midazolam followed by propofol. The depth of the patient's sedation was titrated by continuous monitoring with a bispectral index monitor and a pulse oximetry. A 25-gauge needle was advanced anterior to the lateral aspect of the aorta at the level of the celiac trunk. Subsequently, 3 mL of 1% lidocaine and 10 mL of mixed solution consisting of pure alcohol (9 mL) and contrast agent (1 mL) were injected around each side of the celiac trunk, respectively (**A**). Before the puncture was performed, Doppler mode was used to confirm the absence of intervening vessels. During the puncture, aspirations were negative for blood or cerebrospinal fluid. No problem was observed during the procedure related to the patient's movement, hiccups, or cough. Postprocedural CT scanning showed that neurolytic/contrast agents were distributed on both sides of the celiac trunk (**B**). After awaking from sedation, the

patient reported numbness and weakness in her legs. Neurological examination revealed acute paraplegia. Urgent magnetic resonance imaging (MRI) performed 6 hours after the procedure detected no significant acute changes; however, MRI performed the next day demonstrated diffuse intramedullary T2 hyperintensity below the T-11 level to the conus medullaris, which indicates an acute spinal cord infarction (**C**). Vasospasm of the radicular arteries, which supply the lower two-thirds of the anterior spinal cord, might be provoked due to direct injection or propagation of alcohol close to the arteries. She was treated with intravenous edaravone and underwent rehabilitation. The weakness in her legs gradually improved, although the follow-up MRI obtained 3 months later showed lingering intramedullary T2 hyperintensity, which suggests that the paraplegia is irreversible (**D**).

DISCLOSURE

All authors disclosed no financial relationships relevant to this publication.

Kosuke Minaga, MD, Masayuki Kitano, MD, PhD, Hajime Imai, MD, Takeshi Miyata, MD, Masatoshi Kudo, MD, PhD, *Department of Gastroenterology and Hepatology, Kinki University Faculty of Medicine, Osaka-ayama, Japan*

http://dx.doi.org/10.1016/j.gie.2015.10.044

Commentary

This is the third case in the literature reporting paralysis as an adverse event of EUS-guided celiac plexus neurolysis (EUS-CPN).

Pancreatic cancer–associated pain is mediated by nociceptive fibers arising from the pancreas, which then pass through the celiac plexus and splanchnic nerves and finally reach the spinal cord. It is present in 70% of patients with newly diagnosed pancreatic cancer, and in some of them, it gradually becomes refractory to nonsteroidal anti-inflammatory drugs and opioids. When pain control is imperative to improve patients' quality of life, new techniques appear in the therapeutic arsenal. In 1914, Kappis first described CPN as an analgesic strategy. It consists of a permanent ablation of the celiac plexus neurons by the injection of neurotoxic agents, such as phenol and alcohol. Traditionally, it has been performed under CT or US guidance, with major adverse events reported, such as paraplegia and pneumothorax. EUS allows direct real-time imaging and precise targeting of the celiac plexus, potentially decreasing the morbidity of these traditional approaches. In 1996, Wiersema performed the first EUS-CPN. This approach showed pain reduction in 80% of pancreatic cancer patients. So far, the most commonly reported adverse effects are related to blockade of sympathetic efferent activity and include worsening transient pain, hypotension, diarrhea, and inebriation. Perforation, hemorrhage, and infection are also reported, but their rates are similar to conventional EGD. Despite improved injection-site localization, extremity paraplegia can occur secondary to hypotension or propagation of alcohol causing vasospasm of radicular arteries. The majority of adverse events, including a recently described fatal case, have been reported in patients with chronic pancreatitis–related pain. This case points out that EUS-CPN is not as benign as previously thought, so it should be considered as an alternative only in patients with severe pancreatic cancer–related pain.

Katherine Mejía
Medical Student
Universidad de los Andes
Bogotá, Colombia

Massimo Raimondo, MD
Associate Editor for Focal Points

Metastatic periampullary clear cell renal carcinoma

A 50-year-old man with a background history of metastatic renal cell carcinoma (RCC) presented with acute onset of fever, abdominal pain, and jaundice. A partially covered metal biliary stent had been inserted 12 months earlier when he had a mass at the head of the pancreas mass and secondary biliary obstruction. Laboratory test results demonstrated neutrophilia (18.6×10^9/L), elevated C-reactive protein (66 mg/L), and elevated lipase (2221 mIU/L). Total bilirubin was 34 μmol/L, alkaline phosphatase was 694 U/L, and γ-glutamyltransferase was 481 U/L. Blood cultures were positive for *Klebsiella pneumoniae*. An abdominal CT scan revealed dilatation of the

Liver Cancer

Liver Cancer 2016;5:1–7
DOI: 10.1159/000367760
Published online: December 15, 2015

2235-1795/16/0051-0001$39.50/0
www.karger.com/lic

Editorial

Defect Reperfusion Imaging with Sonazoid®: A Breakthrough in Hepatocellular Carcinoma

Prof. M. Kudo

Editor *Liver Cancer*

The basic concept of contrast-enhanced ultrasonography (CEUS) has been confined to the hepatic nodule, which is detected by B-mode ultrasound (US). This is applicable to contrast agents such as SonoVue® [1, 2]. However, the use of Sonazoid® in combination with a technique termed defect reperfusion US imaging [3–5] has changed the management of hepatocellular carcinoma (HCC) drastically. Sonazoid® has three favorable properties: it allows real-time vascular imaging, stable Kupffer phase imaging lasting up to 60 minutes, and its use is tolerable for multiple scanning. Defect reperfusion US imaging, which is based on reinjection at the Kupffer phase, enables the detection of B-mode ill-defined nodules and locally recurring nodules. In addition, it facilitates the correct diagnosis of nodules detected on screening/surveillance or the detection of additional nodules for staging before treatment. This is a breakthrough technique that will change the clinical practice pattern of HCC management.

Background

Despite advances in diagnostic imaging techniques for HCC such as US, computed tomography (CT) and magnetic resonance imaging (MRI), many challenges remain unresolved, such as differential diagnosis, surveillance, staging, evaluation of treatment response, treatment guidance, identification of local recurring nodules after treatment, and the diagnosis of intrahepatic recurrence after treatment [6–11]. Among the techniques used to overcome these problems, Levovist®-enhanced US has contributed to diagnostic differentiation [12–14], evaluation of malignancy grade [15], evaluation of the therapeutic response to transarterial chemoembolization (TACE) [16–21], and needle insertion guidance [22, 23] to some extent. However, there are still significant limitations in the evaluation of the therapeutic response to radiofrequency ablation (RFA) [24–26], screening and staging.

Liver Cancer

Liver Cancer 2016;5:1–7
DOI: 10.1159/000367760
Published online: December 15, 2015

The main advantages of Sonazoid® are that it facilitates stable Kupffer phase imaging tolerable for repeated scanning from 10 to 60 minutes after its injection and the acquisition of real-time blood flow images at low acoustic power. Sonazoid® is more effective than Levovist® for real-time vascular imaging, it is easier to use, and it allows accurate imaging even with non high-end machines [27, 28]. This reduces the dependence on skills and machines, which may help facilitate the widespread use of CEUS.

Sonazoid®-enhanced US in combination with defect reperfusion imaging, which consists of Sonazoid® reinjection into areas showing defects in the Kupffer phase, is an innovative breakthrough technique that will change the clinical practice of HCC management [4, 5].

Defect Reperfusion Imaging with Sonazoid®

CEUS with Sonazoid® allows the acquisition of stable Kupffer images and real-time fine blood flow images. These features make it a useful technique for the diagnosis of typical HCC, which is depicted by CT but not by B-mode US scanning. Dynamic diagnostic imaging is based on enhancing patterns according to a time sequence or phase. However, by changing the basic idea, combined Kupffer and arterial phase images are obtained by Sonazoid® reinjection at the Kupffer phase.

After intravenous injection of Sonazoid® (0.01 ml/kg), early enhancement is observed in the vascular phase, and the presence or absence of defects is determined by an entire liver scan in the Kupffer phase 10–60 minutes after injection. Subsequently, the probe is applied to the area that shows a defect in the Kupffer phase. An additional injection of Sonazoid® (0.01 ml/kg) is used to determine the presence or absence of arterial blood flow in the defective area (defect reinjection test). A fast wash-in of arterial flow in the Kupffer defect area confirms the diagnosis of HCC [5]. The detection rate of HCC with Sonazoid®-enhanced US is superior to that of dynamic CT [29].

Detection of B-Mode US Undetectable HCC and Treatment Guidance

HCC nodules that cannot be visualized by B-mode US, but which are detected by dynamic CT, defects can be detected at the Kupffer phase by Sonazoid®-enhanced US. Reinjection of Sonazoid® allows the detection of a clear wash-in and staining in the Kupffer defect area (positive defect reperfusion sign). These defects can be treated by RFA. Kupffer phase Sonazoid®-enhanced US-guided RFA is possible in almost all cases of HCC that are not identified by B-mode US, with a sensitivity as high as 100% [30–34].

Response Evaluation after Locoregional Therapy

Treatment response after RFA or TACE is most accurately evaluated with Sonazoid®-enhanced US with a concurrent use of defect reperfusion imaging [35–39].

Liver Cancer

Liver Cancer 2016;5:1–7

DOI: 10.1159/000367760
Published online: December 15, 2015

Detection of Local Progression after RFA

In cases of local progression or recurrence at a different region after RFA, that is not identified by B-mode US, the recurring nodules can be clearly identified in all cases (sensitivity: 100%) using CEUS with the Sonazoid® reinjection technique [40].

Surveillance and Confirmation of HCC

Surveillance of HCC is also possible by Kupffer phase of Sonazoid®-enhanced US [41]. A defect reperfusion US study is performed in cases in which a Kupffer defect is found. Sonazoid® (0.01 ml/kg) is intravenously injected into a patient at high risk of HCC (hepatitis B and C liver cirrhosis) in the outpatient setting. Subsequently, patients then undertake a US for the Kupffer phase imaging at between 10–60 minutes post-injection. When a defective area is identified at the Kupffer phase, reinjection of Sonazoid® is performed to determine the presence or absence of an arterial supply in the Kupffer-defect nodule. If an arterial supply is confirmed, a definitive diagnosis of HCC is also possible [41]. In this way, tiny HCC nodules smaller than 15 mm can be successfully depicted and confirmed.

Diagnosis of Pathologically Early HCC

Nodules showing a hypovascular pattern in the arterial phase on dynamic CT/MRI can show a hypervascular pattern with Sonazoid®-enhanced US, which is the most sensitive technique for the detection of arterial flow among all imaging modalities [29]. This indicates the presence of arterial flow in a well-to-moderately differentiated HCC nodule.

However, pathologically early HCC usually shows a hypovascular pattern at the early arterial phase and low intensity at the Kupffer phase. Also, it is well known that both dysplastic nodules and early HCC are both fed by portal blood flow, which can be also demonstrated by Sonazoid®-enhanced US [42]. This pattern provides an important clue for the diagnosis of pathologically early HCC, although a tumor biopsy is necessary for confirmation. In the diagnosis of pathologically early HCC, gadolinium-ethoxybenzyl-diethylenetriamine pentaacetic acid-enhanced MRI (Gd-DTPA EOB-MRI) is superior to CEUS with Sonazoid®, as stated in the Consensus-based HCC Practice Guidelines proposed by the Japan Society of Hepatology [8]. However, in the diagnosis of pathologically early HCC, Sonazoid®-enhanced US plays an important role to confirm it noninvasively [43, 44].

Intraoperative US

Intraoperative US is the most sensitive tool for the detection of additional liver nodules that are not detected by preoperative imaging. Kupffer defects detected in the Kupffer phase are not always intrahepatic HCC metastases, and defect reperfusion imaging is useful to distinguish true metastatic HCC lesions from the other types of tumors, such as cysts, hemangiomas or focal nodular hyperplasia [27, 45].

Liver Cancer

Liver Cancer 2016;5:1–7
DOI: 10.1159/000367760
Published online: December 15, 2015

Diagnosis of the Gross Pathological Type of HCC

Simple nodular with extra growth, and confluent multinodular type of HCC are biologically more malignant than simple nodular type of HCC [46, 47]. CEUS in the Kupffer phase is a useful technique for the identification of the gross pathological type of HCC, which is important to determine the optimal treatment strategy. Defect reperfusion imaging is used to confirm the gross pathological type of HCC, for which the diagnostic accuracy of Sonazoid®-enhanced US is superior to that of dynamic CT [48, 49].

Summary

The detection of small nodular lesions in coarse liver parenchyma is difficult by B-mode US alone, although dynamic CT or dynamic MRI can detect arterial enhancing nodules with venous washout. Approximately 10% of HCC nodules that are not detected by B-mode US can be clearly identified by defect reperfusion imaging with Sonazoid®. The false positive rate increases when the technique is confined to Kupffer phase scanning. In addition to the Kupffer defect, information on arterial vascularity, i.e., the reinjection method, increases the diagnostic accuracy to 100% even in deeply seated nodules.

This breakthrough method allows the detection of nodules that cannot be visualized by B-mode US, as defects on Kupffer images in the stable Kupffer phase. The presence of arterial blood flow in nodules with Kupffer defects is subsequently determined by the reinjection technique, making this method a breakthrough in diagnostic imaging [4, 5]. CEUS with Sonazoid® reinjection requires no special apparatus or analysis, and is the result of a change in the way of thinking regarding CEUS. For the typical CT image (so-called early enhancement with late washout nodules), defects are easily detected in the Kupffer phase, and arterial perfusion within the defect is subsequently demonstrated by the reinjection test (visualization of staining within the Kupffer defects, which is the reverse phenomenon of early enhancement with late washout). The introduction of this technique has allowed almost 100% accuracy in the detection of lesions observed on CT images that are not visualized on B-mode US images.

If the reinjection test shows no enhancement of a Kupffer defect, this defect differs from the nodule detected by CT. This method then serves to guide needle insertion.

In surveillance, this procedure facilitates screening because Sonazoid® US can be performed in the setting of a routine examination. In addition, operators only need to concentrate on the delineation of Kupffer defects in the Kupffer phase in contrast to routine B-mode US, in which regenerative nodules or dysplastic nodules may mimic malignant ones. If defects are detected, HCC can be confirmed by Sonazoid® reinjection, which provides information on both Kupffer cell function and arterial blood flow on the same cross-sectional image. This dual phase fusion imaging allows detection and definitive diagnosis of HCC with 100% confidence. As a result, Sonazoid® has markedly improved the efficiency of HCC detection.

In the past, CEUS was considered only for nodules previously depicted by B-mode US and was not used as a screening tool. However, this concept changed with the introduction of defect reperfusion imaging using Sonazoid®.

Defect reperfusion imaging is also useful for the localization of recurrent lesions at a previously ablated area, which is difficult by B-mode US because of the inhomogeneous echo pattern mixed with viable lesions, the ablated area, and ablated surrounding liver. In this setting, even skilled operators have difficulties determining the viable area on B-mode US images alone, which corresponds to the enhancing area on CT because of numerous US

Liver Cancer 2016;5:1–7
DOI: 10.1159/000367760
Published online: December 15, 2015

cross-sections [50]. This problem has been readily overcome by defect reperfusion imaging with Sonazoid®.

Defect reperfusion imaging is particularly useful for needle insertion guidance in the treatment of HCC. For invisible nodules on B-mode US, needle insertion can be performed under the guidance of either fusion imaging [51, 52] or SonoVue®-enhanced US. However, fusion imaging requires CT/MRI volume data and special apparatus. In addition, complete concordance of synchronized images from B-mode US that correspond to the cross-sectional plane of CT/MRI volume data is sometimes difficult. Similarly, under SonoVue®-enhanced US, puncture should be performed in a very short time in the early arterial phase.

Conversely, in Sonazoid®-enhanced US, Kupffer defects are detected easily, and whether blood flow is present in defective areas can be determined by the reinjection technique (defect reperfusion imaging) in all cases. Therefore, needle insertion can be easily performed during a stable period in the Kupffer phase, and accurate needle placement followed by sufficient treatment is possible with Sonazoid®-enhanced US.

Conclusions

CEUS with Sonazoid® is useful in the characterization of hepatic tumors when compared with multidetector raw CT. Sonazoid®-enhanced US with defect reperfusion imaging is a breakthrough technique in the diagnosis and treatment of HCC. This innovative technique was developed based on the two major favorable properties of Sonazoid®, namely, the demonstration of real-time blood flow images with low acoustic power, and stable Kupffer phase images tolerable for repeated scanning in the Kupffer phase. Among them, especially the presence of a Kupffer phase is the key of defect reperfusion imaging. This technique will markedly change the clinical practice of HCC management. The method is not possible with SonoVue® or Definity®, which do not have Kupffer phase imaging properties. Although these contrast agents are approved in most parts of the world, the Kuppfer phase imaging technique is only possible using Sonazoid®, which is so far only approved in Japan, Korea, China and Norway. In this respect, Sonazoid® should be made more available worldwide.

References

1 Claudon M, Dietrich CF, Choi BI, Cosgrove DO, Kudo M, Nolsøe CP, Piscaglia F, Wilson SR, Barr RG, Chammas MC, Chaubal NG, Chen MH, Clevert DA, Correas JM, Ding H, Forsberg F, Fowlkes JB, Gibson RN, Goldberg BB, Lassau N, Leen EL, Mattrey RF, Moriyasu F, Solbiati L, Weskott HP, Xu HX, World Federation for Ultrasound in Medicine European Federation of Societies for Ultrasound: Guidelines and good clinical practice recommendations for Contrast Enhanced Ultrasound (CEUS) in the liver - update 2012: A WFUMB-EFSUMB initiative in cooperation with representatives of AFSUMB, AIUM, ASUM, FLAUS and ICUS. Ultrasound Med Biol 2013;39:187–210.
2 Claudon M, Dietrich CF, Choi BI, Cosgrove DO, Kudo M, Nolsøe CP, Piscaglia F, Wilson SR, Barr RG, Chammas MC, Chaubal NG, Chen MH, Clevert DA, Correas JM, Ding H, Forsberg F, Fowlkes JB, Gibson RN, Goldberg BB, Lassau N, Leen EL, Mattrey RF, Moriyasu F, Solbiati L, Weskott HP, Xu HX: Guidelines and good clinical practice recommendations for contrast enhanced ultrasound (CEUS) in the liver—update 2012: a WFUMB-EFSUMB initiative in cooperation with representatives of AFSUMB, AIUM, ASUM, FLAUS and ICUS. Ultraschall Med 2013;34:11–29.
3 Kudo M, Hatanaka K, Chung H, Minami Y, Maekawa K: A proposal of novel treatment-assist technique for hepatocellular carcinoma in the sonazoid-enhanced ultrasonography: Value of defect re-perfusion imaging. Kanzo 2007;48:299–301 (in Japanese).
4 Kudo M: Defect reperfusion imaging, a newly developed novel technology using sonazoid in the treatment of hepatocellular carcinoma. J Med Ultrasound 2008;16:169–176.
5 Kudo M, Hatanaka K, Maekawa K: Newly developed novel ultrasound technique, defect reperfusion ultrasound imaging, using sonazoid in the management of hepatocellular carcinoma. Oncology 2010;78(Suppl 1):40–45.

Liver Cancer 2016;5:1–7
DOI: 10.1159/000367760
Published online: December 15, 2015

6 Murakami T, Tsurusaki M: Hypervascular benign and malignant liver tumors that require differentiation from hepatocellular carcinoma: key points of imaging diagnosis. Liver Cancer 2014;3:85–96.
7 Ichikawa T, Sano K, Morisaka H: Diagnosis of pathologically early HCC with eob-mri: Experiences and current consensus. Liver Cancer 2014;3:97–107.
8 Kudo M, Matsui O, Izumi N, Iijima H, Kadoya M, Imai Y, Okusaka T, Miyayama S, Tsuchiya K, Ueshima K, Hiraoka A, Ikeda M, Ogasawara S, Yamashita T, Minami T, Yamakado K, Liver Cancer Study Group of Japan: JSH consensus-based clinical practice guidelines for the management of hepatocellular carcinoma: 2014 update by the Liver Cancer Study Group of Japan. Liver Cancer 2014;3:458–468.
9 Kudo M: Surveillance, diagnosis, treatment, and outcome of liver cancer in Japan. Liver Cancer 2015;4:39–50.
10 Minami Y, Kudo M: Imaging modalities for assessment of treatment response to nonsurgical hepatocellular carcinoma therapy: Contrast-enhanced US, CT, and MRI. Liver Cancer 2015;4:106–114.
11 Ichikawa S, Ichikawa T, Motosugi U, Sano K, Morisaka H, Enomoto N: Was hypervascular hepatocellular carcinoma visible on previous gadoxetic acid-enhanced magnetic resonance images? Liver Cancer 2015;4:154–162.
12 Kudo. M: Contrast harmonic imaging in the diagnosis and treatment of hepatic tumors.; Springer Verlag. Tokyo, 2003, pp p1-253.
13 Wen YL, Kudo M, Zheng RQ, Ding H, Zhou P, Minami Y, Chung H, Kitano M, Kawasaki T, Maekawa K: Characterization of hepatic tumors: value of contrast-enhanced coded phase-inversion harmonic angio. AJR Am J Roentgenol 2004;182:1019–1026.
14 Ding H, Kudo M, Onda H, Suetomi Y, Minami Y, Maekawa K: Hepatocellular carcinoma: depiction of tumor parenchymal flow with intermittent harmonic power Doppler US during the early arterial phase in dual-display mode. Radiology 2001;220:349–356.
15 Inoue T, Kudo M, Watai R, Pei Z, Kawasaki T, Minami Y, Chung H, Fukunaga T, Awai K, Maenishi O: Differential diagnosis of nodular lesions in cirrhotic liver by post-vascular phase contrast-enhanced US with Levovist: comparison with superparamagnetic iron oxide magnetic resonance images. J Gastroenterol 2005;40:1139–1147.
16 Ding H, Kudo M, Onda H, Suetomi Y, Minami Y, Maekawa K: Contrast-enhanced subtraction harmonic sonography for evaluating treatment response in patients with hepatocellular carcinoma. AJR Am J Roentgenol 2001;176:661–666.
17 Minami Y, Kudo M, Kawasaki T, Kitano M, Chung H, Maekawa K, Shiozaki H: Transcatheter arterial chemoembolization of hepatocellular carcinoma: usefulness of coded phase-inversion harmonic sonography. AJR Am J Roentgenol 2003;180:703–708.
18 Ding H, Kudo M, Onda H, Suetomi Y, Minami Y, Chung H, Kawasaki T, Maekawa K: Evaluation of posttreatment response of hepatocellular carcinoma with contrast-enhanced coded phase-inversion harmonic US: comparison with dynamic CT. Radiology 2001;221:721–730.
19 Raoul JL, Gilabert M, Piana G: How to define transarterial chemoembolization failure or refractoriness: a European perspective. Liver Cancer 2014;3:119–124.
20 Kudo M: Locoregional therapy for hepatocellular carcinoma. Liver Cancer 2015;4:163–164.
21 Tsurusaki M, Murakami T: Surgical and locoregional therapy of HCC. Tace Liver Cancer 2015;4:165–175.
22 Minami Y, Kudo M, Kawasaki T, Chung H, Ogawa C, Shiozaki H: Treatment of hepatocellular carcinoma with percutaneous radiofrequency ablation: usefulness of contrast harmonic sonography for lesions poorly defined with B-mode sonography. AJR Am J Roentgenol 2004;183:153–156.
23 Minami Y, Kudo M, Chung H, Kawasaki T, Yagyu Y, Shimono T, Shiozaki H: Contrast harmonic sonography-guided radiofrequency ablation therapy versus B-mode sonography in hepatocellular carcinoma: prospective randomized controlled trial. AJR Am J Roentgenol 2007;188:489–494.
24 Wen YL, Kudo M, Zheng RQ, Minami Y, Chung H, Suetomi Y, Onda H, Kitano M, Kawasaki T, Maekawa K: Radiofrequency ablation of hepatocellular carcinoma: therapeutic response using contrast-enhanced coded phase-inversion harmonic sonography. AJR Am J Roentgenol 2003;181:57–63.
25 Teng W, Liu KW, Lin CC, Jeng WJ, Chen WT, Sheen IS, Lin CY, Lin SM: Insufficient ablative margin determined by early computed tomography may predict the recurrence of hepatocellular carcinoma after radiofrequency ablation. Liver Cancer 2015;4:26–38.
26 Kang TW: Recent advances in tumor ablation for hepatocellular carcinoma. Liver Cancer 2015;4:176–187.
27 Hatanaka K, Kudo M, Minami Y, Ueda T, Tatsumi C, Kitai S, Takahashi S, Inoue T, Hagiwara S, Chung H, Ueshima K, Maekawa K: Differential diagnosis of hepatic tumors: value of contrast-enhanced harmonic sonography using the newly developed contrast agent, Sonazoid. Intervirology 2008;51(Suppl 1):61–69.
28 Kudo M, Hatanaka K, Maekawa K: Sonazoid-enhanced ultrasound in the diagnosis and treatment of hepatic tumors. J Med Ultrasound 2008;16:130–139.
29 Hatanaka K, Kudo M, Minami Y, Maekawa K: Sonazoid-enhanced ultrasonography for diagnosis of hepatic malignancies: comparison with contrast-enhanced CT. Oncology 2008;75(Suppl 1):42–47.
30 Kudo M: The 2008 Okuda lecture: Management of hepatocellular carcinoma: from surveillance to molecular targeted therapy. J Gastroenterol Hepatol 2010;25:439–452.
31 Minami Y, Kudo M, Hatanaka K, Kitai S, Inoue T, Hagiwara S, Chung H, Ueshima K: Radiofrequency ablation guided by contrast harmonic sonography using perfluorocarbon microbubbles (Sonazoid) for hepatic malignancies: an initial experience. Liver Int 2010;30:759–764.
32 Inoue T, Minami Y, Chung H, Hayaishi S, Ueda T, Tatsumi C, Takita M, Kitai S, Hatanaka K, Ishikawa E, Yada N, Hagiwara S, Ueshima K, Kudo M: Radiofrequency ablation for hepatocellular carcinoma: assistant techniques for difficult cases. Oncology 2010;78(Suppl 1):94–101.

Liver Cancer 2016;5:1–7
DOI: 10.1159/000367760
Published online: December 15, 2015

33 Minami Y, Kudo M: Review of dynamic contrast-enhanced ultrasound guidance in ablation therapy for hepatocellular carcinoma. World J Gastroenterol 2011;17:4952–4959.
34 Minami Y, Okumura N, Yamamoto N, Tsuji N, Kono Y, Kudo M: Quantification of tumor vascularity with contrast-enhanced ultrasound for early response of transcatheter arterial chemoembolization for hepatocellular carcinoma: A report of three cases. J Med Ultrasound 2012;39:15–19.
35 Xia Y, Kudo M, Minami Y, Hatanaka K, Ueshima K, Chung H, Hagiwara S, Inoue T, Ishikawa E, Kitai S, Takahashi S, Tatsumi C, Ueda T, Hayaishi S, Maekawa K: Response evaluation of transcatheter arterial chemoembolization in hepatocellular carcinomas: the usefulness of sonazoid-enhanced harmonic sonography. Oncology 2008;75(Suppl 1):99–105.
36 Andreana L, Kudo M, Hatanaka K, Chung H, Minami Y, Maekawa K, Ruggiero G: Contrast-enhanced ultrasound techniques for guiding and assessing response to locoregional treatments for hepatocellular carcinoma. Oncology 2010;78(Suppl 1):68–77.
37 Inoue T, Kudo M, Hatanaka K, Arizumi T, Takita M, Kitai S, Yada N, Hagiwara S, Minami Y, Sakurai T, Ueshima K, Nishida N: Usefulness of contrast-enhanced ultrasonography to evaluate the post-treatment responses of radiofrequency ablation for hepatocellular carcinoma: comparison with dynamic CT. Oncology 2013;84(Suppl 1):51–57.
38 Minami Y, Kudo M: Therapeutic response assessment of transcatheter arterial chemoembolization for hepatocellular carcinoma: ultrasonography, CT and MR imaging. Oncology 2013;84(Suppl 1):58–63.
39 Minami Y, Nishida N, Kudo M: Therapeutic response assessment of RFA for HCC: contrast-enhanced US, CT and MRI. World J Gastroenterol 2014;20:4160–4166.
40 Inoue T, Kudo M, Hatanaka K, Takahashi S, Kitai S, Ueda T, Ishikawa E, Hagiwara S, Minami Y, Chung H, Ueshima K, Maekawa K: Imaging of hepatocellular carcinoma: qualitative and quantitative analysis of postvascular phase contrast-enhanced ultrasonography with sonazoid. Comparison with superparamagnetic iron oxide magnetic resonance images. Oncology 2008;75(Suppl 1):48–54.
41 Kudo M, Hatanaka K, Kumada T, Toyoda H, Tada T: Double-contrast ultrasound: a novel surveillance tool for hepatocellular carcinoma. Am J Gastroenterol 2011;106:368–370.
42 Kudo M, Hatanaka K, Inoue T, Maekawa K: Depiction of portal supply in early hepatocellular carcinoma and dysplastic nodule: value of pure arterial ultrasound imaging in hepatocellular carcinoma. Oncology 2010;78(Suppl 1):60–67.
43 Inoue T, Kudo M, Maenishi O, Komuta M, Nakashima O, Kojiro M, Maekawa K: Value of liver parenchymal phase contrast-enhanced sonography to diagnose premalignant and borderline lesions and overt hepatocellular carcinoma. AJR Am J Roentgenol 2009;192:698–705.
44 Inoue T, Hyodo T, Korenaga K, Murakami T, Imai Y, Higaki A, Suda T, Takano T, Miyoshi K, Koda M, Tanaka H, Iijima H, Ochi H, Hirooka M, Numata K, Kudo M: Kupffer phase image of Sonazoid-enhanced US is useful in predicting a hypervascularization of non-hypervascular hypointense hepatic lesions detected on Gd-EOB-DTPA-enhanced MRI: a multicenter retrospective study. J Gastroenterol 2015; Epub ahead of print.
45 Mitsunori Y, Tanaka S, Nakamura N, Ban D, Irie T, Noguchi N, Kudo A, Iijima H, Arii S: Contrast-enhanced intraoperative ultrasound for hepatocellular carcinoma: High sensitivity of diagnosis and therapeutic impact. Journal of hepatobiliary-pancreatic sciences 2013;20:234–242.
46 Hui AM, Takayama T, Sano K, Kubota K, Akahane M, Ohtomo K, Makuuchi M: Predictive value of gross classification of hepatocellular carcinoma on recurrence and survival after hepatectomy. J Hepatol 2000;33:975–979.
47 Shirabe K, Aishima S, Taketomi A, Soejima Y, Uchiyama H, Kayashima H, Ninomiya M, Mano Y, Maehara Y: Prognostic importance of the gross classification of hepatocellular carcinoma in living donor-related liver transplantation. Br J Surg 2011;98:261–267.
48 Hatanaka K, Chung H, Kudo M, Haji S, Minami Y, Maekawa K, Hayaishi S, Nagai T, Takita M, Kudo K, Ueda T, Tatsumi C, Kitai S, Ishikawa E, Yada N, Inoue T, Hagiwara S, Ueshima K: Usefulness of the post-vascular phase of contrast-enhanced ultrasonography with sonazoid in the evaluation of gross types of hepatocellular carcinoma. Oncology 2010;78(Suppl 1):53–59.
49 Hatanaka K, Minami Y, Kudo M, Inoue T, Chung H, Haji S: The gross classification of hepatocellular carcinoma: usefulness of contrast-enhanced US. J Clin Ultrasound 2014;42:1–8.
50 Kudo M: Local ablation therapy for hepatocellular carcinoma: current status and future perspectives. J Gastroenterol 2004;39:205–214.
51 Minami Y, Kudo M, Chung H, Inoue T, Takahashi S, Hatanaka K, Ueda T, Hagiwara H, Kitai S, Ueshima K, Fukunaga T, Shiozaki H: Percutaneous radiofrequency ablation of sonographically unidentifiable liver tumors. Feasibility and usefulness of a novel guiding technique with an integrated system of computed tomography and sonographic images. Oncology 2007;72(Suppl 1):111–116.
52 Minami T, Minami Y, Chishina H, Arizumi T, Takita M, Kitai S, Yada N, Inoue T, Hagiwara S, Ueshima K, Nishida N, Kudo M: Combination guidance of contrast-enhanced US and fusion imaging in radiofrequency ablation for hepatocellular carcinoma with poor conspicuity on contrast-enhanced US/fusion imaging. Oncology 2014;87(Suppl 1):55–62.

Liver Cancer

Liver Cancer 2016;5:47–54
DOI: 10.1159/367761
Published online: December 18, 2015

2235-1795/16/0051-0047$39.50/0
www.karger.com/lic

Editorial

Breakthrough Imaging in Hepatocellular Carcinoma

Prof. M. Kudo

Editor *Liver Cancer*

The ultrasound (US) contrast agent, SonoVue®, has been approved for use worldwide. Conversely, Sonazoid®, which was approved in Japan ahead of other countries in January 2007, is also currently used in Korea, China, and Norway, although its use is gradually spreading to other countries. Sonazoid®-enhanced US is considered a breakthrough imaging technology because it has drastically changed clinical practice, especially in the treatment of hepatocellular carcinoma (HCC) [1, 2].

Sonazoid®-enhanced US imaging is divided into two phases, namely the vascular and Kupffer phases, based on the in vivo dynamics of the agent. Sonazoid®-enhanced US is extremely sensitive for the detection of intranodular blood flow in hepatic tumors, and it is superior to the sensitivity of triphasic multidetector-row computerized tomography (MDCT) [3]. In other words, contrast-enhanced US (CEUS) detects arterial blood flow in real time, resulting in 100% sensitivity. This means that the detection sensitivity of CEUS for intranodular arterial blood flow is higher than that of MDCT. It is also well known that CT hepatic angiography (CTHA), in which CT and angiography are performed concurrently, is inferior to CEUS in terms of the detection sensitivity for intranodular arterial blood flow. SonoVue® -enhanced US is normally performed to display intranodular blood flow for a thorough examination of previously detected nodules by B-mode US. However, unlike SonoVue®, the Kupffer phase of Sonazoid®-enhanced US is used to survey the entire liver by depicting Kupffer defects. Intranodular vascularity is subsequently detected by re-injecting Sonazoid® (defect reperfusion imaging) [2, 4], thus enabling the concurrent detection and definitive diagnosis of HCCs. Accordingly, Sonazoid®-enhanced US can be used for visualizing B-mode ill-defined nodules as well as for surveillance and staging, which is not feasible with CEUS using SonoVue®.

The Kupffer phase of Sonazoid®-enhanced US is an extremely important phase for the following reasons:

(1) All hypervascular HCCs are well-to-moderately differentiated HCCs, and thus show decreased or absent Sonazoid® uptake in the Kupffer phase.

(2) Among precancerous lesions such as dysplastic nodules (DNs) and early HCCs [5], those with a poor arterial blood supply, but with a preserved portal venous supply, appear isoecho-

Liver Cancer 2016;5:47–54
DOI: 10.1159/367761
Published online: December 18, 2015

ic relative to surrounding tissues in terms of Sonazoid® uptake in the Kupffer phase.
(3) The differentiation between a DN and a well-differentiated early HCC is difficult because neither show defects in the Kupffer phase. However, hypovascular nodules that are hypoechoic in the Kupffer phase may be diagnosed as early HCCs [6].

In the future, it will be desirable to consider these findings in combination with gadolinium ethoxybenzyl diethylenetriamine pentaacetic acid (Gd-EOB-DPTA)-enhanced magnetic resonance imaging (Gd-EOB-MRI).

Sonazoid®-enhanced US is also useful for the differentiation of various liver tumors. Tumors can be differentiated easily if they display different contrast enhancement patterns [7]. When the US shows characteristic vascular architecture and hemodynamics, it is normally unnecessary to perform CT or MRI to obtain additional information in order to make a definitive diagnosis [4, 7].

In recent years, by applying highly stable Kupffer-phase imaging and real-time vascular imaging in Sonazoid®-enhanced US, a novel and extremely useful US technique called defect reperfusion imaging has been developed [2, 8]. This can accurately localize B-mode ill-defined nodules in typical HCCs that are hypervascular, and that washout in the late venous phase on MDCT [1, 2]. With this technology, B-mode ill-defined nodules are detected first as defects in the stable Kupffer phase, and then Sonazoid® is re-injected to examine whether arterial blood flow is present within the Kupffer defects. This breakthrough diagnostic imaging technique was developed by simply reversing the conventional way of thinking and it requires no special equipment or analysis. In other words, nodules with typical CT findings of early enhancement with late washout are displayed as defects in the Kupffer phase, and then arterial vascularity in the defects are visualized using Sonazoid® re-injection. By incorporating these ideas, nodules that display typical findings on CT images, but that are ill-defined on B-mode US are identified with almost 100% sensitivity. In defect reperfusion imaging, nodules that are not enhanced after the re-injection of Sonazoid® may be identified as nodules that are different from those detected on dynamic CT imaging. Accordingly, this imaging can be used as an innovative technique to assist in the treatment of HCC [9–12]. Furthermore, defect reperfusion imaging is useful in various applications, such as screening for HCC in cases of liver cirrhosis with a coarse parenchyma [13], the identification of local recurrence after treatment, contrast US-guided needle insertion, the evaluation of treatment response following radiofrequency ablation (RFA) [14], or transarterial chemoembolization (TACE) [15–17].

Various imaging modalities including CT, MRI, and B-mode US are widely available in current clinical practice. Therefore, it is important to know when to apply Sonazoid®-enhanced US, as summarized below.
(1) When a screening US shows a nodular lesion with findings indicative of a hemangioma:
CEUS enables the definitive diagnosis of a cavernous hemangioma in the outpatient setting, making dynamic CT imaging and MRI unnecessary.
(2) When a liver mass displays the ‘spoke-wheel’ sign by color Doppler, and the patient is negative for viral hepatitis, tumor markers, clinical signs of liver disease, and in the absence of a known primary neoplasm:
A definitive diagnosis of focal nodular hyperplasia (FNH) is possible if CEUS shows the ‘spoke-wheel’ sign and has iso- or high-uptake in the Kupffer phase. Therefore, angiography only to make a diagnosis of FNH has proved to be unnecessary in recent years. With respect to the ability to visualize the ‘spoke-wheel’ sign, CEUS is superior to other modalities such as angiography, CTHA, and carbon dioxide-enhanced ultrasonography [18–20].
(3) When nodules previously diagnosed as DNs on CTHA, CT during arterial portography (CTAP), or biopsy should be monitored for malignant transformation:
By performing CEUS regularly, it is possible to monitor these nodules in the outpatient set-

Liver Cancer 2016;5:47–54
DOI: 10.1159/367761
Published online: December 18, 2015

tings to identify the appearance of intranodular arterial blood flow or a decline in the uptake of Sonazoid® in the Kupffer phase.
(4) When nodules are not hypervascular in the early arterial phase, but are hypovascular in the portal venous and equilibrium phases in contrast-enhanced CT:
A diagnosis of HCC can be made even in such nodules when arterial vascularity is observed on CEUS, since this technique is more sensitive in the detection of intranodular arterial blood flow than MDCT.
(5) When a navigation system for accurate needle insertion guidance is necessary for B-mode ill-defined HCC:
Defect reperfusion imaging can localize nodules in the Kupffer phase. After the re-injection of Sonazoid® to confirm the presence of arterial blood flow (defect reperfusion imaging), the Kupffer-phase image can be used to guide needle insertion for local ablation.
(6) When HCCs with typical hypervascularity in the arterial-phase CT have washout in the portal venous and equilibrium phases, which are ill-defined in B-mode US (including locally recurrent lesions):
The detection rate of viable HCC is 100% if defect reperfusion imaging is performed after detecting Kupffer-phase defects.
(7) When macroscopic morphologic diagnosis of nodules is needed before treatment:
Because the macroscopic morphology of HCC accurately reflects the malignancy grade of the tumor, morphological information is essential for the establishment of the correct treatment strategy. Among currently available imaging modalities, Sonazoid®-enhanced US most accurately displays the macroscopic morphology of HCC lesions [21, 22].
(8) To evaluate treatment response after RFA or TACE:
CEUS is the most sensitive evaluation method immediately after these procedures. Although fusion imaging is also used in RFA, it is possible to evaluate not only tumor response but also ablative margins by using CEUS[23, 24].
(9) For surveillance and staging of HCC:
In addition to a pilot study [13], a recent multicenter randomized prospective study showed that screening the entire liver by the Kupffer phase of Sonazoid®-enhanced US is a more sensitive method for the early detection of small HCCs compared with screening by B-mode US. It is therefore anticipated that entire liver screening in the Kupffer phase of Sonazoid®-enhanced US will be incorporated into clinical guidelines for the surveillance of HCCs based on this evidence. This imaging approach is also expected to play an important role in the staging of HCCs.
(10) For screening and staging of metastatic liver cancer and cholangiocarcinoma:
Whole-liver scanning in the Kupffer phase shows metastatic liver cancers as defects, thereby revealing a higher number of nodules than MDCT or B-mode US. Therefore, screening in the Kupffer phase of Sonazoid®-enhanced US should be incorporated into clinical practice to establish a treatment strategy for patients who have or are suspected to have 1–2 metastatic liver tumors.

Essentially, CEUS is recommended to increase the diagnostic accuracy of benign tumors (hemangioma, FNH, and DN) in outpatient clinics, and to aid in the screening and staging of metastatic liver cancer and HCC. Because of its high sensitivity in detecting intranodular arterial blood flow, CEUS is also useful for detecting small lesions that contrast-enhanced CT fails to identify.

As described earlier, US has conventionally been used as a screening tool. However, in recent years, CEUS has become an important tool for providing a thorough examination and a definitive diagnosis, demonstrating that it is indeed a breakthrough imaging technology.

Liver Cancer

Liver Cancer 2016;5:47–54
DOI: 10.1159/367761
Published online: December 18, 2015

EOB-MRI

The commercialization of the hepatocyte-specific contrast agent Gd-EOB-DTPA began in 2008, placing it in a relatively new group of MRI contrast agents. This unique liver-specific contrast agent is taken up by hepatic parenchymal cells and is secreted into the bile. Unlike other liver-specific agent such as superparamagnetic iron oxide (SPIO), Gd-EOB-DTPA show the hepatic parenchyma as white 20 minutes post-injection in the hepatocyte-phase of a T1-weighted MRI, while nodules that lack hepatic parenchyma, such as HCC, appear as hypointense signals. For this reason, Gd-EOB-DTPA is occasionally called 'white liver' agent. Compared with SPIO, which turns the entire liver black (also known as 'black liver' agent) in T2-weighted images with poor spatial resolution, Gd-EOB-DTPA is a user-friendly diagnostic imaging modality even for hepatologists who are not specialized in the use of MRI. Therefore, Gd-EOB-MRI is also a breakthrough in diagnostic liver imaging.

After intravenous administration, approximately 50% of Gd-EOB-DTPA is taken up by hepatocytes and excreted into the bile, while the rest is excreted by the kidneys. The uptake of the contrast agent into hepatocytes is known to occur via passive diffusion mediated by organic anion transporter protein 1 (OATP1) in the cell membrane [25], while its excretion from hepatocytes into the bile canaliculi is thought to involve ATP-dependent active transport mediated by multidrug-resistance associated protein 2 (MRP2) [26].

Recent studies show that OATP1B3 (also referred to as OATP8) is responsible for the uptake of Gd-EOB-DTPA in humans [27, 28]. OATP1B3 is expressed in some of moderately- to well-differentiated hypervascular HCCs, and these neoplasms are visualized as hyperintense signals in the hepatocyte phase. However, no association exists between the expression of OATP1B3 and bile production or tumor differentiation [27]. These findings suggest that the expression of the uptake transporter OATP1B3 and the excretion-related transporter MRP2 are normal in DNs, causing no change in the uptake of the contrast agent in the hepatocyte phase. In well-differentiated early HCCs accompanied by stromal invasion, however, the expression of OATP1B3 is decreased, resulting in reduced uptake of the contrast agent, and thus generating hypointense signals in the hepatocyte phase. In well-differentiated as well as moderately- or poorly-differentiated HCCs, the expression of OATP1B3 is reduced or absent, presumably causing hypointense signals in the hepatocyte phase.

However, nodules in approximately 5–10% of hypervascular and moderately-differentiated HCCs are iso-to-hyperintense in the hepatocyte phase, and this type of nodule is known to have a favorable clinical outcome [28–30]. Even among hypervascular HCCs, nodules showing hyperintense signals in the hepatocyte phase have low alpha-fetoprotein and vitamin K antagonist-II levels and a low rate of intrahepatic metastasis, and thus a good prognosis. Based on these findings, it is possible to observe early HCCs in which OATP1B3 expression has not been downregulated during development from a DN to an early HCC and then to a well-to-moderately differentiated HCC. Indeed, in clinical practice, some nodules that are not hypointense in the EOB-MRI hepatocyte phase are subsequently diagnosed as well differentiated HCCs based on histological findings from the biopsy, suggesting that it is not unusual to find well-differentiated HCCs expressing OATP1B3.

Cases opposite to the above scenario, that is, DNs displaying hypointense signals in the hepatocyte phase, may be problematic. In clinical practice, some nodules showing hypointense signals in the hepatocyte phase are subsequently diagnosed as a DN following a biopsy. However, in a study examining resected specimens, but not biopsy samples, all DNs displayed isointensity in the hepatocyte phase [31]. According to expert opinion, in early HCC, it is extremely rare for DNs to be hypointense in the hepatocyte phase of EOB-MRI. Indeed, in our clinical experience, it is also extremely rare for hypointense resected specimens to be diagnosed as DNs [10]. Even when a diagnosis of a DN is made based on biopsy findings, there is

Liver Cancer 2016;5:47–54
DOI: 10.1159/367761
Published online: December 18, 2015

always a possibility of sampling variability. Furthermore, even liver specialized histopathologists have difficulty making a definitive diagnosis of early HCC [5] in the absence of stromal invasion in biopsied samples, despite their similar cellular or structural atypia. Further study is needed to address the diagnostic limitations of histopathological findings from biopsies.

Many early HCCs appear hypovascular in resected specimens, making their diagnosis difficult even by CTAP or CTHA. While many early HCCs show a slight decrease in portal venous blood flow, some are isodense on CTAP. In addition, many early HCCs that are hypointense on the hepatocyte phase of Gd-EOB-MRI are diagnosed as early HCCs upon histological examination [10]. Furthermore, most nodules that do not show decreased signals in the hepatocyte phase are identified as DNs in the resected specimens. Taking into account these findings, when differentiating early HCCs from DNs, the functional diagnostic ability of Gd-EOB-MRI, which sensitively captures early signs of carcinogenesis, is believed to be superior to hemodynamic or functional diagnosis of Kupffer cells such as the Kupffer phase of SPIO-MRI, Sonazoid®-enhanced US, or decreased portal venous flow on CTAP.

The following are unknown: (1) the frequency of DNs that display hypointense signals in the hepatocyte phase of EOB-MRI; (2) the frequency of hypovascular, hypointense nodules in the hepatocyte phase that are pathologically diagnosed as early HCC; (3) the frequency of future hypervascularization among these nodules; and (4) the factors associated with hypervascularization. These four questions should be addressed as soon as possible in multicenter studies with an adequate number of cases. Indeed, there are many reports of hypervascularization of hypovascular, hypointense nodules [32–50]. Tumor diameter and nodule growth speed are reported as risk factors for hypervascularization. These characteristics are therefore important in predicting the hypervascularization of hypovascular nodules. It should be noted that the tumor diameter cutoff in these studies has often been reported around 1 cm. Actually, intensive follow-up of hypovascular nodules that are hypointense in the hepatobiliary phase of EOB-MRI has shown that nodules with a higher rate of growth are more prone to develop into hypervascular nodules, which suggests that nodule growth speed might be included in the algorithm as well.

The next question concerns the proper clinical management of these nodules. To address this issue, a multicenter prospective study must be performed to investigate their rate of malignant transformation. This should be done by obtaining histopathological findings from hypovascular nodules that are identified as hypointense in the hepatocyte phase of Gd-EOB-MRI and by following the natural course of these nodules.

In conclusion, proactive examination using EOB-MRI is recommended in the following settings: (1) the differentiation of early HCC from DNs; (2) staging of HCCs prior to treatment; (3) alternate use of MDCT and Gd-EOB-MRI for screening of HCCs in high-risk patients who are recommended to undergo MDCT or MRI 1–2 times annually [51]; (4) early detection of recurrence by the alternate use of MDCT and Gd-EOB-MRI during follow-up after treatment of HCC; and (5) preoperative detection and evaluation of metastatic liver cancers.

As stated above, CEUS and Gd-EOB-MRI play tremendously important roles in screening, definitive diagnosis, malignant potential, diagnosis of pathological differentiation grade, assessment of treatment response, treatment guidance, and early detection of tumor recurrence.

In this issue of *Liver Cancer*, detailed reviews of these two breakthrough imaging modalities are presented by Piscaglia and Salvatore [52] and Lee [53], and I believe these two articles are of tremendous value for readers of this journal.

Liver Cancer 2016;5:47–54
DOI: 10.1159/367761
Published online: December 18, 2015

References

1 Kudo M, Hatanaka K, Chung H, Minami Y, Maekawa K: A proposal of novel treatment-assist technique for hepatocellular carcinoma in the sonazoid-enhanced ultrasonography: Value of defect re-perfusion imaging. Kanzo 2007;48:299–301 (in Japanese).
2 Kudo M, Hatanaka.K, Maekawa K: Defect reperfusion imaging, a newly developed novel technology using sonazoid in the treatment of hepatocellular carcinoma. J Med Ultrasound 2008;16:169–176.
3 Hatanaka K, Kudo M, Minami Y, Maekawa K: Sonazoid-enhanced ultrasonography for diagnosis of hepatic malignancies: comparison with contrast-enhanced CT. Oncology 2008;75(Suppl 1):42–47.
4 Kudo M, Hatanaka K, Maekawa K: Sonazoid-enhanced ultrasound in the diagnosis and treatment of hepatic tumors. J Med Ultrasound 2008;16:130–139.
5 Kudo M: Early hepatocellular carcinoma: definition and diagnosis. Liver Cancer 2013;2:69–72.
6 Inoue T, Hyodo T, Korenaga K, Murakami T, Imai Y, Higaki A, Suda T, Takano T, Miyoshi K, Koda M, Tanaka H, Iijima H, Ochi H, Hirooka M, Numata K, Kudo M: Kupffer phase image of Sonazoid-enhanced US is useful in predicting a hypervascularization of non-hypervascular hypointense hepatic lesions detected on Gd-EOB-DTPA-enhanced MRI: a multicenter retrospective study. J Gastroenterol 2015.
7 Hatanaka K, Kudo M, Minami Y, Ueda T, Tatsumi C, Kitai S, Takahashi S, Inoue T, Hagiwara S, Chung H, Ueshima K, Maekawa K: Differential diagnosis of hepatic tumors: value of contrast-enhanced harmonic sonography using the newly developed contrast agent, Sonazoid. Intervirology 2008;51(Suppl 1):61–69.
8 Kudo M, Hatanaka K, Maekawa K: Newly developed novel ultrasound technique, defect reperfusion ultrasound imaging, using Sonazoid in the management of hepatocellular carcinoma. Oncology 2010;78:S40–S45.
9 Minami Y, Kudo M, Hatanaka K, Kitai S, Inoue T, Hagiwara S, Chung H, Ueshima K: Radiofrequency ablation guided by contrast harmonic sonography using perfluorocarbon microbubbles (Sonazoid) for hepatic malignancies: an initial experience. Liver Int 2010;30:759–764.
10 Kudo M: The 2008 Okuda lecture: Management of hepatocellular carcinoma: from surveillance to molecular targeted therapy. J Gastroenterol Hepatol 2010;25:439–452.
11 Inoue T, Minami Y, Chung H, Hayaishi S, Ueda T, Tatsumi C, Takita M, Kitai S, Hatanaka K, Ishikawa E, Yada N, Hagiwara S, Ueshima K, Kudo M: Radiofrequency ablation for hepatocellular carcinoma: assistant techniques for difficult cases. Oncology 2010;78(Suppl 1):94–101.
12 Minami Y, Kudo M, Chung H, Kawasaki T, Yagyu Y, Shimono T, Shiozaki H: Contrast harmonic sonography-guided radiofrequency ablation therapy versus B-mode sonography in hepatocellular carcinoma: prospective randomized controlled trial. AJR Am J Roentgenol 2007;188:489–494.
13 Kudo M, Hatanaka K, Kumada T, Toyoda H, Tada T: Double-contrast ultrasound: a novel surveillance tool for hepatocellular carcinoma. Am J Gastroenterol 2011;106:368–370.
14 Teng W, Liu KW, Lin CC, Jeng WJ, Chen WT, Sheen IS, Lin CY, Lin SM: Insufficient ablative margin determined by early computed tomography may predict the recurrence of hepatocellular carcinoma after radiofrequency ablation. Liver Cancer 2015;4:26–38.
15 Tsurusaki M, Murakami T: Surgical and locoregional therapy of HCC. Tace Liver Cancer 2015;4:165–175.
16 Kudo M: Locoregional therapy for hepatocellular carcinoma. Liver Cancer 2015;4:163–164.
17 Raoul JL, Gilabert M, Piana G: How to define transarterial chemoembolization failure or refractoriness: a European perspective. Liver Cancer 2014;3:119–124.
18 Kudo M, Tomita S, Tochio H, Kashida H, Hirasa M, Todo A: Hepatic focal nodular hyperplasia: specific findings at dynamic CEUS with carbon dioxide microbubbles. Radiology 1991;179:377–382.
19 Kudo M, Tomita S, Tochio H, Mimura J, Okabe Y, Kashida H, Hirasa M, Ibuki Y, Todo A: Sonography with intraarterial infusion of carbon dioxide microbubbles (sonographic angiography): value in differential diagnosis of hepatic tumors. AJR Am J Roentgenol 1992;158:65–74.
20 Kudo M, Tomita S, Tochio H, Mimura J, Okabe Y, Kashida H, Hirasa M, Ibuki Y, Todo A: Small hepatocellular carcinoma: diagnosis with US angiography with intraarterial CO2 microbubbles. Radiology 1992;182:155–160.
21 Hatanaka K, Chung H, Kudo M, Haji S, Minami Y, Maekawa K, Hayaishi S, Nagai T, Takita M, Kudo K, Ueda T, Tatsumi C, Kitai S, Ishikawa E, Yada N, Inoue T, Hagiwara S, Ueshima K: Usefulness of the post-vascular phase of contrast-enhanced ultrasonography with sonazoid in the evaluation of gross types of hepatocellular carcinoma. Oncology 2010;78(Suppl 1):53–59.
22 Hatanaka K, Minami Y, Kudo M, Inoue T, Chung H, Haji S: The gross classification of hepatocellular carcinoma: usefulness of CEUS. J Clin Ultrasound 2014;42:1–8.
23 Minami T, Minami Y, Chishina H, Arizumi T, Takita M, Kitai S, Yada N, Inoue T, Hagiwara S, Ueshima K, Nishida N, Kudo M: Combination guidance of CEUS and fusion imaging in radiofrequency ablation for hepatocellular carcinoma with poor conspicuity on CEUS/fusion imaging. Oncology 2014;87(Suppl 1):55–62.
24 Minami Y, Kudo M: Ultrasound fusion imaging of hepatocellular carcinoma: a review of current evidence. Dig Dis 2014;32:690–695.
25 van Montfoort JE, Stieger B, Meijer DK, Weinmann HJ, Meier PJ, Fattinger KE: Hepatic uptake of the magnetic resonance imaging contrast agent gadoxetate by the organic anion transporting polypeptide Oatp1. J Pharmacol Exp Ther 1999;290:153–157.
26 Pascolo L, Petrovic S, Cupelli F, Bruschi CV, Anelli PL, Lorusso V, Visigalli M, Uggeri F, Tiribelli C: Abc protein transport of MRI contrast agents in canalicular rat liver plasma vesicles and yeast vacuoles. Biochem Biophys Res Commun 2001;282:60–66.

Liver Cancer 2016;5:47–54
DOI: 10.1159/367761
Published online: December 18, 2015

27 Narita M, Hatano E, Arizono S, Miyagawa-Hayashino A, Isoda H, Kitamura K, Taura K, Yasuchika K, Nitta T, Ikai I, Uemoto S: Expression of OATP1B3 determines uptake of Gd-EOB-DTPA in hepatocellular carcinoma. J Gastroenterol 2009;44:793–798.
28 Kitao A, Matsui O, Yoneda N, Kozaka K, Kobayashi S, Koda W, Gabata T, Yamashita T, Kaneko S, Nakanuma Y, Kita R, Arii S: Hypervascular hepatocellular carcinoma: correlation between biologic features and signal intensity on gadoxetic acid-enhanced MR images. Radiology 2012;265:780–789.
29 Kitao A, Matsui O, Yoneda N, Kozaka K, Kobayashi S, Sanada J, Koda W, Minami T, Inoue D, Yoshida K, Yamashita T, Yamashita T, Kaneko S, Takamura H, Ohta T, Ikeda H, Nakanuma Y, Kita R, Gabata T: Hepatocellular carcinoma with beta-catenin mutation: Imaging and pathologic characteristics. Radiology 2015;275:708–717.
30 Yamashita T, Kitao A, Matsui O, Hayashi T, Nio K, Kondo M, Ohno N, Miyati T, Okada H, Yamashita T, Mizukoshi E, Honda M, Nakanuma Y, Takamura H, Ohta T, Nakamoto Y, Yamamoto M, Takayama T, Arii S, Wang X, Kaneko S: Gd-EOB-DTPA-enhanced magnetic resonance imaging and alpha-fetoprotein predict prognosis of early-stage hepatocellular carcinoma. Hepatology 2014;60:1674–1685.
31 Ichikawa T, Sano K, Morisaka H: Diagnosis of pathologically early HCC with eob-mri: Experiences and current consensus. Liver Cancer 2014;3:97–107.
32 Matsuda M, Tsuda T, Yoshioka S, Murata S, Tanaka H, Hirooka M, Hiasa Y, Mochizuki T: Incidence for progression of hypervascular HCC in hypovascular hepatic nodules showing hyperintensity on gadoxetic acid-enhanced hepatobiliary phase in patients with chronic liver diseases. Jpn J Radiol. 2014;32(7):405–413.
33 Jang KM, Kim SH, Kim YK, Choi D: Imaging features of subcentimeter hypointense nodules on gadoxetic acid-enhanced hepatobiliary phase MR imaging that progress to hypervascular hepatocellular carcinoma in patients with chronic liver disease. Acta Radiol 2015;56:526–535.
34 Komatsu N, Motosugi U, Maekawa S, Shindo K, Sakamoto M, Sato M, Tatsumi A, Miura M, Amemiya F, Nakayama Y, Inoue T, Fukasawa M, Uetake T, Ohtaka M, Sato T, Asahina Y, Kurosaki M, Izumi N, Ichikawa T, Araki T, Enomoto N: Hepatocellular carcinoma risk assessment using gadoxetic acid-enhanced hepatocyte phase magnetic resonance imaging. Hepatol Res. 2014;44(13):1339–1346.
35 Iannicelli E, Di Pietropaolo M, Marignani M, Briani C, Federici GF, Delle Fave G, David V: Gadoxetic acid-enhanced MRI for hepatocellular carcinoma and hypointense nodule observed in the hepatobiliary phase. Radiol Med (Torino) 2014;119:367–376.
36 Inoue T, Hyodo T, Murakami T, Takayama Y, Nishie A, Higaki A, Korenaga K, Sakamoto A, Osaki Y, Aikata H, Chayama K, Suda T, Takano T, Miyoshi K, Koda M, Numata K, Tanaka H, Iijima H, Ochi H, Hirooka M, Imai Y, Kudo M: Hypovascular hepatic nodules showing hypointense on the hepatobiliary-phase image of Gd-EOB-DTPA-enhanced MRI to develop a hypervascular hepatocellular carcinoma: a nationwide retrospective study on their natural course and risk factors. Dig Dis 2013;31:472–479.
37 Ichikawa S, Ichikawa T, Motosugi U, Sano K, Morisaka H, Enomoto N, Matsuda M, Fujii H, Araki T: Presence of a hypovascular hepatic nodule showing hypointensity on hepatocyte-phase image is a risk factor for hypervascular hepatocellular carcinoma. J Magn Reson Imaging 2014;39:293–297.
38 Toyoda H, Kumada T, Tada T, Niinomi T, Ito T, Sone Y, Kaneoka Y, Maeda A: Non-hypervascular hypointense nodules detected by Gd-EOB-DTPA-enhanced MRI are a risk factor for recurrence of HCC after hepatectomy. J Hepatol 2013;58:1174–1180.
39 Hyodo T, Murakami T, Imai Y, Okada M, Hori M, Kagawa Y, Kogita S, Kumano S, Kudo M, Mochizuki T: Hypovascular nodules in patients with chronic liver disease: risk factors for development of hypervascular hepatocellular carcinoma. Radiology 2013;266:480–490.
40 Kim YK, Lee WJ, Park MJ, Kim SH, Rhim H, Choi D: Hypovascular hypointense nodules on hepatobiliary phase gadoxetic acid-enhanced MR images in patients with cirrhosis: potential of DW imaging in predicting progression to hypervascular HCC. Radiology 2012;265:104–114.
41 Kobayashi S, Matsui O, Gabata T, Koda W, Minami T, Ryu Y, Kozaka K, Kitao A: Intranodular signal intensity analysis of hypovascular high-risk borderline lesions of HCC that illustrate multi-step hepatocarcinogenesis within the nodule on Gd-EOB-DTPA-enhanced MRI. Eur J Radiol 2012;81:3839–3845.
42 Kobayashi S, Matsui O, Gabata T, Koda W, Minami T, Ryu Y, Kozaka K, Kitao A: Relationship between signal intensity on hepatobiliary phase of gadolinium ethoxybenzyl diethylenetriaminepentaacetic acid (Gd-EOB-DTPA)-enhanced MR imaging and prognosis of borderline lesions of hepatocellular carcinoma. Eur J Radiol 2012;81:3002–3009.
43 Kobayashi S, Matsui O, Gabata T, Koda W, Minami T, Ryu Y, Kawai K, Kozaka K: Gadolinium ethoxybenzyl diethylenetriamine pentaacetic Acid-enhanced magnetic resonance imaging findings of borderline lesions at high risk for progression to hypervascular classic hepatocellular carcinoma. J Comput Assist Tomogr 2011;35:181–186.
44 Joishi D, Ueno A, Tanimoto A, Okuda S, Masugi Y, Emoto K, Okuma K, Sakamoto M, Imai Y, Kuribayashi S: Natural course of hypovascular nodules detected on gadoxetic acid-enhanced MR imaging: presence of fat is a risk factor for hypervascularization. Magn Reson Med Sci 2013;12:281–287.
45 Motosugi U: Hypovascular hypointense nodules on hepatocyte phase gadoxetic acid-enhanced MR images: too early or too progressed to determine hypervascularity. Radiology 2013;267:317–318.
46 Takechi M, Tsuda T, Yoshioka S, Murata S, Tanaka H, Hirooka M, Mochizuki T: Risk of hypervascularization in small hypovascular hepatic nodules showing hypointense in the hepatobiliary phase of gadoxetic acid-enhanced mri in patients with chronic liver disease. Jpn J Radiol. 2012;30(9):743–751.

Liver Cancer 2016;5:47–54
DOI: 10.1159/367761
Published online: December 18, 2015

47 Takayama Y, Nishie A, Nakayama T, Asayama Y, Ishigami K, Kakihara D, Ushijima Y, Fujita N, Hirakawa M, Honda H: Hypovascular hepatic nodule showing hypointensity in the hepatobiliary phase of gadoxetic acid-enhanced MRI in patients with chronic liver disease: prediction of malignant transformation. Eur J Radiol 2012;81:3072–3078.
48 Akai H, Matsuda I, Kiryu S, Tajima T, Takao H, Watanabe Y, Imamura H, Kokudo N, Akahane M, Ohtomo K: Fate of hypointense lesions on Gd-EOB-DTPA-enhanced magnetic resonance imaging. Eur J Radiol 2012;81:2973–2977.
49 Motosugi U, Ichikawa T, Sano K, Sou H, Onohara K, Muhi A, Amemiya F, Enomoto N, Matsuda M, Fujii H, Araki T: Outcome of hypovascular hepatic nodules revealing no gadoxetic acid uptake in patients with chronic liver disease. J Magn Reson Imaging 2011;34:88–94.
50 Kumada T, Toyoda H, Tada T, Sone Y, Fujimori M, Ogawa S, Ishikawa T: Evolution of hypointense hepatocellular nodules observed only in the hepatobiliary phase of gadoxetate disodium-enhanced MRI. AJR Am J Roentgenol 2011;197:58–63.
51 Kudo M, Matsui O, Izumi N, Iijima H, Kadoya M, Imai Y, Okusaka T, Miyayama S, Tsuchiya K, Ueshima K, Hiraoka A, Ikeda M, Ogasawara S, Yamashita T, Minami T, Yamakado K, Liver Cancer Study Group of Japan: JSH consensus-based clinical practice guideline for the management of hepatocellular carcinoma: 2014 update by the Liver Cancer Study Group of Japan. Liver Cancer 2014;3:458–468.
52 Salvatore V, Gianstefani A, Negrini G, Allegretti G, Galassi M, Piscaglia F: Imaging diagnosis of hepatocellular carcinoma: Recent advances of contrast-enhanced ultrasonography with SonoVue®. Liver Cancer 2016;5:55–66.
53 Joo I, Lee JM: Recent advances in the imaging diagnosis of hepatocellular carcinoma: Value of gadoxetic acid-enhanced MRI. Liver Cancer 2016;5:67–87.

Contrast-enhanced harmonic endoscopic ultrasonography for differential diagnosis of pancreatic cysts

Authors Ken Kamata[1], Masayuki Kitano[1], Shunsuke Omoto[1], Kumpei Kadosaka[1], Takeshi Miyata[1], Kentaro Yamao[1], Hajime Imai[1], Hiroki Sakamoto[1], Yogesh Harwani[1], Takaaki Chikugo[2], Yasutaka Chiba[3], Ippei Matsumoto[4], Yoshifumi Takeyama[4], Masatoshi Kudo[1]

Institutions Institutions are listed at end of article.

submitted:
7. December 2014
accepted after revision:
18. August 2015

Bibliography
DOI http://dx.doi.org/10.1055/s-0034-1393564
Published online: 25.11.2015
Endoscopy 2016; 48: 35–41

ISSN 0013-726X

Corresponding author
Masayuki Kitano, MD PhD
Department of Gastroenterology and Hepatology
Kinki University Faculty of Medicine
377–2 Ohno-higashi
Osaka-sayama 589–8511
Japan
Fax: +81–72–3672880
m-kitano@med.kindai.ac.jp

Scan this QR-Code to watch the video comment.

Background and study aim: Comparison of fundamental B-mode endoscopic ultrasonography (FB-EUS) and contrast-enhanced harmonic endoscopic ultrasonography (CH-EUS) in the differential diagnosis of pancreatic cysts according to presence of mural nodules.

Patients and methods: Between April 2007 and April 2012, FB-EUS and CH-EUS data were prospectively collected from 581 consecutive patients with pancreatic cysts, and were retrospectively analyzed from 70 with subsequent cyst resection. Presence and height of mural nodules as detected on FB-EUS and CH-EUS were evaluated, and thence accuracies of both methods for diagnosing mucinous versus nonmucinous and malignant versus benign cysts.

Results: On pathological examination 48 cysts were mucinous and 22 were nonmucinous; 30 cysts were malignant (high grade dysplasia or invasive carcinoma) and 40 were benign. If presence of a mural nodule was considered to indicate a mucinous cyst, FB-EUS and CH-EUS accuracies did not differ significantly (respectively: sensitivity 85 % vs. 79 %; specificity 46 % vs. 96 %; accuracy 73 % vs. 84 %, $P=0.057$). If presence of mural nodule was considered to indicate malignancy, CH-EUS was significantly more accurate than FB-EUS (respectively: sensitivity 97 % vs. 97 %; specificity 75 % vs. 40 %; accuracy 84 % vs. 64 %, $P=0.0001$). For diagnosing malignancy by evaluating mural nodule height, the area under the receiver operating characteristic (AUROC) was 0.84 and 0.93 for FB-EUS and CH-EUS, respectively ($P=0.028$). Presence of a mural nodule of height ≥ 4 mm on CH-EUS was a sign of malignancy (false-positive fraction 0.2; true-positive fraction 0.93; odds ratio 56.0).

Conclusions: CH-EUS is more accurate than FB-EUS for diagnosing malignant pancreatic cysts.

Introduction

Pancreatic cyst is a frequent finding on cross-sectional imaging [1]. Mucinous cystic neoplasms (MCNs) and intraductal papillary mucinous neoplasms (IPMNs) have malignant potential; however, these lesions can be followed up without surgical resection when they are asymptomatic and present without high risk features [2]. Serous cystic neoplasms and non-neoplastic cysts are generally not considered at risk for malignant progression. Therefore, after identification a cyst, diagnosis of the cyst type and categorization of the cyst as benign, premalignant, or malignant is critical for guiding subsequent management decisions [3].

Endoscopic ultrasonography (EUS) is superior to other imaging methods in terms of spatial resolution and is widely used to evaluate pancreatic cysts [4–6]. Contrast-enhanced harmonic EUS (CH-EUS) is a new imaging modality that uses an ultrasonographic contrast agent to visualize blood flow in fine vessels and has been shown to be accurate for the differential diagnosis of solid pancreatic tumors [7–11]. CH-EUS may also aid in the diagnosis of pancreatic cysts by enabling assessment of the vascularity of structures such as cyst walls, septa, or mural nodules and the discrimination of contrast-enhancing mural nodules from nonenhancing mucus clots [7].

In this study, we evaluated fundamental B-mode EUS (FB-EUS) and CH-EUS in the diagnosis of mucinous versus nonmucinous and malignant versus nonmalignant pancreatic cysts, based on the evaluation of cyst mural nodules.

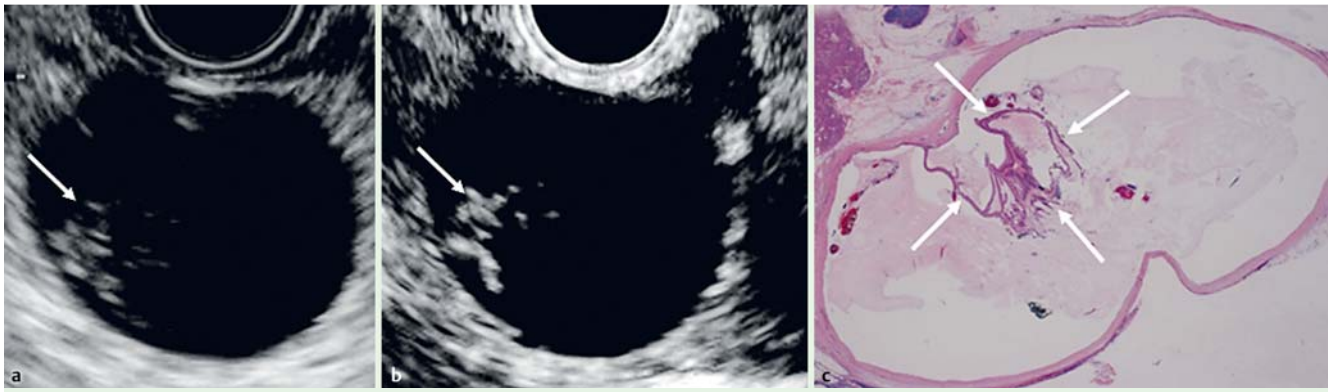

Fig. 1 Contrast-enhanced harmonic endoscopic ultrasound (CH-EUS) for differential diagnosis of pancreatic cysts: a side branch intrapapillary mucinous neoplasm (IPMN) with high grade dysplasia. **a** Fundamental B-mode endoscopic ultrasound (FB-EUS): the protruding component suspected of being a mural nodule is shown in the cystic lesion (arrow). **b** CH-EUS: the protruding component has vascularity (arrow). **c** Pathological examination of the resected specimen (hematoxylin and eosin staining) reveals high grade dysplasia in the part of the mural nodule detected by EUS (arrows).

Patients and methods

Study design

This was a retrospective review of prospectively collected imaging, clinical, and pathological data. The aim was to determine and compare the diagnostic accuracies (and other test performance characteristics) of FB-EUS and CH-EUS for diagnosis of mucinous versus nonmucinous cysts and malignant versus benign cysts based on the presence and height of mural nodules. The "gold standard" for diagnosing pancreatic cystic lesions was histopathological diagnosis of specimens obtained by surgical resection.

Patients

A total of 581 consecutive patients with pancreatic cysts underwent FB-EUS followed by CH-EUS at the Kinki University School of Medicine between April 2007 and April 2012. Of these, 92 patients underwent surgical resection because of features seen on EUS and/or other imaging modalities that suggested malignancy (i.e., size ≥ 3 cm, thickened cyst walls, solid component within cyst, abrupt changes in caliber of pancreatic duct, and/or presence of concomitant pancreatic invasive cancer distinct from the cyst). The remaining 489 patients were managed by follow-up.

Of the 92 patients with surgical resection, 22 patients with concomitant pancreatic invasive cancer distinct from the cyst (n = 11) or with multiple cysts (n = 11) were excluded from this study. Consequently, data were analyzed from 70 patients with solitary pancreatic cysts who underwent surgical resection. For the purpose of the study all surgical specimens were reviewed by expert pathologists to discriminate between mucinous versus nonmucinous and between malignant versus nonmalignant pancreatic cystic lesions.

In line with the Japanese guidelines, EUS-guided fine needle aspiration (EUS-FNA) was not performed [12]. This study was performed with the approval of the ethics committee of the Kinki University School of Medicine.

FB-EUS and CH-EUS

An echoendoscope developed for CH-EUS (GF-UCT260; Olympus Medical Systems, Tokyo, Japan) was used. EUS images were analyzed using an Aloka ProSound SSD α-10 system (Aloka, Tokyo, Japan). After evaluation of all of the pancreas and the cyst using FB-EUS, the imaging mode was changed to the extended pure harmonic detection mode, which synthesized the filtered second-harmonic components with signals obtained from the phase shift for contrast-enhanced harmonic imaging. The transmitting frequency and mechanical index were 4.7 MHz and 0.3, respectively. The ultrasound contrast agent used for CH-EUS was Sonazoid (Daiichi-Sankyo, Tokyo, Japan; GE Healthcare Milwaukee, Wisconsin, USA), which consists of perfluorobutane microbubbles surrounded by a lipid membrane. Immediately before performance of CH-EUS, the contrast agent was reconstituted with 2 mL of sterile water for injection, and a dose of 15 µL/kg bodyweight was prepared in a 2-mL syringe. A bolus injection of the ultrasound contrast agent was administered at a speed of 1 mL/s through a 22-gauge cannula placed in the antecubital vein, followed by a 10-mL saline solution flush to ensure that all the contrast agent was introduced into the circulation.

The CH-EUS examinations for the pancreatic cyst lasted for 60 s from injection of the contrast agent. Video sequences of 60 s were stored and then independently reviewed by two readers (M.K. and H.I.), who have each performed more than 1000 CH-EUS procedures. For this special review of the stored data, the readers were blinded to the final diagnosis. When the independent conclusions of the two reviewers were discordant regarding presence of a mural nodule, they re-evaluated the saved images together until agreement was reached.

Definitions

The reference standard was the pathological finding obtained after surgical resection. IPMNs and MCNs were classified as low, intermediate, or high grade dysplasia, or as invasive carcinoma [13]. Malignancy was defined as high grade dysplasia or invasive carcinoma. IPMNs and MCNs were considered to be mucinous cysts.

On FB-EUS, a mural nodule was defined as a EUS-detectable protrusion of the cyst wall into its lumen. On CH-EUS, a mural nodule was defined as a cyst wall protrusion that showed enhancement after contrast administration. The height of a mural nodule was measured from the nodule base to its top in the axis perpendicular to the cyst wall. **Fig. 1** shows a representative image of a mural nodule as seen at FB-EUS and CH-EUS, and the histopathological appearance.

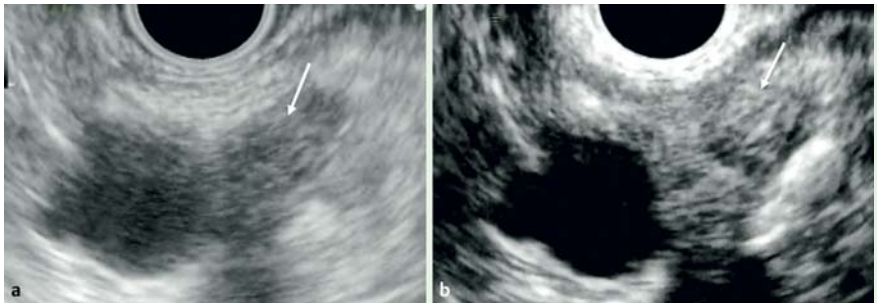

Fig. 2 A side branch intrapapillary mucinous neoplasm (IPMN) with invasive carcinoma. **a** Fundamental B-mode endoscopic ultrasound (FB-EUS): a highly echoic structure is visible in the dilated branch duct (arrow). **b** Contrast-enhanced harmonic endoscopic ultrasound (CH-EUS): the lesions are enhanced and the shape of the lesion is clearly delineated (arrow).

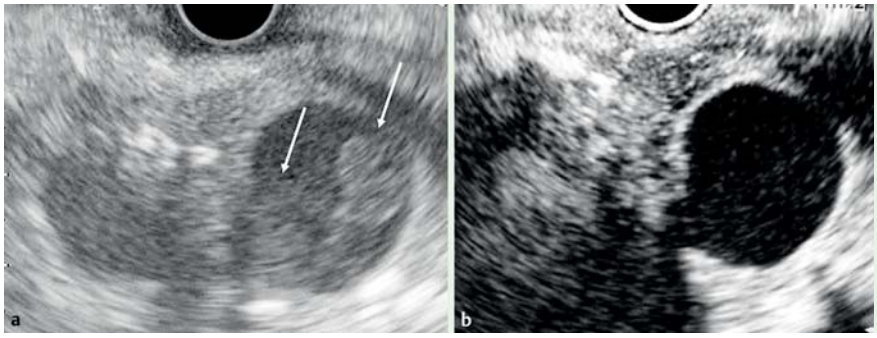

Fig. 3 A case of intrapapillary mucinous neoplasm (IPMN) with low grade dysplasia. **a** Fundamental B-mode endoscopic ultrasound (FB-EUS): a highly echoic structure is visible in the dilated branch duct (arrows). **b** Contrast-enhanced harmonic endoscopic ultrasound (CH-EUS): the lesions are not enhanced.

Statistical analysis

McNemar's test was used to compare the accuracies of FB-EUS and CH-EUS in the diagnosis of mucinous versus nonmucinous and malignant versus benign cysts. For interobserver agreement testing of FB-EUS and CH-EUS, kappa (κ) coefficients of > 0.8, > 0.6, and > 0.4 were considered to indicate excellent, good, and moderate agreement, respectively. The optimal cutoff value of mural nodule height for malignant cysts was derived from the point closest to the top left corner in the receiver operating characteristic (ROC). The difference between FB-EUS and CH-EUS in area under the ROC was evaluated using DeLong's test, which was performed using the R-3.0.3 software. All other analyses were performed using SAS 9.1.3 (SAS Institute, Cary, North Carolina, USA). Differences were considered to be significant when $P < 0.05$.

Table 1 Comparison of contrast-enhanced harmonic endoscopic ultrasound (CH-EUS) and fundamental B-mode endoscopic ultrasound (FB-EUS) for differential diagnosis of pancreatic cysts: patient characteristics and final diagnosis.

Sex (male/female), n/n	31/39
Age, mean (range), years	62 (37–82)
Cyst size, median (range), mm	33 (10–82)
Cyst location	
Head	30
Body/tail	40
Histology	
Mucinous cystic neoplasm (MCN)	6
Benign	4
Malignant*	2
Intraductal papillary mucinous neoplasm (IPMN) (branch-duct type)	42
Benign	14
Malignant*	28
Serous cystic neoplasm	4
Non-neoplastic cyst	18

* For the purpose of the study, both high grade dysplasia and invasive carcinoma were considered to be malignant.

Results

Demographic characteristics and the final pathologic diagnosis of the 70 patients included in the study are shown in **Table 1**. Following surgical resection, 6 MCNs, 42 branch duct IPMNs, 4 serous cystic neoplasms, and 18 non-neoplastic cysts were diagnosed. Of the MCNs, 2 were mucinous cystic adenocarcinomas and 4 were adenomas. Of the IPMNs, 14 were benign (low grade dysplasia 14) and 28 were malignant (high grade dysplasia 9, invasive carcinoma 19). Of the non-neoplastic cysts, 6 were epithelium-lined true cysts and 12 were pseudocysts associated with acute or relapsing chronic pancreatitis.

Comparison of FB-EUS and CH-EUS for identifying mural nodules

Overall, FB-EUS detected mural nodules in 53 of 70 pancreatic cystic lesions (76%) (namely, in 2 MCNs, 39 IPMNs, and 12 non-neoplastic cysts), whereas CH-EUS detected mural nodules in 39 of 70 cases (56%) (in 1 MCN, 37 IPMNs, and 1 non-neoplastic cyst).

Both methods were in agreement on the absence or presence of a mural nodule in 17 and 39 cases, respectively (**Fig. 2**, **Video 1**). There was discrepancy between FB-EUS and CH-EUS in 14 cases; these comprised 1 of 6 MCNs (17%), 11 of 18 non-neoplastic cysts (61%) and 2 of 42 IPMNs (5%) (**Fig. 3**, **Video 2**). In all of these cases, FB-EUS detected nodules that were subsequently not confirmed on CH-EUS.

Testing of interobserver agreement between the two readers for detecting mural nodules revealed good reproducibility for FB-EUS (κ coefficient 0.69, $P < 0.01$) and excellent reproducibility for CH-EUS (κ coefficient 0.83, $P < 0.01$).

FB-EUS and CH-EUS for diagnosing mucinous and malignant cysts

When the presence of a mural nodule was considered indicative of a mucinous cyst, CH-EUS tended to be more accurate than FB-EUS; however, there was no statistically significant difference (**Table 2**).

	FB-EUS		CH-EUS	
	Patients, n/n	% (95 %CI)	Patients, n/n	% (95 %CI)
Sensitivity	41/48	85 % (78 % – 92 %)	38/48	79 % (73 % – 81 %)
Specificity	10/22	46 % (30 % – 59 %)	21/22	96 % (82 % – 99 %)
PPV	41/53	77 % (71 % – 83 %)	38/39	97 % (90 % – 100 %)
NPV	10/17	59 % (39 % – 76 %)	21/31	68 % (58 % – 70 %)
Overall accuracy	51/70	73 %[2] (63 % – 81 %)	59/70	84 %[2] (76 % – 87 %)

Table 2 Mural nodule as a sign of mucinous cyst[1] on fundamental B-mode endoscopic ultrasound (FB-EUS) and contrast-enhanced harmonic endoscopic ultrasound (CH-EUS).

CI, confidence interval; PPV, positive predictive value; NPV, negative predictive value.
[1] Mucinous cysts included branch duct intraductal papillary mucinous neoplasms and mucinous cystic neoplasms
[2] $P = 0.057$ (McNemar's test).

When the presence of a mural nodule was considered indicative of a malignant cyst, CH-EUS was significantly more accurate than FB-EUS (**Table 3**). For diagnosis of malignant cysts, the optimal cutoff value of mural nodule height for was 8 mm for FB-EUS and 4 mm for CH-EUS. The presence of a mural nodule ≥ 8 mm in height on FB-EUS was a sign of malignancy with a false-positive fraction 0.3, true-positive fraction 0.87, and odds ratio 15.17. By contrast, the presence of a mural nodule ≥ 4 mm in height on CH-EUS was a sign of malignancy with a false-positive fraction 0.2, true-positive fraction 0.93, and odds ratio 56.0. The areas under the ROCs for FB-EUS and CH-EUS were 0.84 and 0.93, respectively ($P = 0.028$) (**Fig. 4**). This result suggested that CH-EUS was superior to FB-EUS in distinguishing between malignant and benign cysts.

Discussion

In this study, we assessed the abilities of FB-EUS and CH-EUS to diagnose mucinous versus nonmucinous and/or malignant versus nonmalignant pancreatic cysts by evaluation of mural nodules.

Mural nodules, visualized as projections of epithelial cells, are commonly detected in mucinous cysts but not in serous cystic neoplasms. In our study, most mucinous cysts were IPMNs and mural nodules were detected by EUS in most cases of IPMN. However, there was a discrepancy between FB-EUS and CH-EUS in detecting mural nodules in 1 of 6 MCNs (17 %), 11 of 18 non-neoplastic cysts (61 %) and 2 of 42 (5 %) IPMNs (**Fig. 3**, **Video 2**), indicating that FB-EUS often misinterprets images of mucus clots, necrotic tissue, or sludge as mural nodules. In the current study, the presence of mural nodules distinguished mucinous and/or malignant cysts from other cystic lesions. Relative to FB-EUS, CH-EUS improved the diagnosis of these cystic lesions by more accurately identifying mural nodules.

Video 1

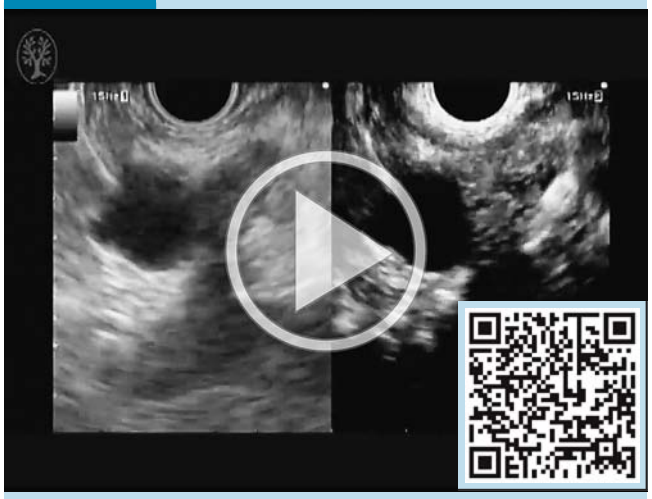

A side branch intrapapillary mucinous neoplasm (IPMN) with invasive carcinoma. Left panel: Fundamental B-mode endoscopic ultrasound (FB-EUS) image. Right panel: Contrast-enhanced harmonic endoscopic ultrasound (CH-EUS) image. Online content including video sequences viewable at: http://dx.doi.org/10.1055/s-0034-1393564

Video 2

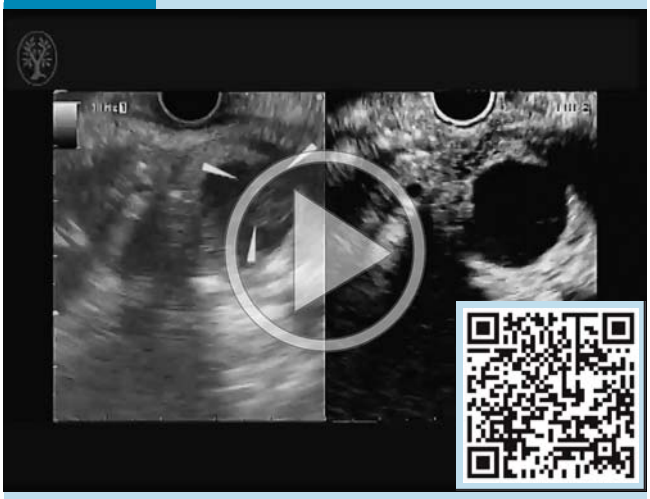

A case of intrapapillary mucinous neoplasm (IPMN) with low grade dysplasia. Left panel: Fundamental B-mode endoscopic ultrasound (FB-EUS) image. Right panel: Contrast-enhanced harmonic endoscopic ultrasound (CH-EUS) image. Online content including video sequences viewable at: http://dx.doi.org/10.1055/s-0034-1393564

	FB-EUS		CH-EUS	
	Patients, n/n	% (95%CI)	Patients, n/n	% (95%CI)
Sensitivity	29/30	97% (86%–99%)	29/30	97% (86%–99%)
Specificity	16/40	40% (32%–42%)	30/40	75% (67%–77%)
PPV	29/53	55% (49%–56%)	29/39	74% (66%–77%)
NPV	16/17	94% (76%–99%)	30/31	97% (87%–99%)
Overall accuracy	45/70	64%[2] (55%–67%)	59/70	84%[2] (75%–87%)

CI, confidence interval; PPV, positive predictive value; NPV, negative predictive value.
[1] Malignancy was defined as high grade dysplasia or invasive carcinoma.
[2] $P = 0.0001$ (McNemar's test).

Table 3 Mural nodule as a sign of malignant cyst[1] on fundamental B-mode endoscopic ultrasound (FB-EUS) and contrast-enhanced harmonic endoscopic ultrasound (CH-EUS).

Imaging information alone is often not sufficient to characterize pancreatic cystic lesions. In cases of diagnostic uncertainty, EUS-FNA may be valuable because of its ability to evaluate viscosity, cytology, chemistry, tumor markers, and molecular arrangement in the cyst fluid [14–25]. The American Society of Gastrointestinal Endoscopy and the International Association of Pancreatology support the use of EUS-FNA for diagnosing pancreatic cysts [24,25].

Surgical resection should be considered for pancreatic cystic lesions if a mural nodule is detected by CH-EUS, even if EUS-FNA does not show malignancy. In this way, the use of CH-EUS and EUS-FNA together may be useful for accurate diagnosis. In line with Japanese guidelines, we did not perform EUS-FNA in this study [12]. In addition, several studies have shown that IPMNs are frequently accompanied by carcinomas that are distinct from the IPMN both at the first medical examination and during follow-up [6,26–28], and such concomitant pancreatic carcinomas may develop even if the IPMN lesion is smaller than 15 mm [6]. Thus, evaluation of the whole pancreas with EUS followed by CH-EUS may be helpful for identifying these carcinomas. However, we did not evaluate concomitant pancreatic cancers that were separate from the cyst in this study. These cases were excluded from the study because the main purpose of surgery was resection of the concomitant pancreatic cancers, rather than the cystic lesions. The utility of CH-EUS for follow-up of pancreatic cystic lesions should be evaluated in a further prospective multicenter study.

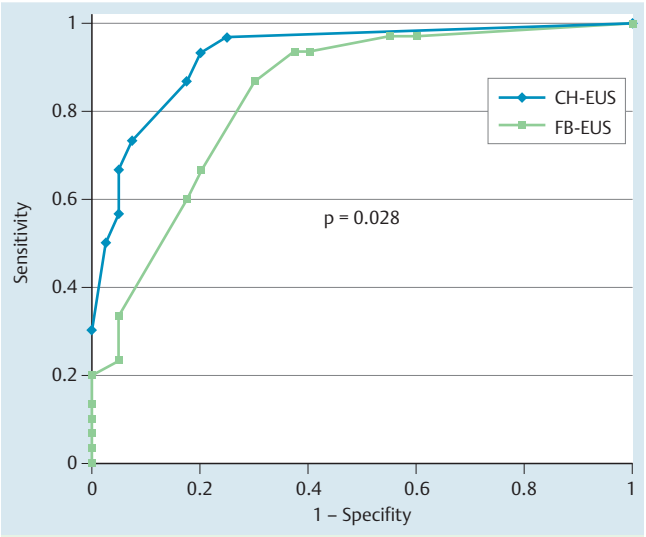

Fig. 4 The receiver operating characteristics (ROC) for the diagnosis of malignant cyst based on mural nodule height on fundamental B-mode endoscopic ultrasound (FB-EUS) and contrast-enhanced harmonic endoscopic ultrasound (CH-EUS).

Several studies have evaluated the presence or size of mural nodules with regard to diagnosis of malignant IPMN [29–35]. Anand et al. reported that the presence of a mural nodule was a predictor of malignancy with an odds ratio of 9.3 [29]. In another report, multivariate analysis revealed that the presence of a mural nodule was a good predictor of malignancy ($P = 0.002$) [30]. Kawada et al. measured mural nodule size by ultrasonography or EUS and reported that the odds ratio of mural nodules larger than 10 mm as a predictor of malignancy was 198 ($P < 0.0001$) and, when the results of cytology were considered in addition to those of mural nodule size, the sensitivity, specificity, and accuracy were 88%, 98%, and 97%, respectively [31]. Hirono et al. reported that a mural nodule of more than 5 mm in height was an independent factor associated with malignancy [32]. In the present study, detection of a mural nodule of height ≥ 8 mm (odds ratio 15.17) by FB-EUS or ≥ 4 mm (odds ratio 56.0) by CH-EUS indicated malignancy, and these results are similar to those of previous reports.

The present study is the first to compare CH-EUS with FB-EUS for diagnosis of pancreatic cystic lesions by evaluation of mural nodule height. CH-EUS identified mural nodules more accurately than FB-EUS. On the other hand, Ohno et al. classified mural nodule vascularity into four patterns using contrast-enhanced EUS, and reported that papillary and invasive nodule patterns are associated with malignancy [33]. Kurihara et al. also evaluated the vascularity of mural nodules of 10 mm or more and reported that a branch-shaped pattern was associated with carcinoma [34]. Several studies, including the present one, have reported that the presence and height of mural nodules are associated with malignancy of IPMNs. However, Koshida et al. have reported on flat-type IPMNs without mural nodules that had a higher recurrence rate and a poorer 5-year survival rate [35]. Therefore, during follow-up a focus may be needed on IPMNs without mural nodules.

This study has several limitations. The study was retrospective; however most of the data used for analysis were derived from prospectively collected databases. In addition, the pathological

diagnoses were verified by review of all resected specimens by expert pathologists. Verification bias cannot be excluded, because the FB-EUS and CH-EUS results might have influenced the decision regarding cyst resection. Only 70 patients with a solitary cyst who underwent surgical resection were enrolled in the study; 22 patients who underwent surgical resection were excluded because they either had multiple cysts, some of which differed in pathological features in individual patients, or had synchronous pancreatic carcinoma distinct from the cyst. For the purpose of the study cysts with high grade dysplasia as well as those with invasive carcinoma were considered to be malignant, and this may explain the high proportion of malignant branch-duct type IPMNs. The presence and height of mural nodules were analyzed in a subjective manner. There was potential bias resulting from the fact that the readers who assessed the FB-EUS and CH-EUS images might have known that there was high suspicion of malignancy in all patients included in the study because all of those patients underwent surgical resection. Moreover, the results of the analysis for the optimal cutoff value for mural nodule height were not validated. In this study, we did not perform EUS-FNA because we followed Japanese guidelines [12]; therefore, we could not compare CH-EUS with EUS-FNA for diagnosis of pancreatic cystic lesions. Further studies comparing the outcomes of CH-EUS and EUS-FNA would elucidate the utility of CH-EUS for managing pancreatic cystic lesions.

In conclusion, our study shows that, compared with FB-EUS, CH-EUS is better at discriminating mural nodules from mucus clots and more accurately distinguishes between malignant and benign pancreatic cysts. These advantages may help to reduce the number of unnecessary surgical procedures in patients with non-malignant cysts.

Competing interests: None

Institutions
[1] Department of Gastroenterology and Hepatology, Kinki University Faculty of Medicine, Osaka-sayama, Japan
[2] Department of Pathology, Kinki University Faculty of Medicine, Osaka-sayama, Japan
[3] Clinical Research Center, Kinki University Hospital, Osaka-sayama, Japan
[4] Department of Surgery, Kinki University Faculty of Medicine, Osaka-sayama, Japan

Acknowledgment

The present study was supported by grants from the Japan Society for the Promotion of Science.

References

1 *Scheiman JM, Hwang JH, Moayyedi P.* American Gastroenterological Association technical review on the diagnosis and management of asymptomatic neoplastic pancreatic cysts. Gastroenterology 2015; 148: 824 – 848
2 *Vege SS, Ziring B, Jain R* et al. American Gastroenterological Association Institute guidelines on the diagnosis and management of asymptomatic neoplastic pancreatic cysts. Gastroenterology 04 2015; 148: 819 – 822
3 *Brugge WR, Lewandrowski K, Lee-Lewandrowski E* et al. Diagnosis of pancreatic cystic neoplasms: a report of the cooperative pancreatic cyst study. Gastroenterology 2004; 126: 1330 – 1336
4 *Koito K, Namieno T, Nagakawa T* et al. Solitary cystic tumor of the pancreas: EUS-pathologic correlation. Gastrointest Endosc 1997; 45: 268 – 276
5 *Kubo H, Nakamura K, Itaba S* et al. Differential diagnosis of cystic tumors of the pancreas by endoscopic ultrasonography. Endoscopy 2009; 41: 684 – 689
6 *Kamata K, Kitano M, Kudo M* et al. Value of EUS in early detection of pancreatic ductal adenocarcinomas in patients with intraductal papillary mucinous neoplasms. Endoscopy 2014; 46: 22 – 29
7 *Kitano M, Sakamoto H, Matsui U* et al. A novel perfusion imaging technique of the pancreas: contrast-enhanced harmonic EUS (with video). Gastrointest Endosc 2008; 67: 141 – 150
8 *Sakamoto H, Kitano M, Suetomi Y* et al. Utility of contrast-enhanced endoscopic ultrasonography for diagnosis of small pancreatic carcinomas. Ultrasound Med Biol 2008; 34: 525 – 532
9 *Fusaroli P, Spada A, Mancino MG* et al. Contrast harmonic echo-endoscopic ultrasound improves accuracy in diagnosis of solid pancreatic masses. Clin Gastroenterol Hepatol 2010; 8: 629 – 634
10 *Napoleon B, Alvarez-Sanchez MV, Gincoul R* et al. Contrast-enhanced harmonic endoscopic ultrasound in solid lesions of the pancreas: results of a pilot study. Endoscopy 2010; 42: 564 – 70
11 *Kitano M, Kudo M, Yamao K* et al. Characterization of small solid tumors in the pancreas: the value of contrast-enhanced harmonic endoscopic ultrasonography. Am J Gastroenterol 2012; 107: 303 – 310
12 *Kitano M, Isayama H, Yamao K* eds. Gastroenterological endoscopy handbook. 1st edn. Nihon Medical Center. Tokyo: Japan Gastroenterological Endoscopy Society; 2012: 111 – 122
13 *Adsay NV, Fukushima N, Furukawa T* et al. Intraductal neoplasms of the pancreas. In: Bosman FT, Hruban RH Cameiro F et al., eds. WHO classification of tumors of the digestive system. WHO classification of tumors. 4th edn. Lyon: IARC; 2010: 304 – 313
14 *Samarasena JB, Nakai Y, Chang KJ* et al. Endoscopic ultrasonography-guided fine-needle aspiration of pancreatic cystic lesions: a practical approach to diagnosis and management. Gastrointest Endosc Clin N Am 2012; 22: 169 – 185
15 *Dal Molin M, Matthaei H, Wu J* et al. Clinicopathological correlates of activating GNAS mutations in intraductal papillary mucinous neoplasm (IPMN) of the pancreas. Ann Surg Oncol 2013; 20: 3802 – 3808
16 *Konda VJ, Meining A, Jamil LH* et al. A pilot study of in vivo identification of pancreatic cystic neoplasms with needle-based confocal laser endomicroscopy under endosonographic guideline. Endoscopy 2013; 45: 1006 – 1013
17 *Pitman MB, Genevay M, Yaeger K* et al. High-grade atypical epithelial cells in pancreatic mucinous cysts are more accurate predictor of malignancy than "positive" cytology. Cancer Cytopathol 2010; 118: 434 – 440
18 *Genevay M, Mino-Kenudson M, Yaeger K* et al. Cytology adds value to imaging studies for risk assessment of malignancy in pancreatic mucinous cysts. Ann Surg 2011; 254: 977 – 983
19 *Jacobson BC, Baron TH, Adler DG* et al. ASGE guideline: the role of endoscopy in the diagnosis and the management of cystic lesions and inflammatory fluid collections of the pancreas. Gastrointest Endosc 2005; 61: 363 – 370
20 *Tanaka M, Fernandez-del Castillo C, Adsay V* et al. International consensus guidelines 2012 for the management of IPMN and MCN of the pancreas. Pancreatology 2012; 12: 183 – 197
21 *Van der Waaij LA, van Dullemen HM, Porte RJ* et al. Cyst fluid analysis in the differential diagnosis of pancreatic cystic lesions: a pooled analysis. Gastrointest Endosc 2005; 62: 383 – 389
22 *Varadarajulu S, Mohamad A.* Eloubeidi. Frequency and significance of acute intracystic hemorrhage during EUS-FNA of cystic lesions of the pancreas. Gastrointest Endosc 2004; 60: 631 – 635
23 *O'Toole D, Palazzo L, Arotcarena R* et al. Assessment of complications of EUS-guided fine-needle aspiration. Gastrointest Endosc 2001; 53: 470 – 474
24 *Williams DB, Sahai AV, Aabakken L* et al. Endoscopic ultrasound guided fine needle aspiration biopsy: a large single centre experience. Gut 1999; 44: 720 – 726
25 *Walsh RM, Zuccaro G, Dumot JA* et al. Predicting success of endoscopic aspiration for suspected pancreatic cystic neoplasms. JOP 2008; 9: 612 – 617
26 *Yamaguchi k, Ohuchida J, Ohtsuka T* et al. Intraductal papillary-mucinous tumor of the pancreas concomitant with ductal carcinoma of the pancreas. Pancreatology 2002; 2: 484 – 490
27 *Uehara H, Nakaizumi A, Ishikawa O* et al. Development of ductal carcinoma of the pancreas during follow-up of branch duct intraductal papillary mucinous neoplasm of the pancreas. Gut 2008; 57: 1561 – 1565
28 *Tada M, Kawabe T, Arizumi M* et al. Pancreatic cancer in patients with pancreatic cystic lesions: a prospective study in 197 patients. Clin Gastroenterol Hepatol 2006; 4: 1265 – 1270

29 *Anand N*, *Sampath K*, *Wu BU* et al. Cyst features and risk of malignancy in intraductal papillary mucinous neoplasms of the pancreas: a meta-analysis. Clin Gastroenterol Hepatol 2013; 11: 913 – 921
30 *Akita H*, *Takeda Y*, *Hoshino H* et al. Mural nodule in branch duct-type intraductal papillary mucinous neoplasm of the pancreas is a marker of malignant transformation and indication for surgery. Am J Surg 2011; 202: 214 – 219
31 *Kawada N*, *Uehara H*, *Nagata S* et al. Predictors of malignancy in branch duct intraductal papillary mucinous neoplasm of the pancreas. JOP 2014; 15: 459 – 464
32 *Hirono S*, *Tani M*, *Kawai M* et al. The carcinoembryonic antigen level in pancreatic juice and mural nodule size are predictors of malignancy for branch duct type intraductal papillary mucinous neoplasm of the pancreas. Ann Surg 2012; 255: 517 – 522
33 *Ohno E*, *Hirooka Y*, *Itoh A* et al. Intraductal papillary mucinous neoplasms of the pancreas: differentiation of malignant and benign tumors by endoscopic ultrasound findings of mural nodules. Ann Surg 2009; 249: 628 – 634
34 *Kurihara N*, *Kawamoto H*, *Kobayashi Y* et al. Vascular patterns in nodules of intraductal papillary mucinous neoplasms depicted under contrast-enhanced ultrasonography are helpful for evaluating malignant potential. Eur J Radiol 2012; 81: 66 – 70
35 *Koshita S*, *Fujita N*, *Noda Y* et al. Invasive carcinoma derived from "flat type" branch duct intraductal papillary mucinous neoplasm of the pancreas: impact of classification according to the height of mural nodule on endoscopic ultrasonography. J Hepatobiliary Pancreat Sci 2015; 22: 301 – 319

Hepatology Research

Hepatology Research 2016; **46**: 3–9 doi: 10.1111/hepr.12542

Special Report

Response Evaluation Criteria in Cancer of the Liver (RECICL) (2015 Revised version)

Masatoshi Kudo, Kazuomi Ueshima, Shoji Kubo, Michiie Sakamoto, Masatoshi Tanaka, Iwao Ikai, Junji Furuse, Takamichi Murakami, Masumi Kadoya and Norihiro Kokudo, for the Liver Cancer Study Group of Japan

Committee for Response Evaluation Criteria in Cancer of the Liver, Liver Cancer Study Group of Japan, Department of Gastroenterology and Hepatology, Kinki University School of Medicine, Osaka-Sayama, Japan

The Response Evaluation Criteria in Solid Tumors (RECIST) is inappropriate to assess the direct effects of treatment on hepatocellular carcinoma (HCC) by locoregional therapies such as radiofrequency ablation (RFA) and transarterial chemoembolization (TACE). Therefore, establishment of response evaluation criteria solely devoted to HCC is needed urgently in clinical practice as well as in clinical trials of HCC treatment, such as molecular-targeted therapies, which cause necrosis of the tumor. The Response Evaluation Criteria in Cancer of the Liver (RECICL) was revised in 2015 by the Liver Cancer Study Group of Japan based on the 2009 version of RECICL, which was commonly used in Japan. Major revised points of the RECICL 2015 is to define the target lesions of two lesions per organ or three lesions per liver, up to a maximum of five lesions. The second revised point is that setting the timing at which the overall treatment response has been changed. The third point is that the definition of treatment effect 1 has been changed to more than 50% tumor enlargement, excluding the area of necrosis after treatment. Overall evaluation of treatment response has been amended to make it possible to evaluate the overall response including extrahepatic lesions by systemic therapy, which is similar to RECIST or modified RECIST. We hope this new treatment response criteria, RECICL, proposed by the Liver Cancer Study Group of Japan will benefit HCC treatment response evaluation in the setting of daily clinical practice and clinical trials, not only in Japan, but also internationally.

Key words: hepatocellular carcinoma, Liver Cancer Study Group of Japan, modified Response Evaluation Criteria in Solid Tumors, Response Evaluation Criteria in Cancer of the Liver, Response Evaluation Criteria in Solid Tumors

INTRODUCTION

THE FIRST VERSION of the Response Evaluation Criteria in Cancer of the Liver (RECICL) was compiled in October 1993 and published in a 1994 issue of *Kanzo*.[1] The revised versions of RECICL were subsequently published in *Kanzo* in 2004[2] and 2009[3] and have been used widely in routine clinical practice. As described in the 2004 RECICL and the version published in *Hepatology Research*,[4] the basic concepts of RECICL are that it: (i) is simple and sufficiently applicable in daily clinical practice; (ii) is internationally acceptable; (iii) is primarily for locoregional treatments (ethanol injection, microwave coagulation and radiofrequency ablation [RFA]) and transcatheter arterial therapy; (iv) is also applicable in radiation therapy and systemic chemotherapy as additional treatment methods; (v) provides separate criteria for the assessment of direct treatment effects on intrahepatic target lesions and overall response; and (vi) complies with the sixth edition of the General Rules for the Clinical and Pathological Study of Primary Liver Cancer.[10] However, because the 2009 version was not applicable in all clinical cases following the introduction of molecular-targeted therapy as a systemic chemotherapy for hepatocellular carcinoma (HCC), we recently revised RECICL for the fourth time. The revision process this time is in line with the concepts used for the 2009 version but includes relatively extensive revision of the definition of treatment effect 1 (TE1) and the assessment of overall response.

In Europe, the World Health Organization (WHO) Handbook for Reporting Results of Cancer Treatment in Solid Tumors (hereinafter the WHO criteria)[5] and Response Evaluation Criteria in Solid Tumors (RECIST, version 1.0)[6] have been used conventionally to assess treatment response in

Correspondence: Dr Masatoshi Kudo, Liver Cancer Study Group of Japan, Department of Gastroenterology and Hepatology, Kinki University School of Medicine, 377-2 Ohno-Higashi, Osaka-Sayama, Osaka 589-8511, Japan. Email: m-kudo@med.kindai.ac.jp
Received 11 March 2015; revision 26 May 2015; accepted 31 May 2015

HCC. RECIST 1.0 was simplified further, and version 1.1[7] is used widely today. However, the WHO criteria and RECIST are both inappropriate for the assessment of direct treatment effects on the target HCC lesion because they use only tumor size reduction as the criterion for treatment effect and do not recognize tumor necrosis as a treatment effect even though the necrosis of HCC is frequently caused by various locoregional treatments. For example, it has been shown that pathological necrosis does not correlate with tumor size reduction assessed by the WHO criteria and RECIST after transarterial chemoembolization (TACE) using lipiodol.[8] For this reason, establishing response evaluation criteria that take into consideration the necrosis of HCC is urgently needed. In 2010, Lencioni *et al.* proposed a modified version of RECIST (mRECIST) that incorporates the necrosis of tumors as a treatment effect into RECIST 1.0 to make the appropriate criteria for HCC.[9] However, the criteria used to evaluate necrosis lack accuracy because unidirectional measurements were used. On the other hand, since the 1990s, tumor necrosis has been assessed using bidirectional measurements to improve the accuracy of treatment response evaluation in RECICL. Therefore, RECICL may be more specific to HCC. In recent years, treatment methods for HCC have changed greatly because of the adoption of molecular-targeted agents. Unlike cytotoxic anticancer drugs, molecular-targeted agents cause not only size reduction but also necrosis in tumors due to their antiangiogenic property. In other words, there is a greater need to establish proper evaluation criteria for tumor necrosis. In the 2009 version, the response evaluation criteria for systemic chemotherapy were supplemented by RECIST. In this revision, RECICL was modified to be all-in-one evaluation criteria that are applicable to all treatment methods by incorporating the overall evaluation criteria of RECIST. RECICL is now applicable to extrahepatic lesions and its features that are specific to HCC remain.

The high incidence of multicentric tumors and of intrahepatic recurrence and metastasis is a biological feature specific to HCC and not to other types of cancer. Consequently, it is not always appropriate to interpret the appearance of a new intrahepatic lesion in the untreated area in the liver as progressive disease (PD). The major goal of RECICL is that it focuses only on the efficacy of various treatment methods (locoregional treatments) for target lesions, and also correlates the treatment effects with prognosis as much as possible in assessing the overall response. This is different from RECIST, which is used to assess the efficacy of one particular therapy. With RECIST, when current therapy is considered ineffective when PD is diagnosed, changing to another treatment method may be considered. Unlike systemic chemotherapy, treatment by transcatheter arterial therapy or ablation therapy is not performed throughout the liver and therefore does not affect newly developed lesions in untreated areas of the liver. In other words, when the latter therapies are repeated for new target lesions, the treatment response of the new lesions is expected to be the same as that observed in previous target lesions. Therefore, even if a new target lesion (i.e. multicentric lesion) appears in a different area, it should neither represent an indication for changing the treatment method nor be used to determine prognosis. This point should be considered when evaluating treatment response in HCC, and RECICL provides the evaluation criteria that fully consider these specific characteristics of HCC.

MAJOR REVISED POINTS IN THE 2015 VERSION OF RECICL (TABLE 1)

1. Up until the 2009 version of RECICL, tumor enlargement of 25% or more was defined as TE1 and was treated as PD. However, a bidirectional enlargement of 25% is roughly equivalent to a unidirectional enlargement of 11% and is a stricter criterion than the definition of 20% enlargement for PD in RECIST 1.1. This 20% unidirectional enlargement in RECIST 1.1 would be equal to a 44% bidirectional enlargement ($1.2 \times 1.2 = 1.44$ times). In this revision, we used an enlargement of 50% as the criterion for TE1 because of its consistency with RECIST and its usability in clinical settings (Table 2).
2. Up until the 2009 version, lesions subject to evaluation (target lesions) were intrahepatic lesions, and when multiple intrahepatic lesions are present, five lesions from largest to smallest were selected as target lesions. However, in accordance with RECIST 1.1, two lesions per organ and a maximum of five lesions in total will be determined as target lesions in the 2015 version. If three or more intrahepatic lesions are present, a maximum of three lesions should be counted as target lesions to comply with the criterion of three or less lesions that are 3 cm or less in the Milan criteria and as an indication for ablation therapy.
3. In the 2015 version, it was clearly stated that response to locoregional treatments should be assessed 1–3 months after completion of therapy or at the last treatment if a series of treatments were given. In chemotherapy (including hepatic arterial infusion), treatment response should be assessed 1–3 months after the first administration of the anticancer agents. If the therapy is ongoing, the assessment should be repeated every 1–3 months. The efficacy of radiation therapy is

Table 1 Differences between Response Evaluation Criteria in Cancer of the Liver (RECICL) 2009 and 2015 versions

	RECICL 2009 version	RECICL 2015 version
Target lesions	Intrahepatic lesions only Maximum of five intrahepatic lesions	Intrahepatic and extrahepatic lesions Two lesions per organ or three lesions per liver, up to a maximum of five lesions
Measurement direction	Bidirectional	(same as 2009 version)
Measurement method	Assess the cross-sectional area of the tumor by multiplying the major axis of the maximum cross-section and the maximum diameter crossing the major axis at a right angle. However, the unstained region and the region of lipiodol accumulation without washout are regarded as necrotized regions.	(same as 2009 version) (same as 2009 version)
Time for evaluation	Immediately after ablation therapy One month or more after TACE or hepatic arterial infusion chemotherapy Six months or less after radiation therapy	One to three months after ablation therapy One to three months after TACE or hepatic arterial infusion chemotherapy (same as 2009 version)
Treatment response of target lesions (treatment effect [TE])		
TE4	Tumor necrosis of 100% or 100% reduction in tumor size	(same as 2009 version)
TE4a	Necrotized area larger than an original tumor (enough ablative margin)	(same as 2009 version)
TE4b	Necrotized area similar in size to an original tumor (insufficient ablative margin)	(same as 2009 version)
TE3	Tumor necrosis of 50–100% or 50–100% reduction in tumor size	(same as 2009 version)
TE2	Effect other than TE3 or TE1	(same as 2009 version)
TE1	Tumor enlargement of >25% regardless of necrosis	Tumor enlargement of >50% (excluding the area of necrosis after treatment)

assessed based on the best treatment response observed during the 6 months of therapy after treatment initiation.

4 Although the evaluation criteria for overall treatment response were supplemented by RECIST in the RECICL 2009 version, we developed new evaluation criteria in line with RECIST 1.1 for the 2015 version. For new lesions that developed after ablation therapy or transarterial chemoembolization, it is important to describe whether the new lesion is (i) inside or (ii) outside the previously treated area to make the information useful in future revisions of the current criteria.

FULL TEXT OF RESPONSE EVALUATION CRITERIA IN CANCER OF THE LIVER

Subjects

SUBJECTS ARE PATIENTS who are treated for the primary lesion and for recurrence. As a rule, contrast-enhanced computed tomography (CT) is performed to assess treatment response in RECICL, the principle targets in the assessment should be clearly visualized on the images, and should be hypervascular in intrahepatic and extrahepatic lesions.

Among all measurable lesions, two lesions per organ and a maximum of five lesions in total are defined as target lesions. If there are three or more lesions in the liver, three nodules should be included in the target lesions. The area of individual target lesions is calculated by multiplying the length of the major axis by the maximum diameter crossing the major axis at a right angle, and the sum of the areas in all target lesions is used as the baseline area. All the remaining lesions are regarded as non-target lesions.

Detailed description

Description of past medical history

1 Methods and date when the definitive diagnosis of HCC was made.

Table 2 Assessment of direct treatment effect on target lesions

Treatment effect (TE)	
TE4	Tumor necrosis of 100% or 100% reduction in tumor size TE4a: necrotized area larger than the original tumor (sufficient ablative margin) TE4b: necrotized area similar in size to the original tumor (insufficient ablative margin)
TE3	Tumor necrosis of 50–100% or 50–100% reduction in tumor size
TE2	Effect other than TE3 or TE1
TE1	Tumor enlargement of ≥50% (excluding the area of necrosis after treatment)

A unidirectional enlargement of 20%, which is defined as progressive disease in RECIST 1.1, is equivalent to a bidirectional enlargement of 44% (1.2 × 1.2 = 1.44 times). Therefore, in the new version, the enlargement of a tumor by 50% is defined as TE1 to be consistent with internationally accepted criteria, RECIST and to be easy to use in the clinical setting.

2 Previous treatment modality (as described in "Description of treatment modalities").
3 Dates of initiation and completion of previous treatment.
4 Methods and date when recurrence was diagnosed.

Descriptions of HCC at the time of treatment initiation

In accordance with the sixth edition of the General Rules for the Clinical and Pathological Study of Primary Liver Cancer (edited by Liver Cancer Study Group of Japan),[10] the descriptions should include the following items:

1 Tumor location.
2 Tumor size, number and vascular invasion. The tumor size is presented as the major axis and maximum diameter crossing the major axis at a right angle.
3 Macroscopic classification.
4 Tumor stage (tumor–node–metastasis [TNM]). Even for tumors that are only assessable by imaging, TNM staging should be described similar to surgical findings and those of the resected specimen.
5 Histological classification or differentiation.

Description of treatment modalities

1 Treatment names: transarterial therapy (hepatic arterial infusion chemotherapy, transarterial embolization [TAE], and transarterial chemoembolization [TACE], and local ablation treatments such as percutaneous ethanol injection, microwave coagulation, and radiofrequency ablation [RFA]); radiation therapy; and systemic chemotherapy (including molecular targeted therapy)
2 Treatment details: for treatments using drugs, the name of the drugs* (anticancer drugs, lipiodol, etc.), route of administration, treatment interval, dose, total number of administrations, and total dose should be described. For other treatment methods, the details should be described appropriately. When the treatment is discontinued, the reason for discontinuation and the presence or absence of adverse effects should be described.
*Chemotherapeutic agents, any agent directly injected into the tumor to induce necrosis such as ethanol, and/or embolization material used in transarterial chemoembolization should be described.
3 Dates of initiation and completion or termination of each treatment.

Assessment of direct treatment effect on the target lesion

1 To assess the treatment effect on the target nodule, the tumor-necrotizing effect or the rate of tumor size reduction are calculated based on the size reduction or disappearance of arterial enhancement of the nodule on dynamic contrast-enhanced CT. In the assessment, the findings of dynamic magnetic resonance imaging (MRI) or contrast-enhanced ultrasonography (US) can substitute the findings of dynamic contrast-enhanced CT.
2 The necrotizing effect is assessed by diagnostic imaging. The percent ratio of the necrotized area to the cross-sectional area of the tumor should be calculated.*
*When various cross-sections are obtained for a single tumor, the total sum of the necrotic areas should be used; however, when the maximum cross-section represents the entire findings of the tumor, assessment could be based on the maximum cross-sectional area.
3 The size reduction rate is calculated using the equation below after calculating the size by multiplying the major axis of the maximum cross-section by the maximum diameter crossing the major axis at a right angle:

$$\text{Size reduction rate} = ([\text{size before treatment}] - [\text{size after treatment}])/(\text{size before treatment}) \times 100$$

4 Target nodule treatment response (treatment effect [TE]). Effects on individual lesions are categorized into four categories based on tumor size reduction observed within a

predetermined period* after initiation of treatment or the maximum tumor-necrotizing effect.** As shown in Table 2, TE4 is equivalent to a complete response (CR) and is defined as 100% tumor-necrotizing effect or 100% tumor size reduction. TE3 is equivalent to partial response (PR) and defined as 50–100% tumor-necrotizing effect or 50–100% tumor size reduction. TE2 is regarded as stable disease (SD) if the effect is neither PR nor PD. TE1 corresponds to PD with an increase in tumor size of 50% or more,*** excluding the area of treatment-induced necrosis.

*Treatment effects are assessed 1–3 months after local ablation treatments (percutaneous ethanol injection, microwave coagulation and RFA), hepatic arterial infusion chemotherapy with or without lipiodol, TAE, TACE or systemic chemotherapy. When a series of treatments are performed, the effects should be also assessed 1–3 months after completion of the last treatment. The effect of radiation therapy is assessed using the best response observed during the 6 months after treatment initiation.

**For local ablation treatments, when the non-stained, low-density area is wider across the entire circumference than the low-density area in the late phase of pretreatment CT scan (sufficient ablative margin), the lesion is regarded as 100% necrotized (TE4a). Although the ideal sufficient ablative margin is more than 5 mm from an edge around the tumor, presence of a smaller sized non-stained area of 5 mm can be regarded as a sufficient margin in this criteria. The disappearance of hypervascularity alone with the lack of a wider non-stained region compared with the low-density area on CT scan is judged as TE4b (insufficient ablative margin). The effect of TAE or TACE is judged as 100% tumor-necrotizing effect (TE4) when the following findings are present: (i) complete tumor disappearance; (ii) lack of tumor hypervascularity on contrast-enhanced CT; (iii) strongly dense lipiodol accumulations; or (iv) shrinkage of lipiodol-accumulated areas across the lesion when lipiodol is used. The effect of radiation therapy is also evaluated using the criteria for necrotizing effects when tumor necrosis is observed.

***Up until the 2009 version of RECICL, tumor enlargement of 25% or more was defined as TE1 and was treated as PD. However, a bidirectional enlargement of 25% is roughly equivalent to a unidirectional enlargement of 11%, and is stricter than the PD criterion of 20% enlargement in RECIST 1.1. To ensure consistency with RECIST 1.1, a unidirectional enlargement of 20% will be equivalent to a bidirectional enlargement of 44% ($1.2 \times 1.2 = 1.44$ times). Therefore, in the 2015 version of RECICL, a 50% enlargement in tumor size is used as the criterion for TE1 because treatment is continued in most patients with PD based on RECIST and because of the usability in clinical settings.

5 When multiple intrahepatic lesions are present, the treatment effect on target nodules is assessed individually for up to a maximum of three lesions.

Overall evaluation of treatment response

1 From the perspective of intrahepatic and extrahepatic treatment effects and the duration of treatment effects, overall treatment response is assessed based on the four-grade system using CR, PR, SD and PD, as shown in Table 3.

2 To use this method to predict the prognosis, TE is determined and recorded at 1–3 months after treatment initiation to assess overall response. However, the effect of radiation therapy is assessed based on the maximum effect observed within 6 months of treatment initiation.

3 Definition of new lesions. In dynamic CT, dynamic MRI (including gadoxetic acid-enhanced magnetic resonance imaging [Gd-EOB-MRI]) and Sonazoid-enhanced US, new intrahepatic lesions are typically observed as hypervascularity in the early phase and washout in the late phase (low-intense nodules on Gd-EOB-MRI hepatocyte phase images or Kupffer defect on Sonazoid-enhanced US images). As a rule, new intrahepatic lesions should be nodules of 10 mm or more. When a new intrahepatic lesion appears after ablation therapy or TACE, it is important to determine whether the location is inside or outside the previously treated area. Extrahepatic lesions should be nodules of 10 mm or more, and lymph nodes with a minor axis of 15 mm or more are regarded as lymph node metastasis.

Table 3 Overall response (evaluation based on the maximum response obtained over a period of 1–3 months or within 6 months in case of radiation therapy)

Target lesions	Non-target lesions	New lesions	Overall response
TE4	TE4	No	CR
TE4	TE3, TE2	No	PR
TE3	Non-TE1	No	PR
TE2	Non-TE1	No	SD
TE1	Any	Yes or no	PD
Any	TE1	Yes or no	PD
Any	Any	Yes	PD

CR, complete response; PD, progressive disease; PR, partial response; SD, stable disease; TE, treatment effect.

Table 4 Reference table for the assessment of treatment effect in liver cancer

Patient	Age	Sex: M or F	ID:		
1. Description of liver cancer					
(1) Medical history					
	Date of definitive diagnosis				
(2) Characteristics of liver cancer					
	Tumor location, number, size, vascular invasion				
	Macroscopic stage				
2. Description of liver cancer					
(1) Treatment for original lesion or recurrence					
(2) Treatment modality (multiple modalities in case of combined therapy)					
(3) Treatment details *If terminated, describe the reason for termination					
(4) Adverse events					
(5) Dates of initiation and completion or termination					
3. Treatment effect on target nodule (TE1, 2, 3, or 4)					
			Assessment results:	Lesion 1 ( )	
Refer to Table 1				Lesion 2 ( )	
(Include 4a and 4b for the assessment of ablation therapy)				Lesion 3 ( )	
				Lesion 4 ( )	
				Lesion 5 ( )	
4. Overall evaluation (CR, PR, SD, PD)			Assessment results:		
Refer to Table 3					
			Appearance of a new lesion after locoregional therapy or TACE		
			a. Inside the previously treated area		
			b. Outside the previously treated area		
Appendix:					

Tumor markers	Before treatment (Time)	Lowest value within 3 months	Within 6 months (radiation therapy only)
AFP	( )	( )	( )
AFP-L3 fraction	( )	( )	( )
PIVKA-II (DCP)	( )	( )	( )

AFP, α-fetoprotein; AFP-L3, *Lens culinaris* agglutinin-reactive fraction of AFP; CR, complete response; DCP, des-γ-carboxyprothrombin; PD, progressive disease; PIVKA-II, protein induced by vitamin K absence/antagonist-II; PR, partial response; SD, stable disease.

Detailed criteria

Necrotizing effects are assessed in accordance with the response evaluation criteria for the treatment of a target nodule.

1 The presence of a non-enhancing area corresponding to the original nodule after treatment on dynamic contrast-enhanced CT using an i.v. bolus injection is regarded as a necrotizing effect. Such non-stained, low-density areas are enhanced less intensely than

the surrounding liver parenchyma in the early and late phases.* In other words, the CT attenuation value of a non-stained, low-density area does not change due to contrast enhancement.

***The early phase of contrast-enhanced CT using a bolus injection represents the hepatic arterial dominant phase, whereas the late phase represents the equilibrium phase.

2 When lipiodol is used, the presence of a region retaining lipiodol homogeneously and densely in the tumor on CT images taken 1 month after therapy is regarded as a necrotizing area. Contrast-enhanced MRI or contrast-enhanced US can be used as an alternative.

3 The lowest levels of three tumor markers (α-fetoprotein [AFP], protein induced by vitamin K absence/antagonist-II and Lens culinaris agglutinin-reactive fraction of AFP) within 3 months (6 months in the case of radiation therapy) described in the sixth revised edition of the General Rules for the Clinical and Pathological Study of Primary Liver Cancer[10] should be recorded as reference values for the overall response evaluation (Table 4).

REFERENCES

1 Liver Cancer Study Group of Japan. Response evaluation criteria in cancer of the liver. *Kanzo* 1994; **35** (2): 193–205. (in Japanese)

2 Liver Cancer Study Group of Japan. Response evaluation criteria in cancer of the liver. *Kanzo* 2004; **45** (7): 380–5. (in Japanese)

3 Kudo M, Kubo S, Takayasu K *et al.* Liver cancer study group of Japan, response evaluation criteria in cancer of the liver (2009 revised version). *Kanzo* 2010; **51** (5): 261–6. (in Japanese)

4 Kudo M, Kubo S, Takayasu K, *et al.* Response evaluation criteria in cancer of the liver (RECICL) proposed by the Liver Cancer Study Group of Japan (2009 revised version). *Hepatol Res* 2010 **40**(7): 686–92.

5 WHO. Handbook for Reporting Results of Cancer Treatment.: Geneva, SwitzerlandWorld Health Organization Offset Publication, 1979.

6 Therasse P, Arbuck SG, Eisenhauer EA, *et al.* New guidelines to evaluate the response to treatment in solid tumors. European Organization for Research and Treatment of Cancer, National Cancer Institute of the United States, National Cancer Institute of Canada. *J Natl Cancer Inst* 2000 **92**(3): 205–16.

7 Eisenhauer EA, Therasse P, Bogaerts J, *et al.* New response evaluation criteria in solid tumours: revised RECIST guideline (version 1.1). *Eur J Cancer* 2009 **45**(2): 228–47.

8 Takayasu K, Arii S, Matsuo N, *et al.* Comparison of CT findings with resected specimens after chemoembolization with iodized oil for hepatocellular carcinoma. *AJR Am J Roentgenol* 2000 **175**(3): 699–704.

9 Lencioni R, Llovet JM. Modified RECIST (mRECIST) assessment for hepatocellular carcinoma. *Semin Liver Dis* 2010 **30**(1): 52–60.

10 Liver Cancer Study Group of Japan. General Rules for the Clinical and Pathological Study of Primary Liver Cancer, 6th revised edn. Tokyo: Liver Cancer Study Group of Japan, Kanehara & Co., 2015. (in Japanese)

J Gastroenterol (2016) 51:144–152
DOI 10.1007/s00535-015-1094-8

The Japanese Society of Gastroenterology

ORIGINAL ARTICLE—LIVER, PANCREAS, AND BILIARY TRACT

Kupffer phase image of Sonazoid-enhanced US is useful in predicting a hypervascularization of non-hypervascular hypointense hepatic lesions detected on Gd-EOB-DTPA-enhanced MRI: a multicenter retrospective study

Tatsuo Inoue[1] · Tomoko Hyodo[2] · Keiko Korenaga[3,4] · Takamichi Murakami[2] · Yasuharu Imai[5] · Atsushi Higaki[3] · Takeshi Suda[6] · Toru Takano[7] · Kennichi Miyoshi[8] · Masahiko Koda[8] · Hironori Tanaka[9,10] · Hiroko Iijima[9] · Hironori Ochi[11] · Masashi Hirooka[11] · Kazushi Numata[12] · Masatoshi Kudo[1]

Received: 26 August 2014 / Accepted: 6 June 2015 / Published online: 15 September 2015

Abstract

Background It remains unknown whether Kupffer-phase images in Sonazoid-enhanced ultrasonography (US) can be used to predict hypervascularization of borderline lesions. Therefore, we aimed to clarify whether Kupffer-phase images in Sonazoid-enhanced ultrasonography can predict subsequent hypervascularization in hypovascular borderline lesions detected on hepatobiliary-phase gadolinium-ethoxybenzyl-diethylenetriamine pentaacetic acid (Gd-EOB-DTPA)-enhanced magnetic resonance imaging.

Methods From January 2008 to March 2012, 616 low-intensity hypovascular nodules were detected in hepatobiliary-phase images of Gd-EOB-DTPA-enhanced MRI at nine institutions. Among these, 167 nodules, which were confirmed as hypovascular by Gd-EOB-DTPA-enhanced MRI and Sonazoid-enhanced US, were evaluated in this study. Potential hypervascularization factors were selected based on their clinical significance and the results of previous reports. The Kaplan–Meier model and log-rank test were used for univariate analysis and the Cox regression model was used for multivariate analysis.

Results The cumulative incidence of hypervascularization of borderline lesions was 18, 37, and 43 % at 1, 2, and 3 years, respectively. Univariate analyses showed that tumor size ($p = 0.0012$) and hypoperfusion on Kupffer-phase images in Sonazoid-enhanced US ($p = 0.004$) were associated with hypervascularization of the tumor. Multivariate analysis showed that tumor size [HR: 1.086, 95 %

✉ Tatsuo Inoue
tatsuoinouejp@yahoo.co.jp

Masatoshi Kudo
m-kudo@med.kindai.ac.jp

1 Department of Gastroenterology and Hepatology, Kinki University School of Medicine, 377-2, Ohno-Higashi, Osaka-Sayama 589-8511, Osaka, Japan

2 Department of Diagnostic Radiology, Kinki University School of Medicine, 377-2, Ohno-Higashi, Osaka-Sayama 589-8511, Osaka, Japan

3 Department of Hepatology and Pancreatology, Kawasaki Medical School, Kurashiki, Japan

4 Department of Gastroenterology and Hepatology, Kohnodai Hospital, National Center for Global Health and Medicine, Chiba, Japan

5 Department of Gastroenterology, Ikeda Municipal Hospital, Osaka, Japan

6 Division of Gastroenterology and Hepatology, Graduate School of Medical and Dental Sciences, Niigata University, Niigata, Japan

7 Division of Radiation Oncology, Graduate School of Medical and Dental Sciences, Niigata University, Niigata, Japan

8 Division of Medicine and Clinical Science, Department of Multidisciplinary Internal Medicine, Tottori University, Tottori, Japan

9 Ultrasound Imaging Center, Hyogo College of Medicine, Nishinomiya, Japan

10 Division of Hepatobiliary and Pancreatic Disease, Department of Internal Medicine, Hyogo College of Medicine, Nishinomiya, Japan

11 Department of Gastroenterology and Metabology, Ehime University Graduate School of Medicine, Matsuyama, Japan

12 Gastroenterological Center, Yokohama City University Medical Center, Yokohama, Japan

confidence interval = 1.027−1.148, $p = 0.004$] and hypo perfusion on Kupffer-phase images [HR: 3.684, 95 % confidence interval = 1.798−7.546, $p = 0.0004$] were significantly different.
Conclusions Kupffer-phase images in Sonazoid-enhanced US and tumor diameter can predict hypervascularization of hypointense borderline lesions detected on hepatobiliary-phase Gd-EOB-DTPA-enhanced MRI.

Keywords Kupffer phase · Sonazoid-enhanced ultrasonography · Gadolinium ethoxybenzyl-diethylenetriamine-pentaacetic acid-enhanced MRI · Hepatocellular carcinoma · Hypervascular transformation

Abbreviations

HCC	Hepatocellular carcinoma
US	Ultrasonography
CT	Dynamic computed tomography
MRI	Magnetic resonance imaging
DNs	Dysplastic nodules
Gd-EOB-DTPA	Gadolinium ethoxybenzyl diethylenetriamine pentaacetic acid
T2WI	T2-weigthed images
CTHA	CT during hepatic arteriography
HRs	Hazard ratios
CIs	Confidence intervals
CTAP	CT during arterial portography

Introduction

Hepatocellular carcinoma (HCC) is one of the most common cancers worldwide and is a major cause of death in patients with cirrhosis.

Recent advances in imaging modalities and periodic follow-up of chronic liver disease, particularly cirrhosis, with ultrasonography (US), dynamic computed tomography (CT), magnetic resonance imaging (MRI), or measurement of tumor markers, have aided in the detection of small, early stage HCC including early HCC, low-grade dysplastic nodules (DNs), and high-grade DNs. The majority of these lesions are hypovascular because these nodules lacking hypervascularity in the arterial phase on imaging modalities and are called borderline lesions [1, 2]. A hepatocyte-specific contrast agent, gadolinium ethoxybenzyl diethylenetriamine pentaacetic acid (Gd-EOB-DTPA) (Primovist®), has unique pharmacodynamics: it is taken up by hepatocytes and subsequently excreted into the bile ducts [3]. Several previous studies showed a significant correlation between the expression level of organic anion transporting polypeptide 1B3 and enhancement ratio in HCCs in hepatobiliary-phase images of Gd-EOB-DTPA-enhanced MR [4–7]. Kogita et al. reported that reduction in Gd-EOB-DTPA uptake might be an early event of hepatocarcinogenesis that occurs before portal blood flow reduction [8]. In fact, the detection of premalignant/borderline lesions, which are difficult to detect on the basis of intratumoral hemodynamic changes, has improved dramatically with the use of Gd-EOB-DTPA-enhanced MRI [9–11]. It is important to identify the borderline lesions that are at risk of hypervascularization. Previous studies have revealed that tumor size, tumor growth rate, presence of fat, and hyperintensity on T1- and T2-weighted images indicate a high probability of hypervascularization of borderline lesions [12–20].

Sonazoid is a second-generation sonographic contrast agent that consists of perfluorobutane gas microbubbles with phospholipid monolayer shells. In addition to a real-time fine vascular image in the vascular phase [21–24], Sonazoid is phagocytosed by Kupffer cells in the liver after administration, which enables persistent and stable enhancement image, called Kupffer-phase imaging. Kupffer-phase imaging is typically performed 10 min after Sonazoid injection, at which time the normal hepatic parenchyma is enhanced, and malignant lesions that contain few or no Kupffer cells are clearly delineated as contrast defects. A few studies have suggested a relationship between enhancement patterns of the Kupffer phase in Sonazoid-enhanced US and histological grading of HCC [25, 26].

Ohama et al. reported a correlation between the hepatobiliary-phase image of Gd-EOB-DTPA-enhanced MR and the Kupffer-phase image in Sonazoid-enhanced US [27]. They concluded that the uptake of Sonazoid begins to decrease later than that of Gd-EOB-DTPA in stepwise hepatocarcinogenesis of borderline lesions. Gd-EOB-DTPA-enhanced MRI can be used to detect many borderline lesions; however, repeated MRI examinations are not suitable because of their cost and severe side effects, such as anaphylactic shock and nephrogenic systemic fibrosis although the onset of severe side effects rarely occurs if subjects are carefully selected [28]. In clinical practice, it is important to evaluate the risk of hypervascularization of borderline lesions by using cost-effective and safe methods. Therefore, we hypothesized that the Kupffer-phase image in Sonazoid-enhanced US could be evaluated to predict hypervascularization of borderline lesions. Thus far, no study has reported the usefulness of Kupffer-phase images in Sonazoid-enhanced US for prediction of hypervascularization of borderline lesions. Therefore, the aim of our study was to evaluate whether the Kupffer-phase image in Sonazoid-enhanced US can be used to predict subsequent hypervascularization in non-hyper borderline lesions detected in the hepatobiliary-phase image of Gd-EOB-DTPA-enhanced MR.

Methods

Patients

The selection of the study population is presented in a flow chart (Fig. 1). In the present study, Gd-EOB-DTPA MR was performed for routine examination or evaluation of a nodule detected by B-mode US. Sonazoid-enhanced US was performed to reevaluate tumor vascularity in the vascular phase and to evaluate uptake of Sonazoid in the Kupffer-phase detected as low intense in the hepatobiliary-phase image of Gd-EOB-DTPA-enhanced MR. Between February 2008 and March 2011, 616 hypovascular nodules with low intensity in hepatobiliary-phase images of Gd-EOB-DTPA-enhanced MR were recruited from nine institutions that participated in the present study. Of these, we excluded patients with Child-Pugh class C because of insufficient enhancement on MR imaging [29]; in addition, 214 patients who did not undergo Sonazoid-US were excluded. Finally, 112 patients with 167 hepatic nodules that were diagnosed as hypovascular hepatic nodules on Gd-EOB-DTPA-enhanced MR and Sonazoid-enhanced US were evaluated in the present study. The baseline characteristics of the patients are shown in Table 1. Our retrospective study design was approved by the institutional review board of Kinki University Faculty of Medicine. The requirement to obtain informed consent was waived.

Image analysis

All images were interpreted independently by an experienced board of certified radiologists, sonologists, and gastroenterologists at each institution who were aware that the patients were at risk for HCC but had no other clinical information. Discrepancies between the readers were resolved by discussion to reach consensus.

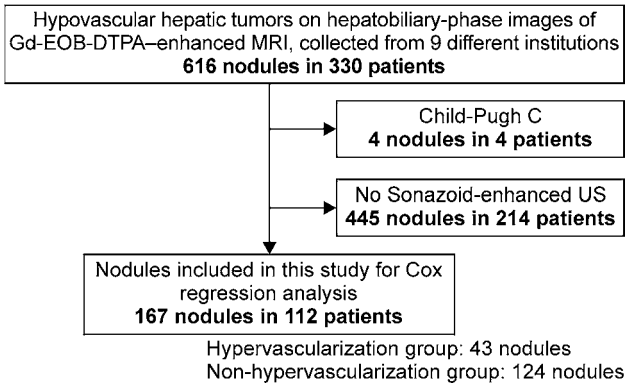

Fig. 1 Flow chart depicting selection of the study population

MR imaging

All the institutions that participated in the present study were equipped with high-field-strength (at least 1.5 T) MRI units. The pulse sequence parameters were set according to the local experience of the readers. The MR machines were 3.0 T (Achieva, Philips Medical Systems, Best, Netherlands; and MAGNETOM Skyra, Siemens, Erlangen, Germany) or 1.5 T systems (Signa Excite HDxt, GE Healthcare, Milwaukee, Wisconsin; Gyroscan Intera Nova and Achieva, Philips Medical Systems; Excelart Vantage Powered by Atlas, Toshiba Medical Systems, Tochigi, Japan; and MAGNETOM Symphony and Avanto, Siemens, Erlangen, Germany). Unenhanced, arterial, portal venous, late phase images were obtained according to the local standard of care. Hepatobiliary phase images were obtained more than 20 min after injection of Gd-EOB-DTPA at each institution.

Ultrasonography

Different US systems were used at the different institutions (Table 2). First, a grayscale US scan was obtained for each lesion. Each focal liver lesion was measured. After baseline US scan evaluation, the sonologist initiated the contrast-specific mode. Before intravenous injection of the microbubble contrast agent Sonazoid (Daiichi Sankyo, Tokyo, Japan), the persistence of the image display on the US machine was set to zero, the signal gain was registered below the noise threshold, and one focus was positioned below the level of the lesion. The contrast-enhanced examination consisted of the early vascular phase, late vascular phase, and Kupffer phase (at least 10 min after the injection of the contrast agent). The real-time images were stored on a hard disk so that the images could be recalled as necessary. We identified vascular patterns in the early vascular phase as isovascular or hypovascular and classified tumor perfusion patterns on Kupffer-phase images as hyper-perfusion, iso-perfusion, or hypo-perfusion.

Evaluation of tumor vascularity

Tumor vascularity was evaluated by Sonazoid-enhanced US and Gd-EOB-DTPA-enhanced MRI at each institution. A non-hypervascular nodule was defined as a nodule that showed non-hypervascularity relative to the surrounding liver parenchyma during the arterial phase of dynamic imaging for both the modalities. Arterial enhancement was assessed by visual inspection. The exclusion criteria for hypointense lesions observed in hepatobiliary-phase images of Gd-EOB-DTPA-enhanced MR were as follows: (a) hypervascularity on initial dynamic MRI and/or early vascular phase of Sonazoid-enhanced US (i.e., exclusion of

Table 1 Baseline characteristics of the patients and imaging findings of the nodules

Parameters	Hypervascularization at follow-up examinations		*p* value*
	Yes ($n = 43$)	No ($n = 124$)	
Tumor diameter	12 ± 4.6	10.4 ± 4.06	0.04
Coexistence of hypervascular HCC (yes/no)	25/18	51/73	0.075
Liver disease (chronic hepatitis/liver cirrhosis/unknown)	8/28/7	44/80	0.13
Etiology (HCV/HBV/other/unknown)	19/12/6/6	69/29/16/10	0.52
Child–Pugh score (A/B/C/unknown)	34/3/0/6	97/14/0/13	0.63
Previous history of HCC treatment (yes/no)	25/18	51/73	0.075
Unenhanced T1-weighted images on MRI (low intensity/iso-hyper intensity)[b]	29/14	84/40	0.56
Fat-containing lesions on in- and opposed-phase images on MRI (yes/no)[b]	10/33	26/98	0.83
Unenhanced T2-weighted images on MRI (hyper intensity/iso-low intensity)[b]	9/34	16/108	0.22
Kupffer-phase image of Sonazoid-enhanced US (hypo-perfusion/iso-hyper perfusion)[b]	15/28	17/107	0.005
Arterial-phase image of dynamic study[a] (hypovascular/isovascular)[b]	23/20	53/71	0.29
Portal-phase image of dynamic study[a] (hypovascular/isovascular)[b]	15/28	52/72	0.47
Serum α-fetoprotein level (AFP) (<12 ng/ml/>12 ng/ml/NA)	17/26/0	65/57/2	0.11
Serum des-γ-carboxy prothrombin (DCP) (<21mAU/ml/ >21 mAU/ml/NA)	16/24/3	60/57/7	0.88
Observation period	483	434	0.74

Data are mean ± SD

When CTHA and CTAP were performed, we assessed the respective imaging findings

HCC hepatocellular carcinoma, *HCV* hepatitis C virus, *HBV* hepatitis B virus, *NA* not assessed

* $p < 0.05$ indicates statistical significance

[a] Dynamic study refers to any of the available modalities (Gd-EOB-DTPA–enhanced MRI, dynamic CT, contrast-enhanced US, CTHA, and CTAP)

[b] Qualitative assessment

Table 2 US equipment and contrast-enhanced modes

Equipment, manufacturer	Scanning mode	No. of lesions scanned	Amount of Sonazoid[a]	Scan time of Kupffer phase (min)	Mechanical index (MI)	High MI burst[b]
GE lOGIQ 7	Coded harmonic angio	1	0.2 ml/body[c]	10	0.25	0.8
GE lOGIQ E9	Phase inversion amplitude modulation	71	0.01 ml/kg		0.26	
Toshiba Aplio XG	Pulse subtraction	94	0.01 ml/kg	10–30	0.2–0.3	0.7–1.0, 1.52
Toshiba Aplio XV			0.5 ml/body			
HITACHI Aloka Prosound alpha-10	Pure harmonic detection mode	1	0.01 ml/kg 0.5 ml/body	10	0.24	–

[a] The amount of Sonazoid was set at each institution

[b] To eliminate background B-mode findings, the high MI contrast mode was used when the tumor showed hyper echogenicity on B-mode US

[c] A total of 0.2 ml Sonazoid was injected

classical HCC and other hypervascular tumors); (b) delayed enhancement on initial dynamic MRI and/or late vascular phase of Sonazoid-enhanced US (i.e., exclusion of slow-filling hemangiomas); (c) strong high intensity on T2-weigthed images (T2WI) (i.e., excluding cysts); and (d) lesion size of less than 3 mm (because the slice thickness for the hepatobiliary phase of Gd-EOB-DTPA-enhanced MR was 3 mm).

Table 3 Stepwise multiple Cox regression analysis

Results of univariate analysis			
Parameters			*p* value*
Age (<70/≥70 years)			0.76
Sex (male/female)			0.29
Tumor size (continuous value)			0.0012
Coexistence of hypervascular HCC (yes/no)			0.17
Liver disease (chronic hepatitis/liver cirrhosis/unknown)			0.87
Etiology of liver disease (HCV/HBV/other/unknown)			0.89
Child-Pugh score (A/B/C/unknown)			0.13
Unenhanced T1-weighted images on MRI (low intensity/iso-hyper intensity)			0.57
Previous history of HCC treatment (yes/no)			0.17
Fat-containing lesions on in- and opposed-phase images on MRI (yes/no)			0.93
Unenhanced T2-weighted images on MRI (hyper intensity/iso-low intensity)			0.43
Kupffer-phase image of Sonazoid-enhanced US (hypo-perfusion/iso-hyper perfusion)			0.004
Arterial-phase image in dynamic study (hypovascular/isovascular)			0.91
Portal-phase image in dynamic study (hypovascular/isovascular)			0.07
Serum α-fetoprotein level (AFP) (<12 ng/ml/≥20 ng/ml/NA)			0.22
Serum des-γ-carboxy prothrombin (DCP) (< 21 mAU/ml/≥ 21 mAU/ml/NA)			0.14
Results of multivariate analysis			
Parameters	Ex (B)	95 % CI	*p* value*
Tumor diameter (mm)	1.086	1.027−1.148	0.004
Kupffer phase (hypo-perfusion)	3.684	1.798−7.546	0.0004
Coexistence of hypervascular HCC	1.465	0.7634−2.811	0.25
History of local therapy for HCC	1.501	0.7993−2.820	0.21
Image of fat-suppressed MR T2-weighted images	1.501	0.6332−2.361	0.55
Fat-containing lesions on in- and opposed-phase images	1.508	0.6895−3.298	0.30

* $p < 0.05$ indicates statistical significance

Definition of hypervascular transformation

During the follow-up period, when a CT hepatic arteriography (CTHA) image, Sonazoid-enhanced US, dynamic CT, and MR in the early phase indicated a region of hyperattenuation relative to the area surrounding the nodule, it was described as hypervascularization. Hypervascularization was confirmed by more than one modality, and the earliest date of the imaging examinations was used as the reference point.

Statistical analysis

All analyses were conducted at the nodule level. R software (Version 2.12.0; R Foundation for Statistical Computing, Vienna, Austria) was used for statistical analysis. To evaluate the independent prognostic significance of baseline covariates for subsequent hypervascularization, a multivariate Cox proportional hazard model was used. Because 26 patients had multiple nodules detected at two or more follow-up examinations, we used the coxph function from the survival package in the R software, with the cluster option. This method accounted for correlation induced by having multiple nodules per patient and used robust variance estimates [30]. Before model selection, bivariate analysis was performed by using Spearman rank correlations to test for collinearity among independent variables. As a result, Spearman correlation coefficients for variables were generally below 0.5, which suggests that multicollinearity was not a concern. Hazard ratios (HRs) and 95 % confidence intervals (CIs) were calculated. Continuous variables were presented as the median and range. Continuous variables such as tumor size and observation period were compared with Mann–Whitney *U* test, and other categorical variables were compared by Fisher's exact test or the Chi-squared test. Based on the analysis of lesions, the cumulative risk of a non-hypervascular tumor transforming into classical HCC was calculated according to the Kaplan–Meier method. We calculated the relative risk using Cox proportional hazard regression analysis. Actuarial analysis of the cumulative incidence of vascularization was performed with the Kaplan–Meier method, and the differences were tested by

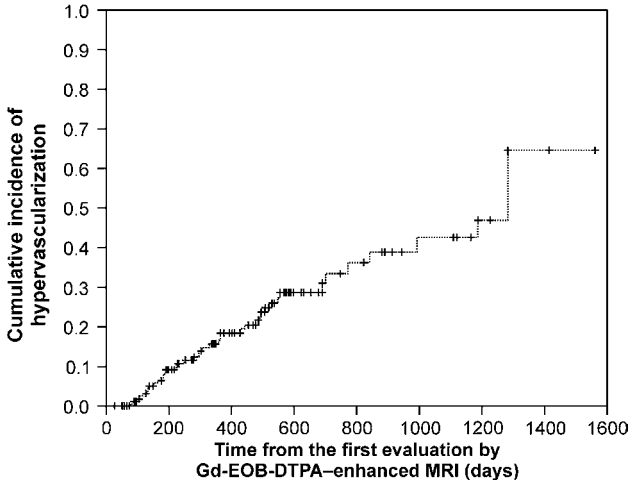

Fig. 2 Cumulative rates for hypervascularization of hypointense lesions. The overall cumulative incidence of hypervascular transformation was 18 % at 12 months, 37 % at 24 months, and 43 % at 18 months. Forty-three (25.7 %) out of the 167 cases showed hypervascular transformation in the arterial phase of dynamic imaging during the follow-up period

the log-rank test. A p value <0.05 was considered to denote a statistically significant difference.

Results

Nodule characteristics

Table 1 shows the characteristics of the nodules that were vascularized and of those that were not. Of the 167 nodules, 43 (25.7 %) showed hypervascular transformation in the arterial phase of dynamic imaging during the follow-up period. Fisher's exact test showed that at the start of follow-up, nodules with and without vascularization showed significant differences with respect to the average tumor diameter ($p = 0.04$) and Kupffer-phase images in Sonazoid-enhanced US ($p = 0.005$).

Cumulative incidence of hypervascular transformation

The overall cumulative incidence of hypervascular transformation was 18 % at 12 months, 37 % at 24 months, and 43 % at 18 months (Fig. 2).

Univariate analysis using the log-rank test revealed that hypoperfusion on Kupffer-phase images of contrast-enhanced US using Sonazoid and tumor diameter were correlated with hypervascular transformation (Table 3). Next, the two significant factors identified by univariate analysis and another four variables, including coexistence of hypervascular HCC, history of local therapy for HCC, fat-suppressed T2-weighted images, and fat-containing lesions on in- and opposed-phase images, were further analyzed by multivariate analysis using the Cox regression model because these 4 variables have been described as important predictors [14]. Consequently, tumor diameter (HR = 1.086; $p = 0.004$, 95 % CI: 1.027, 1.148) and hypo-perfusion on Kupffer-phase images in Sonazoid-enhanced US (HR = 3.684; $p = 0.0004$, 95 % CI: 1.798, 7.546) were identified as independent factors for hypervascular transformation (Table 3). Subsequently, we compared the incidence of hypervascular transformation of tumors with these risk factors based on the Kaplan–Meier curve. The incidence of hypervascularization was significantly higher in the groups with these prognostic factors (Figs. 3, 4). The optimum cut-off point for tumor size was estimated to be 8.6 mm by receiver operating characteristic (ROC) curves (figure not shown).

Discussion

To the best of our knowledge, this study is the first to show the usefulness of Kupffer-phase images in Sonazoid-enhanced US for predicting hypervascularization of non-hypervascular borderline lesions detected in hepatobiliary-phase images of Gd-EOB-DTPA-enhanced MR.

Previously, Kupffer cells were thought to be absent in overt HCC tissues, but recently investigators have shown that Kupffer cells exist in early stage HCCs [31]. Furthermore, the histologic grade of HCC has been shown to correlate with the number of Kupffer cells present. Kupffer cells, the resident liver macrophages, constitute 31 % of the sinusoidal cells [32]. They are more numerous (43 %) in the periportal zone of the lobule. In addition to being more numerous, periportal Kupffer cells are larger, have more lysosomes, and take up more particles than do middle- or central-zone Kupffer cells [33]. Sugihara et al. [34] reported that cancerous tissue of well-differentiated HCCs possesses blood spaces that are similar to the normal sinusoids. Therefore, blood spaces are expected to possess morphologic and functional characteristics similar to those of normal sinusoids but that as tumors grew in size and came to have a lower histologic grade, the blood spaces increased in apparent capillarization and became morphologically different from normal sinusoids. When neovascularization suggested by unpaired artery [35] occurred, normal sinusoids were gradually destroyed and the portal supply declined. Therefore, we speculate that Kupffer cells lose their functional ability to take up microbubbles. Although all most all premalignant/borderline lesions possess portal areas and blood spaces similar to those of normal sinusoids may take up microbubbles in a manner similar to non-nodular adjacent tissue, some of the

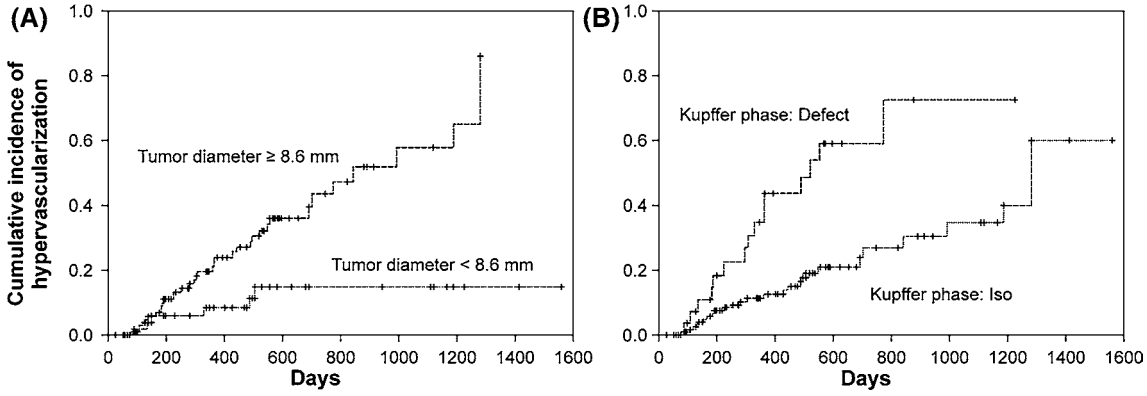

Fig. 3 Cumulative rates for hypervascularization of hypointense lesions. Lesions are stratified according to the tumor size and Kupffer-phase image in Sonazoid-enhanced US. The incidence of hypervascularization was significantly higher when the tumor diameter was greater than 8.6 mm

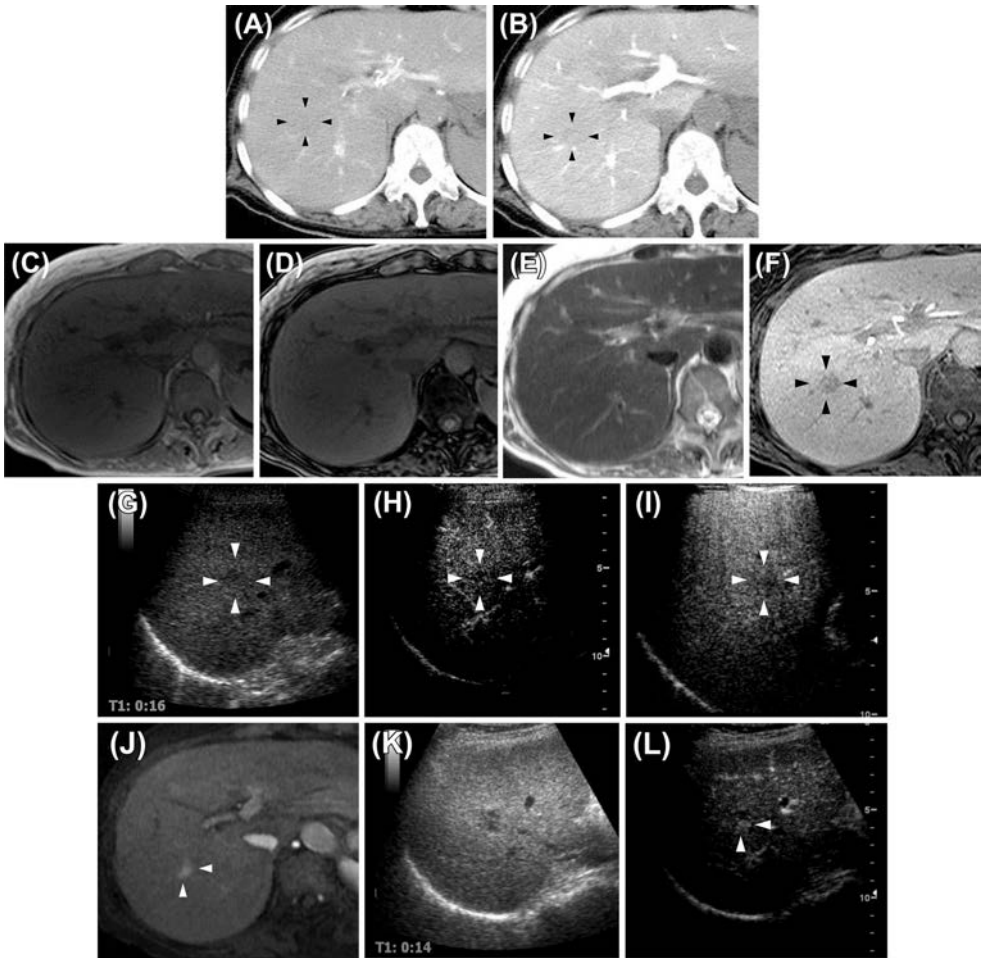

Fig. 4 Case presentation of borderline lesions (*arrowheads* indicate the tumor). **a**, **b** Tumors showing isovascularity on CTHA (**a**) and CTAP(**b**). Initial Gd-EOB-DTPA–enhanced MRI (**c**–**f**). Tumors showing: Isointensity on in-phase (**c**) and opposed-phase images (**d**). **e** Isointensity on T2-weighted image. **f** Low intensity in hepatobiliary-phase image of Gd-EOB-DTPA-enhanced. MRI Initial Sonazoid-enhanced US (**g**–**i**). **g**, **k** Monitor mode, **h**, **i**, **l** contrast mode. Tumors showing: **g**, **h** Hypovascularity in early vascular phase. **i** Hypoperfusion in Kupffer-phase. **j** Hypervascular spot in nodule in arterial-phase of Gd-EOB-DTPA-enhanced MRI at 30 months after start of follow-up. **k**, **l** hypervascular spot in nodule in early vascular phase in Sonazoid-enhanced US

premalignant/borderline lesions might have lost their ability to possess microbubbles resulting in the tumorous perfusion defects observed in Kupffer phase imaging before hypervascularization detected by other imaging modalities. In the present study, 135 out of 167 nodules showed iso-perfusion on the Kupffer-phase image. Although the improved detection ability of Gd-EOB-DTPA-enhanced MRI enabled us to detect many premalignant/borderline lesions, which are difficult to detect on the basis of intratumoral hemodynamic changes, the new challenge is in deciding which lesions should be monitored more carefully. However, by using Sonazoid-enhanced US, Kupffer cell function can be evaluated for tumors that cannot be evaluated by other imaging modalities. Therefore, we evaluated the Kupffer cell function of these premalignant/borderline lesions using Sonazoid, and we found that it can be a useful tool for predicting hypervascularization. Sonazoid-enhanced US is easy to perform, and it is more cost-effective than MRI and does not involve exposure to ionizing radiation, unlike contrast-enhanced CT, CTHA, and CT during arterial portography (CTAP). In general, when non-hypervascular hypointense lesions are detected by Gd-EOB-DTPA-enhanced MRI, we strongly suggest that Sonazoid-enhanced US should be performed to evaluate Kupffer cell function and predict hypervascularization.

Although we conducted a cooperative study, collecting several non-hypervascular tumors and investigating the natural outcome of hypointense lesions in a nationwide manner, this study did have some limitations. The principal limitation of this study was the variation in the equipment used at different institutions. Although this limitation may have been inevitable because of the multicenter nature of the study, the different sensitivities of the different equipment used should be considered in future investigations. Second, this was a retrospective study, which may have introduced bias in data homogeneity. Moreover, the interval between the follow-up examinations varied for each individual and among the patients. Prospective studies with consistent follow-up intervals must be performed to overcome this limitation. In this study, most of the follow-up studies were performed at intervals of 3 and 6 months, which is consistent with the usual practice for follow-up of patients at high risk of HCC [36, 37]. Third, on imaging analysis, our study was potentially limited by consensus review. To minimize operator bias, well-trained radiologists and physicians reviewed the images. However, in the future, assessment of interobserver variability is warranted. Fourth, the ability of Sonazoid-enhanced US to detect hypervascularization in a nodule varies considerably according to depth from the surface of the liver, coarseness of liver parenchyma, and patient's obesity. It would be appropriate to use Gd-EOB-DTPA-enhanced MR only for the evaluation. Finally, no pathologic proof existed for the nodules evaluated in the present study. However, the major purpose of the present study was to evaluate whether the Kupffer-phase image in Sonazoid-enhanced US can predict hypervascular transformation in borderline lesions; we did not aim to distinguish among dysplastic nodules, early HCCs, and well-differentiated HCCs. In conclusion, this study shows that the Kupffer-phase image in Sonazoid-enhanced US is useful for the prediction of hypervascularization of non-hypervascular hypointense hepatic lesions detected on Gd-EOB-DTPA-enhanced MRI.

Conflict of interest The authors declare that they have no conflict of interest.

References

1. Kudo M. Imaging diagnosis of hepatocellular carcinoma and premalignant/borderline lesions. Semin Liver Dis. 1999;19(3):297–309.
2. Krinsky G. Imaging of dysplastic nodules and small hepatocellular carcinomas: experience with explanted livers. Intervirology. 2004;47(3–5):191–8.
3. Schuhmann-Giampieri G, Schmitt-Willich H, Press WR, et al. Preclinical evaluation of Gd-EOB-DTPA as a contrast agent in MR imaging of the hepatobiliary system. Radiology. 1992;183(1):59–64.
4. Kitao A, Zen Y, Matsui O, et al. Hepatocellular carcinoma: signal intensity at gadoxetic acid-enhanced MR imaging–correlation with molecular transporters and histopathologic features. Radiology. 2010;256(3):817–26.
5. Narita M, Hatano E, Arizono S, et al. Expression of OATP1B3 determines uptake of Gd-EOB-DTPA in hepatocellular carcinoma. J Gastroenterol. 2009;44(7):793–8.
6. Leonhardt M, Keiser M, Oswald S, et al. Hepatic uptake of the magnetic resonance imaging contrast agent Gd-EOB-DTPA: role of human organic anion transporters. Drug Metab Dispos. 2010;38(7):1024–8.
7. Kitao A, Matsui O, Yoneda N, et al. The uptake transporter OATP8 expression decreases during multistep hepatocarcinogenesis: correlation with gadoxetic acid enhanced MR imaging. Eur Radiol. 2011;21(10):2056–66.
8. Kogita S, Imai Y, Okada M, et al. Gd-EOB-DTPA-enhanced magnetic resonance images of hepatocellular carcinoma: correlation with histological grading and portal blood flow. Eur Radiol. 2010;20(10):2405–13.
9. Inoue T, Kudo M, Komuta M, et al. Assessment of Gd-EOB-DTPA-enhanced MRI for HCC and dysplastic nodules and comparison of detection sensitivity versus MDCT. J Gastroenterol 2012.
10. Kudo M. Early hepatocellular carcinoma: definition and diagnosis. Liver Cancer. 2013;2(2):69–72.
11. Ichikawa T, Sano K, Morisaka H. Diagnosis of pathologically early HCC with EOB-MRI: experiences and current consensus. Liver Cancer. 2014;3(2):97–107.
12. Kumada T, Toyoda H, Tada T, et al. Evolution of hypointense hepatocellular nodules observed only in the hepatobiliary phase of gadoxetate disodium-enhanced MRI. AJR Am J Roentgenol. 2011;197(1):58–63.
13. Akai H, Matsuda I, Kiryu S, et al. Fate of hypointense lesions on Gd-EOB-DTPA-enhanced magnetic resonance imaging. Eur J Radiol. 2012;81(11):2973–7.
14. Motosugi U, Ichikawa T, Sano K, et al. Outcome of hypovascular hepatic nodules revealing no gadoxetic acid uptake in patients

with chronic liver disease. J Magn Reson Imaging. 2011;34(1):88–94.
15. Takayama Y, Nishie A, Nakayama T, et al. Hypovascular hepatic nodule showing hypointensity in the hepatobiliary phase of gadoxetic acid-enhanced MRI in patients with chronic liver disease: prediction of malignant transformation. Eur J Radiol. 2012;81(11):3072–8.
16. Kobayashi S, Matsui O, Gabata T, et al. Relationship between signal intensity on hepatobiliary phase of gadolinium ethoxybenzyl diethylenetriaminepentaacetic acid (Gd-EOB-DTPA)-enhanced MR imaging and prognosis of borderline lesions of hepatocellular carcinoma. Eur J Radiol. 2012;81(11):3002–9.
17. Hyodo T, Murakami T, Imai Y, et al. Hypovascular nodules in patients with chronic liver disease: risk factors for development of hypervascular hepatocellular carcinoma. Radiology. 2013;266(2):480–90.
18. Higaki A, Ito K, Tamada T, et al. High-risk nodules detected in the hepatobiliary phase of Gd-EOB-DTPA-enhanced MR imaging in cirrhosis or chronic hepatitis: incidence and predictive factors for hypervascular transformation, preliminary results. J Magn Reson Imaging. 2013;37(6):1377–83.
19. Takechi M, Tsuda T, Yoshioka S, et al. Risk of hypervascularization in small hypovascular hepatic nodules showing hypointense in the hepatobiliary phase of gadoxetic acid-enhanced MRI in patients with chronic liver disease. Jpn J Radiol. 2012;30(9):743–51.
20. Inoue T, Hyodo T, Murakami T, et al. Hypovascular hepatic nodules showing hypointense on the hepatobiliary-phase image of Gd-EOB-DTPA-enhanced MRI to develop a hypervascular hepatocellular carcinoma: a nationwide retrospective study on their natural course and risk factors. Dig Dis. 2013;31(5–6):472–9.
21. Moriyasu F, Itoh K. Efficacy of perflubutane microbubble-enhanced ultrasound in the characterization and detection of focal liver lesions: phase 3 multicenter clinical trial. AJR Am J Roentgenol. 2009;193(1):86–95.
22. Murakami T, Imai Y, Okada M, et al. Ultrasonography, computed tomography and magnetic resonance imaging of hepatocellular carcinoma: toward improved treatment decisions. Oncology. 2011;81(Suppl 1):86–99.
23. Kudo M, Hatanaka K, Kumada T, et al. Double-contrast ultrasound: a novel surveillance tool for hepatocellular carcinoma. Am J Gastroenterol. 2011;106(2):368–70.
24. Luo W, Numata K, Morimoto M, et al. Role of Sonazoid-enhanced three-dimensional ultrasonography in the evaluation of percutaneous radiofrequency ablation of hepatocellular carcinoma. Eur J Radiol. 2010;75(1):91–7.
25. Korenaga K, Korenaga M, Furukawa M, et al. Usefulness of Sonazoid contrast-enhanced ultrasonography for hepatocellular carcinoma: comparison with pathological diagnosis and superparamagnetic iron oxide magnetic resonance images. J Gastroenterol. 2009;44(7):733–41.
26. Sugimoto K, Moriyasu F, Saito K, et al. Comparison of Kupffer-phase Sonazoid-enhanced sonography and hepatobiliary-phase gadoxetic acid-enhanced magnetic resonance imaging of hepatocellular carcinoma and correlation with histologic grading. J Ultrasound Med. 2012;31(4):529–38.
27. Ohama H, Imai Y, Nakashima O, et al. Images of Sonazoid-enhanced ultrasonography in multistep hepatocarcinogenesis: comparison with Gd-EOB-DTPA-enhanced MRI. J Gastroenterol 2013.
28. Grobner T, Prischl FC. Gadolinium and nephrogenic systemic fibrosis. Kidney Int. 2007;72(3):260–4.
29. Willatt JM, Hussain HK, Adusumilli S, et al. MR imaging of hepatocellular carcinoma in the cirrhotic liver: challenges and controversies. Radiology. 2008;247(2):311–30.
30. Lin DY. Cox regression analysis of multivariate failure time data: the marginal approach. Stat Med. 1994;13(21):2233–47.
31. Tanaka M, Nakashima O, Wada Y, et al. Pathomorphological study of Kupffer cells in hepatocellular carcinoma and hyperplastic nodular lesions in the liver. Hepatology. 1996;24(4):807–12.
32. Bouwens L, Baekeland M, De Zanger R, et al. Quantitation, tissue distribution and proliferation kinetics of Kupffer cells in normal rat liver. Hepatology. 1986;6(4):718–22.
33. Ruttinger D, Vollmar B, Wanner GA, et al. In vivo assessment of hepatic alterations following gadolinium chloride-induced Kupffer cell blockade. J Hepatol. 1996;25(6):960–7.
34. Sugihara S, Kojiro M, Nakashima T. Ultrastructural study of hepatocellular carcinoma with replacing growth pattern. Acta Pathol Jpn. 1985;35(3):549–59.
35. Kojiro M, Wanless I, Alves V, et al. Pathologic diagnosis of early hepatocellular carcinoma: a report of the international consensus group for hepatocellular neoplasia. Hepatology. 2009;49(2):658–64.
36. Bruix J, Sherman M. Management of hepatocellular carcinoma: an update. Hepatology. 2011;53(3):1020–2.
37. Kudo M, Izumi N, Kokudo N, et al. Management of hepatocellular carcinoma in Japan: consensus-based clinical practice guidelines proposed by the Japan Society of Hepatology (JSH) 2010 updated version. Dig Dis. 2011;29(3):339–64.

World Journal of Gastroenterology

Submit a Manuscript: http://www.wjgnet.com/esps/
Help Desk: http://www.wjgnet.com/esps/helpdesk.aspx
DOI: 10.3748/wjg.v22.i12.3381

World J Gastroenterol 2016 March 28; 22(12): 3381-3391
ISSN 1007-9327 (print) ISSN 2219-2840 (online)

ORIGINAL ARTICLE

Retrospective Cohort Study

Contrast-enhanced harmonic endoscopic ultrasonography for assessment of lymph node metastases in pancreatobiliary carcinoma

Takeshi Miyata, Masayuki Kitano, Shunsuke Omoto, Kumpei Kadosaka, Ken Kamata, Hajime Imai, Hiroki Sakamoto, Naoshi Nisida, Yogesh Harwani, Takamichi Murakami, Yoshifumi Takeyama, Yasutaka Chiba, Masatoshi Kudo

Takeshi Miyata, Masayuki Kitano, Shunsuke Omoto, Kumpei Kadosaka, Ken Kamata, Hajime Imai, Hiroki Sakamoto, Naoshi Nisida, Yogesh Harwani, Masatoshi Kudo, Department of Gastroenterology and Hepatology, Kinki University Faculty of Medicine, Osaka-sayama 589-8511, Japan

Takamichi Murakami, Department of Radiology, Kinki University Faculty of Medicine, Osaka-sayama 589-8511, Japan

Yoshifumi Takeyama, Department of Surgery, Kinki University Faculty of Medicine, Osaka-sayama 589-8511, Japan

Yasutaka Chiba, Division of Biostatistics, Clinical Research Center, Kinki University Faculty of Medicine, Osaka-sayama 589-8511, Japan

Author contributions: Miyata T wrote the manuscript; Miyata T, Kitano M, Imai H, Sakamoto H and Kudo M drafted the study conception and design; Miyata T, Kadosaka K, Harwani Y, Murakami T and Takeyama Y critically revised the article for important intellectual content; Kitano M and Sakamoto H performed the endosonography studies; Omoto S, Kamata K, Nisida N and Takeyama Y performed the pathological evaluations; Kadosaka K and Chiba Y provided statistical analysis; Imai H, Murakami T and Kudo M read images; and Harwani Y critically revised English grammar.

Supported by Grants from the Japan Society for the Promotion of Science and the Japanese Foundation for the Research and Promotion of Endoscopy, No. 22590764 and No. 25461035.

Institutional review board statement: This study was approved by the Institutional Review Board of Kinki University Faculty of Medicine.

Informed consent statement: All patients provided informed consent with regard to the procedures and participation in the study.

Conflict-of-interest statement: We wish to confirm that there are no known conflicts of interest associated with this publication.

Data sharing statement: No additional data are available.

Correspondence to: Masayuki Kitano, MD, PhD, Department of Gastroenterology and Hepatology, Kinki University Faculty of Medicine, 377-2 Ohno-higashi, Osaka-sayama 589-8511, Japan. m-kitano@med.kindai.ac.jp

Received: September 9, 2015
Peer-review started: September 16, 2015
First decision: October 14, 2015
Revised: October 23, 2015
Accepted: December 12, 2015
Article in press: December 14, 2015
Published online: March 28, 2016

Abstract

AIM: To assess the usefulness of contrast-enhanced harmonic endoscopic ultrasonography (CH-EUS) for lymph node metastasis in pancreatobiliary carcinoma.

METHODS: All patients suspected of pancreatobiliary carcinoma with visible lymph nodes after standard EUS between June, 2009 and January, 2012 were enrolled.

In the primary analysis, patients with successful EUS-fine needle aspiration (FNA) were included. The lymph nodes were assessed by several standard EUS variables (short and long axis lengths, shape, edge characteristic and echogenicity), color Doppler EUS variable [central intranodal blood vessel (CIV) presence] and CH-EUS variable (heterogeneous/homogeneous enhancement patterns). The diagnostic accuracy relative to EUS-FNA was calculated. In the second analysis, N-stage diagnostic accuracy of CH-EUS was compared with EUS-FNA in patients who underwent surgical resection.

RESULTS: One hundred and nine patients (143 lymph nodes) fulfilled the criteria. The short axis cut-off $\geqslant$ 13 mm predicted malignancy with a sensitivity and specificity of 72% and 85%, respectively. These values were 72% and 63% for the long axis cut-off $\geqslant$ 20 mm, 62% and 75% for the round shape variable, 81% and 30% for the sharp edge variable, 66% and 61% for the hypoechogenicity variable, 70% and 72% for the CIV-absent variable, and 83% and 91% for the heterogeneous CH-EUS-enhancement variable, respectively. CH-EUS was more accurate than standard and color Doppler EUS, except the short axis cut-off. Notably, three patients excluded because of EUS-FNA failure were correctly N-staged by CH-EUS.

CONCLUSION: CH-EUS complements standard and color Doppler EUS and EUS-FNA for assessment of lymph node metastases.

Key words: Contrast-enhanced harmonic endoscopic ultrasonography; Sensitivity and specificity; Lymph node; Pancreatobiliary carcinoma; Endoscopic ultrasonography-fine needle aspiration

Core tip: Diagnosis of malignant intra-abdominal lymph nodes is often challenging for endoscopists and radiologists. In the present study, the diagnostic accuracy for differentiating malignant from benign lymph nodes of standard endoscopic ultrasonography (EUS), color Doppler EUS, and contrast-enhanced harmonic (CH)-EUS relative to EUS-fine needle aspiration (FNA) was assessed. A secondary objective of the present study was to assess the N-stage diagnostic accuracy of CH-EUS and EUS-FNA in patients who underwent surgical resection. In conclusion, CH-EUS was more accurate than standard and color Doppler EUS, except the short axis cut-off. Notably, three patients excluded because of EUS-FNA failure were correctly N-staged by CH-EUS.

Miyata T, Kitano M, Omoto S, Kadosaka K, Kamata K, Imai H, Sakamoto H, Nisida N, Harwani Y, Murakami T, Takeyama Y, Chiba Y, Kudo M. Contrast-enhanced harmonic endoscopic ultrasonography for assessment of lymph node metastases in pancreatobiliary carcinoma. *World J Gastroenterol* 2016; 22(12): 3381-3391 Available from: URL: http://www.wjgnet.com/1007-9327/full/v22/i12/3381.htm DOI: http://dx.doi.org/10.3748/wjg.v22.i12.3381

INTRODUCTION

Accurate staging by using the tumor, node and metastasis (TNM) classification system is the most important variable for determining the optimal treatment of pancreatobiliary carcinomas. In particular, since the lymph node stage relates not only to the choice of treatment but also to the prognosis, it is essential that the techniques used for N-staging are reliable[1,2]. However, diagnosis of malignant intra-abdominal lymph nodes is often challenging for endoscopists and radiologists[3]. Several studies report that although endoscopic ultrasonography (EUS) (which has good spatial resolution) is useful for the differential diagnosis of malignant and benign lymph nodes, its diagnostic accuracy remains unsatisfactory[4-6]. By contrast, a cyto-pathological diagnosis *via* EUS-fine needle aspiration (FNA) is highly accurate. However, an accurate noninvasive evaluating method[7] is needed for cases in which a lymph node cannot be accessed for EUS-FNA or EUS-FNA does not obtain adequate material for analysis[8]. In addition, noninvasive methods could facilitate EUS-FNA by identifying the target lymph node for EUS-FNA, namely, the lymph node that is most suspicious of malignancy and whose sampling will shape treatment decisions. One such noninvasive evaluation method is vascular imaging. Although color Doppler imaging can evaluate the vasculature in lymph nodes, it has several limitations, including blooming, overpainting and motion artifacts. It is also difficult to evaluate perfusion by using color Doppler imaging. This problem was recently overcome by a revolution in US technology, namely, the invention of US contrast agents that, when combined with contrast harmonic imaging, make it possible to depict the microvasculature in real time[9]. Recently, EUS was equipped with this novel perfusion imaging technique, thus yielding contrast-enhanced harmonic EUS (CH-EUS)[10,11].

In the present study, the diagnostic accuracy for differentiating malignant from benign lymph nodes of standard EUS, color Doppler EUS, and CH-EUS relative to EUS-FNA was assessed. For this, all patients with standard EUS-detected pancreatobiliary carcinomas with apparently visible intra-abdominal lymph nodes who underwent all four procedures during the study period were recruited prospectively and followed up. The CH-EUS variable that was analyzed was the detection of the microvasculature in visible lymph node(s); this was expressed as heterogeneous/homogeneous enhancement. A secondary objective of the present study was to assess the N-stage diagnostic accuracy of CH-EUS and EUS-FNA in patients who

underwent surgical resection.

MATERIALS AND METHODS

Patients and study design

All consecutive patients who were suspected of having pancreatobiliary diseases due to CT, MRI, or transabdominal US results and who then underwent standard EUS between June, 2009 and January, 2012 in a tertiary care referral center in Japan were recruited prospectively (Figure 1). All patients also underwent color Doppler EUS, CH-EUS, and EUS-FNA immediately after the standard EUS procedure. The primary objective of this study was to compare the diagnostic accuracy of standard EUS, color Doppler EUS and CH-EUS in terms of the ability to differentiate malignant nodes from benign nodes. For this primary retrospective analysis, only the patients from whom adequate and accurate EUS-FNA samples were retrieved and who were followed up for at least 12 mo after the standard EUS were included. The patients where a diagnosis was obtained by specimen histology rather than EUS-FNA because of EUS-FNA failure (sample inadequacy or lymph node inaccessibility) were excluded from this analysis because it was sometimes difficult to ensure that the lymph nodes harvested from surgical specimens were the same as those that were identified by imaging.

The study also had a secondary aim, namely, to compare the accuracy of CH-EUS and EUS-FNA in terms of N-stage diagnosis in all of the patients in the original cohort who underwent surgical resection.

The study was approved by the Institutional Review Board of Kinki University Faculty of Medicine. All patients provided informed consent with regard to the procedures and participation in the study.

Equipment

An echoendoscope developed for CH-EUS (Olympus GF-UCT260; Olympus Medical Systems, Tokyo, Japan) was used. An ALOKA ProSound SSD α-10 (Aloka Co Ltd, Tokyo, Japan) was used for US imaging. For CH-EUS, the extended pure harmonic detection mode was used. This mode selectively depicts signals from the microbubbles by simultaneously filtering the harmonic component and synthesizing the phase-shift signals. The preset variables were established for EUS and CH-EUS previously[10,11]. The transmitting frequency and mechanical indices were set at 4.7 MHz and 0.3, respectively. The frame rate was set at 10-15 frame per second. The focus point was set at the distal portion of the target lymph node.

US contrast

Sonazoid (Daiichi-Sankyo, Tokyo, Japan; GE Healthcare, Milwaukee, Wis) was used as the US contrast agent. This second generation US contrast agent is composed of perfluorobutane microbubbles with a median diameter of 2-3 μm[12]. Sonazoid was reconstituted with 2 mL of sterile water for injection. A dose of 0.015 mL/kg body weight was used.

Standard EUS, color Doppler EUS and CH-EUS

During the EUS analyses, the patients were sedated by midazolam and propofol. Standard EUS, color Doppler EUS, and CH-EUS were performed by two endosonographers (Kitano M and Sakamoto H). One was responsible for the endoscopic manipulation and scanning and the other for operating the US image scanner. Both endosonographers (who were qualified by the Japan Gastroenterological Endoscopy Society) have had experience with CH-EUS for more than 10 years: both have performed more than 1000 CH-EUS procedures. Each examination was performed by using the same protocol. Thus, after a pancreatobiliary carcinoma was observed, the trans-gastric or trans-duodenal approach was used to search for intra-abdominal lymph node(s). If an apparently visible lymph node was detected, standard EUS was used to evaluate the size (*i.e*., the short and long axis lengths), shape (round or oval), edge characteristics (sharp or fuzzy), and echogenicity (hypo or hyper) of the lymph node. Thereafter, the imaging modality was changed to color Doppler EUS, which was used to determine whether a central intranodal blood vessel (CIV) was present in the lymph node.

Subsequently, the specific mode for CH-EUS (extended pure harmonic detection mode) was selected and a bolus injection of Sonazoid was administered at a speed of 1 mL/s through a 22-gauge cannula that was placed in the antecubital vein. This was followed by a 10-mL saline solution flush to ensure that all contrast was administered into the circulation system. If there were multiple apparently visible lymph nodes, each was separately assessed by injecting US contrast agent, performing CH-EUS, and then conducting EUS-FNA. These multiple CH-EUS procedures were performed at intervals of at least 10 min, which was found to be sufficient for the US contrast from the preceding CH-EUS procedure to be washed out from all lymph nodes. All movie clips were stored on the hard disk of the scanner for offline analysis.

Image analyses

All standard EUS, color Doppler EUS and CH-EUS variables were measured independently in a blinded fashion by two readers (Kudo M and Imai H). Both have had experience with CH-EUS for more than 8 years: both have read the data of more than 500 CH-EUS procedures. The two readers evaluated the movie clips of the lymph nodes. They were told that the movie clips that they were evaluating were standard EUS/color Doppler/CH-EUS analyses of lymph nodes. However, they were blinded to all CT, MRI, transabdominal US, and standard EUS findings of the primary lesions.

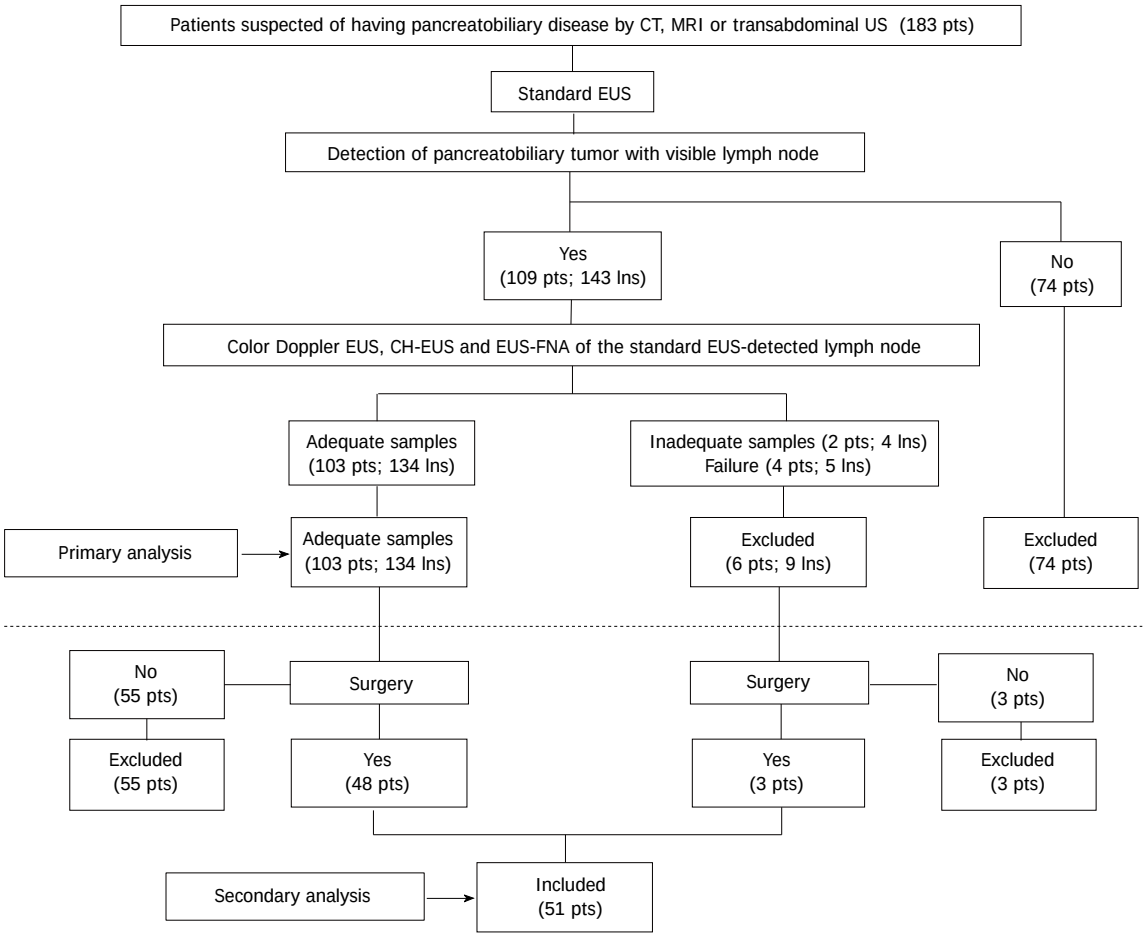

Figure 1 Schematic depiction of patient selection and exclusion criteria. pts: Patients; lns: Lymph nodes. CT: Computed tomography; MRI: Magnetic resonance imaging; EUS: Endoscopic ultrasonography; FNA: Fine needle aspiration.

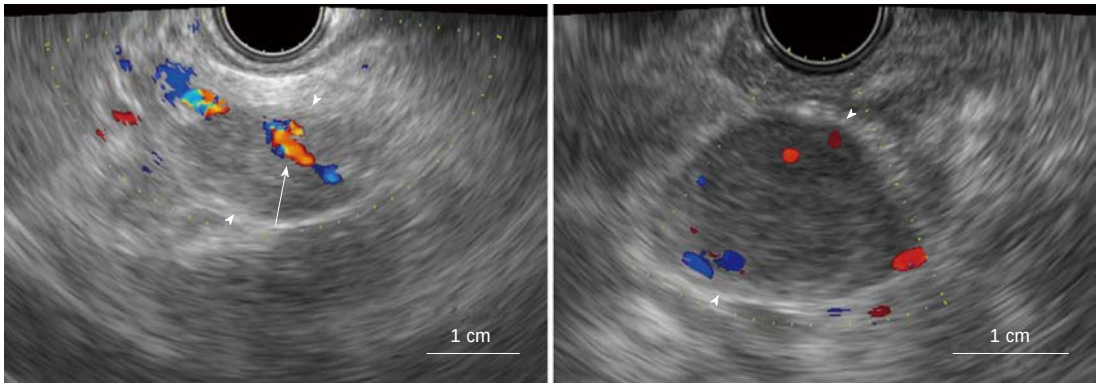

Figure 2 Typical examples of lymph nodes with (A) and without (B) a central intranodal blood vessel on color Doppler endoscopic ultrasonography. An apparently visible lymph node was detected in both A and B (arrowheads). A shows a tubular structure that was ⩾ 1 mm in diameter and was located toward the center of the lymph node and demonstrated blood flow on color Doppler endoscopic ultrasonography (arrow).

Receiver-operating characteristics (ROC) analysis was used to identify the standard EUS-detected short and long axis cut-off values that would optimize diagnosis of the lymph nodes. Based on a previous report[13], the readers predicted that the lymph nodes were malignant if they had a round shape and/or a sharp edge and/or exhibited hypoechogenicity on standard EUS. The color Doppler EUS images were assessed to determine whether CIV was present[4]. CIV was defined as a tubular structure with a well-defined smooth hyperechoic wall that was ⩾ 1 mm in diameter, located toward the center of the lymph node, and demonstrated blood flow on color Doppler EUS (Figure 2A). Based on a previous report[4], the readers predicted that the lymph nodes were malignant if a CIV was absent (Figure 2B). The CH-EUS images were assessed to determine the enhancement patterns, which were classified as being heterogeneous or

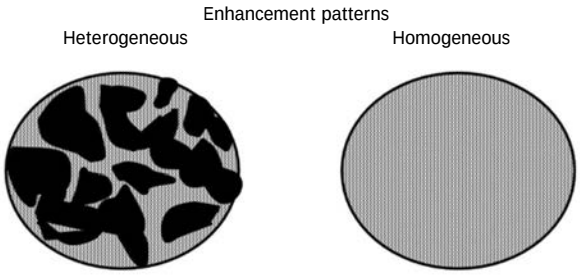

Figure 3 Contrast-enhanced harmonic endoscopic ultrasonography -determined enhancement patterns of the lymph node.

homogenous[14]. Based on a previous report[14], the readers predicted that the lymph nodes were malignant if heterogeneous enhancement was observed (Figures 3 and 4, Video 1).

Both of the blinded readers initially measured the standard EUS (shape, edge characteristics, and echogenicity), color Doppler EUS (CIV presence/absence), and CH-EUS (heterogeneous/homogenous enhancement pattern) variables separately. Interobserver agreement between the two readers in terms of these measurements was assessed by calculating the κ-coefficient (Supplementary Tables 1-1 to 1-5). Thereafter, if there were discrepant findings between the two readers, they reassessed the relevant image(s) together until an agreement was reached.

EUS-guided FNA

The final diagnosis was based on histological and/or cytological analysis of samples obtained by EUS-FNA. After standard EUS, color Doppler EUS, and CH-EUS of each lymph node, EUS-FNA was performed with a 22- or 25-gauge aspiration needle (Echo Tip Ultra, Cook, Winston-Salem, NC, United States). Punctures were repeated until a sample was obtained; the maximum number of passes was five. A cytopathologist was present in the endoscopy room for on-site sample evaluation. After it was confirmed that adequate numbers of cells had been obtained, the samples were processed and evaluated in the pathology department by using Papanicolaou staining for cytology and hematoxylin-eosin staining for histology. If there were multiple apparently visible lymph nodes, EUS-FNA was performed separately on each lymph node: after each aspiration, the needles were changed.

Histology of resected lymph nodes

The lymph nodes that were surgically resected after imaging were also assessed by the pathology department for malignancy. For this, 51 patients were included (Figure 1).

Study design

The primary objective was to compare the diagnostic accuracy of standard EUS, color Doppler EUS and CH-EUS in terms of the primary end-point, which was the ability to differentiate malignant nodes from benign nodes. The secondary end-point was to compare the accuracy of CH-EUS and EUS-FNA in terms of N-stage diagnosis in patients who underwent surgical resection.

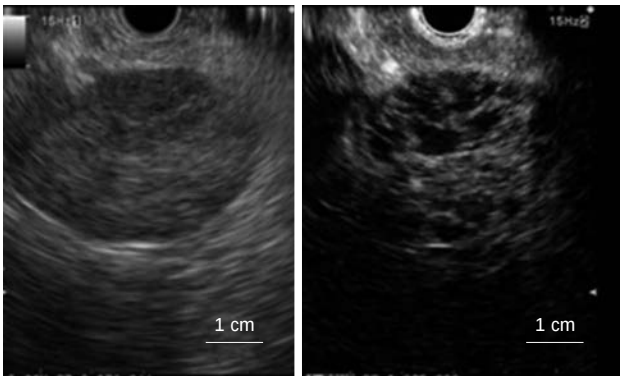

Figure 4 Typical example of a metastatic lymph node that shows heterogeneous enhancement on contrast-enhanced harmonic endoscopic ultrasonography (left, fundamental B mode; right, contrast harmonic mode).

Statistical analyses

All data were analyzed by using SAS software version 8.2 (SAS Institute, Cary, NC, United States). Differences between the EUS methods in terms of malignant lymph node detection were assessed by using McNemar's test. A difference with $P < 0.01$ was regarded as significant. This approach was also used to test differences between benign and malignant lymph nodes in terms of CH-EUS enhancement patterns. McNemar's test was also used to compare CH-EUS and EUS-FNA in terms of their N-stage diagnostic accuracy in the patients who underwent surgical resection.

Interobserver agreement in terms of the EUS variables described above was also assessed. A κ coefficient of > 0.8 was considered to indicate excellent agreement, > 0.6 was considered to indicate good agreement, and > 0.4 was considered to indicate moderate agreement. The sensitivity, specificity and accuracy with which CH-EUS differentiated malignant from benign lymph nodes were calculated and compared to the values of standard and color Doppler EUS findings (short axis, long axis, shape, edge characteristics, echogenicity and CIV). The numbers of cases of discordance are shown in Supplementary Tables 2-1 to 2-6.

RESULTS

Patient recruitment

During the study period, 183 patients suspected of pancreatobiliary disease underwent EUS and were enrolled prospectively. In 109 patients, EUS detected a pancreatobiliary carcinoma and one or more apparently visible intra-abdominal lymph nodes. The total number of detected lymph nodes was 143. The remaining 74 patients were excluded from

Table 1 Characteristics of the patients in the primary analysis

Sex (M:F)	68:35	
Median age	65 (35-82)	
Median size (long axis × short axis) (mm)	18 (8-60) × 9 (4-42)	
Final diagnosis (*n*)	Pancreatic carcinoma	67
	Bile duct carcinoma	21
	Gallbladder carcinoma	11
	Ampullary carcinoma	4

analysis because a pancreatobiliary carcinoma and/or apparently visible intra-abdominal lymph nodes were not detected. All 109 patients with apparently visible intra-abdominal lymph node(s) in standard EUS immediately underwent color Doppler EUS, CH-EUS, and EUS-FNA. In six patients (nine lymph nodes; 6.3% of the 143 apparently visible lymph nodes detected by standard EUS), the EUS-FNA samples of lymph nodes were inadequate (4 lymph nodes from 2 patients) and failed because the lymph node was in an inaccessible location (5 lymph nodes from 4 patients) (Figure 1). These patients were excluded from the primary analysis cohort. Nevertheless, among these 6 patients, 3 patients underwent surgical resection, and were included in the secondary analysis cohort (Figure 1). The remaining 103 patients (134 lymph nodes) were included in the primary analysis cohort (Figure 1).

Diagnostic accuracy of standard EUS, color Doppler EUS and CH-EUS in lymph nodes with histological diagnosis obtained by EUS-FNA (primary analysis)

Table 1 displays the characteristics of these 103 patients for the primary analysis cohort. The male: female ratio was 68:35 and the median age was 65 (range: 35-82) years. The median long and short axis lengths of the 134 lymph nodes were 18 (range: 8-60) and 9 (range: 4-42) mm, respectively. The final diagnoses were pancreatic carcinoma (n = 67), bile duct carcinoma (n = 21), gallbladder carcinoma (n = 11), and ampullary carcinoma (n = 4). Standard EUS, color Doppler EUS and CH-EUS were successfully performed in all patients and associated adverse effects were not observed. Of the 134 lymph nodes, histological and/or cytological analyses of the samples obtained by EUS-FNA revealed that 47 were malignant lymph nodes and 87 were reactive lymph nodes. Adverse effects of EUS-FNA were also not observed. All 103 patients were followed up for at least 12 mo. None of the patients who were deemed to have benign lymph nodes after EUS-FNA and the other tests, and who did not undergo surgical resection of the nodes, exhibited any signs of lymph node malignancy during follow-up, as indicated by twice yearly standard EUS.

Standard EUS

ROC analyses revealed that a short axis of 13 mm or longer and a long axis of 20 mm or longer predicted malignancy with the best sensitivity and specificity (Supplementary Figures 1 and 2). A short axis of 13 mm or longer predicted malignancy with a sensitivity, specificity and accuracy of 72% [95% confidence intervals (CI): 62%-81%)], 85% (95%CI: 79%-90%), and 81% (95%CI: 73%-86%), respectively (Table 2). A long axis of 20 mm or longer predicted malignancy with a sensitivity, specificity and accuracy of 72% (95%CI: 61%-82%), 63% (95%CI: 57%-68%), and 66% (95%CI: 59%-73%), respectively (Table 2). A round shape predicted malignancy with a sensitivity, specificity and accuracy of 62% (95%CI: 51%-72%), 75% (95%CI: 69%-80%), and 70% (95%CI: 62%-77%), respectively (Table 2). A sharp edge predicted malignancy with a sensitivity, specificity and accuracy of 81% (95%CI: 71-89%), 30% (95%CI: 24-34%), and 48% (95%CI: 41-53%), respectively (Table 2). Hypoechogenicity predicted malignancy with a sensitivity, specificity and accuracy of 66% (95%CI: 55%-76%), 61% (95%CI: 55%-66%), and 63% (95%CI: 55%-70%), respectively (Table 2). Interobserver agreement testing revealed good (κ coefficient: 0.63, P < 0.01), moderate (κ coefficient: 0.49, P < 0.01), and moderate (κ coefficient: 0.47, P < 0.01) agreement between the two readers in terms of the shape, edge characteristics, and echogenicity measurements, respectively (Supplementary Tables 2-1 to 2-3).

Color Doppler EUS

The absence of a CIV predicted malignancy with a sensitivity, specificity and accuracy of 70% (95%CI: 59%-80%), 72% (95%CI: 66%-78%), and 72% (95%CI: 64%-78%), respectively (Table 2). Interobserver agreement testing revealed good reproducibility between the two readers in terms of this measurement (κ coefficient: 0.69, P < 0.01) (Supplementary Table 2-4).

Contrast-enhanced harmonic EUS

All 134 lymph nodes yielded high-quality dynamic images on CH-EUS. Interobserver agreement testing revealed excellent reproducibility between the two readers in terms of detecting heterogeneous/homogeneous enhancement patterns (κ coefficient: 0.81, P < 0.01) (Supplementary Table 2-5).

Table 3 lists the number and frequency of lesions in the benign and malignant lymph node groups that had a heterogeneous or homogeneous enhancement pattern after reassessment of discrepant findings by the two blinded readers. Of the 47 malignant lymph nodes, 39 (83%) exhibited heterogeneous enhancement in which the distorted tumor vessels could be clearly visualized (Figures 3 and 4, Video 1). Of the 87 benign lymph nodes, 79 (91%) exhibited homogeneous enhancement (Figures 3 and 5, Video 2). The benign and malignant lymph node groups differed significantly in terms of the frequencies of homogeneous and heterogeneous enhancement (P < 0.01). When heterogeneous enhancement was deemed to indicate malignancy and homogeneous

Table 2 Sensitivity, specificity, and accuracy with which CH-endoscopic ultrasonography, color Doppler endoscopic ultrasonography, and the standard endoscopic ultrasonography variables differentiate malignant from benign lymph nodes

	Sensitivity (95%CI)	Specificity (95%CI)	Accuracy (95%CI)	*P* value[1]
Short axis 13 mm or longer	72% (34/47) (62-81)	85% (74/87) (79-90)	81% (108/134) (73-86)	0.27
Long axis 20 mm or longer	72% (34/47) (61-82)	63% (55/87) (57-68)	66% (89/134) (59-73)	0.001
Round shape	62% (29/47) (51-72)	75% (65/87) (69-80)	70% (94/134) (62-77)	0.008
Sharp edge	81% (38/47) (71-89)	30% (26/87) (24-34)	48% (64/134) (41-53)	< 0.001
Hypoechogenicity	66% (31/47) (55-76)	61% (53/87) (55-66)	63% (84/134) (55-70)	< 0.001
CIV absent	70% (33/47) (59-80)	72% (63/87) (66-78)	72% (96/134) (64-78)	0.009
Heterogeneous (CH-EUS)	83% (39/47) (77-89)	91% (79/87) (86-94)	88% (118/134) (82-93)	

[1]Compared with contrast-enhanced harmonic endoscopic ultrasonography (CH-EUS), as determined by McNemar's test. CIV: Central intranodal blood vessel.

Table 3 Number of lymph nodes in the benign and malignant groups that exhibited heterogeneous and homogeneous enhancement on contrast-enhanced harmonic endoscopic ultrasonography

	Number with each enhancement pattern		
Final diagnosis	Heterogeneous	Homogeneous	Total
Malignancy	39	8	47
Benign	8	79	87
Total	47	87	134

enhancement was deemed to indicate benignity, CH-EUS differentiated malignant from benign lymph nodes with a sensitivity, specificity and accuracy of 83% (95%CI: 77%-89%), 91% (95%CI: 86%-94%), and 88% (95%CI: 82%-93%), respectively (Table 2).

Comparison of EUS imaging methods

CH-EUS diagnosed malignant lymph nodes with a significantly higher diagnostic accuracy than most of the standard EUS variables (P = 0.001 *vs* the 20-mm long axis cut-off, P = 0.008 *vs* the round shape variable, P < 0.001 *vs* the sharp edge variable, and P < 0.001 *vs* the hypoechogenicity variable, as determined by McNemar tests) or the color Doppler EUS CIV variable (P = 0.009). However, CH-EUS did not differ significantly from the 13-mm short axis cut-off variable in terms of differentiating malignant from benign lymph nodes (P = 0.27) (Table 2).

Comparison of CH-EUS and EUS-FNA for N-staging in the surgically resected patients (secondary analysis)

Of the 109 patients in whom EUS detected a pancreato-biliary carcinoma and one or more apparently visible intra-abdominal lymph nodes, 48 patients underwent surgical resection and histological examinations of the resected lymph nodes (Figure 1). In addition, three patients whose EUS-FNA samples of lymph nodes were inadequate or failed EUS-FNA because the lymph node was in an inaccessible location underwent surgical resection, and were included in the secondary analysis cohort (Figure 1, Table 4). Thus, the secondary analysis cohort consisted of 51 patients. Comparison of the EUS-FNA and CH-EUS findings relative to surgical specimen histology revealed that six (including failed due to inadequate sampling and inaccessibility) and five of the 51 patients were misdiagnosed by EUS-FNA and CH-EUS, respectively. Thus, EUS-FNA and CH-EUS diagnosed the N-stage in the patients who underwent surgical resection with an accuracy of 88% and 90%, respectively (P = 0.50).

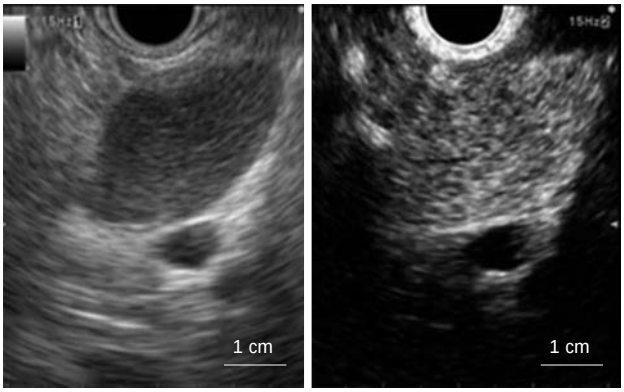

Figure 5 Typical example of a reactive lymph node that shows homogeneous enhancement on contrast-enhanced harmonic endoscopic ultrasonography (left, fundamental B mode; right, contrast harmonic mode).

It should be noted that three patients in the secondary analysis cohort were not included in the primary analysis cohort because EUS-FNA failed due to inadequate sampling or inaccessibility of the lymph nodes. All three patients were correctly N-staged by CH-EUS. One of these three patients was shown by standard and color Doppler EUS to have a long axis of 22 mm, a sharp edge, and to lack a CIV: all of these features predicted that the lymph node was

Table 4 Characteristics of the patients in the secondary analysis

Sex (M:F)	32:19	
Median age	66 (37-79)	
Median size (long axis × short axis) (mm)	20 (8-60) × 10 (4-42)	
Final diagnosis (*n*)	Pancreatic carcinoma	29
	Bile duct carcinoma	12
	Gallbladder carcinoma	7
	Ampullary carcinoma	3

malignant. By contrast, CH-EUS revealed that this lymph node had homogeneous enhancement, which was deemed to indicate a benign lymph node. The patient underwent surgery and indeed, histological examination of the lymph node resected during surgery revealed that it was benign. With regard to the remaining two patients, between two and four of the six standard EUS and color Doppler EUS variables predicted that they were benign. By contrast, CH-EUS revealed that it had heterogeneous enhancement, which was deemed to indicate a malignant lymph node. Indeed, histological examination of the lymph nodes resected during surgery revealed that those lymph nodes were malignant.

DISCUSSION

A study by Gill *et al*[13] identified several morphological characteristics that can be detected by standard EUS that can help to distinguish between malignant and benign lymph nodes. Multivariable analysis revealed that in particular, a round shape, a sharp edge, and a short axis that exceeded 8.3 mm associated significantly with malignant cytology. However, the predictive accuracy of these features was limited. The present study also assessed the ability of a round shape, a sharp edge, hypoechogenicity, a $\geqslant$ 13 mm short axis length, and a $\geqslant$ 20 mm long axis length to distinguish between benign and malignant lymph nodes. However, like Gill *et al*[13], we found that the diagnostic accuracy of these features was limited.

An alternative method is color Doppler EUS. Sawhney *et al*[4] reported that the absence of CIV on color Doppler EUS is a strong and independent predictor of metastatic lymph node. In our study, however, the absence of CIV on color Doppler EUS did not predict malignancy better than the standard EUS variables. This may reflect differences between our study and theirs in terms of the way the lymph nodes were selected: Sawhney *et al*[4] only included lymph nodes that were 10 mm or longer, whereas in the present study, smaller lymph nodes were included (64 had a short axis diameter of less than 10 mm). This difference may relate to the fact that we evaluated all apparently visible lymph nodes found during the standard EUS procedure by color Doppler EUS. Therefore, the lymph nodes evaluated in the current study were relatively smaller than those examined by Sawhney *et al*[4]. Since some small benign lymph nodes may not exhibit CIV, this may have resulted in the relatively lower specificity associated with this variable in our study.

Another alternative method is contrast-enhanced color Doppler EUS with US contrast agent. Kanamori *et al*[15] reported that defective enhancement on contrast-enhanced color Doppler EUS using the first generation US contrast agent Levovist, (Nihon Schering Co., Ltd., Tokyo, Japan) predicted lymph node malignancy significantly more accurately than standard EUS variables. Hocke *et al*[8] also reported that that an irregular appearance of the vessels (or the presence of arterial vessels only) on contrast-enhanced Doppler EUS using the second generation US contrast agent SonoVue (BR1, Bracco, Italy) predicted lymph node malignancy significantly better than standard EUS variables. However, as with the study by Sawhney *et al*[4], the lymph nodes examined in these studies were relatively larger than those in our study.

Recently, the combination of the second generation US contrast agent Sonazoid and low mechanical index imaging techniques has led to CH-EUS being used for perfusion imaging, which facilitates the depiction of tumor vascularity[10,16-18]. Sonazoid resonates with a low acoustic power and thus allows us to perform CH-EUS. We showed previously that this method has an excellent ability to differentiate malignant from benign lesions without Doppler-related artifacts, even when the lesions are small[19]. Heterogeneous enhancement was observed in 39 of 47 (83%) malignant lymph nodes. This is consistent with the observation of a pathology-based study[20] that showed that the vascular architecture of malignant lymph nodes is characterized by caliber fluctuations, an irregular coarse, sinusoid formation, and arteriovenous shunts. In the current study, interobserver agreement regarding CH-EUS results revealed excellent reproducibility between the two readers (κ coefficient: 0.81). Another report also showed that CH-EUS yielded highly reproducible findings with regard to malignant lymph nodes[21]. Indeed, its reproducibility was higher than that of MDCT[22] and all of the standard EUS findings that were measured in the present study. However, it should be noted that in the current study, the readers were experts who had practiced CH-EUS for more than 8 years; each had read the data of more than 500 CH-EUS procedures. It is possible that the reproducibility of CH-EUS findings among beginners may be low, although Gincul *et al*[21] did not detect significant differences between experts and beginners. Fusaroli *et al*[23] also reported that among three parameters (uptake, pattern, and washout) of CH-EUS for solid pancreatic lesion, pancreatic cystic lesion, and submucosal lesion, the reproducibility between experienced and non-experienced endosonographers did not differ significantly. This issue must be validated in future series.

Another alternative method is EUS elastography.

EUS elastography has been presented as a novel technique to assess tissue elasticity and has been used to differentiate between malignant and benign lymph nodes. Several different variables have been used in EUS elastography as a measure of tissue elasticity, namely, color patterns[24-29], strain ratio[30,31], hue histogram analysis[32,33] and artificial neural networks[34,35]. Wei *et al*[36] report a meta-analysis that included seven articles and a large number of lymph nodes (368 patients with 431 lymph nodes). The sensitivity and specificity of EUS elastography for the differential diagnosis of benign and malignant lymph nodes were 88%, and 85%, respectively. The area under the summary receiver operating characteristic curve was 0.9456. However, the sensitivity and specificity of this method varied greatly between studies[36]. Thus, CH-EUS should be compared to EUS elastography in terms of its ability to differentiate malignant from benign lymph nodes in further studies. In addition, it may be useful to evaluate whether these imaging methods could complement each other or other methods.

EUS-FNA is also useful for differentiating malignant from benign lymph nodes. Since EUS-FNA is highly specific in terms of identifying malignant lymph nodes, most cases where EUS-FNA reveals the presence of atypical cells in the lymph nodes have a final diagnosis of malignant lymph node[37]. However, false-positive and false-negative EUS-FNA results remain possible. Jason *et al*[38] report that in their series, the EUS-FNA false-positive and false-negative rates of intra-abdominal lymph node diagnosis were 0.7% and 5.8%, respectively. The present study suffers a limitation in relation to this: we cannot be certain that the EUS-FNA findings of the lymph nodes analyzed in the primary analysis were correct. For this reason, only patients who were followed up for at least 12 mo were included in the primary analysis. None of the patients with apparently benign lymph nodes exhibited signs of lymph node malignancy during this follow-up period.

Another limitation of EUS-FNA is that it cannot be performed in all cases because of intervening vessels and/or the difficult location of the lymph node, which could, for example, lead to an excessively large scope angle or distance from the probe. These problems suggest that CH-EUS technology may complement EUS-FNA-based histological and/or cytological diagnoses. This notion is supported by the four studies that have compared CH-EUS and EUS-FNA previously. All were for pancreatic masses. Napoleon *et al*[39] report that of five adenocarcinomas that had false-negative EUS-FNA results, CH-EUS revealed hypo-enhancement in four. Gincul *et al*[21] also report that all five false-negative EUS-FNA cases were correctly classified by CH-EUS. Moreover, Kitano *et al*[19] report that when CH-EUS was combined with EUS-FNA, the sensitivity of EUS-FNA increased from 92.2% to 100%. Fusaori *et al*[40] also report that CH-EUS increased the detection of malignant pancreatic lesions in difficult cases (patients with chronic pancreatitis or biliary stents) and helped guide EUS-FNA. The present study showed that at least in the patients who underwent surgical resection, CH-EUS and EUS-FNA did not differ in terms of N-staging diagnostic accuracy. However, CH-EUS correctly N-staged three patients in which EUS-FNA sampling failed because of lymph node location or were inadequate. This is the first report to indicate that CH-EUS complements EUS-FNA in terms of N-staging in patients with pancreatobiliary neoplasms.

The present study had some limitations. Multiple lymph nodes in one patient were included in the primary analysis because it was unclear which of these lymph nodes should be sampled; thus, all apparently visible lymph nodes were sampled. This could have introduced a bias in terms of lymph node selection. In addition, EUS-FNA was the gold standard in the primary analysis, even though the accuracy of EUS-FNA may be limited, as discussed above. Histology of resected specimens yields the most accurate diagnosis. However, it is difficult to identify during surgery which lymph nodes were previously evaluated by standard EUS, color Doppler EUS, or CH-EUS. For this reason, EUS-FNA served as the gold standard in the primary analysis.

In conclusion, CH-EUS depicted the microvasculature of intra-abdominal lymph node very clearly. Thus, it may be a useful modality for differentiating malignant from benign lymph nodes in patients with pancreato-biliary carcinomas and may complement standard EUS, color Doppler EUS and EUS-FNA, all of which have limitations. In addition, it may be helpful for determining the lymph nodes that should be subjected to EUS-FNA. In view of the high accuracy described in this study, in the future, CH-EUS may help to detect the in-operable stage better and thereby helps to avoid unnecessary surgery. Hence, CH-EUS will play an important role in determining the optimal treatment of pancreatobiliary carcinomas. However, given that the sample size of this study was relatively small and all CH-EUS procedures were performed in a single medical unit, an additional study that confirms the value of CH-EUS for differentiating malignant from benign lymph nodes is warranted.

COMMENTS

Background

Accurate staging by using the tumor, node and metastasis (TNM) classification system is the most important variable for determining the optimal treatment of pancreatobiliary carcinomas. In particular, since the lymph node stage relates not only to the choice of treatment but also to the prognosis, it is essential that the techniques used for N-staging are reliable.

Research frontiers

A cyto-pathological diagnosis *via* endoscopic ultrasonography (EUS)-fine needle aspiration (FNA) is highly accurate. Noninvasive methods could facilitate EUS-FNA by identifying the target lymph node for EUS-FNA, namely, the lymph node that is most suspicious of malignancy and whose sampling will shape

treatment decisions. Standard EUS can help to distinguish between malignant and benign lymph nodes, although the predictive accuracy of these features was limited. US contrast agents that, when combined with contrast harmonic imaging, make it possible to depict the microvasculature in real time. Recently, EUS was equipped with this novel perfusion imaging technique, thus yielding contrast-enhanced harmonic EUS (CH-EUS).

Innovations and breakthroughs

This is the first study to evaluate the diagnostic accuracy of CH-EUS for differentiating malignant from benign lymph node, compared with standard and color Doppler EUS. CH-EUS was more accurate than standard and color Doppler EUS. Notably, three patients with EUS-FNA failure were correctly N-staged by CH-EUS.

Applications

The results of this study suggest that it may be a useful modality for differentiating malignant from benign lymph nodes in patients with pancreatobiliary carcinomas and may complement EUS-FNA. In addition, it may be helpful for determining the lymph nodes that should be subjected to EUS-FNA. Application of CH-EUS to staging will help patients avoid unnecessary surgery.

Terminology

Color Doppler imaging has several limitations, including blooming, overpainting and motion artifacts. It is also difficult to evaluate perfusion by using color Doppler imaging. This problem was recently overcome by a revolution in US technology, namely, contrast harmonic imaging which makes it possible to depict the microvasculature in real time. Recently, EUS was equipped with this novel perfusion imaging technique, thus yielding CH-EUS.

Peer-review

The authors demonstrated the clinical utility of CH-EUS as a diagnostic tool for detecting lymph node metastasis in patients with pancreatobiliary carcinoma. This paper is informative and interesting for the further developments of imaging approaches.

REFERENCES

1 **Schomas DA**, Quevedo JF, Donahue JM, Nichols FC, Romero Y, Miller RC. The prognostic importance of pathologically involved celiac node metastases in node-positive patients with carcinoma of the distal esophagus or gastroesophageal junction: a surgical series from the Mayo Clinic. *Dis Esophagus* 2010; **23**: 232-239 [PMID: 19515184 DOI: 10.1111/j.1442-2050.2009.00990.x]

2 **Natsugoe S**, Yoshinaka H, Shimada M, Sakamoto F, Morinaga T, Nakano S, Kusano C, Baba M, Takao S, Aikou T. Number of lymph node metastases determined by presurgical ultrasound and endoscopic ultrasound is related to prognosis in patients with esophageal carcinoma. *Ann Surg* 2001; **234**: 613-618 [PMID: 11685023]

3 **Sharma A**, Fidias P, Hayman LA, Loomis SL, Taber KH, Aquino SL. Patterns of lymphadenopathy in thoracic malignancies. *Radiographics* 2004; **24**: 419-434 [PMID: 15026591 DOI: 10.1148/rg.242035075]

4 **Sawhney MS**, Debold SM, Kratzke RA, Lederle FA, Nelson DB, Kelly RF. Central intranodal blood vessel: a new EUS sign described in mediastinal lymph nodes. *Gastrointest Endosc* 2007; **65**: 602-608 [PMID: 17383457 DOI: 10.1016/j.gie.2006.11.057]

5 **Eloubeidi MA**, Wallace MB, Reed CE, Hadzijahic N, Lewin DN, Van Velse A, Leveen MB, Etemad B, Matsuda K, Patel RS, Hawes RH, Hoffman BJ. The utility of EUS and EUS-guided fine needle aspiration in detecting celiac lymph node metastasis in patients with esophageal cancer: a single-center experience. *Gastrointest Endosc* 2001; **54**: 714-719 [PMID: 11726846]

6 **Bhutani MS**, Hawes RH, Hoffman BJ. A comparison of the accuracy of echo features during endoscopic ultrasound (EUS) and EUS-guided fine-needle aspiration for diagnosis of malignant lymph node invasion. *Gastrointest Endosc* 1997; **45**: 474-479 [PMID: 9199903]

7 **Jhala NC**, Jhala DN, Chhieng DC, Eloubeidi MA, Eltoum IA. Endoscopic ultrasound-guided fine-needle aspiration. A cytopathologist's perspective. *Am J Clin Pathol* 2003; **120**: 351-367 [PMID: 14502798 DOI: 10.1309/MFRFJ0XYJLN8NVDP]

8 **Hocke M**, Menges M, Topalidis T, Dietrich CF, Stallmach A. Contrast-enhanced endoscopic ultrasound in discrimination between benign and malignant mediastinal and abdominal lymph nodes. *J Cancer Res Clin Oncol* 2008; **134**: 473-480 [PMID: 17891499 DOI: 10.1007/s00432-007-0309-7]

9 **Quaia E**, Calliada F, Bertolotto M, Rossi S, Garioni L, Rosa L, Pozzi-Mucelli R. Characterization of focal liver lesions with contrast-specific US modes and a sulfur hexafluoride-filled microbubble contrast agent: diagnostic performance and confidence. *Radiology* 2004; **232**: 420-430 [PMID: 15286314 DOI: 10.1148/radiol.2322031401]

10 **Kitano M**, Sakamoto H, Matsui U, Ito Y, Maekawa K, von Schrenck T, Kudo M. A novel perfusion imaging technique of the pancreas: contrast-enhanced harmonic EUS (with video). *Gastrointest Endosc* 2008; **67**: 141-150 [PMID: 18155437 DOI: 10.1016/j.gie.2007.07.045]

11 **Romagnuolo J**, Hoffman B, Vela S, Hawes R, Vignesh S. Accuracy of contrast-enhanced harmonic EUS with a second-generation perflutren lipid microsphere contrast agent (with video). *Gastrointest Endosc* 2011; **73**: 52-63 [PMID: 21184870]

12 **Sontum PC**, Ostensen J, Dyrstad K, Hoff L. Acoustic properties of NC100100 and their relation with the microbubble size distribution. *Invest Radiol* 1999; **34**: 268-275 [PMID: 10196718]

13 **Gill KR**, Ghabril MS, Jamil LH, Hasan MK, McNeil RB, Woodward TA, Raimondo M, Hoffman BJ, Hawes RH, Romagnuolo J, Wallace MB. Endosonographic features predictive of malignancy in mediastinal lymph nodes in patients with lung cancer. *Gastrointest Endosc* 2010; **72**: 265-271 [PMID: 20541192 DOI: 10.1016/j.gie.2010.02.037]

14 **Xia Y**, Kitano M, Kudo M, Imai H, Kamata K, Sakamoto H, Komaki T. Characterization of intra-abdominal lesions of undetermined origin by contrast-enhanced harmonic EUS (with videos). *Gastrointest Endosc* 2010; **72**: 637-642 [PMID: 20646696 DOI: 10.1016/j.gie.2010.04.013]

15 **Kanamori A**, Hirooka Y, Itoh A, Hashimoto S, Kawashima H, Hara K, Uchida H, Goto J, Ohmiya N, Niwa Y, Goto H. Usefulness of contrast-enhanced endoscopic ultrasonography in the differentiation between malignant and benign lymphadenopathy. *Am J Gastroenterol* 2006; **101**: 45-51 [PMID: 16405532 DOI: 10.1111/j.1572-0241.2006.00394.x]

16 **Ding H**, Kudo M, Onda H, Suetomi Y, Minami Y, Maekawa K. Hepatocellular carcinoma: depiction of tumor parenchymal flow with intermittent harmonic power Doppler US during the early arterial phase in dual-display mode. *Radiology* 2001; **220**: 349-356 [PMID: 11477236 DOI: 10.1148/radiology.220.2.r01au07349]

17 **Park BK**, Kim B, Kim SH, Ko K, Lee HM, Choi HY. Assessment of cystic renal masses based on Bosniak classification: comparison of CT and contrast-enhanced US. *Eur J Radiol* 2007; **61**: 310-314 [PMID: 17097844 DOI: 10.1016/j.ejrad.2006.10.004]

18 **Kitano M**, Kamata K, Imai H, Miyata T, Yasukawa S, Yanagisawa A, Kudo M. Contrast-enhanced harmonic endoscopic ultrasonography for pancreatobiliary diseases. *Dig Endosc* 2015; **27** Suppl 1: 60-67 [PMID: 25639788 DOI: 10.1111/den.12454]

19 **Kitano M**, Kudo M, Yamao K, Takagi T, Sakamoto H, Komaki T, Kamata K, Imai H, Chiba Y, Okada M, Murakami T, Takeyama Y. Characterization of small solid tumors in the pancreas: the value of contrast-enhanced harmonic endoscopic ultrasonography. *Am J Gastroenterol* 2012; **107**: 303-310 [PMID: 22008892 DOI: 10.1038/ajg.2011.354]

20 **Shubik P**. Vascularization of tumors: a review. *J Cancer Res Clin Oncol* 1982; **103**: 211-226 [PMID: 6181069]

21 **Gincul R**, Palazzo M, Pujol B, Tubach F, Palazzo L, Lefort C, Fumex F, Lombard A, Ribeiro D, Fabre M, Hervieu V, Labadie M, Ponchon T, Napoléon B. Contrast-harmonic endoscopic ultrasound for the diagnosis of pancreatic adenocarcinoma: a prospective

multicenter trial. *Endoscopy* 2014; **46**: 373-379 [PMID: 24532350 DOI: 10.1055/s-0034-1364969]
22 **Kim JH**, Eun HW, Kim KW, Lee JY, Lee JM, Han JK, Choi BI. Intraductal papillary mucinous neoplasms with associated invasive carcinoma of the pancreas: imaging findings and diagnostic performance of MDCT for prediction of prognostic factors. *AJR Am J Roentgenol* 2013; **201**: 565-572 [PMID: 23971447 DOI: 10.2214/AJR.12.9511]
23 **Fusaroli P**, Kypraios D, Mancino MG, Spada A, Benini MC, Bianchi M, Bocus P, De Angelis C, De Luca L, Fabbri C, Grillo A, Marzioni M, Reggio D, Togliani T, Zanarini S, Caletti G. Interobserver agreement in contrast harmonic endoscopic ultrasound. *J Gastroenterol Hepatol* 2012; **27**: 1063-1069 [PMID: 22414180 DOI: 10.1111/j.1440-1746.2012.07115.x]
24 **Giovannini M**, Hookey LC, Bories E, Pesenti C, Monges G, Delpero JR. Endoscopic ultrasound elastography: the first step towards virtual biopsy? Preliminary results in 49 patients. *Endoscopy* 2006; **38**: 344-348 [PMID: 16680632 DOI: 10.1055/s-2006-925158]
25 **Janssen J**, Schlörer E, Greiner L. EUS elastography of the pancreas: feasibility and pattern description of the normal pancreas, chronic pancreatitis, and focal pancreatic lesions. *Gastrointest Endosc* 2007; **65**: 971-978 [PMID: 17531630 DOI: 10.1016/j.gie.2006.12.057]
26 **Giovannini M**, Thomas B, Erwan B, Christian P, Fabrice C, Benjamin E, Geneviève M, Paolo A, Pierre D, Robert Y, Walter S, Hanz S, Carl S, Christoph D, Pierre E, Jean-Luc VL, Jacques D, Peter V, Andrian S. Endoscopic ultrasound elastography for evaluation of lymph nodes and pancreatic masses: a multicenter study. *World J Gastroenterol* 2009; **15**: 1587-1593 [PMID: 19340900 DOI: 10.3748/wjg.15.1587]
27 **Iglesias-Garcia J**, Larino-Noia J, Abdulkader I, Forteza J, Dominguez-Munoz JE. EUS elastography for the characterization of solid pancreatic masses. *Gastrointest Endosc* 2009; **70**: 1101-1108 [PMID: 19647248 DOI: 10.1016/j.gie.2009.05.011]
28 **Itokawa F**, Itoi T, Sofuni A, Kurihara T, Tsuchiya T, Ishii K, Tsuji S, Ikeuchi N, Umeda J, Tanaka R, Yokoyama N, Moriyasu F, Kasuya K, Nagao T, Kamisawa T, Tsuchida A. EUS elastography combined with the strain ratio of tissue elasticity for diagnosis of solid pancreatic masses. *J Gastroenterol* 2011; **46**: 843-853 [PMID: 21505859 DOI: 10.1007/s00535-011-0399-5]
29 **Hocke M**, Ignee A, Dietrich CF. Advanced endosonographic diagnostic tools for discrimination of focal chronic pancreatitis and pancreatic carcinoma--elastography, contrast enhanced high mechanical index (CEHMI) and low mechanical index (CELMI) endosonography in direct comparison. *Z Gastroenterol* 2012; **50**: 199-203 [PMID: 22298098 DOI: 10.1055/s-0031-1281824]
30 **Larsen MH**, Fristrup CW, Mortensen MB. Intra- and interobserver agreement of endoscopic sonoelastography in the evaluation of lymph nodes. *Ultraschall Med* 2011; **32** Suppl 2: E45-E50 [PMID: 22194049 DOI: 10.1055/s-0031-1273493]
31 **Iglesias-Garcia J**, Larino-Noia J, Abdulkader I, Forteza J, Dominguez-Munoz JE. Quantitative endoscopic ultrasound elastography: an accurate method for the differentiation of solid pancreatic masses. *Gastroenterology* 2010; **139**: 1172-1180 [PMID: 20600020 DOI: 10.1053/j.gastro.2010.06.059]
32 **Dawwas MF**, Taha H, Leeds JS, Nayar MK, Oppong KW. Diagnostic accuracy of quantitative EUS elastography for discriminating malignant from benign solid pancreatic masses: a prospective, single-center study. *Gastrointest Endosc* 2012; **76**: 953-961 [PMID: 22854060 DOI: 10.1016/j.gie.2012.05.034]
33 **Săftoiu A**, Iordache SA, Gheonea DI, Popescu C, Maloş A, Gorunescu F, Ciurea T, Iordache A, Popescu GL, Manea CT. Combined contrast-enhanced power Doppler and real-time sonoelastography performed during EUS, used in the differential diagnosis of focal pancreatic masses (with videos). *Gastrointest Endosc* 2010; **72**: 739-747 [PMID: 20674916 DOI: 10.1016/j.gie.2010.02.056]
34 **Săftoiu A**, Vilmann P, Gorunescu F, Janssen J, Hocke M, Larsen M, Iglesias-Garcia J, Arcidiacono P, Will U, Giovannini M, Dietrich C, Havre R, Gheorghe C, McKay C, Gheonea DI, Ciurea T. Accuracy of endoscopic ultrasound elastography used for differential diagnosis of focal pancreatic masses: a multicenter study. *Endoscopy* 2011; **43**: 596-603 [PMID: 21437851 DOI: 10.1055/s-0030-1256314]
35 **Săftoiu A**, Vilmann P, Gorunescu F, Gheonea DI, Gorunescu M, Ciurea T, Popescu GL, Iordache A, Hassan H, Iordache S. Neural network analysis of dynamic sequences of EUS elastography used for the differential diagnosis of chronic pancreatitis and pancreatic cancer. *Gastrointest Endosc* 2008; **68**: 1086-1094 [PMID: 18656186 DOI: 10.1016/j.gie.2008.04.031]
36 **Xu W**, Shi J, Zeng X, Li X, Xie WF, Guo J, Lin Y. EUS elastography for the differentiation of benign and malignant lymph nodes: a meta-analysis. *Gastrointest Endosc* 2011; **74**: 1001-109; quiz 1001-109; [PMID: 22032315 DOI: 10.1016/j.gie.2011.07.026]
37 **Srinivasan R**, Bhutani MS, Thosani N, Săftoiu A, Rice DC, Ioncică AM, Eapen GA, Gupta P, Jaganmohan S, Artifon EL, Zwischenberger JB. Clinical impact of EUS-FNA of mediastinal lymph nodes in patients with known or suspected lung cancer or mediastinal lymph nodes of unknown etiology. *J Gastrointestin Liver Dis* 2012; **21**: 145-152 [PMID: 22720302]
38 **Korenblit J**, Anantharaman A, Loren DE, Kowalski TE, Siddiqui AA. The role of endoscopic ultrasound-guided fine needle aspiration (eus-fna) for the diagnosis of intra-abdominal lymphadenopathy of unknown origin. *J Interv Gastroenterol* 2012; **2**: 172-176 [PMID: 23687604 DOI: 10.4161/jig.23742]
39 **Napoleon B**, Alvarez-Sanchez MV, Gincoul R, Pujol B, Lefort C, Lepilliez V, Labadie M, Souquet JC, Queneau PE, Scoazec JY, Chayvialle JA, Ponchon T. Contrast-enhanced harmonic endoscopic ultrasound in solid lesions of the pancreas: results of a pilot study. *Endoscopy* 2010; **42**: 564-570 [PMID: 20593334 DOI: 10.1055/s-0030-1255537]
40 **Fusaroli P**, Spada A, Mancino MG, Caletti G. Contrast harmonic echo-endoscopic ultrasound improves accuracy in diagnosis of solid pancreatic masses. *Clin Gastroenterol Hepatol* 2010; **8**: 629-34.e1-2 [PMID: 20417721 DOI: 10.1016/j.cgh.2010.04.012]

P- Reviewer: Arigami T, Hardt PD, Lee CL, Li YM **S- Editor**: Yu J
L- Editor: A **E- Editor**: Zhang DN

Published by **Baishideng Publishing Group Inc**
8226 Regency Drive, Pleasanton, CA 94588, USA
Telephone: +1-925-223-8242
Fax: +1-925-223-8243
E-mail: bpgoffice@wjgnet.com
Help Desk: http://www.wjgnet.com/esps/helpdesk.aspx
http://www.wjgnet.com

ISSN 1007-9327

J Med Ultrasonics (2016) 43:163
DOI 10.1007/s10396-015-0691-8

EDITORIAL ANNOUNCEMENT

Inclusion of Journal of Medical Ultrasonics in MEDLINE

Masatoshi Kudo[1] · **Hiroshi Kanai**[2]

To our members,

Our English-language Journal of Medical Ultrasonics will finally be included in MEDLINE.[1] It will be indexed in PubMed (see footnote 1) beginning with vol. 42 (2015). We are also making arrangements to have past English editions [vol. 28 (2001) to vol. 41 (2014)] included in MEDLINE.

In addition to reporting this news, we would also like to express our gratitude to all those involved for their efforts to get to this point and to all the members who helped increase the number of quality papers published. Thanks to you, the number of papers published in 2015 increased greatly to 88 papers, as compared to 31 papers in 2005 and 35 papers in 2010. It should be noted that quality is being ensured, with the acceptance rate in 2015 being 39 %, versus 95 % in 2005 and 61 % in 2010.

The Editorial Committee plans to step up its efforts, and we would like to ask our members to continue to submit the valuable results of your research.

Masatoshi Kudo, President
Hiroshi Kanai, Editor-in-Chief
The Japan Society of Ultrasonics in Medicine

✉ Hiroshi Kanai
kanai@ecei.tohoku.ac.jp

[1] Department of Gastroenterology and Hepatology, Kinki University School of Medicine, Osaka, Japan

[2] Graduate School of Engineering and Biomedical Engineering, Tohoku University, Miyagi, Japan

[1] Provided by the US National Library of Medicine (NLM), MEDLINE is the world's most widely used online database that indexes biomedical articles. PubMed is a free online service for retrieving MEDLINE data (http://pubmed.gov).

Histologic diagnosis of pancreatic masses using 25-gauge endoscopic ultrasound needles with and without a core trap: a multicenter randomized trial

Authors Ken Kamata[1], Masayuki Kitano[1], Satoru Yasukawa[2], Masatoshi Kudo[1], Yasutaka Chiba[3], Takeshi Ogura[4], Kazuhide Higuchi[4], Nobuyasu Fukutake[5], Reiko Ashida[5], Tomoaki Yamasaki[6], Hiroko Nebiki[6], Satoru Hirose[7], Noriyuki Hoki[7], Masanori Asada[8], Shujiro Yazumi[8], Makoto Takaoka[9], Kazuichi Okazaki[9], Fumihiro Matsuda[10], Yoshihiro Okabe[10], Akio Yanagisawa[2]

Institutions Institutions are listed at end of article.

submitted 8. May 2015
accepted after revision 23. February 2016

Bibliography
DOI http://dx.doi.org/10.1055/s-0042-106294
Published online: 29.4.2016
Endoscopy 2016; 48: 632–638

ISSN 0013-726X

Corresponding author
Masayuki Kitano, MD
Department of Gastroenterology and Hepatology
Kinki University School of Medicine
377-2 Ohno-higashi
Osaka-sayama 589-8511
Japan
m-kitano@med.kindai.ac.jp

Background and study aims: Endoscopic ultrasound-guided fine needle aspiration (EUS-FNA) with 25-gauge needles yields small volume samples that are mainly processed for cytology. Using 25-gauge needles with a core trap may overcome this limitation. This trial compared 25-gauge needles with and without a core trap in terms of their ability to obtain histologic samples from solid pancreatic masses.

Patients and methods: Consecutive patients with solid pancreatic masses who presented to eight Japanese referral centers for EUS-FNA in April–September 2013 were randomized to undergo sampling with a 25-gauge needle with a core trap (ProCore) or a standard 25-gauge needle. Tissue samples were fixed in formalin and processed for histologic evaluation. For the purpose of this study only samples obtained with the first needle pass were used for comparison of: (i) accuracy for the diagnosis of malignancy, (ii) rate of samples with preserved tissue architecture adequate for histologic evaluation, and (iii) sample cellularity.

Results: A total of 214 patients were enrolled. Compared to the first pass with a standard needle (n = 108), the first pass with the ProCore needle (n = 106) provided samples that were more often adequate for histologic evaluation (81.1% vs. 69.4%; $P = 0.048$) and had superior cellularity (rich/moderate/poor, 36%/27%/37% vs. 19%/26%/55%; $P = 0.003$). There were no significant differences between the two needles in sensitivity (75.6% vs. 69.0%, $P = 0.337$) and accuracy (79.2% vs. 75.9%, $P = 0.561$) for the diagnosis of malignancy.

Conclusions: In patients with solid pancreatic masses, a 25-gauge EUS-FNA needle with a core trap provides histologic samples of better quality than a standard 25-gauge needle. There was no difference in accuracy for the diagnosis of malignancy between the needles.

Clinical trial number: UMIN000010021.

Introduction

Endoscopic ultrasound (EUS)-guided fine needle aspiration (FNA) was developed for the pathologic diagnosis of lesions in and adjacent to the digestive tract [1]. In the setting of solid pancreatic masses, EUS-FNA has a diagnostic sensitivity of 54%–96%, a specificity of 96%–98%, and an accuracy of 83%–95% [2–5].

Several studies have shown that compared to 22-gauge and 19-gauge needles, 25-gauge needles are more maneuverable (particularly when difficult regions have to be accessed), can penetrate the mass more easily, and are less likely to yield samples contaminated with blood [6–9]. Moreover, a recently published meta-analysis showed that a 25-gauge FNA needle was more sensitive than a 22-gauge FNA needle for diagnosing solid pancreatic tumors (pooled sensitivity, 93% vs. 85%, respectively) [10]. However, this superiority was only true for cytology-based diagnoses: the 25-gauge needle was inferior to the 22-gauge needle in terms of the accuracy of histology-based diagnosis [11]. This probably reflects the fact that 25-gauge needles usually generate smaller sample volumes than 22-gauge and 19-gauge needles [12]. Rapid on-site evaluation (ROSE) is needed to confirm that the EUS-FNA samples are satisfactory for pathologic diagnosis and to decrease the number of passes, although it is controversial whether ROSE impacts on diagnostic accuracy [13,14].

In order to decrease the number of passes, the adequacy of the sample obtained by each pass needs to be improved. To achieve this, a needle with a core trap was recently developed [15–20]. Compared with the standard needle, the needle with a core trap reduced the number of passes needed to establish a diagnosis, particularly a histology-based diagnosis; however, the diagnostic accuracy and diagnostic yield of the two needles were not significantly different [17,19]. A retro-

spective study focused on the utility of the 25-gauge needle with a core trap and showed excellent cytology-based diagnostic yield for a single pass [20].

The aim of this prospective multicenter randomized controlled trial was to compare the novel 25-gauge needle with a core trap to a standard 25-gauge needle in terms of their ability to provide samples with preserved tissue architecture adequate for histologic evaluation and diagnosis in patients with pancreatic masses.

Patients and methods

Study design and patient enrollment

This multicenter parallel-arm randomized study was approved by the Institutional Review Board of each participating hospital. All patients provided written informed consent. The trial was registered by the University hospital Medical Information Network: number UMIN000010021.

All consecutive patients with solid pancreatic masses who presented to eight referral centers in Japan for EUS-FNA between April and September 2013 were prospectively enrolled through a designated website. Patients were included if they had a solid pancreatic mass as shown by imaging modalities, had no severe comorbidities, required a pathologic diagnosis to determine their treatment, and provided written informed consent. Patients were excluded from the study if they had a high risk of bleeding or did not provide informed consent. An EUS was performed to check for interposing vessels and problems with tumor visualization prior to randomization. Patients in whom such issues were found were also excluded from the study.

The included patients were randomly assigned to two groups with a 1:1 ratio using a random number generator. One group underwent EUS-FNA with the novel 25-gauge needle with a core trap (EchoTip ProCore, Cook Medical, Bloomington, Indiana, USA), while the other group underwent EUS-FNA with a standard 25-gauge needle (EchoTip Ultra, Cook Medical). The two groups were designated as the ProCore and standard needle groups, respectively.

Outcome measures

For the purpose of this study, only samples obtained with the first needle pass were analyzed and used for comparisons of: (i) accuracy for the diagnosis of malignancy (primary outcome), (ii) rate of samples with preserved tissue architecture adequate for histologic evaluation, and (iii) sample cellularity (secondary outcomes).

EUS-FNA technique

EUS-FNA was performed using a linear array echoendoscope (GF-UCT 240 or GF-UCT 260, Olympus Optical, Tokyo, Japan; or EG-530UT2, FUJIFILM, Tokyo, Japan) with the patient under conscious sedation.

The same EUS-FNA technique was used in both groups. After the mass had been punctured, the stylet was slowly pulled out without suction (i.e. the slow-pull technique) while fanning the needle 20 times to and fro within the lesion. Samples were expelled into formalin bottles with the stylet and were processed for histologic analysis; ROSE was not performed. The sample was not split for cytologic, cell block, and histologic examination. To ensure that each patient would receive an accurate diagnosis, additional needle passes were then performed until the endosonographer felt that a sufficient sample had been obtained. Because these additional passes were not analyzed in this study, a technique different from that described above for the first pass could be used.

Tissue processing and histologic assessment

All formalin-fixed samples were brought to one designated facility 1 day after harvest and were processed for histologic evaluation. The same technique was used with each sample (**Fig. 1**). The entire formalin-fixed sample was spread onto a mesh sheet and stained by mercurochrome for easy recognition during processing. The samples were then dehydrated and embedded in paraffin. After the block had been cooled slightly, the mesh sheet was removed to yield the completed paraffin block. Ten slides bearing serial sections were prepared, two of which were stained with hematoxylin and eosin (H&E), the remaining eight slides being stained immunohistochemically.

Two pathologists (S.Y. and A.Y.), blinded to the type of needle used, independently assessed all samples for: (i) cellularity, (ii) preservation of tissue architecture, and (iii) histologic diagnosis. Sample cellularity was classified as rich (≥5000 cells), moderate (100–5000 cells), or poor (<100 cells) (**Fig.2**). The pathologists conferred until a consensus was reached. The pathologists responsible for this study had experience of examining cytology and histology in more than 1000 EUS-FNA cases.

Final diagnosis

In patients who underwent surgical resection of the mass, the final diagnosis was based on surgical pathology. Patients who did not undergo surgical resection were followed up for at least 12 months with ultrasound, computed tomography (CT), magnetic resonance imaging (MRI), and/or EUS every 2–6 months or until their time of death.

Patients were diagnosed with malignant disease if metastatic lesions were identified during imaging examinations, there were signs of disease progression, and/or malignant EUS-FNA results were obtained after the additional passes (the EUS-FNA results of the first pass were not used to determine the final diagnosis). Non-resected patients who did not display these imaging features during follow-up and had no EUS-FNA results suggesting malignancy after additional passes were diagnosed as having benign disease.

Serous cyst neoplasm, neuroendocrine tumor (NET) G1, NET G2, and solid pseudopapillary neoplasm (SPN) were considered benign, whereas pancreatic carcinoma, NET G3, lymphoma, and metastases to the pancreas were considered malignant.

Statistical analysis

On the basis of previous reports [12, 19], it was estimated that the diagnostic accuracy (the primary outcome) would be 80% and 60% in the ProCore and standard needle groups, respectively. Normal approximation revealed that given this difference, a type I error of 0.05, and power of 80%, a sample of 100 patients per group would be required. Assuming a 5% drop-out rate, a target sample size of 210 patients was established.

The two groups were compared in terms of categorical and continuous variables using the chi-squared test (unless any expected value was less than 5, in which case Fisher's exact test was used) and *t* test (unless a Kolmogorov-Smirnov test indicated that the variable was not normally distributed, in which case a Wilcoxon's rank sum test was used), respectively. For the evaluation of sample cellularity, the Cochran-Armitage test was used. The Bre-

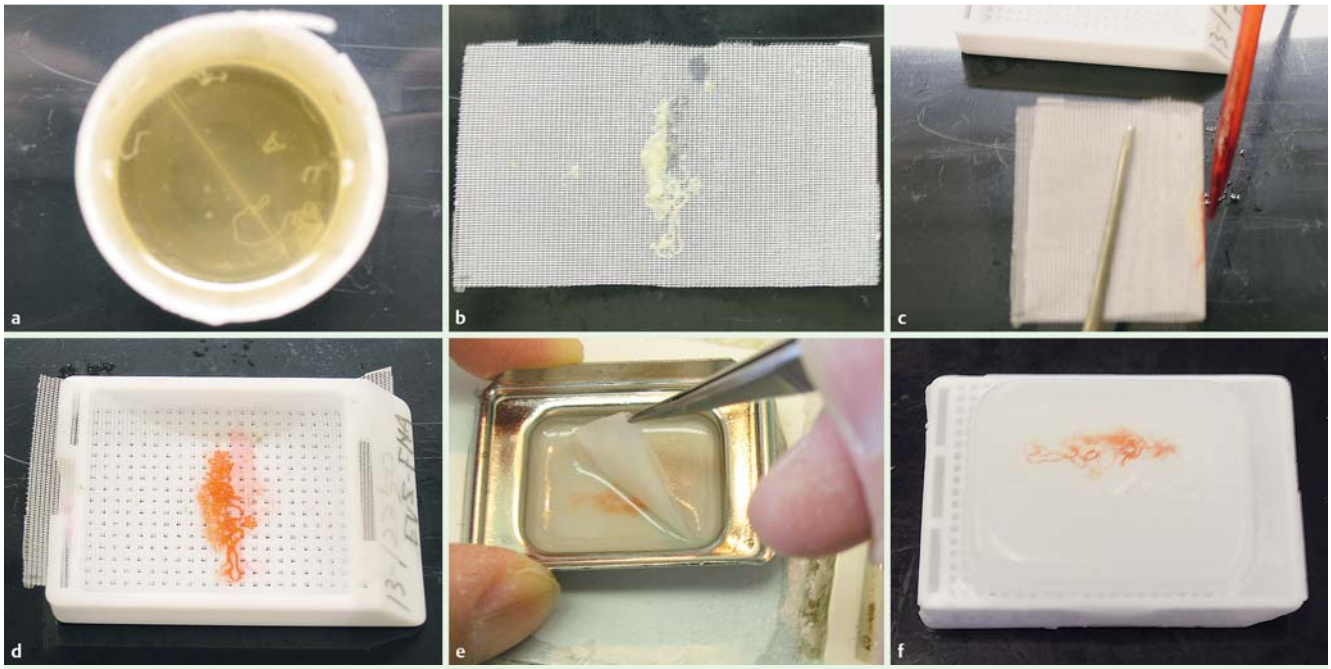

Fig. 1 The processing of samples for histologic evaluation. **a** Samples from endoscopic ultrasound-guided fine needle aspiration were inserted into formalin bottles; **b** the whole sample was spread onto a mesh sheet; **c** the sample was stained by mercurochrome for easy recognition during processing; **d** it was dehydrated and embedded in paraffin; **e** the mesh sheet was removed after the block had been allowed to cool slightly. **f** The completed paraffin block.

slow–Day test for the homogeneity of the odds ratios was performed prior to performing subgroup analysis. All statistical analyses were performed using SAS software version 9.1 (SAS Institute, Cary, North Carolina, USA).

Results

Fig. 3 shows the study flow chart. Of the 225 consecutive patients with a pancreatic mass who presented for EUS-FNA during the study period, 214 patients were enrolled, while 11 were excluded for the following reasons: no informed consent (n=7), high risk of bleeding (n=2), intervening vessels in the puncture route (n=1), and poor visualization of the tumor on EUS (n=1). A total of 106 and 108 patients were randomized into the ProCore and standard needle groups, respectively. The groups did not differ significantly in terms of their demographic characteristics, mean tumor size, and puncture site (**Table 1**).

Table 2 shows the patients' final diagnoses. These diagnoses were based on histologic examination of resected specimens in 61 patients, and on the clinical course/imaging analyses undertaken during follow-up in combination with EUS-FNA results of additional passes in 153 patients. The median follow-up period of those patients followed up was 358 days (range, 10–801 days). The ProCore and standard needle groups did not differ significantly in the number of patients with final diagnoses of pancreatic adenocarcinoma (78% and 72%, respectively; $P=0.303$) and pancreatic malignancy (85% and 78%, respectively; $P=0.181$).

There were no significant complications during or after the EUS-FNA procedure in either group.

The technical success rate (i.e. the successful puncture of the pancreatic mass on the first pass) in both groups was 100%. **Table 3** shows data on the quality of samples obtained in both groups. When compared with the standard needle, the first pass with the ProCore needle provided samples with preserved tissue architecture that were adequate for histologic evaluation significantly more frequently (81.1% vs. 69.4%; $P=0.048$). Analysis of subgroups of patients punctured from the stomach and duodenum did not show significant differences between the groups.

The cellularity of samples obtained with the ProCore needle was significantly superior to the cellularity of samples obtained with the standard needle (rich/moderate/poor cellularity, 36%/27%/37% vs. 19%/26%/55%; $P=0.003$; **Table 3**). **Table 4** shows the performance characteristics of the first pass for the diagnosis of malignancy. No statistically significant differences in accuracy were found in either the analysis of all 214 patients or in the subgroup of 161 patients with samples adequate for histologic evaluation.

The two pathologists differed in their view of whether there were adequate architectural features for diagnostic histology in five patients. Therefore, the agreement for this variable was 97.7% and the *kappa* statistic was 93.9%. The two pathologists also differed in terms of the diagnosis of malignancy in 10 patients, giving an agreement of 95.3% and *kappa* statistic of 90.5% for this variable.

Discussion

The present study showed that in patients with a solid pancreatic mass, the first-pass samples obtained with the novel 25-gauge EUS-FNA needle with a core trap had a significantly better quality than the samples obtained with the standard 25-gauge needle, both in terms of sample cellularity and the rate of samples with preserved tissue architecture that permitted histologic evaluation. However, there was no significant difference between the two needles in terms of their diagnostic accuracy for the diagnosis of malignancy.

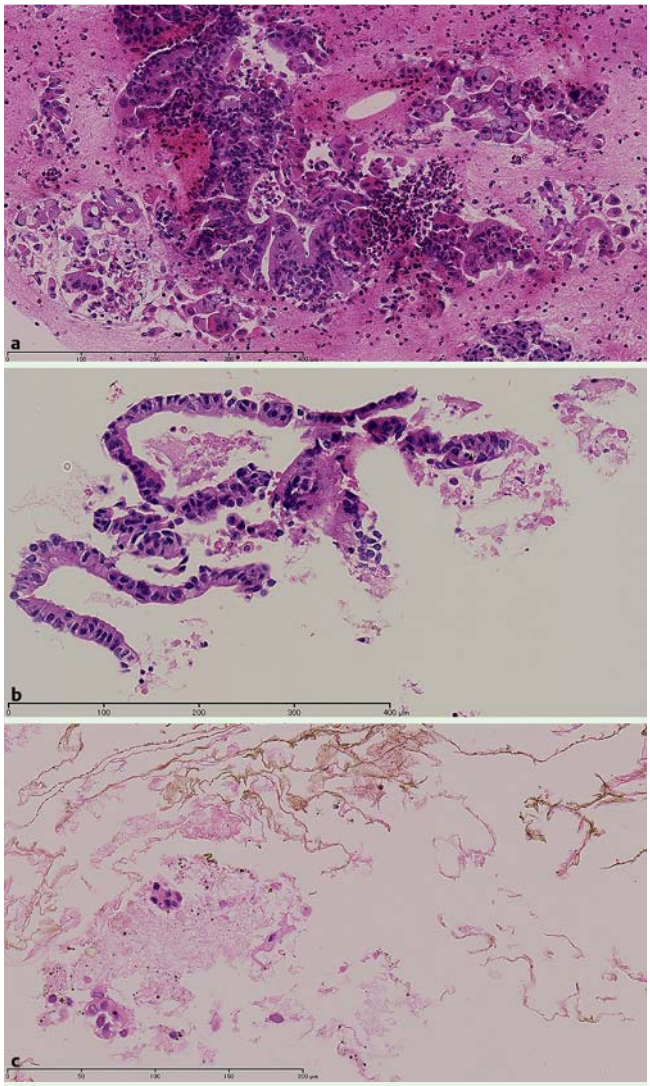

Fig. 2 Histologic views showing examples of different sample cellularities: **a** rich; **b** moderate; and **c** poor.

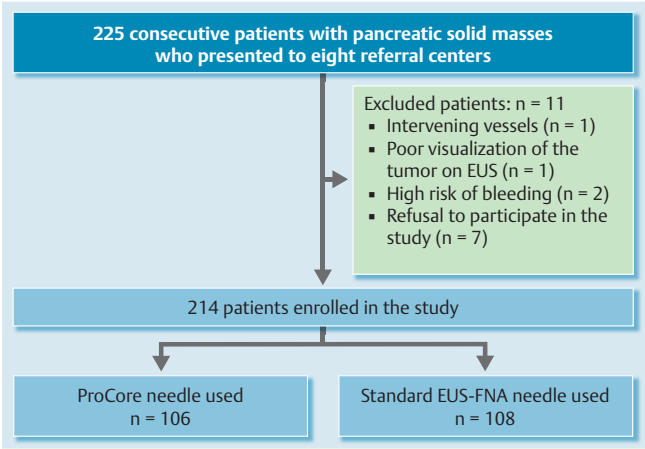

Fig. 3 Study flow chart. EUS-FNA, endoscopic ultrasound-guided fine needle aspiration.

Several studies have compared the performances of EUS-FNA needles with and without a core trap. Hucl et al. [17] reported that in patients with pancreatic masses or lymphadenopathy, less needle passes were required to establish the diagnosis with the 22-gauge core needle than with the standard 22-gauge needle; however, the diagnostic accuracy of both needles was similar. Similarly, a randomized trial comparing a 22-gauge aspiration needle with a 22-gauge core-trap needle in 56 patients with solid pancreatic mass lesions revealed no significant differences in endpoints such as median number of passes required to establish the diagnosis, rates of diagnostic sufficiency, procurement of the histologic core, or the presence of diagnostic histologic specimens [18]. Increasing the number of passes from one to two and three did not significantly increase the sample adequacy and diagnostic accuracy.

Lee et al. [19] also found that compared to a standard 22-gauge or 25-gauge needle, a 22-gauge or 25-gauge ProCore needle did not improve the overall diagnostic accuracy in pancreatic malignancy. However, the ProCore needles did yield higher diagnostic accuracy and sensitivity when the samples were subjected to on-site cytology with the Diff-Quik stain. They also allowed more patients to be diagnosed with malignancy on the first pass.

The advantages of our study include the fact that all of the samples were first-pass samples that were obtained by the same procedure, namely, the slow-pull technique. This technique was used in this study because it is associated with less contamination with blood and results in a higher diagnostic yield when a smaller (25-gauge or 22-gauge) core biopsy needle is used [20, 21]. This is also observed when slow-pull aspiration with a standard 25-gauge EUS-FNA needle is followed by either histologic diagnosis or cytology [22]. Other advantages of our study are that all of the samples were subjected to histologic analysis in a single facility staffed by experienced pathologists, all subjects were consecutive and randomized, and the pathologists were blinded to the type of needle used. Therefore, the study design prevented selection and information bias.

In our study, we found that the first pass of the 25-gauge ProCore needle detected malignancy with a sensitivity of 75.6%. By contrast, Iwashita et al. [20] found that after a single pass with a 25-gauge core biopsy needle, histology detected malignancy in solid pancreatic lesions with a sensitivity of only 63%, although it increased to 87% after four passes (by contrast, cytologic analysis detected malignancy with a sensitivity of 83% after one pass). It has been reported that seven passes are optimal for EUS-FNA of pancreatic lesions in terms of obtaining a correct diagnosis: the diagnostic sensitivity of this approach is 83% [23]. However, the high quality of the tissue obtained by a single pass with the 25-gauge ProCore needle in the present study suggests that fewer passes may be needed when this needle is used.

In our study, the technical success rates with the 25-gauge ProCore and standard needles were both 100%, even though the transduodenal approach was used in 43% (n=93) of the patients. Moreover, the 25-gauge EUS-FNA ProCore needle yielded first-pass samples that retained architectural features in 81.1% of the patients, and the overall diagnostic accuracy with the ProCore needle was 79.2%.

In contrast, Iglesias-Garcia et al. [15] found that EUS-FNA with a 19-gauge core biopsy needle did not yield adequate samples in 2 of their 35 patients with intraintestinal and extraintestinal masses who underwent EUS-FNA via the transduodenal approach. However, the 25-gauge core biopsy needle acquired adequate histologic samples less frequently than the 19-gauge core biopsy needle and its diagnostic accuracy was also lower. Similarly, Sakamoto et al. [11] found that EUS-guided 19-gauge Trucut needle biopsy followed by histologic analysis had an accuracy of 83.3%,

Table 1 Baseline characteristics of the 214 patients with pancreatic masses who underwent endoscopic ultrasound-guided fine needle aspiration.

	ProCore needle (n = 106)	Standard needle (n = 108)	*P* value
Age, median (range), years	68 (43–90)	67 (34–89)	0.660
Sex, male : female, n	53 : 53	59 : 49	0.498
Tumor size, mean ± SD, mm	29.3 ± 15.6	27.9 ± 14.4	0.530
Puncture site, stomach : duodenum, n	56 : 50	65 : 43	0.278

SD, standard deviation.

Table 2 Final diagnoses of the 214 patients with pancreatic masses who underwent endoscopic ultrasound-guided fine needle aspiration.

	ProCore needle (n = 106)	Standard needle (n = 108)	*P* value*
Malignant disease, n (%)	90 (85 %)	84 (78 %)	0.181
Adenocarcinoma	83	78	0.303
Neuroendocrine tumor (grade 3)	2	0	
Metastatic cancer	2	4	
Acinar cell carcinoma	2	0	
Malignant lymphoma	1	0	
Intraductal papillary mucinous carcinoma	0	1	
Cholangiocarcinoma	0	1	
Benign disease, n (%)	16 (15 %)	24 (22 %)	
Chronic pancreatitis	4	8	
Autoimmune pancreatitis	4	6	
Neuroendocrine tumor (grade 1 or 2)	6	6	
Solid pseudopapillary neoplasm	0	2	
Serous cyst neoplasm	2	2	

* *P* value for comparison of the frequencies of diagnoses in both groups of malignant/benign and adenocarcinoma/other disease.

Table 3 Quality of histologic samples obtained at the first needle pass.

	ProCore needle (n = 106)	Standard needle (n = 108)	*P* value
Technical success rate	100 % (106/106)	100 % (108/108)	1.000
Rate of samples adequate for histologic evaluation			
All patients, n = 214	81.1 % (86/106)	69.4 % (75/108)	0.048
Puncture from the stomach, n = 121	76.8 % (43/56)	70.8 % (46/65)	*
Puncture from the duodenum, n = 93	86.0 % (43/50)	67.4 % (29/43)	*
Sample cellularity			
Rich (≥ 5000 cells)	36 % (38/106)	19 % (21/108)	0.003
Moderate (100 – 5000 cells)	27 % (29/106)	26 % (28/108)	
Poor (< 100 cells)	37 % (39/106)	55 % (59/108)	

* Subgroup comparisons were not performed because a Breslow – Day test for homogeneity of the odds ratios was not significant (*P* = 0.2445).

Table 4 Performance characteristics for the diagnosis of malignancy based on histologic evaluation of samples obtained at the first needle pass.

	All samples, n = 214			Samples adequate for histologic evaluation, n = 161		
	ProCore needle (n = 106)	Standard needle (n = 108)	*P* value	ProCore needle (n = 86)	Standard needle (n = 75)	*P* value
Sensitivity (95 %CI)	75.6 % (68/90) (72.4 %–75.6 %)	69.0 % (58/84) (65.5 %–69.0 %)	0.34	89.5 % (68/76) (86.3–89.5)	93.5 % (58/62) (89.8–93.5)	0.55
Specificity (95 %CI)	100 % (16/16) (82.5 %–100 %)	100 % (24/24) (87.7 %–100 %)	1.00	100 % (10/10) (75.8 %–100 %)	100 % (13/13) (81.9 %–100 %)	1.00
PPV (95 %CI)	100 % (68/68) (82.5 %–100 %)	100 % (58/58) (94.9 %–100 %)	1.00	100 % (68/68) (96.4 %–100 %)	100 % (58/58) (95.9 %–100 %)	1.00
NPV (95 %CI)	42.1 % (16/38) (34.7 %–42.1 %)	48.0 % (24/50) (42.1 %–48.0 %)	0.58	55.6 % (10/18) (42.1 %–55.6 %)	76.5 % (13/17) (62.6 %–76.5 %)	0.29
Accuracy (95 %CI)	79.2 % (84/106) (74.0 %–79.2 %)	75.9 % (82/108) (70.4 %–75.9 %)	0.56	90.7 % (78/86) (85.1 %–90.7 %)	94.7 % (71/75) (88.4 %–94.7 %)	0.38

CI, confidence interval; PPV, positive predictive value; NPV, negative predictive value.

whereas EUS-FNA with a 25-gauge needle followed by histology detected malignancy in solid pancreatic masses with poor accuracy (45.8 %). However, they did not examine which needle was better in terms of tissue acquisition and diagnostic yield.

This study has several limitations. First, the final diagnoses of only 61 of the patients were determined by histology after surgical resection; the remaining 153 patients did not undergo surgery and therefore had to be diagnosed on the basis of their clinical course during the >12-month follow-up period (disease-specific death or signs of disease progression). Second, cytology, including ROSE, was not assessed; however, in the present study, we used the whole sample obtained by the first pass for the histologic examination because the aim of our study was to compare the diagnostic accuracy of EUS-FNA with the two needles by a simple standard method. Third, the results of the samples obtained by the additional passes after the first pass were not analyzed. The first pass (single pass) is not sufficient to diagnose pancreatic tumors. At present, best practice with respect to EUS-FNA requires multiple passes [14]. In this study, only the first-pass data were evaluated so as to examine whether the core trap impacted diagnostic accuracy under a simple set of conditions using strictly standardized methods. The imaging results and follow-up outcomes in combination with the later passes were used to determine the final diagnoses in patients who did not undergo surgery. Therefore, we did not use data from the later passes for analysis.

We found that the first pass with the ProCore needle yielded more tissue than the first pass with the standard needle, although there was no significant difference between the two in terms of sensitivity and accuracy. Therefore, the ProCore needle was superior to the standard needle only in terms of diagnostic yield. Several randomized controlled trials have compared ProCore needles with standard needles and all show that fewer passes are needed to establish the diagnosis when using the ProCore needle [17 – 19]; however, no reports have shown that the diagnostic accuracy and diagnostic yield are different.

In conclusion, in patients with solid pancreatic masses, the quality of histologic samples obtained at the first pass with 25-gauge EUS-FNA needles with a core trap is better than the quality of samples obtained with standard 25-gauge needles. Samples obtained with the core needle have better cellularity and are more often adequate for histologic evaluation. However, better sample quality does not translate into improved accuracy for the diagnosis of malignancy, which is similar for both needle types.

Competing interests: None

Institutions

[1] Department of Gastroenterology and Hepatology, Kinki University Faculty of Medicine, Osaka-sayama, Japan
[2] Department of Surgical Pathology, Kyoto Prefectural University of Medicine, Kyoto, Japan
[3] Clinical Research Center, Kinki University Hospital, Osaka-sayama, Japan
[4] The Second Department of Internal Medicine, Osaka Medical College, Takatsuki, Japan
[5] Department of Cancer Survey and Gastrointestinal Oncology, Osaka Medical Center for Cancer and Cardiovascular Diseases, Osaka, Japan
[6] Department of Gastroenterology, Osaka City General Hospital, Osaka, Japan
[7] Department of Gastroenterology, Bell Land General Hospital, Sakai, Japan
[8] Digestive Disease Center, Kitano Hospital, Osaka, Japan
[9] The Third Department of Internal Medicine, Kansai Medical University, Hirakata, Japan
[10] Department of Gastroenterology and Hepatology, Osaka Red Cross Hospital, Osaka, Japan

Acknowledgments

This study was supported by grants from the Japan Society for Promotion of Science (no. 22590764 and 25461035).

References

1 *Dumonceau JM, Polkowski M, Larghi A* et al. Indication, results, and clinical impact of endoscopic ultrasound (EUS)-guided sampling in gastroenterology: European Society of Gastrointestinal Endoscopy (ESGE) Clinical Guideline. Endoscopy 2011; 43: 897 – 912
2 *Hewitt MJ, McPhail MJ, Possamai L* et al. EUS-guided FNA for diagnosis of solid pancreatic neoplasms: a meta-analysis. Gastrointest Endosc 2012; 75: 319 – 331
3 *Itoi T, Sofuni A, Itokawa F* et al. Current status of diagnostic endoscopic ultrasonography in the evaluation of pancreatic mass lesions. Dig Endosc 2011; 23: 17 – 21
4 *Chen G, Liu S, Zhao Y* et al. Diagnostic accuracy of endoscopic ultrasound-guided fine-needle aspiration for pancreatic cancer: a meta-analysis. Pancreatology 2013; 13: 298 – 304
5 *Puli SR, Bechtold ML, Buxbaum JL* et al. How good is endoscopic ultrasound-guided fine-needle aspiration in diagnosing the correct etiology for a solid pancreatic mass? A meta-analysis and systematic review Pancreas 2013; 48: 20 – 26
6 *Siddiqui UD, Rossi F, Rosenthal LS* et al. EUS-guided FNA of solid pancreatic masses: A prospective, randomized trial comparing 22-gaguge and 25-gauge needles. Gastrointest Endosc 2009; 70: 1093 – 1097
7 *Yusuf TE, Ho S, Pavey DA* et al. Retrospective analysis of the utility of endoscopic ultrasound-guided fine-needle aspiration (EUS-FNA) in pancreatic masses, using a 22-gauge or 25-gauge needle system: a multicenter experience. Endoscopy 2009; 41: 445 – 448
8 *Nguyen TT, Lee CE, Whang CS* et al. A comparison of the diagnostic yield and specimen adequacy between 22 and 25 gauge needles for endoscopic ultrasound guided fine-needle aspiration (EUS-FNA) of solid pancreatic lesions (SPL): is big better? Gastrointest Endosc 2008; 67: AB100
9 *Lee JH, Stewart J, Ross WA* et al. Blinded prospective comparison of the performance of 22-gauge and 25-gauge needles in endoscopic ultrasound-guided fine needle aspiration of the pancreas and peri-pancreatic lesions. Dig Dis Sci 2009; 54: 2274 – 2281
10 *Madhoun MF, Wani SB, Rastogi A* et al. The diagnostic accuracy of 22-gauge and 25-gauge needles in endoscopic ultrasound-guided fine needle aspiration of solid pancreatic lesions: a meta-analysis. Endoscopy 2013; 45: 86 – 92
11 *Sakamoto H, Kitano M, Komaki T* et al. Prospective comparative study of the EUS guided 25-gauge FNA needle with the 19-gauge Trucut needle and 22-gauge FNA needle in patients with solid pancreatic masses. J Gastroenterol Hepatol 2009; 24: 384 – 390
12 *Song TJ, Kim JH, Lee SS* et al. The prospective randomized, controlled trial of endoscopic ultrasound-guided fine-needle aspiration using 22G and 19G aspiration needles for solid pancreatic or peripancreatic masses. Am J Gastroenterol 2010; 105: 1739 – 1745
13 *Wani S, Muthusamy VR, Komanduri S* et al. EUS-guided tissue acquisition: an evidence-based approach (with videos). Gastrointest Endosc 2014; 80: 939 – 959
14 *Wani S, Mullady D, Early DS* et al. The clinical impact of immediate on-site cytopathology evaluation during endoscopic ultrasound-guided fine needle aspiration of pancreatic masses: a prospective multicenter randomized controlled trial. Am J Gastroenterol 2015; 110: 1429 – 1439
15 *Iglesias-Garcia J, Poley JW, Larghi A* et al. Feasibility and yield of a new EUS histology needle: results from a multicenter, pooled, cohort study. Gastrointest Endosc 2011; 73: 1189 – 1196
16 *Larghi A, Iglesias-Garcia J, Poley JW* et al. Feasibility and yield of a novel 22-gauge histology EUS needle in patients with pancreatic masses: a multicenter prospective cohort study. Surg Endosc 2013; 27: 3733 – 3738
17 *Hucl T, Wee E, Anuradha S* et al. Feasibility and efficiency of a new 22G core needle: a prospective comparison study. Endoscopy 2013; 45: 792 – 798
18 *Bang JY, Herbert-Magee S, Trevino J* et al. Randomized trial comparing the 22-gauge aspiration and 22-gauge biopsy needles for EUS-guided sampling of solid pancreatic mass lesions. Gastrointest Endosc 2012; 76: 321 – 327

19 *Lee YN*, *Moon JH*, *Kim HK* et al. Core biopsy needle versus standard aspiration needle for endoscopic ultrasound-guided sampling of solid pancreatic masses: a randomized parallel-group study. Endoscopy 2014; 46: 1056 – 1062
20 *Iwashita T*, *Nakai Y*, *Samarasena JB* et al. High single-pass diagnostic yield of a new 25-gauge core biopsy needle for EUS-guided FNA biopsy in solid pancreatic lesions. Gastrointest Endosc 2013; 7: 909 – 915
21 *Kim GH*, *Cho YK*, *Kim EY* et al. Comparison of 22-gauge aspiration needle with 22-gauge biopsy needle in endoscopic ultrasonography-guided subepithelial tumor sampling. Scand J Gastroenterol 2014; 49: 347 – 354
22 *Nakai Y*, *Isayama H*, *Chang K* et al. Slow pull versus suction in endoscopic ultrasound-guided fine-needle aspiration of pancreatic solid masses. Dig Dis Sci 2014; 59: 1578 – 1585
23 *LeBlanc JK*, *Ciaccia D*, *Al-Assi MT* et al. Optimal number of EUS-guided fine needle passes needed to obtain a correct diagnosis. Gastrointest Endosc 2004; 59: 475 – 481

hepatic dysfunction in EPP. Earlier studies in Abcc2/Mrp2-deficient rats unequivocally showed that this organic anion transporter is not responsible for PP deposition into bile, whereas more hydrophilic coproporphyrins do rely on Abcc2/Mrp2 activity for their hepatobiliary excretion.[2] In fact, the mechanism of biliary PP excretion has remained elusive. A passive mode of excretion in which biliary lipids act as acceptors for the hydrophobic PP molecules has been proposed.[3] More recently, evidence has been provided for a role of Abcg2 in hepatobiliary elimination of PP through high-affinity transport of its glycoconjugates and, possibly, by low-affinity transport of unconjugated PP.[4,5] We therefore think that the observed relationship between ABCC2/MRP2 expression and hepatocellular PP deposition in these two patients is not causal in nature. The potential contribution of reduced expression of other transporters in the development of EPP-associated liver disease deserves further investigation.

Vincent W. Bloks[1]
Torsten Plösch, Ph.D.[2]
Johan W. Jonker, Ph.D.[1]
Folkert Kuipers, Ph.D.[1]
[1]Department of Pediatrics
[2]Department of Obstetrics and Gynaecology
University Medical Center Groningen
University of Groningen
Groningen, The Netherlands

REFERENCES

1) Hagiwara S, Nishida N, Park AM, Sakurai T, Kawada A, Kudo M. Impaired expression of multidrug resistance–associated protein 2 and liver damage in erythropoietic protoporphyria. HEPATOLOGY 2015;62:1638-1639.
2) Beukeveld GJ, In 't Veld G, Havinga R, Groen AK, Wolthers BG, Kuipers F. Relationship between biliary lipid and protoporphyrin secretion; potential role of mdr2 P-glycoprotein in hepatobiliary organic anion transport. J Hepatol 1996;24:343-352.
3) Plosch T, Bloks VW, Baller JF, Havinga R, Verkade HJ, Jansen PL, et al. Mdr P-glycoproteins are not essential for biliary excretion of the hydrophobic heme precursor protoporphyrin in a griseofulvin-induced mouse model of erythropoietic protoporphyria. HEPATOLOGY 2002;35:299-306.
4) Jonker JW, Buitelaar M, Wagenaar E, Van Der Valk MA, Scheffer GL, Scheper RJ, et al. The breast cancer resistance protein protects against a major chlorophyll-derived dietary phototoxin and protoporphyria. Proc Natl Acad Sci USA 2002;99:15649-15654.
5) Jonker JW, Musters S, Vlaming ML, Plosch T, Gooijert KE, Hillebrand MJ, et al. Breast cancer resistance protein (Bcrp1/Abcg2) is expressed in the harderian gland and mediates transport of conjugated protoporphyrin IX. Am J Physiol Cell Physiol 2007;292:C2204-C2212.

DOI 10.1002/hep.27993
Potential conflict of interest: Nothing to report.

REPLY:

We read with great interest the Bloks et al. correspondence and appreciate the important point raised by them regarding ABCG2. In the current analysis, we studied ABCG2 expression, and not that of ABCC2/MRP2, by using immunohistochemistry and quantitative polymerase chain reaction (PCR), as cited in the reference 3 of the article.[1] However, we accidentally mixed up the names of these two molecules because they belong to the same ABC transporters and erroneously referred to ABCG2 as ABCC2 during the preparation of the manuscript. Whole-exome sequencing did not show any specific mutation in the *ABCG2* (and in the *ABCC2*) genes in both patients. The anti-ABCG2 antibody for IHC was purchased from ALEXIS Co. (Lausen, Switzerland); the quantitative PCR primers used for measuring ABCG2 expression were TTCGGCTTGCAACAACTATGA (forward) and CACCACGGATAAACTGAGTTCCA (reverse). We are ready to open the detail of the methods so that these can be reproduced.

Regarding the differences in the expression of ABCG2 on hepatocellular protoporphyrin deposition, we understand the concern being pointed out. Probably, it should be ideal to examine expression of ABCG2 in the liver of the older brother in the recovery phase; however, this was difficult owing to the ethical considerations and risk of complications. Therefore, we measured the levels of other membrane transporters, ABCG6 and PEPT1,[1,2] together with ABCG2, by using quantitative PCR. We did not find any differences in ABCG6 and PEPT1 expression between the two brothers; the differences in ABCG2 expression were unique among the genes of transporter proteins examined. This result, at least partially, indicates that the reduction in ABCG2 levels in the older brother was a cause of the liver damage, and not its consequence. We also understand that the potential contribution of other candidate transporters in the development of erythropoietic protoporphyria-associated liver disease deserves further investigation.

Satoru Hagiwara, M.D., Ph.D.
Naoshi Nishida, M.D., Ph.D.

Masatoshi Kudo, M.D., Ph.D.
Department of Gastroenterology and Hepatology
Kinki University School of Medicine
Osaka-Sayama, Japan

REFERENCES

1) Kobuchi H, Moriya K, Ogino T, Fujita H, Inoue K, Shuin T, et al. Mitochondrial localization of ABC transporter ABCG2 and its function in 5-aminolevulinic acid-mediated protoporphyrin IX accumulation. PLoS One 2012;7:e50082.
2) Ogino T, Kobuchi H, Munetomo K, Fujita H, Yamamoto M, Utsumi T, et al. Serum-dependent export of protoporphyrin IX by ATP-binding cassette transporter G2 in T24 cells. Mol Cell Biochem 2011;358:297-307.

View this article online at wileyonlinelibrary.com.
DOI 10.1002/hep.27989
Potential conflict of interest: Nothing to report.

Hypomethylation and Hypohydroxymethylation of DNA in Hepatocellular Carcinoma and Cholangiocarcinoma

TO THE EDITOR:

We read with great interest the article by Udali et al.,[1] who demonstrated that there was significantly reduced DNA methylation in hepatocellular carcinoma (HCC) compared to cholangiocarcinoma (CC) and that there was no difference in DNA hydroxymethylation between HCC and CC. They also reported that high levels of methylcytosine (mCyt) in the DNA of peripheral blood mononuclear cells (PBMCs) were related to a better clinical outcome of patients with HCC or CC. We appreciate their findings and would like to address a few issues that may help to further clarify or interpret their findings.

First, methylation and hydroxymethylation of DNA play important parts in cell differentiation, embryonic development, host adaptations to environmental factors, and pathogenesis. Cytosine methylation is a DNA modification that is, in general, associated with transcriptional silencing. DNA methylation has been linked to dietary, psychological, and environmental factors.[2,3] Thus, it is conceivable that postoperatively patients with HCC or CC would face changes in dietary, psychological, and environmental factors such as B vitamins, oxidative stress, and radiation.[4-6] Therefore, all these factors should be taken into account when the outcome of patients with HCC or CC is assessed, and univariate and multivariate (i.e., Cox proportional hazards model) analyses should be applied. In addition, it should be noted that detection of the content of mCyt and hydroxymethylcytosine in the DNA of PBMCs is not practical and feasible in the clinical setting, and a surrogate parameter that is more clinically measurable would be more useful.

Second, biological samples differ in accessibility and enrichment in tumor cells, as well as organ specificity, among studies on DNA methylation. Blood samples are commonly used in studies on DNA methylation, but aberrant DNA methylation can originate in any organ. How a blood-positive screening assay could point a clinician toward the site of malignancy is challenging.[7] For example, neoplastic tissues from patients with HCC or CC may contain various amounts of DNA with tissue-specific patterns of DNA methylation. Udali et al.[1] measured the global levels of mCyt and hydroxymethylcytosine in HCC and CC tissues and in DNA from PBMCs to define methylation and hydroxymethylation. They found that whereas global methylation and hydroxymethylation in DNA from PBMCs did not differ between HCC and CC, the mCyt content in HCC tissues was significantly lower than that in CC tissues. This observation clearly indicates that tissue-specific DNA methylation, not global methylation in DNA from PBMCs, plays the crucial role in differentiating between HCC and CC; and it is the tissue-specific DNA methylation (i.e., mCyt levels) that should be used as the clinical diagnostic biomarker that differentiates HCC from CC.

Third, the authors followed up the 42 patients (26 HCC and 16 CC) for 48 months to assess survival with regard to DNA methylation and DNA hydroxymethylation. Encouragingly, they observed that the survival rate was greater in patients with mCyt levels in DNA from PBMCs >5.59% than in those with mCyt levels <5.59%. However, the authors did not provide any postoperative data. Generally, it is essential to generate the overall survival rate, such as 1-year, 3-year, or 5-year survival rates, and then determine the factors

TACE Treatment in Patients with Sorafenib-treated Unresectable Hepatocellular Carcinoma in Clinical Practice: Final Analysis of GIDEON[1]

Jean-François Geschwind, MD[2]
Masatoshi Kudo, MD, PhD
Jorge A. Marrero, MD
Alan P. Venook, MD
Xiao-Ping Chen, MD, PhD
Jean-Pierre Bronowicki, MD, PhD
Lucy Dagher, MD
Junji Furuse, MD, PhD
Laura Ladrón de Guevara, MD
Christos Papandreou, MD, PhD
Arun J. Sanyal, MD
Tadatoshi Takayama, MD, PhD
Sheng-Long Ye, MD, PhD
Seung Kew Yoon, MD, PhD
Keiko Nakajima, MD
Robert Lehr, MSc
Stephanie Heldner, BSc
Riccardo Lencioni, MD, PhD

[1] From Vascular and Interventional Radiology, Johns Hopkins University School of Medicine, 600 N Wolfe St, Blalock 545, Baltimore, MD 21287 (J.F.G.); Department of Gastroenterology and Hepatology, Kinki University School of Medicine, Osaka, Japan (M.K.); Department of Internal Medicine, Division of Digestive and Liver Diseases, University of Texas Southwestern Medical Center, Dallas, Tex (J.A.M.); University of California–San Francisco, San Francisco, Calif (A.P.V.); Hepatic Surgery Center, Tongji Hospital, Tongji Medical College, Huazhong University of Science and Technology, Wuhan, China (X.P.C.); Department of Gastroenterology and Hepatology, INSERM U954, University Hospital, University of Lorraine, Nancy, France (J.P.B.); Policlínica Metropolitana, Caracas, Venezuela (L.D.); Kyorin University School of Medicine, Mitaka, Tokyo, Japan (J.F.); Hospital Angeles Clínica Londres, Mexico City, Mexico (L.L.d.G.); University Hospital of Larissa, Larissa, Greece (C.P.); Virginia Commonwealth University Medical Center, Richmond, Va (A.J.S.); Department of Digestive Surgery, Nihon University School of Medicine, Tokyo, Japan (T.T.); Liver Cancer Institute and Zhongshan Hospital, Fudan University, Shanghai, China (S.L.Y.); The Catholic University of Korea, Seoul, Korea (S.K.Y.); Global Medical Affairs, Bayer Healthcare Pharmaceuticals, Whippany, NJ (K.N.); Clinical Statistics, Bayer Healthcare Pharmaceuticals, Whippany, NJ (R.L.); Global Medical Affairs and Pharmacovigilance, Bayer Pharma AG, Berlin, Germany (S.H.); and Division of Diagnostic Imaging and Intervention, Pisa University Hospital and School of Medicine, Pisa, Italy (R.L.). Received March 19, 2015; revision requested May 1; final revision received July 28; accepted August 12; final version accepted October 16. Supported by Bayer Healthcare Pharmaceuticals and Onyx Pharmaceuticals, an Amgen subsidiary. **Address correspondence to** J.F.G. (e-mail: *jeff.geschwind@yale.edu*).

Current Address:
[2] Department of Radiology and Biomedical Imaging, Yale School of Medicine, New Haven, Conn.

Purpose: To evaluate transarterial chemoembolization (TACE) use prior to and concomitantly with sorafenib in patients with unresectable hepatocellular carcinoma (HCC) across different global regions.

Materials and Methods: GIDEON is an observational registry study of more than 3000 HCC patients. Patients with histologically, cytologically, or radiographically diagnosed HCC, and for whom a decision had been made to treat with sorafenib, were eligible. Patients were enrolled into the registry from 39 countries beginning in January 2009, with the last patient follow-up in April 2012. Detailed data on treatment history, treatment patterns, adverse events, and outcomes were collected. All treatment decisions were at the discretion of the treating physicians. Documented approval from local ethics committees was obtained, and all patients provided signed informed consent. Descriptive statistics, including minimum, median, and maximum, were calculated for metric data, and frequency tables for categorical data. Kaplan-Meier estimates with 95% confidence intervals were calculated for survival end points.

Results: A total of 3202 patients were eligible for safety analysis, of whom 2631 (82.2%) were male. Median age was 62 years (range, 15–98 years). A total of 1511 (47.2%) patients underwent TACE prior to sorafenib; 325 (10.1%) underwent TACE concomitantly. TACE prior to sorafenib was more common in Japan and Asia-Pacific compared with all other regions (362 [71.3%] and 560 [60.3%] vs 12–209 [13.3%–37.1%]). Adverse events were reported in 2732 (85.3%) patients overall, with no notable differences in the incidence of adverse events, regardless of TACE treatment history. Overall survival was 12.7 months in prior-TACE patients, 9.2 months in non–prior-TACE patients, 21.6 months in concomitant-TACE patients, and 9.7 months in non–concomitant-TACE patients.

Conclusion: Global variation exists in TACE use in sorafenib-treated HCC patients. The combination of TACE with sorafenib appears to be a well-tolerated and viable therapeutic approach.

Online supplemental material is available for this article.

Hepatocellular carcinoma (HCC) is a leading cause of cancer-related death worldwide (1). HCC is a complex disease of liver cancer with underlying liver dysfunction, commonly arising from viral infections and cirrhosis (2). Therefore, HCC treatment is challenging and effectively amounts to the management of two separate diseases. Treatment decisions in HCC are based on the severity of the cancer and the remaining degree of liver functionality (3). Most patients present with advanced stages of HCC that are incurable with surgical resection. According to most guidelines, transarterial chemoembolization (TACE) is the first-line treatment for patients with intermediate stage HCC that is large or multinodular, unresectable, and without vascular invasion or extrahepatic spread (4–6). Sorafenib (Nexavar; Bayer Pharma, Berlin, Germany) is an oral multikinase inhibitor with antiangiogenic activity and is the only approved systemic treatment for advanced HCC (6). Sorafenib is recommended as a first-line therapy for patients with extensive disease; with confirmed metastasis; who cannot benefit from resection, transplantation, or additional local-regional therapies (LRTs); and who have preserved liver function (6). Currently, TACE and sorafenib are the only noncurative treatments for advanced HCC that have been shown to provide a survival benefit in HCC patients (7–9).

While TACE is widely used in the management of HCC, there is no single, globally accepted therapeutic algorithm for TACE use or for assessment of the response to TACE in clinical practice (10), although scoring systems have been recently developed to inform TACE initiation (selection for transarterial chemoembolization treatment, or STATE) and retreatment (assessment for re-treatment with TACE, or ART) (11,12). However, not all patients who undergo TACE derive clinical benefit, and patients may experience tumor recurrence (13,14). Recurrence may occur because of the proangiogenic effects of hypoxia resulting from TACE-induced necrosis at the tumor site (13). The antiangiogenic effect of sorafenib has the potential to synergistically offset this effect of TACE, and multiple trials have shown promising safety and efficacy data on the use of TACE combined with sorafenib in HCC patients (15–19).

Global investigation of therapeutic decisions in hepatocellular carcinoma and of its treatment with sorafenib (GIDEON) is a nonrandomized observational registry study undertaken to evaluate the safety of sorafenib in patients with unresectable HCC in clinical practice (20). The GIDEON study design allowed for the collection of a large, robust, and clinically relevant global dataset, with a preplanned range of subanalyses across patient subgroups. Data on the use of TACE prior to or concomitantly with sorafenib were collected to allow assessment of TACE and sorafenib use and associated safety and outcomes in a clinical practice setting. The GIDEON study began enrolling patients in 2009 and was completed in 2012, with more than 3000 sorafenib-treated patients enrolled from 39 countries in five global regions. Findings from two interim analyses have been previously reported in approximately 500 and 1500 patients (21,22). Here, we report data from the final analyses of GIDEON.

Advances in Knowledge

- The use of transarterial chemoembolization (TACE) prior to sorafenib varied globally and was more common in Japan (362 of 508; 71.3%) and Asia-Pacific (560 of 928; 60.3%) than in United States (209 of 563; 37.1%) and Europe (368 of 1113; 33.1%).
- Overall, 325 (10.1%) patients underwent TACE concomitant with sorafenib therapy; drug-eluting bead TACE was more commonly used than lipiodol-based TACE in the United States (31/73; 42.5%) and Europe (19/52; 36.5%) compared with other regions (range 0/13–3/125; 0–2.4%).
- The overall safety profile of sorafenib was consistent, irrespective of concomitant TACE administration.
- In this observational study, overall survival in patients treated with sorafenib and concomitant TACE was 21.6 months (95% confidence interval: 18.0, not estimable) compared with 9.7 months (95% confidence interval: 9.2, 10.4) in nonconcomitantly treated patients.

Materials and Methods

The GIDEON study is sponsored by Bayer Healthcare Pharmaceuticals and Onyx Pharmaceuticals, an Amgen subsidiary. J.A.M., R.L., M.K., S.L.Y., and A.P.V. are members of the Global Steering and Publication Committee for the GIDEON study; they were involved in the development of the GIDEON protocol and in data review and interpretation. J.A.M., R.L., M.K., S.L.Y., A.P.V., J.P.B., X.P.C., L.D., J.F., J.F.H.G., L.L.d.G., C.P., A.J.S., T.T., and S.K.Y. were responsible for the provision of patients and data acquisition. K.N., R.L., and S.H. are employees of Bayer

Published online before print
10.1148/radiol.2015150667 **Content code:** VA

Radiology 2016; 279:630–640

Abbreviations:
DEB = drug-eluting bead
GIDEON = global investigation of therapeutic decisions in hepatocellular carcinoma and of its treatment with sorafenib
HCC = hepatocellular carcinoma
LRT = local-regional therapy
TACE = transarterial chemoembolization

Author contributions:
Guarantors of integrity of entire study, J.F.G., L.D., L.L.d.G., A.J.S., S.K.Y., K.N., S.H., R.L.; study concepts/study design or data acquisition or data analysis/interpretation, all authors; manuscript drafting or manuscript revision for important intellectual content, all authors; approval of final version of submitted manuscript, all authors; agrees to ensure any questions related to the work are appropriately resolved, all authors; literature research, M.K., J.A.M., S.L.Y., K.N.; clinical studies, J.F.G., M.K., J.A.M., A.P.V., X.P.C., L.D., J.F., L.L.d.G., A.J.S., T.T., S.L.Y., S.K.Y., K.N.; experimental studies, J.F.G.; statistical analysis, A.J.S., R.L.; and manuscript editing, J.F.G., M.K., J.A.M., A.P.V., J.P.B., L.D., J.F., C.P., A.J.S., T.T., S.L.Y., K.N., S.H.

Conflicts of interest are listed at the end of this article.

Healthcare and were the lead medical advisor, internal statistician, and global study manager, respectively. All authors had access to relevant data and had control of which data were included in the manuscript. The final decision on manuscript content rested with the authors who are not Bayer employees. The GIDEON protocol is available at *https://www.clinicaltrials.gov/ct2/show/NCT00812175?term=NCT00812175&rank=1*, and a synopsis of the study results is publicly available at *http://pharma.bayer.com/en/research-and-development/*. The required documented approval from the appropriate ethics committees and institutional review boards was obtained for all participating centers prior to the study. All patients provided signed, informed consent to be included in the registry. The GIDEON study began enrolling patients in January 2009 and was completed in April 2012.

Patients with a histologic, cytologic, or radiographic diagnosis of unresectable HCC and with a life expectancy of more than 8 weeks were included in the GIDEON study. Exclusion criteria were based on locally approved product information for sorafenib.

Comprehensive case report forms were used to collect patient data. Information on demographics, baseline disease characteristics, previous therapies, and initial sorafenib dose was recorded at the patients' initial visits. Subsequent follow-up visits were at the discretion of the treating physicians, during which data regarding sorafenib dose (including any modifications or discontinuation), concomitant treatments, adverse events, and outcomes (including death) were collected. The independent contract research organization Kantar Health (Munich, Germany) was responsible for data capture, data management, data quality review, and statistical reporting, overseen by Bayer Healthcare Pharmaceuticals.

All treatment decisions, including the administration of treatments concomitantly with sorafenib, were determined entirely at the discretion of the treating physicians. As such, the type, schedule, and other aspects of TACE were not dictated by the study protocol.

Figure 1

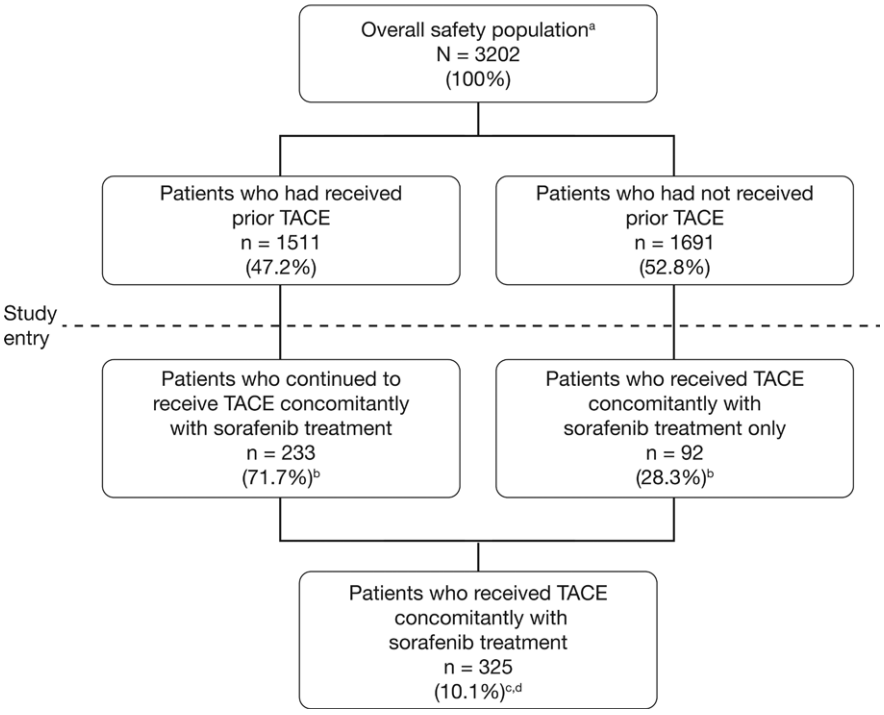

Figure 1: Flowchart of patient selection in GIDEON. [a]Safety population includes all patients who received at least one dose of sorafenib and underwent at least one follow-up assessment after the start of sorafenib treatment. [b]Expressed as a percentage of patients who received TACE concomitantly with sorafenib treatment. [c]Expressed as a percentage of overall safety population. [d]89.9% of the overall patient population did not receive concomitant TACE.

Adverse events were graded according to the National Cancer Institute Common Terminology Criteria for Adverse Events, version 3.0 (National Cancer Institute, Bethesda, Md), and the likely relationship of sorafenib to any adverse event was documented as part of the case report form. Patients who received at least one dose of sorafenib and underwent at least one follow-up examination were evaluable for safety.

The primary objective of GIDEON was to evaluate the safety of sorafenib in patients with HCC under real-life practice conditions. Secondary objectives included evaluating sorafenib efficacy, duration of therapy, and treatment practice across various clinically relevant subsets of patients. Full details of the GIDEON study design and rationale have previously been published (20).

Enrollment was planned for 3000 patients, which was deemed sufficient for full safety evaluation of the overall study population, as well as for specific subgroups that were preplanned in the study design, including analysis based on treatment history, Child-Pugh score, and geographic region (20). The final analysis was performed 12 months after the 3000th patient was enrolled. All baseline and safety data are summarized by using descriptive statistics, including mean, standard deviation, minimum, quartiles, median, and maximum calculated for metric data, and frequency tables for categorical data. Kaplan-Meier estimates and curves were calculated for survival end points.

Results

Patient Disposition

Overall, 3202 patients were eligible for and included in the safety analysis (Fig 1).

Table 1

Use of Prior and Concomitant Therapies by Region

Therapy	Asia-Pacific (*n* = 928)	Europe (*n* = 1113)	Latin America (*n* = 90)	United States (*n* = 563)	Japan (*n* = 508)	Total (*n* = 3202)
Prior therapy						
All LRTs	624 (67.2)	484 (43.5)	25 (27.8)	278 (49.4)	429 (84.4)	1840 (57.5)
TACE*	560 (60.3)	368 (33.1)	12 (13.3)	209 (37.1)	362 (71.3)	1511 (47.2)
Lipiodol based	505 (90.2)	218 (59.2)	10 (83.3)	85 (40.7)	298 (82.3)	1116 (73.9)
DEB	16 (2.9)	133 (36.1)	2 (16.7)	83 (39.7)	6 (1.7)	240 (15.9)
No. of TACE treatments†						
1	228 (40.7)	174 (47.3)	10 (83.3)	124 (59.3)	76 (21.0)	612 (40.5)
2	116 (20.7)	92 (25.0)	1 (8.3)	55 (26.3)	67 (18.5)	331 (21.9)
≥3	216 (38.6)	102 (27.7)	1 (8.3)	30 (14.4)	219 (60.5)	568 (37.6)
Ablation						
Radiofrequency ablation‡	119 (12.8)	166 (14.9)	16 (17.8)	65 (11.5)	195 (38.4)	561 (17.5)
Percutaneous ethanol injection§	25 (2.7)	59 (5.3)	0	6 (1.1)	59 (11.6)	149 (4.7)
Hepatic arterial infusion‖	48 (5.2)	11 (1.0)	2 (2.2)	22 (3.9)	96 (18.9)	179 (5.6)
Radiation						
External#	123 (13.3)	14 (1.3)	0	27 (4.8)	29 (5.7)	193 (6.0)
Radioembolization**	1 (0.1)	1 (< 0.1)	0	2 (0.4)	0	4 (0.1)
Surgery	225 (24.2)	172 (15.5)	5 (5.6)	53 (9.4)	220 (43.3)	675 (21.1)
Systemic therapy	46 (5.0)	42 (3.8)	0	19 (3.4)	59 (11.6)	166 (5.2)
Concomitant therapy						
TACE	125 (13.5)	52 (4.7)	13 (14.4)	73 (13.0)	62 (12.2)	325 (10.1)
Lipiodol based	100 (80.0)	26 (50.0)	12 (92.3)	21 (28.8)	50 (80.6)	209 (64.3)
DEB	3 (2.4)	19 (36.5)	0	31 (42.5)	0	53 (16.3)
No. of TACE treatments						
1	90 (9.7)	35 (3.1)	9 (10.0)	48 (8.5)	43 (8.5)	225 (7.0)
2	24 (2.6)	10 (0.9)	3 (3.3)	19 (3.4)	9 (1.8)	65 (2.0)
≥3	11 (1.2)	7 (0.6)	1 (1.1)	6 (1.1)	10 (2.0)	35 (1.1)
Ablation						
Radiofrequency ablation	14 (1.5)	14 (1.3)	5 (5.6)	12 (2.1)	8 (1.6)	53 (1.7)
Percutaneous ethanol injection	2 (0.2)	3 (0.3)	0	0	0	5 (0.2)
Hepatic arterial infusion	34 (3.7)	1 (< 0.1)	0	1 (0.2)	18 (3.5)	54 (1.7)
Radiation						
External	33 (3.6)	13 (1.2)	0	14 (2.5)	23 (4.5)	83 (2.6)
Radioembolization	0	2 (0.2)	0	1 (0.2)	0	3 (< 0.1)
Surgery	8 (0.9)	2 (0.2)	1 (1.1)	4 (0.7)	3 (0.6)	18 (0.6)

Note.—Data in parentheses are percentages.

* Data missing for 327 patients.

† Based on number of patients who received TACE.

‡ Data missing for 338 patients.

§ Data missing for 353 patients.

‖ Data missing for 341 patients.

Data missing for 3009 patients.

** Data missing for 3198 patients.

TACE subgroups comprised patients who had received TACE treatment prior to sorafenib (47.2%), patients who had not received prior TACE treatment (52.8%), patients who received TACE treatment concomitantly with sorafenib (10.1%), and patients who did not receive concomitant TACE treatment (*n* = 2877; 89.9%). Of the patients who received concomitant TACE treatment, the majority (71.7%) had also received prior TACE treatment.

Use of Prior and Concomitant Therapies

In total, 57.5% of patients had received LRT prior to study entry, although with regional variation. Overall, TACE was the most common prior LRT received (Table 1). Lipiodol (Guebert, Villepinte,

Table 2

Baseline Demographics and Disease Characteristics at Study Entry by Prior and Concomitant TACE

Characteristic	No Prior TACE ($n = 1691$)	Prior TACE ($n = 1511$)	No Concomitant TACE ($n = 2877$)	Concomitant TACE ($n = 325$)	Overall ($n = 3202$)*
No. of men	1349 (79.8)	1282 (84.8)	2362 (82.1)	269 (82.8)	2631 (82.2)
Median age (y)†	62 (18–98)	62 (15–90)	63 (15–98)	58 (18–88)	62 (15–98)
Median body mass index (kg/m^2)†	24.8 (13.9–58.0)	23.8 (14.1–45.1)	24.2 (13.9–58.0)	24.7 (17.2–43.2)	24.2 (13.9–58.0)
Etiology‡					
Hepatitis B	522 (30.9)	648 (42.9)	1030 (35.8)	140 (43.1)	1170 (36.5)
Hepatitis C	545 (32.2)	508 (33.6)	938 (32.6)	115 (35.4)	1053 (32.9)
Alcohol use	483 (28.6)	351 (23.2)	761 (26.5)	73 (22.5)	834 (26.0)
Nonalcoholic steatohepatitis	55 (3.3)	35 (2.3)	80 (2.8)	10 (3.1)	90 (2.8)
BCLC stage§					
A	120 (7.1)	106 (7.0)	192 (6.7)	34 (10.5)	226 (7.1)
B	282 (16.7)	352 (23.3)	536 (18.6)	98 (30.2)	634 (19.8)
C	915 (54.1)	749 (49.6)	1526 (53.0)	138 (42.5)	1664 (52.0)
D	115 (6.8)	58 (3.8)	161 (5.6)	12 (3.7)	173 (5.4)
Child-Pugh status‖					
A	950 (56.2)	1018 (67.4)	1737 (60.4)	231 (71.1)	1968 (61.5)
B	403 (23.8)	263 (17.4)	611 (21.2)	55 (16.9)	666 (20.8)
C	58 (3.4)	16 (1.1)	68 (2.4)	6 (1.8)	74 (2.3)
Metastatic lesion					
HCC confined to liver	731 (43.2)	689 (45.6)	1228 (42.7)	192 (59.1)	1420 (44.3)
Vascular invasion	427 (25.3)	285 (18.9)	660 (22.9)	52 (16.0)	712 (22.2)
Extrahepatic spread	650 (38.4)	622 (41.2)	1180 (41.0)	92 (28.3)	1272 (39.7)

Note.—Unless otherwise indicated, data are number of patients and data in parentheses are percentages.

* Reflects patients with and those without prior TACE or patients with and those without concomitant TACE.

† Data in parentheses are the range.

‡ Data missing/not available for seven patients.

§ BCLC = Barcelona Clinic Liver Cancer. Data missing for four patients and not evaluable for 501 patients.

‖ Score missing for one patient and not evaluable for 493 patients.

France)-based TACE was generally more common than drug-eluting beads (DEB) TACE; however, DEB TACE was more common in the United States and Europe compared with all other regions. Other LRTs used prior to study entry included radiofrequency ablation, percutaneous ethanol injection, and hepatic artery infusion, which also varied regionally (Table 1).

The use of TACE concomitant with sorafenib was similar across the regions, although lower in Europe compared with elsewhere (Table 1). Overall, for concomitant TACE, lipiodol-based TACE was more common than DEB TACE (64.3% vs 16.3%), except for in the United States, where DEB TACE was more common (42.5% vs 28.8%). Concomitant use of treatments other than TACE was reported rarely, with external radiation being the most frequent (2.6%) (Table 1). A small number of patients underwent TACE after sorafenib discontinuation (4.3%), most commonly in Japan (11.8%) (Table E1 [online]).

Patient Baseline Demographics and Disease Characteristics at Study Entry

Baseline demographics and disease characteristics at study entry for prior and concomitant TACE treatment use are shown in Table 2. Disease etiology was similar across all patient subgroups, although variations in Child-Pugh and Barcelona Clinic Liver Cancer stage were observed, as patients who had never received TACE treatment tended to have more severe liver disease at the start of sorafenib therapy compared with those who received prior or concomitant TACE treatment. Vascular invasion was less common in patients who had received prior or concomitant TACE treatment compared with those who had not (Table 2). Extrahepatic spread was lower in patients treated concomitantly with TACE compared with all other subgroups.

Sorafenib Administration

The median daily dose of sorafenib was lower in patients previously treated with TACE compared with those who had not been previously treated with TACE (603.0 mg vs 757.0 mg) (Table 3). The median daily dose of sorafenib was also lower in concomitantly treated TACE patients compared with nonconcomitantly treated patients (587.0 mg vs 698.5 mg). The overall median duration of sorafenib therapy was 15.0 weeks, although it was notably longer

in patients who underwent concomitant TACE (36.4 weeks) compared with patients who did not undergo concomitant TACE (13.1 weeks) (Table 3).

Safety

Overall, treatment-emergent adverse events were reported in 85.3% of patients and drug-related adverse events were reported in 66.0% of patients, with little variation across patient subgroups (Table 4). Serious adverse events and drug-related serious adverse events were reported in 43.3% and 9.3% of patients, respectively. Serious adverse events occurred in 33.5% of patients who underwent concomitant TACE, compared with 44.4% of those who did not. Overall, the most frequent treatment-emergent adverse events (occurring in ≥ 10% of patients) included diarrhea (30.6%), hand-foot skin reaction (27.1%), and fatigue (23.7%) (Table 4). Patients who received concomitant TACE treatment had slightly increased incidences of diarrhea (37.8%) and hand-foot skin reaction (41.5%), compared with the overall study population (30.6% and 27.1%, respectively), but a slightly lower incidence of fatigue (21.8% vs 23.7%). Adverse events resulting in permanent discontinuation of sorafenib were

Table 3

Administration of Sorafenib

Characteristic	No Prior TACE (*n* = 1691)	Prior TACE (*n* = 1511)	No Concomitant TACE (*n* = 2877)	Concomitant TACE (*n* = 25)	Overall (*n* = 3202)*
Daily dose					
No. of patients†	1492	1365	2576	281	2857
Median dose (mg)‡	757.0	603.0	698.5	587.0	688.0
Mean dose (mg)‡	643.1	587.4	621.4	571.6	616.5
Duration of therapy					
No. of patients	1639	1491	2805	325	3130
Median duration (wk)§	13.3	16.7	13.1	36.4	15.0
Mean duration (wk)§	22.8	25.3	21.8	42.6	24.0

* Reflects patients with and those without prior TACE or patients with and those without concomitant TACE.

† Patients for whom dosing data are available.

‡ Average daily dose determined within patient-based actual days on study drug excluding interruptions.

§ Treatment duration is the time from initial visit to last dosing date.

Table 4

Summary of Sorafenib Safety Profile and Incidence of Most Common Treatment-emergent Adverse Events Occurring in 10% or More of Patients

Characteristic	No Prior TACE (*n* = 1691)	Prior TACE (*n* = 1511)	No Concomitant TACE (*n* = 2877)	Concomitant TACE (*n* = 325)	Overall (*n* = 3202)*
Adverse events					
Total (all grades)	1430 (84.6)	1302 (86.2)	2444 (84.9)	288 (88.6)	2732 (85.3)
Drug related	1037 (61.3)	1075 (71.1)	1871 (65.0)	241 (74.2)	2112 (66.0)
Serious (all grades)	811 (48.0)	576 (38.1)	1278 (44.4)	109 (33.5)	1387 (43.3)
Drug-related serious (all grades)	151 (8.9)	146 (9.7)	277 (9.6)	20 (6.2)	297 (9.3)
Grade 3 or 4	497 (29.4)	519 (34.3)	905 (31.5)	111 (34.2)	1016 (31.7)
Drug-related grade 3 or 4	359 (21.2)	395 (26.1)	677 (23.5)	77 (23.7)	754 (23.5)
Grade 5	519 (30.7)	279 (18.5)	742 (25.8)	56 (17.2)	798 (24.9)
Drug-related grade 5	31 (1.8)	15 (1.0)	44 (1.5)	2 (0.6)	46 (1.4)
Resulting in permanent discontinuation of sorafenib	504 (29.8)	500 (33.1)	937 (32.6)	67 (20.6)	1004 (31.4)
Incidence of most common adverse events, all grades					
Diarrhea	502 (29.7)	479 (31.7)	858 (29.8)	123 (37.8)	981 (30.6)
Hand-foot skin reaction	352 (20.8)	517 (34.2)	734 (25.5)	135 (41.5)	869 (27.1)
Fatigue	416 (24.6)	344 (22.8)	689 (23.9)	71 (21.8)	760 (23.7)
Anorexia	250 (14.8)	233 (15.4)	440 (15.3)	43 (13.2)	483 (15.1)
Abdominal pain	236 (14.0)	212 (14.0)	398 (13.8)	50 (15.4)	448 (14.0)
Liver dysfunction	217 (12.8)	178 (11.8)	366 (12.7)	29 (8.9)	395 (12.3)
Rash/desquamation	203 (12.0)	188 (12.4)	337 (11.7)	54 (16.6)	391 (12.2)
Nausea	190 (11.2)	130 (8.6)	279 (9.7)	41 (12.6)	320 (10.0)
Hypertension	141 (8.3)	168 (11.1)	269 (9.4)	40 (12.3)	309 (9.7)
Fever	88 (5.2)	103 (6.8)	158 (5.5)	33 (10.2)	191 (6.0)

Note.—Data are number of patients and data in parentheses are percentages. SAE = serious adverse event.

* Reflects patients with and those without prior TACE or patients with and those without concomitant TACE.

Figure 2

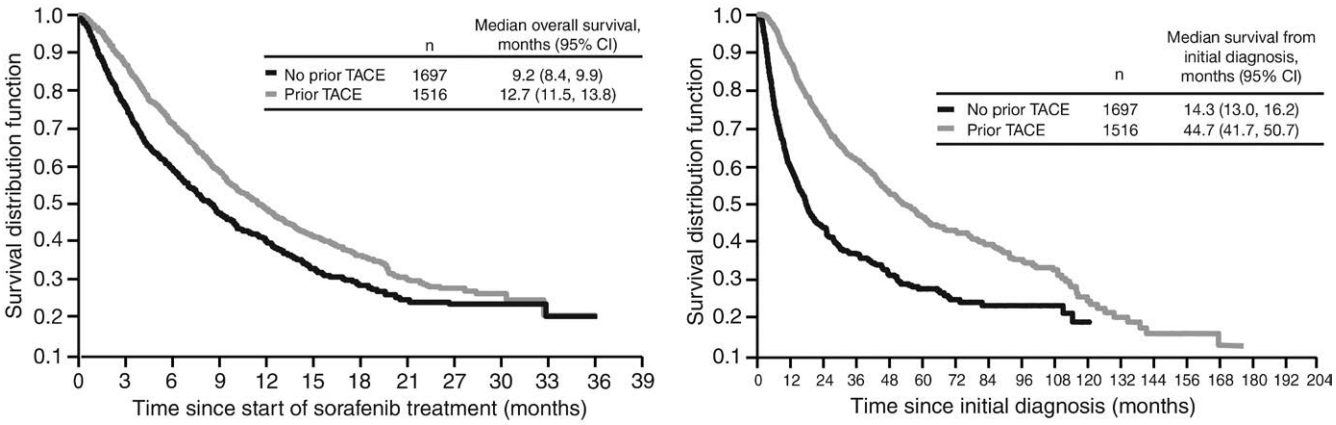

a. b.

Figure 2: Graphs show **(a)** overall survival and **(b)** survival time from initial diagnosis to death in patients who received prior TACE treatment versus patients who had not received prior TACE treatment. *CI* = confidence interval.

Figure 3

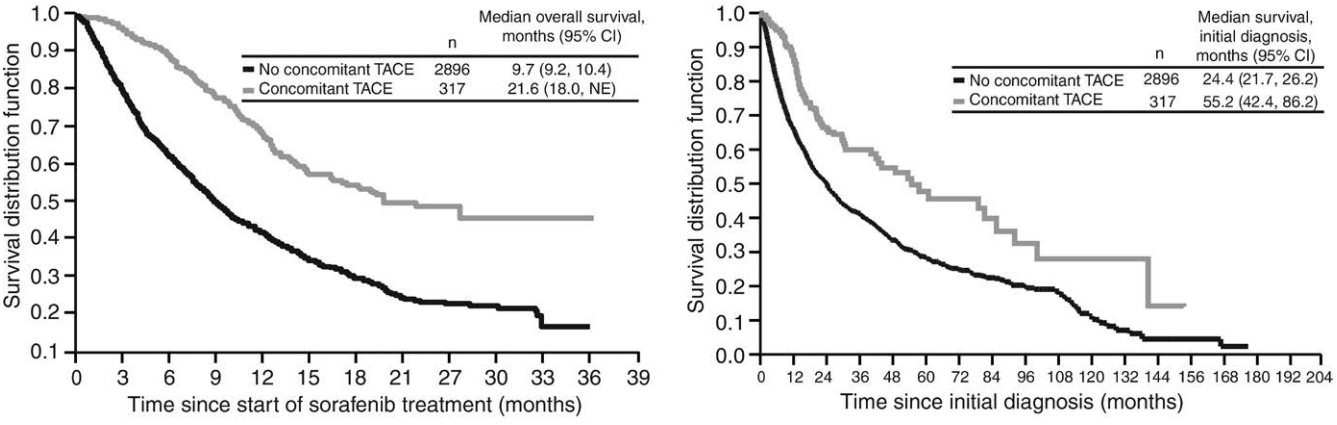

a. b.

Figure 3: Graphs show **(a)** overall survival and **(b)** survival time from initial diagnosis to death in patients who received TACE treatment concomitantly with sorafenib and patients who had not received concomitant TACE treatment. *CI* = confidence interval, *NE* = not evaluable.

least common in concomitantly treated TACE patients compared with other subgroups (20.6% vs 29.8%–33.1%).

Outcomes

Median overall survival was 12.7 months (95% confidence interval [CI]: 11.5, 13.8) in patients who received prior TACE treatment and 9.2 months (95% CI: 8.4, 9.9) in patients who had not received prior TACE treatment (Fig 2a). Patients who had received TACE treatment prior to sorafenib had a notably longer median time from initial diagnosis to death than patients who had not received prior TACE treatment (44.7 months [95% CI: 41.7, 50.7] vs 14.3 months [95% CI: 13.0, 16.2]) (Fig 2b). Concomitantly treated TACE patients had a median overall survival of 21.6 months (95% CI: 18.0, not estimable) and a median time from initial diagnosis to death of 55.2 months (95% CI: 42.4, 86.2), while nonconcomitantly treated patients had a median overall survival time of 9.7 months (95% CI: 9.2, 10.4) and a median time from initial diagnosis to death of 24.4 months (95% CI: 21.7, 26.2) (Fig 3a, 3b). Overall survival was longer in concomitantly treated patients across Barcelona Clinic Liver Cancer stages (Fig 4).

Discussion

The large database generated from systematic data collection in GIDEON offers an opportunity to assess global patterns of LRT use in the treatment of HCC in clinical practice. Final analyses of GIDEON highlighted that almost half of patients received TACE treatment

Figure 4

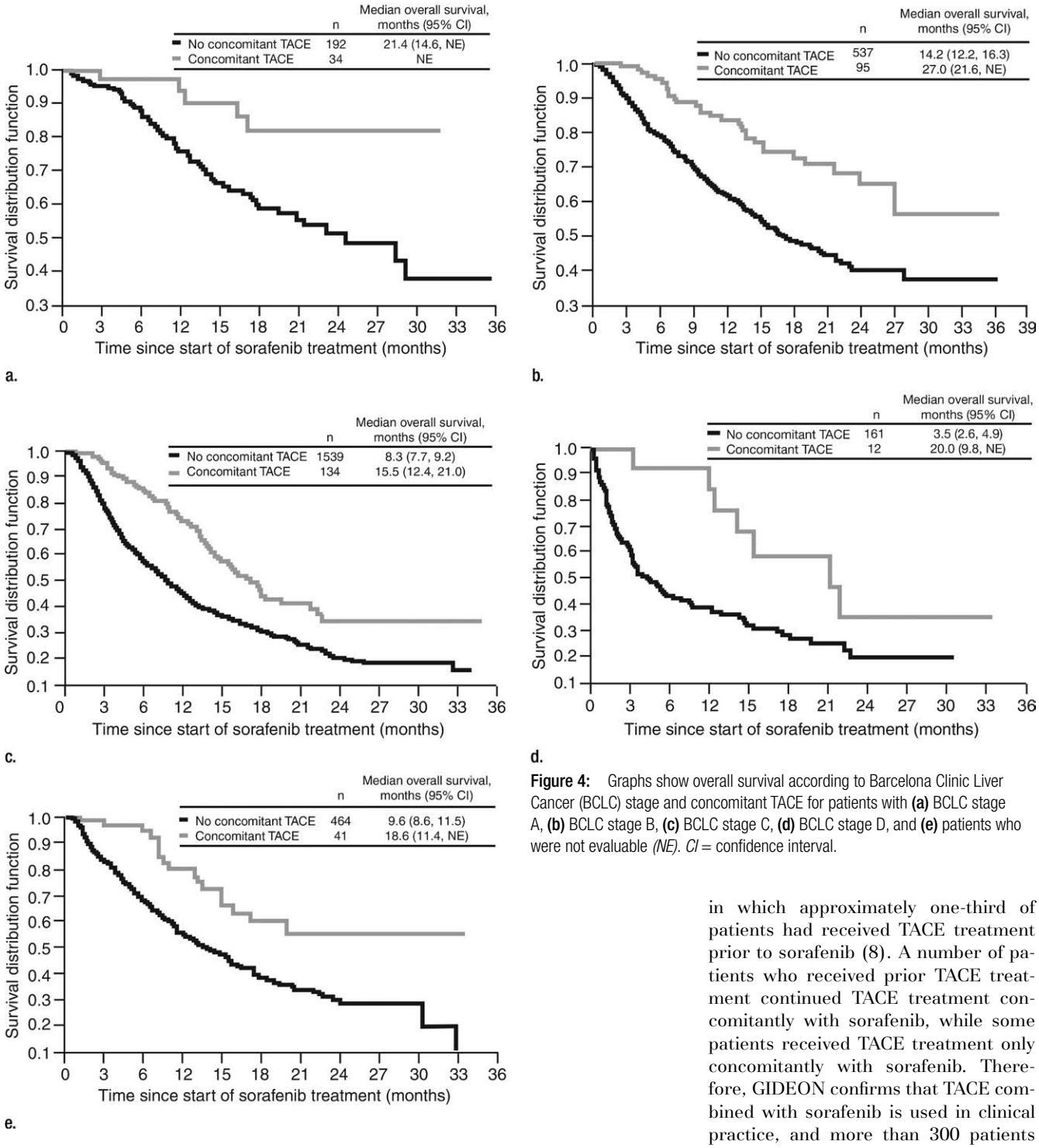

Figure 4: Graphs show overall survival according to Barcelona Clinic Liver Cancer (BCLC) stage and concomitant TACE for patients with **(a)** BCLC stage A, **(b)** BCLC stage B, **(c)** BCLC stage C, **(d)** BCLC stage D, and **(e)** patients who were not evaluable *(NE)*. *CI* = confidence interval.

prior to sorafenib. The observed use of sorafenib following TACE was consistent with the pivotal phase III Sorafenib Hepatocellular Carcinoma Assessment Randomized Protocol trial, which demonstrated the efficacy of sorafenib and in which approximately one-third of patients had received TACE treatment prior to sorafenib (8). A number of patients who received prior TACE treatment continued TACE treatment concomitantly with sorafenib, while some patients received TACE treatment only concomitantly with sorafenib. Therefore, GIDEON confirms that TACE combined with sorafenib is used in clinical practice, and more than 300 patients received this combination. The patterns of TACE use prior to sorafenib varied regionally, consistent with previous reports, particularly in the frequency of

prior TACE and number of prior TACE treatments received per patient (23).

Lipiodol-based TACE was the predominant choice and more common than DEB TACE, perhaps unsurprisingly as DEB is a relatively new method (13,24); for example, DEB TACE was not approved by the China Food and Drug Administration to be the choice of TACE agent except for use in clinical trials. DEB TACE use varied globally and was more common in Western regions. These data may reflect regional variations or delays in the uptake of DEB TACE, and patterns may alter as further safety and efficacy data in representative patient populations are reported (25–27).

With respect to disease characteristics, patients without a history of TACE treatment tended to be at a more advanced stage of disease, likely reflecting that patients with an earlier disease stage may be more likely to receive TACE treatment. Some patients receiving concomitant TACE treatment had extrahepatic spread (28%) or vascular invasion (16%), somewhat contrary to TACE treatment guidelines, which recommend TACE use in intermediate noninvasive HCC (28).

Safety findings in GIDEON were consistent with the known safety profile of sorafenib. There was no evidence of unanticipated adverse events or adverse event patterns in TACE-treated patients, and safety was similar in patients treated with TACE and those never treated with TACE. The combination of TACE with sorafenib appeared to be well tolerated, and safety profiles were broadly similar irrespective of the pattern of TACE use. Sorafenib administration data revealed that duration of sorafenib treatment was longest in patients who received concomitant TACE treatment (over 36 weeks), highlighting the feasibility of the combination.

Patients who received prior TACE treatment tended to have a slightly longer overall survival time compared with those who had not received prior TACE treatment. However, these outcomes data must be interpreted with caution, given the variations in disease characteristics between patients who received prior or concomitant TACE treatment and those never treated with TACE. Patients who underwent a combination of TACE with sorafenib had a longer overall survival compared with all other subgroups. However, data must be interpreted with caution as only a relatively low number of patients received concomitant TACE treatment compared with the other subgroups, and the majority of patients who received concomitant TACE treatment had also received TACE treatment prior to sorafenib.

A number of studies have reported that the combination of sorafenib and TACE resulted in improved overall survival in patients with advanced HCC (17,19,29,30). However, a further study reported no benefit of sorafenib when given sequentially to patients who had responded to TACE (31). Ongoing trials will hopefully help to address key questions in relation to this combination in patients with advanced as well as intermediate stage HCC, including the optimal timing of sorafenib in relation to TACE and the influence of patient characteristics on the safety and efficacy of this combination (32).

Overall, the final analysis of GIDEON highlights global variations in TACE treatment patterns, as observed in the previous interim analysis (21). GIDEON data suggest that although prior TACE and TACE concomitant with sorafenib are tolerable and feasible, consistent with previous reports, variations exist in clinical practice, including the use of different TACE methodologies across global regions. GIDEON data may also reflect variations in decisions regarding when TACE should be performed and when TACE should be stopped (refractory), and thus when systemic therapy should be initiated (10). Repeated courses of TACE with no objective response may detract from the administration of potentially effective systemic therapy as a result of a lack of evidence-based guidelines (33). Further, scoring systems that better inform TACE retreatment are likely to prove useful in improving the approach to TACE use (11,34). The findings from GIDEON provide support for the standardization of TACE treatment practices and the publication of evidence-based guidelines to inform clinical decisions. Moreover, outcomes of HCC patients treated with TACE followed or not followed by sorafenib and the influence of timing to initiate **s**orafenib, or OPTIMIS, is an ongoing, prospective, observational study that will further evaluate the use of TACE and sorafenib in clinical practice.

Because GIDEON is an observational registry study, it is inherently limited by the lack of a randomized, controlled population. In addition, its observational nature means the study is also limited by the potential for selection bias and an inability to control for possible confounding factors. As such, it cannot evaluate if sorafenib in combination with TACE provided a benefit over TACE alone, and the descriptive statistics used do not allow for conclusive analysis of outcomes, so outcomes data must be interpreted with caution. However, GIDEON provides an opportunity to evaluate and understand global treatment patterns in clinical practice for the treatment of unresectable HCC. These data can be used to inform best practice and, ultimately, improve patient treatment and outcomes.

In conclusion, the findings from GIDEON in more than 3000 sorafenib-treated HCC patients highlight that global variation exists in LRT use for the treatment of HCC and in the technical aspects of TACE. Importantly, no safety concerns were noted in the use of TACE treatment either prior to or concomitant with sorafenib treatment. Therefore, TACE treatment prior to and/or concomitant with sorafenib appears to be a viable therapeutic approach in the treatment of unresectable HCC.

Acknowledgments: The authors thank all participating clinical sites that contributed to the GIDEON study. Data management-related activities for the GIDEON study were coordinated and overseen by Anja Laske, BS, and Dalila Lakbir, BS, at Bayer Healthcare Pharmaceuticals. The authors take full responsibility for the scope, direction, and content of the manuscript and have all approved the submitted manuscript. Tanja Torbica, PhD, at Complete HealthVizion provided assistance in the preparation and revision of the draft manuscript, based on detailed

discussion and feedback from all the authors. Editorial assistance was funded by Bayer Healthcare Pharmaceuticals.

Disclosures of Conflicts of Interest: J.F.G. Activities related to the present article: disclosed no relevant relationships. Activities not related to the present article: received grants and personal fees from BTG, Guerbet, Boston Scientific, and Bayer/Onyx and Philips Healthcare Research Grant, Research Grant from the NIH RO1 CA160771, Rolf W. Günther Foundation Educational Grant. Other relationships: disclosed no relevant relationships. **M.K.** disclosed no relevant relationships. **J.A.M.** Activities related to the present article: disclosed no relevant relationships. Activities not related to the present article: received personal fees from Bayer HealthCare and Onyx Pharmaceuticals. Other relationships: disclosed no relevant relationships. **A.P.V.** Activities related to the present article: received grant from Bayer. Activities not related to the present article: disclosed no relevant relationships. Other relationships: disclosed no relevant relationships. **X.P.C.** disclosed no relevant relationships. **J.P.B.** Activities related to the present article: institution received a grant from Bayer, author received consulting and lecture fees from Bayer. Activities not related to the present article: disclosed no relevant relationships. Other relationships: disclosed no relevant relationships. **L.D.** disclosed no relevant relationships. **J.F.** Activities related to the present article: received grant from Bayer. Activities not related to the present article: received personal fees from Chugai, Taiho, Eli Lilly Japan, Bayer, Eisai, Novartis, Ono, Yakult, Takeda, Astellas, Daiichi Sankyo, Sumitomo Dainippom, Bristol-Myers Squibb, Nippon Kayaku, Ajinomoto, Meiji Seika, Sanofy, Mitsubishi Tanabe Pharma, Hisamitsu, Sandoz, Shionogi, Kyowa Hakko Kirin, Merck Serono, Sumitomo Dainippon Pharma, MSD, Sawai, Mochida, Zeria, AstraZeneca, Graxo Smith Kline, Fujifilm, Boehringer Ingelheim, Onco Therapy Science, Otsuka, Janssen, Nobelphama, and J-Pharma. Other relationships: disclosed no relevant relationships. **L.L.d.G.** Activities related to the present article: received personal fees from Bayer. Activities not related to the present article: received personal fees from Bayer. Other relationships: disclosed no relevant relationships. **C.P.** Activities related to the present article: disclosed no relevant relationships. Activities not related to the present article: received grants from Bayer Healthcare. Other relationships: disclosed no relevant relationships. **A.J.S.** Activities related to the present article: disclosed no relevant relationships. Activities not related to the present article: received consultancy fees from Genfit, Tobira, Intercept, Nitto Denko, Immuron, Exhalenz, Merck, Lilly, Bristol Myers, and Astra Zeneca; institution received grants from Gilead, Bristol Myers, Intercept, Immuron, Novartis, Tobira, and Astra Zeneca; institution has patents for Nash Mouse from Virginia Commonwealth University; author receives royalties from Uptodate and Elsevier; author has stock options in Genfit. Other relationships: disclosed no relevant relationships. **T.T.** disclosed no relevant relationships. **S.L.Y.** disclosed no relevant relationships. **S.K.Y.** disclosed no relevant relationships. **K.N.** Activities related to the present article: author has stock ownership from Bayer. Activities not related to the present article: disclosed no relevant relationships. Other relationships: disclosed no relevant relationships. **R.L.** disclosed no relevant relationships. **S.H.** disclosed no relevant relationships. **R.L.** Activities related to the present article: disclosed no relevant relationships. Activities not related to the present article: received consultancy fees from Bayer. Other relationships: disclosed no relevant relationships.

References

1. Bruix J, Gores GJ, Mazzaferro V. Hepatocellular carcinoma: clinical frontiers and perspectives. Gut 2014;63(5):844–855.
2. Gao J, Xie L, Yang WS, et al. Risk factors of hepatocellular carcinoma: current status and perspectives. Asian Pac J Cancer Prev 2012; 13(3):743–752.
3. Forner A, Llovet JM, Bruix J. Hepatocellular carcinoma. Lancet 2012;379(9822):1245–1255.
4. Forner A, Reig ME, de Lope CR, Bruix J. Current strategy for staging and treatment: the BCLC update and future prospects. Semin Liver Dis 2010;30(1):61–74.
5. Kudo M, Izumi N, Kokudo N, et al. Management of hepatocellular carcinoma in Japan: consensus-based clinical practice guidelines proposed by the Japan Society of Hepatology (JSH) 2010 updated version. Dig Dis 2011; 29(3):339–364.
6. National Comprehensive Cancer Network. NCCN clinical practice guidelines in oncology: Hepatobiliary Cancers (Version 2.2014). http://www.nccn.org/professionals/physician_gls/pdf/hepatobiliary.pdf. Accessed June 23, 2015.
7. Llovet JM, Bruix J. Systematic review of randomized trials for unresectable hepatocellular carcinoma: chemoembolization improves survival. Hepatology 2003;37(2):429–442.
8. Llovet JM, Ricci S, Mazzaferro V, et al. Sorafenib in advanced hepatocellular carcinoma. N Engl J Med 2008;359(4):378–390.
9. Cheng AL, Kang YK, Chen Z, et al. Efficacy and safety of sorafenib in patients in the Asia-Pacific region with advanced hepatocellular carcinoma: a phase III randomised, double-blind, placebo-controlled trial. Lancet Oncol 2009;10(1):25–34.
10. Cheng AL, Amarapurkar D, Chao Y, et al. Re-evaluating transarterial chemoembolization for the treatment of hepatocellular carcinoma: consensus recommendations and review by an International Expert Panel. Liver Int 2014;34(2):174–183.
11. Hucke F, Sieghart W, Pinter M, et al. The ART-strategy: sequential assessment of the ART score predicts outcome of patients with hepatocellular carcinoma re-treated with TACE. J Hepatol 2014;60(1):118–126.
12. Hucke F, Pinter M, Graziadei I, et al. How to STATE suitability and START transarterial chemoembolization in patients with intermediate stage hepatocellular carcinoma. J Hepatol 2014;61(6):1287–1296.
13. Lencioni R. Management of hepatocellular carcinoma with transarterial chemoembolization in the era of systemic targeted therapy. Crit Rev Oncol Hematol 2012;83(2): 216–224.
14. Terzi E, Golfieri R, Piscaglia F, et al. Response rate and clinical outcome of HCC after first and repeated cTACE performed "on demand". J Hepatol 2012;57(6):1258–1267.
15. Pawlik TM, Reyes DK, Cosgrove D, Kamel IR, Bhagat N, Geschwind JF. Phase II trial of sorafenib combined with concurrent transarterial chemoembolization with drug-eluting beads for hepatocellular carcinoma. J Clin Oncol 2011;29(30):3960–3967.
16. Sansonno D, Lauletta G, Russi S, Conteduca V, Sansonno L, Dammacco F. Transarterial chemoembolization plus sorafenib: a sequential therapeutic scheme for HCV-related intermediate-stage hepatocellular carcinoma—a randomized clinical trial. Oncologist 2012;17(3):359–366.
17. Bai W, Wang YJ, Zhao Y, et al. Sorafenib in combination with transarterial chemoembolization improves the survival of patients with unresectable hepatocellular carcinoma: a propensity score matching study. J Dig Dis 2013;14(4):181–190.
18. Lencioni R, Llovet JM, Han G, et al. Sorafenib or placebo in combination with transarterial chemoembolization (TACE) with doxorubicin-eluting beads (DEBDOX) for intermediate-stage hepatocellular carcinoma (HCC): phase II, randomized, double-blind SPACE trial [abstr]. J Clin Oncol 2012;30(4 Suppl):LBA154.
19. Chao Y, Chung YH, Han G, et al. The combination of transcatheter arterial chemoembolization and sorafenib is well tolerated and effective in Asian patients with hepatocellular carcinoma: final results of the START trial. Int J Cancer 2015;136(6):1458–1467.
20. Lencioni R, Marrero J, Venook A, Ye SL, Kudo M. Design and rationale for the non-interventional Global Investigation of therapeutic DEcisions in hepatocellular carcinoma and Of its treatment with sorafeNib (GIDEON) study. Int J Clin Pract 2010;64(8):1034–1041.

21. Lencioni R, Kudo M, Ye SL, et al. First interim analysis of the GIDEON (Global Investigation of therapeutic decisions in hepatocellular carcinoma and of its treatment with sorafeNib) non-interventional study. Int J Clin Pract 2012;66(7):675–683.

22. Lencioni R, Kudo M, Ye SL, et al. GIDEON (Global Investigation of therapeutic DEcisions in hepatocellular carcinoma and Of its treatment with sorafeNib): second interim analysis. Int J Clin Pract 2014;68(5):609–617.

23. Geschwind JF, Lencioni R, Marrero JA, et al. Worldwide trends in locoregional therapy for hepatocellular carcinoma (HCC): second interim analysis of the Global Investigation of therapeutic DEcisions in HCC and Of its treatment with sorafeNib (GIDEON) study [abstr]. J Clin Oncol 2012;30(suppl 4):317.

24. Varela M, Real MI, Burrel M, et al. Chemoembolization of hepatocellular carcinoma with drug eluting beads: efficacy and doxorubicin pharmacokinetics. J Hepatol 2007;46(3):474–481.

25. Lammer J, Malagari K, Vogl T, et al. Prospective randomized study of doxorubicin-eluting-bead embolization in the treatment of hepatocellular carcinoma: results of the PRECISION V study. Cardiovasc Intervent Radiol 2010;33(1):41–52.

26. Song MJ, Chun HJ, Song S, et al. Comparative study between doxorubicin-eluting beads and conventional transarterial chemoembolization for treatment of hepatocellular carcinoma. J Hepatol 2012;57(6):1244–1250.

27. Huang K, Zhou Q, Wang R, Cheng D, Ma Y. Doxorubicin-eluting beads versus conventional transarterial chemoembolization for the treatment of hepatocellular carcinoma. J Gastroenterol Hepatol 2014;29(5):920–925.

28. European Association For The Study Of The Liver; European Organisation For Research And Treatment Of Cancer. EASL-EORTC clinical practice guidelines: management of hepatocellular carcinoma. J Hepatol 2012;56(4):908–943.

29. Qu XD, Chen CS, Wang JH, et al. The efficacy of TACE combined sorafenib in advanced stages hepatocellullar carcinoma. BMC Cancer 2012;12:263.

30. Zhao Y, Wang WJ, Guan S, et al. Sorafenib combined with transarterial chemoembolization for the treatment of advanced hepatocellular carcinoma: a large-scale multicenter study of 222 patients. Ann Oncol 2013;24(7):1786–1792.

31. Kudo M, Imanaka K, Chida N, et al. Phase III study of sorafenib after transarterial chemoembolisation in Japanese and Korean patients with unresectable hepatocellular carcinoma. Eur J Cancer 2011;47(14):2117–2127.

32. Cabibbo G, Tremosini S, Galati G, et al. Transarterial chemoembolization and sorafenib in hepatocellular carcinoma. Expert Rev Anticancer Ther 2014;14(7):831–845.

33. Lencioni R, Chen XP, Dagher L, Venook AP. Treatment of intermediate/advanced hepatocellular carcinoma in the clinic: how can outcomes be improved? Oncologist 2010;15(suppl 4):42–52.

34. Sieghart W, Hucke F, Pinter M, et al. The ART of decision making: retreatment with transarterial chemoembolization in patients with hepatocellular carcinoma. Hepatology 2013;57(6):2261–2273.

Images of the Month

Small-Bowel Obstruction Due to Obturator Hernia

Kao-Lang Liu[1], I-Lun Shih[1] and Chin-Chen Chang[1]

Am J Gastroenterol 2016;111:453; doi:10.1038/ajg.2015.310

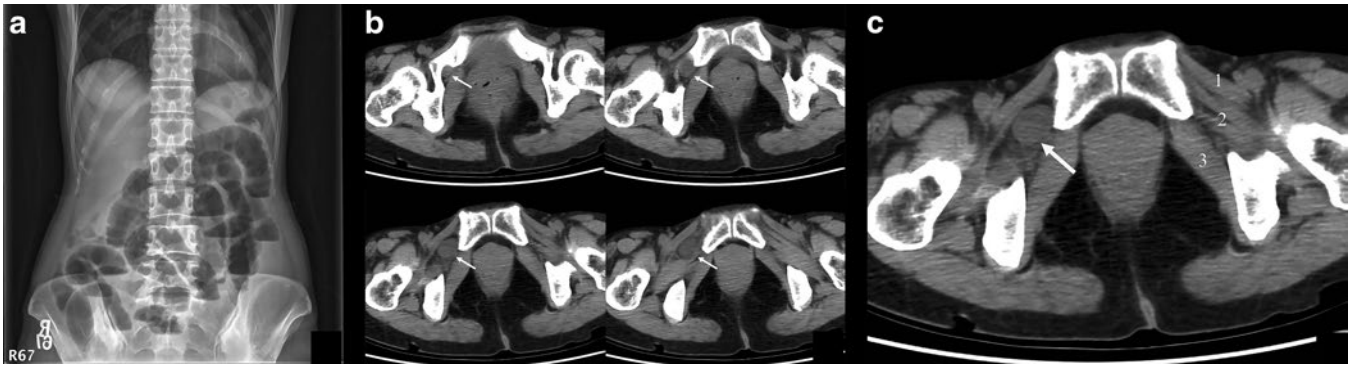

A 48-year-old woman with no history of abdominal surgery had lower abdominal pain without fever or peritoneal signs. The standing plain abdominal radiograph revealed ileus (**a**). Treatment with metoclopramide and bisacodyl with nil per os was unsuccessful. Computed tomography showed a small-bowel obstruction due to focal incarceration of the small bowel between the right obturator externus and pectineus muscles (arrows, **b**). Weakness of the right obturator externus muscle was noted (**c**; 1, pectineus; 2, obturator externus; 3, obturator internus). Awareness of this diagnosis may help in detecting the physical Howship–Romberg sign, leading to early diagnosis and management.

[1]National Taiwan University Hospital and National Taiwan University College of Medicine, Taipei, Taiwan.

Gastric Perineurioma

Shigenaga Matsui[1], Hiroshi Kashida[1] and Masatoshi Kudo[1]

Am J Gastroenterol 2016;111:453; doi:10.1038/ajg.2015.306

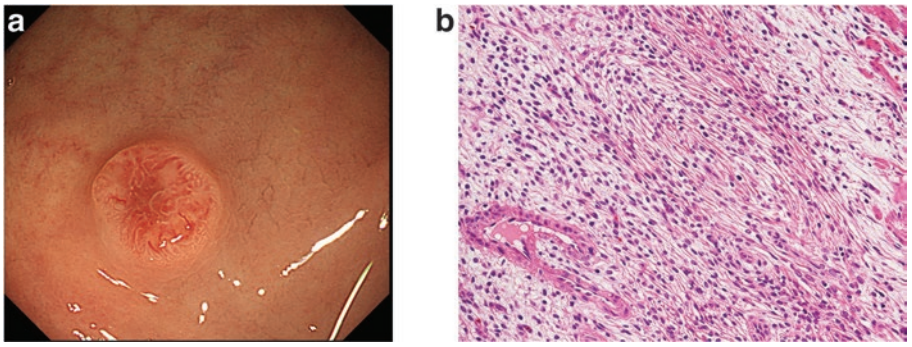

Gastrointestinal endoscopy performed in a 51-year-old woman for screening purposes revealed a small, elevated lesion with a reddish depression at the fornix (**a**). Endoscopic mucosal resection was performed. Histology showed proliferation of band spindle cells with ovoid to elongated nuclei and indistinct cytoplasma. Note the tendency for the tumor cells to be located around vessels in whorls of striking appearance (**b**). Immunohistochemical staining revealed that the spindle cells were positive for GLUT-1 and claudin-1, but the cells were negative for membrane antigen (EMA), S-100 protein, CD117, CD34, and smooth muscle actin. Therefore, this lesion was diagnosed as a gastric perineurioma.

[1]Kinki University, Osaka, Japan.

World Journal of Gastroenterology

Submit a Manuscript: http://www.wjgnet.com/esps/
Help Desk: http://www.wjgnet.com/esps/helpdesk.aspx
DOI: 10.3748/wjg.v22.i21.5132

World J Gastroenterol 2016 June 7; 22(21): 5132-5136
ISSN 1007-9327 (print) ISSN 2219-2840 (online)

CASE REPORT

Modified single transluminal gateway transcystic multiple drainage technique for a huge infected walled-off pancreatic necrosis: A case report

Kosuke Minaga, Masayuki Kitano, Hajime Imai, Kentaro Yamao, Ken Kamata, Takeshi Miyata, Tomohiko Matsuda, Shunsuke Omoto, Kumpei Kadosaka, Tomoe Yoshikawa, Masatoshi Kudo

Kosuke Minaga, Masayuki Kitano, Hajime Imai, Kentaro Yamao, Ken Kamata, Takeshi Miyata, Tomohiko Matsuda, Shunsuke Omoto, Kumpei Kadosaka, Tomoe Yoshikawa, Masatoshi Kudo, Department of Gastroenterology and Hepatology, Kinki University Faculty of Medicine, Osaka-Sayama 589-8511, Japan

Author contributions: Minaga K contributed to manuscript writing, performing endoscopic interventions; Kitano M contributed to drafting conception and design, performing endoscopic interventions; Imai H, Yamao K, Kamata K, Miyata T, Matsuda T, Omoto S, Kadosaka K and Yoshikawa T contributed to writing the manuscript; Kudo M contributed to drafting conception and design; all authors helped to perform the research.

Supported by The Japan Society for the Promotion of Science and the Japanese Foundation for the Research and Promotion of Endoscopy, No. 22590764 and No. 25461035.

Institutional review board statement: This study was approved by the Institutional Review Board of Kinki University Faculty of Medicine.

Informed consent statement: The patient provided informed written consent prior to study enrollment.

Conflict-of-interest statement: All authors declare no conflicts-of-interest related to this article.

Correspondence to: Masayuki Kitano, MD, PhD, Department of Gastroenterology and Hepatology, Kinki University Faculty of Medicine, 377-2 Ohno-Higashi, Osaka-Sayama 589-8511, Japan. m-kitano@med.kindai.ac.jp
Telephone: +81-72-3660221
Fax: +81-72-3672880

Received: January 9, 2016
Peer-review started: January 10, 2016
First decision: February 18, 2016
Revised: February 24, 2016
Accepted: March 18, 2016
Article in press: March 18, 2016
Published online: June 7, 2016

Abstract

We report a successful endoscopic ultrasonography-guided drainage of a huge infected multilocular walled-off necrosis (WON) that was treated by a modified single transluminal gateway transcystic multiple drainage (SGTMD) technique. After placing a wide-caliber fully covered metal stent, follow-up computed tomography revealed an undrained subcavity of WON. A large fistula that was created by the wide-caliber metal stent enabled the insertion of a forward-viewing upper endoscope directly into the main cavity, and the narrow connection route within the main cavity to the subcavity was identified with a direct view, leading to the successful drainage of the subcavity. This modified SGTMD technique appears to be useful for seeking connection routes between subcavities of WON in some cases.

Key words: Endoscopic ultrasonography; Infected pancreatic necrosis; Walled-off necrosis; Endoscopic ultrasonography-guided drainage; Acute pancreatitis

Core tip: Walled-off necrosis (WON) remains difficult to endoscopically manage because of insufficient drainage of solid necrotic tissues. Here, we present a case of successful drainage of a huge WON *via* a modified single transluminal gateway transcystic multiple drainage technique. After placing a wide-caliber covered metal stent, follow-up computed tomography revealed an undrained subcavity of WON. A large fistula created by the metal stent enabled the insertion of an upper endoscope directly into the main cavity, and the narrow connection route within the main cavity to the subcavity was identified with a direct view, leading to the successful drainage of the subcavity.

Minaga K, Kitano M, Imai H, Yamao K, Kamata K, Miyata T, Matsuda T, Omoto S, Kadosaka K, Yoshikawa T, Kudo M. Modified single transluminal gateway transcystic multiple drainage technique for a huge infected walled-off pancreatic necrosis: A case report. *World J Gastroenterol* 2016; 22(21): 5132-5136 Available from: URL: http://www.wjgnet.com/1007-9327/full/v22/i21/5132.htm DOI: http://dx.doi.org/10.3748/wjg.v22.i21.5132

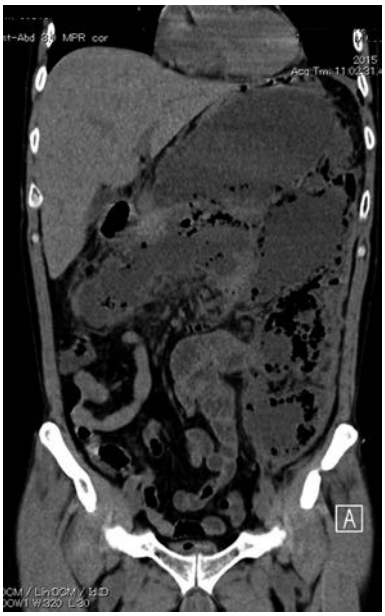

Figure 1 Abdominal computed tomography scan showing a huge multilocular walled-off necrosis replacing the body and tail of the pancreas, which extended to the pelvis. Gas bubbles were observed in the cavity.

INTRODUCTION

Endoscopic ultrasonography (EUS)-guided drainage for pancreatic fluid collection (PFC) is increasingly used as a minimally invasive alternative to surgical and percutaneous drainage[1-3]. However, walled-off necrosis (WON) remains difficult to endoscopically manage because of insufficient drainage of solid necrotic tissues. Various techniques, such as the use of wide-caliber metal stents[4,5], direct endoscopic necrosectomy[6,7] and multiple transluminal gateway technique[8] are reportedly useful for managing WON. However, responses to these advanced techniques remain unsatisfactory in some cases. Recently, a single transluminal gateway transcystic multiple drainage (SGTMD) was developed for treating complicated multilocular WON[9]. Here, we present a case of successful endoscopic drainage of a huge infected multilocular WON *via* a modified SGTMD technique.

CASE REPORT

A 49-year-old male presented with upper abdominal pain and high fever of 7 d duration. He was diagnosed with alcohol-induced severe acute pancreatitis 1 mo before and was discharged 6 d after admission from a neighbouring general hospital. His computed tomography (CT) severity index[10] was 6. He was re-admitted to our hospital with the above-mentioned chief complaints. Laboratory tests revealed elevated C-reactive protein (CRP) and procalcitonin levels (27.8 mg/dL and 6.17 ng/mL, respectively). Elevated levels of kidney function parameters were also noted (blood urea nitrogen level, 77 mg/dL; serum creatinine level, 3.14 mg/dL). An abdominal CT revealed a huge multilocular WON measuring 31 cm × 16 cm, which spread from the pancreas to pelvis (Figure 1). Clinically, infection of the necrosis was assumed. Doripenem was intravenously introduced; however, his clinical symptoms and elevated inflammatory reaction persisted. As the main cavity of WON was close to the gastric lumen, we decided to puncture WON under EUS guidance. EUS-guided transluminal drainage was performed; a wide-caliber fully covered TTS Niti-S esophageal stent (internal diameter, 16 mm; maximum flange diameter, 24 mm; length, 40 mm; Taewoong Medical, Seoul, South Korea) was placed (Figure 2). Through the metal stent, a 7-Fr double-pigtail plastic stent (length, 80 mm) and a 7-Fr nasocystic catheter were inserted (Figure 3). During the procedure, approximately 2.4 L of purulent fluid were suctioned. A follow-up abdominal CT obtained 1 wk after the procedure demonstrated a significant reduction in the size of the main cavity; however, the undrained subcavity remained, which was mainly located in the left anterior pararenal space and extended to the left pelvis (Figure 4). Additional drainage targeting the subcavity was required because high fever continued after the procedure. Because the subcavity was not adjacent to the stomach or duodenum, additional EUS-guided puncture was difficult. CT suggested communication between the subcavity and main cavity; therefore, a SGTMD procedure was considered. Repeated attempts to determine the connection route within the main cavity to the subcavity using an ERCP catheter and 0.025-inch guidewire were unsuccessful. The metal stent was removed, and a large fistula that was created by the metal stent enabled the insertion

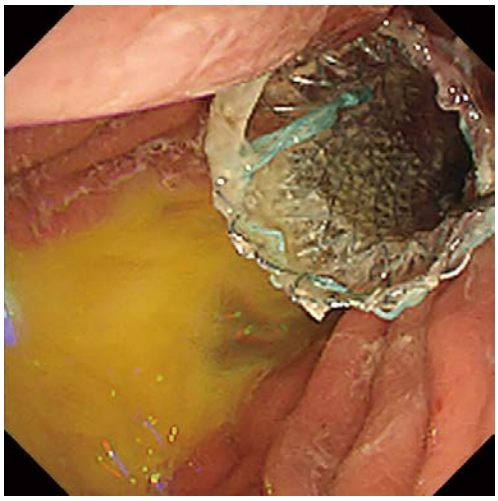

Figure 2 Successful deployment of a wide-caliber fully covered TTS Niti-S **esophageal stent. Purulent fluid was observed in the gastric lumen.**

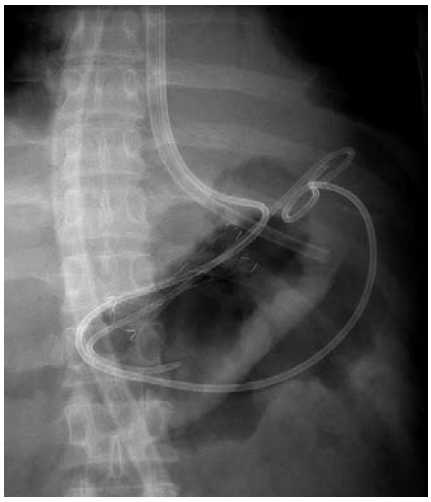

Figure 3 A 7-Fr double-pigtail plastic stent and a 7-Fr nasocystic catheter were deployed through the fully covered metal stent.

of a forward-viewing upper endoscope directly into the main cavity. After the endoscope was advanced into the cavity, a narrow connection route was identified (Figure 5). Contrast medium was injected into the connection. Having confirmed the detection of the subcavity, the guidewire was inserted into the cavity and two 7-Fr double-pigtail plastic stents (lengths, 120 and 80 mm, respectively) were deployed (Figure 6). No procedure-related complications were observed. After additional endoscopic management, high fever resolved over the course of a few days and CRP levels significantly decreased. CT revealed that the subcavity of WON was well drained. The patient completely recovered and was discharged after 3 wk of hospitalization. Follow-up CT obtained 1 month after discharge revealed that WON had mostly collapsed (Figure 7) and the patient remained symptom free.

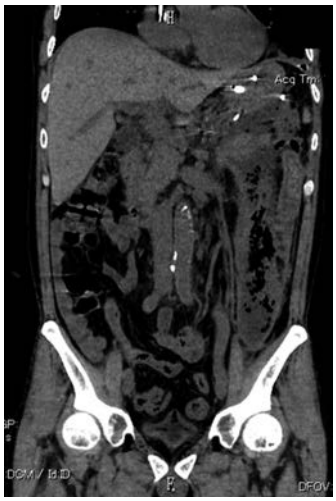

Figure 4 Computed tomography one week after initial drainage showed an undrained subcavity, located mainly at the left anterior pararenal space that extended to the left pelvis.

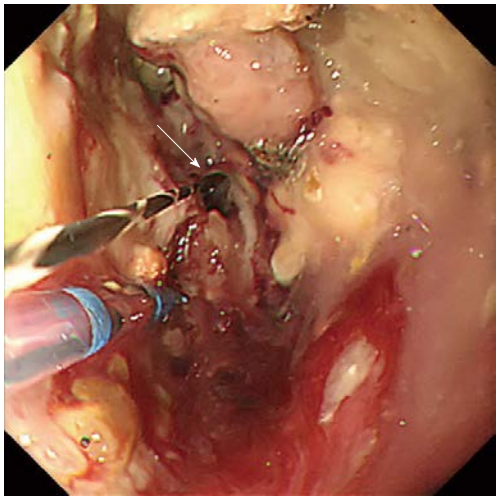

Figure 5 Endoscopic view of the cavity of walled-off necrosis by a modified single transluminal gateway transcystic multiple drainage technique. An upper endoscope was inserted into the walled-off necrosis (WON) through the fistula and a narrow connection route within the main cavity to the subcavity could be identified directly (white arrow).

DISCUSSION

Over the last decade, techniques for pancreatic fluid collection have shifted toward minimally invasive approaches. Since first reported in 1992 by Grimm *et al*[1] EUS-guided transluminal drainage for pancreatic fluid collection has played a pivotal role and spread worldwide as a minimally invasive alternative to surgical and percutaneous drainage[1-3]. However, the clinical response rate of the conventional single transluminal gateway technique deploying single or multiple stenting for treating WON is not satisfactory (described as 45%-63%)[8,11]. Recently, various techniques, such as the use of wide-caliber metal

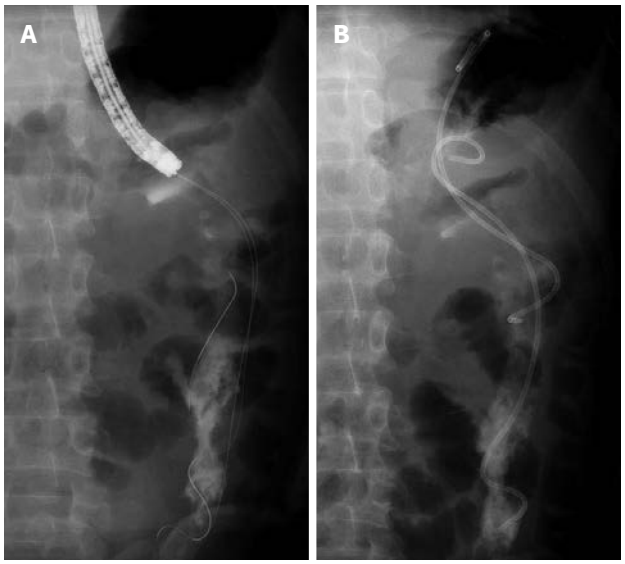

Figure 6 Fluoroscopic view of modified single transluminal gateway transcystic multiple drainage technique. With a direct view of the connection route, a 0.025-inch guidewire was inserted into the subcavity (A) and two 7-Fr double-pigtail plastic stents were deployed (B).

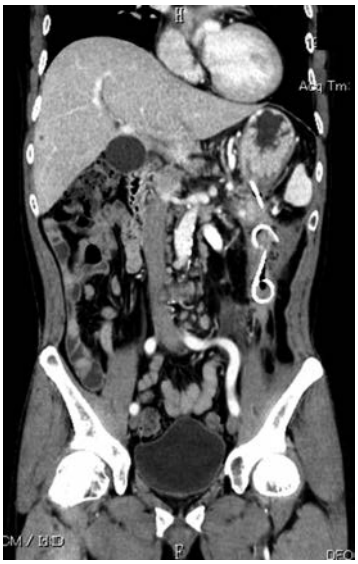

Figure 7 Follow-up computed tomography obtained one month after discharge revealed the WON had mostly collapsed.

stents[4,5], direct endoscopic necrosectomy[6,7] and multiple transluminal gateway technique[8] have improved the clinical success rate of endoscopic management of WON. However, response to these advanced techniques remains unsatisfactory in some cases. Mukai *et al*[9] recently described a novel SGTMD procedure for complicated multilocular WON and reported successful drainage in five cases using this technique. When subcavities are located far from the gastrointestinal lumen, percutaneous approach would have been used conventionally. Mukai *et al*[9] hypothesized that the multilocular cavity may have originally been unilocular and separated into subcavities with tiny, narrow connections during the process of treatment and collapse. They used an ERCP catheter and soft guidewire to locate tiny, narrow connections. In this case, we repeatedly attempted to identify the connection using an ERCP catheter and soft guidewire through the metal stent under fluoroscopic guidance, but the guidewire curled up in the main cavity and failed to locate a connection route. Instead, we inserted the upper endoscope into the cavity through the large fistula, which enabled the narrow connection route to be directly observed. The guidewire was easily and safely advanced into the subcavity, and successful drainage of the subcavity was achieved. This is a modified technique of the previously described SGTMD. In addition to SGTMD, having a direct view to identify the connection route may lead to a higher success rate in some cases.

In this case, the pig-tail stents have been left in place during 6 mo follow-up. This is because the previous studies revealed that stent retrieval was associated with higher PFC recurrence rates[12,13].

In conclusion, we presented a case of successful endoscopic drainage of a huge infected multilocular WON by a modified SGTMD technique with direct endoscope insertion into the cavity. This modified SGTMD technique appears to be useful in seeking connection routes between the subcavities of WON and might avoid the requirement for a more invasive drainage procedure, such as endoscopic or surgical necrosectomy.

COMMENTS

Case characteristics

One month after being diagnosed with alcohol-induced severe acute pancreatitis, a 49-year-old male presented with upper abdominal pain and high fever of 7 d duration.

Clinical diagnosis

The patient had upper abdominal pain and high fever.

Differential diagnosis

Pancreatic pseudocyst.

Laboratory diagnosis

The laboratory findings showed elevated C-reactive protein, procalcitonin levels and renal dysfunction.

Imaging diagnosis

Abdominal computed tomography demonstrated a huge multilocular WON measuring 31 cm × 16 cm, which spread from the pancreas to pelvis.

Pathological diagnosis

Pathological examination was not performed in this case.

Treatment

Endoscopic drainage with a modified single transluminal gateway transcystic multiple drainage (SGTMD) technique was performed.

Related reports

WON remains difficult to endoscopically manage because of insufficient drainage of solid necrotic tissues. Various techniques, such as the use of wide-caliber metal stents, direct endoscopic necrosectomy, multiple transluminal gateway technique and SGTMD technique were developed for treating WON.

Term explanation

Modified SGTMD is a novel alternative technique for drainage of WON which means a single transluminal gateway transcystic multiple drainage with direct endoscope insertion into the cavity.

Experiences and lessons

Modified SGTMD technique appears to be useful in seeking connection routes between the subcavities of WON and might avoid the requirement for a more invasive drainage procedure, such as endoscopic or surgical necrosectomy.

Peer-review

This case report is interesting and well documented.

REFERENCES

1 **Grimm H**, Binmoeller KF, Soehendra N. Endosonography-guided drainage of a pancreatic pseudocyst. *Gastrointest Endosc* 1992; **38**: 170-171 [PMID: 1568613 DOI: 10.1016/S0016-5107(92)70384-8]

2 **Park DH**, Lee SS, Moon SH, Choi SY, Jung SW, Seo DW, Lee SK, Kim MH. Endoscopic ultrasound-guided versus conventional transmural drainage for pancreatic pseudocysts: a prospective randomized trial. *Endoscopy* 2009; **41**: 842-848 [PMID: 19798610 DOI: 10.1055/s-0029-1215133]

3 **Talreja JP**, Shami VM, Ku J, Morris TD, Ellen K, Kahaleh M. Transenteric drainage of pancreatic-fluid collections with fully covered self-expanding metallic stents (with video). *Gastrointest Endosc* 2008; **68**: 1199-1203 [PMID: 19028232 DOI: 10.1016/j.gie.2008.06.015]

4 **Bapaye A**, Itoi T, Kongkam P, Dubale N, Mukai S. New fully covered large-bore wide-flare removable metal stent for drainage of pancreatic fluid collections: results of a multicenter study. *Dig Endosc* 2015; **27**: 499-504 [PMID: 25545957 DOI: 10.1111/den.12421]

5 **Attam R**, Trikudanathan G, Arain M, Nemoto Y, Glessing B, Mallery S, Freeman ML. Endoscopic transluminal drainage and necrosectomy by using a novel, through-the-scope, fully covered, large-bore esophageal metal stent: preliminary experience in 10 patients. *Gastrointest Endosc* 2014; **80**: 312-318 [PMID: 24721519 DOI: 10.1016/j.gie.2014.02.013]

6 **Seifert H**, Wehrmann T, Schmitt T, Zeuzem S, Caspary WF. Retroperitoneal endoscopic debridement for infected peripancreatic necrosis. *Lancet* 2000; **356**: 653-655 [PMID: 10968442 DOI: 10.1016/S0140-6736(00)02611-8]

7 **Yasuda I**, Nakashima M, Iwai T, Isayama H, Itoi T, Hisai H, Inoue H, Kato H, Kanno A, Kubota K, Irisawa A, Igarashi H, Okabe Y, Kitano M, Kawakami H, Hayashi T, Mukai T, Sata N, Kida M, Shimosegawa T. Japanese multicenter experience of endoscopic necrosectomy for infected walled-off pancreatic necrosis: The JENIPaN study. *Endoscopy* 2013; **45**: 627-634 [PMID: 23807806 DOI: 10.1055/s-0033-1344027]

8 **Varadarajulu S**, Phadnis MA, Christein JD, Wilcox CM. Multiple transluminal gateway technique for EUS-guided drainage of symptomatic walled-off pancreatic necrosis. *Gastrointest Endosc* 2011; **74**: 74-80 [PMID: 21612778 DOI: 10.1016/j.gie.2011.03.1122]

9 **Mukai S**, Itoi T, Sofuni A, Itokawa F, Kurihara T, Tsuchiya T, Ishii K, Tsuji S, Ikeuchi N, Tanaka R, Umeda J, Tonozuka R, Honjo M, Moriyasu F. Novel single transluminal gateway transcystic multiple drainages after EUS-guided drainage for complicated multilocular walled-off necrosis (with videos). *Gastrointest Endosc* 2014; **79**: 531-535 [PMID: 24287280 DOI: 10.1016/j.gie.2013]

10 **Balthazar EJ**, Robinson DL, Megibow AJ, Ranson JH. Acute pancreatitis: value of CT in establishing prognosis. *Radiology* 1990; **174**: 331-336 [PMID: 2296641 DOI: 10.1148/radiology.174.2.2296641]

11 **Gardner TB**, Chahal P, Papachristou GI, Vege SS, Petersen BT, Gostout CJ, Topazian MD, Takahashi N, Sarr MG, Baron TH. A comparison of direct endoscopic necrosectomy with transmural endoscopic drainage for the treatment of walled-off pancreatic necrosis. *Gastrointest Endosc* 2009; **69**: 1085-1094 [PMID: 19243764 DOI: 10.1016/j.gie.2008.06.061]

12 **Arvanitakis M**, Delhaye M, Bali MA, Matos C, De Maertelaer V, Le Moine O, Devière J. Pancreatic-fluid collections: a randomized controlled trial regarding stent removal after endoscopic transmural drainage. *Gastrointest Endosc* 2007; **65**: 609-619 [PMID: 17324413 DOI: 10.1016/j.gie.2006.06.083]

13 **Bang JY**, Wilcox CM, Trevino J, Ramesh J, Peter S, Hasan M, Hawes RH, Varadarajulu S. Factors impacting treatment outcomes in the endoscopic management of walled-off pancreatic necrosis. *J Gastroenterol Hepatol* 2013; **28**: 1725-1732 [PMID: 23829423 DOI: 10.1111/jgh.12328]

P- Reviewer: Wronski M **S- Editor**: Qi Y **L- Editor**: A
E- Editor: Zhang DN

Published by **Baishideng Publishing Group Inc**
8226 Regency Drive, Pleasanton, CA 94588, USA
Telephone: +1-925-223-8242
Fax: +1-925-223-8243
E-mail: bpgoffice@wjgnet.com
Help Desk: http://www.wjgnet.com/esps/helpdesk.aspx
http://www.wjgnet.com

ISSN 1007-9327

REFERENCES

1. Imai H, Kitano M, Omoto S, et al. EUS-guided gallbladder drainage for rescue treatment of malignant distal biliary obstruction after unsuccessful ERCP. Gastrointest Endosc. Epub 2016 Jan 4.
2. Fletcher DR, Jones RM. Laparoscopic cholecystjejunostomy as palliation for obstructive jaundice in inoperable carcinoma of pancreas. Surg Endosc 1992;6:147-9.
3. Tarnasky PR, England RE, Lail LM, et al. Cystic duct patency in malignant obstructive jaundice. An ERCP-based study relevant to the role of laparoscopic cholecystojejunostomy. Ann Surg 1995;221:265-71.
4. Isayama H, Kawabe T, Nakai Y, et al. Cholecystitis after metallic stent placement in patients with malignant distal biliary obstruction. Clin Gastroenterol Hepatol 2006;4:1148-53.
5. Nakai Y, Isayama H, Tsujino T, et al. Intraductal US in the assessment of tumor involvement to the orifice of the cystic duct by malignant biliary obstruction. Gastrointest Endosc 2008;68:78-83.

http://dx.doi.org/10.1016/j.gie.2016.01.015

Response:

We thank Dr Nakai and his colleagues for their great interest in and valuable comments to our article.[1] They discussed the utility of observing the cystic duct before carrying out EUS-guided gallbladder drainage (EUS-GBD). We agree that the indications for EUS-GBD are limited because this procedure can be performed only in cases in which cystic duct takeoff is not involved. Therefore, evaluating cystic duct patency before EUS-GBD is important.

Intraductal ultrasonography (IDUS) is the most suitable tool to check cystic duct patency during ERCP, by which tumor involvement of the cystic duct is accurately confirmed.[2] However, it was impossible to use IDUS for confirmation of cystic duct patency before EUS-GBD, because all patients underwent EUS-GBD after ERCP failed in our study.[1] Thus, cystic duct patency was confirmed by EUS before EUS-GBD was performed in all 12 patients.[1] When the cystic duct was entrapped by the tumor, we did not carry out EUS-GBD.

In conclusion, cystic duct patency should be confirmed by EUS before EUS-GBD is performed. If the cystic duct is obstructed by tumor involvement, EUS-guided bile duct drainage or percutaneous transhepatic bile duct drainage rather than EUS-GBD should be used.

DISCLOSURE

All authors disclosed no financial relationships relevant to this publication.

Masayuki Kitano, MD, PhD
Hajime Imai, MD
Ken Kamata, MD, PhD
Masatoshi Kudo, MD, PhD
Department of Gastroenterology and Hepatology
Kinki University School of Medicine
Osaka-sayama, Japan

REFERENCES

1. Imai H, Kitano M, Omoto S, et al. EUS-guided gallbladder drainage for rescue treatment of malignant distal biliary obstruction after unsuccessful ERCP. Gastrointest Endosc. In Press 2016.
2. Isayama H, Kawabe T, Nakai Y, et al. Cholecystitis after metallic stent placement in patients with malignant distal biliary obstruction. Clin Gastroenterol Hepatol 2006;4:1148-53.

http://dx.doi.org/10.1016/j.gie.2016.03.1487

Post-ERCP pancreatitis after biliary cannulation with traditional rendezvous in patients with T-tube

To the Editor:

We read with interest the article by Cantù et al[1] about a new technique of duodenal rendezvous for successful biliary cannulation in patients with a T-tube after orthotopic liver transplantation. Although the sample of the study group in this report was very small (10 duodenal, 10 traditional), the authors reported that this technique is relatively safe with regard to the risk of post-ERCP pancreatitis (PEP), and the procedure time is shorter in duodenal rendezvous than in traditional rendezvous.

Indeed, we have mostly applied the duodenal technique in our clinics for years if we fail in biliary cannulation in patients with a T-tube after liver transplantation, cholecystectomy, or both. We agree with the authors that selective biliary cannulation with this technique is much faster than the traditional rendezvous technique. However, we disagree with the authors with regard to their observation about an increased risk of PEP after traditional rendezvous. At least 2 reports in the literature describe a reduction in PEP after rendezvous cannulation.[2,3] We believe that if the wire through the T-tube is synchronously loosened during its removal from the papilla after grasping with the snare, no significant stretching of the papilla vateri occurs. Moreover, this technique also prevents unintentional engagement with the pancreatic duct, similarly to the duodenal rendezvous technique. Transient asymptomatic hyperamylasemia associated with the traditional rendezvous technique as noted by Cantù et al[1] has very little clinical significance and also is usually not recognized as an adverse event.

It is obvious that most ERCP clinics in the world use and advocate the duodenal technique, and if it fails the traditional technique is used in patients with a T-tube. However, there is no strong evidence in the report by Cantù et al[1] that the traditional rendezvous, if conducted correctly, has an increased risk of PEP compared with duodenal rendezvous. Moreover, some authors recommend a combined approach via traditional rendezvous over standard biliary cannulation to minimize the risk of PEP.[3]

DISCLOSURE

All authors disclosed no financial relationships relevant to this publication.

Ulku Saritas, MD
Medicana Ankara International Hospital
Gastroenterology Clinics
Ankara, Turkey
Yucel Ustundag, MD
Bulent Ecevit University
Department of Internal Medicine
Gastroenterology Clinics
Zonguldak, Turkey

REFERENCES

1. Cantù P, Parzanese I, Melada E, et al. A new duodenal rendezvous technique for biliary cannulation in patients with T-tube after orthotopic liver transplantation (with video). Gastrointest Endosc 2016;83:229-33.
2. Swahn F, Nilsson M, Arnelo U, et al. Rendezvous cannulation technique reduces post-ERCP pancreatitis: a prospective nationwide study of 12,718 ERCP procedures. Am J Gastroenterol 2013;108:552-9.
3. Swahn F, Regnér S, Enochsson L, et al. Endoscopic retrograde cholangiopancreatography with rendezvous cannulation reduces pancreatic injury. World J Gastroenterol 2013;19:6026-34.

http://dx.doi.org/10.1016/j.gie.2016.01.027

Response:

We thank Saritas et al for their interest in our article. In case-control studies, the traditional rendezvous (RV) cannulation results in a lower risk of post-ERCP pancreatitis (PEP) in comparison with cannulation without RV.[1] In this view, the advantages of traditional RV could be secondary to limitation of repeated cannulations of the papillary orifice and prevention of inadvertent cannulation or injection of contrast medium into the pancreatic ducts. In previous studies involving patients referred for cholecystectomy[2] and in our series of patients with biliary adverse events after liver transplantation,[3] mild PEP also occurred after traditional RV had been performed with great caution. The mechanisms leading to PEP during traditional RV are unknown, but instrumentation with the guidewire to pass into the duodenum and retrieval of the wire into the endoscope are probably major factors leading to trauma at the level of the papilla. To minimize as much as possible the risk of PEP in patients after liver transplantation, we have proposed direct duodenal cannulation over the wire during RV procedures. During nonrandomized consecutive cases, we have recorded no PEP after our duodenal RVs, possibly related to reduction of cannulation time compared with traditional RV.

We agree with Saritas et al that a large randomized study is needed to confirm our preliminary data. However, the large number of patients with biliary adverse events after liver transplantation needed for such a study (>200 per arm) makes it difficult to perform in centers with a high workload of liver transplantations, considering that approximately 10% to 15% of biliary adverse events occur yearly. Waiting for the best evidence in this field, we now routinely use duodenal RV as a first step to cannulate when a T tube is present, to avoid the unnecessary risk of pancreatitis in patients who have undergone liver transplantation, and we are glad to share this approach with Saritas et al.

DISCLOSURE

All authors disclosed no financial relationships relevant to this publication.

Paolo Cantù, MD, PhD
Ilaria Parzanese, MD
Gastroenterology and Endoscopy Unit
Ernesto Melada, MD
Giorgio Rossi, MD
Liver Transplant Unit
Dario Conte, MD
Roberto Penagini, MD, PhD
Gastroenterology and Endoscopy Unit
Department of Pathophysiology and Transplantation
Fondazione IRCCS Ca' Granda
Ospedale Maggiore Policlinico
Università degli Studi di Milano
Milan, Italy

REFERENCES

1. Swahn F, Nilsson M, Arnelo U, et al. Rendezvous cannulation technique reduces post-ERCP pancreatitis: a prospective nationwide study of 12,718 ERCP procedures. Am J Gastroenterol 2013;108:552-9.
2. La Greca G, Barbagallo F, Sofia M, et al. Simultaneous laparoendoscopic rendezvous for the treatment of cholecystocholedocholithiasis. Surg Endosc 2010;24:769-80.
3. Cantù P, Parzanese I, Melada E, et al. A new duodenal rendezvous technique for biliary cannulation in patients with T-tube after orthotopic liver transplantation (with video). Gastrointest Endosc 2016;83:229-33.

http://dx.doi.org/10.1016/j.gie.2016.02.012

Management of novel oral anticoagulants for GI endoscopy procedures

To the Editor:

We read with great interest the American Society for Gastrointestinal Endoscopy guideline on the management of antithrombotic agents for patients undergoing GI

Liver Cancer

Liver Cancer 2016;5:175–189
DOI: 10.1159/000367765
Published online: May 3, 2016

2235-1795/16/0053-0175$39.50/0
www.karger.com/lic

Original Paper

Survival Benefit of Locoregional Treatment for Hepatocellular Carcinoma with Advanced Liver Cirrhosis

Satoshi Kitai[a] Masatoshi Kudo[a] Naoshi Nishida[a] Namiki Izumi[b] Michiie Sakamoto[c] Yutaka Matsuyama[d] Takafumi Ichida[e] Osamu Nakashima[f] Osamu Matsui[g] Yonson Ku[h] Norihiro Kokudo[i] Masatoshi Makuuchi[j] for the Liver Cancer Study Group of Japan

[a]Department of Gastroenterology and Hepatology, Kinki University School of Medicine, Osaka-Sayama, [b]Department of Gastroenterology and Hepatology, Musashino Red Cross Hospital, [c]Department of Pathology, Keio University School of Medicine, [d]Department of Biostatistics, School of Public Health, University of Tokyo, Tokyo, [e]Shonan-East General Hospital, Kanagawa, [f]Department of Clinical Laboratory Medicine, Kurume University Hospital, Kurume, [g]Department of Radiology, Kanazawa University Graduate School of Medical Science, Kanazawa, [h]Department of Surgery, Kobe University Graduate School of Medicine, Kobe, [i]Hepato-Biliary-Pancreatic Surgery Division, Artificial Organ and Transplantation Division, Department of Surgery, Graduate School of Medicine, University of Tokyo, [j]Department of Surgery, Japanese Red Cross Medical Center, Tokyo, Japan

Key Words
Best supportive care · Child-Pugh grade C · Local ablation therapy · Transarterial chemoembolization

ABSTRACT

Background & Aims: Hepatocellular carcinoma (HCC) with decompensated liver cirrhosis (LC) is a life-threatening condition, which is amenable to liver transplantation (LT) as the standard first-line treatment. However, the application of LT can be limited due to a shortage of donor livers. This study aimed to clarify the effect of non-surgical therapy on the survival of patients with HCC and decompensated LC. ***Methods:*** Of the 58,886 patients with HCC registered in the nationwide survey of the Liver Cancer Study Group of Japan (January 2000–December 2005), we included 1,344 patients with primary HCC and Child-Pugh (C-P) grade C for analysis in this retrospective study. Among the patients analyzed, 108 underwent LT, 273 were treated by local ablation therapy (LAT), 370 were treated by transarterial chemoembolization

Masatoshi Kudo, MD, PhD
Department of Gastroenterology and Hepatology
Kinki University School of Medicine
377-2, Ohno-Higashi, Osaka-Sayama, Osaka 589-8511 (Japan)
Tel. +81 723 66 0221 (ext: 3149), E-Mail m-kudo@med.kindai.ac.jp

KARGER

Liver Cancer

Liver Cancer 2016;5:175–189
DOI: 10.1159/000367765
Published online: May 3, 2016

(TACE), and 593 received best supportive care (BSC). The effect of LT, LAT, and TACE on overall survival (OS) was analyzed using multivariate and propensity score analyses. ***Results:*** Patient characteristics did not differ significantly between each treatment group and the BSC group, after propensity score matching. LAT (hazard ratio [HR]) =0.568; 95% confidence interval [CI], 0.40-0.80) and TACE (HR=0.691; 95% CI, 0.50-0.96) were identified as significant contributors to OS if the C-P score was less than 11 and tumor conditions met the Milan criteria. ***Conclusions:*** For patients with HCC within the Milan criteria and with a C-P score of 10 or 11, locoregional treatment can be used as a salvage treatment if LT is not feasible.

Introduction

Hepatocellular carcinoma (HCC) is one of the most common malignancies worldwide and the second leading cause of death from cancer [1]. Approximately 80% of patients with HCC have chronic hepatitis and liver cirrhosis (LC), which is attributed to chronic infection with hepatitis B virus (HBV) and/or hepatitis C virus (HCV) [2]. Despite recent advancements in antiviral therapy for viral hepatitis, the prognosis of patients with decompensated LC remains poor, especially in cases with concomitant HCC [3]. Therefore, in addition to tumor stage, it is critical to evaluate liver function for the management of patients with HCC [4, 5].

For HCC with preserved liver function, several treatment options are available including partial hepatectomy [6], liver transplantation (LT) [7–11], local ablation therapy (LAT) [12], and transarterial chemoembolization (TACE) [13–16]. In particular, LT is recommended for patients with advanced LC of Child-Pugh (C-P) grade C and an early stage of HCC [5, 7, 10, 17]. However, the application of LT to patients with HCC has been limited because of the shortage of donor livers. In addition, systemic therapies including sorafenib are not feasible without any survival benefit in HCC cases with C-P grade C [18]. Therefore, it is necessary to know whether conventional locoregional treatment for HCC, such as LAT and TACE, can improve survival even in patients with HCC and C-P grade C. However, there has been a lack of evidence for the value of locoregional treatments in such patients with decompensated LC although several reports state some survival benefit in a small-sized retrospective study [19, 20]. Because best supportive care (BSC) is recommended for patients with HCC and C-P grade C, when LT is not applicable, the benefits of BSC in comparison to locoregional treatments should be assessed in the context of overall survival (OS) in these patients.

We address this important issue using a systematic and multi-pronged approach with a large cohort of patients with HCC and C-P grade C using a Japanese nationwide database. The aim of this study was to evaluate the utility of non-surgical treatment for patients suffering from primary HCC with decompensated LC.

Materials and Methods

Patient Characteristics

Patients included in the analysis were registered in the database of a nationwide survey of the Liver Cancer Study Group of Japan (LCSGJ). The data collection and registration of patients with HCC included in this analysis were performed with the approval of each patient's institution. Obtaining informed consent from patients was not required because of the retrospective design of the study.

The patients were diagnosed with HCC on the basis of histological or radiological examinations as well as clinical criteria [5, 21–23]. A histological examination was performed if the tumor did not present

with typical radiological features or if an increase in any HCC-specific tumor markers (alpha-fetoprotein [AFP], Lens culinaris agglutinin-reactive AFP and des-gamma-carboxy prothrombin) was not detected.

Of the 58,886 patients who were registered in the LCSGJ as having newly diagnosed HCC between January 2000 and December 2005, 42,905 were eligible for this analysis because all of the following data were available in the database including: C-P grade and its constitutive parameters (serum bilirubin level, serum albumin level, prothrombin time (PT), ascites, and hepatic encephalopathy), age, sex, status of HBV and HCV, tumor size, number of tumors, tumor-, node-metastasis (TNM) stage, and treatment modalities (i.e., LT, LAT, TACE, or BSC).

Among them, a total of 1,344 patients were classified as having C-P grade C and were enrolled in this study. Among the enrolled patients, 656 were identified with a C-P score of 10. Likewise, the numbers of patients with C-P scores of 11, 12, 13, 14, and 15 were 384, 186, 73, 38, and 7, respectively. The diagnosis of HCC was mainly established by imaging studies; 189 out of 1,344 patients were diagnosed by biopsy or via operatively extracted specimens. Tumors of 828 patients were within the Milan criteria, whereas 516 did not meet the criteria. To determine the eligibility for locoregional treatment for HCC according to the C-P score, we further classified cases of HCC into two groups as follows: the 'lower score' group (C-P score=10 or 11, n=603) and the "higher score" group (C-P score =12-15, n=143). There were no patients who were treated with radiofrequency ablation (RFA) combined with TACE in this study. The details of the clinical data of the patients are summarized in the tables 1 and 2.

Statistical Analysis

First, we determined which factors significantly affected the OS of patients with HCC and C-P grade C. Accordingly, we compared the OS of patients categorized according to clinical background using Kaplan-Meier analysis, and univariate parameters were analyzed using the log-rank test. Patients were censored at the time of their last clinical visit or death not due to HCC. Variables with a p value of <0.05 on univariate analysis were further subjected to the multivariate analysis using the Cox proportional-hazards regression model to determine independent contributors to OS. Patient characteristics were compared among different treatment groups using Pearson's chi-square test for categorical variables and the Student's t-test for continuous variables.

In order to avoid selection bias of the treatment due to the different backgrounds of patients with HCC, we applied propensity score analyses, which allowed the normalization of patients' characteristics between each treatment group. Propensity score analyses were performed for the two group pairs, LAT vs. BSC, and TACE vs. BSC, to evaluate the benefit of treatment in comparison to BSC. The Kaplan-Meier method and log-rank test were also used for survival analyses of matched patients. Because the propensity score analysis could not compare three groups (i.e., LAT, TACE, and BSC), the utility was compared between each treatment and BSC, according to the hazard ratio (HR) of treatment compared to BSC.

Results

Clinical Factors Associated with Survival in Patients with HCC and C-P Grade C LC

To evaluate which factors contributed to the improvement of OS in patients with HCC and C-P grade C, we analyzed the association between the duration of OS and each clinical parameter. The univariate analysis revealed that a younger age, smaller tumor size, lower AFP level, lower C-P score, lower TNM stage, and receipt of treatment were identified as significant factors contributing to an increased duration of OS (p<0.0001 for each by log-rank test, table 3). The status of hepatitis virus infection also showed borderline significance (p=0.0424).

We subsequently performed a multivariate analysis, which showed that receipt of treatment (p<0.0001), smaller tumor size (p=0.0002), lower AFP levels (p=0.0010), lower TNM stage (p<0.0001), and lower C-P score (p=0.0070) were independent contributors to longer survival (see table 4). In a comparison of OS among the BSC, LT, LAT, and TACE groups with C-P grade C, the LT group showed the longest OS compared to the LAT (p=0.0271) and TACE (p<0.0001) groups, respectively. Conversely, the LAT (p<0.0001) and TACE (p<0.0001) groups showed longer OS than the BSC group for each comparison (see fig. 1a). Similarly, in patients within the Milan criteria, the LT group showed the longest OS than the LAT (p=0.0079) and

Table 1. Characteristics of patients with HCC in each treatment group with C-P scores of 10 or 11

Background factors	BSC	LAT	TACE	Total n=1040	p value
	n=198	n=218	n=187	n=603	
	No. of Patients	No. of Patients	No. of Patients	No. of Patients	
Age (years)					
<60	44	77	61	182	0.009
≥60	154	141	126	421	
Sex					
Male	130	140	114	384	0.611
Female	68	78	73	219	
Hepatitis B and virological status					
B–, C+	128	142	119	389	0.960
B+, C–	24	25	27	76	
B+, C+	3	4	4	11	
B–, C–	38	42	31	111	
Maximum tumor size (cm)					
≤2.0	96	132	84	312	0.009
2.1–3.0	74	68	71	213	
3.1–5.0	28	18	32	78	
No.of tumors					
1	144	164	116	424	0.011
≥2	54	54	71	179	
AFP (ng/ml)					
≤200	93	114	117	324	<0.0001
>200	119	29	75		
TNM stage					
I	71	102	50	223	<0.0001
II	98	92	100	290	
III	29	24	37	90	

TACE (p=0.0010) groups, respectively. On the other hand, the LAT (p<0.0001) and TACE (p<0.0001) groups showed longer OS than the BSC group for each comparison (see fig. 1b).

To determine whether locoregional treatment for HCC showed benefit regardless of the baseline C-P score, we further excluded the LT focusing on the impact of LAT and TACE. We also conducted separate survival analyses in both the lower C-P score and higher C-P score groups. In the lower C-P score group, both the LAT and TACE groups showed longer OS than the BSC group (p<0.0001 for both LAT and TACE groups; see fig. 2a), suggesting that these locoregional treatments might have a survival benefit for patients with HCC and C-P score 10 or 11. The median OS (95% confidence interval [CI]) of patients who received BSC and locoregional treatments were 4.0 months (range 2.9-5.1 months) for the BSC group, 26.0 months (range 22.4-29.6 months) for the LAT group, and 17.0 months (range 14.6-19.4 months) for the TACE group, respectively (p<0.0001 for each comparison; see fig. 2a).

Similarly, in patients with HCC with a higher C-P score, both the LAT and TACE groups had longer OS than the BSC group. The median OS (95% CI) of patients who received BSC and locoregional treatment groups were 2.0 months (range 1.5-2.5 months) for the BSC group, 11.0 months (range 9.4-12.6 months) for the LAT group, and 14.0 months (range 11.9-16.1 months) for the TACE group, respectively (p<0.0001 for each comparison except for LAT vs. TACE; see fig. 2b).

Table 2. Characteristics of patients with HCC in each treatment group with C-P sores of 12–15

Background factors	BSC	LAT	TACE	Total n=1040	p value
	n=93	n=22	n=28	n=143	
	No. of Patients	No. of Patients	No. of Patients	No. of Patients	
Age (years)					
<60	26	8	12	46	0.320
≥60	67	14	16	97	
Sex					
Male	60	17	19	96	0.516
Female	33	5	9	47	
Hepatitis B and C virological status					
B–, C+	47	14	19	80	0.134
B+, C–	15	3	3	21	
B+, C+	1	1	1	3	
B–, C–	24	4	5	33	
Maximum tumor size (cm)					
≤2.0	38	13	10	61	0.489
2.1–3.0	35	7	12	54	
3.1–5.0	20	2	6	28	
No. of tumors					
1	66	18	20	104	0.392
≥2	27	4	8	39	
AFP (ng/ml)					
≤200	47	7	25	79	0.090
>200	54	7	12	73	
TNM stage					
I	24	10	6	40	0.362
II	56	11	18	85	
III	13	1	4	18	

Survival Benefit of Locoregional Treatment for HCC in Patients with Lower and Higher C-P Scores

We also conducted a multivariate analysis to determine the independent variables that had an effect on the duration of OS in patients with HCC and lower C-P scores. Notably, a longer OS was observed even in patients who received locoregional treatment compared to those who received BSC (p<0.0001 for all variables; HR and 95% CI: 0.338 and 0.25-0.45 for LAT vs. BSC, and 0.462 and 0.36-0.58 for TACE vs. BSC, respectively). Tumor size (≤2.0 cm vs. ≥3.1 cm) and the AFP level were also associated with improved OS, with p values of <0.0001 (HR 0.595; 95% CI, 0.45-0.77) and 0.0004 (HR 0.665; 95% CI, 0.53-0.83), respectively (table 5).

For the patients with higher C-P scores, LAT and TACE also had a survival benefit (p=0.0014, HR and 95% CI=0.361 and 0.17-0.68 for LAT vs. BSC, p=0.0018, HR and 95% CI=0.517 and 0.33-0.78 for TACE vs. BSC, respectively). Lower AFP level were also associated with improved OS, with a p value of 0.0008 (HR=0.533; 95% CI, 0.37-0.76). However, tumor size (≤2.0 vs. ≥3.1) showed borderline significance on survival with a p value of 0.0664 (HR=0.662; 95% CI, 0.35-1.03; table 6).

Table 3. Univariate analysis of risk factors for survival in patients with HCC with C-P grade C LC

Background factor	n=1344 No. of patients	Median survival time (months)	Survival rate (%) 1-year	3-year	5-year	p value
Age (years)						
<60	432	18	57.9	31.1	19.9	<0.0001
≥60	911	9	43.3	14.9	5.1	
Sex						
Male	897	11	48.0	18.8	7.4	0.5627
Female	447	11	47.9	21.1	14.4	
Hepatitis B and C virological status						
B–, C+	803	11	46.2	18.7	8.6	0.0424
B+, C–	204	12	49.1	24.4	-	
B+, C+	25	16	59.4	12.4	-	
B–, C–	262	13	51.2	21.2	6.8	
Maximum tumor size (cm)						
≤2.0	441	15	57.3	36.9	26.4	<0.0001
2.1–3.0	335	16	57.2	31.7	18.8	
>3.1	568	4	28.2	13.1	7.9	
No. of tumors						
Solitary	768	11	48.3	21.4	10.5	0.1591
Multiple	576	11	47.5	17.0	8.1	
AFP (ng/ml)						
≤200	448	13	53.3	27.4	18.0	
>200	315	9	26.5	14.0	6.3	<0.0001
Treatment						
Yes (LT, LAT and TACE)	541	18	62.4	27.4	13.5	<0.0001
No (BSC)	803	3	25.7	6.9	2.4	
C-P score						
10 or 11	1040	13	52.5	20.9	9.40	<0.0001
12–15	304	5	32.7	15.0	-	
TNM stage						
I	283	11	59.2	28.1	14.7	<0.0001
II	496	10	48.9	18.9	8.4	
III	301	9	48.8	12.9	5.1	
IV	264	11	45.1	16.5	7.8	

Locoregional Treatment of HCC Showed a Survival Benefit in Cases with C-P Score 10 or 11 by Propensity Score Analyses

The results of the multivariate analysis may be attributed to selection bias of the treatment based upon differences in clinical background inherent to retrospective analyses. As a consequence, we performed analyses using an unbiased method to confirm the benefit of locoregional treatment. Accordingly, we applied propensity score analyses between the BSC and locoregional treatment groups (i.e., LAT and TACE), specifically for HCC cases that met the Milan criteria for tumor status. After propensity score matching, there were no significant differences in the background characteristics between BSC and LAT groups (table 7), as well as between the BSC and TACE groups (table 8), suggesting that these were suitable cohorts for the unbiased analyses.

Table 4. Multivariate analysis of risk factors for survival in patients with C-P grade C LC

Variable	HR	95% CI	p value
Treatment			
No	1	-	-
Yes (LT, LAT, or TACE)	0.406	0.33–0.49	<0.0001
Maximum tumor size (cm)			
>3.1	1	-	-
2.1–3.0	0.536	0.43–0.67	
≤2.0	0.618	0.38–0.50	0.0002
Age (years)			
≥60	1	-	-
<60	0.847	0.69–1.02	0.0923
AFP (ng/ml)			
>200	1		
≤200	0.729	0.60–0.88	0.0010
C-P score			
12–15	1	-	-
10 or 11	0.756	0.62–0.92	0.0070
TNM			
IV	1		
III	0.594	0.45–0.77	
II	0.538	0.42–0.68	
I	0.524	0.35–0.78	<0.0001

After matching, 124 pairs of patients were eligible for the comparison of OS between the BSC and LAT groups in the cohort of C-P score 10 or 11 (table 7); the median follow-up period and 25th-75th percentiles are as follows: 11.0 months and 15.1±12.9 months for the LAT group and 7.0 months and 10.6±12.0 months for the BSC group, respectively. Importantly, patients who underwent LAT showed a lower risk of death than did patients who underwent BSC (p=0.0014, HR=0.568; 95% CI, 0.40-0.80: fig. 3a). The 1-, 2-, and 3-year OS rates of the BSC and LAT groups were 53.1%, 31.4%, and 15.0%, versus 71.9%, 58.5%, and 36.3%, respectively. Similarly, 127 pairs of patients were eligible for OS comparison between the BSC and TACE groups (table 8). The results indicated that the TACE group had a longer OS than the BSC group, even after propensity score matching (median follow-up period and 25th-75th percentiles: 7.0 months and 10.2±11.6 months for the TACE group and 10.0 months and 14.7±13.9 months for the BSC group, respectively; fig. 3b). The HR of receiving TACE for patient survival was 0.691 (95% CI, 0.50–0.96; p=0.0289) compared to BSC. The 1-, 2-, and 3-year OS rates of the BSC and TACE groups were 56.9%, 33.8%, and 15.0%, versus 63.8%, 39.9%, and 22.9%, respectively.

Assessment of Survival Benefit of Locoregional Treatment for HCC by Propensity Score Matching Analyses in Cases with C-P Score 12–15

We also performed propensity analyses for patients with HCC and C-P scores of 12-15. After propensity score matching, 19 patients were eligible for the BSC versus LAT group analysis, and 49 patients were eligible for the BSC versus TACE group analysis. On comparison of OS between locoregional treatment groups and the BSC group, there were no significant differences for OS duration between the LAT and BSC groups (p=0.201, HR=0.601; 95% CI,

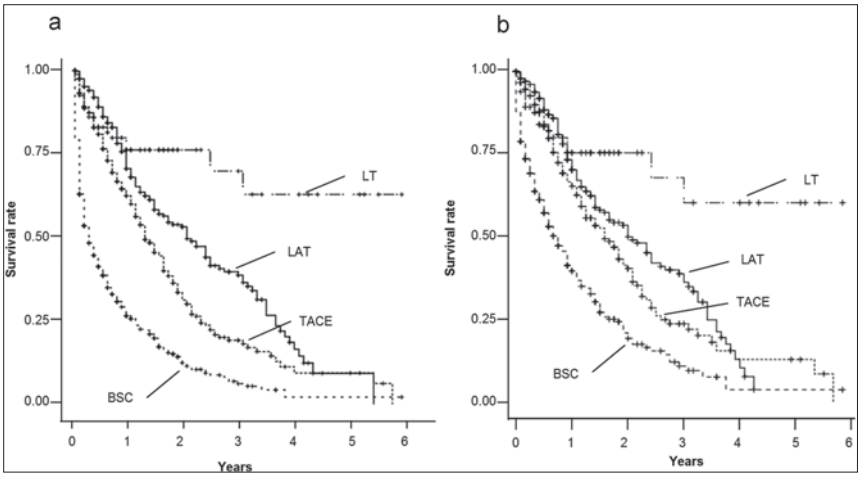

Fig. 1. **a** A comparison of OS among the BSC, LT, LAT, and TACE groups with C-P grade C. Patients who underwent LT, LAT, and TACE had significantly longer OS than patients who received BSC (p<0.0001). Moreover, there was significant difference in OS between the LT and LAT groups (p=0.0271) as well as the LT and TACE groups (p<0.0001). **b** A comparison of OS among the BSC, LT, LAT, and TACE groups with C-P grade C within the Milan criteria. The patients who underwent LT, LAT, and TACE had significantly longer OS than patients who received BSC (p<0.0001). The significant difference of OS was observed between the LT and LAT groups (p=0.0079) as well as the LT and TACE groups (p=0.0010).

0.27-1.36; fig. 3c). Similarly, there were no significant differences for OS duration between the TACE and the BSC groups (p=0.0549, HR=0.626; 95% CI, 0.38-1.03; fig. 3d).

Discussion

The prognosis of HCC with decompensated LC is still unsatisfactory, and LT is the only recommended treatment for patients with HCC and C-P grade C. However, even in patients with HCC meeting the Milan criteria, LT might not be applicable because of the shortage of donor livers. Conversely, the recent developments of novel therapeutic devices help to achieve minimal deterioration of liver function after locoregional treatment [24–27]. From this perspective, it is necessary to re-evaluate the efficacy of locoregional treatments for HCC with decompensated LC, which has been a controversial issue to date. Here, we demonstrate that the locoregional treatments can be effectively used for the treatment of HCC with decompensated LC if the C-P score is 11 or less.

In the present study, the univariate and multivariate analyses revealed that smaller tumor size, lower C-P score, lower serum AFP level, lower TNM stage and receipt of non-surgical HCC treatment were significant factors contributing to an increase in OS. This suggests that these treatments may improve the survival of patients with HCC and C-P grade C. The LT group showed a significantly longer OS than locoregional treatment groups as previously reported [11, 17, 28]. Among patients with a lower C-P score, a longer OS was also observed in patients who underwent locoregional treatment compared to patients who received BSC. For patients with higher C-P scores, LAT, and TACE were also identified as carrying a survival benefit, suggesting that locoregional treatment for HCC may contribute to improvement in OS in these cases.

However, as is inherent with retrospective analyses, the bias of treatment selection can lead to unexpected results regarding the contribution of locoregional treatment to an in-

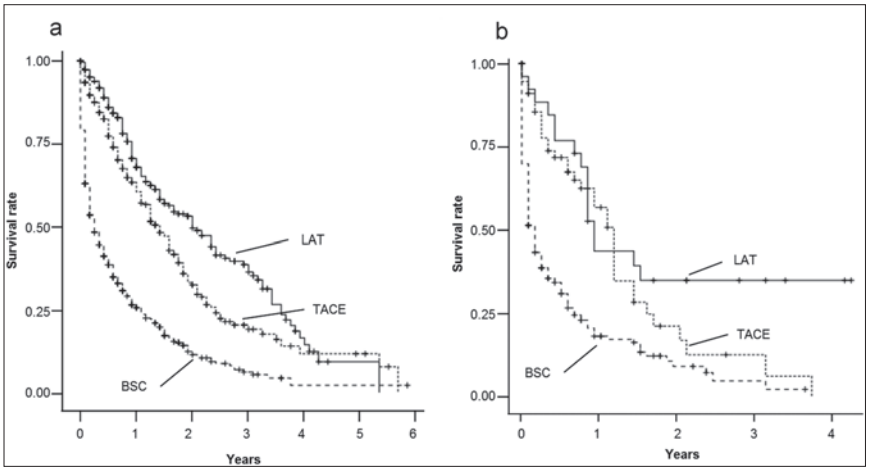

Fig. 2. **a** A comparison of OS among the BSC, LAT, and TACE groups with C-P scores of 10 or 11. Each Kaplan-Meier survival curve represents the OS of patients who underwent LAT, TACE, and BSC. The patients who underwent LAT or TACE had significantly longer OS than patients who received BSC (p<0.0001). **b** A comparison of OS among the BSC, LAT, and TACE groups with C-P scores of 12-15. The Kaplan-Meier survival curves indicate that patients who underwent LAT or TACE had significantly longer OS than patients who received BSC (p<0.0001).

Table 5. Multivariate analysis of risk factors for survival in patients with a C-P score of 10 or 11

Variable	HR	95% CI	p value
Treatment			
LAT vs. BSC	0.338	0.25–0.45	<0.0001
TACE vs. BSC	0.462	0.36–0.58	<0.0001
Age (years)			
<60 vs. ≥60	0.949	0.74–1.19	0.6679
Maximum tumor size (cm)			
≤2.0 vs. 2.1–3.0	1.18	0.88–1.58	0.2590
≤2.0 vs. ≥3.1	0.595	0.45–0.77	<0.0001
AFP (ng/ml)			
≤200 vs. >200	0.665	0.53–0.83	0.0004
Number of tumors			
solitary vs. multiple	0.985	0.79–1.21	0.8935

creased duration of OS. For example, age, background liver function, and the number and size of tumors may affect the selection of treatment. Therefore, we further applied a less-biased method using propensity score matching, and normalized the patients' backgrounds. After the matching, locoregional treatment also showed a significant association with longer survival as compared to the BSC groups in the lower C-P score group. Although there has been a lack of evidence regarding the benefit of locoregional treatment in patients with HCC and C-P grade C, refined techniques using new devices for RFA and TACE may contribute to an improvement in survival, even in patients with HCC that have decompensated LC. To the contrary, in the cohort of higher C-P scores of 12-15, locoregional treatment did not produce a survival benefit, suggesting that LT is the only current treatment showing survival benefit. To further confirm the ineligibility of locoregional treatment in the C-P score 12-15 group, we analyzed the intragroup causes of death as follows: 22 of 44 patients (50%) in the locoregional treatment group

Table 6. Multivariate analysis of risk factors for survival in patients with a C-P score of 12-15

Variable	HR	95% CI	p Value
Treatment			
LAT vs. BSC	0.361	0.17–0.68	0.0014
TACE vs. BSC	0.517	0.33–0.78	0.0018
Age (years)			
<60 vs. ≥60	0.89	0.59–1.30	0.5674
AFP (ng/ml)			
≤200 vs. >200	0.533	0.37–0.76	0.0008
Maximum tumor size (cm)			
≤2.0 vs. 2.1–3.0	0.957	0.52–1.73	0.8879
≤2.0 vs. ≥3.1	0.622	0.35–1.03	0.0664

died of hepatic failure and 13 patients (29.5%) died of cancer; 93 of 136 patients (50.2%) in the BSC group died of hepatic failure and 55 patients (40.4%) died of cancer. This supports the idea that the leading cause of death of the patients with C-P scores of 12-15 was hepatic failure, and cancer-related death was not the main cause even in the BSC group. Therefore it is conceivable that any intervention without improvement of liver decompensation is unlikely to be tolerated, or it will affect the survival for this patient group.

Although the data suggest a survival benefit of locoregional treatment in patients with HCC along with lower scores of C-P grade C, there are certain limitations in this study. First, as the nature of retrospective studies, there may be bias regarding the effect of treatment on OS, even after propensity score matching. For example, the source database is potentially flawed, since only stronger/healthier C-P grade C patients would see a physician and hence become registered. Moreover, significant selection bias occurred at the time of treatment decisions, because stronger/healthier patients tended to be treated. Second, propensity score analyses were performed only for patients with HCC within the Milan criteria in terms of tumor status. Therefore, a treatment benefit for patients with HCC beyond these criteria was not identified in this study. Third, the analysis did not include performance status, a factor that may impact on survival in patients with HCC. Although it was possible that the majority of the patients included in this study should be of a performance status of 0 or 1, the effect of performance status on survival in the treatment of HCC also needs to be confirmed in the future. However, even with these limitations, the results of this study provide sample evidence for the development of future prospective studies.

In conclusion, we provide evidence of a treatment benefit with LAT and TACE in patients with HCC within the Milan criteria and with C-P scores of 10 or 11. The results presented here are of clinical importance because BSC is the only recommended therapy in patients with HCC who have deterioration in liver function. Our data indicate that LAT or TACE could be used as a salvage treatment if LT is not applicable.

Table 7. Comparison of patient characteristics between the BSC and LAT groups with C-P score 10 or 11, matched by propensity score.

Background factors	BSC n=124 No. of Patients	LAT n=124 No. of Patients	p value
Age (years)			
<60	35	35	1
≥60	89	89	
Sex			
Male	80	75	0.5119
Female	44	49	
Hepatitis B and C virological status			
B–, C+	85	83	0.7645
B+, C–	14	13	
B+, C+	1	3	
B–, C–	20	22	
Maximum tumor size (cm)			
≤2	69	72	0.8605
2.1–3.0	47	43	
3.1–5.0	8	9	
No. of tumors			
1	91	90	0.8863
2–3	33	34	
TNM stage			
I	52	54	0.9636
II	56	54	
III	16	16	
Bilirubin (mg/dL)			
<2.0	31	27	0.8303
2.0–3.0	41	42	
>3.0	52	55	
Albumin (g/dL)			
>3.5	0	1	0.5694
2.8–3.5	46	43	
<2.8	78	80	
PT (%)			
>70	4	7	0.645
40–70	107	105	
<40	13	12	
Ascites			
None	44	40	0.86458
Responsive	53	56	
Unresponsive	27	28	
Encephalopathy			
None	69	70	0.9361
Mild	36	37	
Coma	19	17	

Table 8. Comparison of patient characteristics between the BSC and TACE groups with C-P score 10 or 11, matched by propensity score.

Background factors	BSC n=127 No. of Patients	TACE n=127 No. of Patients	p value
Age (years)			
<60	38	32	0.3995
≥60	89	95	
Sex			
Male	81	79	0.7949
Female	46	48	
Hepatitis B and C virological status			
B–, C+	83	86	0.4087
B+, C–	13	16	
B+, C+	2	0	
B–, C–	26	21	
Maximum tumor size (cm)			
≤2	58	58	0.9828
2.1–3.0	48	49	
3.1–5.0	21	20	
No. of tumors			
1	84	85	0.8942
2–3	43	42	
TNM stage			
I	39	36	0.6549
II	64	71	
III	24	20	
Bilirubin (mg/dL)			
<2.0	35	31	0.8488
2.0–3.0	43	45	
>3.0	49	51	
Albumin (g/dL)			
>3.5	2	3	0.8886
2.8–3.5	41	42	
<2.8	84	82	
PT (%)			
>70	7	10	0.7462
40–70	106	104	
<40	14	13	
Ascites			
None	34	32	0.8772
Responsive	50	54	
Unresponsive	43	41	
Encephalopathy			
None	76	75	0.8867
Mild	43	42	
Coma	8	10	

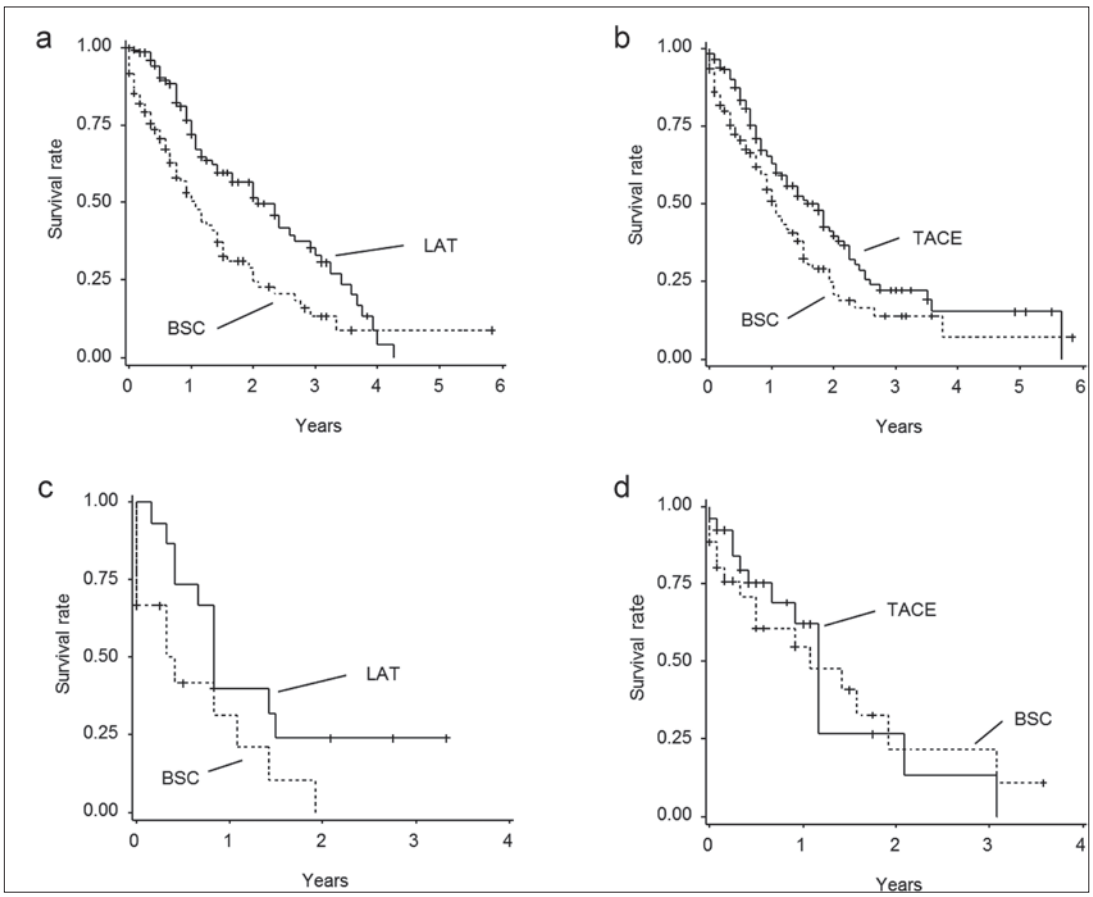

Fig. 3. **a** A comparison of OS between the BSC and LAT groups with C-P scores of 10 or 11, after matching patient backgrounds using propensity score analysis. The Kaplan-Meier curve shows that the LAT group had a lower risk of death than the BSC group (HR 0.568; 95% CI, 0.40-0.80; p=0.0014). **b** A comparison of OS between the BSC and TACE groups with C-P scores of 10 or 11, after matching patient backgrounds using propensity score analysis. The TACE group had a lower risk of death than the BSC group (HR 0.691; 95% CI, 0.50-0.96; p=0.0289). **c** A comparison of OS between the BSC and LAT groups with C-P scores of 12-15, after matching patient backgrounds using propensity score analysis. The LAT group had a lower risk of death than the BSC group (HR 0.601; 95% CI, 0.27-1.36; p=0.201). **d** A comparison of OS between the BSC and TACE groups with C-P scores of 12-15, after matching patient backgrounds using propensity score analysis. The TACE group had a lower risk of death than the BSC group (HR 0.626; 95% CI, 0.38-1.03; p=0.0549).

Grant Support

This work was supported by the Health Labor Sciences Research Grant from The Ministry of Health, Labour and Welfare (H22-Clinical Oncology-General-015), Japan.

Competing Interests

The authors have no competing interests to declare.

Author Contributions

SK, NN, and MK designed the studies, wrote the initial version of the paper, and revised the manuscript. SK, NN, NI, MS, YM, TI, ON, OM, YK, NK, MM, and MK interpreted the data, performed the statistical analyses, and helped with acquisition of data. MK organized collaborations, obtained funding, supervised data collection. SK, NN, NI, MS, YM, TI, ON, OM, YK, NK, MM, and MK helped with acquisition of data.

References

1 Jemal A, Bray F, Center MM, Ferlay J, Ward E, Forman D: Global cancer statistics. CA Cancer J Clin 2011;61:69–90.
2 Perz JF, Armstrong GL, Farrington LA, Hutin YJ, Bell BP: The contributions of hepatitis B virus and hepatitis C virus infections to cirrhosis and primary liver cancer worldwide. J Hepatol 2006;45:529–538.
3 Infante-Rivard C, Esnaola S, Villeneuve JP: Clinical and statistical validity of conventional prognostic factors in predicting short-term survival among cirrhotics. Hepatology 1987;7:660–664.
4 Kudo M, Chung H, Haji S, Osaki Y, Oka H, Seki T, Kasugai H, Sasaki Y, Matsunaga T: Validation of a new prognostic staging system for hepatocellular carcinoma: the JIS score compared with the CLIP score. Hepatology 2004;40:1396–1405.
5 Kudo M, Izumi N, Kokudo N, Matsui O, Sakamoto M, Nakashima O, Kojiro M, Makuuchi M, HCC Expert Panel of Japan Society of Hepatology: Management of hepatocellular carcinoma in Japan: Consensus-Based Clinical Practice Guidelines proposed by the Japan Society of Hepatology (JSH) 2010 updated version. Dig Dis 2011;29:339–364.
6 Faber W, Sharafi S, Stockmann M, Denecke T, Sinn B, Puhl G, Bahra M, Malinowski MB, Neuhaus P, Seehofer D: Long-term results of liver resection for hepatocellular carcinoma in noncirrhotic liver. Surgery 2013;153:510–517.
7 Lee Cheah Y, K H Chow P: Liver transplantation for hepatocellular carcinoma: an appraisal of current controversies. Liver Cancer 2012;1:183–189.
8 Chan SC: Liver transplantation for hepatocellular carcinoma. Liver Cancer 2013;2:338–344.
9 Chan SC, Sharr WW, Chan AC, Chok KS, Lo CM: Rescue Living-donor Liver Transplantation for Liver Failure Following Hepatectomy for Hepatocellular Carcinoma. Liver Cancer 2013;2:332–337.
10 Belghiti J, Fuks D: Liver resection and transplantation in hepatocellular carcinoma. Liver Cancer 2012;1:71–82.
11 Mazzaferro V, Bhoori S, Sposito C, Bongini M, Langer M, Miceli R, Mariani L: Milan criteria in liver transplantation for hepatocellular carcinoma: an evidence-based analysis of 15 years of experience. Liver Transpl 2011;17(Suppl 2):S44–S57.
12 Lin SM: Local ablation for hepatocellular carcinoma in taiwan. Liver Cancer 2013;2:73–83.
13 Lencioni R: Loco-regional treatment of hepatocellular carcinoma. Hepatology 2010;52:762–773.
14 Llovet JM, Bruix J: Systematic review of randomized trials for unresectable hepatocellular carcinoma: Chemoembolization improves survival. Hepatology 2003;37:429–442.
15 Lencioni R: Chemoembolization in patients with hepatocellular carcinoma. Liver Cancer 2012;1:41–50.
16 Llovet JM, Real MI, Montaña X, Planas R, Coll S, Aponte J, Ayuso C, Sala M, Muchart J, Solà R, Rodés J, Bruix J, Barcelona Liver Cancer Group: Arterial embolisation or chemoembolisation versus symptomatic treatment in patients with unresectable hepatocellular carcinoma: a randomised controlled trial. Lancet 2002;359:1734–1739.
17 Mazzaferro V, Regalia E, Doci R, Andreola S, Pulvirenti A, Bozzetti F, Montalto F, Ammatuna M, Morabito A, Gennari L: Liver transplantation for the treatment of small hepatocellular carcinomas in patients with cirrhosis. N Engl J Med 1996;334:693–699.
18 Kudo M: Treatment of advanced hepatocellular carcinoma with emphasis on hepatic arterial infusion chemotherapy and molecular targeted therapy. Liver Cancer 2012;1:62–70.
19 Nouso K, Ito Y, Kuwaki K, Kobayashi Y, Nakamura S, Ohashi Y, Yamamoto K: Prognostic factors and treatment effects for hepatocellular carcinoma in Child C cirrhosis. Br J Cancer 2008;98:1161–1165.
20 Kudo M, Osaki Y, Matsunaga T, Kasugai H, Oka H, Seki T: Hepatocellular carcinoma in Child-Pugh C cirrhosis: prognostic factors and survival benefit of nontransplant treatments. Dig Dis 2013;31:490–498.
21 Bruix J, Sherman M Practice Guidelines Committee, American Association for the Study of Liver Diseases: Management of hepatocellular carcinoma. Hepatology 2005;42:1208–1236.
22 Izumi N: Diagnostic and treatment algorithm of the Japanese society of hepatology: a consensus-based practice guideline. Oncology 2010;78(Suppl 1):78–86.
23 European Association For The Study Of The Liver European Organisation For Research And Treatment Of Cancer: EASL-EORTC clinical practice guidelines: management of hepatocellular carcinoma. J Hepatol 2012;56:908–943.
24 Kudo M: Real practice of hepatocellular carcinoma in Japan: conclusions of the Japan Society of Hepatology 2009 Kobe Congress. Oncology 2010;78(Suppl 1):180–188.

25 Minami Y, Kitai S, Kudo M: Treatment response assessment of radiofrequency ablation for hepatocellular carcinoma: usefulness of virtual CT sonography with magnetic navigation. Eur J Radiol 2012;81:e277–e280.
26 Takayasu K: Superselective transarterial chemoembolization for hepatocellular carcinoma: recent progression and perspective. Oncology 2011;81(Suppl 1):105–110.
27 Takayasu K, Arii S, Ikai I, Omata M, Okita K, Ichida T, Matsuyama Y, Nakanuma Y, Kojiro M, Makuuchi M, Yamaoka Y, Liver Cancer Study Group of Japan: Prospective cohort study of transarterial chemoembolization for unresectable hepatocellular carcinoma in 8510 patients. Gastroenterology 2006;131:461–469.
28 Tamura S, Sugawara Y, Kokudo N: Living donor liver transplantation for hepatocellular carcinoma: the Japanese experience. Oncology 2011;81(Suppl 1):111–115.

Ther Adv Gastroenterol
2016, Vol. 9(4) 483–494
DOI: 10.1177/1756283X16644248

Predictors of pain response in patients undergoing endoscopic ultrasound-guided neurolysis for abdominal pain caused by pancreatic cancer

Kosuke Minaga, Masayuki Kitano, Hiroki Sakamoto, Takeshi Miyata, Hajime Imai, Kentaro Yamao, Ken Kamata, Shunsuke Omoto, Kumpei Kadosaka, Toshiharu Sakurai, Naoshi Nishida, Yasutaka Chiba and Masatoshi Kudo

Abstract

Background: Interventional endoscopic ultrasound (EUS)-guided procedures such as EUS-guided celiac ganglia neurolysis (EUS-CGN) and EUS-guided broad plexus neurolysis (EUS-BPN) were developed to treat abdominal cancer-associated pain; however, these procedures are not always effective. The aim of this study was to explore predictors of pain response in EUS-guided neurolysis for pancreatic cancer-associated pain.

Methods: This was a retrospective analysis of prospectively collected data of 112 consecutive patients who underwent EUS-BPN in our institution. EUS-CGN was added in cases of visible celiac ganglia. The neurolytic-spread area was divided into six sections and evaluated by post-procedural computed tomography scanning. Pain intensity was assessed using a visual analog scale (VAS), and a decrease in VAS scores by $\geqslant$3 points after neurolysis was considered a good pain response. Univariable and multivariable logistic regression analyses were performed to explore predictors of pain response at 1 and 4 weeks, and complications.

Results: A good pain response was obtained in 77.7% and 67.9% of patients at 1 and 4 weeks, respectively. In the multivariable analysis of these patients, the combination method (EUS-BPN plus CGN) was a significant positive predictive factor at 1 week (odds ratio = 3.69, $p = 0.017$) and 4 weeks (odds ratio = 6.37, $p = 0.043$). The numbers of neurolytic/contrast spread areas (mean $\pm$ SD) were 4.98 $\pm$ 1.08 and 4.15 $\pm$ 1.12 in patients treated with the combination method and single method, respectively ($p < 0.001$). There was no significant predictor of complications.

Conclusions: EUS-BPN in combination with EUS-CGN was a predictor of a good pain response in EUS-guided neurolysis for pancreatic cancer-related pain. The larger number of neurolytic/contrast spread areas may lead to better outcomes in patients receiving combination treatment.

Keywords: cancer-associated pain, celiac plexus neurolysis, endoscopic ultrasound, EUS-guided neurolysis, pancreatic cancer, predictor

Correspondence to:
Masayuki Kitano, MD, PhD
Department of Gastroenterology and Hepatology, Kinki University Faculty of Medicine, 377-2 Ohno-Higashi, Osaka-Sayama 589-8511, Japan
m-kitano@med.kindai.ac.jp

Kosuke Minaga, MD
Hiroki Sakamoto, MD, PhD
Takeshi Miyata, MD, PhD
Hajime Imai, MD
Kentaro Yamao, MD
Ken Kamata, MD, PhD
Shunsuke Omoto, MD
Kumpei Kadosaka, MD
Toshiharu Sakurai, MD, PhD
Naoshi Nishida, MD, PhD
Masatoshi Kudo, MD, PhD
Department of Gastroenterology and Hepatology, Kinki University Faculty of Medicine, Osaka-Sayama, Japan

Yasutaka Chiba, PhD
Clinical Research Center, Kinki University Hospital, Osaka-Sayama, Japan

Introduction

Visceral pain secondary to upper abdominal cancer is often difficult to control and poses a challenge to the physician. Celiac plexus neurolysis (CPN) consists of the chemical ablation of the celiac plexus (CP) and it can be used for the treatment of enduring pain caused by abdominal malignancies. Endoscopic ultrasound-guided CPN (EUS-CPN) was first described in 1996 [Wiersema and Wiersema, 1996] and is currently

widely applied to treat upper abdominal cancer-associated pain [Gunaratnam *et al.* 2001; Collins *et al.* 2006; Michaels and Draganov, 2007; Puli *et al.* 2009; Penman and Rösch, 2009; Soweid and Azar, 2010; Kaufuman *et al.* 2010; LeBlanc *et al.* 2011; Sakamoto *et al.* 2011; Zou *et al.* 2012; Seicean, 2014; Seicean *et al.* 2013; Luz *et al.* 2014]. Current National Comprehensive Cancer Network guidelines (available at http://www.nccn.org) recommend EUS-CPN for the treatment of severe cancer-associated pain. Recently, different EUS approaches such as EUS-guided celiac ganglia neurolysis (EUS-CGN) [Levy *et al.* 2008] and EUS-guided broad plexus neurolysis (EUS-BPN) [Sakamoto *et al.* 2010] were developed to improve the efficacy of this technique. In a recent randomized, multicenter, controlled trial, EUS-CGN, a direct injection technique, was more effective than EUS-CPN in relieving pain [Doi *et al.* 2013]. Our group reported a single-center study comparing the pain-relieving efficacy of standard EUS-CPN with that of EUS-BPN that uses a 25-gauge needle to inject both sides of the superior mesenteric artery (SMA), and concluded that EUS-BPN provides better pain relief than EUS-CPN in patients with advanced pancreatic cancer [Sakamoto *et al.* 2010].

In several previous studies, EUS-CPN, -CGN, and -BPN showed satisfactory results and an excellent safety profile, indicating that they are promising methods; however, the efficacy of these techniques is not guaranteed. The aim of the current study was to explore predictors of pain response in patients undergoing EUS-guided neurolysis for abdominal pain caused by pancreatic cancer.

Patients and methods

Patients

This study was a retrospective analysis of prospectively collected data. Our database was reviewed to identify all patients who had undergone initial EUS-guided neurolysis for abdominal pain caused by pancreatic cancer between June 2008 and December 2014 in our institution. Patients who had been followed up at our institution for at least 4 weeks were eligible to enroll in the study. Relevant data were retrieved from the medical records of our institution. This study was approved by the Institutional Review Board of Kinki University Faculty of Medicine and written informed consent was obtained from all patients.

The inclusion criteria were as follows: (1) age older than 20 years; (2) enduring abdominal pain due to confirmed pancreatic cancer diagnosed by EUS-guided fine-needle aspiration (EUS-FNA), endoscopic biopsy or percutaneous biopsy; (3) presence of unresectable advanced pancreatic cancer. The contraindications included Eastern Cooperative Oncology Group performance status of 4, bleeding tendency (prothrombin time international normalized ratio > 1.5 and $< 50{,}000$ platelets) and presence of esophageal or gastric varices.

Pretreatment procedures

Patients were hydrated with an intravenous saline solution (500 ml) before the procedure to minimize the risk of hypotension. Patients were placed in the left lateral decubitus position with moderate sedation using intravenous midazolam with or without propofol. The level of sedation was titrated to optimize the tolerance to the procedure without compromising respiration, using a bispectral index-measuring monitor. Patients were continuously monitored during the procedure with an automated noninvasive blood pressure device, electrocardiogram tracing, and pulse oximetry.

Procedural techniques of EUS-BPN and EUS-CGN

In the present study, EUS-BPN was attempted in all patients and EUS-CGN was added in cases of visible celiac ganglia. EUS-BPN and CGN were performed using a linear array echoendoscope (GF-UCT 260; Olympus, Tokyo, Japan). US images were observed using an ALOKA ProSound SSD α-10 (ALOKA Co. Ltd., Tokyo, Japan). For EUS-BPN, at the level of the SMA, the probe was rotated clockwise toward the patient's left until the SMA origin could no longer be visualized but the aorta could still be seen. A 25-gauge needle (Echo Tip Ultra, Cook Medical, Limerick, Ireland) filled with 0.9% saline solution was prepared and introduced through the biopsy channel and affixed to the hub. The 25-gauge needle was placed under direct EUS visualization adjacent and anterior to the lateral aspect of the aorta at a level above or next to the SMA. An aspiration test was then performed. A volume of 3 ml of 1% lidocaine was injected to prevent transient neurolytic agent-induced pain. Subsequently, a solution consisting of 9 ml of 99.5% absolute alcohol (Maruishi Pharmaceutical, Osaka, Japan) and 1 ml of contrast material (Iopamiron 300, Schering AG, Berlin, Germany; 300 mg d'Iode/ml) was injected

up to 10 ml maximum. The needle was then withdrawn from the patient, flushed with 0.9% saline solution, and the same procedure was performed on the opposite side of the aorta (counterclockwise rotation). Mainly, we chose to inject the neurolytic agents into both sides around the SMA. However, in some patients, the injection areas were decided depending on the locations of intervening vessels, the tumor, and the SMA. If there were intervening vessels with or without direct tumor invasion at the target area, we avoided injecting the neurolytic agents into the area and chose only the opposite side. If the injection target was below the SMA, we injected up to 10 ml of neurolytic agents into each side below the SMA and also around the celiac artery (CA). When we injected neurolytic agents in all four sites (two sides below the SMA and two sides around the CA), a maximum of 40 ml of neurolytic agent was used for EUS-BPN per patient.

One session consisted of EUS-BPN and a subsequent attempt to perform EUS-CGN. After visualization of the celiac trunk, the scope was rotated clockwise, enabling visualization and identification of the left adrenal gland. Most frequently, celiac ganglia could be visualized at the left of the CA, between the aorta and the left adrenal gland, at a level between the CA and the left renal artery. Ganglia were also visualized cephalad to the CA in some cases. Hypoechoic nodular structures linked by hypoechoic threads residing in the periphery of this region were defined as celiac ganglia. EUS-CGN was performed by direct ganglia injection. During EUS-CGN, direct ganglia injection was performed in as many visualized ganglia as possible. For each ganglion, 1–2 ml of the mixed solution described above containing pure alcohol and contrast medium was injected. All visualized celiac ganglia were subjected to the above procedure.

When only EUS-BPN was performed without EUS-CGN, the procedure was categorized as the single method. When EUS-BPN was performed in combination with EUS-CGN, the procedure was categorized as the combination method. Schematic images of EUS-BPN and -CGN are shown in Figures 1 and 2, respectively.

Pain scores

Pain scores were determined using a standardized 11-point continuous visual analog scale (VAS), with '0' indicating no pain, '5' indicating moderate pain and '10' representing the worst pain ever. A good pain response was defined as a decrease in the VAS score by $\geqslant$3 points without additional opioid medication at 1 or 4 weeks after neurolysis. To minimize subjective variations in the evaluation of VAS scores, the same physician (H. I.) explained the pain intensity scale to all patients. The physician was unaware of the detailed endoscopic procedures except that he was informed that the patients were suffering from abdominal pain caused by pancreatic cancer. At each follow-up visit, detailed instructions explaining how to assess the VAS were read aloud and the patients then informed the same physician of the VAS score that best reflected their pain status. The physician recorded the pain rating as well as patients' responses in the analgesic questionnaire.

Computed tomography assessment

Computed tomography (CT) scanning was performed immediately after the procedure to confirm the neurolytic/contrast spread area [Sakamoto *et al.* 2006]. Serial CT images were obtained between the upper and lower limits of the neurolytic/contrast spread. To evaluate the spread pattern, the region including the CA and SMA was divided on the frontal plane into six areas: upper right and left (above the CA), middle right and left (between the CA and SMA), and lower right and left (below the SMA) (Figure 3). The CP is located in the upper and middle areas, whereas the superior mesenteric plexus (SMP) and the inferior mesenteric plexus (IMP) are located in the middle and lower areas. The relationship between the number of areas of neurolytic/contrast spread and the subsequent level of pain response was then analyzed.

Statistical analysis

All statistical analyses were performed using SAS version 9.4 software (SAS Institute Inc., Cary, NC, USA). Univariable and subsequent multivariable analyses were performed using logistic regression to explore predictors of pain response at 1 and 4 weeks and to evaluate complications. The response variables for univariable and multivariable analysis were responders and nonresponders. The explanatory variables for univariable analysis were as follows: age, sex, performance status, initial VAS score, preintervention opioid dose (dose in morphine equivalents), session timing, presence of ascites, tumor size, tumor location, tumor staging, procedure method (combination or single), number of ganglia

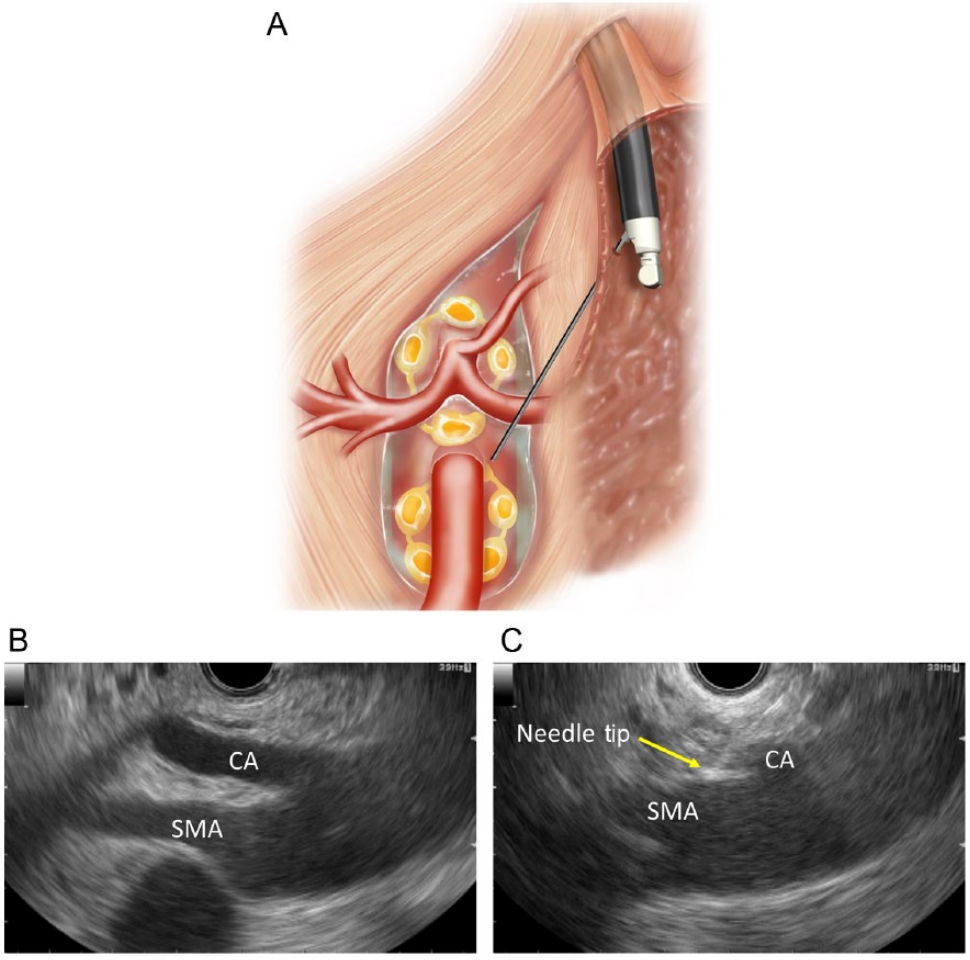

Figure 1. Endoscopic ultrasound-guided broad plexus neurolysis (EUS-BPN).
A. Schematic image of EUS-BPN.
B. EUS image of EUS-guided BPN before needle puncture. The celiac artery (CA), superior mesenteric artery (SMA), and aorta were visualized on EUS.
C. EUS image of EUS-BPN after needle puncture. A 25-gauge needle was advanced adjacent to the SMA. The needle tip is shown by a yellow arrow.

injected, and injected alcohol dose. The session timing means whether EUS-guided neurolysis was performed at initial cancer identification (early neurolysis) or during follow up (late neurolysis). For assessment of the tumor location, the cancers were categorized as pancreatic head *versus* body or tail, and as upper cancer (indicating a localized cancer that had not spread beyond the SMA) *versus* lower cancer (indicating a cancer that had expanded extensively beyond the SMA) [Sakamoto *et al.* 2010]. Candidate variables identified in the univariable analysis with a p value of < 0.1 were included in the multivariable logistic regression analysis.

Patients were divided into five subgroups according to the number of neurolytic/contrast spread areas (six, five, four, three, and two or less areas). In the subgroup analysis, response rates were calculated and compared between the subgroups using logistic regression analysis. The numbers of neurolytic/contrast areas were also measured for the two procedure methods (single or combination) using logistic regression analysis. Statistical significance was set at a p value of < 0.05.

Results

Between June 2008 and December 2014, 112 consecutive patients underwent initial EUS-guided neurolysis and all of them were followed up for at least 4 weeks after the procedure at our institution. Patient demographics, disease, and treatment characteristics are shown in Table 1 for the 112

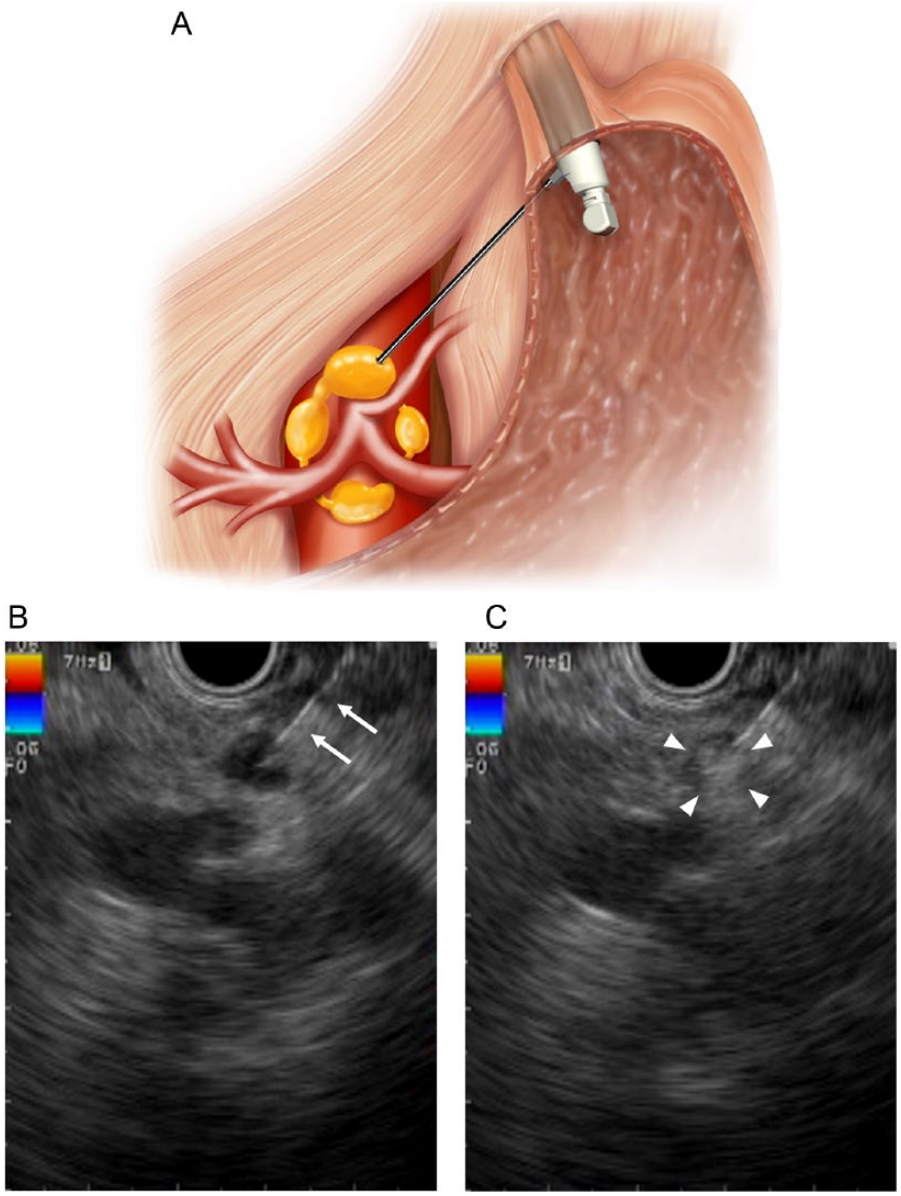

Figure 2. Endoscopic ultrasound-guided celiac ganglia neurolysis (EUS-CGN).
A. Schematic image of EUS-CGN.
B. EUS image of EUS-CGN before injection of neurolytic/contrast agents. A 25-gauge needle (white arrow) was advanced into the ganglion.
C. EUS image of EUS-CGN after injection of neurolytic/contrast agents. The ganglion exhibited a hyperechoic appearance (white arrow heads).

patients with available data for analysis. All patients had malignant tumors histologically confirmed by EUS-FNA ($n = 95$), bile duct biopsy ($n = 3$), bile cytology ($n = 6$), biopsy of liver metastases ($n = 5$), or ascites cytology ($n = 3$). The volumes of injected neurolytic/contrast agents ranged from 5 to 42 ml (mean 20.3 ml). The mean number of injection sites during EUS-BPN was 2.4 (1–4). The number of injection sites depended on the locations of intervening vessels, tumor, the SMA and the CA. We could inject neurolytic/contrast agents into all four sites (both sides around the SMA and both sides around the CA) in only five patients. In one patient, only a unilateral injection with 5 ml of neurolytic agent was possible, because there were many intervening vessels that raised a concern about the risk of bleeding. The rates of good pain response, defined as a decrease in the VAS score by ⩾3 points without additional opioid medication, were 77.7% (87 of 112 patients) and 67.9%

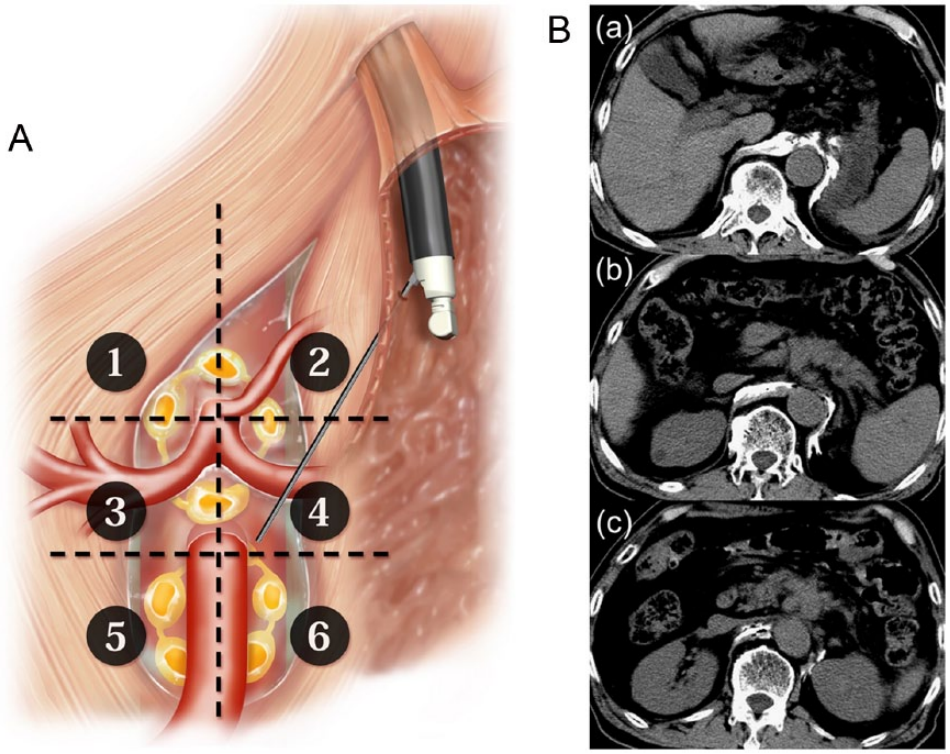

Figure 3. A. Division of the celiac, superior mesenteric, and inferior mesenteric regions into six areas: two upper areas (①, upper right; ②, upper left), two middle areas, (③, middle right; ④, middle left), and two lower areas (⑤, lower right; ⑥, lower left).
B. Post-procedural distribution of neurolytic/contrast agents on computed tomography (CT) immediately after neurolysis. Neurolytic/contrast agents were distributed over all six areas. (a) CT images above the celiac trunk (upper areas), (b) between the celiac trunk and the superior mesenteric trunk (middle areas), and (c) below the superior mesenteric trunk (lower areas) in a case with pancreatic cancer.

Table 1. Demographics and clinical characteristics of patients who underwent endoscopic ultrasound-guided neurolysis (n = 112).

Age, years (mean)	36–89 (64.3)
Sex, male/female	56/56
Performance status 0/1 or 2	92/20
Initial VAS score (mean)	3–10 (7.4)
Preintervention opioid dose, mg* (mean)	0–180 (12.7)
Session timing, early/late neurolysis	35/77
Ascites, slight or mild/none	26/86
Tumor size (mm) (mean)	15–90 (35.9)
Tumor location, head/body or tail	49/63
Tumor location upper/lower	46/66
Tumor staging, IVb/IVa	68/44
Procedure method, combination/single	47/65
Number of ganglia injected (mean)	0–3 (0.6)
Injected alcohol dose, ml (mean)	5–42 (20.3)

VAS, visual analog scale; *dose in morphine equivalents.

(76 of 112 patients) at 1 and 4 weeks after EUS-guided neurolysis, respectively.To explore predictors of pain response at 1 and 4 weeks in patients who underwent EUS-guided neurolysis, the variable data were compared between the responders and the non-responders. At 1 week, age, sex, performance status, initial pain scores, preintervention opioid dose, session timing, presence of ascites, tumor size, tumor staging and injected alcohol dose did not differ significantly between the two groups (Table 2A). However, tumors located in the head of the pancreas and the combination method (EUS-BPN plus CGN) were significant positive predictive factors in the univariable analysis (p = 0.035 and 0.015, respectively) (Table 2A). Candidate predictive variables with $p < 0.1$ in the univariable analysis were then identified. Tumor location (head *versus* body or tail, p = 0.035 and procedure method (combination *versus* single method, p = 0.015) were considered candidate predictors and included in the multivariable logistic regression analysis. The multivariable

Table 2. A. Univariable analysis of factors associated with pain response after 1 week in the enrolled cohort of 112 patients.

Independent variables	OR	95% CI	*p* value
Age, years	1.02	0.97–1.06	0.442
Sex, male/female	0.90	0.37–2.20	0.821
Performance status 1 or 2/0	0.61	0.21–1.79	0.366
Initial VAS score ⩾ 7/< 7	1.94	0.72–5.23	0.192
Preintervention opioid dose	1.00	0.99–1.01	0.976
Session timing, early/late neurolysis	0.48	0.19–1.22	0.123
Ascites slight or mild/none	1.78	0.55–5.75	0.337
Tumor size	0.97	0.94–1.01	0.108
Tumor location, head/body or tail	2.96	1.08–8.11	0.035
Tumor location, upper/lower	0.69	0.28–1.70	0.426
Tumor staging IVb/IVa	1.29	0.52–3.16	0.584
Procedure method, combination/single	3.73	1.29–10.9	0.015
Number of ganglia injected	1.70	0.85–3.40	0.136
Injected alcohol dose	1.00	0.94–1.06	0.913

OR, odds ratio; CI, confidence interval; VAS, visual analog scale.

B. Multivariable analysis of factors affecting pain response after 1 week.

Independent variables	OR	95% CI	*p* value
Tumor location in the head	3.17	0.99–10.2	0.052
Combination method (EUS-BPN plus CGN)	3.69	1.25–10.9	0.017

OR, odds ratio; CI, confidence interval; EUS, endoscopic ultrasound; BPN, broad plexus neurolysis; CGN, celiac ganglia neurolysis.

analysis revealed that the combination method was associated with a good pain response [odds ratio (OR) = 3.69, $p = 0.017$] (Table 2B).Similarly, at 4 weeks, the combination method (EUS-BPN plus CGN) was a significant positive predictive factor in univariable analysis ($p = 0.014$) (Table 3A). In multivariable analysis, the combination method was associated with a good pain response (OR = 6.37, $p = 0.043$) (Table 3B).Six, five, four, three, and two or less neurolytic/contrast spread areas were obtained in 27, 29, 35, 15 and 6 patients, respectively. The response rates at 1 and 4 weeks correlated with the number of neurolytic/contrast spread areas (Figure 4). The number of neurolytic/contrast-spread areas (mean ± SD) were 4.98 ± 1.08 and 4.15 ± 1.12 in patients treated with the combination procedure (EUS-BPN plus CGN, $n = 47$) and single procedure (EUS-BPN alone, $n = 65$), respectively ($p < 0.001$).

Complications occurred in 22.3% of 112 patients. Most of the complications were minor and self-limited, and included transient inebriation (8.0%), transient hypotension (4.5%), transient increase of pain (3.6%), and transient diarrhea (3.6%). Major complications occurred in one patient (0.9%), who developed acute paraplegia after the single method (EUS-BPN alone). In this patient, a total volume of 20 ml was injected into both sides. The number of neurolytic/contrast spread areas was six. MRI performed the next day demonstrated diffuse intramedullary T2 hyperintensity below the T-11 level to the conus medullaris, although the CT scan performed immediately after endoscopic treatment revealed no spread of the neurolytic/contrast agent into the spine. In the univariable analysis, there were no significant predictors of complications.

Discussion

Two meta-analyses of the utility of EUS-guided neurolysis for unresectable abdominal cancer-related pain showed an alleviation rate of approximately 80%, with a treatment duration of approximately 4–5 weeks [Puli *et al.* 2009; Kaufuman *et al.* 2010]. In the present study, cancer-associated pain was relieved by EUS-guided

Table 3. A. Univariable analysis of factors associated with pain response after 4 weeks in the enrolled cohort of 112 patients.

Independent variables	OR	95% CI	*p* value
Age, years	1.02	0.98–1.06	0.261
Sex, male/female	1.00	0.45–2.21	1.00
Performance Status 1 or 2/0	1.13	0.39–3.23	0.821
Initial VAS score ⩾ 7/< 7	1.25	0.49–3.18	0.640
Preintervention opioid dose	1.00	0.99–1.01	0.644
Session timing, early/late neurolysis	0.72	0.31–1.67	0.446
Ascites slight or mild/none	0.86	0.34–2.19	0.758
Tumor size	0.98	0.95–1.01	0.110
Tumor location, head/body or tail	2.16	0.93–4.99	0.072
Tumor location, upper/lower	1.62	0.71–3.70	0.254
Tumor staging IVb/IVa	0.82	0.36–1.86	0.636
Procedure method, combination/ single	3.00	1.25–7.22	0.014
Number of ganglia injected	1.64	0.91–2.95	0.09
Injected alcohol dose	1.01	0.96–1.07	0.620

OR, odds ratio; CI, confidence interval; VAS, visual analog scale.

B. Multivariable analysis of factors affecting pain response after 4 weeks.

Independent variables	OR	95% CI	*p* value
Tumor location in the head	2.10	0.89–5.00	0.091
Combination method (EUS-BPN plus CGN)	6.37	1.06–38.4	0.043
Number of ganglia injected	0.58	0.30–1.66	0.309

OR, odds ratio; CI, confidence interval; EUS, endoscopic ultrasound; BPN, broad plexus neurolysis; CGN, celiac ganglia neurolysis.

neurolysis in approximately 78% and 68% of patients at 1 and 4 weeks, respectively. The remaining patients did not respond to EUS-guided neurolysis. Analysis of the predictors of pain response in patients undergoing EUS-guided neurolysis showed that the combination method was the best predictor of pain response at both 1 and 4 weeks after EUS-guided neurolysis.

Whether bilateral injection of neurolytic agents is superior to central injection during EUS-CPN is controversial. LeBlanc and colleagues randomized 50 patients with pancreatic cancer to central or bilateral EUS-CPN groups, and found no difference in efficacy between the two groups [LeBlanc *et al.* 2013]. Sahai and colleagues evaluated the efficacy of bilateral injection compared with central injection in 160 patients, and found that bilateral injection was the only predictor of >50% of pain reduction by day 7 [Sahai *et al.* 2009]. However, these two reports did not compare the neurolytic spread between the bilateral and central injection methods.

Immediate assessment of the neurolytic spread using CT scanning is useful for the prediction of pain relief, as a wide neurolytic/contrast spread area is associated with a high response rate [Sakamoto *et al.* 2006, 2010]. In another study by Iwata and colleagues, limited distribution of alcohol to the left side of the CA was a significant factor associated with a negative response to EUS-CPN [Iwata *et al.* 2011]. In the present study, the response rates at 1 and 4 weeks correlated with the number of neurolytic/contrast spread areas.

In EUS-CGN, celiac ganglia are visualized by EUS in 62.5–89.4% of patients [Gerke *et al.* 2006; Gleeson *et al.* 2007; Ha *et al.* 2008; Kaufuman *et al.* 2010; Ascunce *et al.* 2011; Wang *et al.* 2012]. A retrospective study by Ascunce and colleagues showed that visualization of the celiac

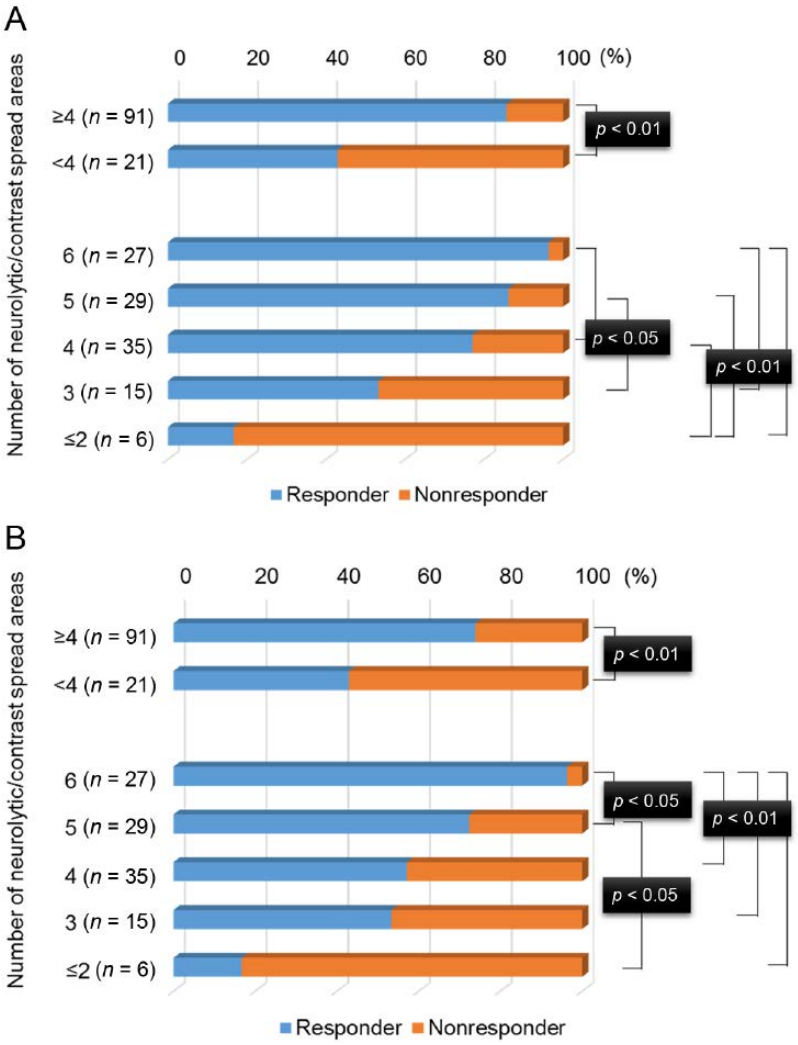

Figure 4. Relationship between neurolytic/contrast spread areas and pain response rate after 1 week (A) and 4 weeks (B). The upper two-bar graph shows a comparison of response rates between patients with at least four and those with less than four neurolytic/contrast spread areas. The lower five-bar graph shows the comparison of response rates between patients with six, five, four, three, and two or less neurolytic/contrast spread areas.

ganglia with direct injection into the ganglia is the best predictor of pain improvement after EUS-CPN [Ascunce *et al.* 2011]. In a recent randomized multicenter trial by Doi and colleagues, EUS-CGN was more effective than EUS-CPN in providing pain relief [Doi *et al.* 2013]. In the present study, additional EUS-CGN (the combination method in this study) led to a better pain response than that achieved with the single method. The number of neurolytic/contrast spread areas was higher in patients receiving combination treatment (EUS-BPN plus CGN) than in those treated with the single method (EUS-BPN alone). The larger number of neurolytic/contrast spread areas may lead to better outcomes in patients receiving combination treatment.

Three articles on the correlation between tumor location and the response to CPN have been published, although the tumor location associated with better pain relief remains controversial [Rykowski and Hilgier, 2000; Ascunce *et al.* 2011; Iwata *et al.* 2011]. Ascunce and colleagues reported that tumors located outside the head of the pancreas are weakly associated with a good response to EUS-CPN and EUS-CGN [Ascunce *et al.* 2011]. On the other hand, Rykowski and Hilgier reported that the posterior transcutaneous CPN technique is more effective in tumors involving the head of the pancreas than in those affecting the body and tail of the pancreas [Rykowski and Hilgier, 2000]. In the present study, multivariable analysis revealed that patients with

tumors located at the pancreatic head tended to respond better than those with tumors at the pancreatic body or tail after 1 week, which is consistent with the results described by Rykowski and Hilgier. Iwata and colleagues reported that EUS-CPN is less effective in patients with direct invasion of the CP [Iwata *et al.* 2011]. Pain caused by direct invasion of the CP is less likely to be induced by tumors of the head of the pancreas than by those of the body or tail [Iwata *et al.* 2011]. Direct cancer invasion from the pancreatic body to the CP may restrict the spread of neurolytic solution and limit the subsequent pain relief.

The CP extends down from the origin of the CA to the origin of the SMA. The SMP and IMP are situated on the lateral and anterior aspects of the aorta between the origin of the SMA and the inferior mesenteric artery. The CP, SMP and IMP are composed of a network of nerve fibers that originate from both sympathetic and parasympathetic nervous systems. Therefore, we hypothesized that pain relief might be achieved in patients with unresectable pancreatic cancer by using EUS-guided broad plexus neurolysis, because this could interrupt extensive nociceptive impulses from the abdomen. In a previous study from our group, EUS-BPN provided patients with advanced abdominal cancer with better pain relief than standard EUS-CPN without incurring serious complications, especially in cases in which the cancer expanded extensively within the abdominal cavity beyond the distribution of the CP [Sakamoto *et al.* 2010]. Only 19% of the EUS-CPN patients achieved satisfactory, long-lasting pain relief, whereas the EUS-BPN procedure was significantly more effective in lower cancer patients, for whom 79% achieved pain relief [Sakamoto *et al.* 2010]. In another study using CT guidance, broader plexus neurolysis, including that of the celiac, inferior mesenteric, and superior hypogastric plexuses produced effective immediate pain relief in all patients without serious adverse events, although 48.6% experienced transient diarrhea [Kitoh *et al.* 2005]. Therefore, in the present study, we performed EUS-BPN as the first line procedure and used tumor location (upper *versus* lower) for explanatory variables to determine the predictors of pain response. The efficacy of this approach did not differ between upper and lower pancreatic cancer patients at 1 and 4 weeks after EUS-guided neurolysis. Lower pancreatic cancer was not a negative predictive factor of good pain responses in patients undergoing EUS-BPN.

In the randomized pilot study by LeBlanc and colleagues comparing the effects of 10 and 20 ml of alcohol injected during neurolysis, there was no difference in complete pain response between the two groups [LeBlanc *et al.* 2011]. Similarly, in the present study, the dose of injected alcohol did not affect the pain response.

With respect to the timing of EUS-guided neurolysis sessions, Wyse and colleagues reported that early EUS-CPN performed at the time of diagnostic- and staging-EUS, provides better pain relief than conventional management, in addition to preventing progressive increases in morphine consumption [Wyse *et al.* 2011]. In the present study, the timing of EUS-guided neurolysis did not affect its efficacy. These results suggest that EUS-guided neurolysis may be effective not only at the time of initial cancer detection (early neurolysis), but also during follow up (late neurolysis), although our study included a smaller number of patients who underwent early neurolysis.

A recent review that included 15 studies of EUS-guided neurolysis found that complications occurred in 21% of 661 patients [Alvarez-Sánchez *et al.* 2014]. Most of the reported complications were minor and self-limited, usually lasting less than 48 hours, and were attributed to disruption of sympathetic activity. In the present study, minor complications occurred in 22.3% of 112 patients and all minor complications were transient and self-limited. There was only one major complication consisting of acute spinal cord infarction with paraplegia in a patient treated by the single method (EUS-BPN alone). Serious complications after EUS-guided neurolysis are uncommon [O'Toole and Schmulewitz, 2009; Alvarez-Sánchez *et al.* 2014]. A recent overview of the safety and complications of EUS-guided neurolysis reported serious complications in 0.2% of EUS-guided neurolysis cases [Luz *et al.* 2014; Alvarez-Sánchez *et al.* 2014], and two cases of acute paraplegia after EUS-guided neurolysis have been reported [Fujii *et al.* 2012; Mittal *et al.* 2012]. In the present study, the complication rate was not related to the predictor of good pain response (procedure methods), suggesting that the combination method provides better pain relief without serious complications.

The present study had several inherent limitations. One potential limitation was that this study

was retrospectively performed in a single institution. The second potential limitation of the present study was the lack of double blinding for the selection of patients for the two procedures. Additional EUS-CGN was performed only when celiac ganglia were detected on EUS, and visible celiac ganglia (42.0%) were detected in a lower proportion of patients than that reported previously (62.5–89.4%). The visibility of some ganglia can be impaired by the hyperechoic appearance of the alcohol injected during EUS-BPN. We feared that the hyperechoic appearance of the ganglia located on the puncture line for EUS-BPN might impair the visibility of the SMA if the ganglia had been treated before EUS-BPN. However, an alternative method using EUS-CGN before EUS-BPN might facilitate visualization of the ganglia. The third limitation was the subjective evaluation of pain. Because pain is difficult to measure objectively, a quantitative analysis of the efficacy of the prospective method is required. The fourth limitation was the short duration of follow up. It was difficult for us to follow up patients for longer than 4 weeks, because some patients were transferred to a hospice and had a short survival time.

Conclusion

The combination method (EUS-BPN plus CGN) was a predictor of better pain relief, suggesting that the combination method might improve the efficacy of EUS-guided neurolysis. The larger number of neurolytic/contrast spread areas might contribute to the better efficacy of the combination method. Further prospective, randomized control studies to compare EUS-BPN with and without EUS-CGN are needed to evaluate the efficacy of the different approaches to EUS-guided neurolysis.

Author contributions

Masayuki Kitano and Hiroki Sakamoto: manuscript writing, drafting conception and design, performing the endoscopic procedure. Kosuke Minaga and Takeshi Miyata: manuscript writing, analyzing the data and providing clinical advice. Hajime Imai, Kentaro Yamao, Ken Kamata, Shunsuke Omoto, Kumpei Kadosaka, Toshiharu Sakurai and Naoshi Nishida: contribution to writing the manuscript and providing clinical advice. Yasutaka Chiba: statistical analysis of data. Masatoshi Kudo: contribution to writing the manuscript, drafting conception and design.

Funding

The present study was supported by grants from the Japan Society for the Promotion of Science (grant numbers 22590764 and 25461035).

Conflict of interest statement

The authors declare that there is no conflict of interest.

References

Alvarez-Sánchez, M., Jenssen, C., Faiss, S. and Napoleon, B. (2014) Interventional endoscopic ultrasonography: an overview of safety and complications. *Surg Endosc* 28: 712–734.

Ascunce, G., Ribeiro, A., Reis, I., Rocha-Lima, C., Sleeman, D., Merchan, J. *et al.* (2011) EUS visualization and direct celiac ganglia neurolysis predicts better pain relief in patients with pancreatic malignancy (with video). *Gastrointest Endosc* 73: 267–274.

Collins, D., Penman, I, Mishra, G. and Draganov, P. (2006) EUS-guided celiac block and neurolysis. *Endoscopy* 38: 935–939.

Doi, S., Yasuda, I., Kawakami, H., Hayashi, T., HIsai, H., Irisawa, A. *et al.* (2013) Endoscopic ultrasound-guided celiac ganglia neurolysis *versus* celiac plexus neurolysis : a randomized multicenter trial. *Endoscopy* 45: 362–369.

Fujii, L., Clain, J., Morris, J. and Levy, M. (2012) Anterior spinal cord infarction with permanent paralysis following endoscopic ultrasound-guided celiac plexus neurolysis. *Endoscopy* 44: E265–E266.

Gerke, H., Silva, R., Jr., Shamoun, D., Johnson, C. and Jensen, C. (2006) EUS characteristics of celiac ganglia with cytologic and histologic confirmation. *Gastrointest Endosc* 64: 35–39.

Gleeson, F., Levy, M., Papachristou, G., Pelaez-Luna, M., Rajan, E., Clain, J. *et al.* (2007) Frequency of visualization of presumed celiac ganglia by endoscopic ultrasound. *Endoscopy* 39: 620–624.

Gunaratnam, N., Sarma, A., Norton, I. and Wiersema, M. (2001) A prospective study of EUS-guided celiac plexus neurolysis for pancreatic cancer pain. *Gastrointest Endosc* 54: 316–324.

Ha, T., Kim, G., Kang, D., Song, G., Kim, S. and Lee, J. (2008) Detection of celiac ganglia with radial scanning endoscopic ultrasonography. *Korean J Intern Med* 23: 5–8.

Iwata, K., Yasuda, I., Enya, M., Mukai, T., Nakashima, M., Doi, S. *et al.* (2011) Predictive factors for pain relief after endoscopic ultrasound-guided celiac plexus neurolysis. *Dig Endosc* 23: 140–145.

Kaufuman, M., Singh, G., Das, S., Concha-Parra, R., Erber, J., Micames, C. *et al.* (2010) Efficacy of endoscopic ultrasound-guided celiac plexus neurolysis for managing abdominal pain associated with chronic pancreatitis and pancreatic cancer. *J Clin Gastroenterol* 44: 127–134.

Kitoh, T., Tanaka, S., Ono, K., Ohfusa, Y., Ina, H. and Otagiri, T. (2005) Combined neurolytic block of celiac, inferior mesenteric, and superior hypogastric plexuses for incapacitating abdominal and/or pelvic pain. *J Anesth* 19: 328–332.

LeBlanc, J., Al-Haddad, M., McHenry, L., Sherman, S., Juan, M., McGreevy., K. *et al.* (2011) A prospective, randomized study of EUS-guided celiac plexus neurolysis for pancreatic cancer: one injection or two? *Gastrointest Endosc* 74: 1300–1307.

LeBlanc, J., Rawl, S., Juan, M., Johnson, C., Kroenke, K., McHenry, L. *et al.* (2013) Endoscopic ultrasound-guided celiac plexus neurolysis in pancreatic cancer: a prospective pilot study of safety using 10 ml *versus* 20 ml alcohol. *Diagn Ther Endosc* 2013: article ID 327036.

Levy, M., Topazian, M., Wiersema, M., Clain, J., Rajan, E., Wang, K. *et al.* (2008) Initial evaluation of the efficacy and safety of endoscopic ultrasound-guided direct Ganglia neurolysis and block. *Am J Gastroenterol* 103: 98–103.

Luz, L., Al-Haddad, M. and DeWitt, J. (2014) EUS-guided celiac interventions in pancreatic cancer pain: an update and controversies for the endosonographer. *Endosc Ultrasound* 3: 213–220.

Michaels, A. and Draganov, P. (2007) Endoscopic ultrasonography guided celiac plexus neurolysis and celiac plexus block in the management of pain due to pancreatic cancer and chronic pancreatitis. *World J Gastroenterol* 13: 3575–3580.

Mittal, M., Rabinstein, A. and Wijdicks, E. (2012) Pearls & oysters: acute spinal cord infarction following endoscopic ultrasound-guided celiac plexus neurolysis. *Neurology* 78: e57–e59.

O'Toole, T. and Schmulewitz, N. (2009) Complication rates of EUS-guided celiac plexus blockade and neurolysis: Results of a large case series. *Endoscopy* 41: 593–597.

Penman, I. and Rösch, T: EUS 2008 Working Group. (2009) EUS 2008 Working Group document: evaluation of EUS-guided celiac plexus neurolysis/block (with video). *Gastrointest Endosc* 69: S28–S31.

Puli, S., Reddy, J., Bechtold, M., Antillon, M. and Brugge, W. (2009) EUS-guided celiac plexus neurolysis for pain due to chronic pancreatitis or pancreatic cancer pain: A meta-analysis and systematic review. *Dig Dis Sci* 54: 2330–2337.

Rykowski, J. and Hilgier, M. (2000) Efficacy of neurolytic celiac plexus block in varying locations of pancreatic cancer: influence on pain relief. *Anethesiology* 92: 347–354.

Sahai, A., Lemedin, V., Lam, E. and Paquin, S. (2009) Central *versus* bilateral endoscopic ultrasound-guided celiac plexus block or neurolysis: a comparative study of short-term effectiveness. *Am J Gastroenterol* 104: 326–329.

Sakamoto, H., Kitano, M., Kamata, K., Komaki, T., Imai, H., Chikugo, T. *et al.* (2010) EUS-guided broad plexus neurolysis over the superior mesenteric artery using a 25-gauge needle. *Am J Gastroenterol* 105: 2599–2606.

Sakamoto, H., Kitano, M., Komaki, T., Imai, H., Kamata, K. and Kudo, M. (2011) Endoscopic ultrasound-guided neurolysis in pancreatic cancer. *Pancreatology* 11: 52–58.

Sakamoto, H., Kitano, M., Nishio, T., Takeyama, Y., Yasuda, C. and Kudo, M. (2006) Value of computed tomography for evaluating the injection site in endosonography-guided celiac plexus neurolysis for pancreatic cancer pain. *Dig Endosc* 18: 206–211.

Seicean, A. (2014) Celiac plexus neurolysis in pancreatic cancer: the endoscopic ultrasound approach. *World J Gastroenterol* 20: 110–117.

Seicean, A., Cainap, C., Gulei, I., Tantau, M. and Seicean, R. (2013) Pain palliation by endoscopic ultrasound-guided celiac plexus neurolysis in patients with unresectable pancreatic cancer. *J Gastrointest Liver Dis* 22: 59–64.

Soweid, A. and Azar, C. (2010) Endoscopic ultrasound-guided celiac plexus neurolysis. *World J Gastrointest Endosc* 2: 228–231.

Wang, K., Jin, Z., Du, Y., Zhan, X., Zou, D., Liu, Y. *et al.* (2012) EUS-guided celiac ganglion irradiation with iodine-125 seeds for pain control in pancreatic carcinoma: a prospective pilot study. *Gastrointest Endosc* 76: 945–952.

Wiersema, M. and Wiersema, L. (1996) Endosonography-guided celiac plexus neurolysis. *Gastrointest Endosc* 44: 656–662.

Wyse, J., Carone, M., Paquin, S., Usatii, M. and Sahai, A. (2011) Randomized, double-blind, controlled trial of early endoscopic ultrasound-guided celiac plexus neurolysis to prevent pain progression in patients with newly diagnosed, painful, inoperable pancreatic cancer. *J Clin Oncol* 29: 3541–3546.

Zou, X., Shen, S., Lv, Y., Li, W. and Zhanq, X. (2012) Endoscopic ultrasound-guided celiac plexus neurolysis for pain management in patients with pancreatic carcinoma reasons to fight a losing battle. *Pancreas* 41: 655–657.

ULTRA SONO GRAPHY

New endoscopic ultrasonography techniques for pancreaticobiliary diseases

Ken Kamata, Masayuki Kitano, Shunsuke Omoto, Kumpei Kadosaka, Takeshi Miyata, Kosuke Minaga, Kentaro Yamao, Hajime Imai, Masatoshi Kudo

Department of Gastroenterology and Hepatology, Kinki University Faculty of Medicine, Osaka-Sayama, Japan

REVIEW ARTICLE

http://dx.doi.org/10.14366/usg.15042
pISSN: 2288-5919 • eISSN: 2288-5943
Ultrasonography 2015;35:169-179

Endoscopic ultrasonography (EUS) is widely used to evaluate pancreaticobiliary diseases, especially pancreatic masses. EUS has a good ability to detect pancreatic masses, but it is not sufficient for the differential diagnosis of various types of lesions. In order to address the limitations of EUS, new techniques have been developed to improve the characterization of the lesions detected by EUS. EUS-guided fine needle aspiration (EUS-FNA) has been used for diagnosing pancreatic tumors. In order to improve the histological diagnostic yield, a EUS-FNA needle with a core trap has recently been developed. Contrast-enhanced harmonic EUS is a new imaging modality that uses an ultrasonographic contrast agent to visualize blood flow in fine vessels. This technique is useful in the diagnosis of pancreatic solid lesions and in confirming the presence of vascularity in mural nodules for cystic lesions. EUS elastography analyzes several different variables to measure tissue elasticity, color patterns, and strain ratio, using analytical techniques such as hue-histogram analysis, and artificial neural networks, which are useful for the diagnosis of chronic pancreatitis and pancreatic cancer.

Keywords: Endosonography; Endoscopic ultrasound-guided fine needle aspiration; Elasticity imaging techniques; Biliary tract; Pancreas; Sonazoid

Received: July 27, 2015
Revised: April 10, 2016
Accepted: April 12, 2016

Correspondence to:
Masayuki Kitano, MD, PhD,
Department of Gastroenterology and Hepatology, Kinki University Faculty of Medicine, 377-2 Ohno-Higashi, Osaka-Sayama 589-8511, Japan

Tel. +81-72-366-0221 (ext. 3525)
Fax. +81-72-367-2880
E-mail: m-kitano@med.kindai.ac.jp

How to cite this article:
Kamata K, Kitano M, Omoto S, Kadosaka K, Miyata T, Minaga K, et al. New endoscopic ultrasonography techniques for pancreaticobiliary diseases. Ultrasonography. 2016 Jul;35(3):169-179.

Introduction

Endoscopic ultrasonography (EUS) is widely used to evaluate pancreaticobiliary diseases, especially pancreatic masses [1–5]. EUS has an adequate ability to detect pancreatic masses, but it is not sufficient for the differential diagnosis of various types of lesions. A recently published report has shown that when pancreatic carcinoma was defined as a hypoechoic lesion, the sensitivity and specificity of conventional EUS were 86% and 18%, respectively [6]. In order to overcome the limitations of EUS, new techniques, such as contrast-enhanced EUS, EUS elastography (EUS-E), and EUS-guided fine needle aspiration (EUS-FNA) have been developed to characterize the lesions detected by EUS.

EUS-FNA

Solid Lesions of the Pancreas

EUS-FNA was developed for the pathological diagnosis of lesions in and adjacent to the digestive

tract and has a diagnostic accuracy of 60% to 90%, depending on the site that is investigated [7]. EUS-FNA is particularly useful for diagnosing pancreatic tumors and assists in making treatment decisions. For these carcinomas, it has a diagnostic sensitivity of 54%–96%, a specificity of 96%–98%, and an accuracy of 83%–95% [8–11]. Various EUS-FNA needles have been developed, including 25-, 22-, and 19-gauge needles. Of particular note, 25-gauge needles are easier to handle and cause fewer complications. Several studies have shown that, in comparison to 22- and 19-gauge needles, 25-gauge needles are more maneuverable and are less likely to yield samples contaminated with blood [12–15]. Additionally, the lesions are more easily penetrated. Moreover, a recently published prospective comparative study showed that 25-gauge FNA needles had a better diagnostic yield in solid pancreatic tumors than 22-gauge FNA needles (pooled sensitivity: 93% for 25-gauge needles vs. 85% for 22-gauge needles) [16]. However, this finding only applied to cytology-based diagnoses, as the 25-gauge needle was inferior to the 22-gauge needle in terms of the accuracy of histology-based diagnoses. In order to improve the diagnostic yield, a histological diagnosis is needed, especially when immunohistological analysis is required (e.g., when a neuroendocrine tumor or malignant lymphoma is suspected). For this reason, a EUS-FNA needle with a core trap was developed recently (Fig. 1) [17–22]. It provides histological core tissue using a 25-gauge needle, even in a single pass, and several studies have shown it to improve the diagnostic yield in solid pancreatic tumors, particularly in the histological diagnosis. Thus, the selection of an optimal FNA needle depends on the purpose of EUS-FNA. The technique used during EUS-FNA is also important for improving accuracy. The fanning technique, which involves sampling multiple areas within a lesion during each pass, was found to be superior to the standard approach because fewer passes were required to establish the diagnosis [23]. The slow-pull technique is a new technique during EUS-FNA procedures. In this technique, after the mass is punctured, the stylet is slowly pulled out without suction [21]. It was found that the slow-pull technique was associated with less contamination with blood and resulted in a higher diagnostic yield when a smaller (25- or 22-gauge) core biopsy needle was used. This pattern was also observed when slow-pull aspiration with a standard 25-gauge EUS-FNA needle was followed by either histological diagnosis or cytology. Thus, many options are available for EUS-FNA, and further study is required to establish the optimal methods for EUS-FNA.

Cystic Lesions of the Pancreas

EUS-FNA is efficient for the differential diagnosis of pancreatic cysts. It also identifies the main pancreatic duct communication by measuring intracystic pancreatic enzymes or tumor markers such as amylase, lipase, and carcinoembryonic antigen (CEA) [24–29]. Brugge et al. [24] reported a 79% accuracy for diagnosing mucinous cystic neoplasms when the cut-off value of CEA was defined as 192 ng/mL. Van der Waaij et al. [25] reported a 98% specificity for identifying mucinous cystic neoplasms as malignant when CEA in the cyst was >800 ng/mL and also indicated that a cyst fluid amylase concentration of <250 U/L virtually excluded the possibility of a pseudocyst. Although EUS-FNA rarely causes complications such as hemorrhage (0.2%–6%) and infection (0.2%–5%), determining how management may be affected by the imaging information is essential before performing EUS-FNA [26–28]. Cyst size is often the most important determinant of success in cyst aspiration and the acquisition of adequate fluid for analysis. Walsh et al. [29] showed that a minimum cyst size of 1.5 cm was needed to obtain at least one variable (cytology, CEA, and amylase) with an 84% success rate, and therefore endorsed using EUS-FNA for pancreatic cysts 1.5 cm or larger. Recently, through-the-needle imaging has been employed for evaluating pancreatic cysts. Needle-based confocal laser endomicroscopy (nCLE) that can be inserted into 19-gauge EUS-FNA needles has been developed to allow observations to be made within the cyst [30,31]. By using nCLE, images of the internal structure of the cyst are obtained, which are similar to histopathological images. This novel technique is expected to be of use for the differential diagnosis of malignant versus non-malignant as well as mucinous versus non-mucinous cystic neoplasms.

Gallbladder Masses

EUS-FNA of gallbladder masses was first reported by Jacobson et al. in 2003 [32]. Although only small case series have been published, the FNA of gallbladder masses has been found to have high sensitivity (80%–100%) and specificity [33–35]. However, the effectiveness of EUS-FNA for the diagnosis of gallbladder tumors is questionable. It is necessary to consider bile leakage and/or seeding related to FNA, although no reports have described severe complications in EUS-FNA for gallbladder tumors.

Contrast-Enhanced EUS

Contrast-enhanced EUS includes contrast-enhanced Doppler EUS and contrast-enhanced harmonic EUS (CH-EUS). Contrast-enhanced Doppler remains limited in terms of real-time vessel imaging due to artifacts such as blooming. CH-EUS selectively depicts harmonic components that are integer multiples of the fundamental frequency [36,37]. When microbubbles oscillate or are broken after receiving a certain range of acoustic power, harmonic components are produced. The harmonic component derived from microbubbles is higher than that obtained from tissues; thus, contrast harmonic

imaging depicts signals from the microbubbles with greater intensity than it depicts signals from the tissue by selectively detecting the harmonic components [36,37]. CH-EUS is a new imaging modality that uses an ultrasonographic contrast agent to visualize blood flow in fine vessels.

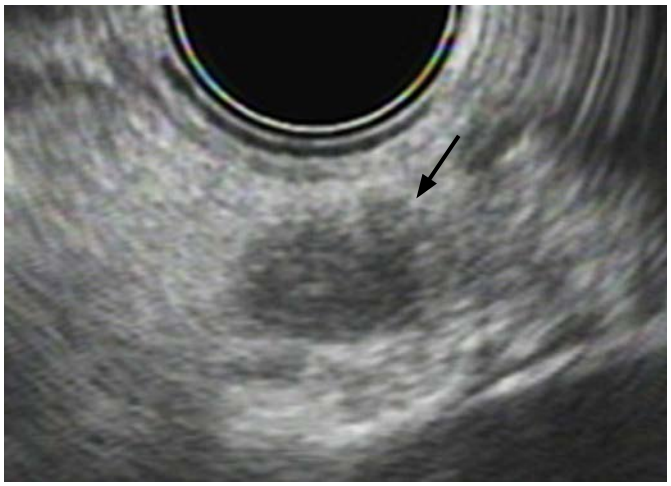

A

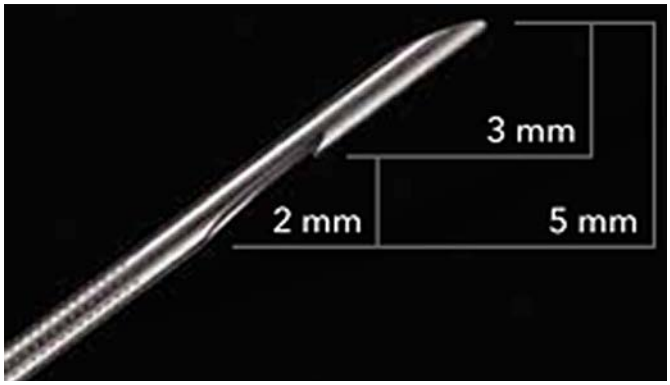

B

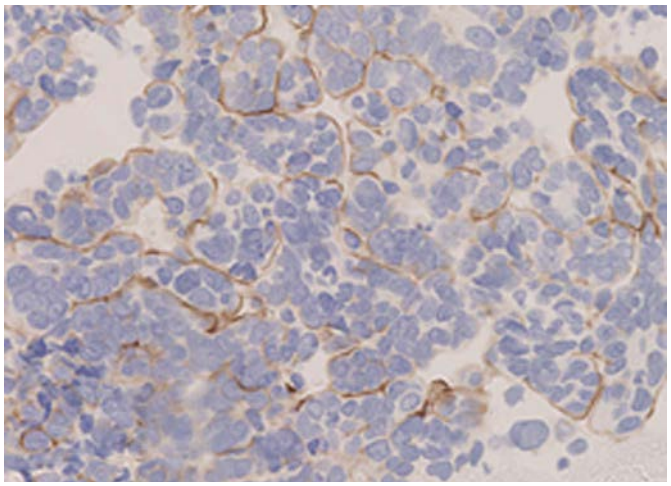

C

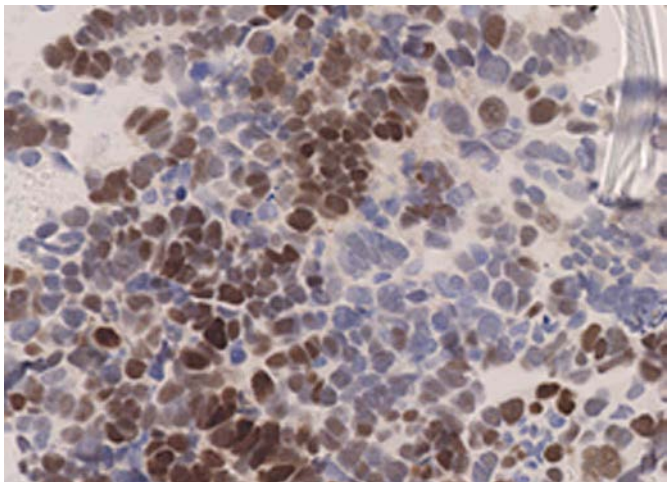

D

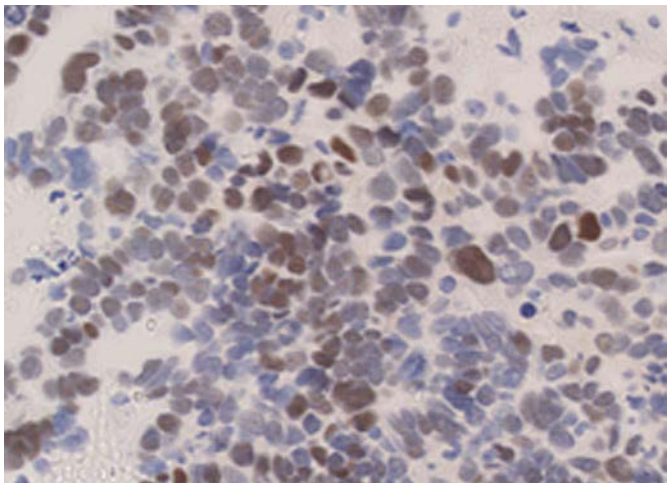

E

Fig. 1. A 50-year-old woman with pancreatic metastasis of ovarian carcinoma as diagnosed by endoscopic ultrasonography-guided fine needle aspiration (EUS-FNA).
A. EUS shows a 12-mm hypoechoic mass (arrow) in the body of the pancreas. B. A 25-gauge needle with a core trap was used for EUS-FNA. The core was located at the top of the needle. C–E. Immunohistochemical studies demonstrate the following results: CA-125 (+) (C), estrogen receptor (++) (D), and progesterone receptor (+) (E) (C–E, ×400).

Solid Lesions of the Pancreas

On CH-EUS, solid pancreatic lesions can be classified into four patterns depending on the enhancement pattern: non-enhancement, hypoenhancement, isoenhancement, and hyperenhancement [6,38–40]. Pancreatic carcinomas possess a certain degree of enhancement, mostly hypoenhancement, whereas benign necrotic tissue does not exhibit enhancement (Fig. 2, Video clip 1). In contrast, most neuroendocrine tumors exhibit hyperenhancement (Fig. 3) [6,38–40]. A recently published meta-analysis has shown that when pancreatic adenocarcinomas were diagnosed based on showing hypoenhancement in CH-EUS, the pooled diagnostic sensitivity and specificity were 94% and 89%, respectively [41]. When CH-EUS was compared to conventional EUS in detecting pancreatic carcinomas, the former (with pancreatic carcinomas defined as hypoenhanced lesions) had better sensitivity and specificity than the latter (96% vs. 86% and 64% vs. 18%, respectively) [6]. Moreover, CH-EUS clearly depicts the outline of ductal carcinomas, even when the conventional EUS finding is uncertain. This could help clarify the location of the target tumor for performing EUS-FNA. CH-EUS and contrast-enhanced computed tomography (CT) are comparable in

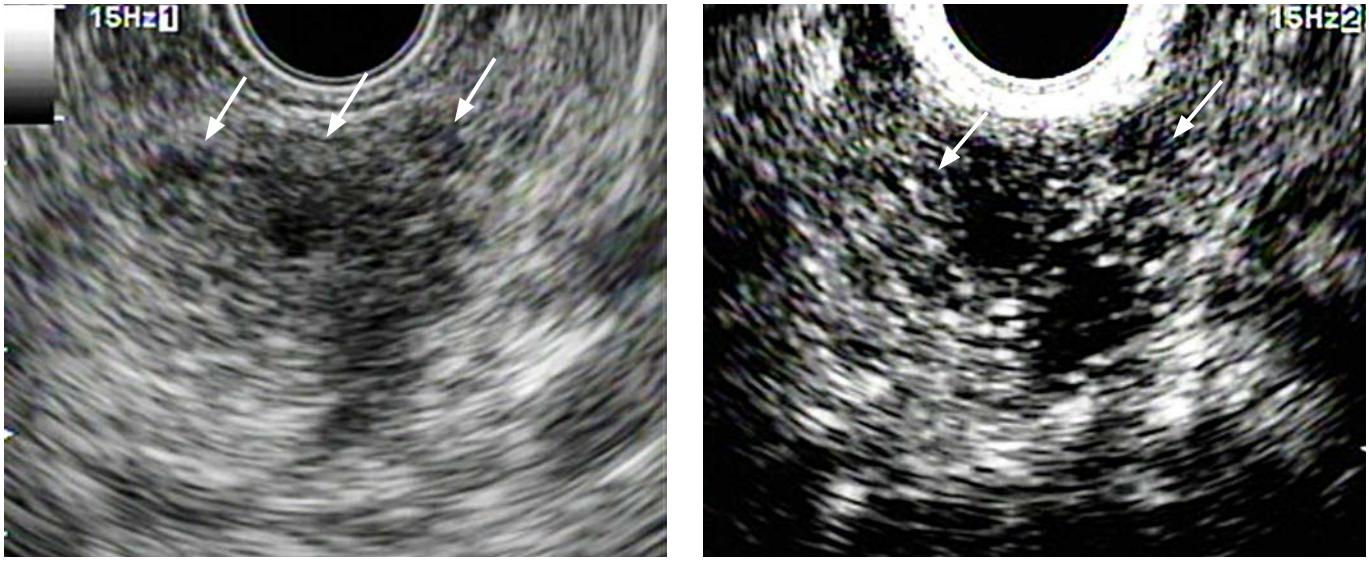

A B

Fig. 2. A 67-year-old man with pancreatic ductal adenocarcinoma.
A. Fundamental B-mode endoscopic ultrasonography (EUS) shows a 20-mm hypoechoic tumor (arrows) in the body of the pancreas. B. Contrast-enhanced harmonic EUS shows hypoenhancement of the lesion (arrows).

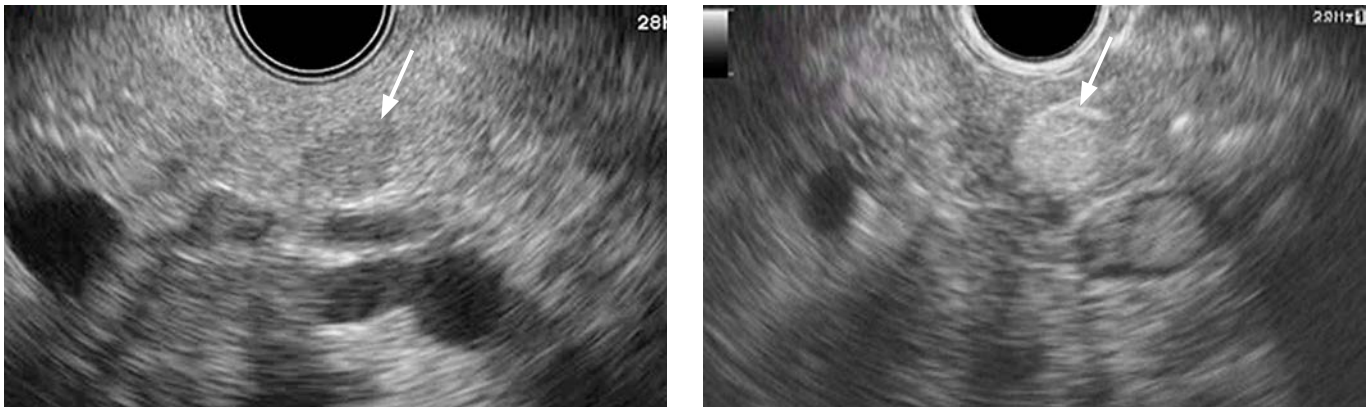

A B

Fig. 3. A 42-year-old woman with a neuroendocrine tumor in the pancreas.
A. Fundamental B-mode endoscopic ultrasonography (EUS) shows a 7-mm hypoechoic tumor (arrow) in the body of the pancreas. B. Contrast-enhanced harmonic EUS demonstrates hyperenhancement of the lesion (arrow).

terms of differentiating pancreatic carcinomas from other masses. However, for small carcinomas (≤2 cm), CH-EUS was found to be superior (sensitivity, 91%; specificity, 94%) in comparison with contrast-enhanced CT (sensitivity, 71%; specificity, 92%) [38]. This shows that CH-EUS is useful for characterizing small neoplasms that contrast-enhanced CT cannot identify. The combination of CH-EUS and EUS-FNA is useful for accurately diagnosing pancreatic cancer. When ductal carcinomas were defined as tumors with hypoenhancement on CH-EUS and/or a positive EUS-FNA result, the sensitivity and specificity were 100% and 92.6%, respectively [38]. Combining CH-EUS with EUS-FNA increased the sensitivity of EUS-FNA from 92.2% to 100%.

Cystic Lesions of the Pancreas

Internal structural features of cystic tumors, including the locularity, cystic component, appearance, and/or the presence of a thick wall and/or mural nodules are important in the differential diagnosis of cystic lesions of the pancreas [42,43]. CH-EUS may also aid in the diagnosis of pancreatic cysts through the assessment of the vascularity of structures such as the cyst wall, septa, or mural nodules, as well as by distinguishing contrast-enhancing mural nodules from non-enhancing mucus clots (Figs. 4, 5, Video clip 2) [37]. It is important to evaluate mural nodules in intraductal papillary mucinous neoplasms in order to perform a differential diagnosis of malignant versus non-malignant. However, standard EUS may misdiagnose mucus clots as mural nodules; therefore, confirming the

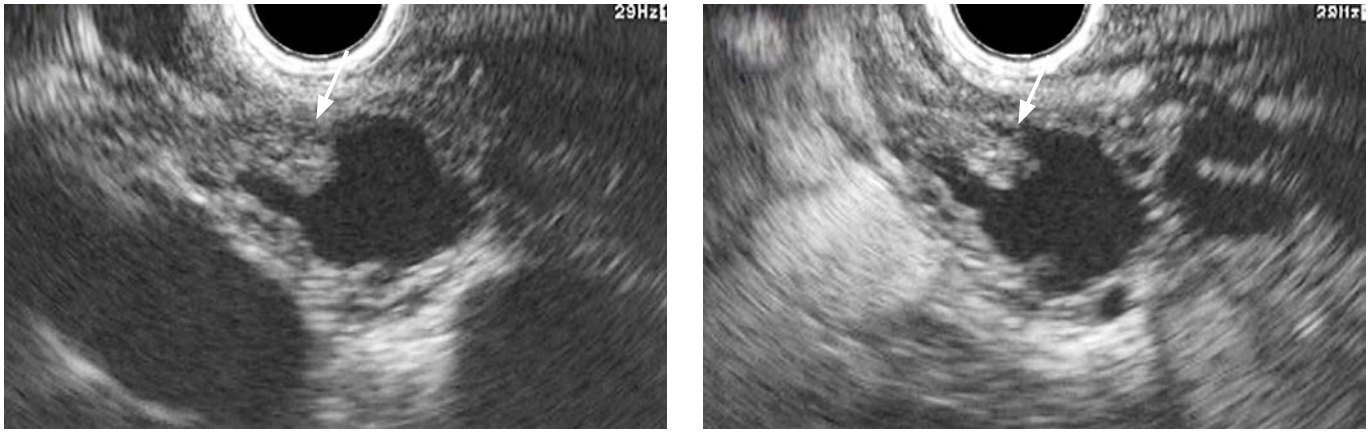

A B

Fig. 4. A 72-year-old man with intrapapillary mucinous neoplasms exhibiting high-grade dysplasia.
A. Fundamental B-mode endoscopic ultrasonography (EUS) shows a mural nodule in the cystic lesion (arrow). B. Contrast-enhanced harmonic EUS demonstrates vascularity in the mural nodule (arrow) on contrast-enhanced harmonic EUS.

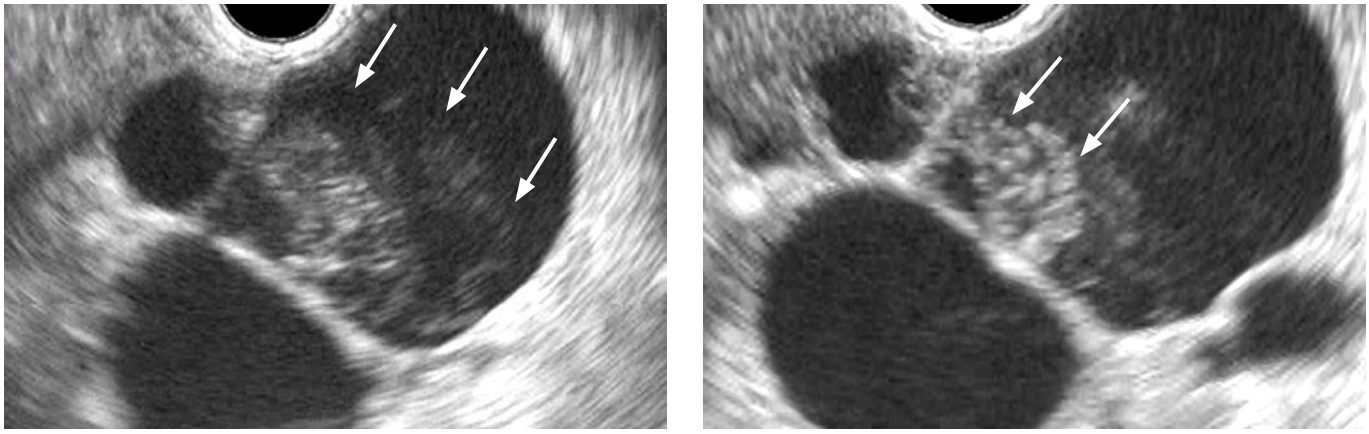

A B

Fig. 5. A 74-year-old man with an intraductal papillary mucinous neoplasm exhibiting high-grade dysplasia.
A. Fundamental B-mode endoscopic ultrasonography (EUS) shows suspicious mural nodules in the cystic lesion (arrows). B. Contrast-enhanced harmonic EUS shows that a part of the lesion had vascularity (arrows), and it was considered to be a true mural nodule.

presence of vascularity in the mural nodule on CH-EUS is important and helps to avoid unnecessary surgical resection. Several studies have evaluated the vascular patterns of mural nodules. Ohno et al. [44] classified mural nodules into four groups based on vascularity (low papillary nodules, polypoid nodules, papillary nodules, and invasive nodules) using contrast-enhanced Doppler EUS, and reported that papillary and invasive nodule patterns were associated with malignancy. Kurihara et al. [45] evaluated the vascularity of mural nodules measuring more than 10 mm using transabdominal ultrasonography and reported that a branch-shaped pattern was associated with carcinoma.

Gallbladder Lesions

Hirooka et al. [46] first reported the usefulness of CH-EUS using sonicated albumin for the diagnosis of gallbladder lesions in 1998. The authors reported that the accuracy of the determination of tumor invasion for conventional EUS was 78.6%, whereas it was 92.9% for CH-EUS. Imazu et al. [47] reported that an inhomogeneous enhancement pattern on CH-EUS for wall thickening of the gallbladder indicated malignancy. They evaluated CH-EUS using a Sonazoid and reported that the sensitivity, specificity, accuracy, positive predictive value, negative predictive value, and area under the receiver operating curve (ROC) of CH-EUS were 89.6%, 98%, 94.4%, 97.7%, 92.2%, and 0.94, respectively. These values are superior to those of conventional EUS. With respect to gallbladder polyps, the presence of irregular intratumoral vessels or perfusion defects seen on CH-EUS was a sensitive and accurate predictor of malignant gallbladder polyps [48]. In that study, it was found that in 93 patients with gallbladder polyps larger than 10 mm in diameter, an irregular vessel pattern determined by CH-EUS aided in the diagnosis of malignant polyps, with a sensitivity and specificity of 90.3% and 96.6%, respectively. The presence of perfusion defects was able to diagnose malignant polyps with a sensitivity and specificity of 90.3% and 94.9%, respectively. Thus, malignant gallbladder lesions can be characterized as showing inhomogeneous enhancement and/or irregular vessels on CH-EUS (Fig. 6). In another small series, Park et al. [49] found that CH-EUS also helped differentiate cholesterol polyps from gallbladder adenomas. They studied 87 patients with gallbladder polyps and found that the sensitivity and specificity of CH-EUS for the differential diagnosis of gallbladder adenomas from cholesterol polyps based on the enhancement pattern were 75.0% and 66.6%, respectively. CH-EUS may be useful for the differential diagnosis of gallbladder lesions, but the clinical efficacy of CH-EUS in deciding on a treatment strategy remains questionable. Moreover, the visual assessment of CH-EUS images is subjective and an additional quantitative analysis is required.

EUS Elastography

The major principle of tissue elastography is that a compressive force is applied to the tissue, causing axial tissue deformation (strain), which is then calculated by comparing the echo sets before and after the compression [50]. EUS-E is an adjunctive imaging technique that allows the tissue elasticity of a solid mass to be assessed during a conventional EUS examination [51,52]. This technique allows the direct visualization of information reflecting strain superimposed on the fundamental B-mode image as a strain distribution map (the elastogram), which, for visualization purposes, is color-coded and displayed next to the fundamental B-mode image on the screen.

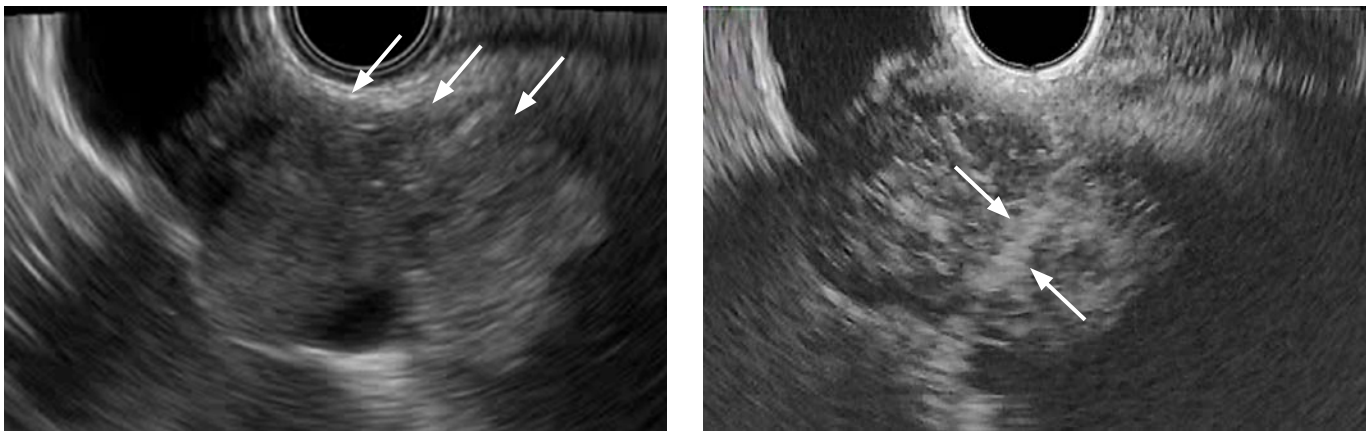

A B

Fig. 6. A 75-year-old man with gallbladder carcinoma.
A. Fundamental B-mode endoscopic ultrasonography (EUS) demonstrates a solid tumor in the gallbladder (arrows). B. Contrast-enhanced harmonic EUS shows heterogeneous enhancement and irregular vessels (arrows) in the lesion.

Red is used for encoding soft tissue, blue for hard tissue, and yellow/green for tissue of intermediate stiffness (Fig. 7). Several different variables have been used in EUS-E as a measure of tissue elasticity, color patterns and strain ratio (SR), using analytical techniques such as hue-histogram analysis, and artificial neural networks [52–55]. The classification of color patterns, which is qualitative, may be limited by its subjectivity, which could lead to differences in interpretation between endosonographers. This is less likely to be a significant problem for the remaining three quantitative variables, which are supplementary to the qualitative variable.

Diagnosis of Malignant Pancreatic Lesions

The primary aim of EUS-E is to distinguish benign and malignant tumors through the assessment of tissue elasticity (with benign tumors being soft while malignant tumors are hard) [56]. The first clinical experience with the qualitative analysis of EUS-E was obtained in 49 patients in 2006, and the authors of that study observed an optimal sensitivity (100%) for both pancreatic malignancies and malignant lymph nodes [52]. Iglesias-Garcia et al. [57] extended this type of analysis by using the following four patterns: homogeneous green, heterogeneous green-predominant, homogeneous blue, and heterogeneous blue-predominant. They found that this method diagnosed pancreatic malignancies with a sensitivity, specificity, and overall accuracy of 100%, 85.5%, and 94%, respectively. Two studies have assessed the accuracy of SR-based EUS-E for diagnosing pancreatic malignancies, with the sensitivity ranging from 93% to 100% and the specificity ranging from 17% to 95% [54,58]. Therefore, SR-based EUS-E results are problematically variable, especially with regard to specificity. In 2012–2013, six meta-analyses have been published on this subject. Pei et al. [59] identified 1,042 patients with solid pancreatic masses and found that EUS-E showed a pooled sensitivity and specificity of 95% (93%–96%) and 69% (63%–75%), respectively, with an area under the ROC curve (AUC) of 0.870 for the differential diagnosis of benign and malignant masses. Mei et al. [60] reported similar data in 1,044 cases: for EUS-E, the pooled sensitivity was 95% (94%–97%), the pooled specificity was 67% (61%–73%), the diagnostic odds ratio was 42.28 (26.90–66.46), and the AUC was 0.905.

Diagnosis of Chronic Pancreatitis

EUS-E is also used for the diagnosis of chronic pancreatitis (CP). Janssen and Papavassiliou [61] compared pancreatic elasticity among healthy patients younger than 60 years of age (group 1) and older than 60 years of age (group 2) with patients with CP (group 3). Histogram analysis of the elastograms (with 0 corresponding to the hardest tissue and 255 indicating the softest tissue) showed that the mean strain values were 110.2±23.9, 80.0±16.4, and 32.4±11.9 in groups 1, 2, and 3, respectively. They identified a cut-off value of

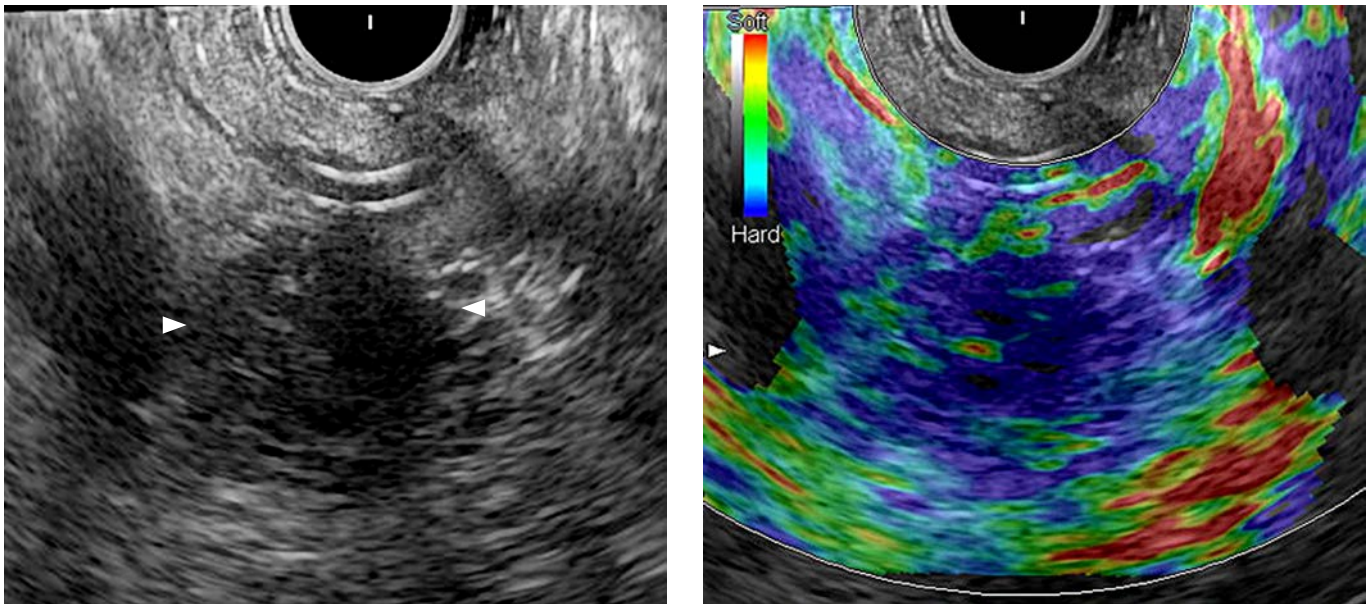

A B

Fig. 7. A 68-year-old man with pancreatic ductal adenocarcinoma.
A. Fundamental B-mode endoscopic ultrasonography (EUS) demonstrates a hypoechoic mass (arrowheads) in the head of the pancreas. B. EUS elastography shows a relatively homogenous hard pattern (predominantly blue) at the site of the tumor in comparison to the surrounding tissues.

50 that was able to distinguish the presence of CP in contrast to healthy people older than 60 years of age with an AUC of 0.993. These results show that the pancreatic parenchyma becomes significantly harder during aging but remains softer than in patients with CP. Itoh et al. [62] evaluated the ability of EUS-E to quantify the degree of fibrosis of the parenchyma surrounding pancreatic tumors in 58 patients undergoing pancreasectomy. On average, EUS-E (performed through software analysis) showed an AUC of 0.90 for the diagnosis of pancreatic fibrosis. Recently, Dominguez-Munoz et al. [63] enrolled 115 patients with CP undergoing EUS in order to evaluate the correlation between EUS-E and pancreatic exocrine insufficiency (PEI). They observed that pancreatic fibrosis was directly correlated with PEI; in particular, patients with PEI (30% of the study population) showed a significantly higher SR than patients with CP with no PEI (4.89 vs. 2.99, P<0.001). They also estimated that the probability of PEI was <5% in patients with a SR <2.5 and >90% in patients with a SR >5.5.

Biliary Tree and Gallbladder Diseases

Few reports have yet evaluated EUS-E of the biliary tree and gallbladder. Since the common bile duct is a hollow organ, the application of EUS-E may be limited when the bile duct is not completely blocked and the mass does not infiltrate beyond the wall. Rustemovic et al. [64] evaluated EUS-E as a method for screening patients with suspected primary sclerosing cholangitis. They found that a hard or mixed elasticity score was observed more frequently in patients with primary sclerosing cholangitis (P<0.001). According to a recent review article, EUS-E can demonstrate a homogeneously hard (blue) elastographic pattern in malignant masses that infiltrate the bile duct and extend beyond the wall, causing stenosis [65].

Conclusion

Technological innovations such as EUS-FNA, CH-EUS, and EUS-E have improved the ability of EUS to detect and characterize pancreaticobiliary lesions. These methods supplement the diagnostic use of conventional EUS.

ORCID: Ken Kamata: http://orcid.org/0000-0003-1568-0769; Masayuki Kitano: http://orcid.org/0000-0001-6885-9223; Shunsuke Omoto: http://orcid.org/0000-0001-7291-3608; Kumpei Kadosaka: http://orcid.org/0000-0003-3993-1673; Takeshi Miyata: http://orcid.org/0000-0003-4702-2197; Kosuke Minaga: http://orcid.org/0000-0001-5407-7925; Kentaro Yamao: http://orcid.org/0000-0003-2497-7740; Hajime Imai: http://orcid.org/0000-0001-6767-7989; Masatoshi Kudo: http://orcid.org/0000-0002-4102-3474

Conflict of Interest

No potential conflict of interest relevant to this article was reported.

Supplementary Material

Video clip 1. In the same patient presented in Fig. 2, the pancreatic cancer shows a gradual hyperenhancement during contrast-enhanced harmonic endoscopic ultrasonography (http://dx.doi.org/10.14366/usg.15042.v001).

Video clip 2. In the same patient presented in Fig. 5, contrast-enhanced harmonic EUS shows the vascularity of the true mural nodule, as distinguished from non-enhancing mucus clots in the cystic lesion (http://dx.doi.org/10.14366/usg.15042.v002).

References

1. Rosch T, Lorenz R, Braig C, Feuerbach S, Siewert JR, Schusdziarra V, et al. Endoscopic ultrasound in pancreatic tumor diagnosis. Gastrointest Endosc 1991;37:347-352.
2. Yasuda K, Mukai H, Nakajima M, Kawai K. Staging of pancreatic carcinoma by endoscopic ultrasonography. Endoscopy 1993;25:151-155.
3. Gress FG, Hawes RH, Savides TJ, Ikenberry SO, Cummings O, Kopecky K, et al. Role of EUS in the preoperative staging of pancreatic cancer: a large single-center experience. Gastrointest Endosc 1999;50:786-791.
4. DeWitt J, Devereaux B, Chriswell M, McGreevy K, Howard T, Imperiale TF, et al. Comparison of endoscopic ultrasonography and multidetector computed tomography for detecting and staging pancreatic cancer. Ann Intern Med 2004;141:753-763.
5. Sakamoto H, Kitano M, Suetomi Y, Maekawa K, Takeyama Y, Kudo M. Utility of contrast-enhanced endoscopic ultrasonography for diagnosis of small pancreatic carcinomas. Ultrasound Med Biol 2008;34:525-532.
6. Fusaroli P, Spada A, Mancino MG, Caletti G. Contrast harmonic echo-endoscopic ultrasound improves accuracy in diagnosis of solid pancreatic masses. Clin Gastroenterol Hepatol 2010;8:629-634.
7. Dumonceau JM, Polkowski M, Larghi A, Vilmann P, Giovannini M, Frossard JL, et al. Indications, results, and clinical impact of endoscopic ultrasound (EUS)-guided sampling in gastroenterology: European Society of Gastrointestinal Endoscopy (ESGE) Clinical Guideline. Endoscopy 2011;43:897-912.
8. Hewitt MJ, McPhail MJ, Possamai L, Dhar A, Vlavianos P, Monahan KJ. EUS-guided FNA for diagnosis of solid pancreatic neoplasms: a meta-analysis. Gastrointest Endosc 2012;75:319-331.
9. Itoi T, Sofuni A, Itokawa F, Irisawa A, Khor CJ, Rerknimitr R. Current status of diagnostic endoscopic ultrasonography in the evaluation of pancreatic mass lesions. Dig Endosc 2011;23 Suppl 1:17-21.
10. Chen G, Liu S, Zhao Y, Dai M, Zhang T. Diagnostic accuracy of endoscopic ultrasound-guided fine-needle aspiration for pancreatic cancer: a meta-analysis. Pancreatology 2013;13:298-304.
11. Puli SR, Bechtold ML, Buxbaum JL, Eloubeidi MA. How good is

endoscopic ultrasound-guided fine-needle aspiration in diagnosing the correct etiology for a solid pancreatic mass?: a meta-analysis and systematic review. Pancreas 2013;42:20-26.
12. Siddiqui UD, Rossi F, Rosenthal LS, Padda MS, Murali-Dharan V, Aslanian HR. EUS-guided FNA of solid pancreatic masses: a prospective, randomized trial comparing 22-gauge and 25-gauge needles. Gastrointest Endosc 2009;70:1093-1097.
13. Yusuf TE, Ho S, Pavey DA, Michael H, Gress FG. Retrospective analysis of the utility of endoscopic ultrasound-guided fine-needle aspiration (EUS-FNA) in pancreatic masses, using a 22-gauge or 25-gauge needle system: a multicenter experience. Endoscopy 2009;41:445-448.
14. Lee JH, Stewart J, Ross WA, Anandasabapathy S, Xiao L, Staerkel G. Blinded prospective comparison of the performance of 22-gauge and 25-gauge needles in endoscopic ultrasound-guided fine needle aspiration of the pancreas and peri-pancreatic lesions. Dig Dis Sci 2009;54:2274-2281.
15. Rastogi A, Wani S, Gupta N, Singh V, Gaddam S, Reddymasu S, et al. A prospective, single-blind, randomized, controlled trial of EUS-guided FNA with and without a stylet. Gastrointest Endosc 2011;74:58-64.
16. Madhoun MF, Wani SB, Rastogi A, Early D, Gaddam S, Tierney WM, et al. The diagnostic accuracy of 22-gauge and 25-gauge needles in endoscopic ultrasound-guided fine needle aspiration of solid pancreatic lesions: a meta-analysis. Endoscopy 2013;45:86-92.
17. Iglesias-Garcia J, Poley JW, Larghi A, Giovannini M, Petrone MC, Abdulkader I, et al. Feasibility and yield of a new EUS histology needle: results from a multicenter, pooled, cohort study. Gastrointest Endosc 2011;73:1189-1196.
18. Larghi A, Iglesias-Garcia J, Poley JW, Monges G, Petrone MC, Rindi G, et al. Feasibility and yield of a novel 22-gauge histology EUS needle in patients with pancreatic masses: a multicenter prospective cohort study. Surg Endosc 2013;27:3733-3738.
19. Hucl T, Wee E, Anuradha S, Gupta R, Ramchandani M, Rakesh K, et al. Feasibility and efficiency of a new 22G core needle: a prospective comparison study. Endoscopy 2013;45:792-798.
20. Bang JY, Hebert-Magee S, Trevino J, Ramesh J, Varadarajulu S. Randomized trial comparing the 22-gauge aspiration and 22-gauge biopsy needles for EUS-guided sampling of solid pancreatic mass lesions. Gastrointest Endosc 2012;76:321-327.
21. Iwashita T, Nakai Y, Samarasena JB, Park DH, Zhang Z, Gu M, et al. High single-pass diagnostic yield of a new 25-gauge core biopsy needle for EUS-guided FNA biopsy in solid pancreatic lesions. Gastrointest Endosc 2013;77:909-915.
22. Lee YN, Moon JH, Kim HK, Choi HJ, Choi MH, Kim DC, et al. Core biopsy needle versus standard aspiration needle for endoscopic ultrasound-guided sampling of solid pancreatic masses: a randomized parallel-group study. Endoscopy 2014;46:1056-1062.
23. Bang JY, Magee SH, Ramesh J, Trevino JM, Varadarajulu S. Randomized trial comparing fanning with standard technique for endoscopic ultrasound-guided fine-needle aspiration of solid pancreatic mass lesions. Endoscopy 2013;45:445-450.
24. Brugge WR, Lewandrowski K, Lee-Lewandrowski E, Centeno BA, Szydlo T, Regan S, et al. Diagnosis of pancreatic cystic neoplasms: a report of the cooperative pancreatic cyst study. Gastroenterology 2004;126:1330-1336.
25. van der Waaij LA, van Dullemen HM, Porte RJ. Cyst fluid analysis in the differential diagnosis of pancreatic cystic lesions: a pooled analysis. Gastrointest Endosc 2005;62:383-389.
26. Varadarajulu S, Eloubeidi MA. Frequency and significance of acute intracystic hemorrhage during EUS-FNA of cystic lesions of the pancreas. Gastrointest Endosc 2004;60:631-635.
27. O'Toole D, Palazzo L, Arotcarena R, Dancour A, Aubert A, Hammel P, et al. Assessment of complications of EUS-guided fine-needle aspiration. Gastrointest Endosc 2001;53:470-474.
28. Williams DB, Sahai AV, Aabakken L, Penman ID, van Velse A, Webb J, et al. Endoscopic ultrasound guided fine needle aspiration biopsy: a large single centre experience. Gut 1999;44:720-726.
29. Walsh RM, Zuccaro G, Dumot JA, Vargo J, Biscotti CV, Hammel J, et al. Predicting success of endoscopic aspiration for suspected pancreatic cystic neoplasms. JOP 2008;9:612-617.
30. Konda VJ, Meining A, Jamil LH, Giovannini M, Hwang JH, Wallace MB, et al. A pilot study of in vivo identification of pancreatic cystic neoplasms with needle-based confocal laser endomicroscopy under endosonographic guidance. Endoscopy 2013;45:1006-1013.
31. Nakai Y, Iwashita T, Park DH, Samarasena JB, Lee JG, Chang KJ. Diagnosis of pancreatic cysts: EUS-guided, through-the-needle confocal laser-induced endomicroscopy and cystoscopy trial: DETECT study. Gastrointest Endosc 2015;81:1204-1214.
32. Jacobson BC, Pitman MB, Brugge WR. EUS-guided FNA for the diagnosis of gallbladder masses. Gastrointest Endosc 2003;57:251-254.
33. Meara RS, Jhala D, Eloubeidi MA, Eltoum I, Chhieng DC, Crowe DR, et al. Endoscopic ultrasound-guided FNA biopsy of bile duct and gallbladder: analysis of 53 cases. Cytopathology 2006;17:42-49.
34. Hijioka S, Hara K, Mizuno N, Imaoka H, Ogura T, Haba S, et al. Diagnostic yield of endoscopic retrograde cholangiography and of EUS-guided fine needle aspiration sampling in gallbladder carcinomas. J Hepatobiliary Pancreat Sci 2012;19:650-655.
35. Varadarajulu S, Eloubeidi MA. Endoscopic ultrasound-guided fine-needle aspiration in the evaluation of gallbladder masses. Endoscopy 2005;37:751-754.
36. Dietrich CF, Ignee A, Frey H. Contrast-enhanced endoscopic ultrasound with low mechanical index: a new technique. Z Gastroenterol 2005;43:1219-1223.
37. Kitano M, Sakamoto H, Matsui U, Ito Y, Maekawa K, von Schrenck T, et al. A novel perfusion imaging technique of the pancreas: contrast-enhanced harmonic EUS (with video). Gastrointest Endosc

2008;67:141-150.
38. Kitano M, Kudo M, Yamao K, Takagi T, Sakamoto H, Komaki T, et al. Characterization of small solid tumors in the pancreas: the value of contrast-enhanced harmonic endoscopic ultrasonography. Am J Gastroenterol 2012;107:303-310.
39. Napoleon B, Alvarez-Sanchez MV, Gincoul R, Pujol B, Lefort C, Lepilliez V, et al. Contrast-enhanced harmonic endoscopic ultrasound in solid lesions of the pancreas: results of a pilot study. Endoscopy 2010;42:564-570.
40. Gincul R, Palazzo M, Pujol B, Tubach F, Palazzo L, Lefort C, et al. Contrast-harmonic endoscopic ultrasound for the diagnosis of pancreatic adenocarcinoma: a prospective multicenter trial. Endoscopy 2014;46:373-379.
41. Gong TT, Hu DM, Zhu Q. Contrast-enhanced EUS for differential diagnosis of pancreatic mass lesions: a meta-analysis. Gastrointest Endosc 2012;76:301-309.
42. Koito K, Namieno T, Nagakawa T, Shyonai T, Hirokawa N, Morita K. Solitary cystic tumor of the pancreas: EUS-pathologic correlation. Gastrointest Endosc 1997;45:268-276.
43. Kubo H, Nakamura K, Itaba S, Yoshinaga S, Kinukawa N, Sadamoto Y, et al. Differential diagnosis of cystic tumors of the pancreas by endoscopic ultrasonography. Endoscopy 2009;41:684-689.
44. Ohno E, Hirooka Y, Itoh A, Ishigami M, Katano Y, Ohmiya N, et al. Intraductal papillary mucinous neoplasms of the pancreas: differentiation of malignant and benign tumors by endoscopic ultrasound findings of mural nodules. Ann Surg 2009;249:628-634.
45. Kurihara N, Kawamoto H, Kobayashi Y, Okamoto Y, Yamamoto N, Tsutsumi K, et al. Vascular patterns in nodules of intraductal papillary mucinous neoplasms depicted under contrast-enhanced ultrasonography are helpful for evaluating malignant potential. Eur J Radiol 2012;81:66-70.
46. Hirooka Y, Naitoh Y, Goto H, Ito A, Hayakawa S, Watanabe Y, et al. Contrast-enhanced endoscopic ultrasonography in gallbladder diseases. Gastrointest Endosc 1998;48:406-410.
47. Imazu H, Mori N, Kanazawa K, Chiba M, Toyoizumi H, Torisu Y, et al. Contrast-enhanced harmonic endoscopic ultrasonography in the differential diagnosis of gallbladder wall thickening. Dig Dis Sci 2014;59:1909-1916.
48. Choi JH, Seo DW, Park DH, Lee SS, Lee SK, Kim MH. Utility of contrast-enhanced harmonic EUS in the diagnosis of malignant gallbladder polyps (with videos). Gastrointest Endosc 2013;78:484-493.
49. Park CH, Chung MJ, Oh TG, Park JY, Bang S, Park SW, et al. Differential diagnosis between gallbladder adenomas and cholesterol polyps on contrast-enhanced harmonic endoscopic ultrasonography. Surg Endosc 2013;27:1414-1421.
50. Gao L, Parker KJ, Lerner RM, Levinson SF. Imaging of the elastic properties of tissue: a review. Ultrasound Med Biol 1996;22:959-977.
51. Saftoiu A, Vilman P. Endoscopic ultrasound elastography: a new imaging technique for the visualization of tissue elasticity distribution. J Gastrointestin Liver Dis 2006;15:161-165.
52. Giovannini M, Hookey LC, Bories E, Pesenti C, Monges G, Delpero JR. Endoscopic ultrasound elastography: the first step towards virtual biopsy?: preliminary results in 49 patients. Endoscopy 2006;38:344-348.
53. Janssen J, Schlorer E, Greiner L. EUS elastography of the pancreas: feasibility and pattern description of the normal pancreas, chronic pancreatitis, and focal pancreatic lesions. Gastrointest Endosc 2007;65:971-978.
54. Dawwas MF, Taha H, Leeds JS, Nayar MK, Oppong KW. Diagnostic accuracy of quantitative EUS elastography for discriminating malignant from benign solid pancreatic masses: a prospective, single-center study. Gastrointest Endosc 2012;76:953-961.
55. Saftoiu A, Vilmann P, Gorunescu F, Janssen J, Hocke M, Larsen M, et al. Accuracy of endoscopic ultrasound elastography used for differential diagnosis of focal pancreatic masses: a multicenter study. Endoscopy 2011;43:596-603.
56. Fusaroli P, Saftoiu A, Mancino MG, Caletti G, Eloubeidi MA. Techniques of image enhancement in EUS (with videos). Gastrointest Endosc 2011;74:645-655.
57. Iglesias-Garcia J, Larino-Noia J, Abdulkader I, Forteza J, Dominguez-Munoz JE. EUS elastography for the characterization of solid pancreatic masses. Gastrointest Endosc 2009;70:1101-1108.
58. Saftoiu A, Iordache SA, Gheonea DI, Popescu C, Malos A, Gorunescu F, et al. Combined contrast-enhanced power Doppler and real-time sonoelastography performed during EUS, used in the differential diagnosis of focal pancreatic masses (with videos). Gastrointest Endosc 2010;72:739-747.
59. Pei Q, Zou X, Zhang X, Chen M, Guo Y, Luo H. Diagnostic value of EUS elastography in differentiation of benign and malignant solid pancreatic masses: a meta-analysis. Pancreatology 2012;12:402-408.
60. Mei M, Ni J, Liu D, Jin P, Sun L. EUS elastography for diagnosis of solid pancreatic masses: a meta-analysis. Gastrointest Endosc 2013;77:578-589.
61. Janssen J, Papavassiliou I. Effect of aging and diffuse chronic pancreatitis on pancreas elasticity evaluated using semiquantitative EUS elastography. Ultraschall Med 2014;35:253-258.
62. Itoh Y, Itoh A, Kawashima H, Ohno E, Nakamura Y, Hiramatsu T, et al. Quantitative analysis of diagnosing pancreatic fibrosis using EUS-elastography (comparison with surgical specimens). J Gastroenterol 2014;49:1183-1192.
63. Dominguez-Munoz JE, Iglesias-Garcia J, Castineira Alvarino M, Luaces Regueira M, Larino-Noia J. EUS elastography to predict pancreatic exocrine insufficiency in patients with chronic pancreatitis. Gastrointest Endosc 2015;81:136-142.
64. Rustemovic N, Cukovic-Cavka S, Opacic M, Petrovecki M, Hrstic I,

Radic D, et al. Endoscopic ultrasound elastography as a method for screening the patients with suspected primary sclerosing cholangitis. Eur J Gastroenterol Hepatol 2010;22:748-753.

65. Cui XW, Ignee A, Braden B, Woenckhaus M, Dietrich CF. Biliary papillomatosis and new ultrasound imaging modalities. Z Gastroenterol 2012;50:226-231.

World Journal of Gastroenterology

Submit a Manuscript: http://www.wjgnet.com/esps/
Help Desk: http://www.wjgnet.com/esps/helpdesk.aspx
DOI: 10.3748/wjg.v22.i16.4264

World J Gastroenterol 2016 April 28; 22(16): 4264-4269
ISSN 1007-9327 (print) ISSN 2219-2840 (online)

CASE REPORT

Urgent endoscopic ultrasound-guided choledochoduodenostomy for acute obstructive suppurative cholangitis-induced sepsis

Kosuke Minaga, Masayuki Kitano, Hajime Imai, Kentaro Yamao, Ken Kamata, Takeshi Miyata, Shunsuke Omoto, Kumpei Kadosaka, Tomoe Yoshikawa, Masatoshi Kudo

Kosuke Minaga, Masayuki Kitano, Hajime Imai, Kentaro Yamao, Ken Kamata, Takeshi Miyata, Shunsuke Omoto, Kumpei Kadosaka, Tomoe Yoshikawa, Masatoshi Kudo, Department of Gastroenterology and Hepatology, Kinki University Faculty of Medicine, Osaka-Sayama 589-8511, Japan

Author contributions: All authors helped to perform the research; Minaga K wrote the manuscript; Kitano M and Kudo M drafted the conception and design; Kitano M performed endoscopic interventions; Imai H, Yamao K, Kamata K, Miyata T, Omoto S, Kadosaka K and Yoshikawa T contributed to writing the manuscript.

Supported by The Japan Society for the Promotion of Science and the Japanese Foundation for the Research and Promotion of Endoscopy, No. 22590764 and 25461035.

Institutional review board statement: This study was approved by the Institutional Review Board of Kinki University Faculty of Medicine.

Informed consent statement: All study participants, or their legal guardian, provided informed written consent prior to study enrollment.

Conflict-of-interest statement: All authors declare no conflicts-of-interest related to this article.

Correspondence to: Masayuki Kitano, MD, PhD, Department of Gastroenterology and Hepatology, Kinki University Faculty of Medicine, 377-2 Ohno-Higashi, Osaka-Sayama 589-8511, Japan. m-kitano@med.kindai.ac.jp

Telephone: +81-72-3660221
Fax: +81-72-3672880

Received: December 10, 2015
Peer-review started: December 12, 2015
First decision: December 30, 2015
Revised: January 7, 2016
Accepted: January 30, 2016
Article in press: January 30, 2016
Published online: April 28, 2016

Abstract

Acute obstructive suppurative cholangitis (AOSC) due to biliary lithiasis is a life-threatening condition that requires urgent biliary decompression. Although endoscopic retrograde cholangiopancreatography (ERCP) with stent placement is the current gold standard for biliary decompression, it can sometimes be difficult because of failed biliary cannulation. In this retrospective case series, we describe three cases of successful biliary drainage with recovery from septic shock after urgent endoscopic ultrasound-guided choledochoduodenostomy (EUS-CDS) was performed for AOSC due to biliary lithiasis. In all three cases, technical success in inserting the stents was achieved and the patients completely recovered from AOSC with sepsis in a few days after EUS-CDS. There were no procedure-related complications. When initial ERCP fails, EUS-CDS can be an effective life-saving endoscopic biliary decompression procedure that shortens the procedure time and prevents post-ERCP pancreatitis, particularly in patients with AOSC-induced sepsis.

Key words: Endoscopic ultrasound-guided biliary drainage; Choledochoduodenostomy; Acute obstructive

suppurative cholangitis; Sepsis; Life-saving endoscopy

Core tip: We present 3 cases of urgent endoscopic ultrasound-guided choledochoduodenostomy (EUS-CDS) performed for acute obstructive suppurative cholangitis (AOSC)-induced sepsis due to benign lesions. In all three cases, technical success in inserting the stents was achieved and the patients completely recovered from AOSC with sepsis in a few days after EUS-CDS. Although endoscopic retrograde cholangiopancreatography (ERCP) with transpapillary stent placement is the current gold standard for biliary decompression, this technique is not always successful. In this situation, EUS-CDS can be an effective life-saving biliary decompression procedure that can shorten the procedure time and prevent post-ERCP pancreatitis, particularly in patients with AOSC-induced sepsis.

Minaga K, Kitano M, Imai H, Yamao K, Kamata K, Miyata T, Omoto S, Kadosaka K, Yoshikawa T, Kudo M. Urgent endoscopic ultrasound-guided choledochoduodenostomy for acute obstructive suppurative cholangitis-induced sepsis. *World J Gastroenterol* 2016; 22(16): 4264-4269 Available from: URL: http://www.wjgnet.com/1007-9327/full/v22/i16/4264.htm DOI: http://dx.doi.org/10.3748/wjg.v22.i16.4264

INTRODUCTION

Acute obstructive suppurative cholangitis (AOSC) due to biliary lithiasis is a life-threatening condition that requires urgent biliary decompression. Endoscopic retrograde cholangiopancreatography (ERCP) with transpapillary stent placement is the current gold standard for biliary decompression. Endoscopic transpapillary stent placement can sometimes be difficult because of failed biliary cannulation. Recently, endoscopic ultrasound (EUS) guided biliary drainage (EUS-BD) has been increasingly used as an alternative in patients with malignant biliary obstruction after failed initial ERCP[1-4]. However, this technique is not usually indicated for benign biliary lesions. Here we describe three cases of successful biliary drainage with full recovery from septic shock after urgent EUS-guided choledochoduodenostomy (EUS-CDS) was performed for AOSC-induced sepsis. All procedures were carried out by a single experienced endoscopist (M.K.) at a tertiary-care referral center. All EUS procedures were performed using a therapeutic linear echoendoscope (GF-UCT260; Olympus Medical Systems, Tokyo, Japan) with carbon dioxide insufflation. The collection of clinical data for this study was approved by the Institutional Review Board of Kinki University Faculty of Medicine and all study participants, or their legal guardian, provided informed written consent prior to study enrollment.

CASE REPORT

Patient 1

An 83-year-old woman with septic shock due to common bile duct (CBD) stones was referred to our hospital. Urgent ERCP had been performed at a neighboring general hospital; however, biliary cannulation was unsuccessful even with needle-knife precut papillotomy. Intravenous norepinephrine had been administered to maintain systolic blood pressure. Her vital signs were as follows: Glasgow coma scale (GCS) conscious level of E3V4M3, blood pressure of 75/55 mmHg, heart rate of 108 beats/min, and body temperature of 39.2 ℃. Laboratory tests showed an elevated inflammatory reaction [white blood cell count (WBC), 38300/μL; serum C-reactive protein (CRP) level, 17.7 mg/dL; and serum procalcitonin (PCT), 64.3 ng/mL]. Elevated levels of serum liver function parameters and bilirubin were also noted [aspartate aminotransferase (AST), 123 IU/L; alanine aminotransferase (ALT), 169 IU/L; alkaline phosphatase (ALP), 220 IU/L; and total bilirubin, 5.2 mg/dL]. Computed tomography (CT) revealed large piled-up CBD stones and dilatation of CBD. Because the intrahepatic bile ducts were not dilated, percutaneous transhepatic biliary drainage (PTBD) seemed to be difficult. Thus, we decided to perform EUS-CDS. The procedure was performed without intubation after administration of a small amount of intravenous midazolam. The depth of the patient's sedation was titrated by continuous monitoring with a bispectral index monitor and a pulse oximetry. On EUS, the dilated CBD was accessed from the duodenum bulb. First, the CBD was punctured using a 19-gauge needle (Sono Tip Pro Control; Medi-Globe, Rosenheim, Germany) under echoendoscopic guidance (Figure 1A). Bile was aspirated, and then contrast medium was injected. A 0.025-inch guidewire (VisiGlide 2; Olympus Medical Systems) was placed into the CBD. The fistula was dilated using a 4-mm balloon catheter (ZARA; Century Medical, Tokyo, Japan) (Figure 1B), and a covered metallic stent (8-mm wide, 80-mm long; WallFlex partially covered stent; Boston Scientific, Natick, MA, United States) and a 6-Fr endoscopic nasobiliary drainage catheter were inserted (Figure 1C). The duration for the procedure was 21 min. The patient completely recovered in a few days and was discharged 14 d after admission. One month later, we removed the metallic stents and inserted two 7-Fr plastic stents *via* the EUS-CDS fistula to keep it patent (Figure 2). When we suggested options for performing rendezvous technique *via* the CDS fistula or surgery to extract the CBD stones, the patient and her family did not choose to undergo these procedures because she did not have any new symptoms. Therefore, we decided to exchange stents semiannually. During 8 mo

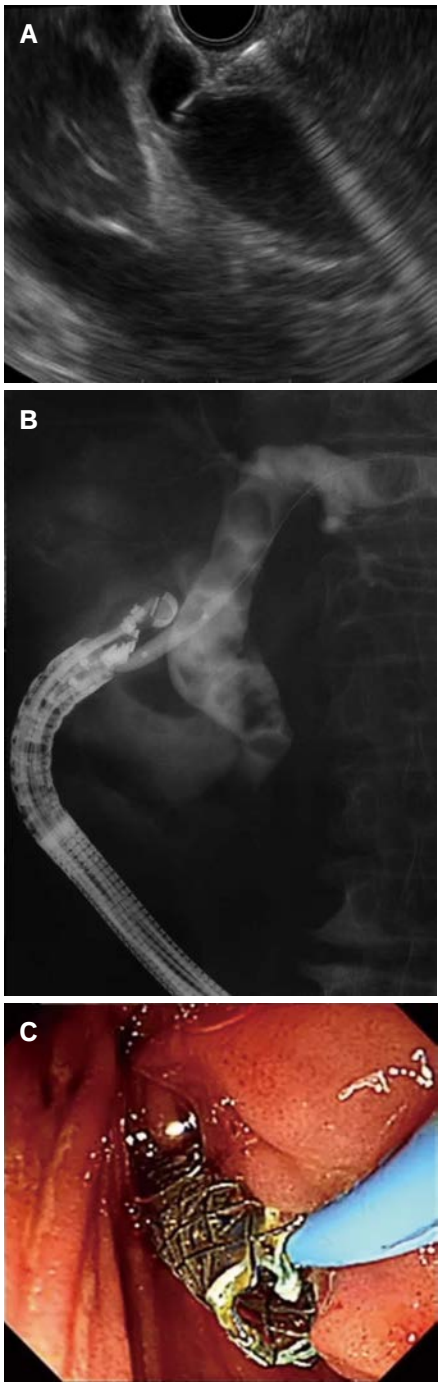

Figure 1 Images of patient 1 who underwent urgent endoscopic ultrasound-guided choledochoduodenostomy. A: EUS-guided common bile duct (CBD) puncture; B: EUS-guided cholangiography showed large piled-up CBD stones. Fistula track was dilated using a 4-mm balloon catheter; C: A covered metallic stent and an endoscopic nasobiliary drainage catheter were successfully placed *via* the duodenum bulb. EUS: Endoscopic ultrasound.

of follow-up, the patient was free of any symptoms and we exchanged the stents endoscopically 6 mo after the initial procedure.

Patient 2

An 85-year-old woman with septic shock due to CBD stones was referred to our hospital. Urgent

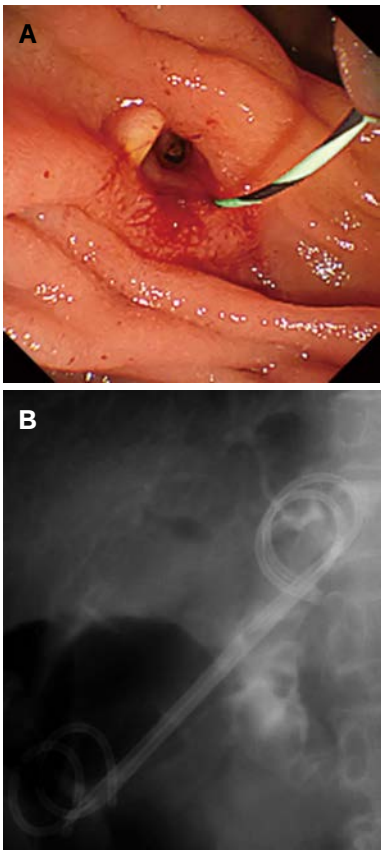

Figure 2 Images of biliary cannulation and plastic stent placement *via* an endoscopic ultrasound-guided choledochoduodenostomy fistula. A: A matured fistula was created where the removed metallic stent was placed. The common bile duct (CBD) was cannulated *via* the EUS-CDS fistula using an ERCP catheter and a guidewire was inserted; B: Two 7-Fr double pigtail plastic stents were placed into the CBD *via* the EUS-CDS fistula. EUS-CDS: Endoscopic ultrasound-guided choledochoduodenostomy; ERCP: Endoscopic retrograde cholangiopancreatography.

ERCP had been attempted at a neighboring general hospital. Biliary cannulation had failed because of the presence of juxtapapillary diverticulum. The patient's vital signs were as follows: GCS conscious level of E2V2M3, blood pressure of 193/92 mmHg, heart rate of 120 beats/min, and body temperature of 39.8 ℃. Laboratory tests showed an elevated inflammatory reaction (WBC, 93600/μL; serum CRP, 11.6 mg/dL; and serum PCT, 30.1 ng/mL). Elevated levels of serum liver function parameters and bilirubin were also remarkable (AST, 567 IU/L; ALT, 372 IU/L; ALP, 1312 IU/L; and total bilirubin, 5.0 mg/dL). CT revealed large multiple CBD stones, and the CBD was dilated approximately 18 mm. Because urgent biliary drainage was required to treat septic shock, we performed EUS-CDS. The intrahepatic bile ducts were slightly dilated on EUS; therefore, the dilated CBD was punctured from the duodenum bulb using a 19-gauge needle. A 0.025-inch guidewire was placed into the CBD. Then, the fistula was dilated using a 7-Fr dilation catheter, and a covered metallic stent (8-mm-wide and 60-mm-long; WallFlex) was placed. The duration

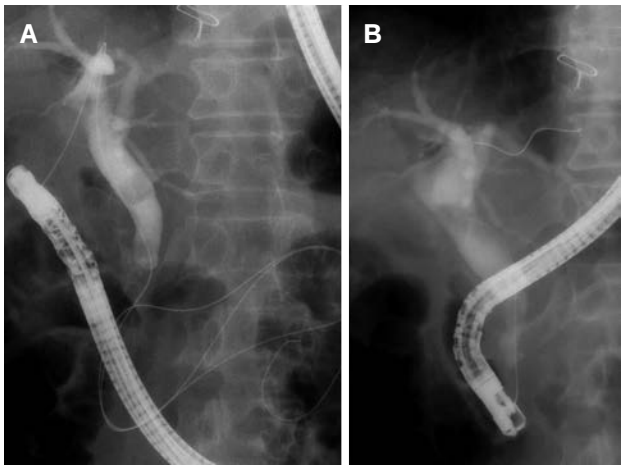

Figure 3 Images of a rendezvous technique *via* the endoscopic **ultrasound-guided choledochoduodenostomy fistula.** A: The common bile duct was cannulated *via* the EUS-CDS fistula and a guidewire was advanced into the duodenum through the papilla; B: The guidewire was caught in the duodenum and transpapillary biliary cannulation was succeeded.

for the procedure was 18 min. The patient recovered completely in a few days and was discharged 12 d after admission. One month later, we removed the metallic stents and inserted two 7-Fr plastic stents *via* the EUS-CDS fistula. We suggested options for performing rendezvous technique or surgery in the same manner as described in case 1, she did not wish for these invasive procedures. Therefore, we decided to exchange stents semiannually. During 4 mo of follow-up, the patient was free of any symptoms.

Patient 3

An 80-year-old man with severe cholangitis due to CBD stones was referred to our hospital. His vital signs were as follows: GCS conscious level of E3V4M5, blood pressure of 170/77 mmHg, heart rate of 102 beats/min, and body temperature of 38.6 ℃. Laboratory tests showed an elevated inflammatory reaction (WBC, 13200/μL and serum CRP, 6.7 mg/dL). Elevated liver function parameters and bilirubin level were also noted (AST, 306 IU/L; ALT, 324 IU/L; ALP, 1510 IU/L; and total bilirubin, 1.8 mg/dL). His platelet count decreased to 96000/μL. He also had disseminated intravascular coagulation (DIC) (defined as an acute DIC score ⩾ 4) complicated by acute cholangitis induced-sepsis. CT revealed two CBD stones with a diameter of 12 mm. Recombinant human soluble thrombomodulin was administered to treat DIC. Then, urgent ERCP was attempted. Deep biliary cannulation failed even after using a double-guidewire technique. To treat the sepsis, we performed EUS-CDS in the same session. The dilated CBD was punctured from the duodenum bulb using a 19-gauge needle. A 0.025-inch guide wire was placed into the CBD. Then, the fistula was dilated using a 7-Fr dilation catheter, and a 7-Fr straight plastic stent (70-mm-long; Flexima, Boston Scientific) was placed. The duration for ERCP and EUS-CDS procedures was 43 min and 18 min, respectively. The patient recovered fully in a few days. One month later, we removed the plastic stent, and because the guidewire was successfully advanced through the papilla, we performed a rendezvous technique *via* the EUS-CDS fistula (Figure 3). After achieving transpapillary biliary cannulation, endoscopic sphincterotomy was performed, and two stones were removed using a retrieval balloon. Follow-up MRCP obtained 6 mo later showed no recurrence of bile duct stones.

DISCUSSION

Acute cholangitis is a systemic infectious disease characterized by acute inflammation and biliary tract infection. AOSC is a severe form of cholangitis in which pus collects in the biliary tract. According to the newly published Updated Tokyo Guidelines for management of acute cholangitis and cholecystitis (TG13), biliary tract drainage should be performed as soon as possible in patients with AOSC[5]; otherwise, translocation of bacteria into the bloodstream causes sepsis, which is a fatal complication of acute cholangitis that induces severe organ damage and high mortality. Endoscopic retrograde biliary stenting is the current gold standard treatment for acute cholangitis due to biliary lithiasis; however, it may be impossible in patients with selective cannulation failure of the major papilla. In this situation, PTBD is an alternative method, but is sometimes difficult when the intrahepatic bile ducts are not dilated.

Since being first reported in 2001 by Giovannini *et al*[1] EUS-BD has been increasingly performed as an alternative in patients with malignant biliary obstruction for failed ERCP[1-4]. Various techniques of EUS-BD have been described, including EUS-CDS, EUS-guided rendezvous (EUS-RV), and EUS-guided antegrade stent placement. Among these, because EUS-RV preserves the anatomical integrity of the biliary tree and avoids permanent fistula creation, it can be a first-line EUS-BD technique in patients with an endoscopically accessible papilla[6]. There still remain technically challenging aspects, including difficulty in negotiating the guidewire across the obstruction and papilla[6]. Furthermore, EUS-RV needs scope exchange and may require a long procedure time[7]. Püspök *et al*[8] indicated that, compared with EUS-RV, EUS-CDS has several advantages. One is that the fistulous tract created by a puncture of the bile duct is immediately sealed within the same session, which minimizes the risk of significant bile leakage. However, the main indication for EUS-CDS was malignant distal biliary obstruction due to pancreato-biliary malignancies. A recent review, which included 36 studies of EUS-CDS, found that EUS-CDS for benign biliary stricture was performed in only two cases[9]. For acute cholangitis due to choledocholithiasis, EUS-CDS was performed

in only one case[10]. Therefore, the indication for benign biliary disease has not been established. In our series, we experienced three cases of successful urgent EUS-CDS for AOSC due to choledocholithiasis, and there were no procedure-related complications in any of the cases. We suggest that patients with AOSC due to biliary lithiasis after failed ERCP could be preferred candidates for EUS-CDS because endoscopic procedure of long duration may lead to causing increase in morbidity and mortality especially in elderly patients with AOSC-induced sepsis.

The drainage of the CBD can be achieved by two different types of stents, metal and plastic. In cases 1 and 2, covered metallic stents were deployed and in case 3, plastic stent was deployed. According to a recent systematic analysis, the post-procedure adverse events were lower in the metallic stents although there were no differences in technical and functional success rates between metallic and plastic stents[11]. In case 3, the patient had increased risk of bleeding due to DIC. Concerning this risk, we avoided to insert a metallic stent for it needs fistula dilation using a balloon catheter. We placed a nasobiliary tube through the metallic stent in case 1 because the previous report recommended the use of a nasobiliary drain for 48 h to decrease the pressure in the punctured bile duct[12]. In case 2, we attempted to place the nasobiliary tube but the guidewire slipped and failed to place it.

In one case, we extracted CBD stones using a RV technique, and in the other two cases, the patients and their families didn't wish for RV technique or surgery due to advanced age, we routinely exchanged the plastic stents to keep the fistula patent. Endoscopic transpapillary biliary stenting remains an effective alternative for patients with stones difficult to manage by conventional endoscopic methods and those who are unfit for surgery or have high surgical risks[13,14]. There is no standardized time period for routine stent replacement of endoscopic transpapillary biliary stenting. Stent patency rates declined rapidly from 94% at 6 mo to 79% at 12 mo and 58% at 24 mo[15]. Therefore we decided to exchange stents semiannually in case 1 and 2.

Recent large studies have identified repeated cannulation attempts with standard approach as a risk factor for post-ERCP pancreatitis (PEP)[16]. It is important to change the procedure early to achieve safe and effective bile cannulation with a shorter procedure time. For prevention of PEP, EUS-CDS is a more advantageous procedure because the pancreas is untouched.

Although endoscopic retrograde biliary stenting has been well-established technique for providing biliary decompression in patients with bile duct obstruction, we believe that EUS-CDS will be a suited salvage to patients whom ERCP cannot be performed. There are still some problems to be solved. One is that bile leak is a concern during EUS-guided biliary interventions and previous studies have demonstrated that biliary leakage into the peritoneal space is the most common complications of EUS-BD[3,4,17]. Therefore, the development of new comfortable stenting device that facilitates simultaneous puncture/dilation is needed. If it becomes available, EUD-CDS will become easier and safer in the future.

The limitations of this study were the small number of patients, lack of a control group, and the inclusion of only a single operator at a single tertiary-care referral center.

In conclusion, with regards to a failed standard ERCP, EUS-CDS can be an effective life-saving biliary decompression procedure that can shorten the procedure time and prevent PEP, particularly in patients with AOSC-induced sepsis. Further long-term studies with a larger cohort are needed to prove the efficacy and safety of this technique.

COMMENTS

Case characteristics

Three elderly patients (1 male, 2 female) presented with sepsis from acute cholangitis.

Clinical diagnosis

Acute obstructive suppurative cholangitis (AOSC) with sepsis due to biliary lithiasis.

Differential diagnosis

Tumors (pancreatic cancer, cholangiocarcinoma, ampullary cancer or metastasis) or benign bile duct stricture/stenosis.

Laboratory diagnosis

The laboratory findings showed an elevated inflammatory reaction and elevated levels of serum liver function parameters and bilirubin.

Imaging diagnosis

Computed tomography revealed common bile duct (CBD) stones and dilatation of CBD.

Pathological diagnosis

Pathological examination was not performed in any of the patients.

Treatment

Urgent endoscopic ultrasound-guided choledochoduodenostomy (EUS-CDS) *via* the duodenum bulb.

Related reports

EUS-CDS is commonly performed in patients with malignant distal biliary obstruction due to pancreato-biliary malignancies. In contrast, there are few reports performing this technique for benign biliary lesions.

Term explanation

EUS-CDS is a novel alternative technique for biliary drainage in patients for whom endoscopic retrograde cholangiopancreatography (ERCP) has failed and who prefer internal rather than percutaneous biliary drainage or surgical bypass procedures.

Experiences and lessons

Urgent EUS-CDS for AOSC-induced sepsis due to biliary lithiasis can be an effective life-saving endoscopic biliary decompression procedure that can

shorten the procedure time and prevent post-ERCP pancreatitis.

Peer-review

This case report is well written and the topic is interesting. This report describes the successful use of EUS-CDS in three patients with AOSC-induced sepsis due to biliary lithiasis.

REFERENCES

1 **Giovannini M**, Moutardier V, Pesenti C, Bories E, Lelong B, Delpero JR. Endoscopic ultrasound-guided bilioduodenal anastomosis: a new technique for biliary drainage. *Endoscopy* 2001; **33**: 898-900 [PMID: 11571690 DOI: 10.1055/s-2001-17324]

2 **Artifon EL**, Aparicio D, Paione JB, Lo SK, Bordini A, Rabello C, Otoch JP, Gupta K. Biliary drainage in patients with unresectable, malignant obstruction where ERCP fails: endoscopic ultrasonography-guided choledochoduodenostomy versus percutaneous drainage. *J Clin Gastroenterol* 2012; **46**: 768-774 [PMID: 22810111 DOI: 10.1097/MCG.0b013e31825f264c]

3 **Kahaleh M**, Hernandez AJ, Tokar J, Adams RB, Shami VM, Yeaton P. Interventional EUS-guided cholangiography: evaluation of a technique in evolution. *Gastrointest Endosc* 2006; **64**: 52-59 [PMID: 16813803]

4 **Park do H**, Jang JW, Lee SS, Seo DW, Lee SK, Kim MH. EUS-guided biliary drainage with transluminal stenting after failed ERCP: predictors of adverse events and long-term results. *Gastrointest Endosc* 2011; **74**: 1276-1284 [PMID: 21963067 DOI: 10.1016/j.gie.2011.07.054]

5 **Miura F**, Takada T, Strasberg SM, Solomkin JS, Pitt HA, Gouma DJ, Garden OJ, Büchler MW, Yoshida M, Mayumi T, Okamoto K, Gomi H, Kusachi S, Kiriyama S, Yokoe M, Kimura Y, Higuchi R, Yamashita Y, Windsor JA, Tsuyuguchi T, Gabata T, Itoi T, Hata J, Liau KH. TG13 flowchart for the management of acute cholangitis and cholecystitis. *J Hepatobiliary Pancreat Sci* 2013; **20**: 47-54 [PMID: 23307003 DOI: 10.1007/s00534-012-0563-1]

6 **Iwashita T**, Yasuda I, Mukai T, Iwata K, Ando N, Doi S, Nakashima M, Uemura S, Mabuchi M, Shimizu M. EUS-guided rendezvous for difficult biliary cannulation using a standardized algorithm: a multicenter prospective pilot study (with videos). *Gastrointest Endosc* 2016; **83**: 394-400 [PMID: 26089103 DOI: 10.1016/j.gie.2015.04.043]

7 **Kim YS**, Gupta K, Mallery S, Li R, Kinney T, Freeman ML. Endoscopic ultrasound rendezvous for bile duct access using a transduodenal approach: cumulative experience at a single center. A case series. *Endoscopy* 2010; **42**: 496-502 [PMID: 20419625 DOI: 10.1055/s-0029-1244082]

8 **Püspök A**, Lomoschitz F, Dejaco C, Hejna M, Sautner T, Gangl A. Endoscopic ultrasound guided therapy of benign and malignant biliary obstruction: a case series. *Am J Gastroenterol* 2005; **100**: 1743-1747 [PMID: 16086710]

9 **Ogura T**, Higuchi K. Technical tips of endoscopic ultrasound-guided choledochoduodenostomy. *World J Gastroenterol* 2015; **21**: 820-828 [PMID: 25624715 DOI: 10.3748/wjg.v21.i3.820]

10 **Horaguchi J**, Fujita N, Noda Y, Kobayashi G, Ito K, Obana T, Takasawa O, Koshita S, Kanno Y. Endosonography-guided biliary drainage in cases with difficult transpapillary endoscopic biliary drainage. *Dig Endosc* 2009; **21**: 239-244 [PMID: 19961522 DOI: 10.1111/j.1443-1661.2009.00899.x]

11 **Wang K**, Zhu J, Xing L, Wang Y, Jin Z, Li Z. Assessment of efficacy and safety of EUS-guided biliary drainage: a systematic review. *Gastrointest Endosc* 2015; Epub ahead of print [PMID: 26542374 DOI: 10.1016/j.gie.2015.10.033]

12 **Giovannini M**, Pesenti Ch, Bories E, Caillol F. Interventional EUS: difficult pancreaticobiliary access. *Endoscopy* 2006; **38** Suppl 1: S93-S95 [PMID: 16802236]

13 **Jain SK**, Stein R, Bhuva M, Goldberg MJ. Pigtail stents: an alternative in the treatment of difficult bile duct stones. *Gastrointest Endosc* 2000; **52**: 490-493 [PMID: 11023565]

14 **Yang J**, Peng JY, Chen W. Endoscopic biliary stenting for irretrievable common bile duct stones: Indications, advantages, disadvantages, and follow-up results. *Surgeon* 2012; **10**: 211-217 [PMID: 22647840 DOI: 10.1016/j.surge.2012.04.003]

15 **Li KW**, Zhang XW, Ding J, Chen T, Wang J, Shi WJ. A prospective study of the efficacy of endoscopic biliary stenting on common bile duct stones. *J Dig Dis* 2009; **10**: 328-331 [PMID: 19906114 DOI: 10.1111/j.1751-2980.2009.00404.x]

16 **Cheng CL**, Sherman S, Watkins JL, Barnett J, Freeman M, Geenen J, Ryan M, Parker H, Frakes JT, Fogel EL, Silverman WB, Dua KS, Aliperti G, Yakshe P, Uzer M, Jones W, Goff J, Lazzell-Pannell L, Rashdan A, Temkit M, Lehman GA. Risk factors for post-ERCP pancreatitis: a prospective multicenter study. *Am J Gastroenterol* 2006; **101**: 139-147 [PMID: 16405547]

17 **Poincloux L**, Rouquette O, Buc E, Privat J, Pezet D, Dapoigny M, Bommelaer G, Abergel A. Endoscopic ultrasound-guided biliary drainage after failed ERCP: cumulative experience of 101 procedures at a single center. *Endoscopy* 2015; **47**: 794-801 [PMID: 25961443 DOI: 10.1055/s-0034-1391988]

P- Reviewer: Amornyotin S, Giannopoulos GA, Kayaalp C, Muguruma N, Skok P, Yan SL **S- Editor**: Qi Y **L- Editor**: A **E- Editor**: Ma S

Published by **Baishideng Publishing Group Inc**
8226 Regency Drive, Pleasanton, CA 94588, USA
Telephone: +1-925-223-8242
Fax: +1-925-223-8243
E-mail: bpgoffice@wjgnet.com
Help Desk: http://www.wjgnet.com/esps/helpdesk.aspx
http://www.wjgnet.com

ISSN 1007-9327

Research Article

JOURNAL OF HEPATOLOGY

Randomized phase II placebo controlled study of codrituzumab in previously treated patients with advanced hepatocellular carcinoma

Ghassan K. Abou-Alfa[1,2,*], Oscar Puig[3], Bruno Daniele[4], Masatoshi Kudo[5], Philippe Merle[6], Joong-Won Park[7], Paul Ross[8], Jean-Marie Peron[9], Oliver Ebert[10], Stephen Chan[11], Tung Ping Poon[12], Massimo Colombo[13], Takuji Okusaka[14], Baek-Yeol Ryoo[15], Beatriz Minguez[16], Takayoshi Tanaka[17], Toshihiko Ohtomo[17], Stacey Ukrainskyj[3], Frederic Boisserie[3], Olga Rutman[3], Ya-Chi Chen[3], Chao Xu[3], Eliezer Shochat[18], Lori Jukofsky[3], Bernhard Reis[18], Gong Chen[3], Laura Di Laurenzio[3], Ray Lee[3], Chia-Jui Yen[19]

[1]*Memorial Sloan Kettering Cancer Center, New York, NY, USA;* [2]*Weill Cornell Medical College, New York, NY, USA;* [3]*Roche Innovation Center New York, Hoffmann-La Roche Inc., USA;* [4]*G. Rummo Hospital, Benevento, Italy;* [5]*Kinki University Hospital, Japan;* [6]*Hopital de la Croix-Rousse, Hepatologie et Gastroenterologie, Lyon, France;* [7]*National Cancer Center, Republic of Korea;* [8]*King's College Hospital, United Kingdom;* [9]*Hopital Purpan, Gastro Enterologie Hepatologie, France;* [10]*II. Medizinische Klinik und Poliklinik, Klinikum rechts der Isar, Technische Universität München, Germany;* [11]*Prince of Wales Hospital, Hong Kong;* [12]*Queen Mary Hospital, Hong Kong;* [13]*Fondazione IRCCS Ospedale Maggiore Policlinico, Italy;* [14]*National Cancer Center Hospital, Japan;* [15]*Asan Medical Center, Republic of Korea;* [16]*Liver Unit, Hospital Universitario Vall dHebron, Barcelona, Spain;* [17]*Chugai Pharmaceutical Co. Ltd., Japan;* [18]*Roche Innovation Center Basel, Hoffmann-La Roche, Switzerland;* [19]*National Cheng-Kung Univ. Hospital, Taiwan*

Background & Aims: Codrituzumab, a humanized monoclonal antibody against Glypican-3 (GPC3) that is expressed in hepatocellular carcinoma (HCC), interacts with CD16/FcγRIIIa and triggers antibody-dependent cytotoxicity. Codrituzumab was studied *vs.* placebo in a randomized phase II trial in advanced HCC patients who had failed prior systemic therapy.

Methods: Patients with advanced HCC who had failed prior systemic therapy, ⩾18 years, Eastern cooperative oncology group (ECOG) 0-1, Child-Pugh A were randomized 2:1 to biweekly codrituzumab 1600 mg *vs.* placebo. Patients were stratified based on GPC3 immunohistochemical expression: 2+/3+, 1+, and 0. Primary endpoint was progression free survival. Secondary endpoints include overall survival (OS), tolerability, pharmacokinetics, and an exploratory endpoint in biomarkers analysis.

Results: 185 patients were enrolled: 125 received codrituzumab and 60 placebo: Median age 64/63, 85/75% male, 46/42% Asian, ECOG 0 65/63%, 74/77% having vascular invasion and/or extrahepatic metastasis. 84%/70% had prior sorafenib. Drug exposure was 98.4% of planned dose, with an identical adverse events profile between the 2 groups. The median progression free survival and overall survival in the codrituzumab *vs.* placebo groups in months were: 2.6 *vs.* 1.5 (hazard ratios 0.97, $p = 0.87$), and 8.7 *vs.* 10 (hazard ratios 0.96, $p = 0.82$). Projected C_{trough} at cycle 3 day 1 based exposure, high CD16/FcγRIIIa on peripheral immune cells, and GPC3 expression in the tumor, were all associated with prolonged progression free survival and overall survival.

Conclusions: Codrituzumab did not show clinical benefit in this previously treated HCC population. Whether higher codrituzumab drug exposure or the use of CD16 and GPC3 as potential biomarkers would improve outcome remain unanswered questions.

Lay summary: Codrituzumab is a manufactured antibody against a liver cancer protein called glypican-3. In this clinical trial, codrituzumab was not found be effective against liver cancer. It was suggested though that a higher dose of codrituzumab or selecting patients with high level of glypican-3 or its mediator CD16 might improve outcome.

Clinical trial registration: This trial is registered at Clinicaltrials.gov (NCT01507168).

Keywords: Hepatocellular carcinoma; Codrituzumab; Glypican-3; CD16.
Received 27 September 2015; received in revised form 30 March 2016; accepted 5 April 2016; available online 13 April 2016

* Corresponding author. Address: Memorial Sloan Kettering Cancer Center, 300 East 66th Street, New York, NY, USA. Tel.: +1 646 888 4184; fax: +1 646 888 4255.
E-mail address: abou-alg@mskcc.org (G.K. Abou-Alfa).

Introduction

Glypican-3 (GPC3) is a member of the glypican family, a group of heparan sulfate proteoglycans linked to the cell surface and which plays an important role in cell growth, differentiation, and migration [1,2]. GPC3 is highly expressed in HCC and has become a useful diagnostic marker for HCC by immunohistochemical (IHC) studies since the adjacent non-tumoral tissue does not express GPC3 [3–8]. GPC3 may promote HCC growth by stimulating the canonical Wnt pathway, and/or interacting

with the IGFII-IGF1R pathway, or it may play a role in fibroblast growth factor (FGF) signaling [9–12]. Therefore, GPC3 may represent a specific tumor marker and a potential target for therapy in HCC [13].

Codrituzumab is a recombinant, humanized monoclonal antibody that binds to human GPC3 with high affinity [14–18]. Codrituzumab interacts with CD16/FcγRIIIa and triggers antibody-dependent cytotoxicity (ADCC) [15]. Non-clinical characterization of codrituzumab demonstrates that it elicits ADCC against GPC3-positive human hepatoma cells lines (SK-03: SK-HEP-1 HCC line engineered to overexpress GPC3; HepG2: hepatoblastoma), using human peripheral blood mononuclear cells (PBMCs) as effector cells [18]. Phase I studies in US [19] and Japan [20] showed that codrituzumab was well tolerated up to 20 mg/kg/wk without dose limiting toxicity.

In this phase II study, codrituzumab was compared with placebo in a randomized way in advanced HCC patients who had failed at least one prior systemic therapy.

Patients and methods

Study population

Patients with histologically confirmed unresectable advanced or metastatic HCC following Barcelona clinic liver cancer (BCLC) classification, who received at least one prior systemic therapy, were eligible. Subjects had to be ⩾18 years of age, with an ECOG score [21] of 0–1, a Child-Pugh score of A, measurable disease as defined by RECIST version 1.1 [22], and adequate organ function defined by platelet count ⩾50×10^9/L, absolute neutrophil count ⩾1,500/μL, hemoglobin ⩾8.0 g/dl, alanine transaminase (ALT or SGPT) and aspartate transaminase (AST or SGOT) ⩽5 × upper limit of normal, total bilirubin ⩽2 mg/dl and creatinine ⩽2 × ULN or calculated Creatinine Clearance ⩾60 ml/min using Cockcroft and Gault formula [23]. Patients with prior organ transplantation or known positive HIV infection were excluded. The study was approved by institutional review boards of participating centers and was conducted in accordance with the Declaration of Helsinki and Good Clinical Practice guidelines.

Study design, dose administration, randomization, and cohort assignment

Patients were randomized in a 2:1 ratio to codrituzumab 1,600 mg intravenously every two weeks after two weekly loading doses *vs.* placebo. Prior to randomization, patients were assigned into 3 cohorts based on the immunohistochemistry (IHC) analysis of GPC3 expression: cohort A (GPC3 IHC 2+/3+), B (GPC3 IHC 1+) and C (GPC3 IHC 0) (Supplementary Fig. 1). Patients were stratified based on the following factors: GPC3 expression status by IHC, region, ECOG performance status (0 *vs.* 1), and presence or absence of macroscopic vascular invasion or extra-hepatic spread. A two-stage adaptive design was used with intention to collect more information in patients who have high GPC3 expression levels and therefore, likely to benefit from codrituzumab treatment.

Efficacy and safety analysis

The primary efficacy endpoint was progression free survival (PFS) based on investigator assessment. Secondary endpoints included overall survival (OS), time to progression, tolerability and safety of codrituzumab *vs.* placebo. Tumor assessment was done by computed tomography at weeks 6, 12 and 18, and every 8 weeks afterwards until progression. Response evaluation was based on investigator assessment using the criteria of RECIST version 1.1 [22]. Human anti-human immunoglobulin test (HAHA) was evaluated in pretreatment, cycles 1, 6, 10, final visit and 28-day off-study visit. The NCI-CTCAE version 4.0 was used to evaluate adverse events.

Pharmacokinetics and exposure-response analysis

Pharmacokinetic (PK) samples were collected from all patients participating in the study. An extensive PK sampling schedule was performed for 40 patients in cycle 1 days 1, 2, 5, 8, 9 and 12 and cycle 6 (days 1, 2, 5 and 11), as well as at the predose in cycles 2, 3, 7, 9, 10, and 11. A sparse PK sampling was performed in cycle 1 (days 1, 3 and 8) and cycle 6 (day 1) as well as at the predose in cycles 9, 10 and 11 for the remaining patients. Additional samples were obtained at the final visit, the 28-day follow-up visit, and at the time of progression of disease for all patients. A population pharmacokinetic (popPK) model was developed using the PK data from 120 patients with evaluable PK data. Individual predose concentrations at Cycle 3 day 1 (C3D1) that correspond to Day 29 were simulated using the popPK model. The target saturation was derived from Michaelis-Menten constant (K_m) within the model [24].

In a post hoc analysis, the codrituzumab arm was divided into low and high exposure subgroups by the trough level on C3D1 and the exposure-efficacy relationship on PFS was explored. To reduce the bias introduced by potentially unbalanced confounding risk factors among the different groups (high exposure, low exposure and placebo), a nearest available Mahalanobis metric matching within calipers defined by the propensity score method was used to create balanced groups of high exposure and placebo and low exposure and placebo separately [25]. These matched groups were then compared for the treatment effects. Hazard ratios (HR) for PFS were calculated for the propensity score matched high *vs.* placebo, and low exposure group *vs.* placebo, respectively.

Biomarkers

GPC-3 IHC was performed in fresh tissue or in tissue prepared within 3 months from formalin-fixed paraffin-embedded blocks of the primary or the metastatic tumor. The percentage of tumor cells stained and the pattern of membrane and/or cytoplasmic positivity were used to infer a clinical score (range 0–3+) assigned according to the criteria described in Supplementary Table 1. CD16MESF (Molecules of Equivalent Soluble Fluorochrome), which represents the level of expression of CD16 in natural killer (NK) cells in the PBMCs, was determined by flow cytometry. Additional biomarker methodological details are presented in the Supplementary material.

Statistical design

All patients enrolled were included in the intent-to-treat population (ITT), and all patients who received at least one dose of codrituzumab were included in the safety population. A data review committee including both internal Roche and external members with expertise in oncology and statistics, not involved in the study, was established to help evaluate the outcome of the first stage of the study and to monitor safety.

The primary analysis of PFS was planned to take place after approximately 112 PFS events in GPC3 IHC 1+/2+/3+ and approximately 79 PFS events in GPC3 IHC 2+/3+ populations have been observed. In case of early termination of tumor GPC3 IHC 1+ at futility analysis, approximately 90 PFS events in tumor GPC3 IHC 2+/3+ would have been required at the final analysis. The analysis was expected approximately 24 months after the first patient was randomized. The clinical study report will be based on this final analysis of PFS.

For biomarker analysis, we used a cutoff value at median or any other percentile to define "biomarker high" *vs.* "biomarker low". We calculated HR, 95% confidence intervals (CI) and corresponding two-sided *p* values for treatment effect for both "biomarker high" and "biomarker low" groups separately, based on Cox proportional hazard regression models, with OS as response variable, and adjusting clinical baseline covariates. Since multiple biomarkers were tested at the same time, False Discovery Rate (FDR) was computed to adjust statistical significance via the Benjamini and Hochberg method [26]. For a given biomarker, we defined significance when FDR <0.05. Kaplan-Meier curves were employed to visualize marginal treatment effect. Different cutoffs (33rd, 50th, and 67th percentiles) of CD16 MESF were explored by calculating HR, CI and *p* values based on 5-fold cross-validation and determined if they remained significant.

Results

Study population

Between February 2012 to March 2013, 259 patients with HCC diagnosis were screened for the study and 185 patients were enrolled in three cohorts: 105 in Cohort A (GPC3 IHC 2+/3+), 56 in Cohort B, (GPC3 IHC 1+), and 24 in Cohort C (GPC3 IHC 0). The main reasons for screening failure include lack of tumor tissue, out of range of Child-Pugh scores and laboratory parameters,

Table 1. Demographics of enrolled patients.

RO5137382 Phase II demographics (ITT population)			
		Codrituzumab (n = 125)	Placebo (n = 60)
Age in years median, (range)		64 (31-81)	62.5 (36-79)
Gender	Male/Female	106/19 (85%/15%)	45/15 (75%/25%)
Race	White	46%	55%
	Asian	46%	42%
	Other	8%	3%
ECOG	0/1	81/44 (65%/35%)	38/22 (63%/37%)
Vascular invasion/ extrahepatic metastasis	Yes/No	93/32 (74%/26%)	46/14 (77%/23%)
Prior surgery	Yes	47 (28%)	26 (29%)
Prior local therapy	Yes	92 (74%)	50 (83%)
Prior sorafenib	Yes/No	105/20 (84%/16%)	42/18 (70%/30%)
Etiology	Hepatitis B	48 (38%)	25 (42%)
	Hepatitis C	34 (27%)	18 (30%)
	Non-alcohol liver damage	14 (11%)	5 (8%)
Child Pugh Score	A5	82 (66%)	43 (72%)
	A6	42 (34%)	17 (28%)

misdiagnosis of HCC, no prior systemic therapy, and others. 125 patients received codrituzumab and 60 received placebo. Demographics are shown in Table 1 and show no major imbalances between the two arms. Approximately 84% and 70% of patients in codrituzumab and placebo arms, respectively, received sorafenib previously. Close to 75% of patients in both arms had vascular invasion and/or extra-hepatic spread.

Patient outcome and safety analysis

The final analysis was triggered after the 128th PFS event on May 6, 2013 and efficacy analyses other than OS are based on a data cutoff date of 13 June 2013 when 150 PFS events had accumulated. By that time, 125 patients were randomized to the codrituzumab arm, and 60 to placebo arm. In the codrituzumab arm, 124 (99.2%) patients discontinued treatment: 4 (3.2%) due to adverse events, 3 (2.4%) due to death, 107 (85.6%) due to progression of disease, and 5 (4.0%) due to withdrawal of consent. In the placebo arm, 60 (100%) discontinued treatment: 3 ((5.0%) due to adverse events, 2 (3.3%) due to death, and 47 (78.3%) due to progression of disease (Fig. 1). The mean dose intensity relative to the scheduled doses was 98.4% on the codrituzumab and 98.8% on the placebo arm. Adverse events were reported in 114 patients who received codrituzumab (94.2%) and 59 patients who received placebo (98.3%) as detailed in Table 2. The major difference between the two groups was the incidence of infusion-related reaction of pyrexia with a 44.6% incidence in the codrituzumab *vs.* 15% in the placebo group. Serious adverse events were reported in 31 patients (25.6%) of the codrituzumab receiving group and 19 patients who received placebo (31.7%). The most common grade

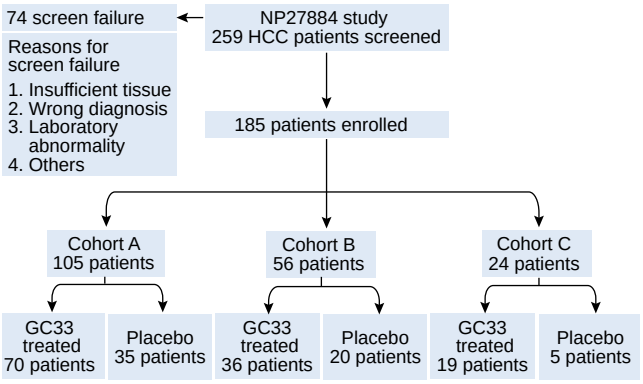

Fig. 1. Consort flow diagram.

Table 2. Common adverse grade 3 or higher event profile with incidence at 10% or higher.

	Codrituzumab	Number of events (%)	Placebo	Number of events (%)
Pyrexia	54 (45%)	1 (0.8%)	9 (15%)	1 (1.7%)
Fatigue	36 (30%)	2 (1.7%)	12 (20%)	-
Nausea	21 (17%)	-	5 (8.3%)	-
Headache	20 (17%)	-	2 (3.3%)	-
Decreased appetite	19 (16%)	-	9 (15%)	2 (3.3%)
Diarrhea	18 (15%)	1 (0.8%)	10 (17%)	-
Abdominal pain	18 (15%)	3 (2.5%)	11 (18%)	2 (3.3%)
Constipation	17 (14%)	-	9 (15%)	1 (1.7%)
Peripheral edema	16 (13%)	1 (0.8%)	8 (13%)	1 (1.7%)
Vomiting	15 (12%)	-	1 (1.7%)	-
Pruritus	14 (12%)	-	6 (10%)	-
Asthenia	13 (11%)	1 (0.8%)	12 (20%)	3 (5.0%)
Cough	15 (12%)	-	5 (8.3%)	1 (1.7%)
Back pain	10 (8.3%)	-	9 (15%)	2 (3.3%)
Ascites	8 (7%)	1 (0.8%)	7 (12%)	4 (6.7%)

3 or higher adverse events were anemia (3.3% for placebo and 4.1% for codrituzumab arm), AST increase (3.3% for the codrituzumab arm and 0% for the placebo arm). Most of the adverse events are very comparable in the codrituzumab arm compared to the placebo arm.

Efficacy

At the time of the recorded 150 PFS events, the median PFS was 2.6 months in the codrituzumab arm and 1.5 months in the placebo arm for all randomized patients (HR, 0.97; 95% CI, 0.67–1.39; $p = 0.87$). OS results are based on a data cutoff date of 11 April 2014.

The median time for OS was 8.7 months for the codrituzumab arm, and 10 months for the placebo arm (HR 0.96; 95% CI, 0.65–1.41; $p = 0.82$). There was one partial response by RECIST 1.1 in the codrituzumab arm. The Kaplan-Meier curves of the PFS and OS are shown in Fig. 2. Similar results were obtained in subgroup analyses for subjects with GPC3 positive tumors (GPC3 1+/2+/3+)

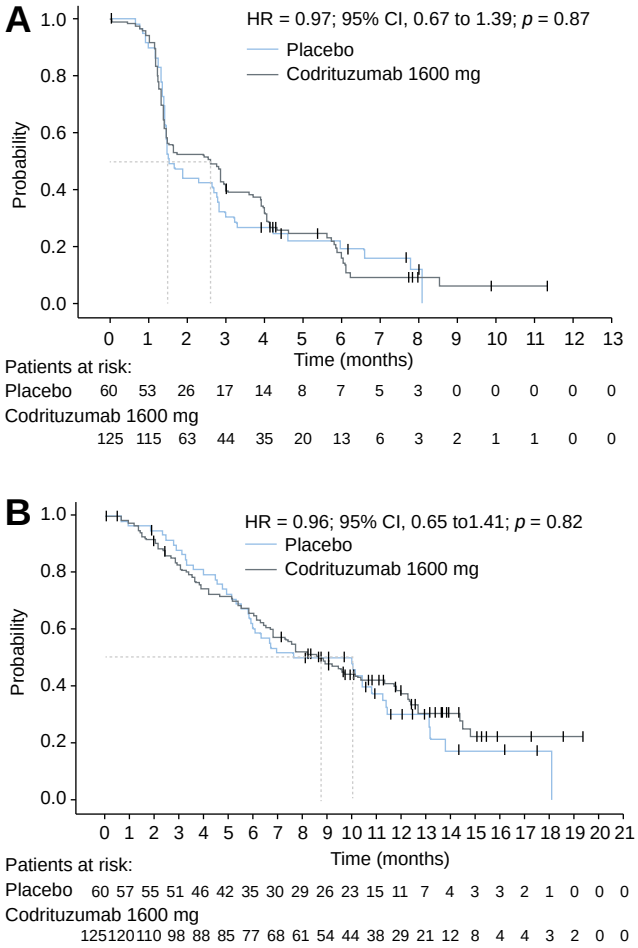

Fig. 2. Kaplan-Meier curves. (A) Kaplan-Meier curve of PFS (150 events) for all randomized patients. (B) Kaplan-Meier curve of OS (118 death events).

and for subjects with high expression of GPC3 (GPC3 2+/3+) (data not shown).

Pharmacokinetic analysis

The pharmacokinetic model developed using data from this study indicates target-mediated drug disposition (TMDD), a non-linear elimination of codrituzumab [24]. The median C3D1 exposure was around 230 μg/ml, which is projected to achieve a target saturation of ~85% based on the popPK TMDD model [24]. The median PFS in each of the four quartiles of C3D1 concentrations were shown in Fig. 3. An exposure-response relationship was observed with longer PFS corresponding to the higher C3D1 exposure, suggesting that sustained high target saturation (inferred by popPK model) may be needed for a beneficial effect of codrituzumab. However, the difference in PFS could also be due to other confounding risk factors in addition to codrituzumab exposure. Therefore, a propensity score method was used for matching potential risk confounding factors between groups [25]. After matching, the patient characteristics were balanced between the high exposure and placebo groups as well as the low exposure and placebo groups (Supplementary Table 2). A longer PFS was found to correspond to a higher exposure (C3D1 trough concentrations ⩾230 μg/ml). The HR of PFS was 0.55 (95% CI: 0.35–0.88, $p = 0.012$) for high exposure group *vs.* placebo and was 1.02 (95% CI: 0.62–1.69, $p = 0.92$) for low exposure group *vs.* placebo, respectively (Fig. 4).

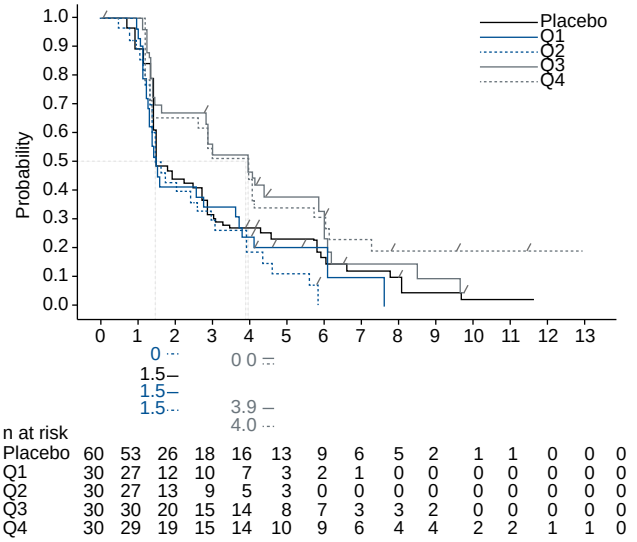

Fig. 3. Kaplan-Meier curves of PFS in the quartiles of drug exposure for codrituzumab and placebo. The table shows the ranges of trough level at Cycle 3 day 1 of the quartiles and their median PFS in months.

GPC3 tumor expression levels are correlated to longer OS

When we focused on GPC3 IHC scores in the high exposure group (C3D1 C_{trough} above median), due to the small number of subjects in each separate IHC subgroup, we pooled together subjects with low GPC3 expression in tumor by IHC (GPC3 IHC 0/1+, "biomarker low") and separated them from subjects with high expression (GPC3 2+/3+, "biomarker high"), which were also pooled together. In this context, there was no difference in PFS between the treatment and placebo in the high GPC3 expression group (HR = 0.59; 95% CI, 0.34–1.05; $P = 0.074$). Subjects with high expression of GPC3 treated with codrituzumab had longer OS than subjects in the placebo group. However, there was no difference in OS between placebo and treatment groups in subjects with low expression of GPC3 (HR = 0.34; 95% CI, 0.17–0.69; $p = 0.003$) (Fig. 5).

Peripheral blood markers of NK cell activity

Several blood peripheral NK cell markers showed statistically significant FDR levels that pass cutoff for multiplicity (FDR <0.05) in the high exposure group (data not shown), but did not predict response in the low exposure group. CD16 MESF assay measures the expression level of CD16 receptor in the surface of NK cells, which binds the Fc portion of IgG1 antibodies to trigger ADCC [27–29]. After covariate adjustment, cross-validated HR in the CD16 MESF "biomarker high" group decreases with the increase of CD16 MESF cutoffs (HR = 0.44 for the 33rd percentile, HR = 0.33 for the 50th percentile, and HR = 0.09 for the 67th percentile), indicating a relationship between the benefit to codrituzumab and CD16 MESF levels. In contrast, there is no such

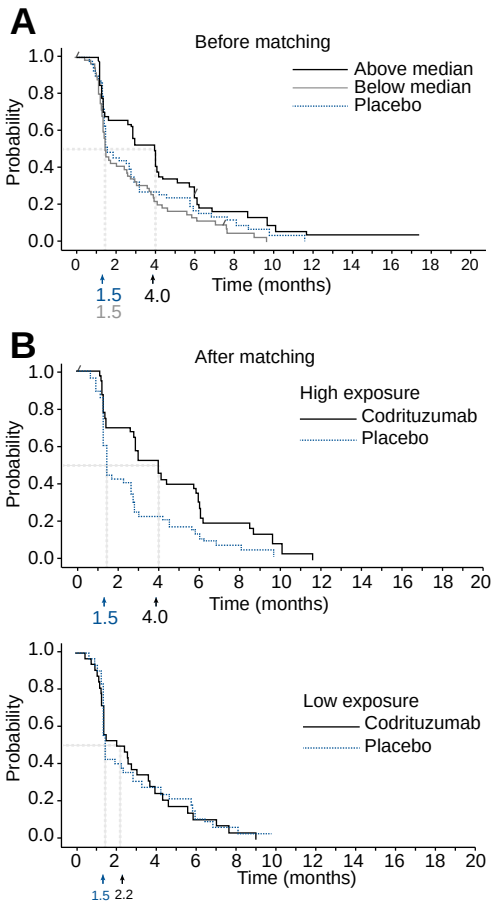

Fig. 4. Kaplan-Meier's curves of PFS in the subgroups of high, low exposure of codrituzumab and placebo after matching by the propensity scores.

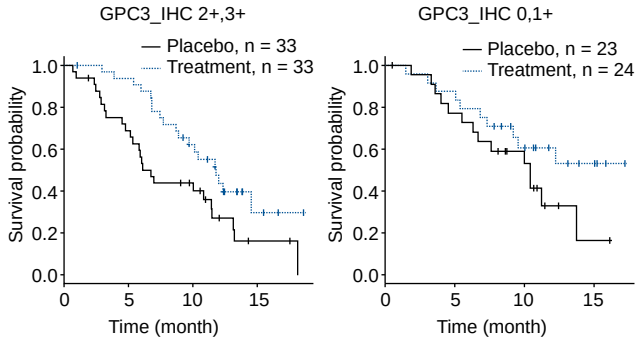

Fig. 5. Kaplan-Meier's curves of OS in the subgroups. High (2+, 3+), low (0, +1) expression levels of GPC3_IHC in subjects with C3D1 C_{trough} above median (the high exposure group) after treatment with codrituzumab or Placebo.

significant treatment effect observed in the CD16 MESF "biomarker low" group (Fig. 6).

Discussion

The study design took into consideration that tumor expression of GPC3 by IHC appeared to correlate with the ADCC activity of codrituzumab in the preclinical models, and assigned patients into 3 cohorts based on their expression of GPC3 by IHC. This study demonstrated no difference in the median durations of PFS and OS of the codrituzumab-treated arm compared to placebo arm in the all-comer population. Codrituzumab was well tolerated.

The retrospective exploratory exposure-response analysis combined with propensity score matching method showed a potential benefit of codrituzumab treatment in high exposure group (C3D1 ⩾230 μg/ml) compared to the placebo group. Such difference was not noted in the low exposure group. From a pharmacokinetic point of view, the current dosing regimen in this study, 1600 mg every two week (Q2W) after 2 weekly doses, was selected to ensure >85% patient population achieving a trough concentration above 50 μg/ml based on antitumor effect in modeling analysis using phase I data. However, this target trough concentration level only corresponds to about 50–60% target saturation, which is inferred by the population PK TMDD model. A dosing regimen to achieve sustained higher target saturation (such as the median trough C3D1 level of 230 μg/ml that corresponds to ~85% target saturation) might have a better chance to yield a therapeutic benefit. This would be consistent with the biological hypothesis that codrituzumab would need to have adequate binding to GPC3 on the tumor cell surface, so that the Fc portion of the antibody will interact with its receptor CD16 on NK cells surface to trigger ADCC.

This however may not necessarily be true, as we continue to lack a full understanding of any correlation between GPC3 expression and codrituzumab potential activity. This is well reflective in the lack of any difference in PFS based on GPC3 expression, albeit a difference in OS between those two groups.

By calculating the propensity scores and matching, we balanced the demographics of the subgroups with high exposure and low exposure *vs.* placebo for further an exploratory biomarker analysis. By splitting the CD16 MESF into 33rd, 50th, and 67th levels, a positive exposure – effect relationship of CD16 MESF was observed. The higher the CD16 expression, the better the response (OS) was observed in codrituzumab therapy. However, it is worth noting that results from the subgroup analyses always need to be interpreted with caution, as the clinical characteristics of each subgroup of patients may not be truly balanced and thus may potentially harbor a selection bias. The hypothetical mechanism of action of codrituzumab is that it first interacts with the GPC3 target on the surface of tumor cells and then subsequently recruits CD16-positive effector cells to exert cell killing seems to align with the observed data. High tumor GPC3 expression and peripheral blood CD16MESF level would therefore be essential for triggering the drug effect. As mentioned above, the result of PK analysis based on the popPK model suggests that codrituzumab may need to achieve high target saturation in tumor cells to induce any beneficial effect. Hence, only those with high exposure, but not those with low exposure, exhibited such a benefit in those biomarker-defined populations.

This argument will however remain within the theoretical realm, considering that most of its aspects are built on retrospective, unplanned, and limited sample size work.

In summary, single agent codrituzumab at the dose used was well tolerated but could not demonstrate benefit in patients with advanced HCC as a second line therapy in an all-comer population. Based on 3 independent analyses, increasing codrituzumab exposure, the high GPC-3 expression, and high CD16 expression in circulating immune cells may help predict the efficacy of codri-

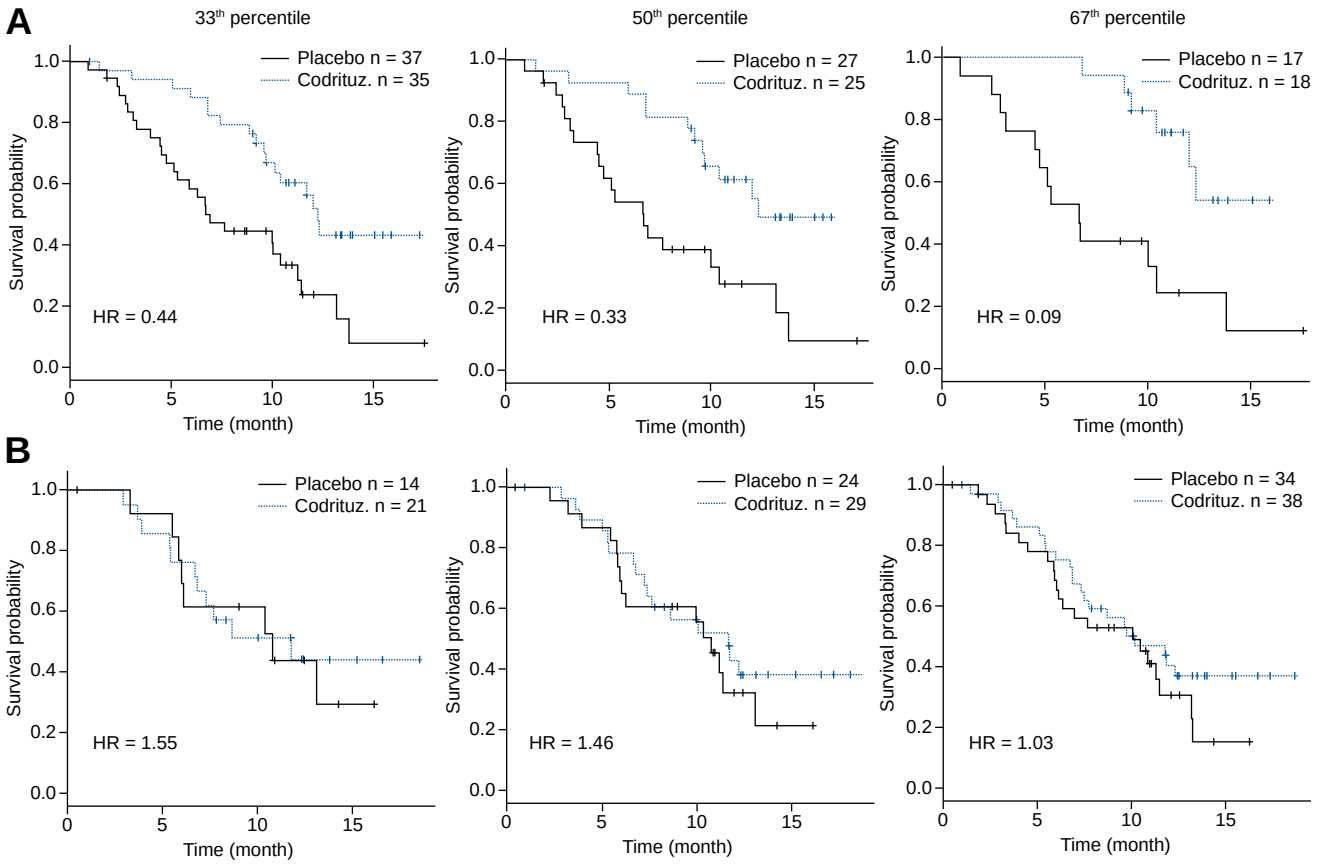

Fig. 6. Increasing cutoff of CD16 MESF levels leads to lower HR and longer surviva. Subjects in high exposure group and CD16 MESF biomarker high levels noted at the 33rd, 50th, and 67th percentiles (A), with no such significant treatment effect observed in the CD16 MESF biomarker low group (B).

tuzumab. Further precise development for codrituzumab in HCC may be worth considering with this perspective in mind.

Financial support

Funding was supported by Chugai Pharmaceutical Co. Ltd. and Hoffmann-La Roche Inc.

Conflict of interest

BD, PM, SC, PR, TP, BM, BR, CJY, JMP, JP, MK, and OE received grants from Roche. BeR, OP, OR, SU, RL, YC, TT, ToO, CX, ES, FB, GC, LD and LJ were employees of Roche. GAA, MC and TO received grants and personal fees from Roche.

Authors' contributions

Conception and design: G.K. Abou-Alfa. Abou-Alfa, R. Lee, T. Tanaka, and T. Ohtomo. Provision of study materials or patients: G.K. Abou-Alfa, Oscar Puig, Bruno Daniele, Masatoshi Kudo, Philippe Merle, Joong-Won Park, Paul Ross, Jean-Marie Peron, Oliver Ebert, Stephen Chan, Tung Ping Poon, Massimo Colombo, Takuji Okusaka, Baek-Yeol Ryoo, Beatriz Minguez, and other participating investigators. Collection and assembly of data: All authors and study sites. Data analysis and interpretation: G.K. Abou-Alfa, O. Puig, L. Jukofsky, B. Reis, S. Ukrainskyj, Frederic Boisserie, O. Rutman, Y.C. Chen, C. Xu, E. Shochat, Gong Chen, L. Di Laurenzio and R. Lee. Pharmacokinetic analysis and modeling: Y.C. Chen. Final approval of manuscript: All authors.

Acknowledgements

We thank James Song, Sandrine Anton Belousov, Christine Rossin, Chia-Huey Ooi, Axel Muehlig, Jasbinder Bajwa, Janine Feng, Bharathi Vennapusa, Monica Reinholz, John Allard, Victor A. Iglesias, Mikiko Nakamura, Yasuo Sugitani and Judy Zhong for help during data processing and analysis.

Supplementary data

Supplementary data associated with this article can be found, in the online version, at http://dx.doi.org/10.1016/j.jhep.2016.04.004.

References

[1] Farooq M, Hwang SY, Park MK, et al. Blocking endogenous glypican-3 expression releases Hep 3B cells from G1 arrest. Mol Cells 2003;15:356–360.
[2] Li M, Choo B, Wong ZM, et al. Expression of OCI-5/glypican 3 during intestinal morphogenesis: regulation by cell shape in intestinal epithelial cells. Exp Cell Res 1997;235:3–12.

[3] Capurro M, Wanless IR, Sherman M, et al. Glypican-3: a novel serum and histochemical marker for hepatocellular carcinoma. Gastroenterology 2003;125:89–97.
[4] Libbrecht L, Severi T, Cassiman D, et al. Glypican-3 expression distinguishes small hepatocellular carcinomas from cirrhosis, dysplastic nodules, and focal nodular hyperplasia-like nodules. Am J Surg Pathol 2006;30:1405–1411.
[5] Llovet JM, Chen Y, Wurmbach E, et al. A molecular signature to discriminate dysplastic nodules from early hepatocellular carcinoma in HCV cirrhosis. Gastroenterology 2006;131:1758–1767.
[6] Wang XY, Degos F, Dubois S, et al. Glypican-3 expression in hepatocellular tumors: diagnostic value for preneoplastic lesions and hepatocellular carcinomas. Hum Pathol 2006;37:1435–1441.
[7] Yamauchi N, Watanabe A, Hishinuma M, et al. The glypican 3 oncofetal protein is a promising diagnostic marker for hepatocellular carcinoma. Mod Pathol 2005;18:1591–1598.
[8] Zhu ZW, Friess H, Wang L, et al. Enhanced glypican-3 expression differentiates the majority of hepatocellular carcinomas from benign hepatic disorders. Gut 2001;48:558–564.
[9] Capurro M, Martin T, Shi W, et al. Glypican-3 binds to frizzled and plays a direct role in the stimulation of canonical Wnt signaling. J Cell Sci 2014;127:1565–1575.
[10] Capurro MI, Xiang YY, Lobe C, et al. Glypican-3 promotes the growth of hepatocellular carcinoma by stimulating canonical Wnt signaling. Cancer Res 2005;65:6245–6254.
[11] Cheng W, Tseng CJ, Lin TT, et al. Glypican-3-mediated oncogenesis involves the Insulin-like growth factor-signaling pathway. Carcinogenesis 2008;29:1319–1326.
[12] Lai JP, Sandhu DS, Yu C, et al. Sulfatase 2 up-regulates glypican 3, promotes fibroblast growth factor signaling, and decreases survival in hepatocellular carcinoma. Hepatology 2008;47:1211–1222.
[13] Nakatsura T, Nishimura Y. Usefulness of the novel oncofetal antigen glypican-3 for diagnosis of hepatocellular carcinoma and melanoma. BioDrugs 2005;19:71–77.
[14] Ishiguro T, Sugimoto M, Kinoshita Y, et al. Anti-glypican 3 antibody as a potential antitumor agent for human liver cancer. Cancer Res 2008;68:9832–9838.
[15] Nakano K, Orita T, Nezu J, et al. Anti-glypican 3 antibodies cause ADCC against human hepatocellular carcinoma cells. Biochem Biophys Res Commun 2009;378:279–284.
[16] Takai H, Ashihara M, Ishiguro T, et al. Involvement of glypican-3 in the recruitment of M2-polarized tumor-associated macrophages in hepatocellular carcinoma. Cancer Biol Ther 2009;8:2329–2338.
[17] Takai H, Kato A, Kato C, et al. The expression profile of glypican-3 and its relation to macrophage population in human hepatocellular carcinoma. Liver Int 2009;29:1056–1064.
[18] Takai H, Kato A, Kinoshita Y, et al. Histopathological analyses of the antitumor activity of anti-glypican-3 antibody (GC33) in human liver cancer xenograft models: The contribution of macrophages. Cancer Biol Ther 2009;8:930–938.
[19] Zhu AX, Gold PJ, El-Khoueiry AB, et al. First-in-man phase I study of GC33, a novel recombinant humanized antibody against glypican-3, in patients with advanced hepatocellular carcinoma. Clin Cancer Res 2013;19:920–928.
[20] Ikeda M, Ohkawa S, Okusaka T, et al. Japanese phase I study of GC33, a humanized antibody against glypican-3 for advanced hepatocellular carcinoma. Cancer Sci 2014;105:455–462.
[21] Oken MM, Creech RH, Tormey DC, et al. Toxicity and response criteria of the Eastern Cooperative Oncology Group. Am J Clin Oncol 1982;5:649–655.
[22] Eisenhauer EA, Therasse P, Bogaerts J, et al. New response evaluation criteria in solid tumours: revised RECIST guideline (version 1.1). Eur J Cancer 2009;45:228–247.
[23] Cockcroft DW, Gault MH. Prediction of creatinine clearance from serum creatinine. Nephron 1976;16:31–41.
[24] Chen YC et al. Application of non-linear popPK with Target Mediated Drug Disposition (TMDD) in Optimization of an Oncology Dosing Regimen. ASCPT 2014 late breaking abstract, March 18–22.
[25] Rubin DB. Bias reduction using Mahalanobis-metric matching. Biometrics 1980;36:293–298.
[26] Hochberg Y, Benjamini Y. More powerful procedures for multiple significance testing. Stat Med 1990;9:811–818.
[27] Alderson KL, Sondel PM. Clinical cancer therapy by NK cells via antibody-dependent cell-mediated cytotoxicity. J Biomed Biotechnol 2011;2011:379123.
[28] Krebs P, Barnes MJ, Lampe K, et al. NK-cell-mediated killing of target cells triggers robust antigen-specific T-cell-mediated and humoral responses. Blood 2009;113:6593–6602.
[29] Tamm A, Schmidt RE. IgG binding sites on human Fc gamma receptors. Int Rev Immunol 1997;16:57–85.

Liver INTERNATIONAL

Liver International ISSN 1478-3223

ORIGINAL ARTICLE

Regional differences in sorafenib-treated patients with hepatocellular carcinoma: GIDEON observational study

Masatoshi Kudo[1], Riccardo Lencioni[2], Jorge A. Marrero[3], Alan P. Venook[4], Jean-Pierre Bronowicki[5], Xiao-Ping Chen[6], Lucy Dagher[7], Junji Furuse[8], Jean-Francois H. Geschwind[9], Laura Ladrón de Guevara[10], Christos Papandreou[11], Arun J. Sanyal[12], Tadatoshi Takayama[13], Seung Kew Yoon[14], Keiko Nakajima[15], Robert Lehr[16], Stephanie Heldner[17] and Sheng-Long Ye[18]

1 Department of Gastroenterology and Hepatology, Kinki University School of Medicine, Osaka, Japan
2 Division of Diagnostic Imaging and Intervention, Pisa University Hospital and School of Medicine, Pisa, Italy
3 Division of Digestive and Liver Diseases, Department of Internal Medicine, University of Texas Southwestern Medical Center, Dallas, TX, USA
4 University of California, San Francisco, CA, USA
5 Department of Gastroenterology and Hepatology, INSERM U954, University Hospital, University of Lorraine, Nancy, France
6 Hepatic Surgery Center, Tongji Hospital, Tongji Medical College, Huazhong University of Science and Technology, Wuhan, China
7 Policlínica Metropolitana, Caracas, Venezuela
8 Kyorin University School of Medicine, Tokyo, Japan
9 Vascular and Interventional Radiology, Johns Hopkins University School of Medicine, Baltimore, MD, USA
10 Hospital Angeles Clínica Londres, Mexico City, Mexico
11 University Hospital of Larissa, Larissa, Greece
12 Virginia Commonwealth University Medical Center, Richmond, VA, USA
13 Department of Digestive Surgery, Nihon University School of Medicine, Tokyo, Japan
14 The Catholic University of Korea, Seoul, Korea
15 Global Medical Affairs, Bayer HealthCare Pharmaceuticals, Whippany, NJ, USA
16 Clinical Statistics, Bayer HealthCare Pharmaceuticals, Whippany, NJ, USA
17 Global Medical Affairs and Pharmacovigilance, Bayer Pharma AG, Berlin, Germany
18 Liver Cancer Institute and Zhongshan Hospital, Fudan University, Shanghai, China

DOI: 10.1111/liv.13096

Abstract

Background & Aims: Treatment approaches for hepatocellular carcinoma (HCC) vary across countries, but these differences and their potential impact on outcomes have not been comprehensively assessed. Data from the multinational GIDEON (Global Investigation of therapeutic DEcisions in HCC and Of its treatment with sorafeNib) registry evaluated differences in patient characteristics, practice patterns and outcomes in HCC across geographical regions in patients who received sorafenib. *Methods:* GIDEON is a non-randomised, observational registry study conducted in 39 countries across five global regions. HCC patients in whom a decision to treat with sorafenib was made in clinical practice and according to local practices were included. *Results:* 3202 patients were evaluable for safety analysis: Asia-Pacific (n = 928), Japan (n = 508), Europe (n = 1113), USA (n = 563) and Latin America (n = 90). Patients in Japan had earlier-stage disease at initial

Abbreviations

AE, adverse event; BCLC, Barcelona Clinic Liver Cancer; BMI, body mass index; CI, confidence interval; EASL, European Association for the Study of the Liver; GIDEON, Global Investigation of therapeutic DEcisions in hepatocellular carcinoma and Of its treatment with sorafeNib; HAI, hepatic arterial infusion; HCC, hepatocellular carcinoma; LRT, locoregional therapy; NASH, non-alcoholic steatohepatitis; NE, not evaluable; PEI, percutaneous ethanol injection; RECIST, Response Evaluation Criteria in Solid Tumours; RFA, radiofrequency ablation; TACE, transarterial chemoembolisation; TNM, tumour node metastasis; WHO, World Health Organization.

Correspondence

Professor Masatoshi Kudo, Department of Gastroenterology and Hepatology, Kinki University School of Medicine, 377-2 Ohno-Higashi, Osaka-Sayama City, Osaka 589-8511, Japan
Tel: +81 72 366 0221 ext. 3149; Fax: +81 72 367 2880
e-mail: m-kudo@med.kindai.ac.jp

Handling editor: Chun-Jen Liu

Received 10 July 2015; Accepted 5 February 2016
Additional Supporting Information may be found at onlinelibrary.wiley.com/doi/10.1111/liv.13096/suppinfo

diagnosis compared with patients in other regions (Barcelona Clinic Liver Cancer stage A; 43.7% vs 9.1–24.3%). Use of locoregional therapies before sorafenib, including transarterial chemoembolisation, was more common in Japan (84.4%) and Asia-Pacific (67.2%) compared with the USA (49.4%) and Europe (43.5%). Treatment patterns with respect to sorafenib also differed, with a shorter duration of treatment reported in the USA and Asia-Pacific. Time from initial diagnosis to death was longer in Japan compared with other regions (median, 79.6 months vs 14.8–25.0 months). *Conclusions:* Data from GIDEON highlight regional variations in the management of HCC and patient outcomes. Greater standardisation of management may help optimise outcomes for HCC patients.

Keywords
GIDEON – hepatocellular carcinoma – liver – Nexavar – sorafenib

Key points

- There are regional differences in the management of HCC, including diagnosis, treatment and monitoring
- A higher proportion of HCC patients in Japan were diagnosed at an earlier disease stage compared with patients in Europe, the USA and other Asian countries
- In Japan, a high proportion of patients received multiple treatments before receiving sorafenib
- Patients in Japan had a longer time from diagnosis to death irrespective of BCLC stage, suggesting that various factors, in addition to early diagnosis, contribute to improved outcomes in this region

Hepatocellular carcinoma (HCC) is the third most common cause of cancer-related deaths worldwide (1). Significant variation exists in HCC aetiology and incidence in different global regions, as endemic hepatitis B virus causes high HCC disease burden in eastern Asia and Africa, whereas hepatitis C virus is the leading cause of HCC in Japan (2, 3). Other risk factors, more commonly observed in western areas, include heavy alcohol consumption (alcoholic cirrhosis) and diabetes (non-alcoholic steatohepatitis) (4). The GLOBOCAN 2008 database estimated that 59.6% of new HCC cases (per year per 100 000 people) were in eastern Asia, 8.1% in Europe and 3.9% in the USA (5), with the incidence in western areas predicted to rise because of increased hepatitis C virus infection rates (6). Hence, HCC is a global problem, and understanding the approach to managing HCC across regions is crucial to improving patient care.

Treatment decisions for HCC depend on both the tumour stage and the degree of underlying liver dysfunction. Treatment options for HCC may include surgical resection, locoregional therapies such as radiofrequency ablation and transarterial chemoembolisation (TACE), and the oral multikinase inhibitor sorafenib (Nexavar®; Bayer Pharma AG, Berlin, Germany) (7, 8). Treatment patterns across the globe vary, and there is no globally standardised approach to managing patients with HCC (9).

Sorafenib is approved for use in patients with unresectable HCC based on improved survival demonstrated in two placebo-controlled, randomised, phase III trials (10, 11). GIDEON (Global Investigation of therapeutic DEcisions in HCC and Of its treatment with sorafeNib) is a non-randomised, observational registry study undertaken in 39 countries to assess the use of sorafenib in clinical practice (12). Patients were enrolled from Asia-Pacific, Europe, Latin America, the USA and Japan. Here, we report results from pre-planned final analyses of GIDEON evaluating regional variations in disease characteristics, treatment practices and outcomes.

Materials and methods

GIDEON enrolled patients with HCC who fulfilled the criteria for systemic therapy and for whom the decision to treat with sorafenib had been made in clinical practice. This study design and rationale have been previously reported (12). GIDEON was undertaken to fulfil a post-approval agreement to licensing agencies, with the primary objective of evaluating sorafenib safety in real-life practice. This study protocol conforms to the ethical guidelines of the 1975 Declaration of Helsinki as reflected in prior approval by the institutions' human research committees. There were 376 participating study centres and approval from an independent ethics committee or institutional review board was obtained for each, including from the Kinki University Hospital Institutional Review Board. Further information on ethical approval for individual centres is available upon request. Informed consent was obtained for all patients who participated in this study.

Inclusion and exclusion criteria for this study were based on local prescribing and product information for sorafenib (12). Data were collected using case report forms. Adverse events were graded according to the National Cancer Institute Common Terminology Criteria for Adverse Events version 3.0 (National Cancer Institute, Bethesda, MD, USA), with the causality relationship of the adverse event to sorafenib documented. The safety population included all patients who received at least one dose of sorafenib and underwent at least one follow-up assessment after the start of sorafenib treatment.

The target enrolment of 3000 patients was determined to be sufficient for the full safety evaluation of the overall sample population and for subgroups within it; regional analyses were pre-planned (12). Descriptive statistics were used to summarise all baseline and safety data.

Results

Patient demographics and disease characteristics

In total, 3202 patients were included in the safety analyses. The majority of patients were male and the median age was 62 years. Differences in aetiology were as expected: hepatitis B virus was the leading cause of HCC in patients in Asia-Pacific (82.3%) while hepatitis C virus was the most common aetiology in patients in the USA (54.9%) and Japan (53.1%) (Table 1).

At initial diagnosis, a considerably greater proportion of patients in Japan had Barcelona Clinic Liver Cancer (BCLC) stage A (43.7%) compared with all other regions, where most patients had BCLC stage B or C (Table 1).

At the time of sorafenib initiation (study entry), most patients in all regions had BCLC stage C, including 54.7% of patients in Japan. The majority of patients (61%) had Child–Pugh A status at the time of sorafenib initiation, although a considerable proportion of patients in the USA had Child–Pugh B status (30.7%), which was higher than in other regions with the exception of Latin America.

Of note, approximately 15% of patients were not evaluable for Child–Pugh status based on the data provided. This was most common in the USA, where 29.5% of enrolled patients did not have all of the data required to calculate the Child–Pugh score.

Treatment practices: before sorafenib initiation

Overall, 21.1% of patients had undergone surgery and 47.2% had received TACE before initiating sorafenib. TACE was the most commonly used locoregional therapy, and patients in Japan were more likely to have received prior TACE. Patients in Japan were also more likely to have received three or more TACE treatments (60.5%) compared with patients in all other regions (Asia-Pacific 38.6%; Europe 27.7%; USA 14.4%; Latin America 8.3%) (Table 2). The reported response rate (complete or partial response) to TACE was 47.9% for patients assessed by modified Response Evaluation Criteria in Solid Tumours. A higher response rate was reported for patients in Japan (84.5%) and Europe (65.2%) compared with patients in the other regions (Table S1).

Marked regional variations were observed in the time from initial diagnosis to the start of sorafenib treatment, with the longest time reported in Japan (median, 24.10 months vs 1.15–3.72 months) (Table 3). Time to the start of sorafenib from prior surgery or from first locoregional therapy was also longer in Japan compared with other regions.

Treatment practices: during sorafenib treatment

The majority of patients received the recommended initial dose of sorafenib of 800 mg. A lower proportion of patients in Japan (45.5%) and the USA (54.4%) received an initial dose of 800 mg compared with patients in Asia-Pacific (76.5%), Europe (82.4%) and Latin America (96.7%) (Table 3). The median daily dose was also lower in Japan and the USA (419 mg and 527 mg, respectively) compared with Asia-Pacific and Europe (800 mg and 780 mg, respectively). Dose modifications were more frequent in the USA (54.9%) and Japan (67.3%) than in other regions (range, 24.4–45.1%).

The median duration of treatment tended to be slightly shorter in Asia-Pacific and the USA (12.6 weeks and 12.7 weeks, respectively) than in Japan (15.9 weeks) and Europe (17.1 weeks). The median interval of radiological tumour assessment during sorafenib treatment was 36 days, which was consistent across regions (Table 3).

The major reasons for discontinuation from sorafenib in all regions were progression, recurrence or relapse of HCC, and adverse events (Table 3). Conversely, loss to follow-up was substantially lower in Japan than in other regions (0.2% vs 5.8–25.0%).

Treatment practices: after sorafenib initiation

A total of 15.5% of patients received non-systemic treatments after initiating sorafenib. TACE was the most common non-systemic therapy received, with 10.1% of patients receiving TACE concomitantly with sorafenib (Table 2). Radiation therapy concomitant with sorafenib was uncommon (2.6%), as were hepatic arterial infusion and radiofrequency ablation (1.7% each).

Sorafenib safety

Safety findings during sorafenib administration showed that sorafenib tolerability was generally similar across the regions, and treatment-emergent adverse events were recorded in 85.3% of patients (Table 4).

Drug-related adverse events were more common in Japan (87.6% vs 48.7–71.9% across other regions); however, the incidence of death was lower (15.2% vs 19.1–33.4%) (Table 4). The most commonly observed drug-related adverse events in all regions were diarrhoea (27.1%), hand-foot skin reaction (26.5%) and fatigue (15.5%). A higher incidence of hand-foot skin reaction was reported in Japan (47.8% vs 12.2–26.3% across other regions), while fatigue was most common in Europe (23.3% vs 4.4–18.1% across other regions).

Table 1. Patient demographics and disease characteristics

	Asia-Pacific (*n* = 928)	Japan (*n* = 508)	Europe (*n* = 1113)	USA (*n* = 563)	Latin America (*n* = 90)	Total (*N* = 3202*)
Patients†, %	29.0	15.9	34.8	17.6	2.8	100
Males†, *n* (%)	809 (87.2)	410 (80.7)	927 (83.3)	440 (78.2)	45 (50.0)	2631 (82.2)
Median age†, years (range)	54 (19–87)	70 (23–90)	66 (15–94)	61 (20–87)	67 (18–98)	62 (15–98)
Median BMI†, kg/m^2 (range)	22.7 (14.7–45.1)	22.7 (13.9–36.6)	25.5 (15.2–43.9)	27.1 (23.6–58.0)	26.6 (20.2–43.0)	24.2 (13.9–58.0)
Aetiology†, *n* (%)						
Hepatitis B	764 (82.3)	123 (24.2)	201 (18.1)	79 (14.0)	3 (3.3)	1170 (36.5)
Hepatitis C	46 (5.0)	270 (53.1)	396 (35.6)	309 (54.9)	32 (35.6)	1053 (32.9)
Alcohol use	150 (16.2)	67 (13.2)	382 (34.3)	221 (39.3)	14 (15.6)	834 (26.0)
NASH	2 (0.2)	12 (2.4)	36 (3.2)	34 (6.0)	6 (6.7)	90 (2.8)
At initial diagnosis						
BCLC stage‡, *n* (%)						
A	84 (9.1)	222 (43.7)	271 (24.3)	95 (16.9)	21 (23.3)	693 (21.6)
B	147 (15.8)	103 (20.3)	288 (25.9)	65 (11.5)	28 (31.1)	631 (19.7)
C	349 (37.6)	90 (17.7)	355 (31.9)	149 (26.5)	21 (23.3)	964 (30.1)
D	24 (2.6)	4 (0.8)	22 (2.0)	33 (5.9)	7 (7.8)	90 (2.8)
Unknown§	294 (31.7)	74 (14.6)	151 (13.6)	186 (33.0)	13 (14.4)	718 (22.4)
Child–Pugh status, *n* (%)						
A	551 (59.4)	380 (74.8)	660 (59.3)	199 (35.3)	41 (45.6)	1831 (57.2)
B	124 (13.4)	23 (4.5)	174 (15.6)	152 (27.0)	26 (28.9)	499 (15.6)
C	11 (1.2)	0	14 (1.3)	43 (7.6)	6 (6.7)	74 (2.3)
Not evaluable§,¶	242 (26.1)	105 (20.7)	265 (23.8)	169 (30.0)	17 (18.9)	798 (24.9)
TNM status**, *n* (%)						
I	75 (8.1)	128 (25.2)	199 (17.9)	89 (15.8)	13 (14.4)	504 (15.7)
II	92 (9.9)	153 (30.1)	178 (16.0)	69 (12.3)	16 (17.8)	508 (15.9)
III (A–C)	295 (31.8)	108 (21.3)	392 (35.2)	147 (26.1)	38 (42.2)	980 (30.6)
IV	182 (19.6)	53 (10.4)	162 (14.6)	93 (16.5)	5 (5.6)	495 (15.5)
Unknown§	258 (27.8)	49 (9.6)	151 (13.6)	132 (23.4)	18 (20.0)	608 (19.0)
At study entry						
BCLC stage†,††, *n* (%)						
A	26 (2.8)	33 (6.5)	95 (8.5)	56 (9.9)	16 (17.8)	226 (7.1)
B	95 (10.2)	162 (31.9)	271 (24.3)	70 (12.4)	36 (40.0)	634 (19.8)
C	567 (61.1)	278 (54.7)	589 (52.9)	204 (36.2)	26 (28.9)	1664 (52.0)
D	46 (5.0)	9 (1.8)	44 (4.0)	66 (11.7)	8 (8.9)	173 (5.4)
Not evaluable¶	194 (20.9)	26 (5.1)	111 (10.0)	166 (29.5)	4 (4.4)	501 (15.6)
Child–Pugh status†,‡‡, *n* (%)						
A	590 (63.6)	432 (85.0)	721 (64.8)	192 (34.1)	33 (36.7)	1968 (61.5)
B	173 (18.6)	58 (11.4)	221 (19.9)	173 (30.7)	41 (45.6)	666 (20.8)
C	16 (1.7)	0	12 (1.1)	43 (7.6)	3 (3.3)	74 (2.3)
Not evaluable¶	149 (16.1)	18 (3.5)	159 (14.3)	154 (27.4)	13 (14.4)	493 (15.4)
TNM status†,§§, *n* (%)						
I	16 (1.7)	14 (2.8)	62 (5.6)	54 (9.6)	9 (10.0)	155 (4.8)
II	53 (5.7)	135 (26.6)	123 (11.1)	64 (11.4)	13 (14.4)	388 (12.1)
III (A–C)	288 (31.0)	129 (25.4)	493 (44.3)	177 (31.4)	51 (56.7)	1138 (35.5)
IV	429 (46.2)	225 (44.3)	303 (27.2)	161 (28.6)	8 (8.9)	1126 (35.2)
Not evaluable¶	142 (15.3)	5 (1.0)	130 (11.7)	105 (18.7)	9 (10.0)	391 (12.2)
Extrahepatic spread†, *n* (%)	500 (53.9)	224 (44.1)	369 (33.2)	169 (30.0)	10 (11.1)	1272 (39.7)

*Safety population (includes all patients who received at least one dose of sorafenib and underwent at least one follow-up assessment after the start of sorafenib treatment).

†Baseline data collected at study entry, which is defined as the start of therapy and is indicated by the initial visit. For aetiology, patients may have multiple responses.

‡Data missing for 106 patients.

§No record was available.

¶Necessary staging data were not collected in routine practice, or the investigator chose not to assess the stage.

**Data missing for 107 patients.

††Data missing for four patients.

‡‡Data missing for one patient.

§§Data missing for four patients.

BCLC, Barcelona Clinic Liver Cancer; BMI, body mass index; NASH, non-alcoholic steatohepatitis; TNM, tumour node metastasis.

Liver International (2016)

Table 2. Treatments for hepatocellular carcinoma before and after sorafenib initiation

n (%)	Asia-Pacific (*n* = 928)	Japan (*n* = 508)	Europe (*n* = 1113)	USA (*n* = 563)	Latin America (*n* = 90)	Total (*N* = 3202*)
Prior therapies						
Surgery	225 (24.2)	220 (43.3)	172 (15.5)	53 (9.4)	5 (5.6)	675 (21.1)
Liver transplantation	31 (3.3)	1 (0.2)	22 (2.0)	27 (4.8)	2 (2.2)	83 (2.6)
LRT† (all)	624 (67.2)	429 (84.4)	484 (43.5)	278 (49.4)	25 (27.8)	1840 (57.5)
TACE‡	560 (60.3)	362 (71.3)	368 (33.1)	209 (37.1)	12 (13.3)	1511 (47.2)
Number of TACE treatments						
1	228 (40.7)	76 (21.0)	174 (47.3)	124 (59.3)	10 (83.3)	612 (40.5)
2	116 (20.7)	67 (18.5)	92 (25.0)	55 (26.3)	1 (8.3)	331 (21.9)
≥3	216 (38.6)	219 (60.5)	102 (27.7)	30 (14.4)	1 (8.3)	568 (37.6)
RFA§	119 (12.8)	195 (38.4)	166 (14.9)	65 (11.5)	16 (17.8)	561 (17.5)
HAI¶	48 (5.2)	96 (18.9)	11 (1.0)	22 (3.9)	2 (2.2)	179 (5.6)
PEI**	25 (2.7)	59 (11.6)	59 (5.3)	6 (1.1)	0	149 (4.7)
Systemic treatment††	46 (5.0)	59 (11.6)	42 (3.8)	19 (3.4)	0	166 (5.2)
Tumour evaluation methods following TACE‡‡						
RECIST	212 (37.9)	179 (49.4)	191 (51.9)	63 (30.1)	3 (25.0)	648 (42.9)
Modified RECIST	183 (32.7)	58 (16.0)	92 (25.0)	25 (12.0)	3 (25.0)	361 (23.9)
Clinical assessment§§	107 (19.1)	96 (26.5)	64 (17.4)	103 (49.3)	5 (41.7)	375 (24.8)
Non-systemic concomitant therapies¶¶						
TACE	125 (13.5)	62 (12.2)	52 (4.7)	73 (13.0)	13 (14.4)	325 (10.1)
Radiation therapy	33 (3.6)	23 (4.5)	13 (1.2)	14 (2.5)	0	83 (2.6)
HAI	34 (3.7)	18 (3.5)	1 (<0.1)	1 (0.2)	0	54 (1.7)
RFA	14 (1.5)	8 (1.6)	14 (1.3)	12 (2.1)	5 (5.6)	53 (1.7)

*Safety population (includes all patients who received at least one dose of sorafenib and underwent at least one follow-up assessment after the start of sorafenib treatment).

†Patients may have received more than one prior treatment.

‡Data missing for 327 patients.

§Data missing for 338 patients.

¶Data missing for 341 patients.

**Data missing for 353 patients.

††Chemotherapy, immunotherapy or others.

‡‡Other criteria used not shown: WHO (*n* = 25), EASL (*n* = 3) and missing/unknown (*n* = 216).

§§Assessment not based on RECIST, modified RECIST or WHO or EASL criteria.

¶¶Therapies given after initiating sorafenib until the end of sorafenib.

EASL, European Association for the Study of the Liver; HAI, hepatic arterial infusion; LRT, locoregional therapy; PEI, percutaneous ethanol injection; RECIST, Response Evaluation Criteria in Solid Tumours; RFA, radiofrequency ablation; TACE, transarterial chemoembolisation; WHO, World Health Organization.

Outcomes

Overall survival from sorafenib initiation was broadly similar across regions, although this was longest for patients in Japan (14.5 months vs 8.5–13.7 months) (Fig. 1A). Time from initial diagnosis of HCC to death was considerably longer in Japan than in other regions (79.6 months vs 14.8–25.0 months) (Fig. 1B). Interestingly, patients in Japan had the longest median survival time from initial diagnosis to death irrespective of BCLC stage at initial diagnosis (Fig. S1A–D).

Discussion

GIDEON is the first global study assessing the use of sorafenib for HCC in clinical practice, allowing for evaluation of regional variations in patient management with the benefit of standardised data collection (12). These data provide insight into differences in the diagnosis and treatment of HCC and provide impetus for improvements in the standardisation of patient management.

Patient characteristics in the GIDEON population were consistent with previous reports (13–15), although the low number of patients with non-alcoholic steatohepatitis suggests that this may have been underreported (4, 16). A relatively high proportion of patients, particularly in the USA, were non-evaluable for Child–Pugh status at the time of sorafenib initiation because of the required elements not being collected by the treating physician. This highlights that patient assessment differs regionally and common scoring systems may not be followed in clinical practice.

In Japan, patients tended to be diagnosed at an earlier disease stage, potentially because of the presence of a national HCC surveillance system (17). Patients in Japan were also more likely to have received a greater number of previous therapies, likely reflecting the trend for earlier

Table 3. Sorafenib administration, patient assessment and discontinuation

	Asia-Pacific (*n* = 928)	Japan (*n* = 508)	Europe (*n* = 1113)	USA (*n* = 563)	Latin America (*n* = 90)	Total (*N* = 3202*)
Initial dose of 800 mg†, *n* (%)	710 (76.5)	231 (45.5)	917 (82.4)	306 (54.4)	87 (96.7)	2251 (70.3)
Daily dose‡, mg						
n§	730	499	1026	530	72	2857
Median	800.0	419.0	780.0	527.0	800.0	688.0
Mean	663.4	487.2	668.1	555.7	748.5	616.5
Dose modification¶, *n* (%)	301 (32.4)	342 (67.3)	502 (45.1)	309 (54.9)	22 (24.4)	1476 (46.1)
Duration of treatment**, weeks						
n§	887	505	1097	551	90	3130
Median	12.60	15.90	17.10	12.70	23.10	15.00
Mean	21.12	23.43	27.19	21.75	30.23	23.99
Total exposure, mg						
n§	730	499	1026	530	72	2857
Median	45 600.00	40 000.00	68 800.00	41 200.00	101 600.00	52 400.00
Mean	80 661.89	66 095.44	111 145.83	72 450.75	135 152.78	88 915.06
Median time to start of sorafenib, months						
n††	737	380	941	475	79	2612
From initial HCC diagnosis	2.56	24.10	3.72	2.76	1.15	3.88
n‡‡	200	202	157	47	4	610
From prior surgery	7.18	26.12	15.16	9.27	3.27	13.91
n§§	588	406	428	246	22	1690
From first LRT	5.0	25.0	10.0	4.0	3.0	9.0
Patient visit interval during sorafenib therapy						
n§	913	500	1106	562	90	3171
Median visit interval, days (range)	60.0 (1.0–478.0)	52.0 (3.0–126.0)	51.0 (1.0–318.0)	45.0 (1.0–283.0)	49.5 (3.0–228.0)	53.0 (1.0–478.0)
Radiological tumour assessment during sorafenib treatment						
n¶¶	185	229	384	164	15	977
Median interval, days (range)	37.0 (7.0–282.0)	35.0 (2.0–205.0)	38.0 (4.0–142.0)	36.0 (3.0–129.0)	33.0 (14.0–106.0)	36.0 (2.0–282.0)
Reasons for discontinuation, *n* (%)						
*n****	958	510	1126	569	92	3255
Progression, recurrence or relapse of HCC	181 (18.9)	188 (36.9)	294 (26.1)	120 (21.1)	3 (3.3)	786 (24.1)
Adverse event or toxicity	89 (9.3)	135 (26.5)	161 (14.3)	95 (16.7)	3 (3.3)	483 (14.8)
Deterioration of general condition	44 (4.6)	51 (10.0)	165 (14.7)	72 (12.7)	5 (5.4)	337 (10.4)
Lost to follow-up	188 (19.6)	1 (0.2)	65 (5.8)	47 (8.3)	23 (25.0)	324 (10.0)
Patient decision (not disease progression)	130 (13.6)	20 (3.9)	81 (7.2)	55 (9.7)	13 (14.1)	299 (9.2)

Table 3 (continued)

	Asia-Pacific (n = 928)	Japan (n = 508)	Europe (n = 1113)	USA (n = 563)	Latin America (n = 90)	Total (N = 3202*)
Progression of liver disease (not HCC)	37 (3.9)	9 (1.8)	84 (7.5)	39 (6.9)	3 (3.3)	172 (5.3)
Death	183 (19.1)	9 (1.8)	128 (11.4)	83 (14.6)	30 (32.6)	433 (13.3)

*Safety population (includes all patients who received at least one dose of sorafenib and underwent at least one follow-up assessment after the start of sorafenib treatment).
†Data missing for one patient; data not shown for 950 patients who received an initial dose of 29 mg, 67 mg, 100 mg, 200 mg, 400 mg or 600 mg.
‡Average daily dose was determined within patient-based actual days on study drug excluding interruptions.
§Patients for whom data are available.
¶Dose increase or reduction calculated by drug administration information relative to previous visit.
**Time from initial visit to last dosing date +1.
††Patients for whom the date of initial diagnosis is known.
‡‡Patients who received prior surgery and for whom the date of initial surgery is known.
§§Patients who received LRT and for whom the date of first LRT is known.
¶¶Includes only patients with respective assessment of radiological progression.
***Patients who were enrolled and treated.
HCC, hepatocellular carcinoma; LRT, locoregional therapy.

diagnosis and highlighting the ongoing need to improve early detection in other regions. Therefore, as one might expect, survival time from initial diagnosis was considerably longer in Japan. However, this was the case irrespective of BCLC stage, suggesting that various medical or social factors, in addition to earlier diagnosis, contributed to the longer survival observed in this region.

In the USA, a higher proportion of patients had Child–Pugh B status or BCLC stage D at the time of sorafenib initiation. This suggests that later diagnosis may consequently affect the point at which sorafenib is used in the treatment course, with patients receiving systemic therapy at a more advanced disease stage. Median overall survival from the time of sorafenib initiation was shortest in the USA, which may reflect the fact patients had more advanced disease when systemic treatment was started.

Regional variation in the response to TACE was observed, with Europe and Japan reporting higher response rates. This highlights that further consensus on TACE use and evaluation is needed, and is emphasised by the fact that a large proportion of patients in most regions received more than three TACE treatments. Recent European Association for the Study of the Liver guidelines suggest that patients who do not respond after two rounds of TACE should be considered for alternative treatments, including sorafenib (18). The recent observational BRIDGE study further highlighted the discrepancy between HCC guidelines and clinical practice, noting that only 14% of patients diagnosed with advanced HCC received sorafenib treatment during their treatment course, despite this being the recommended standard of care in these patients (19).

Together, the data therefore suggest that earlier diagnosis allowing for use of a greater number of treatments may improve patient outcomes. Due to the observational nature of this study and the potential for lead-time bias, it is not possible to make any definitive conclusions.

Despite the prescribing information regarding dose and dose modification being consistent across regions, the USA and Japan both tended to use a lower daily dose with more frequent dose modifications. This did not appear to be based on patient-related factors, but rather reflected the accepted approach of these regions, and may also have been influenced by factors such as reimbursement policies (20). As this study was conducted soon after sorafenib became available, the use of lower doses observed in the USA and Japan may also reflect a gap in education or experience in these regions. Due to the observational nature of this study, it is not possible to reliably correlate sorafenib exposure with outcomes, and the impact of observed differences in sorafenib dosing across regions may warrant further exploration.

Sorafenib tolerability was similar across the regions, consistent with data reported in the phase III Asia-Pacific and SHARP clinical trials (10, 11). Of note, the use of a lower sorafenib dose, as seen in Japan and the USA,

Table 4. Treatment-emergent and drug-related adverse events

n (%)	Asia-Pacific (*n* = 928)	Japan (*n* = 508)	Europe (*n* = 1113)	USA (*n* = 563)	Latin America (*n* = 90)	Total (*N* = 3202*)
Treatment-emergent AEs†,‡						
AEs (all grades)	650 (70.0)	482 (94.9)	983 (88.3)	554 (98.4)	63 (70.0)	2732 (85.3)
Drug-related AEs	452 (48.7)	445 (87.6)	766 (68.8)	405 (71.9)	44 (48.9)	2112 (66.0)
AEs (grade 3 or 4)	190 (20.5)	223 (43.9)	379 (34.0)	212 (37.6)	12 (13.3)	1016 (31.8)
Drug-related AEs (grade 3 or 4)	114 (12.2)	190 (37.4)	305 (27.4)	134 (23.8)	11 (12.2)	754 (23.6)
Serious AEs§ (all grades)	312 (33.6)	209 (41.1)	514 (46.2)	309 (54.9)	43 (47.8)	1387 (43.3)
Drug-related serious AEs (all grades)	32 (3.4)	90 (17.7)	121 (10.9)	42 (7.5)	12 (13.3)	297 (9.3)
AEs leading to permanent discontinuation of sorafenib	187 (20.2)	210 (41.3)	391 (35.1)	204 (36.2)	12 (13.3)	1004 (31.4)
Deaths	177 (19.1)	77 (15.2)	286 (25.7)	188 (33.4)	30 (33.3)	758 (23.7)
Drug-related AEs (all grades)						
Diarrhoea¶	143 (15.4)	182 (35.8)	361 (32.4)	162 (28.8)	20 (22.2)	868 (27.1)
Hand-foot skin reaction**	244 (26.3)	243 (47.8)	224 (20.1)	126 (22.4)	11 (12.2)	848 (26.5)
Fatigue††	41 (4.4)	90 (17.7)	259 (23.3)	102 (18.1)	4 (4.4)	496 (15.5)
Rash/desquamation‡‡	65 (7.0)	74 (14.6)	105 (9.4)	106 (18.8)	8 (8.9)	358 (11.2)
Anorexia§§	44 (4.7)	100 (19.7)	113 (10.2)	48 (8.5)	6 (6.7)	311 (9.7)
Hypertension¶¶	35 (3.8)	123 (24.2)	83 (7.5)	27 (4.8)	3 (3.3)	271 (8.5)
Alopecia***	44 (4.7)	99 (19.5)	44 (4.0)	27 (4.8)	7 (7.8)	221 (6.9)
Nausea†††	34 (3.7)	21 (4.1)	54 (4.9)	98 (17.4)	2 (2.2)	209 (6.5)
Weight loss‡‡‡	3 (0.3)	14 (2.8)	81 (7.3)	37 (6.6)	0	135 (4.2)

*Safety population (includes all patients who received at least one dose of sorafenib and underwent at least one follow-up assessment after the start of sorafenib treatment).
†While on sorafenib treatment and up to 30 days of last dose collected from all available sources.
‡AEs graded by National Cancer Institute Common Terminology Criteria for Adverse Events version 3.0.
§Any AE occurring at any dose that resulted in: death; threat to life; hospitalisation or prolonged existing hospitalisation; persistent or significant disability/incapacity; congenital anomaly/birth defect; or medically important event.
¶Data missing for 17 patients.
**Data missing for nine patients.
††Data missing for 11 patients.
‡‡Data missing for seven patients.
§§Data missing for two patients.
¶¶Data missing for two patients.
***Data missing for four patients.
†††Data missing for three patients.
‡‡‡Data missing for one patient.
AE, adverse event.

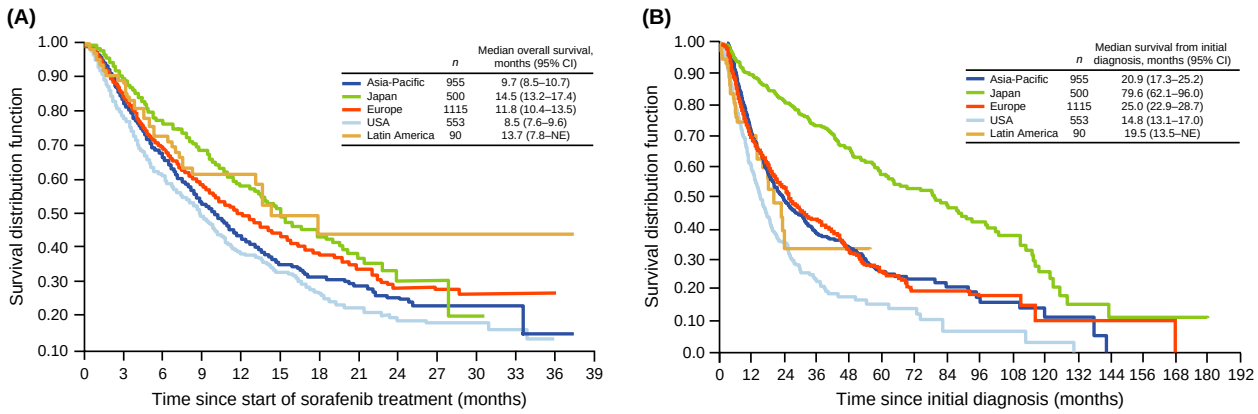

Fig. 1. Overall survival by time from start of treatment (A) and time from initial diagnosis to death (B) by region in the overall population. CI, confidence interval; NE, not evaluable.

did not appear to be associated with a reduced incidence of adverse events.

GIDEON is a non-randomised, observational study and findings are therefore limited by the lack of a randomised study population, the absence of a control arm, and no adjustment for lead-time bias. This said, observational studies allow for large datasets assessing real-life practice situations, thereby enabling evaluation of a wider patient population than is typically seen in randomised controlled trials. The robust data collected in GIDEON therefore contribute valuable information on the current management of HCC and may potentially help inform and improve patient care. It is also important to note that within each region analysed, country-level variations may also exist, and that treatment practices in countries within a given region may not be homogenous.

In summary, considerable regional variation in diagnosis and management of HCC in clinical practice was observed in the GIDEON registry. Sorafenib was well tolerated across all regions, with no new safety concerns reported. These data highlight that global efforts are still required to improve detection of HCC and to standardise treatment approaches to improve patient outcomes – continued sharing of knowledge globally will be central to this effort.

Acknowledgements

The authors would like to thank all clinical sites that contributed to the GIDEON study. The independent contract research organisation Kantar Health GmbH (Munich, Germany) was responsible for data capture, data management, data quality review and statistical reporting, overseen by Anja Laske and Dalila Lakbir at Bayer HealthCare Pharmaceuticals. Tanja Torbica, PhD, at Complete HealthVizion provided assistance in the preparation and revision of the draft manuscript, based on detailed discussion and feedback from all the authors. Editorial assistance was funded by Bayer HealthCare Pharmaceuticals.

Financial support: The GIDEON study was funded by Bayer HealthCare Pharmaceuticals and Onyx Pharmaceuticals, an Amgen subsidiary.

Conflicts of interest: Professors Furuse and Geschwind have received honoraria for advisory arrangements and research grant support from Bayer HealthCare Pharmaceuticals. Professor Marrero has received honoraria for advisory arrangements from Bayer HealthCare Pharmaceuticals and Onyx Pharmaceuticals, an Amgen subsidiary. Professor Venook has received honoraria for advisory arrangements and research grant support from Bayer HealthCare Pharmaceuticals and Onyx Pharmaceuticals, an Amgen subsidiary. Professors Lencioni and Bronowicki have received honoraria for advisory arrangements from Bayer HealthCare Pharmaceuticals. Professor Papandreou has received research grant support from Bayer HealthCare Pharmaceuticals. Dr Nakajima, Mr Lehr and Ms Heldner are employees of Bayer HealthCare Pharmaceuticals. Dr Nakajima has stock ownership with Bayer HealthCare Pharmaceuticals. Drs Kudo, Chen, Dagher, Ladrón de Guevara, Sanyal, Takayama, Yoon and Ye have no relevant disclosures to report.

Trial registration: ClinicalTrials.gov, NCT00812175 (http://www.clinicaltrials.gov/ct2/show/NCT00812175?term=GIDEON&rank=1)

References

1. Maillard E. [Epidemiology, natural history and pathogenesis of hepatocellular carcinoma]. *Cancer Radiother* 2011; **15**: 3–6.
2. Flores A, Marrero JA. Emerging trends in hepatocellular carcinoma: focus on diagnosis and therapeutics. *Clin Med Insights Oncol* 2014; **8**: 71–6.
3. Gao J, Xie L, Yang WS, *et al.* Risk factors of hepatocellular carcinoma - current status and perspectives. *Asian Pac J Cancer Prev* 2012; **13**: 743–52.
4. El-Serag HB, Rudolph KL. Hepatocellular carcinoma: epidemiology and molecular carcinogenesis. *Gastroenterology* 2007; **132**: 2557–76.
5. Ferlay J, Soerjomataram I, Ervik M, *et al.* GLOBOCAN 2012: Estimated Cancer Incidence, Mortality and Prevalence Worldwide in 2012. Available at: http://globocan.iarc.fr. Last updated 2013. Accessed 3 July 2015.
6. El-Serag HB. Epidemiology of viral hepatitis and hepatocellular carcinoma. *Gastroenterology* 2012; **142**: 1264–73.e1.
7. Lencioni R. Chemoembolization for hepatocellular carcinoma. *Semin Oncol* 2012; **39**: 503–9.
8. Rodrìguez de Lope C, Tremosini S, Forner A, Reig M, Bruix J. Management of HCC. *J Hepatol* 2012; **56**(Suppl. 1): S75–87.
9. Abou-Alfa GK, Huitzil-Melendez FD, O'Reilly EM, Saltz LB. Current management of advanced hepatocellular carcinoma. *Gastrointest Cancer Res* 2008; **2**: 64–70.
10. Cheng AL, Kang YK, Chen Z, *et al.* Efficacy and safety of sorafenib in patients in the Asia-Pacific region with advanced hepatocellular carcinoma: a phase III randomised, double-blind, placebo-controlled trial. *Lancet Oncol* 2009; **10**: 25–34.
11. Llovet JM, Ricci S, Mazzaferro V, *et al.* Sorafenib in advanced hepatocellular carcinoma. *N Engl J Med* 2008; **359**: 378–90.
12. Lencioni R, Marrero J, Venook A, Ye SL, Kudo M. Design and rationale for the non-interventional Global Investigation of therapeutic DEcisions in hepatocellular carcinoma and OF its treatment with sorafeNib (GIDEON) study. *Int J Clin Pract* 2010; **64**: 1034–41.
13. Farinati F, Rinaldi M, Gianni S, Naccarato R. How should patients with hepatocellular carcinoma be staged? Validation of a new prognostic system. *Cancer* 2000; **89**: 2266–73.
14. Tandon P, Garcia-Tsao G. Prognostic indicators in hepatocellular carcinoma: a systematic review of 72 studies. *Liver Int* 2009; **29**: 502–10.
15. Lencioni R, Kudo M, Ye SL, *et al.* First interim analysis of the GIDEON (Global Investigation of therapeutic DEcisions in hepatocellular carcinoma and Of its treatment

with sorafeNib) non-interventional study. *Int J Clin Pract* 2012; **66**: 675–83.
16. El-Zayadi AR. Hepatic steatosis: a benign disease or a silent killer. *World J Gastroenterol* 2008; **14**: 4120–6.
17. Johnson P, Berhane S, Satomura S, *et al.* An international collaborative study assessing the role of aetiology and stage in survival in HCC - implications for screening. *J Hepatol* 2014; **60**: S45.
18. European Association for the Study of the Liver, European Organisation for Research and Treatment of Cancer. EASL-EORTC clinical practice guidelines: management of hepatocellular carcinoma. *J Hepatol* 2012; **56**: 908–43.
19. Roayaie S, Jibara G, Tabrizian P, *et al.* How is BCLC stage C HCC treated in real-world practice and what outcomes are obtained? Answers from the BRIDGE database. Abstract 0-014 presented at the International Liver Cancer Association, Kyoto, Japan, 5–7 September 2014.
20. Lim CS, Kwon S, Lee YG, Koh Y, Heo DS. International comparison on the factors influencing reimbursement of expensive cancer drugs. *J Clin Oncol* (Meeting Abstracts) 2013; **31**: 6614 (abstract).

Supporting information

Additional Supporting Information may be found at onlinelibrary.wiley.com/doi/10.1111/liv.13096/suppinfo

EUS-guided gallbladder drainage for rescue treatment of malignant distal biliary obstruction after unsuccessful ERCP

Hajime Imai, MD, Masayuki Kitano, MD, PhD, Shunsuke Omoto, MD, Kumpei Kadosaka, MD, Ken Kamata, MD, PhD, Takeshi Miyata, MD, Kentaro Yamao, MD, Hiroki Sakamoto, MD, PhD, Yogesh Harwani, MD, Masatoshi Kudo, MD, PhD

Osaka-sayama, Japan

Background and Aims: EUS-guided bile duct drainage (EUS-BD) is a well-recognized rescue biliary drainage method after unsuccessful ERCP. EUS-guided gallbladder drainage (EUS-GBD) was recently used to treat acute cholecystitis. The aim of this study was to assess the efficacy and safety of EUS-GBD for malignant biliary stricture–induced obstructive jaundice after unsuccessful ERCP as well as unsuccessful or impractical EUS-BD.

Methods: Between January 2006 and October 2014, 12 patients with obstructive jaundice due to unresectable malignant distal biliary stricture underwent EUS-GBD after ERCP failed. EUS-GBD was performed under the guidance of EUS and fluoroscopy by puncturing the gallbladder with a needle, inserting a guidewire, dilating the puncture hole, and placing a stent. The technical and functional success rates, adverse events rate, overall patient survival time, and stent dysfunction rate during patient survival were measured.

Results: The rates of technical success, functional success, adverse events, and stent dysfunction were 100%, 91.7%, 16.7%, and 8.3%, respectively. The median survival time after EUS-GBD was 105 days (range 15 - 236 days).

Conclusions: EUS-GBD is a possible alternative route for decompression of the biliary system when ERCP is unsuccessful.

ERCP is the criterion standard for treating malignant obstructive jaundice. However, it is sometimes difficult to perform because of the presence of duodenal stenosis and/or previous surgical reconstruction. EUS-guided bile duct drainage (EUS-BD) techniques such as EUS-guided choledochoduodenostomy (EUS-CDS), EUS-guided hepaticogastrostomy (EUS-HGS), EUS-guided antegrade stenting, and EUS-guided rendezvous stenting (EUS-RVS) are alternative biliary drainage methods after unsuccessful ERCP.[1-10] Recently, EUS-guided gallbladder drainage (EUS-GBD) was reported to be useful for acute cholecystitis.[11-22] Moreover, Jang et al[20] showed that EUS-GBD was comparable to percutaneous transhepatic gallbladder drainage in terms of its technical feasibility, efficacy, and safety of the procedures. Thus, when it is difficult to treat malignant distal biliary obstruction by both ERCP and EUS-BD, EUS-GBD may be a suitable alternative. This is because the gallbladder is a large organ on EUS; this makes EUS-GBD access easier than EUS-CDS or EUS-HGS. EUS-GBD is thus used at our institution to treat malignant obstructive jaundice when other methods are unsuccessful or not feasible. The aim of this study was to evaluate the outcomes of EUS-GBD for obstructive jaundice in terms of technical success, functional success, overall patient survival, adverse events, stent patency, and stent dysfunction.

Abbreviations: EUS-BD, EUS-guided bile duct drainage; EUS-CDS, EUS-guided choledochoduodenostomy; EUS-GBD, EUS-guided gallbladder drainage; EUS-HGS, EUS-guided hepaticogastrostomy; EUS-RVS, EUS-guided rendezvous stenting; PTBD, percutaneous transhepatic biliary drainage; SEMS, self-expandable metal stent.

DISCLOSURE: *All authors disclosed no financial relationships relevant to this publication. This study was supported by grants from the Japan Society for the Promotion of Science (nos. 22590764 and 25461035).*

0016-5107/$36.00
http://dx.doi.org/10.1016/j.gie.2015.12.024

Received July 15, 2015. Accepted December 28, 2015.

Current affiliation: Department of Gastroenterology and Hepatology, Kinki University School of Medicine, Osaka-sayama, Japan.

Reprint requests: Masayuki Kitano, MD, PhD, Department of Gastroenterology and Hepatology, Kinki University School of Medicine, 377-2 Ohno-higashi, Osaka-sayama, 589-8511 Japan.

PATIENTS AND METHODS

Patients

Between January 2006 and October 2014, 511 consecutive patients were admitted to our hospital because of obstructive jaundice caused by unresectable malignant distal biliary stricture. These patients were identified by retrospective review of the medical database of our hospital. This study was approved by the institutional review board of the Kinki University Faculty of Medicine.

Obstructive jaundice was diagnosed in all cases on the basis of the characteristic clinical features (jaundice and

fever), laboratory data (elevated bilirubin levels and alkaline phosphatase levels), and imaging studies. The malignant distal biliary obstruction cases that were difficult to treat with ERCP were managed with the following strategy. In all cases in which ERCP failed, we suggested to the patient that percutaneous transhepatic biliary drainage (PTBD) or EUS-BD could be performed. Those who gave written informed consent to undergo EUS-BD then underwent EUS-BD, including EUS-RVS, EUS-CDS, and EUS-HGS. If EUS-BD was difficult because of the presence of duodenal stenosis, thickened bile-duct wall, intervening vessels, and/or nondilation of the intrahepatic bile ducts, we performed EUS-GBD. The case series reported in this article consisted of all patients who underwent EUS-GBD as a rescue treatment because neither ERCP nor EUS-BD could be performed.

EUS-GBD technique

An echoendoscope (GF-UCT240-AL5; Olympus, Tokyo, Japan) was introduced into the stomach or duodenum. The echoendoscopic images were used to ensure that the cystic duct was intact and dilated before EUS-GBD was performed (if the cystic duct was entrapped by tumor, EUS-GBD was not performed). After visualization of the swollen gallbladder adjacent to the antrum or the duodenal bulb, the echoendoscope was manipulated until an appropriate puncture route without interposing vessels was identified. The neck or body of the gallbladder was generally chosen as the ideal target and was then punctured with a 19-gauge needle (EchoTip Ultra; Cook Medical, Bloomington, Ind) under echoendoscopic guidance (Fig. 1A). The gallbladder was irrigated with saline solution to prevent peritonitis caused by bile leaking out of the 19-gauge needle immediately after the gallbladder was punctured. The gallbladder was irrigated more than 10 times with a saline solution–filled 20-mL syringe. Thus, the total irrigation volume was at least 200 mL. Irrigation was continued until the color of the bile became faint. Thereafter, a sufficient length of 0.035-inch guidewire (Revowave; PIOLAX, Yokohama, Japan) was inserted into the gallbladder lumen until there were more than 2 coils in the lumen (Fig. 1B). The puncture tract was then serially dilated with biliary dilation catheters (6F→7F→9F) (Soehendra Biliary Dilation Catheter; Cook Medical) or a balloon dilator (Max Pass, 4 mm; Olympus) over the guidewire. A self-expandable metal stent (SEMS) (Wallflex partially covered stent, 8 mm in diameter, 6 cm in length; Boston Scientific, Marlborough, Mass) was deployed between the gallbladder and the stomach or the duodenum (Figs. 1C and 1D). This new technique was approved by the institutional review board of the Kinki University Faculty of Medicine.

Assessment of outcomes

The outcomes that were assessed were the technical success rate, functional success rate, adverse events rate, overall patient survival time, and rate of stent dysfunction during patient survival. Technical success was defined as successful stent deployment between the gallbladder lumen and the stomach or duodenum. Functional success was defined as a decrease in bilirubin levels to <50% of the pretreatment value within 2 weeks.[5] The incidence of the following adverse events was assessed: peritonitis, bile leakage, bleeding, stent migration, and stent occlusion. Early and late adverse events were defined as those that presented within and after 30 days of stent placement, respectively. Stent dysfunction was defined as the need for endoscopic, surgical, or percutaneous procedures to improve symptoms after placement of the stent.

RESULTS

In 101 of these 511 patients, ERCP could not be performed due to duodenal involvement of the tumor or postsurgical reconstruction. ERCP was attempted in the remaining 410 patients, which was successful in 376 patients and unsuccessful in 34 patients. ERCP was unsuccessful or not feasible in a total of 135 patients. Seven of these patients elected best supportive care. The remaining 128 patients were advised that they could undergo either PTBD or EUS-BD. PTBD was performed in 11 of the 101 patients unable to undergo ERCP and in 4 of the 34 patients in whom ERCP failed. The remaining 113 did not want to undergo PTBD because they wanted to avoid the external drainage tube. EUS-BD, including EUS-RVS, EUS-CDS, and EUS-HGS, was then attempted in these 113 patients. In 12 of these patients, EUS-BD was not possible or failed because of the presence of duodenal stenosis, thickened bile duct walls, intervening vessels, and/or nondilation of the intrahepatic bile ducts. These 12 patients then underwent EUS-GBD (the first case in February 2009), as described in Figure 2. The remaining 101 patients underwent successful EUS-BD. The demographic and clinical characteristics of the 12 patients who underwent EUS-GBD are shown in Table 1. The patients were, on average, 67.3 ± 13.9 years old, and 8 were male. The main primary disease was pancreatic cancer, followed by lymph node metastasis, bile duct cancer, and malignant lymphoma. The EUS-GBD procedure was performed via the stomach in 7 patients and the duodenum in 5 patients. In 7 patients, a plastic double pigtail stent was inserted in the SEMS to prevent stent migration. The technical success and functional success rates were 100% (12/12) and 91.7% (11/12), respectively. The 1 patient who did not exhibit functional success had sustained hyperbilirubinemia for 2 weeks because of rapid tumor progression. Two early adverse events were observed in this study. One was peritonitis that improved with conservative treatment. The other was stent dysfunction that was due to entrapment of the cystic duct by the growing

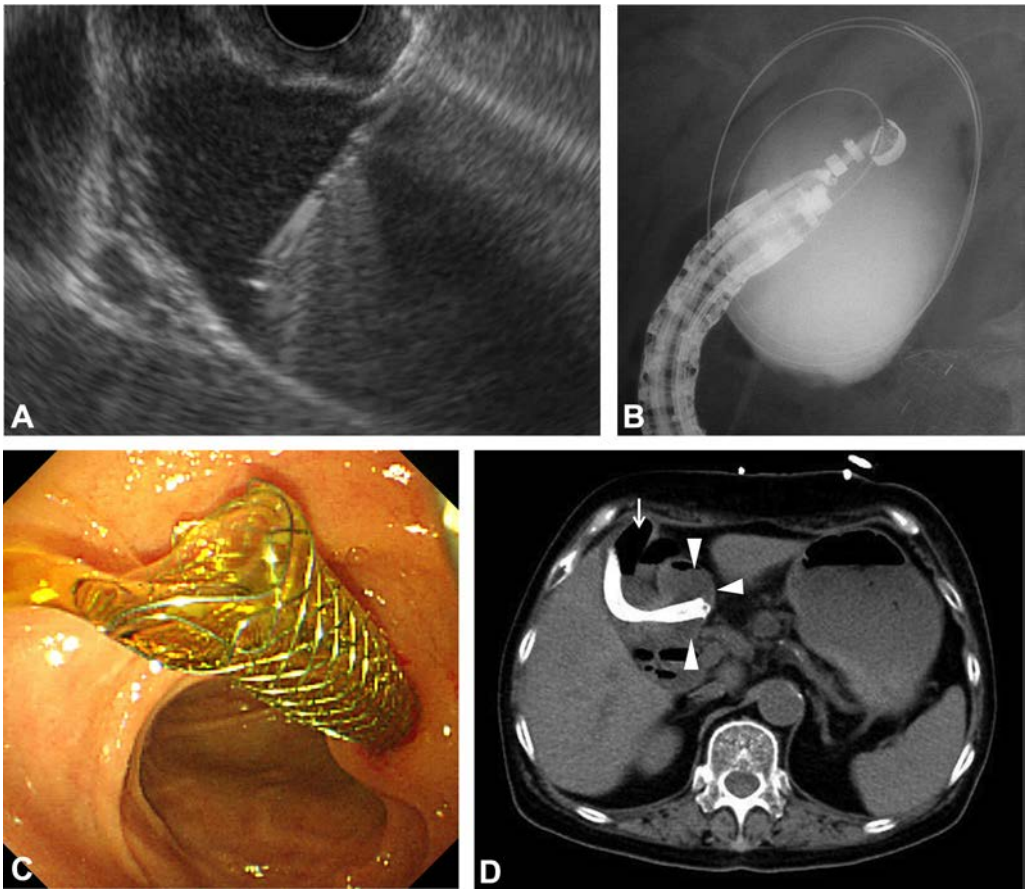

Figure 1. The EUS-guided gallbladder drainage procedure. **A**, Puncture of the gallbladder (EUS image). The neck of the gallbladder is punctured from the gastric antrum with a 19-gauge needle. **B**, Insertion of the guidewire (fluoroscopic image). A sufficient length of a 0.035-inch guidewire is inserted through the needle into the gallbladder so that it forms more than 2 coils in the gallbladder lumen. **C**, Deployment of a metal stent (endoscopic image). A self-expandable metal stent is inserted through the puncture tract into the gallbladder lumen from the duodenal bulb. **D**, Confirmation of deployment of the metal stent (CT image). A self-expandable metal stent is deployed between the gallbladder lumen (*arrow*) and the bulb of the duodenum (*arrowheads*).

tumor. PTBD was performed as a reintervention in this case. There were no late adverse events. No bleeding or stent migration occurred throughout the observation period. Thus, the adverse event rate was 16.7% (2/12), and the stent dysfunction rate was 8.3% (1/12). At the time that the records were subjected to retrospective evaluation (December 31, 2014), all 12 patients had died. The median survival time after EUS-GBD for these patients was 105 days.

Regarding the 101 patients who successfully underwent EUS-BD, the technical success, functional success, and adverse events rates were 92.1%, 84.2%, and 19.8%, respectively.

DISCUSSION

EUS-GBD was recently reported to be useful for acute cholecystitis.[11-22] The current study is the first case series on the feasibility of EUS-GBD for malignant obstructive jaundice. In this study, EUS-GBD was performed when ERCP was unsuccessful or not feasible and EUS-BD was difficult to perform. Several studies have reported on the usefulness of EUS-BD in malignant obstructive jaundice when ERCP is unsuccessful: the functional success and adverse event rates of this procedure were 67% to 100% and 0% to 46%, respectively.[1-10] Our study showed that the functional success and adverse event rates in the 101 patients who were successfully managed with EUS-BD were similar (84.2% and 19.8%, respectively). With regard to the 12 patients who could not be managed with either ERCP or EUS-BD and had to be managed with EUS-GBD, the functional success and adverse event rates appear to be similar to those for EUS-BD (91.7% and 16.7%, respectively). Thus, this study shows that EUS-GBD may be useful as an alternative treatment option for malignant stricture of the distal bile duct after transpapillary drainage has failed.

The main risk of EUS-BD is bile leakage into the peritoneal space, which can cause bile peritonitis. The bile

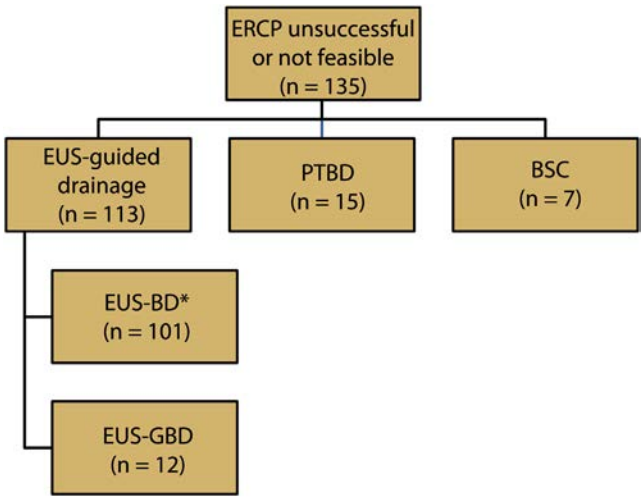

Figure 2. Flow chart representing progress of rescue treatment of malignant distal biliary obstruction after the ERCP was unsuccessful or not feasible. *EUS-BD includes EUS-guided choledochoduodenostomy, hepaticogastrostomy, and rendezvous stenting. *BSC*, best supportive care; *EUS-BD*, EUS-guided bile duct drainage; *EUS-GBD*, EUS-guided gallbladder drainage; *PTBD*, percutaneous transhepatic biliary drainage.

TABLE 1. Demographic, clinical characteristics, and outcomes of patients who underwent EUS-guided gallbladder drainage for malignant distal biliary obstruction

Age, y, mean ± SD	67.3 ± 13.9
Sex, male/female, n	8/4
Primary disease, % (n/N)	
Pancreatic cancer	50.0 (6/12)
Bile duct cancer	16.7 (2/12)
Lymph node metastasis	25.0 (3/12)
Malignant lymphoma	8.3 (1/12)
Technical success rate, % (n/N)	100 (12/12)
Functional success rate, % (n/N)	91.7 (11/12)
Adverse events, % (n/N)	16.7 (2/12)
Overall survival, days median (range)	105 (15–236)
Stent dysfunction during patient survival, % (n/N)	8.3 (1/12)

leakage is caused by migration of the stent and the gap between the fistula and the stent.[11-13] In this case series, several techniques were used to avoid such bile leakage. First, the guidewire was inserted until at least 2 coils were in the lumen. The gallbladder lumen has more space for coiling than the bile duct. Such coiling yields better stability compared with that with the EUS-CDS or HGS technique. Second, we irrigated the gallbladder lumen with saline solution after puncturing the gallbladder and before proceeding to the next step. This irrigation procedure may reduce the chance of peritonitis due to bile leakage during dilation. We also used SEMSs in our study. Compared with plastic stents, SEMSs are better at sealing the gap between the stent and the needle tracts of the gallbladder wall, thus preventing bile leakage.[14] Notably, 2 separate groups have reported that using novel lumen-apposing metal stents with anchor flanges and flares for EUS-GBD results in excellent outcomes.[19,21] Thus, such EUS-GBD–specific stents may yield even better and safer outcomes than SEMSs.

In this study, balloon dilation was chosen as the first-line dilation method rather than cautery dilation because we were afraid of the risk of bleeding due to burning gastroduodenal and gallbladder walls. However, cautery dilation may lead to a rapid procedure. Lumen-apposing metal stents equipped with a cautery tip in the delivery system were recently developed. This allows single-step EUS-GBD from puncture to deployment of the stent with a single maneuver.[23]

This study has a few limitations. First, the number of EUS-GBD patients was small, and all patients were from a single institution. Second, the indications for EUS-GBD were limited because this procedure was only performed in patients in whom EUS-BD was unsuccessful or not feasible. A larger study that compares the efficacy and safety of EUS-GBD and EUS-BD is warranted.

In conclusion, EUS-GBD is a possible alternative route for decompression of the biliary system when conventional ERCP is unsuccessful.

REFERENCES

1. Giovannini M, Moutardier V, Pesenti C, et al. Endoscopic ultrasound-guided bilioduodenal anastomosis: a new technique for biliary drainage. Endoscopy 2001;33:898-900.
2. Will U, Thieme A, Fueldner F, et al. Treatment of biliary obstruction in selected patients by endoscopic ultrasonography (EUS)-guided transluminal biliary drainage. Endoscopy 2007;39:292-5.
3. Burmester E, Niehaus J, Leineweber T, et al. EUS-cholangio-drainage of the bile duct: report of 4 cases. Gastrointest Endosc 2003;57:246-51.
4. Kim YS, Gupta K, Mallery S, et al. Endoscopic ultrasound rendezvous for bile duct access using a transduodenal approach: cumulative experience at a single center. A case series. Endoscopy 2010;42:496-502.
5. Siddiqui AA, Sreenarasimhaiah J, Lara LF, et al. Endoscopic ultrasound-guided transduodenal placement of a fully covered metal stent for palliative biliary drainage in patients with malignant biliary obstruction. Surg Endosc 2011;25:549-55.
6. Nguyen-Tang T, Binmoeller KF, Sanchez-Yague A, et al. Endoscopic ultrasound (EUS)-guided transhepatic anterograde self-expandable metal stent (SEMS) placement across malignant biliary obstruction. Endoscopy 2010;42:232-6.
7. Hara K, Yamao K, Niwa Y, et al. Prospective clinical study of EUS-guided choledochoduodenostomy for malignant lower biliary tract obstruction. Am J Gastroenterol 2011;106:1239-45.
8. Komaki T, Kitano M, Sakamoto H, et al. Endoscopic ultrasonography-guided biliary drainage: evaluation of a choledochoduodenostomy technique. Pancreatology 2011;11(Suppl 2):47-51.
9. Dhir V, Bhandari S, Bapat M, et al. Comparison of EUS-guided rendezvous and precut papillotomy techniques for biliary access (with videos). Gastrointest Endosc 2012;75:354-9.
10. Vila JJ, Perez-Miranda M, Vazquez-Sequeiros E, et al. Initial experience with EUS-guided cholangiopancreatography for biliary and pancreatic duct drainage: a Spanish national survey. Gastrointest Endosc 2012;76:1133-41.

11. Baron TH, Topazian MD. Endoscopic transduodenal drainage of the gallbladder: implications for endoluminal treatment of gallbladder disease. Gastrointest Endosc 2007;65:735-7.
12. Kwan V, Eisendrath P, Antaki F, et al. EUS-guided cholecystenterostomy: a new technique (with videos). Gastrointest Endosc 2007;66:582-6.
13. Lee SS, Park do H, Hwang CY, et al. EUS-guided transmural cholecystostomy as rescue management for acute cholecystitis in elderly or high-risk patients: a prospective feasibility study. Gastrointest Endosc 2007;66:1008-12.
14. Takasawa O, Fujita N, Noda Y, et al. Endosonography-guided gallbladder drainage for acute cholecystitis following covered metal stent deployment. Dig Endosc 2009;21:43-7.
15. Itoi T, Itokawa F, Kurihara T. Endoscopic ultrasonography-guided gallbladder drainage: actual technical presentations and review of the literature (with videos). J Hepatobiliary Pancreat Sci 2011;18:282-6.
16. Song TJ, Park do H, Eum JB, et al. EUS-guided cholecystoenterostomy with single-step placement of a 7F double-pigtail plastic stent in patients who are unsuitable for cholecystectomy: a pilot study (with video). Gastrointest Endosc 2010;71:634-40.
17. Jang JW, Lee SS, Park do H, et al. Feasibility and safety of EUS-guided transgastric/transduodenal gallbladder drainage with single-step placement of a modified covered self-expandable metal stent in patients unsuitable for cholecystectomy. Gastrointest Endosc 2011;74:176-81.
18. Kamata K, Kitano M, Komaki T, et al. Transgastric endoscopic ultrasound (EUS)-guided gallbladder drainage for acute cholecystitis. Endoscopy 2009;41(Suppl 2):E315-6.
19. Itoi T, Binmoeller KF, Shah J, et al. Clinical evaluation of a novel lumen-apposing metal stent for endosonography-guided pancreatic pseudocyst and gallbladder drainage (with videos). Gastrointest Endosc 2012;75:870-6.
20. Jang JW, Lee SS, Song TJ, et al. Endoscopic ultrasound-guided transmural and percutaneous transhepatic gallbladder drainage are comparable for acute cholecystitis. Gastroenterology 2012;142:805-11.
21. De la Serna-Higuera C, Perez-Miranda M, Gil-Simon P, et al. EUS-guided transenteric gallbladder drainage with a new fistula-forming, lumen-apposing metal stent. Gastrointest Endosc 2013;77:303-8.
22. Ogura T, Masuda D, Imoto A, et al. EUS-guided gallbladder drainage and hepaticogastrostomy for acute cholecystitis and obstructive jaundice (with video). Endoscopy 2014;46(Suppl 1 UCTN):E75-6.
23. Teoh AY, Binmoeller KF, Lau JY. Single-step EUS-guided puncture and delivery of a lumen-apposing stent for gallbladder drainage using a novel cautery-tipped stent delivery system. Gastrointest Endosc 2014;88:1171.

Preface

Digestive Diseases

Dig Dis 2016;34:617–619
DOI: 10.1159/000448821

Chronic Liver Diseases and Liver Cancer: State-of-the Art Progress in 2016

Masatoshi Kudo

Department of Gastroenterology and Hepatology, Kindai University Faculty of Medicine, Osaka-Sayama, Japan

The 13th Japan-Korea Liver Symposium was held in Kyoto on May 25–26, 2016, in conjunction with the 89th annual meeting of the Japan Society of Ultrasonics in Medicine, 12th Congress of Asian Federation of Societies for Ultrasound in Medicine and Biology, and 8th Congress of Asian Conference on Ultrasound Contrast Imaging.

Hagiwara et al. [1] evaluated the efficacy of direct-acting antiviral drugs for asunaprevir (ASV) and daclatasvir (DCV) for hepatitis C virus (HCV). The authors found that ASV/DCV combination therapy achieved sustained viral response (SVR) at 24 weeks in 106 of 120 (88%) patients with HCV. They also stated that surveillance of hepatocellular carcinoma (HCC) is very important since risk of HCC development in patients who achieved SVR still exists.

Sugimoto et al. [2] evaluated the efficacy and safety of sofosbuvir plus rivavirin treatment for patients with chronic hepatitis C (CHC) genotype 2. They reported that all patients (17/17) under sofosbuvir plus rivavirin treatment achieved end-of-treatment response. They also found that this combination therapy had an acceptable safety profile and resulted in no discontinuation of the treatment, irrespective of age or the effect of the polymorphisms of the inosine triphosphatase gene.

Nishida et al. [3] also evaluated the safety, tolerability and efficacy of sofosbuvir plus rivavirin therapy in elderly patients infected with HCV genotype 2. They found that 37 of 41 patients achieved SVR 12 (90.2%). They reported that the aged group (>75 years) showed a lower SVR rate (81.3%) at 12 weeks than the non-aged group (<75 years) (96.0%). They concluded that this combination therapy of sofosbuvir plus RBV is tolerable and beneficial not only in younger (<75) patients but also in elderly (>75) patients.

Wu et al. [4] evaluated the two-dimensional shear wave elastography (2D SWE) as compared with real-time tissue elastography (RTE) for assessing liver fibrosis in patients with chronic hepatitis B (CHB). They concluded that 2D SWE obtained by Aixplorer US system (SuperSonic Imaging) was more accurate than RTE obtained by Ascendus (Hitachi) in the assessment of significant fibrosis and cirrhosis in patients with CHB. However, the measurement values and diagnostic performance obtained by 2D SWE are more affected by the inflammation fluctuations.

Yada et al. [5] evaluated the prospective risk analysis of HCC in patients with CHC by ultrasound strain elastography. Respective cumulative liver cancer incidence rates at 5 years in patients whose liver fibrosis index (LFI) determined by RTE of <2.0, 2–2.8 and >2.8 were 0%, 19.9 and 31.4% ($p = 0.011$) respectively. They concluded that measurement of LFI by strain imaging can successfully predict liver cancer risk in patients with chronic HCV infection.

Takita et al. [6] reported the epock-making therapy for polycystic liver disease, monoethanolamine oleate (EO) sclerotherapy. They concluded that EO infusion therapy achieves a fairly high treatment response in the volume reduction (99%) and sustained shrinkage over long-term follow-up. Therefore, this is a breakthrough technique in

KARGER

E-Mail karger@karger.com
www.karger.com/ddi

0257–2753/16/0346–0617$39.50/0

Masatoshi Kudo, MD, PhD
Department of Gastroenterology and Hepatology
Kindai University Faculty of Medicine
377-2 Ohno-Higashi, Osaka-Sayama, Osaka 589-8511 (Japan)
E-Mail m-kudo@med.kindai.ac.jp

the treatment of polycystic liver disease as well as simple cyst and should be a standard of care for this disease.

Chishina et al. [7] evaluated the clinical effect of tolvaptan, a vasopressin receptor antagonist, for refractory ascites in patients with decompensated liver cirrhosis. They concluded that the diuretic effect of tolvaptan may decrease in renal hypofunction patients. They also stated that continuation of tolvaptan administration is an option even though the early treatment effect is poor since its delayed effect was sometimes observed.

Kim et al. [8] evaluated the association of coffee intake and liver enzyme in Korean immigrants and Japanese. They found that coffee may inhibit hepatic damage caused by alcohol drinking and smoking both in Korean immigrants and Japanese.

Arizumi et al. [9] reported a validation study of Kinki criteria, a modified substaging system, in patients with intermediate stage HCC. They concluded that the performance of Kinki criteria is useful in determining the treatment strategy for HCC in the intermediate (BCLC B) stage.

Iwamoto et al. [10] evaluated the ability of Gd-EOB-DTPA enhanced MRI and contrast-enhanced ultrasound (CEUS) using sonazoid in the diagnosis of macroscopic type of 79 surgically resected HCCs. They concluded that the diagnostic performance for macroscopic classification of HCC of CEUS was comparable with that of Gd-EOB-DTPA enhanced MRI. Furthermore, they stated that the combination of the two modalities had a more accurate diagnostic performance.

Minami et al. [11] described US–US fusion imaging in radiofrequency ablation (RFA) for liver metastases. They concluded that US–US fusion imaging can contribute to RFA therapy with a safety margin since the image overlay of US–US fusion imaging allows the evaluation of the ablative margin three-dimensionally in real-time.

Kawasaki et al. [12] described the usefulness of CEUS as treatment guidance at RFA therapy for HCC [13–16] after transcatheter arterial chemoembolization (TACE) [17, 18]. They stated the success rate of initial RFA guided by CEUS was 100% (22/22 HCCs) as compared with that guided by B mode US alone of 83.3% (15/18 HCCs).

Ogawa et al. [19] evaluated the usefulness of SYNAPSE VINCENT in the prediction of embolization area after TACE for HCC. They stated that this new technology, automatic prediction software of SYNAPSE VINCENT, has possibilities to reduce the amount of contrast medium, decrease radiation exposure and improve the therapeutic effect of TACE.

Nagai et al. [20] reported the role of tight junction protein ZO-1 (TJP1) and TWIST expression on postoperative survival of patients with HCC. Apparently, epithelial mesenchymal transition plays a critical role in cancer progression and metastasis. They stated that the upregulation of TWIST and the downregulation of TJP1 were significantly associated with sorter recurrence free survival as well as overall survival after surgical resection. They concluded that the low level of TJP1 and high level of TWIST expression are prognostic factors predicting the prevalence of HCC after surgical resection.

Nishida and Kudo [21] described the clinical significance of epigenetic alterations in human HCC and its association with genetic mutations. They stated that differentiation therapy is one of the potential approaches for HCC with advanced epigenetic alterations. On the other hand, a tumor changing an accumulation of genetic mutations would be good targets for immune reactions; thus, immune checkpoint blockade [22] should be effective for HCCs with genetic hypermutation.

Kudo [23] described the recent trend in the management of HCC, with special emphasis on treatment by regorafenib and immune checkpoint inhibitors. The author clearly states that regorafenib, as second-line systemic treatment, prolongs survival in patients with intermediate and advanced HCC who continued treatment with sorafenib [24–26]. Furthermore, immune checkpoint inhibitors are promising in the management of HCCs since clinical trials of PD-1 antibody, nivolumab, showed promising results in the treatment of advanced HCC.

Finally, I strongly believe that this special issue 'Chronic Liver Diseases and Liver Cancer: State-of-the Art Progress in 2016' will be beneficial and invaluable for all readers who specialize in understanding liver diseases including liver cancer.

References

1 Hagiwara S, Nishida N, Watanabe T, Sakurai T, Ida H, Minami Y, Takita M, Minami T, Iwanishi M, Chishina H, Ueshima K, Komeda Y, Arizumi T, Kudo M: Outcome of asunaprevir/daclatasvir combination therapy for chronic liver disease type C. Dig Dis 2016;34:620–626.

2 Sugimoto K, Kim SK, Kim SR, Kobayashi M, Kato A, Morimoto E, Imoto S, Kim CW, Tanaka Y, Kudo M, Yano Y, Hayashi Y: Efficacy and safety of sofosbuvir plus ribavirin treatment for patients with chronic hepatitis C genotype 2. Dig Dis 2016;34:627–631.

3 Nishida N, Kono M, Minami T, Chishina H, Arizumi T, Takita M, Yada N, Ida H, Hagiwara S, Minami Y, Ueshima K, Sakurai T, Kudo M: Safety, tolerability, and efficacy of sofosbuvir plus ribavirin in elderly patients infected with hepatitis C virus genotype 2. Dig Dis 2016;34:632–639.

4 Wu T, Wang P, Zhang T, Zheng J, Li SY, Zeng J, Kudo M, Zheng RQ: Comparison of two-dimensional shear wave elastography and real-time tissue elastography for assessing liver fibrosis in chronic hepatitis B. Dig Dis 2016;34:640–649.
5 Yada N, Sakurai T, Kudo M, Minami T, Arizumi T, Takita M, Hagiwara S, Ueshima K, Ida H, Nishida N: Prospective risk analysis of hepatocellular carcinoma in patients with chronic hepatitis C by ultrasound strain elastography. Dig Dis 2016;34:650–653.
6 Takita M, Iwanishi M, Minami T, Kono M, Chishina H, Arizumi T, Yada N, Hagiwara S, Minami Y, Ida H, Ueshima K, Nishida N, Kudo M: Monoethanolamine oleate sclerotherapy for polycystic liver disease. Dig Dis 2016;34:654–658.
7 Chishina H, Hagiwara S, Nishida N, Ueshima K, Sakurai T, Ida H, Minami Y, Takita M, Kono M, Minami T, Iwanishi M, Umehara Y, Watanabe T, Komeda Y, Arizumi T, Kudo M: Clinical factors predicting the effect of tolvaptan for refractory ascites in patients with decompensated liver cirrhosis. Dig Dis 2016;34:659–664.
8 Kim SK, Shin MH, Sugimoto K, Kim SR, Imoto S, Kim KI, Taniguchi M, Oh HK, Yano Y, Hayashi Y, Kudo M: Coffee intake and liver enzyme association in Korean immigrants and Japanese: a comprehensive cross-sectional study. Dig Dis 2016;34:665–670.
9 Arizumi T, Ueshima K, Iwanishi M, Minami T, Chishina H, Kono M, Takita M, Kitai S, Inoue T, Yada N, Hagiwara S, Minami Y, Ida H, Sakurai T, Kitano M, Nishida N, Kudo M: Validation of kinki criteria, a modified substaging system, in patients with intermediate stage hepatocellular carcinoma. Dig Dis 2016;34:671–678.
10 Iwamoto T, Imai Y, Kogita S, Igura T, Sawai Y, Fukuda K, Yamaguchi Y, Matsumoto Y, Nakahara M, Morimoto O, Seki Y, Ohashi H, Fujita N, Kudo M, Takehara T: Comparison of contrast-enhanced ultrasound and gadolinium-ethoxybenzyl-diethylenetriamine pentaacetic acid-enhanced MRI for the diagnosis of macroscopic type of hepatocellular carcinoma. Dig Dis 2016;34:679–686.
11 Minami Y, Minami T, Chishina H, Kono M, Arizumi T, Takita M, Yada N, Hagiwara S, Ida H, Ueshima K, Nishida N, KUdo M: US-US fusion imaging in radiofrequency ablation for liver metastases. Dig Dis 2016;34:687–691.
12 Kawasaki T, Hata KY, Kinoshita D, Takayama M, Okuda H, Mizuno S, KUdo M: Radiofrequency ablation guided by contrast-enhanced sonography versus B-mode sonography for hepatocellular carcinoma after transcatheter arterial chemoembolization. Dig Dis 2016;34:692–695.
13 Teng W, Liu KW, Lin CC, Jeng WJ, Chen WT, Sheen IS, Lin CY, Lin SM: Insufficient ablative margin determined by early computed tomography may predict the recurrence of hepatocellular carcinoma after radiofrequency ablation. Liver Cancer 2015;4:26–38.
14 Kudo M: Locoregional therapy for hepatocellular carcinoma. Liver Cancer 2015;4:163–164.
15 Kang TW, Rhim H: Recent advances in tumor ablation for hepatocellular carcinoma. Liver Cancer 2015;4:176–187.
16 Lencioni R, de Baere T, Martin RC, Nutting CW, Narayanan G: Image-guided ablation of malignant liver tumors: recommendations for clinical validation of novel thermal and non-thermal technologies – a western perspective. Liver Cancer 2015;4:208–214.
17 Kudo M: Surveillance, diagnosis, treatment, and outcome of liver cancer in Japan. Liver Cancer 2015;4:39–50.
18 Tsurusaki M, Murakami T: Surgical and locoregional therapy of HCC: TACE. Liver Cancer 2015;4:165–175.
19 Ogawa C, Minami Y, Morita M, Noda A, Arasawa S, Izuta M, Kubo A, Matsunaka T, Tamaki N, Shibatouge M, Kudo M: Prediction of embolization area after conventional transcatheter arterial chemoembolization for hepatocellular carcinoma using SYNAPSE VINCENT. Dig Dis 2016;34:696–701.
20 Nagai T, Arao T, Nishio K, Matsumoto K, Hagiwara S, Sakurai T, Minami Y, Ida H, Ueshima K, Nishida N, Sakai K, Saijo N, Kudo K, Kaneda H, Tamura D, Aomatsu K, Kimura H, Fujita Y, Haji S, Kudo M: Impact of tight junction protein ZO-1 and TWIST expression on postoperative survival of patients with hepatocellular carcinoma. Dig Dis 2016;34:702–707.
21 Nishida N, Kudo M: Clinical significance of epigenetic alterations in human hepatocellular carcinoma and its association with genetic mutations. Dig Dis 2016;34:708–713.
22 Kudo M: Immune checkpoint blockade in hepatocellular carcinoma. Liver Cancer 2015;4:201–207.
23 Kudo M: Recent trends in the management of hepatocellular carcinoma with special emphasis on treatment with regorafenib and immune checkpoint inhibitors. Dig Dis 2016;34:714–730.
24 Arizumi T, Ueshima K, Minami T, Kono M, Chishina H, Takita M, Kitai S, Inoue T, Yada N, Hagiwara S, Minami Y, Sakurai T, Nishida N, Kudo M: Effectiveness of sorafenib in patients with transcatheter arterial chemoembolization (TACE) refractory and intermediate-stage hepatocellular carcinoma. Liver Cancer 2015;4:253–262.
25 Raoul JL, Gilabert M, Piana G: How to define transarterial chemoembolization failure or refractoriness: a European perspective. Liver Cancer 2014;3:119–124.
26 Peck-Radosavljevic M: Drug therapy for advanced-stage liver cancer. Liver Cancer 2014;3:125–131.

Original Article

Digestive Diseases

Dig Dis 2016;34:620–626
DOI: 10.1159/000448822

Outcome of Asunaprevir/Daclatasvir Combination Therapy for Chronic Liver Disease Type C

Satoru Hagiwara Naoshi Nishida Tomohiro Watanabe Toshiharu Sakurai Hiroshi Ida Yasunori Minami Masahiro Takita Tomohiro Minami Mina Iwanishi Hirokazu Chishina Kazuomi Ueshima Yoriaki Komeda Tadaaki Arizumi Masatoshi Kudo

Department of Gastroenterology and Hepatology, Kindai University Faculty of Medicine, Osaka-Sayama, Japan

Key Words
Asunaprevir · Daclatasvir · Hepatocellular carcinoma

Abstract
Objective: Treatment for chronic hepatitis C has recently developed in a very rapid manner. In Japan, in September 2014, IFN-free asunaprevir (ASV) and daclatasvir (DCV) became available for combination therapy. We report the treatment outcomes achieved at our hospital using this combination therapy. ***Methods:*** Sustained virological response (SVR) 24 could be evaluated in 120 of 125 patients with chronic liver disease type C who visited our hospital and were treated with ASV/DCV after September 2014, and these patients were analyzed. ***Results:*** SVR24 was achieved in 106 patients (88%). End-of-treatment response was not achieved in 10 patients (8.3%). Five of them carried multiple-resistant NS3/4A or NS5A region, and administration was discontinued early in 4 patients due to adverse effects. After ASV/DCV treatment, hepatocellular carcinoma (HCC) developed in 2 patients (1.7%) and recurred in 5 (4.2%). ***Conclusions:*** ASV/DCV treatment achieved favorable SVR in elderly and hepatic cirrhosis patients and patients in whom HCC was cured. However, an increase in the incidence of HCC development in patients who markedly respond to direct-acting antivirals treatment is expected and surveillance of HCC becomes more important.

Introduction

It is estimated that more than 700,000 people die of hepatitis C virus (HCV)-related disease annually over the world. In Japan, the actual number of deaths due to hepatocellular carcinoma (HCC) is 31,000/year, being the 4th highest following diseases of the lung, stomach, and the large intestine. HCV is still the most frequent cause of death from HCC [1–3], and development of therapeutic drugs for cure against HCV has long been awaited.

Treatment for chronic hepatitis C has rapidly developed, and direct-acting antiviral drugs (DAA), telaprevir [4–6] and simeprevir [7–11], were approved in 2011 and 2013, respectively, improving the efficacy. However, it is essential that these drugs be combined with PEG-IFN and RBV, thus increasing the tolerability. It is difficult to ad-

KARGER

E-Mail karger@karger.com
www.karger.com/ddi

0257–2753/16/0346–0620$39.50/0

Satoru Hagiwara, MD, PhD
Department of Gastroenterology and Hepatology
Kindai University Faculty of Medicine
377-2 Ohno-Higashi, Osaka-Sayama, Osaka 589-8511 (Japan)
E-Mail hagi-318@hotmail.co.jp

minister these drugs to the elderly and patients with an underlying disease, such as hepatic cirrhosis, depression, and anemia, and many such patients have died of liver cancer.

Because of this background, development of more tolerable treatment methods ensuring efficacy has been much awaited. In Japan, in September 2014, IFN-free asunaprevir (ASV) and daclatasvir (DCV) became available for combination therapy [12–15]. We report the treatment outcomes achieved at our hospital.

Methods

Patients and Treatment Schedule

Sustained virological response (SVR) 24 could be evaluated in 120 of 125 patients with chronic liver disease type C who visited our hospital and were treated with ASV/DCV after September 2014, and these patients were analyzed. The duration of administration of ASV/DCV was 24 weeks, and the course was followed for 24 weeks after treatment completion. DCV was orally administered at 60 mg once a day, and ASV was orally administered at 100 mg twice a day. When liver disorder developed, the dose of ASV was reduced to 100 mg once a day based on judgment by the attending physician.

Resistance Test

Resistances of HCV NS5A and NS3/4A were measured using the PCR-invader method. The rates of mutant virus below 1, 1–20, and 20% or higher were judged as negative, weakly positive, and positive, respectively.

Statistical Analysis

Changes in hepatic spare ability were analyzed using Student t test. $p < 0.05$ was considered significant.

Results

Patients

SVR24 could be evaluated in 120 of 125 patients with chronic liver disease type C who visited our hospital and were treated with ASV/DCV after September 2014, and these patients were analyzed. The median age was 72, and 73 (61%) and 53 (44%) patients were 65 years or older and 75 years or older, respectively, showing that more elderly patients were treated compared with those in a phase 3 clinical study performed in Japan. Seventy-four hepatic cirrhosis patients (63%) were included and the drugs were administered to 34 patients (28%) after cure of liver cancer. Regarding previous treatment, 36 patients (28%) were naïve, IFN was ineffective for 12 patients (10%), the disease relapsed in 8 patients (7%), and 64 patients (54%) were ineligible/intolerable with IFN, being most frequently noted (table 1).

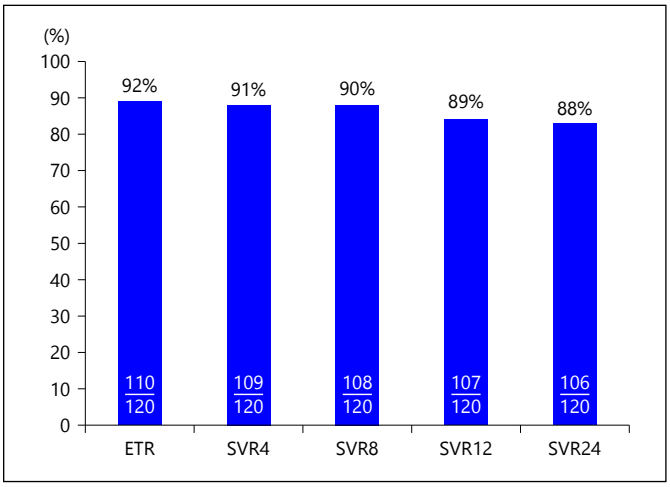

Color version available online

Fig. 1. Antiviral effect (ITT). Of the 120 patients, 110 (92%) achieved the ETR but the disease subsequently relapsed in 4 within 24 weeks after treatment completion. Thus, SVR24 was achieved in 106 patients (88%).

Table 1. Patient background

Characteristics	n = 120
Age, years	
Median (range)	72 (26–87)
>65, n (%)	73 (61)
>75, n (%)	53 (44)
Male gender, n (%)	54 (45)
Cirrhosis, n (%)	74 (63)
History of HCC, n (%)	34 (28)
Prior therapy, n (%)	
Naïve	36 (28)
NR	12 (10)
Relapse	8 (7)
Intolerant	20 (17)
Ineligible	44 (37)

Virological Response

Of the 120 patients, 110 (92%) achieved the end-of-treatment response (ETR), but the disease subsequently relapsed in 4 patients within 24 weeks after treatment completion. Thus, SVR24 was achieved in 106 patients (88%; fig. 1).

Virological Ineffectiveness

ETR was not achieved in 10 patients (8.3%). Five of them carried multiple-resistant NS3/4A or NS5A region, and administration was discontinued early in 4 of them due to adverse effects (table 2). The disease relapsed after completion of 24-week treatment in 4 patients (table 3). Drug resistance and achievement of SVR are depicted in fig. 2.

Table 2. Patients who did not achieve ETR

Age	Sex	Previous treatment	Hepatic cirrhosis	Previous HCC treatment	Drug resistance before DAAs	Adverse effect
60	F	Ineffective	Present	Absent	D168E, Y93H strongly positive	No
65	F	Initial treatment	Present	Absent	Q80L, D168E strongly positive	No
54	M	Relapse	Present	Absent	Q80L, D168V strongly positive	No
71	F	Initial treatment	Present	Absent	Y93H, T54A weakly positive	No
77	F	Ineffective	Absent	Absent	D168V, Y93H weakly positive	No
68	F	Initial treatment	Present	Present	No	No
68	F	Initial treatment	Present	Present	No	Anxiety neurosis discontinued on day 2
76	F	Ineligible (elderly)	Present	Absent	No	Ear noises discontinued on day 13
78	F	Intolerable (malaise)	Absent	Absent	No	Skin eruption discontinued on day 14
72	F	Initial treatment	Present	Present	No	Marked ascites discontinued on day 25

Table 3. Patients with relapse

Age	Gender	Previous treatment	Hepatic cirrhosis	Previous HCC treatment	Drug resistance before DAAs	Adverse effect
68	M	Intolerable (interstitial pneumonia)	Present	Present	D168H, T weakly positive	No
56	F	Intolerable (depression)	Present	Present	No	No
72	F	Initial treatment	Present	Present	No	No
82	M	Ineligible (elderly)	Present	Present	Q80R weakly positive	No

The SVR24 achievement rates were 89, 92, and 33% in Y93H-negative, -weakly positive, and -positive patients, respectively (fig. 2a).

In patients with resistant D168A/E/T/V without resistant NS5A, the rates were 91, 89, and 0% in negative, weakly positive, and positive patients, respectively (fig. 2d). Changes in hepatic spare ability after treatment are depicted in fig. 3.

The serum ALB level was 3.9 ± 0.5 (mean ± SD) at the time of treatment introduction and 4.0 ± 0.4 at treatment completion, showing no change (fig. 3a). When the patients were divided into those with chronic hepatitis and hepatic cirrhosis, significant improvement from 3.7 ± 0.5 to 3.9 ± 0.4 was noted in the hepatic cirrhosis patients (fig. 3c, $p = 0.008$). No significant improvement was noted in the platelet (PLT) count in overall, chronic hepatitis, or hepatic cirrhosis patients (fig. 3a–c).

Adverse Effects that Resulted in the Discontinuation of Medication

Adverse effects that resulted in the discontinuation of medication developed in 8 patients (6.6%), and the most frequent event was serum alanine aminotransferase (ALT) elevation noted in 3 patients (2.5%), but all 3 patients achieved SVR24. Seven (88%) of the 8 patients were with hepatic cirrhosis (table 4).

Patients with HCC Development and Recurrence after ASV/DCV Treatment

After ASV/DCV treatment, HCC developed in 2 patients (1.7%) and recurred in 5 patients (4.2%). Most of these 7 patients were elderly people aged 65 or older, male, and with hepatic cirrhosis. All patients were not previously treated with IFN (table 5). HCC developed or recurred in patients in whom AFP was not converted to negative at the time of DAAs treatment completion. In

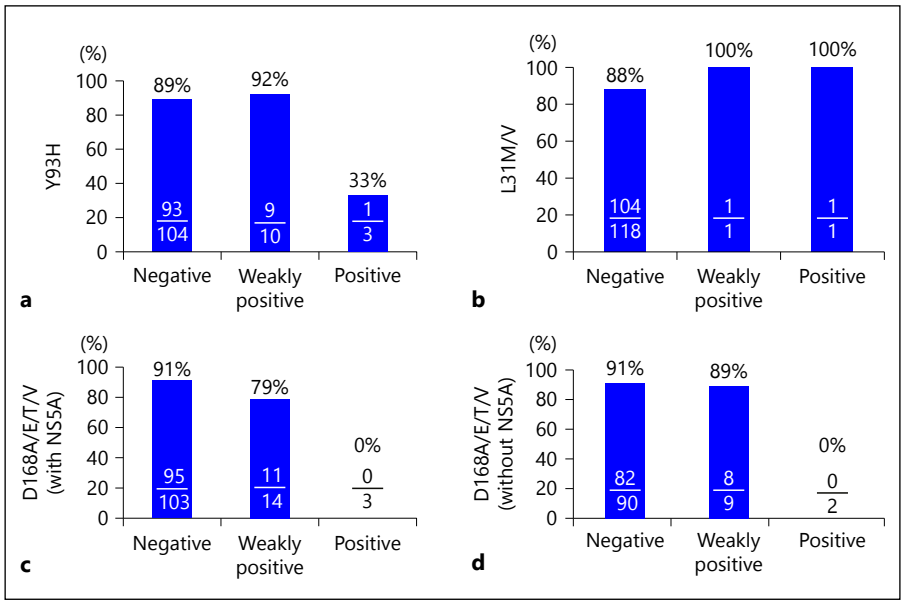

Fig. 2. Drug resistance (PCR-invader) and SVR achievement rate. The SVR24 achievement rates were 89, 92, and 33% in Y93H-negative, -weakly positive, and -positive patients, respectively (**a**). The SVR24 achievement rates were 88, 100, and 100% in L31M/V-negative, -weakly positive, and -positive patients, respectively (**b**). In patients with resistant D168A/E/T/V with resistant NS5A, the rates were 91, 79, and 0% in negative, weakly positive, and positive patients, respectively (**c**). In patients with resistant D168A/E/T/V without resistant NS5A, the rates were 91, 89, and 0% in negative, weakly positive, and positive patients, respectively (**d**).

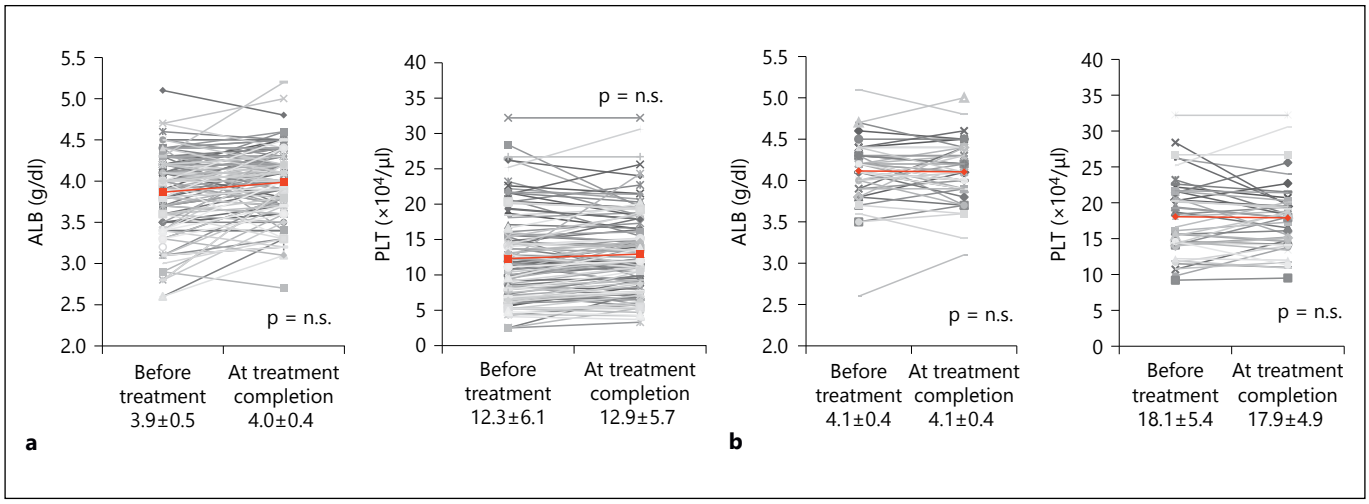

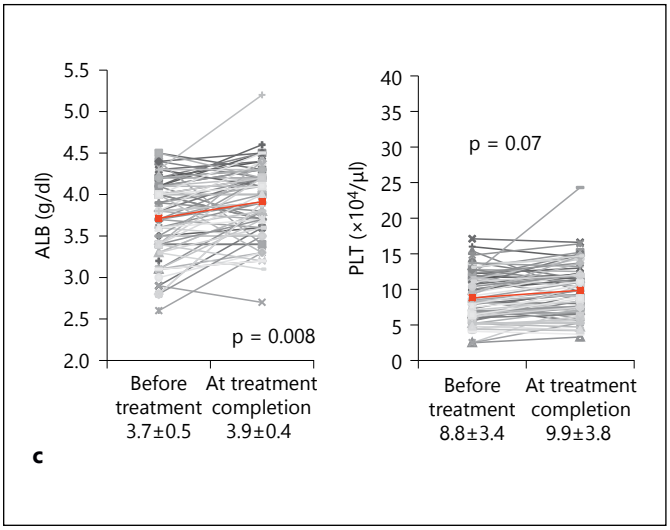

Fig. 3. Changes in hepatic spare ability after treatment. The serum ALB level was 3.9 ± 0.5 (mean ± SD) at the time of treatment introduction and 4.0 ± 0.4 at treatment completion, showing no change (**a**). When the patients were divided into those with chronic hepatitis and hepatic cirrhosis, significant improvement from 3.7 ± 0.5 to 3.9 ± 0.4 was noted in the hepatic cirrhosis patients (**c**, p = 0.008). No significant improvement was noted in the PLT count in overall, chronic hepatitis, or hepatic cirrhosis patients (**a–c**).

Table 4. Adverse effects (discontinued cases)

Adverse effect	Onset time	Outcome	SVR24	Age	Gender	Hepatic cirrhosis
Liver dysfunction (ALT; 103) and systemic malaise	Day 155	Recovered by drug withdrawal alone	○	73	M	Present
Liver dysfunction (ALT275)	Day 150	Recovered by drug withdrawal alone	○	67	F	Present
Liver dysfunction (ALT388)	Day 90	Recovered by drug withdrawal alone	○	70	M	Present
Marked ascites	Day 25	Recovered by drug withdrawal and antidiuretics	×	72	F	Present
SMV thrombosis (antiphospholipid antibody syndrome patient)	Day 89	Recovered by drug withdrawal and surgical therapy	○	56	F	Present
Ear noises	Day 3	Recovered by drug withdrawal alone	×	76	F	Present
Development of anxiety neurosis	Day 2	Recovered by drug withdrawal alone	×	68	F	Present
Skin eruption	Day 14	Recovered by drug withdrawal alone	×	78	F	Absent

Table 5. Patients who developed HCC after DAAs treatment

Number	Age	Gender	Hepatic cirrhosis	Previous IFN treatment	Previous HCC treatment (frequency)	Date of HCC treatment (final day)	ASV/DCV treatment period	Time to HCC development after EOT, days
1	63	M	Absent	Absent	Absent (0)	–	9/5/2014–2/25/2015	244
2	69	M	Present	Absent	Absent (0)	–	4/7/2015–9/21/2015	92
3	80	M	Present	Absent	Present (1)	7/26/2011	1/8/2015–6/25/2015	319
4	77	M	Present	Absent	Present (1)	11/1/2010	4/7/2015–9/22/2015	36
5	82	M	Present	Absent	Present (1)	4/10/2014	3/3/2015–8/18/2015	63
6	65	M	Present	Absent	Present (4)	4/18/2014	1/23/2015–7/19/2015	274
7	72	F	Present	Absent	Present (7)	6/5/2013	3/20/2015–9/5/2015	88

patients in whom HCC developed or recurred despite AFP being converted to negative, DCP elevation was observed (table 6).

Discussion

In the phase 3 clinical study (AI 44726 study) involving ineligible patients untreated/intolerable with IFN-containing treatment and patients who did not respond to previous treatment, the SVR24 achievement rate was 84.7% (188/222). In this study, 106 patients (88%) achieved SVR24. Considering the fact that 53 elderly patients (44%) aged 75 or older and 74 patients with hepatic cirrhosis (63%) were included, the outcome was favorable.

ETR was not achieved in 10 patients (8.3%), and 5 of them carried multiple-resistant NS3/4A or NS5A region. Multiple-resistant patients were found to be mostly positive through the PCR-invader method, thereby clarifying that the frequency of resistant virus influences the treatment effect. Four patients discontinued treatment early due to adverse effects. Achievement of SVR was difficult because treatment was completed after a maximum of 25 days.

When drug resistance and the SVR achievement rate were investigated in detail, the achievement rates were 89, 92, and 33% in Y93H-negative, -weakly positive, and -positive patients, respectively. On analysis of resistant D168A/E/T/V without resistant NS5A, the rates were 91, 89, and 0% in negative, weakly positive, and positive pa-

Table 6. Changes in AFP and DCP

Number	AFP (introduction)	AFP (completion)	AFP (onset of HCC)	DCP (introduction)	DCP (completion)	DCP (onset of HCC)
1	4	4	4	17	20	142
2	351	14	23	18	15	18
3	14	6	5	45	24	43
4	5	2	3	14	15	26
5	8	4	3	96	66	73
6	8	2	3	17	17	15
7	22	28	34	11	19	13

tients, respectively. ETR is unlikely to be achieved in patients with multiple resistance, as described above, but patients with single resistance also became SVR-resistant when the rate of resistant variants was high (20% or higher). The SVR24 achievement rate decreased to 40.5% in patients with resistant Y93H or L31I/M/V in the domestic phase 3 clinical study [15], showing a similar tendency.

The serum ALB level and PLT count were compared before and after treatment to observe changes in the hepatic spare ability after treatment. In hepatic cirrhosis patients, the serum ALB level significantly improved at 24 weeks after treatment completion, and hepatic spare ability improved earlier in patients with more marked reduction of the liver function.

Adverse effects led to the discontinuation of medication in 8 patients (6.6%), and the most frequent adverse effect was serum ALT elevation observed in 3 patients (2.5%). In the domestic phase 3 clinical study (AI 44726 study), treatment was discontinued due to adverse effect–associated liver disorder in 10 patients (4.5%) [15]. Since both DCV and ASV are metabolized by CYP3A4, the frequency of liver disorder increased, particularly in hepatic cirrhosis patients, and attention should be paid because the condition could aggravate, but withdrawal or dose reduction of the drugs due to adverse effects did not result in liver failure or death in our hospital. In addition, all 3 patients with ALT elevation achieved SVR24, and a minimum of 97-day administration was secured. Furthermore, 4 of the 7 patients who discontinued treatment due to adverse effects achieved SVR24 and 12 weeks or longer ASV/DCV administration was secured in all of them. Substantial achievement of SVR can be expected when the duration of administration is 12 weeks or longer.

Reig et al. [16] reported that HCC recurred at a high frequency (27.6%) within a short time (mean 5.7 months) after DAAs treatment in patients in whom HCC had cured. Investigation involving many patients is necessary to conclude whether or not HCC is likely to recur after DAAs treatment. However, elimination of hepatitis C may reduce endogenous IFN, which may release the brake on HCC development, suggesting that more strict liver cancer surveillance is necessary after DAAs treatment compared with that during IFN treatment [3]. Actually, after ASV/DCV treatment, HCC developed in 2 patients (1.7%) and recurred in 5 (4.2%). Since HCC recurred early after DAAs treatment in patients at several years after cure of HCC in cases 3 and 4, the possibility of the influence of DAAs treatment cannot be ruled out. Asahina et al. [17] reported that a decrease in the serum AFP level after IFN treatment is a risk factor for HCC development. In our study, HCC developed or recurred in patients in whom AFP was not converted to negative at the time of DAAs treatment completion, and DCP elevation was observed in patients in whom liver cancer developed or recurred despite AFP being converted to negative, suggesting that AFP and DCP are complementary markers after DAAs treatment similarly to those in normal HCC surveillance [18].

In conclusion, ASV/DCV treatment achieved favorable SVR in elderly and hepatic cirrhosis patients and in patients in whom HCC was cured. However, it has been reported that the risk of HCC development is not immediately reduced after treatment with existing therapeutic drugs, such as IFN, in these patients. Since an increase in the incidence of HCC development in patients who markedly respond to DAAs treatment is expected, surveillance of HCC becomes even more important [19, 20].

Disclosure Statement

There are no conflicts of interest to declare.

References

1 Kudo M, Matsui O, Izumi N, Iijima H, Kadoya M, Imai Y, Okusaka T, Miyayama S, Tsuchiya K, Ueshima K, Hiraoka A, Ikeda M, Ogasawara S, Yamashita T, Minami T, Yamakado K: JSH consensus-based clinical practice guidelines for the management of hepatocellular carcinoma: 2014 update by the liver cancer study group of Japan. Liver Cancer 2014;3:458–468.

2 Kudo M: Surveillance, diagnosis, treatment, and outcome of liver cancer in Japan. Liver Cancer 2015;4:39–50.

3 Clinical practice guidelines for hepatocellular carcinoma differ between Japan, United States, and Europe. Liver Cancer 2015;4:85–95.

4 Jacobson IM, McHutchison JG, Dusheiko G, Di Bisceglie AM, Reddy KR, Bzowej NH, Marcellin P, Muir AJ, Ferenci P, Flisiak R, George J, Rizzetto M, Shouval D, Sola R, Terg RA, Yoshida EM, Adda N, Bengtsson L, Sankoh AJ, Kieffer TL, George S, Kauffman RS, Zeuzem S: Telaprevir for previously untreated chronic hepatitis C virus infection. N Engl J Med 2011;364:2405–2416.

5 Zeuzem S, Andreone P, Pol S, Lawitz E, Diago M, Roberts S, Focaccia R, Younossi Z, Foster GR, Horban A, Ferenci P, Nevens F, Müllhaupt B, Pockros P, Terg R, Shouval D, van Hoek B, Weiland O, Van Heeswijk R, De Meyer S, Luo D, Boogaerts G, Polo R, Picchio G, Beumont M: Telaprevir for retreatment of HCV infection. N Engl J Med 2011;364:2417–2428.

6 Kumada H, Toyota J, Okanoue T, Chayama K, Tsubouchi H, Hayashi N: Telaprevir with peginterferon and ribavirin for treatment-naive patients chronically infected with HCV of genotype 1 in Japan. J Hepatol 2012;56:78–84.

7 Jacobson IM, Dore GJ, Foster GR, Fried MW, Radu M, Rafalsky VV, Moroz L, Craxi A, Peeters M, Lenz O, Ouwerkerk-Mahadevan S, De La Rosa G, Kalmeijer R, Scott J, Sinha R, Beumont-Mauviel M: Simeprevir with pegylated interferon alfa 2a plus ribavirin in treatment-naive patients with chronic hepatitis C virus genotype 1 infection (QUEST-1): a phase 3, randomised, double-blind, placebo-controlled trial. Lancet 2014;384:403–413.

8 Manns M, Marcellin P, Poordad F, de Araujo ES, Buti M, Horsmans Y, Janczewska E, Villamil F, Scott J, Peeters M, Lenz O, Ouwerkerk-Mahadevan S, De La Rosa G, Kalmeijer R, Sinha R, Beumont-Mauviel M: Simeprevir with pegylated interferon alfa 2a or 2b plus ribavirin in treatment-naive patients with chronic hepatitis C virus genotype 1 infection (QUEST-2): a randomised, double-blind, placebo-controlled phase 3 trial. Lancet 2014;384:414–426.

9 Hayashi N, Izumi N, Kumada H, Okanoue T, Tsubouchi H, Yatsuhashi H, Kato M, Ki R, Komada Y, Seto C, Goto S: Simeprevir with peginterferon/ribavirin for treatment-naïve hepatitis C genotype 1 patients in Japan: CONCERTO-1, a phase III trial. J Hepatol 2014;61:219–227.

10 Izumi N, Hayashi N, Kumada H, Okanoue T, Tsubouchi H, Yatsuhashi H, Kato M, Ki R, Komada Y, Seto C, Goto S: Once-daily simeprevir with peginterferon and ribavirin for treatment-experienced HCV genotype 1-infected patients in Japan: the CONCERTO-2 and CONCERTO-3 studies. J Gastroenterol 2014;49:941–953.

11 Kumada H, Hayashi N, Izumi N, Okanoue T, Tsubouchi H, Yatsuhashi H, Kato M, Rito K, Komada Y, Seto C, Goto S: Simeprevir (TMC435) once daily with peginterferon-α-2b and ribavirin in patients with genotype 1 hepatitis C virus infection: the CONCERTO-4 study. Hepatol Res 2015;45:501–513.

12 Chayama K, Takahashi S, Toyota J, Karino Y, Ikeda K, Ishikawa H, Watanabe H, McPhee F, Hughes E, Kumada H: Dual therapy with the nonstructural protein 5A inhibitor, daclatasvir, and the nonstructural protein 3 protease inhibitor, asunaprevir, in hepatitis C virus genotype 1b-infected null responders. Hepatology 2012;55:742–748.

13 Karino Y, Toyota J, Ikeda K, Suzuki F, Chayama K, Kawakami Y, Ishikawa H, Watanabe H, Hernandez D, Yu F, McPhee F, Kumada H: Characterization of virologic escape in hepatitis C virus genotype 1b patients treated with the direct-acting antivirals daclatasvir and asunaprevir. J Hepatol 2013;58:646–654.

14 Suzuki Y, Ikeda K, Suzuki F, Toyota J, Karino Y, Chayama K, Kawakami Y, Ishikawa H, Watanabe H, Hu W, Eley T, McPhee F, Hughes E, Kumada H: Dual oral therapy with daclatasvir and asunaprevir for patients with HCV genotype 1b infection and limited treatment options. J Hepatol 2013;58:655–662.

15 Kumada H, Suzuki Y, Ikeda K, Toyota J, Karino Y, Chayama K, Kawakami Y, Ido A, Yamamoto K, Takaguchi K, Izumi N, Koike K, Takehara T, Kawada N, Sata M, Miyagoshi H, Eley T, McPhee F, Damokosh A, Ishikawa H, Hughes E: Daclatasvir plus asunaprevir for chronic HCV genotype 1b infection. Hepatology 2014;59:2083–2091.

16 Reig M, Mariño Z, Perelló C, Iñarrairaegui M, Ribeiro A, Lens S, Díaz A, Vilana R, Darnell A, Varela M, Sangro B, Calleja JL, Forns X, Bruix J: Unexpected early tumor recurrence in patients with hepatitis C virus-related hepatocellular carcinoma undergoing interferon-free therapy: a note of caution. J Hepatol 2016;pii:S0168-8278(16)30113-1.

17 Asahina Y, Tsuchiya K, Nishimura T, Muraoka M, Suzuki Y, Tamaki N, Yasui Y, Hosokawa T, Ueda K, Nakanishi H, Itakura J, Takahashi Y, Kurosaki M, Enomoto N, Nakagawa M, Kakinuma S, Watanabe M, Izumi N: α-fetoprotein levels after interferon therapy and risk of hepatocarcinogenesis in chronic hepatitis C. Hepatology 2013;58:1253–1262.

18 Toyoda H, Kumada T, Tada T, Sone Y, Kaneoka Y, Maeda A: Tumor markers for hepatocellular carcinoma: simple and significant predictors of outcome in patients with HCC. Liver Cancer 2015;4:126–136.

19 Kudo M: Prediction of hepatocellular carcinoma incidence risk by ultrasound elastography. Liver Cancer 2014;3:1–5.

20 Kudo M: Risk of hepatocellular carcinoma in patients with hepatitis C virus who achieved sustained virological response. Liver Cancer 2016;5:155–161.

Original Article

Digestive Diseases

Dig Dis 2016;34:632–639
DOI: 10.1159/000448824

Safety, Tolerability, and Efficacy of Sofosbuvir Plus Ribavirin in Elderly Patients Infected with Hepatitis C Virus Genotype 2

Naoshi Nishida Masashi Kono Tomohiro Minami Hirokazu Chishina
Tadaaki Arizumi Masahiro Takita Norihisa Yada Hiroshi Ida Satoru Hagiwara
Yasunori Minami Kazuomi Ueshima Tashiharu Sakurai Masatoshi Kudo

Department of Gastroenterology and Hepatology, Kindai University Faculty of Medicine, Osaka-Sayama, Osaka, Japan

Key Words
Sofosbuvir · Ribavirin · Chronic hepatitis C · Genotype 2 · Aged patients

Abstract
Background: An interferon-free regimen including sofosbuvir and ribavirin (RBV) for patients with hepatitis C virus (HCV) genotype 2 (G2) infection leads to a drastic improvement of sustained virological response (SVR). However, the safety, tolerability, and efficacy in patients aged 75 or older have not been completely understood. ***Summary:*** Fifty-six patients with HCV G2 infection who were treated with sofosbuvir and weight-based dose of RBV were enrolled. Thirty-seven patients aged ≥75 and 19 patients aged ≤74 were classified as the aged and non-aged groups, respectively. The aged group was characterized by significantly more number of women, history of hepatocellular carcinoma, low serum albumin (ALB) level, low hemoglobin (Hb) concentration, low estimated glomerular filtration rate (eGFR), and high fibrosis-4 index (p = 0.0029). Forty-one patients were evaluated for SVR at 12 weeks after the end of therapy (SVR12); of them, all but one completed the treatment scheduled for 12 weeks. The aged group showed lower SVR12 rate than the non-aged group (81.3% for aged and 96.0% for non-aged groups). Although the Hb concentration and eGFR are significantly lower in the aged group throughout the clinical course, all patients in the aged group completed the 12-week treatment with a gradual increase of serum ALB level. ***Key Messages:*** The combination of sofosbuvir plus RBV is tolerable and beneficial in patients aged >75. However, intensive management of anemia by dose reduction of RBV is necessary, which could lead to a low SVR12 rate compared to that observed in patients younger than 75 years.

Introduction

Although progress has been made in the treatment of hepatocellular carcinoma (HCC), it is still one of the leading causes of cancer-related death; chronic infection with hepatitis C virus (HCV) is the major cause of HCC emergence in Japan [1, 2]. Thus far, interferon (IFN)-based regimen has been applied for patients with chronic hepatitis C (CHC); the effectiveness and tolerability of IFN-based treatment have been unsatisfactory, especially for aged patients and those with liver cirrhosis [3]. Recently, an IFN-free regimen for CHC was developed, which led to a drastic improvement in sustained virological response (SVR) [4]. With regard to the treatment of CHC patients infected with HCV genotype 2 (G2), data from a

KARGER

E-Mail karger@karger.com
www.karger.com/ddi

0257–2753/16/0346–0632$39.50/0

Naoshi Nishida, MD
Department of Gastroenterology and Hepatology
Kindai University Faculty of Medicine
337-2 Ohno-Higashi, Osaka-Sayama, Osaka 589-8511 (Japan)
E-Mail naoshi@med.kindai.ac.jp

phase III trial on treatment using combination of nucleotide HCV non-structural protein 5B (NS5B) polymerase inhibitor, sofosbuvir, and ribavirin (RBV) for 12 weeks have been published for different ethnic cohorts including the Japanese population; 93–100% of the patients reportedly achieved SVR at 12 weeks (SVR12) after the end of the treatment (EOT) [5–9]. More importantly, the high SVR12 rate could be achieved regardless of age, gender, background status of liver fibrosis, and history of antiviral therapy [6, 8, 9], which have been known to be associated with failure of IFN-based treatment. In the Japanese phase III trial, pharmacokinetic analysis of sofosbuvir and its nucleoside metabolite, GS-331007 was performed [8]. No difference in pharmacokinetics of sofosbuvir and GS-331007 was observed regardless of age and cirrhosis status. However, although no age limits were set for eligibility in these trials, the majority of the enrolled patients were younger than 75 years and efficacy in patients older than 75 years has not been elucidated properly. In addition, regimens including RBV cause anemia and hyperbilirubinemia, especially in aged patients with impaired renal function [10], and the majority of such patients have liver cirrhosis. Therefore, it is important to clarify the safety and tolerability of sofosbuvir plus RBV combination for aged patients with HCV infection. In this study, we compared the safety, tolerability, and efficacy of sofosbuvir plus RBV treatment between patients aged ≥75 and those aged <74.

Materials and Methods

Patients

Between June 2015 and March 2016, 56 patients with CHC caused by HCV G2 who underwent antiviral therapy with sofosbuvir and weight-based dose of RBV were enrolled. The clinical background of the patients before the treatment is as follows; median age (range) was 68 (27–90 years), 29 patients were men and 27 women, 40 patients were treatment-naïve, and 16 had received previous antiviral IFN therapy (5 non-responders, 6 relapsers, and 5 IFN-intolerant). Ten patients had a history of HCC. The median viral load (range) was 6.1 $\log_{10}$ international unit (IU)/ml (2.9–7.1). The median values and ranges of other blood chemical data of the cohort are as follows: 36 IU/l (17–292) for aspartate aminotransferase, 36 IU/l (6–506) for alanine transaminase, 4.2 g/ml (2.3–5.1) for albumin (ALB), 170 × 10^3/μl (42–406) for platelet count, 0.7 mg/dl (0.2–2.1) for total bilirubin (T. Bil), 13.95 g/dl (7.7–18.1) for hemoglobin (Hb) concentration, 74.5 (36–188) for estimated glomerular filtration rate (eGFR), and 3 ng/ml (1–72) for serum α-fetoprotein (AFP) level. The median fibrosis-4 (FIB-4) index was 2.58 (0.545–14.37). Twenty-one patients received a dose reduction of RBV for the management of anemia during treatment. The study was approved by the institutional review boards of the institution involved.

Assessment of Viral Response and Blood Chemical Analyses among Aged (75 Years or Older) and Non-Aged (Younger Than 75 Years) Patients

We compared the viral response and change of blood chemical data during and after the treatment between aged and non-aged patients. For this purpose, the patients were divided into 2 groups based on their age at the initiation of treatment; 37 patients aged ≥75 were classified as the aged group and 19 patients aged <74 comprised the non-aged group. The results for the comparison of the clinical backgrounds between aged and non-aged patients are shown in table 1. The aged group included significantly more female patients (68.4%, 13/19 vs. 37.8%, 14/37, p = 0.0301), and was characterized by history of HCC (36.8%, 7/19 vs. 8.1%, 3/37, p = 0.0223), lower serum ALB level (median and range 4 g/ml, 3.1–4.5 vs. 4.3, 2.3–5.1, p = 0.0165), lower Hb concentration (median and range 13.2 g/dl, 7.7–14.8 vs. 14.4, 9.6–18.1, p = 0.0005), lower eGFR (median and range 69, 36–91 vs. 76, 59–188, p = 0.0075), and higher FIB-4 index (median and range 3.97, 2.00–9.25 vs. 1.97, 0.56–14.4, p = 0.0029) than the non-aged group.

Serum HCV-RNA was quantified at weeks 2, 4, and 12 to evaluate virological response during and at the EOT response (ETR). Similarly, we analyzed viral clearance at weeks 4 and 12 after the EOT (SVR4 and SVR12). Quantification of serum HCV-RNA was performed using the COBAS® TaqMan® HCV Auto Assay System (Roche, USA; lower limit of quantification, 1.2 $\log_{10}$ IU/ml). Standard laboratory and clinical tests were also performed during the clinical course. For the comparison of viral response between aged and non-aged groups, data were compared in an intention-to-treat manner.

Statistical Analysis

Pearson's chi-square test or Fisher's exact test was used to compare categorical variables. For comparisons of continuous variables, the Wilcoxon rank-sum test was applied. All p values were two-sided and $p < 0.05$ was considered statistically significant. All statistical analyses were performed using JMP version 9.0 software (SAS Institute Inc., Cary, N.C., USA).

Results

Clinical Background Associated with the Virological Response at 12 Weeks after the EOT

Of the 56 patients, 41 could evaluate SVR12; 37 achieved SVR12, whereas 4 failed to achieve SVR12 (SVR12 rate = 90.2%, 37/41). RBV dose reduction was performed for 21 (37.5%, 21/56) patients for the management of anemia; 11 of 37 (29.7%) were non-aged patients and 10 of 19 (57.9%) were aged patients. Of the 4 patients who failed to achieve SVR12, 1 who was negative for serum HCV during the treatment, discontinued the treatment at 8 weeks after initiation because of hyperbilirubinemia. Other 3 patients completed the 12-week treatment and showed undetectable serum HCV-RNA at the EOT but failed to achieve SVR12. Of the 4 patients who failed to achieve SVR12, 3 were aged ≥75, were men, had previ-

Table 1. Difference of background characteristics of non-aged (≤74 years of age) and aged patients (≥75 years of age) before antiviral treatment

Backgrounds	Non-aged patients (n = 37)	Aged patients (n = 19)	p value
Gender (male/female)	**23/14**	**6/13**	**0.0301**
Previous treatment (with/without)	10/27	6/13	0.7211
History of HCC emergence (with/without)	**3/34**	**7/12**	**0.0223***
HCV titer, log IU/ml, median (range)	6.1 (3.2–7.1)	6.1 (2.9–6.7)	0.2599
AST, IU/l, median (range)	29 (17–292)	46 (17–68)	0.3648
ALT, IU/l, median (range)	32 (6–506)	38 (8–72)	0.6341
ALB, g/dl, median (range)	**4.3 (2.3–5.1)**	**4 (3.1–4.5)**	**0.0165**
Platelet count, $\times 10^3/\mu l$, median (range)	180 (42–406)	161 (77–288)	0.0805
T. Bil level, mg/dl, median (range)	0.7 (0.2–2.1)	0.7 (0.4–1.7)	0.8754
Hb, g/dl, median (range)	**14.4 (9.6–18.1)**	**13.2 (7.7–14.8)**	**0.0005**
eGFR, median (range)	**76 (59–188)**	**69 (36–91)**	**0.0075**
AFP, ng/ml, median (range)	3 (1–72)	3 (1–55)	0.4051
FIB-4 index, median (range)	**1.97 (0.56–14.4)**	**3.97 (2.00–9.45)**	**0.0029**
FIB-4 index (>3.25/≤3.25)	10/27	10/9	0.0583
Reduction of RBV during the treatment (with/without)	11/26	10/9	0.0937

AST = Aspartate transaminase; ALT = alanine transaminase.

p values by were calculated using Pearson's chi-square test for categorical valuables and Wilcoxon rank sum test for contentious variables are shown. * p values by Fisher's exact test.

Backgrounds showing significant difference between non-aged and aged patients are shown in bold.

ously received antiviral therapy, and had an FIB-4 index >3.25. Similarly, 2 patients received RBV dose reduction and 1 had a history of HCC. Regarding the association between HCV clearance during clinical course and age, no difference was observed in timing of HCV clearance between aged and non-aged groups in which all patients showed undetectable serum HCV-RNA at EOT regardless of age. Although not statistically significant, aged patients showed lower SVR12 rate than non-aged patients did (81.3%, 13/16 for aged and 96.0%, 24/25 for non-aged groups, respectively; fig. 1). One patient who discontinued treatment owing to jaundice was a member of the non-aged group.

Serum ALB, Hb Concentration, and eGFR during the Clinical Course

To determine the safety of sofosbuvir and RBV treatment in aged patients, we compared the serum ALB level, Hb concentration, and eGFR during the clinical course between the aged and non-aged group because these laboratory data were significantly lower in the aged than in the non-aged group (fig. 2). At each time point of the clinical course, Hb concentration and eGFR were significantly lower in the aged than in the non-aged group (p values of each comparison of baseline, at 2 and 4 weeks after the initiation of treatment, at EOT, and at 4 and 12 weeks after the EOT were as follows; p = 0.0005, p = 0.0016, p = 0.0013, p = 0.0064, p = 0.0050, p = 0.0107 for Hb, p = 0.0075, p = 0.0072, p = 0.0043, p = 0.0048, p = 0.0043, p = 0.0179 for eGFR, respectively; fig. 2a, b). Although the serum ALB level was significantly lower in the aged group during the treatment, the difference was not significant after the completion of administration (p = 0.0165, p < 0.0001, p = 0.0018, p = 0.1655, p = 0.1283, p = 0.0501 before treatment, at 2 and 4 weeks after the initiation of treatment, at EOT, and at 4 and 12 weeks after the EOT, respectively; fig. 2c). Despite the low baseline levels of Hb, eGFR, and serum ALB before the treatment in the aged group, all patients aged ≥75 completed the 12-week treatment.

Decrease of the Serum AFP Level after the Treatment

We compared the serum AFP level at 12 weeks after the EOT with the baseline level. Among the 41 patients examined, 38 showed decreased levels of serum AFP after the treatment. The decrease in serum AFP level was observed regardless of age (categorized as ≤74 and ≥75 years; fig. 3a, b). Figure 3 shows the comparison of serum AFP before

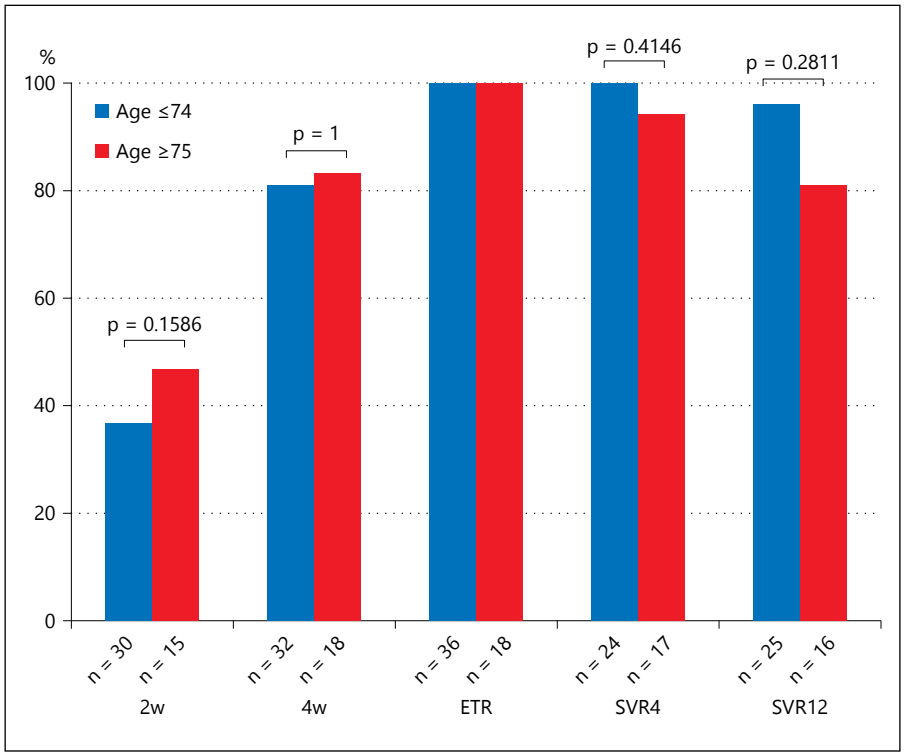

Fig. 1. Comparison of the response rate at each timing between the patients aged >75 and ≤74. Percentages of the patients who showed negative for serum HCV-RNA are shown. Two and 4 weeks denote the response at weeks 2 and 4 during treatment, respectively. ETR denotes end of treatment response, SVR4 and SVR12 denote SVR at 4 and 12 weeks after the EOT. p values by the Wilcoxon rank-sum test are shown.

and after treatment in patients who achieved SVR12 (fig. 3a), and those who failed to achieve SVR12 (fig. 3b). The decrease in serum AFP after the treatment was observed regardless of SVR12 status. We also analyzed the association between percentage decrease of AFP (ΔAFP) after the treatment (calculated as difference in serum AFP before and after the treatment divided by the baseline serum AFP) and FIB-4 index categorized as ≤3.25 and >3.25; fig. 3c). The group with an FIB-4 index of >3.25 showed significantly greater ΔAFP (more decrease of serum AFP after the treatment) than the group with an FIB-4 index of ≤3.25 (p = 0.0249 by the Wilcoxon rank-sum test).

Discussion

CHC is known to be a leading cause of HCC emergence in Japan [11], and approximately 2% of the population have chronic HCV infection [12]. Although the major strain of HCV in Japan is G1, which is known to be resistant to conventional IFN-based therapy, recent advancements in antiviral therapy using direct-acting antiviral agents have drastically improved the HCV response rate [13]. However, G2 is known as a minor strain in Japan and shows favorable response to IFN-based therapy [14, 15]. Therefore, the majority of patients with CHC caused by HCV G2 were believed to achieve SVR upon IFN-based treatment. However, because of side effects of IFN, many patients who are intolerant to IFN-based treatment, such as aged patients and those with liver cirrhosis, remain untreated.

In Europe, CHC patients infected with G2 who were treated with recent IFN-free therapy that combined NS5B polymerase inhibitor, sofosbuvir, with RBV for 12 weeks achieved an SVR12 rate of 93% [5]. Similar results were reported for this combination therapy in several regions, such as Japan, Taiwan, Korea where the reported SVR12 rate was 97, 100, and 97%, respectively [6, 8, 9]. Reportedly, a high SVR12 rate was observed even in patients with liver cirrhosis, treatment-experienced, and elderly patients. However, according to previous reports, almost every patient reported in the literature was younger than 75 years; the efficacy and safety of sofosbuvir plus RBV treatment in patients older than 74 years have not been elucidated [5, 6, 8, 9]. Information regarding the safety, tolerability, and efficacy in aged patients is critical for the management of CHC patients in an aging society such as Japan [16]; we compared the efficacy and safety of this combination therapy between patients aged ≥75 and those aged ≤74.

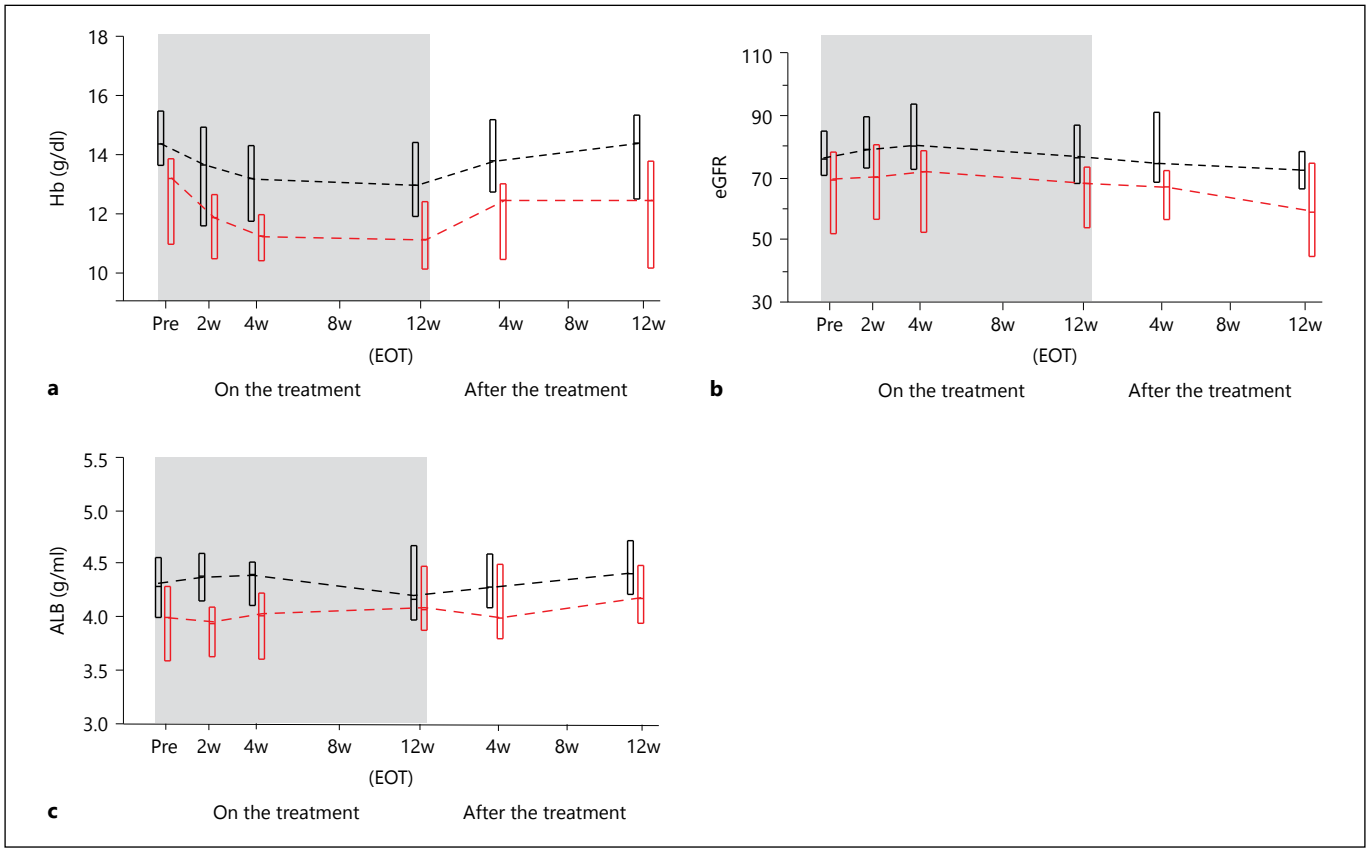

Fig. 2. Hb concentration, eGFR, and serum ALB level during the clinical course in patients aged ≥75 and ≤74. Alterations of Hb concentration (**a**), eGFR (**b**), and serum ALB level (**c**) are shown. Red dashed lines show the data of the patients aged ≥75 and black dashed lines denote that of the patients aged <74. The boxes denote 75% distributions and the lines in the boxes showed median values. p values (by the Wilcoxon rank-sum test) of each comparison between patients aged ≥75 and ≤74 at baseline, at week 2 (2w) and week 4 (4w) on the treatment, at the EOT, and at 4 and 12 weeks after the EOT were as follows; p = 0.0005, p = 0.0016, p = 0.0013, p = 0.0064, p = 0.0050, p = 0.0107 for Hb, p = 0.0075, p = 0.0072, p = 0.0043, p = 0.0048, p = 0.0043, p = 0.0179 for eGFR, and p = 0.0165, p < 0.0001, p = 0.0018, p = 0.1655, p = 0.1283, p = 0.0501 for ALB, respectively.

As shown in table 1, several patient characteristics significantly differ between ≥75 and ≤74 years groups. The aged group includes more women, and patients with a history of HCC. In addition, the aged group shows significantly lower serum ALB level, Hb concentration, and eGFR. We did not perform liver biopsy before the treatment and the presence of liver cirrhosis could not be determined precisely. Therefore, we calculated FIB-4 index as an alternative for assessing the degree of liver fibrosis because an FIB-4 index of >3.25 or ≤3.25 could adequately reflect the presence or absence of advanced liver fibrosis [17]. As expected, the aged group included more patients with FIB-4 index of >3.25.

Although both the aged and non-aged groups represented 100% of the ETR rate, the SVR12 rate of the aged group was 81.3%, which was lower than that of the non-aged groups (SVR12 rate was 96%). Although previous reports suggested a high SVR12 rate irrespective of liver cirrhosis and age [6, 8, 9], the reported cohorts in most previous literature classified the elderly group as the group comprising patients aged ≥65, and did not include patients aged ≥75. Therefore, it might be possible that advanced liver fibrosis and history of HCC that were associated with the presence of liver cirrhosis might be a cause of a lower SVR12 rate in the aged patients. In addition, it is reasonable to speculate that lower Hb concentration and eGFR contribute to the lower SVR rate in the aged patients because many aged patients received RBV dose reduction for anemia management. However, this association is not statistically significant because of the very small number of the patients who failed to achieve SVR12.

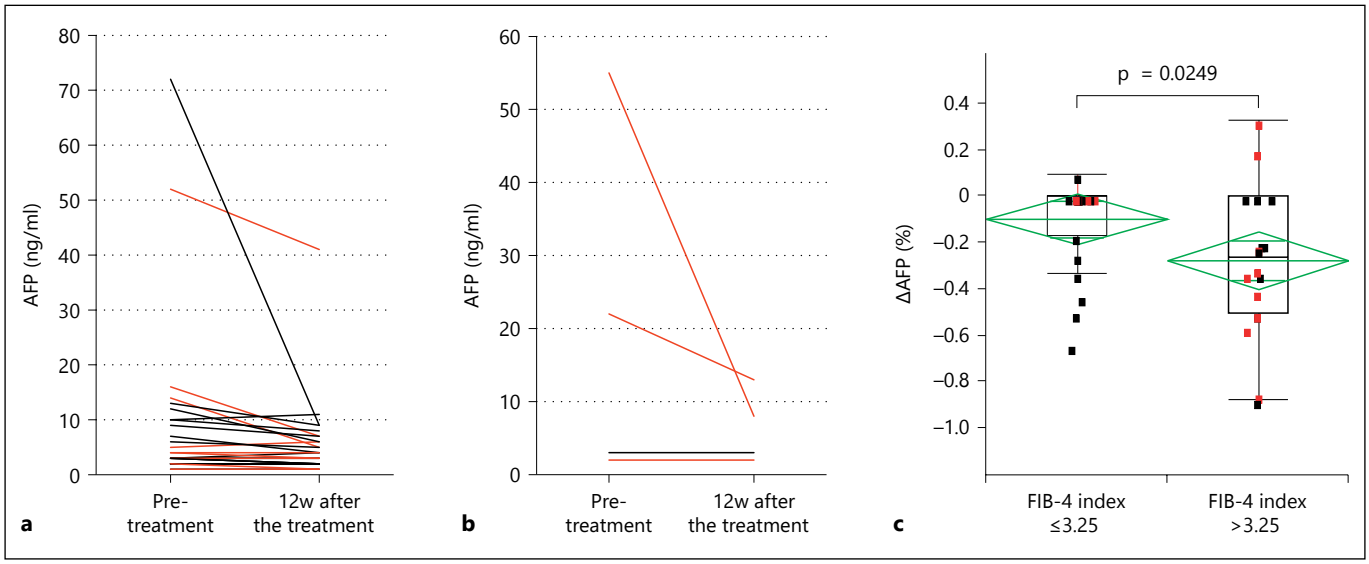

Fig. 3. Alteration of serum AFP before and 12 weeks after the EOT. **a** Alteration of serum AFP of the patients who achieved SVR12, and (**b**) that of the patients who failed to achieve SVR12. The red lines denote the data of the patients aged ≥75 and black lines denote those of the patients aged ≤74. **c** Comparison of percentage difference of serum AFP (ΔAFP) between the patients with FIB-4 index <3.25 and those with FIB-4 index >3.25. The red dots denote the data of the patients aged >75 and black dots denote those of the patients aged ≤74. Black box and whisker plots denote 75 and 95% distributions; lines within boxes show median values; the mean percentage ΔAFP and 95% CI are shown as green diamonds and lines within the diamonds, respectively. The percentage ΔAFP is calculated as difference of the AFP level before and after the treatment divided by baseline AFP level. The minus value denotes decrease of AFP after the treatment. p value by the Wilcoxon rank-sum test is shown.

Consistent with the results from the previous reports [6, 8, 9], all patients were negative for serum HCV at EOT, suggesting a high barrier against the emergence of resistant strain for nucleotide NS5B inhibitor. Of the 4 patients who failed to achieve SVR12, only the patient in the non-aged group discontinued the 12-week treatment because of hyperbilirubinemia. Although this patient was classified as belonging to the non-aged group, the patient was aged 74, had previously received antiviral therapy, had an FIB-4 index >3.25, and showed slightly increased T. Bil level and decreased eGFR at baseline (1.3 mg/dl and 59 for T. Bil level and eGFR, respectively). The serum bilirubin level returned to the baseline after the discontinuation of treatment, suggesting the role of sofosbuvir and/or RBV in hyperbilirubinemia in this patient who had advanced liver fibrosis and impaired renal function, which are frequently observed in aged patients. On the other hand, the other 3 patients who failed to achieve SVR12 are the members of the aged group, and 2 of them received a reduced dose of RBV for the management of anemia. In addition, 2 had previously received antiviral therapy and showed an FIB-4 index of >3.25. The baseline Hb concentration and eGFR in these 3 patients ranged from 13.3 to 14.8 g/dl and from 68 to 69, respectively, and the minimum Hb concentration during the treatment was 10.2–13 g/dl. Therefore, although not statistically significant because of the limited number of non-SVR12 patients, dose reduction of RBV, and low Hb concentration and eGFR at baseline should affect the SVR12 rate especially in patients aged ≥75.

Among the blood chemical tests examined, the serum ALB level, Hb concentration, and eGFR are significantly lower in the aged group; we compared these levels during and after the treatment. RBV dose reduction was performed in 11 of 37 (29.7%) non-aged and 10 of 19 of aged patients (52.6%) for the management of anemia. Although the Hb concentration and eGFR are significantly lower in the aged group throughout the clinical course, no patient showed Hb concentration of less than 10 g/dl and eGFR of less than 50. In addition, a gradual increase of serum ALB level is observed in aged patients, suggesting that the combination of sofosbuvir plus RBV is tolerable and beneficial in patients aged ≥75, although the SVR12 rate is lower in aged than in non-aged patients.

We also examined the decrease of serum AFP before and after the combination treatment. Among the 41 patients for whom serum AFP level before and at 12 weeks after the EOT was evaluated, only 3 showed an increase of AFP and all but

1 patient with the baseline AFP of >5 ng/ml showed a decrease in serum AFP after the treatment, irrespective of age. More importantly, the decrease of AFP was also observed in patients who failed to achieve SVR12 and was more prominent in the patients with an FIB-4 index of >3.25. Because the serum AFP level should be higher in patients with liver cirrhosis, early decrease of AFP could be more prominent in patients with advanced liver fibrosis [18, 19].

In this study, we explored the safety, tolerability, and efficacy of sofosbuvir plus RBV in patients aged ≥75 with HCV G2 infection. The treatment was safe and well tolerable in aged patients with advanced liver fibrosis, history of HCC emergence, low serum ALB level, low Hb concentration, and low eGFR. However, management of anemia by dose reduction of RBV is necessary for such patients, which could lead to a low SVR12 rate compared to the rate in patients younger than 75 years.

Recently, a new combination therapy using sofosbuvir and the NS5A inhibitor velpatasvir has been reported; the SVR for CHC G2 in the sofosbuvir plus velpatasvir group is superior to the rate in the sofosbuvir plus RBV group [20]. In addition, this new combination reportedly shows a high SVR12 rate regardless of genotype and even in cases with decompensated cirrhosis [21, 22]; the development of direct-acting antivirals should lead to the elimination of virus in almost all patients with HCV infection in the near future.

Acknowledgments

This work was supported in part by Grant-in-Aid for Scientific Research (KK160010-01) from the Japanese Society for the Promotion of Science (N.N.).

Disclosure Statement

The authors have no conflicts of interest to disclose.

References

1 Kudo M: Surveillance, diagnosis, treatment, and outcome of liver cancer in Japan. Liver Cancer 2015;4:39–50.
2 Clinical practice guidelines for hepatocellular carcinoma differ between Japan, United States, and Europe. Liver Cancer 2015;4:85–95.
3 Hsu CS, Chao YC, Lin HH, Chen DS, Kao JH: Systematic review: impact of interferon-based therapy on HCV-related hepatocellular carcinoma. Sci Rep 2015;5:9954.
4 Ferenci P: Treatment of hepatitis C in difficult-to-treat patients. Nat Rev Gastroenterol Hepatol 2015;12:284–292.
5 Zeuzem S, Dusheiko GM, Salupere R, Mangia A, Flisiak R, Hyland RH, Illeperuma A, Svarovskaia E, Brainard DM, Symonds WT, Subramanian GM, McHutchison JG, Weiland O, Reesink HW, Ferenci P, Hezode C, Esteban R; VALENCE Investigators: Sofosbuvir and ribavirin in HCV genotypes 2 and 3. N Engl J Med 2014;370:1993–2001.
6 Ahn SH, Lim YS, Lee KS, Paik SW, Lee YJ, Jeong SH, Kim JH, Yoon SK, Yim HJ, Tak WY, Han SY, Yang JC, Mo H, Mathias A, Han L, Knox SJ, Brainard DM, Kim YJ, Byun KS, Kim YS, Heo J, Han KH: A phase 3b study of sofosbuvir plus ribavirin in treatment-naive and treatment-experienced Korean patients chronically infected with genotype 2 hepatitis C virus. J Viral Hepat 2016;23:358–365.
7 Younossi ZM, Stepanova M, Zeuzem S, Dusheiko G, Esteban R, Hezode C, Reesink HW, Weiland O, Nader F, Hunt SL: Patient-reported outcomes assessment in chronic hepatitis C treated with sofosbuvir and ribavirin: the VALENCE study. J Hepatol 2014;61:228–234.
8 Omata M, Nishiguchi S, Ueno Y, Mochizuki H, Izumi N, Ikeda F, Toyoda H, Yokosuka O, Nirei K, Genda T, Umemura T, Takehara T, Sakamoto N, Nishigaki Y, Nakane K, Toda N, Ide T, Yanase M, Hino K, Gao B, Garrison KL, Dvory-Sobol H, Ishizaki A, Omote M, Brainard D, Knox S, Symonds WT, McHutchison JG, Yatsuhashi H, Mizokami M: Sofosbuvir plus ribavirin in Japanese patients with chronic genotype 2 HCV infection: an open-label, phase 3 trial. J Viral Hepat 2014;21:762–768.
9 Kao JH, Chien RN, Chang TT, Peng CY, Hu TH, Lo GH, Wang HY, Chen JJ, Yang JC, Knox SJ, Han L, Mo H, Mathias A, Brainard DM, Sheen IS, Hsu YC, Chu CJ, Chuang WL: A phase 3b study of sofosbuvir plus ribavirin in Taiwanese patients with chronic genotype 2 hepatitis C virus infection. Liver Int 2016;36:1101–1107.
10 Naik GS, Tyagi MG: A pharmacological profile of ribavirin and monitoring of its plasma concentration in chronic hepatitis C infection. J Clin Exp Hepatol 2012;2:42–54.
11 Kudo M, Matsui O, Izumi N, Iijima H, Kadoya M, Imai Y, Okusaka T, Miyayama S, Tsuchiya K, Ueshima K, Hiraoka A, Ikeda M, Ogasawara S, Yamashita T, Minami T, Yamakado K; Liver Cancer Study Group of Japan: JSH consensus-based clinical practice guidelines for the management of hepatocellular carcinoma: 2014 update by the liver cancer study group of Japan. Liver Cancer 2014;3:458–468.
12 Chung H, Ueda T, Kudo M: Changing trends in hepatitis C infection over the past 50 years in Japan. Intervirology 2010;53:39–43.
13 Gotte M, Feld JJ: Direct-acting antiviral agents for hepatitis C: structural and mechanistic insights. Nat Rev Gastroenterol Hepatol 2016;13:338–351.
14 Kohara M, Tanaka T, Tsukiyama-Kohara K, Tanaka S, Mizokami M, Lau JY, Hattori N: Hepatitis C virus genotypes 1 and 2 respond to interferon-alpha with different virologic kinetics. J Infect Dis 1995;172:934–938.
15 Mangia A, Santoro R, Minerva N, Ricci GL, Carretta V, Persico M, Vinelli F, Scotto G, Bacca D, Annese M, Romano M, Zechini F, Sogari F, Spirito F, Andriulli A: Peginterferon alfa-2b and ribavirin for 12 vs. 24 weeks in HCV genotype 2 or 3. N Engl J Med 2005;352:2609–2617.
16 Tanaka J, Kumagai J, Katayama K, Komiya Y, Mizui M, Yamanaka R, Suzuki K, Miyakawa Y, Yoshizawa H: Sex- and age-specific carriers of hepatitis B and C viruses in Japan estimated by the prevalence in the 3,485,648 first-time blood donors during 1995–2000. Intervirology 2004;47:32–40.
17 Vallet-Pichard A, Mallet V, Nalpas B, Verkarre V, Nalpas A, Dhalluin-Venier V, Fontaine H, Pol S: FIB-4: an inexpensive and accurate marker of fibrosis in HCV infection. Comparison with liver biopsy and fibrotest. Hepatology 2007;46:32–36.
18 Toyoda H, Kumada T, Tada T, Sone Y, Kaneoka Y, Maeda A: Tumor markers for hepatocellular carcinoma: simple and significant predictors of outcome in patients with HCC. Liver Cancer 2015;4:126–136.

19 Kudo M: Risk of hepatocellular carcinoma in patients with hepatitis C virus who achieved sustained virological response. Liver Cancer 2016;5:155–161.
20 Foster GR, Afdhal N, Roberts SK, Brau N, Gane EJ, Pianko S, Lawitz E, Thompson A, Shiffman ML, Cooper C, Towner WJ, Conway B, Ruane P, Bourliere M, Asselah T, Berg T, Zeuzem S, Rosenberg W, Agarwal K, Stedman CA, Mo H, Dvory-Sobol H, Han L, Wang J, McNally J, Osinusi A, Brainard DM, McHutchison JG, Mazzotta F, Tran TT, Gordon SC, Patel K, Reau N, Mangia A, Sulkowski M; ASTRAL-2 Investigators; ASTRAL-3 Investigators: Sofosbuvir and velpatasvir for HCV genotype 2 and 3 infection. N Engl J Med 2015;373:2608–2617.
21 Feld JJ, Jacobson IM, Hezode C, Asselah T, Ruane PJ, Gruener N, Abergel A, Mangia A, Lai CL, Chan HL, Mazzotta F, Moreno C, Yoshida E, Shafran SD, Towner WJ, Tran TT, McNally J, Osinusi A, Svarovskaia E, Zhu Y, Brainard DM, McHutchison JG, Agarwal K, Zeuzem S; ASTRAL-1 Investigators: Sofosbuvir and velpatasvir for HCV genotype 1, 2, 4, 5, and 6 infection. N Engl J Med 2015;373:2599–2607.
22 Curry MP, O'Leary JG, Bzowej N, Muir AJ, Korenblat KM, Fenkel JM, Reddy KR, Lawitz E, Flamm SL, Schiano T, Teperman L, Fontana R, Schiff E, Fried M, Doehle B, An D, McNally J, Osinusi A, Brainard DM, McHutchison JG, Brown RS Jr, Charlton M; ASTRAL-4 Investigators: Sofosbuvir and velpatasvir for HCV in patients with decompensated cirrhosis. N Engl J Med 2015;373:2618–2628.

Original Article

Digestive Diseases

Dig Dis 2016;34:654–658
DOI: 10.1159/000448826

Monoethanolamine Oleate Sclerotherapy for Polycystic Liver Disease

Masahiro Takita Mina Iwanishi Tomohiro Minami Masashi Kono Hirokazo Chishina Tadaaki Arizumi Norihisa Yada Satoru Hagiwara Yasunori Minami Hiroshi Ida Kazuomi Ueshima Nishida Naoshi Masatoshi Kudo

Department of Gastroenterology and Hepatology, Kinki University School of Medicine, Osaka-Sayama, Japan

Key Words
Polycystic liver disease · Hepatic cyst · Sclerotherapy therapy · Treatment

Abstract
Objective: The objective of treatment for polycystic liver disease is to reduce the liver volume and reduce or resolve compression symptoms such as abdominal fullness and abdominal pain due to hepatomegaly. Liver cysts are treated internally by puncture and aspiration of the cyst contents or hepatic artery embolization and surgically by cyst fenestration or hepatectomy, but no clear consensus has been reached concerning their selection. We introduced monoethanolamine oleate (EO) sclerotherapy therapy for liver cysts in 1999 and reported its effectiveness. In this study, cases were added, and the results including those of long-term follow-up were evaluated. ***Subjects:*** Twenty-two patients (5 males and 17 females, mean age 65.2) who underwent EO infusion therapy for liver cysts between January 1999 and June 2011 were evaluated. ***Methods:*** Liver cysts were punctured under ultrasound guidance, and a 7Fr pigtail catheter was inserted. After aspirating the cyst contents, EO was infused, and a clamp was applied for 24 h. Then, the catheter was declamped, cyst contents were aspirated again, and the catheter was removed. After the treatment, the cyst size was measured, and the patients were followed up. ***Results:*** Eight simple cysts in 8 patients (simple cyst group) and 21 cysts in 14 patients with multiple cysts (polycystic liver disease group) were treated and followed up over a median of 78 months (0–203 months). The mean volume reduction rate was 99% in the simple cyst group and 91% in the polycystic liver disease group ($p = 0.04$). One procedural accident resulting in liver abscess formation was observed in 1 patient 1 week after discharge, and it required drain placement and antibiotic administration. While mild abdominal pain was observed in a few patients, it was resolved spontaneously under observation. ***Conclusion:*** EO infusion therapy achieves fairly high treatment response in the volume reduction (99%) and sustained shrinkage over long-term follow-up. Therefore, this is a breakthrough technique in the treatment of polycystic liver disease as well as simple cyst and should be a standard of care in the treatment of this disease.

Introduction

In polycystic liver disease, a large number of cysts are formed, and hepatomegaly is caused by an increase in the number and enlargement of cysts. Many patients with polycystic liver disease are asymptomatic, but some show

KARGER

E-Mail karger@karger.com
www.karger.com/ddi

0257–2753/16/0346–0654$39.50/0

Masatoshi Kudo, MD, PhD
Department of Gastroenterology and Hepatology
Kindai University Faculty of Medicine
377-2 Ohno-Higashi, Osaka-Sayama, Osaka 589-8511 (Japan)
E-Mail m-kudo@med.kindai.ac.jp

symptoms associated with hepatomegaly including an abdominal mass, a feeling of abdominal fullness, abdominal discomfort, abdominal pain, and obstruction of the digestive tract. The life prognosis has been reported to be relatively favorable, but life-threatening complications such as intracystic hemorrhage, intracystic infection, bile duct obstruction, and liver failure may occur [1]. Symptoms associated with hepatomegaly exert serious effects on the QOL, but as they are usually nonfatal, the judgment about the timing and therapeutic procedure is occasionally difficult.

Among surgical treatments, hepatectomy is selected if cysts are present diffusely. However, the incidences of perioperative complications such as ascites, pleural effusion, bile spillage, and hemorrhage have been reported to be 20–80%. The recurrence of symptoms has been reported to be 3–33% [2, 3]. Cyst fenestration is selected when large cysts are present in a limited region or when cysts are present on the liver surface. Fenestration is less invasive than hepatectomy, and, recently, it has been found that the procedure may be performed laparoscopically. The most frequent perioperative complication is ascites, the incidence of which is 24%, and the recurrence rate has been reported to be 20% [4, 5].

Internal treatments have also been reported. However, the disease is reported to recur in 78–100% of the patients after drainage alone [6, 7], and concomitant sclerotherapy is recommended. Ethanol infusion therapy has been reported, but caution against pain, symptoms of poisoning, and liver damage is necessary, and the recurrence rate is reportedly 75% [8, 9]. Minocycline hydrochloride infusion therapy is considered to be relatively safe, but there have been few reports on the therapeutic results or reactivation after this procedure [10].

Monoethanolamine oleate (EO) sclerotherapy therapy was performed and reported by Yamamoto et al. [11] in a small number of patients. We also performed the procedure for 17 cysts in 13 patients and previously reported a volume reduction rate of 93.3% and a recurrence rate of 0% [12]. Since we have subsequently encountered additional patients and evaluated long-term courses, the results are reported here.

Subjects and Methods

All patients gave written consent for the study, and the study protocol was approved by the Ethics Committee at our institution.

Twenty-nine cysts in 22 patients who underwent EO infusion therapy for liver cysts between January 1999 and June 2011 were evaluated.

Simple liver cysts were typically visualized on ultrasound images [13] as anechoic smooth borders with strong posterior echo enhancement and an accentuation of echoes beyond the cyst wall. On CT, simple liver cysts appeared as well-demarcated lesions with fluid attenuation and without enhancement after contrast administration. The cysts of PLD typically appeared as multiple homogeneous lesions with fluid attenuation and without wall or content enhancement after IV contrast administration [14].

Under ultrasound guidance, liver cysts were punctured percutaneously using an 18G needle. A guide wire was inserted and a 7Fr pigtail catheter was inserted. Then, the cyst contents were aspirated as much as possible and examined cytologically and by culture. After confirmation of the absence of communication with the bile duct, vessels, or peritoneal cavity by contrast radiography, 5% EO was infused at 10% of the liver volume with a maximum of 120 ml (fig. 1). Until 2007, a clamp was applied for 30 min, during which the body position was changed from the prone position to the left and right recumbent positions every 10 min, and the catheter was declampled and removed after 24 h. From 2007 to 2011, clamping was sustained for 24 h, the catheter was declamped, the cyst contents were discharged again, and the catheter was removed.

The therapeutic effects were followed up by CT or US 1 week, 3, and 6 months after the procedure and every 6 months thereafter and compared between 8 simple cysts in 8 patients and 21 cysts in 14 patients with polycystic liver disease.

Statistical Analysis

Date are expressed as median (range) values. Differences between groups were examined for significance using the t test and Fisher's exact test where appropriate.

Results

Table 1 shows the characteristics of patients. No difference was observed in the gender, age, or symptoms between the simple cyst and polycystic liver disease groups. The median follow-up period was 78 months (0–203 months).

Figure 2 shows the cyst volumes in the simple cyst group. The median cyst volume was 350 ml (26–1,424 ml) before treatment and 4 ml (0–10 ml) after treatment. The median volume reduction rate was 99% (98–100%). No re-enlargement was observed after treatment.

Figure 3 shows the cyst volumes in the polycystic liver disease group. The median cyst volume was 347 ml (61–1,885 ml) before treatment and 14 ml (0–238 ml) after treatment. The median volume reduction rate was 95% (57–100%). No re-enlargement was noted after volume reduction.

Table 2 compares the 2 groups. While no difference was observed in the pre-treatment volume, the volume reduction rate was greater in the simple cyst than polycystic liver disease group ($p = 0.04$).

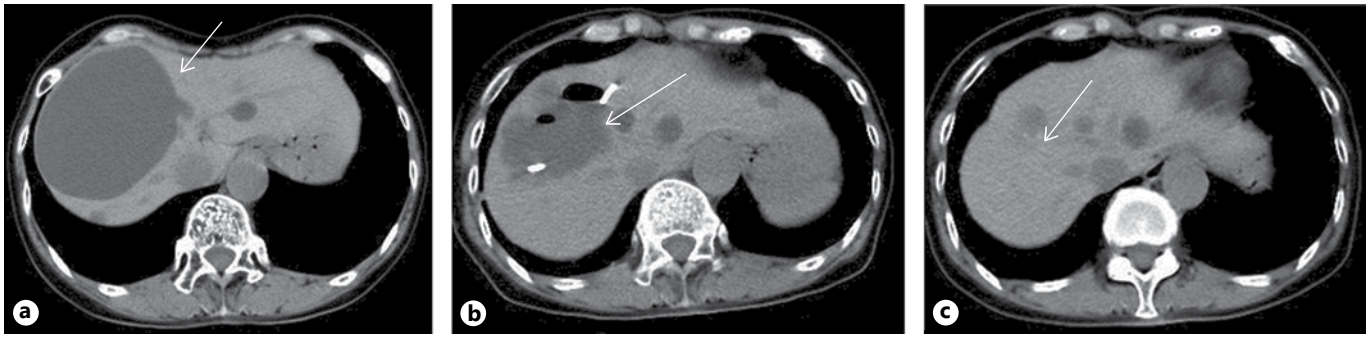

Fig. 1. A 62-year-old woman with polycystic liver disease complaining of a sense of abdominal fullness. **a** Pre-treatment CT scan showing a cyst of 10 cm in diameter in the right hepatic lobe. **b** A drain was placed, the contents were aspirated, EO was infused, the drain was clamped and declamped after 24 h, and CT was performed. The cyst volume had markedly reduced. **c** The cyst had disappeared based on CT conducted 3 years after treatment.

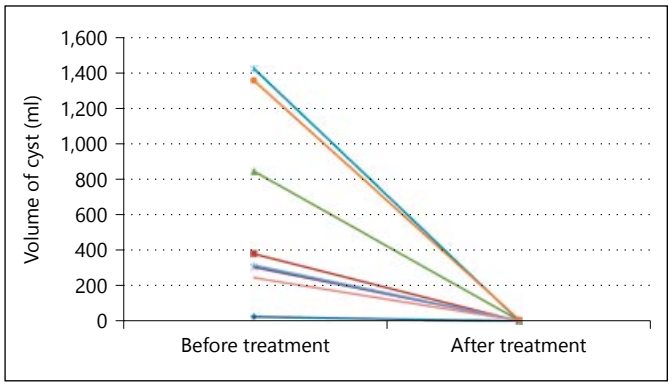

Fig. 2. In the simple cyst group, the median cyst volume was 350 ml (26–1,424 ml) before treatment and 4 ml (0–10 ml) after treatment.

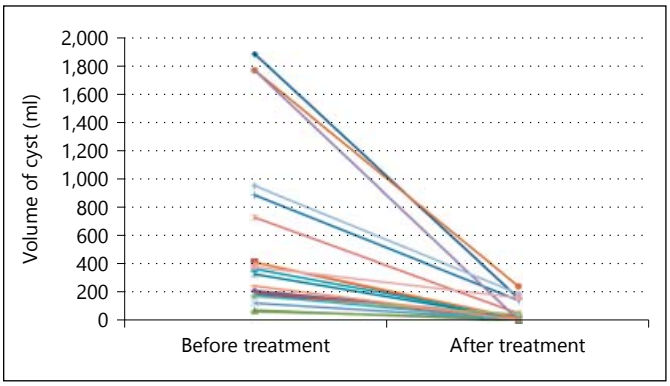

Fig. 3. The cyst volumes before and after treatment in the polycystic liver disease group are shown in figure 2. The median cyst volume was 347 ml (61–1,885 ml) before treatment and 14 ml (0–238 ml) after treatment.

Table 1. Baseline patient characteristics

	Simple cysts	Polycystic liver disease	p value
Gender (M/F)	1/7	3/11	1
Age, years, median (range)	66 (56–79)	65.5 (45–86)	
Symptoms			
Abdominal distension	6/2	4/10	0.07
Epigastralgia	1/7	4/10	0.61

Table 2. Volume reduction rate of the cysts

	Simple cysts	Polycystic liver disease	p value
Number of cysts	8	21	
Cyst volume, ml	350 (26–1,424)	347 (61–1,885)	0.839
Volume reduction rate, %	99 (98–100)	95 (57+100)	0.04

A 64-year-old woman developed fever and abdominal pain 1 week after discharge. Since liver abscess was detected at the treated site, drainage and antibiotic administration were needed. In a 77-year-old woman, the catheter became dislodged after its placement and was removed without repositioning. No other major adverse event was observed.

Discussion

Liver cysts were treated by EO infusion therapy with a volume reduction rate of 99% in the simple cyst group and 95% in the polycystic liver disease group. No re-enlargement was noted, and the results were satisfactory.

Dig Dis 2016;34:654–658
DOI: 10.1159/000448826

After puncture and drainage alone, 78–100% of liver cysts have been reported to recur [6, 7], and its therapeutic effect is limited. On puncture and drainage, samples for cytological examination and culture can be obtained, and the symptoms can be confirmed to be caused by the cysts. Invasive treatments such as ethanol sclerotherapy have been reported to be effective for simple cysts, but the re-enlargement rate of multiple cysts after ethanol sclerotherapy is reportedly 75% or higher [1, 15]. Also, ethanol sclerotherapy is selected for multiple liver cysts in 25% or less of patients. A cause of the unsatisfactory therapeutic results may be insufficient collapsing of multiple cysts by aspiration compared with simple cysts [16, 17]. In addition, pain, symptoms of poisoning, and liver damage may be caused by ethanol infusion therapy. In contrast, minocycline hydrochloride infusion therapy is considered to be performed relatively safety. However, while CR and PR rates have been reported to be 87 and 13%, respectively, there has been no report on the recurrence rate [10], and the long-term results are unclear. In our present study, the volume reduction rate was high in both simple and multiple cysts, no pain was caused by the procedure, and no re-enlargement was observed on long-term follow-up, suggesting the effectiveness of EO infusion therapy.

Regarding hepatic artery embolization, another internal treatment, Takei et al. [18] reported that it could also be performed in patients with a poor general condition and low tolerance to surgery. However, as the procedure has been performed in a small number of patients, and as the response rate is unsatisfactory at 40%, the procedure may be difficult to develop as a standard treatment. On the other hand, EO infusion therapy can be performed at any institution capable of echo-guided puncture similarly to ethanol or Minomycin infusion therapy and is considered to be easier to standardize.

Cyst fenestration is the least invasive among surgical treatments. Drenth et al. [4] reported a recurrence rate of 24%, complication rate of 22%, and mortality rate of 2% in 311 patients. Recently, laparoscopic fenestration has been increasingly reported, but the complication and recurrence rates are similar to those caused by open fenestration [4, 5], and sufficient evaluation is necessary for its application.

There have also been reports of liver transplantation as a treatment for multiple liver cysts. While it is the only radical procedure, it involves marked perioperative invasion with a complication rate of 57–85% and a mortality rate of 3–29% [2–4, 19]. Also, in consideration of the necessity of having the patient continue taking immunosuppressants for the rest of his/her life, it is not recommendable as the first-choice treatment.

Although there was no difference in the therapeutic results between simple cysts and polycystic liver disease in our previous study [12], the results in the simple cyst group were significantly more favorable than those in the polycystic liver disease group in this study. This change may be attributed to the statistical effect of the increase in the number of patients. However, as EO infusion therapy is much superior to ethanol infusion therapy as a treatment for polycystic liver disease, the future of treatment choice is worth considering.

The results of EO sclerotherapy infusion therapy were outstanding. EO infusion therapy achieves a fairly high treatment response in the volume reduction (99%) and sustained shrinkage over long-term follow-up. Therefore, this is a breakthrough technique in the treatment of polycystic liver disease as well as simple cyst and should be a standard of care in this disease.

Disclosure Statement

The authors declare no conflicts of interest regarding the publication of this paper.

Author Contributions

M. Takita drafted the manuscript and wrote the final version of the manuscript. M. Kudo reviewed and approved the last version of the manuscript.

References

1 Erdogan D, van Delden OM, Rauws EA, Busch OR, Lameris JS, Gouma DJ, et al: Results of percutaneous sclerotherapy and surgical treatment in patients with symptomatic simple liver cysts and polycystic liver disease. World J Gastroenterol 2007;13:3095–3100.

2 Aussilhou B, Douflé G, Hubert C, Francoz C, Paugam C, Paradis V, et al: Extended liver resection for polycystic liver disease can challenge liver transplantation. Ann Surg 2010; 252:735–743.

3 Schnelldorfer T, Torres VE, Zakaria S, Rosen CB, Nagorney DM: Polycystic liver disease: a critical appraisal of hepatic resection, cyst fenestration, and liver transplantation. Ann Surg 2009;250:112–118.

4 Drenth JP, Chrispijn M, Nagorney DM, Kamath PS, Torres VE: Medical and surgical treatment options for polycystic liver disease. Hepatology 2010;52:2223–2230.

5 Fiamingo P, Tedeschi U, Veroux M, Cillo U, Brolese A, Da Rold A, et al: Laparoscopic treatment of simple hepatic cysts and polycystic liver disease. Surg Endosc 2003;17:623–626.

6 Saini S, Mueller PR, Ferrucci JT Jr, Simeone JF, Wittenberg J, Butch RJ: Percutaneous aspiration of hepatic cysts does not provide definitive therapy. AJR Am J Roentgenol 1983; 141:559–560.
7 Koperna T, Vogl S, Satzinger U, Schulz F: Nonparasitic cysts of the liver: results and options of surgical treatment. World J Surg 1997;21:850–854; discussion 854–855.
8 Montorsi M, Torzilli G, Fumagalli U, Bona S, Rostai R, De Simone M, et al: Percutaneous alcohol sclerotherapy of simple hepatic cysts. Results from a multicentre survey in Italy. HPB Surg 1994;8:89–94.
9 Mehendale VG, Kamdar MS, Shenoy SN, Chaudhari N, Joshi AM: Non-parasitic hepatic cysts causing obstructive jaundice: two cases. Indian J Gastroenterol 2003;22:26.
10 Cellier C, Cuenod CA, Deslandes P, Auroux J, Landi B, Siauve N, et al: Symptomatic hepatic cysts: treatment with single-shot injection of minocycline hydrochloride. Radiology 1998;206:205–209.
11 Yamamoto K, Sakaguchi H, Anai H, Tanaka T, Morimoto K, Kichikawa K, et al: Sclerotherapy for simple cysts with use of ethanolamine oleate: preliminary experience. Cardiovasc Intervent Radiol 2005;28:751–755.
12 Nakaoka R, Das K, Kudo M, Chung H, Innoue T: Percutaneous aspiration and ethanolamine oleate sclerotherapy for sustained resolution of symptomatic polycystic liver disease: an initial experience. AJR Am J Roentgenol 2009; 193:1540–1545.
13 Mortelé KJ, Ros PR: Cystic focal liver lesions in the adult: differential CT and MR imaging features. Radiographics 2001;21: 895–910.
14 Trinkl W, Sassaris M, Hunter FM: Nonsurgical treatment for symptomatic nonparasitic liver cyst. Am J Gastroenterol 1985;80:907–911.
15 Bean WJ, Rodan BA: Hepatic cysts: treatment with alcohol. AJR Am J Roentgenol 1985;144: 237–241.
16 Spiegel RM, King DL, Green WM: Ultrasonography of primary cysts of the liver. AJR Am J Roentgenol 1978;131:235–238.
17 Kairaluoma MI, Leinonen A, Ståhlberg M, Päivänsalo M, Kiviniemi H, Siniluoto T: Percutaneous aspiration and alcohol sclerotherapy for symptomatic hepatic cysts. An alternative to surgical intervention. Ann Surg 1989; 210:208–215.
18 Takei R, Ubara Y, Hoshino J, Higa Y, Suwabe T, Sogawa Y, et al: Percutaneous transcatheter hepatic artery embolization for liver cysts in autosomal dominant polycystic kidney disease. Am J Kidney Dis 2007;49:744–752.
19 Russell RT, Pinson CW: Surgical management of polycystic liver disease. World J Gastroenterol 2007;13:5052–5059.

Original Article

Digestive Diseases

Dig Dis 2016;34:659–664
DOI: 10.1159/000448828

Clinical Factors Predicting the Effect of Tolvaptan for Refractory Ascites in Patients with Decompensated Liver Cirrhosis

Hirokazu Chishina Satoru Hagiwara Naoshi Nishida Kazuomi Ueshima Toshiharu Sakurai Hiroshi Ida Yasunori Minami Masahiro Takita Masashi Kono Tomohiro Minami Mina Iwanishi Yasuko Umehara Tomohiro Watanabe Yoriaki Komeda Tadaaki Arizumi Masotoshi Kudo

Department of Gastroenterology and Hepatology, Kindai University Faculty of Medicine, Osaka-Sayama, Japan

Key Words
Tolvaptan · Liver cirrhosis · Refractory ascites · Delayed response

Abstract
Objective: Refractory ascites reduces the quality of life of liver cirrhosis patients. Albumin preparation and diuretics, such as furosemide, have been used to treat refractory ascites, but the effect was poor in many patients. In this study, we analyzed patients treated with tolvaptan (TLV) at our hospital and investigated predictors of the effect. ***Methods:*** The subjects were 70 patients for whom TLV was introduced to treat refractory ascites who could be analyzed between November 2013 and March 2015 at our hospital. Patient background before initiation of oral TLV treatment, the dose of diuretics, and each item of biochemical tests of blood and urine were investigated, and factors correlated with the treatment effect were analyzed. An increase of ≥1,000 ml in the daily urine volume from the day before oral treatment or a decrease of ≥1 kg in the body weight within 7 days as an early effect was observed in 33 patients and not observed in 37 patients. TLV treatment was continued for 60 days or longer in 12 of the 37 patients in whom no early effect was observed, and the presence or absence of a delayed effect and predictors of the effect were investigated. A decrease in ascites on abdominal CT with improvement of subjective symptoms at 60 days was defined as a delayed effect. ***Results:*** When early predictors of the effect were investigated by univariate analysis, serum blood urea nitrogen (BUN) and serum creatinine (Cr) were significantly higher in the non-responder group (BUN: $p = 0.03$, Cr: $p = 0.04$), but no factor independently associated with the treatment effect was extracted on multivariate analysis. The delayed effect was noted in 4 (33.3%) of the 12 patients, but no predictor of the effect before treatment was identified. However, reactions, such as an increase in serum Na and reduction of urinary osmotic pressure, were observed early after TLV administration in some patients in whom the delayed effect was observed. ***Conclusions:*** The diuretic effect of TLV may decrease in renal hypofunction patients. Since the delayed effect was noted in a specific ratio of patients, continuation of TLV administration is an option even though the early treatment effect is poor unless ascites aggravates or adverse effects develop.

KARGER

E-Mail karger@karger.com
www.karger.com/ddi

0257–2753/16/0346–0659$39.50/0

Satoru Hagiwara, MD, PhD
Department of Gastroenterology and Hepatology
Kindai University Faculty of Medicine
377-2 Ohno-Higashi, Osaka-Sayama, Osaka 589-8511 (Japan)
E-Mail hagi-318@hotmail.co.jp

Introduction

The cause of death of liver cirrhosis includes liver decompensation and hepatocellular carcinoma (HCC) [1–4]. Ascites, jaundice, or hepatic encephalopathy is the most common symptom of liver decompensation. Liver cirrhosis–associated ascites has been treated with aldosterone antagonists and loop diuretics [5, 6], but even though these are concomitantly used, the response is poor, or adverse effects, such as renal impairment and abnormal electrolytes, develop in some patients. Since tolvaptan (TLV) is a vasopressin (VP) receptor antagonist and it exhibits an aquaretic effect without Na excretion, its indication for fluid retention in liver cirrhosis for which the effects of existing diuretics are insufficient was initially approved as a combination therapy drug in September 2013 [7]. There are also some patients for whom the early effect of TLV is poor, but continued administration exhibits the delayed effect in some patients. In this study, we investigated predictors of the early and delayed effects of TLV.

Methods

Patients

The subjects for this analysis were 70 patients for whom TLV was introduced to treat hepatic edema who could be analyzed between November 2013 and March 2015 at our hospital. Regarding patient background, the median age was 69.8, and there were 40 male and 30 female patients. The cause of liver cirrhosis was HCV in 34 patients, HBV in 9, alcohol in 8, and others in 19. The Child–Pugh Grade was C in 48 patients (about 68.5%). There were 46 patients with HCC, and 18 of them had a VP3 or higher portal vein tumor thrombus. The initial dose of TLV was 3.75 mg/day in 59 patients (about 84%), and the dose was appropriately changed based on the judgment by attending physicians. Regarding diuretics used before introduction of TLV, furosemide was administered at a dose higher than 40 mg/day in 46 patients, and spironolactone was administered at a dose higher than 50 mg/day in 40 patients (table 1).

Evaluation Criteria of Therapeutic Effect

Patient background before the initiation of oral TLV treatment, the dose of diuretics, and each item of biochemical tests of blood and urine was investigated, and factors correlated with the treatment effect were retrospectively analyzed. An increase of ≥1,000 ml in the daily urine volume from the day before oral treatment or a decrease of ≥1 kg in the body weight within 7 days as an early effect was observed in 33 patients and not observed in 37 patients. TLV treatment was continued for 60 days or longer in 12 of the 37 patients in whom no early effect was observed, and the presence or absence of a delayed effect and predictors of the effect were investigated. A decrease in ascites on abdominal CT with improvement of subjective symptoms after 60 days was defined as a delayed effect. Regarding prediction of the delayed effect, patients who received additional treatment, such as treatments with diuretics other than TLV and albumin preparation, were excluded from analysis.

Table 1. Demographics of the enrolled patients (n = 70)

Item	
Age, years	69.8±9.17
Gender (male/female)	40/0
Etiology of liver cirrhosis (HBV/HCV/alcohol/others)	9/34/8/19
Child–Pugh (A/B/C)	1/21/48
HCC (yes/no)	46/24
≥PVTT-Vp3 (yes/no)	18/28
Initial TLV dose (3.75/7.5/15 mg)	59/9/2
Serum albumin, g/dl	2.66±0.51
Serum BUN, mg/dl	26.2±17.3
Serum Cr, mg/dl	1.08±0.51
eGFR	57.4±23.8
Furosemide dose (<40/≥40 mg)	46/24
Spironolactone dose (<50/≥50 mg)	40/30

Date are expressed as mean value (±SD).
PVTT = Portal vein tumor thrombosis.

Statistical Analysis

To investigate the prediction of the early effect, univariate analysis was performed using the Student t test and Fishers exact test. Significant factors on univariate analysis were subjected to multivariate analysis using a logistic regression model. For factors analyzed by multivariate analysis, the cut-off values were calculated by ROC analysis. To investigate prediction of the delayed effect, univariate analysis was performed using the Student t test and Fishers exact test. $p < 0.05$ was regarded as significant.

Results

Predictors of Early Therapeutic Effect

The early effect was observed within 7 days after introduction of TLV in 33 (about 47%) of the 70 patients. Patient background was compared between the 33 responders and 37 non-responders using univariate analysis, but no significant factor was extracted (table 2). On univariate analysis of the blood and urinary test items, serum blood urea nitrogen (BUN) and serum creatinine (Cr) were significantly higher in the non-responder group (BUN: $p = 0.03$, Cr: $p = 0.04$; table 2). Multivariate analysis of these 2 factors was performed using a logistic regression model, but no significant factor was extracted (table 3).

Table 2. Factors associated with early therapeutic effect (univariate analysis)

	Responder (n = 33)	Non-responder (n = 37)	p value
Age, years	71±8.6	78±9.6	0.28
Gender (male/female)	18/15	22/15	0.80
Etiology (HBV/HCV/alcohol/others)	1/17/4/11	8/17/4/8	0.11
Child–Pugh grade (A/B/C)	0/12/21	1/9/27	0.36
HCC complication (yes/no)	18/15	28/9	0.08
PVTT-VP3 or higher (yes/no)	10/8	8/20	0.12
TLV dose (3.75/7.5/15 mg)	27/5/1	32/4/1	0.86
Furosemide dose (<40/≥40 mg)	22/11	24/13	1
Spironolactone dose (<50/≥50 mg)	21/12	19/18	0.34
Serum Na, mEq/l	138.4±3.5	137.3±4.3	0.26
Serum BUN, mg/dl	21.9±12.3	30.1±20.2	0.03*
Serum Cr, mg/dl	0.9±0.3	1.2±0.5	0.04*
eGFR	62.8±23.0	52.8±23.9	0.08
Urinary osmotic pressure, mOsm	515±220	436±101	0.21
Serum albumin, g/dl	2.4±0.5	2.5±0.5	0.19
Serum T-bil, g/dl	2.3±2.2	2.2±1.4	0.70
Serum NH_3, μmol/l	48.3±25.9	38.5±16.5	0.06
Serum ALT, mg/dl	51.5±93.4	40.4±35.7	0.50
Serum PT, %	51.0±19.2	55.9±13.7	0.22
Serum CRP, mg/dl	2.6±3.2	3.4±2.7	0.23

Date are expressed as mean value (±SD).
* Statistically significant ($p < 0.05$).
PVTT = Portal vein tumor thrombosis; T-bil = total bilirubin; ALT = alanine transaminase; PT = prothrombin; CRP = C-reactive protein.

Predictors of Delayed Effect

TLV treatment was continued for 60 days or longer in 12 of the 37 patients for whom the early effect was poor. After 60 days or longer after the introduction of TLV, the delayed effect was observed in 4 (33%) of the 12 patients. Factors associated with the delayed effect were investigated in the items before introduction of TLV, but no significant factor was identified (table 4).

Table 3. Predictors of early therapeutic effect (logistic regression model)

Item	OR	95% CI	p value
BUN, mg/dl		0.109–1.285	0.118
<29	1		
≥29	0.375		
Cr, mg/dl		0.189–1.957	0.404
<0.98	1		
≥0.98	0.608		

Serious Adverse Effect

Grade 2 or severer hepatic encephalopathy developed in 5 patients (7.1%), and hypernatremia (146 mEq/l or higher) developed in 3 patients (4.3%). A 1.5 times or more increase in serum Cr was noted in 12 patients (17.1%), and 3 times or more higher serum Cr than the baseline was noted in 3 patients (4.3%; table 5).

Discussion

As the mechanism of liver cirrhosis, water in liver failure, and abnormal electrolyte, ascites is retained due to portal hypertension and increased arteriovenous shunts, reducing the effective circulating plasma volume, which is considered to cause fluid retention through the renin-angiotensin-aldosterone system enhanced by reduced renal blood flow [8, 9]. Aldosterone antagonists are effective to treat fluid retention accompanying liver cirrhosis [5], but we encounter many patients for whom these drugs are insufficient. On the other hand, a reduced effective circulating plasma volume causes fluid retention through enhancement of VP [8, 9], but no effective therapeutic drug was previously available for this.

TLV shows antagonism against the VP V2 receptor present on the renal collecting duct, which inhibits aqua-

Table 4. Predictors of delayed effect (univariate analysis)

Item	Non-responder (n = 8)	Late responder (n = 4)	p value
Age, years	65±11.5	65±6.3	0.98
Gender (male/female)	5/3	2/2	1
Etiology of liver cirrhosis (HBV/HCV/alcohol/others)	1/1/5/1	1/3/0/0	1
Child–Pugh grade (A/B/C)	1/2/5	0/2/2	0.71
HCC (yes/no)	6/2	2/2	0.54
PVTT-VP3 or higher (yes/no)	0/6	0/2	1
Furosemide dose (<40/≥40 mg)	6/2	3/1	1
Spironolactone dose (<40/≥40 mg)	5/3	2/2	1
Serum Na, mEq/l	139.5±4.2	135±5.5	0.14
Serum albumin, g/dl	2.7±0.4	3.0±0.4	0.25
Serum BUN, mg/dl	41.2±34.8	35.5±26.5	0.77
Serum Cr, mg/dl	1.4±0.8	1.6±0.5	0.73
eGFR	46.8±19.3	35.5±16.6	0.34
Serum T-bil, g/dl	1.5±0.8	0.7±0.2	0.09
Serum CRP, mg/dl	2.4±2.7	2.6±3.3	0.90

Date are expressed as mean value (SD).

PVTT = Portal vein tumor thrombosis; T-bil = total bilirubin; ALT = alanine transaminase; CRP = C-reactive protein.

Table 5. Serious adverse effects

Item	Number (%)
Hepatic encephalopathy (≥grade II)	5 (7.1)
Hypernatremia (≥146 mEq/l)	3 (4.3)
Increase in serum Cr	15 (21.4)
>Baseline × 1.5	12 (17.1)
>Baseline × 3.0	3 (4.3)

porin 2 expression and suppresses reabsorption of water, exhibiting the diuretic effect. In Japan, a phase 3 study was performed involving liver cirrhosis patients for whom the effects of loop diuretics and aldosterone antagonists were insufficient [7]: of 164 patients, 84 and 80 patients were enrolled in the TLV 7.5 mg treatment and placebo groups, respectively. The body weight significantly decreased in the TLV group compared with that in the placebo group. The urine volume significantly increased on days 1 and 7 in the TLV group, but no significant change was noted in the placebo group. The main adverse effects were dry mouth, constipation, renal dysfunction, hepatic encephalopathy, and pruritus, but the severity was mild to moderate. The effect and tolerability of TLV for liver cirrhosis patients were confirmed and the indication for (liver cirrhosis–associated fluid retention for which the effect of other diuretics, such as loop diuretics, is insufficient) was approved in September 2013 for the first time in the world.

There are various reports on the prediction of the effect of TLV. Zhang et al. [10] investigated 39 patients with liver cirrhosis–associated refractory ascites and observed that the effect of TLV decreased in hepatorenal syndrome (HRS) patients. In a TLV single-dose study involving renal failure patients, the effect decreased as estimated glomerular filtration rate (eGFR) decreased [11]. On subanalysis of the phase 3 study performed in Japan, the effect of TLV decreased when BUN was high [12]. As reported in the above studies, the effect of TLV decreases in patients with HRS, renal parenchymal disorder with reduced eGFR, and high BUN, that is, patients in whom intra-vascular dehydration and prerenal impairment are suggested. On investigating predictors of the early effect, serum BUN and serum Cr were extracted as significant factors on univariate analysis, being consistent with previous reports. Our patients were treated with diuretics at a high dose before introduction of TLV: furosemide >40 mg/day in 46 patients (about 66%) and spironolactone >50 mg/day in 40 patients (about 57%). Since furosemide and spironolactone may cause intra-vascular dehydration and prerenal impairment, it may be desirable to introduce TLV before increasing the dose of diuretics.

In addition, there are various reports on the prediction of the effect of TLV centering on heart failure patients. Imamura et al. [13] reported that in a study involving 61 decompensated heart failure patients, many responders were noted in patients in whom urinary osmotic pressure was higher than 352 mOsm/l before TLV administration and it decreased by more than 26% 4–6 h after TLV administration. Iwatani et al. [14] reported that in a study involving 17 patients with heart failure or liver cirrhosis with concomitant CKD with fluid retention, a baseline urinary osmotic pressure higher than 279 mOsm/kg H_2O was associated with 5% or more body weight reduction after 1 week. In our study, the mean baseline urinary osmotic pressure was 515 ± 220 mOsm in the responders and 436 ± 101 mOsm in the non-responders, showing no significant difference ($p = 0.21$), but it was high in the responder group. It is possible that urinary osmotic pressure reflects renal interstitial osmotic pressure, and reduction of its baseline naturally leads to resistance to TLV treatment.

In western countries, TLV is used to treat hyponatremia in heart failure and SIADH patients. In the EVEREST study, a randomized double-blinded placebo-controlled study was performed involving decompensated heart failure patients [15, 16], in which the prognosis of the heart failure patients was not different from that in the placebo group, but TLV administration decreased cardiovascular events in hyponatremia patients with serum Na below 130 mEq/l, confirming the usefulness for hyponatremia patients. In the SALT study, the hyponatremia-improving effect for decompensated liver cirrhosis patients was reported [17].

As described above, various candidates were reported for predictors of the early therapeutic effect, such as baseline serum BUN and Cr, urinary osmotic pressure, and reduction of urinary osmotic pressure and an increase in serum Na after introduction of TLV. On the other hand, there is no report on factors involved in the exhibition of the delayed effect reported by us. There are only a few studies on patients in whom the delayed effect is exhibited, and the investigation is insufficient. We could not also extract pretreatment factors involved in the exhibition of the delayed effect. However, in patients in whom the delayed effect was exhibited, reactions assumed to be influences of TLV, such as reduction of urinary osmotic pressure and an increase in serum Na after introduction of TLV, were observed in some patients. Generally, the effect of TLV is exhibited relatively early, and the plasma TLV level reaches the maximum level 4–6 h after administration [7]. Thus, the exhibition of the effect from the dosing day has been reported. Accordingly, although it is unclear why the action of TLV did not rapidly lead to changes in the body weight, it is possible that V2 receptor antagonism of TLV-induced enhancement of the renin-angiotensin-aldosterone system, or the effect of TLV may be exhibited when the increase in the body weight can be inhibited in patients whose body weight goes on increasing in the clinical course. However, if the effect is defined as early body weight reduction, this reactivity of TLV will be neglected. Thus, the judgment of the effect varies depending on the criteria and timing of judgment of the treatment effect.

Serious adverse effects include grade 2 or severer hepatic encephalopathy and an increase in serum Cr (table 5). The subjects analyzed in our study included many patients with advanced liver cancer and Child–Pugh Grade C poor liver function, suggesting that adverse effects were due to the progression of the primary disease. However, the above adverse effects developed long after the introduction of TLV in some patients. Attention should be paid to the development of adverse effects induced by long-term TLV administration.

It was clarified that, although aimless long-term TLV administration is not recommended, the delayed effect of TLV is exhibited in some patients. Accordingly, even though early responses of the urine volume and body weight are poor, continuation of TLV treatment may be an option when ascites does not aggravate. However, many points remain unclear with regard to the safety of long-term TLV administration for liver cirrhosis patients, and strict observation of the appearance of adverse effects is necessary.

Disclosure Statement

There are no conflicts of interest to declare.

References

1 Kudo M: Surveillance, diagnosis, treatment, and outcome of liver cancer in Japan. Liver Cancer 2015;4:39–50.

2 Kudo M, Matsui O, Izumi N, Iijima H, Kadoya M, Imai Y, Okusaka T, Miyayama S, Tsuchiya K, Ueshima K, Hiraoka A, Ikeda M, Ogasawara S, Yamashita T, Minami T, Yamakado K: JSH consensus-based clinical practice guidelines for the management of hepatocellular carcinoma: 2014 update by the liver cancer study group of Japan. Liver Cancer 2014;3:458–468.

3 Poon RT, Cheung TT, Kwok PC, Lee AS, Li TW, Loke KL, Chan SL, Cheung MT, Lai TW, Cheung CC, Cheung FY, Loo CK, But YK, Hsu SJ, Yu SC, Yau T: Hong Kong consensus recommendations on the management of hepatocellular carcinoma. Liver Cancer 2015;4:51–69.

4 Clinical practice guidelines for hepatocellular carcinoma differ between Japan, United States, and Europe. Liver Cancer 2015;4:85–95.
5 Boyer TD, Warnock DG: Use of diuretics in the treatment of cirrhotic ascites. Gastroenterology 1983;84:1051–1055.
6 Perez-Ayuso RM, Arroyo V, Planas R, Gaya J, Bory F, Rimola A, Rivera F, Rodes J: Randomized comparative study of efficacy of furosemide versus spironolactone in nonazotemic cirrhosis with ascites. Relationship between the diuretic response and the activity of the renin-aldosterone system. Gastroenterology 1983;84:961–968.
7 Sakaida I, Yanase M, Kobayashi Y, Yasutake T, Okada M, Okita K: The pharmacokinetics and pharmacodynamics of tolvaptan in patients with liver cirrhosis with insufficient response to conventional diuretics: a multicentre, double-blind, parallel-group, phase III study. J Int Med Res 2012;40:2381–2393.
8 Janicic N, Verbalis JG: Evaluation and management of hypo-osmolality in hospitalized patients. Endocrinol Metab Clin North Am 2003;32:459–481, vii.
9 Schrier RW, Arroyo V, Bernardi M, Epstein M, Henriksen JH, Rodes J: Peripheral arterial vasodilation hypothesis: a proposal for the initiation of renal sodium and water retention in cirrhosis. Hepatology 1988;8:1151–1157.
10 Zhang X, Wang SZ, Zheng JF, Zhao WM, Li P, Fan CL, Li B, Dong PL, Li L, Ding HG: Clinical efficacy of tolvaptan for treatment of refractory ascites in liver cirrhosis patients. World J Gastroenterol 2014;20:11400–11405.
11 Shoaf SE, Bricmont P, Mallikaarjun S: Pharmacokinetics and pharmacodynamics of oral tolvaptan in patients with varying degrees of renal function. Kidney Int 2014;85:953–961.
12 Sakaida I, Nakajima K, Okita K, Hori M, Izumi T, Sakurai M, Shibasaki Y, Tachikawa S, Tsubouchi H, Oka H, Kobayashi H: Can serum albumin level affect the pharmacological action of tolvaptan in patients with liver cirrhosis? A post hoc analysis of previous clinical trials in Japan. J Gastroenterol 2015;50:1047–1053.
13 Imamura T, Kinugawa K, Nitta D, Fujino T, Inaba T, Maki H, Hatano M, Kinoshita O, Nawata K, Kyo S, Ono M: Novel scoring system using postoperative cardiopulmonary exercise testing predicts future explanation of left ventricular assist device. Circ J 2015;79:560–566.
14 Iwatani H, Kawabata H, Sakaguchi Y, Yamamoto R, Hamano T, Rakugi H, Isaka Y: Urine osmolarity predicts the body weight-reduction response to tolvaptan in chronic kidney disease patients: a retrospective, observational study. Nephron 2015;130:8–12.
15 Konstam MA, Gheorghiade M, Burnett JC Jr, Grinfeld L, Maggioni AP, Swedberg K, Udelson JE, Zannad F, Cook T, Ouyang J, Zimmer C, Orlandi C: Effects of oral tolvaptan in patients hospitalized for worsening heart failure: the EVEREST outcome trial. JAMA 2007;297:1319–1331.
16 Gheorghiade M, Konstam MA, Burnett JC, Jr, Grinfeld L, Maggioni AP, Swedberg K, Udelson JE, Zannad F, Cook T, Ouyang J, Zimmer C, Orlandi C: Short-term clinical effects of tolvaptan, an oral vasopressin antagonist, in patients hospitalized for heart failure: the EVEREST clinical status trials. JAMA 2007;297:1332–1343.
17 Cardenas A, Gines P, Marotta P, Czerwiec F, Oyuang J, Guevara M, Afdhal NH: Tolvaptan, an oral vasopressin antagonist, in the treatment of hyponatremia in cirrhosis. J Hepatol 2012;56:571–578.

Review Article

Digestive Diseases

Dig Dis 2016;34:708–713
DOI: 10.1159/000448863

Clinical Significance of Epigenetic Alterations in Human Hepatocellular Carcinoma and Its Association with Genetic Mutations

Naoshi Nishida Masatoshi Kudo

Department of Gastroenterology and Hepatology, Kindai University Faculty of Medicine, Osaka-Sayama, Japan

Key Words
Hepatocellular carcinoma · DNA methylation · Histone · Chromatin · Mutation

Abstract
Accumulation of genetic and epigenetic alterations is a hallmark of cancer genomes, including those in hepatocellular carcinoma (HCC). Particularly, in human HCC, epigenetic changes are more frequently observed than genetic changes in a variety of cancer-related genes, suggesting a potential role for epigenetic alterations during hepatocarcinogenesis. Several environmental factors, such as inflammation, obesity, and steatosis, are reported to affect the epigenetic status in hepatocytes, which could play a role in HCC development. In addition, genetic mutations in histone modulators and chromatin regulators would be critical for the acceleration of epigenetic alteration. It is also possible that major genetic mutations of HCC, such as *TP53* and *CNTTB1* mutations, are associated with the disturbance of epigenetic integrity. For example, specific *TP53* mutations frequently induced by aflatoxin B1 exposure might affect histone modifiers and nucleosome remodelers. Generally, epigenetic alteration is reversible, because of which dysregulation of transcription takes place, without affecting protein structure. Therefore, differentiation therapy is one of the potential approaches for HCC with advanced epigenetic alterations. On the other hand, a tumor carrying an accumulation of genetic mutations would result in many abnormal proteins that could be recognized as non-self and could be targets for immune reactions; thus, immune-checkpoint blockers should be effective for HCCs with genetic hypermutation. Although the emergence of genetic and epigenetic alterations could be linked to each other and there could be some crossover or convergence between these cancer pathways, characterization of the mutation spectrum of genetic and epigenetic alterations could influence future HCC treatment.

Introduction

It has been well described that the accumulation of genetic and epigenetic changes leads to the clonal selection of cancer cells harboring aggressive tumor behavior, such as metastatic potential and resistance to anticancer drugs [1]. Genetic alterations of cancer-related genes are one of the hallmarks of cancer cells; point mutations, chromosomal rearrangements, and fusion genes could lead to the activation of oncogenes and tumor suppressor genes (TSGs) and play a role in hepatocarcinogenesis [2]. On the other hand, epigenetic changes, such as the alteration of DNA methylation and histone modification in cancer cells, can also induce the activation and inactivation of cancer-related genes. This type of alteration is more frequently observed in a variety of cancer-related genes in hepatocellular carcinoma (HCC) [3]; recent studies have revealed that epigenetic alterations are related to genetic

KARGER

E-Mail karger@karger.com
www.karger.com/ddi

0257–2753/16/0346–0708$39.50/0

Naoshi Nishida, MD, PhD
Department of Gastroenterology and Hepatology
Kindai University Faculty of Medicine
377-2 Ohno-Higashi, Osaka-Sayama 589-8511 (Japan)
E-Mail naoshi@med.kindai.ac.jp

and chromosomal alterations [3]. In this review, we focus on the induction of epigenetic change during human hepatocarcinogenesis, particularly in the context of genetic and epigenetic association with cancer development, and discuss the significance of epigenetic instability in the treatment of this disease.

Induction of Epigenetic Instability

The emergence of cancer cells is mainly attributed to the deregulation of major cellular signaling pathways, induced by modifications in cancer-related genes. It is well known that genetic information is encoded in the nucleotide sequences and affects the protein structure. On the other hand, the epigenetic code is determined by histone modifications, which defines the chromatin status and regulates the transcription of corresponding genes (fig. 1). Two types of protein complexes mainly regulate histone modification; the polycomb group (PcG) protein complex is known to induce a repressive histone modification and inactivates gene expression, whereas the trithorax group (TrxG) protein complex is responsible for the emergence of active histone modifications and induces transcription [4] (fig. 1). Several studies have shown the deregulation of the PcG and TrxG components in human cancer, including HCC [4]. Furthermore, genetic mutations in histone modifier and nucleosome remodeler genes, such as the myeloid/lymphoid or mixed-lineage leukemia (MLL), a methyltransferase of histone H3 lysine 4 (H3K4), and the AT-rich interaction domain-containing proteins 1A and 1B, which are known members of the nucleosome remodelers, have been reported by exome sequencing of HCC tissues [5]. This evidence suggests that genetic change induces epigenetic instability during human hepatocarcinogenesis.

Emergence of Epimutation during HCC Development

As stated above, several types of cancers, including HCC, show dysregulation of the molecules responsible for epigenetic integrity, such as the molecules involved in histone modification, chromatin remodeling, and DNA methylation [4]; genetic mutation in these types of molecules have been reported in recent studies by deep sequencing methods [2]. In addition, associations between the CpG island methylator phenotype and mutations in chromatin regulators have also been reported in colorectal cancer [6]; genetic and epigenetic alterations in the

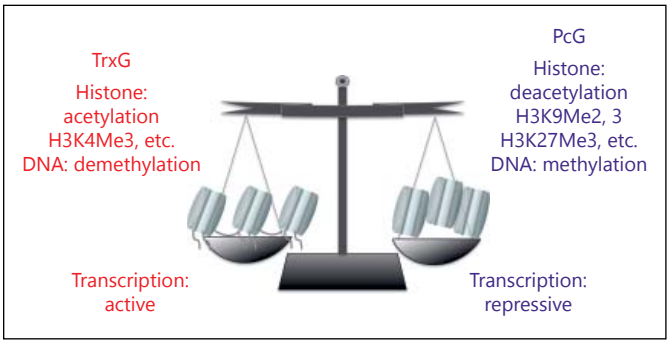

Fig. 1. A nucleosome status and active and repressive histone marks. A nucleosome consists of a DNA segment winding around 8 histone proteins cores; types of histone modification determine the chromatin status and corresponding gene expression. TrxG proteins induce active histone marks, such as H3K4 trimethylation (H3K4Me3), histone acetylation, and DNA demethylation that lead to relaxed chromatin status and activate gene transcription. PcG complex is responsible for inducing repressive histone marks, H3K9Me2, H3K9Me3, H3K27Me3, histone deacetylation, and DNA methylation. These modifications are associated with condensed chromatin status and the inactivation of transcriptions.

histone modifiers and nucleosome remodelers could be critical to maintain the integrity of the epigenetic code.

On the other hand, environmental factors, such as inflammation, aging, and obesity, could affect the epigenetic status and accelerate carcinogenesis [7]. For example, reactive oxygen species induce hypermethylation of the E-cadherin promoter by increasing the expression of transcription factor Snail expression and recruiting histone deacetylase 1 and DNA methyltransferase 1 (DNMT1) [8]. O'Hagan et al. [9] reported that oxidative stress and DNA damage could lead to the recruitment of the DNMT1 and PcG complex to damaged chromatin in colorectal cancer cell lines. Inflammatory cytokines derived from immune cells, such as interleukin (IL)-1β, IL-6, and prostaglandin E2, could also be a cause of abnormal DNA methylation [10–12]. An in vivo study using human liver chimeric mice showed that interferon-γ from natural killer cells was responsible for the induction of abnormal DNA methylation induced by the hepatitis virus [13]. Steatosis induced by hyperalimentation could also be a risk factor for epigenetic alteration in hepatocytes. For example, obesity reportedly accelerates hypermethylation of the genes that usually emerge during the aging process [14]. Another report showed that sterol regulatory element-binding protein-1 could induce HDCA8, which leads to the deacetylation of histone H4 and the formation of trimethylated histone H3 lysine 27 (H3K27me3) in combination with the enhancer of zeste homolog 2 (EZH2)

Dig Dis 2016;34:708–713
DOI: 10.1159/000448863

in steatohepatitis liver induced by obesity [15]. As obesity is a known risk factor of HCC, this evidence suggests that hyperalimentation and steatosis could also accelerate hepatocarcinogenesis through the disruption of epigenetic integrity.

Association between Mutation of Cancer-Related Genes and Epigenetic Alterations

TP53 and β-catenin (*CTNNB1*) are the most frequently mutated cancer-related genes in human HCC [2]. Previously, we have reported that the presence of *TP53* mutation is associated with genome-wide hypomethylation and a high degree of chromosomal alteration, whereas *CTNNB1* mutation is more frequently observed in HCC with advanced regional hypermethylation in known TSGs [16, 17]. Recently, it was reported that HCC with genomic instability and *TP53* mutation represents overexpression of ubiquitin-like with PHD and RING finger domains 1 (UHRF1) [18]. UHRF1 overexpression reportedly induces the destabilization of DNMT1, DNA hypomethylation, and *TP53*-mediated senescence; *TP53* mutation and UHRF1 overexpression induces abrogation of cellular senescence and accelerates the development of HCC carrying DNA hypomethylation that is induced by the ubiquitin ligase activity of UHRF1 and subsequent degradation of DNMT1 [18]. On the other hand, it is also reported that cancer cells expressing stabilized mutant β-catenin show the stabilization of DNMT1 owing to the protein–protein interaction between β-catenin and DNMT1 [19], which could be a cause of regional hypermethylation of the TSGs. Therefore, it is conceivable that diverse mutations of hepatocarcinogenesis also determine the epigenetic status critical for HCC development.

Another report suggests the role of a certain type of gain-of-function p53 mutation in epigenetic dysregulation. The *TP53* mutation at codon 249 (R249S) could induce the transcription of MLL and the association with the switch/sucrose non-fermentable nucleosome remodeling complex [20]. In addition, R249S mutation could induce the transcription of SET domain bifurcated 1 (SETDB1), which is known as a histone H3 lysine 9 (H3K9) methyltransferase; SETDB1 could also suppress the degradation of the R249S mutation and play a role in hepatocarcinogenesis [21]. The codon 249 is known as a mutational hotspot of the *TP53* gene in aflatoxin B1 (AFB1)-induced hepatocarcinogenesis, which is a well-known carcinogen for HCC [22]; induction of the R249S mutation is also reportedly associated with exposure to AFB1 [23]. Therefore, it is possible that some carcinogens induce epigenetic alterations and contribute to the emergence of human HCC.

However, the dysregulation of microRNA (miRNA) expression, usually attributed to the alteration of DNA methylation, could also be an accelerator of epigenetic instability [24]. For example, miRNA-29, which is downregulated in HCC, reportedly targets epigenetic regulators such as DNMT3A and SETDB1 [25]. This evidence suggests a role for deregulated miRNAs in the alteration of epigenetic status.

Cancer Stem Cells, Epigenetic Regulators, and Treatment of HCC Based on Genetic and Epigenetic Profiles

A subpopulation of cancer cells shows stem cell–like properties, such as self-renewal capacity and pluripotency, in HCC [26, 27]. However, the origin of the cancer cells showing stem cell features, or cancer stem cell (CSC), is still controversial [1]. It is possible that the disturbance of epigenetic programing in hepatic progenitor cells leads to CSC in HCC. On the other hand, de-differentiation of HCC cells derived from mature hepatocytes could also be the reason for acquisition of stem cell properties [28]. Holczbauer et al. [29] studied mouse primary hepatic progenitor cells, lineage-committed hepatoblasts, and differentiated adult hepatocytes by transducing oncogenic H-Ras and simian vacuolating virus 40 large T antigen, and found that all transduced cells acquired markers of CSC/progenitor cells and self-renewal capacity in vitro, irrespective of their origins. These cells formed tumors that presented both HCC- and cholangiocarcinoma-like features in mice, suggesting that progenitor cells, as well as mature hepatocytes, could be a source of CSCs of HCC [29].

On the other hand, epigenetic mechanisms, such as histone modification and DNA methylation, have been shown to play a critical role in the regulation of chromatin structure and gene transcription essential for development. Several reports suggest that genes critical for tissue differentiation show 'bivalent' patterns consisting of the repressive histone mark, H3K27, by PcG proteins, as well as the active histone mark, methylated H3K4 in embryonic stem (ES) cells [30]. Subsequent induction of additional histone modulation and dimethylated H3K9 (H3K9Me2) and trimethylated H3K9 (H3K9Me3), reportedly lead to the methylation of the corresponding gene promoter and inactivation of TSGs responsible for

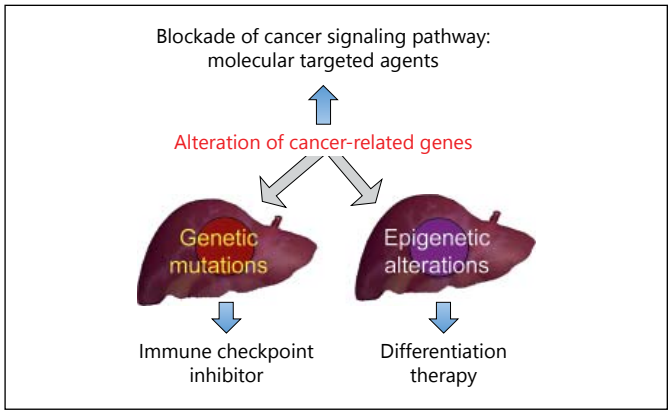

Fig. 2. Accumulation of genetic mutations, epigenetic alterations, and strategy of HCC treatment. Accumulation of alteration of cancer-related genes in HCC leads to the activation of caner signaling pathways. Therefore, the inhibition of caner-signaling pathways using molecular targeted agents should be considered. In addition, if the tumors carry genetic hypermutation, immune checkpoint inhibitors should be effective because mutated proteins could be targets for immune reaction. On the other hand, differentiation therapy, but not immune checkpoint inhibitors, combined with molecular targeted agents should be taken into consideration if HCC carries advanced epigenetic alterations without hypermutations because this type of HCC express less mutated proteins and epigenetic alteration could be reversible.

cancer development [31]. In addition, a transcription factor involved in ES cell proliferation, renewal, and pluripotency, such as Nanog, shows increased expression in HCC, and expresses stem cell markers through DNA hypomethylation [32]. On the other hand, Wen et al. reported a chromosomal region with H3K9Me2 modification, termed large organized chromatin K9 modifications (LOCKs), which bind to the nuclear lamina and are associated with the downregulation of genes within these regions. In differentiated cells, large fractions of the genome are marked by H3K9Me2 LOCKs in a tissue-specific manner, and the lamina-LOCK association can be maintained during cell division [33]. However, the LOCKs are lost and chromosomal positioning is relatively distant from the nuclear membrane in ES cells as well as from cancer cells. This suggests that an increase in chromosomal regions vulnerable to epigenetic changes leads to an induction of the epigenetic instability phenotype; therefore, ES cells and tissue progenitor cells carrying a disturbance in epigenetic integrity could be the origin of CSCs [34].

On the other hand, several reports have presented studies regarding the reprogramming of epigenetic modulations in HCC cell lines. Treatment with epigenetic modulators, such as DNMT1 inhibitor, affects the cell population showing CSC properties [35]. It is also known that HCCs expressing the oncofetal transcription factor Sal-like protein 4 (SALL4) show aggressive tumor behavior; blocking SALL4 inhibited tumor formation in vivo and reversing the transcription profile to one similar to those of mature hepatocytes [36]. We have also reported that the treatment of HCC cells with HDAC and DNMT inhibitors induces alteration of SALL4 expression [37]. Glioma cells showing the CSC phenotype and those with a differentiated phenotype show transition to each other based on the status of EZH2, which is a component of PcG [38]. This evidence suggests the potential of differentiation therapy using epigenetic modulators in HCC.

Conclusion

In this report, we focused on the origin of epigenetic alterations and their respective roles in hepatocarcinogenesis. Generally, the alteration of epigenetic status implies a disturbance of differentiation in the individual cells. However, epigenetic alterations usually do not induce mutated proteins showing abnormal structure, which could be a unique characteristic of cancers with advanced epigenetic changes. In this respect, differentiation therapy combined with molecular target agents acting on cancer signaling pathways is an attractive approach for this type of HCC (fig. 2). However, the accumulation of genetic alterations induces a number of mutant proteins that could be recognized as non-self-proteins and could be targets of immune reactions [39]. Therefore, immune-checkpoint blockers could be effective for HCCs with genetic hypermutation (fig. 2). Although the emergence of genetic and epigenetic alterations could be linked with each other, and there could be some crossover or convergence between these cancer pathways, the mutation spectrum of genetic and epigenetic alterations should be taken into consideration for future treatment of HCC.

Disclosure Statement

The authors have no conflicts of interest to disclose.

Author Contributions

N.N. drafted the manuscript and wrote the final version. M.K. approved the final version of the manuscript.

Dig Dis 2016;34:708–713
DOI: 10.1159/000448863

References

1 Marquardt JU, Andersen JB, Thorgeirsson SS: Functional and genetic deconstruction of the cellular origin in liver cancer. Nat Rev Cancer 2015;15:653–667.
2 Nishida N, Kudo M: Recent advancements in comprehensive genetic analyses for human hepatocellular carcinoma. Oncology 2013; 84(suppl 1):93–97.
3 Nishida N, Kudo M: Alteration of epigenetic profile in human hepatocellular carcinoma and its clinical implications. Liver Cancer 2014;3:417–427.
4 Mills AA: Throwing the cancer switch: reciprocal roles of polycomb and trithorax proteins. Nat Rev Cancer 2010;10:669–682.
5 Totoki Y, Tatsuno K, Covington KR, Ueda H, Creighton CJ, Kato M, Tsuji S, Donehower LA, Slagle BL, Nakamura H, Yamamoto S, Shinbrot E, Hama N, Lehmkuhl M, Hosoda F, Arai Y, Walker K, Dahdouli M, Gotoh K, Nagae G, Gingras MC, Muzny DM, Ojima H, Shimada K, Midorikawa Y, Goss JA, Cotton R, Hayashi A, Shibahara J, Ishikawa S, Guiteau J, Tanaka M, Urushidate T, Ohashi S, Okada N, Doddapaneni H, Wang M, Zhu Y, Dinh H, Okusaka T, Kokudo N, Kosuge T, Takayama T, Fukayama M, Gibbs RA, Wheeler DA, Aburatani H, Shibata T: Trans-ancestry mutational landscape of hepatocellular carcinoma genomes. Nat Genet 2014;46:1267–1273.
6 Tahara T, Yamamoto E, Madireddi P, Suzuki H, Maruyama R, Chung W, Garriga J, Jelinek J, Yamano HO, Sugai T, Kondo Y, Toyota M, Issa JP, Estecio MR: Colorectal carcinomas with CpG island methylator phenotype 1 frequently contain mutations in chromatin regulators. Gastroenterology 2014;146:530–538. e535.
7 Semi K, Yamada Y: Induced pluripotent stem cell technology for dissecting the cancer epigenome. Cancer Sci 2015;106:1251–1256.
8 Lim SO, Gu JM, Kim MS, Kim HS, Park YN, Park CK, Cho JW, Park YM, Jung G: Epigenetic changes induced by reactive oxygen species in hepatocellular carcinoma: methylation of the E-cadherin promoter. Gastroenterology 2008;135:2128–2140, 2140.e1–e8.
9 O'Hagan HM, Wang W, Sen S, Destefano Shields C, Lee SS, Zhang YW, Clements EG, Cai Y, Van Neste L, Easwaran H, Casero RA, Sears CL, Baylin SB: Oxidative damage targets complexes containing DNA methyltransferases, SIRT1, and polycomb members to promoter CpG Islands. Cancer Cell 2011;20:606–619.
10 Hmadcha A, Bedoya FJ, Sobrino F, Pintado E: Methylation-dependent gene silencing induced by interleukin 1beta via nitric oxide production. J Exp Med 1999;190:1595–1604.
11 Isomoto H, Mott JL, Kobayashi S, Werneburg NW, Bronk SF, Haan S, Gores GJ: Sustained IL-6/STAT-3 signaling in cholangiocarcinoma cells due to SOCS-3 epigenetic silencing. Gastroenterology 2007;132:384–396.
12 Xia D, Wang D, Kim SH, Katoh H, DuBois RN: Prostaglandin E2 promotes intestinal tumor growth via DNA methylation. Nat Med 2012;18:224–226.
13 Okamoto Y, Shinjo K, Shimizu Y, Sano T, Yamao K, Gao W, Fujii M, Osada H, Sekido Y, Murakami S, Tanaka Y, Joh T, Sato S, Takahashi S, Wakita T, Zhu J, Issa JP, Kondo Y: Hepatitis virus infection affects DNA methylation in mice with humanized livers. Gastroenterology 2014;146:562–572.
14 Horvath S, Erhart W, Brosch M, Ammerpohl O, von Schonfels W, Ahrens M, Heits N, Bell JT, Tsai PC, Spector TD, Deloukas P, Siebert R, Sipos B, Becker T, Rocken C, Schafmayer C, Hampe J: Obesity accelerates epigenetic aging of human liver. Proc Natl Acad Sci U S A 2014;111:15538–15543.
15 Tian Y, Wong VW, Wong GL, Yang W, Sun H, Shen J, Tong JH, Go MY, Cheung YS, Lai PB, Zhou M, Xu G, Huang TH, Yu J, To KF, Cheng AS, Chan HL: Histone deacetylase HDAC8 promotes insulin resistance and β-catenin activation in NAFID-associated hepatocellular carcinoma. Cancer Res 2015;75: 4803–4816.
16 Nishida N, Nishimura T, Nagasaka T, Ikai I, Goel A, Boland CR: Extensive methylation is associated with beta-catenin mutations in hepatocellular carcinoma: evidence for two distinct pathways of human hepatocarcinogenesis. Cancer Res 2007;67:4586–4594.
17 Nishida N, Kudo M, Nishimura T, Arizumi T, Takita M, Kitai S, Yada N, Hagiwara S, Inoue T, Minami Y, Ueshima K, Sakurai T, Yokomichi N, Nagasaka T, Goel A: Unique association between global DNA hypomethylation and chromosomal alterations in human hepatocellular carcinoma. PLoS One 2013; 8:e72312.
18 Mudbhary R, Hoshida Y, Chernyavskaya Y, Jacob V, Villanueva A, Fiel MI, Chen X, Kojima K, Thung S, Bronson RT, Lachenmayer A, Revill K, Alsinet C, Sachidanandam R, Desai A, SenBanerjee S, Ukomadu C, Llovet JM, Sadler KC: UHRF1 overexpression drives DNA hypomethylation and hepatocellular carcinoma. Cancer Cell 2014;25:196–209.
19 Song J, Du Z, Ravasz M, Dong B, Wang Z, Ewing RM: A protein interaction between β-catenin and DNMT1 regulates WNT signaling and DNA methylation in colorectal cancer cells. Mol Cancer Res 2015;13:969–981.
20 Pfister NT, Fomin V, Regunath K, Zhou JY, Zhou W, Silwal-Pandit L, Freed-Pastor WA, Laptenko O, Neo SP, Bargonetti J, Hoque M, Tian B, Gunaratne J, Engebraaten O, Manley JL, Borresen-Dale AL, Neilsen PM, Prives C: Mutant p53 cooperates with the SWI/SNF chromatin remodeling complex to regulate VEGFR2 in breast cancer cells. Genes Dev 2015;29:1298–1315.
21 Fei Q, Shang K, Zhang J, Chuai S, Kong D, Zhou T, Fu S, Liang Y, Li C, Chen Z, Zhao Y, Yu Z, Huang Z, Hu M, Ying H, Chen Z, Zhang Y, Xing F, Zhu J, Xu H, Zhao K, Lu C, Atadja P, Xiao ZX, Li E, Shou J: Histone methyltransferase SETDB1 regulates liver cancer cell growth through methylation of p53. Nat Commun 2015;6:8651.
22 Hsu IC, Metcalf RA, Sun T, Welsh JA, Wang NJ, Harris CC: Mutational hotspot in the p53 gene in human hepatocellular carcinomas. Nature 1991;350:427–428.
23 Szymanska K, Chen JG, Cui Y, Gong YY, Turner PC, Villar S, Wild CP, Parkin DM, Hainaut P: TP53 R249S mutations, exposure to aflatoxin, and occurrence of hepatocellular carcinoma in a cohort of chronic hepatitis B virus carriers from Qidong, China. Cancer Epidemiol Biomarkers Prev 2009;18:1638–1643.
24 Cao Q, Mani RS, Ateeq B, Dhanasekaran SM, Asangani IA, Prensner JR, Kim JH, Brenner JC, Jing X, Cao X, Wang R, Li Y, Dahiya A, Wang L, Pandhi M, Lonigro RJ, Wu YM, Tomlins SA, Palanisamy N, Qin Z, Yu J, Maher CA, Varambally S, Chinnaiyan AM: Coordinated regulation of polycomb group complexes through microRNAs in cancer. Cancer Cell 2011;20:187–199.
25 Parpart S, Roessler S, Dong F, Rao V, Takai A, Ji J, Qin LX, Ye QH, Jia HL, Tang ZY, Wang XW: Modulation of miR-29 expression by α-fetoprotein is linked to the hepatocellular carcinoma epigenome. Hepatology 2014;60: 872–883.
26 Oishi N, Yamashita T, Kaneko S: Molecular biology of liver cancer stem cells. Liver Cancer 2014;3:71–84.
27 Recent advances in bioinformatics reveal the molecular heterogeneity of hepatocellular carcinoma. Liver Cancer 2014;3:68–70.
28 Chaffer CL, Brueckmann I, Scheel C, Kaestli AJ, Wiggins PA, Rodrigues LO, Brooks M, Reinhardt F, Su Y, Polyak K, Arendt LM, Kuperwasser C, Bierie B, Weinberg RA: Normal and neoplastic nonstem cells can spontaneously convert to a stem-like state. Proc Natl Acad Sci U S A 2011;108:7950–7955.
29 Holczbauer A, Factor VM, Andersen JB, Marquardt JU, Kleiner DE, Raggi C, Kitade M, Seo D, Akita H, Durkin ME, Thorgeirsson SS: Modeling pathogenesis of primary liver cancer in lineage-specific mouse cell types. Gastroenterology 2013;145:221–231.
30 Ohm JE, McGarvey KM, Yu X, Cheng L, Schuebel KE, Cope L, Mohammad HP, Chen W, Daniel VC, Yu W, Berman DM, Jenuwein T, Pruitt K, Sharkis SJ, Watkins DN, Herman JG, Baylin SB: A stem cell-like chromatin pattern may predispose tumor suppressor genes to DNA hypermethylation and heritable silencing. Nat Genet 2007;39:237–242.
31 Schlesinger Y, Straussman R, Keshet I, Farkash S, Hecht M, Zimmerman J, Eden E, Yakhini Z, Ben-Shushan E, Reubinoff BE, Bergman Y, Simon I, Cedar H: Polycomb-mediated methylation on Lys27 of histone H3 pre-marks genes for de novo methylation in cancer. Nat Genet 2007;39:232–236.

32 Wang XQ, Ng RK, Ming X, Zhang W, Chen L, Chu AC, Pang R, Lo CM, Tsao SW, Liu X, Poon RT, Fan ST: Epigenetic regulation of pluripotent genes mediates stem cell features in human hepatocellular carcinoma and cancer cell lines. PLoS One 2013;8:e72435.
33 Wen B, Wu H, Shinkai Y, Irizarry RA, Feinberg AP: Large histone H3 lysine 9 dimethylated chromatin blocks distinguish differentiated from embryonic stem cells. Nat Genet 2009;41:246–250.
34 Doi A, Park IH, Wen B, Murakami P, Aryee MJ, Irizarry R, Herb B, Ladd-Acosta C, Rho J, Loewer S, Miller J, Schlaeger T, Daley GQ, Feinberg AP: Differential methylation of tissue- and cancer-specific CpG island shores distinguishes human induced pluripotent stem cells, embryonic stem cells and fibroblasts. Nat Genet 2009;41:1350–1353.
35 Raggi C, Factor VM, Seo D, Holczbauer A, Gillen MC, Marquardt JU, Andersen JB, Durkin M, Thorgeirsson SS: Epigenetic reprogramming modulates malignant properties of human liver cancer. Hepatology 2014;59:2251–2262.
36 Yong KJ, Gao C, Lim JS, Yan B, Yang H, Dimitrov T, Kawasaki A, Ong CW, Wong KF, Lee S, Ravikumar S, Srivastava S, Tian X, Poon RT, Fan ST, Luk JM, Dan YY, Salto-Tellez M, Chai L, Tenen DG: Oncofetal gene SALL4 in aggressive hepatocellular carcinoma. N Engl J Med 2013;368:2266–2276.
37 Nishida N, Chishina H, Arizumi T, Takita M, Kitai S, Yada N, Hagiwara S, Inoue T, Minami Y, Ueshima K, Sakurai T, Kudo M: Identification of epigenetically inactivated genes in human hepatocellular carcinoma by integrative analyses of methylation profiling and pharmacological unmasking. Dig Dis 2014;32:740–746.
38 Natsume A, Ito M, Katsushima K, Ohka F, Hatanaka A, Shinjo K, Sato S, Takahashi S, Ishikawa Y, Takeuchi I, Shimogawa H, Uesugi M, Okano H, Kim SU, Wakabayashi T, Issa JP, Sekido Y, Kondo Y: Chromatin regulator PRC2 is a key regulator of epigenetic plasticity in glioblastoma. Cancer Res 2013;73:4559–4570.
39 Le DT, Uram JN, Wang H, Bartlett BR, Kemberling H, Eyring AD, Skora AD, Luber BS, Azad NS, Laheru D, Biedrzycki B, Donehower RC, Zaheer A, Fisher GA, Crocenzi TS, Lee JJ, Duffy SM, Goldberg RM, de la Chapelle A, Koshiji M, Bhaijee F, Huebner T, Hruban RH, Wood LD, Cuka N, Pardoll DM, Papadopoulos N, Kinzler KW, Zhou S, Cornish TC, Taube JM, Anders RA, Eshleman JR, Vogelstein B, Diaz LA Jr: PD-1 blockade in tumors with mismatch-repair deficiency. N Engl J Med 2015;372:2509–2520.

Original Article

Digestive Diseases

Dig Dis 2016;34:687–691
DOI: 10.1159/000448857

US–US Fusion Imaging in Radiofrequency Ablation for Liver Metastases

Yasunori Minami Tomohiro Minami Hirokazu Chishina Masashi Kono
Tadaaki Arizumi Masahiro Takita Norihisa Yada Satoru Hagiwara Hiroshi Ida
Kazuomi Ueshima Naoshi Nishida Masatoshi Kudo

Department of Gastroenterology and Hepatology, Kindai University Faculty of Medicine, Osaka-Sayama, Osaka, Japan

Key Words
Ablative margin · Liver metastasis · Radiofrequency ablation · US–US fusion imaging

Abstract
Objective: Radiofrequency ablation (RFA) induces gas bubbles in ablation zones, and the ablative margin cannot be evaluated accurately on ultrasound (US) during and immediately after RFA. This study assessed the usefulness of US–US fusion imaging to visualize the ablative margin of RFA for liver metastasis. ***Methods:*** RFA guided by US–US fusion imaging was performed on 12 targeted tumors in 10 patients. Secondary hepatic malignancies included patients with colorectal cancer (n = 4), breast cancer (n = 2), lung cancer (n = 1), gastrointestinal stromal tumor (n = 1), pancreatic neuroendocrine tumor (n = 1), and adrenocortical carcinoma (n = 1). The maximal diameter of the tumors ranged from 0.8 to 4.0 cm (mean ± SD 1.6 ± 0.9 cm). ***Results:*** The mean number of electrode insertions was 1.6 per session (range 1–3). Technically, effective ablation was achieved in a single session in all patients, and safety ablative margins were confirmed on contrast-enhanced CT for early assessment of tumor response. There were no serious adverse events or procedure-related complications. During the follow-up period (median 220 days, range 31–417 days), none of the patients showed local tumor progression. ***Conclusion:*** US–US fusion imaging could show the tumor images before ablation and the ablative area on US in real time. The image overlay of US–US fusion imaging made it possible to evaluate the ablative margin three dimensionally according to the US probe action. Therefore, US–US fusion imaging can contribute to RFA therapy with a safety margin, that is, the so-called precise RFA.

Introduction

Liver metastasis is one of the critical factors that determines the prognosis of patients with advanced stage cancer. Although surgery can be a therapeutic choice for cure in patients with liver metastases, difficulties of surgical resection may be related to the size, site, and number of tumors, vascular and extrahepatic involvement, as well as poor liver function. There is a need for an effective and less invasive technique for the treatment of unresectable hepatic malignancies. Recently, several local ablative techniques have been reported to be effective in patients considered for liver-directed therapies. In particular, radiofrequency ablation (RFA) [1–4] has resulted in a higher rate of complete necrosis of metastatic lesions in the liver [5–8]. The advantages of minimal invasiveness and good survival with RFA have had a positive impact on the clinical management of patients with liver metastasis [9, 10].

KARGER

E-Mail karger@karger.com
www.karger.com/ddi

0257–2753/16/0346–0687$39.50/0

Masatoshi Kudo, MD, PhD
Department of Gastroenterology and Hepatology
Kindai University Faculty of Medicine
377-2 Ohno-Higashi, Osaka-Sayama, Osaka 589-8511 (Japan)
E-Mail m-kudo@med.kindai.ac.jp

For technical success of the RFA procedure, the tumor and a safety margin must be included in the ablation zone [11]. The local recurrence rate differs markedly depending on whether or not a 5 mm ablative margin is secured to eradicate potential microscopic invasion [12, 13]. However, ultrasound (US) is often restricted by the formation of gas bubbles that cause strong acoustic scattering within the ablated area; the targeted region can be obscured by an irregular hyperechoic zone, so the safety margin cannot be evaluated accurately on US during and immediately after RFA [14]. Failure to establish a sufficient ablative safety margin is an independently significant risk factor for local tumor progression on multivariate analysis [15]. Local tumor progression after RFA is frequently encountered in patients with liver metastasis.

Recent advancements in technology permit two-dimensional (2D) multiplanar reconstruction images of CT or MRI to display in the same plane as US images in real time. It was reported that fusion imaging–guided RFA was useful in the treatment of hepatic malignancies that were inconspicuous on B-mode US [16–21]. Moreover, the application of fusion imaging allows display of the tumor before and during/after ablation on the same US images side by side, and the imaging overlays can show the tumor image before ablation within an ablated hyperechoic zone in real time. Therefore, the image overlay of US–US fusion imaging can visualize the ablative margin three dimensionally according to the US probe action. The purpose of this study was to assess the usefulness of US–US fusion imaging in RFA for liver metastasis.

Materials and Methods

Patient Selection and Eligibility

Approval for this retrospective study was obtained from the local ethical review board. Written informed consent to perform RFA was obtained from all patients before treatment.

This cohort study was conducted as a retrospective analysis in a single institution. This study included patients with liver metastasis who underwent RFA and who had undergone dynamic CT 1 month previously. Between October 2014 and March 2016, 10 patients (5 men, 5 women; age range 41–89; mean age ± SD 60.9 ± 12.2 years) with 12 liver metastases were analyzed. Secondary hepatic malignancies included patients with colorectal cancer (n = 4), breast cancer (n = 2), lung cancer (n = 1), gastrointestinal stromal tumor of the stomach (n = 1), pancreatic neuroendocrine tumor (n = 1), and adrenocortical carcinoma (n = 1). Before RFA, all patients with liver metastasis had undergone systemic chemotherapy after surgical resection of the primary tumor. Nine patients had not been treated previously for these hepatic lesions. One patient with a metastasis had shown local tumor progression after RFA. The maximal diameter of the tumors ranged from 0.5 to 4.0 cm (mean ± SD 1.6 ± 0.9 cm) on dynamic CT. The distance from the skin to the deepest edge of the tumor on sonography ranged from 1 to 9 cm (mean ± SD 4.1 ± 2.7 cm).

Patients were considered eligible for RFA if the diagnosis of liver metastasis was confirmed by typical radiologic findings. Additional eligibility criteria included less than 3 nodules ≤3 cm each; good liver function (Child–Pugh class A or B); absent or trace ascites; albumin level of more than 2.0 g/dl; alanine aminotransferase and aspartate aminotransferase levels of less than 5 times the upper normal limit; total serum bilirubin level of less than 3.0 mg/dl; prothrombin time-international normalized ratio less than 1.5; serum creatinine level of less than 2.0 mg/dl; and platelet count of at least 30,000/mm^3. The exclusion criteria were as follows: poor patient cooperation; patients with target lesions that could be confidently localized on contrast-enhanced US (CEUS); and a target lesion located in a sonographically blind area (e.g., anterior subphrenic area of the right liver). All patient characteristic data at baseline were collected and reviewed before RFA.

Equipment

A US machine (LOGIQ E9, GE Healthcare, Chalfont St. Giles, UK) coupled with a low magnetic field generator was used. Two electromagnetic position sensors connected with a position-sensing unit were attached on the probe (4.0 MHz curvilinear C1–6, GE) through a bracket. Both the transmitter and the sensors were connected to a position-sensing unit embedded in the US machine.

Patients were treated using the RFA (VIVA RF ablation system; STARMed Co., Goyang, Gyeonggi, South Korea). Twenty-centimeter-long, 17-gauge, monopolar internally cooled electrodes (VIVA RF electrode; STARMed) were used to deliver radiofrequency energy, and the active metallic tip could be adjusted in 5 mm intervals up to 3 cm long. A 200-W, 480-kHz monopolar radiofrequency generator regulated by impedance (VIVA RF generator, STARMed) and having 3 styles of power distribution (General, Auto, Continuance modes) was used as the energy source.

A multidetector CT (LightSpeed VCT, GE Healthcare, Chalfont St. Giles, UK) was used for diagnosis. Triple-phase contrast-enhanced CT scans were performed with a 5.0-mm slice thickness at 30, 60, and 180 s after initiating the injection of contrast medium to obtain hepatic arterial, portal venous and equilibrium phase images, respectively. A total of 100 ml of nonionic contrast material containing 300 mg of iodine/ml (Iomeprol, Eisai Co., Tokyo, Japan) was injected intravenously at a rate of 3 ml/s using an automatic power injector.

US–US Fusion Imaging and RFA Procedure

Before inserting the radiofrequency needle, the three-dimensional (3D) US volume was obtained by scanning the liver in a manual sweeping manner with the patient in a breath-holding state. The scanning area had to include not only the tumor but also intrahepatic vessels around the tumor. This 3D volume data contained the spatial information in the generated magnetic field. A cross-section of the 3D US volume was selected based on the largest diameter dimension of the tumor, and 2 green squares on the screen were arranged to fix a perpendicular line through the center of the tumor image. Then, 6 rotated sections passing through the tumor center were automatically displayed. Thereafter, the region of interest was manually drawn along the tumor border in each rotated sections, with the result that the tumor border could be

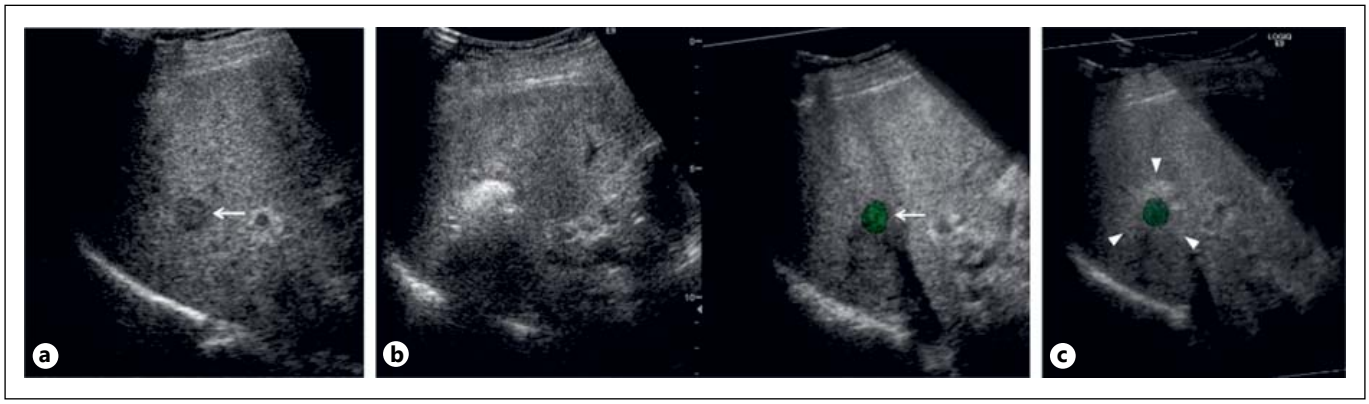

Fig. 1. A 89-year-old man with liver metastasis from colon cancer. **a** CEUS shows the tumor of 1.1 cm as a defect image (arrow) in segment 5 of liver during the post-vascular phase. **b** US–US fusion imaging displays a cross-sectional image of 3D US volume before ablation (right) and a real-time image of CEUS after ablation (left). The tumor is colored green (arrow). **c** The overlay image shows the green-colored tumor inside the ablative hyperechoic zone. Then, the ablative margin is revealed.

traced three dimensionally. The interior was colorized, and 3D-US volume data were stored within the US machine.

Immediately after ablation, the clinical role of US is markedly limited because of the initial hyperechoic ablated zone, the so-called echogenic cloud, and the resultant acoustic shadowing. This echogenic cloud persists for a period ranging from 15 min to 6 h after RFA [22]. As the acoustic shadowing gradually disappeared, the 3D-US volume data was fused with the real-time 2D US image. These 2 images were displayed simultaneously on a split-screen display, and then this fusion imaging allowed comparison of the tumor images before ablation and the ablative area on US in real time. Moreover, the 2 images could be overlaid, and the image overlay allowed easy visualization of the ablative margin on US.

All RFA procedures were performed by 3 experienced hepatologists (M.T., Y.M., and H.I., with 5, 19 and 20 years of experience, respectively). The tip length choice for the active RF electrode was 0.5–1.0 cm over the tumor size. Under auto mode, power was usually begun at 40 W with a 2-cm exposed-tip RF electrode or at 50 W with a 3-cm exposed-RF tip. After a few times of power roll-off, the RFA procedure was terminated if the ablative hyperechoic zone had expanded over the tumor with the safety margin.

Assessment of Technical Effectiveness and Follow-Up

A few days after treatment, the technical effectiveness of ablation was assessed based on contrast-enhanced CT scan findings. A tumor was considered to have been successfully ablated when there were no longer any enhanced regions within the entire tumor during the arterial phase and at least a 0.5 cm margin of apparently normal hepatic tissue surrounding the tumor during the portal phase. Part of the tumor was diagnosed as remaining viable when images of the ablated area showed nodular peripheral enhancement [23, 24].

If 1-month follow-up CT images showed successful ablation and no new tumors, 3-phase contrast-enhanced CT scans were repeated at 3-month intervals. All patients were followed for at least 1 month after RFA and underwent at least one follow-up CT examination by 2 radiologists who had more than 20 years of experience. Any complications were recorded.

Results

In the post-vascular phase, all of the 10 liver metastases (83%) were depicted as defects with a clear margin, and 2 nodules (17%) were depicted as defects with an unclear margin. The mean number of electrode insertions was 1.6 per session (median 1, range 1–3). The technical effectiveness of ablation was achieved in a single session in all patients, and safety ablative margins were confirmed on contrast-enhanced CT for early assessment of tumor response (fig. 1). There were no serious adverse events or procedure-related complications (e.g., hemorrhage, infection, hepatic failure or death). Grade 1 to 2 pain on the Common Toxicity Criteria of the National Cancer Institute was the most common side effect, reported by 6 patients.

Follow-up time ranged from 31 to 417 days (mean 206 days, median 220 days). During the follow-up period, none of the patients showed local tumor progression. However, a single patient demonstrated distant multiple metastases in the liver.

Discussion

The ablative margin of RFA cannot be fully evaluated on B-mode US and/or CEUS. However, this US–US fusion image overlay is a revolutionary technology, allowing us to visualize the ablative margin three dimensionally. To the best of our knowledge, this is the first report to display the ablative margin of RFA on US. Our study showed that good local control was obtained by RFA

guided by US–US fusion imaging in patients with liver metastasis, although local tumor progression is often encountered in such patients after RFA. Our results could confirm the sufficient ablative margin of RFA by design in patients with liver metastasis.

US–US fusion imaging has 3 clinical applications in RFA therapy. The first is the real-time monitoring of RFA lesion formation. Clinicians can employ B-mode US to observe the bubble-related hyperechoic region and preliminarily evaluate the ablation zones comparing the pre-ablation image of the tumor using US–US fusion imaging. The second application is related to decision making about additional ablation. We could confirm any lesion with a poor ablative margin during the session, and then extend the necrotic area by additional ablation. The third is visualization of the safety margin on US. Although the endpoint of conventional RFA cannot be based on objective evidence with US, US–US fusion imaging offers an evidence-based quality improvement in RFA therapy.

Many have reported that the local recurrence rate increased with larger size of tumor in RFA [25–28]. A larger tumor requires multiple ablations to prevent recurrence, and it is often difficult to obtain a sufficient ablative margin over the whole nodule with larger hepatic malignancies. However, US–US fusion imaging enables obtaining a safety margin even for larger tumors because it allows 3D visualization of the ablative margin. However, this US–US fusion imaging system still has room for improvement. The setup process of US–US fusion imaging requires multiple steps and it is complicated. Especially, it is complicated to trace the border of the tumor for colorization of the tumor on 6 rotated images. We strongly anticipate the resolution of these disadvantages by simplifying the setup process of US–US fusion imaging.

The principal limitation of this study was its retrospective design. The second was that this study could suffer from selection bias because the patients were enrolled according to the tumor size and/or number for RFA indication.

Another limitation is the preliminary nature of this study with a relatively small number of patients and a short follow-up time. Further prospective studies of this technique with larger number of patients are warranted.

In conclusion, US–US fusion imaging could show tumor images before ablation and the ablative area on US in real time. The image overlay of US–US fusion could visualize the ablative margin of RFA on US. Therefore, US–US fusion imaging can contribute to RFA therapy with a safety margin, that is, the so-called precise RFA.

Disclosure Statement

The authors declare that no conflict of interest exists.

References

1 Teng W, Liu KW, Lin CC, Jeng WJ, Chen WT, Sheen IS, Lin CY, Lin SM: Insufficient ablative margin determined by early computed tomography may predict the recurrence of hepatocellular carcinoma after radiofrequency ablation. Liver Cancer 2015;4:26–38.

2 Kudo M: Locoregional therapy for hepatocellular carcinoma. Liver Cancer 2015;4:163–164.

3 Kang TW, Rhim H: Recent advances in tumor ablation for hepatocellular carcinoma. Liver Cancer 2015;4:176–187.

4 Lencioni R, de Baere T, Martin RC, Nutting CW, Narayanan G: Image-guided ablation of malignant liver tumors: recommendations for clinical validation of novel thermal and non-thermal technologies – a western perspective. Liver Cancer 2015;4:208–214.

5 Livraghi T, Solbiati L, Meloni F, Ierace T, Goldberg SN, Gazelle GS: Percutaneous radiofrequency ablation of liver metastases in potential candidates for resection: the 'test-of-time approach'. Cancer 2003;97:3027–3035.

6 Oshowo A, Gillams A, Harrison E, Lees WR, Taylor I: Comparison of resection and radiofrequency ablation for treatment of solitary colorectal liver metastases. Br J Surg 2003;90:1240–1243.

7 Abdalla EK, Vauthey JN, Ellis LM, Ellis V, Pollock R, Broglio KR, Hess K, Curley SA: Recurrence and outcomes following hepatic resection, radiofrequency ablation, and combined resection/ablation for colorectal liver metastases. Ann Surg 2004;239:818–825; discussion 825–827.

8 Minami Y, Kudo M, Hatanaka K, Kitai S, Inoue T, Hagiwara S, Chung H, Ueshima K: Radiofrequency ablation guided by contrast harmonic sonography using perfluorocarbon microbubbles (sonazoid) for hepatic malignancies: an initial experience. Liver Int 2010;30:759–764.

9 Shady W, Petre EN, Gonen M, Erinjeri JP, Brown KT, Covey AM, Alago W, Durack JC, Maybody M, Brody LA, Siegelbaum RH, D'Angelica MI, Jarnagin WR, Solomon SB, Kemeny NE, Sofocleous CT: Percutaneous radiofrequency ablation of colorectal cancer liver metastases: factors affecting outcomes – a 10-year experience at a single center. Radiology 2016;278:601–611.

10 Minami Y, Kudo M: Radiofrequency ablation of liver metastases from colorectal cancer: a literature review. Gut Liver 2013;7:1–6.

11 Goldberg SN, Grassi CJ, Cardella JF, Charboneau JW, Dodd GD 3rd, Dupuy DE, Gervais D, Gillams AR, Kane RA, Lee FT Jr, Livraghi T, McGahan J, Phillips DA, Rhim H, Silverman SG: Image-guided tumor ablation: standardization of terminology and reporting criteria. J Vasc Interv Radiol 2005;16:765–778.

12 Minami Y, Nishida N, Kudo M: Therapeutic response assessment of RFA for HCC: contrast-enhanced US, CT and MRI. World J Gastroenterol 2014;20:4160–4166.

13 Minami Y, Kudo M: Imaging modalities for assessment of treatment response to nonsurgical hepatocellular carcinoma therapy: contrast-enhanced US, CT, and MRI. Liver Cancer 2015;4:106–114.

14 Leyendecker JR, Dodd GD 3rd, Halff GA, McCoy VA, Napier DH, Hubbard LG, Chintapalli KN, Chopra S, Washburn WK, Esterl RM, Cigarroa FG, Kohlmeier RE, Sharkey FE: Sonographically observed echogenic response during intraoperative radiofrequency ablation of cirrhotic livers: pathologic correlation. AJR Am J Roentgenol 2002;178:1147–1151.
15 White RR, Avital I, Sofocleous CT, Brown KT, Brody LA, Covey A, Getrajdman GI, Jarnagin WR, Dematteo RP, Fong Y, Blumgart LH, D'Angelica M: Rates and patterns of recurrence for percutaneous radiofrequency ablation and open wedge resection for solitary colorectal liver metastasis. J Gastrointest Surg 2007;11:256–263.
16 Hirooka M, Iuchi H, Kumagi T, Shigematsu S, Hiraoka A, Uehara T, Kurose K, Horiike N, Onji M: Virtual sonographic radiofrequency ablation of hepatocellular carcinoma visualized on CT but not on conventional sonography. AJR Am J Roentgenol 2006;186(5 suppl):S255–S260.
17 Minami Y, Kudo M, Chung H, Inoue T, Takahashi S, Hatanaka K, Ueda T, Hagiwara H, Kitai S, Ueshima K, Fukunaga T, Shiozaki H: Percutaneous radiofrequency ablation of sonographically unidentifiable liver tumors. Feasibility and usefulness of a novel guiding technique with an integrated system of computed tomography and sonographic images. Oncology 2007;72(suppl 1):111–116.
18 Minami Y, Chung H, Kudo M, Kitai S, Takahashi S, Inoue T, Ueshima K, Shiozaki H: Radiofrequency ablation of hepatocellular carcinoma: value of virtual CT sonography with magnetic navigation. AJR Am J Roentgenol 2008;190:W335–W341.
19 Kitada T, Murakami T, Kuzushita N, Minamitani K, Nakajo K, Osuga K, Miyoshi E, Nakamura H, Kishino B, Tamura S, Hayashi N: Effectiveness of real-time virtual sonography-guided radiofrequency ablation treatment for patients with hepatocellular carcinomas. Hepatol Res 2008;38:565–571.
20 Lee JY, Choi BI, Chung YE, Kim MW, Kim SH, Han JK: Clinical value of CT/MR-US fusion imaging for radiofrequency ablation of hepatic nodules. Eur J Radiol 2012;81:2281–2289.
21 Song KD, Lee MW, Rhim H, Cha DI, Chong Y, Lim HK: Fusion imaging-guided radiofrequency ablation for hepatocellular carcinomas not visible on conventional ultrasound. AJR Am J Roentgenol 2013;201:1141–1147.
22 Kim YS, Rhim H, Lim HK, Choi D, Lee MW, Park MJ: Coagulation necrosis induced by radiofrequency ablation in the liver: histopathologic and radiologic review of usual to extremely rare changes. Radiographics 2011;31:377–390.
23 Dromain C, de Baere T, Elias D, Kuoch V, Ducreux M, Boige V, Petrow P, Roche A, Sigal R: Hepatic tumors treated with percutaneous radio-frequency ablation: CT and MR imaging follow-up. Radiology 2002;223:255–262.
24 Sainani NI, Gervais DA, Mueller PR, Arellano RS: Imaging after percutaneous radiofrequency ablation of hepatic tumors: part 2, abnormal findings. AJR Am J Roentgenol 2013;200:194–204.
25 Lin SM, Lin CJ, Lin CC, Hsu CW, Chen YC: Randomised controlled trial comparing percutaneous radiofrequency thermal ablation, percutaneous ethanol injection, and percutaneous acetic acid injection to treat hepatocellular carcinoma of 3 cm or less. Gut 2005;54:1151–1156.
26 Germani G, Pleguezuelo M, Gurusamy K, Meyer T, Isgrò G, Burroughs AK: Clinical outcomes of radiofrequency ablation, percutaneous alcohol and acetic acid injection for hepatocelullar carcinoma: a meta-analysis. J Hepatol 2010;52:380–388.
27 Tanis E, Nordlinger B, Mauer M, Sorbye H, van Coevorden F, Gruenberger T, Schlag PM, Punt CJ, Ledermann J, Ruers TJ: Local recurrence rates after radiofrequency ablation or resection of colorectal liver metastases. Analysis of the European organisation for research and treatment of cancer #40004 and #40983. Eur J Cancer 2014;50:912–919.
28 Künzli BM, Abitabile P, Maurer CA: Radiofrequency ablation of liver tumors: actual limitations and potential solutions in the future. World J Hepatol 2011;3:8–14.

Original Article

Digestive Diseases

Dig Dis 2016;34:696–701
DOI: 10.1159/000448859

Prediction of Embolization Area after Conventional Transcatheter Arterial Chemoembolization for Hepatocellular Carcinoma Using SYNAPSE VINCENT

Chikara Ogawa[a, b] Yasunori Minami[a] Masahiro Morita[b] Teruyo Noda[b] Soichi Arasawa[b] Masako Izuta[b] Atsushi Kubo[b] Toshihiro Matsunaka[b] Hiroyuki Tamaki[b] Mitsushige Shibatoge[b] Masatoshi Kudo[a]

[a]Department of Gastroenterology and Hepatology, Kindai University Faculty of Medicine, Osaka-Sayama, and
[b]Department of Gastroenterology and Hepatology, Takamatsu Red Cross Hospital, Takamatsu, Japan

Key Words
SYNAPSE 3-dimensional · VINCENT · Hepatocellular carcinoma · Transcatheter arterial chemoembolization · Automatic prediction of the embolization area

Abstract
Purpose: Transcatheter arterial chemoembolization (TACE) is one of the most effective therapeutic options for hepatocellular carcinoma (HCC) and it is important to protect residual liver function after treatment as well as the effect. To reduce the liver function deterioration, we evaluated the automatic software to predict the embolization area of TACE in 3 dimensions. ***Materials and Methods:*** Automatic prediction software of embolization area was used in chemoembolization of 7 HCCs. Embolization area of chemoembolization was evaluated within 1 week CT findings after TACE and compared simulated area using automatic prediction software. ***Results:*** The maximal diameter of these tumors is in the range 12–42 mm (24.6 ± 9.5 mm). The average time for detecting tumor-feeding branches was 242 s. The total time to detect tumor-feeding branches and simulate the embolization area was 384 s. All cases could detect all tumor-feeding branches of HCC, and the expected embolization area of simulation with automatic prediction software was almost the same as the actual areas, as shown by CT after TACE. ***Conclusion:*** This new technology has possibilities to reduce the amount of contrast medium used, protect kidney function, decrease radiation exposure, and improve the therapeutic effect of TACE.

Introduction

Transcatheter arterial chemoembolization (TACE) is one of the most effective therapeutic options for patients with intermediate hepatocellular carcinoma (HCC) [1–11]. Ultraselective chemoembolization is an alternative approach to improve local control, and is associated with a reduced incidence of adverse effects [12–14].

However, it is often difficult to determine the relationship between multiple overlapping vessels from two-dimensional (2D) angiographic images [15, 16]. In order to improve this problem, there have been many reports of utility of CT during hepatic angiography (CTHA) and

KARGER

E-Mail karger@karger.com
www.karger.com/ddi

0257–2753/16/0346–0696$39.50/0

Masatoshi Kudo, MD, PhD
Department of Gastroenterology and Hepatology
Kindai University Faculty of Medicine
377-2 Ohno-Higashi, Osaka-Sayama, Osaka 589-8511 (Japan)
E-Mail m-kudo@med.kindai.ac.jp

cone-beam CT (CBCT) [17–21]. Recently, the development and usefulness of built-in CBCT software that automatically identifies the feeding vessel have been reported [22–24]. However, it has not come into widespread use, as it is a high-end expensive machine.

In this study, we investigated a new and simple method for easy and reliable identification of the tumor vessel during TACE, allowing display of predicted embolized regions, display of embolized volume capacity and the ratio of embolized regions of the entire liver using a three-dimensional (3D) volume analyzer system.

Materials and Methods

Patients

A total of 6 patients with 7 HCCs were evaluated in this study. All patients were diagnosed by dynamic CT and/or contrast-enhanced MRI using gadolinium ethoxybenzyl diethylenetriamine pentaacetic acid prior angiography. CT during arterial portography (CTAP) and CTHA were performed in all patients to increase the reliability of diagnoses.

Equipment

The local area network system is connected to a computer with SYNAPSE VINCENT – called SYNAPSE 3D internationally (Fujifilm Medical Co., Tokyo, Japan), a medical imaging and information management system, in Takamatsu Red Cross Hospital.

CTHA was performed using a 64-slice multidetector-row CT scanner (Aquilion 64, Toshiba Medical Systems, Tokyo, Japan; Discovery CT750HD, GE Healthcare, Milwaukee, Wis., USA) with the following scan parameters: reconstructed slice thickness 1 mm; rotation time 0.5 s; pitch factor 0.791–0.984; X-ray tube parameters 120 kV, 300–400 or auto mA.

Digital subtraction angiography (DSA; Infinix Celeve-i DP, Toshiba Medical Systems, Tokyo, Japan) was performed from the celiac artery to evaluate hepatic artery anatomy. A micro-catheter was inserted through 3 or 4-Fr catheter and placed in the proper or common hepatic artery for hepatic arteriography. CTHA was performed using 15–20 ml nonionic contrast medium diluted to 150 mgI/ml of iodine per milliliter (Iopamidol, Bayer Yakuhin, Osaka, Japan) diluted with saline (1:1 ratio), and then CT scanning was performed at 5 and 30 s after initiating injection using an automatic power injector at rate 1.5–2.0 ml/s.

Evaluation

DICOM data from CTHA taken directly before TACE were analyzed by uploading data into the 3D image volume analyzer SYNAPSE 3D [25]. Liver analysis software, a specific application of SYNAPSE 3D, was used to identify liver parenchymal hepatic arteries and tumors and confirm the tumor-feeding vessel. Then we confirmed the embolized region from the site of medication injection on 3D imaging to check that the tumor was included in the embolized region before calculating total liver volume, predicted embolized volume and the ratio of total liver volume to predicted embolized volume (fig. 1). Miriplatin hydrate (Miripla®; Dainippon Sumitomo Pharma Co., Osaka, Japan), which has the same diaminocyclohexane structure as oxaliplatin, is a lipophilic derivative that can be suspended in lipiodol. Miriplatin-lipiodol suspension was injected, followed by gelatin sponge particle (Gelpart; Nippon Kayaku, Tokyo) after confirming that TACE could be safety performed without causing any post-TACE liver failure. Approximately 1 week after TACE, all cases underwent CT to confirm whether the treatment had been effective and compare the actual embolized region with the predicted region according to SNAPSE 3D results before TACE was performed (fig. 2).

Result

The maximum diameter of these lesions ranged from 12 to 42 mm (24.6 ± 9.5). The feeding arteries, total liver volume, predicted embolized volume, and the ratio of total liver volume to predicted embolized volume were able to be detected successfully in all patients using SYNAPSE 3D. The quantitative retention of iodized oil in tumor tissue and liver parenchyma was documented in percentiles of the volume. The average time for detecting tumor-feeding branches was 242 s. The extract of liver parenchyma and tumor using SYNAPSE 3D were 78 and 64 s, respectively (table 1).

Compared CT of 1 week after TACE, we confirmed that the extent of embolization was approximately the same for all cases and did not find severe decreases in liver function, including liver failure.

Discussion

HCC tumors are fed exclusively by the hepatic artery [26], and successful TACE leads to tumor necrosis [27]. The liver parenchyma is rarely damaged because it is mostly fed by the portal vein [1, 28]. To successfully perform TACE, the feeding arteries of HCC including hepatic artery and ectopic perihepatic arteries should be evaluated before treatment [29]. Injection of an emulsion of iodized oil and cytostatic agents into the hepatic artery leads to selective deposition of the emulsion in the tumor [1, 28]. There have been several reports in the past that interventional radiology (IVR), including CTHA, has improved the survival of patients with HCC and efficacy of TACE [17, 18]. In recent years, there have been many reports about the usefulness of using CBCT because identification of the tumor feeding vessel can often be difficult during TACE [21–24]. Furthermore, rotating images using 3D analysis software to recognize and identify feeding vessels is effective, as there are limitations to feeding ves-

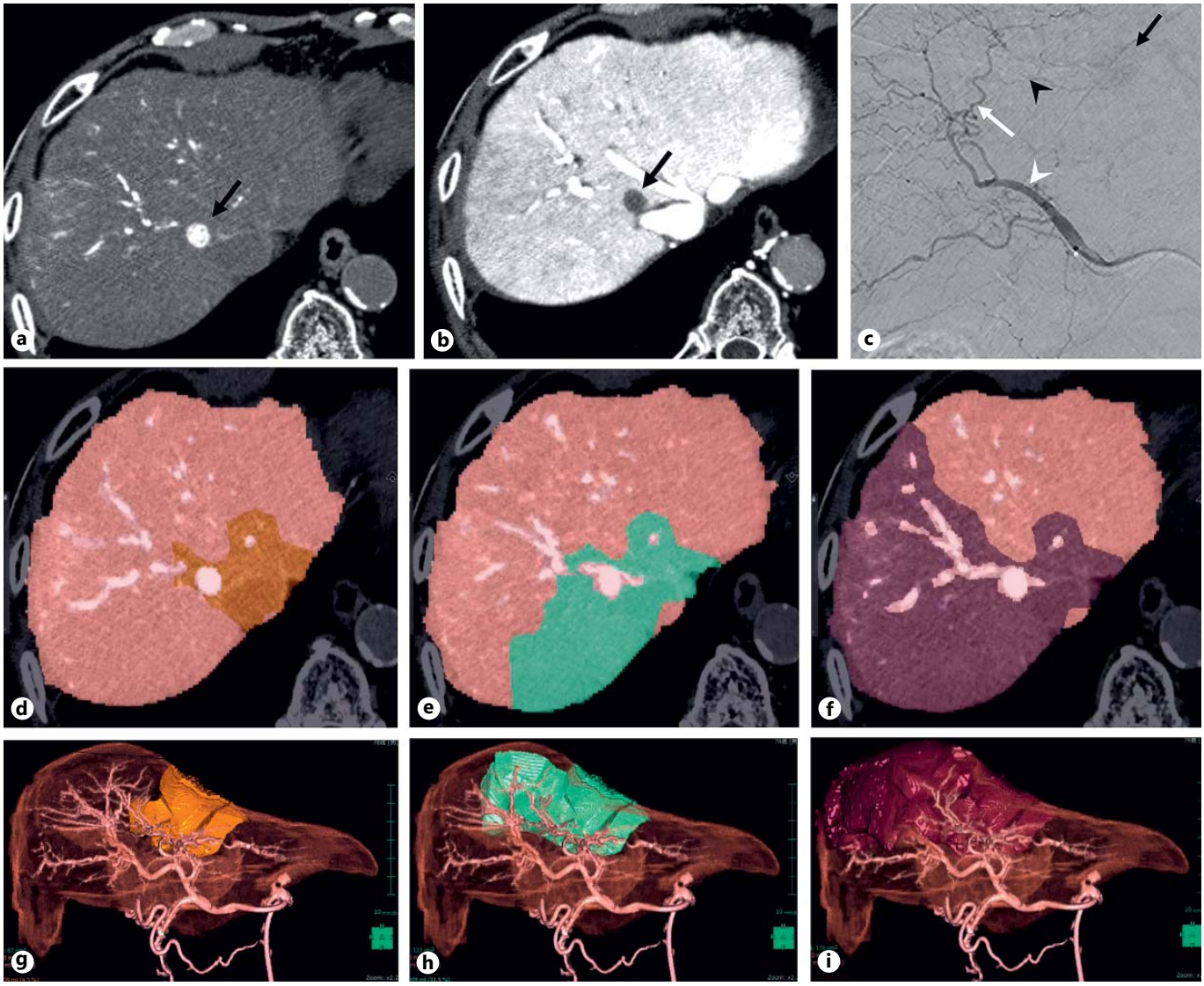

Fig. 1. Images from a 80-year-old man with an HCC lesion 12 mm in diameter. **a** First-phase CTHA showed hyperattenuation in segment 8 (arrow). **b** CTAP showed hypoattenuation in segment 8 (arrow). **c** DSA of right hepatic artery showed faint tumor stain in segment 8 (arrow). **d** Estimated territories of blood vessels from the more peripheral anterior superior subsegmental artery at axial plane (arrowhead in **c**). **e** Estimated territories of blood vessels from the peripheral anterior superior subsegmental artery at axial plane (white arrow in **c**). **f** Estimated territories of blood vessels from the anterior superior artery at axial plane (white arrowhead in **c**). **g** Coronal plane at the same site in **d**. **h** Coronal plane at the same site in **e**. **i** Coronal plane at the same site in **f**.

sel identification when using 2D imaging [22–24]. Selective injection of medication near the tumor has been reported to improve treatment effectiveness, in addition to being useful for preventing decreased hepatic residual capacity [12, 13]. However, the fact that high-cost IVR-CT or CBCT machines were previously required for predicting embolized regions on 3D images, the frequent use of contrast medium, and increased radiation exposure are associated issues. It is also difficult to display the embolized volume as part of the entire liver volume in numerical terms.

SYNAPSE 3D is commonly used in many hospitals all over Japan and sold globally. One of the famous applications of SYNAPSE 3D, liver analysis, was originally developed for the simulation of the resection range for hepatectomy [30], and usefulness of the clinical application of the virtual ultrasound software included in liver analysis has also been indicated [31]. And using this

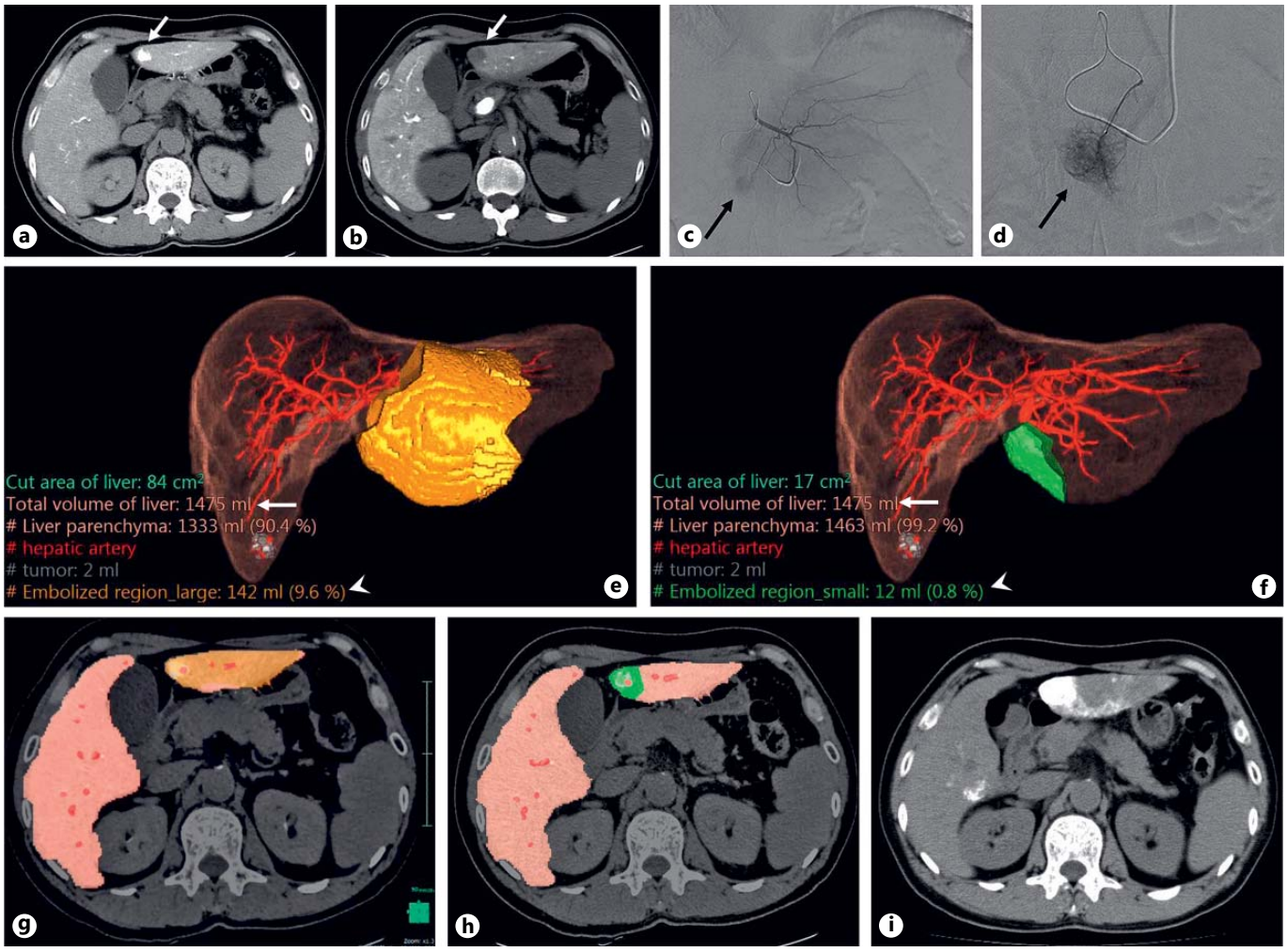

Fig. 2. Images from a 65-year-old man with HCC lesion 16 mm in diameter. Chemoembolization was performed from subsegmental artery (A3 in **d**). **a** First-phase CTHA showed hyperattenuation in segment 3 (white arrow). **b** CTAP showed hypoattenuation in segment 3 (white arrow). **c** Selective DSA of A3 showed tumor stain in segment 3 (arrow). **d** Selective DSA of the more peripheral subsegmental artery (A3) showed tumor stain in segment 3 (arrow). **e** Predicted embolized region from A3 at coronal plane (same site in **c**). SYNAPSE 3D estimated that the total liver volume was 1,475 ml (white arrow), predicted embolized volume was 142 ml and the ratio of total liver volume to predicted embolized volume was 9.6% automatically (white arrowhead). **f** Predicted embolized region from A3 at coronal plane (same site in **d**). SYNAPSE 3D estimated that the total liver volume was 1,475 ml (white arrow), predicted embolized volume was 12 ml and the ratio of total liver volume to predicted embolized volume was 0.8% automatically (white arrowhead). **g** Coronal plane at the same site in **c**. **h** Coronal plane at the same site in **d**. **i** CT obtained 1 week after TACE showed that iodized oil was retained approximately the same for predicted embolized region made by SYNAPSE 3D.

software, we can perform colorized fusion system in colored display on the US monitor [32]. There are 2 types of SYNAPSE 3D systems. There is a standalone system with the software installed on a single PC and a server system that connects to many electronic medical records within hospital via a server using a LAN cable. The server system has recently become the most commonly used system, and SYNAPSE 3D can now be used anywhere at any time within our hospital to access over 100 electronic medical record terminals including the angiography room. The application liver analysis can automatically extract vessels and tumors and can estimate territories of blood vessels from the extracted blood vessels and extracted liver region from multidetector CT findings.

In this study, we confirmed the embolized region on 3D imaging and calculate total liver volume, predicted embolized volume, and the ratio of total liver volume to

Table 1. A total of 6 cases with 7 HCCs were measured the time to estimate the embolized regions

	Work time						Average
	case 1	case 2	case 3	case 4	case 5	case 6	
Extract of liver parenchyma	1.40	1.01	1.08	1.12	0.49	1.43	1.18
Extract of hepatic artery	3.54	3.53	3.26	4.22	4.17	4.19	4.02
Extract of tumor	1.25	0.51	0.24	0.48	2.37	0.18	1.04
Total time	6.59	5.45	4.58	6.22	7.43	6.20	6.24

The average time for detecting tumor-feeding branches was 242 s. The extract of liver parenchyma and tumor using SYNAPSE 3D were 78 and 64 s, respectively.

predicted embolized volume. While TACE is much less invasive than hepatectomy, an overwhelmingly large number of eligible cases have poorer hepatic reserve capacity than cases considered eligible for surgery. Therefore, it is important to identify and confirm the embolized range on 3D imaging, as the residual liver volume and extent of resection range are important findings for post treatment liver failure and complications in surgical cases, and to convert the embolized volume to numerical terms in TACE cases.

As the method outlined here uses software that is already widely used, there is no need to purchase any additional expensive equipment. If the hospital has already introduced the currently mainstream server system, TACE simulation can be performed prior to TACE and in parallel with treatment. This method can reduce the amount of contrast medium used, protect kidney function, and decrease radiation exposure. It is also highly significant from the perspective of sharing information between the treatment team, as other doctors and radiologists, as well as the physician performing TACE, can perform TACE treatment simulations.

Conclusion

The new technology using 3D volume analyzer system before TACE to identify the tumor-feeding branch and tumor and predict the embolized regions, display of embolized volume capacity, and the ratio of embolized regions of entire liver is useful to increase the effect of TACE and reduce the amount of contrast medium used, protect kidney function, and decrease radiation exposure.

Disclosure Statement

The authors have no conflicts of interest to declare.

References

1 Nakamura H, Hashimoto T, Oi H, Sawada S: Transcatheter oily chemoembolization of hepatocellular carcinoma. Radiology 1989;170:783–786.

2 Matsui O, Kadoya M, Yoshikawa J, Gabata T, Arai K, Demachi H, Miyayama S, Takashima T, Unoura M, Kogayashi K: Small hepatocellular carcinoma: treatment with subsegmental transcatheter arterial embolization. Radiology 1993;188:79–83.

3 Takayasu K, Arii S, Ikai I, Omata M, Okita K, Ichida T, Matsuyama Y, Nakanuma Y, Kojiro M, Makuuchi M, Yamaoka Y: Prospective cohort study of transarterial chemoembolization for unresectable hepatocellular carcinoma in 8510 patients. Gastroenterology 2006;131:461–469.

4 Llovet JM, Real MI, Montana X, Planas R, Coll S, Aponte J, Ayuso C, Sala M, Muchart J, Sola R, Rodes J, Bruix J: Arterial embolisation or chemoembolisation versus symptomatic treatment in patients with unresectable hepatocellular carcinoma: a randomised controlled trial. Lancet 2002;359:1734–1739.

5 Sergio A, Cristofori C, Cardin R, Pivetta G, Ragazzi R, Baldan A, Girardi L, Cillo U, Burra P, Giacomin A, Farinati F: Transcatheter arterial chemoembolization (TACE) in hepatocellular carcinoma (HCC): the role of angiogenesis and invasiveness. Am J Gastroenterol 2008;103:914–921.

6 Lencioni R: Chemoembolization in patients with hepatocellular carcinoma. Liver Cancer 2012;1:41–50.

7 Kudo M, Matsui O, Izumi N, Iijima H, Kadoya M, Imai Y, Okusaka T, Miyayama S, Tsuchiya K, Ueshima K, Hiraoka A, Ikeda M, Ogasawara S, Yamashita T, Minami T, Yamakado K: JSH consensus-based clinical practice guidelines for the management of hepatocellular carcinoma: 2014 update by the liver cancer study group of Japan. Liver Cancer 2014;3:458–468.

8 Kudo M: Surveillance, diagnosis, treatment, and outcome of liver cancer in Japan. Liver Cancer 2015;4:39–50.

9 Kudo M: Locoregional therapy for hepatocellular carcinoma. Liver Cancer 2015;4:163–164.

10 Tsurusaki M, Murakami T: Surgical and locoregional therapy of HCC: TACE. Liver Cancer 2015;4:165–175.

11 Arizumi T, Ueshima K, Minami T, Kono M, Chishina H, Takita M, Kitai S, Inoue T, Yada N, Hagiwara S, Minami Y, Sakurai T, Nishida N, Kudo M: Effectiveness of sorafenib in patients with transcatheter arterial chemoembolization (TACE) refractory and intermediate-stage hepatocellular carcinoma. Liver Cancer 2015;4:253–262.
12 Miyayama S, Matsui O, Yamashiro M, Ryu Y, Kaito K, Ozaki K, Takeda T, Yoneda N, Notsumata K, Toya D, Tanaka N, Mitsui T: Ultraselective transcatheter arterial chemoembolization with a 2-f tip microcatheter for small hepatocellular carcinomas: relationship between local tumor recurrence and visualization of the portal vein with iodized oil. J Vasc Interv Radiol 2007;18:365–376.
13 Miyayama S, Mitsui T, Zen Y, Sudo Y, Yamashiro M, Okuda M, Yoshie Y, Sanada T, Notsumata K, Tanaka N, Matsui O: Histopathological findings after ultraselective transcatheter arterial chemoembolization for hepatocellular carcinoma. Hepatol Res 2009;39:374–381.
14 Iwamoto S, Yamaguchi T, Hongo O, Iwamoto H, Sanefuji H: Excellent outcomes with angiographic subsegmentectomy in the treatment of typical hepatocellular carcinoma: a retrospective study of local recurrence and long-term survival rates in 120 patients with hepatocellular carcinoma. Cancer 2010;116:393–399.
15 Lewandowski RJ, Geschwind JF, Liapi E, Salem R: Transcatheter intraarterial therapies: rationale and overview. Radiology 2011;259:641–657.
16 Lencioni R, Crocetti L: Local-regional treatment of hepatocellular carcinoma. Radiology 2012;262:43–58.
17 Nelson RC, Chezmar JL, Sugarbaker PH, Bernardino ME: Hepatic tumors: comparison of CT during arterial portography, delayed CT, and MR imaging for preoperative evaluation. Radiology 1989;172:27–34.
18 Toyoda H, Kumada T, Sone Y: Impact of a unified CT angiography system on outcome of patients with hepatocellular carcinoma. AJR Am J Roentgenol 2009;192:766–774.
19 Ning R, Chen B, Yu R, Conover D, Tang X, Ning Y: Flat panel detector-based cone-beam volume CT angiography imaging: system evaluation. IEEE Trans Med Imaging 2000;19:949–963.
20 Orth RC, Wallace MJ, Kuo MD: C-arm cone-beam CT: general principles and technical considerations for use in interventional radiology. J Vasc Interv Radiol 2008;19:814–820.
21 Minami Y, Murakami T, Kitano M, Sakurai T, Nishida N, Kudo M: Cone-beam CT angiography for hepatocellular carcinoma: current status. Dig Dis 2015;33:759–764.
22 Deschamps F, Solomon SB, Thornton RH, Rao P, Hakime A, Kuoch V, de Baere T: Computed analysis of three-dimensional cone-beam computed tomography angiography for determination of tumor-feeding vessels during chemoembolization of liver tumor: a pilot study. Cardiovasc Intervent Radiol 2010;33:1235–1242.
23 Miyayama S, Yamashiro M, Hashimoto M, Hashimoto N, Ikuno M, Okumura K, Yoshida M, Matsui O: Identification of small hepatocellular carcinoma and tumor-feeding branches with cone-beam CT guidance technology during transcatheter arterial chemoembolization. J Vasc Interv Radiol 2013;24:501–508.
24 Minami Y, Yagyu Y, Murakami T, Kudo M: Tracking navigation imaging of transcatheter arterial chemoembolization for hepatocellular carcinoma using three-dimensional cone-beam CT angiography. Liver Cancer 2014;3:53–61.
25 Ohshima S: Volume analyzer SYNAPSE VINCENT for liver analysis. J Hepatobiliary Pancreat Sci 2014;21:235–238.
26 Nakashima T, Okuda K, Kojiro M, Jimi A, Yamaguchi R, Sakamoto K, Ikari T: Pathology of hepatocellular carcinoma in Japan. 232 consecutive cases autopsied in ten years. Cancer 1983;51:863–877.
27 Nakamura H, Tanaka T, Hori S, Yoshioka H, Kuroda C, Okamura J, Sakurai M: Transcatheter embolization of hepatocellular carcinoma: assessment of efficacy in cases of resection following embolization. Radiology 1983;147:401–405.
28 Shibata J, Fujiyama S, Sato T, Kishimoto S, Fukushima S, Nakano M: Hepatic arterial injection chemotherapy with cisplatin suspended in an oily lymphographic agent for hepatocellular carcinoma. Cancer 1989;64:1586–1594.
29 Chen GW, Song B, Li ZL, Yuan Y: Ectopic blood supply of hepatocellular carcinoma as depicted by angiography with computed tomography: associations with morphological features and therapeutic history. PLoS One 2013;8:e71942.
30 Oshiro Y, Yano H, Mitani J, Kim S, Kim J, Fukunaga K, Ohkohchi N: Novel 3-dimensional virtual hepatectomy simulation combined with real-time deformation. World J Gastroenterol 2015;21:9982–9992.
31 Ogawa C, Minami Y, Morioka Y, Noda A, Arasawa S, Izuta M, Kubo A, Matsunaka T, Tamaki N, Shibatouge M, Kudo M: Virtual sonography for novice sonographers: usefulness of SYNAPSE VINCENT® with precheck imaging of tumor location. Oncology 2014;87(suppl 1):50–54.
32 Ogawa C, Minami Y, Noda T, Arasawa S, Izuta M, Kubo A, Matsunaka T, Tamaki H, Shibatoge M, Kudo M: Initial experience performing percutaneous ultrasound examination with real-time virtual sonography with color display. Oncology 2015;89(suppl 2):11–18.

Review Article

Digestive Diseases

Dig Dis 2016;34:714–730
DOI: 10.1159/000448864

Recent Trends in the Management of Hepatocellular Carcinoma with Special Emphasis on Treatment with Regorafenib and Immune Checkpoint Inhibitors

Masatoshi Kudo

Department of Gastroenterology and Hepatology, Kindai University Faculty of Medicine, Osaka-Sayama, Japan

Key Words
Hepatocellular carcinoma · Regorafenib · Programmed cell death-1 antibody · Nivolumab · Pembrolizumab

Abstract
Hepatocellular carcinoma (HCC) is the fifth most common cancer and the third leading cause of cancer deaths worldwide. Sonazoid-enhanced ultrasound and gadolinium ethoxybenzyl diethylenetriamine pentaacetic acid-enhanced MRI are the most important imaging modalities in diagnosing HCC. There are 2 non-contradictory HCC treatment algorithms in Japan. Hepatic arterial infusion chemotherapy plays an important role in the treatment of advanced HCC with main or branch portal vein invasion. Regorafenib, as a second-line systemic treatment, prolongs survival in patients with intermediate and advanced HCC who progressed on sorafenib. In recent clinical trials, immune check point inhibitors show promising results for the treatment of HCC. This review describes recent trends in the management of HCC.

Introduction

This article reviews recent important topics on the management of hepatocellular carcinoma (HCC).

According to GLOBOCAN 2012, 745,533 individuals worldwide died of HCC, with Asians accounting for 566,886 (76%) of these deaths (fig. 1). In Japan, the number of deaths from liver cancer peaked at 34,510 in 2004, gradually declining thereafter. Deaths from liver cancer were surpassed for the first time by deaths from pancreatic cancer in 2013, with deaths from the former dipping below 30,000 (to 29,543) for the first time in 2014 (fig. 2). The number of HCC-related deaths is expected to continue to decline until 2029 (to about 25,000), with no expected steep decline in this number for the following 15 years (fig. 3). Due to the consistent rate of cancer development in hepatitis C virus-infected patients who achieve a sustained viral response, and the rate of liver cancers related to hepatitis B virus infection, nonalcoholic steatohepatitis, and alcohol overconsumption, a sharp decline in the number of HCC patients is not likely to occur.

Role of Imaging Techniques in the Diagnostic Algorithm for HCC

Multistep Development of HCC and Changes in Intranodular Blood Flow

A majority of HCCs develop infection that is secondary to hepatitis B/C through a multistep carcinogenic process. As the biological malignancy of a hepatic lesion increases, so does blood flow from the hepatic artery into hypovascular nodules. Most tumorous nodules that have dedifferentiated to moderately or poorly differentiated HCCs are arterially hypervascularized. During this pro-

KARGER

E-Mail karger@karger.com
www.karger.com/ddi

0257–2753/16/0346–0714$39.50/0

Masatoshi Kudo, MD, PhD
Department of Gastroenterology and Hepatology
Kindai University Faculty of Medicine
377-2 Ohno-Higashi, Osaka-Sayama, Osaka 589-8511 (Japan)
E-Mail m-kudo@med.kindai.ac.jp

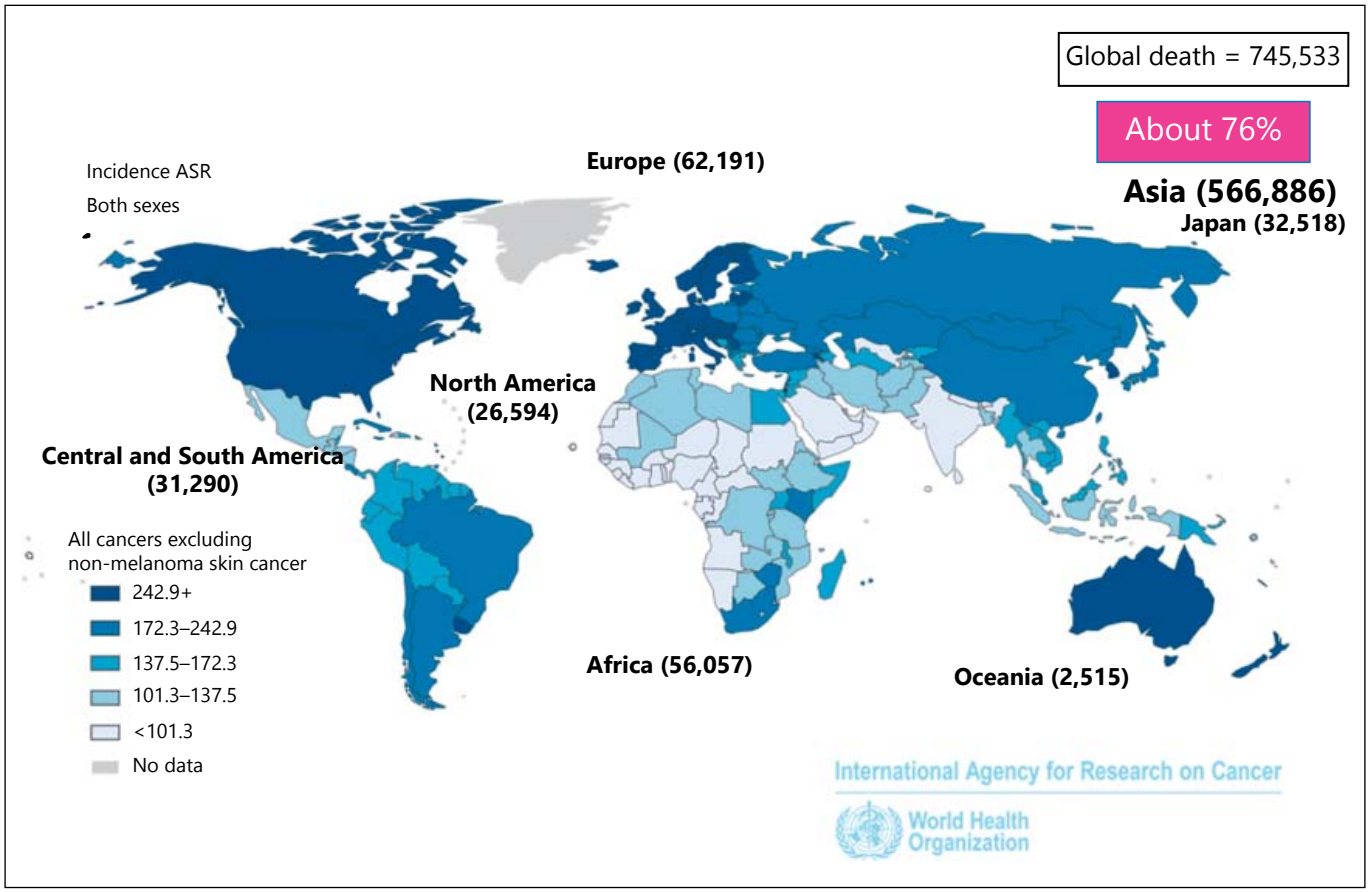

Fig. 1. Liver cancer death in the world.

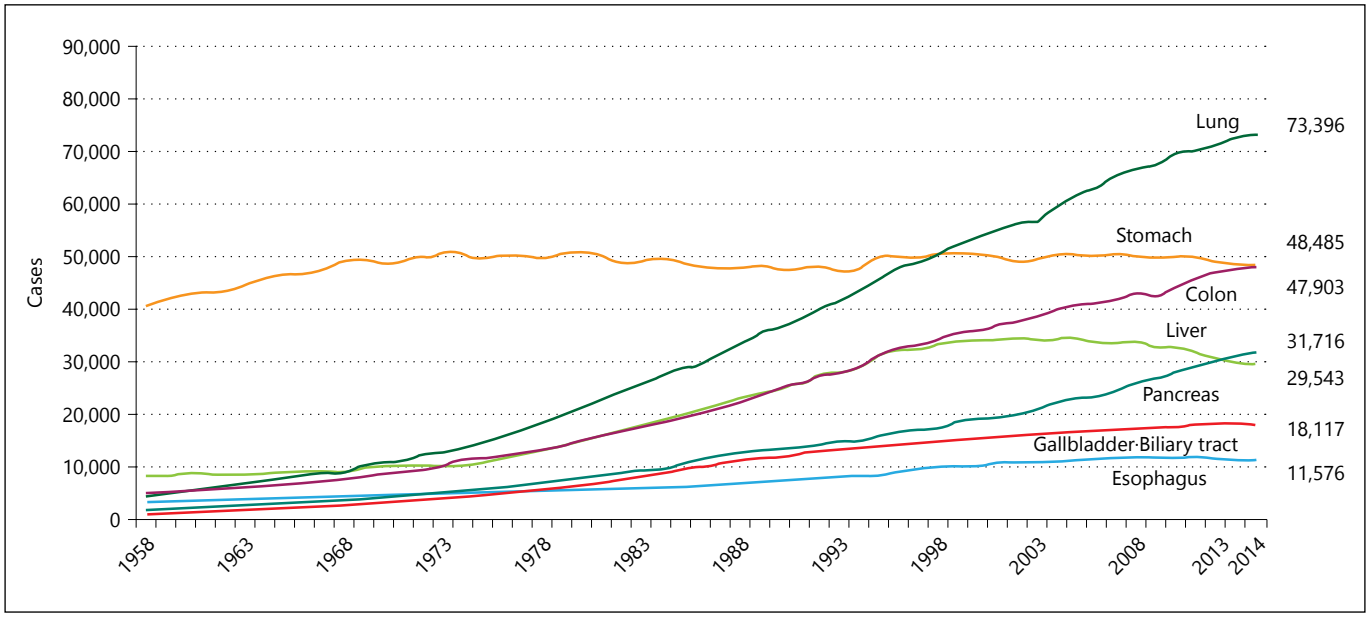

Fig. 2. Numbers of cancer deaths in Japan.

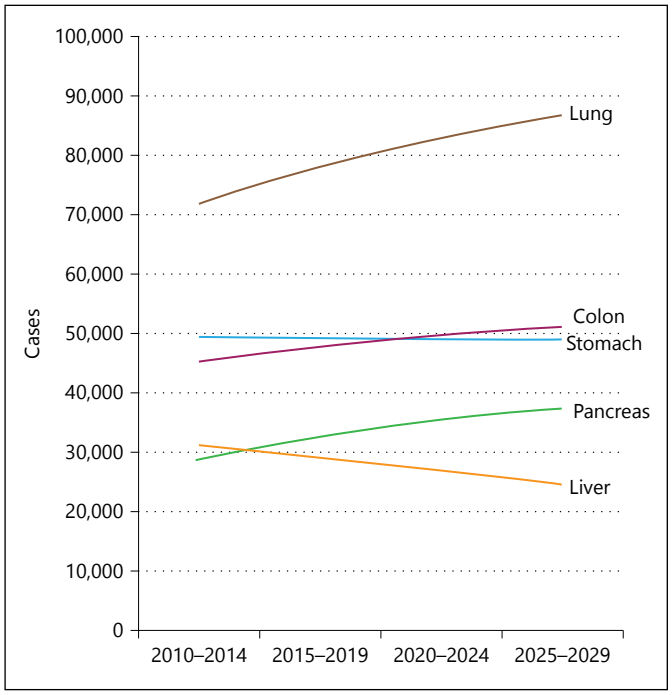

Fig. 3. Estimated cancer mortality.

cess, portal blood flow gradually decreases from the 'present portal flow' state, making hypervascular HCCs eligible for treatment.

Roles of Sonazoid-Enhanced Ultrasonography

Sonazoid-enhanced ultrasonography (US) has 2 benefits in the diagnostic algorithm for HCC. The first is that contrast-enhanced US (CEUS) [1, 2] is sensitive in detecting hypervascularity in nodules that cannot be identified by gadolinium ethoxybenzyl diethylenetriamine pentaacetic acid-enhanced MRI (EOB-MRI) or dynamic multidetector CT (MDCT) [3], as CEUS allows for real-time visualization and does not overlook the influx of arterial blood into these nodules. Thus, nodules diagnosed as 'hypovascular' by EOB-MRI or dynamic MDCT should be evaluated by CEUS to assess the degree of intranodular arterial vascularity.

As for the second benefit, true hypovascular nodules showing hypointensity in both the hepatocyte phase of EOB-MRI and the Kupffer phase of Sonazoid CEUS are likely to be highly malignant and to readily develop into typical hypervascular HCCs. Thus, most hypovascular nodules showing hypointensity on both the hepatocyte phase of EOB-MRI [4, 5] and the Kupffer phase of Sonazoid CEUS can be diagnosed as pathologically early HCC without a biopsy.

Roles of Dynamic CT/MRI

Early enhancement during the arterial phase and washout during the portal/venous phase of dynamic CT/MRI are considered typical of HCC and are widely used for its diagnosis [3, 6]. However, dynamic CT/MRI may not be sensitive enough to diagnose either moderately differentiated HCC with fatty deposition or poorly differentiated HCC of high-grade malignancy, as some of these tumors do not show clear early enhancement during the arterial phase [3]. The arterial phase of dynamic CT/MRI is also associated with a reduced ability to detect a lesion due to incorrect timing of image acquisition, and it may require increased temporal resolution or a more precise setting of the timing of acquisition. Moreover, because the iodinated contrast medium used in dynamic CT has a lower enhancement effect than the gadolinium used in dynamic MRI, some of the lesions detectable by dynamic MRI may not be visualized by dynamic CT.

Dynamic CT has a higher spatial resolution and can visualize intraportal tumor thrombi not visualized by the hepatocyte enhancement phase of EOB-MRI. Furthermore, EOB-MRI is associated with artifacts due to various causes, whereas dynamic CT is associated with a lower incidence of artifacts. Dynamic CT also appears to be more accurate than EOB-MRI when used to differentiate HCC from hemangioma. Thus, in diagnosing HCC, dynamic CT may play a role complementary to EOB-MRI, thereby compensating for the shortcomings of the latter.

Roles of Gd-EOB-MRI

Ability of Gd-EOB-DTPA-Enhanced MRI to Detect HCC

Gd-EOB-DTPA-enhanced MRI (EOB-MRI) has a significantly higher sensitivity and a significantly higher Az value, as determined by alternative free-response receiver-operating characteristic analysis, than MDCT for detecting hypervascular HCCs, and can better detect small hypervascular HCCs. In a regular screening program with EOB-MRI, we found that an increasing number of hypervascular HCCs and HCCs with a nodule-in-nodule appearance (which are undetectable by MDCT) exhibit early enhancement during the arterial phase of EOB-MRI, and are detected as clear hypointense nodules during the hepatocyte phase [7–10]. Previous studies comparing the ability of EOB-MRI and MDCT to detect hypervascular HCCs show the diagnostic performance of EOB-MRI to be better than, or at least equivalent to, that of MDCT.

These findings also apply to hypovascular HCCs. Hypovascular well-differentiated HCCs, that is, early HCCs undetectable by CT during hepatic arteriography (CTHA) or arterial portography (CTAP), by MDCT, or by superparamagnetic iron oxide-enhanced-MRI, have been visualized as hypointense nodules in the hepatocyte phase of EOB-MRI, suggesting the usefulness of EOB-MRI for diagnosing early HCCs [8–11].

A comparison of the diagnostic performance of various modalities for pathologically early HCCs found that only hypointensity during the hepatocyte phase of EOB-MRI had a sensitivity close to 100% (97%) [4, 12]. This finding suggested that the hepatocyte phase of EOB-MRI may show the highest diagnostic performance for early HCCs [4, 12]. A comparison of the rates at which the hepatocyte phase of EOB-MRI, the Kupffer phase of Sonazoid CEUS, T2-weighted imaging (T2WI), diffusion-weighted imaging (DWI), and T1-weighted imaging (T1WI) detect progressing HCCs, early HCCs, and dysplastic nodules (DNs) found that the hepatocyte phase of EOB-MRI had a detection rate of 93% for progressing HCCs (with the remaining 7% detected as hyperintense nodules), and a detection rate of 95% for early HCCs. In addition, 33% of DNs were detected as faint hypointense nodules. In comparison, the Kupffer phase of Sonazoid CEUS detected 100% of progressing HCCs but only 11% of early HCCs. Thus, the hepatocyte phase of EOB-MRI appears superior for detecting early HCCs. Another advantage of EOB-MRI is that the protocol also includes T2WI, DWI, and T1WI, providing different images within a single modality.

Risk Factors for Hypervascularization of Hypovascular Hypointense Nodules at the Hepatocyte Phase of EOB-MRI

Many Japanese studies that investigated risk factors for hypervascularization of hypovascular nodules showing hypointensity in the hepatocyte phase of EOB-MRI [13–19] found that tumor diameter and nodular growth were significant factors and, thus, may predict hypervascularization of hypovascular hypointense nodules. Many of these studies set the cut-off for tumor diameter at around 1 cm, and follow-up of hypovascular nodules showing hypointensity in the hepatocyte phase of EOB-MRI revealed that those with higher growth rates were more likely to be hypervascularized. This finding suggests that nodular growth should be included in the diagnostic algorithm for HCC, although hypervascularization may also be detected early by intensive follow-up with EOB-MRI. In another study, in which hypovascular nodules showing hypointensity during the hepatocyte phase of EOB-MRI were monitored for changes in tumor diameter after hypervascularization, the median tumor diameter was 1.2 cm and many hypovascular nodules ≤1 cm in diameter also underwent hypervascularization. EOB-MRI showed higher diagnostic performance than other diagnostic modalities for both hypervascular and early HCCs, suggesting that EOB-MRI should be the first-choice modality after US screening in diagnostic algorithms for HCC.

Diagnostic Algorithm for HCC Proposed by the Japan Society of Hepatology

Figure 4 shows an overview of the 2015 version of the diagnostic algorithm for HCC based on the final consensus recommendation by the Japan Society of Hepatology (JSH). The basic screening protocols for patients with chronic hepatitis B/C consist of US and the measurement of 3 tumor markers every 6 months, although patients with hepatitis B/C-related cirrhosis (ultra-high risk groups) should be similarly screened every 3–4 months. The JSH guidelines also recommend that ultra-high risk patients undergo contrast-enhanced CT/MRI, preferably Gd-EOB-MRI, every 6–12 months [20]. This algorithm is simple and consists mainly of Gd-EOB-MRI, which shows high detection rates and good diagnostic performance for both hypervascular and hypovascular HCCs, high performance in differentiating among tumorous lesions, and high objectivity and reproducibility.

In the first step, a lesion is classified by the following EOB-MRI findings: (1) hypervascular with washout, (2) hypervascular without washout, or (3) hypovascular. A hypervascular lesion with washout in patients at high or ultra-high risk of HCC is diagnosed as HCC, whereas a hypervascular lesion without washout should be diagnosed as HCC if it is hypointense in the hepatocyte phase. The latter should undergo screening by other imaging modalities such as dynamic CT or MRI to exclude hemangiomas, as they show findings similar to those of HCC on EOB-MRI. A hypervascular tumor without washout that is isointense or hyperintense in the hepatocyte phase of EOB-MRI should be biopsied. A hypovascular lesion that is isointense on EOB-MRI should be assessed by CEUS for intranodular arterial flow to determine whether it is truly hypovascular or not. The lesion should be diagnosed as HCC if it is hypervascular on Sonazoid CEUS or shows any defect in the Kupffer phase; in this case, optional biopsy may be performed. Lesions 1–1.5 cm in size found to be hypovascular on CEUS, with no

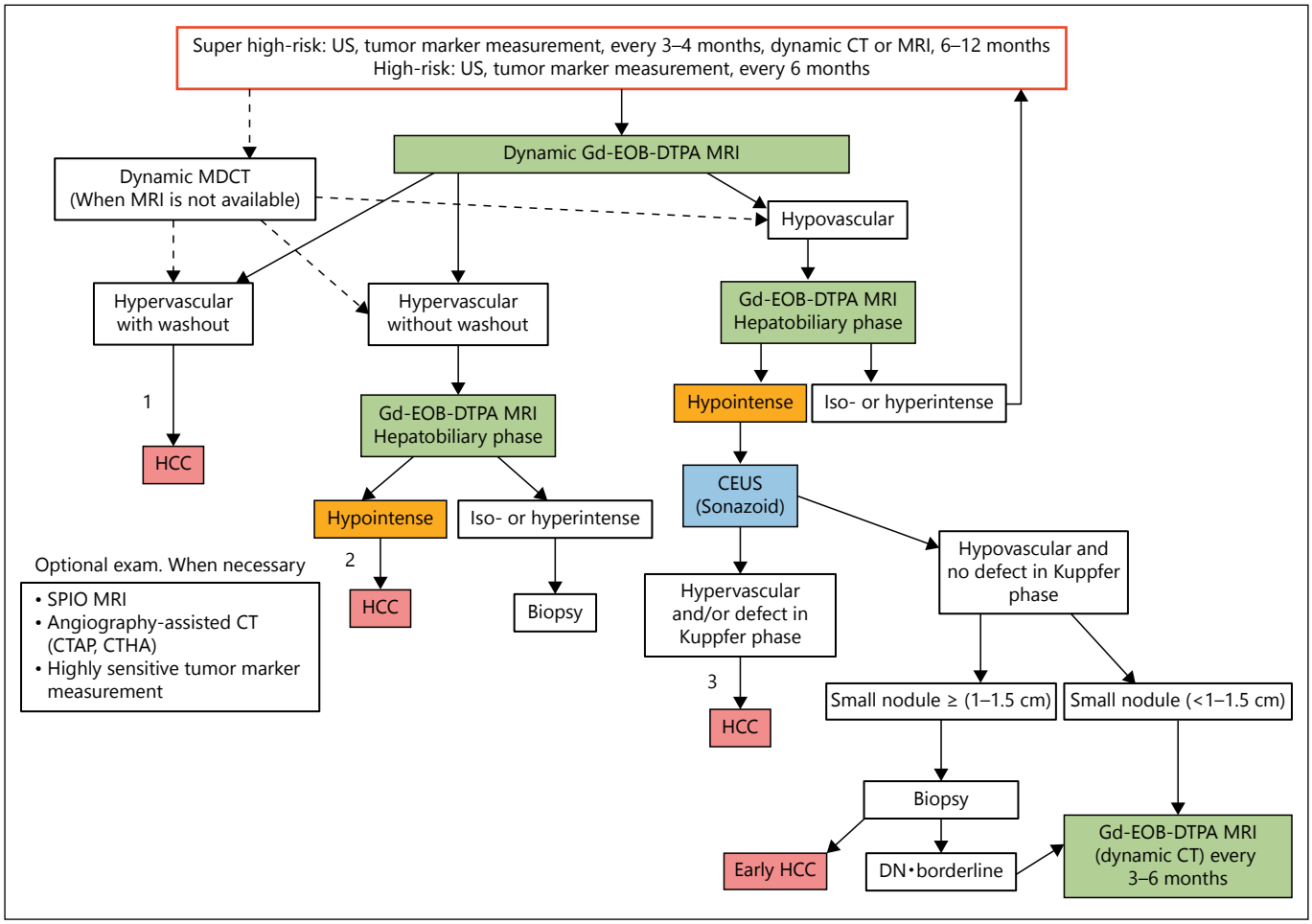

Fig. 4. Surveillance and diagnostic algorithm of HCC (proposed by liver cancer study group of Japan 2015). [1] Cavernous hemangioma may show hypointensity on equilibrium (transitional) phase of dynamic Gd-EOB-DTPA MRI (pseudo-washout). It should be excluded by other sequences of MRI and/or other imaging modalities. [2] Cavernous hemangioma usually shows hypointensity on hepatobiliary phase of Gd-EOB-DTPA MRI. It should be excluded by other sequenced of MRI and/or other imaging modalities. [3] Biopsy may be considered for confirmation.

defect in the Kupffer phase, should be biopsied and followed-up by EOB-MRI every 3–6 months if malignancy has been ruled out. Small nodules (1–1.5 cm) found to be hypovascular on Sonazoid CEUS and to have no defect should also be assessed by EOB-MRI every 3–6 months. Institutions unable to perform EOB-MRI at initial screening or follow-up should substitute dynamic MDCT.

Treatment Algorithm for HCC Proposed by the JSH

In Japan, 2 types of treatment algorithms have been proposed for HCC: the HCC treatment algorithm described in the JSH Evidence-based Clinical Practice Guidelines for HCC, revised in 2013 [21], and the JSH consensus-based Clinical Practice Guidelines for HCC (2014) [20]. In North America and Europe, a treatment algorithm based on BCLC staging has been established as the standard clinical practice guideline [22, 23].

Evidence-Based Treatment Algorithm

This treatment algorithm was initially developed in 2005 by a group led by Maku-uchi of the Japanese Ministry of Health, Labour and Welfare, and was subsequently revised in 2009 and 2013. In this algorithm, the recommended treatment is based on the extent of liver damage, as assessed by the Child–Pugh classification, tumor number, and tumor size. Surgical resection is considered the first-line treatment for patients with a single tumor and Child–Pugh grade A or B liver damage, with ablation considered

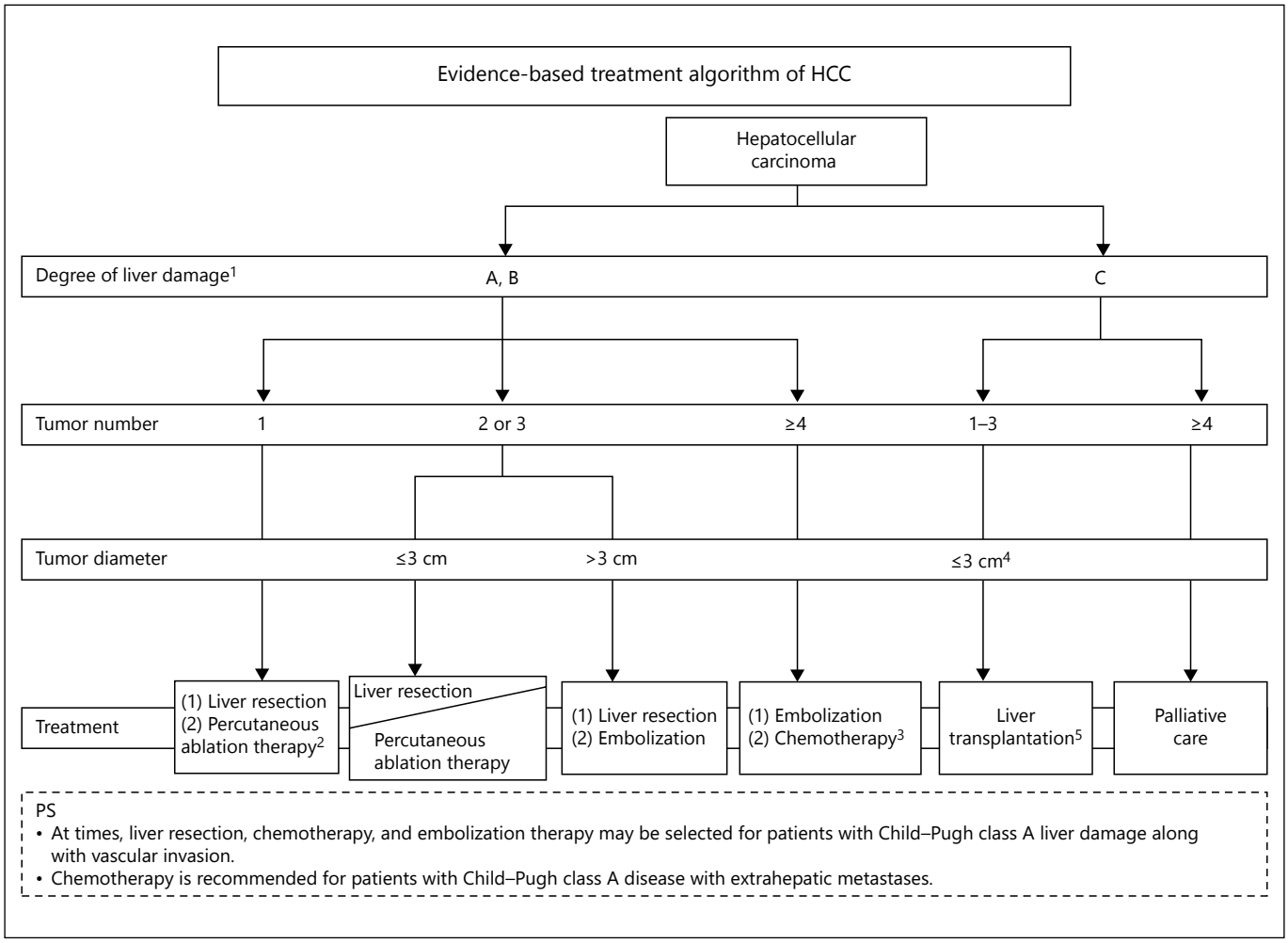

Fig. 5. Evidence-based treatment algorithm of HCC. [1] The Child–Pugh classification may also be used when non-surgical treatment is considered. [2] Can be selected for tumors with a diameter of ≤3 cm. [3] Oral administration and/or hepatic arterial infusion are available. [4] A single tumor ≤5 cm or 2–3 tumors ≤3 cm in diameter. [5] Patients aged ≤65 years.

second-line treatment. Resection or local therapy is considered the first-line treatment for patients with Child–Pugh grade A or B and 2 or 3 tumors <3 cm in size, whereas resection or transarterial chemoembolization (TACE) is recommended for patients with 2 or 3 tumors ≥3 cm in size. TACE or hepatic arterial infusion chemotherapy (HAIC) is recommended for patients with more than 4 tumors. Liver transplantation is recommended for patients with Child–Pugh grade C liver damage and more than 3 tumors <3 cm in size or a single tumor <5 cm in size (i.e., within the Milan criteria), whereas palliative therapy is recommended for patients with more than 4 tumors (fig. 5).

The 2013 version of this algorithm includes a footnote recommending hepatectomy, systemic therapy such as sorafenib or HAIC, or TACE for patients classified as Child–Pugh grade A with vascular invasion, and recommending sorafenib or HAIC for Child–Pugh grade A patients with extrahepatic metastasis. In addition, local ablation therapy may benefit patients with tumors <3 cm in size.

Consensus-Based Treatment Algorithm

Because of the differences in HCC treatment between Japan and Western countries, a Japan-specific algorithm, called the JSH consensus, was originally proposed in 2007 [24] and has since been revised twice [20, 25]. In the treatment algorithm based on the JSH consensus, patients are classified according to the presence/absence of an extrahepatic lesion, liver functional reserve, the presence/absence of vascular invasion, tumor number, and tumor di-

ameter, along with treatments including curative treatment (hepatectomy or local ablation) [26–29], TACE [20, 30–32], HAIC [33–35], sorafenib [36–38], liver transplantation [39], and palliative treatment. This algorithm is in good agreement with the evidence-based treatment algorithm but also includes treatments widely accepted in Japan for which no evidence is available but for which a consensus has been reached. For example, in real-world situations, lesions diagnosed as pathologically early HCC by biopsy, CTHA/CTAP, or Gd-EOB-MRI are treated by local ablation [40, 41].

According to the Evidence-based Clinical Practice Guidelines for HCC, hypovascular tumors are classified as 'atypical nodules' and defined as lesions without early enhancement, for which follow-up is recommended. However, hypovascular tumors further examined by CTAP, EOB-MRI, the Kupffer phase of Sonazoid CEUS, or biopsy, and subsequently confirmed to be 'pathological early HCC,' are often considered eligible for treatment because these lesions are highly likely to progress to classical HCC based on experience in Japan and on many studies using EOB-MRI. These lesions are more likely to be treated by minimally invasive local ablation than by surgical resection as the latter may be overtreatment. Hypovascular lesions with few or no malignant features require extensive and careful follow-up. These hypovascular early HCCs/high-grade DNs should be handled differently than other types of hypervascular HCCs.

With regard to specific algorithms for typical HCCs, resection or ablation is recommended for patients with less than 3 tumors <3 cm in size, without an extrahepatic lesion or vascular invasion, and with preserved liver function. For this group of patients, even ablation is expected to provide reliable and favorable outcomes. Patients with 1–3 tumors >3 cm should be treated by surgical resection or TACE [35, 42, 43]. The addition of ablation to prior transarterial treatment (e.g., TACE or lipiodol-TAI) may improve the curability of these lesions.

TACE or HAIC is selected for most patients with more than 4 tumors, although HAIC has been performed empirically without definitive evidence. Patients with more than 5 or 6 tumors may also benefit from ablation combined with TACE or HAIC. Surgical resection may also be considered for patients with more than 4 lesions. Transplantation may be performed in patients with Child–Pugh A/B liver function who are relatively young, have experienced early or repeated recurrence, and have met the Milan criteria.

Patients with vascular invasion may be candidates for resection if the extent of invasion involves a segmental portal branch (Vp1) and if resection is feasible. TACE may also be selected if the extent of invasion is no further than Vp1 or Vp2. HAIC may be performed in patients with branch (Vp3) or main (Vp4) portal vein invasion, usually with implantation of a reservoir. Sorafenib is another option for HCC patients with Child–Pugh class A liver function and Vp1–3 portal invasion; however, it is not recommended for patients with Vp4 invasion because the drug may cause hepatic failure. In addition, a recent prospective randomized study (the SILIUS trial) suggested that HAIC is preferable for patients with main portal vein invasion (Vp4) [44].

Liver transplantation should be considered for patients with poor liver function (classified as Child–Pugh C) without vascular invasion and who are within the Milan criteria and aged ≤65. Experimental treatments for Child–Pugh C patients without hepatic encephalopathy or refractory ascites and with a serum bilirubin concentration ≤3 mg/dl include ablation and subsegmental TACE. Retrospective studies using propensity score matching [45–47] showed a survival benefit in patients with Child–Pugh score 10 or 11; however, there have been no randomized clinical trials. Further prospective clinical studies are needed to address this issue.

Child–Pugh C patients with vascular invasion or an extrahepatic lesion should receive best supportive care (BSC), including radiotherapy for palliative pain relief. However, intrahepatic lesions in Child–Pugh A/B patients, in whom the occurrence of extrahepatic spread is not a prognostic factor, should be treated according to the algorithm as if there is no extrahepatic spread, as the algorithm is thought to provide better outcomes [48, 49].

Sorafenib is the treatment of choice for patients with extrahepatic spread and Child–Pugh A liver function reserve. Sorafenib or HAIC is recommended for patients with vascular invasion, in particular Vp1–3, with HAIC also recommended for patients with Vp4. Sorafenib can also be an option for patients with Child–Pugh A class liver function unresponsive to TACE or HAIC (fig. 6).

Regorafenib as Second-Line Systemic Treatment

On June 30, 2016, positive data from the RESORCE trial of regorafenib, an inhibitor of a broad range of kinases (including VEGFR, PDGFR, FGFR, TIE2, KIT, RET, and RAF), were presented at the World Congress on Gastrointestinal Cancer [50]. Median overall survival (OS), the primary endpoint of the study, was significantly greater in patients who received regorafenib than placebo as second-line therapy (10.6 vs. 7.8 months; HR 0.62;

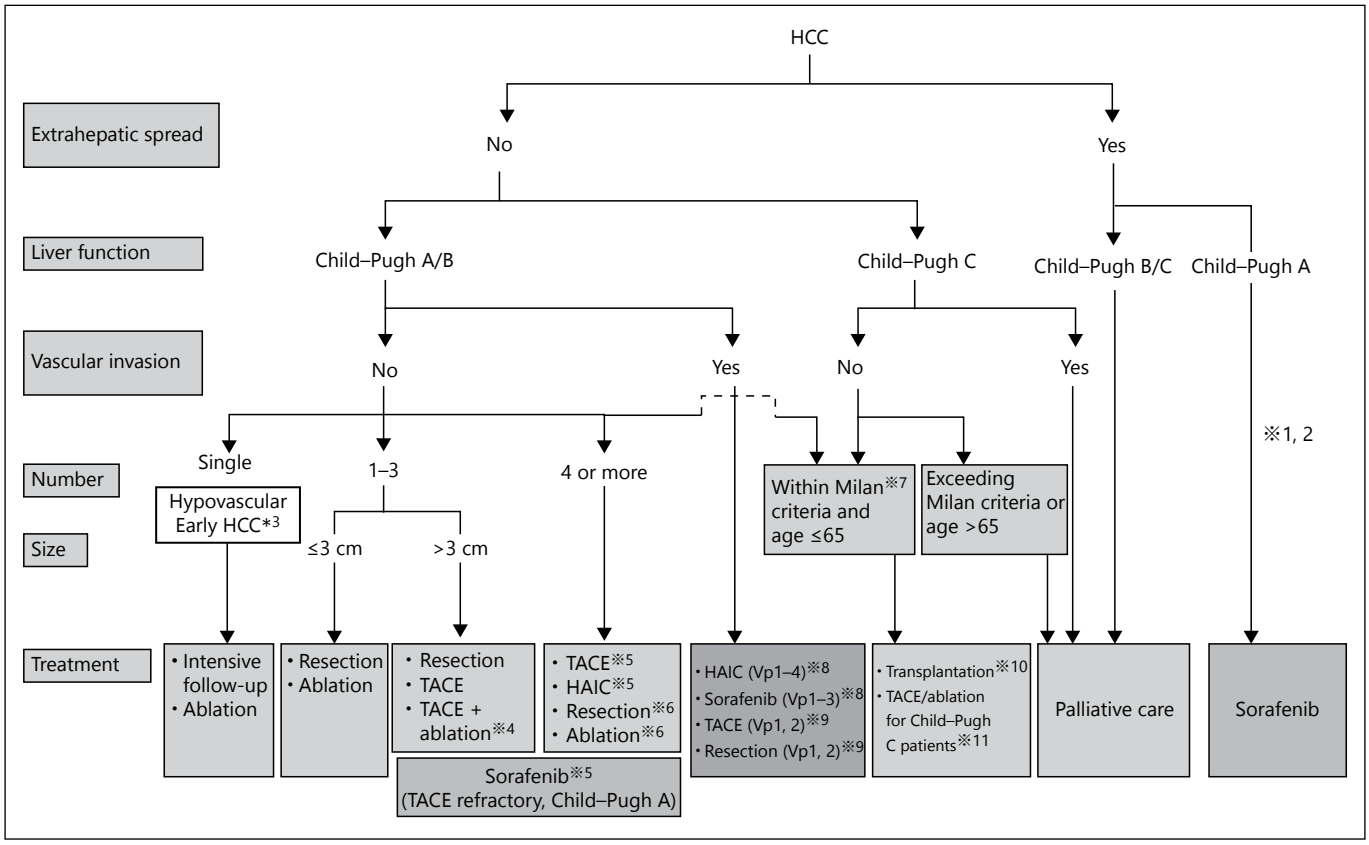

Fig. 6. JSH-LCSGJ consensus-based treatment algorithm for HCC revised in 2014 [20].

Table 1. Results of RESORCE trial [50]

	Regorafenib	Placebo	HR	p value
Number	379	194		
BCLC C, %	88	87		
Treatment duration, months	3.6 (0.03–29.4)	1.9 (0.2–27.4)		
OS, months	10.6	7.8	0.62 (0.50–0.78)	<0.001
PFS, months	3.1	1.5	0.46 (0.37–0.56)	<0.001
TTP, months	3.2	1.5	0.44 (0.36–0.55)	
DCR, %	65.2	36.1		<0.001
ORR, %	10.6	4.1		<0.005
Adverse events (≥grade 3), %	79.7	58.5		

TTP = Time to progression; DCR = disease control rate; ORR = overall response rate.

95% CI 0.50–0.78; p < 0.001; table 1). Importantly, however, the study design may have contributed to the positive outcome. First, the study included a group of patients who progressed while on sorafenib, but these patients were required to have received ≥400 mg of sorafenib for at least 20 of 28 days prior to enrollment in the RESORCE trial; patients who discontinued sorafenib due to poor tolerability were excluded. Second, vascular invasion and extrahepatic spread were treated as independent stratification factors (table 2).

Post-progression survival (PPS) is defined as the interval between a diagnosis of progressive disease (PD) and patient death; OS can be expressed by the equation OS = PFS + PPS, where PFS is progression-free survival. Even

Table 2. Design of the RESORCE trial

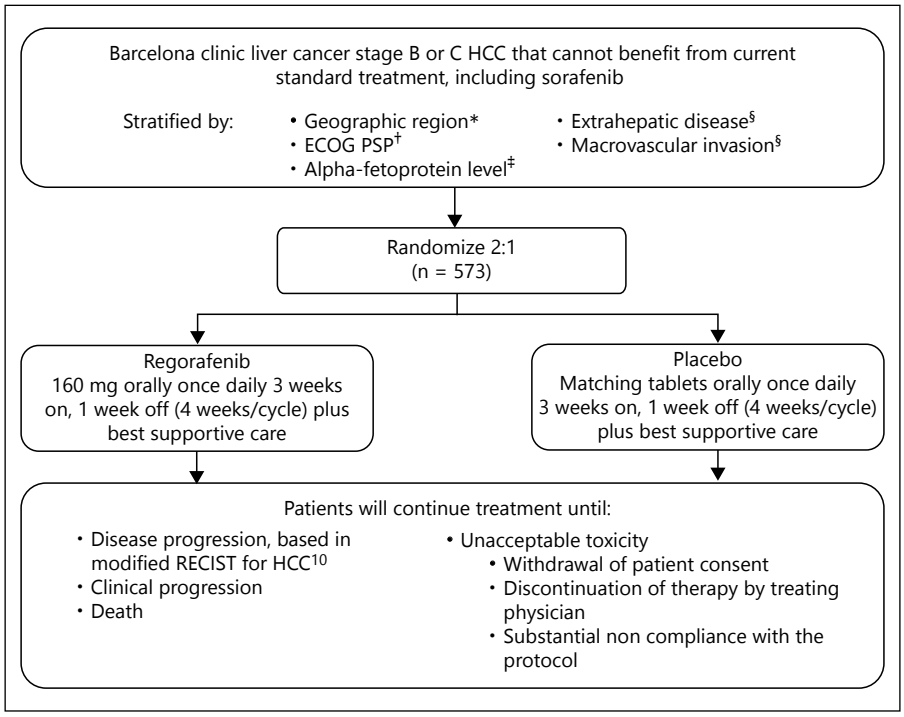

if PFS differs significantly, OS may not differ if PPS is sufficiently long. Indeed, a clinical trial of sorafenib revealed that OS showed greater correlation with PPS than with PFS [51]. Locoregional therapy is the mainstay of treatment for HCC, but molecular targeted agents are indicated when locoregional therapy is no longer practical. However, even after following the recommended therapeutic guidelines, locoregional therapy is often administered to patients in a generally stable condition after the end of a trial. This rarely occurs in patients with other types of cancer. Rather, it is unique to HCC due to the availability of powerful locoregional therapies such as intra-arterial infusion chemotherapy and TACE. Thus, if PPS is prolonged by effective post-trial treatments, OS may not differ significantly [52]. In addition, clinical trials of agents other than regorafenib use intolerability to sorafenib as an inclusion criterion; however, this is thought to augment the influence of post-trial treatments. Patients who progress after the administration of sorafenib are defined as unresponsive to sorafenib; they have relatively poor hepatic function and are in poor overall condition. By contrast, patients defined as intolerant to sorafenib and who discontinue the treatment due to adverse effects remain in a relatively stable condition. Clinically stable patients are more likely to be subjected to various post-trial treatments, particularly locoregional therapy, regardless of whether they receive a second-line agent or a placebo during the trial. This finding is supported by subanalysis of a phase II trial of axitinib, showing that OS was longer in the axitinib than in the placebo arm after excluding patients who discontinued therapy due to adverse events (AEs) [53]. Thus, clinical trials of second-line agents should enroll only those patients unresponsive to sorafenib, as in the RESORCE trial (table 2).

The decision to exclude patients intolerant to sorafenib from the clinical trial of regorafenib was due primarily to the similar toxicological profiles of the 2 agents (sorafenib and regorafenib), resulting from their structural similarity (fig. 7). However, by excluding patients intolerant to sorafenib, post-trial treatments were prohibited. This trial design resulted in a shorter PPS and therefore a greater difference in OS, thereby clarifying the benefits of regorafenib therapy.

Recent Topics on TACE

Heterogeneity of Intermediate-Stage HCC

The BCLC staging system defines intermediate-stage HCCs as BCLC stage B. This staging system has been incorporated into the AASLD [22] and EASL-EORTC [23] guidelines. By contrast, the concept of intermediate-stage

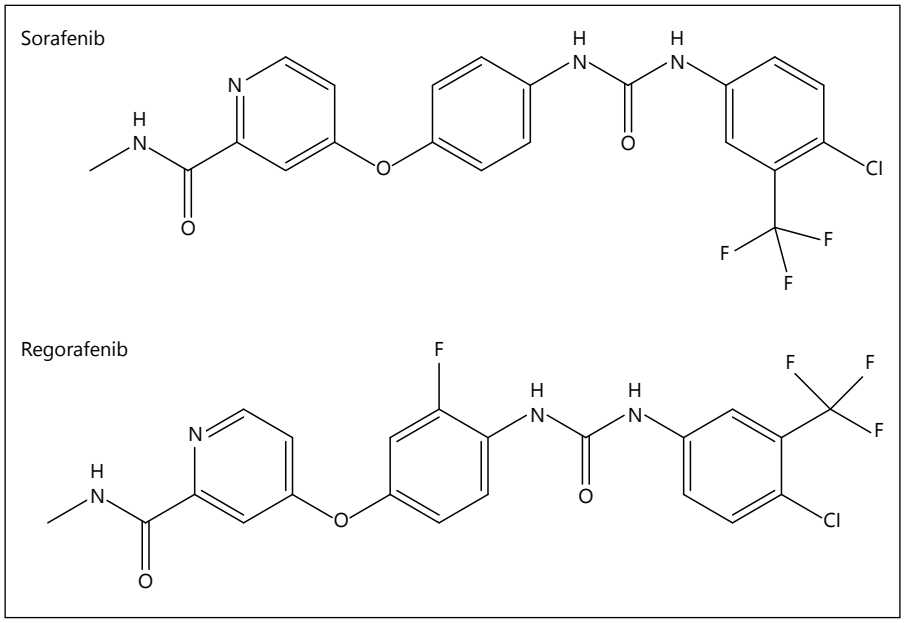

Fig. 7. Chemical structure of sorafenib and regorafenib.

HCC has not been incorporated into the JSH evidence-based [21], JSH consensus-based [54], and APASL [55] guidelines. Among Japanese patients with HCC, this intermediate-stage population would correspond to those with Child–Pugh A/B liver function, more than 4 tumors or a maximum tumor diameter >3 cm, and without vascular invasion or extrahepatic spread. The BCLC staging system recommends TACE as the only treatment option for patients with intermediate-stage HCC. However, the intermediate-stage population consists of various subpopulations, ranging from patients with disease close to early stage disease who are administered treatment with curative intent, to those with disease close to end stage disease with a Child–Pugh score of 9, making them suitable only for liver function-preserving treatment or BSC. Sub-staging of this heterogeneous intermediate stage population is important, as is designing treatment strategies for each substage.

The BCLC stage-B population consists of patients with various levels of liver function, with Child–Pugh scores ranging from 5 to 9. Patients with more than 4 tumors, including those with multiple tumors in both lobes (>20 tumors), are also included in the intermediate stage category provided there is no vascular invasion or distant metastasis and that their performance status is 0. In addition, because there are no restrictions in tumor size, all tumors ≥3 cm are included in this category. Patients with 3 tumors measuring slightly over 3 cm and those with one tumor measuring 5–10 cm may be considered eligible for surgical resection if liver function is well preserved. Moreover, ablation following TACE may be considered for patients with more than 4 nodules or a nodule measuring >3 cm but ≤5 cm, as extensive ablation with bipolar radiofrequency may provide good outcomes. Conventional subsegmental lipiodol TACE (cTACE) may be performed with curative intent. In patients with more than 5 or 6 tumors, a catheter may be advanced to the peritumoral area in a super-selective manner, followed by lipiodol injection and embolization with a gelatin sponge. This may result in partial infarction of the liver and, in some patients, a complete response (CR) without liver function damage. Although super-selective cTACE is a highly advanced therapeutic technique that can be curative in some patients, its applicability is restricted by both tumor size and number. Thus, few patients in countries outside Japan are eligible for super-selective cTACE with curative intent, as Japan has established a surveillance system to detect small nodules [48, 56].

TACE using drug-eluting beads containing anti-cancer agents (DEB-TACE) has also become increasingly popular in Japan. DEB-TACE is more likely to be performed as palliative therapy or for mass reduction purposes in patients with huge or multiple HCCs. DEB-TACE is preferred to cTACE for patients with a large HCC requiring multiple treatment sessions, as it is less toxic to liver function and post-embolization syndrome is mild. Moreover, cTACE is not indicated for super-multiple lesions affecting both lobes, both because it is ineffective and because it may lead to decompensated liver function.

HAIC or sorafenib may be effective in some of these patients. Because even DEB-TACE is not very effective against super-multiple nodules, HAIC or sorafenib may be preferred as first-line treatment.

If both the number and size of tumors are small (within the Milan criteria), treatment modalities that minimally affect liver function are required for patients with impaired liver function as post-procedure outcomes are dependent on the remaining liver function. Super-selective cTACE may be preferred to minimize the reduction of liver function and to maximize the tumor response. DEB-TACE or HAIC is recommended for patients with liver function corresponding to a Child–Pugh score of 7 and many or huge tumors; this is because these treatments can also minimize the reduction of liver function. Treatment strategies in most patients with poor liver functional reserve, corresponding to a Child–Pugh score of 8–9, should be similar to those for Child–Pugh C. Thus, although super-selective cTACE and ablation are options if both the number and maximum diameter of tumors are limited, BSC or liver transplantation may also be considered according to the extended criteria. Sorafenib may be a good first-line option for patients with super-multiple lesions in both lobes and good liver functional reserve.

Sub-Classification of Intermediate-Stage HCCs and Treatment Strategies

As intermediate-stage HCCs are heterogeneous, they may be sub-classified [57] using a staging system that incorporates the 'beyond Milan' and 'up-to-7' criteria [58], a new concept combining the number and diameter of tumors. However, in this system, Child–Pugh scores classified as substages B1, B2, and B3 have been described as 'a score of 5, 6, or 7,' 'a score ranging from 5 to 6,' or just 'a score of 7.' In addition, with respect to the first option, this system seems to be similar to the original BCLC system, as it recommends TACE as first-line therapy. As post-TACE outcomes become poorer with substage advancement from B1 to B4, this new system is better than the original system for predicting outcomes. Moreover, although portal vein tumor thrombus (PVT) is not included in the original BCLC criteria for intermediate-stage HCCs, all criteria for substages B1–B4 include the absence of PVT, suggesting that the reference to PVT can be deleted. Although the new system suggests liver transplantation as an option for patients with Child–Pugh scores of 5, 6, and 7, this may not be practical in Japan, where liver transplantation is not considered a standard treatment option. Moreover, although the new system recommends TACE or radioembolization as the first treatment option for patients with substage B2, radioembolization has not been approved in Japan. Rather, HAIC is a treatment of choice for patients in Japan with multiple intrahepatic lesions in both lobes.

Kinki Criteria

The modified Bolondi classification (table 3; fig. 8) [59] assigns patients into 3 categories: 2 based on liver function (Child–Pugh scores of 5–7 or 8–9) and one based on tumor status (beyond the Milan criteria, but within (in) or beyond (out) the 'up-to-7' criteria [28]). This classification system is similar to the Bolondi sub-staging system, but it is simpler and easier-to-use. According to this modified system, patients classified as substage B1 may be eligible for surgical resection and ablation. Resection may also be an option for patients with Child–Pugh A liver function and 1 or 2 large tumors. Ablation may be a good option for patients with 4–6 small HCCs, as well as for those with large tumors measuring up to 5 cm, as TACE followed by ablation will provide a large ablation area. Super-selective cTACE with curative intent can be applied to each tumor in patients with several small tumors. If super-selective catheterization is not feasible, then DEB-TACE or B-TACE may be an alternative.

DEB-TACE should be applied repeatedly and actively to patients with substage B2 classified as beyond the 'up-to-7' criteria with large HCCs, as well as being a good option for patients with large HCCs. By contrast, cTACE and DEB-TACE are not very effective for patients with multiple HCCs beyond the 'up-to-7' criteria; rather, HAIC or sorafenib may be selected for these patients. cTACE may also be selected but it is not recommended because it damages liver function. Thus, sorafenib may be a good alternative for patients with multiple tumors who are likely to be unresponsive to TACE and for patients classified as 'beyond the up-to-7' and likely to be unresponsive to cTACE or DEB-TACE [35, 60, 61].

BSC may be selected for patients classified as substage B3, similar to patients classified as Child–Pugh C. By contrast, super-selective cTACE or ablation should be carefully applied to each tumor in patients classified as substage-B3 that meet the 'up-to-7' criteria, as these modalities may result in complete necrosis and survival benefits, similar to findings in HCC patients with Child–Pugh C liver function [45, 46]. Liver transplantation should also be considered for patients meeting the 'up-to-7' classification, based on extended criteria or after achieving down-staging. HAIC may be considered for 'beyond the up-to-7' patients, as it may minimize the im-

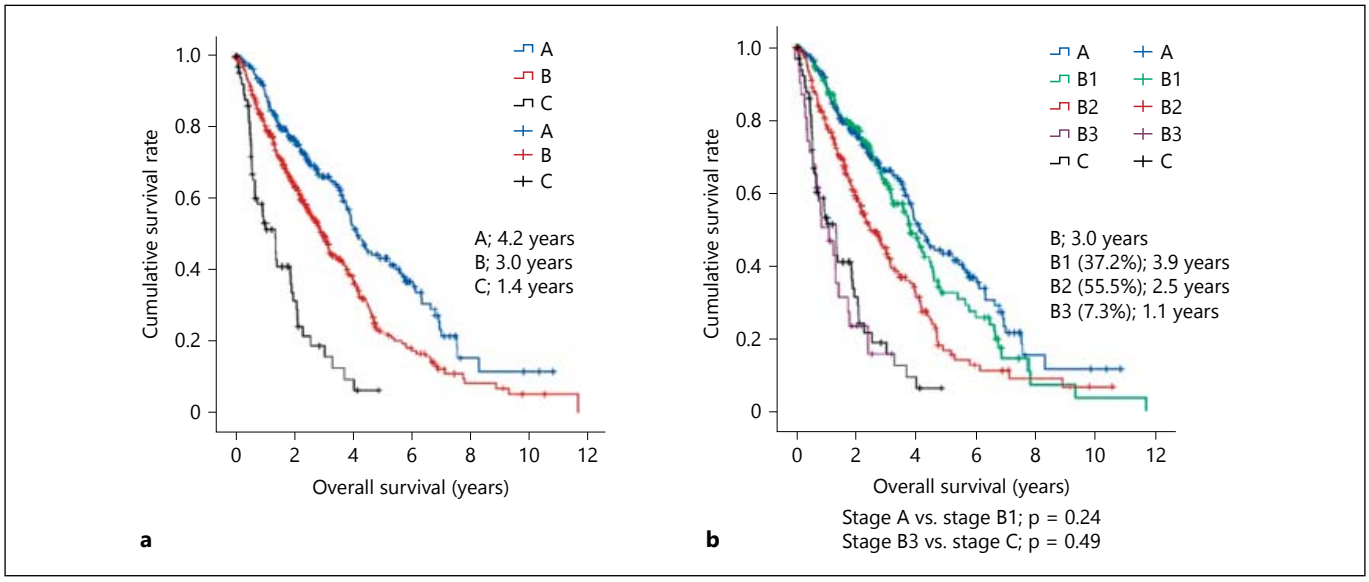

Fig. 8. a, **b** Intermediate stage HCC OS of TACE according to substage (Kinki criteria). Adapted from Arizumi et al. [62].

Table 3. Sub-classification and treatment strategy of intermediate stage HCC (Kinki criteria)

BCLC sub-stage	B1	B2	B3	
Child–Pugh score	5–7	5–7	8, 9	
Beyond Milan and within up-to-7	In	Out	Any	
			in	out
Sub-stage			B3-a	B3-b
Concept of treatment strategy	Curative intent	Non curative, palliative	Curative intent if within up-to-7	Palliative, no treatment
Treatment option	Resection Ablation Superselective c-TACE	DEB-TACE[1] HAIC[2] Sorafenib[3]	Transplantation Ablation Superselective cTACE	HAIC Selective DEB-TACE
Alternative	DEB-TACE (large, C-P 7) B-TACE[4]	cTACE	DEB-TACE B-TACE	BSC

[1] DEB-TACE (drug eluting beads-TACE) is recommended for huge tumors >6 cm.
[2] HAIC (hepatic arterial infusion chemotherapy) is recommended for multiple tumors >6.
[3] Sorafenib is recommended for patients with liver function of Child–Pugh score 5 and 6.
[4] B-TACE (Baloon-occluded TACE) is recommended for fewer tumors.

pairment of liver function, similar to patients classified as substage B2.

Our study analyzed data for patients who underwent cTACE in our hospital according to this sub-classification system [62]. Patients classified as BCLC A, B, and C were well stratified, as were those classified as substages B1, B2, and B3 (fig. 8a). In addition, substage B1 patients had a survival curve similar to that of BCLC A patients, suggesting that the B1 subgroup should be considered for super-selective cTACE or other curative treatment options. The survival curve for patients classified as substage B3 overlapped with that for BCLC C patients (fig. 8b).

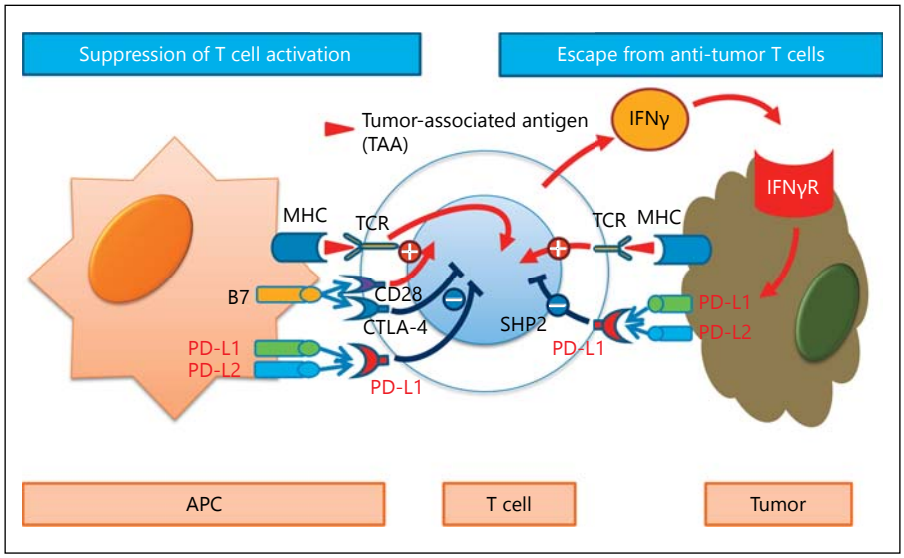

Fig. 9. Immune checkpoint molecule: PD-1.

These findings suggest that repeating cTACE in patients classified as substage B3 would only result in outcomes expected for BCLC C patients. Thus, based on the treatment strategy for Child–Pugh C patients, BSC may be selected as an alternative treatment for 'beyond the up-to-7' patients, whereas patients with the 'up-to-7' criteria in should be treated by super-selective cTACE, ablation, or HAIC to minimize damage to liver function. These results also suggest that BCLC stage-B HCCs should be subclassified as described above and that the treatment strategy should consider both liver function (CP score) and tumor factors (up-to-7 or beyond 7).

Immune Checkpoint Inhibitors in HCCs

Cancer-related antigens on tumor cells are recognized by antigen-presenting cells (APCs), which activate immature T cells in the lymph nodes, converting them to CD8-positive activated T cells (the priming phase). These cells travel through the circulation to reach the vicinity of the tumor, where they start attacking tumor cells through enzymes such as perforin and granzyme (the effector phase). Following recognition of a cancer-derived antigen by a T-cell receptor, the T cells begin to attack the cancer by secreting cytokines such as interferon gamma, which stimulates cancer cells to express molecules to protect themselves, such as PD-L1 and PD-L2, which bind to PD-1. The binding of these ligands to PD-1 sends a negative signal to cytotoxic T lymphocytes, attenuating T cell aggressiveness (i.e., immune escape or immune tolerance; fig. 9). By contrast, the administration of an anti-PD-1 antibody blocks the binding of PD-1 to PD-L1 or PD-L2 expressed on APCs or on tumor cells, releasing the brake for the immune response and restoring the ability of immune system cells to attack tumor cells (fig. 10). Thus, unlike conventional chemotherapies and molecularly targeted drugs, these antibodies act by restoring the original function of the immune system, allowing it to attack cancer cells [63–75]. An antibody against PD-L1 is thought to have the same effect [76]. PD-L1 is a predictive biomarker for the effect of anti-PD-1 antibodies [77]. The Kupffer phase of Sonazoid CEUS may also predict response to treatment with an anti-PD-1 antibody [78].

Interim analysis of a phase I/II clinical study of the anti-PD-1 antibody, nivolumab, in HCC patients (CA209-040 trial) was presented at the annual meeting of the American Society of Clinical Oncology (ASCO) held in Chicago between May 29 and June 2, 2015 [79]. The dose escalation part of the study confirmed that nivolumab was safe at doses up to 10 ml/kg in non-infected, HCV-infected, and HBV-infected patients. Moreover, the dose escalation part of the study assessed the efficacy of nivolumab at doses between 0.1 and 10 ml/kg. A total of 47 patients was examined, including 33 (70%) with extrahepatic metastasis, 6 (13%) with vascular invasion, and 32 (68%) with prior history of treatment with sorafenib, suggesting that the study population comprised patients with relatively advanced cancer. These patients were treated with an anti-PD-1 antibody and the results of an interim analysis performed on March 12, 2015, were reported. At

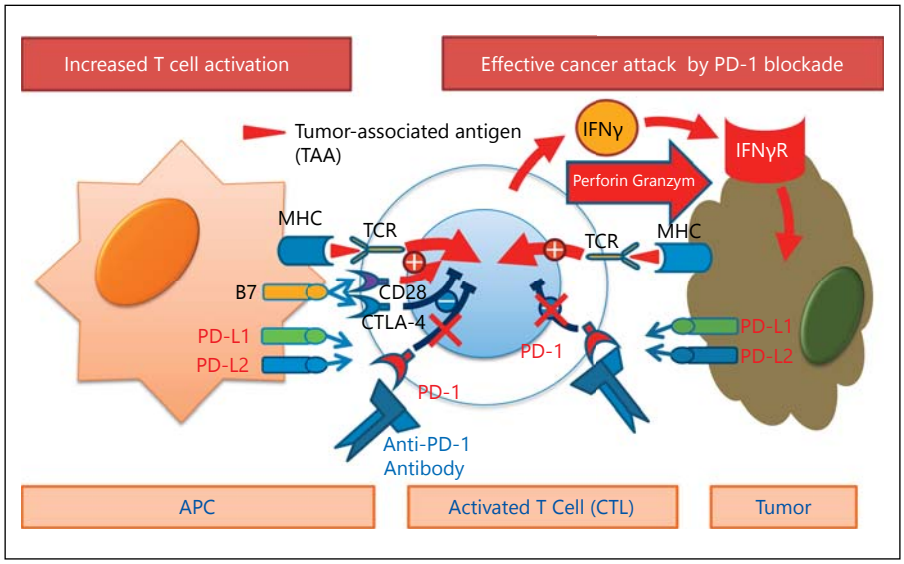

Fig. 10. Immune checkpoint blockade: anti-PD-1 antibody.

Table 4. Investigator-assessed best overall response (RECIST version 1.1) of anti-PD-1 antibody, nivolumab, for HCC (dose-escalation on cohort) [80]

	Uninfected (n = 23)	HCV (n = 10)	HBV (n = 15)	Total (n = 48)
Objective response, n (%)	3 (13)	3 (30)	1 (7)	7 (15)
Complete response	2 (9)	1 (10)	0	3 (6)
Partial response	1 (4)	2 (20)	1 (7)	4 (8)
Stable disease	13 (57)	5 (50)	6 (40)	24 (50)
Progressive disease	6 (26)	2 (20)	7 (47)	15 (31)
Not evaluable	1 (4)	0	1 (7)	2 (4)
Ongoing response, n (%)	1 (33)	0	0	1 (14)

that time, 17 patients were still on treatment, whereas 30 had completed or discontinued treatment. A total of 26, 2, and 2 patients discontinued treatment due to progression, CR, and AEs, respectively. Of the AE-related discontinuations, one was due to increased bilirubin concentration and the other to an AE not related to the study drug. The only CTCAE grade-IV AE was increased lipase levels, and the only grade-III abnormalities were increased AST and increased ALT, which were observed in 5 (11%) and 4 (9%) patients, respectively. No anticipated events of concern, such as serious liver disorders and autoimmune diseases, were observed.

Efficacy was very good, with an overall objective response rate of 19% (8 patients, including 2 (5%) with CR), a disease control rate (defined as the percentage of patients who achieved stable disease or better response) of 67% (28 patients), and PD reported in only 14 (33%) patients.

A waterfall plot showed tumor response in the uninfected and hepatitis B and C cohorts. Of note was the durability of the response. The 2 patients who achieved CR within 3 months remained in CR after 18 months of treatment. Another patient was in SD for about 11 months and subsequently achieved PR close to CR at around 13 months. Moreover, all of the patients who achieved PR or SD remained in the same response category thereafter, with none of these patients developing resistance to treatment or progressing to PD. These observations show that responses to anti-PD-1 antibody therapy may be comparable in patients with liver and other types of cancer. This is an important characteristic of immune checkpoint inhibitors. As mentioned above, the 2 patients who achieved CR within 3 months of treatment remained in CR for more than 18 months, despite discontinuing treatment with anti-PD-1 antibody within a few months after achieving CR. Most of the patients who achieved PR also

Table 5. Investigator-assessed best overall response (RECIST version 1.1) of anti-PD-1 antibody, nivolumab, for HCC (dose-escalation cohort) [81]

	Uninfected: sorafenib naïve/intolerant (n = 54)	Uninfected: sorafenib progressors (n = 58)	HCV (n = 51)	HBV (n = 51)	Total (n = 214)
Objective response, n (%)	11 (20)	11 (19)	7 (14)	6 (12)	35 (16)
Complete response	0	2 (3)	0	0	2 (1)
Partial response	11 (20)	9 (16)	7 (14)	6 (12)	33 (15)
Stable disease	32 (59)	27 (47)	29 (57)	23 (45)	111 (52)
Progressive disease	11 (20)	18 (31)	12 (24)	22 (43)	63 (29)
Not evaluable	0	2 (3)	3 (6)	0	5 (2)

showed a response within 3 months, with only 1 patient requiring about 4 months to achieve PR. The presentation at the ASCO meeting included a patient with multiple HCC lesions in both lobes, which completely disappeared after 6 weeks of treatment, accompanied by a reduction in alpha-fetoprotein concentration from 21,000 to 283 ng/ml. In another case presentation, an HCC measuring ≥10 cm continued to decrease in size (to about 2 cm by week 48), clearly demonstrating a durable response. Moreover, the 12-month OS rate was as high as 62%. These results are highly promising given the poor baseline tumor status of the study population.

At the ASCO meeting in 2016, the updated data for the 48 patients in the dose escalation part and 214 patients in the dose expansion part of the study were reported. Response rates in these 2 groups were 15 and 16%, respectively [80, 81] (tables 4 and 5).

To date, the CA209-040 trial has yielded several major findings: (1) monotherapy with the anti-PD-1 antibody nivolumab has a manageable safety profile when used to treat HCC, with a level of safety comparable with that for other types of cancer; (2) nivolumab is safe in patients with HBV or HCV infection; and (3) the response rate to nivolumab is high for an immunotherapeutic agent; moreover, the response is durable, with this durable response observed at all nivolumab dose levels and in all HCC etiology groups (i.e., uninfected and hepatitis B and C cohorts).

At present, phase 3 trials of nivolumab and pembrolizumab are underway, as is a trial of combination therapy with an anti-PD-1 antibody (PD-L1 antibody) and an anti-CTLA-4 antibody. The results of these trials are eagerly awaited.

Disclosure Statement

The author declares no conflicts of interest regarding the publication of this paper.

References

1 Liu GJ, Wang W, Lu MD, Xie XY, Xu HX, Xu ZF, et al: Contrast-enhanced ultrasound for the characterization of hepatocellular carcinoma and intrahepatic cholangiocarcinoma. Liver Cancer 2015;4:241–252.

2 Minami Y, Kudo M: Imaging modalities for assessment of treatment response to nonsurgical hepatocellular carcinoma therapy: contrast-enhanced US, CT, and MRI. Liver Cancer 2015;4:106–114.

3 Murakami T, Tsurusaki M: Hypervascular benign and malignant liver tumors that require differentiation from hepatocellular carcinoma: key points of imaging diagnosis. Liver Cancer 2014;3:85–96.

4 Ichikawa T, Sano K, Morisaka H: Diagnosis of pathologically early HCC with EOB-MRI: experiences and current consensus. Liver Cancer 2014;3:97–107.

5 Ichikawa S, Ichikawa T, Motosugi U, Sano K, Morisaka H, Enomoto N: Was hypervascular hepatocellular carcinoma visible on previous gadoxetic acid-enhanced magnetic resonance images? Liver Cancer 2015;4:154–162.

6 Chen BB, Murakami T, Shih TT, Sakamoto M, Matsui O, Choi BI, et al: Novel imaging diagnosis for hepatocellular carcinoma: consensus from the 5th Asia-Pacific primary liver cancer expert meeting (APPLE 2014). Liver Cancer 2015;4:215–227.

7 Fujita N, Nishie A, Kubo Y, Asayama Y, Ushijima Y, Takayama Y, et al: Hepatocellular carcinoma: clinical significance of signal heterogeneity in the hepatobiliary phase of gadoxetic acid-enhanced MR imaging. Eur Radiol 2014;25:211–220.

8 Rhee H, Kim MJ, Park MS, Kim KA: Differentiation of early hepatocellular carcinoma from benign hepatocellular nodules on gadoxetic acid-enhanced MRI. Br J Radiol 2012;85:e837–e844.

9 Inoue T, Kudo M, Komuta M, Hayaishi S, Ueda T, Takita M, et al: Assessment of Gd-EOB-DTPA-enhanced MRI for HCC and dysplastic nodules and comparison of detection sensitivity versus MDCT. J Gastroenterol 2012;47:1036–1047.

10 Eso Y, Marusawa H, Osaki Y: Education and imaging. Hepatobiliary and pancreatic: detection of early hepatocellular carcinoma by enhanced magnetic resonance imaging. J Gastroenterol Hepatol 2012;27:416.

11 Kudo M: Early hepatocellular carcinoma: definition and diagnosis. Liver Cancer 2013;2:69–72.

12 Ichikawa T: Diagnosis of pathological early HCC with EOB-MRI: Japanese experience. Liver Cancer 2014;3:149.

13 Joishi D, Ueno A, Tanimoto A, Okuda S, Masugi Y, Emoto K, et al: Natural course of hypovascular nodules detected on gadoxetic acid-enhanced MR imaging: presence of fat is a risk factor for hypervascularization. Magn Reson Med Sci 2013;12:281–287.
14 Motosugi U: Hypovascular hypointense nodules on hepatocyte phase gadoxetic acid-enhanced MR images: too early or too progressed to determine hypervascularity. Radiology 2013;267:317–318.
15 Takechi M, Tsuda T, Yoshioka S, Murata S, Tanaka H, Hirooka M, Mochizuki T: Risk of hypervascularization in small hypovascular hepatic nodules showing hypointense in the hepatobiliary phase of gadoxetic acid-enhanced MRI in patients with chronic liver disease. Jpn J Radiol 2012;30:743–751.
16 Takayama Y, Nishie A, Nakayama T, Asayama Y, Ishigami K, Kakihara D, et al: Hypovascular hepatic nodule showing hypointensity in the hepatobiliary phase of gadoxetic acid-enhanced MRI in patients with chronic liver disease: prediction of malignant transformation. Eur J Radiol 2012;81:3072–3078.
17 Akai H, Matsuda I, Kiryu S, Tajima T, Takao H, Watanabe Y, et al: Fate of hypointense lesions on Gd-EOB-DTPA-enhanced magnetic resonance imaging. Eur J Radiol 2012;81:2973–2977.
18 Motosugi U, Ichikawa T, Sano K, Sou H, Onohara K, Muhi A, et al: Outcome of hypovascular hepatic nodules revealing no gadoxetic acid uptake in patients with chronic liver disease. J Magn Reson Imaging 2011;34:88–94.
19 Kumada T, Toyoda H, Tada T, Sone Y, Fujimori M, Ogawa S, Ishikawa T: Evolution of hypointense hepatocellular nodules observed only in the hepatobiliary phase of gadoxetate disodium-enhanced MRI. AJR Am J Roentgenol 2011;197:58–63.
20 Kudo M, Matsui O, Izumi N, Iijima H, Kadoya M, Imai Y, et al: JSH consensus-based clinical practice guidelines for the management of hepatocellular carcinoma: 2014 update by the liver cancer study group of Japan. Liver Cancer 2014;3:458–468.
21 Kokudo N, Hasegawa K, Akahane M, Igaki H, Izumi N, Ichida T, et al: Evidence-based clinical practice guidelines for hepatocellular carcinoma: the Japan society of hepatology 2013 update (3rd JSH-HCC guidelines). Hepatol Res 2015;45:123–127.
22 Bruix J, Sherman M: Management of hepatocellular carcinoma: an update. Hepatology 2011;53:1020–1022.
23 Llovet JM, Ducreux M, et al: EASL-EORTC clinical practice guidelines: management of hepatocellular carcinoma. J Hepatol 2012;56:908–943.
24 Kudo M, Okanoue T; Japan Society of Hepatology: Management of hepatocellular carcinoma in Japan: consensus-based clinical practice manual proposed by the Japan society of hepatology. Oncology 2007;72(suppl 1):2–15.
25 Kudo M, Izumi N, Kokudo N, Matsui O, Sakamoto M, Nakashima O, et al: Management of hepatocellular carcinoma in Japan: consensus-based clinical practice guidelines proposed by the Japan society of hepatology (JSH) 2010 updated version. Dig Dis 2011;29:339–364.
26 Teng W, Liu KW, Lin CC, Jeng WJ, Chen WT, Sheen IS, et al: Insufficient ablative margin determined by early computed tomography may predict the recurrence of hepatocellular carcinoma after radiofrequency ablation. Liver Cancer 2015;4:26–38.
27 Kudo M: Locoregional therapy for hepatocellular carcinoma. Liver Cancer 2015;4:163–164.
28 Kang TW, Rhim H: Recent advances in tumor ablation for hepatocellular carcinoma. Liver Cancer 2015;4:176–187.
29 Lencioni R, de Baere T, Martin RC, Nutting CW, Narayanan G: Image-guided ablation of malignant liver tumors: recommendations for clinical validation of novel thermal and non-thermal technologies – a Western perspective. Liver Cancer 2015;4:208–214.
30 Clinical practice guidelines for hepatocellular carcinoma differ between Japan, United States, and Europe. Liver Cancer 2015;4:85–95.
31 Hsu C, Chen BB, Chen CH, Ho MC, Cheng JC, Kokudo N, et al: Consensus development from the 5th Asia-Pacific primary liver cancer expert meeting (APPLE 2014). Liver Cancer 2015;4:96–105.
32 Minami Y, Yagyu Y, Murakami T, Kudo M: Tracking navigation imaging of transcatheter arterial chemoembolization for hepatocellular carcinoma using three-dimensional cone-beam CT angiography. Liver Cancer 2014;3:53–61.
33 Ueshima K, Kudo M, Tanaka M, Kumada T, Chung H, Hagiwara S, et al: Phase I/II study of sorafenib in combination with hepatic arterial infusion chemotherapy using low-dose cisplatin and 5-fluorouracil. Liver Cancer 2015;4:263–273.
34 Obi S, Sato S, Kawai T: Current status of hepatic arterial infusion chemotherapy. Liver Cancer 2015;4:188–199.
35 Arizumi T, Ueshima K, Minami T, Kono M, Chishina H, Takita M, et al: Effectiveness of sorafenib in patients with transcatheter arterial chemoembolization (TACE) refractory and intermediate-stage hepatocellular carcinoma. Liver Cancer 2015;4:253–262.
36 Peck-Radosavljevic M: Drug therapy for advanced-stage liver cancer. Liver Cancer 2014;3:125–131.
37 Kudo M: Biomarkers and personalized sorafenib therapy. Liver Cancer 2014;3:399–404.
38 Shao YY, Hsu CH, Cheng AL: Predictive biomarkers of antiangiogenic therapy for advanced hepatocellular carcinoma: where are we? Liver Cancer 2013;2:93–107.
39 Akamatsu N, Sugawara Y, Kokudo N: Living donor liver transplantation for patients with hepatocellular carcinoma. Liver Cancer 2014;3:108–118.
40 International Consensus Group for Hepatocellular Neoplasia: Pathologic diagnosis of early hepatocellular carcinoma: a report of the International consensus group for hepatocellular neoplasia. Hepatology 2009;49:658–664.
41 Theise ND, Park YN, Curado MP, Sakamoto M, Franceschi S, Torbenson M, et al: Hepatocelular carcinoma; in Bosman FT, Carneiro F, Hruban RH, Theise ND (eds): WHO Classification of Tumours of the Digestive System. Lyon, IARC, 2010, pp 205–216.
42 Raoul JL, Gilabert M, Piana G: How to define transarterial chemoembolization failure or refractoriness: a European perspective. Liver Cancer 2014;3:119–124.
43 Tsurusaki M, Murakami T: Surgical and locoregional therapy of HCC: TACE. Liver Cancer 2015;4:165–175.
44 Kudo M, Ueshima K, Yokosuka O, Obi S, Izumi N, Aikata H, et al: Prospective randomized controlled phase III trial comparing the efficacy of sorafenib versus sorafenib in combination with low-dose cisplatin/fluorouracil hepatic arterial infusion chemotherapy in patients with advanced hepatocellular carcinoma. EASL 2016:abstr LB04.
45 Kitai S, Kudo M, Nishida N, Izumi N, Sakamoto M, Matsuyama Y, et al: Survival benefit of locoregional treatment for hepatocellular carcinoma with advanced liver cirrhosis. Liver Cancer 2016;5:175–189.
46 Kudo M, Osaki Y, Matsunaga T, Kasugai H, Oka H, Seki T: Hepatocellular carcinoma in Child-Pugh C cirrhosis: prognostic factors and survival benefit of nontransplant treatments. Dig Dis 2013;31:490–498.
47 Nouso K, Kokudo N, Tanaka M, Kuromatsu R, Nishikawa H, Toyoda H, et al: Treatment of hepatocellular carcinoma with Child-Pugh C cirrhosis. Oncology 2014;87(suppl 1):99–103.
48 Kudo M: Surveillance, diagnosis, treatment, and outcome of liver cancer in Japan. Liver Cancer 2015;4:39–50.
49 Poon RT, Cheung TT, Kwok PC, Lee AS, Li TW, Loke KL, et al: Hong Kong consensus recommendations on the management of hepatocellular carcinoma. Liver Cancer 2015;4:51–69.
50 Bruix J, Merle P, Granito A, Huang YH, Bodoky G, Yokosuka O, et al: LBA-03: efficacy and safety of regorafenib versus placebo in patients with hepatocellular carcinoma (HCC) progressing on sorafenib: results of the international, randomized phase 3 RESORCE trial. Ann Oncol 2016;27(suppl 2):ii1–ii3.
51 Terashima T, Yamashita T, Takata N, Nakagawa H, Toyama T, Arai K, et al: Post-progression survival and progression-free survival in patients with advanced hepatocellular carcinoma treated by sorafenib. Hepatol Res 2016;46:650–656.

52 Reig M, Rimola J, Torres F, Darnell A, Rodriguez-Lope C, Forner A, et al: Postprogression survival of patients with advanced hepatocellular carcinoma: rationale for second-line trial design. Hepatology 2013;58:2023–2031.
53 Kudo M, Park JW, Obi S, Qin S, Assenat E, Umeyama Y, et al: Regional differences in efficacy/safety/biomarkers in a randomised study of axitinib in 2nd line patients (pts) with advanced hepatocellular carcinoma (HCC). J Clin Oncol 2016;34(suppl 4S):abstr 329.
54 Arii S, Sata M, Sakamoto M, Shimada M, Kumada T, Shiina S, et al: Management of hepatocellular carcinoma: Report of Consensus Meeting in the 45th Annual Meeting of the Japan Society of Hepatology (2009). Hepatol Res 2010;40:667–685.
55 Omata M, Lesmana LA, Tateishi R, Chen PJ, Lin SM, Yoshida H, et al: Asian Pacific association for the study of the liver consensus recommendations on hepatocellular carcinoma. Hepatol Int 2010;4:439–474.
56 Kudo M: Japan's successful model of nationwide hepatocellular carcinoma surveillance highlighting the urgent need for global surveillance. Liver Cancer 2012;1:141–143.
57 Bolondi L, Burroughs A, Dufour JF, Galle PR, Mazzaferro V, Piscaglia F, et al: Heterogeneity of patients with intermediate (BCLC B) hepatocellular carcinoma: proposal for a subclassification to facilitate treatment decisions. Semin Liver Dis 2012;32:348–359.
58 Mazzaferro V, Bhoori S, Sposito C, Bongini M, Langer M, Miceli R, Mariani L: Milan criteria in liver transplantation for hepatocellular carcinoma: an evidence-based analysis of 15 years of experience. Liver Transpl 2011;17(suppl 2):S44–S57.
59 Kudo M, Arizumi T, Ueshima K, Sakurai T, Kitano M, Nishida N: Subclassification of BCLC B stage hepatocellular carcinoma and treatment strategies: proposal of modified Bolondi's subclassification (Kinki criteria). Dig Dis 2015;33:751–758.
60 Ogasawara S, Chiba T, Ooka Y, Kanogawa N, Motoyama T, Suzuki E, et al: Efficacy of sorafenib in intermediate-stage hepatocellular carcinoma patients refractory to transarterial chemoembolization. Oncology 2014;87:330–341.
61 Arizumi T, Ueshima K, Chishina H, Kono M, Takita M, Kitai S, et al: Validation of the criteria of transcatheter arterial chemoembolization failure or refractoriness in patients with advanced hepatocellular carcinoma proposed by the LCSGJ. Oncology 2014;87(suppl 1):32–36.
62 Arizumi T, Ueshima K, Iwanishi M, Minami T, Chishina H, Kono M, et al: Validation of a modified substaging system (Kinki criteria) for patients with intermediate-stage hepatocellular carcinoma. Oncology 2015;89(suppl 2):47–52.
63 Sznol M, Chen L: Antagonist antibodies to PD-1 and B7-H1 (PD-L1) in the treatment of advanced human cancer. Clin Cancer Res 2013;19:1021–1034.
64 Herbst RS, Soria JC, Kowanetz M, Fine GD, Hamid O, Gordon MS, et al: Predictive correlates of response to the anti-PD-L1 antibody MPDL3280A in cancer patients. Nature 2014;515:563–567.
65 Shih K, Arkenau HT, Infante JR: Clinical impact of checkpoint inhibitors as novel cancer therapies. Drugs 2014;74:1993–2013.
66 Philips GK, Atkins M: Therapeutic uses of anti-PD-1 and anti-PD-L1 antibodies. Int Immunol 2015;27:39–46.
67 Mahoney KM, Freeman GJ, McDermott DF: The next immune-checkpoint inhibitors: PD-1/PD-L1 blockade in melanoma. Clin Ther 2015;37:764–782.
68 Harshman LC, Drake CG, Wargo JA, Sharma P, Bhardwaj N: Cancer immunotherapy highlights from the 2014 ASCO meeting. Cancer Immunol Res 2014;2:714–719.
69 Topalian SL, Drake CG, Pardoll DM: Targeting the PD-1/B7-H1(PD-L1) pathway to activate anti-tumor immunity. Curr Opin Immunol 2012;24:207–212.
70 Merelli B, Massi D, Cattaneo L, Mandalà M: Targeting the PD1/PD-L1 axis in melanoma: biological rationale, clinical challenges and opportunities. Crit Rev Oncol Hematol 2014;89:140–165.
71 Le DT, Uram JN, Wang H, Bartlett BR, Kemberling H, Eyring AD, et al: PD-1 blockade in tumors with mismatch-repair deficiency. N Engl J Med 2015;372:2509–2520.
72 Droeser RA, Hirt C, Viehl CT, Frey DM, Nebiker C, Huber X, et al: Clinical impact of programmed cell death ligand 1 expression in colorectal cancer. Eur J Cancer 2013;49:2233–2242.
73 Ribas A: Tumor immunotherapy directed at PD-1. N Engl J Med 2012;366:2517–2519.
74 Hamid O, Robert C, Daud A, Hodi FS, Hwu WJ, Kefford R, et al: Safety and tumor responses with lambrolizumab (anti-PD-1) in melanoma. N Engl J Med 2013;369:134–144.
75 Kudo M: Immune checkpoint blockade in hepatocellular carcinoma. Liver Cancer 2015;4:201–207.
76 Brahmer JR, Tykodi SS, Chow LQ, Hwu WJ, Topalian SL, Hwu P, et al: Safety and activity of anti-PD-L1 antibody in patients with advanced cancer. N Engl J Med 2012;366:2455–2465.
77 Gao Q, Wang XY, Qiu SJ, Yamato I, Sho M, Nakajima Y, et al: Overexpression of PD-L1 significantly associates with tumor aggressiveness and postoperative recurrence in human hepatocellular carcinoma. Clin Cancer Res 2009;15:971–979.
78 Tochio H, Sugahara M, Imai Y, Tei H, Suginoshita Y, Iwasaki N, et al: Hyper-enhanced rim surrounding liver metastatic tumors in the postvascular phase of sonazoid-enhanced ultrasonography: a histological indication of the presence of Kupffer cells. Oncology 2015;89(suppl 2):1–3.
79 El-Khoueiry AM, Melero I, Crocenzi TS, et al: Phase I/II safety and antitumor activity of nivolumab in patients with advanced hepatocellular carcinoma (HCC): CA209-040. J Clin Oncol 2015;33(suppl):abstr LBA101.
80 El-Khoueiry AB, Sangro B, Yau TC, Crocenzi TS, Welling TH, Yeo W, et al: Phase I/II safety and antitumor activity of nivolumab (nivo) in patients (pts) with advanced hepatocellular carcinoma (HCC): interim analysis of the CheckMate-040 dose escalation study. J Clin Oncol 2016;34(suppl):abstr 4012.
81 Sangro B, Melero I, Yau TC, Hsu C, Kudo M, Crocenzi TS, et al: Safety and antitumor activity of nivolumab (nivo) in patients (pts) with advanced hepatocellular carcinoma (HCC): interim analysis of dose-expansion cohorts from the phase 1/2 CheckMate-040 study. J Clin Oncol 2016;34(suppl):abstr 4078.

Original Article

Digestive Diseases

Dig Dis 2016;34:665–670
DOI: 10.1159/000448832

Coffee Intake and Liver Enzyme Association in Korean Immigrants and Japanese: A Comprehensive Cross-Sectional Study

Soo Ki Kim[a] Myung-Hee Shin[f] Kayo Sugimoto[b, c] Soo Ryang Kim[a]
Susumu Imoto[a] Ke Ih Kim[b] Miyuki Taniguchi[a] Hyun-Kyung Oh[g]
Yoshihiko Yano[d] Yoshitake Hayashi[c] Masatoshi Kudo[e]

[a]Department of Gastroenterology and [b]Department of Pharmacy, Kobe Asahi Hospital, [c]Division of Molecular Medicine and Medical Genetics, Department of Pathology, and [d]Division of Center Infectious Diseases, Department of Pathology, Kobe University Graduate School of Medicine, Kobe, [e]Department of Gastroenterology and Hepatology, Kindai University Faculty of Medicine, Osaka-Sayama, Japan; [f]Department of Social and Preventive Medicine, Sungkyunkwan University School of Medicine, Suwon, and [g]Department of Preventive Medicine, College of Medicine, Hanyang University, Seoul, South Korea

Key Words
Coffee intake · Liver enzymes · Indigenous Japanese · Korean immigrants · Alcohol drinking and smoking

Abstract
Objectives: Significant inverse association between coffee intake and the levels of liver enzymes has been reported. We demonstrated higher prevalence of metabolic syndrome in Korean immigrants (KIs) than in indigenous Japanese (IJs). The aim of this study was to investigate whether the association between coffee intake and liver enzyme levels was different between the 2 ethnic groups. ***Methods:*** This study is a cross-sectional study including a total of 966 subjects comprising KIs and IJs. The association between the quintiles of coffee intake and dichotomous values of liver enzymes was evaluated by logistic regression analysis in KIs, IJs, a high-risk group (current smokers or alcohol drinkers ≥45 g/day), and a low-risk group (non-smokers and alcohol drinkers <45 g/day). ***Results:*** In KIs, a significant inverse association between coffee intake and serum aspartate aminotransferase (AST) levels was observed. In the IJs, a significant inverse association between coffee intake and serum alanine aminotransferase levels was observed. In the high-risk group, a significant inverse association between coffee intake and serum AST and gamma-glutamyltransferase levels was observed. ***Conclusion:*** No difference was observed between KIs and IJs regarding the association between coffee and liver enzymes. Coffee might inhibit hepatic damage by alcohol drinking and smoking.

Introduction

Potential physiological benefits associated with coffee intake may be related to several different antioxidant compounds in coffee [1–3]. Coffee intake may, thereby,

KARGER

E-Mail karger@karger.com
www.karger.com/ddi

0257–2753/16/0346–0665$39.50/0

Myung-Hee Shin, MD, MPH, PhD
Department of Social and Preventive Medicine
Sungkynkwan University School of Medicine
300 Chunchun-dong, Jangan-gu, Suwon 440-746 (Korea)
E-Mail mhshin@skku.edu

Table 1. Subject characteristics (mean ± SD)

	Men		p value	Women		p value
	KIs (n = 192)	IJs (n = 295)		KIs (n = 292)	IJs (n = 187)	
Coffee, ml	266.3±204.3	286.0±299.8	0.4063	285.1±192.8	223.6±184.2	0.0011
Coffee, g	13.6±11.3	12.9±13.7	0.5618	15.1±12.7	11.0±10.5	0.0004
AST, U/l	25.2±12.2	24.9±19.6	0.8042	22.4±16.9	21.6±10.1	0.4877
ALT, U/l	27.3±17.5	29.2±26.9	0.3467	19.6±20.7	18.3±12.1	0.3834
GGT, U/l	78.2±96.2	63.0±76.0	0.0643	29.3±43.1	27.6±26.7	0.5910

inhibit inflammation and reduce cardiovascular and other inflammatory diseases [4]. Coffee intake reduces the risk of liver cirrhosis and hepatocellular carcinoma [5–11], and a significant inverse association between coffee intake and the levels of liver enzymes has been described [12–14] – for example, the level of gamma-glutamyltransferase (GGT) especially in heavy alcohol drinkers and heavy cigarette smokers [12, 15, 16]. These reports suggest that coffee intake may inhibit the elevation of serum GGT levels induced by smoking and drinking.

Our recent comparative study has revealed a higher prevalence of metabolic syndrome in Korean immigrants (KIs) than in indigenous Japanese (IJs) [17]. Assuming an ethnological difference in metabolic capacity, we investigated whether the association between coffee intake and liver enzyme (serum aspartate aminotransferase (AST), serum, alanine aminotransferase (ALT), and serum GGT) levels was different between the 2 ethnic groups. Also, we conducted a stratified analysis of risk groups in terms of smoking and alcohol-drinking habits.

Materials and Methods

Subjects

A detailed method of the Korean Immigrant Study (KIS) is described elsewhere [17]. In short, the KIS is a cohort study initiated to elucidate the effects of environmental change, genetic susceptibility, and their interaction on hypertension, diabetes, metabolic syndrome, and other health-related outcomes by comparing KIs and IJs. The subjects recruited for this study were KIs who had emigrated at least 15 years earlier and IJs at a ratio of 1:1. The study was broadcast by introductory conferences held in various Korean-Japanese societies, gatherings, companies, and schools (to recruit parents) as well as at Korean consulates in Kobe and Osaka located in western Japan. Subjects were recruited through individual or group applications. Individuals were examined at Kobe Asahi hospital, and groups of 5 or more who were unable to visit the hospital, were examined by our research personnel (nurses and clinical technicians) at subject sites. A total of 966 were enrolled in the study between April 2005 and February 2008.

Exposure Measurements

Levels of smoking and alcohol drinking were measured using a detailed life-style questionnaire. Information on coffee intake in terms of the frequency and amount consumed was obtained using the food frequency questionnaire by the Japan Public Health Center-based prospective study. Health examinations and biospecimen collection were done for all subjects. Liver enzymes such as serum AST, serum ALT, and serum GGT levels were measured with the Hitachi 7170 autoanalyzer.

Statistical Analysis

The χ^2 test and Student's t test were used to compare demographic characteristics, hepatic enzyme (serum AST, serum ALT, and serum GGT) levels and coffee intake by KIs and IJs. Several liver enzymes were categorized into normal (AST: ≥10–<40 IU/l; ALT: <30 IU/l for men and <20 IU/l for women; GGT: <70 IU/l for men and <30 IU/l for women) and abnormal levels. A high-risk group comprised of current smoker or alcohol drinkers (≥45 g/day) and a low-risk group comprised of non-smokers and non-drinkers of alcohol (<45 g/day). The association between the quintiles of coffee intake (quintile 1 (<3 g/day) = lowest intake, quintile 5 (≥25 g/day) = highest intake) and dichotomous values of liver enzymes was evaluated by logistic regression analysis, adjusted for age, gender, race, alcohol drinking (continuous variables, g/day), and body mass index (BMI; continuous variables, kg/m^2) in KIs and IJs and in the high-risk and low-risk groups. The SAS system version 9.2 was used for all analyses.

Informed written consent was obtained from each subject and the study protocol conformed to the ethical guidelines approved by the Ethics Committee in Kobe Asahi Hospital and Samsung Medical Center.

Results

Among women, coffee intake was significantly higher in KIs than in IJs (15.1 vs. 11.0 g; p = 0.0004) but no significant difference was observed in serum AST, ALT, and GGT levels between the 2 (table 1).

In all subjects, a significant inverse association was observed between coffee intake (categorical values) and liver enzyme levels (dichotomous values): AST (p = 0.0296), ALT (p = 0.0102), and GGT (p = 0.0269; table 2). There

Table 2. Association between coffee intake and liver enzymes in all subjects (n = 966)

Coffee intake, g/day	n	n (%)	OR (95% CI)*	p value for trend
OR for abnormal AST				
Quintile 1 (<3)	139	14 (10.1)	1.00	
Quintile 2 (≥3, <7.5)	165	13 (7.9)	0.96 (0.41–2.26)	
Quintile 3 (≥7.5, <12.355)	220	12 (5.5)	0.70 (0.29–1.68)	0.0296
Quintile 4 (≥12.355, <25)	153	11 (7.2)	0.96 (0.40–2.35)	
Quintile 5 (≥25)	203	3 (1.5)	0.19 (0.05–0.73)	
OR for abnormal ALT				
Quintile 1 (<3)	139	57 (41.0)	1.00	
Quintile 2 (≥3, <7.5)	165	48 (29.1)	0.65 (0.39–1.08)	
Quintile 3 (≥7.5, <12.355)	220	68 (30.9)	0.73 (0.45–1.19)	0.0102
Quintile 4 (≥12.355, <25)	153	41 (26.8)	0.55 (0.32–0.93)	
Quintile 5 (≥25)	203	45 (22.2)	0.50 (0.30–0.83)	
OR for abnormal GGT				
Quintile 1 (<3)	139	44 (31.7)	1.00	
Quintile 2 (≥3, <7.5)	165	42 (25.5)	0.83 (0.49–1.41)	
Quintile 3 (≥7.5, <12.355)	220	55 (25.0)	0.80 (0.49–1.32)	0.0269
Quintile 4 (≥12.355, <25)	153	34 (22.2)	0.70 (0.40–1.21)	
Quintile 5 (≥25)	203	36 (17.7)	0.55 (0.32–0.94)	

* OR is adjusted for gender, race, age, alcohol drinking (continuous variables, g/day), and BMI (continuous variables, kg/m^2).

Liver enzymes were categorized normal as follows: 10≤ AST <40, ALT <30 (men) or <20 (women), GGT <70 (men) or <30 (women).

was no difference in the association between coffee intake and liver enzyme levels based on gender (data not shown). Coffee intake (categorical values) and liver enzyme levels (dichotomous values) showed a significant inverse association in KIs (serum AST; p = 0.0013), while coffee intake was not associated with serum GGT and serum ALT (p = 0.1118, p = 0.1064) levels. Similarly, a significant inverse association was observed in IJs (serum ALT level; p = 0.0201), while coffee intake was not associated with serum AST (p = 0.6975) and serum GGT (p = 0.1622) levels (table 3).

In the high-risk group, the association between coffee intake (categorical values) and liver enzyme levels (dichotomous values) showed a significant inverse association in serum AST (p = 0.0200) and GGT (p = 0.0131) levels, while coffee intake was not associated with the serum ALT level (p = 0.2449). In the low-risk group, on the other hand, a significant inverse association was observed in the serum ALT level (p = 0.0387) at quintile 4 (≤12.14–<25 g), but not a significant one at quintile 5 (≥25 g), while coffee intake was not associated with serum AST (p = 0.7141) and serum GGT (p = 0.5450) levels (table 4).

Discussion

An inverse association between serum GGT levels and coffee intake in men and women has been reported [12]. Coffee intake is significantly related to decreased serum ALT and AST levels among men [12, 13]. We demonstrated a significant inverse association between coffee intake and the level of liver enzymes such as serum AST, ALT, and GGT, respectively, adjusted for gender, race, age, alcohol drinking, and BMI, which affect these enzymes.

There are no studies that bring out the association between coffee intake and liver enzymes affected by both alcohol drinking and smoking. In this study, a significant inverse association was observed between coffee intake and serum AST levels in high-risk (heavy drinkers or smokers) subjects, but coffee intake was not associated with the serum ALT level. Coffee effectively modifies the association between alcohol drinking and serum AST levels but not between alcohol drinking and serum ALT levels. Also, alcohol and cigarettes are positively related to serum AST levels but not to serum ALT levels [13]. Therefore, since serum ALT levels are less sensitive on nonspecific markers of alcohol- and cigarette-related liver dam-

Table 3. Association between coffee intake and liver enzymes on the KIs group or the IJs group

Coffee intake, g/day	KIs (n = 484)				Coffee intake, g/day	IJs (n = 482)			
	n	n (%)	OR (95% CI)*	p value for trend		n	n (%)	OR (95% CI)*	p value for trend
OR for abnormal AST									
Quintile 1 (<5)	83	11 (13.3)	1.00		Quintile 1 (<2.57)	88	6 (6.8)	1.00	
Quintile 2 (≥5, <9.64)	83	3 (3.6)	0.28 (0.07–1.14)		Quintile 2 (≥2.57, <6.707)	92	10 (10.9)	2.80 (0.83–9.46)	
Quintile 3 (≥9.64, <13)	83	6 (7.2)	0.54 (0.17–1.72)	0.0013	Quintile 3 (≥6.707, <10.42)	91	2 (2.2)	0.46 (0.08–2.62)	0.6975
Quintile 4 (≥13, <25)	67	1 (1.5)	0.07 (0.01–0.77)		Quintile 4 (≥10.42, <25)	90	11 (12.2)	2.95 (0.89–9.83)	
Quintile 5 (≥25)	112	1 (0.9)	0.05 (0.01–0.49)		Quintile 5 (≥25)	91	2 (2.2)	0.53 (0.09–3.05)	
OR for abnormal ALT									
Quintile 1 (<5)	83	29 (34.9)	1.00		Quintile 1 (<2.57)	88	39 (44.3)	1.00	
Quintile 2 (≥5, <9.64)	83	27 (32.5)	0.93 (0.46–1.87)		Quintile 2 (≥2.57, <6.707)	92	25 (27.2)	0.52 (0.27–1.01)	
Quintile 3 (≥9.64, <13)	83	26 (31.3)	0.90 (0.45–1.81)	0.1118	Quintile 3 (≥6.707, <10.42)	91	26 (28.6)	0.62 (0.32–1.19)	0.0201
Quintile 4 (≥13, <25)	67	13 (19.4)	0.39 (0.17–0.90)		Quintile 4 (≥10.42, <25)	90	29 (32.2)	0.66 (0.34–1.26)	
Quintile 5 (≥25)	112	29 (25.9)	0.72 (0.37–1.41)		Quintile 5 (≥25)	91	16 (17.6)	0.35 (0.17–0.72)	
OR for abnormal GGT									
Quintile 1 (<5)	83	26 (31.3)	1.00		Quintile 1 (<2.57)	88	26 (29.6)	1.00	
Quintile 2 (≥5, <9.64)	83	24 (28.9)	1.04 (0.51–2.10)		Quintile 2 (≥2.57, <6.707)	92	22 (23.9)	0.91 (0.46–1.81)	
Quintile 3 (≥9.64, <13)	83	25 (30.1)	1.08 (0.54–2.18)	0.1064	Quintile 3 (≥6.707, <10.42)	91	17 (18.7)	0.66 (0.32–1.37)	0.1622
Quintile 4 (≥13, <25)	67	13 (19.4)	0.57 (0.25–1.27)		Quintile 4 (≥10.42, <25)	90	22 (24.4)	0.92 (0.46–1.83)	
Quintile 5 (≥25)	112	22 (19.6)	0.64 (0.32–1.29)		Quintile 5 (≥25)	91	14 (13.9)	0.55 (0.26–1.17)	

* OR is adjusted for gender, age, alcohol drinking (continuous variables, g/day), and BMI (continuous variables, kg/m^2).
Liver enzymes were categorized normal as follows: 10≤ AST<40, ALT <30 (men) or <20 (women), GGT <70 (men) or <30 (women).

Table 4. Association between coffee intake and liver enzymes on low-risk groups or high-risk groups

Coffee intake, g/day	Low-risk group (n = 560)				Coffee intake, g/day	High-risk group (n = 392)			
	n	n (%)	OR (95% CI)**	p value for trend		n	n (%)	OR (95% CI)**	p value for trend
OR for abnormal AST									
Quintile 1 (<3)	77	2 (2.6)	1.00		Quintile 1 (<3)	62	12 (19.4)	1.00	
Quintile 2 (≥3, <7.5)	99	4 (4.0)	1.60 (0.28–9.21)		Quintile 2 (≥3, <7.782)	77	10 (13.0)	0.80 (0.30–2.16)	
Quintile 3 (≥7.5, <12.14)	134	4 (3.0)	1.31 (0.23–7.64)	0.7141	Quintile 3 (≥7.782, <12.5)	72	7 (9.7)	0.56 (0.19–1.65)	0.0200
Quintile 4 (≥12.14, <25)	88	5 (5.7)	2.43 (0.44–13.3)		Quintile 4 (≥12.5, <25)	63	6 (9.5)	0.63 (0.21–1.93)	
Quintile 5 (≥25)	119	1 (0.8)	0.37 (0.03–4.36)		Quintile 5 (≥25)	82	2 (2.4)	0.16 (0.03–0.78)	
OR for abnormal ALT									
Quintile 1 (<3)	77	27 (35.1)	1.00		Quintile 1 (<3)	62	30 (48.4)	1.00	
Quintile 2 (≥3, <7.5)	99	27 (27.3)	0.74 (0.38–1.44)		Quintile 2 (≥3, <7.782)	77	24 (31.2)	0.60 (0.28–1.29)	
Quintile 3 (≥7.5, <12.14)	134	44 (32.8)	0.97 (0.52–1.82)	0.0387	Quintile 3 (≥7.782, <12.5)	72	19 (26.4)	0.42 (0.18–0.94)	0.2449
Quintile 4 (≥12.14, <25)	88	18 (20.5)	0.47 (0.22–0.97)		Quintile 4 (≥12.5, <25)	63	23 (36.5)	0.75 (0.33–1.67)	
Quintile 5 (≥25)	119	25 (21.0)	0.54 (0.27–1.07)		Quintile 5 (≥25)	82	20 (24.4)	0.52 (0.24–1.15)	
OR for abnormal GGT									
Quintile 1 (<3)	77	15 (19.5)	1.00		Quintile 1 (<3)	62	29 (46.8)	1.00	
Quintile 2 (≥3, <7.5)	99	18 (18.2)	0.94 (0.43–2.06)		Quintile 2 (≥3, <7.782)	77	26 (33.8)	0.68 (0.33–1.41)	
Quintile 3 (≥7.5, <12.14)	134	26 (19.4)	0.92 (0.44–1.95)	0.5450	Quintile 3 (≥7.782, <12.5)	72	24 (33.3)	0.65 (0.31–1.35)	0.0131
Quintile 4 (≥12.14, <25)	88	16 (18.2)	0.85 (0.37–1.92)		Quintile 4 (≥12.5, <25)	63	18 (28.6)	0.55 (0.25–1.19)	
Quintile 5 (≥25)	119	20 (16.8)	0.77 (0.35–1.71)		Quintile 5 (≥25)	82	16 (19.5)	0.37 (0.17–0.81)	

* Current smoker or alcohol drinker ≥45; high-risk group.
** OR is adjusted for gender, race, age, alcohol drinking (continuous variables, g/day), and BMI (continuous variables, kg/m^2).
Liver enzymes were categorized normal as follows: 10≤ AST <40, ALT <30 (men) or <20 (women), GGT <70 (men) or (women).

age, the possible protective effect of coffee on such damage is less likely to be detected in terms of serum ALT levels. In this study, the association between coffee intake and serum ALT levels in the low-risk group was most significant in quintile 4 but not in quintile 5 with the highest intake of coffee. Therefore, a significant inverse association between coffee intake and serum ALT levels was unlikely in the low-risk group. Maximal inverse association between coffee and serum GGT levels in heavy alcohol drinkers has been reported [12, 16], and coffee might inhibit the adverse effect of smoking on serum GGT levels [15]. Cigarette smoking has an adverse effect on the cytochrome P-448 system (3-methylcholanthreneinducible) in the liver, resulting in the impairment of the clearance of several drugs and possible companion drugs [18]. Because of extended noxious agents, the positive association between cigarette smoking and elevation of serum GGT levels is provocative. Smoking raises serum GGT levels [19, 20] just as alcohol intake is well known to do [20, 21]. We demonstrated that abnormal serum GGT levels were significantly lower with increased coffee intake in the high-risk group, while the association between coffee intake and serum GGT levels was not significant in the low-risk group. Several studies have suggested that caffeine, one of the components of coffee, may have antioxidant effects that could be beneficial if oxidative stress plays a role in liver injury [22, 23]. Although it is difficult to infer a clinically significant association between liver enzyme levels and coffee intake in heavy drinking or smoking subjects, some observations and our results suggest that coffee intake might inhibit the elevation of serum AST and GGT levels induced by alcohol drinking or smoking. Although coffee intake might protect against liver cell damage induced by alcohol drinking or smoking, a limitation in this study was our inability to observe the duration of smoking and alcohol-drinking habits.

We have reported that blood pressure and abdominal obesity are significantly higher in IJs than in KIs [17]. In this study, no difference was observed between KIs and IJs in the levels of serum ALT, AST, and GGT. A significant inverse association between coffee intake and serum AST levels was observed in KIs but not in IJs; however, a significant inverse association between coffee intake and serum ALT levels was observed in IJs but not in KIs. Coffee intake was not significantly related to serum GGT levels in either group. Taken together, these findings suggest that there is no particular difference between KIs and IJs in terms of the association between coffee intake and liver enzymes. Further analysis of a large-scale multicenter study is needed to confirm the effects of coffee intake on liver enzymes in these 2 ethnic groups.

Conclusion

A significant inverse association was observed between coffee intake and liver enzyme levels, such as AST, ALT, and GGT in all subjects. There was no particular difference between KIs and IJs regarding the association between coffee intake and liver enzymes. Coffee intake might protect against hepatic damage by alcohol drinking and smoking.

Acknowledgment

We are indebted to Ms. Mika Matsui for her assistance in the preparation of this manuscript.

Disclosure Statement

The authors declare that they have no financial conflict of interest.

References

1 Salazar-Martinez E, Willett WC, Ascherio A, Manson JE, Leitzmann MF, Stampfer MJ, Hu FB: Coffee consumption and risk for type 2 diabetes mellitus. Ann Intern Med 2004;140:1–8.

2 Nawrot P, Jordan S, Eastwood J, Rotstein J, Hugenholtz A, Feeley M: Effects of caffeine on human health. Food Addit Contam 2003;20:1–30.

3 Gonthier MP, Verny MA, Besson C, Rémésy C, Scalbert A: Chlorogenic acid bioavailability largely depends on its metabolism by the gut microflora in rats. J Nutr 2003;133:1853–1859.

4 Andersen LF, Jacobs DR Jr, Carlsen MH, Blomhoff R: Consumption of coffee is associated with reduced risk of death attributed to inflammatory and cardiovascular diseases in the Iowa Women's health study. Am J Clin Nutr 2006;83:1039–1046.

5 Bravi F, Bosetti C, Tavani A, Bagnardi V, Gallus S, Negri E, Franceschi S, La Vecchia C: Coffee drinking and hepatocellular carcinoma risk: a meta-analysis. Hepatology 2007;46:430–435.

6 Tanaka K, Hara M, Sakamoto T, Higaki Y, Mizuta T, Eguchi Y, Yasutake T, Ozaki I, Yamamoto K, Onohara S, Kawazoe S, Shigematsu H, Koizumi S: Inverse association between coffee drinking and the risk of hepatocellular carcinoma: a case-control study in Japan. Cancer Sci 2007;98:214–218.

7 Freedman ND, Everhart JE, Lindsay KL, Ghany MG, Curto TM, Shiffman ML, Lee WM, Lok AS, Di Bisceglie AM, Bonkovsky HL, Hoefs JC, Dienstag JL, Morishima C, Abnet CC, Sinha R: Coffee intake is associated with lower rates of liver disease progression in chronic hepatitis C. Hepatology 2009;50:1360–1369.

8 Inoue M, Yoshimi I, Sobue T, Tsugane S: Influence of coffee drinking on subsequent risk of hepatocellular carcinoma: a prospective study in Japan. J Natl Cancer Inst 2005;97:293–300.
9 Recent advances in bioinformatics reveal the molecular heterogeneity of hepatocellular carcinoma. Liver Cancer 2014;3:68–70.
10 Nishida N, Kudo M: Alteration of epigenetic profile in human hepatocellular carcinoma and its clinical implications. Liver Cancer 2014;3:417–427.
11 Kudo M: Surveillance, diagnosis, treatment, and outcome of liver cancer in Japan. Liver Cancer 2015;4:39–50.
12 Tanaka K, Tokunaga S, Kono S, Tokudome S, Akamatsu T, Moriyama T, Zakouji H: Coffee consumption and decreased serum gamma-glutamyltransferase and aminotransferase activities among male alcohol drinkers. Int J Epidemiol 1998;27:438–443.
13 Honjo S, Kono S, Coleman MP, Shinchi K, Sakurai Y, Todoroki I, Umeda T, Wakabayashi K, Imanishi K, Nishikawa H, Ogawa S, Katsurada M, Nakagawa K, Yoshizawa N: Coffee consumption and serum aminotransferases in middle-aged Japanese men. J Clin Epidemiol 2001;54:823–829.
14 Ruhl CE, Everhart JE: Coffee and caffeine consumption reduce the risk of elevated serum alanine aminotransferase activity in the United States. Gastroenterology 2005;128:24–32.
15 Nakanishi N, Nakamura K, Nakajima K, Suzuki K, Tatara K: Coffee consumption and decreased serum gamma-glutamyltransferase: a study of middle-aged Japanese men. Eur J Epidemiol 2000;16:419–423.
16 Kono S, Shinchi K, Imanishi K, Todoroki I, Hatsuse K: Coffee and serum gamma-glutamyltransferase: a study of self-defense officials in Japan. Am J Epidemiol 1994;139:723–727.
17 Shin MH, Kim MK, Li ZM, Oh HK, Kim SR, Taniguchi M, Fang J: Comparison of prevalence of metabolic syndrome between Korean emigrants and host country residents in Japan and China – the Korean emigrant study. Epidemiol Health 2010;32:e2010005.
18 Joeres R, Klinker H, Heusler H, Epping J, Zilly W, Richter E: Influence of smoking on caffeine elimination in healthy volunteers and in patients with alcoholic liver cirrhosis. Hepatology 1988;8:575–579.
19 Brenner H, Rothenbacher D, Arndt V, Schuberth S, Fraisse E, Fliedner TM: Distribution, determinants, and prognostic value of gamma-glutamyltransferase for all-cause mortality in a cohort of construction workers from southern Germany. Prev Med 1997;26:305–310.
20 Jang ES, Jeong SH, Hwang SH, Kim HY, Ahn SY, Lee J, Lee SH, Park YS, Hwang JH, Kim JW, Kim N, Lee DH: Effects of coffee, smoking, and alcohol on liver function tests: a comprehensive cross-sectional study. BMC Gastroenterol 2012;12:145.
21 Sharpe PC: Biochemical detection and monitoring of alcohol abuse and abstinence. Ann Clin Biochem 2001;38(pt 6):652–664.
22 Day CP, James OF: Steatohepatitis: a tale of two 'hits'? Gastroenterology 1998;114:842–845.
23 Berson A, De Beco V, Lettéron P, Robin MA, Moreau C, El Kahwaji J, Verthier N, Feldmann G, Fromenty B, Pessayre D: Steatohepatitis-inducing drugs cause mitochondrial dysfunction and lipid peroxidation in rat hepatocytes. Gastroenterology 1998;114:764–774.

Original Article

Digestive Diseases

Dig Dis 2016;34:650–653
DOI: 10.1159/000448865

Prospective Risk Analysis of Hepatocellular Carcinoma in Patients with Chronic Hepatitis C by Ultrasound Strain Elastography

Norihisa Yada Toshiharu Sakurai Tomohiro Minami Tadaaki Arizumi Masahiro Takita Satoru Hagiwara Hiroshi Ida Kazuomi Ueshima Naoshi Nishida Masatoshi Kudo

Department of Gastroenterology and Hepatology, Kindai University Faculty of Medicine, Osaka-Sayama, Japan

Key Words
Ultrasound strain elastography · Real-time tissue elastography · Prospective risk · Liver cancer · Chronic hepatitis C

Abstract
Objective: We have reported about real-time tissue elastography (RTE), which displays relative strain by measuring the relative distortion of the tissue, and found this information to be useful for diagnosing liver fibrosis. However, its use in predicting hepatocellular carcinoma has not been reported as yet. Here, we investigated RTE to predict liver carcinogenesis in patients with chronic hepatitis C virus (HCV) infection. ***Methods:*** We enrolled 160 patients with chronic HCV, who were followed up for 39.9 ± 22.9 weeks (median). They underwent RTE and then ultrasounds every 3–6 months. ***Results:*** Respective cumulative liver cancer incidences for years 1, 2, 3, 4, and 5 were, for the entire cohort: 2.0, 5.6, 8.8, 13.1, and 23.9%; for those whose liver fibrosis index (LFI) was ≤2.0: 0.0, 0.0, 0.0, 0.0, and 0.0%; for those whose LFI was 2–2.8: 0.0, 7.4, 7.4, 13.2 and 19.9%; and for those whose LFI was >2.8: 12.9, 12.9, 21.7, 31.4, and 31.4% (p = 0.011; log-rank test). ***Conclusions:*** Measurements of LFI by strain imaging can effectively predict liver cancer risk in patients with chronic HCV infection.

Introduction

Hepatocellular carcinoma (HCC) has high mortality worldwide. Background diseases associated with HCC include viral hepatitis [1], alcoholic hepatic disease, and nonalcoholic steatohepatitis. As liver cancer risk among patients with chronic viral hepatitis is higher in older people, men, and those with severe liver fibrosis [2–4], accurate monitoring of liver fibrosis is very important in managing viral hepatitis. Conventionally, liver fibrosis is diagnosed using liver biopsy, but this method is invasive and can involve sampling errors. Ultrasound elastography has thus attracted much attention as a noninvasive liver fibrosis diagnostic tool. 'Ultrasound elastography' includes a variety of devices that can be classified into 2 groups by the measured physical quantity.

Shear-wave imaging calculates tissue stiffness by measuring the velocity of a shear wave that propagates through

KARGER

E-Mail karger@karger.com
www.karger.com/ddi

0257–2753/16/0346–0650$39.50/0

Masatoshi Kudo
Department of Gastroenterology and Hepatology
Kindai University Faculty of Medicine
377-2 Ohno-Higashi, Osaka-Sayama, Osaka 589-8511 (Japan)
E-Mail m-kudo@med.kindai.ac.jp

the tissue. In contrast, strain imaging displays, in color, the relative strain by measuring the relative distortion of the tissue [5–7]. Liver stiffness measured by shear wave imaging is useful not only in diagnosing severe liver fibrosis but also for liver carcinogenesis risk assessment [8–10]. We had also found real-time tissue elastography (RTE), a type of strain imaging, to be useful for diagnosing liver fibrosis [11–16], but its use in predicting liver cancer prediction has not been reported.

Therefore, in this study, we investigated the performance of RTE in predicting liver carcinogenesis in patients with chronic hepatitis C virus (HCV) infection.

Patients and Methods

Patients

This was a single-center prospective study that was performed at the Kindai University Hospital (Osaka-Sayama, Japan). We enrolled consecutive patients with chronic HCV infection who were initially tested by RTE between August 2010 and September 2012 and had not received anti-viral therapy at that time. After screening test results were received, patients could undergo antiviral therapy. RTE and blood tests were performed on the same day. Patients were excluded if they consumed >20 g alcohol per day. Patients with histories of autoimmune hepatitis, primary biliary hepatitis, primary sclerosing cholangitis, hemochromatosis, α1-antitrypsin deficiency, or Wilson's disease were also excluded. The study protocol conformed to the Declaration of Helsinki and was approved by the Ethics Committee at the Kindai University Faculty of Medicine. Each patient provided informed consent to participate in the study.

Clinical and Laboratory Assessments

Relevant clinical data recorded were age, gender, weight, height, body mass index (BMI), and waist circumference. Blood samples were collected after overnight fasting on the same day as the patient's RTE. Laboratory tests, including serum albumin, aspartate aminotransferase (AST), alanine aminotransferase (ALT), total bilirubin, platelet count, and prothrombin time, were assessed using automated methods.

Real-Time Tissue Elastography

RTE was performed after overnight fasting with ultrasound (EUB-8500 or HI VISION Ascendus; Hitachi, Tokyo, Japan) and EUP-L52 linear type probe (3–7 MHz; Hitachi, Tokyo, Japan), by a previously reported method [14, 15]. Another analyst calculated the liver fibrosis index (LFI) as the median LFI from 10 still RTE images [12–15].

Diagnosis of HCC

Patients underwent ultrasound examination and testing for tumor markers every 3–6 months. When HCC was suspected, contrast-enhanced CT (CE-CT) or gadolinium-ethoxybenzyl diethylenetriaminepentaacetic acid-enhanced MRI (EOB-MRI) was performed. HCC was diagnosed by early vascular phase hyperenhancement and late-phase washout phenomenon in CE-CT or EOB-MRI.

Table 1. Patients' baseline characteristics according to hepatic carcinogenesis

	HCC (n = 21)	Non HCC (n = 139)	p value
Age, years	66.6±10.0	58.6±13.5	0.003†
Male, n (%)	12 (57.1)	64 (46.0)	0.358
Height, cm	157.4±10.8	159.8±9.6	0.353
Weight, kg	57.2±11.0	59.5±12.5	0.394
Waist circumference, cm	83.5±7.8	83.8±11.2	0.962
BMI, kg/m^2	23.0±2.8	23.2±3.7	0.78
Serum albumin, g/dl	3.8±0.4	4.2±0.5	0.044*
Total bilirubin, mg/dl	0.8±0.4	0.8±0.4	0.855
AST, IU/l	91.4±48.8	56.3±44.6	0.084
ALT, IU/l	81.5±52.3	64.6±68.1	0.408
Platelet count, 10^9/l	11.6±6.0	18.1±7.1	0.018*
Prothrombin time, %	74.8±8.3	90.3±19.7	0.06
LFI	2.72±0.32	1.97±0.72	0.005†

Values are expressed as the mean ± SD or n (%). LFI, age, serum albumin and platelet count differed significantly between the HCC and non-HCC groups.

* $p < 0.05$; † $p < 0.01$.

Statistical Analysis

Descriptive statistics are shown as mean ± SD, median (minimum and maximum), or percentage, as appropriate. Comparisons between the groups were carried out using Wilcoxon signed-rank tests and confirmed using nonparametric Mann–Whitney U tests between groups. Patients were censored at the time of death if they had not developed HCC, at their last visit for those lost to follow-up, or at the end of the study period. Cumulative HCC incidence was estimated by the Kaplan–Meier method. Log-rank test was used to evaluate significance. $p < 0.05$ was considered significant. Analysis was performed using SPSS Statistics 20 (IBM, Armonk, N.Y., USA).

Results

Demographics and Baseline Features

We enrolled 160 patients, including 86 men and 74 women, whose median age was 63.0 (range 23–85 years). Their median follow-up period was 39.9 ± 22.9 weeks. At the end of the study period, 21 patients (13.1%) had developed HCC. This cancer group had a significantly higher mean LFI (2.72 ± 0.32) than did the non-cancer group (1.97 ± 0.72; $p = 0.005$). The cancer group had significantly lower median serum albumin and platelet count than the non-cancer group, but the 2 groups did not significantly differ by gender, height, weight, waist circumference, BMI, total bilirubin, and ALT. AST tended to be higher (but not significantly so) in the cancer group (91.4 ± 48.8) than in the non-cancer group (56.3 ± 44.6; $p = 0.084$; table 1). Prothrombin time tend-

ed to be lower (but not significantly so) in the cancer group (74.8 ± 8.3) than in the non-cancer group (90.3 ± 19.7; p = 0.06; table 1). In total, 130 patients received antiviral therapy after enrolment. Of these patients, a significantly higher percentage of those in the non-cancer group reached sustained viral response (SVR) to interferon therapy (75/116; 64.7%) than did those in the cancer group (5/14; 35.7%).

Liver Cancer Incidence

We stratified 160 patients into 3 groups based on LFI (fig. 1). Respective cumulative liver cancer incidences for years 1, 2, 3, 4, and 5 were, for the entire cohort: 2.0, 5.6, 8.8, 13.1, and 23.9%; for those whose LFI was ≤2.0: 0.0, 0.0, 0.0, 0.0, and 0.0%; for those whose LFI was 2–2.8: 0.0, 7.4, 7.4, 13.2 and 19.9%; and for those whose LFI was >2.8: 12.9, 12.9, 21.7, 31.4, and 31.4% (p = 0.011; log-rank test; table 2).

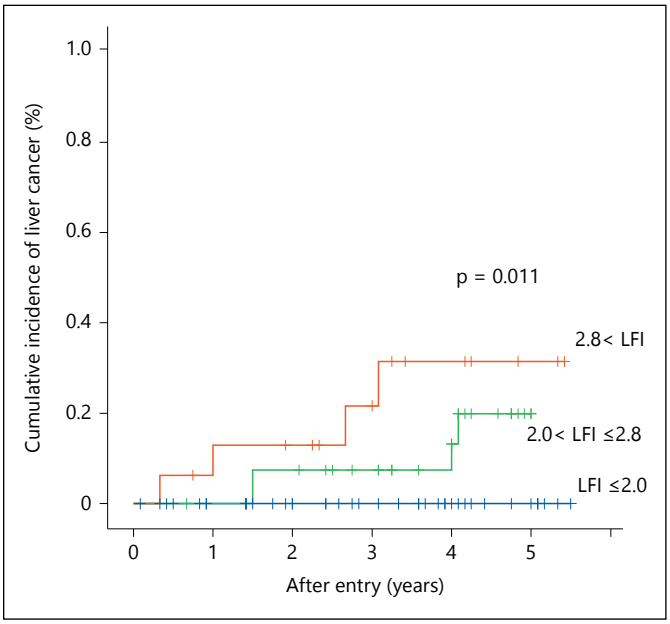

Fig. 1. Cumulative liver cancer incidences based on LFI. We stratified 160 patients into 3 groups based on LFI. Liver cancer incidence for patients whose LFI was >2.8 was significantly higher in each year (p = 0.011; log-rank test).

Table 2. Cumulative liver cancer incidences based on LFI

	Cumulative liver cancer incidences, %				
	1 year	2 years	3 years	4 years	5 years
LFI					
_2.0	0.0	0.0	0.0	0.0	0.0
2.0–2.8	0.0	7.4	7.4	13.2	19.9
>2.8	12.9	12.9	21.7	31.4	31.4
Total	2.0	5.6	8.8	13.1	23.9

Liver cancer incidence for patients whose LFI was >2.8 was significantly higher in each year (p = 0.011; log-rank test).

Discussion

Ultrasound elastography is internationally recognized as a useful tool for noninvasive diagnosis of liver fibrosis. Transient elastography uses shear-wave imaging, which measures the propagation speed of shear waves generated in liver tissue. According to Young's modulus, $E = 3\rho Vs^2$ where E (kPa) is liver stiffness, Vs (m/s) is shear wave propagation velocity, and ρ (g/cm^2) is density. As hepatic fibrosis progresses, liver stiffness increases. As shear-wave velocity can also be affected by inflammation, jaundice, and hepatic congestion [17–21], measuring liver stiffness can also help evaluate the risk for liver cancer, portal hypertension, or decompensation in chronic liver disease.

The other elastography technology, strain imaging, measures the relative distortion in the region of interest, and displays it in a color map. In RTE, relatively hard sites are shown in blue as areas of low distortion, softer sites in red as low strain area, and intermediate areas in green. These colors were mapped and displayed in 256-level gradation in real-time. As liver fibrosis progresses, the blue area increases and the image texture becomes increasingly distorted. The multiple regression equation for diagnosis of hepatic fibrosis uses feature values from RTE images to calculate the LFI, and is widely used to analyze RTE color map patterns objectively [13–16, 22].

The use of strain imaging for diagnosing liver fibrosis has not been widely reported; and to our knowledge, its use to assess liver cancer risk has not been reported at all. Therefore, we plan a prospective study to evaluate the performance of RTE for carcinogenetic risk assessment in patients with chronic HCV infection.

Our study showed RTE to identify high-risk patients with significant reliability. We found patients who entered the study with lower levels of fibrosis to have relatively low carcinogenic risk; most patients reached SVR by anti-viral treatment. Conversely, those with high LFI retained high cancer risk after viral clearance compared with the low-LFI cases, which indicates the need for careful follow-up for high LFI cases.

As this study used a very small sample, a larger study is needed to verify our findings.

Conclusions

Measurements of LFI by strain imaging to assess relative strain are useful in predicting liver cancer risk in patients with chronic HCV infection.

Acknowledgments

This research is supported by the Research Program on Hepatitis from Japan Agency for Medical Research and Development, AMED.

Disclosure Statement

The authors declare that they have no conflicts of interest.

References

1 Kawanaka M, Nishino K, Nakamura J, Oka T, Urata N, Goto D, Suehiro M, Kawamoto H, Kudo M, Yamada G: Quantitative levels of hepatitis B virus DNA and surface antigen and the risk of hepatocellular carcinoma in patients with hepatitis B receiving long-term nucleos(t)ide analogue therapy. Liver Cancer 2014;3:41–52.

2 Kudo M: Surveillance, diagnosis, treatment, and outcome of liver cancer in Japan. Liver Cancer 2015;4:39–50.

3 Kudo M, Matsui O, Izumi N, Iijima H, Kadoya M, Imai Y, Okusaka T, Miyayama S, Tsuchiya K, Ueshima K, Hiraoka A, Ikeda M, Ogasawara S, Yamashita T, Minami T, Yamakado K: JSH consensus-based clinical practice guidelines for the management of hepatocellular carcinoma: 2014 update by the liver cancer study group of Japan. Liver Cancer 2014;3:458–468.

4 Clinical practice guidelines for hepatocellular carcinoma differ between Japan, United States, and Europe. Liver Cancer 2015;4:85–95.

5 Shiina T: JSUM ultrasound elastography practice guidelines: basics and terminology. J Med Ultrason (2001) 2013;40:309–323.

6 Kudo M, Shiina T, Moriyasu F, Iijima H, Tateishi R, Yada N, Fujimoto K, Morikawa H, Hirooka M, Sumino Y, Kumada T: JSUM ultrasound elastography practice guidelines: liver. J Med Ultrason (2001) 2013;40:325–357.

7 Shiina T, Nightingale KR, Palmeri ML, Hall TJ, Bamber JC, Barr RG, Castera L, Choi BI, Chou YH, Cosgrove D, Dietrich CF, Ding H, Amy D, Farrokh A, Ferraioli G, Filice C, Friedrich-Rust M, Nakashima K, Schafer F, Sporea I, Suzuki S, Wilson S, Kudo M: WFUMB guidelines and recommendations for clinical use of ultrasound elastography: part 1: basic principles and terminology. Ultrasound Med Biol 2015;41:1126–1147.

8 Masuzaki R, Tateishi R, Yoshida H, Goto E, Sato T, Ohki T, Imamura J, Goto T, Kanai F, Kato N, Ikeda H, Shiina S, Kawabe T, Omata M: Prospective risk assessment for hepatocellular carcinoma development in patients with chronic hepatitis C by transient elastography. Hepatology 2009;49:1954–1961.

9 Jung KS, Kim SU, Ahn SH, Park YN, Kim DY, Park JY, Chon CY, Choi EH, Han KH: Risk assessment of hepatitis B virus-related hepatocellular carcinoma development using liver stiffness measurement (FibroScan). Hepatology 2011;53:885–894.

10 Kudo M: Prediction of hepatocellular carcinoma incidence risk by ultrasound elastography. Liver Cancer 2014;3:1–5.

11 Tatsumi C, Kudo M, Ueshima K, Kitai S, Ishikawa E, Yada N, Hagiwara S, Inoue T, Minami Y, Chung H, Maekawa K, Fujimoto K, Kato M, Tonomura A, Mitake T, Shiina T: Non-invasive evaluation of hepatic fibrosis for type C chronic hepatitis. Intervirology 2010;53:76–81.

12 Fujimoto K, Kato M, Tonomura A, Yada N, Tatsumi C, Oshita M, Wada S, Ueshima K, Ishida T, Furuta T, Yamasaki M, Tsujimoto M, Motoki M, Mitake T, Shiina T, Kudo M, Hayashi N: Non-invasive evaluation method of the liver fibrosis using real-time tissue elastograpy – usefulness of judgment liver fibrosis stage by liver fibrosis index (LF index). Kanzo 2010;59:539–541.

13 Fujimoto K, Kato M, Kudo M, Yada N, Shiina T, Ueshima K, Yamada Y, Ishida T, Azuma M, Yamasaki M, Yamamoto K, Hayashi N, Takehara T: Novel image analysis method using ultrasound elastography for noninvasive evaluation of hepatic fibrosis in patients with chronic hepatitis C. Oncology 2013;84(suppl 1):3–12.

14 Yada N, Kudo M, Morikawa H, Fujimoto K, Kato M, Kawada N: Assessment of liver fibrosis with real-time tissue elastography in chronic viral hepatitis. Oncology 2013;84(suppl 1):13–20.

15 Yada N, Kudo M, Kawada N, Sato S, Osaki Y, Ishikawa A, Miyoshi H, Sakamoto M, Kage M, Nakashima O, Tonomura A: Noninvasive diagnosis of liver fibrosis: utility of data mining of both ultrasound elastography and serological findings to construct a decision tree. Oncology 2014;87(suppl 1):63–72.

16 Yada N, Sakurai T, Minami T, Arizumi T, Takita M, Inoue T, Hagiwara S, Ueshima K, Nishida N, Kudo M: Ultrasound elastography correlates treatment response by antiviral therapy in patients with chronic hepatitis C. Oncology 2014;87(suppl 1):118–123.

17 Arena U, Vizzutti F, Corti G, Ambu S, Stasi C, Bresci S, Moscarella S, Boddi V, Petrarca A, Laffi G, Marra F, Pinzani M: Acute viral hepatitis increases liver stiffness values measured by transient elastography. Hepatology 2008;47:380–384.

18 Sagir A, Erhardt A, Schmitt M, Häussinger D: Transient elastography is unreliable for detection of cirrhosis in patients with acute liver damage. Hepatology 2008;47:592–595.

19 Millonig G, Reimann FM, Friedrich S, Fonouni H, Mehrabi A, Büchler MW, Seitz HK, Mueller S: Extrahepatic cholestasis increases liver stiffness (FibroScan) irrespective of fibrosis. Hepatology 2008;48:1718–1723.

20 Colli A, Pozzoni P, Berzuini A, Gerosa A, Canovi C, Molteni EE, Barbarini M, Bonino F, Prati D: Decompensated chronic heart failure: increased liver stiffness measured by means of transient elastography. Radiology 2010;257:872–878.

21 Millonig G, Friedrich S, Adolf S, Fonouni H, Golriz M, Mehrabi A, Stiefel P, Pöschl G, Büchler MW, Seitz HK, Mueller S: Liver stiffness is directly influenced by central venous pressure. J Hepatol 2010;52:206–210.

22 Yada N, Sakurai T, Minami T, Arizumi T, Takita M, Hagiwara S, Ueshima K, Ida H, Nishida N, Kudo M: A newly developed shear wave elastography modality: with a unique reliability index. Oncology 2015;89(suppl 2):53–59.

Original Article

Digestive Diseases

Dig Dis 2016;34:627–631
DOI: 10.1159/000448823

Efficacy and Safety of Sofosbuvir Plus Ribavirin Treatment for Patients with Chronic Hepatitis C Genotype 2

Kayo Sugimoto[a, c] Soo Ki Kim[d] Soo Ryang Kim[d] Mana Kobayashi[c] Airi Kato[c] Eri Morimoto[c] Susumu Imoto[d] Chi Wan Kim[e] Yasuhito Tanaka[f] Masatoshi Kudo[g] Yoshihiko Yano[b] Yoshitake Hayashi[a]

[a]Division of Molecular Medicine and Medical Genetics, Department of Pathology, and [b]Division of Center Infectious Diseases, Department of Pathology, Kobe University Graduate School of Medicine, [c]Department of Pharmacy, [d]Department of Gastroenterology, and [e]Department of Surgery, Kobe Asahi Hospital, Kobe, [f]Department of Virology and Liver Unit, Nagoya City University Graduate School of Medical Sciences, Nagoya, and [g]Department of Gastroenterology and Hepatology, Kindai University Faculty of Medicine, Osaka-Sayama, Japan

Key Words
Chronic hepatitis C genotype 2 · Hemoglobin decrease · Inosine triphosphatase gene · Sofosbuvir plus ribavirin · Virological response

Abstract
Objectives: The efficacy of sofosbuvir plus ribavirin (RBV) treatment for hepatitis C virus (HCV) genotype 2 focusing on virological response was compared with that of pegylated interferon (peg-IFN) plus RBV treatment. Safety of the former focusing on the decline in hemoglobin levels was compared with that of the latter and assessed in terms of age and inosine triphosphatase (ITPA). ***Methods:*** Patients (n = 17) receiving sofosbuvir plus RBV and those (n = 24) receiving peg-IFN plus RBV diagnosed with chronic HCV genotype 2 were enrolled in this study, and the efficacy and safety of both treatments were assessed. ***Results:*** Rapid virological response was attained with sofosbuvir plus RBV treatment compared with peg-IFN plus RBV treatment. All patients under sofosbuvir plus RBV treatment achieved end-of-treatment response compared with 70% who sustained viral response under the peg-IFN plus RBV treatment, with the former demonstrating greater virological response. The decline in hemoglobin levels under the former treatment was greater than that under the latter and in patients over 65 years of age with ITPA gene major. ***Conclusion:*** Efficacy and safety of sofosbuvir plus RBV treatment were clearly demonstrated compared with those of peg-IFN plus RBV treatment. The decline in hemoglobin levels was not related to the discontinuation of the former treatment, irrespective of age or the effect of the ITPA gene.

Introduction

Antiviral therapy for hepatitis C virus (HCV) is crucial to prevent the development of hepatocellular C virus [1–3].

Sofosbuvir (Gilead Sciences) is an oral nucleotide analogue inhibitor of HCV-specific NS5B polymerase that has recently been approved in the United States, Europe, and Japan for the treatment of chronic HCV infection [4–6]. The labeled use for patients with chronic genotype 2 HCV infection is sofosbuvir and ribavirin (RBV) for

KARGER

E-Mail karger@karger.com
www.karger.com/ddi

0257–2753/16/0346–0627$39.50/0

Soo Ryang Kim, MD
Department of Gastroenterology
Kobe Asahi Hospital, 3-5-25 Bououji-cho
Nagata-ku, Kobe 653-0801 (Japan)
E-Mail asahi-hp@arion.ocn.ne.jp

12 weeks. In phase 3 studies, this treatment for patients infected with HCV genotype 2 showed sustained virological response 12 (SVR12) in 97% of treatment-naive patients, 93% of patients ineligible to receive interferon, and 86–90% of previously treated patients [6–9].

Although this treatment was safe and efficacious compared with pegylated interferon (peg-IFN) plus RBV treatment, the adverse events of hemolytic anemia attributed to RBV remained unresolved.

In phase 3 trials of sofosbuvir and RBV in Japanese patients with chronic HCV genotype 2 infection, the decline in hemoglobin levels has been greater in patients aged 65 and older than in those aged under 65 [6].

Polymorphisms of the inosine triphosphatase (ITPA) gene in chromosome 20 (20p13) influence RBV-induced anemia, as demonstrated in a Genome-Wide Association Study [10].

Single nucleotide polymorphism (SNP) at rs1127354 for proline-to-threonine substitution (P32T) in the second of 8 exons in the ITPA gene, as well as that at rs7270101 in the second intron, affects the expression of ITPA [11–14].

In our hospital, the efficacy of a 12-week treatment with sofosbuvir plus RBV given to naive and previously treated chronic HCV genotype 2 infection patients with cirrhosis was compared with that of peg-IFN plus RBV received by patients with the same infection but without liver cirrhosis. Moreover, the safety of sofosbuvir plus RBV treatment and its effect on the decline in hemoglobin concentration – the most common adverse event – was compared with that of peg-IFN plus RBV treatment and assessed in terms of age and the ITPA gene.

Patients and Methods

Patients ≥20 years of age, body weight >40 kg, with chronic hepatitis C (CHC) genotype 2 infection (HCV RNA level 4 log IU/ml at screening) were included in the study.

Seventeen patients (10 men and 7 women, 59.2 ± 15.7 years of age, 8 naive and 9 peg-IFN experienced), including 8 over 65 years of age, were for 12 weeks administered sofosbuvir 400 mg/day per os and RBV twice daily per os (600 mg/day for BW ≤60 kg, 800 mg/day for BW >60–≤80 kg or 1,000 mg/day for BW >80 kg; table 1). Patients (n = 5) with Child–Pugh A liver cirrhosis were treated in our hospital from 2015 to 2016.

The primary endpoint was to determine the proportion of patients with undetectable HCV RNA levels at end-of-treatment response (ETR) due to the short follow-up period after the approval of medical insurance coverage in Japan.

Twenty-four patients (16 men and 8 women, 49.1 ± 13.0 years of age) with median HCV RNA level 6.2 log IU/ml were administered PEG-IFN α-2b (Pegintron®; Schering-Plough, Kenilworth, N.J., USA) 1.5 mg/kg BW subcutaneously once a week and RBV (Rebetol®; Schering-Plough) 600, 800 mg/day per os for 24 weeks according to the standard treatment protocol for Japanese patients established by the hepatitis study group of the Ministry of Health, Labour and Welfare, Japan. The patients received >80% of the scheduled dosage of peg-IFN and RBV. Patients with liver cirrhosis were excluded from this study and treated in our hospital from 2008 to 2014 [15].

Table 1. Patient baseline characteristics

	Sofosbuvir and RBV (n = 17)	Peg-IFN and RBV (n = 24)
Age, years*	59.2±15.7	49.1±13.0
Gender, men/women	10/7	16/8
ALT, U/l*	49.6±34.3	67.8±91.6
AFP, ng/ml*	5.9±4.6	8.6±20.6
PLT, $\times 10^4/mm^3$*	15.7±4.4	20.1±6.6
HCVRNA, KIU/ml*	6.1±0.7	6.2±0.8
Cirrhosis, n	5	0

* Data are shown as means ± SD.

The primary end point was to determine the proportion of patients with SVR at the end of week 24 of treatment (SVR24).

Included in the study were patients demonstrating hemoglobin levels ≥11 g/dl (women) or ≥12 g/dl (men), platelet count $\geq 9 \times 10^4/mm^3$, HCV RNA ≥5.0 log IU/ml, neutrophil count ≥1,500/mm^3, and thyroid stimulating hormone levels within normal limits. Excluded were those demonstrating human immunodeficiency virus or hepatitis B coinfection, creatinine clearance <50 ml/min, liver disease other than CHC, evidence of advanced liver disease such as liver cirrhosis (Child–Pugh B and C) under sofosbuvir plus RBV treatment, preexisting psychiatric conditions, or a history of severe psychiatric disorder. Informed written consent was obtained from each patient, and the study protocol conformed to the ethical guidelines approved by the Ethics Committee of Kobe Asahi Hospital [16].

Viral Kinetics

HCV RNA levels and genotype were examined through the COBAS TaqMan HCV test, with a lower limit of quantification of 17 IU/ml. Virological response was defined as undetectable HCV RNA-HCV clearance, during treatment, of serum HCV RNA to a concentration of ≤17 IU/ml [17].

HCV RNA levels were assessed during the treatment, and virological responses were examined at baseline weeks 4, 8, 12, 24, and 48.

Patients clearing HCV viremia (<17 IU/ml) at week 4 were categorized as achieving rapid virological response (RVR).

Patients clearing HCV virus (<17 IU/ml) at week 12 under the sofosbuvir plus RBV treatment and at week 24 under the peg-IFN plus RBV treatment were categorized as ETR.

SNP Genotyping of ITPA

Genetic polymorphisms in SNPs of the ITPA gene (rs1127354) were determined with the use of ABI TaqMan Probes (Applied Biosystems, Carlsbad, Calif., USA) [18]. In Caucasian patients, 2 SNPs (rs1127354 and rs7270101) are associated with ITPA en-

Table 2. Virological response to sofosbuvir plus RBV and -IFN plus RBV treatment

Response	Sofosbuvir and RBV (n = 17), %	Peg-IFN and RBV (n = 24), %	p value
4 weeks	16 (94.1) (RVR)	10 (41.67)	0.0021
8 weeks	17 (100)	23 (95.8)	
12 weeks	17 (100) (ETR)	24 (100)	
24 weeks		24 (100) (ETR)	
48 weeks		17 (70.8) (SVR24)	

zyme activity [10, 19]; however, there are no variants in rs7270101 among Japanese populations [18, 20, 21].

In this study, the ITPA at rs1127354 (major allele) was defined as homozygous (CC) for the major sequence and the ITPA minor allele as homozygous (AA) or heterozygous (CA) for the minor sequence.

Hemoglobin Assessment

Hemoglobin was examined at weeks 1, 2, 4, 8, and 12 of treatment.

Statistical Analysis

The rate of RVR in the sofosbuvir plus RBV group was compared with that of RVR in the peg-IFN plus RBV group by Fisher's exact test or the chi-square test. The Mann–Whitney U test was used to compare the mean change in the level of serum hemoglobin between the 2 groups, between patients aged ≥65 and those <65, between patients with the major ITPA gene and those with the minor ITPA gene.

Variables with a p value <0.05 were considered statistically significant. All statistical analyses were carried out with the use of Excel Statistics 2011 by SSRI.

Results

Efficacy

The patients (n = 17) treated with sofosbuvir plus RBV for 12 weeks achieved ETR: 94% (16/17) achieves RVR at week 4, and 100% (17/17) at week 8. The 24 patients treated with peg-IFN plus RBV achieved virological response: 41.7% (10/24) at week 4 (RVR), 96% (23/24) at week 8, 100% (24/24) at week 12 and 100% (24/24) at week 24 (ETR); also, 70.8% (17/24) achieved virological response at week 48 (SVR24; table 2).

Safety

Comparisons of hemoglobin levels showed the following: the level in the peg-IFN plus RBV treatment group (24 patients) showed a greater decline than in the sofosbuvir plus RBV treatment group (17 patients) at week 8 (–2.6 ± 1.3 vs. –1.5 ± 1.6, p = 0.046) and at week 12 (–2.8 ± 1.4 vs. –1.7 ± 1.5, p < 0.001; fig. 1); in the sofosbuvir plus RBV treatment group, the level in patients aged ≥65 (8 patients) showed a larger decline than in those aged <65 (9 patients) at week 2 (–1.7 ± 0.8 vs. –0.53 ± 0.8, p = 0.008), at week 8 (–2.5 ± 1.0 vs. –0.5 ± 1.4, p = 0.009) and at week 12 (–2.6 ± 1.4 vs. –0.8 ± 1.1, p = 0.019; fig. 2); the level in

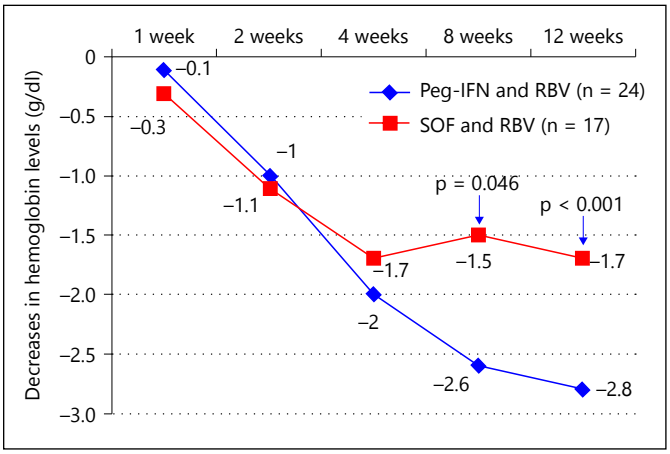

Fig. 1. Comparison of the decline in hemoglobin levels in the sofosbuvir plus RBV treatment group and the peg-IFN plus RBV treatment group. The decline in hemoglobin levels was larger in patients under peg-IFN plus RBV treatment at week 8 (–2.6 ± 1.3 vs. –1.5 ± 1.6, p = 0.046) and at week 12 (–2.8 ± 1.4 vs. –1.7 ± 1.5, p < 0.001).

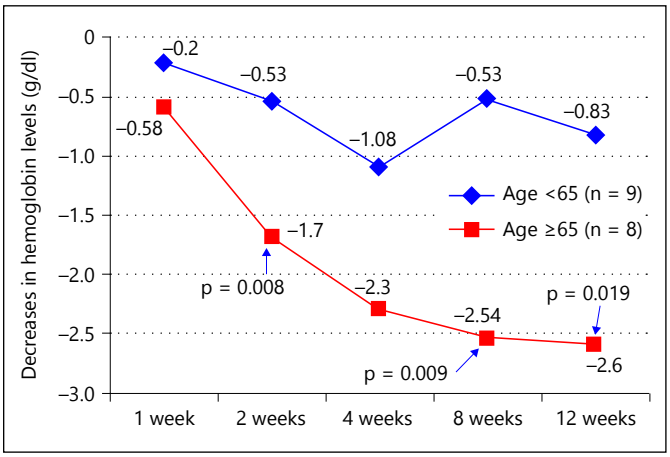

Fig. 2. Comparison of hemoglobin levels between patients aged <65 and those aged ≥65 in the sofosbuvir plus RBV treatment group. Hemoglobin decreased more in patients aged ≥65 than in those aged <65 at week 2 (–1.7 ± 0.8 vs. –0.53 ± 0.8, p = 0.008), at week 8 (–2.5 ± 1.0 vs. –0.5 ± 1.4, p = 0.009) and at week 12 (–2.6 ± 1.4 vs. –0.8 ± 1.1, p = 0.019).

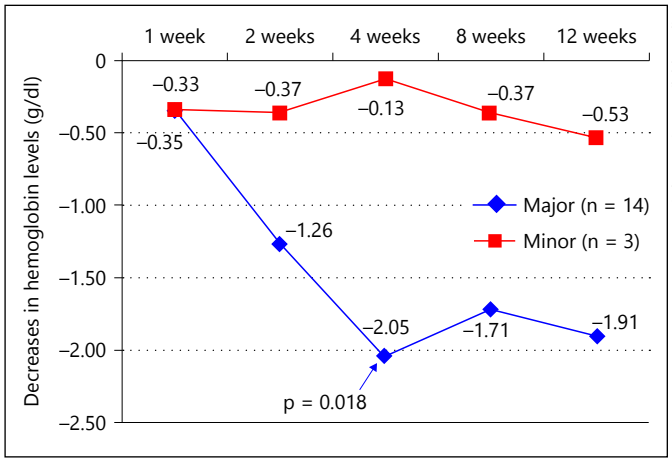

Fig. 3. Comparison of the decline in hemoglobin levels between ITPA gene major and minor. Hemoglobin decreased more in patients with ITPA gene major than in those with ITPA gene minor at week 4 (−2.1 ± 1.0 vs. −0.1 ± 0.9, p = 0.018).

ITPA gene major (14 patients) showed a greater decline than in ITPA gene minor (3 patients) at week 4 (−2.1 ± 1.0 vs. −0.1 ± 0.9, p = 0.018; fig. 3).

Discussion

In this study, the efficacy of sofosbuvir plus RBV treatment was demonstrated by the achievement of virological response in 94% of patients at week 4 (RVR), in 100% at week 4 (RVR), in 100% at week 8 and in 100% at week 12 (ETR). Thus, such early virological response including the high rate of RVR, nearly 100% SVR12 or SVR24 is achievable as previously reported [17, 22].

Treatment with peg-IFN plus RBV provided virological response in 40% (10/24), 95.8% (23/24), 100% (24/24), 100% (24/24) (ETR) at weeks 4, 8, 12, and 24 respectively, and demonstrated SVR in 70.8% of patients at week 24 (SVR24). Sofosbuvir plus RBV treatment, in contrast, was superior to peg-IFN plus RBV treatment in terms of virological response. The difference in SVR and the estimated SVR between the 2 treatments may be related to the virological response at week 4 (RVR).

Hemoglobin decline was markedly greater under peg-IFN plus RBV treatment than under sofosbuvir plus RBV treatment at weeks 4 and 8.

We therefore speculate that the decline in hemoglobin with peg-IFN plus RBV may be related not only to RBV but also to peg-IFN.

The decline in the levels of hemoglobin signifies the greater safety of sofosbuvir plus RBV treatment than that of peg-IFN plus RBV treatment.

The degree of hemoglobin decline in patients with sofosbuvir plus RBV treatment was greater in patients aged 65 and older than in those aged under 65, at weeks 2, 8, and 12 after treatment, which is consistent with that of a previous study [6]. Also, this decline was observed more in patients with ITPA gene major than in those with ITPA gene minor at week 4.

During the peg-IFN plus RBV treatment, patients infected with HCV-1 carrying the CC genotype at rs1127354 are more susceptible to developing anemia than those with CA/AA genotypes, and the decline in hemoglobin is greater in patients with the AA than in those with AC/CC genotypes at rs7270101 [10].

In this study, these observations have been reflected in patients under sofosbuvir plus RBV treatment, as well as in Japanese patients infected with HCV-1 receiving PEG-IFN-α-2b and RBV [23].

This is the first report describing the relation between ITPA and anemia in patients infected with HCV-2 and receiving sofosbuvir plus RBV treatment.

In our study, none of the patients discontinued sofosbuvir plus RBV treatment and none needed blood transfusion.

Because of the short duration of treatment, all patients including those over 65 years of age demonstrated tolerance for the treatment.

Monitoring the decline in hemoglobin levels is necessary, however, not only during treatment but also after treatment, especially in patients aged ≤65, in view of the slow recovery of these levels.

In conclusion, treatment with the all-oral, interferon-free combination of sofosbuvir and RBV resulted in high rates of virological response and proved safe in patients with chronic HCV genotype 2 infection, as well as in previously treated patients and in those with cirrhosis.

In view of the small number of patients in our study, a large-scale study is needed to clarify and confirm our conclusions.

Acknowledgment

We are indebted to Ms. Mika Matsui for her assistance in the preparation of the manuscript.

Disclosure Statement

The authors declare that they have no financial conflict of interest.

References

1 Kudo M: Surveillance, diagnosis, treatment, and outcome of liver cancer in Japan. Liver Cancer 2015;4:39–50.

2 Clinical practice guidelines for hepatocellular carcinoma differ between Japan, United States, and Europe. Liver Cancer 2015;4:85–95.

3 Kudo M, Matsui O, Izumi N, Iijima H, Kadoya M, Imai Y, Okusaka T, Miyayama S, Tsuchiya K, Ueshima K, Hiraoka A, Ikeda M, Ogasawara S, Yamashita T, Minami T, Yamakado K: JSH consensus-based clinical practice guidelines for the management of hepatocellular carcinoma: 2014 update by the liver cancer study group of Japan. Liver Cancer 2014;3:458–468.

4 US Food and drug administration: FDA Approves Sorafenib (nexavar) for the Treatment of Unresectable Hepatocellular Carcinoma. http://wwwfdagov/CDER/Offices/OODP/whatsnew/sorafenibhtm (accessed October 3, 2015).

5 Kane RC, Farrell AT, Madabushi R, Booth B, Chattopadhyay S, Sridhara R, Justice R, Pazdur R: Sorafenib for the treatment of unresectable hepatocellular carcinoma. Oncologist 2009;14:95–100.

6 Omata M, Nishiguchi S, Ueno Y, Mochizuki H, Izumi N, Ikeda F, Toyoda H, Yokosuka O, Nirei K, Genda T, Umemura T, Takehara T, Sakamoto N, Nishigaki Y, Nakane K, Toda N, Ide T, Yanase M, Hino K, Gao B, Garrison KL, Dvory-Sobol H, Ishizaki A, Omote M, Brainard D, Knox S, Symonds WT, McHutchison JG, Yatsuhashi H, Mizokami M: Sofosbuvir plus ribavirin in Japanese patients with chronic genotype 2 HCV infection: an open-label, phase 3 trial. J Viral Hepat 2014;21:762–768.

7 Lawitz E, Mangia A, Wyles D, Rodriguez-Torres M, Hassanein T, Gordon SC, Schultz M, Davis MN, Kayali Z, Reddy KR, Jacobson IM, Kowdley KV, Nyberg L, Subramanian GM, Hyland RH, Arterburn S, Jiang D, McNally J, Brainard D, Symonds WT, McHutchison JG, Sheikh AM, Younossi Z, Gane EJ: Sofosbuvir for previously untreated chronic hepatitis C infection. N Engl J Med 2013;368:1878–1887.

8 Jacobson IM, Gordon SC, Kowdley KV, Yoshida EM, Rodriguez-Torres M, Sulkowski MS, Shiffman ML, Lawitz E, Everson G, Bennett M, Schiff E, Al-Assi MT, Subramanian GM, An D, Lin M, McNally J, Brainard D, Symonds WT, McHutchison JG, Patel K, Feld J, Pianko S, Nelson DR: Sofosbuvir for hepatitis C genotype 2 or 3 in patients without treatment options. N Engl J Med 2013;368:1867–1877.

9 Zeuzem S, Dusheiko GM, Salupere R, Mangia A, Flisiak R, Hyland RH, Illeperuma A, Svarovskaia E, Brainard DM, Symonds WT, Subramanian GM, McHutchison JG, Weiland O, Reesink HW, Ferenci P, Hézode C, Esteban R: Sofosbuvir and ribavirin in HCV genotypes 2 and 3. N Engl J Med 2014;370:1993–2001.

10 Fellay J, Thompson AJ, Ge D, Gumbs CE, Urban TJ, Shianna KV, Little LD, Qiu P, Bertelsen AH, Watson M, Warner A, Muir AJ, Brass C, Albrecht J, Sulkowski M, McHutchison JG, Goldstein DB: ITPA gene variants protect against anaemia in patients treated for chronic hepatitis C. Nature 2010;464:405–408.

11 Arenas M, Duley J, Sumi S, Sanderson J, Marinaki A: The ITPA c.94C>A and g.IVS2+21A>C sequence variants contribute to missplicing of the ITPA gene. Biochim Biophys Acta 2007;1772:96–102.

12 Cao H, Hegele RA: DNA polymorphisms in ITPA including basis of inosine triphosphatase deficiency. J Hum Genet 2002;47:620–622.

13 Stepchenkova EI, Tarakhovskaya ER, Spitler K, Frahm C, Menezes MR, Simone PD, Kolar C, Marky LA, Borgstahl GE, Pavlov YI: Functional study of the P32T ITPA variant associated with drug sensitivity in humans. J Mol Biol 2009;392:602–613.

14 Sumi S, Marinaki AM, Arenas M, Fairbanks L, Shobowale-Bakre M, Rees DC, Thein SL, Ansari A, Sanderson J, De Abreu RA, Simmonds HA, Duley JA: Genetic basis of inosine triphosphate pyrophosphohydrolase deficiency. Hum Genet 2002;111:360–367.

15 Kim SR, El-Shamy A, Imoto S, Kim KI, Sugimoto K, Kim SK, Tanaka Y, Hatae T, Hasegawa Y, Fujinami A, Ohta M, Hotta H, Kudo M: Prediction of response to pegylated interferon/ribavirin combination therapy for chronic hepatitis C genotypes 2a and 2b and high viral load. Dig Dis 2013;31:426–433.

16 Sugimoto K, Kim SR, Kim SK, Imoto S, Tohyama M, Kim KI, Ohtani A, Hatae T, Yano Y, Kudo M, Hayashi Y: Comparison of daclatasvir and asunaprevir for chronic HCV 1b infection with telaprevir and simeprevir plus peginterferon and ribavirin, with a focus on the prevention of occurrence and recurrence of hepatocellular carcinoma. Oncology 2015;89(suppl 2):42–46.

17 Cho Y, Cho EJ, Lee JH, Yu SJ, Yoon JH, Kim YJ: Sofosbuvir-based therapy for patients with chronic hepatitis C: early experience of its efficacy and safety in Korea. Clin Mol Hepatol 2015;21:358–364.

18 Matsuura K, Tanaka Y, Watanabe T, Fujiwara K, Orito E, Kurosaki M, Izumi N, Sakamoto N, Enomoto N, Yatsuhashi H, Kusakabe A, Shinkai N, Nojiri S, Joh T, Mizokami M: ITPA genetic variants influence efficacy of PEG-IFN/RBV therapy in older patients infected with HCV genotype 1 and favourable IL28B type. J Viral Hepat 2014;21:466–474.

19 Thompson AJ, Fellay J, Patel K, Tillmann HL, Naggie S, Ge D, Urban TJ, Shianna KV, Muir AJ, Fried MW, Afdhal NH, Goldstein DB, McHutchison JG: Variants in the ITPA gene protect against ribavirin-induced hemolytic anemia and decrease the need for ribavirin dose reduction. Gastroenterology 2010;139:1181–1189.

20 Sakamoto N, Tanaka Y, Nakagawa M, Yatsuhashi H, Nishiguchi S, Enomoto N, Azuma S, Nishimura-Sakurai Y, Kakinuma S, Nishida N, Tokunaga K, Honda M, Ito K, Mizokami M, Watanabe M: ITPA gene variant protects against anemia induced by pegylated interferon-α and ribavirin therapy for Japanese patients with chronic hepatitis C. Hepatol Res 2010;40:1063–1071.

21 Kurosaki M, Tanaka Y, Tanaka K, Suzuki Y, Hoshioka Y, Tamaki N, Kato T, Yasui Y, Hosokawa T, Ueda K, Tsuchiya K, Kuzuya T, Nakanishi H, Itakura J, Takahashi Y, Asahina Y, Matsuura K, Sugauchi F, Enomoto N, Nishida N, Tokunaga K, Mizokami M, Izumi N: Relationship between polymorphisms of the inosine triphosphatase gene and anaemia or outcome after treatment with pegylated interferon and ribavirin. Antivir Ther 2011;16:685–694.

22 Kao JH, Chien RN, Chang TT, Peng CY, Hu TH, Lo GH, Wang HY, Chen JJ, Yang JC, Knox SJ, Han L, Mo H, Mathias A, Brainard DM, Sheen IS, Hsu YC, Chu CJ, Chuang WL: A phase 3b study of sofosbuvir plus ribavirin in Taiwanese patients with chronic genotype 2 hepatitis C virus infection. Liver Int 2016;36:1101–1107.

23 Ochi H, Maekawa T, Abe H, Hayashida Y, Nakano R, Kubo M, Tsunoda T, Hayes CN, Kumada H, Nakamura Y, Chayama K: ITPA polymorphism affects ribavirin-induced anemia and outcomes of therapy – a genome-wide study of Japanese HCV virus patients. Gastroenterology 2010;139:1190–1197.

Original Article

Digestive Diseases

Dig Dis 2016;34:692–695
DOI: 10.1159/000448858

Radiofrequency Ablation Guided by Contrast-Enhanced Sonography versus B-Mode Sonography for Hepatocellular Carcinoma after Transcatheter Arterial Chemoembolization

Toshihiko Kawasaki[a] Kan-yun Hata[a] Daisuke Kinoshita[a] Masaki Takayama[a]
Hideyuki Okuda[a] Shigeto Mizuno[b] Masatoshi Kudo[c]

[a]Department of Gastroenterology and Hepatology and [b]Department of Endoscopy, Kindai University Nara Hospital, and [c]Department of Gastroenterology and Hepatology, Kindai University, Faculty of Medicine, Osaka-Sayama, Japan

Key Words
Hepatocellular carcinoma · Radiofrequency ablation · Transcatheter arterial chemoembolization · Contrast-enhanced sonography

Abstract
Purpose: Contrast-enhanced sonography increases negative enhancement in the Kupffer phase after transcatheter arterial chemoembolization (TACE) for hepatocellular carcinoma (HCC). We compared contrast-enhanced sonography with B-mode sonography for guidance of radiofrequency ablation (RFA) of HCC after TACE. ***Methods:*** After TACE was performed, 18 nodules in 12 patients were treated by B-mode sonography guided RFA, while 22 nodules in 18 patients were treated by contrast-enhanced sonography-guided RFA. ***Results:*** The success rate of initial RFA was 83.3% (15/18 nodules) in the B-mode sonography group. On the other hand, the success rate was 100% (22/22 nodules) in the contrast-enhanced sonography group and the difference was significant (p = 0.046). ***Conclusion:*** These findings suggest that RFA guided by Kupffer phase contrast-enhanced sonography after TACE is a promising therapeutic option for curing HCC.

Introduction

It has been reported that percutaneous radiofrequency ablation (RFA) of hepatocellular carcinoma (HCC) [1–3] guided by contrast-enhanced sonography is especially useful in patients whose lesions are poorly defined by B-mode sonography [4–7]. Clinical application of a new perflubutane microbubble contrast agent (Sonazoid®; Daiichi-Sankyo, Japan) has improved the utility of contrast-enhanced sonography-guided RFA as a treatment strategy for HCC [8–11].

KARGER

E-Mail karger@karger.com
www.karger.com/ddi

0257–2753/16/0346–0692$39.50/0

Masatoshi Kudo, MD, PhD
Department of Gastroenterology and Hepatology
Kindai University Faculty of Medicine
377-2 Ohno-Higashi, Osaka-Sayama, Osaka 589-8511 (Japan)
E-Mail m-kudo@med.kindai.ac.jp

RFA guided by contrast-enhanced sonography can be performed during two phases, which are the arterial phase and the Kupffer phase. The positive enhancement time is very short (about 10 s) during the arterial phase of contrast-enhanced sonography, which means that only experienced operators can employ this method. On the other hand, the negative enhancement time is longer than 1 h, allowing almost all operators to use this method. The degree of contrast enhancement varies widely among patients when contrast-enhanced sonography is performed in the Kupffer phase, and negative enhancement is almost absent in some cases.

We paid attention to the fact that negative enhancement during the Kupffer phase is increased after transcatheter arterial chemoembolization (TACE), and we performed RFA guided by contrast-enhanced sonography after TACE to assess its utility.

Methods

Patients

The subjects were 30 patients (18 men and 12 women; age range 53–82) with 37 nodules of untreated hypervascular HCC. Between October 2005 and May 2007, 18 nodules in 12 patients (6 men and 6 women; age range 58–80) were treated by B-mode sonography-guided RFA after TACE. Between June 2007 and December 2009, 22 nodules in 18 patients (12 men and 6 women; age range 53–82) were treated by contrast-enhanced sonography-guided RFA after TACE. The ethics committee of our institution approved the study protocol and written informed consent was obtained from all patients at the time of enrollment. This study conforms to the provisions of the Declaration of Helsinki.

Transcatheter Arterial Chemoembolization

First, the subjects underwent TACE in a standard manner from 5 to 12 days before RFA. All patients underwent hepatic angiography before TACE. Then an emulsion of iodized oil and 30–50 mg of a chemotherapy agent (epirubicin) was injected through a catheter, followed by an injection of gelatin sponge pieces. If the tumor was a solitary lesion, the tip of the catheter was advanced into the segmental or subsegmental arteries feeding the tumor. Otherwise, the tip was placed into the right or left branch of the hepatic artery. The volume of emulsion injected was determined from the tumor volume (maximum emulsion volume: 10 ml).

Ultrasound Unit

The ultrasound unit was an SSA-790A (Aplio™XG; Toshiba) with a 3.75 MHz convex transducer (PVT-375BT; Toshiba). B-mode studies were conducted by wideband harmonic imaging (pulse subtraction) with transmission and reception frequencies of 3.75 and 7.5 MHz, respectively. After a conventional B-mode examination, contrast-enhanced sonography was performed with phase-inversion harmonic imaging. The contrast agent (Sonazoid® at 0.01 ml/kg) was administered intravenously by bolus injection via an antecubital vein, followed by flushing with normal saline (10 ml).

Radiofrequency Ablation

Patients in both groups were treated using an RF3000™ radiofrequency ablation system (Boston Scientific) with 3.0 cm LeVeen CoAccess™ needles. In the B-mode sonography group, insertion of the radiofrequency electrodes was only guided by B-mode sonography. In the contrast-enhanced sonography group, insertion of the radiofrequency electrodes was guided by the Kupffer phase contrast-enhanced image.

Assessment of Response

A few days after RFA, the response was assessed by performing 3-phase contrast-enhanced CT, with interpretation of the scans by consensus between 2 experienced radiologists. Tumor ablation was considered successful when there was no enhancement of either the entire tumor or a 0.5 cm margin of apparently normal tissue surrounding the tumor. Residual viable tumor was diagnosed when CT revealed nodular peripheral enhancement, and the residual tumor was managed by additional RFA within a few days of post-treatment CT.

Statistical Analysis and Follow-Up

We compared the success rate of initial RFA between the 2 groups by using the chi-square test and statistical significance was accepted at $p < 0.05$.

If 1-month follow-up CT showed complete ablation and no new tumors, 3-phase contrast-enhanced CT was repeated at 3-month intervals. All patients were monitored for at least 6 months after RFA and underwent at least 2 follow-up CT examinations. The complications related to treatment were also documented.

Results

In the B-mode sonography group, the success rate of initial RFA was 83.3% (15/18 nodules) On the other hand, it was 100% (22/22 nodules) in the contrast-enhanced sonography group and the difference was significant ($p = 0.046$).

During follow-up, no patient in either group showed local tumor progression. There were no serious side effects or procedural complications (hemorrhage, infection, needle track seeding, hepatic failure, and death) in either group.

Discussion

It is difficult to perform RFA in patients with HCC lesions that are poorly defined on B-mode sonography, and solving this issue is one of the important themes in the treatment of HCC. Contrast-enhanced sonography is one of the possible solutions and is a low-invasive method with few side effects. However, only experienced operators can carry out RFA guided by contrast-

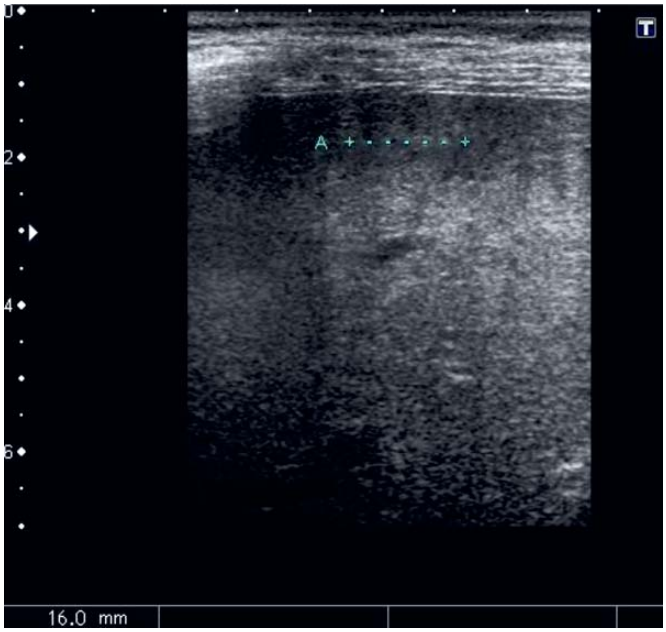

Fig. 1. This HCC nodule was hard to identify by B-mode ultrasonography even with a high-resolution, high-frequency linear transducer (PLT-805AT, 8 MHz).

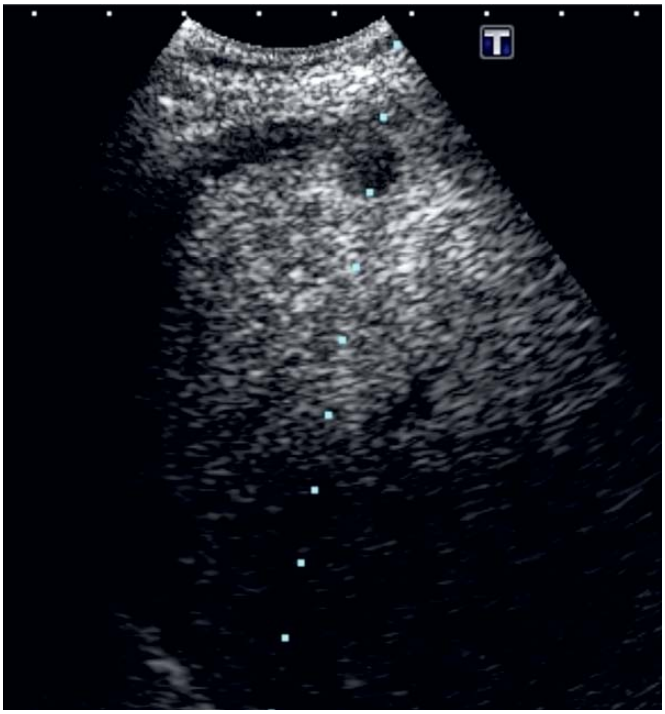

Fig. 2. After TACE, the same HCC nodule was easy to identify by Kupffer phase contrast-enhanced ultrasonography.

enhanced sonography in the arterial phase because the positive enhancement time is very short. Performing RFA guided by contrast-enhanced sonography in the Kupffer phase is also difficult in some cases because the extent of enhancement varies widely among individuals.

On the other hand, RFA is easier to perform with guidance by Kupffer phase contrast-enhanced sonography easy after TACE because negative enhancement in the Kupffer phase is increased. In this study, success rate of initial RFA was 100% (22/22 nodules) in the contrast-enhanced sonography group, and this was significantly superior to the success rate in the B-mode group. In the contrast-enhanced group, 8 out of 22 nodules were difficult to identify using only B-mode ultrasonography (fig. 1). However, it was easy to identify these nodules by contrast-enhanced ultrasonography in the Kupffer phase (fig. 2).

In conclusion, this study showed that RFA guided by Kupffer phase contrast-enhanced sonography after TACE is a promising therapeutic modality for HCC.

Disclosure Statement

The authors declare that they have no conflict of interest.

References

1 Teng W, Liu KW, Lin CC, Jeng WJ, Chen WT, Sheen IS, Lin CY, Lin SM: Insufficient ablative margin determined by early computed tomography may predict the recurrence of hepatocellular carcinoma after radiofrequency ablation. Liver Cancer 2015;4:26–38.

2 Kudo M: Locoregional therapy for hepatocellular carcinoma. Liver Cancer 2015;4:163–164.

3 Kang TW, Rhim H: Recent advances in tumor ablation for hepatocellular carcinoma. Liver Cancer 2015;4:176–187.

4 Minami Y, Kudo M, Kawasaki T, Chung H, Ogawa C, Shiozaki H: Percutaneous radiofrequency ablation guided by contrast-enhanced harmonic sonography with artificial pleural effusion for hepatocellular carcinoma in the hepatic dome. AJR Am J Roentgenol 2004;182:1224–1226.

5 Minami Y, Kudo M, Kawasaki T, Chung H, Ogawa C, Shiozaki H: Treatment of hepatocellular carcinoma with percutaneous radiofrequency ablation: usefulness of contrast harmonic sonography for lesions poorly defined with B-mode sonography. AJR Am J Roentgenol 2004;183:153–156.
6 Minami Y, Kudo M, Chung H, Kawasaki T, Yagyu Y, Shimono T, Shiozaki H: Contrast harmonic sonography-guided radiofrequency ablation therapy versus B-mode sonography in hepatocellular carcinoma: prospective randomized controlled trial. AJR Am J Roentgenol 2007;188:489–494.
7 Lencioni R, de Baere T, Martin RC, Nutting CW, Narayanan G: Image-guided ablation of malignant liver tumors: recommendations for clinical validation of novel thermal and non-thermal technologies – a western perspective. Liver Cancer 2015;4:208–214.
8 Kisaka Y, Hirooka M, Koizumi Y, Abe M, Matsuura B, Hiasa Y, Onji M: Contrast-enhanced sonography with abdominal virtual sonography in monitoring radiofrequency ablation of hepatocellular carcinoma. J Clin Ultrasound 2010;38:138–144.
9 Masuzaki R, Shiina S, Tateishi R, Yoshida H, Goto E, Sugioka Y, Kondo Y, Goto T, Ikeda H, Omata M, Koike K: Utility of contrast-enhanced ultrasonography with sonazoid in radiofrequency ablation for hepatocellular carcinoma. J Gastroenterol Hepatol 2011;26:759–764.
10 Dohmen T, Kataoka E, Yamada I, Miura K, Ohshima S, Shibuya T, Segawa D, Sato W, Anezaki Y, Ishii H, Kamada K, Goto T, Ohnishi H: Efficacy of contrast-enhanced ultrasonography in radiofrequency ablation for hepatocellular carcinoma. Intern Med 2012;51:1–7.
11 Chan AK, Hegarty C, Klass D, Yoshida E, Chung S, Liu DM, Ho SG, Harris AC: The role of contrast-enhanced ultrasound in guiding radiofrequency ablation of hepatocellular carcinoma: a retrospective study. Can Assoc Radiol J 2015;66:171–178.

Original Article

Digestive Diseases

Dig Dis 2016;34:679–686
DOI: 10.1159/000448855

Comparison of Contrast-Enhanced Ultrasound and Gadolinium-Ethoxybenzyl-Diethylenetriamine Pentaacetic Acid-Enhanced MRI for the Diagnosis of Macroscopic Type of Hepatocellular Carcinoma

Takayuki Iwamoto[a] Yasuharu Imai[a] Sachiyo Kogita[a] Takumi Igura[a] Yoshiyuki Sawai[a] Kazuto Fukuda[a] Yoshitaka Yamaguchi[a] Yasushi Matsumoto[a] Masanori Nakahara[a] Osakuni Morimoto[b] Yasushi Seki[c] Hiroshi Ohashi[d] Norihiko Fujita[c] Masatoshi Kudo[e] Tetsuo Takehara[f]

[a]Department of Gastroenterology, [b]Department of Gastroenterological Surgery, [c]Department of Radiology, and [d]Department of Pathology, Ikeda Municipal Hospital, Ikeda, [e]Department of Gastroenterology and Hepatology, Kindai University Faculty of Medicine, Osaka-Sayama, and [f]Department of Gastroenterology and Hepatology, Osaka University Graduate School of Medicine, Suita, Japan

Key Words

Hepatocellular carcinoma · Macroscopic type · Contrast-enhanced ultrasonography · Sonazoid · Gadolinium-ethoxybenzyl-diethylenetriamine pentaacetic acid-enhanced magnetic resonance imaging

Abstract

Objective: We compared the efficacy of contrast-enhanced ultrasound sonography (CEUS) with sonazoid and gadolinium-ethoxybenzyl-diethylenetriamine pentaacetic acid (Gd-EOB-DTPA)-enhanced MRI for the assessment of macroscopic classification of nodular hepatocellular carcinoma (HCC). ***Methods:*** Seventy-seven consecutive patients with 79 surgically resected HCCs who underwent both preoperative CEUS and Gd-EOB-DTPA-enhanced MRI were enrolled in this retrospective study. Based on the macroscopic diagnosis of resected specimens, nodules were categorized into the simple nodular (SN) and non-SN type HCC. Two hepatologists independently assessed image datasets of the post-vascular phase of CEUS and hepatobiliary phase of Gd-EOB-DTPA-enhanced MRI to compare their diagnostic performance. ***Results:*** Gd-EOB-DTPA-enhanced MRI enabled the evaluation of macroscopic classification in a significantly larger number of nodules than CEUS (78/79 (98.7%) vs. 70/79 (88.6%), $p < 0.05$). Of 70 nodules that could be evaluated by both modalities, 41 and 29 nodules were pathologically categorized as SN and non-SN, respectively. The areas under the receiver operating characteristic curve (AUC) for non-SN did not differ between CEUS and Gd-EOB-DTPA-enhanced MRI (reader 1: 0.748 for CEUS, 0.808 for MRI; reader 2: 0.759 for CEUS, 0.787 for MRI). The AUC of combined CEUS and Gd-EOB-DTPA-enhanced MRI for SN HCC was 0.855 (reader 1) and 0.824 (reader 2), indicating higher AUC values for the combined modalities. ***Conclusions:*** The diagnostic performance for macroscopic classification of nodular HCC of CEUS was comparable with that of Gd-EOB-DTPA-enhanced MRI, although some HCCs could not be evaluated by CEUS owing to lower detectability. The combination of the 2 modalities had a more accurate diagnostic performance.

KARGER

E-Mail karger@karger.com
www.karger.com/ddi

0257–2753/16/0346–0679$39.50/0

Yasuharu Imai, MD, PhD
Department of Gastroenterology
Ikeda Municipal Hospital
3-1-18, Johnan, Ikeda, Osaka 563-8510 (Japan)
E-Mail yasuimai@hosp.ikeda.osaka.jp

Introduction

Primary liver cancer is one of the most common cancers worldwide. It is much more common in men than in women. Most primary liver cancers occurring worldwide are hepatocellular carcinoma (HCC) [1]. In Japan, primary liver cancer, 95% of which is HCC, is ranked as the third most common cause of death from malignant neoplasms in men and fifth in women [2]. The macroscopic type of HCC has been reported to be associated with prognosis [3, 4], and the macroscopic type of HCC was classified into 5 types in the General Rules of Clinical and Pathological Study of Primary Liver Cancer in Japan [5]. Determination of the macroscopic type of HCC is important for prognostication and to select appropriate therapeutic methods [6, 7]. Because the macroscopic type of HCC is usually evaluated based on the section of maximum diameter of resected HCC specimens, it cannot be evaluated in patients who do not undergo hepatectomy. Recently, some imaging modalities have been reported to be useful for the assessment of macroscopic findings of HCC.

Contrast-enhanced ultrasound sonography (CEUS) with sonazoid (Sonazoid®, Daiichi Sankyo, Tokyo, Japan) is useful for the diagnosis of HCC [8, 9]. It provides persistent and stable enhancement during the post-vascular phase, as well as real-time fine vascular images during the vascular phase [10–12]. CEUS with sonazoid has been reported to be a useful method to predict macroscopic findings of HCC [13, 14].

Gadolinium-ethoxybenzyl diethylenetriamine pentaacetic acid (Gd-EOB-DTPA) is one of the liver-specific contrast agents for MRI [15]. Gd-EOB-DTPA is selectively taken up by hepatocytes and excreted into bile ducts [16]. Liver tumor cells can be identified as hypointense areas in the hepatobiliary phase of Gd-EOB-DTPA-enhanced MRI [17]. These images are highly sensitive for detecting liver tumors such as HCC and metastatic liver tumors [18–22]. Fujinaga et al. [23] reported the utility of the hepatobiliary phase of Gd-EOB-DTPA-enhanced MRI in the diagnosis of the macroscopic type of HCC. Tada et al. [24] also reported that Gd-EOB-DTPA-enhanced MRI was non-inferior to angiography-assisted CT in the assessment of the macroscopic findings in nodular HCC.

The purpose of this study was to retrospectively compare the diagnostic performance of CEUS with Gd-EOB-DTPA-enhanced MRI for the assessment of the macroscopic type of HCC.

Methods

Patients

This retrospective study was approved by our Institutional Review Board and the requirement for informed consent was waived. This study was conducted in compliance with the provisions of the Declaration of Helsinki. At our institution between March 2008 and August 2015, 131 consecutive patients with HCC underwent surgical resection. The inclusion criteria of this study were as follows: (1) patients who had pathologically diagnosed nodular type of HCC; (2) patients who underwent both CEUS and Gd-EOB-DTPA-enhanced MRI within 2 months of hepatic resection between March 2008 and August 2015; and (3) patients who did not undergo preoperative treatment including radiofrequency ablation therapy, percutaneous ethanol injection, or transarterial chemoembolization. The small nodular type with an indistinct margin (SN-IM) and the infiltrative type (IF) of HCC were excluded from this study. In total, we included 79 nodules from 77 enrolled patients. The characteristics of the 77 patients are presented in table 1. Seventy patients and 7 patients were classified into Child–Pugh classes A and B, respectively. The mean tumor size was 25.7 ± 13.5 mm (mean ± SD; range 8–75 mm).

CEUS Examinations

CEUS images were conducted using a LOGIQ 7 or E9 US system (GE Healthcare, Milwaukee, Wis., USA). Detection of the hepatic nodules by tissue harmonic grayscale imaging was per-

Table 1. Baseline characteristics of 77 patients

Age, years, mean ± SD (range)	70±9 (44–85)
Gender (male/female)	56/21
Etiology (HBV-related/HCV-related/alcoholic/others)	12/46/5/14
Child–Pugh classification (A/B)	70/7
Tumor size, mm, mean ± SD (range)	25.7±13.5 (8.0–75.0)
Pathological macroscopic type (SN/SN-EG/CMN)	43/23/13
Tumor size according to macroscopic type	
SN, mm, mean ± SD (range)	24.2±12.5 (8.0–55.0)
Non-SN, mm, mean ± SD (range)	27.7±14.6 (10.0–75.0)

HBV = Hepatitis B virus; HCV = hepatitis C virus.

formed by using convex or linear probes with a frequency of 2–5 or 4–9 MHz, respectively. The coded phase inversion mode with a mechanical index of 0.2–0.3 was used to perform CEUS. The focal point was set just under the bottom of the lesion. CEUS was carried out with sonazoid as a contrast agent. The recommended dose for the imaging of liver lesions is 0.015 ml/kg of body weight. Half of the recommended dose of sonazoid (0.0075 ml/kg) was administered as a quick bolus intravenously. The examination consisted of an early-vascular phase, a late-vascular phase, and a post-vascular phase (10–20 min after the injection of sonazoid). The post-vascular phase images were obtained after the destruction of bubbles with a high mechanical index of 0.8–1.0 [25].

MR Examinations

Gd-EOB-DTPA-enhanced MRI was performed using a 1.5 T MR scanner (Signa EXCITE HD version 12 (GE Healthcare)) [26]. Unenhanced, arterial, portal, late, and hepatobiliary phase images were obtained just before and after 25, 70, 180 s, and 20 min, respectively, after bolus injection of 25 μmol/kg body weight (0.1 ml/kg) Gd-EOB-DTPA (Primovist®, Bayer-Schering Pharma, Osaka Japan) at a rate of 2.0 ml/s, using T1-weighted three-dimensional gradient-echo sequences in a single breath hold (18–20 s). Liver acquisition with volume acceleration with fat saturation was used as a sequence, and the MR parameters were TR 4.5 ms; TE 2.2 ms; flip angle 12°; SENSE factor 2; slice thickness 5 mm; slice interval 2.5 mm; matrix 192 × 320; and field of view 360 mm.

Definition of Pathological Macroscopic Findings

The pathological macroscopic findings of resected specimens of nodular type HCC were classified into 3 types based on the definition of General Rules of Clinical and Pathological Study of Primary Liver Cancer in Japan [5] as follows: simple nodular (SN), SN with extranodular growth (SN-EG), and confluent multinodular (CMN). Pathological macroscopic classification of the resected specimens was determined by the consensus of 2 hepatologists with more than 10 years of experience in hepatobiliary surgery. In this study, we defined both SN-EG and CMN tumors as non-SN HCC. Tumor size was defined as the maximum diameter of the resected tumor specimen.

Imaging Analysis

The image datasets of the post-vascular phase of CEUS and the hepatobiliary phase of Gd-EOB-DTPA-enhanced MRI were reviewed independently by 2 blinded readers with more than 10 years of experience in hepatobiliary imaging who were unaware of the patients' pathological and clinical data. The all-axial hepatobiliary phase MR images were read on a picture archiving and communication system. For CEUS, post-vascular phase movie images that covered the whole tumor were recorded and used for the review. During one session, image sets consisting of a mixture of MR images of half of the patients and CEUS images of the other half were presented in random order. During the other session, the remaining image sets were presented in random order. To minimize recall bias, each reading session was separated by a 4-week interval. The images of the post-vascular phase of CEUS and the hepatobiliary phase of Gd-EOB-DTPA-enhanced MRI were classified into 3 types along with the macroscopic types of HCC. Diagnostic criteria of each type are as follows: SN HCC, round tumors with a clear and smooth margin (fig. 1a–c); SN-EG HCC, round tumors with a clear smooth margin and a protruding portion (fig. 1d–f); CMN HCC, lobulated tumors with a clear margin (fig. 1g–i). Both SN-EG and CMN types were defined as non-SN HCC.

Assessments for both CEUS and Gd-EOB-DTPA-enhanced MRI images were made independently by the 2 readers based on a 4-point grading scale (definitive SN = 1, probable SN = 2, probable non-SN = 3, definitive non-SN = 4).

Statistical Analysis

For comparisons of quantitative values between the SN and non-SN groups, the Mann–Whitney U test and Fisher's exact test were used for continuous and categorical variables, respectively. Sensitivity, specificity, positive and negative predictive values (NPV), and diagnostic accuracy of CEUS and Gd-EOB-DTPA-enhanced MRI for non-SN HCC were calculated and were expressed with a 95% CI . The McNemar test and Fisher's exact probability test were used for statistical comparison of sensitivity, specificity, and accuracy; and for positive and NPV, respectively. The receiver operating characteristic (ROC) curve was used to assess the diagnostic performance of CEUS, Gd-EOB-DTPA-enhanced MRI and the combination of the 2 imaging modalities. The area under the ROC curve was expressed as AUC. The diagnostic accuracy was defined as low (AUC 0.50–0.70), moderate (AUC 0.70–0.90), or high (AUC 0.90–1.0) [27]. The paired t test was used to compare AUCs. Interobserver agreement between the 2 readers of the 4-point scale used to evaluate diagnostic performance was determined by the unweighted κ statistic regarding SN HCC (score 1 or 2) or non-SN HCC (score 3 or 4), with a value of 0.00 indicating poor agreement; 0.01–0.20, slight agreement; 0.21–0.40, fair agreement; 0.41–0.60, moderate agreement; 0.61–0.80, good agreement; and 0.81–1.00, excellent agreement [28].

All statistical analyses were performed with EZR (Saitama Medical Center, Jichi Medical University, Saitama, Japan), which is a graphical user interface for R (The R Foundation for Statistical Computing, Vienna, Austria). More precisely, it is a modified version of R commander designed to add statistical functions frequently used in biostatistics. All p values were derived from 2-tailed tests, with $p < 0.05$ considered to indicate statistical significance.

Results

Evaluation of Macroscopic Type of HCC by CEUS and Gd-EOB-DTPA-Enhanced MRI

Of the 79 HCCs, the evaluation of macroscopic type of HCC was possible in 70 (88.6%) nodules on CEUS, while the remaining 9 HCCs could not be evaluated by CEUS because of signal attenuation or isoechoic nodules in the post-vascular phase. Gd-EOB-DTPA-enhanced MRI-enabled evaluation of macroscopic findings in 78 (98.7%) nodules; one HCC was not detected by the hepatobiliary phase. Therefore, a significantly larger number of nodules could be evaluated by Gd-EOB-DTPA-enhanced MRI than by CEUS ($p < 0.05$).

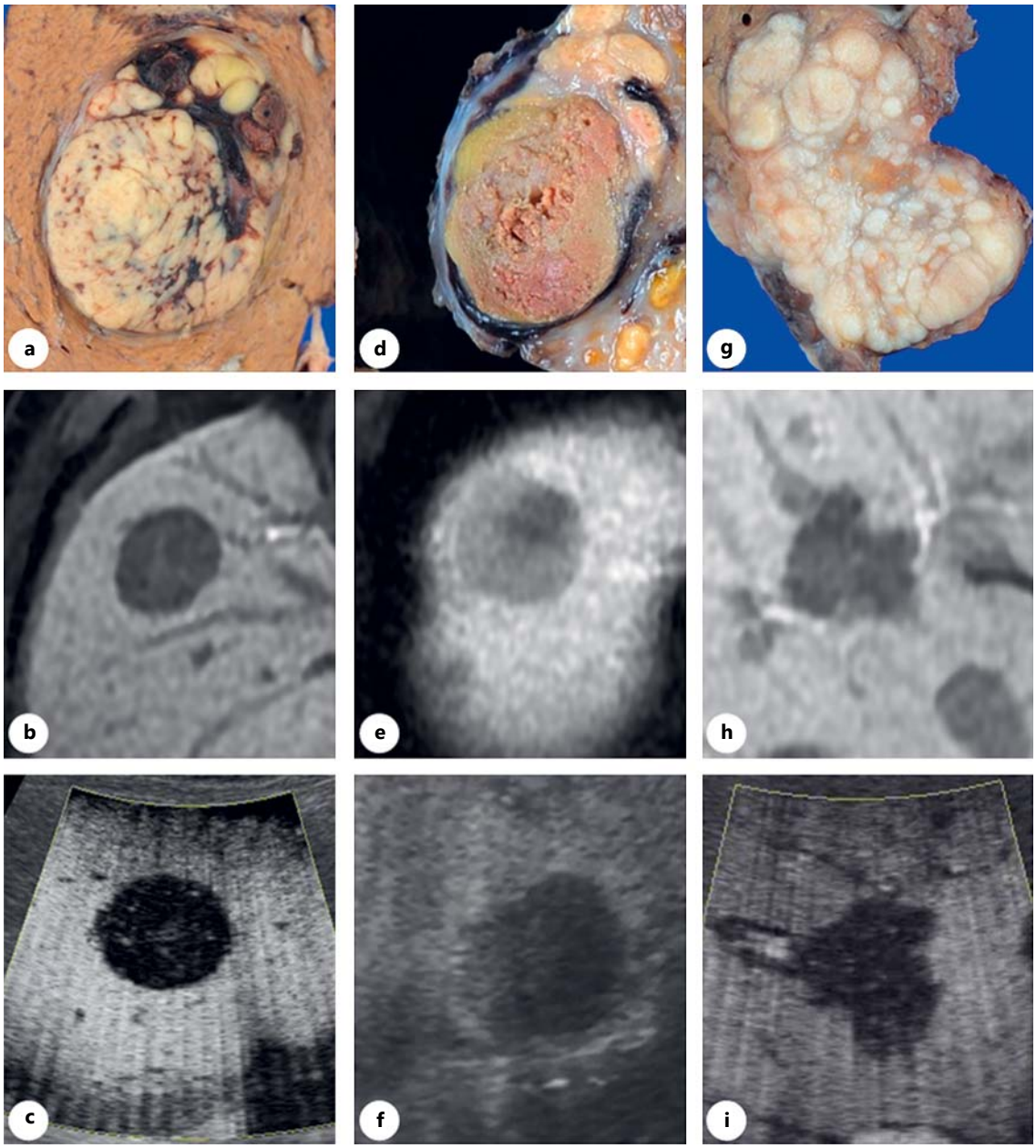

Fig. 1. a–c A 54-year-old woman with cirrhosis related to hepatitis B. **a** Macroscopic type of SN HCC; **b** hepatobiliary phase of Gd-EOB-DTPA-enhanced MRI; **c** post-vascular phase of CEUS. **d–f** A 79-year-old woman with cirrhosis related to hepatitis C. **d** A macroscopic type of SN-EG HCC; **e** hepatobiliary phase of Gd-EOB-DTPA-enhanced MRI; **f** post-vascular phase of CEUS. **g–i** A 78-year-old woman with cirrhosis related to hepatitis C. **g** A macroscopic type of CMN HCC; **h** hepatobiliary phase of Gd-EOB-DTPA-enhanced MRI; **i** post-vascular phase of CEUS.

Macroscopic Diagnosis

Based on the macroscopic pathological examination of the 70 nodules of the 68 patients that were evaluated by both the post-vascular phase of CEUS and the hepatobiliary phase of Gd-EOB-DTPA-enhanced MRI, 41 HCCs were pathologically categorized as SN and the remaining 29 were categorized as non-SN. The mean size of the SN and non-SN tumors was 24.4 ± 12.8 mm (range 8–55 mm) and 27.8 ± 13.5 mm (range 13–75 mm), respectively. There was no difference between the tumor sizes of the SN and non-SN tumors (p = 0.223).

Diagnostic Performance Analysis for Classification of Macroscopic Type of HCC by Blinded Readers

The sensitivity, specificity, accuracy, positive predictive values, and NPV for diagnosing SN HCC of the 70 nodules are shown in table 2. The sensitivity, specificity, and accuracy evaluated by reader 1 were 0.72, 0.71, and 0.71 for CEUS, respectively, and 0.86, 0.66, and 0.74 for Gd-EOB-DTPA-enhanced MRI, respectively. The sensitivity, specificity, and accuracy evaluated by reader 2 were 0.76, 0.81, and 0.79 for CEUS and 0.76, 0.75, and 0.76 for Gd-EOB-DTPA-enhanced MRI, respectively. The values evaluated by readers 1 and 2 had no significant differences between CEUS and Gd-EOB-DTPA-enhanced MRI.

The ROC curves for both imaging modalities for diagnosing non-SN HCC are shown in figure 2a and b. The AUC values evaluated by reader 1 for CEUS and Gd-EOB-DTPA-enhanced MRI were 0.748 (95% CI 0.630–0.865) and 0.808 (95% CI 0.711–0.906), respectively ($p = 0.404$), indicating a moderate diagnostic value. The AUC values evaluated by reader 2 for CEUS and Gd-EOB-DTPA-enhanced MRI were 0.759 (95% CI 0.681–0.893) and 0.787 (95% CI 0.759–0.787), respectively ($p = 0.651$). There was no difference between the AUC values of CEUS and Gd-EOB-DTPA-enhanced MRI for both readers.

Figure 2c and d shows the ROC curve using the combination of CEUS and Gd-EOB-DTPA-enhanced MRI. The AUC values evaluated by readers 1 and 2 using the combination for diagnosis of non-SN HCC were 0.855 (95% CI 0.764–0.947) and 0.824 (95% CI 0.721–0.927), respectively, resulting in higher diagnostic values. There was statistical significance between CEUS and the combination of 2 modalities evaluated by reader1 ($p = 0.036$).

Interobserver agreement was fair for both CEUS (κ value: 0.45) and Gd-EOB-DTPA-enhanced MRI (κ value: 0.52).

Table 2. Comparison of diagnostic performance of CEUS and Gd-EOB-DTPA-enhanced MRI

	Reader 1 (n = 70)		Reader 2 (n = 70)	
	CEUS/MRI	p value	CEUS/MRI	p value
Sensitivity	0.72/0.86	0.289	0.76/0.76	1
Specificity	0.71/0.66	0.789	0.81/0.75	0.773
Accuracy	0.71/0.74	0.503	0.79/0.76	0.815
PPV	0.64/0.64	0.580	0.73/0.69	0.454
NPV	0.78/0.87	0.270	0.83/0.82	0.574

Discussion

Various factors related to the recurrence and survival after HCC resection have been reported, such as tumor diameter, vascular invasion, intrahepatic metastasis, advanced fibrosis, and macroscopic type of HCC [29–35]. Kanai et al. [3] reported that SN-EG HCCs had a significantly higher rate of portal vein tumor thrombus and/or intrahepatic metastasis than SN HCCs, and that patients with SN HCCs had a better overall survival than those with SN-EG and CMN HCCs. Hui et al. [4] also reported that the rate of microscopic vascular invasion significantly increased from SN nodular to SN-EG nodular and then to CMN nodular. SN nodular was significantly associated with a lower recurrence rate and a higher disease-specific survival.

Several modalities including CEUS, angiography-assisted CT, and Gd-EOB-DTPA-enhanced MRI, have been reported to be useful for the diagnosis of macroscopic type of nodular HCC. Hatanaka et al. [13] reported the utility of CEUS with sonazoid for predicting the macroscopic type of nodular HCC in comparison with contrast-enhanced CT (CECT). They used arterial vascular images and post-vascular CEUS images for the evaluation of the macroscopic type of nodular HCC and found that the diagnostic accuracy of CEUS and CECT for the macroscopic type of HCC were 86.9% and 65.6%, respectively.

Tada et al. [14] also reported the utility of CEUS with sonazoid for diagnosing the macroscopic type of small nodular HCCs. They compared arterial phase, portal phase, and post-vascular phase of CEUS for the diagnosis of macroscopic type of small nodular HCC and found the AUC values for the shape of enhancement in the late arterial phase and the shape of the post-vascular image were high, 0.824 and 0.878, respectively. Moreover, they reported that the combination of the shape of enhancement in the late arterial phase and the shape of the post-vascular image for the diagnosis of non-SN HCC resulted in a higher AUC value.

In this study, we compared the diagnostic performance of CEUS and Gd-EOB-DTPA-enhanced MRI for the assessment of macroscopic type of HCC. We found that EOB-DTPA-enhanced MRI was able to evaluate macroscopic findings of HCC in a significantly larger number of nodules owing to its higher detectability as compared with CEUS. It was difficult to evaluate the macroscopic findings of nodules by CEUS in the deep area of the liver or under the diaphragm because of signal attenuation. Additionally, 3 nodules of hypovascular well-differentiated

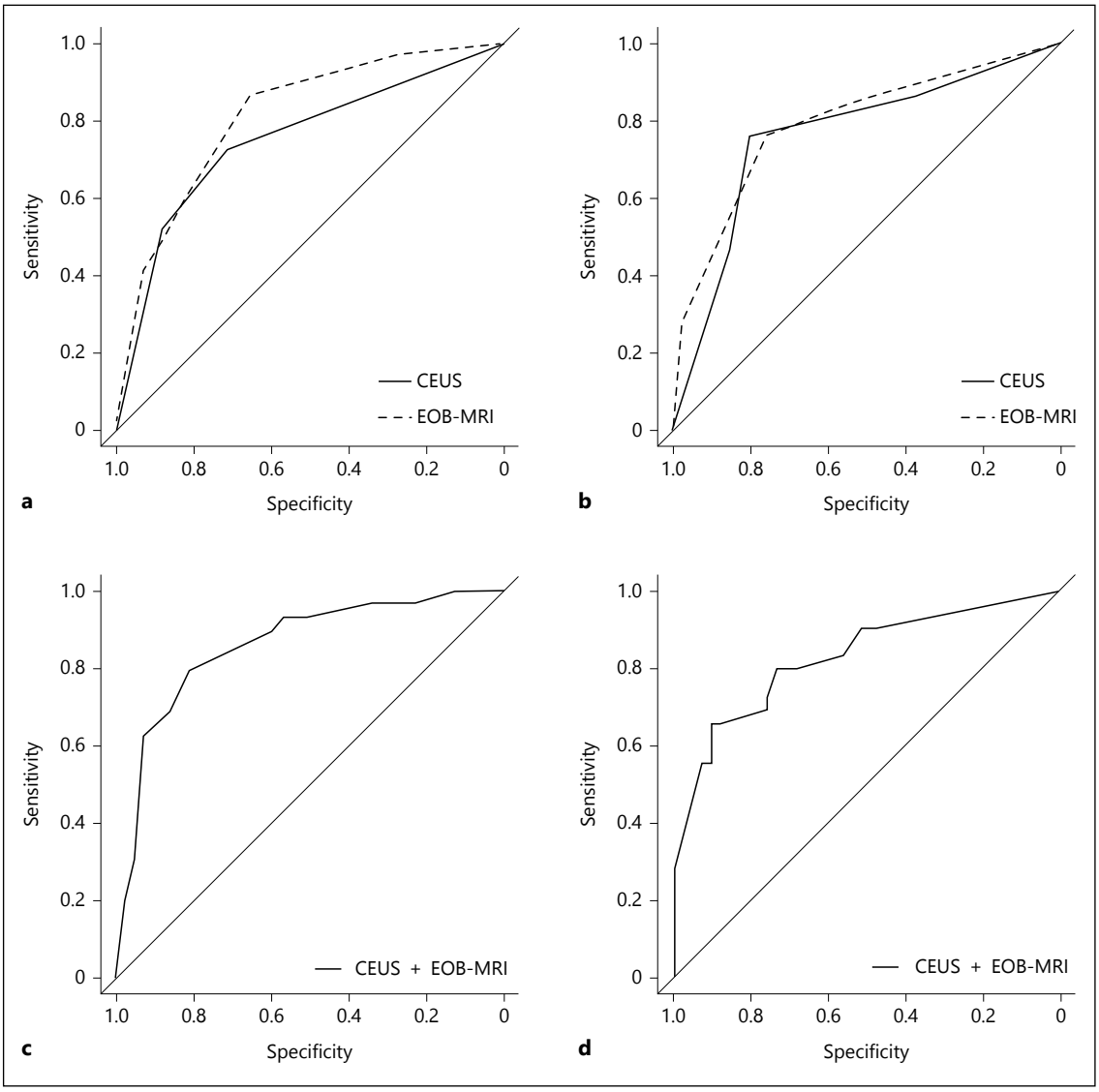

Fig. 2. ROC curves of the diagnosis of non-SN HCC based on a 4-point scale in 70 nodules evaluated by both modalities. **a** The AUCs evaluated by reader 1 for CEUS (solid line) and Gd-EOB-DTPA-enhanced MRI (dotted line) were 0.748 and 0.808, respectively. **b** The AUCs evaluated by reader 2 for CEUS (solid line) and Gd-EOB-DTPA-enhanced MRI (dotted line) were 0.759 and 0.787, respectively. **c** The AUC evaluated by reader 1 for the combination of CEUS and Gd-EOB-DTPA-enhanced MRI was 0.855. **d** The AUC evaluated by reader 2 for the combination of CEUS and Gd-EOB-DTPA-enhanced MRI was 0.824.

HCCs in this study were depicted as an isoechoic nodule on the post-vascular phase of CEUS. All of these nodules showed hypointensity on the hepatobiliary phase of Gd-EOB-DTPA-enhanced MRI. These results are compatible with the report by Ohama et al. [36] that described that most hypovascular well-differentiated HCCs are depicted as an isoechoic nodule during the post-vascular phase of CEUS, whereas almost all hypovascular well-differentiated HCCs show hypointensity on the hepatobiliary phase of Gd-EOB-DTPA-enhanced MRI.

We compared the diagnostic performance of CEUS with that of Gd-EOB-DTPA-enhanced MRI in 70 nodules evaluated by both modalities. We found the AUC values for the diagnosis of non-SN HCC were comparable between CEUS and Gd-EOB-DTPA. Moreover, the combination of CEUS and Gd-EOB-DTPA-enhanced MRI for the diagnosis of non-SN HCC yielded a higher AUC value.

Kobayashi et al. [37] recently reported the usefulness of combining Gd-EOB-DTPA-enhanced MRI and CEUS

for diagnosing the macroscopic classification of small HCC. They divided macroscopic findings of resected specimens into 5 types (SN-IM, small nodular type with distinct margin, SN-EG, CMN, and IF) and compared the diagnostic ability of Gd-EOB-DTPA-enhanced MRI, CEUS, and a combination of both modalities for diagnosing non-SN. They found the AUC values for Gd-EOB-DTPA-enhanced MRI and CEUS were 0.786 and 0.784, respectively. Moreover, they reported the AUC value for the combination of Gd-EOB-DTPA-enhanced MRI and CEUS for the diagnosis of non-SN HCC was 0.876. These results are consistent with ours, suggesting strongly that combined Gd-EOB-DTPA-enhanced MRI and CEUS are very useful for the prediction of macroscopic type of HCC.

There are some limitations to this study. First, this study was conducted retrospectively and the number of nodules is not large. A larger prospective study is needed to confirm our findings. Second, the criteria for determining extranodular growth are not clear. Therefore, the evaluation of macroscopic findings of HCC is a subjective assessment by individual readers. Third, we only evaluated the shape of the post-vascular phase in CEUS and the hepatobiliary phase of Gd-EOB-DTPA-enhanced MRI. The evaluation of the vascular phase of CEUS and the arterial phase of Gd-EOB-DTPA-enhanced MRI might have improved the diagnostic quality. Fourth, we did not evaluate the outcomes of patients with non-SN HCC. It is important to analyze survival and recurrence rates in patients with non-SN HCC in the future.

The diagnostic performance for macroscopic classification of nodular HCC of CEUS was comparable with that of Gd-EOB-DTPA-enhanced MRI, although some HCCs could not be evaluated by CEUS owing to lower detectability. The combination of the 2 modalities had a more accurate diagnostic performance.

Disclosure Statement

The authors declare that no financial or other conflicts of interest exist related to the content of the article.

References

1 Torre LA, Bray F, Siegel RL, Ferlay J, Lortet-Tieulent J, Jemal A: Global cancer statistics, 2012. CA Cancer J Clin 2015;65:87–108.
2 Umemura T, Ichijo T, Yoshizawa K, Tanaka E, Kiyosawa K: Epidemiology of hepatocellular carcinoma in Japan. J Gastroenterol 2009; 44(suppl 19):102–107.
3 Kanai T, Hirohashi S, Upton MP, Noguchi M, Kishi K, Makuuchi M, Yamasaki S, Hasegawa H, Takayasu K, Moriyama N, et al: Pathology of small hepatocellular carcinoma. A proposal for a new gross classification. Cancer 1987; 60:810–819.
4 Hui AM, Takayama T, Sano K, Kubota K, Akahane M, Ohtomo K, Makuuchi M: Predictive value of gross classification of hepatocellular carcinoma on recurrence and survival after hepatectomy. J Hepatol 2000;33:975–979.
5 Liver Cancer Study Group of Japan: General Rules for the Clinical and Pathological Study of Primary Liver Cancer, ed 3. Tokyo, Kanehara & Co., Ltd., 2010.
6 Kudo M, Matsui O, Izumi N, Iijima H, Kadoya M, Imai Y, Okusaka T, Miyayama S, Tsuchiya K, Ueshima K, Hiraoka A, Ikeda M, Ogasawara S, Yamashita T, Minami T, Yamakado K: JSH consensus-based clinical practice guidelines for the management of hepatocellular carcinoma: 2014 update by the liver cancer study group of Japan. Liver Cancer 2014;3:458–468.
7 Kudo M: Surveillance, diagnosis, treatment, and outcome of liver cancer in Japan. Liver Cancer 2015;4:39–50.
8 Clinical practice guidelines for hepatocellular carcinoma differ between Japan, United States, and Europe. Liver Cancer 2015;4:85–95.
9 Liu GJ, Wang W, Lu MD, Xie XY, Xu HX, Xu ZF, Chen LD, Wang Z, Liang JY, Huang Y, Li W, Liu JY: Contrast-enhanced ultrasound for the characterization of hepatocellular carcinoma and intrahepatic cholangiocarcinoma. Liver Cancer 2015;4:241–252.
10 Sontum PC, Ostensen J, Dyrstad K, Hoff L: Acoustic properties of NC100100 and their relation with the microbubble size distribution. Invest Radiol 1999;34:268–275.
11 Ramnarine KV, Kyriakopoulou K, Gordon P, McDicken NW, McArdle CS, Leen E: Improved characterisation of focal liver tumours: dynamic power Doppler imaging using NC100100 echo-enhancer. Eur J Ultrasound 2000;11:95–104.
12 Korenaga K, Korenaga M, Furukawa M, Yamasaki T, Sakaida I: Usefulness of sonazoid contrast-enhanced ultrasonography for hepatocellular carcinoma: comparison with pathological diagnosis and superparamagnetic iron oxide magnetic resonance images. J Gastroenterol 2009;44:733–741.
13 Hatanaka K, Chung H, Kudo M, Haji S, Minami Y, Maekawa K, Hayaishi S, Nagai T, Takita M, Kudo K, Ueda T, Tatsumi C, Kitai S, Ishikawa E, Yada N, Inoue T, Hagiwara S, Ueshima K: Usefulness of the post-vascular phase of contrast-enhanced ultrasonography with sonazoid in the evaluation of gross types of hepatocellular carcinoma. Oncology 2010; 78(suppl 1):53–59.
14 Tada T, Kumada T, Toyoda H, Ito T, Sone Y, Kaneoka Y, Maeda A, Okuda S, Otobe K, Takahashi K: Utility of contrast-enhanced ultrasound with perflubutane for diagnosing the macroscopic type of small nodular hepatocellular carcinomas. Eur Radiol 2014;24: 2157–2166.
15 Ichikawa T, Sano K, Morisaka H: Diagnosis of pathologically early HCC with EOB-MRI: experiences and current consensus. Liver Cancer 2014;3:97–107.
16 Schuhmann-Giampieri G, Schmitt-Willich H, Press WR, Negishi C, Weinmann HJ, Speck U: Preclinical evaluation of Gd-EOB-DTPA as a contrast agent in MR imaging of the hepatobiliary system. Radiology 1992;183: 59–64.
17 Hamm B, Staks T, Muhler A, Bollow M, Taupitz M, Frenzel T, Wolf KJ, Weinmann HJ, Lange L: Phase I clinical evaluation of Gd-EOB-DTPA as a hepatobiliary MR contrast agent: safety, pharmacokinetics, and MR imaging. Radiology 1995;195:785–792.
18 Vogl TJ, Kummel S, Hammerstingl R, Schellenbeck M, Schumacher G, Balzer T, Schwarz W, Muller PK, Bechstein WO, Mack MG, Sollner O, Felix R: Liver tumors: comparison of MR imaging with Gd-EOB-DTPA and Gd-DTPA. Radiology 1996;200:59–67.

19 Huppertz A, Balzer T, Blakeborough A, Breuer J, Giovagnoni A, Heinz-Peer G, Laniado M, Manfredi RM, Mathieu DG, Mueller D, Reimer P, Robinson PJ, Strotzer M, Taupitz M, Vogl TJ: Improved detection of focal liver lesions at MR imaging: multicenter comparison of gadoxetic acid-enhanced MR images with intraoperative findings. Radiology 2004;230:266–275.
20 Bluemke DA, Sahani D, Amendola M, Balzer T, Breuer J, Brown JJ, Casalino DD, Davis PL, Francis IR, Krinsky G, Lee FT Jr, Lu D, Paulson EK, Schwartz LH, Siegelman ES, Small WC, Weber TM, Welber A, Shamsi K: Efficacy and safety of MR imaging with liver-specific contrast agent: U.S. multicenter phase III study. Radiology 2005;237:89–98.
21 Saito K, Kotake F, Ito N, Ozuki T, Mikami R, Abe K, Shimazaki Y: Gd-EOB-DTPA enhanced MRI for hepatocellular carcinoma: quantitative evaluation of tumor enhancement in hepatobiliary phase. Magn Reson Med Sci 2005;4:1–9.
22 Huppertz A, Haraida S, Kraus A, Zech CJ, Scheidler J, Breuer J, Helmberger TK, Reiser MF: Enhancement of focal liver lesions at gadoxetic acid-enhanced MR imaging: correlation with histopathologic findings and spiral CT – initial observations. Radiology 2005; 234:468–478.
23 Fujinaga Y, Kadoya M, Kozaka K, Shinmura R, Matsui O, Takayama T, Yamamoto M, Kokudo N, Kawasaki S, Arii S: Prediction of macroscopic findings of hepatocellular carcinoma on hepatobiliary phase of gadolinium-ethoxybenzyl-diethylenetriamine pentaacetic acid-enhanced magnetic resonance imaging: correlation with pathology. Hepatol Res 2013; 43:488–494.
24 Tada T, Kumada T, Toyoda H, Ito T, Sone Y, Okuda S, Ogawa S, Igura T, Imai Y: Diagnostic accuracy for macroscopic classification of nodular hepatocellular carcinoma: comparison of gadolinium ethoxybenzyl diethylenetriamine pentaacetic acid-enhanced magnetic resonance imaging and angiography-assisted computed tomography. J Gastroenterol 2015; 50:85–94.
25 Makino Y, Imai Y, Fukuda K, Seki Y, Kogita S, Sawai Y, Igura T, Kurokawa M, Takamura M: Sonazoid-enhanced ultrasonography for the diagnosis of an intrapancreatic accessory spleen: a case report. J Clin Ultrasound 2011; 39:344–347.
26 Kogita S, Imai Y, Okada M, Kim T, Onishi H, Takamura M, Fukuda K, Igura T, Sawai Y, Morimoto O, Hori M, Nagano H, Wakasa K, Hayashi N, Murakami T: Gd-EOB-DTPA-enhanced magnetic resonance images of hepatocellular carcinoma: correlation with histological grading and portal blood flow. Eur Radiol 2010;20:2405–2413.
27 Swets JA: Measuring the accuracy of diagnostic systems. Science 1988;240:1285–1293.
28 Kundel HL, Polansky M: Measurement of observer agreement. Radiology 2003;228:303–308.
29 Kondo K, Chijiiwa K, Makino I, Kai M, Maehara N, Ohuchida J, Naganuma S: Risk factors for early death after liver resection in patients with solitary hepatocellular carcinoma. J Hepatobiliary Pancreat Surg 2005;12:399–404.
30 Ariizumi S, Kitagawa K, Kotera Y, Takahashi Y, Katagiri S, Kuwatsuru R, Yamamoto M: A non-smooth tumor margin in the hepatobiliary phase of gadoxetic acid disodium (Gd-EOB-DTPA)-enhanced magnetic resonance imaging predicts microscopic portal vein invasion, intrahepatic metastasis, and early recurrence after hepatectomy in patients with hepatocellular carcinoma. J Hepatobiliary Pancreat Sci 2011;18:575–585.
31 Nathan H, Schulick RD, Choti MA, Pawlik TM: Predictors of survival after resection of early hepatocellular carcinoma. Ann Surg 2009;249:799–805.
32 Ikai I, Arii S, Kojiro M, Ichida T, Makuuchi M, Matsuyama Y, Nakanuma Y, Okita K, Omata M, Takayasu K, Yamaoka Y: Reevaluation of prognostic factors for survival after liver resection in patients with hepatocellular carcinoma in a Japanese nationwide survey. Cancer 2004;101:796–802.
33 Grazi GL, Cescon M, Ravaioli M, Ercolani G, Gardini A, Del Gaudio M, Vetrone G, Cavallari A: Liver resection for hepatocellular carcinoma in cirrhotics and noncirrhotics. Evaluation of clinicopathologic features and comparison of risk factors for long-term survival and tumour recurrence in a single centre. Aliment Pharmacol Ther 2003;17(suppl 2):119–129.
34 Eguchi S, Takatsuki M, Hidaka M, Soyama A, Tomonaga T, Muraoka I, Kanematsu T: Predictor for histological microvascular invasion of hepatocellular carcinoma: a lesson from 229 consecutive cases of curative liver resection. World J Surg 2010;34:1034–1038.
35 Pawlik TM, Poon RT, Abdalla EK, Zorzi D, Ikai I, Curley SA, Nagorney DM, Belghiti J, Ng IO, Yamaoka Y, Lauwers GY, Vauthey JN: Critical appraisal of the clinical and pathologic predictors of survival after resection of large hepatocellular carcinoma. Arch Surg 2005; 140:450–457; discussion 457–458.
36 Ohama H, Imai Y, Nakashima O, Kogita S, Takamura M, Hori M, Seki Y, Sawai Y, Igura T, Fukuda K, Makino Y, Morimoto O, Ohsawa M, Sakamoto M, Murakami T: Images of sonazoid-enhanced ultrasonography in multistep hepatocarcinogenesis: comparison with Gd-EOB-DTPA-enhanced MRI. J Gastroenterol 2014;49:1081–1093.
37 Kobayashi T, Aikata H, Hatooka M, Morio K, Morio R, Kan H, Fujino H, Fukuhara T, Masaki K, Ohno A, Naeshiro N, Nakahara T, Honda Y, Murakami E, Kawaoka T, Tsuge M, Hiramatsu A, Imamura M, Kawakami Y, Hyogo H, Takahashi S, Chayama K: Usefulness of combining gadolinium-ethoxybenzyl-diethylenetriamine pentaacetic acid-enhanced magnetic resonance imaging and contrast-enhanced ultrasound for diagnosing the macroscopic classification of small hepatocellular carcinoma. Eur Radiol 2015;25:3272–3281.

Original Article

Digestive Diseases

Dig Dis 2016;34:671–678
DOI: 10.1159/000448834

Validation of Kinki Criteria, a Modified Substaging System, in Patients with Intermediate Stage Hepatocellular Carcinoma

Tadaaki Arizumi Kazuomi Ueshima Mina Iwanishi Tomohiro Minami Hirokazu Chishina Masashi Kono Masahiro Takita Satoshi Kitai Tatsuo Inoue Norihisa Yada Satoru Hagiwara Yasunori Minami Hiroshi Ida Toshiharu Sakurai Masayuki Kitano Naoshi Nishida Masatoshi Kudo

Department of Gastroenterology and Hepatology, Kindai University Faculty of Medicine, Osaka-Sayama, Japan

Key Words
Barcelona Clinic Liver Cancer stage B · Hepatocellular carcinoma · Kinki criteria · Transarterial chemoembolization

Abstract
Background: The standard treatment option that is available for patients with Barcelona Clinic Liver Cancer (BCLC) stage B hepatocellular carcinoma (HCC) is transarterial chemoembolization (TACE). However, the condition of the patients with BCLC stage B disease is heterogeneous showing different tumor statuses and Child–Pugh scores; treatment strategies other than TACE are frequently employed for the patients in this stage. Based on the subclassification system proposed by Bolondi et al. [Semin Liver Dis 2012;32:348–359], we developed the Kinki criteria focusing on a substaging for BCLC stage B disease, which is simpler and should be more suitable in actual clinical setting in Japan. In this study, we evaluated the performance of Kinki criteria. ***Summary:*** This study included 1,633 HCC patients who received first-line treatment at the Kindai University Hospital. Patients were classified into subgroups based on the Kinki criteria and the survival time was estimated for each group. There were 156 (33.3%) patients in subclass B1, 278 (59.3%) in B2, and 35 (7.4%) in B3. The median overall survival times and 95% CI for BCLC B subclasses B1, B2, and B3 were 4.3 years (3.7–4.9), 2.9 years (2.2–3.4), and 1.1 years (0.5–1.8), respectively ($p < 0.001$). ***Key Messages:*** Classification of HCC patients in BCLC stage B based on the Kinki criteria showed statistically significant differences in survival, indicating the performance of Kinki criteria, which takes Child–Pugh score and tumor status into account for determining treatment options for HCC in BCLC stage B.

Introduction

Hepatocellular carcinoma (HCC) is one of the leading causes of cancer-related death in patients with chronic liver disease; more than 700,000 of new cases are being diagnosed annually worldwide [1, 2]. The total number of deaths from liver cancer in Japan has obviously decreased after it reached its peak in 2004. In Japan, according to the recent analysis in 2012, 30,690 people died from liver cancer [3]. HCC may develop into a tumor with intrahepatic metastasis and further progress to tumors with extrahepatic metastases. The stage of HCC has been determined

KARGER

E-Mail karger@karger.com
www.karger.com/ddi

0257–2753/16/0346–0671$39.50/0

Masatoshi Kudo, MD, PhD
Department of Gastroenterology and Hepatology
Kindai University Faculty of Medicine
377-2 Ohno-Higashi, Osaka-Sayama 589-8511 (Japan)
E-Mail m-kudo@med.kindai.ac.jp

using the Barcelona Clinic Liver Cancer (BCLC) staging system. This system classifies the HCC into 5 stages, as stage 0, A, B, C, and D; BCLC stage B is considered an intermediate stage where transarterial chemoembolization (TACE) is recommended as the standard treatment option. According to the criteria, BCLC stage B disease includes a diverse status of the HCC patients with Child–Pugh scores 5–9 points and number of tumor of ≥4 in both lobes without vascular invasion or distant metastasis [4–7].

Although TACE is recommended for the treatment of patients with BCLC stage B disease [8, 9], TACE is reportedly not effective in patients with tumors size ≥7 cm in diameter and in those with tumor number ≥4 because TACE is less effective in cases with large and multiple tumors and it also impairs the hepatic function [10]. Zhong et al. [11, 13] and Lin et al. [12] reported that in patients with BCLC stage B and Child–Pugh A, the cumulative survival rate for surgical resection was significantly higher than that for TACE. Yin et al. [14] also reported the usefulness of surgical resection in a randomized clinical trial comparing the effectiveness of resection and TACE in patients with liver cancers beyond the Milan criteria. These reports suggested that surgical resection could be the best option for HCC patients with BCLC stage B disease. Furthermore, in some patients, TACE resistance due to the repeated TACE procedure should end up in the selection of other treatment strategies, including sorafenib and hepatic arterial infusion chemotherapy (HAIC) [15–21]. Although TACE is the most frequently selected treatment for the patients in BCLC stage B, other treatment options should be applied depending on the condition of individual patients in the clinical setting.

In a study investigating the indications for liver transplantation, Mazzaferro et al. [22] compared the Milan criteria, which are the conventional eligibility criteria for liver transplantation, with the up-to-7 criteria, and reported that these 2 sets of criteria showed no significant differences in cumulative survival rates after liver transplantation for HCC patients. Bolondi et al. [23] subdivided BCLC stage B into 4 subclasses (B1–B4) taking the Child–Pugh score, the up-to-7 criteria, portal vein thrombosis (PVT), and performance status (PS) into consideration. In terms of disease prognosis, this new substaging system is reportedly useful in the stratification of intermediate stage HCC patients because prognosis worsens as disease progresses. However, the Child–Pugh scores for subclasses B1–B3 were assigned in a complex manner. For example, subclasses B1, B2, and B3 were assigned the Child–Pugh scores of 5–7, 5–6, and 7 points, respectively. In addition, because PVT and PS have never been a defining factor for intermediate-stage HCC, these PVT and PS factors should be deleted from the substaging system. TACE is recommended as a first treatment option by the Bolondi substaging system, which appears to show no substantial difference in treatment strategies from the original BCLC stage.

Based on the concept proposed by Bolondi et al. [23], we proposed the Kinki criteria, which classified the BCLC B stage into 3 substages using the Child–Pugh classification (5–7 or 8, 9 points), the beyond Milan, and the up-to-7 criteria. Our substaging that is based on the Bolondi's subclassification is simple and easy to use compared to the Bolondi's substaging. Previously, we reported that the Kinki criteria could be well stratified based on the survival in patients who underwent TACE [24]. In this study, we further evaluated the performance of the Kinki criteria in the HCC patients irrespective of the type of treatment.

Material and Methods

Patients

Between 2001 and 2015, 1,633 patients who had received HCC treatment for the first time at the Kindai University Hospital and satisfied the inclusion criteria were selected for this retrospective study. All patients met the diagnostic criteria for HCC according to the American Association for the Study of the Liver guidelines. Clinicopathological variables including patient demographics, tumor staging (including the number of focal lesions and maximum diameter of contrast-enhancing disease), Child–Pugh class, and BCLC prognostic score were collected at the time of referral to our unit, prior to treatment [5]. The inclusion criteria for this study were HCC diagnosis based on histological examination or radiological findings, that is, an early enhancement followed by late washout by contrast-enhanced CT or dynamic MRI, PS of 0, and Child–Pugh class A or B. The exclusion criteria were concomitant antineoplastic treatment, without any treatment but best supportive care, and patients whose details were unknown because of missing medical records. Patients who died before the first imaging assessment were classified as having disease progression. Overall, survival (OS) was calculated from the date when treatment was first availed and the date of death. The study was approved by the research ethics committee at our institution. We posted research content at the outpatient department and on a website; we also gave the patients the right to refuse participation in the study.

Modified Bolondi Classification (Kinki Criteria)

For the determination of a substage based on the Kinki Criteria, the patients were classified to 3 substages according to Child–Pugh scores of 5–7 or 8, 9 points, and the beyond Milan and status of up-to-7 criteria were determined based on the number and diameter of the tumors. Subclass B1 is defined by Child–Pugh score

Table 1. Subclassification and treatment strategy of intermediate-stage HCC according to the modified Bolondi subclassification (Kinki criteria)

BCLC substage	B1	B2	B3	
Child–Pugh score	5–7	5–7	8, 9	
Beyond Milan and within up-to-7 criteria	In	Out	Any	
			In	Out
			B3-a	B3-b
Concept of treatment strategy	Curative intent	Non curative, palliative	Curative intent if within up-to-7 criteria	Palliative, no treatment
Treatment options	Resection Ablation Superselective cTACE	DEB-TACE[1] HAIC[2] Sorafenib[3]	Transplantation Ablation Superselective cTACE	HAIC Selective DEB-TACE
Alternatives	DEB-TACE (large, Child–Pugh score 7) B-TACE[4]	cTACE	DEB-TACE B-TACE HAIC	BSC

[1] DEB-TACE is recommended for patients with very large tumors (>6 cm).
[2] HAIC is recommended for patients with multiple tumors (>6 cm).
[3] Sorafenib is recommended for patients with liver function of Child–Pugh scores 5 and 6.
[4] B-TACE (balloon-occluded TACE) is recommended for patients with fewer tumors.

5–7 and within the up-to-7 criteria, subclass B2 is defined by Child–Pugh score of 5–7 and beyond the up-to-7 criteria, and subclass B3 is defined by Child–Pugh score 8, 9 and any status of up-to-7 criteria, respectively (table 1) [25].

Statistical Analysis

Univariate survival analysis was performed using the Kaplan–Meier method and the OS analysis ended at the time of death or it was censored at the time of the last follow-up visit. The survivals were compared between the groups using the log-rank test. For multiple comparisons, the Bonferroni correction was applied. p value <0.05 was considered to be the statistically significant difference. All analyses were performed using the SPSS Medical Pack for Windows version 10.0 (SPSS, Inc., Chicago, Ill., USA).

Results

Baseline Characteristics

Among the 1,633 patients who received HCC treatment for the first time during the clinical course of their disease, the tumors of 968 (59.3%), 469 (28.7%), and 196 (12.0%) patients were staged BCLC A, BCLC B, and BCLC C, respectively. The first-line treatment included radiofrequency ablation (RFA) in 694 patients (42.5%), resection in 200 patients (12.2%), conventional TACE (cTACE) in 550 patients (33.7%), TACE using drug-eluting beads (DEB-TACE) in 26 patients (1.6%) patients, sorafenib therapy in 114 patients (7.0%), and HAIC in 49 patients (3.0%).

Modified Bolondi Classification (Kinki Criteria)

Of the 469 BCLC stage B patients, 167 patients (35.6%) were within and 302 patients (64.4%) were beyond the up-to-7 criteria, respectively; and 264 (56.3%), 112 (23.9%), 58 (12.4%), 28 (6.0%), and 7 (1.5%) patients had Child–Pugh scores 5, 6, 7, 8, and 9, respectively. These patients were then classified according to the Kinki criteria as follows: 156 patients (33.3%) were classified into subclass B1, 278 patients (59.3%) into subclass B2, and 35 patients (7.4%) into subclass B3. The BCLC stage B group included 19 patients treated with RFA, 81 with surgical resection, 321 with cTACE, 17 with DEB-TACE, 12 with HAIC, and 19 with sorafenib. Within the BCLC stage B group, the distributions of patients according to treatment with RFA, surgical resection, cTACE, DEB-TACE, HAIC, and sorafenib were 16, 25, 113, 1, 1, and 0 patients, respectively, for BCLC subclass B1; 1, 55, 181, 13, 10, and 18 patients, respectively, for BCLC subclass B2; and 2, 1, 27, 3, 1, and 1 patients, respectively, for BCLC subclass B3 (fig. 1).

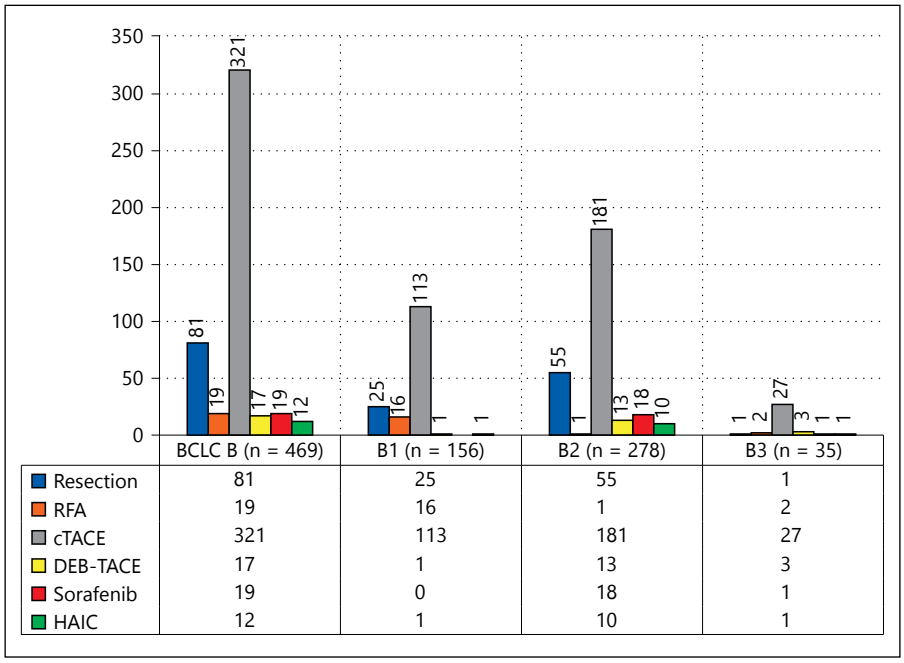

Fig. 1. Breakdown of the treatment strategies selected for the patients according to the subclasses of the Kinki criteria.

OS of the Patients

The median OS for all patients was 4.9 years (95% CI 4.5–5.4). We compared the OS times in BCLC stage A, BCLC stage B, and BCLC stage C groups using the Kaplan–Meier estimates. The comparisons of the survival curves showed that the median OS was 7.1 years (95% CI 6.5–8.1) in the BCLC stage A group, 3.2 years (95% CI 2.8–3.7) in the BCLC stage B group, and 0.7 years (95% CI 0.6–1.0) in the BCLC stage C group ($p < 0.001$; fig. 2). In the BCLC stage B group, the OS times were compared between patients who were categorized as within or beyond the up-to-7 criteria, demonstrating median survival times of 4.2 years (95% CI 3.5–4.8) and 2.5 years (95% CI 2.1–3.2), respectively ($p = 0.004$; fig. 3a). In addition, the duration of OS were compared between patients having Child–Pugh scores of 5, 6, 7, 8, and 9. The median OS times in patients with Child–Pugh scores 5, 6, 7, 8, and 9 were 3.9 years (95% CI 3.3–4.4), 2.4 years (95% CI 1.6–3.1), 2.4 years (95% CI 1.3–3.4), 1.3 years (95% CI 0.8–1.9), and 0.4 years (95% CI 0.1–0.7), respectively ($p < 0.001$). Pairwise comparisons confirmed a significantly longer OS period in the group of patients with Child–Pugh score 5 than in those with Child–Pugh score 6 ($p < 0.001$). Similarly, the OS time was significantly longer in the group of patients with Child–Pugh score 7 than those in the group with Child–Pugh score 8 ($p = 0.001$). In contrast, no significant differences in OS were detected between the groups of the Child–Pugh score 6 and Child–Pugh score 7 ($p = 0.68$), and between the groups of the Child–Pugh score 8 and Child–Pugh score 9 ($p = 0.98$; fig. 3b).

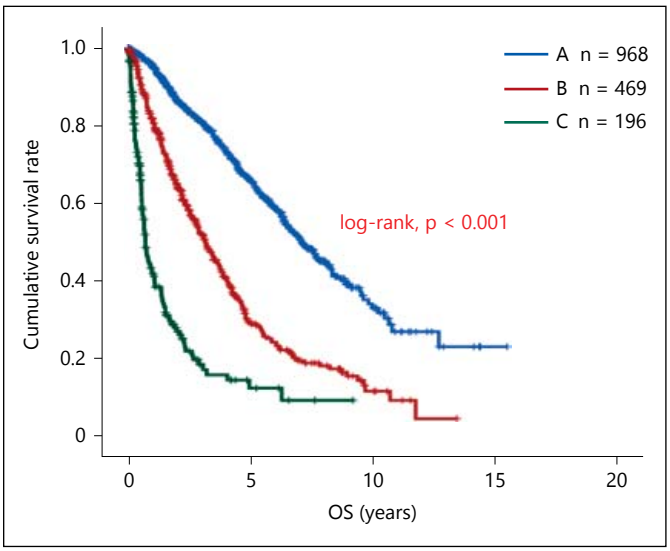

Fig. 2. OS according to the BCLC staging system. The comparisons of the survival curves showed that the median OS was 7.1 (95% CI 6.5–8.1) years in the BCLC stage A group, 3.2 (95% CI 2.8–3.7) years in the BCLC stage B group, and 0.7 (95% CI 0.6–1.0) years in the BCLC stage C group ($p < 0.001$).

Subsequently, the BCLC stage B patients were classified into the B1–B3 subclasses using the Kinki criteria, and OS times were compared between the patients in the A,

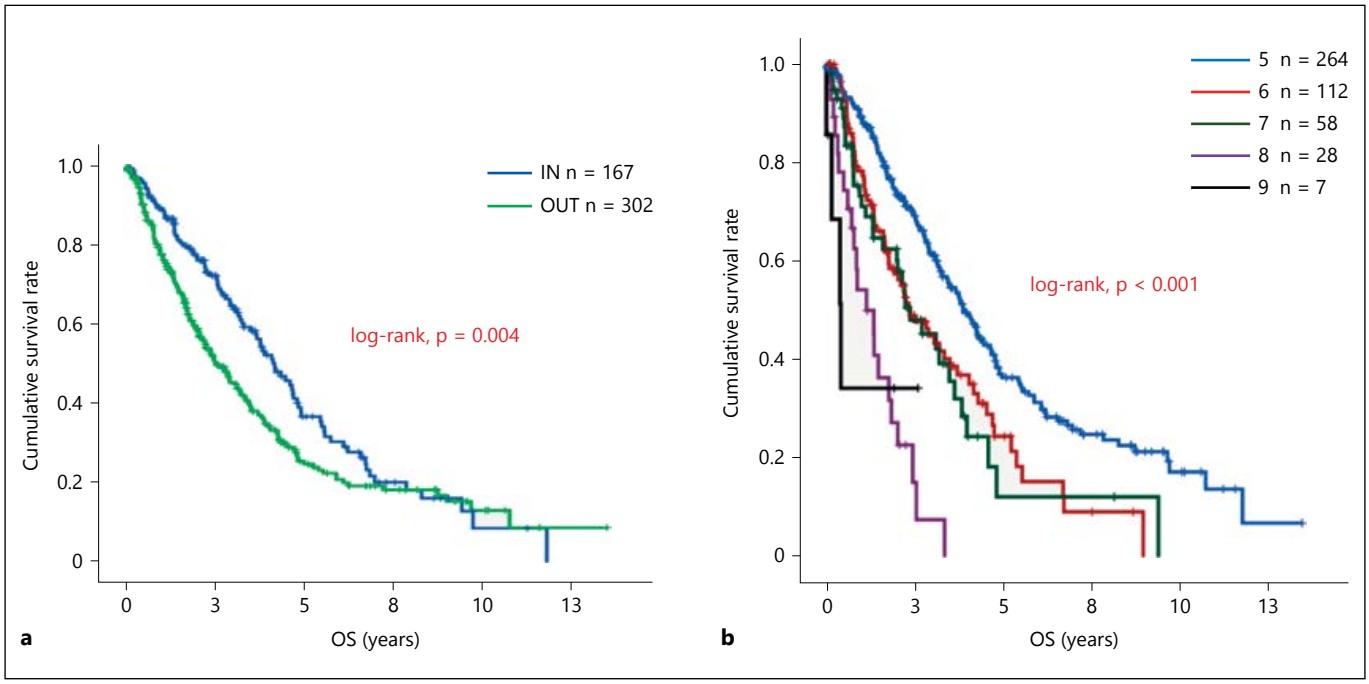

Fig. 3. OS according to up-to-7 criteria (**a**) and Child–Pugh score (**b**). In the BCLC stage B patients, the OS was compared between the within and beyond cases according to the up-to-7 criteria, demonstrating median survival of 4.2 (95% CI 3.5–4.8) and 2.5 years (95% CI 2.1–3.2), respectively (p = 0.004). The OS among patients having Child–Pugh scores of 5, 6, 7, 8, and 9 points were compared. The median OS was 3.9 (95% CI 3.3–4.4) years in patients with Child–Pugh scores of 5; 2.4 (95% CI 1.6–3.1) years in patients with Child–Pugh scores of 6; 2.4 (95% CI 1.3–3.4) years in patients with Child–Pugh scores of 7; 1.3 (95% CI 0.8–1.9) years in patients with Child–Pugh scores of 8; and 0.4 (95% CI 0.1–0.7) years in patients with Child–Pugh scores of 9 (p < 0.001).

B1, B2, B3, and C groups. The median OS times for patients with BCLC stage A, B1, B2, B3, and C were 7.1 years (95% CI 6.5–8.1), 4.3 years (95% CI 3.7–4.9), 2.9 years (95% CI 2.2–3.4), 1.1 years (95% CI 0.5–1.8), and 0.7 years (95% CI 0.6–1.0; p < 0.001). Pairwise comparisons confirmed a significantly longer OS in the patients with BCLC stage A than those in the BCLC subclass B1 group (p < 0.001). Similarly, the OS time was significantly longer in patients with BCLC subclass B1 than those in the BCLC subclass B2 (p = 0.007), and it was significantly longer in the BCLC subclass B2 than those in the BCLC subclass B3 group (p < 0.001). In contrast, no significant differences were detected between the OS times of the patients with BCLC subclass B3 and with BCLC stage C (p = 0.97; fig. 4).

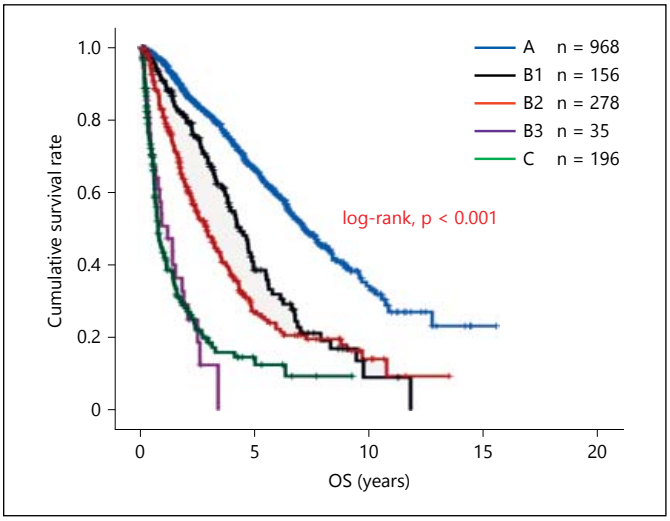

Fig. 4. OS according to the modified Bolondi subclassification (Kinki criteria). The median OS was 7.1 (95% CI 6.5–8.1) years in the BCLC stage A group, and 4.3 (95% CI 3.7–4.9) years in the BCLC subclass stage B1 group, 2.9 (95% CI 2.2–3.4) years in the BCLC subclass stage B2 group, 1.1 (95% CI 0.5–1.8) years in the BCLC subclass stage B3 group, and 0.7 (95% CI 0.6–1.0) years in the BCLC stage C group (p < 0.001).

Discussion

Because the BCLC stage B disease encompasses a diverse and heterogeneous group of patients in terms of liver function, tumor diameter, and the number of tumors, we proposed the Kinki criteria for the subclassification of

the patients having this disease stage. At our hospital, treatment strategies other than cTACE had been selected as first-line treatment in approximately 30% of the patients with BCLC stage B HCC. Although alternative treatment to the cTACE had been applied for them, patients were stratified into subclasses based on the Kinki criteria and statistically significant differences were observed between the subclasses.

In this study, we also examined the patients according to the Child–Pugh score. The OS times did not differ significantly between patients with Child–Pugh scores of 8 and 9, and the outcomes were poor in patients with either score. However, the OS of patients with Child–Pugh score 7 was significantly longer than that of patients with Child–Pugh score 8. There was no statistically significant difference between the OS times of patients with Child–Pugh scores of 6 and 7. In the Bolondi subclassification, the patients with Child–Pugh scores of 6 and 7 were classified into subclasses B2 and B3, respectively. In this study, although a statistically significant difference was observed between the OS times of patients with Child–Pugh scores of 5 and 6, there was no statistically significant difference between the OS times of patients with Child–Pugh scores of 6 and 7. Thus, it might not be necessary to classify patients with Child–Pugh scores of 6 and 7 into different subclasses. We classified these patients into one subclass, which makes our substaging system unique – simpler than that of the Bolondi subclassification system.

TACE is the only recommended standard therapy for BCLC stage B HCC [6]. However, in our hospital, approximately 30% of the patients who were diagnosed with BCLC stage B HCC and received first-line treatment had been treated by other treatment methods than cTACE. Although cTACE is generally accepted as palliative therapy, super-selective cTACE might help achieve complete cure in some patients [26, 27]. However, recurrent tumors after TACE might be resistant to TACE [18, 28–31]; it is difficult to achieve effective embolization after the repeated TACE procedure because the feeding vessels are irregularly narrowed due to granulomatous arteritis [32]. Thus, first-line treatment strategies should be as curative as possible. Because it is possible to achieve complete cure in subclass B1 patients [33], some of them were treated with surgical procedures or RFA. In those treated with cTACE, super selective cTACE was performed in an attempt to obtain complete cure. In subclass B2, treatment with sorafenib or HAIC was selected in some patients who were expected to be no response to TACE because of multiple tumors in both of the lobes. Moreover, because subclass B3 patients have impaired liver function, cTACE might cause serious complications; some subclass B3 patients with impaired liver function were treated with HAIC. Among patients within the up-to-7 criteria, some BCLC subclass B3 patients were treated with RFA, while their liver function was carefully monitored. Although TACE is frequently selected for the treatment of BCLC stage B HCC patients, other treatment strategies should be better for the survival in some patients.

We previously reported that statistically significant differences were observed in the survival times of patients treated with cTACE who were stratified into subclasses based on the Kinki criteria. In this study, we stratified patients treated with other treatment strategies as well as those treated with cTACE, and statistically significant differences were also observed between the survival times of subclasses, which are consistent with the findings of our previous study conducted only in patients treated with cTACE. In our previous study, we had not shown a statistically significant difference between the survival times of patients with BCLC stage A and subclass B1 disease. However, in this study, we showed a statistically significant difference between the survival times of patients in both groups because among the patients in the BCLC stage A group, some patients received curative treatment such as surgical resection or RFA. When the Kinki criteria were applied only to patients with BCLC stage B disease, they were stratified into the subclasses as described in our previous report. However, there was no clear distinction between subclass B3 and BCLC stage C patients, and no statistically significant difference in survival time was observed between these groups. It appears that it is possible to achieve complete cure in patients with subclass B1 stage disease via the selection of a more curative treatment option or through super selective cTACE. Although complete cure might be difficult to achieve in patients with subclass B2 disease, aggressive treatment modalities should be administered to improve liver function. Particularly in this subclass, tumor status should be carefully considered while selecting the appropriate treatment strategy. In patients with subclass B3 disease, because aggressive treatment is highly likely to worsen survival outcomes owing to impaired liver function, we suggest the selection of treatment strategies that exert few adverse effects on the liver function.

Conclusion

Patients with BCLC stage B HCC were stratified into subclasses according to the Kinki criteria, and statistically significant differences were observed between the sur-

vival times of different subclasses. Although TACE is recommended for the treatment of BCLC stage B patients, various other treatment strategies are frequently selected in the actual clinical setting. The Kinki criteria appears to be effective in the subclassification of BCLC stage B patients, which is very diverse even in terms of only tumor factors and liver function. The findings of this single-center retrospective study suggesting the effectiveness of Kinki criteria for selecting the appropriate treatment option should be validated in multicenter and prospective studies in the future.

Disclosure Statement

Authors declare no conflict of interest.

References

1 Forner A, Llovet JM, Bruix J: Hepatocellular carcinoma. Lancet 2012;379:1245–1255.
2 Bruix J, Gores GJ, Mazzaferro V: Hepatocellular carcinoma: clinical frontiers and perspectives. Gut 2014;63:844–855.
3 Kudo M: Surveillance, diagnosis, treatment, and outcome of liver cancer in Japan. Liver Cancer 2015;4:39–50.
4 Liccioni A, Reig M, Bruix J: Treatment of hepatocellular carcinoma. Dig Dis 2014;32:554–563.
5 Llovet JM, Bru C, Bruix J: Prognosis of hepatocellular carcinoma: the BCLC staging classification. Semin Liver Dis 1999;19:329–338.
6 Bruix J, Sherman M: Management of hepatocellular carcinoma: an update. Hepatology 2011;53:1020–1022.
7 European Association for the Study of the Liver; European Organisation for Research and Treatment of Cancer: EASL-EORTC clinical practice guidelines: management of hepatocellular carcinoma. J Hepatol 2012;56:908–943.
8 Kudo M: Locoregional therapy for hepatocellular carcinoma. Liver Cancer 2015;4:163–164.
9 Tsurusaki M, Murakami T: Surgical and locoregional therapy of HCC: TACE. Liver Cancer 2015;4:165–175.
10 Yamakado K, Miyayama S, Hirota S, Mizunuma K, Nakamura K, Inaba Y, Maeda H, Matsuo K, Nishida N, Aramaki T, Anai H, Koura S, Oikawa S, Watanabe K, Yasumoto T, Furuichi K, Yamaguchi M: Subgrouping of intermediate-stage (BCLC stage B) hepatocellular carcinoma based on tumor number and size and Child-Pugh grade correlated with prognosis after transarterial chemoembolization. Jpn J Radiol 2014;32:260–265.
11 Zhong JH, Ke Y, Gong WF, Xiang BD, Ma L, Ye XP, Peng T, Xie GS, Li LQ: Hepatic resection associated with good survival for selected patients with intermediate and advanced-stage hepatocellular carcinoma. Ann Surg 2014;260:329–340.
12 Lin CT, Hsu KF, Chen TW, Yu JC, Chan DC, Yu CY, Hsieh TY, Fan HL, Kuo SM, Chung KP, Hsieh CB: Comparing hepatic resection and transarterial chemoembolization for Barcelona clinic liver cancer (BCLC) stage B hepatocellular carcinoma: change for treatment of choice? World J Surg 2010;34:2155–2161.
13 Zhong JH, Xiang BD, Gong WF, Ke Y, Mo QG, Ma L, Liu X, Li LQ: Comparison of long-term survival of patients with BCLC stage B hepatocellular carcinoma after liver resection or transarterial chemoembolization. PLoS One 2013;8:e68193.
14 Yin L, Li H, Li AJ, Lau WY, Pan ZY, Lai EC, Wu MC, Zhou WP: Partial hepatectomy vs. transcatheter arterial chemoembolization for resectable multiple hepatocellular carcinoma beyond Milan criteria: a RCT. J Hepatol 2014;61:82–88.
15 Ogasawara S, Chiba T, Ooka Y, Kanogawa N, Motoyama T, Suzuki E, Tawada A, Kanai F, Yoshikawa M, Yokosuka O: Efficacy of sorafenib in intermediate-stage hepatocellular carcinoma patients refractory to transarterial chemoembolization. Oncology 2014;87:330–341.
16 Kudo M, Matsui O, Izumi N, Kadoya M, Okusaka T, Miyayama S, Yamakado K, Tsuchiya K, Ueshima K, Hiraoka A, Ikeda M, Ogasawara S, Yamashita T, Minami T: Transarterial chemoembolization failure/refractoriness: JSH-LCSGJ criteria 2014 update. Oncology 2014;87(suppl 1):22–31.
17 Arizumi T, Ueshima K, Chishina H, Kono M, Takita M, Kitai S, Inoue T, Yada N, Hagiwara S, Minami Y, Sakurai T, Nishida N, Kudo M: Validation of the criteria of transcatheter arterial chemoembolization failure or refractoriness in patients with advanced hepatocellular carcinoma proposed by the LCSGJ. Oncology 2014;87(suppl 1):32–36.
18 Arizumi T, Ueshima K, Minami T, Kono M, Chishina H, Takita M, Kitai S, Inoue T, Yada N, Hagiwara S, Minami Y, Sakurai T, Nishida N, Kudo M: Effectiveness of sorafenib in patients with transcatheter arterial chemoembolization (TACE) refractory and intermediate-stage hepatocellular carcinoma. Liver Cancer 2015;4:253–262.
19 Raoul JL, Gilabert M, Piana G: How to define transarterial chemoembolization failure or refractoriness: a European perspective. Liver Cancer 2014;3:119–124.
20 Obi S, Sato S, Kawai T: Current status of hepatic arterial infusion chemotherapy. Liver Cancer 2015;4:188–199.
21 Ueshima K, Kudo M, Tanaka M, Kumada T, Chung H, Hagiwara S, Inoue T, Yada N, Kitai S: Phase I/II study of sorafenib in combination with hepatic arterial infusion chemotherapy using low-dose cisplatin and 5-fluorouracil. Liver Cancer 2015;4:263–273.
22 Mazzaferro V, Llovet JM, Miceli R, Bhoori S, Schiavo M, Mariani L, Camerini T, Roayaie S, Schwartz ME, Grazi GL, Adam R, Neuhaus P, Salizzoni M, Bruix J, Forner A, De Carlis L, Cillo U, Burroughs AK, Troisi R, Rossi M, Gerunda GE, Lerut J, Belghiti J, Boin I, Gugenheim J, Rochling F, Van Hoek B, Majno P: Predicting survival after liver transplantation in patients with hepatocellular carcinoma beyond the Milan criteria: a retrospective, exploratory analysis. Lancet Oncol 2009;10:35–43.
23 Bolondi L, Burroughs A, Dufour JF, Galle PR, Mazzaferro V, Piscaglia F, Raoul JL, Sangro B: Heterogeneity of patients with intermediate (BCLC B) hepatocellular carcinoma: proposal for a subclassification to facilitate treatment decisions. Semin Liver Dis 2012;32:348–359.
24 Arizumi T, Ueshima K, Iwanishi M, Minami T, Chishina H, Kono M, Takita M, Kitai S, Inoue T, Yada N, Hagiwara S, Ida H, Minami Y, Sakurai T, Kitano M, Nishida N, Kudo M: Validation of a modified substaging system (Kinki criteria) for patients with intermediate-stage hepatocellular carcinoma. Oncology 2015;89(suppl 2):47–52.
25 Kudo M, Arizumi T, Ueshima K, Sakurai T, Kitano M, Nishida N: Subclassification of BCLC B stage hepatocellular carcinoma and treatment strategies: proposal of modified Bolondi's subclassification (Kinki criteria). Dig Dis 2015;33:751–758.
26 Miyayama S, Matsui O, Yamashiro M, Ryu Y, Kaito K, Ozaki K, Takeda T, Yoneda N, Notsumata K, Toya D, Tanaka N, Mitsui T: Ultraselective transcatheter arterial chemoembolization with a 2-F tip microcatheter for small hepatocellular carcinomas: relationship between local tumor recurrence and visualization of the portal vein with iodized oil. J Vasc Interv Radiol 2007;18:365–376.
27 Matsui O, Kadoya M, Yoshikawa J, Gabata T, Arai K, Demachi H, Miyayama S, Takashima T, Unoura M, Kogayashi K: Small hepatocellular carcinoma: treatment with subsegmental transcatheter arterial embolization. Radiology 1993;188:79–83.

28 Miyayama S, Matsui O, Zen Y, Yamashiro M, Hattori Y, Orito N, Matsui K, Tsuji K, Yoshida M, Sudo Y: Portal blood supply to locally progressed hepatocellular carcinoma after transcatheter arterial chemoembolization: observation on CT during arterial portography. Hepatol Res 2011;41:853–866.
29 Wang B, Xu H, Gao ZQ, Ning HF, Sun YQ, Cao GW: Increased expression of vascular endothelial growth factor in hepatocellular carcinoma after transcatheter arterial chemoembolization. Acta Radiol 2008;49:523–529.
30 Zen C, Zen Y, Mitry RR, Corbeil D, Karbanova J, O'Grady J, Karani J, Kane P, Heaton N, Portmann BC, Quaglia A: Mixed phenotype hepatocellular carcinoma after transarterial chemoembolization and liver transplantation. Liver Transpl 2011;17:943–954.
31 Kojiro M, Sugihara S, Kakizoe S, Nakashima O, Kiyomatsu K: Hepatocellular carcinoma with sarcomatous change: a special reference to the relationship with anticancer therapy. Cancer Chemother Pharmacol 1989;23(suppl):S4–S8.
32 Ishikura H, Sotozaki Y, Adachi H, Sato M, Yoshiki T: Granulomatous arteritis with massive eosinophilic leukocyte infiltration and transient peripheral eosinophilia subsequent to transarterial embolization therapy with a gelatin sponge. Acta Pathol Jpn 1991;41:618–622.
33 Lin CC, Cheng YT, Chen M WT, Lin SM: The effectiveness of multiple electrode radiofrequency ablation in patients with hepatocellular carcinoma with lesions more than 3 cm in size and Barcelona clinic liver cancer stage A to B2. Liver Cancer 2016;5:8–20.

Original Article

Digestive Diseases

Dig Dis 2016;34:640–649
DOI: 10.1159/000448825

Comparison of Two-Dimensional Shear Wave Elastography and Real-Time Tissue Elastography for Assessing Liver Fibrosis in Chronic Hepatitis B

Tao Wu[a] Ping Wang[a] Ting Zhang[a] Jian Zheng[a] Shuoyang Li[b] Jie Zeng[a]
Masatoshi Kudo[c] Rongqin Zheng[a]

[a]Department of Medical Ultrasonic, The Third Affiliated Hospital of Sun Yat-sen University, and [b]Department of Radiology, The First Affiliated Hospital of Sun Yat-sen University, Guangzhou, China; [c]Department of Gastroenterology and Hepatology, Kindai University Faculty of Medicine, Osaka-Sayama, Japan

Key Words
Shear-wave elastography · Real-time tissue elastography
Hepatitis B virus · Liver fibrosis

Abstract
Background: Noninvasive assessment of liver fibrosis has important clinical significance. Different techniques including two-dimensional shear-wave elastography (2D SWE) and real-time tissue elastography (RTE) are reported to be useful for the noninvasive diagnosis of hepatic fibrosis. All these techniques are affected by many factors. How to choose a reasonable method needs further studies. ***Purpose:*** This study was conducted to comparatively assess the diagnostic performance of 2D SWE and RTE in patients with Chronic Hepatitis B (CHB) and influence of inflammation on the stiffness values obtained by both techniques, so as to objectively assess the reasonable choice between these 2 elastography techniques for noninvasive assessment of hepatic fibrosis in clinical practice. ***Materials and Methods:*** Four-hundred and thirty-seven patients with CHB meeting the inclusion criteria were enrolled in the study. All patients underwent liver stiffness measurements by using 2D SWE and RTE on the same day. Histologic fibrosis was staged and inflammation activity was graded based on the METAVIR scoring system on liver biopsy specimens. ***Results:*** The liver stiffness values by using 2D SWE and RTE both increased in parallel with the degree of liver fibrosis and the grade of inflammation. However, the diagnostic efficacy of significant fibrosis and cirrhosis using 2D SWE was significantly higher than that of RTE. The 2D SWE measurement values were statistically different in different alanine aminotransferase (ALT) levels and METAVIR activity grades; however, no statistically significant differences were observed by using RTE. The diagnostic efficacy of 2D SWE significantly varied with elevated ALT levels compared with RTE. ***Conclusion:*** 2D SWE was more accurate than RTE in the assessment of significant fibrosis and cirrhosis in patients with CHB. Compared with RTE, the measurement values and diagnostic performance obtained by 2D SWE were prone to be more easily affected by the inflammation fluctuations.

T.W. and P.W. contributed equally to this work.

Rongqin Zheng, MD, PhD
Department of Ultrasound
The Third Affiliated Hospital of Sun Yat-sen University
No. 600 Tianhe Road, Guangzhou 510630 (China)
E-Mail zhengrq@mail.sysu.edu.cn

Masatoshi Kudo, MD, PhD
Department of Gastroenterology and Hepatology
Kinki University School of Medicine
377-2 Ohno-Higashi, Osaka-Sayama, Osaka 589-8511 (Japan)
E-Mail m-kudo@med.kindai.ac.jp

KARGER

E-Mail karger@karger.com
www.karger.com/ddi

0257–2753/16/0346–0640$39.50/0

Introduction

The assessment of liver fibrosis has important significance in deciding on the best therapeutic option and for predicting the prognosis of chronic liver diseases such as hepatitis B virus (HBV) infection or nonalcoholic fatty liver disease [1, 2], which has a risk of causing hepatocellular carcinoma [3–7] and liver failure. Liver biopsy (LB) has been considered as the 'gold standard' for the assessment of liver fibrosis in clinical practice; however, as an invasive procedure, it has some potential risks and complications, such as bleeding and pain and sometimes even death [8–11], which may cause patients discomfort during biopsy. Therefore, it is urgently necessary to assess liver fibrosis noninvasively in the increasing number of patients with chronic liver diseases.

Elastography, mainly consisting of shear-wave elastography and strain elastography, is reported to be useful for the noninvasive diagnosis of hepatic fibrosis by measuring liver stiffness and has become a hot research topic in recent years [12–18]. Transient elastography (TE), a shear-wave elastography, is now accepted as a noninvasive and validated method for the detection of significant fibrosis and cirrhosis, a role that has been confirmed by considerable scientific evidence [19–22]. However, several studies have also noted that the results of liver stiffness measurements (LSMs) by TE can be affected by many factors including necroinflammatory activity, extrahepatic cholestasis, and obesity [23–27]. Acute inflammation can lead to increased stiffness values and thus affects the accuracy and application scope of TE evaluations [28]. Two-dimensional shear-wave elastography (2D SWE) is a newly introduced shear-wave elastography. In recent years, an increasing number of studies have confirmed its noninvasive liver fibrosis evaluation capacity [29, 30]. As a shear-wave elastography, 2D SWE might also be affected by inflammation or other factors. Real-time tissue elastography (RTE) of the strain elastography has been demonstrated to noninvasively assess liver fibrosis by several studies [31–33]. Moreover, RTE may not be affected by inflammation [34, 35], although the literature is inconclusive on this topic.

Until now, no report has compared 2D SWE and RTE in the assessment of liver fibrosis or has a study explored the influence of inflammation on these 2 measurement values. Thus, this study intends to apply these 2 techniques consecutively in patients with CHB and aims to comparatively evaluate the diagnostic performance of their assessments of liver fibrosis and the influence of inflammation on both measurement values in hopes of objectively guiding reasonable option of elastography for noninvasive assessment of hepatic fibrosis in clinical practice.

Patients and Methods

Patients and Study Procedures

This was a single-center, cross-sectional study. Our institutional Ethics Committee approved the study protocols, and the participants were enrolled after obtaining their written informed consent. We enrolled 437 consecutive patients with CHB who were admitted to our hospital to undergo percutaneous ultrasound-guided LB followed by 2D SWE and RTE examination between September 2011 and July 2014. In these patients, CHB was defined as the presence of hepatitis B surface antigen and HBV DNA was present in the serum. The exclusion criteria included the following: failure of 2D SWE or RTE examination, lack of consent for the 2D SWE or RTE examination, chronic hepatitis caused by another hepatitis virus or disease, biopsy samples less than 15 mm long or with fewer than 6 portal tracts under the microscope. Blood samples were obtained on the day of LB examination. The following data were collected from all patients: gender; age; body mass index (BMI); biochemical tests of alanine aminotransferase (ALT), aspartate aminotransferase, alkaline phosphatase, and gamma-glutamyl transferase; total bilirubin and serum albumin levels; platelet counts; and prothrombin activity (table 1).

First, we calculated the correlation between the LSMs and the histological liver analysis findings, and then we compared the diagnosis performance of significant fibrosis (≥F2) and cirrhosis (F4) by 2D SWE and RTE, and third, we analyzed the influence of inflammation on the values obtained by 2D SWE and RTE. Finally, we divided the patients into 2 groups based on the ALT levels and compared their diagnostic performance using the cut-off calculated from all patients in these 2 groups.

Liver Stiffness Measurement

A single sonographer with 8 years of US experience and at least 3 months of experience performing 2D SWE and RTE examinations who was blinded to the clinical data performed 2D SWE and RTE using an Aixplorer US system (SuperSonic Imagine, Aix-en-Provence, France) with a SC6-1 convex broadband probe (1–6 MHz) and a HI-VISION Ascendus (Hitachi Aloka Medical, Tokyo, Japan) with an EUP-L52 linear probe (3–7 MHz), respectively.

Two-Dimensional Shear-Wave Elastography

2D SWE was performed with the patient in the supine position and the right arm at maximum abduction. The probe was positioned in the intercostal spaces of the right lobe of the liver. The operator chose the target area of the liver guided by a conventional, real-time B-mode image. As the patients held their breath, the 2D SWE was launched, and we placed the stiffness sample box, approximately 4 × 3 cm, at least 1 cm under the liver capsule and in an area of liver parenchyma free of large vessels. Five 2D SWE images were obtained for each patient and the median value of the 5 LSMs was used for the statistical analysis [15, 30]. A 2D SWE examination was considered a failure if no valid measurement was obtained in the sample box [30].

Table 1. Demographic data, blood tests, and histologic results in patients with CHB

Characteristics	n = 437
Gender, men, n (%)	334 (76.4)
Age, years, mean (SD; range)	35.8 (10.2; 18–85)
BMI, kg/m^2, mean (SD; range)	21.8 (3.0; 14.4–32.9)
AST, IU/l, median (IQR; range)	33 (25–49; 9–474)
ALT, IU/l, median (IQR; range)	43 (28–72; 4–976)
Alkaline phosphatase, IU/l, mean (SD; range)	75.3 (32.3; 27–324)
Gamma-glutamyl transferase, IU/l, median (IQR; range)	32.0 (20.0–64.0; 7–1,333)
Total bilirubin, μmol/l, median (IQR; range)	13.8 (10.5–18.4; 3.7–247.7)
Serum albumin, g/l, median (IQR; range)	43.9 (40.7–46.2; 24.1–51.4)
Platelets count, 10^3/mm^3, median (IQR; range)	186 (150–224; 47–472)
Prothrombin activity, n (%), mean (SD; range)	98.6 (13.2; 57–139)
Fibrosis score, METAVIR, n (%)	
F0	78 (17.8)
F1	153 (35.0)
F2	83 (19.0)
F3	62 (14.2)
F4	61 (14.0)
Activity grade, METAVIR, n (%)	
A0	14 (3.2)
A1	200 (45.8)
A2	123 (28.1)
A3	100 (22.9)

Real-Time Tissue Elastography

The examinations were also performed on the right lobe of the liver through the intercostal spaces. The appropriate position was selected as guided by the B-mode images. The patients were asked to stop breathing for approximately 5–10 s, and then we placed the ROI of the strain image, approximately 2.5 × 2.5 cm, more than 1 cm below the surface of the liver in the selected position. Additionally, we avoided placing the ROI deep inside the liver, near large vessels or in a position attenuated by the lungs or ribs. The best RTE images were selected for the final analysis. An average liver fibrosis index (LFI) of the best 3–5 images for each patient was used for the statistical analysis. An RTE examination was considered a failure because of no valid measurement in the ROI and no a sufficient number of suitable RTE images [31].

Liver Histologic Assessment

A percutaneous LB was performed in the right liver lobe with a 16-gauge Magnum needle (Bard, Tempe, Ariz), guided by US. LB specimens were fixed in formalin and embedded in paraffin. Two liver pathologists (with more than 10 and 20 years of experience), who were blinded to the 2D SWE and RTE results, conducted the pathology tests. Every qualified specimen was longer than 1.5 cm and contained at least 6 portal tracts. Liver fibrosis was staged on a 0–4 scale and the inflammation activity was graded on a 0–3 scale according to the METAVIR scoring system; stage F0, no fibrosis; F1, portal fibrosis without septa; F2, portal fibrosis and a few septa; F3, numerous septa without cirrhosis; and F4, cirrhosis. Significant fibrosis was defined as stage F2 or higher, and cirrhosis was defined as stage F4. Necroinflammatory activity was graded as follows: A0 = none, A1 = mild, A2 = moderate and A3 = severe [36].

Statistical Analysis

The one-sample Kolmogorov–Smirnov test was used to test the normal distribution of quantitative variables. When the quantitative variables were normally distributed, the results are expressed as mean values and SDs; otherwise, medians and interquartile ranges (25th–75th percentile) are reported. Qualitative variables are summarized as counts and percentages. The ages of male and female patients were compared using the unpaired t test. Spearman correlation coefficients were used to analyze the correlation between the 2D SWE and RTE results and the histologic fibrosis stages. The 2D SWE results were not normally distributed; therefore, Kruskal–Wallis one-way analysis of variance by rank was used to test the equality of the median 2D SWE measurements across different fibrosis stages. The RTE results were normally distributed; therefore, the t test was used to test the equality of the LFI across different fibrosis stages. The diagnostic performances of 2D SWE and RTE was assessed with receiver operating characteristic (ROC) curves and the sensitivity, specificity, positive and negative predictive values, and positive and negative likelihood ratio of maximizing the Youden index were calculated. Differences between the areas under the ROC curves (AUROCs) were compared with a Delong test [37]. Differences between the sensitivity, specificity, positive and negative predictive values, and positive and negative likelihood ratios were compared using the Altman test [38]. $p < 0.05$ was considered statistically significant. The analysis was performed using SPSS statistics version 20 (IBM, Armonk, N.Y., USA) and Med-Calc version 12.7.0 (MedCalc Software, Mariakerke, Belgium).

Table 2. Relationship between the LSMs, LFI and the METAVIR fibrosis stage

METAVIR fibrosis stage	n	2D SWE, median LSMs (IQR, kPa)	RTE LFI, mean ± SD
F0	78	5.96 (5.44, 6.54)	1.95±0.43
F1	153	6.3 (5.55, 7.19)	2.31±0.45
F2	83	8.42 (7.13, 11.0)	2.36±0.58
F3	62	12.28 (9.7, 16.02)	2.70±0.54
F4	61	17.4 (13.82, 24.18)	2.88±0.58

Table 3. Relationship between the LSMs, LFI and the METAVIR activity stage

METAVIR activity grade	n	2D SWE, median LSMs (IQR, kPa)	RTE LFI, mean ± SD
A0	14	5.38 (5.08, 6.20)	2.11±0.46
A1	200	6.36 (5.76, 7.52)	2.06±0.47
A2	123	8.18 (6.88, 11.32)	2.32±0.60
A3	100	15.4 (11.18, 21.63)	2.72±0.64

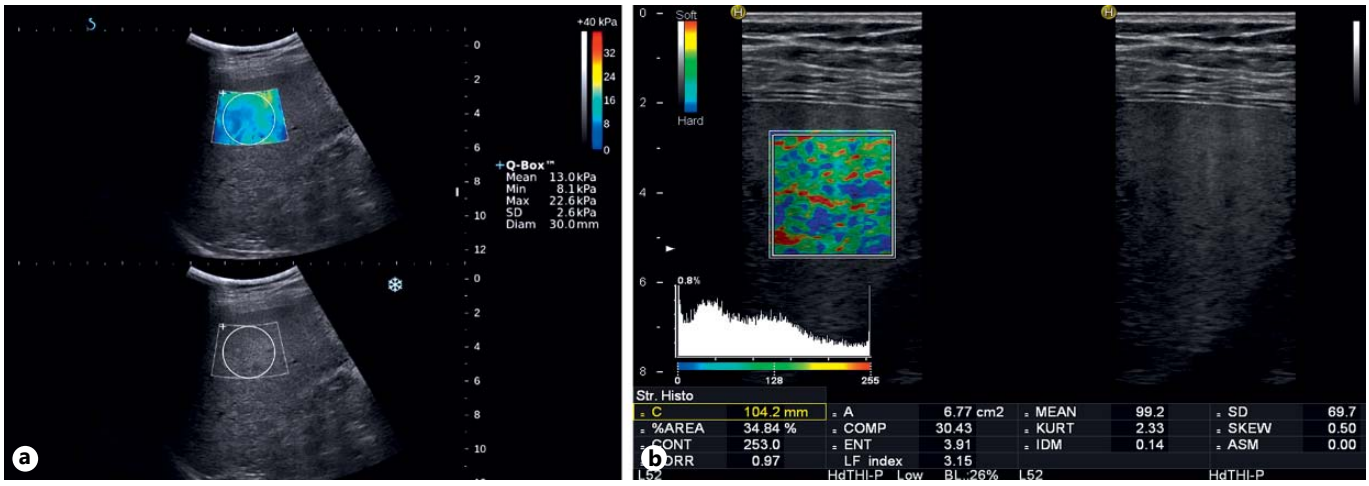

Fig. 1. 2D SWE (**a**) and RTE (**b**) measurement in the liver of a 42-year-old man with fibrosis stage F4.

Results

Patients

We performed both 2D SWE and RTE in 453 patients between September 2011 and July 2014, and we excluded 16 patients from our study: in 1 patient, neither 2D SWE nor RTE examination was completed, and in 15 patients, RTE examination was not completed. The success rate of 2D SWE and RTE was 99.7% (452/453) and 96.5% (437/453), respectively. The reasons for failure included the inability to optimally perform a breath hold (n = 3), liver atrophy (n = 3), and poor penetration of the ultrasound (n = 10). The failure cases were not included for the statistical analysis. The clinical characteristics and laboratory information of the 437 patients are shown in table 1.

The Relationship between the LSMs, LFI and the Histological Liver Analysis Findings

The correlation coefficients between the 2D SWE and RTE results and the METAVIR fibrosis stage were 0.745 and 0.520, respectively. The correlation coefficients between the 2D SWE and RTE results and the METAVIR activity stage were 0.684 and 0.408, respectively. The LSMs of 2D SWE and RTE for each stage are shown in tables 2 and 3 (fig. 1–3).

Comparison of Diagnostic Performance of 2D SWE and RTE for Significant Fibrosis and Cirrhosis

The AUROCs of the 2D SWE and RTE for predicting significant fibrosis (F0–1 vs. F2–4) were 0.903 and 0.754, respectively. For cirrhosis (F0–3 vs. F4), the AUROCs of the 2D SWE and RTE were 0.926 and 0.813, respectively (table 4). Comparisons of the AUROCs of 2D SWE and RTE indicated significant differences in the values obtained for significant fibrosis and cirrhosis ($p < 0.01$; fig. 4, 5).

The Influence of Inflammation on the LSM Obtained by 2D SWE and RTE

We divided the patients into 3 groups based on the severity of their hepatic fibrosis (F0–1, F2–3, and F4). In

Table 4. Diagnostic performance of the 2D SWE and RTE cut-off values for predicting significant fibrosis (F0–1 vs. F2–4) and cirrhosis (F0–3 vs. F4)

	2D SWE		RTE	
	≥F2 (95% CI)	F4 (95% CI)	≥F2 (95% CI)	F4 (95% CI)
AUC	0.903 (0.871–0.929)	0.926 (0.897–0.949)	0.754 (0.711–0.793)	0.813 (0.773–0.848)
Cut-off	8.2	11.256	2.14	2.3533
Sensitivity, %	78.16 (71.9–83.6)	91.80 (81.9–97.3)	76.70 (70.3–82.3)	81.97 (70.0–90.6)
Specificity, %	85.28 (80.0–89.6)	84.31 (80.2–87.8)	63.20 (56.6–69.4)	65.16 (60.1–70.0)
PPV, %	82.6 (76.5–87.6)	48.7 (39.2–58.2)	65.0 (58.7–71.0)	27.6 (21.3–34.7)
NPV, %	81.4 (75.9–86.1)	98.4 (96.4–99.5)	75.3 (68.6–81.2)	95.7 (92.4–97.8)
Positive LR	5.31 (3.9–7.3)	5.75 (4.5–7.4)	2.08 (1.7–2.5)	2.35 (2.0–2.8)
Negative LR	0.26 (0.2–0.3)	0.12 (0.05–0.2)	0.37 (0.3–0.5)	0.28 (0.2–0.5)

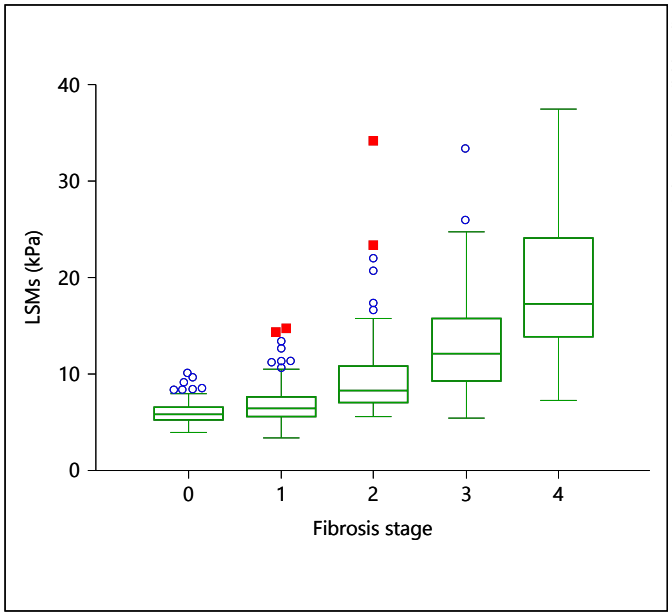

Fig. 2. Relationships between hepatic fibrosis stages and LSMs of 2D SWE. There was a high correlation between LSM of 2D SWE and the stages of hepatic fibrosis (r = 0.745).

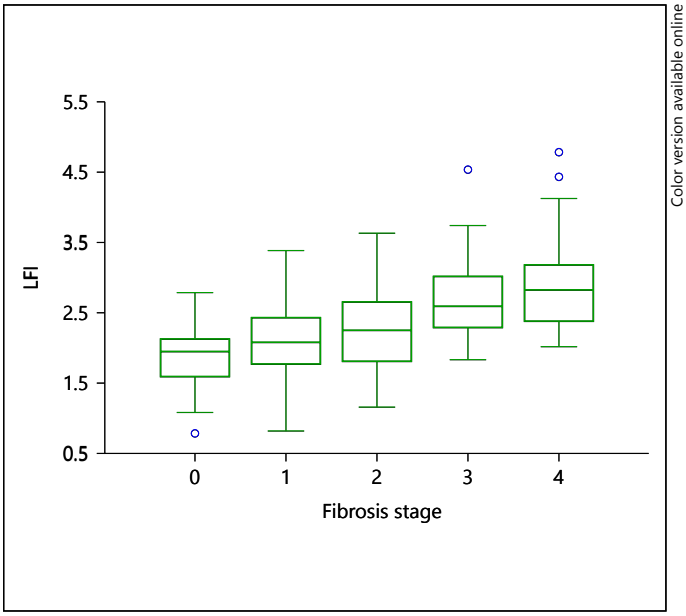

Fig. 3. Relationships between hepatic fibrosis stages and LFI of RTE. There was a medium correlation between LFI of RTE and the stages of hepatic fibrosis (r = 0.520).

each group, we continued to group the patients according to their ALT levels (<2 time the upper limit of normal (ULN) and ≥2 × ULN) or METAVIR activity grade (A0–1 and A2–3, respectively), and then we compared the measurement values (tables 5–8). The 2D SWE measurement values were statistically and significantly different for different ALT levels and METAVIR activity grades, while the RTE measurement values were not statistically and significantly different for different ALT levels and METAVIR activity grades.

A Comparison of the Diagnostic Performance of Predicting Significant Fibrosis and Cirrhosis by 2D SWE and RTE Based on ALT Levels

We divided the patients into 2 groups based on ALT levels that were 2 times the ULN: 336 patients were in the less than 2 times the ULN group, and 101 patients were in the ≥2 times the ULN group. Table 9 shows the diagnostic performance of the calculated 2D SWE and RTE cut-off values for predicting significant fibrosis and cirrhosis in the different groups and their comparison.

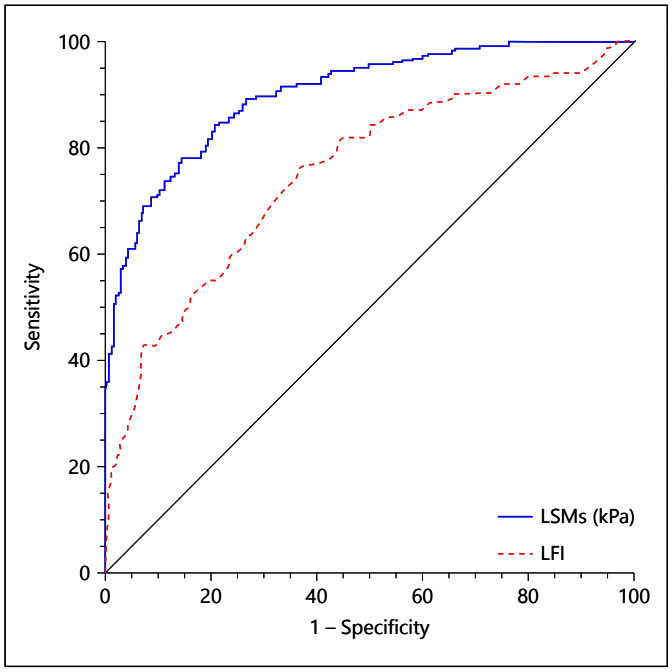

Fig. 4. Comparison of the AUROC of the 2D SWE and RTE for predicting significant fibrosis (F0–1 vs. F2–4). 2D SWE was significantly superior to RTE.

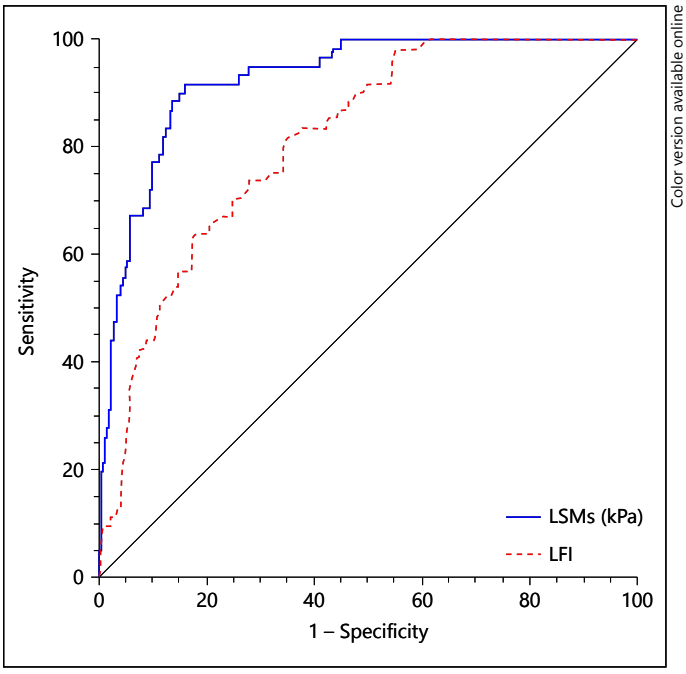

Fig. 5. Comparison of the AUROC of the 2D SWE and RTE for predicting cirrhosis (F0–3 vs. F4). 2D SWE was significantly superior to RTE.

Discussion

In this study, the liver stiffness values of SWE and RTE increased in parallel with the degree of liver fibrosis and the grade of inflammation, which is consistent with the previous literatures [28, 39, 40]. However, the diagnostic efficacy of 2D SWE for significant fibrosis and cirrhosis was significantly higher than that of RTE, which may be due to the following reasons. First, 2D SWE was used to assess liver fibrosis by measuring the absolute hardness of the liver, whereas RTE was used to evaluate liver fibrosis by the relative hardness values from the deformation of liver parenchyma caused by the heart beating, so RTE is easily affected by the strength of the heartbeat. Second, the RTE operational skills and experience and image evaluation requirements were relatively stricter than those of 2D SWE. In this study, 16 of 453 patients failed to undergo the RTE examination, while only 1 of 453 patients failed to complete the 2D SWE examination; thus, RTE may require more training and practice. The above factors may have contributed to the poorer diagnostic performance of RTE compared to 2D SWE. Compared with other studies, the diagnostic efficacy of RTE in this study was lower. Yada et al. [35] evaluated liver stiffness with RTE in patients with CHB and chronic hepatitis C, and they found that the AUROCs for the prediction of F2 or a higher stage of fibrosis (F0–1 vs. F2–4) and for diagnosing cirrhosis (F0–3 vs. F4) by RTE were 0.800 and 0.846, respectively. In our study, the AUROCs for significant fibrosis and cirrhosis were 0.754 and 0.813, respectively. The different populations and patient etiology might explain these different results. Different methods for evaluating the images might provide another explanation. Our study did not use the offline evaluation system. In other studies, RTE was mostly based on dynamic image offline evaluations so that remeasurements could be performed effectively avoiding a single measurement by an operator accompanied with measurement error. Meanwhile, RTE and operation experience are closely related, such that the lack of experience in the early stages of this study had an impact on the results.

Furthermore, our results showed that based on either the ALT level (<2 × ULN and ≥2 × ULN) or METAVIR activity grade (A0–1 and A2–3), different levels of inflammation significantly affected the 2D SWE results. Specifically, the median 2D SWE measurement value of fibrosis stages (F0–1, F2–3, and F4) significantly increased with apparent inflammation activity ($p < 0.05$), as shown in tables 5 and 7, but it had little effect on the RTE results, as

Table 5. Comparison of the 2D SWE LSMs for different ALT levels

ALT	2D SWE, median LSMs (IQR, kPa)					
	F0–1	n	F2–3	n	F4	n
<2 × ULN	6.16 (5.4, 6.95)	191	9.52 (7.67, 12.28)	106	17.0 (12.08, 21.36)	39
≥2 × ULN	7.57 (6.22, 9.34)	40	11.68 (8.92, 15.7)	39	21.3 (15.95, 28.8)	22
Z value	–4.894		–2.854		–2.02	
p value	0.000		0.004		0.043	

Table 6. Comparison of the RTE measurement values for different ALT levels

ALT	RTE LFI, mean ± SD					
	F0–1	n	F2–3	n	F4	n
<2 × ULN	2.03±0.45	191	2.47±0.60	106	2.87±0.58	39
≥2 × ULN	2.11±0.52	40	2.35±0.58	39	2.90±0.61	22
t value	–1.074		1.101		–0.224	
p value	0.284		0.273		0.823	

Table 7. Comparison of the 2D SWE LSMs for different METAVIR activity grades

METAVIR grade	2D SWE, median LSMs (IQR, kPa)					
	F0–1	n	F2–3	n	F4	n
A0–1	6.19 (5.48, 6.97)	186	8.09 (6.97, 10.98)	28		0
A2–3	7.16 (6.05, 8.07)	45	10.23 (8.20, 14.29)	117	17.4 (13.82, 24.18)	61
Z value	–3.178		–2.74			
p value	0.001		0.006		Not applicable	

Table 8. Comparison of the RTE measurement values for different METAVIR activity grades

METAVIR grade	RTE LFI, mean ± SD					
	F0–1	n	F2–3	n	F4	n
A0–1	2.03±0.45	186	2.30±0.53	28		0
A2–3	2.07±0.53	45	2.47±0.61	117	2.88±0.58	61
t value	–0.549		–1.338			
p value	0.583		0.183		Not applicable	

demonstrated in tables 6 and 8. Acute inflammation or noticeable inflammation fluctuations cause cell edema and increase the pressure among hepatocytes and the absolute hardness of liver. Then either TE or 2D SWE measurement values increase and this have been proven in this study and other literatures [24, 25, 28]. In contrast, RTE evaluates liver stiffness by measuring the relative stiffness of the liver. Pressure changes among hepatocytes, and hemodynamic changes induced by inflammation fluctuations are related to diffuse liver changes. Pathologic differences within the liver tissue were small, and therefore, the RTE measurement value was large-

Table 9. Diagnostic performance of the 2D SWE and RTE calculated cut-off values for predicting significant fibrosis (F0–1 vs. F2–4) and cirrhosis (F0–3 vs. F4) in the different groups

	2D SWE		RTE	
	≥F2[a] (95% CI)	F4[b] (95% CI)	≥F2[c] (95% CI)	F4[d] (95% CI)
Cut-off*	8.2	11.256	2.14	2.3533
ALT <2 × ULN				
Sensitivity, %	73.10 (65.1–80.1)	84.62 (69.5–94.1)	75.17 (67.3–82.0)	79.49 (63.5–90.7)
Specificity, %	91.10 (86.1–94.7)	88.55 (84.4–91.9)	65.45 (58.2–72.2)	64.98 (59.3–70.4)
PPV, %	86.2 (78.8–91.7)	49.3 (36.8–61.8)	62.3 (54.7–69.5)	23.0 (16.1–31.0)
NPV, %	81.7 (75.8–86.7)	97.8 (95.2–99.2)	77.6 (70.4–83.8)	96.0 (92.3–98.3)
Positive LR	8.21 (5.2–13.1)	7.39 (5.2–10.4)	2.18 (1.8–2.7)	2.27 (1.8–2.8)
Negative LR	0.30 (0.2–0.4)	0.17 (0.08–0.4)	0.38 (0.3–0.5)	0.32 (0.2–0.6)
ALT ≥2 × ULN				
Sensitivity, %	85.25 (73.8–93.0)	100.00 (84.6–100.0)	78.69 (66.3–88.1)	86.36 (65.1–97.1)
Specificity, %	62.50 (45.8–77.3)	68.35 (56.9–78.4)	52.50 (36.1–68.5)	65.82 (54.3–76.1)
PPV, %	77.6 (65.7–87.0)	46.8 (32.1–61.9)	71.6 (59.3–82.0)	41.3 (27.0–56.8)
NPV, %	73.5 (55.6–87.1)	100.0 (93.4–100.0)	61.8 (43.6–77.8)	94.5 (84.9–98.9)
Positive LR	2.27 (1.5–3.4)	3.16 (2.3–4.4)	1.66 (1.2–2.4)	2.53 (1.8–3.6)
Negative LR	0.24 (0.1–0.5)	0	0.41 (0.2–0.7)	0.21 (0.07–0.6)

* Cut-off liver stiffness values were calculated for all the patients.

[a] The differences in the sensitivity and specificity are statistically significant between groups with p values of 0.0177 and <0.0001, respectively, while the PPV and NPV are not statistically significant between groups with p values of 0.0545 and 0.0972, respectively.

[b] The differences in the sensitivity and specificity are statistically significant between groups with p values of <0.0001 and <0.0001, respectively, while the PPV and NPV are not statistically significant between groups with p values of 0.7435 and 0.2876, respectively.

[c] The differences in the specificity and NPV are statistically significant between groups with p values of 0.0251 and 0.0023, respectively, while the sensitivity and PPV are not statistically significant between groups with p values of 0.553 and 0.111, respectively.

[d] The difference in the PPV is statistically significant between groups with a p value of 0.0006, while differences in the sensitivity, specificity, and NPV are not statistically significant between groups with p values of 0.1613, 0.9711, and 0.7114, respectively.

ly unaffected, which is similar to the results published in the previous literatures [34, 35]. However, liver fibrosis in HBV is closely connected with inflammation activity. A selective bias may exist in our study because of the imbalance of samples, such as the relatively fewer number of patients with F4 and F0–1. Thus, it is necessary to enlarge and balance the sample numbers of future studies.

To further explore the influence of inflammation activity on the diagnostic performance of 2D SWE and RTE, the cut-off values presented in table 4 were applied to calculate diagnostic parameters (such as the sensitivity and specificity) at different ALT levels (<2 × ULN and ≥2 × ULN) for predicting significant fibrosis (F0–1 vs. F2–4) and cirrhosis (F0–3 vs. F4). The results demonstrated that the main parameters, including all sensitivity and specificity results for 2D SWE, significantly varied with elevated ALT (≥2 × ULN; $p < 0.05$), but only the specificity of RTE for predicting significant fibrosis (F0–1 vs. F2–4) decreased significantly. These results suggest that in clinical practice, when ALT levels are ≥2 times the ULN, the diagnostic efficacy of 2D SWE is significantly decreased, leading to unreliable results. Patients should be advised to objectively reassess their liver fibrosis by 2D SWE after inflammation subsides, and RTE might be another selectable technique for assessing liver fibrosis for these patients.

There are several limitations to this study. First, the biopsy pathologic examination (specimens longer than 1.5 cm containing at least 6 portal tracts) in our study was not as strict as the pathologic standard of the American Association for the Study of Liver Diseases (specimens 2–3 cm long containing at least 11 portal tracts). In this study, all biopsies that measured longer than 15 mm were categorized correctly according to the reference value by using the METAVIR scoring system. Second, the distributions of pathological staging in HBV patients were unbalanced: F1 patients accounted for 35% of the total cases (153/437) and the relatively few A0 patients

accounted for only 3% of the overall cases (14/437). Last, all patients in our study had relatively low BMIs, which may lead to differences between our results and those of other studies. However, the lower BMI in all patients may reduce the influence of steatosis on stiffness measurements.

Conclusions

For patients with CHB, the diagnostic performance of 2D SWE for the assessment of liver fibrosis is better than that of RTE. The stiffness values obtained by 2D SWE are prone to be affected by inflammation fluctuations, so the patients with acute inflammation should choose a reasonable method for clinical noninvasive assessment of hepatic fibrosis.

Acknowledgement

This research is partially supported by the Research Program on Hepatitis from Japan Agency for Medical Research and Development, AMED.

Disclosure Statement

The authors declare that no conflicts of interest exist.

References

1 Poynard T, Mathurin P, Lai CL, Guyader D, Poupon R, Tainturier MH, Myers RP, Muntenau M, Ratziu V, Manns M, Vogel A, Capron F, Chedid A, Bedossa P; PANFIBROSIS Group: A comparison of fibrosis progression in chronic liver diseases. J Hepatol 2003;38:257–265.

2 McPherson S, Henderson E, Burt AD, Day CP, Anstee QM: Serum immunoglobulin levels predict fibrosis in patients with non-alcoholic fatty liver disease. J Hepatol 2014;60:1055–1062.

3 Kudo M, Matsui O, Izumi N, Iijima H, Kadoya M, Imai Y, et al; Liver Cancer Study Group of Japan: JSH consensus-based clinical practice guidelines for the management of hepatocellular carcinoma: 2014 update by the liver cancer study group of Japan. Liver Cancer 2014;3:458–468.

4 Kudo M: Surveillance, diagnosis, treatment, and outcome of liver cancer in Japan. Liver Cancer 2015;4:39–50.

5 Poon RT, Cheung TT, Kwok PC, Lee AS, Li TW, Loke KL, et al: Hong Kong consensus recommendations on the management of hepatocellular carcinoma. Liver Cancer 2015;4:51–69.

6 Kawanaka M, Nishino K, Nakamura J, Oka T, Urata N, Goto D, et al: Quantitative levels of hepatitis B virus DNA and surface antigen and the risk of hepatocellular carcinoma in patients with hepatitis B receiving long-term nucleos(t)ide analogue therapy. Liver Cancer 2014;3:41–52.

7 Kudo M: Prediction of hepatocellular carcinoma incidence risk by ultrasound elastography. Liver Cancer 2014;3:1–5.

8 Gebo KA, Herlong HF, Torbenson MS, Jenckes MW, Chander G, Ghanem KG, El-Kamary SS, Sulkowski M, Bass EB: Role of liver biopsy in management of chronic hepatitis C: a systematic review. Hepatology 2002;36(suppl 1):S161–S172.

9 Seeff LB, Everson GT, Morgan TR, Curto TM, Lee WM, Ghany MG, Shiffman ML, Fontana RJ, Di Bisceglie AM, Bonkovsky HL, Dienstag JL; HALT-C Trial Group: Complication rate of percutaneous liver biopsies among persons with advanced chronic liver disease in the HALT-C trial. Clin Gastroenterol Hepatol 2010;8:877–883.

10 Stotland BR, Lichtenstein GR: Liver biopsy complications and routine ultrasound. Am J Gastroenterol 1996;91:1295–1296.

11 Cadranel JF, Rufat P, Degos F: Practices of liver biopsy in France: results of a prospective nationwide survey. For the group of epidemiology of the French association for the study of the liver (AFEF). Hepatology 2000;32:477–481.

12 Friedrich-Rust M, Wunder K, Kriener S, Sotoudeh F, Richter S, Bojunga J, Herrmann E, Poynard T, Dietrich CF, Vermehren J, Zeuzem S, Sarrazin C: Liver fibrosis in viral hepatitis: noninvasive assessment with acoustic radiation force impulse imaging versus transient elastography. Radiology 2009;252:595–604.

13 Ferraioli G, Tinelli C, Dal Bello B, Zicchetti M, Filice G, Filice C; Liver Fibrosis Study Group: Accuracy of real-time shear wave elastography for assessing liver fibrosis in chronic hepatitis C: a pilot study. Hepatology 2012;56:2125–2133.

14 Franchi-Abella S, Corno L, Gonzales E, Antoni G, Fabre M, Ducot B, Pariente D, Gennisson JL, Tanter M, Corréas JM: Feasibility and diagnostic accuracy of supersonic shear-wave elastography for the assessment of liver stiffness and liver fibrosis in children: a pilot study of 96 patients. Radiology 2016;278:554–562.

15 Zheng J, Guo H, Zeng J, Huang Z, Zheng B, Ren J, Xu E, Li K, Zheng R: Two-dimensional shear-wave elastography and conventional US: the optimal evaluation of liver fibrosis and cirrhosis. Radiology 2015;275:290–300.

16 Cassinotto C, Lapuyade B, Mouries A, Hiriart JB, Vergniol J, Gaye D, Castain C, Le Bail B, Chermak F, Foucher J, Laurent F, Montaudon M, De Ledinghen V: Non-invasive assessment of liver fibrosis with impulse elastography: comparison of supersonic shear imaging with ARFI and FibroScan®. J Hepatol 2014;61:550–557.

17 Ferraioli G, Parekh P, Levitov AB, Filice C: Shear wave elastography for evaluation of liver fibrosis. J Ultrasound Med 2014;33:197–203.

18 Kobayashi K, Nakao H, Nishiyama T, Lin Y, Kikuchi S, Kobayashi Y, Yamamoto T, Ishii N, Ohashi T, Satoh K, Nakade Y, Ito K, Yoneda M: Diagnostic accuracy of real-time tissue elastography for the staging of liver fibrosis: a meta-analysis. Eur Radiol 2015;25:230–238.

19 Sandrin L, Fourquet B, Hasquenoph JM, Yon S, Fournier C, Mal F, Christidis C, Ziol M, Poulet B, Kazemi F, Beaugrand M, Palau R: Transient elastography: a new noninvasive method for assessment of hepatic fibrosis. Ultrasound Med Biol 2003;29:1705–1713.

20 Foucher J, Chanteloup E, Vergniol J, Castéra L, Le Bail B, Adhoute X, Bertet J, Couzigou P, de Lédinghen V: Diagnosis of cirrhosis by transient elastography (FibroScan): a prospective study. Gut 2006;55:403–408.

21 Kim JH, Kim MN, Han KH, Kim SU: Clinical application of transient elastography in patients with chronic viral hepatitis receiving antiviral treatment. Liver Int 2015;35:1103–1115.

22 Fernandez M, Trépo E, Degré D, Gustot T, Verset L, Demetter P, Devière J, Adler M, Moreno C: Transient elastography using Fibroscan is the most reliable noninvasive method for the diagnosis of advanced fibrosis and cirrhosis in alcoholic liver disease. Eur J Gastroenterol Hepatol 2015;27:1074–1079.

23 Viganò M, Massironi S, Lampertico P, Iavarone M, Paggi S, Pozzi R, Conte D, Colombo M: Transient elastography assessment of the liver stiffness dynamics during acute hepatitis B. Eur J Gastroenterol Hepatol 2010;22:180–184.

24 Sagir A, Erhardt A, Schmitt M, Häussinger D: Transient elastography is unreliable for detection of cirrhosis in patients with acute liver damage. Hepatology 2008;47:592–595.

25 Wong GL, Wong VW, Choi PC, Chan AW, Chim AM, Yiu KK, Chan FK, Sung JJ, Chan HL: Increased liver stiffness measurement by transient elastography in severe acute exacerbation of chronic hepatitis B. J Gastroenterol Hepatol 2009;24:1002–1007.

26 Fraquelli M, Rigamonti C, Casazza G, Conte D, Donato MF, Ronchi G, Colombo M: Reproducibility of transient elastography in the evaluation of liver fibrosis in patients with chronic liver disease. Gut 2007;56:968–973.

27 Millonig G, Reimann FM, Friedrich S, Fonouni H, Mehrabi A, Büchler MW, Seitz HK, Mueller S: Extrahepatic cholestasis increases liver stiffness (FibroScan) irrespective of fibrosis. Hepatology 2008;48:1718–1723.

28 Arena U, Vizzutti F, Corti G, Ambu S, Stasi C, Bresci S, Moscarella S, Boddi V, Petrarca A, Laffi G, Marra F, Pinzani M: Acute viral hepatitis increases liver stiffness values measured by transient elastography. Hepatology 2008; 47:380–384.

29 Song P, Mellema DC, Sheedy SP, Meixner DD, Karshen RM, Urban MW, Manduca A, Sanchez W, Callstrom MR, Greenleaf JF, Chen S: Performance of 2-dimensional ultrasound shear wave elastography in liver fibrosis detection using magnetic resonance elastography as the reference standard: a pilot study. J Ultrasound Med 2016;35:401–412.

30 Zeng J, Liu GJ, Huang ZP, Zheng J, Wu T, Zheng RQ, Lu MD: Diagnostic accuracy of two-dimensional shear wave elastography for the non-invasive staging of hepatic fibrosis in chronic hepatitis B: a cohort study with internal validation. Eur Radiol 2014;24:2572–2581.

31 Wu T, Ren J, Cong SZ, Meng FK, Yang H, Luo Y, Lin HJ, Sun Y, Wang XY, Pei SF, Zheng Y, He Y, Chen Y, Hu Y, Yang N, Li P, Kudo M, Zheng RQ: Accuracy of real-time tissue elastography for the evaluation of hepatic fibrosis in patients with chronic hepatitis B: a prospective multicenter study. Dig Dis 2014;32: 791–799.

32 Ochi H, Hirooka M, Koizumi Y, Miyake T, Tokumoto Y, Soga Y, Tada F, Abe M, Hiasa Y, Onji M: Real-time tissue elastography for evaluation of hepatic fibrosis and portal hypertension in nonalcoholic fatty liver diseases. Hepatology 2012;56:1271–1278.

33 Koizumi Y, Hirooka M, Kisaka Y, Konishi I, Abe M, Murakami H, Matsuura B, Hiasa Y, Onji M: Liver fibrosis in patients with chronic hepatitis C: noninvasive diagnosis by means of real-time tissue elastography – establishment of the method for measurement. Radiology 2011;258:610–617.

34 Fujimoto K, Kato M, Kudo M, Yada N, Shiina T, Ueshima K, Yamada Y, Ishida T, Azuma M, Yamasaki M, Yamamoto K, Hayashi N, Takehara T: Novel image analysis method using ultrasound elastography for noninvasive evaluation of hepatic fibrosis in patients with chronic hepatitis C. Oncology 2013;84(suppl 1):3–12.

35 Yada N, Kudo M, Morikawa H, Fujimoto K, Kato M, Kawada N: Assessment of liver fibrosis with real-time tissue elastography in chronic viral hepatitis. Oncology 2013; 84(suppl 1):13–20.

36 Bedossa P, Poynard T: An algorithm for the grading of activity in chronic hepatitis C. The METAVIR cooperative study group. Hepatology 1996;24:289–293.

37 DeLong ER, DeLong DM, Clarke-Pearson DL: Comparing the areas under two or more correlated receiver operating characteristic curves: a nonparametric approach. Biometrics 1988;44:837–845.

38 Altman DG, Machin D, Bryant TN, Gardner MJ (eds): Statistics with Confidence, ed 2. BMJ Books, 2000.

39 Tada T, Kumada T, Toyoda H, Ito T, Sone Y, Okuda S, Tsuji N, Imayoshi Y, Yasuda E: Utility of real-time shear wave elastography for assessing liver fibrosis in patients with chronic hepatitis C infection without cirrhosis: comparison of liver fibrosis indices. Hepatol Res 2015;45:E122–E129.

40 Tamaki N, Kurosaki M, Matsuda S, Nakata T, Muraoka M, Suzuki Y, Yasui Y, Suzuki S, Hosokawa T, Nishimura T, Ueda K, Tsuchiya K, Nakanishi H, Itakura J, Takahashi Y, Matsunaga K, Taki K, Asahina Y, Izumi N: Prospective comparison of real-time tissue elastography and serum fibrosis markers for the estimation of liver fibrosis in chronic hepatitis C patients. Hepatol Res 2014;44:720–727.

Original Article

Digestive Diseases

Dig Dis 2016;34:702–707
DOI: 10.1159/000448860

Impact of Tight Junction Protein ZO-1 and TWIST Expression on Postoperative Survival of Patients with Hepatocellular Carcinoma

Tomoyuki Nagai[a, b] Tokuzo Arao[b] Kazuto Nishio[b] Kazuko Matsumoto[b] Satoru Hagiwara[a] Toshiharu Sakurai[a] Yasunori Minami[a] Hiroshi Ida[a] Kazuomi Ueshima[a] Naoshi Nishida[a] Kazuko Sakai[b] Nagahiro Saijo[b] Kanae Kudo[b] Hiroyasu Kaneda[b] Daisuke Tamura[b] Keiichi Aomatsu[b] Hideharu Kimura[b] Yoshihiko Fujita[b] Seiji Haji[c] Masatoshi Kudo[a]

Departments of [a]Gastroenterology and Hepatology, [b]Genome Biology, and [c]Surgery, Kindai University Faculty of Medicine, Osaka-Sayama, Japan

Key Words
Epithelial-mesenchymal transition · Tight junction protein ZO-1 · TWIST · Survival · Hepatocellular carcinoma

Abstract
Background: Epithelial-mesenchymal transition (EMT) is considered to play a critical role in cancer progression and metastasis. However, the impact of EMT on the prognosis of hepatocellular carcinoma (HCC) is still elusive. In this study, we examined the relationship between the expression of EMT markers and recurrence-free survival (RFS) and overall survival (OS) in HCC patients after hepatic resection. ***Summary:*** The mRNA expression of 15 genes related to EMT was assessed by quantitative real-time polymerase chain reaction in cancerous tissues from 72 patients who underwent hepatic resection of HCC between January 2005 and December 2010 at our hospital. The upregulation of TWIST and the downregulation of tight junction protein ZO-1 (TJP1) were significantly associated with shorter RFS as well as OS. Increased levels of TWIST and decreased levels of TJP1 should be predictive markers for poor prognosis in patients with HCC after hepatectomy; those could serve as potential biomarkers for the treatment of HCC. ***Key Messages:*** A low level of TJP1 and high level of TWIST expression were prognostic factors predicting HCC after hepatic resection.

Introduction

Hepatocellular carcinoma (HCC) is the fifth most common cause of cancer-related death in the world annually, and the development of new primary tumors, recurrences, and metastasis are the most common causes of mortality among patients with HCC [1–3]. HCC develops predominantly in an established background of chronic liver diseases mainly caused by persistent infection of hepatitis B [4] and/or hepatitis C virus, alcoholic liver disease, or non-alcoholic steatohepatitis [5, 6]. Meanwhile, growing evidence indicates that the epithelial-mesenchymal transition (EMT), a developmental process by which epithelial cells reduce intercellular adhesions and acquire fibroblastoid properties, has important roles in the acquisition of the invasive and metastatic potentials of cancer progression [7–10]. We have recently

KARGER

E-Mail karger@karger.com
www.karger.com/ddi

0257–2753/16/0346–0702$39.50/0

Naoshi Nishida, MD
Department of Gastroenterology and Hepatology
Kindai University Faculty of Medicine
337-2 Ohno-Higashi, Osaka-Sayama, Osaka 589-8511 (Japan)
E-Mail naoshi@med.kindai.ac.jp

reported that sorafenib [11, 12] exerts a potent inhibitory activity against the EMT by inhibiting MAPK signaling and SNAI1 expression in HCC [13]. Chen et al. [14] reported that sorafenib inhibits transforming growth factor β1-mediated EMT and apoptosis in mouse hepatocytes. These papers reported that the anti-EMT effect of sorafenib may prolong overall survival (OS) in patients with unresectable HCC. Based on the previous analyses, it is conceivable that analyzing the relationship of the expressions of EMT markers with survival of HCC patients will provide critical information for the management of this disease. As EMT is critical for the invasiveness and metastasis of cancers, we specifically focused on the expression profiles of the 15 genes related to EMT in the context of survival of the HCC patients who had undergone hepatic resection. Here, we show the unique expression profile of the EMT-related molecules that affect the prognosis of the HCC patients who underwent hepatic resection.

Table 1. Patient characteristics

Age, years, median (range)	71 (40–80)
Gender (male/female)	54/18
TNM (I/II/III/IV)	4/20/28/20
Cause of disease (HBV, HCV/non B, non C)	13/39/20
Child–Pugh (5/6/7)	60/10/2
Histology (well/mod/poor)	16/46/10
Tumor size (<5/≥5 cm)	43/29
Previous therapy (yes/none)	23/49
Vascular invasion (yes/no)	34/38
Tumor number (1/2/≥3)	34/18/20
AFP, median (range)	15 (1–23,811)
PIVKA-II, average (SD)	101 (10–46,416)

Total 72 patients who underwent hepatic resection for HCC at Kinki University from 2005 to 2010.

Materials and Methods

Patients

Clinical research included 72 patients who underwent hepatic resection for primary HCC between January 2005 and December 2010 in the Department of Surgery, Kinki University Hospital. The mean age (range) of patients is 71 (40–80), 54 are male and 18 are female. The numbers of the patients carrying each stage of HCC are as follows: 4 for stage I, 20 for stage II, 28 for stage III and 20 for stage IV. Details of the patient characteristics and the clinical backgrounds are summarized in table 1.

RNA Extraction, cDNA Synthesis, and Real-Time Reverse-Transcription Polymerase Chain Reaction

We examined the mRNA expression of the following EMT-related molecules: Snail, Slug, zinc finger E-box binding homeobox 1, zinc finger E-box binding homeobox 2, TWIST, E-cadherin, N-cadherin, vimentin, fibronectin (FIN), discoidin domain receptor 2 (DDR2), S100 calcium-binding protein A4 (S100A4), tight junction protein ZO-1 (TJP1), forkhead box protein C2 (FOXC2), SIX homeobox 1 (SIX1), and Goosecoid (GSC). The mRNA was extracted from frozen surgical HCC samples. Real-time reverse-transcription (RT)-polymerase chain reaction (PCR) amplification was performed for quantification of target mRNA using glyceraldehyde 3-phosphate dehydrogenase (GAPD) as an internal control for normalization.

The condition of real-time RT-PCR has been described previously [15]. Briefly, 1 μg of total RNA from the cultured cells was converted to cDNA using a GeneAmp RNA-PCR kit (Applied Biosystems, Calif., USA). Amplification was performed using a Thermal Cycler Dice (Takara, Otsu, Japan) in accordance with the manufacturer's instructions under the following conditions: 95°C for 6 min, 40 cycles of 95°C for 15 s and 60°C for 1 min. GAPD was used to normalize the expression levels in the subsequent quantitative analyses. To amplify the target genes, the following primers were purchased from TaKaRa (Yotsukaichi, Japan): *CDH1* (E-cadherin), forward: 5′-TTA AAC TCC TGG CCT CAA GCA ATC-3′ and reverse: 5′-TCC TAT CTT GGG CAA AGC AAC TG-3′; *CDH2*, forward: 5′-CGA ATG GAT GAA AGA CCC ATC C-3′ and reverse: 5′-GGA GCC ACT GCC TTC ATA GTC AA-3′; SNAI1 (Snail1), forward: 5′-TCT AGG CCC TGG CTG CTA CAA-3′ and reverse: 5′-ACA TCT GAG TGG GTC TGG AGG TG-3′; SNAI2 (Snail12), forward: 5′-ATG CAT ATT CGG ACC CAC ACA TTA C-3′ and reverse: 5′-AGA TTT GAC CTG TCT GCA AAT GCT C-3′; VIM (vimentin), forward: 5′-TGA GTA CCG GAG ACA GGT GCA G-3′ and reverse: 5′-TAG CAG CTT CAA CGG CAA AGT TC-3′; FIN, forward: 5′-GGA GCA AAT GGC ACC GAG ATA-3′ and reverse: 5′-GAG CTG CAC ATG TCT TGG GAA C-3′; DDR2, forward: 5′-CCC AGC TGT CAG ATC AAC AGG TTA-3′ and reverse: 5′-TCA GGA CAA ATG GCT GGT TGA G-3′; S100A4, forward: 5′-GGG TGA CAA GTT CAA GCT CAA CAA-3′ and reverse: 5′-ATC ATG GCG ATG CAG GAC AG-3′; TJP1, forward: 5′-CGG GAC TGT TGG TAT TGG CTA GA-3′ and reverse: 5′-GGC CAG GGC CAT CAT AGT AAA GTT TG-3′; FOXC2, forward: 5′-CTA CAG CTA CAT CGC GCT CAT CA-3′ and reverse: 5′-ACT GGT AGA TGC CGT TCA AGG TG-3′; SIX1, forward: 5′-AAT GCC ATT ACT CAT GCC CTC A-3′ and reverse: 5′-CCA GGT TGC CAG ATT CGT TG-3′; GSC, forward: 5′-CAC CTC CGC GAG GAG AAA GT-3′ and reverse: 5′-GAC GAC GAC GTC TTG TTC CAC-3′; GAPD, forward: 5′-GCA CCG TCA AGG CTG AGA AC-3′ and reverse: 5′-ATG GTG GTG AAG ACG CCA GT-3′.

Cell Culture and Migration Assay

The human HCC cell lines Huh7 were maintained in DMEM medium (Sigma, St. Louis, Mo., USA) supplemented with 10% fetal bovine serum (FBS), penicillin, and streptomycin (Sigma) in a humidified atmosphere of 5% CO_2 at 37°C. The migration assays were performed using the Boyden-chamber methods and polycarbonate membranes with an 8-μm pore size (Chemotaxicell; Kurabo, Tokyo, Japan), as previously described [13]. The membranes were coated with FIN on the outer side and dried for 2 h at room temperature. The cells to be analyzed (2×10^4 cells/well) were then seeded onto the upper chambers with 200 μl of migrat-

Table 2. Univariate Cox regression analyses of RFS and OS of the patient characteristics and the expression of 15 genes related to EMT. Multivariate Cox regression analyses of RFS and OS of the patient characteristics of the patient characteristics and the expression of 15 genes related to EMT

	RFS			OS		
	univariate, p value	multivariate		univariate, p value	multivariate	
		HR (95% CI)	p value		HR (95% CI)	p value
Age, years	0.22		NA	0.88		NA
Gender (male/female)	0.86		NA	0.46		NA
TNM stage (I + II/III + IV)	0.17		NA	0.03*	9.22 (1.121–75.84)	0.039*
HBV history (no/yes)	0.71		NA	0.58		NA
HCV history (no/yes)	0.48		NA	0.59		NA
Child–Pugh (5/>5)	0.233		NA	0.168		NA
Histology (well + mod/poor)	0.003*	1.657 (0.721–3.81)	0.234	0.008*	5.526 (1.385–22.05)	0.015*
Tumor size (<5/≥5 cm)	0.28		NA	0.03*		NA
Previous therapy (no/yes)	0.752		NA	0.604		NA
Vascular invasion (no/yes)	0.02*	1.844 (0.947–3.59)	0.072	0.003*		NA
Tumor number (1/≥2)	0.06	1.891 (0.961–3.72)	0.065	0.48		NA
AFP (≤20/>20)	0.00017*	3.099 (1.514–6.344)	0.002*	0.07	1.427 (0.46–4.432)	0.538
PIVKA-II (≤120/>120)	0.21		NA	0.046*	3.331 (1.054–11.823)	0.041*
CDH1	0.68		NA	0.66		NA
CDH2	0.28		NA	0.12		NA
Snail	0.79		NA	0.79		NA
Slug	0.88		NA	0.83		NA
ZEB1	0.65		NA	0.37		NA
ZEB2	0.90		NA	0.65		NA
TWIST	0.004*	2.027 (1.143–3.595)	0.016*	0.019*	2.553 (1.309–4.979)	0.006*
Vimentin	0.51		NA	0.08		NA
FIN	0.61		NA	0.35		NA
DDR2	0.66		NA	0.33		NA
S100A4	0.48		NA	0.73		NA
TJP1	0.045*	0.45 (0.14–1.451)	0.181	0.002*	0.148 (0.027–0.805)	0.027*
FOXC2	0.83		NA	0.46		NA
SIX1	0.77		NA	0.87		NA
GSC	0.41		NA	0.98		NA

Variables with $p < 0.1$ in univariate analysis were adopted for multivariate analysis. TNM stage was included; other covariates including tumor size and vascular inavasion were excluded.

NA = Not applicable. * $p < 0.05$.

ing medium (DMEM containing 0.5% FBS), and the upper chambers were placed into the lower chambers of 24-well culture dishes containing 600 μl of DMEM containing 10% FBS. After incubation for 24 h, the media in the upper chambers were aspirated and the non-migrated cells on the inner sides of the membranes were removed using a cotton swab. The cells that had migrated to the outer side of the membranes were fixed with 4% paraformaldehyde for 10 min and stained with 0.1% Giemsa stain solution for 15 min; they were then counted using a light microscope. The experiment was performed in triplicate.

Western Blot Analysis

The following antibodies were used in this study: TJP1 and β-actin antibody and HRP-conjugated secondary antibody (Cell Signaling Technology, Beverly, Mass., USA). All the experiments were performed in duplicate. The western blot analysis was performed as described previously [10].

Transfection of Small Interfering RNA

Three different sequences of small interfering RNA (siRNA) targeting human TJP1 (Hs-TJP1-5302, Hs-TJP1-7406) and those of 2 scramble control siRNA were purchased from Sigma Aldrich Japan (Tokyo). The details of the conditions of transfection have been described previously [13].

Statistical Analysis

Statistical analyses were performed to calculate the SD and to test for statistical significances between the samples using a Student t test and Pearson chi-square test. The gene expression data were normalized by means of the log10 transform. Univariate Cox regression analyses were run for each gene, as summarized in table 2. Subsequently, a multivariate Cox proportional hazard model was applied to identify independent prognostic factors for recurrence-free survival (RFS) and OS. The analysis of OS after hepatic resection was calculated using the Kaplan–Meier method, and the

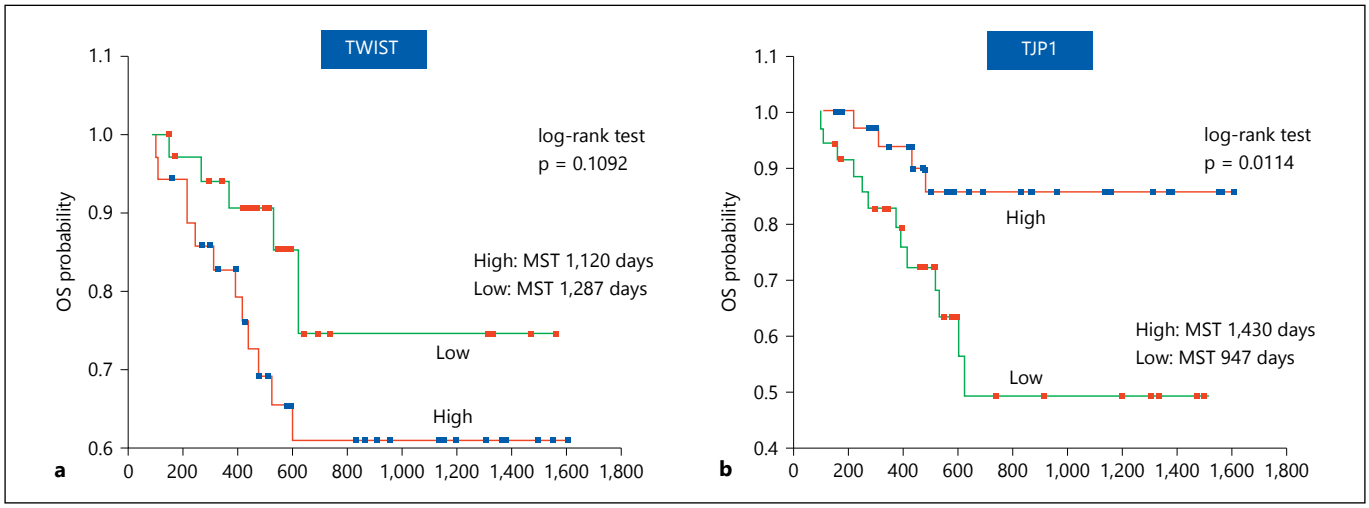

Fig. 1. Low-TJP-1 expression is associated with worse clinical outcomes in HCC after operation. Kaplan–Meier survival curves for high-TWIST expression versus low-TWIST expression (**a**) and high-TJP-1 expression versus low-TJP-1 expression in 72 HCC patients and p values = 0.1092 (**a**) and p values = 0.0114 (**b**).

differences in survivals between the groups were examined by the log-rank test. A p value of <0.05 is considered statistically significant. All statistical analyses were done with SPSS 19.0 (SPSS Inc., Chicago, Ill., USA).

Results

The TJP1 as a Protective Gene and the TWIST as a Risk Gene for the Survival of HCC Patients

For identification of prognostic factors associated with RFS and OS, we examined the expression of 15 kinds of EMT-related genes in HCC tissues and analyzed the RFS and OS of the patients. The follow-up was completed on December 31, 2010, with median follow-up time of 17 months (range 3.3–53.5 months). Patients' characteristics and factors revealed to be significant in univariate analysis were subsequently applied into the multivariate Cox proportional hazards regression model. The associations between patients' backgrounds and RFS and OS by univariate Cox regression analysis are shown in table 2. Poorly differentiated phenotype, the presence of vascular invasion, and high serum level of alpha-fetoprotein (AFP) are significantly associated with RFS. Similarly, larger tumor size, TNM stage, vascular invasion, and high levels of AFP and prothrombin induced by vitamin K absence-II (PIVKA-II) are significantly associated with OS. In addition, the expression of TWIST and TJP1 are correlated with RFS and OS by univariate Cox regression analysis (table 2).

Figure 1 showed survival curve of the patients with high expression and low expression of TWIST and TJP1. Low expression of TWIST shows a trend with longer OS in HCC patients after hepatic resection (fig. 1a). And the high expression of TJP1 is significantly associated with longer OS in those patients (fig. 1a). The high expression of TJP1 is related to longer OS. Multivariate analysis revealed that AFP levels (>20) and high expression of TWIST were independent predictors for shorter RFS (table 2). Regarding the OS, high expression of TWIST, low expression of TJP1, poorly differentiated phenotype, high serum level of PIVKA-II, and stage were the variables related to shorter OS (table 2). Therefore, TJP1 is considered a protective gene (a hazard ratio of less than 1) and TWIST a risk gene (a hazard ratio of more than 1) for patients' survival.

Knocking Down of TJP1-Induced Migration of HCC Cell line

Previously, we reported that sorafenib suppressed the EMT and cellular migration in an HCC cell line, Huh7. Therefore, we performed a migration assay using the Boyden-chamber method. The siRNA knockdown of TJP1 strongly induced migration of an HCC cell line Huh7 (fig. 2).

Discussion

In this study, we demonstrated that the low expression of TJP1 was significantly associated with poor survival in HCC patients after hepatic resection. Yang et al. [16] re-

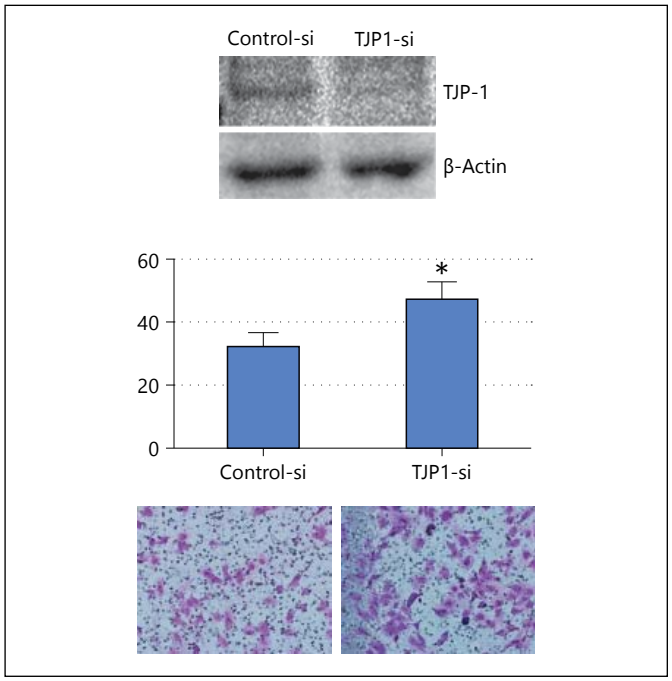

Fig. 2. Cells transfected with si-TJP-1 showed higher potential for invasion. By transwell assay, si-TJP-1-transfected cells penetrated into the lower chamber when compared to the action of si-control cells.

ported that the coexpression of Snail and TWIST was associated with the worst prognosis for HCC patients. On the other hand, our data demonstrated that the low level of TJP1 is also an independent factor for poor prognosis in HCC patents, which have not been reported so far. TJP1 is a 210–225 kDa protein that is found at the submembranous domain of tight junction in epithelia and endothelia; it represents a scaffolding function and reportedly plays an important role in signal transduction by clustering critical membrane proteins [17, 18]. TJP1 also known to establish a link between occluding and the actin cytoskeleton, and play a role on the regulation of gene expression mediated by the signal from the tight junction [19–21]. Orban et al. [22] reported that the expression of occludin and TJP1 mRNA in HCC was lower than those in normal liver tissue, while the protein expression of occludin and TJP1 was higher in metastatic lesion compared with those in normal liver. Ohtani et al. [23] reported the expression of tight-junction–associated proteins in human gastric cancer. Kaihara et al. [24] also reported the association between the dedifferentiation of tumors and decreased expression of adhesion molecules; E-cadherin and TJP1 are closely related to liver metastasis of colorectal cancer. Ni et al. [25] reported that increased TJP1 expression predicted valuable prognosis in non-small cell lung cancer. Decreased TJP1 expression was also shown to be associated with increased invasiveness in breast cancer [26]. In addition, the altered expression of the tight junction protein, such as TJP1, should play an important role in the process of cell dissociation. TWIST is also considered one of the major EMT regulators [22]. Taking these facts into consideration, understanding the role of TJP1 and TWIST expression in human cancer is quite important from both basic and clinical aspects.

The results of our analysis revealed that RFS and OS were independently influenced by different prognostic factors. For example, the multivariate Cox proportional hazards regression model revealed that TWIST was an independent factor of RFS and OS. And there was a trend between with the high expression of TWIST and shorter OS ($p = 0.1092$). The analysis of survival curves with the Kaplan–Meier method for high-TWIST expression versus low-TWIST expression is not significantly different. The one of reason is that the groups of high- and low-TWIST expression are divided in the median.

On the other hand, TJP1 was not found to be an independent prognostic factor affecting the RFS. It is probably due to the different follow-up schedule of the patients among the physicians; the date of recurrence was not defined precisely. Therefore, RFS should be affected by the variation of follow-up schedule among the physicians greater than the way in which OS is affected. On the other hand, the high expression of TJP1 and low expression of TWIST are significantly associated with longer OS, suggesting the critical role of TJP1 as a tumor suppressor and TWIST as an oncogenic protein on survival of the HCC patients.

Although TJP1 is known as an epithelial marker, its function is still largely unclear. To confirm the biological function of TJP1, we knocked down TJP1 using siRNA in a Huh7 HCC cell line, which accelerated a migration of Huh7. Therefore, it is possible that TJP1 may act as a metastatic suppressor because knockdown of TJP1 led to an increased migration of Huh7 cells. In conclusion, we found that the low expression of TJP1 is associated with poor prognosis; it could be a predictive factor for poor prognosis in patients with HCC after hepatic resection and may serve as a potential biomarker.

Disclosure Statement

The authors have no conflicts of interest to disclose.

References

1 Torre LA, Bray F, Siegel RL, Ferlay J, Lortet-Tieulent J, Jemal A: Global cancer statistics, 2012. CA Cancer J Clin 2015;65:87–108.
2 Yamamoto J, Kosuge T, Takayama T, Shimada K, Yamasaki S, Ozaki H, Yamaguchi N, Makuuchi M: Recurrence of hepatocellular carcinoma after surgery. Br J Surg 1996;83:1219–1222.
3 Kudo M: Surveillance, diagnosis, treatment, and outcome of liver cancer in Japan. Liver Cancer 2015;4:39–50.
4 Kawanaka M, Nishino K, Nakamura J, Oka T, Urata N, Goto D, Suehiro M, Kawamoto H, Kudo M, Yamada G: Quantitative levels of hepatitis B virus DNA and surface antigen and the risk of hepatocellular carcinoma in patients with hepatitis B receiving long-term nucleos(t)ide analogue therapy. Liver Cancer 2014;3:41–52.
5 Kudo M, Matsui O, Izumi N, Iijima H, Kadoya M, Imai Y, Okusaka T, Miyayama S, Tsuchiya K, Ueshima K, Hiraoka A, Ikeda M, Ogasawara S, Yamashita T, Minami T, Yamakado K: JSH consensus-based clinical practice guidelines for the management of hepatocellular carcinoma: 2014 update by the liver cancer study group of Japan. Liver Cancer 2014;3:458–468.
6 Clinical practice guidelines for hepatocellular carcinoma differ between Japan, United States, and Europe. Liver Cancer 2015;4:85–95.
7 Brockhausen J, Tay SS, Grzelak CA, Bertolino P, Bowen DG, d'Avigdor WM, Teoh N, Pok S, Shackel N, Gamble JR, Vadas M, McCaughan GW: miR-181a mediates TGF-β-induced hepatocyte EMT and is dysregulated in cirrhosis and hepatocellular cancer. Liver Int 2015;35:240–253.
8 Yamada S, Fuchs BC, Fujii T, Shimoyama Y, Sugimoto H, Nomoto S, Takeda S, Tanabe KK, Kodera Y, Nakao A: Epithelial-to-mesenchymal transition predicts prognosis of pancreatic cancer. Surgery 2013;154:946–954.
9 Bae SY, Kim HJ, Lee KJ, Lee K: Translationally controlled tumor protein induces epithelial to mesenchymal transition and promotes cell migration, invasion and metastasis. Sci Rep 2015;5:8061.
10 Xu J, Li X, Yang H, Chang R, Kong C, Yang L: SIN1 promotes invasion and metastasis of hepatocellular carcinoma by facilitating epithelial-mesenchymal transition. Cancer 2013;119:2247–2257.
11 Peck-Radosavljevic M: Drug therapy for advanced-stage liver cancer. Liver Cancer 2014;3:125–131.
12 Arizumi T, Ueshima K, Minami T, Kono M, Chishina H, Takita M, Kitai S, Inoue T, Yada N, Hagiwara S, Minami Y, Sakurai T, Nishida N, Kudo M: Effectiveness of sorafenib in patients with transcatheter arterial chemoembolization (TACE) refractory and intermediate-stage hepatocellular carcinoma. Liver Cancer 2015;4:253–262.
13 Nagai T, Arao T, Furuta K, Sakai K, Kudo K, Kaneda H, Tamura D, Aomatsu K, Kimura H, Fujita Y, Matsumoto K, Saijo N, Kudo M, Nishio K: Sorafenib inhibits the hepatocyte growth factor-mediated epithelial mesenchymal transition in hepatocellular carcinoma. Mol Cancer Ther 2011;10:169–177.
14 Chen YL, Lv J, Ye XL, Sun MY, Xu Q, Liu CH, Min LH, Li HP, Liu P, Ding X: Sorafenib inhibits transforming growth factor β1-mediated epithelial-mesenchymal transition and apoptosis in mouse hepatocytes. Hepatology 2011;53:1708–1718.
15 Matsumoto K, Arao T, Tanaka K, Kaneda H, Kudo K, Fujita Y, Tamura D, Aomatsu K, Tamura T, Yamada Y, Saijo N, Nishio K: mTOR signal and hypoxia-inducible factor-1 alpha regulate CD133 expression in cancer cells. Cancer Res 2009;69:7160–7164.
16 Yang MH, Chen CL, Chau GY, Chiou SH, Su CW, Chou TY, Peng WL, Wu JC: Comprehensive analysis of the independent effect of twist and snail in promoting metastasis of hepatocellular carcinoma. Hepatology 2009;50:1464–1474.
17 Fanning AS, Anderson JM: PDZ domains: fundamental building blocks in the organization of protein complexes at the plasma membrane. J Clin Invest 1999;103:767–772.
18 Itoh M, Furuse M, Morita K, Kubota K, Saitou M, Tsukita S: Direct binding of three tight junction-associated MAGUKs, ZO-1, ZO-2, and ZO-3, with the COOH termini of claudins. J Cell Biol 1999;147:1351–1363.
19 Morita K, Furuse M, Fujimoto K, Tsukita S: Claudin multigene family encoding four-transmembrane domain protein components of tight junction strands. Proc Natl Acad Sci U S A 1999;96:511–516.
20 Furuse M, Hirase T, Itoh M, Nagafuchi A, Yonemura S, Tsukita S, Tsukita S: Occludin: a novel integral membrane protein localizing at tight junctions. J Cell Biol 1993;123:1777–1788.
21 Saitou M, Fujimoto K, Doi Y, Itoh M, Fujimoto T, Furuse M, Takano H, Noda T, Tsukita S: Occludin-deficient embryonic stem cells can differentiate into polarized epithelial cells bearing tight junctions. J Cell Biol 1998;141:397–408.
22 Orban E, Szabo E, Lotz G, Kupcsulik P, Paska C, Schaff Z, Kiss A: Different expression of occludin and ZO-1 in primary and metastatic liver tumors. Pathol Oncol Res 2008;14:299–306.
23 Ohtani S, Terashima M, Satoh J, Soeta N, Saze Z, Kashimura S, Ohsuka F, Hoshino Y, Kogure M, Gotoh M: Expression of tight-junction-associated proteins in human gastric cancer: downregulation of claudin-4 correlates with tumor aggressiveness and survival. Gastric Cancer 2009;12:43–51.
24 Kaihara T, Kusaka T, Nishi M, Kawamata H, Imura J, Kitajima K, Itoh-Minami R, Aoyama N, Kasuga M, Oda Y, Hattori M, Fujimori T: Dedifferentiation and decreased expression of adhesion molecules, E-cadherin and ZO-1, in colorectal cancer are closely related to liver metastasis. J Exp Clin Cancer Res 2003;22:117–123.
25 Ni S, Xu L, Huang J, Feng J, Zhu H, Wang G, Wang X: Increased ZO-1 expression predicts valuable prognosis in non-small cell lung cancer. Int J Clin Exp Pathol 2013;6:2887–2895.
26 Hoover KB, Liao SY, Bryant PJ: Loss of the tight junction MAGUK ZO-1 in breast cancer: relationship to glandular differentiation and loss of heterozygosity. Am J Pathol 1998;153:1767–1773.

Med Oncol (2016) 33:114
DOI 10.1007/s12032-016-0827-8

ORIGINAL PAPER

Prognostic sub-classification of intermediate-stage hepatocellular carcinoma: a multicenter cohort study with propensity score analysis

Ramya Ramaswami[1] · David J. Pinato[1,2] · Keiichi Kubota[3] · Mitsuru Ishizuka[3] · Tadaaki Arizumi[4] · Masatoshi Kudo[4] · Jeong Won Jang[5] · Young Woon Kim[5] · Mario Pirisi[6,7] · Elias Allara[6] · Rohini Sharma[1]

Received: 2 August 2016 / Accepted: 24 August 2016 / Published online: 6 September 2016

Abstract There is significant heterogeneity in the clinicopathological characteristics of intermediate hepatocellular carcinoma (IHCC). This also translates to treatment as transarterial chemoembolization (TACE) is used as first-line therapy for patients with IHCC; however, in Asia liver resection (LR) is preferred. Prognostic tools are required to help guide clinicians in deciding treatment options. This study evaluates the prognostic impact of the Intermediate Stage Score (ISS) on overall survival (OS) in a large, multicenter cohort study of patients with IHCC treated with TACE or surgery LR. Consecutive patients from centers in Japan, Korea, Italy and the United Kingdom who underwent TACE or LR between 2001 and 2015 were enrolled. Propensity score (PS) adjustment was used to remove residual confounding and applied to LR ($n = 162$) and TACE ($n = 449$) to determine the prognostic significance of ISS. Among 611 patients, 75 % were men and 25 % women, with a mean age of 70 years. ISS is a valid prognostic tool in the BCLC-B population with a median OS ISS 1–51, 2–38.3, 3–24.3, 4–15.6, 5–16 months ($p < 0.0001$). ISS was analyzed within each treatment modality, and this was a valid prognostic score among those treated with TACE and LR ($p < 0.001$ vs. $p = 0.008$). In the PS-adjusted model, ISS retained its prognostic utility in TACE and LR groups ($p < 0.001$ vs. $p = 0.007$). ISS optimizes prognostic prediction in IHCC, reducing clinical heterogeneity, and is a useful tool for patients treated for TACE or LR.

Keywords Hepatocellular cancer · Transarterial chemoembolization · Liver resection · Prognosis · Multicenter

✉ Rohini Sharma
r.sharma@imperial.ac.uk

1 Department of Surgery and Cancer, Imperial College London Hammersmith Hospital, Du Cane Road, London W12 0HS, UK

2 Department of Medical Oncology, The Royal Marsden NHS Foundation Trust, Downs Road, Sutton SM2 5PT, UK

3 Department of Surgery, Dokkyo Medical University, Dokkyo, Japan

4 Department of Gastroenterology and Hepatology, Kinki University School of Medicine, Osaka-Sayama, Osaka, Japan

5 Department of Internal Medicine, The Catholic University of Korea Incheon St. Mary's Hospital, Seoul, Republic of Korea

6 Department of Translational Medicine, Università degli Studi del Piemonte Orientale "A. Avogadro", Via Solaroli 17, 28100 Novara, Italy

7 Interdisciplinary Research Center of Autoimmune Diseases, Università degli Studi del Piemonte Orientale "A. Avogadro", Via Solaroli 17, 28100 Novara, Italy

Introduction

Hepatocellular carcinoma (HCC) is one of the leading causes of cancer-related death in patients with liver cirrhosis, with more than new 700,000 cases diagnosed yearly worldwide [1, 2]. Over the past few decades, it has become clear that the natural history of HCC strongly depends on anatomical stage, underlying liver function and overall patients' physical status: this has led to the development of several prognostic algorithms with intent to optimize treatment [3–7].

The Barcelona Clinic Liver Cancer (BCLC) stage includes prognostic variables such as tumor stage, performance status, and Child–Turcotte–Pugh (CTP) class [8]. Prospective validation of the BCLC staging system has demonstrated reliable prognostic subdivision of HCC [9, 10]. Due to its association with treatment allocation, the

BCLC algorithm has received formal endorsement by organizations such the European Association for the Study of the Liver (EASL) and the American Association for the Study of Liver Diseases (AASLD) [11–13]. However, there is marked heterogeneity in the reported 3-year survival in BCLC-B stage disease of 10–40 %. Therefore, formulating appropriate treatment strategies for the individual patient is difficult within this nebulous BCLC-B staging system.

According to the BCLC staging system, transarterial chemoembolization (TACE) is recommended as first-line treatment for patients with IHCC or BCLC-B. Two randomized controlled trials have shown an approximate 50 % reduction in mortality in patients treated with TACE compared to controls [14, 15]. A significant OS benefit from TACE has been further consolidated by two separate meta-analyses [16], which however re-defined the magnitude of benefit of TACE due to patient and procedural heterogeneity, resulting in some of the pooled studies not meeting their primary survival endpoints [17].

Issues such as the relative efficacy of TACE and the risk of adverse events among this group of patients results in the use of sorafenib, trial therapies or best supportive care [18, 19]. Alternatively, clinicians who do not adhere to BCLC guidelines offer other treatments such as resection or transarterial radioembolization (TARE) if IHCC patients meet local criteria [20, 21]. Therefore, despite the presence of consensus guidelines, there is variation in treatment in patients with BCLC-B disease. There is an urgent need for improved prognostication and subsequent stratification of management for patients with IHCC.

Bolondi et al. [22] created a prognostic score to further subdivide patients with IHCC in an effort to improve treatment allocation among this complex group. The Intermediate Stage Score (ISS) consists of five stages and includes CTP classification, ECOG performance status, portal vein thrombus and specific size criteria (Table 1). On the basis of the score, the authors recommended that patients can be offered first-line options such as TACE while patients with advanced stage (Quasi-C) should receive sorafenib [22]. There have been mixed outcomes in demonstrating the efficacy of this score. Two studies have demonstrated an association between ISS and OS among patients treated with bland transarterial embolization (TAE) and TACE ($N = 580, 466$) [23, 24]. However, in a separate European study, the score did not achieve prognostic significance ($N = 254$) [25]. Our intent was to validate the prognostic ability of the ISS in patients with intermediate-stage HCC (BCLC-B) by using propensity score analysis in diverse Eastern and Western populations treated with either surgical resection (LR) or TACE.

Materials and methods

Patient population

All centers in this study were involved in prospective collection of data from patients with a diagnosis of HCC made according to radiological or histological criteria, between 2001 and 2015. Patients were recruited from Hammersmith Hospital, London, St Mary's Hospital, Seoul, University of Novara, and, Dokkyo Medical University, Dokkyo and Kinki University, Osaka). Informed consent was obtained from all patients recruited in this study in accordance with the Declaration of Helsinki and Good Clinical Practice (GCP) guidelines. Ethical approval for this study was obtained from the East London Research Ethics Committee.

Clinical variables were retrieved include patient demographics, complete blood count, albumin, aspartate and alanine aminotransferases (AST, ALT), alkaline phosphatase (ALP) alpha-fetoprotein (AFP), the international normalized ratio (INR) value and underlying etiology of liver disease was also identified. Patients with IHCC (BCLC-B) were categorized into five groups as per the criteria described by Bolondi et al. [22] (Table 1). Liver functional reserve was estimated using the CTP classification.

Table 1 BCLC-B sub-classification by Bolondi et al

BCLC sub-stage (ISS)	B1 (1)	B2 (2)	B3 (3)	B4 (4)	Quasi-C (5)
Child–Pugh score	5–6–7	5–6	7	8–9	5–6
Beyond milan and within Ut-7	In	Out	Out	Any	Any
ECOG PS	0	0	0	0–1	0
Portal vein thrombosis	No	No	No	No	Yes
1st line treatment	TACE	TACE or TARE		Best Supportive Care	Sorafenib
Alternative	LT TACE + Ablation	Sorafenib	Research trials TACE Sorafenib	LT	TACE or TARE

Proposed sub-classification and management recommendations for intermediate hepatocellular carcinoma as detailed by Bolondi et al. [15]

BCLC barcelona liver clinic, *ECOG* Eastern Cooperative Oncology Group, *PS* performance status, *LT* liver transplantation, *TACE* transarterial chemoembolization, *TARE* transarterial radioembolization

Tumor staging was described as the number of focal hepatic lesions and maximum diameter detected during contrast enhancement phase on computerized tomography. The Milan criteria and up-to-seven criteria (Up-to-7) were used to categorize size for calculating the ISS. The Milan criteria is defined as a single lesion <5 cm, up to three lesions <3 cm, the absence of gross vascular invasion or nodal or distant metastases [26]. Within the Up-to-7 criteria, seven is the sum of the size (centimeters) and the number of tumors for any given HCC [27].

Statistical analysis

Continuous variables were presented as a median and range, and associations were tested using Mann–Whitney U or Student's t test as appropriate. Categorical variables with absolute or relative frequencies were tabulated and or Fisher's exact test, where appropriate. The OS rates for various ISS levels in all patients were analyzed using Kaplan–Meier method, and log-rank test was used to compare survival time. Univariate analyses of prognostic variables were completed with the Cox proportional hazards model. All statistical analyses were completed using two-sided test, and statistical significance was achieved where $p < 0.05$.

The date of HCC diagnosis till the date of death, loss to follow-up or study censoring (1st January 2016) was used to calculate overall survival. All patients were monitored with routine follow-up till the dates of death, loss to follow-up or study censoring.

Propensity score adjustment (PS) is a statistical method to reduce the effect of residual confounding in two groups

Table 2 Patient demographic at initial HCC diagnosis

Baseline characteristic	All patients (%), median, range $N = 611$	TACE intervention (%), median, range $N = 449$	LR intervention (%), median, range $N = 162$	p value
Age, years	70 (28–89)	72 (33–89)	68 (28–84)	<0.0001
Gender				0.39
Male	460 (75.3)	334 (74.4)	126 (77.8)	
Female	151 (24.7)	115 (25.6)	36 (22.2)	
Aetiology				
Hepatitis B infection	102 (16.7)	64 (14.3)	38 (23.4)	0.01
Hepatitis C infection	369 (60.4)	268 (59.7)	101 (62.3)	0.36
Alcohol related	97 (15.9)	97 (21.6)	–	–
Child–Turcotte–Pugh class				0.0003
A5	274 (44.8)	221 (49.2)	53 (32.7)	
A6	201 (32.9)	128 (28.5)	73 (45.0)	
B7	101 (16.5)	69 (15.4)	32 (19.8)	
B8	27 (4.4)	23 (5.1)	4 (2.5)	
B9	7 (1.2)	7 (1.5)	–	
Maximum tumor diameter				<0.0001
<7 cm	509 (83.3)	403 (89.8)	106 (65.4)	
≥7 cm	102 (16.7)	46 (10.2)	56 (34.6)	
Portal vein thrombus				–
Present	5 (1.1)	5 (1.1)	–	
Absent	444 (98.9)	444 (98.9)	–	
AFP, ng/mL	33 (1– > 1000)	32 (1– > 1000)	43.5 (1– > 1000)	0.44
Platelet count, $\times 10^9$/L	128 (26–470)	123 (26–453)	146 (44–470)	0.0008
ISS				<0.0001
1	104 (17.0)	42 (9.4)	62 (38.3)	
2	384 (62.8)	309 (68.8)	75 (46.3)	
3	84 (13.8)	63 (14.0)	21 (13.0)	
4	34 (5.6)	30 (6.7)	4 (2.5)	
5	5 (0.8)	5 (1.1)	–	
Median OS in months (95 % CI)	37 (33, 39.3)	34.8 (29.6, 38.9)	40 (34,47)	0.09

AFP alpha-fetoprotein, *INR* international normalized ratio, *BScore* scoring system for intermediate HCC, *OS* overall survival, *TACE* transarterial chemoembolization, *LR* liver resection

Table 3 Univariate analysis of factors that predict overall survival in patients with intermediate hepatocellular carcinoma (IHCC) treated with TACE or LR

Baseline characteristic	Hazard ratio (HR)	95 % confidence interval (CI)	*p* value
Age, years	1.01	0.99–1.01	0.32
Gender (F vs. M)	1.40	1.11–1.77	0.005
Aetiology			
Hepatitis B infection	0.69	0.51–0.93	0.01
Hepatitis C infection	1.23	0.99–1.53	0.06
Child–Turcotte–Pugh class			
A5			
A6	1.24	0.98–1.57	0.08
B7	1.62	1.20–2.19	0.002
B8	2.56	1.58–4.13	0.00
B9	3.22	1.19–8.72	0.02
Maximum tumor diameter (<7 vs. ≥7 cm)	1.11	0.86–1.43	0.42
Portal Vein Thrombus	1.51	0.48–4.71	0.48
AFP, ng/mL	1.00	0.99–1.00	0.07
Platelet Count, $\times 10^9$/L	0.99	0.996–0.999	0.03
ISS			
1	–	–	
2	1.39	1.03–1.87	0.03
3	2.29	1.55–3.39	0.00
4	3.19	1.95–5.23	0.00
5	2.27	0.71–7.29	0.17

[28]. In this study, PS was used to reduce the effect of residual confounding in the cohort by adjusting for confounding variables that are not accounted for within ISS classification, such as age, gender, hepatitis status and INR that impact treatment options. Cox regression analysis was used to determine the effect of ISS adjusted for PS quartiles in TACE and LR treatment groups. An interaction test was performed to determine the statistical significance of ISS in TACE and LR groups. Statistical analyses were performed using R version 3.1.2 (ww.r-project.org) and SAS 9.4 (SAS Institute Inc. Cary, North Carolina).

Results

Patient characteristics

Our study population consisted of 611 BCLC-B patients diagnosed with HCC across five centers (Table 2). The majority of patients underwent TACE (73.4 %) as first anticancer treatment, while 27.6 % were offered liver resection. Patients undergoing liver resection were younger ($p < 0.001$), while a higher proportion of patients undergoing TACE were Hepatitis B positive ($p = 0.01$). Five patients treated with TACE had portal vein thrombosis (PVT) and were classified as 'Quasi C' or ISS 5. There was a significant difference in the CTP classification between LR and TACE, with a higher proportion of patients with CTP > A6 receiving TACE ($p < 0.01$). The median OS (OS) of the overall population was 37 months (95 % confidence interval (CI) 33.0–39.3 months). The 1- and 3-year survival rates were 84.1, and 21.9 %, respectively. There was no significant difference between the median OS between TACE and LR subgroups (34.8 vs. 40 months, $p = 0.09$).

ISS characteristics and OS

In univariate analyses of the cohort, male gender, positive hepatitis B status and INR were variables that were significant for increased mortality and were not within the ISS prognostic score (Table 3). There was a difference in the ISS categories between TACE and LR groups, with a higher proportion of patients with ISS 2 or greater treated with TACE and those with an ISS of 2 or less treated with LR ($p < 0.0001$). There were no significant differences in baseline characteristics between ISS groups (Table 4). Due to the small number of patients with ISS 4 and 5, these were analyzed together to improve statistical validity. Significant differences in OS were observed between the

Table 4 Sub-classification of BCLC-B with intermediate stage score (ISS) and corresponding characteristics

Factors	Total	ISS 1 ($n = 104$)	ISS 2 ($n = 384$)	ISS 3 ($n = 84$)	ISS 4 ($n = 34$)	ISS 5 ($n = 5$)	p value
Age, median years	70	67.4	69.7	68.9	66.1	65.8	0.07
Gender							0.088
Male	460 (75.3)	77 (74.0)	294 (76.6)	61 (72.6)	24 (70.6)	4 (80.0)	
Female	151 (24.7)	27 (25.9)	90 (23.4)	23 (27.3)	10 (29.4)	1 (20.0)	
Aetiology							
Hepatitis B infection	102 (16.7)	26 (25.0)	61 (15.9)	10 (11.9)	5 (14.7)	–	0.33
Hepatitis C infection	369 (60.4)	60 (57.7)	242 (63.0)	43 (51.2)	20 (58.8)	4 (80.0)	0.54
Alcohol related	97 (15.9)	11 (10.6)	57 (14.8)	19 (22.6)	9 (26.5)	1 (20.0)	0.34
Alpha-fetoprotein	33 (1– > 1000)	2279.4	5903.6	3923.2	1262.9	4525.5	0.96
Child–Turcotte–Pugh class							<0.0001
A5	274 (44.8)	53 (50.9)	219 (57.0)	–	–	2 (40.0)	
A6	201 (32.9)	35 (33.7)	164 (42.7)	–	–	1 (20.0)	
B7	101 (16.5)	16 (15.4)	–	84 (100)	–	2 (40.0)	
B8	27 (4.4)	–	–	–	27 (100)	–	
B9	7 (1.2)	–	–	–	7 (100)	–	
Maximum tumor diameter							0.0004
<7 cm	509 (83.3)	104 (100)	309 (80.5)	65 (77.4)	28 (82.4)	3 (60.0)	
≥7 cm	102 (16.7)	–	75 (19.5)	19 (22.6)	6 (17.6)	1 (20.0)	
Median overall survival in months	37	51	38.3	24.3	15.6	16	<0.0001

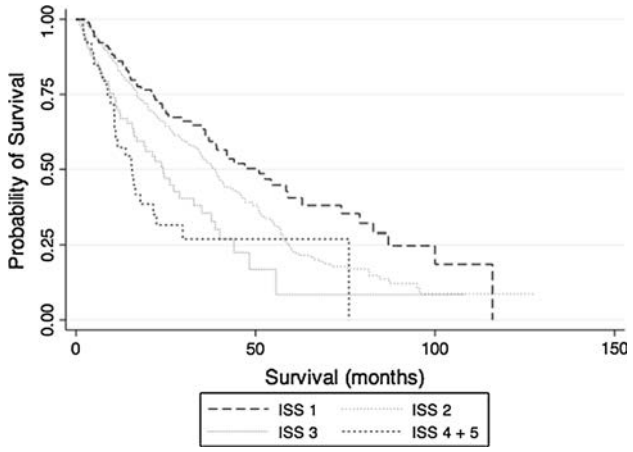

Fig. 1 Cumulative mortality stratified by intermediate stage score (ISS) for all patients with intermediate hepatocellular carcinoma

different ISS groups ranging from 51 (ISS 1) to 16 months (ISS 4 and 5; $p < 0.001$), (Table 3; Fig. 1).

ISS retains prognostic utility in propensity score adjustment analysis

When considering the prognostic utility of the ISS according to treatment received, ISS was significant in TACE ($p = 0.0003$) and LR ($p = 0.008$). ISS retained its prognostic ability following PS adjustment. In the PS-adjusted model, among patients undergoing LR, ISS of 4 and 5 implied poor prognosis compared to ISS 1 [hazard ratio (HR) 2.13 (95 % CI 0.64, 7.02)], such that ISS was a prognostic score among patients treated with LR [Likelihood ratio test (LRT) $p = 0.007$]. This comparison between ISS 4 and 5 to ISS 1 was evident for patients treated with TACE [HR 3.59 (95 % CI 2.07, 7.57)], (LRT $p < 0.001$, Table 5). On assessing the prognostic value of ISS on either treatment, there was no evidence of a difference in ISS subgroups between LR and TACE groups ($p = 0.23$).

Discussion

This is the first large, multi-center study to validate the prognostic ability of the ISS in patients with BCLC-B stage disease, independent of treatment received. Bolondi and colleagues divided BCLC-B stage disease into sub-classifications based on trial results and expert opinion in an effort to reduce heterogeneity in survival in this otherwise disparate patient group. While their method has been validated in a number of papers, this the largest study incorporating both Eastern and Western populations that adheres to the BCLC-B classification. As such this is the first study to explore the use of LR within the BCLC-B classification, albeit in small numbers. PS has been used to reduce

Table 5 Propensity score-adjusted Cox proportional hazards model of ISS on overall survival within TACE and LR population and overall likelihood ratio test (LRT), and interaction test to determine effect of ISS between treatments

	TACE intervention, hazard ratio (95 % CI)		LR intervention median OS in months (95 % CI)$^{+}$		p value[a]
ISS 1	–	$p < 0.001$	–	$p = 0.007$	0.226
ISS 2	1.30 (0.79–2.14)		1.66 (1.06–2.59)		
ISS 3	1.97 (1.08–3.58)		2.98 (1.61–5.51)		
ISS 4 + 5	3.95 (2.07–7.57)		2.13 (0.64–7.02)		

[a] Log likelihood ratio test of interaction

confounders between LR and TACE groups, adding to the robust nature of the results obtained.

A plethora of prognostic scores have recently been introduced aiming to improve treatment selection in patients with BCLC-B stage disease [29–31]. These scores such as the Hepatoma Arterial Embolization Prognostic score (HAP score) and Selection for Transarterial chemoembolization Treatment (STATE) score have derived prognostic variables within a cohort and subsequently validated the scores within an external population [30, 31]. The recently proposed ART and HAP scores have attracted significant attention recently particularly as prognostic markers in patients receiving TACE. The HAP score consists of two measures of tumor burden (AFP and size of largest tumor) and two measures of liver function (albumin and bilirubin) [30]. However, the original study included patients with BCLC-A, B and C disease, as well as concerns regarding the independent prognostic ability of bilirubin, may impact on the overall utility of this score. The ART score while useful in determining retreatment with TACE does not contribute to prognostic sub-classification within BCLC-B. Recently Ogasawara and colleagues derived the CHIP score as a means to delineate survival heterogeneity in BCLC-B stage tumors [32]. However, in their paper when compared to the ISS, their novel score showed no real difference in prognostic ability.

The variables included in the ISS are similar to previously identified scores including markers of liver function such albumin, bilirubin, and tumor burden. The main difference with the ISS is that it incorporates three measures of tumor burden; up-to-7 criteria, size of the largest tumor and number of tumors. We report considerable variation in OS from 15.6 to 51 months in our population suggesting that the variables used by Bolondi et al. are useful in delineating prognosis further within this patient group.

A key strength of this study is that we used patient datasets derived from different academic institutions in both Europe and Asia. While TACE is the recommended treatment for BCLC-B patients according to American and European guidelines, in Asian centers, it is not uncommon to propose surgical management [33, 34]. We have shown that ISS retains its prognostic ability in LR or TACE in BCLC-B stage disease prior to and following PS-adjusted analysis. Resection of liver lesions beyond the Milan criteria in BCLC-B population has been shown to improve OS compared to TACE treatment [35], and though beyond the remit of this study, these results suggest that surgical intervention may be a useful treatment modality in a carefully selected population group, and does warrant further investigation in a larger population group within a prospective study design. ISS appears a useful prognostic tool within each treatment category, and there is no evidence of a difference in the effects of ISS subgroups between treatment groups.

However, the inclusion of 'Quasi C sub-classification' (ISS 5) and patients with portal vein thrombosis involves a subgroup recognized to possess a poorer prognosis with variable treatment options [36]. While we have demonstrated the prognostic accuracy of the ISS, we have not validated the treatment allocation aspect of the score as proposed by Bolondi et al., an aspect that has not been corroborated in any study. In this context, reflection is required on the use of liver transplant for patients with BCLC-B disease given the poorer overall prognosis of this patient group compared with BCLC-A in the context of global organ shortages. We suggest, therefore, that the role of the ISS is in prognostication rather than as treatment allocation per se.

This is a significant time for the management of HCC as new therapies emerge on the horizon. Useful prognostic tools that improve patient selection are crucial in order to ensure that safe, appropriate and effective therapies are administered in a timely manner. It is evident from this large multi-centered study that the ISS offers a useful tool for clinicians to stratify treatment options, such as TACE and LR, in the BCLC-B population.

Acknowledgments Our sincere thanks to Dr. Bindu Kalesan who provided advise on the statistical methods used within this paper.

Funding No specific funding was obtained to support the conduct of this study.

Compliance with ethical standards

Conflict of interest The authors have no conflicts of interests to disclose.

References

1. Surveillance, Research, Program. National Cancer Institute Fast stats: an interactive tool for access to SEER cancer statistics. http://seer.cancer.gov/faststats. (2011).
2. Bruix J, Gores GJ, Mazzaferro V. Hepatocellular carcinoma: clinical frontiers and perspectives. Gut. 2014;63(5):844–55.
3. Chevret S, Trinchet JC, Mathieu D, Rached AA, Beaugrand M, Chastang C. A new prognostic classification for predicting survival in patients with hepatocellular carcinoma. J Hepatol. 1999;3:133–41.
4. Llovet JM, Bruix J. Prospective validation of the Cancer of the Liver Italian Program (CLIP) score: a new prognostic system for patients with cirrhosis and hepatocellular carcinoma. Hepatology. 2000;32:679–80.
5. Chung H, Kudo M, Takahashi S. Comparison of three current staging systems for hepatocellular carcinoma: Japan integrated staging score, new Barcelona Clinic Liver Cancer staging classification, and Tokyo score. J Gastroenterol Hepatol. 2008; 23:445–52.
6. Chan SL, Mo FK, Johnson PJ. Prospective validation of the Chinese University Prognostic Index and comparison with other staging systems for hepatocellular carcinoma in an Asian population. J Gastroenterol Hepatol. 2011;26:340–7.
7. Leung TW, Tang AM, Zee B, Lau WY, Lai PB, Leung KL, et al. Construction of the Chinese University Prognostic Index for hepatocellular carcinoma and comparison with the TNM staging system, Okuda staging system, and the Cancer of the Liver Italian Program staging system: a study based on 926 patients. Cancer. 2002;94:1760–9.
8. Forner A, Llovet JM, Bruix J. Hepatocellular Carcinoma. Lancet. 2012;379(9822):1245–55.
9. Cillo U, Vitale A, Grigoletto F, Farinati F, Brolese A, Zanus G, et al. Prospective validation of the Barcelona Clinic Liver Cancer staging system. J Hepatol. 2006;44(4):723–31.
10. Llovet JM, Bru C, Bruix J. Prognosis of hepatocellular carcinoma: the BCLC staging classification. Semin Liver Dis. 1999;19:329–38.
11. Bruix J, Sherman M, Llovet JM, Beaugrand M, Lencioni R, Burroughs AK, et al. Clinical management of hepatocellular carcinoma. Conclusions of the Barcelona-2000 EASL conference. European Association for the Study of the Liver. J Hepatol. 2001;35(3):421–30.
12. Bruix J, Sherman M. Management of hepatocellular carcinoma. Hepatology. 2005;42:1208–36.
13. Bruix J, Sherman M. American Association for the Study of Liver Disease. Management of hepatocellular carcinoma: an update. Hepatology. 2011;53(3):1020–2.
14. Lo CM, Ngan H, Tso WK, Liu CL, Lam CM, Poon RT, et al. Randomized controlled trial of transarterial lipiodol chemoembolization for unresectable hepatocellular carcinoma. Hepatology. 2002;35(5):1164–71.
15. Llovet JM, Real MI, Montana X, Planas R, Coll S, Aponte J, et al. Arterial embolisation or chemoembolisation versus symptomatic treatment in patients with unresectable hepatocellular carcinoma: a randomised controlled trial. Lancet. 2002;359(9319):1734–9.
16. Llovet JM, Bruix J. Systematic review of randomized trials for unresectable hepatocellular carcinoma: chemoembolization improves survival. Hepatology. 2003;37(2):429–42.
17. Camma C, Schepis F, Orlando A, Albanese M, Shahied L, Trevisani F, et al. Transarterial chemoembolization for unresectable hepatocellular carcinoma: meta-analysis of randomized controlled trials. Radiology. 2002;225(1):47–54.
18. Raoul JL, Sangro B, Forner A, Mazzaferro V, Piscaglia F, Bolondi L, et al. Evolving strategies for the management of intermediate-stage hepatocellular carcinoma: available evidence and expert opinion on the use of transarterial chemoembolization. Cancer Treat Rev. 2011;37:212–20.
19. Bruix J, Raoul JL, Sherman M, Mazzaferro V, Bolondi L, Craxi A, et al. Efficacy and safety of sorafenib in patients with advanced hepatocellular carcinoma: subanalyses of a phase III trial. J Hepatol. 2012;57(4):821–9.
20. Salem R, Lewandowski RJ, Mulcahy MF, Riaz A, Ryu RK, Ibrahim S, Atassi B, et al. Radioembolization for hepatocellular carcinoma using Yttrium-90 microspheres: a comprehensive report of long-term outcomes. Gastroenterology. 2010;138:52–64.
21. Sangro B, Carpanese L, Cianni R, Golfieri R, Gasparini D, Ezziddin S, et al. Survival after yttrium-90 resin microsphere radioembolization of hepatocellular carcinoma across Barcelona clinic liver cancer stages: a European evaluation. Hepatology. 2011;54:868–78.
22. Bolondi L, Burroughs A, Dufour JF, Galle PR, Mazzaferro V, Piscaglia F, et al. Heterogeneity of patients with intermediate (BCLC B) hepatocellular carcinoma: proposal for a subclassification to facilitate treatment decisions. Semin Liver Dis. 2012;32:348–59.
23. Wang JH, Kee KM, Lin CY, Hung CH, Chen CH, Lee CM, et al. Validation and modification of a proposed substaging system for patients with intermediate hepatocellular carcinoma. J Gastroenterol Hepatol. 2015;30(2):358–63.
24. Ha Y, Shim JH, Kim SO, Kim KM, Lim YS, Lee HC. Clinical appraisal of the recently proposed Barcelona Clinic Liver Cancer stage B subclassification by survival analysis. J Gastroenterol Hepatol. 2014;29(4):787–93.
25. Weinmann A, Koch S, Sprinzi M, Kloeckner R, Schulze-Bergkamen H, Duber C, et al. Survival analysis of proposed BCLC-B subgroups in hepatocellular carcinoma patients. Liver Int. 2015;35(2):591–600.
26. Mazzaferro V, Regalia E, Doci R, Andreola S, Pulvirenti A, Bozzetti F, et al. Liver transplantation for the treatment of small hepatocellular carcinomas in patients with cirrhosis. N Engl J Med. 1996;334(11):693–9.
27. Mazzaferro V, Llovet JM, Miceli R, Bhoori S, Schiavo M, Mariani L, et al. Predicting survival after liver transplantation in patients with hepatocellular carcinoma beyond the Milan criteria: a retrospective, exploratory analysis. Lancet Oncol. 2009;10(1):35–43.
28. Austin PC. An introduction to propensity score methods for reducing the effects of confounding in observational studies. Multivar Behav Res. 2011;46(3):399–424.
29. Sieghart W, Hucke F, Peck-Radosavljevic M. Transarterial chemoembolization: modalities, indication, and patient selection. J Hepatol. 2015;62(5):1187–95.
30. Kadalayil L, Benini R, Pallan L, O'Beirne J, Marelli L, Yu D, et al. A simple prognostic scoring system for patients receiving transarterial embolisation for hepatocellular cancer. Ann Oncol. 2013;24:2565–70.
31. Hucke F, Pinter M, Graziadei I, Bota S, Vogel W, Muller C, et al. How to STATE suitability and START transarterial chemoembolization in patients with intermediate stage hepatocellular carcinoma. J Hepatol. 2014;61(6):1287–96.

32. Ogasawara S, Chiba T, Ooka Y, Kanogawa N, Motoyama T, Suzuki E, et al. A prognostic score for patients with intermediate-stage hepatocellular carcinoma treated with transarterial chemoembolization. PLoS ONE. 2015;10(4):e0125244.
33. Zhang DZ, Wei XD, Wang XP. Comparison of hepatic resection and transarterial chemoembolization for solitary hepatocellular carcinoma. World J Gastroenterol. 2015;21(15):4635–43.
34. Kudo M, Han KH, Kokudo N, Cheng AL, Choi BI, Furuse J, et al. Liver cancer working group report. Jpn J Clin Oncol. 2010;40(Suppl 1):i19–27.
35. Hsu CY, Hsia CY, Huang YH, Su CW, Lin HC, Pai JT, et al. Comparison of surgical resection and transarterial chemoembolization for hepatocellular carcinoma beyond the Milan criteria: a propensity score analysis. Ann Surg Oncol. 2012;19(3):842–9.
36. Quirk M, Kim YH, Saab S, Lee EW. Management of hepatocellular carcinoma with portal vein thrombosis. World J Gastroenterol. 2015;21(12):3462–71.

World Journal of Gastroenterology

Submit a Manuscript: http://www.wjgnet.com/esps/
Help Desk: http://www.wjgnet.com/esps/helpdesk.aspx
DOI: 10.3748/wjg.v22.i30.6917

World J Gastroenterol 2016 August 14; 22(30): 6917-6924
ISSN 1007-9327 (print) ISSN 2219-2840 (online)

ORIGINAL ARTICLE

Basic Study

Evaluation of anti-migration properties of biliary covered self-expandable metal stents

Kosuke Minaga, Masayuki Kitano, Hajime Imai, Yogesh Harwani, Kentaro Yamao, Ken Kamata, Takeshi Miyata, Shunsuke Omoto, Kumpei Kadosaka, Toshiharu Sakurai, Naoshi Nishida, Masatoshi Kudo

Kosuke Minaga, Masayuki Kitano, Hajime Imai, Yogesh Harwani, Kentaro Yamao, Ken Kamata, Takeshi Miyata, Shunsuke Omoto, Kumpei Kadosaka, Toshiharu Sakurai, Naoshi Nishida, Masatoshi Kudo, Department of Gastroenterology and Hepatology, Kindai University Faculty of Medicine, Osaka-Sayama 589-8511, Japan

Author contributions: All authors helped to perform the research; Kitano M and Kudo M drafted conception and design; Minaga K and Kitano M performed the experiments, analyzed the data, and wrote the manuscript; Imai H, Harwani Y, Yamao K, Kamata K, Miyata T, Omoto S, Kadosaka K, Sakurai T, Nishida N and Kudo M contributed to writing the manuscript.

Supported by Japan Society for the Promotion of Science and the Japanese Foundation for the Research and Promotion of Endoscopy, No. 22590764 and No. 25461035.

Institutional review board statement: This study was approved by the Institutional Review Board of Kindai University Faculty of Medicine.

Conflict-of-interest statement: All authors declare no conflicts-of-interest related to this article.

Data sharing statement: No additional data are available.

Correspondence to: Masayuki Kitano, MD, PhD, Department of Gastroenterology and Hepatology, Kindai University Faculty of Medicine, 377-2 Ohno-Higashi, Osaka-Sayama 589-8511, Japan. m-kitano@med.kindai.ac.jp
Telephone: +81-72-3660221
Fax: +81-72-3672880

Received: February 17, 2016
Peer-review started: February 19, 2016
First decision: March 31, 2016
Revised: April 4, 2016
Accepted: April 15, 2016
Article in press: April 15, 2016
Published online: August 14, 2016

Abstract

AIM: To assess anti-migration potential of six biliary covered self-expandable metal stents (C-SEMSs) by using a newly designed phantom model.

METHODS: In the phantom model, the stent was placed in differently sized holes in a silicone wall and retracted with a retraction robot. Resistance force to migration (RFM) was measured by a force gauge on the stent end. Radial force (RF) was measured with a RF measurement machine. Measured flare structure variables were the outer diameter, height, and taper angle of the flare (ODF, HF, and TAF, respectively). Correlations between RFM and RF or flare variables were analyzed using a linear correlated model.

RESULTS: Out of the six stents, five stents were braided, the other was laser-cut. The RF and RFM of each stent were expressed as the average of five replicate measurements. For all six stents, RFM and RF decreased as the hole diameter increased. For all six stents, RFM and RF correlated strongly when the stent had not fully expanded. This correlation was not observed in the five braided stents excluding the laser cut stent. For all six stents, there was a strong correlation between RFM and TAF when the stent fully expanded. For the five braided stents, RFM after full stent expansion correlated strongly with all three stent flare structure variables (ODF, HF, and TAF). The laser-

cut C-SEMS had higher RFMs than the braided C-SEMSs regardless of expansion state.

CONCLUSION: RF was an important anti-migration property when the C-SEMS did not fully expand. Once fully expanded, stent flare structure variables plays an important role in anti-migration.

Key words: Biliary stricture; Self-expandable metal stent; Radial force; Resistance force to migration; Anti-migration property

Core tip: Ability of prevention of migration is very important to improve the results of covered self-expandable metal stents (C-SEMSs) for biliary stricture. This study aims to assess the anti-migration potential of six C-SEMSs by using a newly designed phantom model which allows the resistance force to migration (RFM) measurement of the stents. We found that RFM and radial force correlated strongly when the stent had not fully expanded. Once fully expanded, stent flare structure variables affected the anti-migration property of the stent. We concluded that several stent properties, including radial force and flare structure should be considered when selecting C-SEMS.

Minaga K, Kitano M, Imai H, Harwani Y, Yamao K, Kamata K, Miyata T, Omoto S, Kadosaka K, Sakurai T, Nishida N, Kudo M. Evaluation of anti-migration properties of biliary covered self-expandable metal stents. *World J Gastroenterol* 2016; 22(30): 6917-6924 Available from: URL: http://www.wjgnet.com/1007-9327/full/v22/i30/6917.htm DOI: http://dx.doi.org/10.3748/wjg.v22.i30.6917

INTRODUCTION

Endoscopic biliary stent placement in patients with biliary malignancy plays a pivotal role in relieving obstructive jaundice[1-8]. The biliary stents used to palliate malignant biliary obstruction should have a long patency duration. Since the self-expandable metal stent (SEMS) has an especially long patency, it is widely recognized to be an effective standard biliary endoprosthesis[9-12]. Covered SEMSs (C-SEMSs) have also been developed to prevent tumor in growth through the stent mesh. One disadvantage of C-SEMSs is that they are more prone to migration than uncovered SEMSs[13-17]. As a result, biliary C-SEMS have been provided with anti-migration mechanical properties, including higher radial force (RF), an anchoring flap, and specific stent flare structures[18-20]. A recent study comparing covered and uncovered SEMSs showed that neither of the stents with uncovered flare ends and relatively low axial force did not migrate[21]. Moreover, the C-SEMS associated with a significantly longer stent patency duration and longer patient survival time without stent dysfunction. Thus, anti-migration systems may not only prevent C-SEMS migration, they may also prevent stent dysfunction and prolong patency.

Of the various anti-migration properties, RF may be particularly important in preventing SEMS migration. RF is the radially outward expanding force that maintains the luminal patency at the stricture once the SEMS is deployed. Other anti-migration features, including stent structures, covering material, and flare structures may also contribute to the anti-migration potential of the stent. The present study was conducted to determine the contributions of RF and other anti-migration features of six currently commercially available C-SEMSs in Japan. The resistance force to retraction in the axial direction is denoted in this study as the resistance force to migration (RFM) and was measured by using a phantom model of biliary stricture.

MATERIALS AND METHODS

Samples

Table 1 lists the six commercially available C-SEMSs in Japan and their structures, stent materials, cover materials, and manufacturers. The six stents had four types of structures: braided with cross wire (Wallflex), braided with hook wire (ComVi and SUPREMO stents), braided with both hook and cross wires (BONA and HANARO stents), and a laser-cut structure (ZEO stent). Thus, there were five braided and one laser-cut stents. The stents were made of either nitinol (all except Wallflex) or platinum-cored nitinol (Wallflex) and their cover membranes were composed of silicone (Wallflex, BONA, HANARO, and SUPREMO), expanded polytetrafluoroethylene (ComVi), or polyurethane (ZEO). All stents were 10 mm in outer diameter and 80 mm in length.

Method of measuring RFM

A phantom model of inducing biliary SEMS migration was created by using a retraction robot, a 3-mm thick silicone wall (Shin-etsu chemical, Tokyo, Japan), and a force gauge (Model DPRS5T, Imada, Tokyo, Japan). The metal stents were fixed into a round hole in the silicone wall that had a diameter of 6, 8, or 10 mm. A force gauge was fixed to the distal end of the stent. The phantom model was placed in a box and the temperature was maintained at 37 ℃ by injecting heated air. During the experiments, the distal end of the stent (with the attached force gauge) was retracted at a speed of 1 mm/s. by using the retraction robot (Figure 1). The force of the resistance of the stent to the retraction (*i.e.*, RFM) was measured from the time stent retraction started until the time the distal end of the stent was dislocated from the silicone wall. The maximum value of resistance force during

Table 1 The biliary covered self-expandable metal stents that were tested

C-SEMS	Structure	Stent material	Cover material	ODF (mm)	HF (mm)	TAF (degree)	Manufacturer
Wallflex stent (fully covered)	Braided Cross wire	Platinum-cored nitinol	Silicone	11.8	1.9	11.3	Boston scientific
BONA stent	Braided Cross and hook wire	Nitinol	Silicone	13.4	3.2	21.8	Standard Sci Tech
HANARO stent	Braided Cross and hook wire	Nitinol	Silicone	13.4	3.2	16.7	M.I. Tech
ComVi stent	Braided Hook wire	Nitinol	e-PTFE	9.7	0	0	Taewoong
SUPREMO stent	Braided Hook wire	Nitinol	Silicone	12.2	2	16.7	Taewoong
ZEO stent	Laser-cut	Nitinol	Polyurethane	11.1	1.9	26.6	Zeon

All stents are 10 mm in diameter × 80 mm in length. C-SEMS: Covered self-expandable metal stent; e-PTFE: Expanded polytetrafluoroethylene; HF: Height of the flare; ODF: Outer diameter of the flare; TAF: Taper angle of the flare.

Figure 1 Resistance force to migration measurement machine. The machine consists of a retraction robot (arrows), a silicone wall (arrowheads), and a force gauge (Model DPRS5T, Imada, Tokyo, Japan). The covered self-expandable metal stent is fixed into a round hole in the silicone wall (arrowheads) and its distal end is connected to the force gauge device. The stent is retracted from the wall at a speed of 1 mm/s. by using the retraction robot (arrows).

retraction was used for analysis.

Method of measuring RF

RF was measured as described previously[18]. Thus, the RF measurement machine (Model RTA310, Blockwise Engineering, Tempe, AZ, United States) was placed in a box where the temperature was maintained at 37 ℃ by injecting heated air. The SEMS sample in its fully expanded state was placed in the cylindrical space of the machine and the cylinder was contracted, thereby causing the SEMS to shrink to its minimum size (2 mm). The force on the cylinder was then reversed so that the SEMS expanded automatically until it achieved its fully expanded state. The force that expanded the SEMS (*i.e.*, the RF) was continuously recorded by a force gauge that was deployed inside the cylinder. The force required to expand the SEMS to an outer diameter of 6, 8, and 10 mm was recorded and used for analysis.

Measurement of stent structure variables

Stent structure was expressed as outer diameter of the fully expanded stent (ODES; mm), outer diameter of the compressed stent (ODCS; mm), outer diameter of the flare (ODF; mm), height of the flare [HF = (ODF-ODES)/2; mm], length of the flare (LF; mm), and taper angle of the flare (TAF = HF/LF; degree) (Figure 2). The three key stent structure variables were ODF, HF, and TAF.

Statistical analysis

The RF and RFM of each stent were expressed as the average of five replicate measurements. The correlations between RFM and RF or stent flare structure variables were analyzed by simple linear regression and correlation analysis, and expressed by correlation coefficient (r). For these correlation analyses, either all six stents or only the five braided stents were included. A correlation was deemed to be strong if $r \geqslant 0.7$. All statistical analyses were performed by using the statistical software SAS 9.4. (SAS Institute Inc., Cary, NC, United States).

RESULTS

*Comparison of six C-SEMSs in terms of RFM, RF, and **stent flare structure variables***

Figure 3A shows the RFM measurement results when the hole of the wall (ODCS) was 6, 8, and 10 mm in diameter. For all six stents, the RFM dropped as the

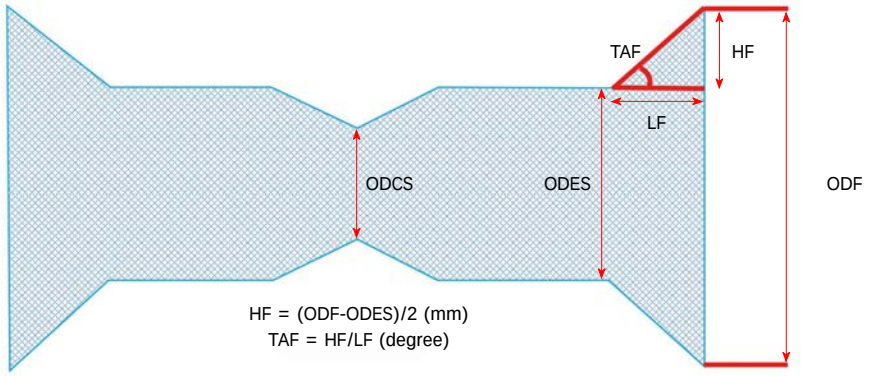

Figure 2 Schematic depiction of a stent. Stent structure is expressed as outer diameter of the fully expanded stent (ODES; mm), outer diameter of the compressed stent (ODCS; mm), outer diameter of the flare (ODF; mm), height of the flare [HF = (ODF-ODES)/2; mm], length of the flare (LF; mm), and taper angle of the flare (TAF = HF/LF; degree).

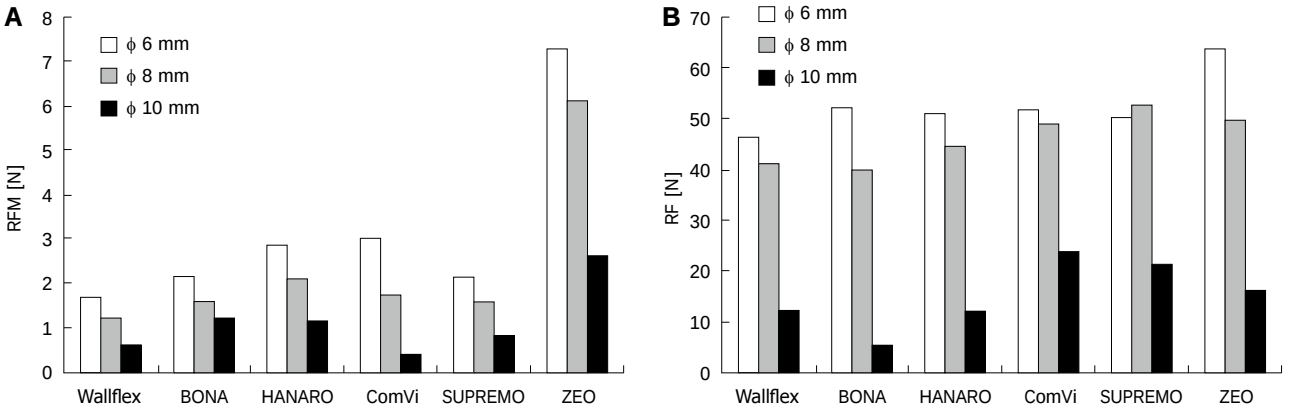

Figure 3 Resistance force to migration and radial force of 6 stents. A: The resistance force to migration (RFM) of each stent when the outer diameter of the compressed stent was 6, 8, or 10 mm. B: The radial force (RF) of each stent when the outer diameter of the compressed stent was 6, 8, or 10 mm.

hole diameter (ODCS) increased. The laser-cut ZEO stent had the highest RFM at all three hole diameters (6, 8, and 10 mm ODCS). Figure 3B shows the RF measurement results during expansion, namely, at the times when the ODCS was 6, 8, and 10 mm. For all six stents, the RF decreased as the ODCS increased. At the ODCS of 6 mm, the laser-cut ZEO stent had the highest RF. At the ODCSs of 8 and 10 mm, the braided stents SUPREMO and ComVi had the highest RFs, followed by the laser-cut ZEO stent. Table 1 shows the stent flare structure variables (ODF, HF, and TAF) of the stents. The BONA and HANARO stents both had the highest ODFs and HFs. The laser-cut ZEO stent had the highest TAF. Of the five braided stents, BONA had the highest TAF.

Relationship between RFM and RF

For all six C-SEMSs, the coefficients for the correlation between RFM and RF when the ODCS was 6, 8, and 10 mm were 0.849, 0.387, and 0.103, respectively (Figure 4A-C). Thus, the correlation was only strong when the ODCS was 6 mm. When excluding the laser cut stent, the correlation coefficients between RFM and RF when the ODCS was 6 mm, 8 mm and 10 mm were 0.262, -0.230 and -0.143, respectively (Figure 4D-F). Thus, the RFM of the five braided stents did not correlate strongly with RF regardless of the ODCS.

Relationship between RFM and stent flare structure variables

For all six SEMSs, the coefficients for the correlation between RFM and ODF when the ODCS was 6, 8, and 10 mm were -0.359, -0.257, and 0.098, respectively. The correlation coefficients between RFM and HF were -0.359, -0.020, and -0.134, respectively. The correlation coefficients between RFM and TAF were 0.484, 0.594, and 0.837 mm, respectively (Figure 5A-C). Thus, for all six stents, RFM did not correlate well with ODF and HF. It correlated better with TAF but only achieved a strong correlation when the ODCS was 10 mm.

When excluding the laser cut stent, the coefficients for the correlation between RFM and ODF when the ODCS was 6 mm, 8 mm and 10 mm were -0.301, 0.271, and 0.952, respectively. The correlation coefficients between RFM and HF were -0.327, 0.242, and 0.943, respectively. The correlation coefficients between RFM and TAF were -0.454, 0.089, and 0.906, respectively (Figure 5D-F). Thus, for the braided stents, RFM correlated strongly with all stent structure

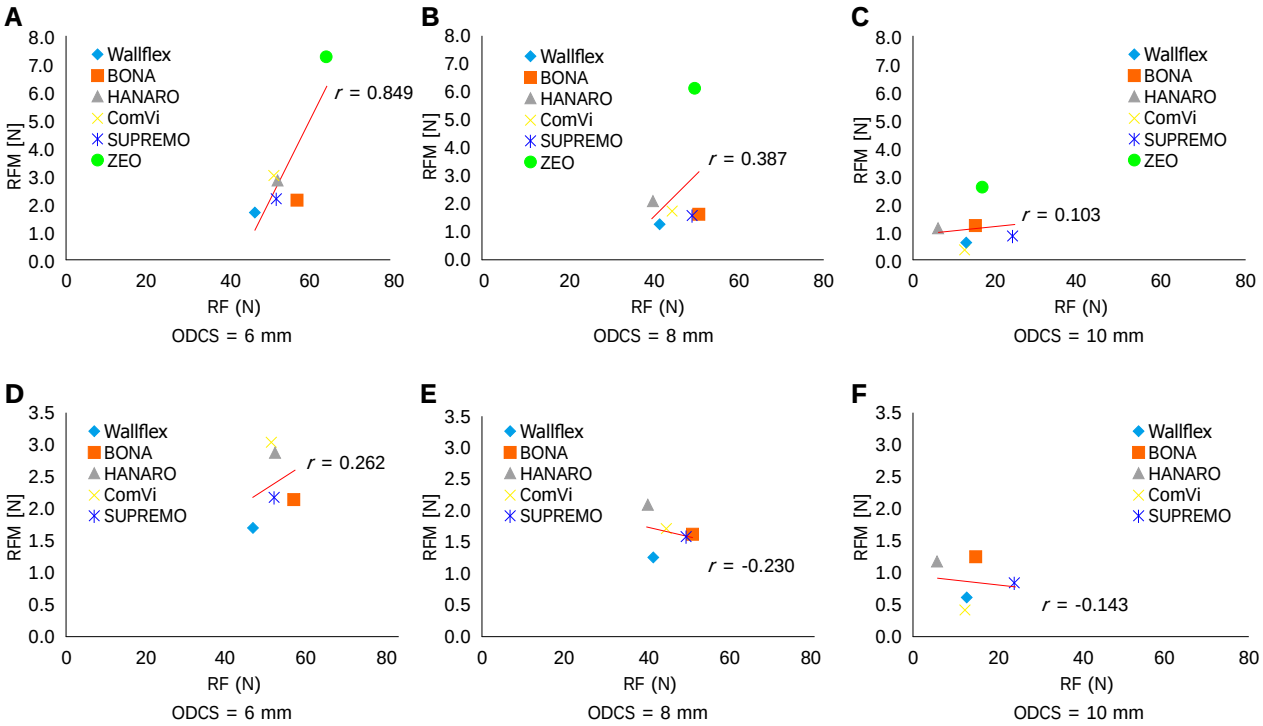

Figure 4 Relationship between resistance force of migration and radial force. A-C: The relationship between RFM and RF in all six stents when the outer diameter of the compressed stent was 6 (A), 8 (B), or 10 mm (C); D-F: The relationship between RFM and RF in just the five braided stents when the outer diameter of the compressed stent was 6 (D), 8 (E), or 10 mm (F). A simple linear regression model was used. RFM: Resistance force of migration; RF: Radial force.

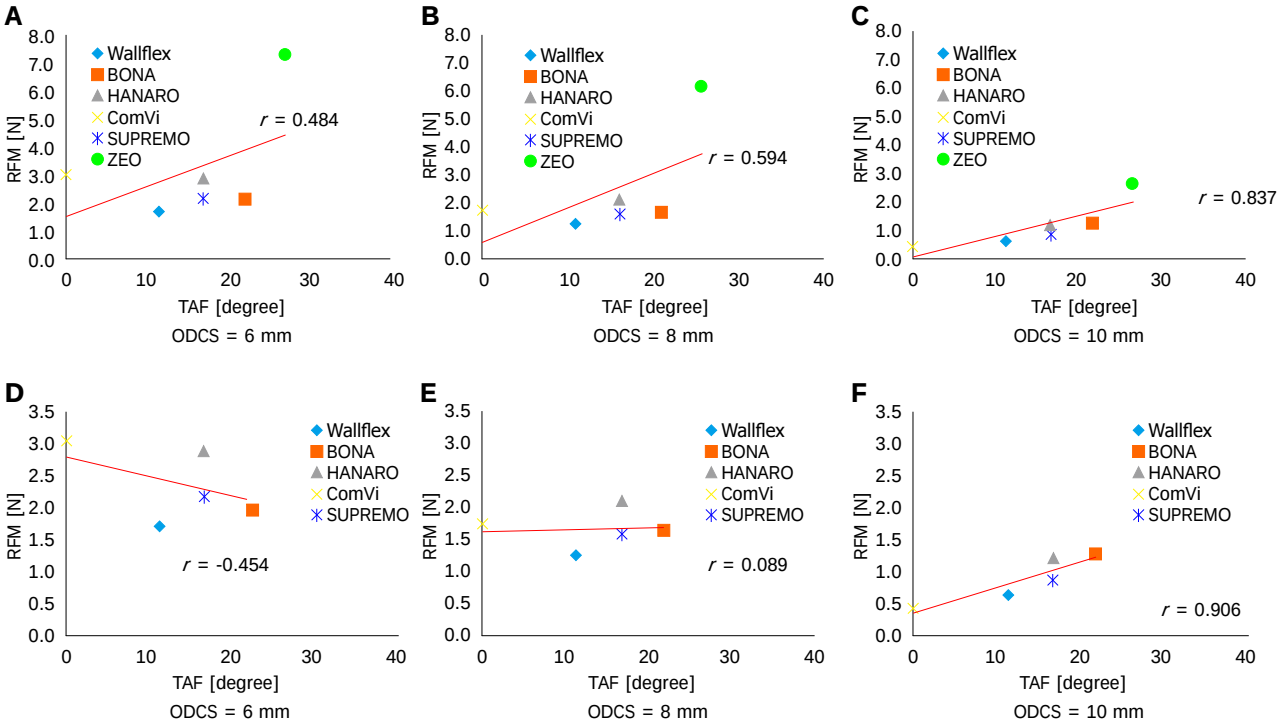

Figure 5 Relationship between resistance force of migration and taper of the flare. A-C: The relationship between RFM and TAF in all six stents when the outer diameter of the compressed stent was 6 (A), 8 (B), or 10 mm (C); D-F: The relationship between RFM and TAF in just the five braided stents when the outer diameter of the compressed stent was 6 (D), 8 (E), or 10 mm (F). A simple linear regression model was used. RFM: Resistance force of migration; TAF: Taper of the flare.

variables when the ODCS was 10 mm.

Thus, overall, when all six stents were considered, their RFM correlated strongly with RF at 6 mm and TAF at 10 mm. Other variables did not correlate with RFM. By contrast, when only the braided stents were considered, their RFM did not correlate with RF but did

correlate with all three flare variables at 10 mm.

DISCUSSION

Although C-SEMSs tend to show a higher rate of stent migration than uncovered SEMSs[13-17], they associate with significantly longer patency than uncovered SEMSs in some reports[13,21,22]. To reduce their migration, C-SEMSs have been equipped with various anti-migration mechanical properties, namely, different stent frameworks, membrane materials, higher RF, different flare structures, and the presence of an anchoring flap[18-20]. However, to the best of our knowledge, only three studies have examined whether the anti-migration features of biliary SEMSs actually prevent migration[19,20,23]. When Park *et al*[19] compared the anti-migration effects of two types of SEMSs, they concluded that the anchoring design was superior to the flare-end design. Isayama *et al*[20] designed a novel C-SEMS with flare and bank structures and reported the low rate of stent migration of this C-SEMS. Recently, Nakai *et al*[23] suggested that if RF is low C-SEMSs can easily slip through the biliary stricture. Their study revealed that RF but not axial force was associated with C-SEMS migration in patients with distal malignant biliary obstruction due to pancreatic cancer[23]. In the present study, we assessed the anti-migration potential of six C-SEMSs by using a new phantom model to measure RFM.

We found several key relationships between RFM and stent variables. First, for all six stents, RFM correlated strongly with RF only when the stent did not fully expand (*i.e.*, the ODCS was 6 mm) (r = 0.849); this was not observed when the stent fully expanded (*i.e.*, the ODCS was 10 mm). It was also not observed when the five braided stents were examined. Recent article indicated that low RF was one of the significant risk factors for early C-SEMS migration[23]. Considering this clinical outcome, RF may remain playing a pivotal role to prevent migration of the stent, when the stent does not fully expand due to compression by a growing tumor.

Second, for all six stents, there was a strong correlation between RFM and TAF when the stent fully expanded (r = 0.837); a correlation with RFM was not observed for the other two flare variables (ODF and HF). However, when only the five braided stents were assessed, they showed strong correlations between RFM and all three flare variables at 10 mm expansion (ODF, r = 0.952; HF, r = 0.943; TAF, r = 0.906).

When Isayama *et al*[18] measured the RF of 14 different SEMSs, including five C-SEMSs, they found that the RF *vs* diameter curves exhibited two characteristics. In addition, the values during expansion were different from those during contraction. We hypothesized that the expansion process is most appropriate for measuring the anti-migration potential of stents in the setting of biliary stricture. Therefore, we used the values of RF during expansion at different outer diameters (*i.e.*, when the ODCS was 6, 8, and 10 mm). Regarding our six stents, RF only correlated closely with RFM when the stent did not fully expand (6 mm). This suggests that RF may play an important role in preventing migration during stent deployment until full expansion is achieved.

The present study also showed that when the stent did not fully expand (6 mm), the laser-cut C-SEMS had a higher RF than any of the five braided C-SEMSs. However, the laser-cut C-SEMS also had a higher RFM than the braided SEMSs at all three ODCSs (6, 8, and 10 mm). These observations suggest that the high RFM of the laser-cut C-SEMS was caused not only by its high RF but also by its other properties. In other words, the scaly framework of this laser-cut stent may have contributed to its anti-migration potential.

When all stents were considered, a close correlation between RFM and the stent flare property TAF was observed when the stent fully expanded; this correlation was not observed when the stent did not fully expand or for the other two stent flare properties. However, when the laser-cut C-SEMS was excluded from the analysis, extremely close correlations between RFM and all three stent flare properties was observed. These results indicate that an effective stent flare structure, particularly a high TAF, is very important for preventing the migration of the stent after deployment and full expansion.

The present study has some limitations. First, this phantom model may not reflect the real clinical situation of biliary strictures. In the real clinical situation, stent migration may be caused by several factors, including duodenum motility and bile flow. By contrast, our phantom model only measures the resistance of the stents to mechanical retraction from a silicone wall. Second, we could not assess the mechanical properties of C-SEMS other than RFM, RF and flare structure in our analysis. Other properties such as axial force may associate with anti-migration potential. However, axial force occurs only in a tortuous bile duct. As the stent was not bent in our phantom model, relationship between axial force and RFM could not be assessed. Third, only one laser-cut C-SEMS was used in the experiments. Other SEMSs should be evaluated in terms of their anti-migration potential by using this phantom model.

In conclusion, RF plays an important role in anti-migration when the C-SEMS has not yet fully expanded. However, in the fully expanded state, stent flare structure variables may strongly affect the anti-migration property of the stent. The laser-cut stent appears to have an extremely high resistance to migration whether or not the stent fully expands. Thus, several stent properties, including RF, flare structure, and stent framework should be considered

when selecting C-SEMS for biliary stricture.

ACKNOWLEDGMENTS

We thank Mr. Chimyon Gon, MT from Research and Development Center, Zeon Corporation for technical assistance regarding the radial force and resistance force to migration measurements.

COMMENTS

Background

Biliary covered self-expandable metal stents (C-SEMSs) tend to migrate more frequently than uncovered SEMSs. Mechanical anti-migration properties of C-SEMS such as the stent frame work, flare structure and radial force (RF) may prevent this. However, to our knowledge, only three studies have examined whether the anti-migration features of biliary SEMSs actually prevent migration

Research frontiers

Of the various anti-migration properties, RF may be particularly important in preventing SEMS migration. RF is the radially outward expanding force that maintains the luminal patency at the stricture once the SEMS is deployed. Other anti-migration features, including stent structures, covering material, and flare structures may also contribute to the anti-migration potential of the stent.

Innovations and breakthroughs

This is the first study to assess the anti-migration potential of biliary C-SEMSs by using a phantom model which enabled to measure the resistance force to migration (RFM) of the stents. According to the results of our study, RF was an important anti-migration property when the C-SEMS did not fully expand. Once fully expanded, stent flare structure variables may strongly affect the anti-migration property of the stent.

Applications

The results of this study suggest that several stent properties, including RF, flare structure, and stent framework should be considered when selecting C-SEMS for biliary stricture to reduce stent-related complications. This study highlights the problem of C-SEMS migration faced by clinicians and provides useful information for stent selection in future clinical practice.

Terminology

RFM in this study denotes the resistance force of the stents to retraction in the axial direction and this force was measured by using a phantom model of biliary stricture.

Peer-review

In this *in vitro* study, the authors evaluated resistance force against migration and its correlations with RF and the flare structure of six commonly-used C-SEMSs. This study highlights the problem of C-SEMS migration faced by clinicians and provides useful information for stent selection in future clinical practice.

REFERENCES

1 **Soehendra N**, Reynders-Frederix V. Palliative bile duct drainage - a new endoscopic method of introducing a transpapillary drain. *Endoscopy* 1980; **12**: 8-11 [PMID: 7353562 DOI: 10.1055/s-2007-1021702]

2 **Huibregtse K**, Tytgat GN. Palliative treatment of obstructive jaundice by transpapillary introduction of large bore bile duct endoprosthesis. *Gut* 1982; **23**: 371-375 [PMID: 7076014 DOI: 10.1136/gut.23.5.371]

3 **Walta DC**, Fausel CS, Brant B. Endoscopic biliary stents and obstructive jaundice. *Am J Surg* 1987; **153**: 444-447 [PMID: 3578663 DOI: 10.1016/0002-9610(87)90787-2]

4 **Speer AG**, Cotton PB, Russell RC, Mason RR, Hatfield AR, Leung JW, MacRae KD, Houghton J, Lennon CA. Randomised trial of endoscopic versus percutaneous stent insertion in malignant obstructive jaundice. *Lancet* 1987; **2**: 57-62 [PMID: 2439854 DOI: 10.1016/S0140-6736(87)92733-4]

5 **Huibregtse K**, Cheng J, Coene PP, Fockens P, Tytgat GN. Endoscopic placement of expandable metal stents for biliary strictures--a preliminary report on experience with 33 patients. *Endoscopy* 1989; **21**: 280-282 [PMID: 2482170 DOI: 10.1055/s-2007-1012969]

6 **Irving JD**, Adam A, Dick R, Dondelinger RF, Lunderquist A, Roche A. Gianturco expandable metallic biliary stents: results of a European clinical trial. *Radiology* 1989; **172**: 321-326 [PMID: 2664861 DOI: 10.1148/radiology.172.2.2664861]

7 **Lammer J**, Klein GE, Kleinert R, Hausegger K, Einspieler R. Obstructive jaundice: use of expandable metal endoprosthesis for biliary drainage. Work in progress. *Radiology* 1990; **177**: 789-792 [PMID: 2243991 DOI: 10.1148/radiology.177.3.2243991]

8 **Smith AC**, Dowsett JF, Russell RC, Hatfield AR, Cotton PB. Randomised trial of endoscopic stenting versus surgical bypass in malignant low bileduct obstruction. *Lancet* 1994; **344**: 1655-1660 [PMID: 7996958 DOI: 10.1016/S0140-6736(94)90455-3]

9 **Davids PH**, Groen AK, Rauws EA, Tytgat GN, Huibregtse K. Randomised trial of self-expanding metal stents versus polyethylene stents for distal malignant biliary obstruction. *Lancet* 1992; **340**: 1488-1492 [PMID: 1281903 DOI: 10.1016/0140-6736(92)92752-2]

10 **Knyrim K**, Wagner HJ, Pausch J, Vakil N. A prospective, randomized, controlled trial of metal stents for malignant obstruction of the common bile duct. *Endoscopy* 1993; **25**: 207-212 [PMID: 8519239 DOI: 10.1055/s-2007-1010294]

11 **Lammer J**, Hausegger KA, Flückiger F, Winkelbauer FW, Wildling R, Klein GE, Thurnher SA, Havelec L. Common bile duct obstruction due to malignancy: treatment with plastic versus metal stents. *Radiology* 1996; **201**: 167-172 [PMID: 8816539 DOI: 10.1148/radiology.201.1.8816539]

12 **Prat F**, Chapat O, Ducot B, Ponchon T, Pelletier G, Fritsch J, Choury AD, Buffet C. A randomized trial of endoscopic drainage methods for inoperable malignant strictures of the common bile duct. *Gastrointest Endosc* 1998; **47**: 1-7 [PMID: 9468416 DOI: 10.1016/S0016-5107(98)70291-3]

13 **Isayama H**, Komatsu Y, Tsujino T, Sasahira N, Hirano K, Toda N, Nakai Y, Yamamoto N, Tada M, Yoshida H, Shiratori Y, Kawabe T, Omata M. A prospective randomised study of "covered" versus "uncovered" diamond stents for the management of distal malignant biliary obstruction. *Gut* 2004; **53**: 729-734 [PMID: 15082593 DOI: 10.1136/gut.2003.018945]

14 **Park DH**, Kim MH, Choi JS, Lee SS, Seo DW, Kim JH, Han J, Kim JC, Choi EK, Lee SK. Covered versus uncovered wallstent for malignant extrahepatic biliary obstruction: a cohort comparative analysis. *Clin Gastroenterol Hepatol* 2006; **4**: 790-796 [PMID: 16716757]

15 **Kullman E**, Frozanpor F, Söderlund C, Linder S, Sandström P, Lindhoff-Larsson A, Toth E, Lindell G, Jonas E, Freedman J, Ljungman M, Rudberg C, Ohlin B, Zacharias R, Leijonmarck CE, Teder K, Ringman A, Persson G, Gözen M, Eriksson O. Covered versus uncovered self-expandable nitinol stents in the palliative treatment of malignant distal biliary obstruction: results from a randomized, multicenter study. *Gastrointest Endosc* 2010; **72**: 915-923 [PMID: 21034892 DOI: 10.1016/j.gie.2010.07.036]

16 **Telford JJ**, Carr-Locke DL, Baron TH, Poneros JM, Bounds BC, Kelsey PB, Schapiro RH, Huang CS, Lichtenstein DR, Jacobson BC, Saltzman JR, Thompson CC, Forcione DG, Gostout CJ, Brugge WR. A randomized trial comparing uncovered and partially covered self-expandable metal stents in the palliation of distal malignant biliary obstruction. *Gastrointest Endosc* 2010; **72**: 907-914 [PMID: 21034891 DOI: 10.1016/j.gie.2010.08.021]

17 **Lee JH**, Krishna SG, Singh A, Ladha HS, Slack RS, Ramireddy S, Raju GS, Davila M, Ross WA. Comparison of the utility

of covered metal stents versus uncovered metal stents in the management of malignant biliary strictures in 749 patients. *Gastrointest Endosc* 2013; **78**: 312-324 [PMID: 23591331 DOI: 10.1016/j.gie.2013.02.032]

18 **Isayama H**, Nakai Y, Toyokawa Y, Togawa O, Gon C, Ito Y, Yashima Y, Yagioka H, Kogure H, Sasaki T, Arizumi T, Matsubara S, Yamamoto N, Sasahira N, Hirano K, Tsujino T, Toda N, Tada M, Kawabe T, Omata M. Measurement of radial and axial forces of biliary self-expandable metallic stents. *Gastrointest Endosc* 2009; **70**: 37-44 [PMID: 19249766 DOI: 10.1016/j.gie.2008.09.032]

19 **Park DH**, Lee SS, Lee TH, Ryu CH, Kim HJ, Seo DW, Park SH, Lee SK, Kim MH, Kim SJ. Anchoring flap versus flared end, fully covered self-expandable metal stents to prevent migration in patients with benign biliary strictures: a multicenter, prospective, comparative pilot study (with videos). *Gastrointest Endosc* 2011; **73**: 64-70 [PMID: 21184871 DOI: 10.1016/j.gie.2010.09.039]

20 **Isayama H**, Kawakubo K, Nakai Y, Inoue K, Gon C, Matsubara S, Kogure H, Ito Y, Tsujino T, Mizuno S, Hamada T, Uchino R, Miyabayashi K, Yamamoto K, Sasaki T, Yamamoto N, Hirano K, Sasahira N, Tada M, Koike K. A novel, fully covered laser-cut nitinol stent with antimigration properties for nonresectable distal malignant biliary obstruction: a multicenter feasibility study. *Gut Liver* 2013; **7**: 725-730 [PMID: 24312715 DOI: 10.5009/gnl.2013.7.6.725]

21 **Kitano M**, Yamashita Y, Tanaka K, Konishi H, Yazumi S, Nakai Y, Nishiyama O, Uehara H, Mitoro A, Sanuki T, Takaoka M, Koshitani T, Arisaka Y, Shiba M, Hoki N, Sato H, Sasaki Y, Sato M, Hasegawa K, Kawabata H, Okabe Y, Mukai H. Covered self-expandable metal stents with an anti-migration system improve patency duration without increased complications compared with uncovered stents for distal biliary obstruction caused by pancreatic carcinoma: a randomized multicenter trial. *Am J Gastroenterol* 2013; **108**: 1713-1722 [PMID: 24042190]

22 **Saleem A**, Leggett CL, Murad MH, Baron TH. Meta-analysis of randomized trials comparing the patency of covered and uncovered self-expandable metal stents for palliation of distal malignant bile duct obstruction. *Gastrointest Endosc* 2011; **74**: 321-327.e1-3 [PMID: 21683354 DOI: 10.1016/j.gie.2011.03.1249]

23 **Nakai Y**, Isayama H, Kogure H, Hamada T, Togawa O, Ito Y, Matsubara S, Arizumi T, Yagioka H, Mizuno S, Sasaki T, Yamamoto N, Hirano K, Tada M, Koike K. Risk factors for covered metallic stent migration in patients with distal malignant biliary obstruction due to pancreatic cancer. *J Gastroenterol Hepatol* 2014; **29**: 1744-1749 [PMID: 24720610 DOI: 10.1111/jgh.12602]

P- Reviewer: Hu B **S- Editor**: Gong ZM **L- Editor**: A
E- Editor: Ma S

Published by **Baishideng Publishing Group Inc**
8226 Regency Drive, Pleasanton, CA 94588, USA
Telephone: +1-925-223-8242
Fax: +1-925-223-8243
E-mail: bpgoffice@wjgnet.com
Help Desk: http://www.wjgnet.com/esps/helpdesk.aspx
http://www.wjgnet.com

ISSN 1007-9327

Liver Cancer

Liver Cancer 2016;5:190–197
DOI: 10.1159/000367775
Published online: May 10, 2016

2235-1795/16/0053-0190$39.50/0
www.karger.com/lic

Original Paper

Survival Analysis over 28 Years of 173,378 Patients with Hepatocellular Carcinoma in Japan

Masatoshi Kudo[a] Namiki Izumi[b] Michiie Sakamoto[c]
Yutaka Matsuyama[d] Takafumi Ichida[e] Osamu Nakashima[f]
Osamu Matsui[g] Yonson Ku[h] Norihiro Kokudo[i]
Masatoshi Makuuchi[j] for the Liver Cancer Study Group of Japan

[a]Department of Gastroenterology and Hepatology, Kindai University Faculty of Medicine, Osaka-Sayama, [b]Department of Gastroenterology and Hepatology, Musashino Red Cross Hospital, Musashino, [c]Department of Pathology, Keio University School of Medicine, Shinjuku, [d]Department of Biostatistics, School of Health Sciences and Nursing, University of Tokyo, Tokyo, [e]Department of Gastroenterology, Shizuoka Hospital Juntendo University School of Medicine, Shizuoka, [f]Department of Clinical Laboratory Medicine, Kurume University Hospital, Kurume, [g]Department of Radiology, Kanazawa University Graduate School of Medical Science, Kanazawa, [h]Department of Surgery, Kobe University Graduate School of Medicine, Kobe, [i]Department of Hepato-Biliary and Pancreatic Surgery, University of Tokyo Graduate School of Medicine, Tokyo, [j]Department of Surgery, Japanese Red Cross Medical Center, Tokyo, Japan

Key Words
Hepatic arterial infusion chemotherapy · Hepatocellular carcinoma · Liver Cancer Study Group of Japan · Nationwide survey · Overall survival

Abstract
Background: Beginning in 1967, the Liver Cancer Study Group of Japan (LCSGJ) started a nationwide prospective registry of all patients with hepatocellular carcinoma (HCC) diagnosed at more than 700 institutions. To determine the effectiveness of surveillance and treatment methods longitudinally, we analyzed improvements over time in overall survival (OS) of 173,378 patients with HCC prospectively entered into the LCSGJ registry between 1978 and 2005. ***Methods:*** All patients from more than 700 institutions throughout Japan with HCC were entered into the LCSGJ registry. Patients were grouped by years of diagnosis, with OS and 5-year OS rates being calculated. We also assessed OS and 5-year OS rates in patients who underwent resection, local ablation, transarterial chemoembolization (TACE), and hepatic arterial infusion chemotherapy (HAIC) and in those with baseline serum alpha-fetopro-

Masatoshi Kudo, MD
Department of Gastroenterology and Hepatology,
Kindai University Faculty of Medicine
377-2 Ohnohigashi, Osaka-Sayama, 589-8511 (Japan)
Tel. +81 72 366 0221, E-Mail m-kudo@med.kindai.ac.jp

tein (AFP) levels ≥400 ng/ml. ***Results:*** The 5- and 10-year OS rates in the cohort of 173,378 patients were 37.9% and 16.5%, respectively. However, over time, the mean maximum tumor size decreased significantly, whereas 5-year OS rates and median survival time increased significantly. Similar findings were observed separately in patients who underwent resection, local ablation, TACE, and HAIC, as well as in patients with AFP levels ≥400 ng/ml. ***Conclusion:*** The establishment of a nationwide HCC surveillance program in Japan has contributed to longer median OS and increased OS rates in patients diagnosed with this disease. These findings suggest that the establishment of a surveillance program in other countries with patients at risk for HCC may provide significant survival benefits.

Introduction

Worldwide, hepatocellular carcinoma (HCC) is the sixth most common cancer and the third most common cause of cancer deaths [1]. Globally, about 80% of patients with HCC are in Asian countries [2, 3]. In Japan, the incidence of HCC and the associated death rates began to increase sharply in 1975, peaking at 34,510 and 27.4/100,000, respectively in 2004. However, these decreased to 33,662 and 26.7/100,000, respectively by 2006 [4]. The primary cause of HCC in Japan is infection with hepatitis C virus (HCV), which is observed in about 70% of all patients. This is followed by infection with hepatitis B virus in 15–22%, and non-viral causes, which is predominantly alcohol associated, in the remaining 8–15% of patients. The survival of Japanese patients with HCC can be predicted by the Japan Integrated Staging score [5]. Risk factors for the development of HCC, methods of prevention, diagnosis and treatment modalities were recently reviewed [6].

Beginning in 1967, the Liver Cancer Study Group of Japan (LCSGJ) started a nationwide prospective registry of patients with HCC. Patients were followed-up after diagnosis with surveys published every two years [7, 8]. In the 18th and most recent follow-up survey for the period 2004–2005, 20,153 patients were newly diagnosed with HCC and 30,677 previously diagnosed patients were being followed-up at 544 institutions [8], respectively. This follow-up survey showed that, of 17,804 measurable tumors in patients initially diagnosed in the period 2004–2005, 855 (4.80%) were ≤1 cm, 5,106 (28.68%) were 1–2 cm, 4,272 (23.99%) were 2–3 cm, 3,833 (21.53%) were 3–5 cm, and 3,738 (21.00%) were 5–10 cm in diameter, respectively. This survey also showed that, of 18,255 patients initially diagnosed in the period 2004–2005, 10,539 (57.73%) had one tumor, 3,157 (17.29%) had two tumors, 1,437 (7.87%) had three tumors, and 3,122 (17.10%) had four or more tumors. Overall survival (OS) was inversely related to both the maximum tumor size in 24,410 patients and to the number of tumors in 24,233 patients who underwent resection from the period 1994 to 2005. In addition, of 18,619 patients surveyed in the period 2004–2005, only 904 (4.86%) had evidence of extrahepatic spread at the time of diagnosis. Of 17,804 patients surveyed in the same period, 13,074 (73.4%) had serum alpha-fetoprotein (AFP) levels <200 ng/ml and 14,074 (79.0%) had serum AFP levels <400 ng/ml, respectively.

Methods of treatment for HCC can be potentially curative or palliative. Potentially curative treatments include resection, local ablation, and liver transplantation. Palliative treatments include transarterial chemoembolization (TACE), hepatic arterial infusion chemotherapy (HAIC), and systemic chemotherapy, each of which has advantages and disadvantages [9–14]. More recently, the multiple tyrosine kinase inhibitor, sorafenib, has shown efficacy in patients with HCC [15, 16]. Response criteria for patients with HCC have been recently redefined [17, 18].

Although the two-yearly surveys by the LCSGJ have assessed the incidence of HCC by demographic and clinical characteristics in addition to the survival rates of these patients, these "snapshot" surveys are only able to assess these parameters at specific points in time. It is important to determine the effectiveness of surveillance and treatment methods longitudinally. We therefore analyzed the improvements in OS in 173,378 patients who were prospectively entered into the LCSGJ registry between 1978 and 2005 and assorted into 5-year intervals by date of diagnosis. We also analyzed improvements in OS over time in patients who underwent resection, local ablation, TACE, and HAIC.

Patients and Methods

The LCSGJ Surveillance System

The LCSGJ surveillance system registers all patients in Japan diagnosed with HCC. According to the Japanese HCC practice guidelines, high risk patients are those with chronic hepatitis B and/or C virus infection or liver cirrhosis. In addition, very high risk patients are those with hepatitis B or C virus associated cirrhosis [19, 20].

Follow-up methods for Japanese patients at high risk for HCC has included ultrasonography of the liver and measurements of the serum concentrations of tumor markers including AFP, the lectin-binding fraction of AFP (AFP-L3), and prothrombin induced in the absence of vitamin K (PIVKA-II), also known as des-γ-carboxy-prothrombin (DCP), every six months. In very high risk patients, follow-up has consisted of ultrasonography and measurements of AFP, PIVKA-II, and/or AFP-L3 every 3–4 months. At the discretion of their physicians, these patients have also undergone dynamic computed tomography (CT)/magnetic resonance imaging (MRI) every 6–12 months [19, 20].

The LCSGJ HCC Registry

The LCSGJ registry consists of all patients diagnosed with HCC at more than 700 institutions and who were prospectively registered between 1978 and 2005, with data taken from the fifth through the eighteenth follow-up survey [7]. A total of 173,378 patients with HCC were prospectively registered between 1978 and 2005. Improvements in OS over time were assessed by dividing patients into 5-year groups. We also assessed improvements in OS in patients who underwent resection, local ablation, TACE, and HAIC over the same time periods.

The maximum tumor size at the time of diagnosis and the number of tumors were measured by ultrasonography. The tumor stage at diagnosis was defined, and AFP, PIVKA-II, and AFP-L3 concentrations were measured, as described [17].

Statistical Methods

OS was calculated by the Kaplan-Meier method, with differences between groups determined by the log rank test. Differences among three or more groups were also determined by same latter method.

Results

OS over Time

A total of 173,378 patients with HCC were prospectively registered into the LCSGJ HCC registry between 1978 and 2005. The 5- and 10-year OS rates of this cohort were 37.9% and 16.5%, respectively. The mean maximum tumor size was found to decrease over time (table 1). In addition, when 5-year OS rates were assessed in patients assorted by the year of diagnosis into 5-year intervals, these rates increased over time, from 3.7% in the 1978–1980 period to 42.7% in the 2001–2005 period, with the difference between each period and the preceding period being statistically significant ($p<0.0001$ each; fig. 1a). In addition, the median survival time in patients divided by 5-year intervals also increased over time, from three months in the

Table 1. Maximum tumor size at the time of initial detection in patients with HCC assorted by year of diagnosis

	Mean maximum tumor size (cm)				
Year	≤2.0	2.1-3.0	3.1-5.0	5.1-10.0	≥10.1
1978–1980	1.3%	4.2%	3.2%	26.3%	65.1%
1981–1985	5.3%	18.0%	15.6%	28.8%	32.3%
1986–1990	14.5%	25.8%	21.5%	21.6%	16.5%
1991–1995	20.8%	23.3%	25.0%	17.2%	13.7%
1996–2000	17.3%	24.5%	23.6%	19.6%	15.0%
2001–2005	31.2%	24.5%	22.3%	15.5%	6.5%

Percentages are shown of patients with HCC in each time period assorted by maximum tumor size at the time of diagnosis.

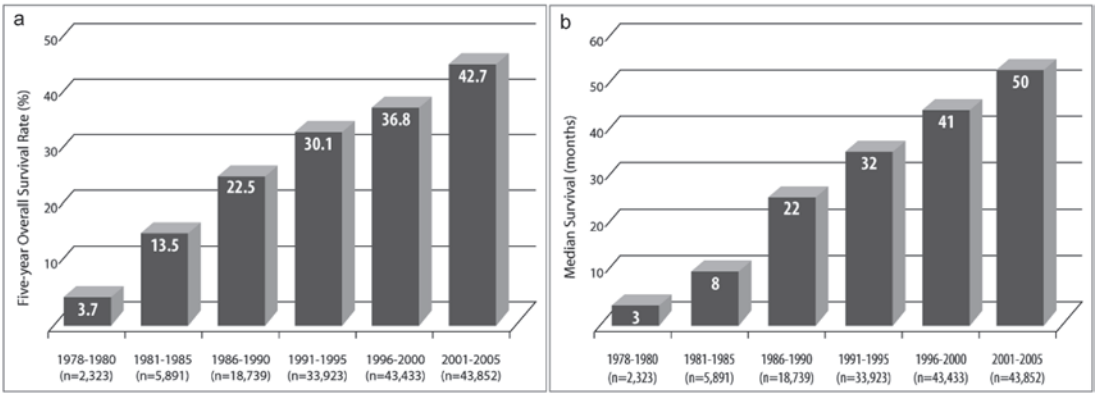

Fig. 1. Five-year OS rates (**a**) and (**b**) median OS over 5-year intervals in patients with HCC. The differences between each period and the preceding period were statistically significant (p<0.0001 each).

1978–1980 period to 50 months in the 2001–2005 period, with the difference between each period and the preceding period also being statistically significant (p<0.0001 each; fig. 1b).

OS as a Function of Treatment

To assess whether changes in OS over time were a function of initial treatment, patients were divided into those undergoing resection, local ablation, TACE and HAIC and further subdivided into 5-year intervals by year of their diagnosis with HCC. We found that the 5-year OS rates in 42,713 patients who underwent resection increased over time, from 14.5% in the 1978–1980 period to 58.4% in the 2001–2005 period (table 2), as did median survival, from 13 months in the 1978–1980 period to 74 months in the 2001–2005 period (table 3). Similarly, we observed increases over time in 5-year OS rates in 37,196 patients who underwent local ablation, from 32.8% in the 1986–1990 period to 47.6% in the 2001–2005 period, and median survival, from 41 months in the 1986–1990 period to 59 months in the 2001–2005 period. Five-year OS rates also increased over time in 61,460 patients who underwent TACE, from 5.4% in the 1978–1980 period to 35.0% in the 2001–2005 period, as did median survival, from nine months in the 1978–1980 period to 42 months in the 2001–2005 period. Furthermore, 5-year OS rates increased over time, from 2.5% in the 1978–1980 period to 31.9% in the 2001–2005 period, in 14,246 patients who received HAIC as initial treatment,

Table 2. Five-year OS rates (%) in patients who underwent resection, ablation, TACE, and HAIC assorted by year of initial diagnosis

	Resection (n=42,713)		Ablation (n=37,196)		TACE (n=61,460)		HAIC (n=14,246)	
	n	5-year OS rate,%	n	5-year OS rate,%	n	5-year OS rate,%	n	5-year OS rate,%
1978–1980	505	14.5			93	5.4	889	2.5
1981–1985	2,363	28.7*			1,682	17.8*	1,755	8.3*
1986–1990	5,959	40.5*	1,962	32.8	8,423	22.3*	1,821	14.6*
1991–1995	9,822	49.5*	7,246	37.7*	14,806	26.2*	1,079	16.0
1996–2000	11,562	54.5*	12,923	43.1*	18,037	30.5*	3,198	32.0*
2001–2005	12,502	58.4*	15,065	47.6*	18,419	35.0*	5,504	31.9

*p<0.0001 compared with the preceding time period.

Table 3. Median OS (months) in patients who underwent resection, ablation, TACE, and HAIC assorted by year of initial diagnosis

	Resection (n=42,713)		Ablation (n=37,196)		TACE (n=61,460)		HAIC (n=14,246)	
	n	Median OS, months	n	Median OS, months	n	Median OS, months	n	Median OS, months
1978–1980	505	13			93	9	889	4
1981–1985	2,363	28			1,682	17	1,755	7
1986–1990	5,959	46	1,962	41	8,423	27	1,821	12
1991–1995	9,822	60	7,246	47	14,806	32	1,079	10
1996–2000	11,562	69	12,923	53	18,037	37	3,198	33
2001–2005	12,502	74	15,065	59	18,419	42	5,504	31

as did median survival, from four months in the 1978–1980 period to 31 months in the 2001–2005 period.

We also assessed 5-year OS rates over time in HCC patients with AFP levels ≥400 ng/ml at the time of diagnosis. We found that OS rates increased steadily over time, with the differences between each 5-year period and the preceding 5-year period being statistically significant (fig. 2).

Discussion

The results shown here, taken from the two-yearly nationwide registry maintained by the LCSGJ, clearly show that, over 28 years, the 5-year OS rates have markedly improved in patients with HCC. Although these improvements are largely due to the appropriate and intensive treatment of patients by established treatment modalities, including potentially curative treatment (resection or ablation) and mass reductive/palliative treatment (TACE or HAIC), they are also due to the establishment of the LCSGJ surveillance program throughout Japan. In addition, the establishment of additional treatment options, including molecular targeted agents such as sorafenib and their inclusion in established treatment algorithms, are expected to bring further improvements in survival in patients with HCC in Japan.

The improvements we observed in the 5-year OS rates and median OS could be correlated with the improvements in surveillance and treatment modalities over the 28-year time span.

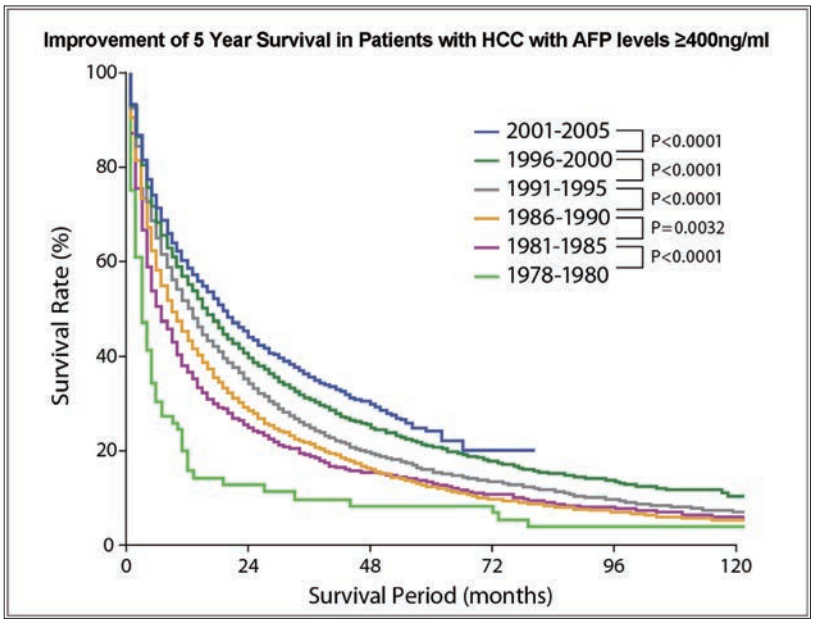

Fig. 2. Kaplan-Meier analysis of OS in patients with AFP levels ≥400 ng/ml at the time of diagnosis as a function of the period of diagnosis: 1978-1980 (light green), 1981-1985 (pink), 1986-1990 (yellow), 1991-1995 (gray), 1996-2000 (dark green), and 2001-2005 (blue). p<0.0001 for all differences between each period and the preceding period, except for p<0.0032 for 1986-1990 vs. 1981-1985.

The inclusion of ultrasound examinations and measurements of serum AFP concentration was instituted in the Japanese nationwide surveillance program in 1980. Hepatic resection and TACE were instituted as potentially curative and palliative treatments in 1985. In 1990, helical CT/MRI was introduced for diagnosis, percutaneous ethanol injection therapy was instituted in patients with HCC, and interferon treatment was instituted in patients with chronic HCV infection. In 1995, HAIC was instituted to treat HCC and measurements of DCP and AFP-L3 were instituted for patient surveillance and diagnosis. Radiofrequency ablation was instituted for curative treatment, multidetector-row CT for surveillance and diagnosis was introduced in 2000, and sorafenib was approved for the systemic treatment of patients with HCC in 2009.

Comparisons with Other Countries

Five-year OS rates for patients in the United States with liver and intrahepatic bile duct cancer have also shown slight improvements over time, from 3% for patients diagnosed in the 1975–1977 period to 11% for patients diagnosed in the 2001–2007 period [21–23]. In Korea, where guidelines recommend that individuals be monitored for HCC beginning at the age of 30 years old, the 5-year OS rates are higher than in the US, improving from 10.7% for patients diagnosed in the 1993–1995 period to 18.9% for patients diagnosed in the 2001–2005 period [24]. Nevertheless, they remain lower than those in Japan, perhaps due to the longer duration of the surveillance program and its complete nationwide establishment in Japan, but which is not the case in Korea.

Over time, approximately 62% of patients with HCC in Japan have undergone potentially curative treatments (resection or ablation) as initial therapy. In comparison, only about 30%

of patients in Western countries are eligible for potentially curative treatments at the time of their initial diagnosis [25]. The higher numbers of Japanese patients eligible for potentially curative treatment are likely to be due to the earlier detection and treatment of HCC, which is ultimately due to the establishment of comprehensive surveillance programs in patients at risk for HCC. This has undoubtedly resulted in increased 5-year OS rates in countries with surveillance programs, indicating that surveillance of patients at risk can lead to early detection and treatment [26]. The application of process-of-care quality indicators to measure evidence-practice gaps has been applied to the liver cancer registry and this may improve the quality of care in these patients [27]. Other differences between Japanese and Western populations are probably negligible in their contribution to differences in OS rates. These include differences in genetics, diet, and disease characteristics.

In conclusion, our findings show that the establishment of a nationwide HCC surveillance program in Japan has contributed to increased OS rates. These findings indicate the need for the establishment of national surveillance programs worldwide of patients at risk for HCC.

Disclosure Statement

The authors declare that they have no financial conflict of interest.

References

1 Ferlay J, Shin HR, Bray F, Forman D, Mathers C, Parkin DM: Estimates of worldwide burden of cancer in 2008: GLOBOCAN 2008. Int J Cancer 2010;127:2893–2917.
2 Asia-Pacific Working Party on Prevention of Hepatocellular Carcinoma: Prevention of hepatocellular carcinoma in the Asia-Pacific region: consensus statements. J Gastroenterol Hepatol 2010;25:657–663.
3 Song P, Tang W, Tamura S, Hasegawa K, Sugawara Y, Dong J, Kokudo N: The management of hepatocellular carcinoma in Asia: a guideline combining quantitative and qualitative evaluation. Biosci Trends 2010;4:283–287.
4 Umemura T, Ichijo T, Yoshizawa K, Tanaka E, Kiyosawa K: Epidemiology of hepatocellular carcinoma in Japan. J Gastroenterol 2009;44(Suppl 19):102–107.
5 Kudo M, Chung H, Haji S, Osaki Y, Oka H, Seki T, Kasugai H, Sasaki Y, Matsunaga T: Validation of a new prognostic staging system for hepatocellular carcinoma: the JIS score compared with the CLIP score. Hepatology 2004;40:1396–1405.
6 El-Serag HB: Hepatocellular carcinoma. N Engl J Med 2011;365:1118–1127.
7 Ikai I, Arii S, Okazaki M, Okita K, Omata M, Kojiro M, Takayasu K, Nakanuma Y, Makuuchi M, Matsuyama Y, Monden M, Kudo M: Report of the 17th Nationwide Follow-up Survey of Primary Liver Cancer in Japan. Hepatol Res 2007;37:676–691.
8 Ikai I, Kudo M, Arii S, Omata M, Kojiro M, Sakamoto M, et al: Report of the 18th Nationwide Follow-up Survey of Primary Liver Cancer in Japan. Hepatol Res 2010;40:1043–1059.
9 Takayasu K, Arii S, Ikai I, Omata M, Okita K, Ichida T, Matsuyama Y, Nakanuma Y, Kojiro M, Makuuchi M, Yamaoka Y, Liver Cancer Study Group of Japan: Prospective cohort study of transarterial chemoembolization for unresectable hepatocellular carcinoma in 8510 patients. Gastroenterology 2006;131:461–469.
10 Hasegawa K, Makuuchi M, Takayama T, Kokudo N, Arii S, Okazaki M, Okita K, Omata M, Kudo M, Kojiro M, Nakanuma Y, Takayasu K, Monden M, Matsuyama Y, Ikai I: Surgical resection vs. percutaneous ablation for hepatocellular carcinoma: a preliminary report of the Japanese nationwide survey. J Hepatol 2008;49:589–594.
11 Fujita T: Hepatectomy versus radiofrequency ablation for early hepatocellular carcinoma. J Hepatol 2009;50:1051–1052, author reply 1052–1053.
12 Takayasu K, Arii S, Ikai I, Kudo M, Matsuyama Y, Kojiro M, Makuuchi M, Liver Cancer Study Group of Japan: Overall survival after transarterial lipiodol infusion chemotherapy with or without embolization for unresectable hepatocellular carcinoma: propensity score analysis. AJR Am J Roentgenol 2010;194:830–837.
13 Eguchi S, Kanematsu T, Arii S, Omata M, Kudo M, Sakamoto M, Takayasu K, Makuuchi M, Matsuyama Y, Monden M, Liver Cancer Study Group of Japan: Recurrence-free survival more than 10 years after liver resection for hepatocellular carcinoma. Br J Surg 2011;98:552–557.
14 Mazzaferro V, Regalia E, Doci R, Andreola S, Pulvirenti A, Bozzetti F, Montalto F, Ammatuna M, Morabito A, Gennari L: Liver transplantation for the treatment of small hepatocellular carcinomas in patients with cirrhosis. N Engl J Med 1996;334:693–699.

15 Llovet JM, Ricci S, Mazzaferro V, Hilgard P, Gane E, Blanc JF, de Oliveira AC, Santoro A, Raoul JL, Forner A, Schwartz M, Porta C, Zeuzem S, Bolondi L, Greten TF, Galle PR, Seitz JF, Borbath I, Häussinger D, Giannaris T, Shan M, Moscovici M, Voliotis D, Bruix J, SHARP Investigators Study Group: Sorafenib in advanced hepatocellular carcinoma. N Engl J Med 2008;359:378–390.
16 Cheng AL, Kang YK, Chen Z, Tsao CJ, Qin S, Kim JS, Luo R, Feng J, Ye S, Yang TS, Xu J, Sun Y, Liang H, Liu J, Wang J, Tak WY, Pan H, Burock K, Zou J, Voliotis D, Guan Z: Efficacy and safety of sorafenib in patients in the Asia-Pacific region with advanced hepatocellular carcinoma: a phase III randomised, double-blind, placebo-controlled trial. Lancet Oncol 2009;10:25–34.
17 Kudo M, Ueshima K, Kubo S, Sakamoto M, Tanaka M, Ikai I, Furuse J, Murakami T, Kadoya M, Kokudo N Liver Cancer Study Group of Japan (Committee for Response Evaluation Criteria in Cancer of the Liver, Liver Cancer Study Group of Japan): Response Evaluation Criteria in Cancer of the Liver (RECICL) proposed by the Liver Cancer Study Group of Japan (2016 Revised Version). Hepatol Res 2016;46:3-9.
18 Lencioni R, Llovet JM: Modified RECIST (mRECIST) assessment for hepatocellular carcinoma. Semin Liver Dis 2010;30:52–60.
19 Makuuchi M, Kokudo N, Arii S, Futagawa S, Kaneko S, Kawasaki S, Matsuyama Y, Okazaki M, Okita K, Omata M, Saida Y, Takayama T, Yamaoka Y: Development of evidence-based clinical guidelines for the diagnosis and treatment of hepatocellular carcinoma in Japan. Hepatol Res 2008;38:37–51.
20 Kudo M, Izumi N, Kokudo N, Matsui O, Sakamoto M, Nakashima O, Kojiro M, Makuuchi M, HCC Expert Panel of Japan Society of Hepatology: Management of hepatocellular carcinoma in Japan: Consensus-Based Clinical Practice Guidelines proposed by the Japan Society of Hepatology (JSH) 2010 updated version. Dig Dis 2011;29:339–364.
21 Altekruse SF, McGlynn KA, Dickie LA, Kleiner DE: Hepatocellular carcinoma confirmation, treatment, and survival in surveillance, epidemiology, and end results registries, 1992-2008. Hepatology 2012;55:476–482.
22 Ries. LAG, Melbert D, Krapcho M, et al (eds.). SEER Cancer Statistics Review, 1975–2005, National Cancer Institute, Bethesda, MD. Available at: http://seer.cancer.gov/csr/1975_2005/,2008. Accessed February 27, 2012.
23 American Cancer Society. Cancer facts and figures 2012.
24 Park JW, Korean Liver Cancer Study Group and National Cancer Center: [Practice guideline for diagnosis and treatment of hepatocellular carcinoma]. Korean J Hepatol 2004;10:88–98.
25 Llovet JM, Burroughs A, Bruix J: Hepatocellular carcinoma. Lancet 2003;362:1907–1917.
26 El-Serag HB, Davila JA: Surveillance for hepatocellular carcinoma: in whom and how? Therap Adv Gastroenterol 2011;4:5–10.
27 Higashi T, Hasegawa K, Kokudo N, Makuuchi M, Izumi N, Ichida T, Kudo M, Ku Y, Sakamoto M, Nakashima O, Matsui O, Matsuyama Y, Sobue T, Liver Cancer Study Group of Japan: Demonstration of quality of care measurement using the Japanese liver cancer registry. Hepatol Res 2011;41:1208–1215.

Liver Cancer

Liver Cancer 2016;5:155–161
DOI: 10.1159/000443563
Published online: May 3, 2016

2235-1795/16/0053-0155$39.50/0
www.karger.com/lic

Editorial

Risk of Hepatocellular Carcinoma in Patients with Hepatitis C Virus Who Achieved Sustained Virological Response

Prof. M. Kudo

Editor *Liver Cancer*

Introduction

The recent development of interferon-free direct-acting antivirals (DAAs) has had a significant impact on the already great advances made in the treatment of hepatitis C. Combination therapy with pegylated interferon, ribavirin and simeprevir has achieved a sustained virological response (SVR) rate of approximately 70% in patients with hepatitis C caused by the genotype Ib virus. Combination therapy using daclatasvir and asunaprevir, which was approved in Japan in September 2014, has increased the SVR rate to approximately 95%. A clinical trial testing sofosbuvir–ledipasvir combination therapy (approved in September 2015 in Japan and October and November 2014 in the USA and EU, respectively) showed an SVR rate of nearly 100% in patients with genotype 1b hepatitis C virus. Combination therapy with ombitasvir and paritaprevir, which has a powerful therapeutic effect (SVR rate ≥95%), also became available in Japan from November 2015. Because interferon-based therapy is not possible in patients aged >70 years, in patients with cirrhosis, or in patients with a low platelet count, the above DAAs (which have extremely low rates of adverse effects) are extensively indicated. DAAs can be administered to almost all hepatitis C patients, including the elderly and those with compensated liver cirrhosis, and rapidly eradicate hepatitis C viruses; high SVR rates are achieved even in elderly cirrhotic patients with a high risk of liver cancer. Consequently, a new clinical problem has emerged, namely, the development of liver cancer after SVR [1–12]. Thus, two new unmet needs have arisen in the clinical setting: (1) finding the best possible way to assess the risk of liver cancer development after SVR is achieved and (2) establishing a liver cancer screening program for these patients [13, 14].

Liver Cancer 2016;5:155–161
DOI: 10.1159/000443563
Published online: May 3, 2016

α-Fetoprotein (AFP)

It is well known that liver cancer can develop in elderly patients and patients with advanced fibrosis who have achieved SVR after interferon-based therapy [1–12]. Nationwide data reveal that 2.4% (109/4,542) of Japanese patients who achieved SVR developed liver cancer during an observation period of approximately 5.5 years [15]. The longest interval between SVR and cancer onset was more than 15 years. The same study also showed that advanced fibrosis, hypoalbuminemia before interferon treatment, and high baseline AFP levels were strongly associated with the development of hepatocellular carcinoma (HCC).

When treatment with DAAs became available, the initial concern was that the drugs would be inferior to interferon-based therapy in terms of reducing the risk of liver cancer development. However, now that several tens of thousands of patients with hepatitis C have been treated with DAAs in Japan, it is clear that AFP levels, a surrogate marker of HCC development, drop to ≤10 ng/ml after achieving SVR, thereby dispelling this initial concern. These low AFP levels also suggest that both DAAs and interferon-based therapies will reduce the cancer risk.

A large-scale cohort study revealed that old age, advanced fibrosis, male gender, and high post-treatment AFP levels are risk factors for post-SVR HCC development [16]. In addition to high AFP levels, high alanine transaminase levels and platelet counts are reportedly risk factors for cancer development after treatment with interferon-based therapy, regardless of whether SVR is achieved [17–19].

Two different cut-offs have been suggested for AFP levels after interferon-based treatment: 6 ng/ml [17] and 10 ng/ml [19]. The risk of HCC development appears to be high in patients whose AFP levels remain ≥10 ng/ml after antiviral treatment (figs. 1 and 2). Regardless of whether SVR is achieved, surveillance needs to be continued in such patients to detect HCC at an early stage. It is recommended that elderly patients or patients with advanced fibrosis who have post-treatment AFP levels ≥10 ng/ml be identified as a high-intermediate risk group. This group should be tested for three types of tumor marker (AFP, prothrombin induced in the absence of vitamin K [PIVKA-II], and the lectin-binding fraction of AFP [AFP-L3]) and undergo ultrasonography every 6–12 months.

Mac-2 Binding Protein Glycosylation Isomer (M2BPGi)

The carbohydrate M2BPGi is a serum marker of liver fibrosis [20] that was developed by Sysmex Corp. (Kobe, Japan) and a team led by Dr. Hisashi Narimatsu (Research Centre for Medical Glycoscience, National Institute of Advanced Industrial Science and Technology, Tokyo, Japan). Carbohydrate epitopes developed as markers of liver fibrosis have been used to diagnose fibrosis in patients with hepatitis C, hepatitis B, and non-alcoholic fatty liver disease. In recent years, their utility as markers of HCC development in hepatitis C patients has been of particular interest. The rate of HCC in patients with hepatitis C gradually increases from 0.5%, to 1.5%, 3%, 5%, and 8% as hepatic fibrosis progresses from stage F0 to F1, F2, F3, and F4, respectively. Yamasaki et al. measured M2BPGi levels in 707 patients with chronic hepatitis C who had undergone liver biopsy and found that progression of fibrosis correlated well with M2BPGi levels [21]. More precisely, the proportion of patients with F0–F1 and F4 was clearly different in those with an M2BPGi cutoff index (COI) ≤1 (80.6% and 1.3%, respectively) and in those with an M2BPGi COI ≥8 (3.1% and 78.1%, respectively). Furthermore, the cumulative incidence of HCC increased as M2BPGi levels increased regardless of fibrosis stage (fig. 3) [21].

Liver Cancer 2016;5:155–161
DOI: 10.1159/000443563
Published online: May 3, 2016

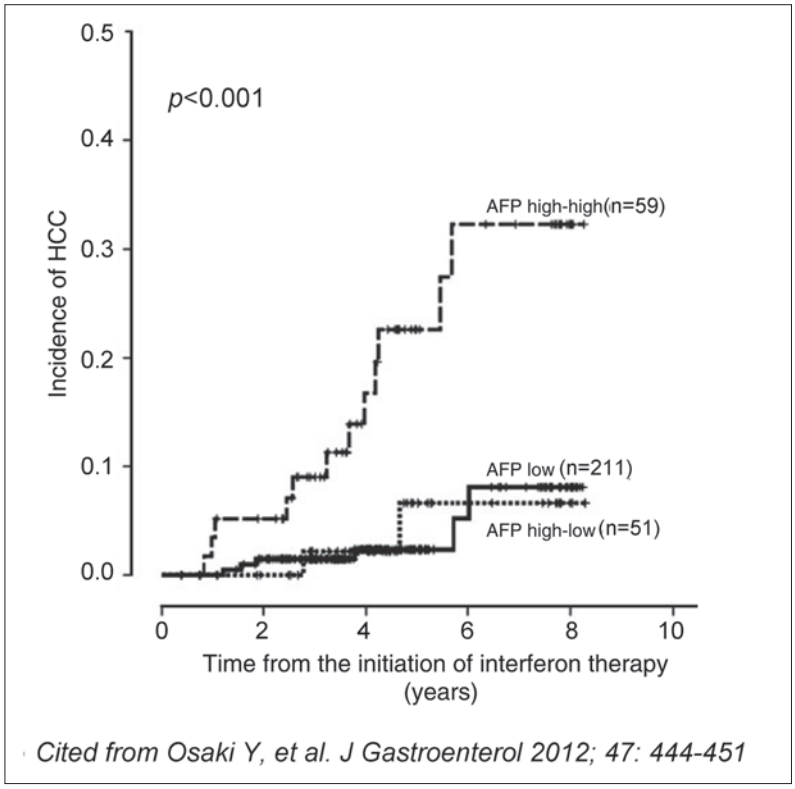

Fig. 1. Kaplan–Meier estimates of the incidence of HCC after interferon therapy for hepatitis C. The solid line denotes the AFP-low group (AFP levels before interferon therapy <10 ng/ml), the dotted line denotes the AFP high-low group (baseline AFP levels ≥10 ng/ml, average AFP integration level <10 ng/ml), and the dashed line denotes the AFP high-high group (both baseline and average AFP integration levels ≥10 ng/ml). Reproduced with permission from Osaki Y, et al. [19]

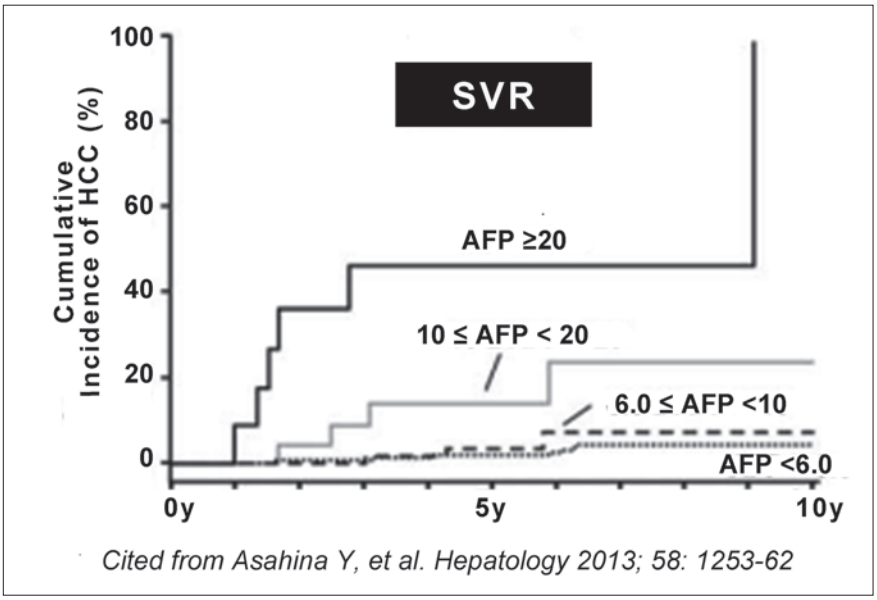

Fig. 2. Cumulative incidence of HCC in chronic hepatitis C patients according to post-interferon treatment AFP level. Patients with SVR after treatment of hepatitis C were stratified according to post-IFN treatment AFP levels (log-rank test: p<0.0001). Reproduced with permission from Asahina Y, et al. [17]

Liver Cancer 2016;5:155–161
DOI: 10.1159/000443563
Published online: May 3, 2016

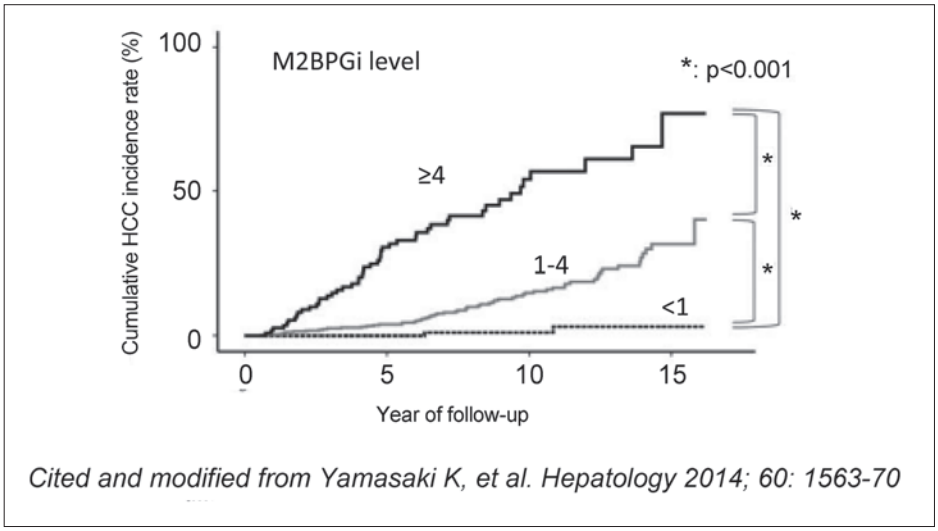

Fig. 3. Cumulative incidence of HCC according to M2BPGi levels in patients with hepatitis C, as analyzed using the Kaplan–Meier method. Black solid, gray solid, and dotted lines denote stratified M2BPGi levels ≥4, 1–4, and <1, respectively. The HCC incidence differed significantly between the three groups ($p<0.001$, log-rank test) and increased with increasing M2BPGi levels. Reproduced with permission from Yamasaki K, et al. [21]

Multivariate analysis using the Cox proportional hazards model was performed to identify factors contributing to the development of HCC. Fibrosis stage (F0–F1, F2, F3, F4), AFP (<6, 6–20, ≥20 ng/ml), age (<57 or ≥57 years old), interferon therapy (no therapy versus SVR) were significantly associated with the risk of HCC. It should be noted that fibrosis stage F4 versus stages F0–F1 was the only significant factor indicative of increased risk of HCC development as far as the fibrosis stage is concerned, whereas an M2BPGi COI of 1–4 (hazard ratio 5.2, $p=0.029$) and of ≥4 (hazard ratio 8.3, $p=0.007$) were significant factors versus an M2BPGi COI ≤1. This finding indicates that M2BPGi is a more useful factor for predicting the development of HCC than the fibrosis stage is [21].

Analysis of the time-dependent area under the receiver operating characteristic (AUROC) curve was also used to compare the predictive performances of M2BPGi, AFP, and platelet count. M2BPGi levels (based on AUROC analysis that examined the period from year 1 to year 13 after liver biopsy) were superior to AFP levels and platelet counts for predicting HCC development in years 3 and 5.

The above data were derived by comparing the incidence of HCC development in the overall cohort of patients with chronic hepatitis C. A similar approach could be used to predict the risk of cancer development in the subgroup of hepatitis C patients who achieved SVR after antiviral treatment.

Sasaki et al. measured M2BPGi levels in 238 patients with hepatitis C and found that they were significantly higher in the 16 patients (6.8%) who developed HCC after achieving SVR than in the remaining 222 patients (93.2%) who did not. Multivariate analysis also revealed that the M2BPGi level is an independent predictive factor for HCC development (fig. 4) [22].

Tamaki et al. used a cumulative scoring system in which an annual change in the M2BPGi level of ≥0.3, an AFP level of ≥10 ng/ml, and an M2BPGi COI of ≥4.2 were individually counted as one point (or as zero points when they were less than these values). They found that HCC development was rarely confirmed in patients with a cumulative score of zero, whereas the risk of HCC development gradually increased as the cumulative score increased from 1

Liver Cancer 2016;5:155–161
DOI: 10.1159/000443563
Published online: May 3, 2016

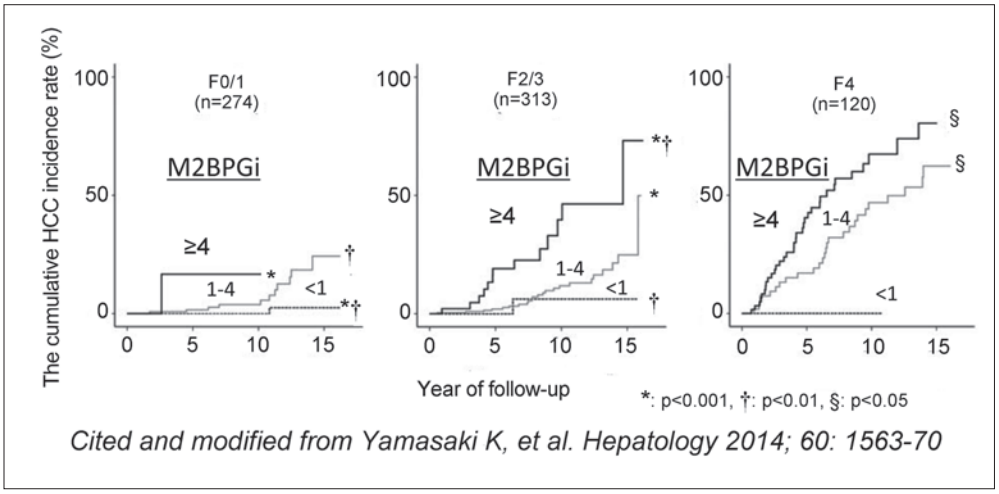

Fig. 4. Cumulative incidence of HCC in patients with hepatitis C according to M2BPGi levels stratified according to the fibrosis stage as analyzed using the Kaplan–Meier method. Black solid, gray solid, and dotted lines denote stratified M2BPGi levels ≥4, 1–4, and <1, respectively. The HCC incidence increased with increasing M2BPGi levels. Reproduced with permission from Yamasaki K, et al. [21]

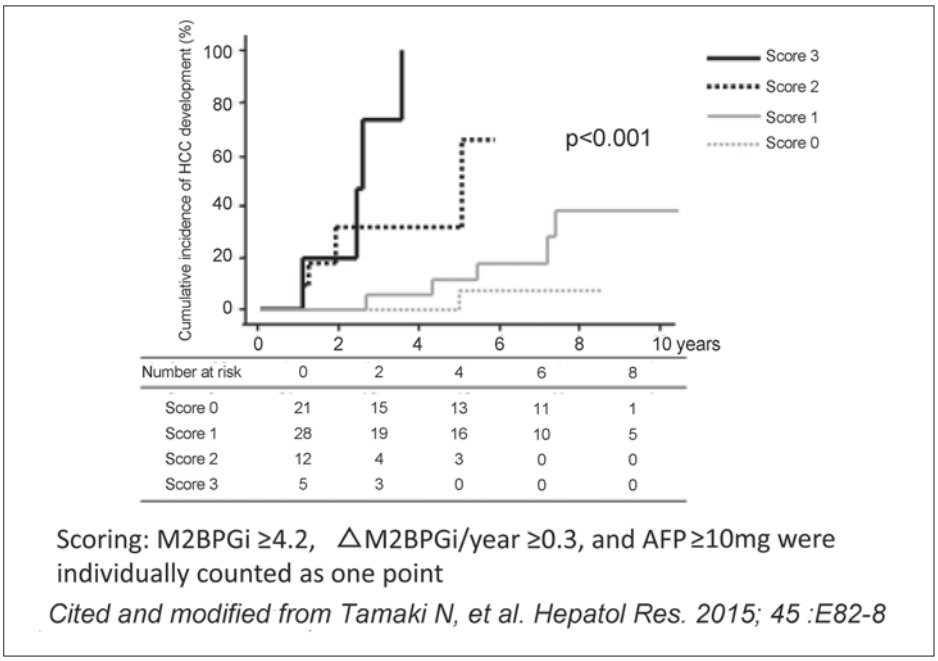

Fig. 5. Association between the risk score and the cumulative incidence of HCC development in chronic hepatitis C patients. M2BPGi ≥4.2, ΔM2BPGi/year ≥0.3, and AFP ≥10 ng/ml each contributed one point to the overall score. M2BPGi <4.2, ΔM2BPGi/year <0.3, and AFP <10 ng/ml each contributed zero points to the overall score. Patients were classified into four groups according to their total score (0, 1, 2, or 3). Reproduced with permission from Tamaki N, et al. [23]

to 3 (fig. 5) [23]. Clearly, blood tests measuring the above three factors provide a certain level of prediction regarding post-SVR cancer risk. This finding also supports the notion that the M2BPGi level is useful for predicting HCC development in those with chronic hepatitis C who have achieved SVR after antiviral therapy.

Liver Cancer 2016;5:155–161
DOI: 10.1159/000443563
Published online: May 3, 2016

Conclusion

In the future, M2BPGi will play an extremely important role in predicting HCC development in hepatitis C patients who achieve SVR after antiviral therapy. This factor can be used alongside post-treatment AFP levels, for which a consensus on its predictive utility has almost been reached. Additionally, a scoring system that combines AFP and M2BPGi levels appears to be beneficial. The growing clinical problems associated with the rapidly emerging era of DAA therapy may be reduced by considering post-treatment AFP and M2BPGi levels in addition to old age, male gender, and low platelet count when analyzing the post-SVR HCC risk in patients with chronic hepatitis C. This approach will also be useful for introducing different screening intervals determined according to the results of individual risk analysis.

Although evidence indicating that both AFP and M2BPGi levels in hepatitis C patients after achievement of SVR are important for assessing the post-SVR risk of developing HCC has come only from Japan, these two serum markers will be of particular significance when developing screening strategies for post-SVR HCC development. It is anticipated that M2BPGi testing will soon be available in the clinical setting in other parts of the world, including Asian and Western countries.

References

1 Asahina Y, Tsuchiya K, Tamaki N, Hirayama I, Tanaka T, Sato M, Yasui Y, Hosokawa T, Ueda K, Kuzuya T, Nakanishi H, Itakura J, Takahashi Y, Kurosaki M, Enomoto N, Izumi N: Effect of aging on risk for hepatocellular carcinoma in chronic hepatitis C virus infection. Hepatology 2010;52:518–527.
2 Nagaoki Y, Aikata H, Miyaki D, Murakami E, Hashimoto Y, Katamura Y, Azakami T, Kawaoka T, Takaki S, Hiramatsu A, Waki K, Imamura M, Kawakami Y, Takahashi S, Chayama K: Clinical features and prognosis in patients with hepatocellular carcinoma that developed after hepatitis C virus eradication with interferon therapy. J Gastroenterol 2011;46:799–808.
3 Ohki T, Tateishi R, Sato T, Masuzaki R, Imamura J, Goto T, Yamashiki N, Yoshida H, Kanai F, Kato N, Shiina S, Yoshida H, Kawabe T, Omata M: Obesity is an independent risk factor for hepatocellular carcinoma development in chronic hepatitis C patients. Clin Gastroenterol Hepatol 2008;6:459–464.
4 Kobayashi S, Takeda T, Enomoto M, Tamori A, Kawada N, Habu D, Sakaguchi H, Kuroda T, Kioka K, Kim SR, Kanno T, Ueda T, Hirano M, Fujimoto S, Jomura H, Nishiguchi S, Seki S: Development of hepatocellular carcinoma in patients with chronic hepatitis C who had a sustained virological response to interferon therapy: A multicenter, retrospective cohort study of 1124 patients. Liver Int 2007;27:186–191.
5 Hirakawa M, Ikeda K, Arase Y, Kawamura Y, Yatsuji H, Hosaka T, Sezaki H, Akuta N, Kobayashi M, Saitoh S, Suzuki F, Suzuki Y, Kumada H: Hepatocarcinogenesis following HCV RNA eradication by interferon in chronic hepatitis patients. Intern Med 2008;47:1637–1643.
6 Tanaka A, Uegaki S, Kurihara H, Aida K, Mikami M, Nagashima I, Shiga J, Takikawa H: Hepatic steatosis as a possible risk factor for the development of hepatocellular carcinoma after eradication of hepatitis C virus with antiviral therapy in patients with chronic hepatitis C. World J Gastroenterol 2007;13:5180–5187.
7 Tokita H, Fukui H, Tanaka A, Kamitsukasa H, Yagura M, Harada H, Okamoto H: Risk factors for the development of hepatocellular carcinoma among patients with chronic hepatitis C who achieved a sustained virological response to interferon therapy. J Gastroenterol Hepatol 2005;20:752–758.
8 Ikeda M, Fujiyama S, Tanaka M, Sata M, Ide T, Yatsuhashi H, Watanabe H: Risk factors for development of hepatocellular carcinoma in patients with chronic hepatitis C after sustained response to interferon. J Gastroenterol 2005;40:148–156.
9 Iwasaki Y, Takaguchi K, Ikeda H, Makino Y, Araki Y, Ando M, Kobashi H, Kobatake T, Tanaka R, Tomita M, Senoh T, Kawaguchi M, Shimoe T, Manabe K, Kita K, Shimamura J, Sakaguchi K, Shiratori Y: Risk factors for hepatocellular carcinoma in hepatitis C patients with sustained virologic response to interferon therapy. Liver Int 2004;24:603–610.
10 Makiyama A, Itoh Y, Kasahara A, Imai Y, Kawata S, Yoshioka K, Tsubouchi H, Kiyosawa K, Kakumu S, Okita K, Hayashi N, Okanoue T: Characteristics of patients with chronic hepatitis C who develop hepatocellular carcinoma after a sustained response to interferon therapy. Cancer 2004;101:1616–1622.
11 Kasahara A, Hayashi N, Mochizuki K, Takayanagi M, Yoshioka K, Kakumu S, Iijima A, Urushihara A, Kiyosawa K, Okuda M, Hino K, Okita K, Osaka Liver Disease Study Group: Risk factors for hepatocellular carcinoma and its incidence after interferon treatment in patients with chronic hepatitis C. Hepatology 1998;27:1394–1402.

Liver Cancer 2016;5:155–161
DOI: 10.1159/000443563
Published online: May 3, 2016

12 Dohmen K, Kawano A, Takahashi K, Shigematsu H, Tanaka H, Haruno M, Yanagita K, Ichiki Y, Mori T, Hayashida K, Shimoda S, Ishibashi H, Nomura H: The incidence and risk factors for the development of hepatocellular carcinoma after peginterferon plus ribavirin therapy for chronic hepatitis C. Hepatogastroenterology 2013;60:2034–2038.
13 Kudo M: Surveillance, diagnosis, treatment, and outcome of liver cancer in Japan. Liver Cancer 2015;4:39–50.
14 Kudo M: Clinical practice guidelines for hepatocellular carcinoma differ between Japan, United States, and Europe. Liver Cancer 2015;4:85–95.
15 Sato A, Sata M, Ikeda K, Kumada T, Izumi N, Asahina Y, Osaki Y, Chayama K, Kaneko S, Sakai A, Onji M, Hiasa Y, Omura T, Ozeki I, Yokosuka O, Shiina S, Itsubo M, Nishiguchi S, Hirano K, Ide T, Sakisaka S, Yamasaki T, Hidaka I, Tanaka M, Kim SR, Ichida T: Clinical characteristics of patients who developed hepatocellular carcinoma after hepatitis C virus eradication with interferon therapy: current status in Japan. Intern Med 2013;52:2701–2706.
16 Nagaoki Y, Aikata H, Nakano N, Shinohara F, Nakamura Y, Hatooka M, Morio K, Kan H, Fujino H, Kobayashi T, Fukuhara T, Masaki K, Ono A, Nakahara T, Kawaoka T, Miki D, Tsuge M, Hiramatsu A, Imamura M, Takahashi S, Kawakami Y, Ochi H, Chayama K, Hiroshima Liver Study Group: Development of hepatocellular carcinoma in patients with hepatitis C virus infection who achieved sustained virological response following interferon therapy: a large-scale, long-term cohort study. J Gastroenterol Hepatol 2015 Nov 19. doi: 10.1111/jgh.13236. [Epub ahead of print] .
17 Asahina Y, Tsuchiya K, Nishimura T, Muraoka M, Suzuki Y, Tamaki N, Yasui Y, Hosokawa T, Ueda K, Nakanishi H, Itakura J, Takahashi Y, Kurosaki M, Enomoto N, Nakagawa M, Kakinuma S, Watanabe M, Izumi N: α-Fetoprotein levels after interferon therapy and risk of hepatocarcinogenesis in chronic hepatitis C. Hepatology 2013;58:1253–1262.
18 Oze T, Hiramatsu N, Yakushijin T, Miyazaki M, Yamada A, Oshita M, Hagiwara H, Mita E, Ito T, Fukui H, Inui Y, Hijioka T, Inada M, Katayama K, Tamura S, Yoshihara H, Inoue A, Imai Y, Hayashi E, Kato M, Miyagi T, Yoshida Y, Tatsumi T, Kasahara A, Hamasaki T, Hayashi N, Takehara T, Osaka Liver Forum: Post-treatment levels of α-fetoprotein predict incidence of hepatocellular carcinoma after interferon therapy. Clin Gastroenterol Hepatol 2014;12:1186–1195.
19 Osaki Y, Ueda Y, Marusawa H, Nakajima J, Kimura T, Kita R, Nishikawa H, Saito S, Henmi S, Sakamoto A, Eso Y, Chiba T: Decrease in alpha-fetoprotein levels predicts reduced incidence of hepatocellular carcinoma in patients with hepatitis C virus infection receiving interferon therapy: a single center study. J Gastroenterol 2012;47:444–451.
20 Kuno A, Ikehara Y, Tanaka Y, Ito K, Matsuda A, Sekiya S, Hige S, Sakamoto M, Kage M, Mizokami M, Narimatsu H: A serum "sweet-doughnut" protein facilitates fibrosis evaluation and therapy assessment in patients with viral hepatitis. Sci Rep 2013;3:1065. doi: 10.1038/srep01065. Epub 2013 Jan 15
21 Yamasaki K, Tateyama M, Abiru S, Komori A, Nagaoka S, Saeki A, Hashimoto S, Sasaki R, Bekki S, Kugiyama Y, Miyazoe Y, Kuno A, Korenaga M, Togayachi A, Ocho M, Mizokami M, Narimatsu H, Yatsuhashi H: Elevated serum levels of Wisteria floribunda agglutinin-positive human Mac-2 binding protein predict the development of hepatocellular carcinoma in hepatitis C patients. Hepatology 2014;60:1563–1570.
22 Sasaki R, Yamasaki K, Abiru S, Komori A, Nagaoka S, Saeki A, Hashimoto S, Bekki S, Kugiyama Y, Kuno A, Korenaga M, Togayachi A, Ocho M, Mizokami M, Narimatsu H, Ichikawa T, Nakao K, Yatsuhashi H: Serum wisteria floribunda agglutinin-positive mac-2 binding protein values predict the development of hepatocellular carcinoma among patients with chronic hepatitis C after sustained virological response. PLoS ONE 2015;10:e0129053.
23 Tamaki N, Kurosaki M, Kuno A, Korenaga M, Togayachi A, Gotoh M, Nakakuki N, Takada H, Matsuda S, Hattori N, Yasui Y, Suzuki S, Hosokawa T, Tsuchiya K, Nakanishi H, Itakura J, Takahashi Y, Mizokami M, Narimatsu H, Izumi N: Wisteria floribunda agglutinin positive human Mac-2-binding protein as a predictor of hepatocellular carcinoma development in chronic hepatitis C patients. Hepatol Res 2015;45:E82–88.

HEPATOLOGY

HEPATOLOGY, VOL. 64, NO. 3, 2016

Randomized, Open-Label Phase 2 Study Comparing Frontline Dovitinib Versus Sorafenib in Patients With Advanced Hepatocellular Carcinoma

Ann-Lii Cheng,[1] Sumitra Thongprasert,[2] Ho Yeong Lim,[3] Wattana Sukeepaisarnjaroen,[4] Tsai-Shen Yang,[5] Cheng-Chung Wu,[6] Yee Chao,[7] Stephen L. Chan,[8] Masatoshi Kudo,[9] Masafumi Ikeda,[10] Yoon-Koo Kang,[11] Hongming Pan,[12] Kazushi Numata,[13] Guohong Han,[14] Binaifer Balsara,[15] Yong Zhang,[15] Ana-Marie Rodriguez,[16] Yi Zhang,[15] Yongyu Wang,[15] and Ronnie T. P. Poon[17]

Angiogenesis inhibition by the vascular endothelial growth factor receptor (VEGFR) and platelet-derived growth factor receptor (PDGFR) inhibitor sorafenib provides survival benefit in hepatocellular carcinoma (HCC); however, angiogenic escape from sorafenib may occur due to angiogenesis-associated fibroblast growth factor receptor (FGFR) pathway activation. In addition to VEGFR and PDGFR, dovitinib inhibits FGFR. Frontline oral dovitinib (500 mg/day, 5 days on, 2 days off; n = 82) versus sorafenib (400 mg twice daily; n = 83) was evaluated in an open-label, randomized phase 2 study of Asian-Pacific patients with advanced HCC. The primary and key secondary endpoints were overall survival (OS) and time to tumor progression (TTP) as determined by a local investigator, respectively. Patients included in the study were ineligible for surgical and/or locoregional therapies or had disease progression after receiving these therapies. The median OS (95% confidence interval [CI]) was 8.0 (6.6-9.1) months for dovitinib and 8.4 (5.4-11.3) months for sorafenib. The median TTP (95% CI) per investigator assessment was 4.1 (2.8-4.2) months and 4.1 (2.8-4.3) months for dovitinib and sorafenib, respectively. Common any-cause adverse events included diarrhea (62%), decreased appetite (43%), nausea (41%), vomiting (41%), fatigue (35%), rash (34%), and pyrexia (30%) for dovitinib and palmar-plantar erythrodysesthesia syndrome (66%) and decreased appetite (31%) for sorafenib. Subgroup analysis revealed a significantly higher median OS for patients in the dovitinib arm who had baseline plasma soluble VEGFR1 (sVEGFR1) and hepatocyte growth factor (HGF) below median levels versus at or above the median levels (median OS [95% CI]: sVEGFR1, 11.2 [9.0-13.8] and 5.7 [4.3-7.0] months, respectively [P = .0002]; HGF, 11.2 [8.9-13.8] and 5.9 [5.0-7.6] months, respectively [P = 0.0002]). *Conclusion:* Dovitinib was well tolerated, but activity was not greater than sorafenib as a frontline systemic therapy for HCC. Based on these data, no subsequent phase 3 study has been planned. (HEPATOLOGY 2016;64:774-784)

Abbreviations: AE, adverse event; BCLC, Barcelona Clinic Liver Cancer; CI, confidence interval; ECOG PS, Eastern Cooperative Oncology Group performance status; FGFR, fibroblast growth factor receptor; HCC, hepatocellular carcinoma; HGF, hepatocyte growth factor; OS, overall survival; PDGFR, platelet-derived growth factor receptor; PK, pharmacokinetics; PPES, palmar-plantar erythrodysesthesia syndrome; RECIST, Response Evaluation Criteria in Solid Tumors; sVEGFR1, soluble vascular endothelial growth factor receptor-1; TKI, tyrosine kinase inhibitor; TTP, time to tumor progression; ULN, upper limit of normal; VEGFR, vascular endothelial growth factor receptor.

Received September 4, 2015; accepted April 2, 2016.

Additional Supporting Information may be found article at onlinelibrary.wiley.com/doi/10.1002/hep.28600/suppinfo.

View this article online at wileyonlinelibrary.com.

DOI 10.1002/hep.28600

Potential conflict of interest: Masafumi Ikeda advises and is on the speakers' bureau for Bayer Yakuhin, Bristol-Myers Squibb, and Eli Lilly. He advises Nano Carrier and Eisai. He is on the speakers' bureau for Novartis, Abbott, Yakult, Taiho, Kowa, Nippon Kayaku, and Chugai. Masatoshi Kudo is on the speakers' bureau for Bayer and received grants from MSD, Eisai, Ajinomoto, Otsuka, and Bristol-Myers Squibb. Ann-Lii Cheng consults for Novartis, Eisai, Merck Serono, Merck Sharp & Dohme, and Bayer. Stephen L. Chan advises Novartis. Yoon-Koo Kang consults, advises, and received grants from Novartis and Bayer. Binaifer Balsara is employed by Novartis. Yi Zhang is employed by Novartis. Yong Zhang is employed by Novartis. Ana-Marie Rodriguez is employed by Novartis. Yongyu Wang is employed by Novartis. All other authors have nothing to disclose.

Overexpression of fibroblast growth factor receptors (FGFRs) FGFR1, FGFR2, FGFR3, or FGFR4 and corresponding FGF ligands (FGF2, FGF8, FGF17, or FGF18) has been observed in human hepatocellular carcinoma (HCC) tumors.[1-3] HCC accounts for approximately 80% of primary liver cancer cases, the majority of which are diagnosed at an advanced stage of disease and are not candidates for surgical interventions.[4,5] FGF2, a potent angiogenic factor in HCC, has been shown to augment vascular endothelial growth factor (VEGF)-mediated HCC development and angiogenesis, and perhaps may evade resistance to VEGFR modulating agents.[6-8]

Sorafenib (Nexavar; Whippany, NJ), a multikinase inhibitor of vascular endothelial growth factor receptor (VEGFR) and platelet-derived growth factor receptor (PDGFR), was the first effective antiangiogenic therapy for advanced HCC and remains the only approved treatment for this disease.[9,10] Although sorafenib was shown to improve overall survival (OS) and radiological time to tumor progression (TTP) in Asian-Pacific patients with advanced HCC (median OS, 6.5 months; median TTP, 2.8 months), better systemic therapy remains an unmet need for patients with HCC in the Asia-Pacific region.

Dovitinib is a potent inhibitor of FGFRs, VEGFRs, and PDGFRβ, with antitumor activity mediated by a dual mechanism of action, including antiproliferative and antiangiogenic effects.[11,12] Preliminary efficacy for dovitinib has been reported in patients with metastatic renal cell carcinoma, metastatic melanoma, breast cancer, multiple myeloma, and acute myeloid leukemia.[12-15] In phase 1 studies in solid tumors, the maximum tolerated dose was determined to be 500 mg/day on a 5 days on, 2 days off schedule.[12,16] Dovitinib activity has been evaluated in multiple preclinical xenograft models in HCC. In the sorafenib-sensitive PLC5 HCC model, dovitinib inhibited tumor growth in a dose-dependent manner.[17] Furthermore, in patient-derived HCC xenograft models, dovitinib demonstrated antitumor activity superior to that of sorafenib and antiangiogenic effects that correlated with FGFR, PDGFRβ, and VEGFR2 signaling pathway activation.[18,19] These data support an investigation of dovitinib in patients with HCC. Here, we present the efficacy and safety results of a phase 2 study of frontline dovitinib versus sorafenib in patients with advanced HCC.

Materials and Methods

STUDY DESIGN AND TREATMENT

This phase 2, open-label, multicenter, randomized study conducted in the Asia-Pacific region evaluated the efficacy and safety of dovitinib compared with sorafenib in patients with advanced HCC. The protocol and all amendments were reviewed by the Independent Ethics Committee or Institutional Review Board for each study site. The study was conducted according to the ethical principles of the Declaration of Helsinki.

Patients were stratified according to Eastern Cooperative Oncology Group performance status (ECOG PS; 0 versus 1) and were randomized 1:1 to receive oral dovitinib at 500 mg/day on a 5 days on, 2 days off schedule or sorafenib at the standard dose, 400 mg continuously twice daily, until disease progression, unacceptable toxicity, death, or discontinuation for any

ARTICLE INFORMATION:

From the [1]National Taiwan University Hospital and National Taiwan University Cancer Center, Taipei, Taiwan; [2]Chiangmai University, Chiangmai, Thailand; [3]Samsung Medical Center, Seoul, South Korea; [4]Srinagarind Hospital, Khon Kaen, Thailand; [5]Chang Gung Memorial Hospital, Taoyuan, Taiwan; [6]Taichung Veterans General Hospital, Taichung, Taiwan; [7]Taipei Veterans General Hospital, Taipei, Taiwan; [8]Prince of Wales Hospital and The Chinese University of Hong Kong, Shatin, Hong Kong; [9]Kinki University School of Medicine, Osaka, Japan; [10]National Cancer Center Hospital East, Kashiwa, Japan; [11]Asan Medical Center, Seoul, South Korea; [12]Sir Run Run Shaw Hospital, Zhejiang University Medical College, Zhejiang, China; [13]Yokohama City University Medical Center, Yokohama, Japan; [14]Xijing Hospital, Fourth Military Medical University, Xi'an Shaanxi, China; [15]Novartis Pharmaceuticals Corporation, East Hanover, NJ; [16]Novartis Pharma AG, Basel, Switzerland; [17]Queen Mary Hospital, Pok Fu Lam, Hong Kong.

ADDRESS CORRESPONDENCE AND REPRINT REQUESTS TO:

Ann-Lii Cheng, M.D., Ph.D.
National Taiwan University Hospital
Room 5443, 4F, 5 West, No. 1, Changde Street
Zhongzheng District
Taipei City 100, Taiwan
Tel: +886-2-23123456 (extension 67011)
Fax: +886-2-23711174
E-mail: alcheng@ntu.edu.tw

reason. Treatment crossover was not planned; however, some patients on the dovitinib arm were given sorafenib as subsequent therapy in countries where sorafenib was clinically available, based on the investigator's judgment. Dose adjustments and interruptions (up to 3 weeks) were allowed for patients unable to tolerate dovitinib or sorafenib study doses. Dovitinib dose reduction for toxicity could not be re-escalated; however, when deemed appropriate by the treating physician, treatment after interruption was resumed on the next day of planned dosing, with every effort made to return to the original 5 days on, 2 days off dosing schedule as soon as possible. Local prescribing information was used to guide sorafenib dose and/or schedule adjustments.

STUDY POPULATION

Patients aged ≥18 years with an ECOG PS of ≤1 and advanced stage B or C HCC according to the American Association for the Study of Liver Diseases guidelines[20] and the Barcelona Clinic Liver Cancer (BCLC) staging classification[21] were eligible for this study. Patients were required to have at least one lesion as assessed by computed tomography or magnetic resonance imaging scans per the Response Evaluation Criteria in Solid Tumors (RECIST) version 1.1. Patients included in the study were either not eligible for surgical and/or locoregional therapies or had disease progression after receiving these therapies. All patients were required to have adequate bone marrow, liver, and renal function, and a current cirrhotic status of Child–Pugh Class A (5-6 points) with no encephalopathy. Patients were excluded from the study if they had received any systemic HCC therapy or sorafenib-based locoregional therapy, received a liver transplant or were awaiting immediate transplantation, or were currently receiving full-dose anticoagulation treatment with therapeutic doses of warfarin or antiplatelet therapy. Patients with clinically significant third space fluid accumulation (i.e., ascites requiring tapping despite use of diuretics, or pleural effusion that either required tapping or is associated with shortness of breath), or impaired cardiac function or clinically significant cardiac diseases were also excluded. Patients were required to stop treatment with any locoregional therapies, radiotherapy (except palliative radiotherapy for bone lesions, within 2 weeks), and major surgery within 4 weeks before study entry. Patients were permitted to receive prophylactic or antiviral treatment as needed, per institutional guidelines. All patients provided written informed consent to participate in the study.

EFFICACY ASSESSMENTS

Tumor response was evaluated locally at investigator sites and centrally by an independent radiologist according to RECIST version 1.1. Criteria for disease progression were also based on RECIST version 1.1. All target and nontarget lesions were assessed by chest, abdomen, and pelvis computed tomography or magnetic resonance imaging scans at baseline and every 6 weeks after the start of dovitinib or sorafenib treatment until radiological progression (see Supporting Information).

SAFETY ASSESSMENTS

Adverse events (AEs) occurring on or after the first dose day through 30 days after the end of treatment were recorded. National Cancer Institute Common Terminology Criteria for Adverse Events version 4.03 was used for grading. Hematology, blood chemistry, thyroid and cardiac function, and vital signs were also monitored throughout the study.

PHARMACOKINETICS AND BIOMARKER ASSESSMENTS

Blood samples for full pharmacokinetics (PK) analysis were collected from patients receiving dovitinib on day 1 of week 1 (postdose 1, 3, 6, and 24 hours) and on day 5 of week 2 (predose), week 4 (predose and postdose 1, 3, 6, and 24 hours), and week 6 (predose). Full PK blood sampling was used to estimate dovitinib PK parameters in patients with advanced HCC. A minimum of 18 patients who received dovitinib were enrolled for full PK analysis; the remaining patients in the dovitinib arm participated in sparse PK blood sampling, in which only the postdose 1-hour sample was collected on postdose collection days (day 1 of week 1 and day 5 of week 4).

For plasma pharmacodynamics analysis, blood samples were collected at baseline and predose on day 1 of week 1; day 5 of week 2, 4, and 6; day 1 (±3 days) of week 13; every 12 weeks thereafter; and at the end of treatment. Circulating growth factors, including hepatocyte growth factor (HGF), and soluble receptors, including soluble VEGFR1 (sVEGFR1), were evaluated as core pharmacodynamics biomarkers for FGFR and VEGFR and were measured by way of enzyme-linked immunosorbent or multiplex assays.

STATISTICAL ANALYSIS

The primary endpoint of the study was OS, defined as the time from date of randomization to

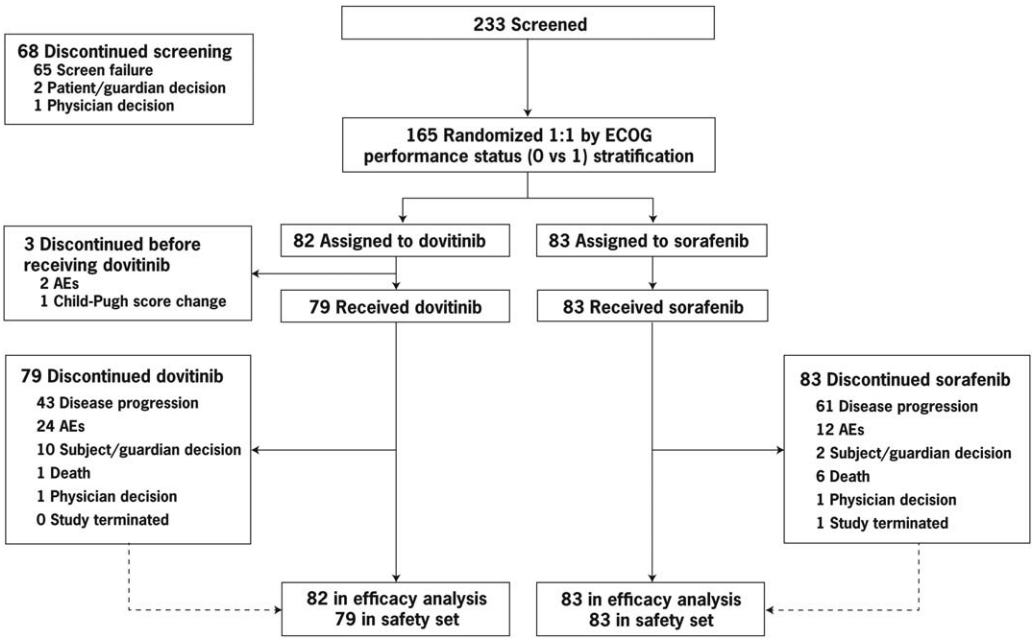

FIG. 1. CONSORT diagram of patient disposition. AE, adverse event; ECOG PS, Eastern Cooperative Oncology Group performance status.

date of death from any cause. If survival status for a patient was unknown at the time of data cutoff, the OS was censored at the last date of contact. Patients who discontinued dovitinib or sorafenib treatment were followed for survival every 6 weeks. Final OS analysis was performed after ≥130 deaths were observed.

The key secondary endpoint was radiologic TTP according to the assessment of a local investigator, which was defined as the time from the date of randomization to the date of first documented radiological disease progression. Patients who did not have a disease progression event were censored on the date of last adequate tumor assessment before the date of data analysis cutoff, start of antineoplastic therapy, or death. Death due to progression without documented radiological disease progression did not represent a disease progression event. Additional secondary endpoints were local investigator-assessed disease control rate (sum of patients with best overall response of complete response, partial response, or stable disease), time to definitive ECOG PS deterioration by ≥1 point (time from the date of randomization to either the date of definitive deterioration of the ECOG PS by ≥1category of the score from baseline or death, whichever came first), and safety.

The study population used for efficacy analyses included all patients who had been randomized. The safety and exploratory PK and biomarker (dovitinib arm only) populations for analysis comprised all patients who received at least one dose of study medication. Descriptive statistics were used to summarize patient demographics, baseline disease characteristics, AEs, PK parameters, and biomarker data, only allowing for an exploratory comparison between the two arms. A Cox proportional hazard model stratified by stratification factor (ECOG PS [0 versus 1]) was used to estimate the hazard ratio and its 95% confidence interval (CI). OS was analyzed using the Kaplan–Meier method, and the median OS along with 95% CIs were determined by treatment group.

Results

PATIENT DEMOGRAPHICS AND DISPOSITION

A total of 165 patients were randomized 1:1 to dovitinib (n = 82) or sorafenib (n = 83), stratified by ECOG PS (Fig. 1). Patient demographics were well balanced between the treatment arms (Table 1). All

TABLE 1. Patient Demographics and Baseline Characteristics

Characteristic	Treatment Arm: Dovitinib (n = 82)	Treatment Arm: Sorafenib (n = 83)
Age, years, median (range)	56 (27-82)	56 (27-83)
Sex, n (%)		
Men	73 (89)	67 (81)
Women	9 (11)	16 (19)
Race, n (%)		
Asian	82 (100)	83 (100)
Ethnicity, n (%)		
East Asian	54 (66)	51 (61)
Japanese	8 (10)	11 (13)
Southeast Asian	19 (23)	20 (24)
South Asian	1 (1)	0 (0)
Other	0 (0)	1 (1)
ECOG PS, n (%)		
0	52 (63)	53 (64)
1	30 (37)	29 (35)
Missing	0 (0)	1 (1)
Histologic grade, n (%)		
Moderately differentiated	14 (17)	13 (16)
Poorly differentiated	5 (6)	11 (13)
Unknown	61 (74)	55 (66)
Well differentiated	2 (2)	4 (5)
BCLC stage at baseline, n (%)		
Stage B	2 (2)	2 (2)
Stage C	80 (98)	81 (98)
Metastatic site of cancer, n (%)		
Adrenal	2 (2.4)	2 (2.4)
Ascites (malignant)	4 (4.9)	2 (2.4)
Bone	7 (8.5)	5 (6.0)
Liver	1 (1.2)	0 (0)
Lung	46 (56.1)	42 (50.6)
Mesenteric lymph nodes	5 (6.1)	9 (10.8)
Other	23 (28.0)	21 (25.3)
Pancreas	1 (1.2)	1 (1.2)
Para-aortic lymph nodes	4 (4.9)	6 (7.2)
Paracardiac lymph nodes	1 (1.2)	0 (0)
Pericardial effusion (malignant)	0 (0)	1 (1.2)
Peritoneum	3 (3.7)	5 (6.0)
Pleura	0 (0)	1 (1.2)
Pleural effusion (malignant)	0 (0)	2 (2.4)
Pulmonary lymph nodes	1 (1.2)	3 (3.6)
Retroperitoneal lymph nodes	1 (1.2)	4 (4.8)
Skin	0 (0)	1 (1.2)
Spleen	1 (1.2)	0 (0)
Supraclavicular lymph nodes	1 (1.2)	0 (0)
Time from primary diagnosis to start of study drug, months, n (%)		
<6	41 (50)	39 (47)
6 to <12	11 (13)	12 (14)
12 to <24	6 (7)	12 (14)
≥24	21 (26)	20 (24)
Missing	3 (4)	0 (0)
Child-Pugh class, n (%)		
A	82 (100)	82 (99)
B	0 (0)	1 (1)

Abbreviations: BCLC, Barcelona Clinic Liver Cancer classification; ECOG PS, Eastern Cooperative Oncology Group performance status.

patients (100%) were Asian-Pacific, with a median age of 56 years (range, 27-83 years), and a majority were men (85%) with an ECOG PS of 0 at baseline (64%). Most patients had BCLC stage C (98%) and Child–Pugh class A (99%) HCC with unknown histological grade (70%). Many patients received prior antineoplastic therapy (56%), including local HCC therapies (56%), surgery (36%), or radiotherapy (7%). Of the local HCC therapies, 35% of patients received antineoplastic medication and 12% received two or more regimens.

All patients discontinued study treatment (Fig. 1), most frequently due to progressive disease (dovitinib, 52%; sorafenib, 73%) or an AE (dovitinib, 29%; sorafenib, 14%). In the dovitinib arm, three patients did not receive the study drug due to AEs (pulmonary embolism [n = 1] and decreased platelets [n = 1]) or change in Child-Pugh score from 6 to 7 at baseline (n = 1) that occurred after study randomization but prior to receiving the first dose. In patients who received at least one dose of the study drug, the median duration of exposure was 2.5 (range, 0.0-11.7) months in the dovitinib arm and 3.2 (range, 0.1-23.5) months in the sorafenib arm. A majority of patients (dovitinib, 72%; sorafenib, 63%) required dose adjustment or interruption for AEs, most commonly including increased bilirubin (14%), aspartate aminotransferase (13%), or alanine aminotransferase (11%), fatigue (11%), and diarrhea (10%) in the dovitinib arm, and palmar-plantar erythrodysesthesia syndrome (PPES; 30%) and increased aspartate aminotransferase (11%) in the sorafenib arm.

EFFICACY

A total of 136 OS events were observed (dovitinib, n = 69; sorafenib, n = 67), with a median follow-up of 113.9 weeks (26.2 months). The median OS (95% CI) was 34.6 (28.6-39.4) weeks (8.0 [6.6-9.1] months) and 36.7 (23.3-49.3) weeks (8.4 [5.4-11.3] months) for dovitinib and sorafenib, respectively, with a hazard ratio (95% CI) of 1.27 (0.90-1.79). Kaplan–Meier curves of the two treatment arms cross between 30 and 36 weeks (6.9 and 8.3 months), with a separation in curves in favor of dovitinib before crossing and in favor of sorafenib after crossing (Fig. 2A). The drop in the Kaplan–Meier plot for the dovitinib arm between 24 and 42 weeks was not due to toxicity; patients who died within 24-42 weeks (5.5-9.7 months) from randomization lived for 6.9-37.1 weeks (1.6-8.5 months) after discontinuing dovitinib (Supporting Table 1).

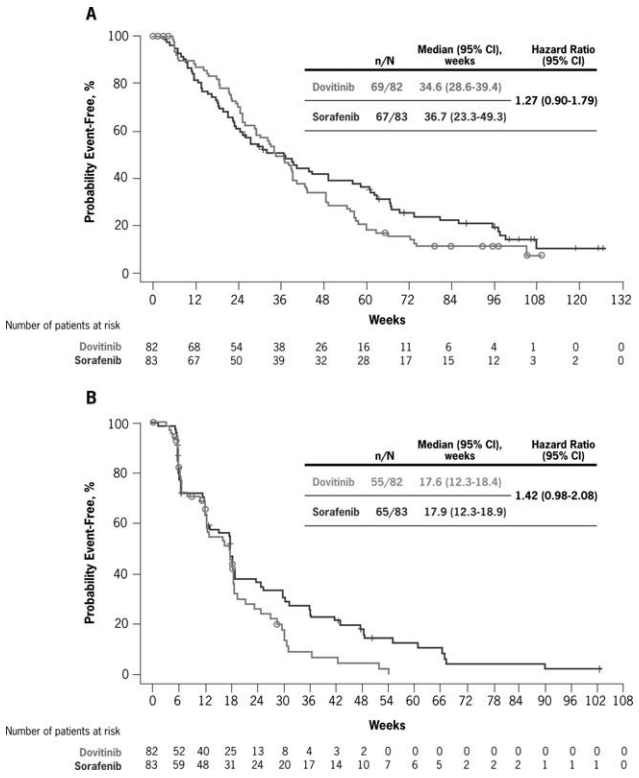

FIG. 2. (A) Overall survival by treatment arm. (B) Time to progression per local investigator assessment by treatment arm. CI, confidence interval; N, number of patients included in the analysis; n, number of events included in the analysis.

The median TTP (95% CI) according to the local investigator's assessment was 17.6 (12.3-18.4) weeks (4.1 [2.8-4.2] months) for dovitinib and 17.9 (12.3-18.9) weeks (4.1 [2.8-4.3] months) for sorafenib (hazard ratio [95% CI], 1.42 [0.98-2.08]). Kaplan–Meier curves for the treatment arms were almost identical until 18 weeks (4.1 months), when the curves separate in favor of sorafenib (Fig. 2B).

The disease control rate according to the local investigator's assessment was lower in the dovitinib arm than the sorafenib arm (57% versus 64%; Table 2). Although the disease control rate was lower for dovitinib than it was for sorafenib, a higher number of patients in the dovitinib arm showed a decrease in best percentage change from baseline in sum of diameters based on RECIST version 1.1 compared with the sorafenib arm (49% versus 41%), and a lower number of patients showed an increase (35% versus 47%) (Supporting Fig. 1). In addition, the number of patients with progressive disease was also lower in the dovitinib arm (21% versus 27%).

Definitive deterioration of ECOG PS was observed in 48% of patients in both treatment arms. The median time to definitive deterioration of ECOG PS (95% CI) was 22.3 (12.6-34.0) weeks (5.1 [2.9-7.8] months) and 21.3 (13.6-not estimable) weeks (4.9 [3.1-not estimable] months) for patients treated with dovitinib and sorafenib, respectively (Supporting Table 2).

SAFETY

All patients experienced at least one AE regardless of study relationship during the study (Table 3). In the dovitinib arm, the most common AEs of any grade, regardless of cause, were diarrhea (62%), decreased appetite (43%), nausea (41%), vomiting (41%), fatigue (35%), rash (34%), and pyrexia (30%). PPES (66%), diarrhea (42%), and decreased appetite (31%) were common in the sorafenib arm. In the dovitinib arm, the most common grade 3/4 AEs, regardless of cause, were increased aspartate aminotransferase (20%), increased alanine aminotransferase (17%), fatigue (14%), hypertension (13%), diarrhea (11%), increased blood bilirubin (11%), and decreased neutrophil count (10%). Common grade 3 and 4 AEs for the sorafenib arm were increased aspartate aminotransferase (24%), PPES (16%), and hypertension (11%).

Serious AEs were experienced by 51% patients in the dovitinib arm and 41% patients in the sorafenib arm (Supporting Table 3), most commonly pyrexia (13% versus 6%). Other serious AEs occurring in 4% of patients were decreased appetite, hepatic encephalopathy, fatigue, and increased blood bilirubin in the dovitinib arm and gastrointestinal hemorrhage in the sorafenib arm. All other serious AEs occurred in ≤2% of patients.

During the study, including up to 30 days after the end of treatment, a total of 18 patients died, five (6%) in the dovitinib arm and 13 (16%) in the sorafenib arm (Supporting Table 4). The most common cause of death was disease progression (dovitinib, n = 4 [5%];

TABLE 2. Best Overall Response by Investigator Assessment

	Dovitinib (n = 82)	Sorafenib (n = 83)
Disease control rate, n (%)	47 (57)	53 (64)
95% CI	46%-68%	53%-74%
Best overall response, n (%)		
Complete response	0 (0)	1 (1)
Partial response	5 (6)	8 (10)
Stable disease	42 (51)	44 (53)
Progressive disease	17 (21)	22 (27)
Unknown	18 (22)	8 (10)

TABLE 3. AEs Regardless of Study Drug Relationship (≥10% Any Grade in Either Treatment Arm)

	Treatment Arm					
	Dovitinib (n = 79)			Sorafenib (n = 83)		
AE	Any Grade	Grade 3	Grade 4	Any Grade	Grade 3	Grade 4
Any	79 (100)	52 (66)	12 (15)	83 (100)	49 (59)	10 (12)
Diarrhea	49 (62)	9 (11)	0 (0)	35 (42)	1 (1)	0 (0)
Decreased appetite	34 (43)	6 (8)	0 (0)	26 (31)	4 (5)	0 (0)
Nausea	32 (41)	4 (5)	0 (0)	16 (19)	0 (0)	0 (0)
Vomiting	32 (41)	1 (1)	0 (0)	10 (12)	1 (1)	0 (0)
Fatigue	28 (35)	11 (14)	0 (0)	13 (16)	2 (2)	0 (0)
Rash	27 (34)	1 (1)	0 (0)	18 (22)	2 (2)	0 (0)
Pyrexia	24 (30)	1 (1)	0 (0)	23 (28)	1 (1)	0 (0)
Increased AST	23 (29)	15 (19)	1 (1)	22 (26)	17 (20)	3 (4)
Increased blood bilirubin	21 (27)	7 (9)	2 (2)	19 (23)	7 (8)	0 (0)
Decreased weight	19 (24)	1 (1)	0 (0)	17 (20)	0 (0)	0 (0)
Hypertension	17 (22)	10 (13)	0 (0)	20 (24)	9 (11)	0 (0)
Increased ALT	17 (22)	13 (16)	1 (1)	17 (20)	8 (10)	0 (0)
Insomnia	17 (22)	0 (0)	0 (0)	9 (11)	0 (0)	0 (0)
Constipation	16 (20)	1 (1)	0 (0)	12 (14)	0 (0)	0 (0)
Peripheral edema	14 (18)	1 (1)	0 (0)	11 (13)	0 (0)	0 (0)
Decreased platelet count	14 (18)	6 (8)	0 (0)	8 (10)	4 (5)	0 (0)
Upper abdominal pain	13 (16)	0 (0)	0 (0)	11 (13)	1 (1)	0 (0)
Stomatitis	13 (16)	1 (1)	0 (0)	11 (13)	0 (0)	0 (0)
Cough	13 (16)	0 (0)	0 (0)	8 (10)	0 (0)	0 (0)
Abdominal pain	12 (15)	3 (4)	0 (0)	17 (20)	3 (4)	0 (0)
Headache	12 (15)	0 (0)	0 (0)	4 (5)	0 (0)	0 (0)
Decreased neutrophil count	12 (15)	8 (10)	0 (0)	2 (2)	0 (0)	0 (0)
PPES	11 (14)	1 (1)	0 (0)	55 (66)	13 (16)	0 (0)
Ascites	10 (13)	2 (2)	0 (0)	9 (11)	4 (5)	0 (0)
Anemia	10 (13)	1 (1)	0 (0)	7 (8)	3 (4)	0 (0)
Hypoalbuminemia	10 (13)	1 (1)	0 (0)	6 (7)	0 (0)	0 (0)
Dizziness	10 (13)	1 (1)	0 (0)	2 (2)	0 (0)	0 (0)
Dyspnea	9 (11)	1 (1)	1 (1)	8 (10)	3 (4)	0 (0)
Thrombocytopenia	9 (11)	4 (5)	1 (1)	2 (2)	1 (1)	0 (0)
Acne	9 (11)	0 (0)	0 (0)	0 (0)	0 (0)	0 (0)
Abdominal distension	8 (10)	0 (0)	0 (0)	9 (11)	1 (1)	0 (0)
Pruritus	8 (10)	0 (0)	0 (0)	5 (6)	0 (0)	0 (0)
Alopecia	1 (1)	0 (0)	0 (0)	19 (23)	0 (0)	0 (0)

Data are presented as n (%).
Abbreviations: AE, adverse event; ALT, alanine aminotransferase; AST, aspartate aminotransferase; PPES, palmar-plantar erythrodysesthesia.

sorafenib, n = 12 [14%]). Other causes of death were coronary artery disease (dovitinib only, n = 1) and cerebral hemorrhage (sorafenib only, n = 1).

DOVITINIB PK AND BIOMARKERS

PK analysis of patients with varying degrees of hepatic function and impairment who received dovitinib revealed that exposure was comparable between patients with mild hepatic function impairment and normal hepatic function (Table 4).

Subgroup analysis revealed that higher median OS was achieved by patients in both the dovitinib arm and the sorafenib arm who had baseline plasma sVEGFR1 and HGF below the median levels compared with patients who had baseline plasma sVEGFR1 and HGF at or above the median levels (Fig. 3); however, statistical significance for this association was achieved only with dovitinib (sVEGFR1, $P = 0.0002$; HGF, $P = 0.0002$). The prognostic effect of baseline HGF and sVEGFR1 was not apparent compared with TTP as determined by the local investigator.

Discussion

Currently available treatment options for patients with HCC include the VEGFR and PDGFR inhibitor sorafenib, which has been shown to delay HCC progression through antiangiogenic effects.[9,10] However, clinical benefits observed with sorafenib are usually limited, as angiogenic escape from sorafenib may

TABLE 4. Dovitinib Exposure by Hepatic Function

PK Parameter	Normal Hepatic Function	Mild Hepatic Impairment	Moderate Hepatic Impairment
n, week 1/week 4	19/9	47/14	4/NA
AUC_{last}, h · ng/mL (CV%)			
Week 1, day 1	5291 (29)	5641 (32)	5589 (19)
Week 4, day 5	5986 (42)	6251 (28)	NA
C_{max}, ng/mL (CV%)			
Week 1, day 1	289 (28)	321 (34)	309 (25)
Week 4, day 5	329 (43)	355 (28)	NA
T_{max}, h			
Week 1, day 1	6	6	3
Week 4, day 5	6	6	NA

Values for AUC_{last} and C_{max} are the geometric mean (CV%) and values for T_{max} are the median. Hepatic function definitions: normal = total bilirubin $\leq$ ULN and AST and ALT $\leq$ ULN; mild = total bilirubin $\leq$ ULN and ALT and/or AST $>$ ULN (both below 5× ULN), or 1× ULN $<$ total bilirubin $\leq$ 1.5× ULN and AST and ALT $\leq$ 5× ULN; and moderate = 1.5× ULN $<$ total bilirubin $\leq$ 3× ULN and AST and ALT $\leq$ 5× ULN.
Abbreviations: AUC_{last}, area under the concentration time curve from time zero until the last time point sampled; C_{max}, maximum concentration; CV%, coefficient of variation; NA, not assessed; PK, pharmacokinetics; T_{max}, time to C_{max}; ULN, upper limit of normal.

occur due to FGFR pathway activation.[22] In addition to VEGFR and PDGFR, dovitinib inhibits FGFR[23] and has been hypothesized to provide more effective and sustainable antitumor activity in patients with advanced HCC. However, in this randomized phase 2 study, dovitinib activity was not greater than that of sorafenib as frontline therapy in Asian-Pacific patients with advanced HCC.

In this study, the median OS was similar for dovitinib and sorafenib (34.6 versus 36.7 weeks [8.0 versus 8.4 months]). Similarly, the median TTP as determined by the local investigator did not differ with dovitinib and sorafenib treatment in this study (17.6 versus 17.9 weeks [4.0 versus 4.1 months]). These results are similar to those of studies evaluating other tyrosine kinase inhibitors (TKIs) versus sorafenib, although differences in toxicity and OS have been observed [24].

It is interesting to note that the OS and TTP results in this study are higher than those reported for sorafenib in the phase 3 Asia-Pacific HCC trial (median OS, 6.5 months; median TTP, 2.8 months).[9] Although patient demographics and disease characteristics were similar, overall baseline ECOG PS was more favorable for patients in this study (dovitinib: 0, 63%; 1, 37%; 2, 0%; missing, 0%; sorafenib: 0, 64%; 1, 35%; 2, 0%; missing, 1%) than in the phase 3 Asia-Pacific HCC trial (sorafenib: 0, 25%; 1, 69%; 2, 5%), which may have contributed to the higher activity observed for sorafenib in this study. Similar results were noted in Asian subpopulations in studies of other TKIs versus sorafenib, in which the ECOG PS of 0 (~50%-65%) and median OS (8.5-8.9 months) were comparable to those reported here.[25-27] The effect of ECOG PS on median OS was revealed in some of these TKI versus sorafenib studies, because patients (regardless of region) with ECOG PS 0 had a higher median OS than those with ECOG PS 1.[25,26] For example, in a phase 3 study evaluating linifanib versus sorafenib in HCC, the median OS for ECOG PS 0 compared with ECOG PS 1 was 10.2 versus 8.5 months for sorafenib and 10.2 versus 7.2 months for linifanib[26]; in a phase 3 study of brivanib versus sorafenib, the median OS for ECOG PS 0 compared with ECOG PS 1 was 12.8 versus 6.5 months for sorafenib and 11.6 versus 6.6 months for brivanib.[25] Likewise, ECOG performance status was identified as a prognostic indicator for OS in the SHARP study,[10,28] where risk of death was reduced in patients with ECOG PS 0 (hazard ratio, 0.68 [95% CI, 0.50-0.95]) compared with ECOG PS $\geq$1 (hazard ratio, 0.71 [95% CI, 0.52-0.96]).[10] Therefore, the differences in results between this study and the phase 3 Asia-Pacific HCC trial[9] may be reflective of the difference in patient ECOG PS. However, it should also be noted that in this and more recently reported TKI studies, patients may have tolerated sorafenib better than those in the phase 3 Asia-Pacific HCC trial, because sorafenib AE management has improved greatly in recent years.[29]

The data presented here support the observation from randomized phase 3 studies of sorafenib in patients with HCC, in which median OS and TTP with sorafenib were lower in an Asian-Pacific population compared with a population that was primarily from Europe and North America (OS, 6.5 versus 10.7 months; TTP, 2.8 versus 5.5 months).[9,10] This result may potentially be attributed to differences in

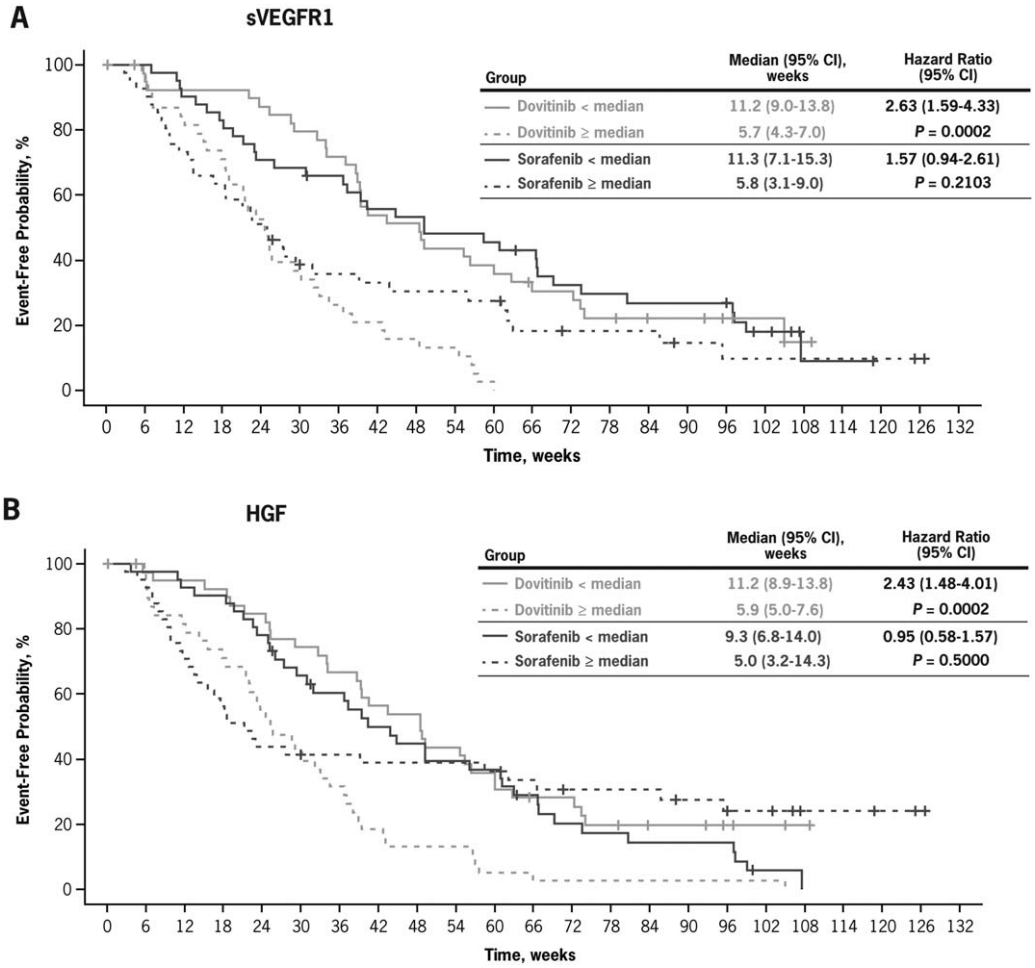

FIG. 3. Overall survival (OS) by baseline plasma levels of (A) soluble vascular endothelial growth factor receptor 1 (sVEGFR1) and (B) hepatocyte growth factor (HGF). The false discovery rate *P* values were adjusted for multiplicity only at the biomarker level within a specific analysis. Therefore, interpretation based on *P* values should be made with caution and in context, considering the point estimates and 95% confidence intervals (CI) of the parameters provided for these biomarker data.

symptomatic disease and extrahepatic metastases at presentation, etiology (e.g., hepatitis B or C infection, alcohol), and varying regional treatment practices.[9,10,30-32] For example, prevalence of hepatitis B infection in this study (dovitinib, 72%; sorafenib 64%) was more similar to that observed in the Asian subpopulation (~65%) than in the non-Asian subpopulation (~20%) in a recently reported study comparing sunitinib versus sorafenib, which may explain why the median OS for sorafenib in this study (8.4 months) was more similar to that observed in the Asian subpopulation (8.8 months) than the non-Asian subpopulation (15.1 months). This is consistent with the association of hepatitis B infection with poor prognosis in patients with advanced HCC, as well as additional subgroup analyses in recently reported TKI versus sorafenib studies demonstrating improved median OS in patients without hepatitis B.[25-27,30] However, although these data indicate that population variations need to be considered when comparing activity between TKI trials, it is important to note that etiology was not found to be a significant predictor of OS in the SHARP trial or the Asia-Pacific study of sorafenib.[9,10] Instead, recent studies have identified tumor stage, Child-Pugh class, and as significant predictors of OS.[33,34]

The results of the AE analysis in this study were consistent with the known safety profile of dovitinib[35-38] and did not identify any new safety concerns associated with the use of dovitinib in patients with

advanced HCC. The most common AEs experienced by patients on dovitinib and sorafenib were diarrhea (62% versus 42%), decreased appetite (43% versus 31%), nausea (41% versus 19%), vomiting (41% versus 12%), fatigue (35% versus 16%), rash (34% versus 22%), pyrexia (30% versus 28%), and PPES (14% versus 66%), respectively. Overall, treatment with dovitinib was shorter and interruptions due to AEs were more frequent, potentially indicating poorer tolerance to this agent; however, this could be attributed partly to the open label design of the study.

Dovitinib exposure in patients with mild hepatic function impairment was comparable to exposure in patients with normal hepatic function. Association of median OS with sVEGFR1 and HGF baseline plasma levels achieved statistical significance for dovitinib.

Pattern of progression has recently been noted as a key parameter in HCC. For example, a recent analysis of patients with advanced HCC treated with sorafenib showed that the emergence of new extrahepatic metastases was an independent predictor of poor prognosis.[39] Although patterns of progression (e.g., intrahepatic versus extrahepatic) and their association with postprogression survival were not assessed in this study, these factors may be worth exploring in future studies evaluating dovitinib in HCC.

In conclusion, though generally well tolerated, dovitinib did not appear to have improved activity over sorafenib in patients with advanced HCC in this study, and OS analyses did not demonstrate any benefit. Based on the data presented, there are no plans for a subsequent phase 3 study.

Acknowledgment: We thank Peter J. Simon and Amanda L. Kauffman for medical editorial assistance. We also thank Mahtab Marker for assistance with biomarker statistical analysis for this trial.

REFERENCES

1) Uematsu S, Higashi T, Nouso K, Kariyama K, Nakamura S, Suzuki M, et al. Altered expression of vascular endothelial growth factor, fibroblast growth factor-2 and endostatin in patients with hepatocellular carcinoma. J Gastroenterol Hepatol 2005;20:583-588.
2) Gauglhofer C, Sagmeister S, Schrottmaier W, Fischer C, Rodgarkia-Dara C, Mohr T, et al. Up-regulation of the fibroblast growth factor 8 subfamily in human hepatocellular carcinoma for cell survival and neoangiogenesis. HEPATOLOGY 2011; 53:854-864.
3) Kin M, Sata M, Ueno T, Torimura T, Inuzuka S, Tsuji R, et al. Basic fibroblast growth factor regulates proliferation and motility of human hepatoma cells by an autocrine mechanism. J Hepatol 1997;27:677-687.
4) Madkhali AA, Fadel ZT, Aljiffry MM, Hassanain MM. Surgical treatment for hepatocellular carcinoma. Saudi J Gastroenterol 2015;21:11-17.
5) Thomas MB, Zhu AX. Hepatocellular carcinoma: the need for progress. J Clin Oncol 2005;23:2892-2899.
6) Ribatti D, Vacca A, Nico B, Sansonno D, Dammacco F. Angiogenesis and anti-angiogenesis in hepatocellular carcinoma. Cancer Treat Rev 2006;32:437-444.
7) Yoshiji H, Kuriyama S, Yoshii J, Ikenaka Y, Noguchi R, Hicklin DJ, et al. Synergistic effect of basic fibroblast growth factor and vascular endothelial growth factor in murine hepatocellular carcinoma. HEPATOLOGY 2002;35:834-842.
8) Wang L, Park H, Chhim S, Ding Y, Jiang W, Queen C, et al. A novel monoclonal antibody to fibroblast growth factor 2 effectively inhibits growth of hepatocellular carcinoma xenografts. Mol Cancer Ther 2012;11:864-872.
9) Cheng AL, Kang YK, Chen Z, Tsao CJ, Qin S, Kim JS, et al. Efficacy and safety of sorafenib in patients in the Asia-Pacific region with advanced hepatocellular carcinoma: a phase III randomised, double-blind, placebo-controlled trial. Lancet Oncol 2009;10:25-34.
10) Llovet JM, Ricci S, Mazzaferro V, Hilgard P, Gane E, Blanc JF, et al. Sorafenib in advanced hepatocellular carcinoma. N Engl J Med 2008;359:378-390.
11) Lopes de Menezes DE, Peng J, Garrett EN, Louie SG, Lee SH, Wiesmann M, et al. CHIR-258: a potent inhibitor of FLT3 kinase in experimental tumor xenograft models of human acute myelogenous leukemia. Clin Cancer Res 2005;11:5281-5291.
12) Angevin E, Lopez-Martin JA, Lin CC, Gschwend JE, Harzstark A, Castellano D, et al. Phase I study of dovitinib (TKI258), an oral FGFR, VEGFR, and PDGFR inhibitor, in advanced or metastatic renal cell carcinoma. Clin Cancer Res 2013;19:1257-1268.
13) Sarker D, Molife R, Evans TR, Hardie M, Marriott C, Butzberger-Zimmerli P, et al. A phase I pharmacokinetic and pharmacodynamic study of TKI258, an oral, multitargeted receptor tyrosine kinase inhibitor in patients with advanced solid tumors. Clin Cancer Res 2008;14:2075-2081.
14) André F, Bachelot T, Campone M, Dalenc F, Perez-Garcia JM, Hurvitz SA, et al. Targeting FGFR with dovitinib (TKI258): preclinical and clinical data in breast cancer. Clin Cancer Res 2013;19:3693-3702.
15) Takiuchi H, Gotoh M, Yoshida M, Kii T, Yamashita K, Sunakawa Y, et al. A phase I study of dovitinib (TKI258) in Japanese patients with advanced solid tumors. ASCO Annual Meeting Abstracts 2012; Abstract 3088.
16) Kim KB, Chesney J, Robinson D, Gardner H, Shi MM, Kirkwood JM. Phase I/II and pharmacodynamic study of dovitinib (TKI258)-an inhibitor of fibroblast growth factor receptors and VEGF receptors-in patients with advanced melanoma. Clin Cancer Res 2011;17:7451-7461.
17) Tai WT, Cheng AL, Shiau CW, Liu CY, Ko CH, Lin MW, et al. Dovitinib induces apoptosis and overcomes sorafenib resistance in hepatocellular carcinoma through SHP-1-mediated inhibition of STAT3. Mol Cancer Ther 2012;11: 452-463.
18) Huynh HT, Chow P, Soo CK, Shi M. Dovitinib (TKI258), a multikinase inhibitor of FGFR, PDGFR, and VEGFR tyrosine

kinases, induces growth suppression in mouse models of human hepatocellular carcinoma (HCC). AACR Annual Meeting 2010; Abstract LB-364.
19) Huynh H, Chow PK, Tai WM, Choo SP, Chung AY, Ong HS, et al. Dovitinib demonstrates antitumor and antimetastatic activities in xenograft models of hepatocellular carcinoma. J Hepatol 2012;56:595-601.
20) Bruix J, Sherman M, American Association for the Study of Liver Diseases. Management of hepatocellular carcinoma: an update. HEPATOLOGY 2011;53:1020-1022.
21) Llovet JM, Di Bisceglie AM, Bruix J, Kramer BS, Lencioni R, Zhu AX, et al. Design and endpoints of clinical trials in hepatocellular carcinoma. J Natl Cancer Inst 2008;100:698-711.
22) Bergers G, Hanahan D. Modes of resistance to anti-angiogenic therapy. Nat Rev Cancer 2008;8:592-603.
23) Lee SH, Lopes de Menezes D, Vora J, Harris A, Ye H, Nordahl L, et al. In vivo target modulation and biological activity of CHIR-258, a multitargeted growth factor receptor kinase inhibitor, in colon cancer models. Clin Cancer Res 2005;11: 3633-3641.
24) Chan SL, Yeo W. Development of systemic therapy for hepatocellular carcinoma at 2013: updates and insights. World J Gastroenterol 2014;20:3135-3145.
25) Johnson PJ, Qin S, Park JW, Poon RT, Raoul JL, Philip PA, et al. Brivanib versus sorafenib as first-line therapy in patients with unresectable, advanced hepatocellular carcinoma: results from the randomized phase III BRISK-FL study. J Clin Oncol 2013;31:3517-3524.
26) Cainap C, Qin S, Huang WT, Chung IJ, Pan H, Cheng Y, et al. Linifanib versus sorafenib in patients with advanced hepatocellular carcinoma: results of a randomized phase III trial. J Clin Oncol 2015;33:172-179.
27) Cheng AL, Kang YK, Lin DY, Park JW, Kudo M, Qin S, et al. Sunitinib versus sorafenib in advanced hepatocellular cancer: results of a randomized phase III trial. J Clin Oncol 2013;31: 4067-4075.
28) Llovet JM, Pena CE, Lathia CD, Shan M, Meinhardt G, Bruix J; SHARP Investigators Study Group. Plasma biomarkers as predictors of outcome in patients with advanced hepatocellular carcinoma. Clin Cancer Res 2012;18:2290-2300.
29) Bolondi L, Craxi A, Trevisani F, Daniele B, Di Costanzo GG, Fagiuoli S, et al. Refining sorafenib therapy: lessons from clinical practice. Future Oncol 2015;11:449-465.
30) Cantarini MC, Trevisani F, Morselli-Labate AM, Rapaccini G, Farinati F, Del Poggio P, et al. Effect of the etiology of viral cirrhosis on the survival of patients with hepatocellular carcinoma. Am J Gastroenterol 2006;101:91-98.
31) Llovet JM, Burroughs A, Bruix J. Hepatocellular carcinoma. Lancet 2003;362:1907-1917.
32) de Villa V, Lo CM. Liver transplantation for hepatocellular carcinoma in Asia. Oncologist 2007;12:1321-1331.
33) Tsukui Y, Mochizuki H, Hoshino Y, Kawakami S, Kuno T, Fukasawa Y, et al. Factors contributing to the overall survival in patients with hepatocellular carcinoma treated by sorafenib. Hepatogastroenterology 2012;59:2536-2539.
34) Li J, Wang L, Cong N, Shi C, Bu W, Song J, et al. Efficacy of sorafenib for advanced hepatocellular carcinoma and prognostic factors. Hepatogastroenterology 2014;61:954-957.
35) Angevin E, Lopez JA, Pande A, Moldovan C, Shi M, Soria JC, et al. TKI258 (dovitinib lactate) in metastatic renal cell carcinoma (mRCC) patients refractory to approved targeted therapies: a phase I/II dose finding and biomarker study. J Clin Oncol 2009;27(Suppl. 15): Abstract 3563.
36) Kang YK, Yoo C, Ryoo BY, Lee JJ, Tan E, Park I, et al. Phase II study of dovitinib in patients with metastatic and/or unresectable gastrointestinal stromal tumours after failure of imatinib and sunitinib. Br J Cancer 2013;109:2309-2315.
37) Milowsky MI, Dittrich C, Duran I, Jagdev S, Millard FE, Sweeney CJ, et al. Phase 2 trial of dovitinib in patients with progressive FGFR3-mutated or FGFR3 wild-type advanced urothelial carcinoma. Eur J Cancer 2014;50:3145-3152.
38) Infante JR, Ramanathan RK, George D, Tan E, Quinlan M, Liu A, et al. A randomized, crossover phase 1 study to assess the effects of formulation (capsule vs tablet) and meal consumption on the bioavailability of dovitinib (TKI258). Cancer Chemother Pharmacol 2015;75:729-737.
39) Ogasawara S, Chiba T, Ooka Y, Suzuki E, Kanogawa N, Saito T, et al. Post-progression survival in patients with advanced hepatocellular carcinoma resistant to sorafenib. Invest New Drugs 2016;34:255-260.

Supporting Information

Additional Supporting Information may be found article at onlinelibrary.wiley.com/doi/10.1002/hep.28600/suppinfo.

Nucleotide-binding oligomerization domain 1 acts in concert with the cholecystokinin receptor agonist, cerulein, to induce IL-33-dependent chronic pancreatitis

T Watanabe[1,2,3], Y Sadakane[2], N Yagama[2], T Sakurai[4], H Ezoe[2], M Kudo[4], T Chiba[1] and W Strober[3]

Nucleotide-binding oligomerization domain 1 (NOD1) fulfills important host-defense functions via its responses to a variety of gut pathogens. Recently, however, we showed that in acute pancreatitis caused by administration of cholecystokinin receptor (CCKR) agonist (cerulein) NOD1 also has a role in inflammation via its responses to gut commensal organisms. In the present study, we explored the long-term outcome of such NOD1 responsiveness in a new model of chronic pancreatitis induced by repeated administration of low doses of cerulein in combination with NOD1 ligand. We found that the development of chronic pancreatitis in this model requires intact NOD1 and type I IFN signaling and that such signaling mediates a macrophage-mediated inflammatory response that supports interleukin (IL)-33 production by acinar cells. The IL-33, in turn, has a necessary role in the induction of IL-13 and TGF-β1, factors causing the fibrotic reaction characteristic of chronic pancreatitis. Interestingly, the Th2 effects of IL-33 were attenuated by the concomitant type I IFN response since the inflammation was marked by clear increases in IFN-γ and TNF-α production but only marginal increases in IL-4 production. These studies establish chronic pancreatitis as an IL-33-dependent inflammation resulting from synergistic interactions between the NOD1 and CCKR signaling pathways.

INTRODUCTION

Pancreatic inflammatory disease can occur as an acute or a chronic form of inflammation that differ from one another both clinically and pathologically. Acute pancreatitis refers to new-onset pancreatic inflammation occurring in a previously un-inflamed pancreas that may subside prior to causing permanent changes in the pancreas or may cause permanent changes if recurrent; in contrast, chronic pancreatitis refers to on-going pancreatic inflammation of varying severity in a pancreas already reflecting permanent inflammatory changes.[1,2] In addition, the presence of long-standing inflammation in chronic pancreatitis is not simply due to the continuation of the inflammatory process present in the acute disease. Instead, it results from the activation of new pathological processes that cause the development of inflammation only evident in chronic pancreatitis such as severe pancreatic atrophy and fibrosis. It is these new features of inflammation that cause the insufficiency in both exocrine and endocrine pancreatic function typical of chronic pancreatitis.[2,3]

A well-accepted hypothesis regarding the pathogenesis of both acute and chronic pancreatitis is that pancreatic inflammation is initiated by various environmental factors (such as excessive drinking of alcohol) capable of causing pathologic triggering of the cholecystokinin receptor (CCKR) signaling pathway within pancreatic acinar cells and subsequently, the excessive conversion of trypsinogen to trypsin.[4,5] This, in turn, leads to autodigestion of pancreatic tissue and the influx of inflammatory cells that cause the pancreatic inflammation.[1,2] This concept of pancreatitis pathogenesis is fully supported by the fact that mutations in a molecule that

[1]Department of Gastroenterology and Hepatology, Kyoto University Graduate School of Medicine, Kyoto, Kyoto, Japan. [2]Center for Innovation in Immunoregulative Technology and Therapeutics, Kyoto University Graduate School of Medicine, Kyoto, Kyoto, Japan. [3]Mucosal Immunity Section, Laboratory of Host Defenses, National Institute of Allergy and Infectious Diseases, National Institutes of Health, Bethesda, Maryland, USA and [4]Department of Gastroenterology and Hepatology, Kinki University Graduate School of Medicine, Osaka-sayama, Osaka, Japan. Correspondence: T Watanabe (tmhrwtnb@kuhp.kyoto-u.ac.jp).

Received 1 July 2015; accepted 5 December 2015; published online 27 January 2016. doi:10.1038/mi.2015.144

inhibits cationic trypsinogen activation, the serine protease inhibitor Kazal type 1 (SPINK1) or mutations in cationic trypsinogen (PRSS1) cause hereditary pancreatitis in humans due to constitutive activation of trypsinogen.[6] However, autodigestion of acinar cells by activated trypsin may not completely account for development of pancreatitis in all cases since pancreatitis can arise from very diverse factors.[7] In addition, it has been reported that mice that are genetically deficient in trypsinogen nevertheless exhibit pancreatic and systemic inflammation similar to that in wild-type mice subjected to acute and chronic experimental cerulein-induced pancreatitis.[8,9] Given the fact that cerulein, a CCKR agonist, is a strong inducer of trypsinogen activation,[10] these studies thus alert us to the possibility that excessive activation of trypsinogen is not the only mechanism contributing to the development of pancreatitis.[11]

In line with this idea, evidence has recently emerged that factors relating to innate immune responses activated by microbe-associated molecular patterns (MAMPs)[12,13] and damage-associated molecular patterns (DAMPs)[14] also contribute to the development of pancreatitis. This was first suggested by the fact that bacterial colonization of the inflamed pancreas occurs in severe forms of acute pancreatitis characterized by local and extrapancreatic complications and, in fact, infection of necrotic pancreatic tissue is one of the most important causes of mortality in acute pancreatitis.[1] The relationship between bacterial colonization and the severity of the pancreatitis is also supported by studies showing that bowel sterilization via antibiotic treatment reduces or prevents pancreatic inflammation, infection, and mortality in various experimental pancreatitis models.[15,16] In addition, DAMPs released from autodigested pancreatic tissue have been shown to amplify the inflammation through the activation of innate immune receptors.[17,18]

In studies further supporting the role of innate factors in the pathogenesis of pancreatitis we have previously shown that nucleotide-binding oligomerization domain 1 (NOD1), an intracellular innate immune receptor that detects small peptide components derived from bacterial wall peptidoglycan may also contributes to the development of pancreatitis.[15] In particular, we showed that NOD1 signaling arising from the detection of intestinal microflora by pancreatic acinar cells is necessary for cerulein-induced acute pancreatitis.[15] Moreover, we established a novel model of acute pancreatitis that is induced by the synergistic activity of low dose of cerulein (that does not itself induce pancreatitis) and FK156, an activator of NOD1 that mimics the effect of NOD1 ligand expression by gut bacteria breaching the mucosal barrier.[15] Whereas these previous studies established the importance of NOD1-mediated innate immune responses in acute pancreatitis, they did not provide information about the role of these responses in the chronic form of this disease. To address this question we created a model of chronic pancreatitis induced by repeated administration of low-dose cerulein and NOD1 ligand (FK565) and have used this model to explore the immune mechanisms driving chronic pancreatitis. We showed that in this model, chronic activation of NOD1 in pancreatic acinar cells gives rise to a fibroinflammatory disorder of the pancreas mediated by innate interleukin (IL)-33 and adaptive IL-13 responses.

RESULTS

Repeated injection of low-dose cerulein together with NOD1 ligand (FK565) induces chronic pancreatitis

In a previous study, we established a new model of acute pancreatitis that is induced by administration of low doses of the CCKR agonist, cerulein, together with a single dose of NOD1 ligand.[15] Neither of these agents was capable of causing pancreatitis when administered alone and it was thus clear that the induction of pancreatitis required their synergistic interaction. To better analyze the consequences of this interaction we developed a model of chronic pancreatitis in which C57BL/6 mice were subjected to combination cerulein/FK565 treatment administered twice a week for 7 weeks; this combination treatment consisted of an intraperitoneal (IP) injection of FK565 (NOD1 ligand; 50 μg) and three hourly IP injections of a low dose of cerulein (20 $\mu g\,kg^{-1}$). In the studies below we refer to this method of inducing chronic pancreatitis as the FK565-cerulein CP regimen.

As shown in **Figure 1a,b**, the effect of administration of the FK565-cerulein CP regimen differed markedly from the effects of administration of FK565 alone or cerulein alone (administered at the same dose as in the administration of the FK565-cerulein CP regimen). Thus, as shown in **Figure 1a** and **Supplementary Figure S1a** online, mice subjected to repeated administration of FK565 alone did not exhibit elevated serum levels of amylase or a positive chronic pancreatitis pathology score, whereas mice subjected to repeated administration of cerulein alone exhibited mild pancreatitis as indicated by the presence of increased serum amylase levels and increased pathology scores; evidently, even low-dose cerulein can cause pancreatitis when administered repeatedly. A different picture was obtained with administration of the FK565-cerulein CP regiment since in this case the mice exhibited full-blown chronic pancreatitis as indicated by the presence of increased serum amylase levels, decreased pancreatic weight and a very high pathology score. The fact that serum amylase levels were not as high as in mice with mild pancreatitis induced by administration of cerulein alone reflects the fact that administration of the FK565-cerulein CP regimen causes pancreatic atrophy and associated fibrosis (see below).

As shown in **Figure 1b**, the above findings were corroborated by H&E staining and other tissue staining studies described below and previously.[19] With respect to H&E staining, repeated administration of FK565 caused no changes in pancreatic architecture, whereas repeated administration of cerulein alone led to decreased acinar cell adhesion and expanded peri-acinar extracellular spaces containing a low number of immune cells. In contrast, mice administered the FK565-cerulein CP regimen exhibited extensive loss of normal acinar architecture, acinar cell loss and a large increase in infiltrating immune cells. These findings fit nicely with tissue staining studies to detect the

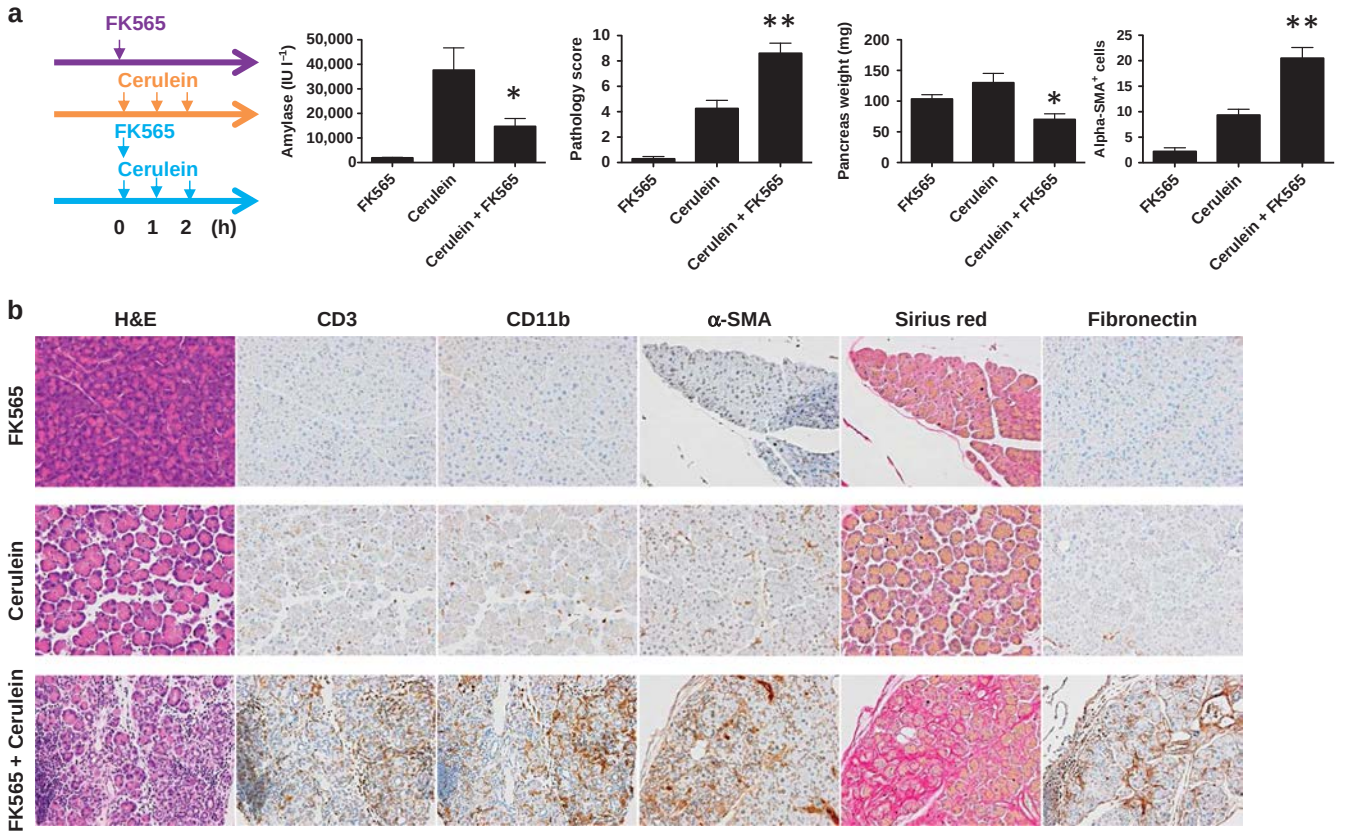

Figure 1 Induction of chronic pancreatitis in mice treated with NOD1 ligand and a low-dose cerulein. (**a**) Experimental protocol (Left): C57BL6 mice were administered FK565 (NOD1 ligand, 50 μg) alone ($n=7$), a low-dose cerulein (20 μg kg^{-1}) for a total of three times ($n=8$), or FK565 followed by a low-dose cerulein (20 μg kg^{-1}) for a total of three times ($n=10$). Mice received each regimen twice a week for a total of 14 times and then sera and pancreatic tissues were obtained. Serum levels of amylase, pathological scores of the pancreas, pancreatic weight, and the numbers of pancreatic α-SMA$^+$ cells per high power fields obtained from mice 3 h after the last injection of cerulein. Results are expressed as mean ± s.e.m. and are a pool of two independent experiments. *$P<0.05$, **$P<0.01$ as compared with cerulein alone. (**b**) Representative picture of the pancreas tissue stained with hematoxylin and eosin (H&E) staining, anti-CD3 Ab, anti-CD11b Ab, anti-SMA Ab, Sirius red, and anti-fibronectin Ab. Magnification × 400. Ab, antibody; NOD1, nucleotide-binding oligomerization domain 1.

presence of CD3$^+$ cells (T cells) and CD11b$^+$ cells (myeloid cells such as macrophages), which showed very mild increases of these cells in mice administered cerulein alone but massive increases of these cells in mice administered the FK565-cerulein CP regimen. Moreover, as shown in **Supplementary Figure S1b**, flow-cytometric analysis revealed that total number of innate immune cells such as CD11b$^+$ myeloid cells, F4-80$^+$ macrophages, and CD11c$^+$ dendritic cells was increased in the pancreas of mice treated with the FK565-cerulein CP regimen as compared with those treated with cerulein alone. In contrast, mice in both groups exhibited similar total numbers of pancreatic Gr-1$^+$ granulocytes. Finally, in studies to evaluate the presence of pancreatic fibrosis, tissue was stained to detect pancreatic stellate cells (PSCs) expressing α-smooth muscle actin (SMA), i.e., cells previously shown to be associated with pancreatic tissue fibrosis.[20] Whereas tissue from mice administered cerulein alone exhibited only a barely detectable increase in α-SMA$^+$ cells, mice administered the FK565-cerulein CP regimen exhibited a large increase in α-SMA$^+$ cells (**Figure 1a,b**). These findings were accompanied by robust staining of tissue from mice administered the FK565-cerulein CP regimen (but not administered cerulein alone) to detect the presence of collagen (with Sirius Red) and fibronectin. Taken together, these data offer strong evidence that the administration of the FK565-cerulein CP regimen induces chronic pancreatitis characterized by disruption of acinar architecture, massive infiltration of immune cells, and fibrosis.

Chronic pancreatitis induced by the administration of the FK565-cerulein CP regimen requires NOD1 signaling and downstream induction of type I interferon

In previous studies, we showed that development of acute pancreatitis induced by a single injection of NOD1 ligand and low-dose cerulein depends on the activation of the NOD1 signaling pathway accompanied by its downstream induction of type I interferon (IFN) and activation of the type I IFN signaling pathway.[15] We therefore determined whether chronic pancreatitis in the model described above develops in mice deficient in these pathways due to NOD1 or type I IFN receptor (IFNAR) gene deletions. As shown in **Figure 2a**, and **Supplementary Figures S2a and S2b**, serum levels of

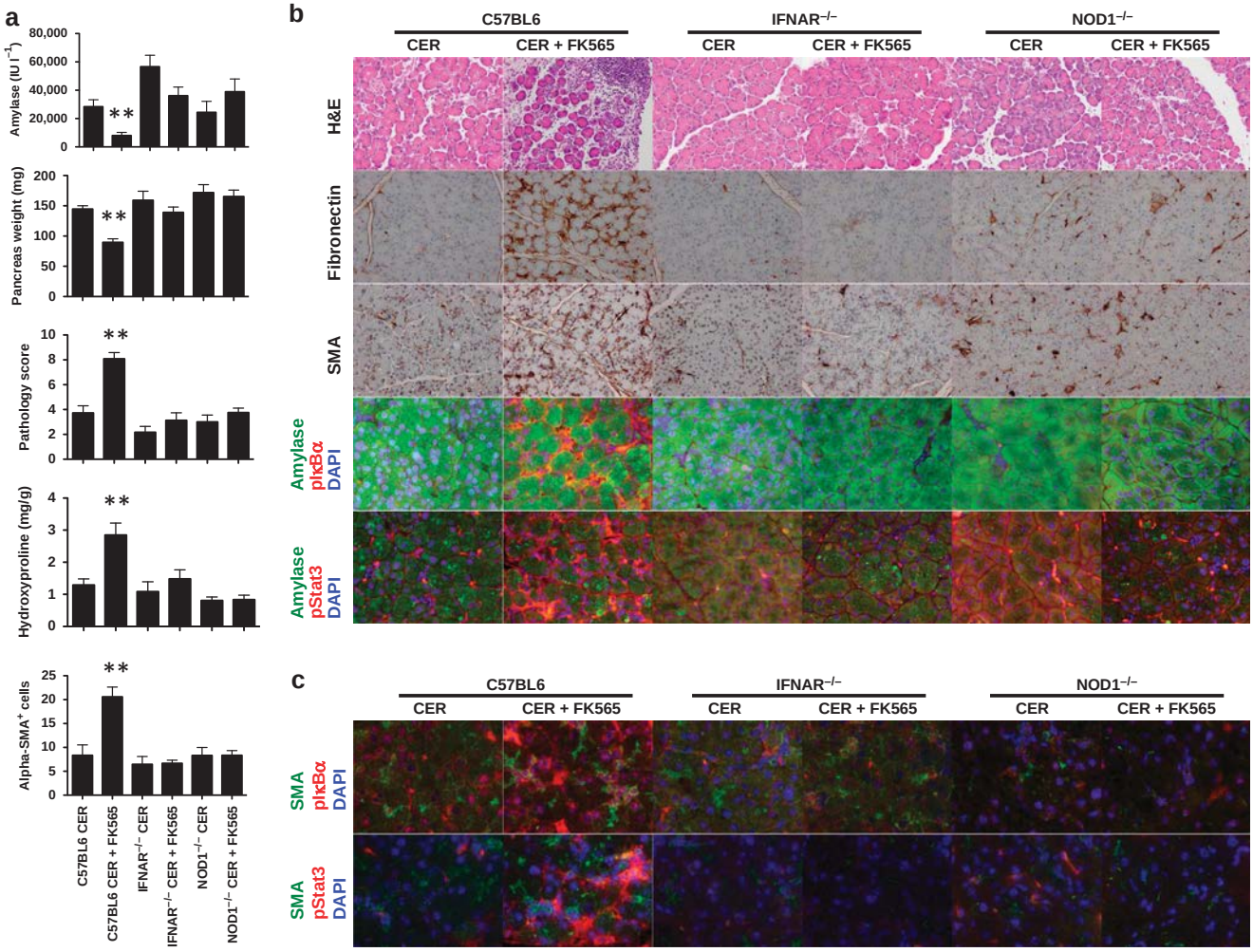

Figure 2 Induction of chronic pancreatitis in mice treated with NOD1 ligand and a low-dose cerulein requires intact NOD1 and type I IFN receptor signaling pathways. (**a**) C57BL6 mice, IFNAR-deficient mice (IFNAR$^{-/-}$), or NOD1-deficient mice (NOD1$^{-/-}$) were administered a low-dose cerulein for a total three of times, or FK565 followed by a low-dose cerulein for a total of three times as described in **Figure 1**. Mice received each regimen twice a week for a total of 14 times and then sera and pancreatic tissues were obtained. Total numbers of mice in each group were as follows; C57BL6 cerulein (CER): $n=11$, C57BL6 CER + FK565: $n=11$, IFNAR$^{-/-}$ CER: $n=6$, IFNAR$^{-/-}$ CER + FK565: $n=8$, NOD1$^{-/-}$ CER: $n=10$, NOD1$^{-/-}$ CER + FK565: $n=8$. Serum levels of amylase, pancreatic weight, pathological scores of the pancreas, pancreatic levels of hydroxyproline, and the numbers of pancreatic α-SMA^{+} cells per high-power fields obtained from mice 3 h after the last injection of cerulein. Results are expressed as mean ± s.e.m. and are a pool of two independent experiments. $^{**}P<0.01$ as compared with cerulein alone in each group. (**b**) Representative picture of the pancreas tissue stained with H&E, anti-fibronectin and anti-SMA, magnification × 400 (top three lines). Representative picture of dual immunofluorescence of the pancreas tissue stained with anti-amylase Ab (green color) or anti-pIκBα Ab (red color) or anti-pStat3 Ab (red color). Nuclei were stained with DAPI, magnification × 800 (bottom two lines). (**c**) Representative picture of dual immunofluorescence of the pancreas tissue stained with anti-SMA Ab (green color) or anti-pIκBα Ab (red color) or anti-pStat3 Ab (red color). Nuclei were stained with DAPI, magnification × 1200. H&E; hematoxylin and eosin; IFN, iterferon.

amylase and pancreas weight were again significantly reduced and pathology scores were again increased in C57BL/6 mice administered the FK565-cerulein CP regimen as compared with mice administered repeated cerulein alone. However, these differences were abolished in mice with NOD1 or IFNAR deficiency since in this case the deficient mice subjected to administration of the FK565-cerulein CP regimen did not manifest more pancreatitis than the deficient mice subjected to cerulein treatment alone. This effect of NOD1 or IFNAR deficiency on induction of chronic pancreatitis was verified with tissue staining studies that showed that pancreatic tissue from wild-type mice and deficient mice administered cerulein alone were indistinguishable upon H&E staining as well as upon tissue staining to detect fibronectin or α-SMA: in addition, as shown in **Figure 2a,b**, the FK565-cerulein CP regimen induced marked expression of pancreatic fibronectin and α-SMA in wild-type mice, but not in NOD1 or IFNAR-deficient mice.

In further and separate studies to quantify the above findings, pancreatic fibrosis was assessed by a hydroxyproline assay and the number of α-SMA^{+} cells/high-powered field was determined. As shown in **Figure 2a**, these studies revealed that pancreatic levels of hydroxyproline were much higher in wild-type mice treated with FK565-cerulein CP regimen as

compared with those treated with cerulein alone. In addition, no increases were seen in the pancreatic levels of hydroxyproline or in the number of α-SMA$^+$ PSCs in NOD1- or IFNAR-deficient mice treated with cerulein alone or with the FK565-cerulein CP regimen as compared with wild-type mice treated with cerulein alone. Taken together, these data strongly suggest that the development of chronic pancreatitis induced by the administration of the FK565-cerulein CP regimen requires intact NOD1 and type I IFN signaling pathways.

As also shown previously, development of acute pancreatitis induced by a single injection of NOD1 ligand and low-dose cerulein required activation of NF-κB and signal transducer and activator of transcription 3 (Stat3) in acinar cells, each dependent on complementary NOD1 and cerulein signaling. To determine whether such activation of NF-κB and Stat3 also occurs in the chronic pancreatitis model developed here we analyzed the expression of phospho-IκBα (pIκBα) and phospho-Stat3 (pStat3) in the pancreas of C57BL/6 mice administered the FK565-cerulein CP regimen. As shown in **Figure 2b**, expression of pIκBα was seen in both amylase-positive acinar cells as well as in amylase-negative cells localized in the peri-acinar cell space. In addition, expression of pStat3 was also detected in amylase-positive pancreatic acinar cells and in amylase-negative cells localized in the peri-acinar space, although in this case, expression in amylase-positive acinar cells was lower than in amylase-negative cells. As expected, in a view of their relative lack of pancreatic inflammation in response to administration of FK565-cerulein CP regimen, NOD1-, or IFNAR-deficient mice exhibited little if any pIκBα and pStat3 expression.

The observation that cells residing in the peri-acinar cell space express both pIκBα and pStat3 prompted us to investigate whether these cells were the PSCs mentioned above that are known to contribute to pancreatic inflammation and fibrosis. As shown in **Figure 2c**, the number of peri-acinar α-SMA$^+$ PSCs expressing both pIκBα and pStat3 was in fact increased in the pancreas of C57BL/6 mice administered the FK565-cerulein CP regimen as compared with those treated with cerulein alone. In contrast, α-SMA$^+$ PSCs expressing pIκBα and pStat3 were barely seen in the pancreas of NOD1- or IFNAR-deficient mice regardless of the mode of treatment. Thus, administration of the FK565-cerulein CP regimen caused NOD1-type I IFN-dependent activation of PSCs as well as acinar cells.

Expression of proinflammatory mediators is enhanced in chronic pancreatitis induced by administration of the FK565-cerulein CP regimen

As repeated injection of FK565 and cerulein induces activation of signaling pathways mediated by NF-κB, Stat3, and type I IFN in the pancreas of C57BL/6 mice, we determined the expression of proinflammatory mediators related to these pathways in mice with chronic pancreatitis. As shown in **Figure 3a**, expression of IFN-β was markedly enhanced in pancreatic lysates of C57BL/6 mice when mice were administered the FK565-cerulein CP regimen, but not when administered cerulein alone. In contrast, administration of the FK565-cerulein CP regimen did not augment the expression of IFN-β in NOD1- or IFNAR-deficient mice. Consistent with these results, administration of FK565-cerulein CP regimen augmented expression of CXCL9 and CXCL10, chemokines whose production depends upon type I IFN signaling.[21] In a similar vein, pancreatic expression of NF-κB-related proinflammatory mediators such as CCL2, TNF-α, and IL-6 was enhanced in C57BL/6 mice treated with the FK565-cerulein CP regimen. Again, such increases were not seen in NOD1- or IFNAR-deficient mice, in the latter case because type I IFN production is necessary for the influx of proinflammatory myeloid cells that produce NF-κB-dependent factors. As shown in **Figure 3b**, these pancreatic cytokine and chemokine production profiles were consistent with the elevated serum levels of IFN-β, CXCL9, CCL2, and IL-6 exhibited by mice administered FK565-cerulein CP regimen but not cerulein alone.

As shown in **Figure 3a**, a similar picture was obtained with respect to cytokines usually produced in adaptive immune responses inasmuch as administration of the FK565-cerulein CP regimen markedly enhanced the pancreatic expression of IFN-γ in C57BL/6 mice, but not in NOD1- or IFNAR-deficient mice. In addition, pancreatic expression of Th2 cytokines such as IL-4 and IL-5 was also enhanced in C57BL/6 mice treated with the FK565-cerulein CP regimen as compared with those with the cerulein alone, although the degree of enhancement was much smaller for these Th2 cytokines than for Th1 cytokines.

The above evaluation of soluble mediators induced by the administration of the FK565-cerulein CP regimen also included analysis of mediators associated with pancreatic fibrosis. This included determination of pancreatic lysate and serum levels of TGF-β1, IL-33, and IL-13, factors that have been previously identified as inducers of hepatic and intestinal fibrosis.[22,23] Thus, as shown in **Figure 3a**, pancreatic lysates of C57BL/6 mice administered the FK565-cerulein CP regimen, but not mice administered cerulein alone, exhibited markedly enhanced expression of IL-33, IL-13, and TGF-β1 and this enhanced expression was also evident in the level of serum IL-33. Again, such enhanced expression was not seen in the pancreatic lysates of NOD1- or IFNAR-deficient mice. Finally, as shown in **Supplementary Figure S2c,d**, IL-33 was highly expressed in C57BL/6 mice administered the FK565-cerulein CP regimen but not mice administered cerulein alone and such expression was not seen in mice deficient in IFNAR and NOD1. Taken together, these data indicate that administration of the FK565-cerulein CP regimen induces NOD1- and type I IFN-dependent expression of proinflammatory and profibrogenic mediators in the pancreas of mice.

Chronic pancreatitis requires NOD1 expression in non-hematopoietic cells

Having defined the cytokine and chemokine profiles accompanying chronic pancreatitis induced by the administration of

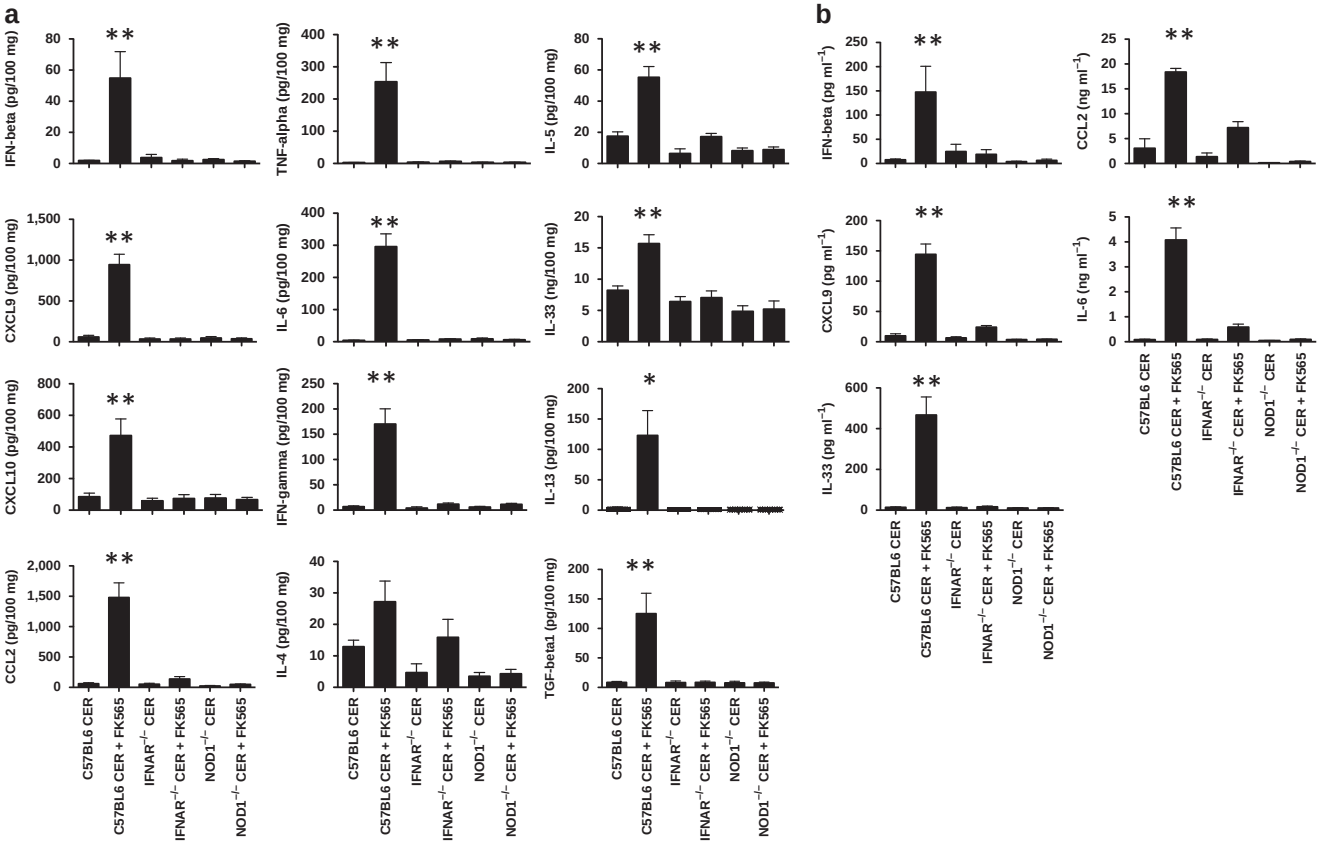

Figure 3 Profiles of cytokines and chemokines expression in mice treated with a low-dose cerulein and NOD1 ligand. C57BL6 mice, IFNAR-deficient (IFNAR$^{-/-}$), or NOD1-deficient (NOD1$^{-/-}$) mice were administered a low-dose cerulein (CER) for a total of three times or FK565 followed by a low-dose cerulein for a total of three times as described in **Figure 2**. Mice received each regimen twice a week for a total of 14 times and then sera and pancreatic lystes were prepared. Concentrations of cytokines and chemokines in pancreatic lysates (**a**) and serum (**b**) were determined by ELISA. Levels of cytokines and chemokines in the pancreas are shown as values per 100 mg pancreatic tissue. Results are expressed as mean ± s.e.m. and are a pool of two independent experiments. *$P<0.05$, **$P<0.01$ as compared with cerulein alone. ELISA, enzyme-linked immunosorbent assay; IFN, interferon.

the FK565-cerulein CP regimen, we turned our attention in defining the cellular origin of NOD1 and type I IFN signaling shown above to be necessary for this inflammation. NOD1 is expressed in hematopoietic cells such as antigen presenting cells as well as in non-hematopoietic cells such as pancreatic acinar cells.[13] To determine whether NOD1 was acting in hematopoietic cells and/or non-hematopoietic cells in the chronic pancreatitis model induced by administration of the FK565-cerulein CP regimen we conducted studies of pancreatitis induction in bone marrow (BM)-chimeric mice. The latter consisted of irradiated NOD1-intact green fluorescent protein (GFP)-transgenic mice and irradiated NOD1-deficient mice reconstituted with NOD1-deficient GFP transgene-negative BM cells and NOD1-intact GFP transgene-positive BM cells that were prepared according to our previous report.[15]

As shown in **Figure 4a** and **Supplementary Figure S3a**, serum levels of amylase was significantly lower and pathology score was significantly higher in NOD1-intact mice transplanted with NOD1-deficient BM cells, but not in NOD1-deficient mice transplanted with NOD1-intact BM cells upon administration of the FK565-cerulein CP regimen, as compared with, similarly reconstituted mice administered cerulein alone. In addition, as shown in **Figure 4b**, serum levels of IFN-β, CXCL9, IL-33, and CCL2 were significantly higher in NOD1-intact mice transplanted with NOD1-deficient BM cells, but not NOD1-deficient mice transplanted with NOD1-intact BM cells, upon administration of the FK565-cerulein CP regimen, as compared with similarly reconstituted mice administered cerulein alone. As shown in **Figure 4a,c**, these findings were consistent with tissue staining studies that showed that NOD1-intact mice transplanted with NOD1-deficient BM cells, but not NOD1-deficient mice transplanted with NOD1-intact BM cells displayed increased expression of fibronectin, α-SMA, and IL-33 in pancreatic tissue following administration of the FK565-cerulein CP regimen vs. cerulein alone.

In further studies of BM-chimeric mice we examined the cellular location of pIκBα and pStat3 in mice with chronic pancreatitis. To this end, we first established that amylase-expressing pancreas acinar cells were GFP-positive in irradiated NOD1-intact GFP-transgene-positive mice

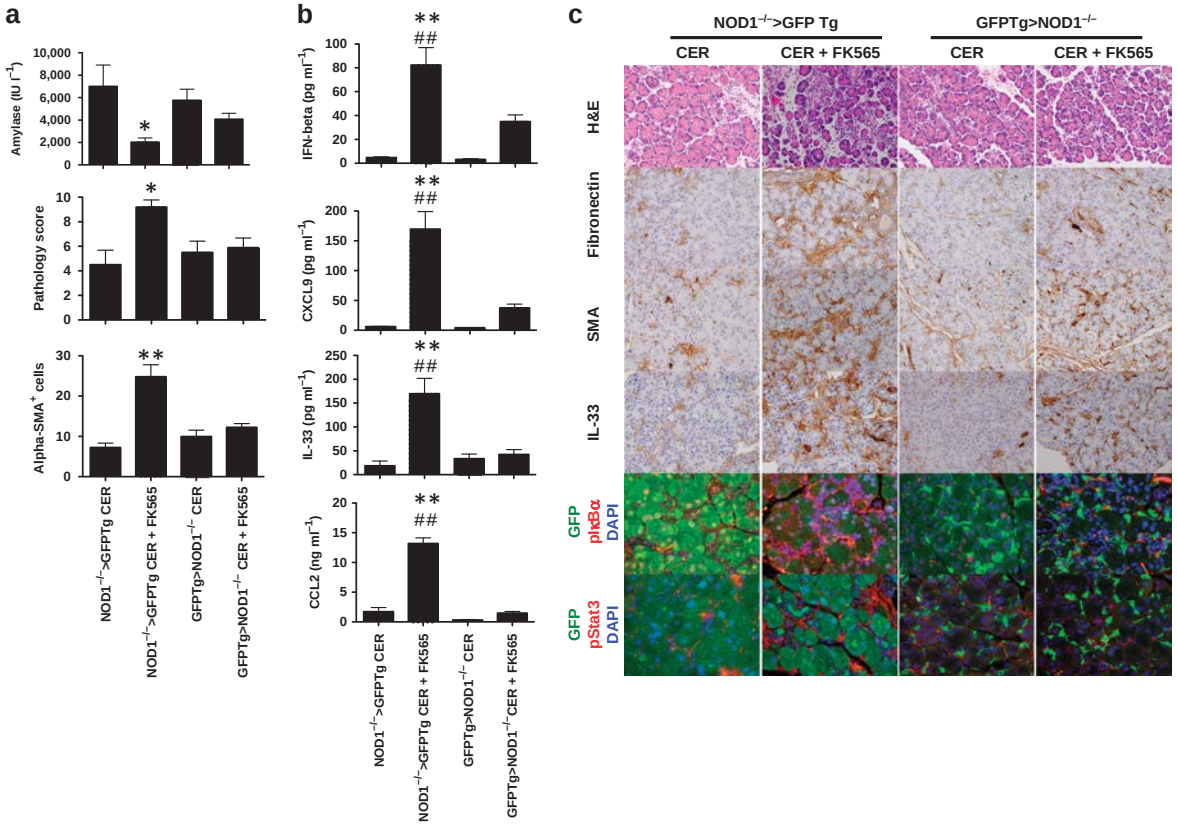

Figure 4 NOD1 expression in pancreatic acinar cells is necessary for the development of chronic pancreatitis induced by a low-dose cerulein and NOD1 ligand. Irradiated GFP-transgenic (GFP-Tg) NOD1-intact mice and NOD1-deficient mice were reconstituted with bone marrow (BM) cells from NOD1-deficient mice and GFP-Tg mice, respectively. These mice were referred to as NOD1$^{-/-}$>GFP Tg and GFPTg>NOD1$^{-/-}$, respectively. NOD1$^{-/-}$>GFP Tg mice and GFPTg>NOD1$^{-/-}$ mice were administered a low-dose cerulein for a total of three times, or FK565 followed by a low-dose cerulein for a total of three times as described in **Figure 1**. Mice received each regimen twice a week for a total of 11 times and then sera and pancreatic tissues were obtained. Total numbers of mice in each group were as follows; NOD1$^{-/-}$>GFP Tg cerulein (CER): $n=6$, NOD1$^{-/-}$>GFP Tg CER + FK565: $n=5$, GFPTg>NOD1$^{-/-}$ CER: $n=5$, GFPTg>NOD1$^{-/-}$ CER + FK565: $n=9$. (**a**) Serum levels of amylase, pathological scores of the pancreas, and the numbers of pancreatic α-SMA^{+} cells per high-power fields obtained from mice three hours after the last injection of cerulein. Results are expressed as mean ± s.e.m. and are a pool of three independent experiments. *$P<0.05$, **$P<0.01$ as compared with cerulein alone. (**b**) Concentrations of cytokines and chemokines in the serum were determined by ELISA. Results are expressed as mean ± s.e.m. and are a pool of three independent experiments. **$P<0.01$ as compared with NOD1$^{-/-}$>GFP Tg mice treated with cerulein alone, $^{\#\#}P<0.01$ as compared with GFPTg>NOD1$^{-/-}$ mice treated with cerulein and FK565. (**c**) Representative picture of the pancreas tissue stained with H&E, anti-fibronectin Ab, anti-SMA Ab or anti-IL-33 Ab magnification × 400 (top four lines). Representative picture of dual immunofluorescence of the pancreas tissue stained with anti-GFP Ab (green color) or anti-pIκBα Ab (red color) or anti-pStat3 Ab (red color). Nuclei were stained with DAPI, magnification × 800 (bottom two lines). GFP, green fluorescent protein; H&E; hematoxylin and eosin; NOD1, nucleotide-binding oligomerization domain 1.

reconstituted with GFP-negative NOD1-deficient BM cells, whereas they were GFP-negative in irradiated NOD1-deficient GFP-transgene-negative mice reconstituted with GFP-positive NOD1-intact BM cells (data not shown). Thus, the status of GFP expression in acinar cells reflected the GFP status of the recipient. As shown in **Figure 4c**, expression of pIκBα was markedly enhanced not only in the GFP-positive acinar cells but also in the GFP-negative hematopoietic cells in the pancreas of irradiated NOD1-intact GFP-transgene-positive mice reconstituted with GFP-negative NOD1-deficient BM cells upon administration of the FK565-cerulein CP regimen. In addition, expression of pStat3 was markedly enhanced in GFP-negative hematopoietic cells in the pancreas of irradiated NOD1-intact GFP-transgene-positive mice reconstituted with GFP-negative NOD1-deficient BM cells upon administration of the FK565-cerulein CP regimen as compared with reconstituted mice administered cerulein alone. In contrast, such expression of pIκBα and pStat3 was barely seen in the pancreas of irradiated NOD1-deficient GFP-transgene-negative mice reconstituted with GFP-positive NOD1-intact BM cells upon administration of the FK565-cerulein CP regimen. Collectively, the above data obtained from BM chimeric mice strongly suggest that NOD1 expression in non-hematopoietic cells, i.e., pancreatic acinar cells, is necessary for the development of chronic pancreatitis.

Chronic pancreatitis is associated with-type I IFN receptor expression in non-hematopoietic or hematopoietic cells

We next conducted additional BM chimera studies to determine whether type I IFN receptor (IFNAR) was acting in hematopoietic cells and/or non-hematopoietic cells in the

development of the chronic pancreatitis developing in mice administered the FK565-cerulein CP regimen. BM-chimeric mice consisting of irradiated IFNAR-intact GFP-transgenic positive mice and irradiated IFNAR-deficient mice, reconstituted with IFNAR-deficient GFP-transgene-negative BM cells and IFNAR-intact GFP-transgene-positive BM cells, respectively, were prepared. As shown in **Supplementary Figures S3b and S4a**, the administration of the FK565-cerulein CP regimen induced equivalent levels of chronic pancreatitis as judged by pathology scores in both irradiated IFNAR-intact GFP-transgene-positive mice and irradiated IFNAR-deficient mice reconstituted with IFNAR-deficient GFP transgene-negative BM cells and IFNAR-intact GFP transgene-positive BM cells, respectively, as compared with both types of BM chimeric mice administered cerulein alone. As shown in **Supplementary Figure S4b**, consistent with the pathology scores, serum levels of IFN-β, CXCL9, IL-33, and CCL2 were significantly higher in both types of BM chimeric mice administered the FK565-cerulein CP regimen as compared with those treated with cerulein alone. Furthermore, as shown in **Supplementary Figures S4a,c**, administration of the FK565-cerulein CP regimen but not cerulein alone induced pancreatic expression of fibronectin, α-SMA, and IL-33 in both types of BM chimeric mice. These data suggest that type I IFNR expression in non-hematopoietic or hematopoietic cells is sufficient for the development of chronic pancreatic inflammation induced by administration of the FK565-cerulein CP regimen.

IL-33 production by acinar cells is regulated by pancreatic myeloid cells

As shown above (**Figure 3**) as well as in a previous study of experimental pancreatitis induced by bile duct blockade,[24,25] pancreatitis is associated with an increased expression of IL-33. These findings, plus the fact that IL-33 is released by cells undergoing necrosis and acinar cell necrosis is a central feature of chronic pancreatitis, suggested to us that this cytokine has an important if not key role in the pathogenesis of chronic pancreatitis induced by the administration of the FK565-cerulein CP regimen.

In initial studies addressing the origin of IL-33 in this model, we considered the possibility that IL-33 was being produced by acinar cells or PSCs, the cell mentioned above that has been implicated in the development of pancreatic fibrosis and shown previously to express nuclear IL-33.[26] Indeed, as shown in **Supplementary Figure S2c**, IL-33 expression was observed in the peri-acinar cell space of the pancreas where PSCs are found in C57BL/6 mice administered the FK565-cerulein CP regimen. However, as also shown in **Supplementary Figure S2d**, dual immunofluorescence studies revealed that most α-SMA$^+$ PSCs were negative for IL-33 staining. This suggested that PSCs are not the main cellular source of this cytokine and that IL-33 in the peri-acinar space originates from necrotic acinar cells.

To further investigate pancreatic acinar cell production of IL-33, we determined the effect of cerulein and/or FK565 on such production in cultures of pancreatic acinar cells obtained from wild-type mice or acinar cells obtained from mice that had been subjected to the FK565-cerulein CP regimen. As shown in **Supplementary Figure S5a**, stimulation of wild-type acinar cells with either cerulein or FK565 induced increased production of IL-33 and the two stimuli acting together induced enhanced IL-33 production. Furthermore, such production was reduced in cells from either IFNAR- or NOD1-deficient mice. These data suggest that type I IFN produced by NOD1 ligand and/or cerulein-stimulated wild-type acinar cells leads to a modest level of IL-33 production by acinar cells. As shown in **Supplementary Figure S5b**, acinar cells obtained from the pancreas of a mouse that had been subjected *in vivo* to the FK565-cerulein CP regimen produced IL-33 at a level similar to those of naive wild-type acinar cells cultured with NOD1 ligand and cerulein; however, when co-cultured with CD11b$^+$ myeloid cells they produced strikingly increased amounts of IL-33, which returned to baseline in the presence of anti-TNF-α Ab or anti-IFNAR Ab. This suggests that type I IFN is acting on myeloid cells to produce TNF-α and the latter is inducing acinar cells to produce large amounts of IL-33. Taken together, these data suggest that pancreatic acinar cells are the main producers of IL-33 in this model of chronic pancreatitis and that pancreatic myeloid cells augment such IL-33 production through a TNF-α-mediated signaling pathway dependent on type I IFN signaling.

IL-33 has a critical role in the chronic pancreatic inflammation induced by the administration of the FK565-cerulein CP regimen

Previous studies have shown that IL-33 acts through ST2 to induce a wide variety of proinflammatory cytokines via a MyD88 signaling pathways and thus promotes the development of both inflammation and fibrosis.[23,27,28] We therefore investigated the role of IL-33 in the pathogenesis of chronic pancreatitis, induced by the administration of the FK565-cerulein CP regimen, with studies in which IL-33 function is blocked by inhibition of ST2 signaling. To this end, we determined the extent of pancreatitis in C57BL/6 mice administered the FK565-cerulein CP regimen or cerulein alone and treated with control Ab or neutralizing anti-ST2 Ab.[29]

As shown in **Figure 5a** and **Supplementary Figure S6a**, serum levels of amylase and pancreatic weight were significantly higher in mice administered the FK565-cerulein CP regimen and treated with anti-ST2 Ab as compared with mice treated with control Ab and the severity of pancreatitis as evaluated by pathology score in these mice was significantly reduced. In addition, as shown in **Figure 5a,b**, mice administered the FK565-cerulein CP regimen and treated with anti-ST2 Ab exhibited a pancreatitis profile similar to that in mice administered cerulein alone and control Ab as judged by serum levels of amylase and pathology score. Thus, anti-ST2 Ab treatment of mice administered the FK565-cerulein CP regimen exhibited the less severe pancreatitis and reduced pancreatic fibrosis characteristic of mice administered cerulein alone and control antibody.

As shown in **Figure 5c**, consistent with this amelioration in the level of inflammation and fibrosis, pancreatic extracts of

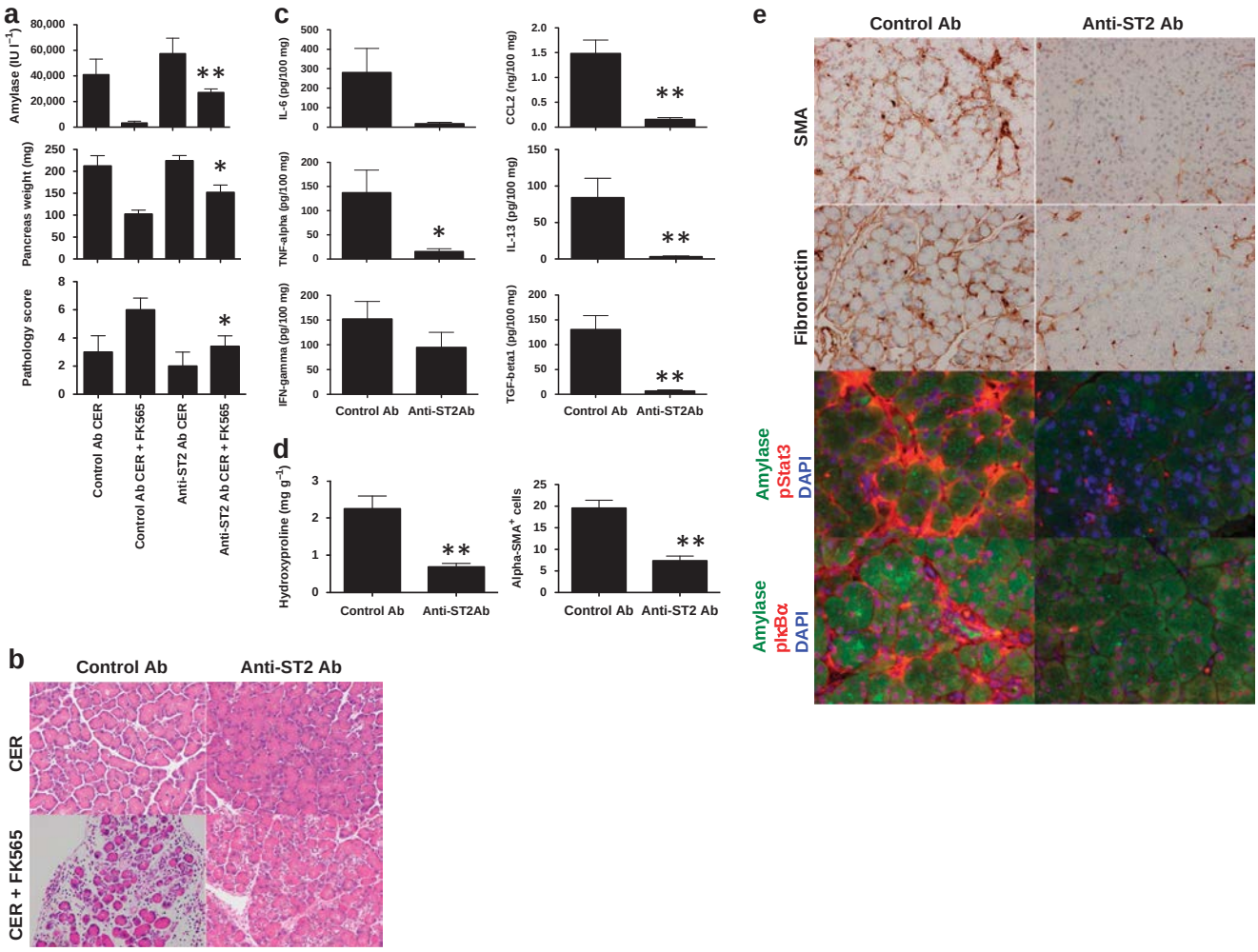

Figure 5 The interaction between IL-33 and ST2 is necessary for the development of chronic pancreatitis induced by a low-dose cerulein and NOD1 ligand. C57BL6 mice were administered a low-dose cerulein (CER) for a total of three times, or FK565 followed by a low-dose cerulein for a total of three times as described in **Figure 1**. Mice were also treated with intraperitoneal injection of control Ab (100 μg, $n=3$; cerulein alone group, $n=5$; cerulein and FK565 group) or anti-ST2 antibody (100 μg, $n=3$; cerulien alone group, $n=5$; cerulein and FK565 group) before the initiation of each treatment regimen. Mice received each regimen twice a week for a total of 14 times after which sera and pancreatic tissues were obtained. (**a**) Serum levels of amylase, pancreatic weight, and pathological scores of the pancreas obtained from mice three hours after the last injection of cerulein. Results are expressed as mean ± s.e.m. $^{*}P<0.05$, $^{**}P<0.01$ as compared with mice treated with control Ab, cerulein, and FK565. (**b**) Representative picture of the pancreas tissue stained with H&E, magnification × 400. (**c**) Concentrations of cytokines and chemokines in pancreatic lysates from mice treated with FK565-cerulein chronic pancreatitis regimen and control Ab or anti-ST2 Ab were determined by ELISA. Levels of cytokines and chemokines in the pancreas are shown as values per 100 mg pancreatic tissue. Results are expressed as mean ± s.e.m. $^{*}P<0.05$, $^{**}P<0.01$ as compared with control Ab. (**d**) Pancreatic levels of hydroxyproline and the numbers of α-SMA^{+} cells in mice treated with FK565-cerulein chronic pancreatitis regimen and control Ab or anti-ST2 Ab. $^{**}P<0.01$ as compared with control Ab. (**e**) Representative picture of the pancreas tissue stained with anti-SMA Ab and anti-fibronectin Ab, magnification x400. Representative picture of dual immunofluorescence of the pancreas tissue stained with anti-amylase Ab (green color) or anti-pStat3 Ab (red color) or anti-pIκBα Ab (red color). Mice received FK565-cerulein chronic pancreatitis regimen with control Ab or anti-ST2 Ab. Nuclei were stained with DAPI, magnification × 800. Ab, antibody; H&E, hematoxylin and eosin; IL, interleukin; NOD1, nucleotide-binding oligomerization domain 1.

mice administered the FK565-cerulein CP regimen and treated with anti-ST2 Ab contained markedly decreased amounts of both proinflammatory mediators such as IL-6, TNF-α, and CCL2 and profibrogenic cytokines such as IL-13 and TGF-β1. In contrast, the same pancreatic extracts exhibited no significant reduction in IFN-γ content. Furthermore, as shown in **Figure 5d,e**, consistent with the reduction in profibrogenic cytokines, pancreatic extracts from mice administered the FK565-cerulein CP regimen and treated with anti-ST2 Ab contained reduced levels of hydroxyproline, and pancreatic tissue from these mice exhibited reduced numbers of α-SMA^{+} cells and reduced fibronectin and α-SMA-staining (**Figure 5d,e**). Finally, anti-ST2 Ab treatment led to reduced pancreatic tissue staining for detection of pStat3 and pIκBα. Collectively, these studies show that blockade of IL-33-ST2 signaling inhibits the profibrotic features of the chronic pancreatic inflammation induced by administration of the FK565-cerulein CP regimen.

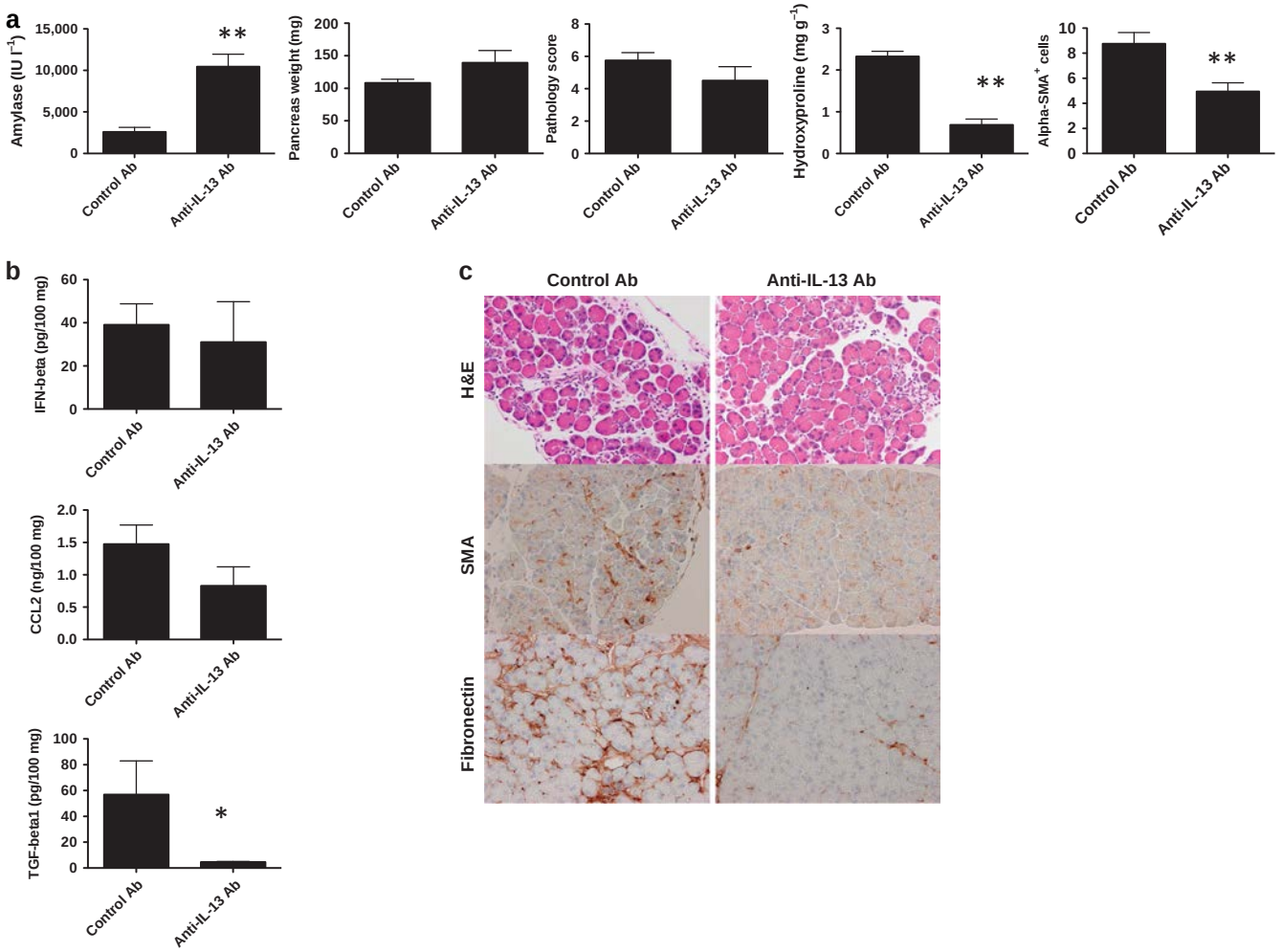

Figure 6 IL-13 is necessary for the development of pancreatic fibrosis induced by a low-dose cerulein and NOD1 ligand. C57BL6 mice were administered FK565 followed by a low-dose cerulein for a total of three times as described in **Figure 1**. Mice were also treated with intraperitoneal injection of control Ab (100 μg, $n=4$) or anti-IL-13 antibody (100 μg, $n=4$) before the initiation of FK565-cerulein treatment regimen. Mice received each regimen twice a week for a total of 14 times and then sera and pancreatic tissues were obtained. (**a**) Serum levels of amylase, pancreatic weight, pathological scores of the pancreas, pancreatic levels of hydroxyproline, and the numbers of α-SMA$^+$ cells obtained from mice 3 h after the last injection of cerulein. Results are expressed as mean ± s.e.m.**$P<0.01$ as compared with control Ab. (**b**) Concentrations of cytokines and chemokines in pancreatic lysates were determined by ELISA. Levels of cytokines and chemokines in the pancreas are shown as values per 100 mg pancreatic tissue. Results are expressed as mean ± s.e.m. *$P<0.05$ as compared with control Ab. (**c**) Representative picture of the pancreas tissue stained with H&E, anti-SMA Ab and anti-fibronectin Ab, magnification × 400. Ab, antibody; ELISA, enzyme-linked immunosorbent assay; H&E; hematoxylin and eosin; IL, interleukin; NOD1, nucleotide-binding oligomerization domain 1.

IL-13-mediated signaling pathways mediate fibrosis in chronic pancreatitis induced by the administration of the FK565-cerulein CP regimen

As shown above, IL-33 signaling via ST2 induces IL-13 production and tissue fibrosis as shown by increased tissue expression of hydroxyproline and α-SMA. This finding raised the possibility that IL-13 is a major profibrotic factor in the chronic pancreatitis induced by administration of the FK565-cerulein CP regimen. To investigate this possibility, C57BL/6 mice administered the FK565-cerulein CP regimen were treated with neutralizing Ab against IL-13 or control Ab at the time of each FK565-cerulein administration. As shown in **Figure 6a,b** and **Supplementary Figure S6b**, serum levels of amylase and pancreatic weight was higher in mice treated with anti-IL-13 Ab as compared with mice treated with control Ab, but anti-IL-I3 Ab treatment had little effect on pathology score. These changes were not associated with changes in pancreatic extract content of IFN-β or CCL2 but were associated with dramatic reduction in content of TGF-β1 and decreases in pancreatic expression of α-SMA, hydroxyproline, and fibronectin (**Figure 6a–c**). Thus, whereas IL-33 induction of IL-13 does not influence the severity of inflammation in this chronic fibrosis model, it is likely to be a major pathway by which IL-33 causes pancreatic fibrosis and atrophy.

IL-13 induced by IL-33 in chronic pancreatitis originates mainly from T cells

Recent studies have shown that IL-33 activates innate lymphoid cell type 2 (ILC2) to promote IL-13-mediated tissue

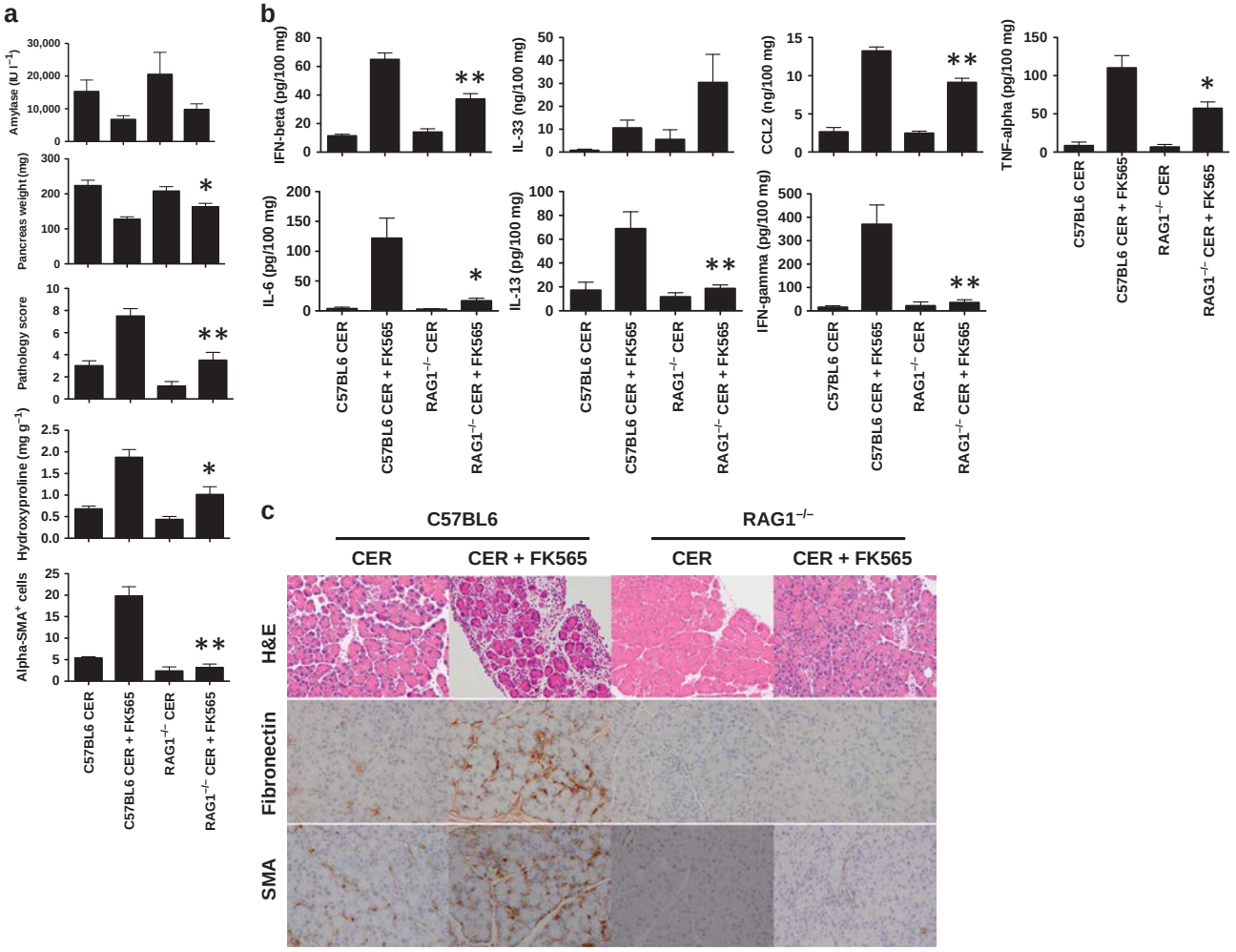

Figure 7 Development of chronic pancreatitis induced by NOD1 ligand and a low-dose cerulein requires adaptive immune responses (**a**) C57BL6 mice and RAG1-deficient mice (RAG1$^{-/-}$) were administered a low-dose cerulein for a total of three times, or FK565 followed by a low-dose cerulein for a total of three times as described in **Figure 1**. Mice received each regimen twice a week for a total of 14 times and then sera and pancreatic tissues were obtained. Total numbers of mice in each group were as follows; C57BL6 cerulein (CER): $n=9$, C57BL6 CER + FK565: $n=9$, RAG1$^{-/-}$ CER: $n=9$, RAG1$^{-/-}$ CER + FK565: $n=9$. Serum levels of amylase, pathological scores of the pancreas, pancreatic weight, pancreatic levels of hydroxyproline, and the numbers of α-SMA^{+} cells obtained from mice three hours after the last injection of cerulein. Results are expressed as mean ± s.e.m. and are a pool of two independent experiments. *$P<0.05$, **$P<0.01$ as compared with C57BL6 mice treated with FK565 and cerulein. (**b**) Concentrations of cytokines and chemokines in pancreatic lysates were determined by ELISA. Levels of cytokines and chemokines in the pancreas are shown as values per 100 mg pancreatic tissue. Results are expressed as mean ± s.e.m. **$P<0.01$, *$P<0.05$ as compared with C57BL6 mice treated with cerulein and FK565. (**c**) Representative picture of the pancreas tissue stained with H&E, anti-fibronectin and anti-SMA, magnification × 400. ELISA, enzyme-linked immunosorbent assay; H&E; hematoxylin and eosin; NOD1, nucleotide-binding oligomerization domain 1.

fibrosis.[23,27,30] We therefore conducted studies to determine if ILC2 and/or conventional T cells were the origin of IL-13 in the chronic pancreatitis induced by administration of the FK565-cerulein CP regimen. In initial studies addressing this question, we determined the type of cells producing IL-13 in the pancreas by dual immunofluorescence analysis and found that most of IL-13-producing cells were CD3^{+} T cells (data not shown). Second, we isolated pancreatic mononuclear cells from C57BL/6 mice treated with the FK565-cerulein CP regimen and then pancreatic mononuclear cells were stimulated with anti-CD3 Ab and CD28 Ab to measure the production of IL-13. As shown in **Supplementary Figure S7**, CD4^{+} pancreatic mononuclear cells, but not CD4^{+} cells-depleted pancreatic mononuclear cells produced a large amount of IL-13.

Finally, in more definitive studies, we compared the chronic pancreatitis induced by administration of the FK565-cerulein CP regimen or repeated administration of cerulein alone in C57BL/6 mice to that induced in RAG-1-deficient mice lacking T cells. As shown in **Figure 7** and **Supplementary Figure S6c**, differences in serum amylase levels between mice administered cerulein alone and those administered the FK565-cerulein CP regimen were generally equivalent in RAG1-deficient and wild-type mice; nevertheless, the RAG1-dificient mice exhibited a significant reduction in pathology score and increase in pancreatic weight as compared with the wild-type mice. In accompanying studies it was found that production of proinflammatory mediators produced in innate immune responses such as IFN-β, CCL2, TNF-α, and IL-6 was

significantly reduced in the RAG1-deficient mice administered the FK565-cerulein CP regimen as compared with wild-type mice (**Figure 7b**). Strikingly, production of proinflammatory mediators produced mainly in adaptive immune responses, IFN-γ and IL-13, were even more decreased in the pancreas of RAG1-deficient mice administered the FK565-cerulein CP regimen. Thus, T-cell-mediated adaptive immune cytokines enhance innate immune-related proinflammatory cytokine responses to cause inflammation in the FK565-cerulein CP model. Finally, RAG-1-deficient mice manifested reduced expression of hydroxyproline, fibronectin, and α-SMA upon administration of the FK565-cerulein CP regimen (**Figure 7a,c**). Thus, these data are compatible with the view that conventional T cells are mainly responsible for the development of both the persistent inflammation and the fibrosis in this chronic pancreatitis model. Nevertheless, it remains possible that ILC2 also contribute to the inflammation and further work exploring this possibility is necessary. Whether the adaptive IL-13 T-cell response was driven by pancreatic autoantigens or microbiome-related stimuli awaits further study.

NOD1-deficient mice are resistant to the induction of chronic pancreatitis induced by high-dose cerulein

The above studies establish a new model of chronic pancreatitis induced by the repeated administration of NOD1 ligand (FK565) and low-dose cerulein. However, since low-dose administration of cerulein was incapable of inducing pancreatitis on its own, it remained possible that NOD1 ligand administration was acting as an adjuvant that is merely enhancing the low-dose cerulein effect and does not have a unique pathogenic role. This possibility was rendered unlikely by our previous studies showing that high-dose cerulein administration is a poor inducer of acute pancreatitis in NOD1-deficient mice.[15] Despite these findings, we conducted studies to determine whether high-dose cerulein administration can induce chronic pancreatitis in the absence of NOD1 signaling and thus under these circumstances where NOD1 signaling may be dispensable. Accordingly, C57BL/6 mice and NOD1-deficient mice were subjected to four hourly injection of high doses of cerulein (100 μg kg^{-1}) twice a week for a total of 7 weeks. As shown in **Supplementary Figure S8**, NOD1-deficient mice were resistant to the induction of chronic pancreatitis by high-dose cerulein as assessed by chronic pancreatitis scores and induction of high pancreatic hydroxyproline levels. Perhaps more importantly, pancreatic expression of IL-33 was strikingly lower in NOD1-deficient mice as compared with wild-type mice. These data thus provide further support for the unique and indispensable role of the NOD1-mediated innate immune response in the development of chronic pancreatitis.

DISCUSSION

In this manuscript we describe a new model of chronic pancreatitis induced by the repeated administration of NOD1 ligand (FK565) and low-dose cerulein. Importantly, both NOD1 ligand and cerulein administration were essential to the induction of the chronic pancreatitis since NOD1 ligand alone did not induce any pancreatic inflammation and administration of cerulein alone led to a mild pancreatic inflammation that lacked the key feature of the chronic disease such as pancreatic atrophy and fibrosis. Given the pivotal role of NOD1 as a pattern recognition receptor responding to intestinal microflora, the findings in this study support the notion that NOD1-mediated innate immune responses occurring in acinar cells following their exposure to circulating bacteria are a necessary condition for the development of chronic pancreatitis initiated by a cause of excessive trypsinogen activation, such as cerulein administration.

Using this model, we were able to identify key proinflammatory mediators responsible for the innate and adaptive immune responses involved in the development of chronic pancreatitis. At first sight, the most obvious of these was NOD1 itself, as, as alluded to above, it was necessary to include NOD1 ligand in the pancreatitis-inducing regimen. However, it could be argued that the role of NOD1 in this model was to act as an enabler of the effect of low-dose cerulein administration as the latter was incapable of inducing pancreatitis on its own and NOD1 does not itself have a unique pathogenic role in the inflammation. This possibility, however, does not fit with the observation that NOD1 stimulation of acinar cells was necessary for the production of type I IFN and other factors shown to be involved in the inflammation (see further discussion below). Perhaps more importantly, this possibility was ruled out by the fact that even high-dose cerulein administration was not able to induce full-blown chronic pancreatitis in the absence of intact NOD1 signaling. Another set of observations pointing to the importance of the role of NOD1 in this chronic pancreatitis model came from studies of BM chimeras, which showed that the development of chronic pancreatitis depended on the expression of NOD1 in the non-hematopoietic cellular compartment. i.e., acinar cells. These studies thus correlated with the observation that stimulation of acinar cells with NOD1 ligand and cerulein led to their production of factors driving the pancreatic inflammation such as CCL2 (as shown in our previous study)[15] and IL-33 (as shown in the present study). Finally, it should be mentioned that while the administration of NOD1 ligand provided the stimulus for the NOD1 response in this model, under more physiologic conditions, the source of such stimulation is likely to be commensal bacteria that enter the circulation as a result of impaired gut epithelial barrier function.

Type I IFN is another key mediator of the chronic pancreatitis in that mice deficient in the receptor for type I IFN (IFNAR) were unable to develop pancreatitis. BM chimera studies conducted in part with mice lacking IFNAR expression disclosed that both hematopoietic cells and non-hematopoietic cells expressing IFNAR participate in the development of chronic pancreatitis, and thus suggested that type I IFN signaling of both acinar cells and infiltrating macrophages are involved in the pancreatic inflammation. This NOD1-induced type I IFN signals acinar cell induction of Stat3

and other factors necessary for optimal acinar cell production of CCL2, a chemokine essential to the migration of $CCR2^+$ macrophages into the pancreas.[15] Its role in macrophage signaling was delineated in studies of other investigators showing that recruitment of $Ly6C^{hi}$ monocytes to a site of inflammation is uniquely dependent on type I IFN induction of monocyte CCR2 expression, the receptor for CCL2.[31] Thus type I IFN is involved both in the production of CCL2 by acinar cells and in the expression of the CCL2 receptor, CCR2, in macrophages, i.e., events that together facilitate the proinflammatory macrophage infiltration of the pancreas.

Another role of type I IFN in the inflammatory process underlying chronic pancreatitis (in addition to its role in macrophage recruitment described above) relates to the possibility that it induces proinflammatory responses by macrophages that have already entered the pancreas. This possibility arises from a previous study showing that in cerulein-induced pancreatitis myeloid cells recruited into the pancreas produce proinflammatory cytokines such as TNF-α, which have the capacity to induce necroptosis in pancreatic acinar cells.[32] Whether type I IFN is a stimulant of such acinar cell-damaging TNF-α production in the chronic pancreatitis model described here, is suggested by our observation that acinar cells co-cultured with pancreatic $CD11b^+$ cells from mice being subjected to chronic pancreatitis induction, release greatly increased amounts of IL-33 (a possible result of acinar cell necroptosis) and that such IL-33 release is inhibited by both anti-IFNAR Ab and anti-TNF-α Ab. These *in vitro* findings are consistent with the fact that IFNAR-deficient mice exhibit decreased expression of pancreatic TNF-α upon exposure to the FK565-cerulein CP regimen. Thus, type I IFN induces the production of TNF-α by macrophages in this model as shown by Mancuso *et al.*, who reported that type I IFN signaling is required for macrophage production of TNF-α and other proinflammatory cytokines upon stimulation with live bacteria.[33] Taken together, these data suggest that type I IFN production in chronic pancreatitis is not only responsible for the recruitment of infiltrating macrophages, but also for the stimulation of such macrophages, their production of TNF-α and the subsequent effect of the latter on induction and/or release of IL-33 from damaged pancreatic acinar cells. As such, type I IFN has a multifaceted and central role in the pathogenesis of this model of chronic pancreatitis. Finally, it is important to mention that NOD1 induction of type I IFN due to acinar cell exposure to gut microflora may have effects on a broad range of phagocytic mononuclear cell function. This possibility comes from recent findings showing that gut microflora have been implicated in the activation of phagocytic mononuclear cell activity leading to NK-cell activation.[34]

Yet another essential proinflammatory mediator necessary for the development of chronic pancreatitis in this model is IL-33, a cytokine released by distressed or dying cells such as the acinar cells harboring excessive amounts of trypsin as a result of cerulein administration. The involvement of this cytokine was shown by the fact that mice deficient in either NOD1 or IFNAR did not mount an increased IL-33 response, indicating that abrogation of the pancreatitis prevented the production of this cytokine. More to the point, it was shown by the fact that blockade of IL-33 signaling by administration of an antibody that blocks IL-33 access to its receptor, anti-ST2 Ab, prevents the development of chronic pancreatitis as well as the effects of cytokines induced by IL-33, IL-13, and TGF-β1 that are responsible for the fibrosis accompanying chronic pancreatitis. Interestingly, however, the cytokine profile in the pancreatic tissue of mice with the FK565-cerulein chronic pancreatitis model was not a typical IL-33-associated Th2 response accompanied by high levels of IL-4, since in this case, the IL-4 increase was marginal. We attribute this cytokine pattern to the finding that type I IFN induction of Th1 cytokines such as IFN-γ and TNF-α were also prominent components of the pancreatic cytokine profile and it is therefore likely that these cytokines were counter-regulating certain aspects of the usual IL-33 response. In any case, the interplay of the IL-33 response and the type I IFN response led to a complex cytokine pattern that contains both Th2 and Th1 elements. One question arising from the presence of both Th1 and Th2 cytokines in this chronic pancreatitis model is the types of immune cells producing IFN-γ and IL-13. As mentioned below, we have provided evidence that $CD4^+$ T cells are main producers of IL-13. The cells producing IFN-γ have not been identified in this study; however, since RAG-1-deficient mice treated with the FK565-cerulein CP regimen exhibited a marked decrease in pancreatic IFN-γ expression, we assume that T cells are main producers of this cytokine. This idea is supported by the finding of Bonilla *et al.*, who showed effective induction of $CD8^+$ T cells producing IFN-γ by IL-33.[35]

IL-33 is an alarmin-type nuclear cytokine that is released from damaged non-hematopoietic cells.[25] It is therefore not unexpected that circulating levels of IL-33 are increased in patients with acute pancreatitis, a condition associated with acinar cell disruption. It was nevertheless unclear from prior studies whether the IL-33 produced in pancreatitis has a proinflammatory or anti-inflammatory effect. In one study, focused on mice with acute pancreatitis induced by a choline-deficient (ethionine-supplemented) diet or high-dose cerulein administration it was found that lack of IL-33 receptor (ST2) expression was associated with more severe inflammation.[36] Similarly, mice with ST2 deficiency exhibited more severe pancreatitis due to Coxsackievirus B5 infectlon as compared with wild-type mice.[37] In this case, the more severe disease was attributed to decreased IL-4-mediated M2 macrophage activity leading to decreased regulatory T-cell function; however, IL-33 administration led to decreased viral titer so that its beneficial effect could have been owing to a direct or indirect effect on viral replication. The above studies supporting an anti-inflammatory role for IL-33, however, were challenged by Kempuraj *et al.*, who found that acute pancreatitis caused by pancreatic duct ligation was made worse by administration of IL-33 and that the latter was associated with increased NF-κB activation and cytokine/chemokine release.[24] Similarly, IL-33 was found to have a proinflammatory effect on pancreatic

carcinoma cells.[38] The present study, in that it provides unequivocal evidence that IL-33 has a proinflammatory and profibrotic effect in chronic pancreatitis is, at first sight, in apparent conflict with some of the prior studies; however, this apparent conflict may be explained by the fact that the role of IL-33 was examined in experimental pancreatitis induced by different methods than that used here and by the fact that, for the most part, in these studies the effect of IL-33 on fibrosis was not evaluated.

PSCs have been shown to be the major source of extracellular matrix necessary for the development of pancreatic fibrosis.[20] A variety of proinflammatory factors such as IL-6, TNF-α, and IL-33, all of which are expressed in the mice with chronic pancreatitis due to administration of the FK565-cerulein CP regimen, have been identified as stimulators of PSC development and function.[20,26] Type I IFN can be considered an additional factor involved in such development in this model since IFNAR-deficient mice exhibited lack of α-SMA expression; however, in this case the effect may be indirect in that type I IFN is acting as an upstream initiator of the inflammatory cascade. In complementary studies we have identified IL-13 as a critical activator of PSCs in this model of chronic pancreatitis. This was evident from studies that showed that neutralization of IL-13 signaling reduced the expression of α-SMA. As discussed below, such activating IL-13 originates from T cells that are part of an adaptive immune response; it is thus clear that while PSC development during chronic pancreatitis depends not only on innate cytokine responses but also on adaptive cytokine responses. Finally, although activated PSCs have been reported to be the source of IL-33 in pancreatic inflammation,[26] our immunofluorescence studies suggest that IL-33 expressed in the peri-acinar spaces is not co-localized with the marker of PSC, α-SMA. Thus, we assume that in this chronic pancreatitis model PSCs are not the main source of IL-33 and this cytokine is more likely to be originating from pancreatic acinar cells.

As shown in recent studies, ILC2s activated by IL-33 have been implicated as a critical player of tissue fibrosis.[23,27,28] ILC2 contributes to the progression of lung and liver fibrosis by producing a large amount of Th2 cytokines such as IL-5 and IL-13 in response to IL-33.[23,27,28] Since pancreatic expression of IL-33 and IL-13 is markedly increased in our model of chronic pancreatitis, it was rational to assume that activation of ILC2 producing IL-13 was also involved in the development of chronic pancreatic inflammation and fibrosis. In fact, neutralization of IL-33 or IL-13 signaling pathways protects mice from chronic pancreatic inflammation and fibrosis in our model. It should be noted, however, that RAG1-deficient mice are completely protected from chronic pancreatitis with diminished pancreatic expression of IL-13, whereas expression of innate immune mediators such as IFN-β, IL-33, and CCL2 were preserved. In addition, we found pancreatic $CD4^+$ T cells isolated from mice treated with the FK565-cerulein CP regimen produced a large amount of IL-13 upon stimulation with anti-CD3 Ab and CD28 Ab. On the basis of these data, we speculate that T cells rather than ILC2s are major source of IL-13 in this model of chronic pancreatitis and that chronic fibroinflammatory responses are mediated by classical Th2 cells.[39] Confirmation of this idea awaits further study addressing phenotypic analysis of ILC2 and Th2 cells in this model and we cannot exclude the possibility that collaborative interactions between ILC2s and Th2 cells exacerbate chronic fibroinflammatory responses of the pancreas as suggested by a recent study.[40]

In conclusion, we have established a unique model of chronic pancreatitis induced by repetitive administration of low-dose cerulein and NOD1 ligand. This model exhibits key characteristics of chronic pancreatitis occurring in human disease, namely, pancreatic atrophy and fibrosis and establishes that these characteristics are caused by the production of IL-33 and its downstream product, IL-13. The fact that activation of NOD1 has a central role in this model suggests the possibility that human chronic pancreatitis is caused by initial intrapancreatic events that lead to the entry of commensal organisms into the pancreas and the subsequent stimulation of proinflammatory innate and adaptive immune mechanisms that sustain prolonged pancreatitis. However, studies in humans with pancreatitis will be necessary to explore this possibility.

METHODS

Mice. C57BL/6 mice were purchased from Japan SLC (Hamamatsu, Japan). NOD1-deficient mice, IFNAR-deficient mice, and GFP-transgenic mice were used as described previously.[21] RAG1-deficient mice were kindly provided by Dr K Suzuki (Kyoto University Graduate School of Medicine). Mice were reared under specific pathogen free conditions. Animal use adhered to the Kyoto University animal-care guidelines, and protocols of animal experiments were approved by the review boards of Kyoto University.

Induction of pancreatitis. Mice received IP injection of FK565 (50 μg, Astellas Pharma, Tokyo, Japan) in combination with IP injection of cerulein (20 μg kg^{-1}, Sigma, St Louis, MO). Mice received each treatment regimen twice a week for a total of 14 times and then sera and pancreas tissue were obtained. In some experiments, mice were treated with anti-ST2 Ab (100 μg per mouse, R&D systems, Minneapolis, MN), anti-IL-13 Ab (100 μg per mouse, eBioscience, San Diego, CA) or rat IgG (100 μg per mouse, Sigma). In some experiments, mice received four hourly IP injection of cerulein (100 μg kg^{-1}) twice a week for a total of 14 times. Serum levels of amylase were determined by the biochemical analyzer, SPOTCHEM (Arkray, Kyoto, Japan). Pancreatic lysate were prepared as described previously.[15] Pancreatic levels of hydroxyproline were determined by the hydroxyproline assay kit (QuickZyme Biosciences, Leiden, The Netherlands).

Bone marrow transplantation. For the generation of BM-chimeric mice, recipient mice were irradiated 10 Gray and reconstituted with BM cells (2×10^6 per each recipient mouse) from the donor mice via the tail vein injection. Mice were used for the induction of experimental pancreatitis at 6–8 weeks after the BM transplantation.

Enzyme-linked immunosorbent assay. Protein concentrations of cytokines and chemokines were determined by eBioscience ELISA kits for mouse IL-6, CCL2, TNF-α, IFN-γ, IL-33, and IL-13. R&D systems ELISA kits were used for the measurement of mouse IFN-β, CXCL9, and CXCL10. Concentration of TGF-β1 was determined by Promega ELISA kit (Madison, WI).

Immunofluoresence and immunohistochemical analysis. Pancreas tissues were harvested and fixed in 10% formalin. Deparaffinized

sections were incubated with anti-IL-33 Ab (Abcam, Cambridge, MA), anti-SMA Ab (Abcam),[41,42] anti-fibronectin Ab (Abcam),[43] anti-CD3 Ab (Abcam),[44] and anti-CD11b Ab (Abcam).[45] Protein expression was visualized by the Dako Envison+ system (DAKO JAPAN, Tokyo, Japan). For the immunofluorescence analysis, deparaffinized sections were incubated with mouse anti-IL-33 Ab (Abcam), rabbit anti-SMA Ab (Abcam), mouse anti-SMA Ab (Abcam), mouse anti-pIκBα (CST, Cambridge, MA),[15] rabbit anti-amylase (Sigma),[15] rabbit anti-GFP (CST), or mouse anti-pStat3 (CST)[15] followed by the incubation with Alexa 488 or Alexa 546-conjugated anti-mouse or rabbit IgG (Invitrogen, Carlsbad, CA). Sirius Red staining was performed by using Picosirius red stain kit (Polysciences Inc., Warrington, PA). At least two immunohistochemical and immunofluorescence photographs were taken by microscopy (Biozero BZ-8100, Keyence, Osaka, Japan) from each slide prepared from mice treated with cerulein and/or FK565. The degree of pancreatic infiltration of PSCs was determined by counting the number of α-SMA$^+$ cells in high-power fields in each slide. Pathological scores of chronic pancreatitis was determined as previously described with some modifications.[46] Within pancreatic sections, areas of abnormal pancreatic tissue architecture were graded as follows: 0 = absent, 1 = rare, 2 = minimal < 10%, 3 = moderate 10–50%, and 4 = severe > 50%. Within these areas, glandular atrophy were graded as follows: 0 = absent, 1 = minimal < 10%, 2 = moderate 10–50%, and 3 = severe > 50%. In addition, the presence of immune cells was graded as: 0 = absent, 1 = minimal, 2 = mild, 3 = moderate, and 4 = severe. The total histological score is given as the pancreatic tissue architecture plus the glandular atrophy plus the presence of immune cells.

Isolation of pancreatic acinar cells and immune cells. Pancreatic acinar cells ($5x10^5$ per ml) were isolated as described previously[47] and stimulated with cerulein (10^{-10} M) and FK565 (100 ng ml^{-1}) for 24 h. Pancreatic immune cells were isolated as described previously.[48] Pancreatic immune cells were stained with PE or FITC-conjugated Gr-1 (Miltenyibiotec, Auburn, CA), F4-80 (Biolegend, San Diego, CA), CD11b (eBioscience), or CD11c Ab (eBioScience) for the flow-cytometric analysis (Accuri C6 cytometer, BD Bioscience, San Jose, CA). CD4$^+$ cells or CD11b$^+$ cells were isolated from pancreatic immune cells by using CD4 or CD11b microbeads (Mitenyibiotec). The purity of CD4$^+$ cells or CD11b$^+$ cells was more than 80% as assessed by flow-cytometric analysis. Pancreatic immune cells were stimulated with anti-CD3 Ab (5 μg ml^{-1}, eBioscinece) and anti-CD28 Ab (10 μg ml^{-1}, BD Bioscience) for 48 h to determine the production of IL-13. In the coculture experiments composed of pancreatic acinar cells (5×10^5 per ml) and CD11b$^+$ cells (5×10^5 per ml), neutralizing Ab against TNF-α (R&D systems) or IFNAR (BD Bioscience) was added at the concentration of 50 μg ml^{-1}.

Statistical analysis. Student's t test was used to evaluate the significance of the differences. Statistical analysis was performed with the Prism (Graphpad, software, La Jolla, CA). A value of $P < 0.05$ was regarded as statistically significant.

SUPPLEMENTARY MATERIAL is linked to the online version of the paper at http://www.nature.com/mi

ACKNOWLEDGMENTS

This work was supported by Grant-in-Aid for Scientific Research (25293172, 15K15370) from the Japan Society for the Promotion of Science, the Japanese Society of Gastroenterology, the Kato Memorial Trust for Nambyo Research, and the Special Coordination Funds by the Ministry of Education, Culture, Sports, Science and Technology of Japan and Astellas Pharma. in Creation of Innovation Centers for Advanced Interdisciplinary Research Areas Program, and the Health and Labor Sciences Research Grants for Research on Intractable Diseases from the Ministry of Health, Labor and Welfare, Japan.

AUTHOR CONTRIBUTIONS

Study concept and design; TW, WS. Acquisition of data; TW, YS, NY, HE. Analysis and interpretation of data; TW, WS. Drafting of the manuscript; TW, TS, WS. Study supervision; MK, TC, WS.

DISCLOSURE

The authors declare no conflict of interest.

REFERENCES

1. Frossard, J.L., Steer, M.L. & Pastor, C.M. Acute pancreatitis. *Lancet* **371**, 143–152 (2008).
2. Braganza, J.M., Lee, S.H., McCloy, R.F. & McMahon, M.J. Chronic pancreatitis. *Lancet* **377**, 1184–1197 (2011).
3. Steer, M.L., Waxman, I. & Freedman, S. Chronic pancreatitis. *N. Engl. J. Med.* **332**, 1482–1490 (1995).
4. Sah, R.P. & Saluja, A. Molecular mechanisms of pancreatic injury. *Curr. Opin. Gastroenterol.* **27**, 444–451 (2011).
5. Saluja, A.K., Lerch, M.M., Phillips, P.A. & Dudeja, V. Why does pancreatic overstimulation cause pancreatitis?. *Annu. Rev. Physiol.* **69**, 249–269 (2007).
6. Whitcomb, D.C. Genetic aspects of pancreatitis. *Annu. Rev. Med.* **61**, 413–424 (2010).
7. Etemad, B. & Whitcomb, D.C. Chronic pancreatitis: diagnosis, classification, and new genetic developments. *Gastroenterology* **120**, 682–707 (2001).
8. Dawra, R. *et al.* Intra-acinar trypsinogen activation mediates early stages of pancreatic injury but not inflammation in mice with acute pancreatitis. *Gastroenterology* **141**, 2210–2217 e2212 (2011).
9. Sah, R.P., Dudeja, V., Dawra, R.K. & Saluja, A.K. Cerulein-induced chronic pancreatitis does not require intra-acinar activation of trypsinogen in mice. *Gastroenterology* **144**, 1076–1085 e1072 (2013).
10. Yamaguchi, H., Kimura, T., Mimura, K. & Nawata, H. Activation of proteases in cerulein-induced pancreatitis. *Pancreas* **4**, 565–571 (1989).
11. Ji, B. & Logsdon, C.D. Digesting new information about the role of trypsin in pancreatitis. *Gastroenterology* **141**, 1972–1975 (2011).
12. Akira, S. & Takeda, K. Toll-like receptor signalling. *Nat. Rev. Immunol.* **4**, 499–511 (2004).
13. Strober, W., Murray, P.J., Kitani, A. & Watanabe, T. Signalling pathways and molecular interactions of NOD1 and NOD2. *Nat. Rev. Immunol.* **6**, 9–20 (2006).
14. Kono, H. & Rock, K.L. How dying cells alert the immune system to danger. *Nat. Rev. Immunol.* **8**, 279–289 (2008).
15. Tsuji, Y., Watanabe, T., Kudo, M., Arai, H., Strober, W. & Chiba, T. Sensing of commensal organisms by the intracellular sensor NOD1 mediates experimental pancreatitis. *Immunity* **37**, 326–338 (2012).
16. Mithofer, K., Fernandez-del Castillo, C., Ferraro, M.J., Lewandrowski, K., Rattner, D.W. & Warshaw, A.L. Antibiotic treatment improves survival in experimental acute necrotizing pancreatitis. *Gastroenterology* **110**, 232–240 (1996).
17. Hoque, R., Malik, A.F., Gorelick, F. & Mehal, W.Z. Sterile inflammatory response in acute pancreatitis. *Pancreas* **41**, 353–357 (2012).
18. Hoque, R. *et al.* TLR9 and the NLRP3 inflammasome link acinar cell death with inflammation in acute pancreatitis. *Gastroenterology* **141**, 358–369 (2011).
19. Ulmasov, B., Oshima, K., Rodriguez, M.G., Cox, R.D. & Neuschwander-Tetri, B.A. Differences in the degree of cerulein-induced chronic pancreatitis in C57BL/6 mouse substrains lead to new insights in identification of potential risk factors in the development of chronic pancreatitis. *Am. J. Pathol.* **183**, 692–708 (2013).
20. Masamune, A. & Shimosegawa, T. Pancreatic stellate cells–multi-functional cells in the pancreas. *Pancreatology* **13**, 102–105 (2013).
21. Watanabe, T. *et al.* NOD1 contributes to mouse host defense against Helicobacter pylori via induction of type I IFN and activation of the ISGF3 signaling pathway. *J. Clin. Invest.* **120**, 1645–1662 (2010).

22. Fichtner-Feigl, S., Strober, W., Geissler, E.K. & Schlitt, H.J. Cytokines mediating the induction of chronic colitis and colitis-associated fibrosis. *Mucosal Immunol.* **1 Suppl 1**, S24–S27 (2008).
23. McHedlidze, T. *et al.* Interleukin-33-dependent innate lymphoid cells mediate hepatic fibrosis. *Immunity* **39**, 357–371 (2013).
24. Kempuraj, D., Twait, E.C., Williard, D.E., Yuan, Z., Meyerholz, D.K. & Samuel, I. The novel cytokine interleukin-33 activates acinar cell proinflammatory pathways and induces acute pancreatic inflammation in mice. *PLoS ONE* **8**, e56866 (2013).
25. Cayrol, C. & Girard, J.P. IL-33: an alarmin cytokine with crucial roles in innate immunity, inflammation and allergy. *Curr. Opin. Immunol.* **31C**, 31–37 (2014).
26. Masamune, A., Watanabe, T., Kikuta, K., Satoh, K., Kanno, A. & Shimosegawa, T. Nuclear expression of interleukin-33 in pancreatic stellate cells. *Am. J. Physiol. Gastrointest. Liver Physiol.* **299**, G821–G832 (2010).
27. Li, D. *et al.* IL-33 promotes ST2-dependent lung fibrosis by the induction of alternatively activated macrophages and innate lymphoid cells in mice. *J. Allergy Clin. Immunol.* **134**, 1422–1432 e1411 (2014).
28. Seidelin, J.B., Rogler, G. & Nielsen, O.H. A role for interleukin-33 in T(H)2-polarized intestinal inflammation?. *Mucosal Immunol.* **4**, 496–502 (2011).
29. Monticelli, L.A. *et al.* Innate lymphoid cells promote lung-tissue homeostasis after infection with influenza virus. *Nat. Immunol.* **12**, 1045–1054 (2011).
30. Li, J. *et al.* Biliary repair and carcinogenesis are mediated by IL-33-dependent cholangiocyte proliferation. *J. Clin. Invest.* **124**, 3241–3251 (2014).
31. Lee, P.Y. *et al.* Type I interferon modulates monocyte recruitment and maturation in chronic inflammation. *Am. J. Pathol.* **175**, 2023–2033 (2009).
32. He, S. *et al.* Receptor interacting protein kinase-3 determines cellular necrotic response to TNF-alpha. *Cell* **137**, 1100–1111 (2009).
33. Mancuso, G. *et al.* Type I IFN signaling is crucial for host resistance against different species of pathogenic bacteria. *J. Immunol.* **178**, 3126–3133 (2007).
34. Ganal, S.C. *et al.* Priming of natural killer cells by nonmucosal mononuclear phagocytes requires instructive signals from commensal microbiota. *Immunity* **37**, 171–186 (2012).
35. Bonilla, W.V. *et al.* The alarmin interleukin-33 drives protective antiviral CD8(+) T cell responses. *Science* **335**, 984–989 (2012).
36. Ouziel, R. *et al.* The ST2 pathway is involved in acute pancreatitis: a translational study in humans and mice. *Am. J. Pathol.* **180**, 2330–2339 (2012).
37. Sesti-Costa, R. *et al.* The IL-33/ST2 pathway controls coxsackievirus B5-induced experimental pancreatitis. *J. Immunol.* **191**, 283–292 (2013).
38. Schmieder, A., Multhoff, G. & Radons, J. Interleukin-33 acts as a pro-inflammatory cytokine and modulates its receptor gene expression in highly metastatic human pancreatic carcinoma cells. *Cytokine* **60**, 514–521 (2012).
39. Ochi, A. *et al.* MyD88 inhibition amplifies dendritic cell capacity to promote pancreatic carcinogenesis via Th2 cells. *J. Exp. Med.* **209**, 1671–1687 (2012).
40. Liu, B., Lee, J.B., Chen, C.Y., Hershey, G.K. & Wang, Y.H. Collaborative interactions between type 2 innate lymphoid cells and antigen-specific CD4+ Th2 cells exacerbate murine allergic airway diseases with prominent eosinophilia. *J. Immunol.* **194**, 3583–3593 (2015).
41. Zhang, S.M. *et al.* Interferon regulatory factor 8 modulates phenotypic switching of smooth muscle cells by regulating the activity of myocardin. *Mol. Cell Biol.* **34**, 400–414 (2014).
42. Hagiwara, K. *et al.* Molecular and cellular features of murine craniofacial and trunk neural crest cells as stem cell-like cells. *PLoS ONE* **9**, e84072 (2014).
43. Conway, M.J. *et al.* Mosquito saliva serine protease enhances dissemination of dengue virus into the mammalian host. *J. Virol.* **88**, 164–175 (2014).
44. Simons, B.W. *et al.* A human prostatic bacterial isolate alters the prostatic microenvironment and accelerates prostate cancer progression. *J. Pathol.* **235**, 478–489 (2015).
45. Rommer, A. *et al.* EVI1 inhibits apoptosis induced by antileukemic drugs via upregulation of CDKN1A/p21/WAF in human myeloid cells. *PLoS ONE* **8**, e56308 (2013).
46. van Westerloo, D.J. *et al.* Therapeutic effects of troglitazone in experimental chronic pancreatitis in mice. *Am. J. Pathol.* **166**, 721–728 (2005).
47. Gout, J. *et al.* Isolation and culture of mouse primary pancreatic acinar cells. *J. Vis. Exp.* **78**, e50514 (2013).
48. Arai, Y. *et al.* Plasmacytoid dendritic cell activation and IFN-alpha production are prominent features of murine autoimmune pancreatitis and human igg4-related autoimmune pancreatitis. *J. Immunol.* **195**, 3033–3044 (2015).

JGH Journal of Gastroenterology and Hepatology

JGHF

doi:10.1111/jgh.13318

HEPATOLOGY

Unique features associated with hepatic oxidative DNA damage and DNA methylation in non-alcoholic fatty liver disease

Naoshi Nishida, Norihisa Yada, Satoru Hagiwara, Toshiharu Sakurai, Masayuki Kitano and Masatoshi Kudo

Department of Gastroenterology and Hepatology, Kinki University Faculty of Medicine, Osaka-sayama, Japan

Key words
hepatocarcinogenesis, methylation, nonalcoholic steatohepatitis, oxidative stress, tumor suppressor gene.

Accepted for publication 8 February 2016.

Correspondence
Dr Naoshi Nishida, Department of Gastroenterology and Hepatology, Kinki University Faculty of Medicine, 337-2 Ohno-higashi, Osaka-sayama, Osaka 589-8511, Japan. Email: naoshi@med.kindai.ac.jp

Disclosures: This work was supported in part by a grant-in-aid for scientific research (KAKENHI: 24590997) from the Japanese Society for the Promotion of Science (N. Nishida) a grant from the Smoking Research Foundation (N. Nishida), the Japan Health Foundation (N. Nishida). The authors declare that they have no conflict of interest.

Abstract

Background and Aim: Non-alcoholic fatty liver disease (NAFLD) is an increasing cause of hepatocellular carcinoma (HCC). Previously, we reported that DNA oxidation induced epigenetic alteration of tumor suppressor genes (TSGs) and contributed to HCC emergence. Here, we examine the associations between clinicopathological characteristics of NAFLD and advanced oxidative DNA damage that is associated with TSG methylation in the NAFLD liver.

Methods: Liver biopsies from 65 NAFLD patients were analyzed for clinicopathological features and oxidative DNA damage using immunohistochemistry of 8-hydroxydeoxyguanosine (8-OHdG). Abnormal DNA methylation in the promoters of 6 TSGs, *HIC1*, *GSTP1*, *SOCS1*, *RASSF1*, *CDKN2A*, and *APC*, was examined using MethyLight. Associations between clinicopathological characteristics, methylation of TSGs, and accumulation of 8-OHdG were analyzed.

Results: We found that aspartate aminotransferase/alanine aminotransferase ratio, the fibrosis-4 index, and serum α-fetoprotein (AFP) level were associated with degree of 8-OHdG, and AFP was an independent factor among them ($P = 0.0271$). Regarding pathological findings, hepatocellular ballooning and stage of fibrosis were also associated with oxidative DNA damage ($P = 0.0021$ and 0.0054); ballooning was an independent risk for detecting high degree of 8-OHdG in hepatocytes (odds ratio 7.38, 95% confidence interval 1.41-49.13, $P = 0.0171$). Accumulation of methylated TSGs was significantly associated with deposition of 8-OHdG ($P = 0.0362$).

Conclusions: Patients with high serum AFP and high degree of ballooning showed accumulation of oxidative DNA damage that could be a seed of DNA methylation responsible for hepatocarcinogenesis. These characteristics could be risk of HCC; such patients require urgent intervention such as lifestyle modification.

Introduction

Nonalcoholic fatty liver disease (NAFLD) is a disorder defined by the deposition of an excess amount of fat in hepatocytes with no or little consumption of alcohol; the entire spectrum of NAFLD includes simple steatosis and nonalcoholic steatohepatitis (NASH) that is a severe from of NAFLD.[1]

Ludwig *et al*., characterized the unique pathologic features of NASH;[2] Brunt et al also proposed a grading and staging system of NASH, with grading assessed using degree of steatosis, ballooning, inflammation, and staging determined using the status of fibrosis.[3] For the diagnosis of the entire spectrum of NAFLD, Kleiner et al. developed a scoring system for encompassing the severity of NAFLD that took the degree of steatosis, inflammation and ballooning into account.[4] As it is possible that there could be a transition from non-NASH to NASH, determination of clinicopathological features of NAFLD that predict undesirable outcome, such as emergence of hepatocellular carcinoma (HCC), is critical, even for patients who have never been diagnosed with NASH according to the previous criteria.

On the other hand, several reports have shown an association between oxidative stress in the liver and steatosis; patients with NASH showed higher levels of oxidative DNA damage compared to other liver disorders.[5,6] In addition, NASH patients with HCC reportedly had a severer oxidative DNA damage in hepatocytes than those without HCC.[6] Oxidative DNA damage could accelerate carcinogenesis through the alteration of histone modification that could lead to the epigenetic inactivation of tumor suppressor genes (TSGs).[7,8] According to our previous findings, an increased number of methylated TSGs was closely associated with shorter time-to-HCC emergence in patients with chronic hepatitis C (CHC).[9] Given the above background, it is conceivable that oxidative stress induces DNA damage and epigenetic alteration in TSGs in hepatocytes that drive hepatocarcinogenesis in patients

with NAFLD. Therefore, for prediction of HCC emergence from NAFLD, it is important to know the clinicopathological characteristics that best reflect the degree of oxidative DNA damage that is associated with TSG methylation and future HCC emergence. However, no reports have clarified the characteristic clinicopathological findings that reflect the oxidative DNA damage in NAFLD.

In this study, we addressed this important issue and identified unique clinicopathological findings that are closely associated with oxidative DNA damage and abnormal methylation of TSGs in the liver of NAFLD. The findings obtained here will help identify specific laboratory and pathological features related to the risk of HCC emergence among patients with NAFLD, which is critical for management of this disease.

Methods

Patients. From October 2010 to February 2014, a total of 65 liver biopsies were performed for diagnosis of NAFLD and enrolled in this study. The details of the patients at the time of biopsy and the inclusion criteria are summarized in Table S1. We also studied HCC and their surrounding non-cancerous liver of the 16 NAFLD-related HCC patients who underwent surgery to analyze the relationship between DNA methylations and corresponding gene expressions. Their characteristics are also shown in Table S2. Informed consent was obtained from each patient and the study protocol conforms to the ethical guidelines of the 1975 Declaration of Helsinki. This study was approved by our institution's research committee.

Histological examinations and immunohistochemistry. Histological findings were evaluated using the NASH activity score (NAS) system described by Kleiner et al.[4] A staging of fibrosis was also evaluated using the system described by Brunt et al.[3] Peal's Prussian blue staining was performed and the degree of iron deposition was evaluated using the criteria described previously.[10]

For evaluation of oxidative DNA damage and lipid oxidation, immunohistochemistry (IHC) staining of 8-hydroxydeoxyguanosine (8-OHdG) and 4-hydroxy-2-nonenal (4-HNE) were performed. The avidin-biotin complex method was applied using a mouse monoclonal antibody against 8-OHdG and 4-HNE (clone N45.1 and HNEJ-2; NIKKEN SEIL Co. Ltd., Tokyo, Japan) at a concentration of 1 μg/mL.[11] Figure 1 and Fig. S1 show the representatives of 8-OHdG and 4-HNE staining, respectively; classifications of degree of 8-OHdG and 4-HNE levels based on the IHC staining are described in Table S3.

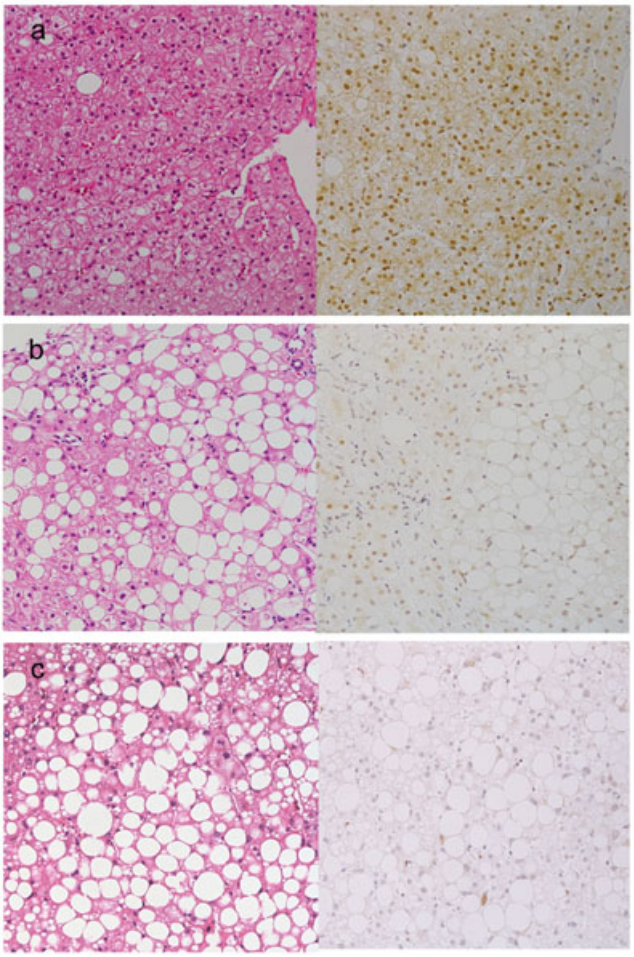

Figure 1 Immunohistochemical staining of 8-OHdG using liver biopsy from patients with nonalcoholic fatty liver disease. (a) A representative case of strong 8-OHdG staining, (b) moderate 8-OHdG staining, and (c) weak 8-OHdG staining. The left picture shows hematoxylin and eosin staining, and the right shows 8-OHdG staining (magnification × 200).

Quantification of DNA methylation on the promoter of tumor suppressor genes and corresponding gene expression. For the analysis of the relationship between oxidative DNA damage and presence of abnormally methylated sequences in the promoter of TSGs in the paraffin-embedded NAFLD biopsy specimens, we selected 6 TSGs, *HIC1*, *GSTP1*, *SOCS1*, *RASSF1*, *CDKN2A*, and *APC* because this set of genes was most frequently and densely methylated in human HCC [12]. For detection of methylation, we used MethyLight assays; the methylation-specific primers and TaqMan probes for each gene were reported previously.[9] Real-time PCRs were carried out three times per experiment. We used PCR of methylation-independent and methylation-specific *Alu* sequence as a positive and an endogenous control of amplification as well as a reference for normalization of input DNA.[13] A relative quantification of methylation level was calculated by dividing the target locus/*Alu* ratio of a sample by that of *Sss*I-treated and non-treated DNA standard (CpGenome Human Methylated and Non-Methylated DNA; Merck Millipore, Darmstadt, Germany). We also applied combined bisulfite restriction assay (COBRA) for semi-quantification of DNA methylation; the details were described previously.[12] For the quantification of corresponding gene expression, we applied quantitative PCR (qPCR) using the TaqMan™ Gene Expression Assays (Applied Biosystems, Foster City, CA); the details are described in Table S4.

Chromatin Immunoprecipitation and quantitative Real-Time PCR. For the detection of alteration of chromatin modification after induction of oxidative stress, we applied chromatin immunoprecipitation (ChIP)-qPCR using antibodies against histone H4 acetylated at lysine 16 (Ack16H4) and histone H3 trimethylated at lysine 4 (3MeK4H3) as active histone markers, histone H3 trimethylated at lysine 27 (3MeK27H3) as a repressive histone marker, and 8-OHdG as a DNA oxidation marker after the treatment of human fetal liver-derived Hc cell line with hydrogen peroxide (H_2O_2). Details of ChIP-qPCR assays were already reported previously.[11]

Statistical analysis. Statistical analyses used in this study are summerized in Table S5.

Results

Relationship between clinical background and oxidative DNA damage in hepatocytes. We tried to identify the clinical features of NAFLD patients who show extensive DNA damage by oxidation. The immunohistochemical analysis of 8-OHdG revealed that 17, 24, and 24 biopsy specimens showed strong, moderate, and weak staining, respectively (Fig. 1). Table 1 indicates the details of the relationship between clinical factors and degree of 8-OHdG staining. There is a borderline association between degree of 8-OHdG staining and sex and height, where moderate/strong 8-OHdG staining is more frequent in female and shorter height ($P = 0.0465$, and 0.0428 for sex and height, respectively). We also identified fibrosis-4 (Fib-4) index was positively correlated with degree of 8-OHdG staining ($P = 0.0340$ by the Wilcoxon rank sum test). In addition, we found a significant association of 8-OHdG staining with serum aspartate aminotransferase (AST)/alanine aminotransferase (ALT) ratio as well as α-fetoprotein (AFP) level, where patients with moderate/strong 8-OHdG staining had higher serum AST/ALT ratio and AFP ($P = 0.0216$ and $P = 0.0395$ for AST/ALT ratio and AFP level respectively, Table 1 and Fig. 2). To examine the robustness of the significance, we also analyzed the associations using parametric t-test. Again, we found significant association of 8-OHdG staining with AFP, but not with AST/ALT or FiB-4 index ($P = 0.0161$, 0.4525 and 0.0621 for AFP, AST/ALT ratio and Fib-4 index, respectively, Fig. 2). We subsequently conducted multivariate analysis, and found that AFP was most closely associated with increased 8-OHdG staining, although not statistically significant. Fib-4 index includes AST and ALT level; those are confounding factors with the AST/ALT ratio. Thus, we eliminated the Fib-4 index from the analysis, and found that high serum AFP level was independently associated with moderate/strong 8-OHdG staining ($P = 0.0271$, Table 1).

Relationship between pathological findings and oxidative DNA damage in hepatocytes. We examined the characteristic pathological finding of NAFLD that best reflects oxidative DNA damage. For this purpose, we evaluated the histologic feature of NAFLD according to the items of NAFLD activity score [4], and also determined the degree of fibrosis using the staging system of Brunt et al.[3] The proportion of patients with each score and stage are shown in Table S1.

We found that increased NAS score was related to strong 8-OHdG staining ($P = 0.0017$, Table 2). Interestingly, among the items in the NAS score, ballooning is the only factor that shows an association with the degree of 8-OHdG staining ($P = 0.0021$), although inflammation tends to be severe in the liver with moderate/strong 8-OHdG staining (Table 2). We also analyzed the association between the components of Brunt's classification and 8-OHdG staining dividing grade and fibrosis stage into two categories (grade: 1 vs. ≥2, and stage: ≤2 vs. ≥3), and found that fibrosis stage, but not grade, also showed an association with 8-OHdG staining ($P = 0.0054$ and 0.1888 for stage and grade, respectively, Table 2). Multivariate analysis reveals that ballooning is independently associated with the degree of 8-OHdG ($P = 0.0454$, Table 2). We calculated the OR for relative risk of showing moderate/strong 8-OHdG staining, and found that increased ballooning score was associated with increased OR in dose-dependent manner (OR = 7.38, 3.18, and 2.32 for ballooning score 2 vs. 0, 1 vs. 0, and 2 vs. 1, respectively, Fig. 3a). Between serum AFP and ballooning score, ballooning is identified as an independent factor for predicting moderate/strong 8-OHdG staining through multivariate analysis ($P = 0.0186$ and 0.0906 for ballooning and AFP, respectively). Furthermore, the combination of ballooning and fibrosis stage shows clear association with 8-OHdG levels ($P = 0.0106$, Fig. 2b).

Degree of oxidative DNA damage is associated with DNA methylation of tumor suppressor genes in the liver of NAFLD. Because oxidative DNA damage could be a cause of abnormal DNA methylation, we analyzed the association between degree of 8-OHdG staining and methylation events of TSGs.[9,12] Methylation events in the promoter of the *CDKN2A* gene are detected in 36 tissues (55.4%) among

Table 1 Association between clinical factors and 8-OHdG staining in hepatocyte

Clinical factors	8-OHdG staining		*P* value	
	Weak ($n = 24$)	Moderate/strong ($n = 41$)	Univariate*	Multivariate**
Age	57 (44.5-65.75)	59 (47.5-63.5)	0.6882	-
Sex (male/female)	13/11	12/29	**0.0465**	0.3062 (0.4445)
Height (cm)	162.6 (158.5-167.0)	157.5 (152.8-163.3)	**0.0428**	0.9311 (0.8525)
Weight (kg)	75.6 (67.0-89.1)	74.4 (60.0-82.0)	0.4506	-
Body mass index	27.9 (25.6-31.7)	28.1 (24.7-33.6)	0.8704	-
AST (IU/L)	38 (25.25-61.75)	49 (29.5-77)	0.0972	-
ALT (IU/L)	51 (29-100)	62 (34-84)	0.7597	-
AST/ALT	0.61 (0.52-1.16)	0.83 (0.67-1.15)	**0.0216**	0.3000 (0.7490)
γ-glutamyltransferase (IU/L)	40 (24.75-72.25)	46 (32.5-79.5)	0.2828	-
Total cholesterol (mg/dL)	187.5 (166.25-215.75)	202 (176.5-231)	0.2563	-
HDL-cholesterol (mg/dL)	52 (43-61.5)	45 (37-57)	0.1468	-
Triglyceride (mg/dL)	112 (100.25-149.5)	138 (91-202.5)	0.1850	-
Uric acid (mg/dL)	6.25 (5.05-7.8)	5.3 (4.4-76.7)	0.0782	-
Total protein (g/dL)	7.4 (6.925-7.7)	7.4 (7.0-7.6)	0.7642	-
Albumin (g/dL)	4.55 (4.125-4.7)	4.5 (4.2-4.7)	0.8751	-
C-reactive protein (mg/dL)	0.129 (0.075-0.208)	0.169 (0.076-0.336)	0.3696	-
Ferritin (ng/mL)	134 (26-217)	106.5 (65.25-204.5)	0.8696	-
Serum iron (μg/dL)	100 (72.5-117.5)	97 (76.25-124.25)	0.9154	-
Total iron binding capacity (μg/dL)	392 (321.75-408.5)	347 (302.5-388)	0.0642	-
Unsaturated iron binding capacity (μg/dL)	259 (224-322.5)	256 (198.75-299)	0.2183	-
ANA[†] (titer ≥40/<40)	3/13	10/30	0.7346	-
IgG (mg/dL)	1328 (1882-1440)	1297 (1142.5-1467)	0.7999	-
IgA (mg/dL)	252 (205.75-347.75)	228 (167.5-378.5)	0.6559	-
IgM (mg/dL)	76 (58-134)	91 (66-127.5)	0.4943	-
Hyaluronic acid (ng/mL)	50.5 (27.25-85.2)	51 (27-121.2)	0.4795	-
Type III procollagen -N-peptide (ng/mL)	0.60 (0.53-0.77)	0.62 (0.52-0.75)	0.6667	-
Type IV collagen (ng/mL)	124 (98-153)	135 (108-196)	0.1702	-
Type IV collagen 7S (ng/mL)	4.8 (3.75-5.675)	5.1 (3.85-7.35)	0.3030	-
Fib-4[‡] index	1.25 (0.71-1.91)	1.84 (1.23-3.16)	**0.0340**	0.2307
Fasting blood sugar (mg/mL)	105.5 (91.5-115.5)	100 (87.5-123.5)	0.7237	-
IRI[§] (μU/mL)	13.7 (9.5-22.4)	13.0 (9.4-16.3)	0.5444	-
HOMA-R[¶]	3.59 (2.50-5.88)	2.91 (2.07-3.99)	0.1320	-
HbA1c (NGSP, %)	6.0 (5.6-7.0)	6.1 (5.6-7.0)	0.7104	-
AFP (ng/mL)	2 (2-3.75)	3 (2-8.5)	**0.0395**	0.1948 (**0.0271**)
PIVKA-II (mAU/mL)	25 (17.5-26)	22 (15-27)	0.3916	-
Diabetes mellitus (with/without)	10/14	18/23	0.8606	-
Hypertension (with/without)	8/16	21/20	0.1615	-
Hyperlipidenia (with/without)	8/16	14/27	0.9467	-

Each column representing 8-OHdG staining shows median (25^{th}-75^{th} percentile) for a continuous variable and number of patients for a categorical variable.

**P* values of univariate analysis were calculated using Pearson's chi-squared test for categorical variables and Wilcoxon rank sum test for continuous variables. $P < 0.05$ are shown in bold.

***P* values by multiple logistic regression analysis. The variables that showed *p* values of < 0.05 in univariate analysis were included in the model. Because the Fib-4 index includes aspartate aminotransferase (AST) and alanine aminotransferase (ALT) levels and could be a confounding variable with AST/ALT, we eliminated the Fib-4 index and re-calculated the *p* values of multivariate analysis; these are shown in parentheses. $P < 0.05$ are shown in bold.

[†]ANA; antinuclear antibody measured by indirect fluorescent antibody.

[‡]Fib-4 index = age (yr) × AST (IU/L)/PLT (10^9/L) × ALT (IU/L)$^{1/2}$

[§]IRI; immunoreactive insulin. Diabetic patients treated with insulin were excluded.

[¶]HOMA-R; homeostasis model assessment ratio. Patients with FBS > 140 mg/mL were excluded.

Abbrevations: AST – aspartate aminotransferase, ALT – alanine aminotransferase, Fib-4 – fibrosis-4, HbA1c - glycated hemoglobin, AFP – α-fetoprotein, PIVKA-II – protein induced by Vitamin K absence or antagonists-II

the liver biopsies obtained from 65 NAFLD patients. Similarly, abnormal methylations are detected in 29 (44.6%), 20 (30.8%), 18 (27.7%), 15 (23.1%), and 15 (23.1%) tissues for *APC*, *RASSF1*, *GSTP1*, *SOCS1*, and *HIC1*, respectively. The methylation levels of each gene are shown in Table S6; relationships between oxidative markers and methylation events of each

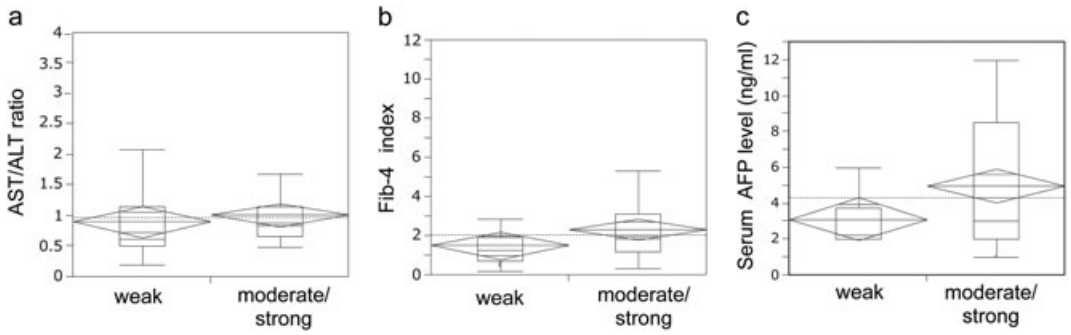

Figure 2 Distribution of AST/ALT ratio, Fib-4 index, and serum AFP level in the context of degree of 8-OHdG staining. Degree of 8-OHdG staining was classified into "weak" ($n = 24$) and "moderate and strong" groups ($n = 41$). Dashed horizontal line through each of the three boxes shows the mean of AST/ALT ratio (a), Fib-4 index (b) and AFP (c), respectively. Diamond and lines in the diamond indicate the means values and 95% confidence intervals of each subgroup; boxes and whiskers denote 75% and 95% distributions, and the lines in the boxes showed median values, respectively. The *P* values by the Wilcoxon rank-sum test and student t test were 0.4525 and 0.0216 for AST/ALT ratio (a), 0.0621 and 0.0340 for Fib-4 index (b), and 0.0161 and 0.0395 for AFP (c), respectively.

Table 2 Association between pathological findings and 8-OHdG staining

Pathological findings	8-OHdG staining		*P* value	
	Weak ($n = 24$)	Moderate/strong ($n = 41$)	Univariate*	Multivariate**
NAS score: ≤2 / 3-4 / 5≤	10/11/3	3/22/16	**0.0017**	-
Steatosis score: 1 / 2-3	13/11	19/22	0.5425	-
Lobular inflammation score: 0-1 / 2-3	20/4	28/13	0.1830	-
Hepatocellular Ballooning score: 0 / 1-2	12/12	6/35	**0.0021**	**0.0454**
Brunt classification				
Grade: 1 / ≥2	14/10	17/24	0.1888	-
Stage: ≤2 / ≥3	21/3	22/19	**0.0054**	0.0734
Iron deposition†				
Grade: ≤1 / ≥2	16/4	18/12	0.1375	-

* *P* values by Pearson's chi-squared test or Fisher's exact test.
** *P* values by multiple logistic regression analysis.
† 15 samples were not determined for iron deposition.
NAS ; NASH activity score

sample are illustrated in Figure 4a. The lipid oxidation marker, 4-HNE, is closely associated with the degree of oxidative DNA damage ($P = 0.0003$, Fig. S2). Eighteen patients showed >3 methylated TSGs, whereas 47 patients showed <2 methylated TSGs. A significant association is detected between high degree of 8-OHdG and 4-HNE staining and increased number of methylated TSGs in the liver of NAFLD patients ($P = 0.0362$ and 0.0166 for 8-OHdG and 4-HNE, respectively; Fig. 4b,c). Among the 6 TSGs, methylation of the *RASSF1* is most positively correlated with progression of 8-OHdG deposit ($P = 0.0065$, Fig. S3a), whereas, methylation of the *CDKN2A* is detected regardless of the degree of 8-OHdG staining. This trend is also observed in the 4-HNE staining (Fig. S3b). Then, we calculated ORs for detecting increased oxidative damage; methylation of *RASSF1* is most positively (OR = 10.9 and 3.97 for 8-OHdG and 4-HNE, receptively), and the *CDKN2A* is negatively (OR = 0.30 and 0.23 for 8-OHdG and 4-HNE) correlated with increase of 8-OHdG and 4-HNE (Table S7).

Association of methylation events and expression of the corresponding genes. We confirmed the association of methylation event with suppression of the corresponding gene expression using NAFLD-related HCC cases. Increase of methylation level and decrease of expression is observed in all the 6 TSGs examined in HCCs compared to the corresponding NAFLD livers (Fig. S4 and S5). In addition, negative correlation is detected for all the TSGs between the DNA methylation and gene expression levels (Fig. S6).

For the nest step, we induced oxidative stress on Hc cell using H_2O_2 and analyzed the alteration of histone modification and DNA methylation. For this purpose, we selected the promoter of *CDKN2A* because this locus did not show any DNA methylation in Hc cells. As shown in Fig. S7a, increase of repressive histone marker (3MeK27H3) and decrease of active histone marker (3MeK4H3 and Ack16H4) is detected after the treatment with H_2O_2. In addition, induction of DNA methylation is observed in the promoter of *CDKN2A* after the treatment (Fig. S7b).

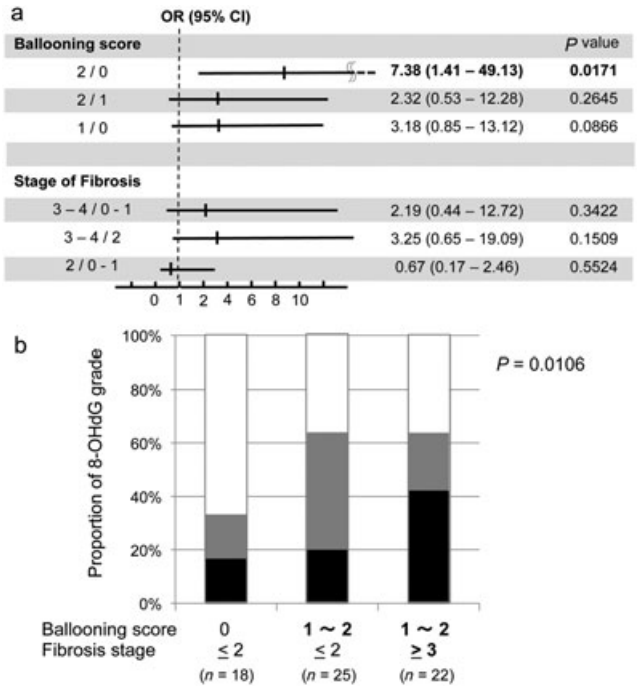

Figure 3 Associations between ballooning score, stage of fibrosis, and degree of 8-OHdG staining. (a) Odds ratios (OR) of each ballooning score and stage of fibrosis for relative risk of detecting moderate/strong 8-OHdG staining are shown. Compared to a ballooning score of 0, score of 2 shows an OR of 7.38 ($P = 0.0171$). Similarly, the OR of ballooning score 1 vs. 0 is 3.18 ($P = 0.0866$). (b) Classification of samples based on the combination of ballooning and fibrosis is associated with 8-OHdG levels. Ballooning score and fibrosis stage were determined by the criteria described by Kleiner et al. and Brunt et al. Among 65 samples, 18 showed a ballooning score of 0 and fibrosis stage of ≤2. Of these samples, 3 showed strong 8-OHdG staining, and 3 and 12 showed moderate and weak 8-OHdG staining, respectively. Similarly, 25 had a ballooning score of 1 or 2 (1-2) and fibrosis stage of ≤2. Five had strong 8-OHdG staining, 11 had moderate staining, and 9 had weak staining. Twenty-two had a ballooning score of 1 or 2 (1-2) and fibrosis stage of ≥3. The degree of 8-OHdG staining was strong in 9 samples, moderate in 10 samples, and weak in 3 samples. *P* value was calculated by Pearson's chi-squared test. □, weak; ■, moderate; ■, strong.

Discussion

Recent advancements in antiviral therapy will likely contribute to a reduction in viral hepatitis-associated HCC.[14] On the contrary, NAFLD-related liver cirrhosis and HCC is increasing due to a prevalence of metabolic disorders.[15] Therefore, detection of a high-risk population for HCC emergence is a top priority for management of NAFLD, where HCC could emerge even in the liver without severe fibrosis.[15] More importantly, as there is no effective treatment for NASH with advanced fibrosis,[1] an intervention for NAFLD patients should be conducted in the early stage of disease.

Previously, we reported that number of methylated TSGs in CHC was closely associated with emergence of HCC in cases without any history of liver cancer.[9] As oxidative stress is also considered to play a critical role in the pathogenesis of NAFLD,[5,15] it is conceivable that 8-OHdG could be a predictive marker for HCC development even in NAFLD patients.[9,11] In this study, we evaluated the clinical and pathological findings that were related to the accumulation of 8-OHdG in hepatocytes, which is important for identifying NAFLD patients at increased risk for developing HCC.

Among the clinical variables analyzed, sex and height showed a borderline association with accumulation of 8-OHdG. However, a multivariate analysis failed to show a significant association. As postmenopausal female generally represent shorter high, it could be possible that postmenopausal female might be prone to DNA oxidation in hepatocyte. However, these parameters could be accidentally selected because of small cohort of the patients. On the other hand, serum AST/ALT ratio, AFP level and Fib-4 index are closely associated with severe accumulation of 8-OHdG. It is known that the AST/ALT ratio and AFP level could be markers for severity of hepatocyte injury.[16] In addition, high serum AFP level is independently associated with moderate/strong 8-OHdG staining. Importantly, serum AFP level reportedly acts as a predictive marker of HCC emergence in CHC patients with sustained virological response.[17] Hepatocellular damage could also lead to a high Fib-4 index because AST and ALT levels are required for the index calculation, although Fib-4 is known as a surrogate marker of liver fibrosis.[18] We also confirmed that degree of 8-OHdG was significantly associated with 4-HNE levels that could be another marker of oxidative damage. Therefore, a high degree of 8-OHdG should be a consequence of continuous oxidative stress and cellular damage, and increased serum AFP reflects the accumulation of 8-OHdG in hepatocytes.

We also found a strong association between NAS score and 8-OHdG staining. It is reported that hepatic 8-OHdG significantly correlate with necro-inflammation grade.[5] In this study, inflammation score tend to be higher in the liver with strong oxidative DNA damage; however, ballooning is most closely associated with accumulation of 8-OHdG, which has not been reported so far. Ballooning reflects hepatocellular injury, and more importantly, it is correlated with insulin resistance.[19] Our analysis also showed that patients with a high degree of ballooning showed high HOMA-R, although not significant ($P = 0.0862$, data not shown). Although the underlying pathogenesis of ballooning remains elusive, oxidative fat injury, endoplasmic reticulum dysfunction, and cytoskeletal injury are observed in ballooned hepatocytes,[20] suggesting that these cells are under severe oxidative stress. Although we found that fibrosis stage was also associated with oxidative DNA damage, ballooning was the only independent pathologic factor associated with 8-OHdG levels in hepatocytes. It is possible that continuous cellular damage by oxidation could lead to induction of 8-OHdG and ballooning as well as fibrosis, and the former could be an earlier sign for determining

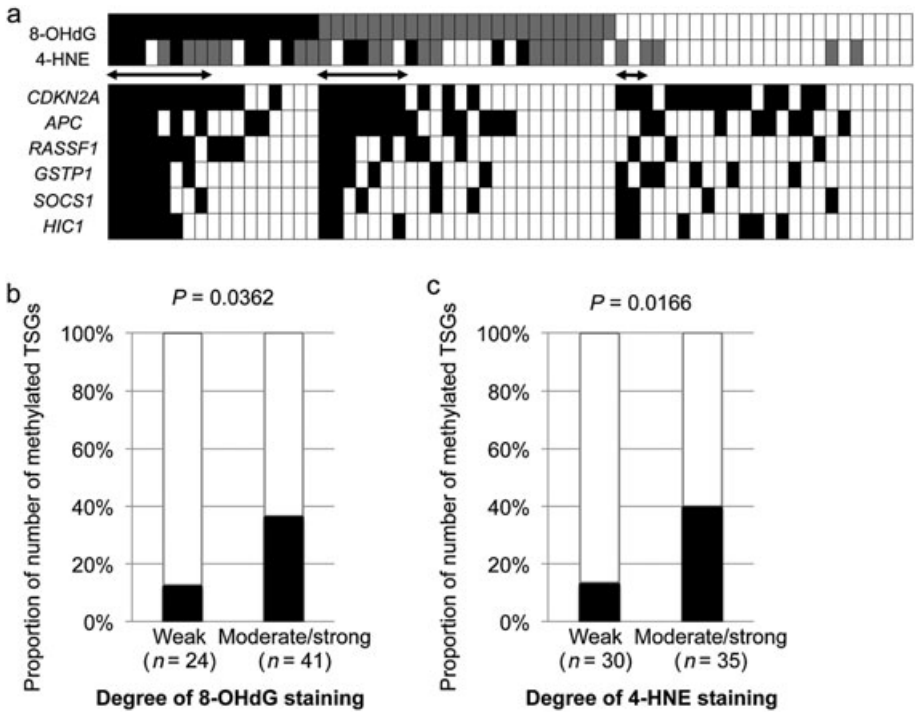

Figure 4 Association of 8-OHdG and 4-HNE levels with number of methylated tumor suppressor genes. (a) Among 65 samples, 17 (26%) showed strong, 24 (37%) were moderate and 24 (37%) showed weak stating of 8-OHdG by IHC. Similarly, 12 samples (18%) showed strong, 23 (35%) were moderate, and 30 (46%) showed weak staining of 4-HNE. Black cells represent the samples with strong IHC staining, grays were moderate, and whites show samples with weak IHC staining for 8-OHdG and 4-HNE. Similarly, among 65 samples, 18 (28%) showed number of methylated TSGs >3 and 47 (72%) had number of methylated TSGs <2, respectively. The black arrows represent the cases with methylated TSGs >3. For the methylation of *APC*, *CDKN2A*, *RASSF1*, *GSTP1*, *SOCS1*, and *HIC1*, black cells denote samples with methylation and white cells denote non-methylated samples. (b) Among 41 samples with moderate/strong 8-OHdG staining, 15 showed >3 methylated TSGs (15/41; 37%). On the contrary, only 3 of 24 samples (3/24; 12.5%) with weak 8-OHdG staining carried >3 methylated TSGs. *P* values were calculated by Pearson's chi-squared test. (c) Among 35 samples with moderate/strong 4-HNE staining, 14 showed >3 methylated TSGs (14/35; 40%).; only 4 of 30 samples (4/30; 13.3%) with weak 4HNE staining carried >3 methylated TSGs. □, Number of methylated TSGs ≤ 2; ■, Number of methylated TSGs ≥ 3.

the risk of HCC. Therefore, it is conceivable that increase of ballooning accompanied by advanced liver fibrosis is the biggest risk for HCC emergence as the combination of ballooning and fibrosis showed clear association with 8-OHdG levels (Fig. 3b).

Finally, we analyzed the methylation levels of 6 TSGs and compared them with those of normal liver that were reported previously.[12] Although assays and individual CpG sites of quantification were different, considerable levels of methylation were detected in NAFLD-liver compared to those of normal liver; their methylation levels were inversely correlated with corresponding gene expressions. Among the TSGs examined, methylation of *RASSF1* was most related to the severe oxidative damage whereas methylation of *CDKN2A* was detected even in early stage of oxidative injury. Although these trends were detected by chance, it might be possible that the *CDKN2A* (*INK4a/ARF*) locus was vulnerable for methylation, and thus, could be an earlier event for oxidative stress-related DNA methylation compared to the *RASSF1*.

As we found that there was a clear association of degree of 8-OHdG with accumulation of methylated TSGs, the degree of 8-OHdG in the livers of NAFLD patients could be a surrogate marker of epigenetic alteration related to hepatocarcinogenesis. However, oxidative stress might also be a risk of carcinogenesis through methylation-independent pathway, we could not determine which was a stronger factor because prospective observation of HCC emergence had not performed. Previously, we reported that TSG methylations were more closely associated with HCC emergence than oxidative DNA damage in HCV-positive livers;[9,11] it should also be confirmed prospectively in NAFLD-related hepatocarcinogenesis. In addition, there are likely to be multiple genes that show abnormal DNA methylation in NASH-related HCC,[11,21] and therefore identifying the driver DNA methylation responsible for hepatocarcinogenesis is required for future analysis.

In this report, we identified that serum AFP level and degree of ballooning showed clear and independent associations with accumulation of oxidative DNA damage in hepatocytes, which could be the seeds of epigenetic alteration of TSGs responsible for hepatocarcinogenesis. Therefore, NAFLD patients showing increased AFP and severe hepatocyte ballooning require intervention through lifestyle modification as well as intensive follow-up for emergence of HCC.

Acknowledgments

The authors thank Ms. Ikuko Kagami and Ms. Mari Kakii for technical assistance.

References

1 Chalasani N, Younossi Z, Lavine JE *et al.* The diagnosis and management of non-alcoholic fatty liver disease: practice Guideline by the American Association for the Study of Liver Diseases, American College of Gastroenterology, and the American Gastroenterological Association. *Hepatology* 2012; **55**: 2005–23.
2 Ludwig J, Viggiano TR, McGill DB, Oh BJ. Nonalcoholic steatohepatitis: Mayo Clinic experiences with a hitherto unnamed disease. *Mayo Clin. Proc.* 1980; **55**: 434–8.
3 Brunt EM, Janney CG, Di Bisceglie AM, Neuschwander-Tetri BA, Bacon BR. Nonalcoholic steatohepatitis: a proposal for grading and staging the histological lesions. *Am. J. Gastroenterol.* 1999; **94**: 2467–74.
4 Kleiner DE, Brunt EM, Van Natta M *et al.* Design and validation of a histological scoring system for nonalcoholic fatty liver disease. *Hepatology* 2005; **41**: 1313–21.
5 Seki S, Kitada T, Yamada T, Sakaguchi H, Nakatani K, Wakasa K. In situ detection of lipid peroxidation and oxidative DNA damage in non-alcoholic fatty liver diseases. *J. Hepatol.* 2002; **37**: 56–62.
6 Tanaka S, Miyanishi K, Kobune M *et al.* Increased hepatic oxidative DNA damage in patients with nonalcoholic steatohepatitis who develop hepatocellular carcinoma. *J. Gastroenterol.* 2013; **48**: 1249–58.
7 O'Hagan HM, Wang W, Sen S *et al.* Oxidative damage targets complexes containing DNA methyltransferases, SIRT1, and polycomb members to promoter CpG Islands. *Cancer Cell* 2011; **20**: 606–19.
8 Nishida N, Kudo M. Oxidative stress and epigenetic instability in human hepatocarcinogenesis. *Dig. Dis.* 2013; **31**: 447–53.
9 Nishida N, Kudo M, Nagasaka T, Ikai I, Goel A. Characteristic patterns of altered DNA methylation predict emergence of human hepatocellular carcinoma. *Hepatology* 2012; **56**: 994–1003.
10 Rowe JW, Wands JR, Mezey E *et al.* Familial hemochromatosis: characteristics of the precirrhotic stage in a large kindred. *Medicine* 1977; **56**: 197–211.
11 Nishida N, Arizumi T, Takita M *et al.* Reactive oxygen species induce epigenetic instability through the formation of 8-hydroxydeoxyguanosine in human hepatocarcinogenesis. *Dig. Dis.* 2013; **31**: 459–66.
12 Nishida N, Nagasaka T, Nishimura T, Ikai I, Boland CR, Goel A. Aberrant methylation of multiple tumor suppressor genes in aging liver, chronic hepatitis, and hepatocellular carcinoma. *Hepatology* 2008; **47**: 908–18.
13 Weisenberger DJ, Siegmund KD, Campan M *et al.* CpG island methylator phenotype underlies sporadic microsatellite instability and is tightly associated with BRAF mutation in colorectal cancer. *Nat. Genet.* 2006; **38**: 787–93.
14 Liang TJ, Ghany MG. Current and future therapies for hepatitis C virus infection. *New Engl J. Med.* 2013; **368**: 1907–17.
15 Hashimoto E, Tokushige K. Hepatocellular carcinoma in non-alcoholic steatohepatitis: Growing evidence of an epidemic? *Hepatol Res.* 2012; **42**: 1–14.
16 Borges LP, Borges VC, Moro AV, Nogueira CW, Rocha JB, Zeni G. Protective effect of diphenyl diselenide on acute liver damage induced by 2-nitropropane in rats. *Toxicology* 2005; **210**: 1–8.
17 Asahina Y, Tsuchiya K, Nishimura T *et al.* alpha-fetoprotein levels after interferon therapy and risk of hepatocarcinogenesis in chronic hepatitis C. *Hepatology* 2013; **58**: 1253–62.
18 Sterling RK, Lissen E, Clumeck N *et al.* Development of a simple noninvasive index to predict significant fibrosis in patients with HIV/HCV coinfection. *Hepatology* 2006; **43**: 1317–25.
19 Brunt EM, Kleiner DE, Wilson LA, Belt P, Neuschwander-Tetri BA, Network NCR. Nonalcoholic fatty liver disease (NAFLD) activity score and the histopathologic diagnosis in NAFLD: distinct clinicopathologic meanings. *Hepatology* 2011; **53**: 810–20.
20 Caldwell S, Ikura Y, Dias D *et al.* Hepatocellular ballooning in NASH. *J. Hepatol.* 2010; **53**: 719–23.
21 Murphy SK, Yang H, Moylan CA *et al.* Relationship between methylome and transcriptome in patients with nonalcoholic fatty liver disease. *Gastroenterology* 2013; **145**: 1076–87.

Supporting Information

Additional supporting information may be found in the online version of this article at the publisher's web-site:

Figure S1. Representatives of immunohistochemical (IHC) staining of 4-hydroxy-2-nonenal (4-HNE) in NAFLD livers.
Figure S2. Relationship between lipid oxidation and oxidative DNA damage in NAFLD liver.
Figure S3. Relationship between each degree of oxidative damage and progression of methylation event of individual genes in NAFLD liver.
Figure S4. Representative images of COBRA for each methylation locus in NAFLD-related HCC and non-cancerous liver.
Figure S5 Methylation level and corresponding gene expression in NAFLD-related HCC and non-cancerous liver.
Figure S6. Correlation between methylation level and corresponding gene expression in NAFLD patients.
Figure S7. Alteration of 8-OHdG levels, histone modification and methylation status after H_2O_2 treatment at the CDKN2A (INK4a/ARF) locus.
Table S1. Clinicopathological findings of the NAFLD patients at the time of biopsy.
Table S2. Clinicopathological findings of the 16 NAFLD-related HCC patients at the time of surgery.
Table S3. Classification of degree of oxidative DNA damage and lipid oxidation based on immunohistochemistry (IHC) staining.
Table S4. Details of reaction conditions for expression assay of the genes of interest.
Table S5. Statistical analyses used in this study.
Table S6. Methylation level of each gene in NAFLD liver analyzed using MethyLight.
Table S7. Odds ratios of methylation at each locus for detecting increased oxidative damage markers.

Liver Cancer

Liver Cancer 2016;5:269–279
DOI: 10.1159/000449338
Published online: September 14, 2016

2235-1795/16/0054-0269$39.50/0
www.karger.com/lic

Original Paper

Feasibility of Extracted-Overlay Fusion Imaging for Intraoperative Treatment Evaluation of Radiofrequency Ablation for Hepatocellular Carcinoma

Yuki Makino[a] Yasuharu Imai[a] Takumi Igura[a] Sachiyo Kogita[a]
Yoshiyuki Sawai[a] Kazuto Fukuda[a] Takayuki Iwamoto[a]
Junya Okabe[a] Manabu Takamura[b] Norihiko Fujita[b]
Masatoshi Hori[c] Tetsuo Takehara[d] Masatoshi Kudo[e]
Takamichi Murakami[f]

Departments of [a]Gastroenterology and [b]Radiology, Ikeda Municipal Hospital, Ikeda, Departments of [c]Radiology and [d]Gastroenterology and Hepatology, Osaka University Graduate School of Medicine, Suita, Departments of [e]Gastroenterology and Hepatology and [f]Radiology, Kinki University Faculty of Medicine, Osaka-Sayama, Japan

Key Words
Contrast-enhanced ultrasonography · Extracted-overlay fusion imaging · Hepatocellular carcinoma · Multimodality fusion imaging · Radiofrequency ablation

Abstract
Background and Aims: Extracted-overlay fusion imaging is a novel computed tomography/magnetic resonance–ultrasonography (CT/MR-US) imaging technique in which a target tumor with a virtual ablative margin is extracted from CT/MR volume data and synchronously overlaid on US images. We investigated the applicability of the technique to intraoperative evaluation of radiofrequency ablation (RFA) for hepatocellular carcinoma (HCC). ***Methods:*** This retrospective study analyzed 85 HCCs treated with RFA using extracted-overlay fusion imaging for guidance and evaluation. To perform RFA, an electrode was inserted targeting the tumor and a virtual 5-mm ablative margin overlaid on the US image. Following ablation, contrast-enhanced US (CEUS) was performed to assess the ablative margin, and the minimal ablative margins were categorized into three groups: (I) margin <0 mm (protrusion), (II) margin 0 to <5 mm, and (III) margin ≥5 mm. Margin assessment was based on the positional relationship between the overlaid tumor plus margin and the perfusion defect of the ablation

Yasuharu Imai, MD, PhD
Department of Gastroenterology, Ikeda Municipal Hospital
3-1-18 Johnan, Ikeda, Osaka 563-8510 (Japan)
Tel. +81 72 751 2881, E-Mail yasuimai@hosp.ikeda.osaka.jp

KARGER

Liver Cancer 2016;5:269–279
DOI: 10.1159/000449338
Published online: September 14, 2016

zone. Tumors in group I underwent repeat ablation until they were in groups II or III. The final classifications were compared with those obtained by retrospectively created fusion images of pre- and post-RFA CT or MR imaging (CT-CT/MR-MR fusion imaging). ***Results:*** Treatment evaluation was impossible using CEUS in six HCCs because the tumors were located far below the body surface. Of the remaining 79 HCCs, the categorizations of minimal ablative margins between CEUS extracted-overlay fusion imaging and CT-CT/MR-MR fusion imaging were in agreement for 72 tumors (91.1%) (Cohen's quadratic-weighted kappa coefficient 0.66, good agreement, $p<0.01$). ***Conclusions:*** Extracted-overlay fusion imaging combined with CEUS is feasible for the evaluation of RFA and enables intraoperative treatment evaluation without the need to perform contrast-enhanced CT.

Introduction

The introduction of multimodality fusion imaging technology has improved the effectiveness of radiofrequency ablation (RFA) for hepatocellular carcinoma (HCC). Computed tomography/magnetic resonance–ultrasonography (CT/MR-US) fusion imaging, which enables the synchronous display of real-time US images and cross-sectional multiplanar reconstruction CT or MR images, is reportedly useful for RFA treatment guidance [1–7]. Moreover, although pre- and post-RFA CT or MR images have been conventionally compared side-by-side to evaluate therapeutic responses, pre- and post-RFA CT-CT/MR-MR fusion images have made it possible to more accurately measure minimal ablative margins [8–14].

The CT/MR-US extracted-overlay fusion imaging technique was developed recently [15]. In this novel technique, a target tumor with a virtual ablative margin is extracted from CT/MR volume data and synchronously overlaid on US images (fig. 1). By virtue of the clear visualization of the tumor and ablative margin, this technique provides effective RFA treatment guidance. This technique has potential for evaluation of RFA treatment by combination with contrast-enhanced US (CEUS) [16–18]. In the present study, we analyzed the feasibility of extracted-overlay fusion imaging for intraoperative and quantitative RFA treatment evaluation, and compared the results with those of CT-CT/MR-MR fusion imaging.

Patients and Methods

Patients and Tumors

Our institutional review board approved this retrospective study, and informed consent was waived. The two inclusion criteria were as follows: (1) HCCs that underwent radical RFA using a Cool-tip RF Ablation System (Covidien, Boulder, CO, USA) and extracted-overlay fusion imaging from March 2013 to January 2014, and (2) HCCs for which CT-CT/MR-MR fusion imaging was available for RFA treatment evaluation using CT or MR images taken ≤2 months before RFA and within 1 month after RFA. Of 101 consecutive patients with 139 HCC nodules who underwent RFA during that period, 68 patients with 85 HCCs that met the inclusion criteria were analyzed. The patients' clinical characteristics are presented in table 1. The diagnosis of HCC was established based on typical contrast-enhanced CT or MR imaging features [19]. When typical imaging findings were not observed, a tumor biopsy was performed to confirm the diagnosis of HCC.

CT/MR-US Fusion Imaging and Extracted-Overlay Fusion Imaging

Volume Navigation (GE Healthcare, Milwaukee, WI, USA) installed in a LOGIQ E9 imaging system (GE Healthcare) was used for CT/MR-US fusion imaging. The imaging modality that most clearly depicted the target tumor was used to produce the reference images. For extracted-overlay fusion imaging, a tumor was segmented from CT or MR imaging volume data and a 5-mm virtual ablative margin was added

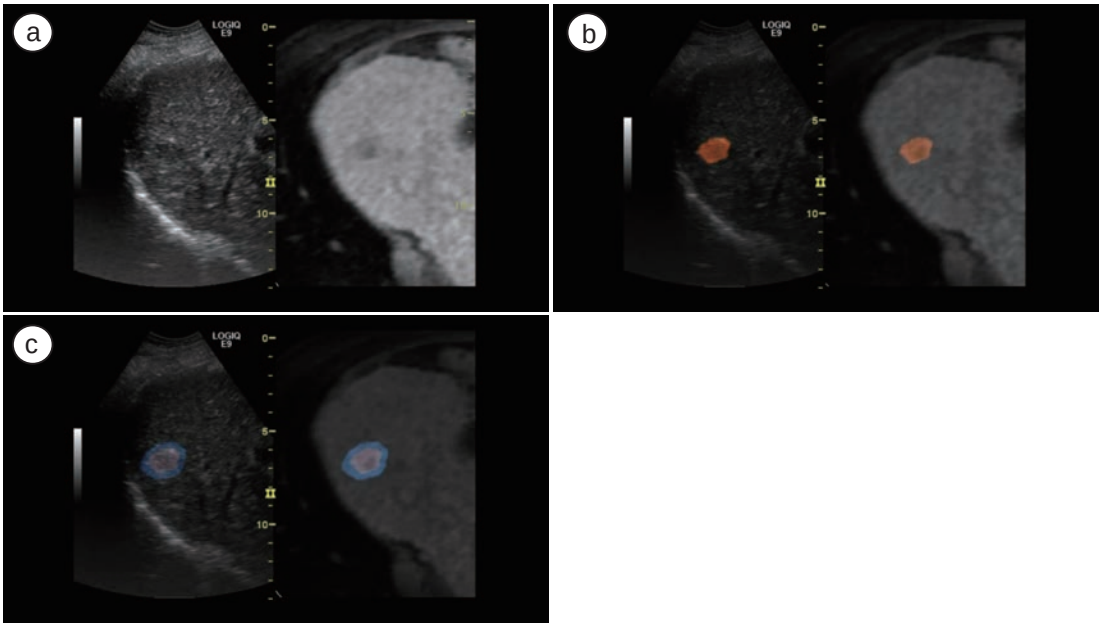

Fig. 1. Extracted-overlay fusion imaging in a 66-year-old woman with HCC in segment VIII. The tumor identified on the hepatobiliary-phase Gd-EOB-DTPA-MR image was used as the reference image and was overlaid on the real-time ultrasonography (US) image. **a** Conventional MR-US fusion imaging. **b** The extracted-overlay fusion image overlies the target tumor only. **c** The extracted-overlay fusion image overlies the target tumor (pink portion) and a 5-mm virtual ablative margin (blue portion) is added.

Table 1. Characteristics of 68 patients with 85 HCCs treated with RFA using extracted-overlay fusion imaging

Characteristic	Value
Age (years)	76 (52–89) †
Gender (male/female)	41/27
Etiology (HBV/HCV/others)	9/52/7
Tumor diameter (mm)	11.9 (4.4–37.0) †
Tumor vascularity (hypervascular/hypovascular)	75/10
Imaging modalities used for the extracted-overlay function (arterial phase of dynamic CT/portal phase of dynamic CT/CTHA/CTAP/ arterial phase of Gd-EOB-DTPA-enhanced MR imaging /hepatobiliary phase of Gd-EOB-DTPA-enhanced MR imaging)	10/2/7/5/1/60
Size of the exposed tip of the Cool-tip needle (2 cm/3 cm)	74/11
Number of ablations per tumor at the first treatment session	2 (1–5) †
Number of treatment sessions per tumor before complete ablation (1/2/3)	80/4/1
Follow-up period (months)	17 (3–27) †

†Median (range). HBV=hepatitis B virus; HCV=hepatitis C virus; CTHA=CT during hepatic arteriography; CTAP=CT during arterial portography.

to the segmented tumor on an image processing workstation (Advantage Workstation VolumeShare 4; GE Healthcare). These procedures have been described in detail in the literature [3, 5, 15].

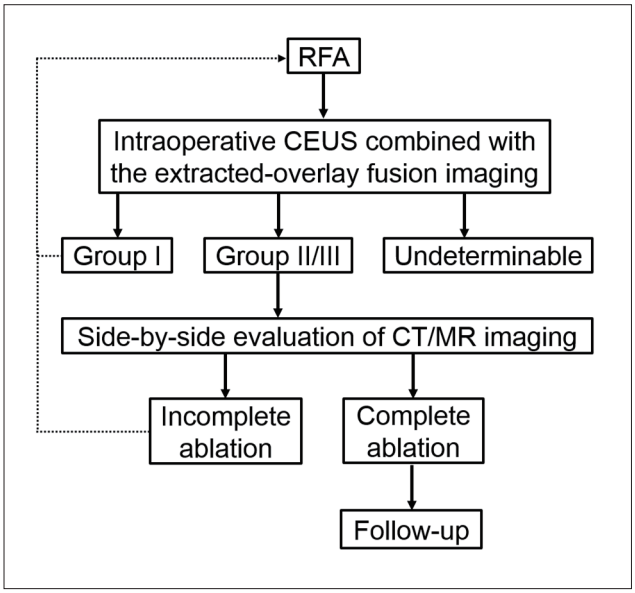

Fig. 2. Flow chart of the treatment procedures in this study.

RFA Procedures and Intraoperative Treatment Evaluation by CEUS Using Extracted-Overlay Fusion Imaging

A flow chart of the treatment and evaluation procedures is presented in fig. 2. One of three hepatologists with more than 10 years' experience performed the RFA procedure using a single 2- or 3-cm Cool-tip electrode. Using extracted-overlay fusion imaging, an electrode was inserted, the overlaid image of the tumor with a 5-mm margin was targeted, and ablation was conducted. Overlapping ablation was added as necessary. Following ablation, the therapeutic effect was assessed by CEUS using 0.0075 ml/kg of perfluorobutane microbubble (Sonazoid; Daiichi-Sankyo, Tokyo, Japan). The perfusion defect of the ablation zone was scanned in the vascular phase (0–120 s after administration of Sonazoid), with the image of the tumor plus a 5-mm margin overlaid on the CEUS image. Any additional tumors were subsequently evaluated. The RFA operator classified the minimal ablative margins into three groups based on the positional relationship between the overlaid tumor plus margin and the perfusion defect: (I) margin <0 mm (tumor extends outside the ablation zone), (II) margin 0 to <5 mm, and (III) margin ≥5 mm (fig. 3). The CEUS criterion for complete ablation was classification as group II or III. Tumors in group I underwent immediate repeat ablation until they were classified into group II or III.

RFA Treatment Evaluation by Side-by-Side CT or MR Imaging and Subsequent Follow-Up

The effectiveness of RFA treatment was evaluated by dynamic CT or gadolinium ethoxybenzyl diethylenetriamine pentaacetic acid-enhanced MR (Gd-EOB-DTPA-MR) imaging within 30 days after RFA. A radiologist with more than 10 years' experience in abdominal radiology compared the pre- and post-RFA images side by side. The two criteria for complete ablation were no signs of early enhancement and circumferential extension of the ablation zone beyond the estimated tumor boundary. The tumor underwent repeat ablation until both criteria were satisfied. After complete ablation, a follow-up contrast-enhanced CT/MR image was obtained every 3 to 4 months. Local tumor progression was defined as the appearance of early enhancement and washout adjacent to the ablation zone.

Retrospective Treatment Evaluation by CT-CT/MR-MR Fusion Imaging

One radiologist with more than 10 years' experience in abdominal radiology and who was blinded to the intraoperative CEUS data created CT-CT or MR-MR fusion images for this study. Minimal ablative margins were measured three-dimensionally and classified into three groups in the same manner as that done for intraoperative CEUS (fig. 4). The detailed procedures of fusion image creation have been described in previous reports [8, 13].

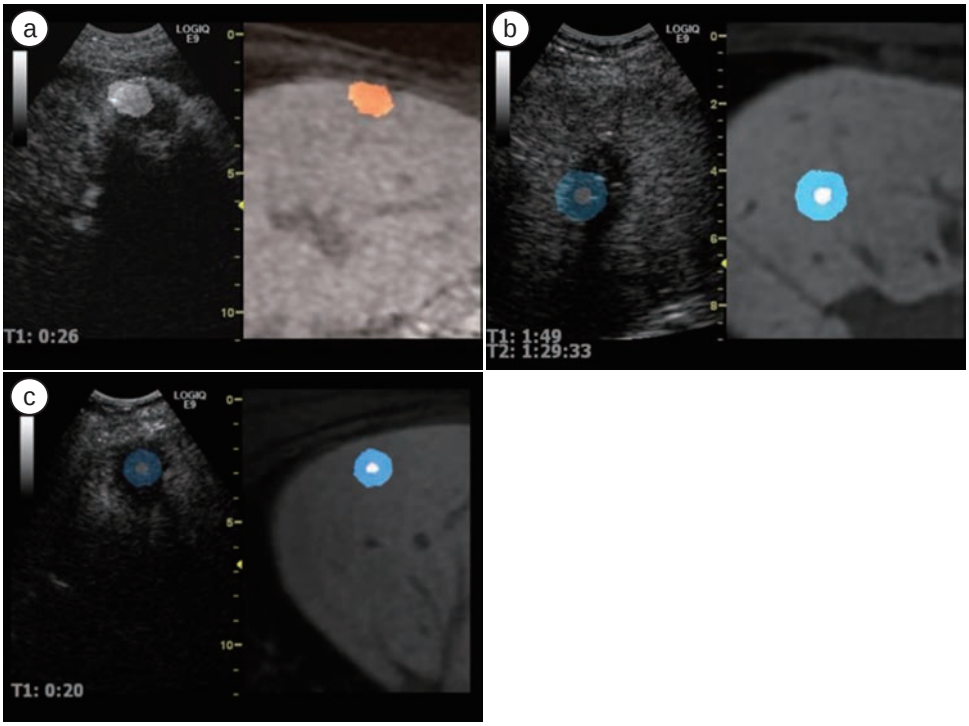

Fig. 3. Categorization of minimal ablative margins after RFA using extracted-overlay fusion imaging combined with CEUS. **a** Group I: margin <0 mm (tumor extends outside the ablation zone); **(b)** group II: margin 0 to <5 mm; **(c)** group III: margin ≥5 mm.

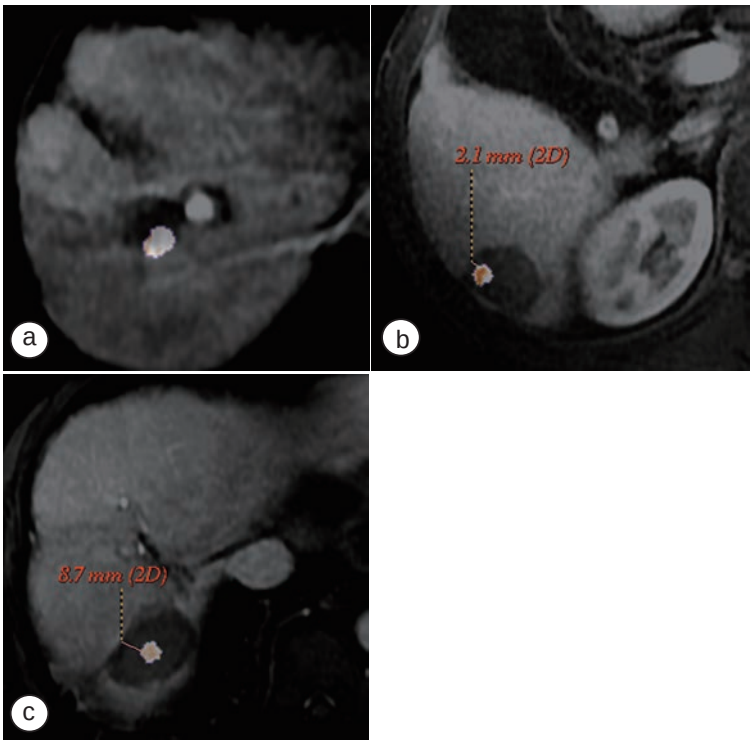

Fig. 4. Categorization of minimal ablative margins after RFA by CT-CT/MR-MR fusion imaging. **a** Group I: margin <0 mm (tumor extends outside the ablation zone); **(b)** group II: margin 0 to <5 mm; **(c)** group III: margin ≥5 mm. MR-MR fusion images are presented in this figure.

Image Acquisition

Dynamic CT and CT angiography were performed using a 64-channel multidetector row helical CT system (Discovery CT 750HD; GE Healthcare) with slice thicknesses of 1.25 and 0.625 mm, respectively. MR images were acquired with a 1.5-T MR system (Signa Excite HD 1.5T; GE Healthcare). The slice thicknesses of the dynamic- and hepatobiliary-phase Gd-EOB-DTPA-MR images were 3 or 5 mm. The protocols for image acquisition have been described in the literature [13, 15].

Statistical Analysis

We evaluated the rate of concordance of the judgments of complete/incomplete ablation between intraoperative CEUS and side-by-side CT/MR evaluation after RFA. The overall agreement of the classification of the minimal ablative margin (i.e., into groups I, II, or III) between intraoperative CEUS and CT-CT/MR-MR fusion imaging was expressed by Cohen's quadratic-weighted kappa coefficient (poor agreement, k=0-0.20; slight agreement, k=0.21–0.40; moderate agreement, k=0.41–0.60; good agreement, k=0.61–0.80; excellent agreement, k=0.81–1.00). The cumulative local tumor progression rate for each ablative margin group was estimated by the Kaplan–Meier method, and statistical significance was analyzed by the log-rank test. SPSS version 18.0 software (SPSS, Chicago, IL, USA) was used for all statistical analyses, and a p value of less than 0.05 was considered to be statistically significant.

Results

All patients were treated without severe complications. Moving images of the treatment procedures and intraoperative CEUS are presented in Electronic Supplementary Material 1 (for all online suppl.material, see www.karger.com/doi/10.1159/000443561). The preparation of extracted-overlay fusion imaging, including image processing on a workstation and image alignment on an US unit, took less than 25 min in all cases. Treatment evaluation using intraoperative CEUS took less than 10 min for all tumors.

Treatment Evaluation of the First RFA Session

In 6 of the 85 HCCs (7.1%) the therapeutic response was impossible to evaluate because of CEUS signal attenuation problems with tumors located distant from the body surface. In the remaining 79 HCCs, the intraoperative CEUS evaluations were compared with both the side-by-side CT/MR evaluations and the retrospectively created CT-CT/MR-MR fusion imaging evaluations.

During intraoperative CEUS of the first RFA treatment session, the number of tumors evaluated as belonging to groups I, II, and III were 2 (2.5%), 71 (89.9%), and 6 (7.6%), respectively. Complete ablation (groups II and III) was achieved in 77 HCCs (97.5%) according to the CEUS criteria. It was impossible to perform additional ablation during the first treatment session for two HCCs in group I because of the patients' physical exhaustion. The median tumor diameters in groups I, II, and III were 16.1 (15.0–17.2) mm, 12.0 (4.4–37.0) mm, and 10.2 (8.7–13.4) mm, respectively.

During the side-by-side CT/MR evaluation after the first treatment session, 75 of 79 HCCs (94.9%) were judged to be completely ablated, and treatment was thus ended for these 75 patients. Four HCCs (5.1%) were considered to be incompletely ablated. The judgment regarding complete or incomplete ablation was in agreement between CEUS and side-by-side CT/MR evaluation in 77 of 79 HCCs (97.5%) (table 2).

Next, we retrospectively created CT-CT/MR-MR fusion imaging using images recorded before and after the first treatment session and categorized tumor ablation margins into three groups in the same manner as was done for CEUS. This new categorization was compared with that obtained by intraoperative CEUS after the first treatment session in 79 HCCs. The median registration error of CT-CT/MR-MR fusion imaging was 1.3 mm (range, 0.44–2.9 mm), and the median minimal ablative margin was 1.6 mm (range, −28.3 to 10.4 mm).

Table 2. Judgment of complete or incomplete ablation by intraoperative CEUS with extracted-overlay fusion imaging and by side-by-side CT/MR evaluation

		Side-by-side CT/MR evaluation		
		Incomplete	Complete	Total
CEUS	Incomplete	2	0	2
	Complete	2	75	77
	Total	4	75	79

Table 3. Categorization of minimal ablative margin by intraoperative CEUS with extracted-overlay fusion imaging and by CT-CT/MR-MR fusion imaging after the first treatment session

		CT-CT/MR-MR fusion imaging			
		Group I	Group II	Group III	Total
CEUS	Group I	2	0	0	2
	Group II	6	65	0	71
	Group III	0	1	5	6
	Total	8	66	5	79

Group I: margin <0 mm (tumor extends outside the ablation zone); group II: margin 0 to <5 mm; group III: margin ≥5 mm.

The numbers and median diameters of HCCs in groups I, II, and III were 8 (10.1%) and 14.7 (6.7–19.7) mm, 66 (83.5%) and 11.8 (4.4–37.0) mm, and 5 (6.3%) and 10.1 (8.7–23.6) mm, respectively. The categorization of minimal ablative margins after the first treatment session assessed using intraoperative CEUS corresponded with that of CT-CT/MR-MR fusion imaging in 72 HCCs (91.1%), and the overall agreement was good (k=0.66; 95% confidence interval, 0.42–0.90; p<0.01) (table 3).

Treatment Evaluation after the Final RFA Session and Cumulative Local Tumor Progression Rate

After the first RFA treatment session, repeat ablation was conducted in four HCCs judged to be incompletely ablated by intraoperative CEUS and/or by side-by-side CT/MR evaluation (table 2), resulting in complete ablation based on both CEUS and side-by-side CT/MR criteria. After the final RFA treatment session, the numbers of tumors in groups I, II, and III were 0 (0.0%), 73 (92.4%), and 6 (7.6%), respectively, based on intraoperative CEUS evaluation. The 1-year cumulative local tumor progression rates in groups II and III were 8.9% and 0.0%, respectively (fig. 5).

Discussion

The effectiveness of RFA treatment has conventionally been assessed by side-by-side comparison of pre- and post-RFA CT images [8–14, 20]. However, because this side-by-side interpretation tends to be inaccurate, several new methods have been developed for more accurate treatment evaluation, such as nonenhanced MR imaging [21], superparamagnetic iron oxide-MR imaging [22, 23], Gd-EOB-DTPA-MR imaging [24], and iodized oil retention [25]. CT-CT/MR-MR fusion imaging was recently developed and is considered to be a useful imaging modality for RFA evaluation in terms of its accuracy, quantitative nature, noninvasiveness, and applicability to hypovascular lesions [8–14]. In the present study, we analyzed the clinical

Liver Cancer

Liver Cancer 2016;5:269–279
DOI: 10.1159/000449338
Published online: September 14, 2016

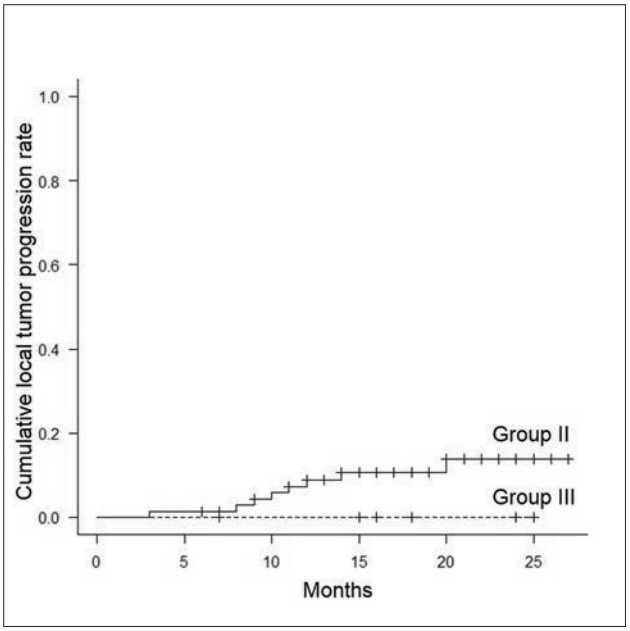

Fig. 5. Cumulative local tumor progression rate of two groups categorized by intraoperative CEUS using extracted-overlay fusion imaging. The 1-year cumulative local tumor progression rates in groups II and III were 8.9% and 0.0%, respectively.

feasibility of extracted-overlay fusion imaging combined with CEUS, a novel CT/MR-US fusion imaging technique [15], for intraoperative RFA treatment evaluation.

By comparing intraoperative CEUS extracted-overlay fusion imaging evaluations with conventional side-by-side CT/MR evaluations, we investigated the concordance rate of the judgment of complete ablation. A high rate of concordance was observed between intraoperative CEUS and side-by-side CT/MR evaluations after RFA (table 2). Only 2 of 79 HCCs (2.5%) judged to be completely ablated on CEUS were categorized as incompletely ablated according to the side-by-side CT/MR evaluation criteria and therefore required additional treatment sessions. These results suggest that intraoperative CEUS using extracted-overlay fusion imaging is reliable when used to determine the necessity of additional ablation.

We next analyzed the accuracy of the quantitative evaluation of the minimal ablative margin by comparison of intraoperative CEUS extracted-overlay fusion imaging with CT-CT/MR-MR fusion imaging. The minimal ablative margins were categorized into three groups that are reportedly related to local tumor progression [8, 13, 20, 25]. Good agreement was observed between the evaluations based on intraoperative CEUS and CT-CT/MR-MR fusion imaging (table 3). The cumulative local tumor progression rate was stratified according to the intraoperative CEUS categorization (fig. 5). Although the data regarding the cumulative local tumor progression rate are still preliminary, these results suggest the accuracy of quantitative treatment evaluation using intraoperative CEUS with extracted-overlay fusion imaging.

The primary advantage of extracted-overlay fusion imaging combined with CEUS is that the tumor with a virtual safety margin is visible during and after RFA, and the therapeutic effect can subsequently be evaluated using CEUS immediately after ablation, without the need to perform contrast-enhanced CT. When incomplete ablation is suspected on intraoperative CEUS, additional ablation can be immediately performed. This greatly reduces the patients'

physical and mental burden, the length of the hospital stay, and the medical expenses associated with RFA treatment (e.g., cost of the RFA electrodes and CT or MR imaging acquisition for treatment evaluation).

The second advantage of extracted-overlay fusion imaging combined with CEUS is that it enables quantitative measurement of the minimal ablative margin. This imaging technique enables the judgment of whether a ≥5-mm margin can be achieved in addition to the determination of complete ablation of the tumor itself. Thus, the performance of repeat ablation until the tumor and 5-mm virtual margin are completely encompassed by the perfusion defect on CEUS may be an effective strategy to achieve a ≥5-mm margin and thereby prevent local tumor progression from the microsatellite lesions around the tumor [26]. In this study, our aim was the complete ablation of the target tumor itself, not the provision of a ≥5-mm margin. Consequently, some tumors showed local tumor progression post-ablation. However, local tumor progression was not observed at all in group III. Therefore, if the therapeutic goal is set as the achievement of a ≥5-mm margin in all cases, the local tumor progression rate will likely be further improved. The third advantage is the noninvasiveness of CEUS. This technique does not cause radiation exposure and can be applied to patients with poor renal function or who are allergic to iodine.

A disadvantage of extracted-overlay fusion imaging is that it is influenced by the tumor location. In the present study, treatment evaluation was impossible using CEUS in 6 HCCs (7.1%) located far below the body surface because of signal attenuation. Moreover, 5 of 8 HCCs (62.5%) regarded as incompletely ablated on CT-CT/MR-MR fusion imaging after the first treatment session were located just beneath the diaphragm. Registration of US and CT/MR reference images might be somewhat inaccurate in this region because of the lack of appropriate landmarks such as branching vessels. Therefore, careful assessment should be performed for HCCs located deep below the body surface or just beneath the diaphragm.

The limitations of this study are its retrospective nature and the inclusion of only a small number of patients. Prospective studies are needed to assess whether this novel evaluation method will eliminate the necessity for contrast-enhanced CT after RFA.

In conclusion, extracted-overlay fusion imaging combined with CEUS is clinically feasible for intraoperative and quantitative evaluation of the effectiveness of RFA treatment and could improve the efficacy of RFA.

Conflict of Interest

All authors declare that there are no conflicts of interest.

References

1 Wood BJ, Kruecker J, Abi-Jaoudeh N, Locklin JK, Levy E, Xu S, Solbiati L, Kapoor A, Amalou H, Venkatesan AM: Navigation systems for ablation. J Vasc Interv Radiol 2010;21(Suppl):S257–S263.
2 Krücker J, Xu S, Venkatesan A, Locklin JK, Amalou H, Glossop N, Wood BJ: Clinical utility of real-time fusion guidance for biopsy and ablation. J Vasc Interv Radiol 2011;22:515–524.

3 Makino Y, Imai Y, Igura T, Ohama H, Kogita S, Sawai Y, Fukuda K, Ohashi H, Murakami T: Usefulness of the multimodality fusion imaging for the diagnosis and treatment of hepatocellular carcinoma. Dig Dis 2012;30:580–587.
4 Kunishi Y, Numata K, Morimoto M, Okada M, Kaneko T, Maeda S, Tanaka K: Efficacy of fusion imaging combining sonography and hepatobiliary phase MRI with Gd-EOB-DTPA to detect small hepatocellular carcinoma. AJR Am J Roentgenol 2012;198:106–114.
5 Makino Y, Imai Y, Ohama H, Igura T, Kogita S, Sawai Y, Fukuda K, Takamura M, Ohashi H, Murakami T: Ultrasonography fusion imaging system increases the chance of radiofrequency ablation for hepatocellular carcinoma with poor conspicuity on conventional ultrasonography. Oncology 2013;84(Suppl 1):44–50.
6 Lee MW, Rhim H, Cha DI, Kim YJ, Choi D, Kim YS, Lim HK: Percutaneous radiofrequency ablation of hepatocellular carcinoma: fusion imaging guidance for management of lesions with poor conspicuity at conventional sonography. AJR Am J Roentgenol 2012;198:1438–1444.
7 Jung EM, Friedrich C, Hoffstetter P, Dendl LM, Klebl F, Agha A, Wiggermann P, Stroszcynski C, Schreyer AG: Volume navigation with contrast enhanced ultrasound and image fusion for percutaneous interventions: first results. PLoS ONE 2012;7:e33956.
8 Makino Y, Imai Y, Igura T, Hori M, Fukuda K, Sawai Y, Kogita S, Ohama H, Matsumoto Y, Nakahara M, Zushi S, Kurokawa M, Isotani K, Takamura M, Fujita N, Murakami T: Utility of computed tomography fusion imaging for the evaluation of the ablative margin of radiofrequency ablation for hepatocellular carcinoma and the correlation to local tumor progression. Hepatol Res 2013;43:950–958.
9 Kim YS, Lee WJ, Rhim H, Lim HK, Choi D, Lee JY: The minimal ablative margin of radiofrequency ablation of hepatocellular carcinoma (> 2 and < 5 cm) needed to prevent local tumor progression: 3D quantitative assessment using CT image fusion. AJR Am J Roentgenol 2010;195:758–765.
10 Kim KW, Lee JM, Klotz E, Kim SJ, Kim SH, Kim JY, Han JK, Choi BI: Safety margin assessment after radiofrequency ablation of the liver using registration of preprocedure and postprocedure CT images. AJR Am J Roentgenol 2011;196:W565–W572.
11 Tomonari A, Tsuji K, Yamazaki H, Aoki H, Kang JH, Kodama Y, Sakurai Y, Maguchi H: Feasibility of fused imaging for the evaluation of radiofrequency ablative margin for hepatocellular carcinoma. Hepatol Res 2013;43:728–734.
12 Passera K, Selvaggi S, Scaramuzza D, Garbagnati F, Vergnaghi D, Mainardi L: Radiofrequency ablation of liver tumors: quantitative assessment of tumor coverage through CT image processing. BMC Med Imaging 2013;13:3.
13 Makino Y, Imai Y, Igura T, Hori M, Fukuda K, Sawai Y, Kogita S, Fujita N, Takehara T, Murakami T: Comparative evaluation of three-dimensional Gd-EOB-DTPA-enhanced MR fusion imaging with CT fusion imaging in the assessment of treatment effect of radiofrequency ablation of hepatocellular carcinoma. Abdom Imaging 2015;40:102–111.
14 Sakakibara M, Ohkawa K, Katayama K, Imanaka K, Ishihara A, Hasegawa N, Kimura H: Three-dimensional registration of images obtained before and after radiofrequency ablation of hepatocellular carcinoma to assess treatment adequacy. AJR Am J Roentqenol 2014;202:W487–W495. [Medline]
15 Makino Y, Imai Y, Igura T, Kogita S, Sawai Y, Fukuda K, Hori M, Kudo M, Murakami T: Usefulness of the extracted-overlay function in CT/MR-ultrasonography fusion imaging for radiofrequency ablation of hepatocellular carcinoma. Dig Dis 2013;31:485–489.
16 Guibal A, Bertin C, Egels S, Savier E, Grenier PA, Lucidarme O: Contrast-enhanced ultrasound (CEUS) follow-up after radiofrequency ablation or cryoablation of focal liver lesions: treated-area patterns and their changes over time. Eur Radiol 2013;23:1392–1400.
17 Inoue T, Kudo M, Hatanaka K, Arizumi T, Takita M, Kitai S, Yada N, Hagiwara S, Minami Y, Sakurai T, Ueshima K, Nishida N: Usefulness of contrast-enhanced ultrasonography to evaluate the post-treatment responses of radiofrequency ablation for hepatocellular carcinoma: comparison with dynamic CT. Oncology 2013;84(Suppl 1):51–57.
18 Numata K, Fukuda H, Morimoto M, Kondo M, Nozaki A, Oshima T, Okada M, Takebayashi S, Maeda S, Tanaka K: Use of fusion imaging combining contrast-enhanced ultrasonography with a perflubutane-based contrast agent and contrast-enhanced computed tomography for the evaluation of percutaneous radiofrequency ablation of hypervascular hepatocellular carcinoma. Eur J Radiol 2012;81:2746–2753.
19 Onishi H, Kim T, Imai Y, Hori M, Nagano H, Nakaya Y, Tsuboyama T, Nakamoto A, Tatsumi M, Kumano S, Okada M, Takamura M, Wakasa K, Tomiyama N, Murakami T: Hypervascular hepatocellular carcinomas: detection with gadoxetate disodium-enhanced MR imaging and multiphasic multidetector CT. Eur Radiol 2012;22:845–854.
20 Nakazawa T, Kokubu S, Shibuya A, Ono K, Watanabe M, Hidaka H, Tsuchihashi T, Saigenji K: Radiofrequency ablation of hepatocellular carcinoma: correlation between local tumor progression after ablation and ablative margin. AJR Am J Roentgenol 2007;188:480–488.
21 Koda M, Tokunaga S, Miyoshi K, Kishina M, Fujise Y, Kato J, Matono T, Okamoto K, Murawaki Y, Kakite S: Assessment of ablative margin by unenhanced magnetic resonance imaging after radiofrequency ablation for hepatocellular carcinoma. Eur J Radiol 2012;81:2730–2736.
22 Mori K, Fukuda K, Asaoka H, Ueda T, Kunimatsu A, Okamoto Y, Nasu K, Fukunaga K, Morishita Y, Minami M: Radiofrequency ablation of the liver: determination of ablative margin at MR imaging with impaired clearance of ferucarbotran—feasibility study. Radiology 2009;251:557–565.
23 Koda M, Tokunaga S, Miyoshi K, Kishina M, Fujise Y, Kato J, Matono T, Murawaki Y, Kakite S, Yamashita E: Ablative margin states by magnetic resonance imaging with ferucarbotran in radiofrequency ablation for hepatocellular carcinoma can predict local tumor progression. J Gastroenterol 2013;48:1283–1292.

Liver Cancer

Liver Cancer 2016;5:269–279

DOI: 10.1159/000449338
Published online: September 14, 2016

24 Okubo H, Kokubu S, Komiyama M, Yamagata H, Uchiyama A, Miyazaki A, Watanabe S: Radiofrequency ablation of hepatocellular carcinoma: the feasibility of magnetic resonance imaging with gadolinium ethoxybenzyl diethylene triamine pentaacetic acid for evaluating the ablative margin. Hepatol Res 2010;40:1034–1041.
25 Nishikawa H, Inuzuka T, Takeda H, Nakajima J, Sakamoto A, Henmi S, Matsuda F, Eso Y, Ishikawa T, Saito S, Kita R, Kimura T, Osaki Y: Percutaneous radiofrequency ablation therapy for hepatocellular carcinoma: a proposed new grading system for the ablative margin and prediction of local tumor progression and its validation. J Gastroenterol 2011;46:1418–1426.
26 Okusaka T, Okada S, Ueno H, Ikeda M, Shimada K, Yamamoto J, Kosuge T, Yamasaki S, Fukushima N, Sakamoto M: Satellite lesions in patients with small hepatocellular carcinoma with reference to clinicopathologic features. Cancer 2002;95:1931–1937.

Annals of Oncology 27: 2090–2096, 2016
doi:10.1093/annonc/mdw323
Published online 29 August 2016

Sorafenib plus hepatic arterial infusion chemotherapy with cisplatin versus sorafenib for advanced hepatocellular carcinoma: randomized phase II trial

M. Ikeda[1*], S. Shimizu[1], T. Sato[2], M. Morimoto[3], Y. Kojima[4], Y. Inaba[5], A. Hagihara[6], M. Kudo[7], S. Nakamori[8], S. Kaneko[9], R. Sugimoto[10], T. Tahara[11], T. Ohmura[12], K. Yasui[13], K. Sato[14], H. Ishii[15], J. Furuse[16] & T. Okusaka[17]

[1]Department of Hepatobiliary and Pancreatic Oncology, National Cancer Center Hospital East, Kashiwa; [2]Department of Biostatistics, Kyoto University School of Public Health, Kyoto; [3]Department of Hepatobiliary and Pancreatic Medical Oncology, Kanagawa Cancer Center, Yokohama; [4]Department of Gastroenterology, National Center for Global Health and Medicine Center Hospital, Tokyo; [5]Department of Diagnostic and Interventional Radiology, Aichi Cancer Center Hospital, Nagoya; [6]Department of Hepatology, Osaka City University Hospital, Osaka; [7]Department of Gastroenterology and Hepatology, Kinki University School of Medicine, Osaka; [8]Department of Hepatobiliary and Pancreatic Surgery, Osaka National Hospital, Osaka; [9]Department of Gastroenterology, Kanazawa University Hospital, Kanazawa; [10]Department of Hepato-Biliary-Pancreatology, National Hospital Organization Kyushu Cancer Center, Fukuoka; [11]Department of Gastroenterology, Saiseikai Utsunomiya Hospital, Tochigi; [12]Department of Gastroenterology, Sapporo Kosei General Hospital, Sapporo; [13]Department of Molecular Gastroenterology and Hepatology, Kyoto Prefectural University of Medicine, Kyoto; [14]Institute for Advancement of Clinical and Translational Science, Kyoto University Hospital, Kyoto; [15]Clinical Research Center, Shikoku Cancer Center, Matsuyama; [16]Department of Medical Oncology, Kyorin University, Tokyo; [17]Department of Hepatobiliary and Pancreatic Oncology, National Cancer Center Hospital, Tokyo, Japan

Received 24 April 2016; revised 11 July 2016; accepted 4 August 2016

Background: Sorafenib (Sor) is acknowledged as a standard therapy for advanced hepatocellular carcinoma (HCC). This trial was conducted to evaluate the effect of addition of hepatic arterial infusion chemotherapy with cisplatin (SorCDDP) to Sor for the treatment of advanced HCC.

Patients and methods: We conducted a multicenter open-labeled randomized phase II trial in chemo-naïve patients with advanced HCC with Child-Pugh scores of 5–7. Eligible patients were randomly assigned 2:1 to receive SorCDDP (sorafenib: 400 mg bid; cisplatin: 65 mg/m^2, day 1, every 4–6 weeks) or Sor (400 mg bid). The primary end point was overall survival.

Results: A total of 108 patients were randomized (Sor, $n = 42$; SorCDDP, $n = 66$). The median survival in the Sor and SorCDDP arms were 8.7 and 10.6 months, respectively [stratified hazard ratio (95% confidence interval), 0.60 (0.38–0.96), $P = 0.031$]. The median time to progression and the response rate were, respectively, 2.8 months and 7.3% in the Sor arm and 3.1 months and 21.7% in the SorCDDP arm. The adverse events were more frequent in the SorCDDP arm than in the Sor arm, but well-tolerated.

Conclusion: SorCDDP yielded favorable overall survival when compared with Sor in patients with advanced HCC.

Clinical Trial registration: UMIN-CTR (http://www.umin.ac.jp/ctr/index-j.htm), identification number: UMIN000005703.

Key words: cisplatin, hepatic arterial infusion chemotherapy, hepatocellular carcinoma, sorafenib, randomized phase II trial

introduction

Sorafenib is currently acknowledged as a standard therapy for advanced hepatocellular carcinoma (HCC), and is available worldwide [1]. After the introduction of sorafenib, a number of phase III trials of various molecular-targeted agents versus sorafenib as first-line chemotherapy have been conducted, but none of the agents examined so far has shown superior survival benefit to sorafenib [1].

Hepatic arterial infusion chemotherapy (HAIC) is employed to treat patients with advanced HCC [2, 3]. This treatment modality is associated with increased local concentrations of the anticancer agents in the tumor and reduced systemic distribution of the drugs, and a stronger antitumor effect and lower incidence of systemic adverse reactions may be expected when compared with systemic chemotherapy. In fact, high response rates, favorable long-term outcomes, and acceptable toxicities with some chemotherapeutic regimens of HAIC have been

*Correspondence to: Dr Masafumi Ikeda, Department of Hepatobiliary and Pancreatic Oncology, National Cancer Center Hospital East, 6-5-1 Kashiwanoha, Kashiwa 277–8577, Japan. Tel: +81-4-7133-1111; Fax: +81-4-7133-0335; E-mail: masikeda@east.ncc.go.jp

reported [2, 3]. However, no consensus has been reached as to its place as a standard treatment of advanced HCC. Among HAI regimens, cisplatin alone can be easily administered using the Seldinger technique, without the need for an indwelling reservoir system [4]. In addition, sorafenib has been shown to interact with platinum transporter proteins [5], and to exert a synergistic anticancer effect with cisplatin in preclinical research [6]. Clinical trials of sorafenib used in combination with cisplatin have been carried out for various cancers [7–9], and favorable outcomes have been reported. Herein, we report the results of a randomized phase II trial of sorafenib plus HAIC with cisplatin (SorCDDP) versus sorafenib alone (Sor). The primary end point was the overall survival, while the secondary end points were the time to progression, response rate, and adverse events.

methods-patients and methods

patient eligibility

The patient inclusion criteria were as follows: advanced HCC confirmed histologically or by typical findings of hypervascular tumor on computed tomography (CT) or angiography and elevated serum alpha-fetoprotein (AFP), or protein induced by vitamin K absence or antagonist-II level; unsuitable for surgical resection, liver transplantation, local ablative therapy or transarterial chemoembolization (TACE); no prior history of chemotherapy; age 20–79 years old; presence of intrahepatic tumors affecting the prognosis irrespective of the presence of extrahepatic tumors; Eastern Cooperative Oncology Group Performance Status 0–1; adequate organ function [neutrophil count ≥1500 /mm^3, hemoglobin ≥8.5 g/dl, platelet count ≥60 000 /mm^3, serum total bilirubin ≤2.0 mg/dl, serum albumin ≥2.8 g/dl, aspartate aminotransferase (AST) and alanine aminotransferase (ALT) ≤5 times the upper limits of normal, serum creatinine ≤1.2 mg/dl, creatinine clearance ≥60 ml/min]; Child-Pugh score 5–7; HAIC technically feasible; written informed consent.

The main exclusion criteria were as follows: refractory pleural effusion or ascites; hepatic encephalopathy; severe and active co-morbidity or concomitant malignancy; allergic reaction to iodine contrast medium precluding angiography; pregnant and lactating females; females of childbearing age unless using effective contraception; and unsatisfactory general condition. Patients with hepatitis B or C virus infection were eligible for enrollment in this trial, provided they fulfilled the eligibility criterion pertaining to hepatic reserve.

treatments

The enrolled patients were randomly assigned 2:1 to the SorCDDP arm or the Sor arm. Randomization was done centrally using a minimization method with biased-coin assignment [10]. The dynamic allocation factors were the presence of portal vein tumor thrombosis and extrahepatic metastasis. In patients of the SorCDDP arm, based on the results of a phase I trial [11], sorafenib (Nexavar®, Bayer Health Care Pharmaceuticals; West Haven, CT, USA) was administered orally at a dose of 400 mg bid, and cisplatin (IA call®, Nippon Kayaku Co., Ltd; Tokyo, Japan) was administered concurrently at 65 mg/m^2/cycle via a catheter placed in the proper, right, or left hepatic artery, or another feeding artery, every 4–6 weeks. In patients of the Sor arm, sorafenib was administered orally at a dose of 400 mg bid. The sorafenib treatment in both arms was continued until tumor progression or unacceptable toxicity, and the HAIC with cisplatin was administered up to a maximum of six cycles until radiological or symptomatic tumor progression, unacceptable toxicity, or technical difficulty in repeating the HAIC. If the protocol therapies were discontinued, the patient was allowed to receive other anticancer treatment at the physician's discretion.

The occurrence of grade 4 hematological toxicity, grade 3 non-hematological toxicity was generally considered as indication for suspending the sorafenib administration. When the toxicities improved by at least one grade when compared with the suspension criteria, the treatment was resumed at a reduced dose of 400 mg daily. If additional dose reduction was required, the dose was reduced further to a single administration of 400 mg every other day.

The criteria for administering HAIC with cisplatin were as follows: neutrophil count ≥1200/mm^3, platelet count ≥50 000/mm^3, serum total bilirubin ≤3.0 mg/dl, serum AST or ALT levels ≤5 times the upper limit of normal, and a serum creatinine level ≤1.5 mg/dl. If the above parameters did not fall within the starting criteria, the HAIC with cisplatin was postponed until the criteria were fulfilled.

response and toxicity assessment

Evaluation of the tumor response by dynamic CT or MRI was carried out every 6 weeks using the modified Response Evaluation Criteria in Solid Tumors (RECIST) [12]. The responses were evaluated centrally by three independent reviewers. Overall survival was measured from the date of enrollment to the date of death or the date of the last follow-up. Time to progression was defined as the time from the date of enrollment to the first documentation of disease progression or death. Assessment of adverse events was based on the National Cancer Institute Common Toxicity Criteria, version 4.0.

statistical analysis

This was a multicenter open-labeled randomized phase II trial. The primary end point was overall survival stratified by the allocation factors, including the presence/absence of portal vein tumor thrombosis and extrahepatic metastases. If the median survival associated with Sor were assumed as 7.0 months and that of SorCDDP as 9.5 months, the hazard ratio (HR) was 0.74. SorCDDP would be judged as being favorable if the HR is 0.74 or lower. A total of 105 patients were needed to estimate the 1-year survival rate with an accuracy of ±10%. This study did not have sufficient statistical power to permit formal statistical comparison between the two arms.

The differences in the categorical data between the two groups were analyzed by Wilcoxon's test. The overall survival time and time to progression were estimated by using the Kaplan–Meier method and the curves were compared using the log-rank test. HRs of the treatment effects were estimated using a Cox regression model, and stratified results by dynamic allocation factors, including the presence/absence of portal vein tumor thrombosis and extrahepatic metastasis, as well as unstratified results, were presented. This clinical trial was conducted with the approval of the review board of each participating institution and in accordance with the Declaration of Helsinki. This trial is registered with UMIN-CTR (http://www.umin.ac.jp/ctr/index-j.htm), identification number (UMIN000005703). Patient registration, random treatment allocation, and data collection were managed by the Japan Clinical Research Support Unit data center. The integrity of the data was ensured through careful review by the staff of the data center, the coordinating investigators (MI and SS), and the trial statistician (TS). All the data were fixed on 28 December 2014, and all the analyses of efficacy were carried out based on the full analysis set (FAS) by the TS using SAS 9.4 and JMP Pro 11.

results

patient characteristics

From June 2011 to December 2013, a total of 108 patients were enrolled and randomized into the two treatment arms (Figure 1). Forty-two patients were assigned to the Sor arm and 66 patients to the SorCDDP arm. While the planned random assignment was 2:1, the actual randomization ratio was 1.6:1, which was within random error. One patient from each of the arms could not receive the chemotherapy (development of paraplegia due to disease progression in one patient of the Sor arm,

and withdrawal of informed consent in one patient of the SorCDDP arm). Therefore, the FAS included 41 patients in the Sor arm and 65 patients in the SorCDDP arm.

The patient characteristics of the 106 patients of the FAS are presented in Table 1. Seropositivity for hepatitis C viral antibody was more frequent in the Sor arm ($n = 20$, 48.8%) than in the SorCDDP arm ($n = 18$, 27.7%), and portal vein tumor thrombosis was less frequent in the Sor arm ($n = 17$, 41.5%) than in the SorCDDP arm ($n = 40$, 61.5%). In terms of all other variables, the patient characteristics were well-balanced.

treatments

By the data cutoff point, the protocol treatment had been discontinued in 41 patients of the Sor arm and 62 patients of the SorCDDP arm. The median number of cisplatin administrations and the median total dose of cisplatin in the SorCDDP arm were two times (range, 1–6 times) and 222 mg (range, 70–709 mg), respectively. The median dose intensity (range) was 488 mg/day (146–800 mg) in the Sor arm and 540 mg/day (193–800 mg) in the SorCDDP arm ($P = 0.70$). The proportion of patients in whom dose reduction of sorafenib was necessitated was 49.2% in the Sor arm and 63.4% in the SorCDDP arm. The median treatment duration (range) was 86 days (16–449 days) in the Sor arm and 75 days (4–881 days) in the SorCDDP arm ($P = 0.58$). After termination of the protocol treatment, 24 patients (59%) in the Sor arm and 40 patients (61.5%) in the SorCDDP arm received subsequent therapies, as follows: HAIC (8 and 19 patients, respectively), TACE (8 and 14 patients, respectively), local ablation (1 and 2 patients, respectively), other systemic chemotherapy (11 and 32 patients, respectively), palliative resection (2 and 5 patients, respectively), and radiotherapy (0 and 9 patients, respectively).

efficacy

At the final analysis, 37 patients of the Sor arm and 49 patients of the SorCDDP arm had died. The median survivals in the Sor and SorCDDP arms were 8.7 and 10.6 months, respectively (Figure 2A). The HR stratified by the allocation factors, including the presence/absence of portal vein tumor thrombosis and extrahepatic metastases (95% CI), was 0.60 (0.38–0.96), and P-value was 0.031. The crude HR [95% confidence interval (CI)] was 0.68 (0.44–1.049) ($P = 0.073$). The forest plot showing the pre-specified subgroup analyses of overall survival is shown in Figure 3. The patient subgroup with serum AFP <400 ng/ml showed a better overall survival in the SorCDDP arm (median 14.8 months) than in the Sor arm (median 8.7 months) ($P = 0.042$). At the data cutoff point, disease progression was

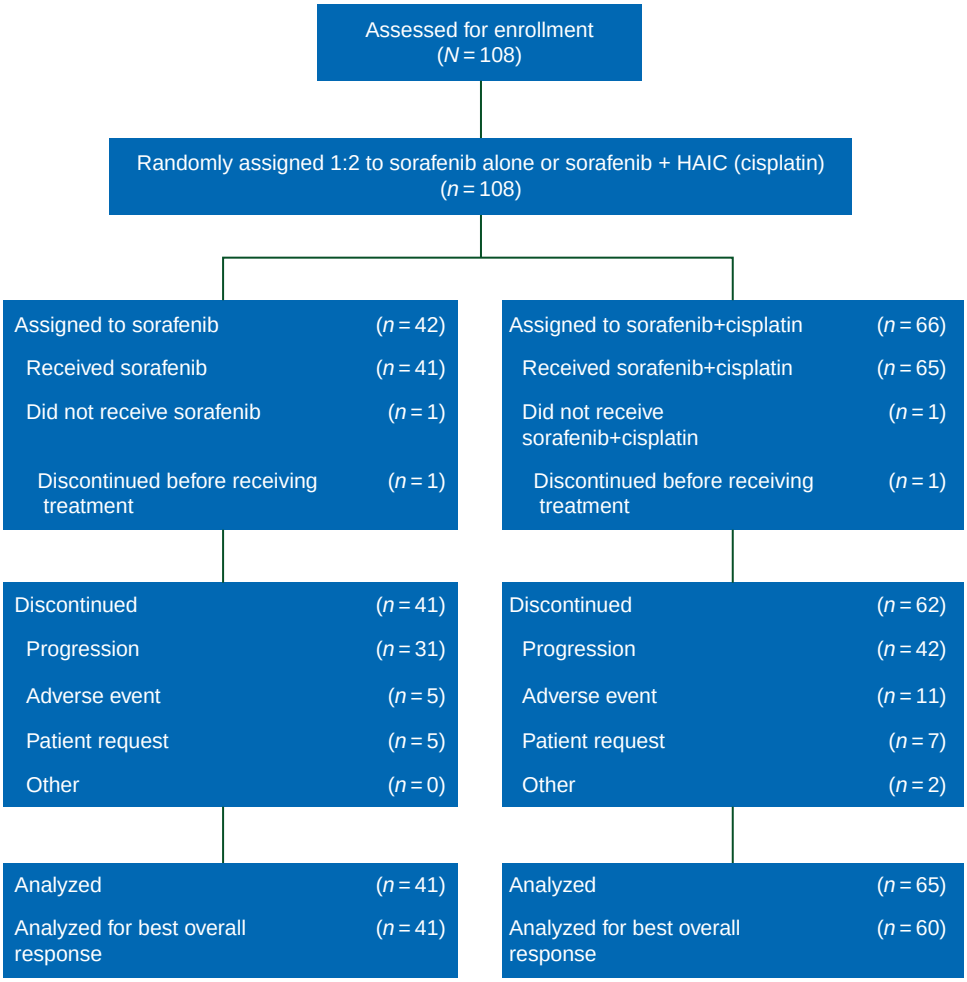

Figure 1. Consort diagram.

observed in 39 patients in the Sor arm and 61 patients in the SorCDDP arm. The median time to progression was 2.8 months in the Sor arm and 3.1 months in the SorCDDP arm (Figure 2B). The crude HR was 0.78 (95% CI, 0.52–1.16,

Table 1. Baseline patient characteristics

Characteristics	Sorafenib alone ($n = 41$)		Sorafenib + HAIC (cisplatin) ($n = 65$)	
	Number of patients	%	Number of patients	%
Age, years				
Median	64		66	
Range	42–78		25–79	
Sex				
Male	32	78.1	56	86.2
Female	9	22.0	9	13.8
ECOG performance status				
0	33	80.5	50	76.9
1	8	19.5	15	23.1
Etiology				
Hepatitis B	9	22.0	22	33.8
Hepatitis C	20	48.8	18	27.7
Child-Pugh score				
5	27	65.9	38	58.5
6	12	29.3	19	29.2
7	2	4.9	8	12.3
Ascites	4	9.8	10	15.4
Previous therapy	21	51.2	33	50.8
Resection	6		17	
PEI/RFA	7		8	
TACE	14		23	
Radiation	1		1	
Other	2		1	
BCLC stage				
B	16	39.0	19	29.2
C	25	61.0	46	70.8
Portal vein tumor thrombosis	17	41.5	40	61.5
Vp1	0		4	10.0
Vp2	4	23.5	9	22.5
Vp3	7	41.4	14	35.0
Vp4	6	35.3	13	32.5
Extrahepatic spread	13	31.7	19	29.2
Lung	6		8	
Bone	3		1	
Lymph node	6		10	
Adrenal	1		1	
Other	2		4	
Number of tumors				
1	4	9.8	8	12.3
2	3	7.3	5	7.7
3	1	2.4	1	1.5
4	3	7.3	5	7.7
≥5	30	73.2	46	70.8
Maximum tumor size, cm				
Median	5.2		5.1	
Range	1.1–17.5		1.0–20.0	
Serum α-fetoprotein, ng/ml				
Median	188		223.5	
Range	2–749 412		1.2–394 944	
PIVKA II, mAU/ml				
Median	1790		1772	
Range	9–1 410,000		10–261 920	

ECOG, Eastern Cooperative Oncology Group; PEI/RFA, percutaneous ethanol injection/radiofrequency ablation; TACE, transarterial chemoembolization; BCLC, Barcelona Clinic Liver Cancer Group; Vp1, tumor thrombosis distal to the second branches of the portal vein; Vp2, tumor thrombosis in the second branches of the portal vein; Vp3, tumor thrombosis in the first branches of the portal vein; Vp4, tumor thrombosis in the main trunk of the portal vein or the opposite side branch of the portal vein; PIVKA II, protein induced by vitamin K absence or antagonist-II.

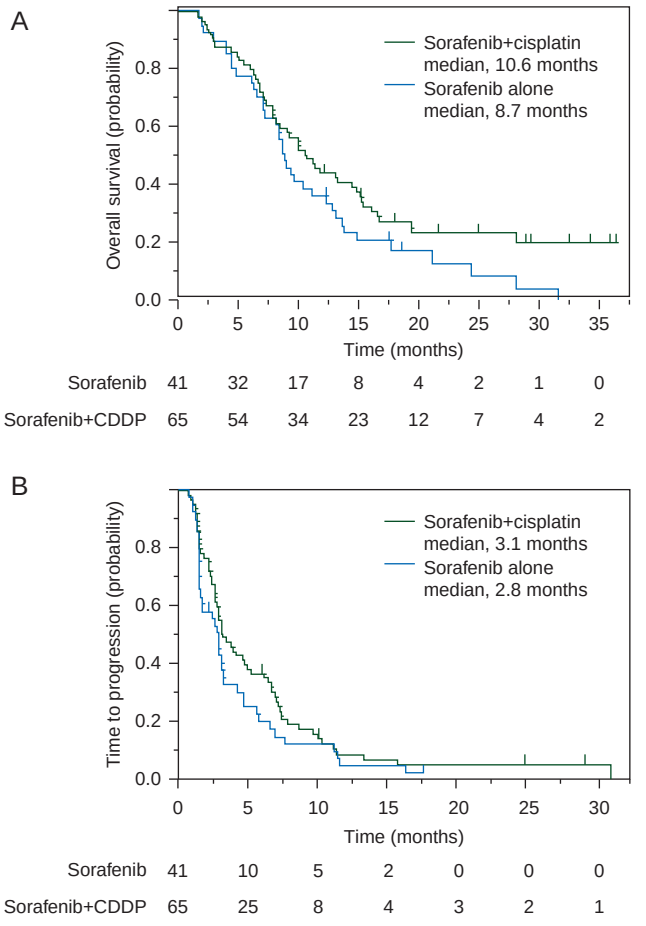

Figure 2. Kaplan–Meier curves of overall survival (A) and time to progression (B) in the sorafenib arm (blue line) and sorafenib plus hepatic arterial infusion chemotherapy with cisplatin arm (green line). The tick marks indicate censored cases.

$P = 0.212$) and the HR stratified by the allocation factors was 0.78 (95% CI, 0.50–1.21, $P = 0.257$).

In the judgment by the central review, the number of patients evaluable by the modified RECIST criteria was 41 in the Sor arm and 60 patients in the SorCDDP arm. The response rate (95% CI) was 7.3% (1.5–19.9%) in the Sor arm and 21.7% (12.1–34.2%) in the SorCDDP arm ($P = 0.09$) (supplementary Figure 1, available at *Annals of Oncology* online).

adverse events

The adverse events in both the arms during the entire treatment period until the final analysis are presented in Table 2. Neutropenia, leukocytopenia, decreased hemoglobin, thrombocytopenia, hyponatremia, nausea, and hiccups of all grades were more frequent in the SorCDDP arm than in the Sor arm. There were two treatment-related deaths in this series: one developed liver failure 9 months after the initiation of SorCDDP therapy, and the other developed pulmonary infection 2 months after the initiation of Sor therapy.

discussion

In this study, SorCDDP yielded favorable overall survival when compared with Sor in patients with advanced HCC. The pre-specified HR stratified by the allocation factors (95% CI) was 0.60 (0.38–0.96), and *P*-value was 0.031. Because we had set the condition that SorCDDP would be judged as favorable if the HR for overall survival was 0.74 or lower, the primary end point of this study was met. In the pre-specified subgroup analysis of overall survival, the SorCDDP arm showed more favorable overall survival than the Sor arm in all the subgroups, and the efficacy of SorCDDP can be anticipated in almost all subjects who are suitable candidates for sorafenib treatment. In this trial, patients with hepatitis C viral infection showed a more favorable overall survival following sorafenib treatment than those with hepatitis B viral infection. However, it remains unknown whether patients with hepatitis C viral infection actually benefitted more from this treatment or not, because of the small sample size of this study. Furthermore, the overall survival in the SorCDDP arm was better than that in the Sor arm among the patients with serum AFP <400 ng/ml [crude HR, 0.53 (95% CI, 0.28–0.99)], whereas no difference was observed between the SorCDDP arm and the Sor arm among the patients with serum AFP ≥400 ng/ml. AFP may be one of the predictive biomarkers in patients receiving SorCDDP therapy, although the reason remains unknown.

Recently, immuno-oncology agents, such as tremelimumab [13] and nivolumab [14], have been introduced as promising agents for advanced HCC. The characteristics of these agents

		Sorafenib alone		Sorafenib + Cisplatin				
	Patients	Median OS (months)	Events/ Patients	Median OS (months)	Events/ Patients	P	HR	95% CI
Full analysis set								
	106	8.7	37	10.6	49	.073	0.677	0.440 to 1.040
Refractory to TACE								
Yes	33	8.3	12/13	7.4	16/20	.461	0.749	0.347 to 1.619
No	73	9.4	25/28	11.6	33/45	.120	0.663	0.393 to 1.118
Portal vein tumor thrombosis								
Yes	57	7.1	15/17	9.1	32/40	.086	0.579	0.308 to 1.090
No	49	11.6	22/24	12.9	17/25	.173	0.646	0.342 to 1.220
Extrahepatic spread								
Yes	32	7.0	12/13	9.9	16/19	.177	0.595	0.277 to 1.277
No	74	9.9	25/28	13.0	33/46	.219	0.721	0.428 to 1.217
ECOG performance status								
0	83	8.7	30/33	10.8	37/50	.130	0.689	0.424 to 1.120
1	23	8.7	7/8	10.4	12/15	.374	0.654	0.256 to 1.676
Child-Pugh class								
A	96	8.8	35/39	11.6	42/57	.051	0.641	0.408 to 1.007
B	10	3.4	2/2	5.1	7/8	.081	0.203	0.028 to 1.470
Hepatitis C								
Yes	38	9.5	17/20	13.0	13/18	.265	0.662	0.318 to 1.376
No	68	8.0	20/21	10.4	36/47	.104	0.635	0.366 to 1.103
Hepatitis B								
Yes	31	7.0	9/9	8.1	16/22	.092	0.498	0.217 to 1.143
No	75	9.9	28/32	11.6	33/43	.205	0.721	0.434 to 1.198
Serum α-fetoprotein								
≥400 ng/mL	50	8.3	18/19	8.5	27/31	.617	0.859	0.472 to 1.564
<400 ng/mL	56	8.7	19/22	14.8	22/34	.042	0.530	0.284 to 0.986

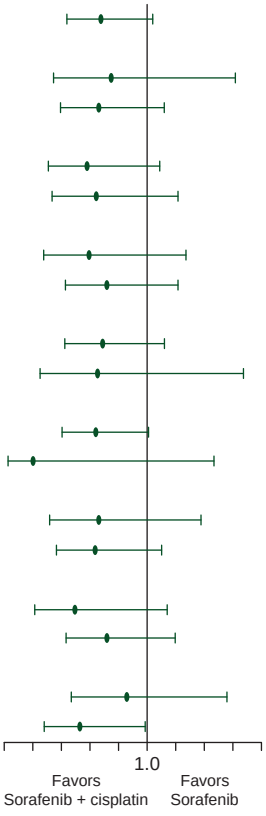

Figure 3. Forest plots showing subgroup analyses of the overall survival. TACE, transarterial chemoembolization; ECOG, Eastern Cooperative Oncology Group; OS, overall survival; HR, hazard ratio; CI, confidence interval.

Table 2. Adverse events

	Sorafenib alone arm						Sorafenib + HAIC (cisplatin) arm					
	All grades		Grade 3		Grade 4		All grades		Grade 3		Grade 4	
	No. of pts	(%)	No. of pts	(%)	No. of pts	(%)	No. of pts	(%)	No. of pts	(%)	No. of pts	(%)
WBC decreased	18	43.9	0	0	0	0	49	75.4	12	18.5	0	0
Neu decreased	18	43.9	0	0	0	0	39	60	8	12.3	2	3.1
Hb decreased	30	73.2	2	4.9	1	2.4	58	89.2	6	9.2	2	3.1
Plt decreased	33	80.5	1	2.4	0	0	58	89.2	19	29.2	0	0
Bilirubin increased	29	70.7	5	12.2	0	0	48	73.8	6	9.2	2	3.1
AST increased	41	100	8	19.5	3	7.3	65	100	21	32.3	1	1.5
ALT increased	37	90.2	7	17.1	1	2.4	61	93.8	12	18.5	1	1.5
γGTP increased	37	90.2	14	34.1	2	4.9	63	96.9	21	32.3	3	4.6
Hypoalbuminemia	32	78	3	7.3	0	0	63	96.9	2	3.1	0	0
Cr increased	11	26.8	0	0	0	0	25	38.5	1	1.5	0	0
Hyponatremia	22	53.7	5	12.2	0	0	53	81.5	18	27.7	0	0
Amylase increased	21	52.5	0	0	0	0	41	64.1	10	15.6	1	1.6
Fatigue	16	39	1	2.4	–	–	28	43.1	7	10.8	–	–
Malaise	17	41.5	–	–	–	–	31	47.7	–	–	–	–
Appetite loss	22	53.7	1	2.4	0	0	45	69.2	4	6.2	2	3.1
Nausea	8	19.5	0	0	–	–	27	41.5	0	0	–	–
Vomiting	5	12.2	0	0	0	0	12	18.5	0	0	0	0
Diarrhea	17	41.5	1	2.4	0	0	23	35.4	4	6.2	0	0
Hand–foot synd	26	63.4	7	17.1	–	–	41	63.1	9	13.8	–	–
Skin rash	11	26.8	2	4.9	0	0	12	18.5	3	4.6	0	0
Hypertension	24	58.5	9	22	0	0	32	49.2	19	29.2	0	0
Hiccups	0	0	0	0	–	–	6	9.2	0	0	–	–

WBC, white blood count; Neu, neutrophils; Hb, hemoglobin; Plt, platelets; AST, aspartate aminotransferase; ALT, alanine aminotransferase; γGTP, γ-glutamyl transpeptidase; Cr, creatinine; synd, syndrome; pts, patients.

are a high response rate and long-lasting antitumor efficacy. In our study also, the response rate in the SorCDDP arm (21.7%) was threefold higher than that in the Sor arm (7.3%), and some patients in the SorCDDP arm showed long-lasting survival over 2 years. With regard to time to progression, the stratified HR by the allocation factors was 0.78 (95% CI, 0.59–1.21), and it was slightly worse than that of overall survival. In some phase III trials conducted for HCC, significant difference was observed in the time to progression or progression-free survival, but not in the overall survival [1]. Eventually, a negative result was concluded. However, in this study, the results were completely opposite. The most important difference between this study and these aforementioned trials may be in the anticancer treatments used: in this study, sorafenib was combined with a cytotoxic agent, while in the aforementioned phase III trials, it was used in combination with other molecular-targeted agents. Among patients showing marked tumor shrinkage on account of the favorable tumor shrinkage effect of SorCDDP, even a slight increase in the tumor size could result in their being classified as showing disease progression, whereas these patients may also show a prolonged overall survival because of the smaller tumor burden. This might also be the reason for the more favorable improvement of the overall survival than the time to progression.

The frequencies of the adverse events in the SorCDDP arm, except for those of neutropenia, leukocytopenia, hypohemoglobinemia, thrombocytopenia, hyponatremia, nausea and hiccups, were similar to those in the Sor arm. These adverse events were not severe. HAIC with cisplatin had only a mild toxicity profile [4] and the toxicities were not overlapped with the adverse effects of sorafenib. Therefore, SorCDDP therapy was also considered to be well-tolerated.

Intra-arterial administration of cisplatin was generally thought to be troublesome, requiring the insertion of a catheter into the tumor-feeding arteries. Recently, a phase III trial of sorafenib plus intra-arterial cisplatin and 5-fluorouracil versus sorafenib alone demonstrated no survival benefit [15]. One of the reasons could be the difficulty in placing the indwelling reservoir system. However, cisplatin is easily administered without the need for an indwelling reservoir system. Furthermore, this combined treatment is medico-economically very viable, because the additional cost of the angiographic procedure and cisplatin is approximately $2000 per session, which is less than the cost of the recently administered molecular-targeted agents or immuno-oncology agents.

In conclusion, this study demonstrated favorable overall survival in the SorCDDP arm when compared with that in the Sor arm in patients with advanced HCC, suggesting the effectiveness of HAIC against advanced HCC. However, since this study was only a randomized phase II trial, we could not arrive at any definitive conclusion with regard to the usefulness of sorafenib plus HAIC with cisplatin in the treatment of advanced HCC. A further phase III trial is being planned to confirm these results.

acknowledgements

We thank all the patients and their families for their participation in this study. We thank the members of the Japan Clinical

Research Support Unit Data Center for their support with the data management (Ms Youko Yoshimoto, Ms Rei Aida, and Mr Takashi Ando), the members of the study committee for safety and efficacy monitoring (Dr Yasuhiro Matsumura, Dr Kei Muro, and Dr Keigo Osuga), the members of the study committee for response evaluation (Dr Tatsushi Kobayashi, Dr Nobumasa Mizuno, and Dr Eiichiro Suzuki), and all the investigators of this trial.

funding

This work was supported in part by the National Cancer Center Research and Development Fund (23-A-22).

disclosure

MI has received payment for lectures from Bayer Yakuhin and Nippon Kayaku; has been a consultant for Bayer Yakuhin; and has received research funding from Bayer Yakuhin. SS has received payment for lectures from Nippon Kayaku. YI has received payment for lectures from Bayer Yakuhin and Nippon Kayaku; and has received research funding from Bayer Yakuhin and Nippon Kayaku. AH has been on the speakers' bureau for Bayer Yakuhin. TO has received payment for lectures from Bayer Yakuhin. JF has received payment for lectures from Bayer Yakuhin and Nippon Kayaku; has been on advisory arrangements for Bayer Yakuhin; and received research funding from Bayer Yakuhin and Nippon Kayaku. TO has received research funding from Bayer Yakuhin and has received payment for lectures from Nippon Kayaku. All remaining authors have declared no conflicts of interest.

references

1. Abou-Alfa GK, Venook AP. The antiangiogenic ceiling in hepatocellular carcinoma: does it exist and has it been reached? Lancet Oncol 2013; 14: e283–e288.
2. Ikeda M, Mitsunaga S, Shimizu S et al. Current status of hepatocellular carcinoma in Japan. Chin Clin Oncol 2013; 240.
3. Kudo M. Treatment of advanced hepatocellular carcinoma with emphasis on hepatic arterial infusion chemotherapy and molecular targeted therapy. Liver Cancer 2012; 1: 62–70.
4. Yoshikawa M, Ono N, Yodono H et al. Phase II study of hepatic arterial infusion of a fine-powder formulation of cisplatin for advanced hepatocellular carcinoma. Hepatol Res 2008; 38: 474–483.
5. Heim M, Scharifi M, Zisowsky J et al. The Raf kinase inhibitor BAY 43-9006 reduces cellular uptake of platinum compounds and cytotoxicity in human colorectal carcinoma cell lines. Anticancer Drugs 2005; 16: 129–136.
6. Wei Y, Shen N, Wang Z et al. Sorafenib sensitizes hepatocellular carcinoma cell to cisplatin via suppression of Wnt/beta-catenin signaling. Mol Cell Biochem 2013; 381: 139–144.
7. Sun W, Powell M, O'Dwyer PJ et al. Phase II study of sorafenib in combination with docetaxel and cisplatin in the treatment of metastatic or advanced gastric and gastroesophageal junction adenocarcinoma: ECOG 5203. J Clin Oncol 2010; 28: 2947–2951.
8. Paz-Ares LG, Biesma B, Heigener D et al. Phase III, randomized, double-blind, placebo-controlled trial of gemcitabine/cisplatin alone or with sorafenib for the first-line treatment of advanced, nonsquamous non-small-cell lung cancer. J Clin Oncol 2012; 30: 3084–3092.
9. Xue C, Huang Y, Huang PY et al. Phase II study of sorafenib in combination with cisplatin and 5-fluorouracil to treat recurrent or metastatic nasopharyngeal carcinoma. Ann Oncol 2013; 24: 1055–1061.
10. Pocock SJ, Simon R. Sequential treatment assignment with balancing for prognostic factors in the controlled clinical trial. Biometrics 1975; 31: 103–115.
11. Hagihara A, Ikeda M, Ueno H et al. Phase I study of combination chemotherapy using sorafenib and transcatheter arterial infusion with cisplatin for advanced hepatocellular carcinoma. Cancer Sci 2014; 105: 354–358.
12. Lencioni R, Llovet JM. Modified RECIST (mRECIST) assessment for hepatocellular carcinoma. Semin Liver Dis 2010; 30: 52–60.
13. Sangro B, Gomez-Martin C, de la Mata M et al. A clinical trial of CTLA-4 blockade with tremelimumab in patients with hepatocellular carcinoma and chronic hepatitis C. J Hepatol 2013; 59: 81–88.
14. El-Khoueiry AB, Melero I, Crocenzi TS et al. Phase I/II safety and antitumor activity of nivolumab in patients with advanced hepatocellular carcinoma (HCC): CA209-040. J Clin Oncol 2015;33 (suppl; abstr LBA101).
15. Ueshima KM, Yokosuka O et al. Prospective randomized controlled phase III trial comparing the efficacy of sorafenib versus sorafenib in combination with low-dose cisplatin/fluorouracil hepatic arterial infusion chemotherapy in patients with advanced hepatocellular carcinoma. J Hepatol 2016; 64: S209–S210 (Abstr LB04).

Liver Cancer

Liver Cancer 2016;5:235–244
DOI: 10.1159/000449335
Published online: September 14, 2016

2235-1795/16/0054-0235$39.50/0
www.karger.com/lic

Editorial

Regorafenib as Second-Line Systemic Therapy May Change the Treatment Strategy and Management Paradigm for Hepatocellular Carcinoma

Prof. M. Kudo

Editor *Liver Cancer*

Introduction

At the European Society of Medical Oncology World Congress of Gastrointestinal Cancer held in Barcelona, Spain, on 30th June 2016, positive outcomes were reported by the Study of Regorafenib after Sorafenib in Patients with Hepatocellular Carcinoma (RESORCE) trial, which investigated the efficacy of regorafenib as second-line therapy after sorafenib failure [1]. In this clinical trial, the group who received regorafenib achieved a survival benefit of approximately 2.8 months compared to the placebo group. Overall survival (OS) was 10.6 months in the regorafenib arm compared with 7.8 months in the placebo arm, with a hazard ratio (HR) of 0.62 (95% confidence interval [CI]: 0.50–0.78; p<0.001). These are groundbreaking results.

The positive outcome achieved by this second-line systemic therapy is a major development, especially after the numerous reports of failures in clinical studies of first-and second-line systemic therapeutic agents (table 1). Regorafenib therapy is expected to significantly prolong life expectancy by approximately 2.8 months in patients with hepatocellular carcinoma (HCC) who develop progressive disease (PD) during sorafenib therapy. This development will certainly lead to drastic changes in the treatment strategy and management paradigm for HCC.

Design of the RESORCE Trial

The RESORCE trial enrolled 573 patients with advanced HCC corresponding to Barcelona Clinic Liver Cancer (BCLC) stage B or C who were unresponsive to sorafenib. The patients were divided into placebo and regorafenib arms at a 1:2 ratio for the daily administration of placebo and oral regorafenib (160 mg), respectively, for three weeks on and one week off

Liver Cancer 2016;5:235–244
DOI: 10.1159/000449335
Published online: September 14, 2016

Table 1. Phase III Clinical Trials of Japanese Participation for HCC

Target population		Design	Trial name	Presentation	Publication
Early	Adjuvant (prevention of recurrence)	1. Peretinoin vs Placebo*	NIK-333	ASCO 2010	JG 2014
		2. Sorafenib vs Placebo*	STORM	ASCO 2014	Lancet-O 2015
		3. Peretinoin vs Placebo	NIK-333/K-333	Ongoing	
Intermediate	Improvement of TACE	1. TACE ± Sorafenib*	Post-TACE	ASCO-GI 2010	EJC 2011
		2. TACE ± Brivanib*	BRISK-TA	ILCA 2013	Hepatol 2014
		3. TACE ± Orantinib*	ORIENTAL	EASL 2015	
Advanced	First line	1. Sorafenib vs Sunitinib*	SUN1170	ASCO 2011	JCO 2013
		2. Sorafenib vs Brivanib*	BRISK-FL	AASLD 2012	JCO 2013
		3. Sorafenib vs Linifanib*	LiGHT	ASCO-GI 2013	JCO 2015
		4. Sorafenib ± HAIC*	SILIUS	EASL 2016	
		5. Sorafenib vs Lenvatinib	REFLECT	Ongoing	
		6. Sorafenib vs Nivolumab	CheckMate 459	Ongoing	
	Second line	1. Brivanib vs Placebo*	BRISK-PS	EASL 2012	JCO 2013
		2. Everolimus vs Placebo*	EVOLVE-1	ASCO-GI 2014	JAMA 2014
		3. Ramucirumab vs Placebo*	REACH	ESMO 2014	Lancet-O 2015
		4. S-1 vs Placebo*	S-CUBE	ASCO 2015	
		5. Regorafenib vs Placebo#	RESORCE	WCGC 2016	
		6. Tivantinib vs Placebo	JET-HCC	Ongoing	
		7. Ramucirumab vs Placebo	REACH-2	Ongoing	
		8. Pembrolizumab vs Placebo	KEYNOTE-240	Ongoing	

*Randomized controlled trial (RCT) halted or negative results. #RCT positive result. HAIC=Hepatic arterial infusion chemotherapy.

(four weeks/cycle) (fig. 1). Geographic region, performance status on the Eastern Cooperative Oncology Group scale, α-fetoprotein level (≥400 or <400 ng/mL), macrovascular invasion, and extrahepatic disease were used as allocation factors. This study excluded patients who were intolerant of sorafenib and who discontinued the treatment because of side effects. It enrolled only those patients who discontinued sorafenib because of evidence of PD on imaging studies. In addition, patients were included only if they had received ≥400 mg sorafenib for at least 20 of 28 days immediately prior to radiologically detected PD. In other words, this trial was designed (1) to ensure regorafenib tolerance among patients, and to reduce the occurrence of the drug-specific skin symptoms because the compound is structurally similar to sorafenib [2,3] (fig. 2) and (2) to reduce the effect of post-trial treatment on OS in both the placebo and treatment arms by using a homogeneous group of patients who developed PD due to sorafenib failure.

In general, post-progression survival (PPS) is defined as the time interval between the diagnosis of PD after primary treatment and the patient's death, and OS is the sum of PPS and progression-free survival (PFS). Therefore, even significant differences in PFS can be canceled out because PPS is prolonged. Indeed, OS showed a stronger correlation with PPS than with PFS in a clinical trial of sorafenib [4]. Because HCC responds extremely well to locoregional therapy, it is often used as post-trial treatment even in cases in which locoregional therapy is no longer applicable and molecular targeted agents are subsequently administered in accordance with the protocol, provided that the patient's general condition is stable. This rarely happens with other types of cancer and is therefore essentially unique to HCC, owing to the availability of powerful locoregional therapies such as intra-arterial infusion chemotherapy [5–7], transcatheter arterial chemoembolization (TACE) [8, 9], and radiofrequency ablation [10–12]. These post-trial treatments are capable of canceling out any difference in the primary endpoint OS by prolonging PPS [13]. Indeed, previous clinical trials of second-line agents other than regorafenib have always included patients intolerant

Liver Cancer 2016;5:235–244
DOI: 10.1159/000449335
Published online: September 14, 2016

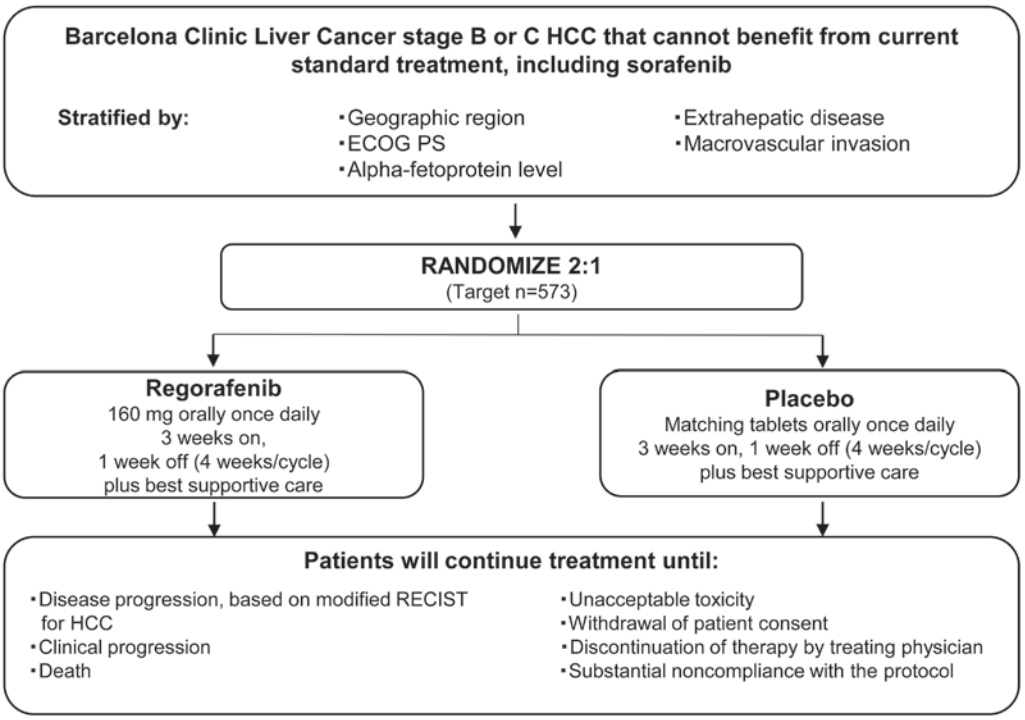

Fig. 1. Design of the RESORCE Trial. ECOG PS=Eastern Cooperative Oncology Group Performance Status; RECIST=Response Evaluation Criteria in Solid Tumors.

to sorafenib, which may have increased the influence of post-trial treatment and thus contributed to their negative outcomes. Patients unresponsive to sorafenib are those who develop PD during sorafenib therapy and are likely to have relatively poor hepatic function and overall general condition. By contrast, patients intolerant to sorafenib are those who discontinue the treatment because of side effects; these patients are in relatively stable conditions because of negligible amounts of internalized sorafenib, and a lack of HCC progression. Because of their clinical stability, patients intolerant to sorafenib are inevitably treated by locoregional therapy or various other post-trial treatments, including the re-administration of sorafenib, regardless of whether they received an actual second-line agent or placebo during the trial. With this in mind, clinical trials of second-line agents should enroll only patients who are unresponsive to sorafenib [14]. The RESORCE trial was the first clinical study to reflect this point in the trial design (fig. 1). The benefit of excluding patients intolerant to sorafenib was demonstrated in the subanalysis of a previous phase II study of axitinib, which generated an excellent HR and a significant study outcome [15, 16].

The second noteworthy point in the design of the RESORCE trial is that the allocation factors of macrovascular invasion and extrahepatic disease were treated as independent stratification factors. In general, the designs of previous clinical trials of molecular targeted agents involved allocation factors specifying "vascular invasion and/or extrahepatic spread" or "neither." However, because vascular invasion is an extremely poor prognostic factor for HCC, assigning vascular invasion to the same category as extrahepatic spread may have influenced the outcome of these clinical trials. For example, when the treatment group contains more patients with vascular invasion but the placebo group includes more patients with extrahepatic spread, such sampling bias will put the treatment group at a significant disadvantage. In fact,

Liver Cancer 2016;5:235–244
DOI: 10.1159/000449335
Published online: September 14, 2016

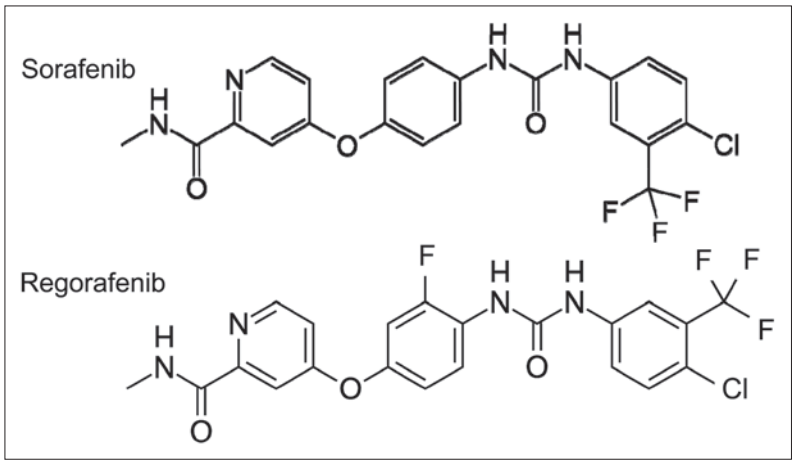

Fig. 2. Chemical structure of Regorafenib is very similar to that of Sorafenib.

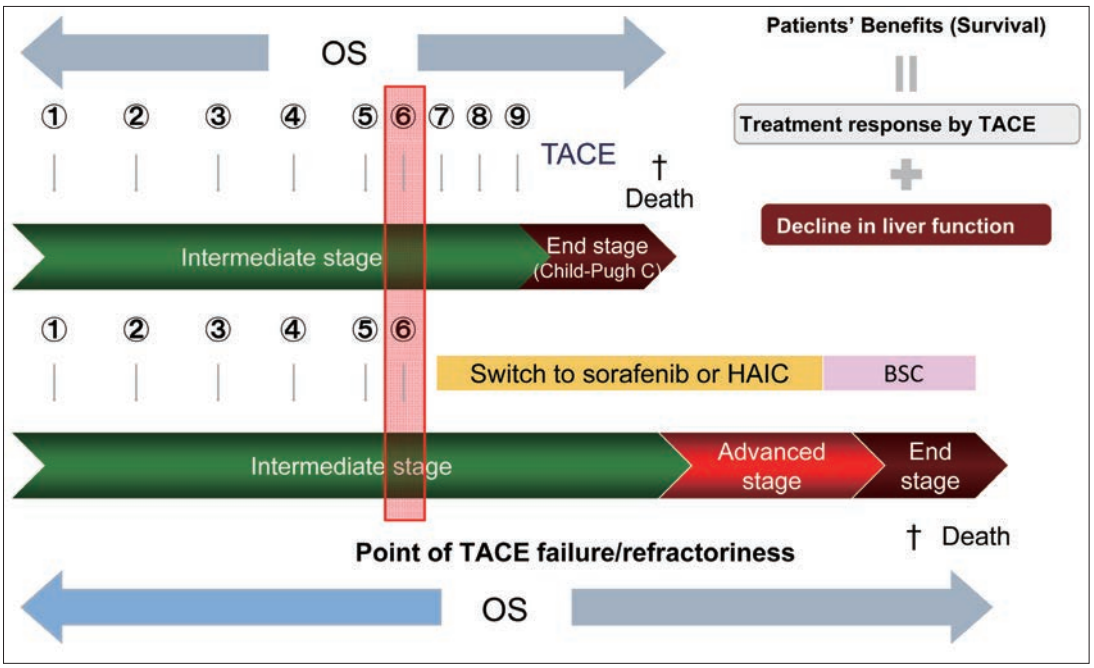

Fig. 3. Switching from repeated TACE to sorafenib may prolong the survival of patients with HCC at the point of TACE failure/refractoriness. Reproduced with permission from Kudo M, et al. [23]

such allocation imbalance apparently contributed to a negative outcome in a clinical trial of brivanib as second-line therapy [17] (table 2).

The design of the RESORCE trial is excellent because it reflects what was learned from the negative outcomes of past trials and the reasons for those outcomes.

Liver Cancer 2016;5:235–244
DOI: 10.1159/000449335
Published online: September 14, 2016

Table 2. Imbalance between Brivanib and Placebo Arm in BRISK-PS Trial

Demographic or Characteristic				
	Brivanib (n=263)		Placebo (n=132)	
	No.	%	No.	%
Reason for sorafenib discontinuation				
Progression	227	86	116	88
Intolerance	35	13	16	12
Distant metastasis	171	65	84	64
Vascular invasion	81	31	24	18
Portal vein invasion and/or thrombosis	65	25	16	12

Modified with permission from Llovet JM, et al. [17]

Table 3. Results of the RESORCE Trial

	Regorafenib	Placebo	
n	379	194	
BCLC stage C (%)	88%	87%	
Treatment duration (M)	3.6 (0.03–29.4)	1.9 (0.2–27.4)	
OS (M)	10.6	7.8	HR=0.62 (0.50–0.78) p<0.001
PFS (M)	3.1	1.5	HR=0.46 (0.37–0.56) p<0.001
TTP (M)	3.2	1.5	HR=0.44 (0.36–0.55)
DCR (%)	65.2	36.1	p<0.001
ORR (%)	10.6	4.1	p<0.005
Adverse events (≥ grade 3) (%)	79.7	58.5	

M=Month.

Results of the RESORCE Trial

In the RESORCE trial of regorafenib, the primary endpoint OS in the treatment group was favorable, with a HR of 0.62 relative to the placebo group (95% CI: 0.50–0.78; p<0.001). Despite being a second-line agent, regorafenib extended the median OS to 10.6 months compared with 7.8 months in the placebo arm, which was a groundbreaking result (table 3). PFS was 3.1 months in the regorafenib arm and 1.5 months in the placebo arm, with a HR of 0.46 (95% CI: 0.37–0.56; p<0.001). In addition, compared with 1.5 months in the placebo arm, regorafenib extended time to progression (TTP) to 3.2 months, with a HR of 0.44 (95% CI: 0.36–0.55; p<0.001). Furthermore, the disease control rate (DCR) was 65.2% in the regorafenib arm and 36.1% in the placebo arm, with a significant intergroup difference. Similarly, the overall response rate (ORR) was 10.6% in the regorafenib arm and 4.1% in the placebo arm, with a significant intergroup difference (table 3).

Liver Cancer 2016;5:235–244
DOI: 10.1159/000449335
Published online: September 14, 2016

Impact of These Positive Results on HCC Management

To date, numerous clinical trials of second-line agents have failed to produce a good outcome (table 1), which makes the positive outcome of the phase III trial of regorafenib even more important. In the past, treatment strategies were designed without scientific evidence after first-line therapy with sorafenib because of the lack of second-line therapies with proven survival benefits. However, from now on, the survival of patients with advanced HCC can be improved by transitioning to second-line therapy with regorafenib. This will require the correct administration of sorafenib and a longer treatment period. There is no doubt that regorafenib will improve the prognosis of patients with advanced HCC even after the development of PD due to sorafenib failure, provided that sorafenib is administered properly.

Furthermore, sequential therapy with sorafenib and regorafenib will require re-establishing the appropriate timing of sorafenib administration. This is because transitioning to second-line therapy while maintaining Child-Pugh Class A liver function can be difficult if patients are treated with sorafenib for the first time after the HCC has progressed to an advanced stage.

What happens when sorafenib is administered to patients with intermediate-stage HCC? Conventionally, TACE is first-line treatment for intermediate-stage HCC [18]. Superselective TACE is regarded as an effective treatment method that can produce survival benefits and favorable response without adversely affecting hepatic functional reserve. Regarding patients with large-sized HCC or multiple bilobar nodules, these lesions are treated with repeated TACE, which seldom produces good results, or may even adversely affect hepatic functional reserve. Therefore, it will be important in the future to determine the optimal time to switch to sorafenib-regorafenib sequential therapy in patients who are unresponsive to TACE [19].

Systemic Therapy at the Point of TACE Failure/Refractoriness

The definition of TACE failure/refractoriness by the Japan Society of Hepatology was validated previously [20]. Two studies compared the prognosis of patients who switched to sorafenib therapy after confirmation of TACE failure/refractoriness to that of patients who continued to undergo repeated TACE [21, 22]. These studies showed that survival benefits were better in patients who switched to sorafenib therapy at the time of TACE failure/refractoriness [23] (fig. 3). This suggests that prognosis will be improved by accurately defining the time point of TACE failure/refractoriness in accordance with this definition and switching to systemic therapy with effective chemotherapeutic agents, namely, sorafenib and regorafenib. The positive outcome of the RESORCE trial underscores the importance of protocolizing the treatment for HCC such that when there is TACE failure/refractoriness, that the switch to systemic therapy is performed in a timely manner.

Indication of Systemic Therapy in BCLC B Substages

As previously reported in many studies, patients with BCLC stage B HCC constitute an extremely heterogeneous group that includes a subgroup of patients who are unresponsive to TACE (fig. 4). The patients unresponsive to TACE benefit more in terms of survival if they start sorafenib therapy without undergoing TACE. This should be investigated in the future by conducting a randomized clinical trial of TACE and systemic therapy. Specifically, the Kinki criteria classify BCLC stage B HCC, which is intermediate-stage HCC, into substages B1, B2,

Liver Cancer 2016;5:235–244
DOI: 10.1159/000449335
Published online: September 14, 2016

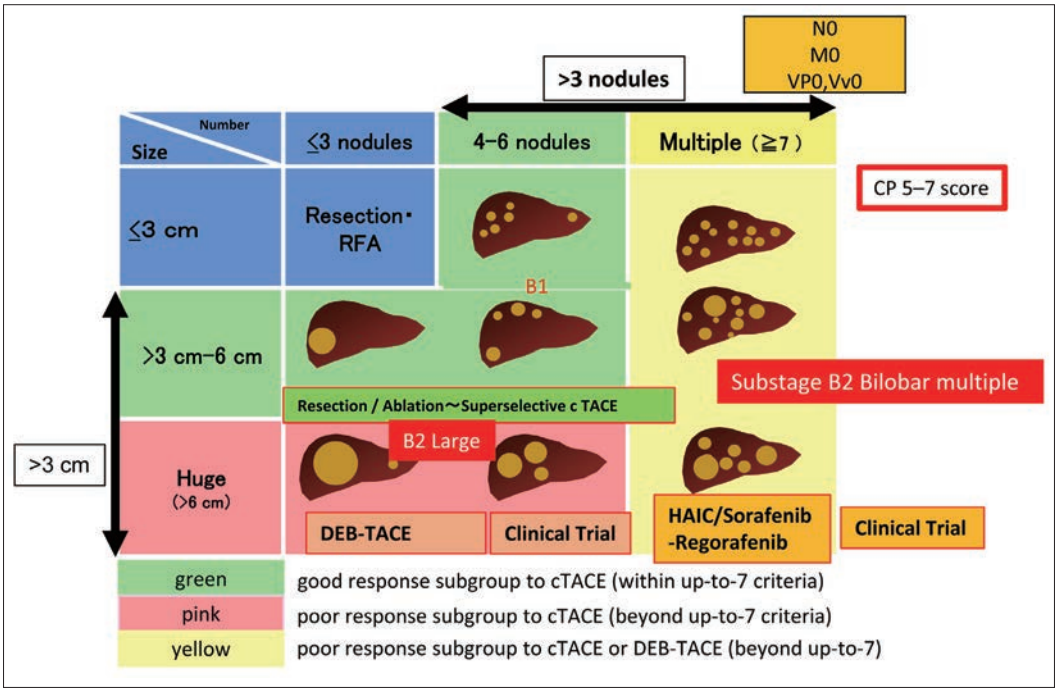

Fig. 4. Heterogeneity and treatment strategy of intermediate-stage HCC. Substage B2 may be a candidate for clinical trials of TACE combination therapy with tyrosine kinase inhibitors or immunotherapy. Modified with permission from Kudo M, et al. [25]

and B3 [24, 25] (table 4). Compared with substage B1 HCC, TACE is clearly not effective in substage B2 HCC, which in turn often reduces hepatic functional reserve. Therefore, patients with substage B2 HCC may easily develop TACE unresponsiveness (fig. 4). Further studies should be aimed at determining whether this group of patients will benefit in terms of survival if they undergo systemic therapy either with targeted therapy or immune checkpoint inhibitors (table 5) [26] from the outset without TACE (fig. 5).

Conclusion

The positive results of the RESORCE trial will have a huge impact on the management of HCC. In particular, to obtain survival benefits from systemic therapy, it is necessary to determine the onset of TACE unresponsiveness or to identify patients with a HCC substage that is predisposed to TACE unresponsiveness, and then to initiate systemic therapy in these patients as early as possible. These issues should be clarified in future clinical trials.

Liver Cancer 2016;5:235–244
DOI: 10.1159/000449335
Published online: September 14, 2016

Table 4. Subclassification of Intermediate-Stage HCC: Kinki Criteria

BCLC Substage	B1	B2	B3	
Child-Pugh score	5–7	5–7	8–9	
Beyond Milan and up-to-7 criteria	IN	OUT	ANY	
			IN	OUT
Sub-substage			B3a	B3b
Concept of treatment strategy	Curative intent	Non-curative, Palliative	Curative intent if within up-to-7	Palliative, No treatment
Treatment option	Resection Ablation Superselective cTACE	DEB-TACE (>6 cm) HAIC (>6 tumors) Sorafenib (CP-A)	Transplantation Ablation Superselective cTACE	HAIC Selective DEB-TACE BSC
Alternative	DEB-TACE (large, CP-7) B-TACE (fewer tumors)	cTACE	DEB-TACE B-TACE, HAIC	BSC

cTACE=conventional transarterial chemoembolization using lipiodol mixed with anticancer drugs; DEB=drug-eluting bead; B-TACE=balloon-occluded transarterial chemoembolization; CP=Child-Pugh; BSC=best supportive care. Reproduced with permission from Kudo M, et al. [25]

Table 5. Objective Response by Nivolumab

	Uninfected: Sorafenib Naïve/ Intolerant (n=54)	Uninfected: Sorafenib Progressors (n=58)	HCV (n=51)	HBV (n=51)	Total (n=214)
Objective response, n (%)	11 (20)	11 (19)	7 (14)	6 (12)	35 (16)
Partial response	0	2 (3)	0	0	2 (1)
Stable disease	32 (59)	27 (47)	29 (57)	23 (45)	111 (52)
Progressive disease	11 (20)	18 (31)	12 (24)	22 (43)	63 (29)
Not evaluable	0	2 (3)	3 (6)	0	5 (2)

HCV=hepatitis C virus; HBV=hepatitis B virus. Reproduced with permission from El-Khoueiry AB, et al. [26]

Liver Cancer 2016;5:235–244
DOI: 10.1159/000449335
Published online: September 14, 2016

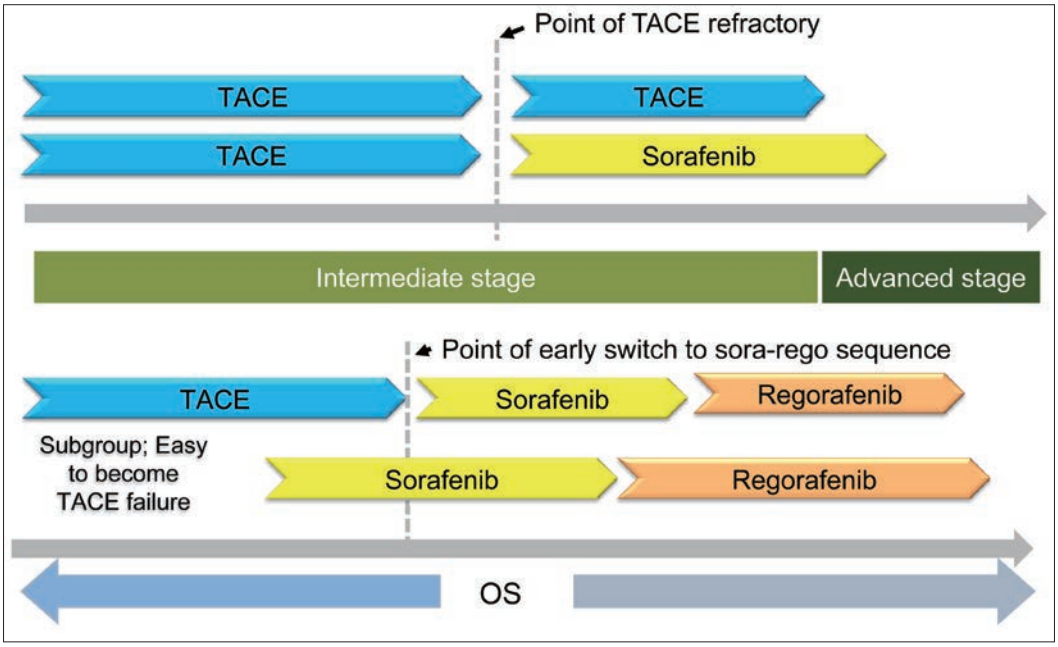

Fig. 5. Treatment strategy for sorafenib-regorafenib sequential therapy. Identification of the subgroup that easily develops TACE failure/refractoriness may be important. For that subgroup, systemic therapy may be a more adequate treatment strategy than TACE for improving patient survival/benefit.

References

1 Bruix J, Merle P, Granito A, Huang YH, Bodoky G, Yokosuka O, Rosmorduc O, Breder V, Gerolami R, Masi G, Ross Paul J, Qin S, Song T, Bronowicki JP, Ollivier-Hourmand I, Kudo M, Leberre M, Baumhauer A, Meinhardt G, Han G, on behalf of the RESORCE Investigators: Efficacy and safety of regorafenib versus placebo in patients with hepatocellular carcinoma (HCC) progressing on sorafenib: Results of the international, randomized phase 3 RESORCE trial. Ann Oncol 2016; 27 (suppl 2): ii140-ii141. (abstr #LBA-03).
2 Bruix J, Tak WY, Gasbarrini A, Santoro A, Colombo M, Lim HY, Mazzaferro V, Wiest R, Reig M, Wagner A, Bolondi L: Regorafenib as second-line therapy for intermediate or advanced hepatocellular carcinoma: multicentre, open-label, phase II safety study. Eur J Cancer 2013;49:3412–3419.
3 Wilhelm SM, Carter C, Tang L, Wilkie D, McNabola A, Rong H, Chen C, Zhang X, Vincent P, McHugh M, Cao Y, Shujath J, Gawlak S, Eveleigh D, Rowley B, Liu L, Adnane L, Lynch M, Auclair D, Taylor I, Gedrich R, Voznesensky A, Riedl B, Post LE, Bollag G, Trail PA: BAY 43-9006 exhibits broad spectrum oral antitumor activity and targets the RAF/MEK/ERK pathway and receptor tyrosine kinases involved in tumor progression and angiogenesis. Cancer Res 2004;64:7099–7109.
4 Terashima T, Yamashita T, Takata N, Nakagawa H, Toyama T, Arai K, Kitamura K, Yamashita T, Sakai Y, Mizukoshi E, Honda M, Kaneko S: Post-progression survival and progression-free survival in patients with advanced hepatocellular carcinoma treated by sorafenib. Hepatol Res 2016;46:650–656.
5 Ueshima K, Kudo M, Tanaka M, Kumada T, Chung H, Hagiwara S, Inoue T, Yada N, Kitai S: Phase I/II study of sorafenib in combination with hepatic arterial infusion chemotherapy using low-dose cisplatin and 5-fluorouracil. Liver Cancer 2015;4:263–273.
6 Obi S, Sato S, Kawai T: Current status of hepatic arterial infusion chemotherapy. Liver Cancer 2015;4:188–199.
7 Lin CC, Hung CF, Chen WT, Lin SM: Hepatic arterial infusion chemotherapy for advanced hepatocellular carcinoma with portal vein thrombosis: Impact of early response to 4 weeks of treatment. Liver Cancer 2015;4:228–240.
8 Kudo M: Locoregional therapy for hepatocellular carcinoma. Liver Cancer 2015;4:163–164.
9 Tsurusaki M, Murakami T: Surgical and locoregional therapy of HCC: TACE. Liver Cancer 2015;4:165–175.
10 Kang TW, Rhim H: Recent advances in tumor ablation for hepatocellular carcinoma. Liver Cancer 2015;4:176–187.
11 Lencioni R, de Baere T, Martin RC, Nutting CW, Narayanan G: Image-guided ablation of malignant liver tumors: Recommendations for clinical validation of novel thermal and non-thermal technologies – a western perspective. Liver Cancer 2015;4:208–214.
12 Kudo M: Surveillance, diagnosis, treatment, and outcome of liver cancer in Japan. Liver Cancer 2015;4:39–50.

Liver Cancer 2016;5:235–244
DOI: 10.1159/000449335
Published online: September 14, 2016

13 Reig M, Rimola J, Torres F, Darnell A, Rodriguez-Lope C, Forner A, Llarch N, Ríos J, Ayuso C, Bruix J: Post-progression survival of patients with advanced hepatocellular carcinoma: rationale for second-line trial design. Hepatology 2013;58:2023–2031.
14 Kudo M, Ueshima K, Minami Y, Nishida N: Molecular targeted therapy for hepatocellular carcinoma: Impact of regorafenib and consideration on trial designs of novel investigational agents. Liver Cancer 2016 (in press).
15 Kudo M, Park JW, Obi S, Qin S, Assenat E, Umeyama Y, Chakrabarti D, Valota O, Fujii Y, Martini JF, Williams JA, Kang YK: Regional differences in efficacy/safety/biomarkers in a randomised study of axitinib in 2nd line patients (pts) with advanced hepatocellular carcinoma (HCC). J Clin Oncol 34, 2016 (suppl 4S; 2016 Gastrointestinal Cancers Symposium; abstr 329).
16 Kang YK, Yau T, Park JW, Lim HY, Lee TY, Obi S, Chan SL, Qin S, Kim RD, Casey M, Chen C, Bhattacharyya H, Williams JA, Valota O, Chakrabarti D, Kudo M: Randomized phase II study of axitinib versus placebo plus best supportive care in second-line treatment of advanced hepatocellular carcinoma. Ann Oncol 2015;26:2457–2463.
17 Llovet JM, Decaens T, Raoul JL, Boucher E, Kudo M, Chang C, Kang YK, Assenat E, Lim HY, Boige V, Mathurin P, Fartoux L, Lin DY, Bruix J, Poon RT, Sherman M, Blanc JF, Finn RS, Tak WY, Chao Y, Ezzeddine R, Liu D, Walters I, Park JW: Brivanib in patients with advanced hepatocellular carcinoma who were intolerant to sorafenib or for whom sorafenib failed: results from the randomized phase III BRISK-PS study. J Clin Oncol 2013;31:3509–3516.
18 Llovet JM, Ducreux M, et al European Association For The Study Of The Liver European Organisation For Research And Treatment Of Cancer: EASL-EORTC clinical practice guidelines: management of hepatocellular carcinoma. J Hepatol 2012;56:908–943.
19 Kudo M, Matsui O, Izumi N, Iijima H, Kadoya M, Imai Y, Okusaka T, Miyayama S, Tsuchiya K, Ueshima K, Hiraoka A, Ikeda M, Ogasawara S, Yamashita T, Minami T, Yamakado K, Liver Cancer Study Group of Japan: JSH consensus-based clinical practice guidelines for the management of hepatocellular carcinoma: 2014 update by the Liver Cancer Study Group of Japan. Liver Cancer 2014;3:458–468.
20 Arizumi T, Ueshima K, Chishina H, Kono M, Takita M, Kitai S, Inoue T, Yada N, Hagiwara S, Minami Y, Sakurai T, Nishida N, Kudo M: Validation of the criteria of transcatheter arterial chemoembolization failure or refractoriness in patients with advanced hepatocellular carcinoma proposed by the LCSGJ. Oncology 2014;87(Suppl 1):32–36.
21 Ogasawara S, Chiba T, Ooka Y, Kanogawa N, Motoyama T, Suzuki E, Tawada A, Kanai F, Yoshikawa M, Yokosuka O: Efficacy of sorafenib in intermediate-stage hepatocellular carcinoma patients refractory to transarterial chemoembolization. Oncology 2014;87:330–341.
22 Arizumi T, Ueshima K, Minami T, Kono M, Chishina H, Takita M, Kitai S, Inoue T, Yada N, Hagiwara S, Minami Y, Sakurai T, Nishida N, Kudo M: Effectiveness of sorafenib in patients with transcatheter arterial chemoembolization (TACE) refractory and intermediate-stage hepatocellular carcinoma. Liver Cancer 2015;4:253–262.
23 Kudo M, Matsui O, Izumi N, Kadoya M, Okusaka T, Miyayama S, et al: Transarterial Chemoembolization Failure/Refractoriness: JSH-LCSGJ Criteria 2014 Update. Oncology 2014;87(Suppl 1):22–31.
24 Arizumi T, Ueshima K, Iwanishi M, Minami T, Chishina H, Kono M, Takita M, Kitai S, Inoue T, Yada N, Hagiwara S, Ida H, Minami Y, Sakurai T, Kitano M, Nishida N, Kudo M: Validation of a modified substaging system (Kinki criteria) for patients with intermediate-stage hepatocellular carcinoma. Oncology 2015;89(Suppl 2):47–52.
25 Kudo M, Arizumi T, Ueshima K, Sakurai T, Kitano M, Nishida N: Subclassification of BCLC B stage hepatocellular carcinoma and treatment strategies: Proposal of modified Bolondi's subclassification (Kinki criteria). Dig Dis 2015;33:751–758.
26 El-Khoueiry AB, Sangro B, Yau TC, Crocenzi TS, Welling TH, Yeo W, et al: Phase I/II safety and antitumor activity of nivolumab (nivo) in patients (pts) with advanced hepatocellular carcinoma (HCC): Interim analysis of the CheckMate-040 dose escalation study. J Clin Oncol 34, 2016 (suppl; 2016 ASCO Annual Meeting; abstr 4012) .

REPLY:

We read with great interest the correspondence from Sachar and Ma and appreciate their pointing out the important issues regarding cholestasis. As suggested, cholestasis could be one of the main causes of hepatic disorders in patients with erythropoietic protoporphyria.[1,2] Indeed, the liver biopsy from the older brother also showed protoporphyrin (PP) deposition in the bile system. However, PP was predominantly observed in the hepatocytes with hepatocyte swelling and necrosis accompanied. Therefore, based on the histological findings and immunohistochemistry, we concluded that the liver damage should be mainly attributed to hepatocyte necrosis, primarily caused by PP deposition in the hepatocytes. Although an increase of the alkaline phosphatase level reflects cholestasis, elevated total bilirubin may reflect damage to hepatocytes as well as cholestasis. On the contrary, the liver biopsy from the younger brother, who had not suffered from liver dysfunction, showed more PP in the biliary system than the liver from the older brother but no PP in the hepatocytes. This evidence also supports the idea that PP deposition in hepatocytes is unique to liver damage, at least in the presented cases, and that the expression of ABCG2, a PP efflux transporter, should be involved in the pathogenesis. For PP detection in pathological specimens, we applied a polarized light microscope; a Maltese cross was confirmed during the observation, indicating that PP deposits were present in hepatocytes.

The author also argued that down-regulation of ABCG2 might be a consequence of liver injury because severe inflammation could affect the expression of proteins. We also addressed this issue; we analyzed the expression of other membrane transporters, ABCG6 and PEPT1. We did not find any differences in the expression of these transporters between the two brothers. Therefore, the difference in ABCG2 expression is specific among transporters; it is conceivable that the reduction of ABCG2 is not a result of liver injury. We already discussed this issue in a previous reply.[3]

Concerning age as a risk factor for liver damage, both brothers reported in our study were young, showing only a 2-year difference in age. In addition, the older brother had developed hepatic disorders when he was 16 years old, suggesting that the difference in age should not primarily affect the pathogenesis of the cases.

Satoru Hagiwara, M.D., Ph.D.
Naoshi Nishida, M.D., Ph.D.
Masatoshi Kudo, M.D., Ph.D.
Department of Gastroenterology and Hepatology
Kinki University School of Medicine
Osaka-Sayama, Japan

REFERENCES

1) Lyoumi S, Abitbol M, Rainteau D, Karim Z, Bernex F, Oustric V, et al. Protoporphyrin retention in hepatocytes and Kupffer cells prevents sclerosing cholangitis in erythropoietic protoporphyria mouse model. Gastroenterology 2011;141:1509-1519.
2) Casanova-González MJ, Trapero-Marugán M, Jones EA, Moreno-Otero R. Liver disease and erythropoietic protoporphyria: a concise review. World J Gastroenterol 2010;16:4526-4531.
3) Hagiwara S, Nishida N, Kudo M. Reply. HEPATOLOGY 2016;63:1744-1745.

View this article online at wileyonlinelibrary.com.
DOI 10.1002/hep.28248
Potential conflict of interest: Nothing to report.

Receptor Interacting Protein Kinase 1 (RIPK1) in Hepatocytes Does Not Mediate Murine Acetaminophen Toxicity

TO THE EDITOR:

Dara et al. reported in HEPATOLOGY that receptor interacting protein kinase 1 (RIPK1)—a kinase harboring pleiotropic functions in programmed cell death[1]—mediates acetaminophen-induced necrosis and liver injury.[2] To show this, the investigators used an experimental approach featuring repetitive injections of an antisense oligonucleotide to facilitate a knockdown of RIPK1 in liver cells, leading to protection of mice. To stimulate the discussion on this important and timely topic, we would like to add our own findings on RIPK1 in this context.

Using cre-loxP technology, we have generated a new mouse line with conditional ablation of *Ripk1* specifically in liver parenchymal cells (LPCs; $RIPK1^{LPC\text{-}KO}$). With this gold-standard method, we could reach a complete loss of RIPK1 expression in hepatocytes, as demonstrated by western blotting analysis from whole liver

A Strange Periampullary Discovery

Mohd Amer Alsamman[1] and Joshua Max[1]

Am J Gastroenterol 2016;111:1515; doi:10.1038/ajg.2016.409

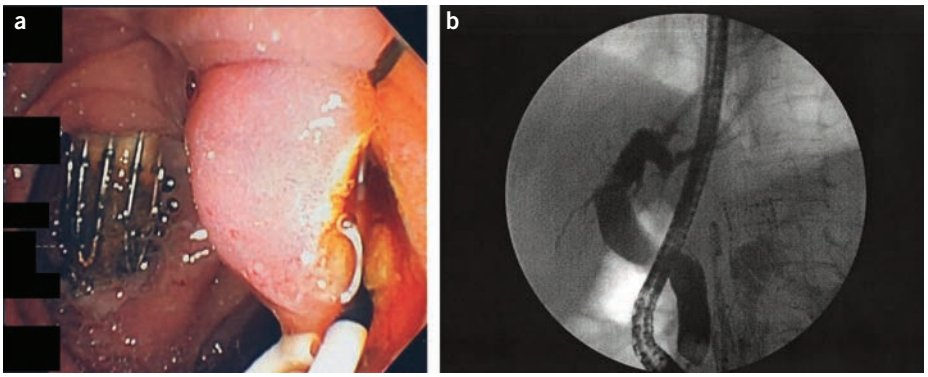

A 77-year-old man had a known history of aortoenteric fistula following abdominal aortic aneurysm repair that had been occluded with plugs and treated with extra-anatomic bypass. He presented to our facility with elevated liver enzymes and diffuse abdominal pain. Imaging was significant for marked dilation of the extrahepatic bile duct to 19 mm. Endoscopic retrograde cholangiopancreatography (ERCP) showed erosion of the aortic stent into the duodenum adjacent to the papilla (shown on the left of the ampulla in **a**). ERCP also revealed papillary stenosis with pancreatic and biliary ductal dilation (**b**), which was treated with biductal stenting; this resulted in temporary relief of the patient's abdominal pain. We hypothesize that the inflammatory milieu surrounding the aortic graft, in close proximity to the major papilla, was responsible for the papillary stenosis. The patient underwent explant of his aortic graft at another facility but expired in postoperative recovery. (Informed consent was obtained from the patient's next of kin to publish these images.)

[1]TriHealth–Good Samaritan Hospital, Cincinnati, Ohio, USA.

Needle-Tract Seeding on the Proximal Gastric Wall After EUS-Guided Fine-Needle Aspiration of a Pancreatic Mass

Kosuke Minaga[1], Masayuki Kitano[1], Eisuke Enoki[1], Hiroshi Kashida[1] and Masatoshi Kudo[1]

Am J Gastroenterol 2016;111:1515; doi:10.1038/ajg.2016.307

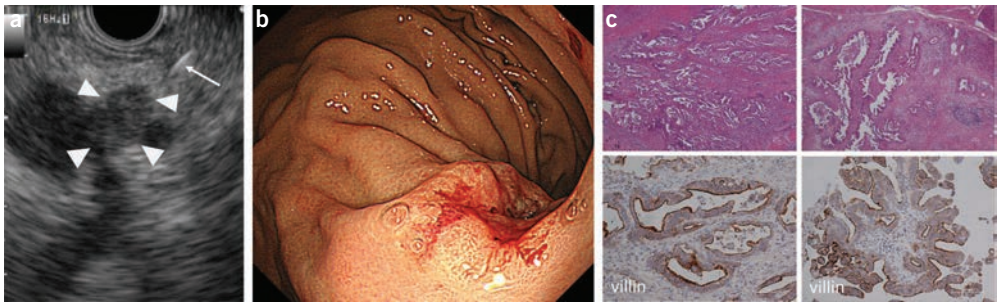

A 72-year-old woman with a small pancreatic mass was referred to our hospital for detailed examination. Endoscopic ultrasonography (EUS) revealed a 10-mm hypoechoic mass in the pancreatic body (**a**, arrowheads). EUS-guided fine-needle aspiration (EUS–FNA) was performed through the posterior gastric wall (**a**, arrow), and cytohistology revealed an adenocarcinoma. The patient underwent distal pancreatectomy for T1N0M0 pancreatic adenocarcinoma. Follow-up management included surveillance of remnant pancreas with EUS and enhanced computed tomography every 6 months for early detection of recurrence. EUS 24 months after the operation revealed a 3-cm mass with ulcer at the posterior gastric wall on endoscopic view (**b**). A biopsy confirmed adenocarcinoma. The mass was near the previous EUS-FNA puncture site, and no masses had been detected on the EUS 6 months previously. Because imaging studies demonstrated no other metastatic lesions, a gastrectomy was performed. (**c**) Microscopy showed a well-differentiated tubular adenocarcinoma (**c**, upper left), which was pathologically similar to the primary pancreatic lesion (**c**, upper right). By immunohistochemistry, adenocarcinoma of the stomach was strongly positive for CK7 and villin (**c**, lower left); weakly positive for maspin, MUC1, MUC5AC, and MUC6; and negative for CDX-2 and MUC2, which was identical to the findings for the primary pancreatic adenocarcinoma (**c**, lower right). These findings suggested that EUS-FNA caused needle-tract seeding on the gastric wall. (Informed consent was obtained from the patient to publish these images.)

[1]Kinki University Faculty of Medicine, Osaka-Sayama, Japan.

Pathology International

Pathology International 2016; **66**: 640–642 doi:10.1111/pin.12457

Letter to the Editor

Bile duct adenoma in patient with chronic hepatitis C: As a benign neoplasm by pathological and imaging studies

To the Editor:

An old man with chronic hepatitis C was admitted to Kobe Asahi Hospital for further examination of a 7 mm hypoechoic nodule in segment five (S5). He had no history of alcohol intake, blood transfusion, or drug abuse.

Six years earlier, the patient had been under treatment with pegylated interferon and ribavirin, discontinuing because of adverse effects.

On admission, a physical examination showed no remarkable abnormality, lymphadenopathy or splenomegaly. Serum hepatitis C virus (HCV) RNA 6.9logIU/mL (real time polymerase chain reaction (PCR)), and HCV genotype 2. Serum hepatitis B virus (HBV) was negative for surface antigen. Laboratory examinations revealed the following values: platelets 13.9 × 10 4 /μL (13.4–34.9), alanine aminotransferase 25 U/L (5–40). The levels of tumor markers were as follows: alpha-fetoprotein (AFP) 2.1 ng/mL (< 10.0), protein-induced vitamin K absence (PIVKA II) 16 mAU/mL (<40), carcinoembryonic antigen (CEA) 2.0 ng/mL (0–5), carbohydrate antigen 19–9 (CA19–9) 7.0 U/mL (<37.0).

Ultrasonography (US) disclosed a 7 mm hypoechoic nodule in S5. Contrast-enhanced US (CE-US) revealed a hypervascular nodule in the early vascular phase, and defect in the post-vascular phase (Fig. 1a); gadolinium ethoxybenzyl diethylenetriamine pentaacetic acid magnet resonance imaging (Gd-EOB-DTPA-MRI) revealed a hypervascular nodule in the early phase, isointense in the delayed phase and defect in the hepatobiliary phase; and contrast-enhanced computed tomography (CE-CT), a hypervascular nodule in the early phase and isodense in the delayed phase. As a hypervascular nodule, pathologies such as hepatocellular carcinoma (HCC), cholangiolocellular carcinoma (CoCC), cholangiocellular carcinoma (CCC), hemangioma, hypervascular metastatic cancer, hepatocellular adenoma, hypervascular hyperplastic nodules, angiomyolipoma, peliosis hepatis, dysplastic nodules, inflammatory pseudotumors and bile duct adenoma (BDA) need to be differentiated, however, HCC was suspected from the above imaging studies and the background of chronic hepatitis C.

In the present case, although imaging modalities including Gd-EOB-DTPA enhanced MRI had been carried out twice,

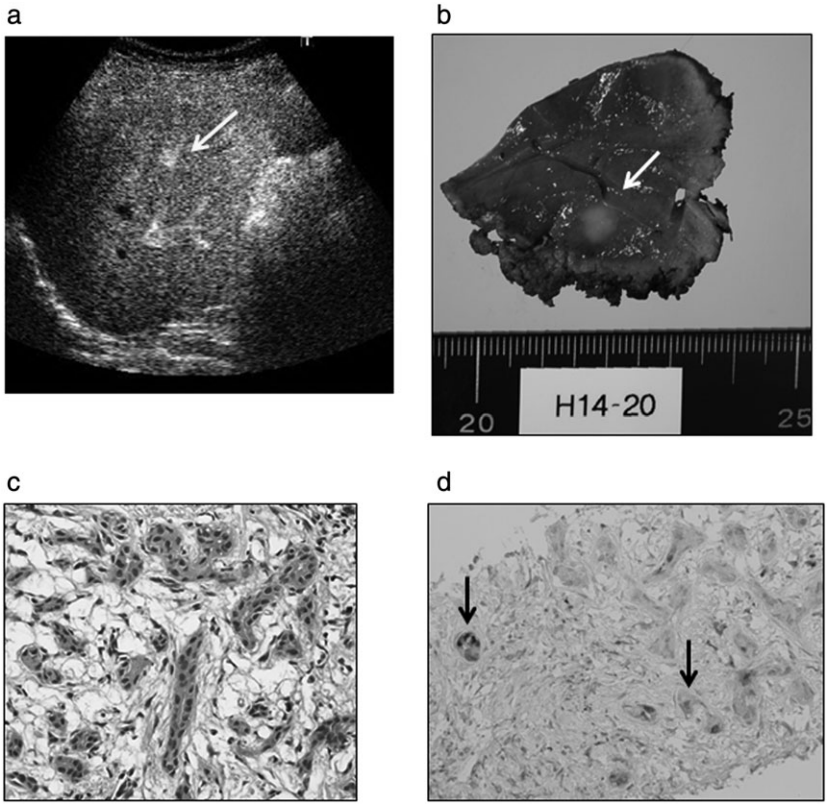

Figure 1 (**a**) Imaging findings: CE-US, hypervascularity in the early vascular phase. (**b**) Pathological findings: Gross finding, 7 mm relatively well-defined yellowish nodule without capsule formation. (**c**) Pathological findings: HE staining (high magnification). The bile ducts within the nodule show a cord-like, anastomosing (the so-called "antler-like") pattern. Cellular atypia is minimal. (**d**) Pathological findings: Immunostaining for $p16^{INK4a}$. The tumor ducts are positively stained.

two or three years earlier, no tumor was detected, and the growth was considered a neoplasm. The nodule was resected under the written consent of the patient.

Grossly, the resected nodule contained a relatively well-defined yellowish white tumorous nodule (7 mm) with a soft rubbery consistency (Fig. 1b). At low magnification, the histological specimen appeared nonencapsulated, replacing the background area of chronic hepatitis and growing in a tubular, cord-like, anastomosing, the so-called "antler-like", pattern.

At high magnification, it revealed a proliferation of small bile ducts with slight to moderate cellular and structural atypia within a loose fibrous stroma (Fig. 1c). Initially, BDA was suspected from the histological findings, however, CoCC needed to be ruled out. Alcian blue and Periodic acid-Schiff staining were negative.

Morphometrically, the size of small bile ducts ranged between 15 and 30 μm, that of the non-neoplastic interlobular ducts and cholangioles of the background was 15–30 μm and less than 15 μm, respectively. The size of the small bile ducts of the nodule was almost the same as interlobular bile ducts in the background.

Immunohistochemical analysis showed proliferating small bile ducts positive for bcl-2 (100%), NCAM (100%), cytokeratin-7 (CK-7) (100%), cytokeratin-19 (CK-19) (100%), p53 (<5%), MIB-1 (6.9%) and $p16^{INK4a}$ (moderate) (Fig. 1d); low positivity for Ki67-index(0–2%), negative for Hep-Par-1, c-kit, MUC1, MUC5AC, MUC6, glu-1, trypsin, CD-10, EZH2 and EMA. CoCC was therefore ruled out, and the above histopathological findings led to our diagnosis of the nodule as BDA. Although BRAF V600E mutation was examined by immunohistochemistry (Anti-BRAF V600E antibody, Clone: VE1, Roche) and direct PCR sequencing (Expand High Fidelity PCR system, Roche Diagnostics), to determine malignant potential, no such mutation was detected. The background of the liver revealed chronic hepatitis (stage F1, grade A1).

BDA has previously been called cholangioma, benign cholangioma, or cholangioadenoma, and simply BDA and is often confused with bile duct hamartoma, however, it has now been established as a pathologically distinct entity.[1]

Most cases of BDA composed of bile duct cells, a rare benign tumor, are found incidentally during laparotomy or at autopsy.[1] Clinical, gross, and histopathologic features of 152 cases reviewed and found asymptomatic, have been discovered incidentally during intra-abdominal surgery (103 cases) and at autopsy (49 cases).[2]

BDA appears as a small whitish nodule measuring <2 cm (mostly 5 mm to 1.0 cm in diameter) and locates immediately below the liver capsule. It is usually found in the normal liver, but on rare occasions also in the cirrhotic liver. Histologically it reveals a nonencapsulated tumor composed of a proliferation of small bile ducts within a fibrous stroma.[2]

It also needs to be differentiated from CoCC and ductular reaction (DR).

CoCC has traditionally been classified as a special type of CCC, but is now considered a stem-cell subtype of combined HCC-CCC.[2]

Immunostaining of the cells may be positive for CK-19, c-kit, NCAM and EpCAM. Cellular atypia is not very severe.

Immunohistochemical stains positive for $p16^{INK4a}$ and negative for EZH2 have been significantly useful in differentiating between BDA and CoCC.[3] In the present case, the absence of significant structural and cellular atypia and stromal invasion, and immunohistochemical positivity for $p16^{INK4a}$ and negativity for c-kit and EZH2 ruled out the diagnosis of CoCC.

DR is a reactive lesion at the portal tract interface comprising increased bile ductules with an accompanying complex of stromal and inflammatory cells. Generally, the gross size of DR is less than 2 mm [4] and its nodule formation has not been reported to date; also, the microscopic size of the cholangiole (ductule) is less than 15 μm; therefore, we ruled out the diagnosis of DR.

The existence of a recurrent molecular alteration such as a BRAF mutation strongly supports the hypothesis that BDAs are true neoplasms and should no longer be designated as reactive processes or hamartomas. BRAF V600E mutations have been identified in 8/15 (53%) BDAs; also V600E mutations have been identified in two of four intrahepatic CCCs associated with BDA; that the rate of BRAF mutation in intrahepatic CCC is rather low (5–10%) suggests that BRAF mutated ICC might arise from BDA.[5]

Two studies have described its pathogenesis more as reactive proliferation than a true neoplasm[2,4]: Recently, Aishima et al. described 35 BDAs divided into the EMA-cytoplasmic type (n = 14) and EMA-luminal type (n = 21), the former, showing a proliferation of cuboidal to low-columnar cells forming an open lumen with NCAM(+)/MUC6(−), have resembled interlobular bile ducts; the latter, showing uniform cuboidal cells with narrow lumen and NCAM(++) / MUC6(++), have resembled ductular reactions, thus suggesting that BDA may be more reactive proliferation than a neoplastic lesion.[4] However, on the basis of gross and histopathological findings, immunohistochemical analysis, and from the viewpoint of morphometry, the present case suggested a neoplasm derived from the interlobular bile duct, despite its benign features and the negative result of BRAF mutation.

ACKNOWLEDGMENTS

The authors thank Professor S Aishima, Professor Y Zen and Doctor M Nakano for histopathological advice, and Ms. M Matsui for excellent technical assistance.

DISCLOSURE STATEMENT

None declared.

Soo Ki Kim,[1] Soo Ryang Kim,[1] Susumu Imoto,[1] Chi Wan Kim,[1] Toshiyuki Matsuoka,[2] Osamu Nakashima,[3] Motoko Sasaki,[4] Tsutomu Kumabe,[5] Masatoshi Kudo,[6] Toshio Fukusato[7] and Fukuo Kondo[8]

[1]*Department of Gastroenterology, Kobe Asahi Hospital, Kobe,* [2]*Department of Radiology, Osaka City University Medical School, Osaka,* [3]*Kurume University Hospital Department of Clinical Laboratory Medicine, Fukuoka,* [4]*Department of Human Pathology, Kanazawa University Graduate School of Medicine, Kanazawa,* [5]*Kumabe Clinic, Kumamoto,* [6]*Department of Gastroenterology and Hepatology, Kinki University School of Medicine, Osakasayama,* [7]*Department of Pathology, Teikyo University School of Medicine, and* [8]*Department of Pathology, Teikyo University Hospital, Japan*

REFERENCES

1 Allaire G, Rabi L, Ishak K, Sesterhenn I. Bile duct adenoma. A study of 152 cases. *Am J Surg Pathol* 1988; **12**: 708–15.
2 WHO. *Classification of Tumours of the Digestive System*. Lyon: *IARC Press*, 2010; 225–7.
3 Sasaki M, Matsubara T, Kakuda Y, Sato Y, Nakanuma Y. Immunostaining for polycomb group protein EZH2 and senescent marker $p16^{INK4a}$ may be useful to differentiate cholangiolocellular carcinoma from ductular reaction and bile duct adenoma. *Am J Surg Pathol* 2014 Mar; **38**: 364–9.
4 Aishima S, Tanaka Y, Kubo Y, Shirabe K, Maehara Y, Oda Y. Bile duct adenoma and von Meyenburg complex-like duct arising in hepatitis and cirrhosis: Pathogenesis and histological characteristics. *Pathol Int* 2014 Nov; **64**: 551–9.
5 Pujals A, Amaddeo G, Castain C *et al.* Author information BRAF V600E mutations in bile duct adenomas. *Hepatology* 2015 Jan; **61**: 403–5.

Research Article

JOURNAL OF HEPATOLOGY

Survival benefit of liver resection for hepatocellular carcinoma associated with portal vein invasion

Takashi Kokudo[1,2], Kiyoshi Hasegawa[1], Yutaka Matsuyama[3], Tadatoshi Takayama[4], Namiki Izumi[5], Masumi Kadoya[6], Masatoshi Kudo[7], Yonson Ku[8], Michiie Sakamoto[9], Osamu Nakashima[10], Shuichi Kaneko[11], Norihiro Kokudo[1,*], for the Liver Cancer Study Group of Japan

[1]*Hepato-Biliary-Pancreatic Surgery Division, Department of Surgery, Graduate School of Medicine, University of Tokyo, Japan;* [2]*Division of Gastroenterological Surgery, Saitama Cancer Center, Japan;* [3]*Department of Biostatistics, School of Public Health, The University of Tokyo, Japan;* [4]*Department of Digestive Surgery, Nihon University School of Medicine, Japan;* [5]*Department of Gastroenterology, Musashino Red Cross Hospital, Japan;* [6]*Department of Radiology, Shinshu University School of Medicine, Japan;* [7]*Department of Gastroenterology and Hepatology, Kinki University School of Medicine, Japan;* [8]*Division of Hepato-Biliary-Pancreatic Surgery, Department of Surgery, Kobe University Graduate School of Medicine, Japan;* [9]*Department of Pathology, Keio University School of Medicine, Japan;* [10]*Department of Clinical Laboratory Medicine, Kurume University Hospital, Japan;* [11]*Department of Gastroenterology, Kanazawa University Hospital, Japan*

Background & Aims: The presence of portal vein tumor thrombosis (PVTT) in patients with hepatocellular carcinoma (HCC) is regarded as indicating an advanced stage, and liver resection (LR) is not recommended. The aim of this study was to evaluate the survival benefit of LR for HCC patients with PVTT through the analysis of the data from a Japanese nationwide survey.

Methods: We analyzed data for 6474 HCC patients with PVTT registered between 2000 and 2007. Of these patients, 2093 patients who underwent LR and 4381 patients who received other treatments were compared. The propensity scores were calculated and we successfully matched 1058 patients (66.1% of the LR group).

Results: In the Child-Pugh A patients, the median survival time (MST) in the LR group was 1.77 years longer than that in the non-LR group (2.87 years *vs.* 1.10 years; p <0.001) and 0.88 years longer than that in the non-LR group (2.45 years *vs.* 1.57 years; p <0.001) in a propensity score-matched cohort. A subgroup analysis revealed that LR provides a survival benefit regardless of age, etiology of HCC, tumor marker elevation, and tumor number. The survival benefit was not statistically significant only in patients with PVTT invading the main trunk or contralateral branch. In the LR group, the postoperative 90-day mortality rate was 3.7% (68 patients).

Conclusions: As long as the PVTT is limited to the first-order branch, LR is associated with a longer survival outcome than non-surgical treatment.

Lay summary: The presence of portal vein tumor thrombosis in patients with hepatocellular carcinoma is regarded as indicating an advanced stage, and liver resection is not recommended. We performed a multicenter, nationwide study to assess the survival benefit of liver resection in hepatocellular carcinoma patients with portal vein tumor thrombosis using propensity score-based matching. As long as the portal vein tumor thrombosis is limited to the first-order branch, liver resection is associated with a longer survival outcome than non-surgical treatment.

Keywords: Hepatocellular carcinoma; Liver resection; Portal vein tumor thrombosis; Propensity score-match; Nationwide survey.

Received 12 January 2016; received in revised form 20 May 2016; accepted 30 May 2016; available online 4 June 2016

* Corresponding author. Address: 7-3-1 Hongo, Bunkyo-ku, Tokyo, Japan. Tel.: +81 338155411; fax: +81 356843989.

E-mail address: KOKUDO-2SU@h.u-tokyo.ac.jp (N. Kokudo).

Abbreviations: HCC, hepatocellular carcinoma; AASLD/BCLC, American Association for the Study of the Liver Disease/Barcelona Clinic for Liver Cancer; PVTT, portal vein tumor thrombosis; MST, median survival time; LR, liver resection; CI, confidence interval; TACE, transcatheter arterial chemoembolization; HR, hazard ratio.

Introduction

Patients with advanced hepatocellular carcinoma (HCC) showing macroscopic vascular invasion have been reported to have an extremely poor prognosis [1]. According to the American Association for the Study of the Liver Disease/Barcelona Clinic for Liver Cancer (AASLD/BCLC) Staging System and treatment guidelines, portal vein invasion, or portal vein tumor thrombosis (PVTT), is regarded as an advanced stage of the disease with almost zero hope for a cure [2]. The only proposed treatment option for this group of patients is sorafenib chemotherapy, and the reported median survival time (MST) of patients with advanced HCC treated with sorafenib is as short as 10.7 months [3]. Therefore, surgical intervention may play some role in the treatment of selected patients.

As a result of recent advances in surgical techniques and perioperative management, liver resection (LR) has become a reasonably safe treatment option with an acceptable mortality and morbidity rate [4,5]. Aggressive surgical resection for HCC with vascular invasion has been proposed by several tertiary centers [6–11]. However, the number of patients enrolled in these studies is generally small, and the reports suffer from substantial selection bias.

The aim of this study was to evaluate the survival benefit of LR for HCC patients with portal vein invasion through the analysis of a large-scale cohort study based on the latest data available from a Japanese nationwide survey.

Patients and methods

Patients

Since 1965, the Liver Cancer Study Group of Japan has been performing nationwide surveys of patients with primary liver cancer. Patients are registered and followed up as reported previously [12]. The collection and registration of data for patients with HCC were performed with the approval of each institution participating in the nationwide survey. The number of registered institutions was 645, accounting for approximately one-third of all HCC patients treated in Japan. To analyze recent results, we set the study period from 2000 to 2007 (latest data available). The presence of PVTT was determined based on the radiological findings. PVTT was categorized into main trunk/contralateral branch (Vp4), first-order branch (Vp3), second-order branch (Vp2), and third-order branch (Vp1), according to the Japanese staging system [13]. R1 resection was defined as a complete macroscopic resection with a positive pathological margin, and R2 resection was defined as a macroscopic positive margin that was extracted from the registry data. Postoperative mortality was defined as any death other than tumor progression within 90 days of surgery.

Statistical analysis

Statistical analyses were performed using the JMP software, version 11.0 (SAS Institute Inc., Cary, NC). Categorical variables were analyzed using the Chi-square test. Continuous variables were analyzed using the Wilcoxon rank-sum test and the Student's *t* test after propensity score matching. The overall survival curves were determined using the Kaplan-Meier method and were compared using the log-rank test. Propensity scores were created using logistic regression modeling the probability of a patient undergoing LR based on age, sex, viral infection (hepatitis B and/or C virus), positive serum alpha-fetoprotein ($\geqslant$15 ng/ml), serum albumin (g/dl), $\log_{10}$ (total bilirubin [mg/dl]), prothrombin time (%), platelet count (10^4/μl), gastroesophageal varices, multiple tumors ($\geqslant$3), and extent of PVTT. Since the $\log_{10}$ (total bilirubin) showed a normal distribution for the entire cohort, this parameter was used instead of the serum total bilirubin level. A 1:1 match without replacement was performed using logit (propensity score) through the nearest available matching, setting the caliper as 0.05. A multivariate analysis was performed using a Cox proportional hazards model and the backward elimination procedure. A *p* value of less than 0.10 was set as the cut-off value for the elimination. The following 8 variables were examined as potential risk factors: age >70 years, gastroesophageal varices, platelet count <100,000/μl, positive serum alpha-fetoprotein ($\geqslant$15 ng/ml), number of tumors $\geqslant$3, tumor size (cm), vp4, and LR. R2 resection, liver cirrhosis, and poor cancer cell differentiation were also examined in patients who underwent LR. All the statistical analyses were 2-tailed. *p* values less than 0.05 were considered to indicate statistical significance.

Results

A total of 77,268 patients with HCC were registered between 2000 and 2007. Among these patients, 8550 patients missing data regarding PVTT, 59,652 patients without PVTT, and 53 patients missing data regarding their survival time were excluded. Among the remaining 9013 patients with PVTT, 1178 Child-Pugh C patients, 1173 patients with distant metastasis, and 188 patients with unavailable data were excluded. The final 6474 patients with PVTT were included in the present analysis. The extent of PVTT was as follows: Vp1, 1772 patients (27.4%); Vp2, 1475 patients (22.8%); Vp3, 1942 patients (30.0%); and Vp4, 1285 patients (19.8%).

The MST after diagnosis according to the extent of PVTT was as follows: Vp1, 2.67 years (95% confidence interval [CI], 2.48–3.01); Vp2, 1.51 years (95% CI, 1.36–1.65); Vp3, 0.78 years (95% CI, 0.70–0.83); and Vp4, 0.50 years (95% CI, 0.45–0.56). Hepatitis C virus infection, defined as a positive status for hepatitis C virus antibody, was seen in 3421 patients (53.3%). Hepatitis B virus infection, defined as a positive hepatitis B surface antigen status, was present in 1495 patients (23.3%).

Of the 6474 patients with PVTT, 2093 patients underwent LR (LR group) and 4381 patients received other treatments (non-LR group). In the non-LR group, 1852 patients (42.3%) received transcatheter arterial chemoembolization (TACE), 1371 patients (31.3%) received chemotherapy or hepatic arterial infusion chemotherapy, 188 patients (4.3%) received ablation therapy, 859 (19.6%) patients received best-supportive care, and 111 patients (2.5%) underwent other treatments. Since sorafenib was only available beginning in 2009 in Japan, none of the patients received sorafenib as an initial treatment. Table 1 shows the characteristics of the patients according to treatment procedure; the non-LR group tended to have unfavorable characteristics for survival.

In the Child-Pugh A patients, the MST after diagnosis for the LR group was 1.77 years longer than that for the non-LR group (2.87 years [95% CI, 2.60–3.37] *vs.* 1.10 years [95% CI, 1.03–1.17]; p <0.001) (Fig. 1A). The survival rates at 1, 3, and 5 years after diagnosis were 74.8%, 49.1%, and 39.1% for the LR group, and 53.1%, 25.3%, and 16.0% for the non-LR group. In the non-LR group, the MST after diagnosis according to treatments was as follows: TACE, 1.38 years (95% CI, 1.20–1.52); chemotherapy or hepatic arterial infusion chemotherapy, 0.88 years (95% CI, 0.82–0.99); and best-supportive care, 0.36 years (95% CI, 0.30–0.48). A multivariate analysis performed to determine the risk factors for overall survival also identified non-LR treatment

Table 1. Baseline characteristics of the 6474 patients with portal vein tumor thrombus according to treatment type.

Patient characteristics	LR group (n = 2093)*	Non-LR group (n = 4381)*	*p* value
Age (years)	63.2 (10.9)	66.4 (10.4)	<0.001
Sex (male/female)	1744/349 (83/17)	3490/891 (80/20)	<0.001
Hepatitis B virus infection	602 (29.0)	893 (20.6)	<0.001
Hepatitis C virus infection	925 (44.6)	2496 (57.4)	<0.001
Child-Pugh class (A/B)	1877/216 (90/10)	2512/1869 (57/43)	<0.001
Serum albumin (g/dl)	3.83 (0.51)	3.48 (0.57)	<0.001
Serum total bilirubin (mg/dl)	0.87 (0.79)	1.41 (1.63)	<0.001
Prothrombin time (%)	84.9 (14.4)	79.4 (15.0)	<0.001
Platelet count (10^4/μl)	18.1 (8.13)	16.0 (9.01)	<0.001
Gastroesophageal varices	255 (12.8)	1772 (41.0)	<0.001
Multiple tumors (≥3)	470 (22.6)	2365 (54.3)	<0.001
Tumor size (cm)	8.12 (4.66)	7.75 (4.96)	<0.001
Alpha-fetoprotein (≥15 ng/ml)	1515 (72.9)	3455 (79.4)	<0.001
Extent of PVTT			
Vp4	206 (9.8)	1079 (24.6)	
Vp3	466 (22.3)	1476 (33.7)	
Vp2	528 (25.2)	947 (21.6)	
Vp1	893 (42.7)	879 (20.1)	<0.001

Data are the mean (standard deviation) or number (%) unless otherwise indicated.
Chi-square test and Wilcoxon rank-sum test were used for comparison.
*Missing data were not imputed for baseline characteristics.
LR, liver resection; PVTT, portal vein tumor thrombosis.

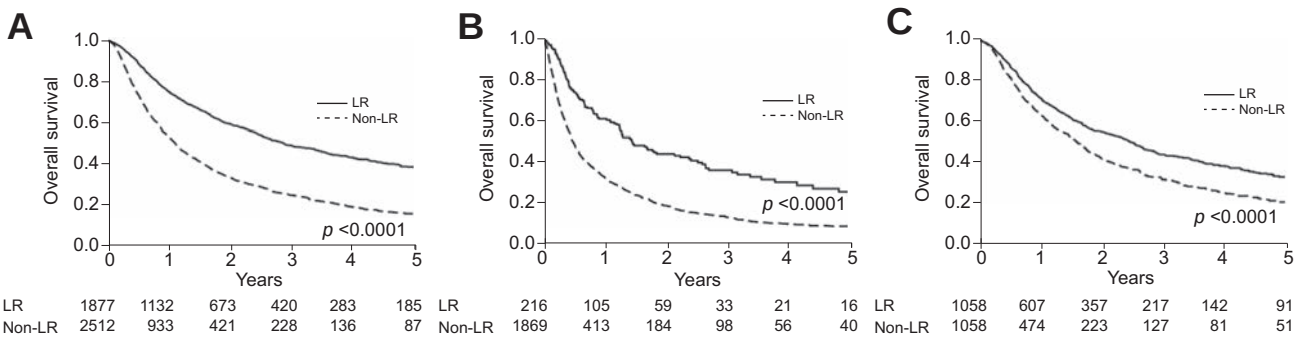

Fig. 1. Kaplan-Meier estimates for survival according to treatment type. (A) 4389 Child-Pugh A patients with portal vein tumor thrombus. (B) 2085 Child-Pugh B patients with portal vein tumor thrombus. (C) 2116 Child-Pugh A patients with portal vein tumor thrombus who were matched by propensity score. Numbers below the x-axis indicate the number of patients at risk. The log-rank test was used for comparison.

(hazard ratio [HR], 1.74 [95% CI, 1.58–1.92]; p <0.001) as one of the most significant risk factors (Supplementary Table 1).

On the other hand, in Child-Pugh B patients, the MST after diagnosis for the LR group was 0.96 years longer than that for the non-LR group (1.44 years [95% CI, 1.23–2.22] *vs.* 0.48 years [95% CI, 0.44–0.52]; p <0.001) (Fig. 1B). The survival rates at 1, 3, and 5 years after diagnosis were 61.3%, 35.2%, and 25.6% for the LR group, and 32.2%, 13.0%, and 7.9% for the non-LR group. In the non-LR group, the MST after diagnosis according to treatments was as follows: TACE, 0.77 years (95% CI, 0.63–0.91); chemotherapy or hepatic arterial infusion chemotherapy, 0.50 years (95% CI, 0.44–0.56); and best-supportive care, 0.19 years (95% CI, 0.17–0.22).

To confirm the survival benefit of LR in Child-Pugh A patients with PVTT, the propensity scores were calculated for 1600 patients in the LR group and 2127 patients in the non-LR group. We successfully matched 1058 patients in the LR group (66.1% of the LR group) and 1058 patients in the non-LR group based on their propensity scores. In the non-LR group, 554 patients (52.4%) received TACE, 299 patients (28.3%) received chemotherapy or hepatic arterial infusion chemotherapy, 73 patients (6.9%) received ablation therapy, 97 (9.2%) patients received best-supportive care, and 35 patients (3.3%) underwent other treatments. Table 2 shows that the main characteristics of these patients did not differ between the two groups. The MST after diagnosis in the LR group was 0.88 years longer than that in the non-LR group (2.45 years [95% CI, 2.15–2.67] *vs.* 1.57 years [95% CI, 1.43–1.72]; p <0.001) (Fig. 1C). Furthermore, the survival rates at 1, 3, and 5 years after diagnosis were 70.9%, 43.5%, and 32.9% for the LR group and 62.9%, 31.6%, and 20.1% for the non-LR group. A multivariate analysis performed to determine the risk factors for overall survival in the propensity score-matched patient groups also identified non-LR treatment (HR, 1.43 [95% CI, 1.26–1.63]; p <0.001) as a significant risk factor (Supplementary Table 2).

A subgroup analysis was then performed for the propensity score-matched patient groups (Fig. 2). In these subgroups, LR showed a survival benefit for both the age >70 years subgroup (HR, 0.63 [95% CI, 0.51–0.79]; p <0.001) and the age ⩽70 years subgroup (HR, 0.74 [95%CI, 0.64–0.86]; p <0.001). The survival benefit of LR was significant regardless of the etiology of the

Table 2. Baseline characteristics of the 2116 Child-Pugh A patients with portal vein tumor thrombus matched by propensity score according to treatment type.

Patient characteristics	LR group (n = 1058)	Non-LR group (n = 1058)	p value
Age (years)	65.0 (10.3)	65.3 (10.5)	0.482
Sex (male/female)	856/202 (80.9/19.1)	862/196 (81.5/18.5)	0.739
Viral infection	755 (71.4)	759 (71.7)	0.847
Serum albumin (g/dl)	3.82 (0.45)	3.82 (0.45)	0.996
Serum total bilirubin (mg/dl)	0.88 (0.57)	0.85 (0.59)	0.305
Prothrombin time (%)	85.3 (13.2)	85.4 (13.1)	0.962
Platelet count (10^4/μl)	17.5 (7.73)	17.2 (8.56)	0.342
Gastroesophageal varices	166 (15.7)	167 (15.8)	0.952
Multiple tumors (≥3)	343 (32.4)	338 (32.0)	0.816
Alpha-fetoprotein (≥15 ng/ml)	792 (74.9)	792 (74.9)	1.000
Extent of PVTT			
Vp 4	138 (13.0)	147 (13.9)	
Vp 3	288 (27.2)	280 (26.5)	
Vp 2	279 (26.4)	279 (26.4)	
Vp 1	353 (33.4)	352 (33.3)	0.941

Data are the mean (standard deviation) or number (%) unless otherwise indicated.
Chi-square test and Student's t test were used for comparison.
LR, liver resection; PVTT, portal vein tumor thrombosis.

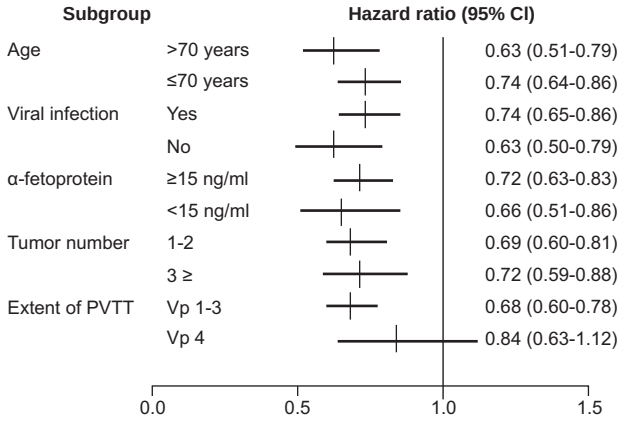

Fig. 2. Hazard ratios for death associated with liver resection in the subgroups of patients matched by propensity score. PVTT, portal vein tumor thrombosis; CI, confidence interval.

Table 3. Operative procedures and outcomes.

	Vp1 (n = 819)*	Vp2 (n = 475)*	Vp3 (n = 404)*	Vp4 (n = 179)*
Major hepatectomy§	379 (49.0)	310 (68.4)	338 (87.1)	158 (90.8)
Extent of resection				
R1	333 (61.1)	215 (65.4)	134 (45.0)	51 (38.1)
R2	64 (11.7)	73 (22.2)	139 (46.6)	81 (60.5)
Median survival time (yr)	4.13 (95% CI 3.40-5.81)	2.49 (95% CI 1.92-3.08)	1.58 (95% CI 1.22-2.17)	0.91 (95% CI 0.75-1.23)
Recurrence-free survival (yr)	1.23 (95% CI 1.04-1.73)	0.82 (95% CI 0.65-1.05)	0.56 (95% CI 0.46-0.69)	0.38 (95% CI 0.29-0.45)
Site of the first recurrence				
Intrahepatic	263 (36.2)	168 (39.3)	149 (41.3)	88 (56.4)
Distant metastasis	71 (9.8)	35 (8.2)	34 (9.4)	17 (10.9)
Both	35 (4.8)	47 (11.0)	47 (13.0)	16 (10.3)
90-day mortality	19 (2.4)	14 (3.0)	21 (5.3)	14 (8.2)

Data are the mean (standard deviation) or number (%) unless otherwise indicated.
*Missing data were not imputed for baseline characteristics.
§More than three Couinaud's segments.
CI, confidence interval.

Table 4. Multivariate analysis to identify prognostic factors associated with survival after liver resection.

Risk factors	*p* value	Hazard ratio (95% CI)
Liver cirrhosis	0.011	1.25 (1.05-1.48)
Tumor size (cm)	<0.001	1.02 (1.01-1.04)
Number of tumors ≥3	0.016	1.27 (1.05-1.53)
Serum alpha-fetoprotein ≥15 ng/ml	<0.001	1.53 (1.25-1.87)
Vp4	<0.001	1.63 (1.27-2.06)
R2 resection	<0.001	1.59 (1.32-1.91)

underlying liver disease, the presence of viral infection subgroup (HR, 0.74 [95% CI, 0.65–0.86]; p <0.001), and the absence of viral infection subgroup (HR, 0.63 [95% CI, 0.50–0.79]; p <0.001). The alpha-fetoprotein level did not affect the survival benefit in either the positive serum alpha-fetoprotein ($\geqslant$15 ng/ml) subgroup (HR, 0.72 [95% CI, 0.63–0.83]; p <0.001) or the negative subgroup (HR, 0.66 [95% CI, 0.51–0.86]; p = 0.002). The tumor number did not affect the survival benefit either: single or two tumors subgroup (HR, 0.69 [95% CI, 0.60–0.81]; p <0.001), and multiple tumors ($\geqslant$3) subgroup (HR, 0.72 [95% CI, 0.59–0.88]; p = 0.002). Although the HR was favorable for LR, compared with non-LR treatment, in the Vp4 patient subgroup, it was not statistically significant (p = 0.242).

The operative procedures and outcomes in the LR group according to the extent of PVTT are shown in Table 3. Along with PVTT progression, the rate of major hepatectomy and R2 resection increased. The MST after surgery according to the extent of PVTT was as follows: Vp1, 4.13 years (95% CI, 3.40–5.81); Vp2, 2.49 years (95% CI, 1.92–3.08); Vp3, 1.58 years (95% CI, 1.22–2.17); and Vp4, 0.91 years (95% CI, 0.75–1.23). The recurrence-free survival after surgery according to the extent of PVTT was as follows: Vp1, 1.23 years (95% CI, 1.04–1.73); Vp2, 0.82 years (95% CI, 0.65–1.05); Vp3, 0.56 years (95% CI, 0.46–0.69); and Vp4, 0.38 years (95% CI, 0.29–0.45). The most frequent site of recurrence was intrahepatic for all extents of PVTT. The postoperative 90-day mortality rate was 3.7% (68 patients) for the entire population and increased according to the extent of PVTT (Vp1: 2.4%, Vp2: 3.0%, Vp3:5.3%, Vp4: 8.2%). In the LR group, 374 patients (19.9%) also underwent TACE, which did not prolong the MST (2.27 years [95% CI, 1.75–3.30] *vs.* 2.73 years [95% CI, 2.48–3.08]; p = 0.075). A multivariate analysis performed to determine the risk factors for overall survival after LR identified liver cirrhosis (HR, 1.25 [95% CI, 1.05–1.48]; p = 0.011), Vp4 (HR, 1.63 [95% CI, 1.27–2.06]; p <0.001), tumor size (HR, 1.02 [95% CI, 1.01–1.04]; p <0.001), number of tumors $\geqslant$3 (HR, 1.27 [95% CI, 1.05–1.53]; p = 0.016), serum alpha-fetoprotein $\geqslant$15 ng/ml (HR, 1.53 [95% CI, 1.25–1.87]; p <0.001), and R2 resection (HR, 1.59 [95% CI, 1.32–1.91]; p <0.001) as significant risk factors (Table 4).

Discussion

The current study revealed that LR has a significant survival benefit with an acceptable postoperative mortality rate for patients with PVTT, even in the propensity score-matched patient groups. In the subgroup analysis, this survival benefit was confirmed regardless of age, etiology of HCC, tumor marker elevation, and tumor number. Liver cirrhosis and R2 resection were risk factors for survival after LR. These results clearly demonstrated that as long as the PVTT is limited to first-order or peripheral branches and the liver function is preserved, LR is the first treatment of choice when a non-R2 resection is possible.

The presence of PVTT is classified as advanced stage HCC in the AASLD/BCLC staging system, and surgical resection has not been recommended for more than a decade [2]. We have to admit that there may be other unidentified biases requiring adjustment, even in the propensity score-based matching analysis; however, the median time of prolonged survival was 1.77 years for the overall cohort and 0.88 years for the propensity score-matched cohort. Since a randomized controlled trial comparing curative resection and palliative treatment would be difficult to conduct, the propensity score-based matching analysis used in the present study provides the second- best evidence available for this issue. Although surgical treatment for PVTT is technically demanding and a major hepatectomy is often required, the present findings justify the consideration of surgical treatment for HCC patients with PVTT.

LR for HCC patients with PVTT was initially reported in Japan in 1990 [14]. After this report, multiple eastern studies have revealed the possible survival benefit of LR in HCC patients with PVTT [10,11,15–19]. Although most of the studies were single center retrospective analyses, their results suggest that PVTT should not be considered as a contraindication for LR in eastern

countries [13,20]. Recently, Liu *et al.* [21] reported a single center retrospective study demonstrating the survival benefit of LR compared with TACE in propensity score-matched patient groups. Several recent western reports have also demonstrated a preferable prognosis after LR for HCC patients with PVTT [22–25]. Together with recently reported evidence, our study certainly confirms that PVTT should not be considered as a contraindication for LR.

Sorafenib has been established as a new standard treatment option for advanced HCC [2,3]. The effectiveness of sorafenib for HCC patients with PVTT has also been reported [26,27]. Since sorafenib became available in Japan in 2009, hardly any patients received sorafenib during the presently reported study period. Therefore, the prognosis of the non-LR group might be slightly better now thanks to the introduction of sorafenib. However, sorafenib is essentially a palliative treatment, and the expected survival time is normally no longer than 2 years. In addition, the median gain in survival enabled by sorafenib is only 0.23 years [3]. Considering that in the LR group, 420 patients (22.4%) lived for more than 3 years and the survival gain was 0.88 years compared with the non-LR group, the survival benefit of LR in patients with PVTT is evident, even in the era of sorafenib.

The surgical indications for PVTT invading the main trunk or contralateral branch, i.e., Vp4, are controversial [11,15,28]. In our data, the survival benefit of LR in the Vp4 patients group was not statistically significant, and the R2 resection rate was relatively high. Considering that a complete resection is extremely difficult in Vp4 patients, the surgical indications for Vp4 patients require further investigation. Neoadjuvant and/or adjuvant treatment including sorafenib and/or radiotherapy together with LR may be a promising treatment strategy for Vp4 patients [26,27].

Other than LR and sorafenib, TACE, hepatic arterial infusion chemotherapy, systemic chemotherapy, radiotherapy, and their combinations have been proposed as possible treatments for PVTT [18,29]. Since the MST after TACE was significantly better than that for best-supportive care (1.38 years *vs.* 0.36 years), TACE may be a suitable treatment for patients with PVTT. However, the rate of complications was not available, and the patient backgrounds were not uniform. Thus, further investigation in the era of sorafenib treatment is needed.

Recently, yttrium-90 radioembolization and other new radiation procedures showed a good prognosis, with an MST ranging from 1.31 years to 2.11 years for Vp1-3 patients [30–33]. However, the number of patients enrolled in these studies is relatively small, and LR was performed in patients with a good response [31]. Although yttrium-90 radioembolization is not performed in Japan, considering that the MST in Vp1-3 patients in our population was 2.90 years, there is no evidence of the superiority of these treatments to LR in patients with PVTT. Although the results of the radiotherapies are promising, future study is essential for comparison with the results of the present study.

One of the limitations of our study is that the data was analyzed retrospectively. Although we tried to eliminate the selection bias of the LR group through propensity score-based matching, the possibility of other biases that were not considered in the present study certainly exists. However, this is the largest case series to be reported and considering the prolongation of survival through LR, this study demonstrates that LR should be considered for patients with PVTT before resorting to palliative treatment, including sorafenib.

Although this article demonstrated the survival benefit of LR in HCC patients with PVTT through a large-scale multi-institutional study, the study was limited to patients in Japan, and the etiology of HCC is mainly viral infection, especially infection with the hepatitis C virus. In the subgroup analysis, the survival benefit of LR was significant among patients regardless of viral infection, indicating the applicability of this result to western countries where non-virus related HCC is more frequent. However, these results should be validated using an international database.

In conclusion, LR is associated with a longer survival outcome than non-surgical treatment in HCC patients with PVTT. As long as the PVTT is limited to a first-order branch, LR should be the first treatment of choice, especially in patients with good liver function.

Financial support

The study's baseline survey was funded by the Grant-in-aid for a nationwide follow-up survey of primary liver cancer.

Conflict of interest

Norihiro Kokudo reports grants from Dainippon Sumitomo and Bayer outside the submitted work. All other authors who have taken part in this study declared that they do not have anything to disclose regarding funding or conflict of interest with respect to this manuscript.

Authors' contributions

TK, KH, and NK had full access to the data. All authors were involved in study design, conduct, analysis of data, interpretation, or writing the reports.

Supplementary data

Supplementary data associated with this article can be found, in the online version, at http://dx.doi.org/10.1016/j.jhep.2016.05.044.

References

Author names in bold designate shared co-first authorship

[1] Thomas MB, Jaffe D, Choti MM, Belghiti J, Curley S, Fong Y, et al. Hepatocellular carcinoma: consensus recommendations of the National Cancer Institute Clinical Trials Planning Meeting. J Clin Oncol 2010;28:3994–4005.
[2] Forner A, Llovet JM, Bruix J. Hepatocellular carcinoma. Lancet 2012;379:1245–1255.
[3] Llovet JM, Ricci S, Mazzaferro V, Hilgard P, Gane E, Blanc JF, et al. Sorafenib in advanced hepatocellular carcinoma. N Engl J Med 2008;359:378–390.
[4] Imamura H, Seyama Y, Kokudo N, Maema A, Sugawara Y, Sano K, et al. One thousand fifty-six hepatectomies without mortality in 8 years. Arch Surg 2003;138:1198–1206.

[5] Kenjo A, Miyata H, Gotoh M, Kitagawa Y, Shimada M, Baba H, et al. Risk stratification of 7,732 hepatectomy cases in 2011 from the National Clinical Database for Japan. J Am Coll Surg 2014;218:412–422.
[6] Yamamoto Y, Ikoma H, Morimura R, Shoda K, Konishi H, Murayama Y, et al. Post-hepatectomy survival in advanced hepatocellular carcinoma with portal vein tumor thrombosis. World J Gastroenterol 2015;21:246–253.
[7] **Shaohua L**, **Qiaoxuan W**, Peng S, Qing L, Zhongyuan Y, Ming S, et al. Surgical strategy for hepatocellular carcinoma patients with portal/hepatic vein tumor thrombosis. PLoS One 2015;10 e0130021.
[8] Kokudo T, Hasegawa K, Yamamoto S, Shindoh J, Takemura N, Aoki T, et al. Surgical treatment of hepatocellular carcinoma associated with hepatic vein tumor thrombosis. J Hepatol 2014;61:583–588.
[9] Torzilli G, Belghiti J, Kokudo N, Takayama T, Capussotti L, Nuzzo G, et al. A snapshot of the effective indications and results of surgery for hepatocellular carcinoma in tertiary referral centers: is it adherent to the EASL/AASLD recommendations?: an observational study of the HCC East-West study group. Ann Surg 2013;257:929–937.
[10] Inoue Y, Hasegawa K, Ishizawa T, Aoki T, Sano K, Beck Y, et al. Is there any difference in survival according to the portal tumor thrombectomy method in patients with hepatocellular carcinoma? Surgery 2009;145:9–19.
[11] Minagawa M, Makuuchi M, Takayama T, Ohtomo K. Selection criteria for hepatectomy in patients with hepatocellular carcinoma and portal vein tumor thrombus. Ann Surg 2001;233:379–384.
[12] Hasegawa K, Kokudo N, Makuuchi M, Izumi N, Ichida T, Kudo M, et al. Comparison of resection and ablation for hepatocellular carcinoma: a cohort study based on a Japanese nationwide survey. J Hepatol 2013;58:724–729.
[13] Kudo M, Izumi N, Kokudo N, Matsui O, Sakamoto M, Nakashima O, et al. Management of hepatocellular carcinoma in Japan: Consensus-Based Clinical Practice Guidelines proposed by the Japan Society of Hepatology (JSH) 2010 updated version. Dig Dis 2011;29:339–364.
[14] Kumada K, Ozawa K, Okamoto R, Takayasu T, Yamaguchi M, Yamamoto Y, et al. Hepatic resection for advanced hepatocellular carcinoma with removal of portal vein tumor thrombi. Surgery 1990;108:821–827.
[15] Kojima H, Hatano E, Taura K, Seo S, Yasuchika K, Uemoto S. Hepatic resection for hepatocellular carcinoma with tumor thrombus in the major portal vein. Dig Surg 2015;32:413–420.
[16] Shi J, Lai EC, Li N, Guo WX, Xue J, Lau WY, et al. Surgical treatment of hepatocellular carcinoma with portal vein tumor thrombus. Ann Surg Oncol 2010;17:2073–2080.
[17] Chen XP, Qiu FZ, Wu ZD, Zhang ZW, Huang ZY, Chen YF, et al. Effects of location and extension of portal vein tumor thrombus on long-term outcomes of surgical treatment for hepatocellular carcinoma. Ann Surg Oncol 2006;13:940–946.
[18] **Minagawa M**, **Makuuchi M**. Treatment of hepatocellular carcinoma accompanied by portal vein tumor thrombus. World J Gastroenterol 2006;12:7561–7567.
[19] Poon RT, Fan ST, Ng IO, Wong J. Prognosis after hepatic resection for stage IVA hepatocellular carcinoma: a need for reclassification. Ann Surg 2003;237:376–383.
[20] **Yau T**, **Tang VY**, **Yao TJ**, Fan ST, Lo CM, Poon RT. Development of Hong Kong Liver Cancer staging system with treatment stratification for patients with hepatocellular carcinoma. Gastroenterology 2014;146:1691–1700.
[21] Liu PH, Lee YH, Hsia CY, Hsu CY, Huang YH, Chiou YY, et al. Surgical resection *vs.* transarterial chemoembolization for hepatocellular carcinoma with portal vein tumor thrombosis: a propensity score analysis. Ann Surg Oncol 2014;21:1825–1833.
[22] Pesi B, Ferrero A, Grazi GL, Cescon M, Russolillo N, Leo F, et al. Liver resection with thrombectomy as a treatment of hepatocellular carcinoma with major vascular invasion: results from a retrospective multicentric study. Am J Surg 2015;210:35–44.
[23] Roayaie S, Jibara G, Taouli B, Schwartz M. Resection of hepatocellular carcinoma with macroscopic vascular invasion. Ann Surg Oncol 2013;20:3754–3760.
[24] Chirica M, Scatton O, Massault PP, Aloia T, Randone B, Dousset B, et al. Treatment of stage IVA hepatocellular carcinoma: should we reappraise the role of surgery? Arch Surg 2008;143:538–543.
[25] Pawlik TM, Poon RT, Abdalla EK, Ikai I, Nagorney DM, Belghiti J, et al. Hepatectomy for hepatocellular carcinoma with major portal or hepatic vein invasion: results of a multicenter study. Surgery 2005;137:403–410.
[26] Kermiche-Rahali S, Di Fiore A, Drieux F, Di Fiore F, François A, Scotté M. Complete pathological regression of hepatocellular carcinoma with portal vein thrombosis treated with sorafenib. World J Surg Oncol 2013;11:171.
[27] Irtan S, Chopin-Laly X, Ronot M, Faivre S, Paradis V, Belghiti J. Complete regression of locally advanced hepatocellular carcinoma induced by sorafenib allowing curative resection. Liver Int 2011;31:740–743.
[28] Peng ZW, Guo RP, Zhang YJ, Lin XJ, Chen MS, Lau WY. Hepatic resection *vs.* transcatheter arterial chemoembolization for the treatment of hepatocellular carcinoma with portal vein tumor thrombus. Cancer 2012;118:4725–4736.
[29] Takayasu K, Arii S, Ikai I, Omata M, Okita K, Ichida T, et al. Prospective cohort study of transarterial chemoembolization for unresectable hepatocellular carcinoma in 8510 patients. Gastroenterology 2006;131:461–469.
[30] **Edeline J**, **Crouzet L**, Campillo-Gimenez B, Rolland Y, Pracht M, Guillygomarc'h A, et al. Selective internal radiation therapy compared with sorafenib for hepatocellular carcinoma with portal vein thrombosis. Eur J Nucl Med Mol Imaging 2016;43:635–643.
[31] **Garin E**, **Rolland Y**, Edeline J, Icard N, Lenoir L, Laffont S, et al. Personalized dosimetry with intensification using 90Y-loaded glass microsphere radioembolization induces prolonged overall survival in hepatocellular carcinoma patients with portal vein thrombosis. J Nucl Med 2015;56:339–346.
[32] Memon K, Kulik L, Lewandowski RJ, Mulcahy MF, Benson AB, Ganger D, et al. Radioembolization for hepatocellular carcinoma with portal vein thrombosis: impact of liver function on systemic treatment options at disease progression. J Hepatol 2013;58:73–80.
[33] **Xi M**, **Zhang L**, Zhao L, Li QQ, Guo SP, Feng ZZ, et al. Effectiveness of stereotactic body radiotherapy for hepatocellular carcinoma with portal vein and/or inferior vena cava tumor thrombosis. PLoS One 2013;8 e63864.

INTERNAL MEDICINE

□ CASE REPORT □

Cases with Refractory Ascites and a Delayed Response to Tolvaptan

Satoru Hagiwara, Naoshi Nishida, Hirokazu Chishina, Hiroshi Ida, Toshiharu Sakurai, Yoriaki Komeda, Masayuki Kitano and Masatoshi Kudo

Abstract

The patient was a 67-year-old female with liver cirrhosis due to hepatitis C. She was administered furosemide at 20 mg/day and spironolactone at 25 mg/day, but the ascites did not improve. Despite the additional administration of tolvaptan at 3.75 mg/day, the response to ascites was still poor. While the dose of tolvaptan was thereafter increased to 7.5 mg/day on the 7th hospital day, the ascites still persisted. However, she continued to receive tolvaptan (7.5 mg/day) because the worsening of her subjective symptoms was mild and she wished to do so. The ascites was later found to have almost completely disappeared on computed tomography (CT) at 6 months.

Key words: tolvaptan, liver cirrhosis, refractory ascites, delayed response

(Intern Med 55: 3273-3277, 2016)
(DOI: 10.2169/internalmedicine.55.7035)

Introduction

Conventionally, aldosterone antagonists and loop diuretics have been used for the management of ascites associated with liver cirrhosis (1, 2). However, some patients show poor responses or adverse reactions, such as renal dysfunction and electrolyte abnormalities, especially with high-dose administration and combined use. Tolvaptan is a vasopressin receptor antagonist and it shows a diuretic effect without Na excretion. It was approved as a concomitant medication for fluid retention in liver cirrhosis patients that insufficiently respond to existing diuretics for the first time in the world in September 2013 (3). Reportedly, there are some non-responders to tolvaptan, while others exhibit a delayed response after sustained administration. We herein report a patient in whom tolvaptan began to show an effect at least 2 months after the start of its administration.

Case Report

The patient was a 67-year-old female. During outpatient treatment for hepatitis C at a local clinic, hepatpcellular carcinoma (HCC) was detected in the right lobe of the liver, and percutaneous radiofrequency ablation was performed at our hospital on November, 2012. The patient was thereafter followed up at our hospital as an outpatient, but she developed anorexia and abdominal fullness in April 2014. Despite the administration of furosemide at 20 mg/day and spironolactone at 25 mg/day, the ascites did not decrease. The patient was admitted for the treatment of ascites on May, 2014. She had a history of cerebral infarction, but no particular familial history. She also had no history of interferon therapy for hepatitis C. The blood chemical analyses at the time of admission are shown in Table 1. The Child-Pugh score was 10 with grade C. Hyponatremia and marked renal dysfunction were also noted. The platelet count was markedly reduced at 37,000 cells/mL. Both alpha-fetoprotein (AFP) and des-gamma carboxyprothrombin (DCP) were mildly increased. Abdominal computed tomography (CT) before admission showed an irregularity of the liver surface, and the marked accumulation of ascites was observed. No signs of any recurrence of HCC were observed (Fig. 1a).

The course after admission is presented in Fig. 2. On admission, her body weight was 37.6 kg, and the daily urine volume was around 900 mL. While the administration of tolvaptan was initiated at 3.75 mg on the 1st hospital day, the urine volume did not increase with a slight increase in

Department of Gastroenterology and Hepatology, Kindai University Faculty of Medicine, Japan
Received for publication December 23, 2015; Accepted for publication March 21, 2016
Correspondence to Dr. Naoshi Nishida, naoshi@med.kindai.ac.jp

Table 1. **Laboratory Data on Admission.**

Blood count		*Urinalysis*	
WBC	3,400μL	Urine osmolarity	N.E.
Hb	10.3g/dL	Decrease rate	N.E.
PLT	3.7×10^{4}/μL		
Coagulability		*Dose of diuretics*	
PT	65.6%	Furosemide	20mg/day
Biochemical values		Spironolactone	25mg/day
Na	130mEq/L	*Initail dose of tolvaptan*	3.75mg/day
K	3.9mEq/L		
BUN	72mg/dL	*Complication by HCC*	None(after cure)
Cr	2.19mg/dL		
eGFR	18	*TM*	
Alb	2.6g/dL	AFP	13ng/mL
T-bil	0.4mg/dL	DCP	50mAU/mL
ALT	28IU/L		
CRP	0.3mg/dL		

WBC: white blood cell, Hb: hemoglobin, PLT: platelet, PT: prothrombin time, Na: sodium, K: potassium, BUN: blood urea nitrogen, Cr: creatinine, eGFR: estimated glomerular filtration rate, Alb: albumin, T-Bil: total bilirubin, ALT: alanine aminotransferase, N.E.: not evaluate, CRP: C-reactive protein, TM: tumor marker, HCC: hepatocellular carcinoma

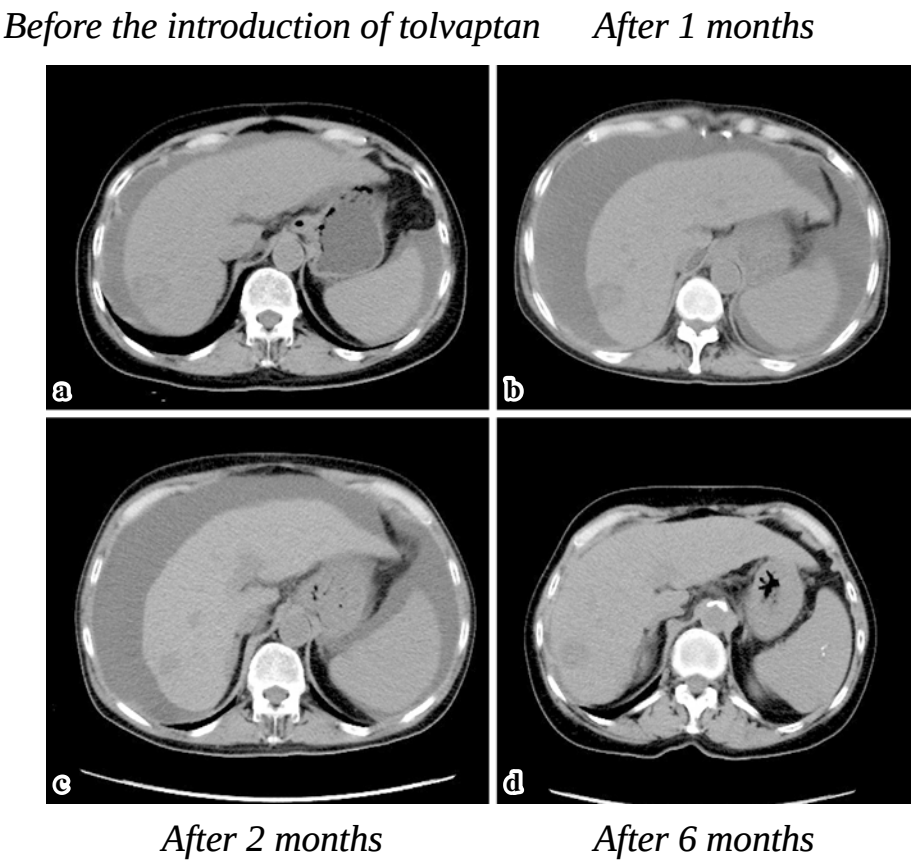

Figure 1. **(a) Abdominal CT performed 2 months before TLV administration showed cirrhosis with massive ascites. (b) A comparison of the abdominal CT performed 2 months before TLV administration with that performed 1 month after TLV administration revealed an increase in ascites. (c) A comparison of abdominal CT performed 1 month after TLV administration with that performed 2 months after TLV administration showed no significant increase or decrease in ascites. (d) Abdominal CT performed 6 months after TLV administration showed a significant decrease in ascites.**

her body weight; the dose of tolvaptan was thene increased to 7.5 mg on the 7th hospital day. Thereafter, although the urine volume showed no marked increase, the increase of her body weight became mild, and the patient was discharged on the 12th hospital day at her request. The water intake underwent a change of approximately 1,000 mL/day,

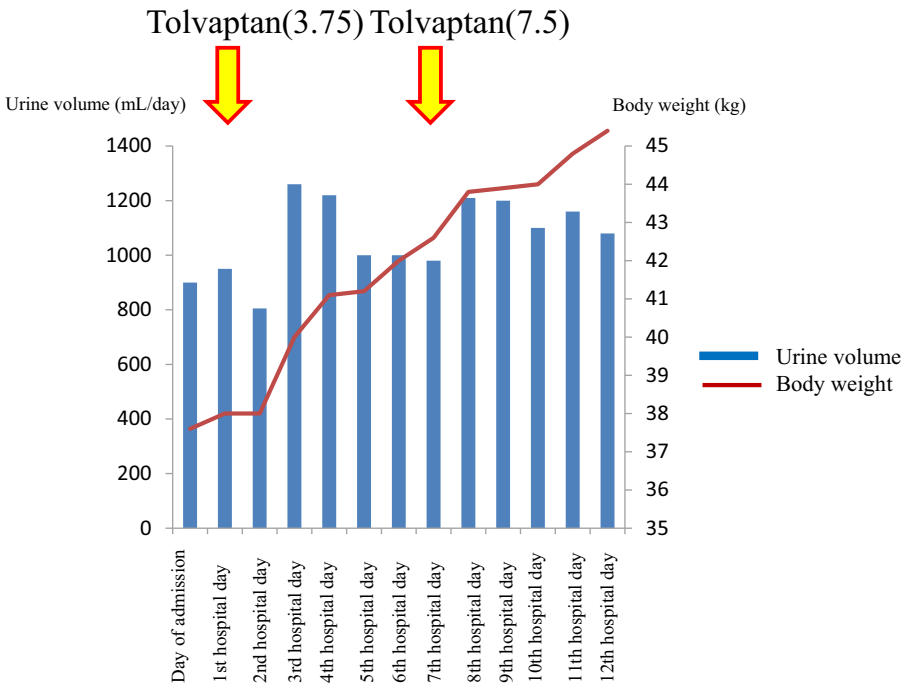

Figure 2. **Clinical course after admission; Despite the administration of tolvaptan at 3.75 mg on the 1st hospital day, no increase in urine volume or decrease in body weight was noted. Therefore, the dose of tolvaptan was increased to 7.5 mg on the 7th hospital day, but there was still no increase in urine volume or decrease in body weight.**

but the intake of fluids included with her meals clearly increased because the symptoms of anorexia also improved after admission. A comparison of the abdominal CT performed 2 months before tolvaptan administration with that performed 1 month after tolvaptan administration showed an increase in ascites (Fig. 1b), and the patient had clearly gained weight from 37.6 kg immediately before tolvaptan administration to 52.2 kg. However, she continued to receive only tolvaptan at 7.5 mg/day without any other additional treatment, such as cell-free and concentrated ascites reinfusion therapy (CART) because the worsening of her subjective symptoms was mild and she wished to do so. A comparison of the CT performed 1 month after tolvaptan administration with that performed 2 months after tolvaptan administration revealed no significant increase or decrease in ascites (Fig. 1c). However, she showed a weight loss from 52.2 to 49.9 kg; therefore, she continued to receive tolvaptan at 7.5 mg/day. After tolvaptan administration, no additional treatment for ascites was given. The abdominal CT performed at 6 months revealed the ascites to have markedly decreased (Fig. 1d). Therefore, the oral administration of furosemide was discontinued, and the administration of only spironolactone at 25 mg and tolvaptan at 7.5 mg was continued. After the beginning of tolvaptan administration, no adverse reaction such as liver and kidney dysfunction was observed.

Discussion

In cirrhotic patients, splanchnic vasodilation, an increase of portal vein pressure and portosystemic shunt result in a decreased effective arterial blood volume. A consequent decrease in the renal blood flow is considered to induce fluid retention through the activation of the renin-angiotensin-aldosterone system (4, 5). Although, aldosterone receptor antagonists are effective for the treatment of fluid retention associated with liver cirrhosis (1), it is insufficient in many patients. Fluid retention is also caused by the activation of vasopressin (VP) through the decrease in the circulating plasma volume (4, 5), but there is still no available medication that has been shown to be effective for the activation of VP.

Tolvaptan is an antagonist for vasopressin V2 receptors in the collecting ducts of the kidney, and it exerts a diuretic effect by suppressing the expression of aquaporin 2. In Japan, a phase 3 comparative study of tolvaptan was carried out in cirrhosis patients who responded poorly to the administration of loop diuretics and anti-aldosterone agents (3). According to the phase 3 study, the urine volume significantly increased on Days 1 and 7 in the tolvaptan group, but no significant change was observed in the placebo group. Thirst, constipation, kidney dysfunction, hepatic encephalopathy, and itching were noted as major adverse reactions, but their severity was only mild to moderate.

Various studies have been reported regarding the prediction of the effect of tolvaptan. Zhang et al. investigated 39 liver cirrhosis patients accompanied by refractory ascites, and observed the effect of tolvaptan to be attenuated in the patients with hepatorenal syndrome (HRS) (6). The effect of tolvaptan has also been reported to decrease as the estimated

Table 2. Time-course of Laboratory Data.

	On admission	After 14 days	After 1 month	After 2 months	After 6 months
Blood count					
WBC	3,400μL	3,900μL	5,200μL	4,000μL	2,700μL
Hb	10.3g/dL	9.8g/dL	10.9g/dL	8.3g/dL	9.9g/dL
PLT	3.7×10^{4}/μL	6.2×10^{4}/μL	10.8×10^{4}/μL	7.6×10^{4}/μL	10.9×10^{4}/μL
Coagulability					
PT	65.6%	75.8%	77.7%	62.6%	70.9%
Biochemical values					
Na	130mEq/L	140mEq/L	143mEq/L	144mEq/L	141mEq/L
K	3.9mEq/L	4.9mEq/L	5.0mEq/L	4.9mEq/L	4.7mEq/L
BUN	72mg/dL	27mg/dL	30mg/dL	23mg/dL	29mg/dL
Cr	2.19mg/dL	1.34mg/dL	1.45mg/dL	1.22mg/dL	1.20mg/dL
eGFR	18	31	29	35	35
Alb	2.6g/dL	2.4g/dL	2.9g/dL	2.6g/dL	2.8g/dL
T-bil	0.4mg/dL	0.4mg/dL	0.7mg/dL	0.5mg/dL	0.7mg/dL
ALT	28IU/L	27IU/L	27IU/L	20IU/L	34IU/L
CRP	0.33mg/dL	0.23mg/dL	0.25mg/dL	0.55mg/dL	0.04mg/dL

WBC: white blood cell, Hb: hemoglobin, PLT: platelet, PT: prothrombin time, Na: sodium, K: potassium, BUN: blood urea nitrogen, Cr: creatinine, eGFR: estimated glomerular filtration rate, Alb: albumin, T-Bil: total bilirubin, ALT: alanine aminotransferase, CRP: C-reactive protein

glemerular filtration rate (eGFR) decreased in renal failure patients in a single-dose study of tolvaptan (7). In a phase 3 clinical study in Japan, the effect of tolvaptan decreased when blood urea nitrogen (BUN) was high in a subanalysis (8). In addition, the effect of tolvaptan decreased in patients demonstrating renal parenchymal disorder with HRS and a decreased eGFR and those with high BUN, i.e., patients suggested to have intravascular volume depletion and prerenal renal dysfunction. The present patient had severe anorexia and prerenal renal dysfunction with 72 mg/dL BUN and 2.19 mg/dL creatinine (Cr) before admission, and these conditions may have been the cause of the poor effect of tolvaptan early after the initiation of administration. However, the symptoms of anorexia improved after admission, where the renal function markedly improved and BUN and Cr on day 14 after the initiation of tolvaptan administration were 27 and 1.34 mg/dL, respectively (Table 2). On the other hand, no reduction in the body weight or ascites was observed for at least 2 months after the initiation of tolvaptan administration. Thus, it is difficult to explain the cause of the poor effect of tolvaptan early after the initiation of administration with renal dysfunction alone. However, although both the ascites and the body weight (37.6→52.2 kg) clearly increased one month after the introduction of tolvaptan compared with those before introduction, no change in body weight was observed over the next month (52.2→49.9 kg). Therefore, it is conceivable that the renal dysfunction caused by dehydration could have blocked the effect of tolvaptan in the early course of tolvaptan treatment. Thereafter the effect of tolvaptan gradually increased after the initial course.

We herein presented a case showing a delayed effect of tolvaptan. Therefore, even when the initial responses of the urine volume and body weight are not remarkable, the continuation of tolvaptan administration should be considered if there is no exacerbation of ascites. Although the safety of long-term tolvaptan therapy has been reported (9), further studies involving more patients are needed before any definitive conclusions can be made.

The authors state that they have no Conflict of Interest (COI).

References

1. Boyer TD, Warnock DG. Use of diuretics in the treatment of cirrhotic ascites. Gastroenterology **84**: 1051-1055, 1983.
2. Pérez-Ayuso RM, Arroyo V, Planas R, et al. Randomized comparative study of efficacy of furosemide versus spironolactone in nonazotemic cirrhosis with ascites. Relationship between the diuretic response and the activity of the renin-aldosterone system. Gastroenterology **84**: 961-968, 1983.
3. Sakaida I, Yanase M, Kobayashi Y, et al; ASCITES Clinical Pharmacology Group. The pharmacokinetics and pharmacodynamics of tolvaptan in patients with liver cirrhosis with insufficient response to conventional diuretics: a multicentre, double-blind, parallel-group, phase III study. J Int Med Res **40**: 2381-2393, 2012.
4. Janicic N, Verbalis JG. Evaluation and management of hypoosmolality in hospitalized patients. Endocrinol Metab Clin North Am **32**: 459-481, 2003.
5. Schrier RW, Arroyo V, Bernardi M, et al. Peripheral arterial vasodilation hypothesis: a proposal for the initiation of renal sodium and water retention in cirrhosis. Hepatology **8**: 1151-1157, 1988.
6. Zhang X, Wang SZ, Zheng JF, et al. Clinical efficacy of tolvaptan for treatment of refractory ascites in liver cirrhosis patients. World J Gastroenterol **20**: 11400-11405, 2014.
7. Shoaf SE, Bricmont P, Mallikaarjun S. Pharmacokinetics and pharmacodynamics of oral tolvaptan in patients with varying degrees of renal function. Kidney Int **85**: 953-961, 2014.
8. Sakaida I, Nakajima K, Okita K, et al. Can serum albumin level affect the pharmacological action of tolvaptan in patients with liver cirrhosis? A post hoc analysis of previous clinical trials in Japan. J Gastroenterol **50**: 1047-1053, 2015.
9. Kogiso T, Tokushige K, Hashimoto E, et al. Safety and efficacy of long-term tolvaptan therapy for decompensated liver cirrhosis. Hepatol Res **46**: E194-E200, 2016.

Through-the-mesh technique after endoscopic ultrasonography-guided hepaticogastrostomy: a novel re-intervention method

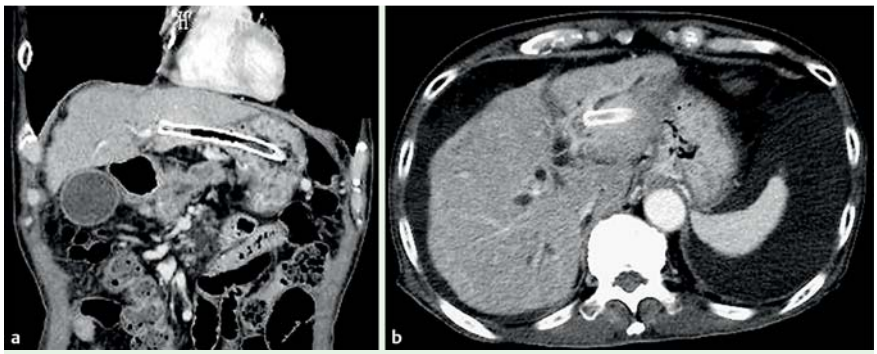

Fig. 1 Computed tomography (CT) images showing: **a** a covered metal stent deployed between the left intrahepatic bile duct and the stomach; **b** a dilated intrahepatic bile duct.

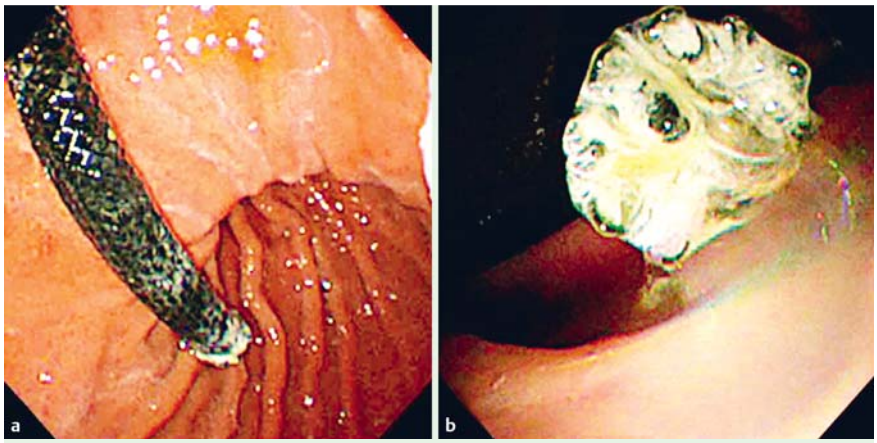

Fig. 2 Gastroscopy showing the occluded metal stent. The length of stent in the gastric lumen was about 5 cm.

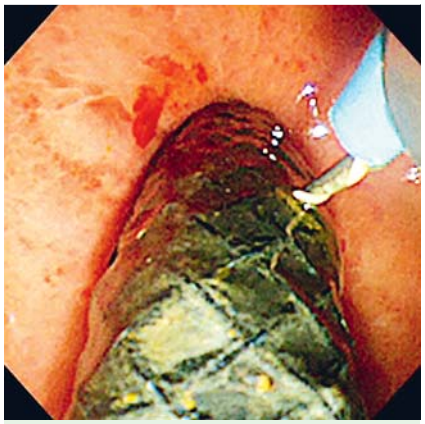

Fig. 3 A 0.025-inch stiff guidewire was inserted to penetrate the stent cover membrane near the gastric puncture site.

Video 1

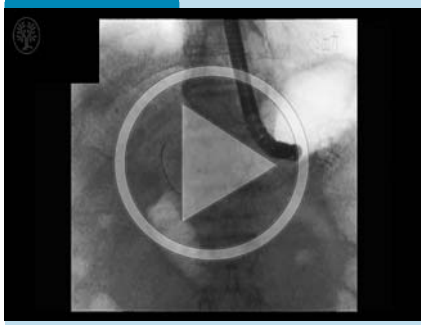

An additional metal stent was deployed through the mesh of the previously placed hepaticogastrostomy (HGS) stent to cover the malignant distal biliary stricture in an antegrade fashion as treatment for HGS stent occlusion.

Endoscopic ultrasonography-guided hepaticogastrostomy (EUS-HGS) is increasingly used to manage failed endoscopic biliary drainage in patients with malignant biliary obstruction [1–3]. A recent study showed that, for EUS-HGS, a stent ≥ 3 cm in length in the luminal portion may be suitable to prevent stent migration and achieve long-term stent patency [4]. However, such a placement can sometimes make re-intervention difficult. Here, we describe a novel re-intervention technique for HGS stent occlusion.

A 75-year-old man with advanced pancreatic cancer presented with a recurrence of jaundice 11 months after undergoing EUS-HGS using a covered metal stent (Niti-S Biliary Covered Stent; 8 × 100 mm; Taewoong Medical, Seoul, Korea) for distal malignant biliary obstruction (**Fig. 1 a**). Computed tomography (CT) revealed a dilated intrahepatic and extrahepatic bile duct (**Fig. 1 b**), and gastroscopy confirmed stent occlusion (**Fig. 2**). Re-intervention was attempted via the HGS route; however, insertion of an endoscopic retrograde cholangiopancreatography (ERCP) catheter into the intrahepatic bile duct through the proximal end of the HGS stent failed.

Re-intervention through the stent mesh was then attempted. A 0.025-inch stiff guidewire was inserted, penetrating the stent cover membrane close to the gastric puncture site (**Fig. 3**). Next, a 6-mm fine-gauge balloon catheter (REN; 3-Fr tip; Kaneka Medix, Osaka, Japan) was inserted into the bile duct, breaking through and opening the stent cover membrane. After successfully advancing the guidewire through the distal biliary stricture into the duodenum, an additional metal stent (BileRush selective; 10 × 60 mm, 5.7-Fr delivery system; Piolax, Kanagawa, Japan) was inserted through the mesh of the HGS stent to cover the biliary stricture in an antegrade fashion (**Fig. 4**; **Video 1**).

The postoperative period was uneventful and the patient's jaundice resolved in a few days. This "through-the-mesh" technique is simple and safe, and could be a useful re-intervention option after EUS-HGS.

Endoscopy_UCTN_Code_CPL_1AL_2AD

Competing interests: None

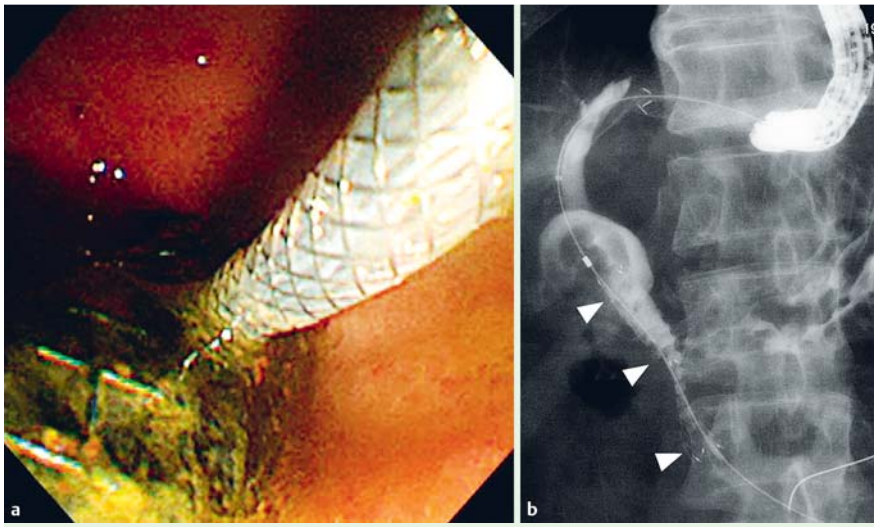

Fig. 4 An additional uncovered metal stent with a fine-gauge delivery system that was inserted to cover the distal biliary stricture in an antegrade fashion through the mesh of the previously deployed stent: **a** in endoscopic view; **b** on fluoroscopy.

Kosuke Minaga[1], Mamoru Takenaka[1], Takeshi Miyata[1], Yasuhiro Ueda[1], Masayuki Kitano[2], Masatoshi Kudo[1]

[1] Department of Gastroenterology and Hepatology, Kindai University Faculty of Medicine, Osaka-Sayama, Japan

[2] Second Department of Internal Medicine, Wakayama Medical University School of Medicine, Wakayama, Japan

References

1 *Burmester E, Niehaus J, Leineweber T* et al. EUS-cholangio-drainage of the bile duct: report of 4 cases. Gastrointest Endosc 2003; 57: 246 – 251

2 *Poincloux L, Rouquette O, Buc E* et al. Endoscopic ultrasound-guided biliary drainage after failed ERCP: cumulative experience of 101 procedures at a single center. Endoscopy 2015; 47: 794 – 801

3 *Wang K, Zhu J, Xing L* et al. Assessment and safety of EUS-guided biliary drainage: a systematic review and meta-analysis. Gastrointest Endosc 2016; 83: 1218 – 1227

4 *Ogura T, Yamamoto K, Sano T* et al. Stent length is impact factor associated with stent patency in endoscopic ultrasound-guided hepaticogastrostomy. J Gastroenterol Hepatol 2015; 30: 1748 – 1752

Bibliography

DOI http://dx.doi.org/10.1055/s-0042-117714
Endoscopy 2016; 48: E369–E370

Stuttgart · New York
ISSN 0013-726X

Corresponding author

Mamoru Takenaka, MD, PhD
Department of Gastroenterology and Hepatology
Kindai University Faculty of Medicine
377-2 Ohno-Higashi
Osaka-Sayama, 589-8511
Japan
Fax: +81-72-3672880
mamoxyo45@gmail.com

Hepaticogastrostomy guided by real-time contrast-enhanced harmonic endoscopic ultrasonography: a novel technique

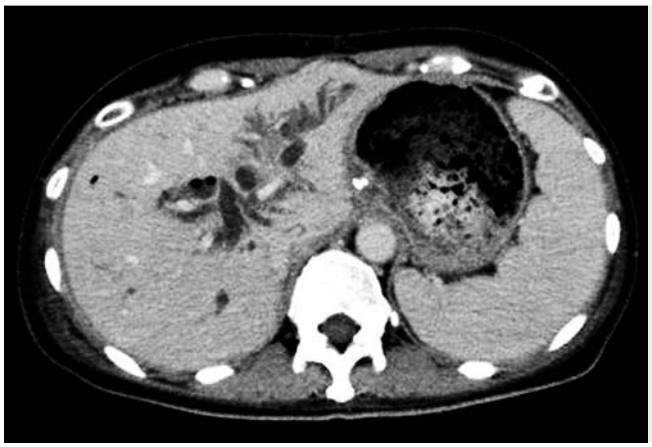

Fig. 1 Contrast-enhanced computed tomography (CT) image showing a dilated left intrahepatic bile duct.

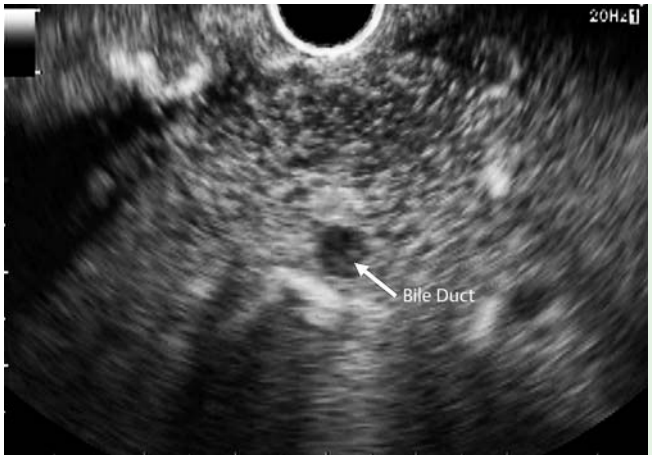

Fig. 2 Contrast-enhanced harmonic endoscopic ultrasonography (EUS) image in the post-vascular phase showing the intrahepatic bile duct as a contrast defect.

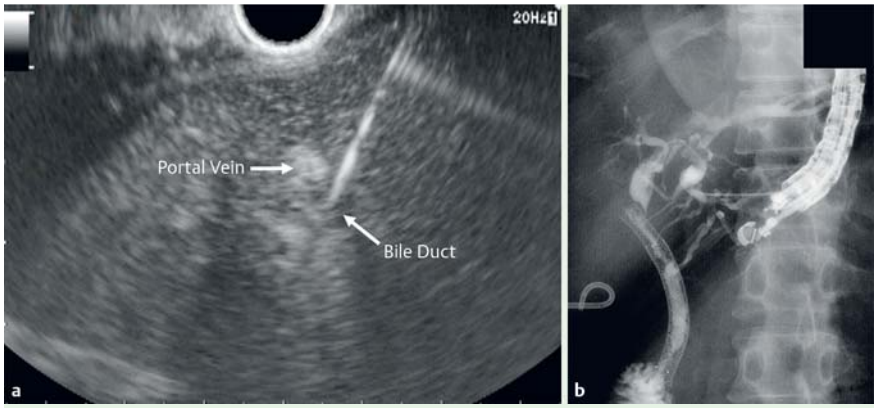

Fig. 3 Hepaticogastrostomy guided by real-time contrast-enhanced harmonic endoscopic ultrasonography (EUS). The dilated intrahepatic bile duct has been punctured using a 19-gauge aspiration needle and, after aspiration of bile, a small amount of contrast medium has been injected.

Video 1

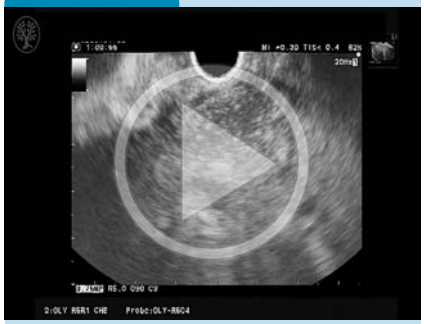

A sonographic contrast agent (Sonazoid) is injected to enhance the contrast between the bile duct and the hepatic parenchyma during endoscopic ultrasonography (EUS)-guided hepaticogastrostomy. After intravenous infusion of Sonazoid, the dilated intrahepatic bile duct could be identified and was punctured with a 19-gauge aspiration needle, which allowed hepaticogastrostomy to be safely carried out.

Endoscopic ultrasonography-guided hepaticogastrostomy (EUS-HGS) has recently been developed as an alternative biliary drainage technique for failed endoscopic retrograde cholangiopancreatography (ERCP) [1–3]. A recent review revealed its overall technical success rate to be 82 % [4], but puncturing the left intrahepatic bile duct (LIBD) is occasionally challenging. Here we present a case in which EUS-HGS was successfully performed under real-time contrast-enhanced harmonic EUS guidance.

A 55-year-old woman with obstructive jaundice secondary to gastric cancer was referred to our hospital. She had previously undergone endoscopic transpapillary metal stenting for biliary obstruction caused by lymph node metastasis. Stent occlusion occurred 6 months after stent deployment and an ERCP was attempted; however, the ampulla was inaccessible because of a duodenal stricture.

As computed tomography (CT) scanning revealed a dilated LIBD (▶ **Fig. 1**), EUS-HGS was performed. Although the left hepatic lobe could be visualized well with an echoendoscope from the stomach, the LIBD was invisible. The contrast between the bile duct and the hepatic parenchyma was enhanced by performing contrast-enhanced harmonic EUS. Immediately after an intravenous infusion of sonographic contrast agent (Sonazoid; Daiichi-Sankyo, Tokyo, Japan) had been administered, the dilated LIBD could be identified (▶ **Fig. 2**) and was punctured with a 19-gauge aspiration needle (▶ **Fig. 3**). After the fistula had been dilated, a covered metal stent was successfully deployed (▶ **Video 1**). The strong contrast between the liver par-

enchyma and the LIBD lasted until the stent had been deployed.

Sonazoid, a unique ultrasound contrast agent, is phagocytosed by Kupffer cells in the liver, which enables persistent and stable image enhancement [5]. When the normal hepatic parenchyma is enhanced, the bile ducts are clearly delineated as contrast defects as they do not contain Kupffer cells. In this patient, the bile duct was filled with sludge and debris, which may have impaired the visibility of the dilated LIBD on conventional EUS. In such cases, EUS-HGS under real-time contrast-enhanced imaging may be useful to clearly visualize and decisively puncture the LIBD.

Endoscopy_UCTN_Code_TTT_1AS_2AD

Competing interests: None

Kosuke Minaga, Masayuki Kitano, Tomoe Yoshikawa, Shunsuke Omoto, Ken Kamata, Kentaro Yamao, Masatoshi Kudo

Department of Gastroenterology and Hepatology, Kindai University Faculty of Medicine, Osaka-Sayama, Japan

References

1 *Burmester E*, *Niehaus J*, *Leineweber T* et al. EUS-cholangio-drainage of the bile duct: report of 4 cases. Gastrointest Endosc 2003; 57: 246 – 251
2 *Itoi T*, *Sofuni A*, *Itokawa F* et al. Endoscopic ultrasonography-guided biliary drainage. J Hepatobiliary Pancreat Sci 2010; 17: 611 – 616
3 *Artifon EL*, *Marson FP*, *Gaidhane M* et al. Hepaticogastrostomy or choledochoduodenostomy for distal malignant biliary obstruction after failed ERCP: is there any difference? Gastrointest Endosc 2015; 81: 950 – 959
4 *Ogura T*, *Higuchi K*. Technical tips for endoscopic ultrasound-guided hepaticogastrostomy. World J Gastroenterol 2016; 22: 3945 – 3951
5 *Park HS*, *Kim YJ*, *Yu MH* et al. Real-time contrast-enhanced sonographically guided biopsy or radiofrequency ablation of focal liver lesions using perflurobutane microbubbles (sonazoid): value of Kupffer-phase imaging. J Ultrasound Med 2015; 34: 411 – 421

Bibliography
DOI http://dx.doi.org/10.1055/s-0042-109059
Endoscopy 2016; 48: E228–E229

Stuttgart · New York
ISSN 0013-726X

Corresponding author
Masayuki Kitano, MD, PhD
Department of Gastroenterology and Hepatology
Kindai University Faculty of Medicine
377-2 Ohno-Higashi
Osaka-Sayama, 589-8511
Japan
Fax: +81-72-3672880
m-kitano@med.kindai.ac.jp

J Gastroenterol
DOI 10.1007/s00535-016-1204-2

The Japanese Society of Gastroenterology

ORIGINAL ARTICLE—LIVER, PANCREAS, AND BILIARY TRACT

Safety and efficacy of sorafenib in Japanese patients with hepatocellular carcinoma in clinical practice: a subgroup analysis of GIDEON

Masatoshi Kudo[1] · Masafumi Ikeda[2] · Tadatoshi Takayama[3] · Kazushi Numata[4] · Namiki Izumi[5] · Junji Furuse[6] · Takuji Okusaka[7] · Masumi Kadoya[8] · Satoshi Yamashita[9] · Yuichiro Ito[9] · Norihiro Kokudo[10]

Received: 24 February 2016 / Accepted: 24 March 2016

Abstract

Background GIDEON was a prospective, global, non-interventional study evaluating the safety of sorafenib in patients with unresectable hepatocellular carcinoma in real-world practice. The aim of this subgroup analysis was to assess the safety and efficacy of sorafenib as used by Japanese patients.

Methods In Japan, 508 patients were valid for safety analysis. Efficacy and safety were evaluated by the Child-Pugh score.

Results The number of patients with Child-Pugh A and B was 432 (85.0 %) and 58 (11.4 %), respectively. The median overall survival time and time to progression in patients with Child-Pugh A and Child-Pugh B were 17.4 and 4.9 months, 3.7 and 2.3 months, respectively. The most common drug-related adverse events (AEs) included hand-foot skin reaction (47.8 %), diarrhea (35.8 %) and hypertension (24.2 %). The incidences of all or drug-related AEs were similar between patients with Child-Pugh A and B. However, all or drug-related serious AEs, AEs resulting in permanent discontinuation of sorafenib and deaths were observed more frequently in patients with Child-Pugh B compared with Child-Pugh A. Duration of treatment tended to be shorter as the Child-Pugh score worsened.

Conclusions Sorafenib was well tolerated by Japanese HCC patients in clinical settings. Patients with Child-Pugh B had shorter duration of treatment and higher incidence of SAEs. It is important to carefully evaluate patients' conditions and assess the benefit and risk before making a decision to treat patients with sorafenib.

Keywords Hepatocellular carcinoma · Sorafenib · Japanese · GIDEON

✉ Masatoshi Kudo
m-kudo@med.kindai.ac.jp

[1] Department of Gastroenterology and Hepatology, Kinki University School of Medicine, 377-2 Ohno-Higashi, Osaka-Sayama, Osaka 589-8511, Japan

[2] Department of Hepatobiliary and Pancreatic Oncology, National Cancer Center Hospital East, Chiba, Japan

[3] Department of Digestive Surgery, Nihon University School of Medicine, Tokyo, Japan

[4] Gastroenterological Center, Yokohama City University Medical Center, Kanagawa, Japan

[5] Department of Gastroenterology and Hepatology, Musashino Red Cross Hospital, Tokyo, Japan

[6] Department of Internal Medicine, Medical Oncology, School of Medicine, Kyorin University, Tokyo, Japan

[7] Department of Hepatobiliary and Pancreatic Oncology, National Cancer Center Hospital, Tokyo, Japan

[8] Department of Radiology, Shinshu University School of Medicine, Nagano, Japan

[9] Medical Affairs Oncology and Hematology, Bayer Yakuhin, Ltd., Osaka, Japan

[10] Hepato-Biliary-Pancreatic Surgery Division, Department of Surgery, Graduate School of Medicine, University of Tokyo, Tokyo, Japan

Introduction

Hepatocellular carcinoma (HCC) is the second-leading cause of cancer-related death in men and the sixth in women worldwide [1, 2]. The major risk factors for HCC are hepatitis C virus (HCV), hepatitis B virus, alcohol

Published online: 22 April 2016

consumption, non-alcoholic steatohepatitis and diabetes mellitus [3, 4]. The majority of cases of HCC (70–90 % of cases) develop as a consequence of cirrhosis [5]—consequently, many patients have liver dysfunction and a high comorbidity rate. Not surprisingly, heterogeneity in the etiology, clinical symptoms and behavior of HCC makes it difficult to manage [6].

The mortality rate associated with HCC has declined by 37 %, primarily because of increased patient surveillance [7]; however, there are still many patients with unresectable HCC. Worldwide standards for the treatment of unresectable HCC have only recently been established [7–9]. Progress made in the understanding of the molecular mechanisms involved in the development and proliferation of tumors has enabled the development of effective therapeutic agents (i.e., targeted molecular therapy) for progressive HCC [10, 11].

Sorafenib is an oral multikinase inhibitor that has an inhibitory effect on tumor growth and angiogenesis [12], and it is a first-line treatment option for unresectable HCC [13]. The effect of sorafenib on prolongation of overall survival (OS) has been demonstrated in two previous phase 3, placebo-controlled, randomized studies [14, 15].

The Global Investigation of Therapeutic Decisions in Hepatocellular Carcinoma and Of Its Treatment With SorafeNib (GIDEON) was a prospective, global, non-interventional study conducted under the guidance of the European Medicines Agency [16]. The primary objective was to evaluate the safety of sorafenib in patients with unresectable HCC under real-world practice across different geographic regions as well as in a series of subgroups; 3371 patients participated from 39 countries, including Japan. Two interim analyses and a final analysis have been performed, as specified in the protocol [17, 18]. In the first and second interim analyses, 500 and 1500 patients were followed up, respectively, for $\geq$4 months; in the final analysis, $\geq$3000 patients were followed up for $\geq$12 months.

In Japan, GIDEON was conducted as a specific drug use-results survey under the regulation of postmarketing surveillance. Before the start of this study, all-case postmarketing surveillance was conducted separately, as required by the Japanese Ministry of Health, Labour and Welfare [19, 20]. The aim of the all-case postmarketing surveillance was to investigate unexpected drug-related adverse events (AEs), the incidence of drug-related AEs and the factors that might affect drug safety and efficacy. Patient registration was initiated after the completion of the registration for the all-case surveillance.

It is important to assess the safety and efficacy of sorafenib in daily practice and also understand the differences in the characteristics of HCC patients between Japan and other countries.

Here we report the results of the efficacy and safety analyses of sorafenib in 517 Japanese patients who participated in GIDEON.

Methods

Study design and objectives

The GIDEON study included patients who were eligible for systemic therapy and for whom the decision to treat with sorafenib had been made under real-world practice. Full details of the study design have been previously published [16].Efficacy analyses included OS and time to progression (TTP) by Child-Pugh score and Barcelona Clinic Liver Cancer (BCLC) status. Incidences of all or drug-related AEs and their details by Child-Pugh score were evaluated for the safety analyses. Patient demographics and baseline characteristics, incidences of drug-related AEs, BCLC stage, median OS, TTP and treatment history at baseline were obtained by region. In addition, the relationship between the number of transcatheter arterial chemoembolization (TACE) sessions before sorafenib administration and the response rate were analyzed. Child-Pugh score at the time of sorafenib administration by the number of TACE sessions was also calculated.

This study was conducted in accordance with Good Postmarketing Surveillance Practice, the principles of the Declaration of Helsinki, and all applicable laws and regulations. The protocol was reviewed and approved by the institutional review boards of all participating study sites. All patients provided written informed consent for participation before enrollment in the study (NCT00812175).

Patients

Patients eligible for the study were outpatients diagnosed histologically, cytologically or radiographically with unresectable HCC, had a life expectancy of $\geq$8 weeks and were candidates for systemic therapy. The decision to provide treatment with sorafenib was made by the patient's physicians. The exclusion criteria were based on the local product information for sorafenib [16].

Data collection and analytical methods

All study data were collected using the case report forms as previously reported for the study [16]. AEs were graded and other safety variables were summarized descriptively in accordance with the National Cancer Institute Common Terminology Criteria for Adverse Events version 3.0 (CTCAE). The safety analysis population included patients who received $\geq$1 dose of sorafenib and underwent $\geq$1

follow-up assessment. Patients in the intent-to-treat (ITT) population had received ≥1 dose of sorafenib.

Results

Patient baseline characteristics

A total of 508 patients were analyzed for safety. The patients demographic and baseline characteristics by Child-Pugh score and BCLC stage at the start of therapy are shown in Table 1.

Median age was 70 years, and approximately 80 % of the patients were males; 85 % of the patients were Child-Pugh A and 11.4 % were Child-Pugh B; 54.7 % of the patients were classified as BCLC stage C. A worse Eastern Cooperative Oncology Group (ECOG) score correlated with a worse Child-Pugh score. The ECOG score was similar among patients with BCLC stages A and B but tended to be higher in patients with BCLC stage C.

Sorafenib administration

Sorafenib administration by Child-Pugh score and BCLC stage at the start of therapy is shown in Table 2. Among the patients with Child-Pugh A, a similar proportion received an initial daily dose of 400 mg (47.0 %) versus 800 mg (46.3 %). A slightly higher proportion of patients with Child-Pugh B (53.4 %) than Child-Pugh A (47.0 %) received an initial daily dose of 400 mg.

Of the patients with BCLC stage B, 50.0 and 40.7 % received an initial daily dose of 400 and 800 mg, respectively. The proportion of patients with BCLC stage C (53.6 %) who received an initial daily dose of 800 mg was slightly higher than for those with BCLC stage B (40.7 %).

The average daily dose of sorafenib, 419.0 mg, was similar to that received by patients with Child-Pugh A and B scores and with BCLC stages A and B (400.0 mg); that of BCLC stage C was slightly higer (471.0 mg).

The median treatment duration with sorafenib was 15.90 weeks. Treatment duration tended to become shorter

Table 1 Demographic and baseline characteristics by initial dose, Child-Pugh Score and BCLC stage at start of therapy

Characteristics	Total ($n = 508$)	CP classification[a]		BCLC stage[b]			
		A ($n = 432$)	B ($n = 58$)	A ($n = 33$)	B ($n = 162$)	C ($n = 278$)	D ($n = 9$)
Patients, %	100	85.0	11.4	6.5	31.9	54.7	1.8
Sex, *n* (%)							
Male	410 (80.7)	355 (82.2)	41 (70.7)	22 (66.7)	137 (84.6)	225 (80.9)	6 (66.7)
Female	98 (19.3)	77 (17.8)	17 (29.3)	11 (33.3)	25 (15.4)	53 (19.1)	3 (33.3)
Median age, years (range)	70.0 (23–90)	70.0 (23–90)	71.5 (35–86)	74.0 (31–87)	73.0 (39–90)	69.0 (23–89)	67.0 (57–78)
Age groups, *n* (%)							
<65 years	159 (31.3)	133 (30.8)	19 (32.8)	7 (21.2)	42 (25.9)	96 (34.5)	3 (33.3)
65– < 75 years	185 (36.4)	166 (38.4)	17 (29.3)	10 (30.3)	59 (36.4)	103 (37.1)	3 (33.3)
>75 years	164 (32.3)	133 (30.8)	22 (37.9)	16 (48.5)	61 (37.7)	79 (28.4)	3 (33.3)
ECOG PS at start of therapy, *n* (%)							
0	406 (79.9)	354 (81.9)	39 (67.2)	31 (93.9)	144 (88.9)	202 (72.7)	7 (77.8)
1	87 (17.1)	65 (15.0)	17 (29.3)	1 (3.0)	16 (9.9)	66 (23.7)	1 (11.1)
2	5 (1.0)	5 (1.2)	0	0	0	4 (1.4)	0
3	1 (0.2)	0	1 (1.7)	0	0	0	1 (11.1)
TNM stage at entry of study, *n* (%)							
Stage I	14 (2.8)	12 (2.8)	0	13 (39.4)	1 (0.6)	0	0
Stage II	135 (26.6)	121 (28.0)	11 (19.0)	19 (57.6)	103 (63.6)	9 (3.2)	0
Stage IIIA	97 (19.1)	80 (18.5)	14 (24.1)	1 (3.0)	49 (30.2)	46 (16.5)	0
Stage IIIB	10 (2.0)	9 (2.1)	1 (1.7)	0	4 (2.5)	6 (2.2)	0
Stage IIIC	22 (4.3)	21 (4.9)	1 (1.7)	0	1 (0.6)	20 (7.2)	0
Stage IV	225 (44.3)	184 (42.6)	31 (53.4)	0	4 (2.5)	197 (70.9)	9 (100.0)

BCLC Barcelona Clinic Liver Cancer, *CP* Child-Pugh, *ECOG PS* Eastern Cooperative Oncology Group Performance Status, *TNM* tumor-node-metastasis

[a] For CP classification, 18 patients were not evaluable

[b] For BCLC stage, 26 patients were not evaluable

Table 2 Study drug administration summary by Child-Pugh and BCLC stage at start of therapy

	Total ($n = 508$)	CP classification					BCLC stage			
		A, < 7 ($n = 432$)	B, 7–9 ($n = 58$)	B, 7 ($n = 42$)	B, 8 ($n = 12$)	B, 9 ($n = 4$)	A ($n = 33$)	B ($n = 162$)	C ($n = 278$)	D ($n = 9$)
Initial sorafenib dose, *n* (%)										
200 mg	21 (4.1)	20 (4.6)	1 (1.7)	1 (2.4)	0	0	3 (9.1)	10 (6.2)	7 (2.5)	0
400 mg	246 (48.4)	203 (47.0)	31 (53.4)	24 (57.1)	4 (33.3)	3 (75.0)	23 (69.7)	81 (50.0)	119 (42.8)	4 (44.4)
600 mg	8 (1.6)	8 (1.9)	0	0	0	0	0	4 (2.5)	3 (1.1)	1 (11.1)
800 mg	231 (45.5)	200 (46.3)	26 (44.8)	17 (40.5)	8 (66.7)	1 (25.0)	6 (18.2)	66 (40.7)	149 (53.6)	4 (44.1)
Average daily dose[a], mg	419.0	425.0	400.0	400.0	584.5	400.0	400.0	400	471.0	412.0
Median treatment duration[b], week	15.90	17.40	7.60	8.80	5.70	10.35	23.60	17.70	13.20	16.10

CP Child-Pugh, *BCLC* Barcelona Clinic Liver Cancer stage

[a] Determined by actual days on the study drug, excluding interruptions

[b] From initial visit to last dosing date

as the Child-Pugh score worsened; patients with Child-Pugh A and Child-Pugh B had median treatment durations of 17.40 and 7.60 weeks, respectively.

Efficacy analyses

A total of 500 patients were analyzed for efficacy in the ITT analysis. The difference between the safety and ITT population was due to reasons such as exclusion of patients who had a history of sorafenib treatment. OS and TTP by Child-Pugh score and BCLC stage per Response Evaluation Criteria in Solid Tumors (RECIST) v1.0 are shown in Figs. 1 and 2.

The median OS in patients with Child-Pugh A (17.4 months; Fig. 1a) was longer than in those with Child-Pugh B (4.9 months), suggesting that the Child-Pugh score is a prognostic factor. Similarly, the median TTP in patients with Child-Pugh A (3.7 months; Fig. 1b) was

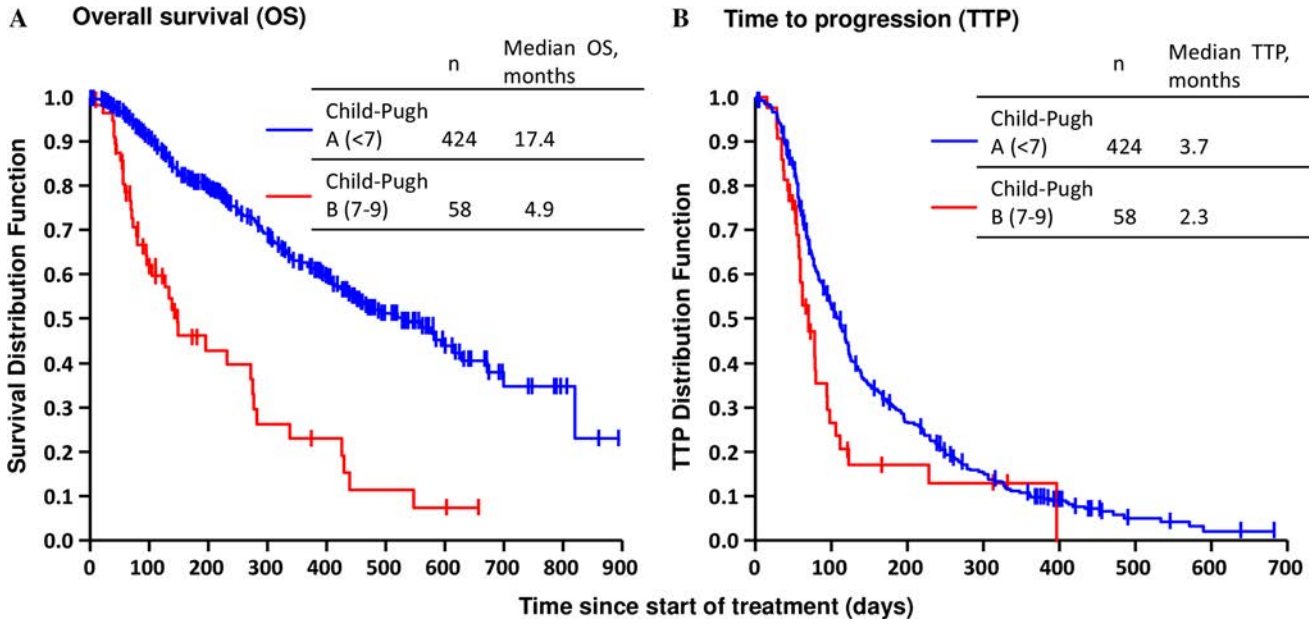

Fig. 1 Kaplan-Meier curve of OS and TTP (intent-to-treat population): **a** OS by baseline Child-Pugh status; **b** TTP by baseline Child-Pugh status. *OS* overall survival, *TTP* time to progression

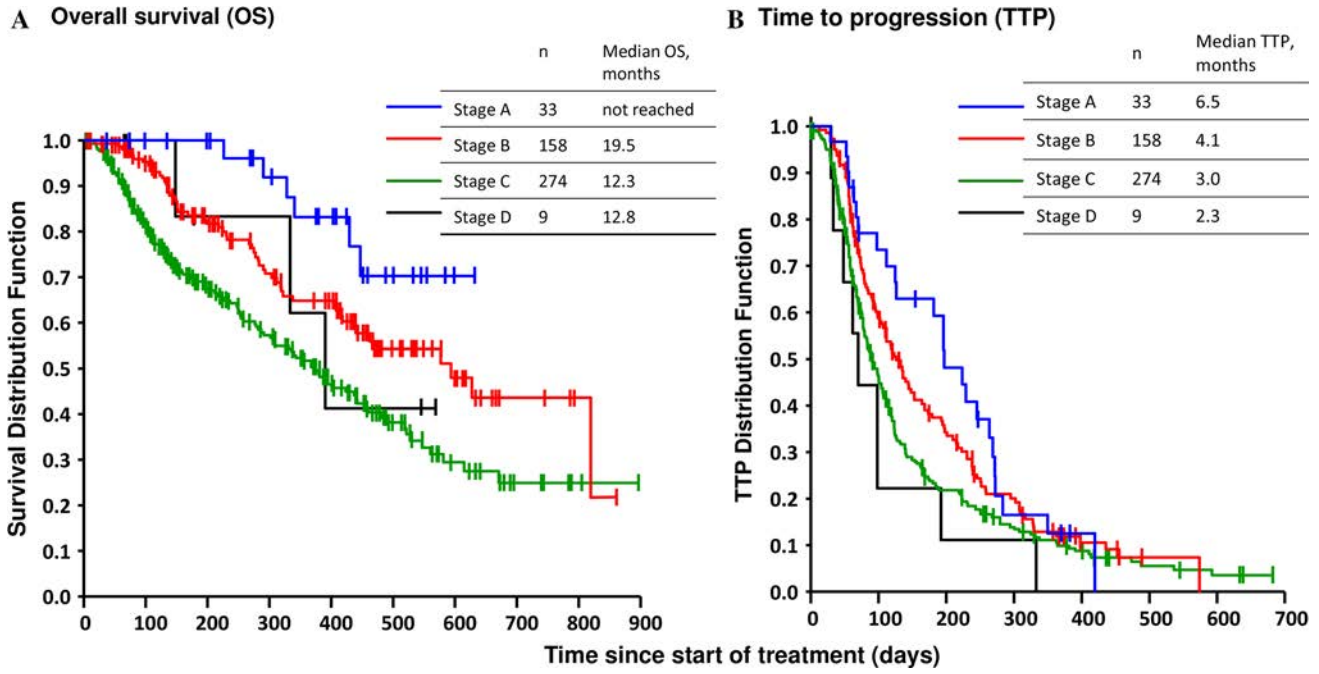

Fig. 2 Kaplan-Meier curve of OS and TTP (intent-to-treat population): **a** OS by BCLC classifications; **b** TTP by BCLC classifications. *BCLC* Barcelona Clinic Liver Cancer, *OS* overall survival, *TTP* time to progression

longer than in patients with Child-Pugh B (2.3 months), but the difference was not as remarkable as that seen for OS. The TTP by modified RECIST (mRECIST) also showed a similar trend (data not shown).

Although the median OS in patients with BCLC stage A was not reached, OS tended to be shorter with more advanced BCLC stage (Fig. 2a). Median OS was longer in patients with better liver function; median OS in patients with BCLC stage B of Child-Pugh A and Child-Pugh B were 20.7 (95 % CI 15.4–unknown) and 8.9 (95 % CI 4.6–14.4) months, respectively. TTP, as measured by RECIST, tended to be shorter with more advanced BCLC stage (Fig. 2b); TTP in patients with BCLC stage A was 6.5 (95 % CI 4.1–8.8) months, 4.1 (3.4–5.0) months in patients with stage B and 3.0 (2.6–3.5) months in patients with stage C. TTP by mRECIST showed a similar tendency (data not shown).

Safety analyses

A summary of AEs by Child-Pugh score and BCLC stage at the start of sorafenib therapy is shown in Table 3.

The incidence of AEs and drug-related AEs in patients with Child-Pugh A and Child-Pugh B were similar (94.9 % and 94.8, 88.2 and 86.2 %, respectively)

The incidence of serious AEs (SAEs) and drug-related SAEs in patients with Child-Pugh B was higher than in patients with Child-Pugh A (69.0 % and 37.0, 32.8 and 16.2 %, respectively). The incidence of AEs leading to permanent discontinuation of sorafenib was 38.7 % in patients with Child-Pugh A and 51.7 % in patients with Child-Pugh B. The incidence of treatment-emergent death occurring up to 30 days after discontinuation of sorafenib was 11.8 % in patients with Child-Pugh A and 34.5 % in patients with Child-Pugh B.

Drug-related AEs reported more frequently in patients with Child-Pugh A than with B included hand-foot skin reaction (HFSR), hypertension, alopecia, hoarseness, decreased platelet count, pruritus and rash/desquamation. However, vomiting and abnormal laboratory tests were reported more often in patients with Child-Pugh B than with A.

The drug-related AEs of the hepatic system of liver dysfunction, hypoalbuminemia, and hepatic encephalopathy were observed more frequently in patients with Child-Pugh B than Child-Pugh A. Among drug-related SAEs, the incidence rates of liver dysfunction, hepatic encephalopathy, gastric ulcer and abnormal laboratory tests were also higher in patients with Child-Pugh B.

Comparison with other geographic regions in GIDEON

Patient baseline characteristics, incidence of drug-related AEs, BCLC stage, median OS and TTP, and treatment history in the five geographic regions of the GIDEON study (Asia-Pacific, European Union, Latin America, USA and Japan) are summarized in Table 4 [21]. In Japanese patients, the median age was higher (70 years) and a

Table 3 Overview of safety data by Child-Pugh classification

Adverse events[a], *n* (%)	Total ($n = 508$)	CP classification			
		A, < 7 ($n = 432$)	B, 7–9 ($n = 58$)	B, 7 ($n = 42$)	B, 8 ($n = 12$)
AEs, all grades	482 (94.9)	410 (94.9)	55 (94.8)	39 (92.9)	12 (100.0)
Drug-related AEs, all grades	445 (87.6)	381 (88.2)	50 (86.2)	36 (85.7)	12 (100.0)
AEs, grade 3 or 4	223 (43.9)	195 (45.1)	23 (39.7)	19 (45.2)	3 (25.0)
Drug-related AEs, grade 3 or 4	190 (37.4)	161 (37.3)	24 (41.4)	19 (45.2)	5 (41.7)
SAEs[b], all grades	209 (41.1)	160 (37.0)	40 (69.0)	28 (66.7)	9 (75.0)
Drug-related SAEs[b], all grades	90 (17.7)	70 (16.2)	19 (32.8)	16 (38.1)	3 (25.0)
AEs resulting in permanent discontinuation of sorafenib[c]	210 (41.3)	167 (38.7)	30 (51.7)	24 (57.1)	6 (50.0)
Deaths[d]	77 (15.2)	51 (11.8)	20 (34.5)	12 (28.6)	6 (50.0)
Any drug-related AEs ≥5 %, %	87.6	88.2	86.2	85.7	100.0
Hand-foot skin reaction	47.8	49.5	37.9	35.7	58.3
Diarrhea	35.8	37.3	24.1	26.2	16.7
Hypertension	24.2	25.5	15.5	16.7	16.7
Alopecia	19.5	21.3	5.2	4.8	8.3
Anorexia	19.7	18.3	20.7	21.4	25.0
Fatigue	17.7	17.6	20.7	26.2	8.3
Rash/desquamation	14.6	15.7	8.6	9.5	8.3
Hoarseness	10.8	11.3	6.9	9.5	0
Decreased platelet count	9.1	10.0	5.2	7.1	0
Pyrexia	5.7	5.6	5.2	4.8	0
Pruritus	4.7	5.1	1.7	2.4	0
Amylase increased	5.5	5.6	6.9	9.5	0
Hypophosphatemia	4.1	4.2	5.2	4.8	8.3
Vomiting	2.4	1.9	5.2	2.4	16.7
Abnormal laboratory tests	2.2	1.4	6.9	9.5	0
Incidence of hepatic system drug-related AEs (≥5 %), %					
ALT increased	7.3	7.2	6.9	2.4	25.0
AST increased	7.9	8.1	5.2	2.4	16.7
Hyperbilirubinemia	5.5	5.3	6.9	2.4	25.0
Liver dysfunction	4.5	3.7	12.1	14.3	8.3
Hypoalbuminemia	3.1	2.8	6.9	7.1	8.3
Hepatic encephalopathy	2.4	2.1	5.2	4.8	8.3
Incidence of drug-related SAE[b] (≥2 %), %					
Any drug-related SAE	17.7	16.2	32.8	38.1	25.0
Liver dysfunction	2.2	1.4	8.6	9.5	8.3
Hepatic encephalopathy	1.4	1.2	3.4	4.8	0
Gastric ulcer	0.8	0.5	3.4	4.8	0
Abnormal laboratory tests	0.8	0.5	3.4	4.8	0

AE adverse event, *ALT* alanine aminotransferase, *AST* aspartate aminotransferase, *CP* Child-Pugh, *SAE* serious adverse event

[a] Graded as per the National Cancer Institute Common Terminology Criteria for Adverse Events, version 3.0

[b] An SAE/drug-related SAE is defined as any AE/drug-related AE occurring at any dose that results in any of the following outcomes: death, life-threatening illness, hospitalization or prolongation of existing hospitalization, persistent or significant disability/incapacity, congenital anomaly/birth defect or medically important event

[c] Any AEs

[d] Treatment-emergent deaths occurring up to 30 days after last sorafenib dose

Table 4 Background difference by region

	Total ($n = 3202$)	Asia-Pacific ($n = 928$)	Europe ($n = 1113$)	Latin America ($n = 90$)	USA ($n = 563$)	Japan ($n = 508$)
Patients, %	100	28.9	34.8	2.8	17.6	15.9
Median (range) age, years	62 (15–98)	54 (19–87)	66 (15–94)	67 (18–98)	61 (20–87)	70 (23–90)
Daily dose, mg						
Median	688.0	800.0	780.0	800.0	527.0	419.0
Mean	616.5	663.4	668.1	748.5	555.7	487.2
Etiology, %						
Hepatitis B	36.5	82.3	18.1	3.3	14.0	24.2
Hepatitis C	32.9	5.0	35.6	35.6	54.9	53.1
Alcohol use	26.0	16.2	34.3	15.6	39.3	13.2
NASH	2.8	0.2	3.2	6.7	6.0	2.4
Treatment-emergent AEs, %						
Drug-related AEs, all grades	66.0	48.7	68.8	48.9	71.9	87.6
Drug-related AEs, grade 3 or 4	23.6	12.2	27.4	12.2	23.8	37.4
Drug-related SAEs[a], all grades	9.3	3.4	10.9	13.3	7.5	17.7
AEs leading to permanent discontinuation of sorafenib[b]	31.4	20.2	35.1	13.3	36.2	41.3
Deaths[c]	23.7	19.1	25.7	33.3	33.4	15.2
BCLC stage at the initial diagnosis						
A	21.6	9.1	24.6	23.3	16.9	43.7
B	19.7	15.8	25.9	31.1	11.5	20.3
C	30.1	37.6	31.9	23.3	26.5	17.7
D	2.8	2.6	2.0	7.8	5.9	0.8
BCLC stage at the start of sorafenib therapy						
A	7.1	2.8	8.5	17.8	9.9	6.5
B	19.8	10.2	24.3	40.0	12.4	31.9
C	52.0	61.1	52.9	28.9	36.2	54.7
D	5.4	5.0	4.0	8.9	11.7	1.8
Median (range) time from the initial diagnosis to death, months						
BCLC stage A	59.2 (51.9–67.5)	54.0 (10.3–NA)	49.3 (42.3–58.0)	23.3 (17.2–NA)	24.9 (18.4–53.5)	91.0 (76.6–113.1)
BCLC stage B	29.9 (25.6–39.0)	31.0 (18.4–47.7)	27.3 (23.0–33.1)	22.2 (12.9–NA)	19.7 (11.1–36.8)	47.9 (40.9–86.2)
BCLC stage C	10.6 (9.4–12.4)	10.3 (8.6–13.4)	11.0 (8.9–13.0)	11.2 (3.1–NA)	8.5 (6.2–10.2)	27.7 (16.6–40.8)
BCLC stage D	8.9 (6.2–13.1)	8.9 (8.6–14.8)	11.0 (4.2–21.7)	NA	7.5 (4.5–12.8)	13.1 (NA–NA)
Overall	25.5 (23.9–28.3)	20.9 (17.3–25.2)	25.0 (22.9–28.7)	19.5 (13.5–NA)	14.8 (13.1–17.0)	79.6 (62.1–96.0)
Median OS from the start of sorafenib therapy, months	10.9	9.7	11.8	13.7	8.5	14.5
Median TTP from the start of sorafenib therapy, months	4.8	3.8	6.4	15.2	5.5	3.4
Median time from initial diagnosis to the start of sorafenib therapy, months	3.9	2.6	3.7	1.2	2.8	24.1
Previous therapy, %						
Surgical treatment	21.1	24.2	15.5	5.6	9.4	43.3
Transplant	2.6	3.3	2.0	2.2	4.8	0.2
All locoregional therapy	57.5	67.2	43.5	27.8	49.4	84.4
TACE	47.2	60.3	33.1	13.3	37.1	71.3

Table 4 continued

	Total ($n = 3202$)	Asia-Pacific ($n = 928$)	Europe ($n = 1113$)	Latin America ($n = 90$)	USA ($n = 563$)	Japan ($n = 508$)
RFA	17.5	12.8	14.9	17.8	11.5	38.4
HAI	5.6	5.2	1.0	2.2	3.9	18.9
PEI	4.7	2.7	5.3	0	1.1	11.6
Systemic therapy	5.2	5.0	3.8	0	3.4	11.6

AE adverse event, *BCLC* Barcelona Clinic Liver Cancer, *HAI* hepatic arterial infusion chemotherapy, *NA* not applicable, *NASH* nonalcoholic steatohepatitis, *OS* overall survival, *PEI* percutaneous ethanol injection, *RFA* radiofrequency ablation, *SAE* serious adverse event, *TACE* transcatheter arterial chemo-embolization, *TTP* time to progression

[a] A drug-related SAE is defined as any drug-related AE occurring at any dose that results in any of the following outcomes: death; life-threatening condition; hospitalization or prolongation of existing hospitalization; persistent or significant disability/incapacity; congenital anomaly/birth defect; medically important event

[b] Any AEs

[c] Treatment-emergent deaths occurring up to 30 days after the last sorafenib dose

history of locoregional therapy was also higher (84.4 %) than for other regions. Particularly, TACE was conducted more frequently in Japanese patients (71.3 %). Infection with HCV was etiologically associated with 53.1 % of HCC cases in Japan, which was comparable to the USA. Japan experienced the highest incidence of drug-related AEs, including CTCAE grades 3 and 4, drug-related SAEs and AEs resulting in permanent discontinuation of sorafenib, but the lowest rate of deaths. In Japan, 43.7 % of patients had BCLC stage A at the time of initial diagnosis, but the majority of patients had progressed to stage B (31.9 %) or C (54.7 %) by the initiation of sorafenib therapy. Regardless of BCLC stage, Japanese patients showed a longer time from initial diagnosis to death than those in other regions. In addition, the median OS from the start of sorafenib therapy was longest, but the median TTP was shorter than in other regions.

Effects of the number of transcatheter arterial chemoembolization sessions on the tumor response rate and Child-Pugh status

The relationships between the number of TACE sessions and its tumor response rate before the start of sorafenib therapy and between the number of TACE sessions and Child-Pugh score at initiation of sorafenib therapy are shown in Table 5. It has been shown that there is no significant correlation between the tumor reduction rate (World Health Organization and RECIST criteria) and the pathologic necrosis rate after TACE with lipiodol [22]. The response evaluation criteria that take account of the tumor necrosis are thus required in liver cancer treatment. Therefore, it is common in Japan to determine the treatment effect using the modified RECIST and the response evaluation criteria in cancer of the liver [23, 24].

The number of TACE sessions was higher in Japan than in other regions; however, patients with ≥6 TACE sessions tended to have lower complete and partial response rates. In addition, when the number of TACE sessions before sorafenib therapy was ≥6, the percentage of patients with Child-Pugh B was higher at initiation of sorafenib therapy.

Discussion

GIDEON was a large-scale, prospective, noninterventional study with ≥3300 patients from 39 countries evaluating the safety and efficacy of sorafenib and the factors that affect decision making with regard to treatment options. The median treatment duration of sorafenib in patients with Child-Pugh B was shorter than in patients with Child-Pugh A. Although the incidence of all or drug-related AEs was similar between Child-Pugh A and B, the incidence of all or drug-related SAEs, the number of AEs resulting in permanent discontinuation of sorafenib and deaths was higher in patients with Child-Pugh B. The incidence of drug-related AEs of hepatic-related events, such as liver dysfunction, hypoalbuminemia and hepatic encephalopathy, was higher in patients with Child-Pugh B than with Child-Pugh A. The incidence of drug-related AEs was analyzed by patient-year in consideration of the treatment duration of sorafenib. The results showed that drug-related AEs and liver function in patients with Child-Pugh A and Child-Pugh B were 1.59 and 2.67, 0.07 and 0.37 events per patient-year, respectively (data not shown). It is necessary to fully weigh the benefits versus risks associated with sorafenib treatment in patients with Child-Pugh B. Furthermore, when Cox regression analysis was given for parameters used in the Child-Pugh classification (excluding hepatic encephalopathy) at the time of treatment initiation

Table 5 Summary of response to TACE

TACE session	Patients, *n*	Tumor response[a], %						CP classification, %		
		CR	Non-CR	Responder	Nonresponder	Disease control	Progressors	A	B	Not evaluable
1	362	18.5	67.1	68.2	17.4	78.4	7.2	85.4	11.0	3.6
2	286	12.2	75.2	68.5	18.9	77.6	9.8	83.2	12.9	3.8
3	219	12.8	74.9	67.1	20.6	76.7	11.0	82.6	12.3	5.0
4	161	8.1	77.0	61.5	23.6	75.8	9.3	80.7	13.0	6.2
5	112	8.9	78.6	62.5	25.0	75.0	12.5	83.9	10.7	5.4
6	75	5.3	78.7	56.0	28.0	69.3	14.7	82.7	16.0	1.3
7	47	2.1	80.8	57.4	25.5	72.3	10.6	76.6	21.3	2.1
8	33	3.0	75.8	39.4	39.4	60.6	18.2	72.7	27.3	0.0
9	21	4.8	71.4	42.9	33.3	61.9	14.3	71.4	28.6	0.0

CP Child-Pugh, *CR* complete response, *TACE* transcatheter arterial chemoembolization

[a] For tumor response, a total rate of each category did not reach 100 % because of the missing or unevaluable patients

with sorafenib, albumin and bilirubin levels were identified as contributing factors to the OS, with the hazard ratio for bilirubin being the highest (data not shown). The results of global analysis had shown that ascites, albumin and bilirubin levels were factors affecting the OS, which were similar to those of the Japanese subgroup analysis [25].

Before the start of this study in Japan, all-case surveillance was conducted separately under the regulations of postmarketing surveillance [19, 20]. The incidence of drug-related AEs was 90.2 %. Frequently observed drug-related AEs included HSFR (51.4 %), liver dysfunction (26.4 %), diarrhea (25.1 %) and hypertension (21.6 %) [19, 20]. The results of Japanese subgroup analyses showed that drug-related AEs were observed in 87.6 % of patients. Frequently observed drug-related AEs included hand-foot skin reaction (47.8 %), liver dysfunction (4.5 %), diarrhea (35.8 %) and hypertension (24.2 %).

Reasons for the low incidence of liver dysfunction may be that a safety bulletin (liver failure and hepatic encephalopathy) was issued from the Japanese Proper Use Advisory Committee immediately after initiation of registration and that there was routine monitoring (e.g., periodic liver function tests followed by appropriate dose reduction or interruption) during sorafenib treatment.

The incidence of drug-related AEs of liver dysfunction was less than 1 % in the sorafenib arm in the Phase III SHARP and Asia-Pacific trial. In the SHARP trial, times to deterioration of liver function (Child-Pugh classification) were similar between the sorafenib and placebo arm (data not shown).

Compared with other regions, the mean time from the initial diagnosis to death in Japan tended to be longer irrespective of BCLC stage. This difference could be the result of early detection or because patients in Japan had more treatment opportunities than those in other regions. In addition, TTP from the start of sorafenib therapy in Japanese patients was the shortest among patients worldwide; Japan's early monitoring by imaging appears to be the major reason why Japanese patients have the shortest TTP [26, 27].

The present results also showed that the incidence of AEs resulting to permanent discontinuation of sorafenib in Japanese patients was 41.3 %, a higher rate than seen in other regions. The incidence of HFSR was 4.1 %, which was the second highest rate after liver dysfunction (4.3 %) (data not shown). Although the HFSR itself is not a life-threatening AE, it can decrease patient quality of life, cause infection and pain, limit daily activities and lead to a complex medical situation.

It has been reported that the incidence of HFSR differs between Japanese and non-Japanese patients [28]. The incidence of hand-foot skin reaction in the all-case surveillance and in this study was high: 51.4 and 47.8 %, respectively, higher than for other Asian countries (31.7 % in Korean patients [29]). Although the discontinuation rate due to HFSR is low, the cause is not fully understood, and future studies will be needed.

Incidence of drug-related AEs was highest in Japan, but treatment-emergent death occurring up to 30 days after discontinuation of sorafenib was lowest compared with other regions. Ealier discontinuation of sorafenib treatment may be related to the apparent lower rate of treatment-emergent death.

The number of TACE sessions performed before sorafenib therapy was higher for Japanese patients than for those in other regions. Patients with $\geq$6 TACE sessions tended to have lower response rates, and there was a higher proportion of Child-Pugh B patients at initiation of

sorafenib therapy. TACE failure/refractoriness was defined by the Japan Society of Hepatology in 2010 and revised in 2014 [30, 31], which was after patient registration began in the GIDEON study. In TACE-refractory patients with intermediate-stage HCC, the deterioration of liver function is accelerated when TACE is continued, and conversion to sorafenib significantly improves the median OS [32, 33]. Therefore, in the case of uncontrolled tumors by TACE, TACE should not be repeated and alternative treatments, such as sorafenib, are recommended.

GIDEON did not include a control group or randomization. The number of patients with Child-Pugh B was much smaller than with Child-Pugh A; therefore, the results should be interpreted with caution. Japanese patients were not registered in the Phase III SHARP and the Asia-Pacific trial [14, 15]. Thus, obtaining background information and treatment trends from real-world practice data in Japanese patients may provide a valuable contribution to the future of HCC treatment. In this subgroup analysis of Japanese patients, there was an earlier diagnosis, more frequent treatment with TACE before sorafenib therapy and a tendency toward longer OS irrespective of BCLC stage at the time of initial diagnosis compared with other regions.

In conclusion, sorafenib was well tolerated by Japanese HCC patients in clinical settings. Patients with Child-Pugh B had a shorter duration of treatment and higher incidence of SAEs. Therefore, it is critical to evaluate the patient's benefit and risk before making a decision to treat with sorafenib for patients with Child-Pugh B.

Acknowledgments We thank the participating patients and staff of the study centers. Editorial assistance in the preparation of this manuscript was provided by WysiWyg Co., Ltd., with financial support from Bayer Yakuhin, Ltd.; the authors retained editorial control over the content. This work was funded by Bayer Yakuhin, Ltd.

Compliance with ethical standards

Conflict of interest Kudo has received lecture fees from Bayer Yakuhin, Kowa and Taiho Pharma, and grants from Chugai Pharmaceutical, Otsuka Pharmaceutical, Takeda Pharmaceutical, Taiho Pharma, Sumitomo Dainippon Pharma, Daiichi Sankyo, MSD and Eisai. Ikeda has received lecture fees from Bayer Yakuhin, and research grants from Bayer Yakuhin, Merck Serono, Kyowa Hakko Kirin, Yakult, Taiho Pharma, Eli Lilly Japan, Boehringer Ingelheim, Kowa, Ono Pharmaceutical, Eisai, AstraZeneca, GlaxoSmithKline and Zeria Pharmaceutical. Izumi has received lecture fees from Gilead Sciences, Otsuka Pharmaceutical, Bristol-Myers Squibb and Bayer Yakuhin. Furuse has received research grants from Taiho Pharma, Merck Serono, Zeria Pharmaceutical, Eli Lilly Japan, Janssen Pharmaceutical, Daiichi Sankyo, Sumitomo Dainippon Pharma and J-Pharma, and lecture fees from Taiho Pharma and Yakult. Okusaka has received research grants from Chugai Pharmaceutical, Eli Lilly Japan, Eisai, Novartis Pharma, Takeda Pharmaceutical, Yakult, OncoTherapy Science, Taiho Pharma, Boehringer Ingelheim Japan, Kowa, Kyowa Hakko Kirin, Merck Serono, Ono Pharmaceutical, Pfizer Japan, AstraZeneca, Sumitomo Dainippon Pharma, Zeria Pharmaceutical and GlaxoSmithKline. Kokudo has received research grants from Sumitomo Dainippon Pharma and Taiho Pharma. Yamashita and Ito are employees of Bayer Yakuhin, Ltd.The other authors declare that they have no conflicts of interest.

References

1. El-Serag HB. Epidemiology of viral hepatitis and hepatocellular carcinoma. Gastroenterology. 2012;142:1264–73.
2. Jemal A, Bray F, Center MM, et al. Global cancer statistics. CA Cancer J Clin. 2011;61:69–90.
3. El-Serag HB, Hampel H, Javadi F. The association between diabetes and hepatocellular carcinoma: a systematic review of epidemiologic evidence. Clin Gastroenterol Hepatol. 2006;4:369–80.
4. Gao J, Xie L, Yang WS, et al. Risk factors of hepatocellular carcinoma–current status and perspectives. Asian Pac J Cancer Prev. 2012;13:743–52.
5. Okuda H. Hepatocellular carcinoma development in cirrhosis. Best Pract Res Clin Gastroenterol. 2007;21:161–73.
6. Thomas MB, Zhu AX. Hepatocellular carcinoma: the need for progress. J Clin Oncol. 2005;23:2892–9.
7. Zhang BH, Yang BH, Tang ZY. Randomized controlled trial of screening for hepatocellular carcinoma. J Cancer Res Clin Oncol. 2004;130:417–22.
8. Llovet JM, Burroughs A, Bruix J. Hepatocellular carcinoma. Lancet. 2003;362:1907–17.
9. Lopez PM, Villanueva A, Llovet JM. Systematic review: evidence-based management of hepatocellular carcinoma-an updated analysis of randomized controlled trials. Aliment Pharmacol Ther. 2006;23:1535–47.
10. Farazi PA, DePinho RA. Hepatocellular carcinoma pathogenesis: from genes to environment. Nat Rev Cancer. 2006;6:674–87.
11. Minguez B, Tovar V, Chiang D, et al. Pathogenesis of hepatocellular carcinoma and molecular therapies. Curr Opin Gastroenterol. 2009;25:186–94.
12. Wilhelm SM, Carter C, Tang L, et al. BAY 43-9006 exhibits broad spectrum oral antitumor activity and targets the RAF/MEK/ERK pathway and receptor tyrosine kinases involved in tumor progression and angiogenesis. Cancer Res. 2004;64:7099–109.
13. Bruix J, Sherman M, American Association for the Study of Liver Diseases. Management of hepatocellular carcinoma: an update. Hepatology. 2011;53:1020–2.
14. Cheng AL, Kang YK, Chen Z, et al. Efficacy and safety of sorafenib in patients in the Asia-Pacific region with advanced hepatocellular carcinoma: a phase III randomised, double-blind, placebo-controlled trial. Lancet Oncol. 2009;10:25–34.
15. Llovet JM, Ricci S, Mazzaferro V, et al. Sorafenib in advanced hepatocellular carcinoma. N Engl J Med. 2008;359:378–90.
16. Lencioni R, Marrero J, Venook A, et al. Design and rationale for the non-interventional global investigation of therapeutic decisions in hepatocellular carcinoma and of its treatment with sorafenib (GIDEON) study. Int J Clin Pract. 2010;64:1034–41.
17. Lencioni R, Kudo M, Ye SL, et al. GIDEON (global investigation of therapeutic decisions in hepatocellular carcinoma and of its

treatment with sorafenib): second interim analysis. Int J Clin Pract. 2014;68:609–17.
18. Lencioni R, Kudo M, Ye SL, et al. First interim analysis of the GIDEON (global investigation of therapeutic decisions in hepatocellular carcinoma and of its treatment with sorafenib) non-interventional study. Int J Clin Pract. 2012;66:675–83.
19. Ito Y. Inuyama L. Results of a prospective postmarketing all-patient surveillance study for sorafenib in Japanese patients with unresectable hepatocellular carcinoma. In: Paper presented at 9th Japan Association of Molecular Targeted Therapy for HCC, Tokyo; 2014 (**In Japanese**).
20. Post-Marketing Surveillance Manager. Nexavar® Tablets 200 Mg (nonproprietary nane: sorafenib tosylate tablets) specific drug use investigation interim report (unresectable hepatocellular carcinoma). Osaka: Bayer Yakuhin Ltd; 2012.
21. Kudo M, Lencioni R, Ye SL, et al. Regional differences in treatment history, practices, and outcomes: final analysis of GIDEON (global investigation of therapeutic decisions in hepatocellular carcinoma and of its treatment with sorafenib). In: Paper presented at 7th Annual Conference of the International Liver Cancer Association, Washington D.C.; 2013.
22. Takayasu K, Arii S, Matsuo N, et al. Comparison of CT findings with resected specimens after chemoembolization with iodized oil for hepatocellular carcinoma. AJR Am J Roentgenol. 2000;175:699–704.
23. Kudo M, Kubo S, Takayasu K, et al. Response evaluation criteria in cancer of the liver (RECICL) proposed by the Liver Cancer Study Group of Japan (2009 revised version). Hepatol Res. 2010;40:686–92.
24. Lencioni R, Llovet JM. Modified RECIST (mRECIST) assessment for hepatocellular carcinoma. Semin Liver Dis. 2010;30:52–60.
25. Bronowicki JP, Kudo M, Lencioni R, et al. GIDEON: a retrospective analysis of prognostic factors[Abstract]. J Hepatol. 2015;62(suppl 2):S451.
26. Johnson P, Berhane S, Satomura S, et al. An international collaborative study assessing the role of aetiology and stage in survival in HCC-implications for screening. J Hepatol. 2014;60(suppl):S45–6.
27. Kudo M. Japan's successful model of nationwide hepatocellular carcinoma surveillance highlighting the urgent need for global surveillance. Liver Cancer. 2012;1:141–3.
28. Yoshino T, Komatsu Y, Yamada Y, et al. Randomized phase III trial of regorafenib in metastatic colorectal cancer: analysis of the CORRECT Japanese and non-Japanese subpopulations. Invest New Drugs. 2015;33:740–50.
29. Kim DY, Kim HJ, Han KH, et al. Real-life experience of sorafenib treatment for hepatocellular carcinoma in Korea: From GIDEON data. In: Paper presented at 24th conference of the Asian Pacific Association for the Study of the Liver, Istanbul; 2015.
30. Kudo M, Izumi N, Kokudo N, et al. Management of hepatocellular carcinoma in Japan: consensus-based clinical practice guidelines proposed by the Japan Society of Hepatology (JSH) 2010 updated version. Dig Dis. 2011;29:339–64.
31. Kudo M, Matsui O, Izumi N, et al. Transarterial chemoembolization failure/refractoriness: JSH-LCSGJ criteria 2014 update. Oncology. 2014;87(Suppl 1):22–31.
32. Ogasawara S, Chiba T, Ooka Y, et al. Efficacy of sorafenib in intermediate-stage hepatocellular carcinoma patients refractory to transarterial chemoembolization. Oncology. 2014;87:330–41.
33. Arizumi T, Ueshima K, Minami T, et al. Effectiveness of sorafenib in patients with transcatheter arterial chemoembolization (TACE) refractory and intermediate-stage hepatocellular carcinoma. Liver Cancer. 2015;4:253–62.

Research Article

JOURNAL OF HEPATOLOGY

Observational registry of sorafenib use in clinical practice across Child-Pugh subgroups: The GIDEON study

Jorge A. Marrero[1,*], Masatoshi Kudo[2], Alan P. Venook[3], Sheng-Long Ye[4], Jean-Pierre Bronowicki[5], Xiao-Ping Chen[6], Lucy Dagher[7], Junji Furuse[8], Jean-Francois H. Geschwind[9], Laura Ladrón de Guevara[10], Christos Papandreou[11], Tadatoshi Takayama[12], Arun J. Sanyal[13], Seung Kew Yoon[14], Keiko Nakajima[15], Robert Lehr[16], Stephanie Heldner[17], Riccardo Lencioni[18]

[1]*Department of Internal Medicine, Division of Digestive and Liver Diseases, University of Texas Southwestern Medical Center, Dallas, TX, USA;* [2]*Department of Gastroenterology and Hepatology, Kinki University School of Medicine, Osaka, Japan;* [3]*Medical Oncology and Translational Research, University of California, San Francisco, CA, USA;* [4]*Liver Cancer Institute and Zhongshan Hospital, Fudan University, Shanghai, China;* [5]*University Henri Poincaré by University of Lorraine, Nancy, France;* [6]*Hepatic Surgery Center, Tongji Hospital, Tongji Medical College, Huazhong University of Science and Technology, Wuhan, China;* [7]*Policlínica Metropolitana, Caracas, Venezuela;* [8]*Kyorin University School of Medicine, Mitaka, Tokyo, Japan;* [9]*Vascular and Interventional Radiology, Johns Hopkins University School of Medicine, Baltimore, MD, USA;* [10]*Hospital Angeles Clínica Londres, Mexico City, Mexico;* [11]*University Hospital of Larissa, Larissa, Greece;* [12]*Department of Digestive Surgery, Nihon University School of Medicine, Tokyo, Japan;* [13]*Virginia Commonwealth University Medical Center, Richmond, VA, USA;* [14]*The Catholic University of Korea, Seoul, Republic of Korea;* [15]*Global Medical Affairs, Bayer HealthCare Pharmaceuticals, Inc., Montville, NJ, USA;* [16]*Clinical Statistics, Bayer HealthCare Pharmaceuticals, Inc., Montville, NJ, USA;* [17]*Global Medical Affairs and Pharmacovigilance, Bayer HealthCare Pharmaceuticals, Inc., Berlin, Germany;* [18]*Division of Diagnostic Imaging and Intervention, Pisa University Hospital and School of Medicine, Pisa, Italy*

Background & Aims: GIDEON (Global Investigation of therapeutic DEcisions in hepatocellular carcinoma and Of its treatment with sorafeNib) is a prospective, observational registry study evaluating the safety of sorafenib and treatment practices in hepatocellular carcinoma patients. This large global database allowed for assessment of the use and tolerability of sorafenib in patients with liver dysfunction.

Methods: Baseline characteristics and medical/treatment history were collected in patients for whom a decision to treat with sorafenib had been made. Adverse event, dosing, and outcomes data were collected during follow-up.

Results: In the overall safety population (n = 3202), 1968 patients (61%) had Child-Pugh A status and 666 (21%) had Child-Pugh B. The majority of Child-Pugh A (72%) and Child-Pugh B (70%) patients received an initial sorafenib dose of 800 mg, consistent with the label, and dose reduction rates were 40% and 29%, respectively. The type and incidence of adverse events were generally consistent across Child-Pugh subgroups. The incidence of drug-related adverse events leading to discontinuation was similar between Child-Pugh A and Child-Pugh B patients (17% and 21%). In the intent-to-treat population (n = 3213), median overall survival (months [95% confidence interval]) was longer in Child-Pugh A patients (13.6 [12.8–14.7]) compared with Child-Pugh B patients (5.2 [4.6–6.3]).

Conclusions: In clinical practice, the safety profile of sorafenib appeared to be consistent across Child-Pugh A and Child-Pugh B patients. Findings suggest sorafenib may be safely used in some Child-Pugh B patients and indicate the importance of careful patient evaluation when making treatment decisions.

Lay summary: The GIDEON (Global Investigation of therapeutic DEcisions in hepatocellular carcinoma and Of its treatment with sorafeNib) study is a large prospective registry of patients with liver cancer who were treated with sorafenib. The aims were to evaluate the safety and tolerability of sorafenib among those in which the liver was not functioning properly. The study showed that the safety profile of sorafenib was consistent across patients with preserved liver function and those in which the liver was not functioning properly, and therefore, suggesting that sorafenib may be a valid treatment for some patients with liver impairment.

Keywords: Hepatocellular carcinoma; HCC; Sorafenib; Nexavar; Child-Pugh; GIDEON.

Received 16 April 2015; received in revised form 28 June 2016; accepted 3 July 2016; available online 25 July 2016

* Corresponding author. Address: Department of Internal Medicine, Division of Digestive and Liver Diseases, University of Texas Southwestern Medical Center, 5323 Harry Hines Boulevard, Dallas, TX 75390, USA. Tel.: +1 214 645 6340; fax: +1 214 645 6257.

E-mail address: jorge.marrero@utsouthwestern.edu (J.A. Marrero).

Abbreviations: HCC, hepatocellular carcinoma; GIDEON, Global Investigation of therapeutic DEcisions in hepatocellular carcinoma and Of its treatment with sorafeNib; AE, adverse event; BCLC, Barcelona Clinic Liver Cancer; ECOG PS, Eastern Cooperative Oncology Group performance status; TNM, tumor node metastasis; CI, confidence interval; INR, international normalized ratio.

Introduction

Liver cancer is the second leading cause of cancer-related death worldwide [1]. The majority of primary liver cancer presents as hepatocellular carcinoma (HCC), the incidence of which is rising

in many parts of the world [2]. The vast majority of HCC cases occur in the setting of liver cirrhosis, usually because of chronic hepatitis C or hepatitis B viral infections, alcohol consumption, non-alcoholic steatohepatitis, or diabetes [3]. The degree of underlying liver disease, as well as the tumor stage and patients' general condition, must therefore be considered when making treatment decisions for HCC. Most HCC patients have advanced disease at diagnosis, or present with recurrent disease following potentially curative treatments [4]. Therefore, systemic therapy with the oral multikinase inhibitor sorafenib (Nexavar®; Bayer Pharma AG, Berlin, Germany) plays a key role in the management of HCC [5].

Sorafenib was approved for the treatment of unresectable HCC after two phase III trials (Sorafenib HCC Assessment Randomized Protocol [SHARP] and Asia-Pacific) demonstrated significant improvements in overall survival [6,7]. Sorafenib is the first-line therapy in patients with advanced HCC [8]; however, pivotal trials, like most clinical trials in HCC, included only patients with Child-Pugh A status in order to avoid confounding results because of the presence of liver dysfunction [7]. Hence, data on the use and safety of sorafenib in HCC patients with Child-Pugh B status are currently limited [9].

The GIDEON (Global Investigation of therapeutic DEcisions in HCC and Of its treatment with sorafeNib) trial was a prospective, observational registry study undertaken to evaluate the safety and use of sorafenib in HCC patients under real-life practice conditions, and, in particular, to gather more comprehensive data on the use of sorafenib in patients with Child-Pugh B liver function. GIDEON is one of the largest efforts ever undertaken in patients with HCC, and allows for a broad evaluation of disease characteristics, treatment practices, and safety across patient subgroups.

Here we present data from the final analysis of GIDEON, including how liver function was assessed, patient and disease characteristics, treatment practices, adverse events, and outcomes, in HCC patients with advanced liver dysfunction treated with sorafenib.

Patients and methods

Study design

GIDEON included patients for whom a decision to treat with sorafenib was made by their physician in clinical practice. All decisions concerning patient assessment, including liver function, sorafenib dose, and duration of treatment, were solely at the discretion of the attending physician and not mandated by the study protocol.

Eligible patients were those diagnosed histologically, cytologically, or radiographically with HCC, with a life expectancy of more than 8 weeks. Exclusion criteria were based on the prescribing information for sorafenib. Full details of the study design, including further inclusion criteria, have been previously published [10]. GIDEON enrollment began in January 2009 and the last patient follow-up occurred in April 2012. Final analysis was undertaken at 12-month follow-up following the enrollment of 3000 sorafenib-treated patients.

Data collection and analyses

All patients provided informed and signed consent. GIDEON was conducted within an approved indication in accordance with the guidelines of the European Medicines Agency and the US Food and Drug Administration relating to non-interventional and post-authorization safety studies and Good Clinical Practice, as outlined in Directive 2001/20/EC [11]. Documented approval from appropriate ethics committees and institutional review boards was obtained in accordance with local laws, regulations, and organizations.

Adverse events (AEs) were graded according to the National Cancer Institute Common Terminology Criteria for Adverse Events version 3.0. Patients who received at least one dose of sorafenib and underwent at least one follow-up assessment were evaluable for safety, while the intent-to-treat population comprised any patient who received one or more doses of sorafenib. For evaluation of liver dysfunction, Child-Pugh score was calculated based on the composite score of five variables: bilirubin, albumin, ascites, encephalopathy, and international normalized ratio [12]. All data were collected by the treating physician via case report forms.

Target enrollment was based on an overall sample of 3,000 patients, the number determined sufficient for comprehensive evaluation of safety for the overall population, as well as specified subgroups [10]. All data were collected and monitored centrally and summarized with descriptive statistics.

Results

Patient disposition

A total of 3,371 patients were enrolled from 39 countries across five regions (USA, Europe, Japan, Latin America, and Asia-Pacific). The safety population comprised 3,202 patients and the intent-to-treat population comprised 3,213 patients. Within the safety population, 2,708 patients had known Child-Pugh status at the start of sorafenib therapy; of these, 73% (n = 1968) had Child-Pugh A, 25% (n = 666) had Child-Pugh B, and 3% (n = 74) had Child-Pugh C (Fig. 1). In the intent-to-treat population, 2717 patients had known Child-Pugh status (n = 1975 [73%] Child-Pugh A, n = 669 [25%] Child-Pugh B, and n = 73 [3%] Child-Pugh C).

Overall, in the safety population, 15% (n = 494) of patients did not have all of the required information in order to be evaluable for Child-Pugh status. The most commonly absent assessments were international normalized ratio/prothrombin time and albumin. Notably, the USA had the highest frequency of missing values for all of the assessments, with 30% of patients non-evaluable for Child-Pugh score (Supplementary Table 1).

Baseline patient demographics and disease characteristics

The median age was 64 years for Child-Pugh A patients and 61 years for Child-Pugh B patients, and the majority of patients in all Child-Pugh subgroups were male (Table 1). The proportion of patients with Child-Pugh A status was highest in Japan (75%) and lowest in the USA (46%). Barcelona Clinic Liver Cancer (BCLC) and TNM stages were similar between Child-Pugh A and Child-Pugh B patients (Table 1).

Sorafenib administration by Child-Pugh status

Overall, sorafenib dosing was similar irrespective of Child-Pugh score. The majority of Child-Pugh A and Child-Pugh B patients received the recommended initial dose of 800 mg (72% and 70%, respectively), while this was slightly lower for patients with Child-Pugh C status (62%). The median daily dose was also comparable between Child-Pugh A and Child-Pugh B patients (677 mg and 742 mg, respectively). A slightly higher proportion of Child-Pugh A patients (40%) had a dose reduction at any time during the study period compared with Child-Pugh B patients (29%) (Table 2).

The initial sorafenib dose and the proportion of patients with a dose reduction or increase were also comparable across

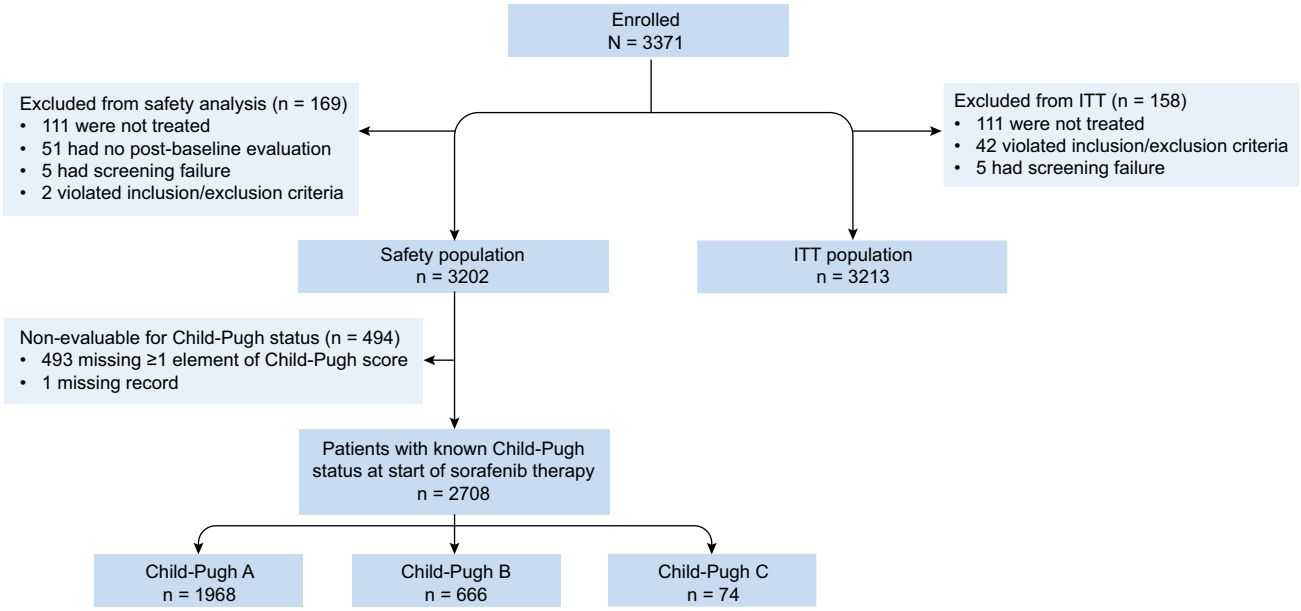

Fig. 1. Patient disposition. ITT, intent-to-treat.

patients with baseline bilirubin levels of less than 2.0 mg/dl, 2.0–3.0 mg/dl, or greater than 3.0 mg/dl (Supplementary Table 2).

The median duration of treatment was longer in Child-Pugh A patients (17.6 weeks) compared with Child-Pugh B patients (9.9 weeks) and Child-Pugh C patients (5.6 weeks) (Table 2). Similarly, Child-Pugh B7 patients tended to have a longer duration of therapy (11.1 weeks) than Child-Pugh B8 patients (9.3 weeks) and Child-Pugh B9 patients (7.6 weeks).

The proportion of patients discontinuing within 8 weeks was lower for Child-Pugh A patients (26%) compared with Child-Pugh B patients (42%), with 38%, 44%, and 49% of B7, B8, and B9 patients discontinuing within 8 weeks, respectively. The proportion of Child-Pugh A and Child-Pugh B patients remaining on sorafenib for more than 28 weeks was 33% and 20%, respectively (Table 2). Those patients who continued sorafenib beyond 28 weeks tended to have higher baseline albumin, lower baseline bilirubin, and no ascites (Supplementary Table 3).

Sorafenib safety assessments

The overall incidence of AEs and drug-related AEs was comparable between Child-Pugh A and Child-Pugh B patients, as was the incidence of grade 3 or 4 AEs; however, serious AEs were more common in Child-Pugh B patients. The incidence of serious AEs was higher in Child-Pugh B patients with a score of 8 or 9 compared with Child-Pugh B patients with a score of 7 (Table 3). The safety profile according to BCLC–Child-Pugh cross-classification was generally consistent with the data across Child-Pugh subgroups. For Child-Pugh A patients, a higher proportion of deaths was seen for those with BCLC C or D status compared with those with BCLC A or B status (Supplementary Table 4).

The most commonly reported AEs across all Child-Pugh subgroups were diarrhea, hand-foot skin reaction, and fatigue. The incidence of individual AEs and drug-related AEs was similar in Child-Pugh A and Child-Pugh B patients, with the exception of hand-foot skin reaction, which was more common in Child-Pugh A patients (Table 4).

The majority of AEs grade 3 or higher occurred during the first 4 weeks of treatment in both Child-Pugh A and Child-Pugh B patients (Fig. 2). The rate of the most common AEs, calculated as event per patient-year, was also comparable in these groups (Supplementary Table 5).

In total, AEs leading to permanent discontinuation were more common in Child-Pugh B (40%) and C (43%) patients than in Child-Pugh A patients (29%), although the incidences of drug-related AEs leading to discontinuation were similar (21%, 15%, and 17%, respectively). The incidences of individual AEs and drug-related AEs leading to permanent discontinuation were also similar in Child-Pugh A and Child-Pugh B subgroups. The types of AEs leading to sorafenib discontinuation were various, with no AE leading to discontinuation in more than 5% of patients overall (Supplementary Table 6). In Child-Pugh B patients, AEs leading to discontinuation occurred most commonly during the first 4 weeks of treatment (Supplementary Table 7).

The overall incidence of AEs leading to permanent discontinuation was similar in patients with baseline bilirubin less than 2.0 mg/dl (85%) and 2.0–3.0 mg/dl (84%), although this was higher in patients with bilirubin greater than 3.0 mg/dl (95%). The overall incidence of drug-related AEs and the incidence of drug-related AEs leading to permanent discontinuation were comparable irrespective of bilirubin level (Supplementary Table 8).

Survival

In the intent-to-treat population, median overall survival was longer in Child-Pugh A patients (13.6 months) than in Child-Pugh B patients (5.2 months) and Child-Pugh C patients (2.6 months), as anticipated (Fig. 3A). Median overall survival in Child-Pugh B7 patients (6.2 months) was considerably shorter than in Child-Pugh A patients, but was longer than in Child-

Table 1. Baseline patient and disease characteristics by Child-Pugh score.

	Child-Pugh score[a,b]					
	A (<7)	B7	B8	B9	B (7-9)[c]	C (>9)
Patients, n (% of total)	1968 (61)	359 (11)	182 (6)	122 (4)	666 (21)	74 (2)
Median age, years (range)	64 (15-94)	61 (19-87)	62 (32-84)	56 (31-79)	61(19-87)	58 (29-82)
Gender, n (%)						
Male	1618 (82)	302 (84)	143 (79)	94 (77)	542 (81)	61 (82)
Female	350 (18)	57 (16)	39 (21)	28 (23)	124 (19)	13 (18)
ECOG PS, n (%)[a,d]						
0 or 1	1741 (89)	278 (77)	124 (68)	77 (63)	481 (72)	44 (59)
≥2	142 (7)	58 (16)	47 (26)	36 (30)	142 (21)	27 (37)
BCLC stage, n (%)[a,e]						
A	158 (8)	22 (6)	10 (6)	5 (4)	37 (6)	0
B	435 (22)	74 (21)	36 (20)	26 (21)	136 (20)	0
C	1124 (57)	199 (55)	106 (58)	66 (54)	373 (56)	1 (1)
D	60 (3)	15 (4)	7 (4)	8 (7)	30 (5)	66 (89)
TNM status, n (%)[a,f,g]						
I	104 (5)	10 (3)	9 (5)	9 (7)	28 (4)	5 (7)
II	287 (15)	33 (9)	18 (10)	10 (8)	61 (9)	10 (14)
III	701 (36)	158 (44)	80 (44)	46 (38)	286 (43)	25 (34)
IV	717 (36)	119 (33)	55 (30)	41 (34)	215 (32)	22 (30)
Bilirubin (mg/dl)[h]						
<2.0	1906 (97)	262 (73)	76 (42)	28 (23)	367 (55)	6 (8)
2.0-3.0	61 (3)	87 (24)	66 (36)	43 (35)	197 (30)	21 (28)
>3.0	1 (<0.1)	10 (3)	40 (22)	51 (42)	102 (15)	47 (64)
Albumin (g/L)[i]						
>35.0	1480 (75)	68 (19)	16 (9)	2 (2)	86 (13)	2 (3)
28.0-35.0	482 (25)	224 (62)	131 (72)	63 (52)	420 (63)	19 (26)
<28.0	1 (<0.1)	67 (19)	35 (19)	57 (47)	160 (24)	53 (72)
International normalized ratio (seconds)[j]						
<1.7	1942 (99)	324 (90)	158 (87)	96 (79)	581 (87)	41 (55)
1.7-2.3	24 (1)	23 (6)	16 (9)	24 (20)	63 (9)	17 (23)
>2.3	0	12 (3)	8 (4)	2 (2)	22 (3)	16 (22)
Encephalopathy, n (%)[k]						
Absent	1960 (100)	347 (97)	177 (97)	112 (92)	637 (96)	52 (70)
Moderate (stage I or II)	7 (<1)	12 (3)	5 (3)	9 (7)	26 (4)	19 (26)
Severe (stage III or IV)	0	0	0	1 (1)	1 (<1)	2 (3)
Ascites, n (%)[l]						
Absent	1830 (93)	190 (53)	70 (39)	34 (28)	294 (44)	8 (11)
Slight	138 (7)	144 (40)	62 (34)	49 (40)	256 (38)	25 (34)
Moderate	0	25 (7)	50 (28)	39 (32)	116 (17)	41 (55)
HCC features, n (%)[a]						
Extrahepatic spread	813 (41)	138 (38)	59 (32)	44 (36)	242 (36)	18 (24)
Vascular invasion	432 (22)	100 (28)	61 (34)	29 (24)	191 (29)	22 (30)
Etiology of liver disease, n (%)[m]						
Hepatitis B	763 (39)	122 (34)	53 (29)	41 (34)	218 (33)	19 (26)
Hepatitis C	628 (32)	134 (37)	72 (40)	43 (35)	251 (38)	34 (46)
Alcohol use[n]	435 (22)	121 (34)	67 (37)	49 (40)	237 (36)	28 (38)

[a]Recorded at study entry (which is defined as start of therapy and is indicated by the initial visit); [b]Child-Pugh status missing for one patient; [c]three patients recorded as having Child-Pugh B but specific score not recorded; [d]data missing for 194 patients; [e]data missing for four patients; 501 patients non-evaluable; [f]data missing for four patients; 391 patients non-evaluable; [g]TNM assessment based on radiological evaluation; [h]data missing for 128 patients; [i]data missing for 223 patients; [j]data missing for 370 patients; [k]data missing for 132 patients; [l]data missing for 113 patients; ascites assessed clinically or radiologically; [m]based on patients with recorded etiology (n = 3195); patients may have more than one etiology; [n]alcohol use was defined as any patient for whom the treating physician recorded alcohol as a potential cause of liver dysfunction. ECOG PS, Eastern Cooperative Oncology Group performance status; TNM, tumor node metastasis.

Pugh B8 patients (4.8 months) and Child-Pugh B9 patients (3.7 months) (Fig. 3B). Median overall survival according to BCLC by Child-Pugh cross-classification followed a similar trend, as patients with Child-Pugh A and BCLC stage B had longer overall survival compared with patients with Child-Pugh B and BCLC stage B (19.5 months *vs.* 10.0 months), and patients with

Table 2. Sorafenib administration across Child-Pugh subgroups.

	Child-Pugh score[a,b]					
	A (<7) (n = 1968)	B7 (n = 359)	B8 (n = 182)	B9 (n = 122)	B (7-9)[c] (n = 666)	C (>9) (n = 74)
Initial dose, n (%)						
800 mg	1415 (72)	253 (70)	129 (71)	79 (65)	464 (70)	46 (62)
400 mg	482 (25)	91 (25)	47 (26)	35 (29)	173 (26)	21 (28)
Median daily dose[d], mg	677.0	725.0	756.5	753.0	741.5	603.5
Dose reduction, n (%)	784 (40)	110 (31)	54 (30)	30 (25)	194 (29)	19 (26)
Dose increase, n (%)	413 (21)	52 (14)	25 (14)	23 (19)	100 (15)	8 (11)
Median time from diagnosis to initiation of sorafenib, mo	4.9	2.8	2.5	2.4	2.5	1.3
Median treatment duration[e], wk	17.6	11.1	9.3	7.6	9.9	5.6
Duration of treatment[f]						
≤8 wk	510 (26)	137 (38)	80 (44)	60 (49)	279 (42)	41 (55)
>8-28 wk	781 (40)	125 (35)	58 (32)	38 (31)	222 (33)	22 (30)
>28 wk	651 (33)	78 (22)	41 (23)	17 (14)	136 (20)	8 (11)

[a]Recorded at study entry (which is defined as start of therapy and is indicated by the initial visit); [b]Child-Pugh status missing for one patient; [c]three patients recorded as having Child-Pugh B but specific score not recorded; [d]based on patients with available data (n = 2857); [e]based on patients with available data (n = 3130); [f]data missing for 72 patients.

Table 3. Overall safety profile of sorafenib by Child-Pugh score.

n (%)	Child-Pugh score[a,b]					
	A (<7) (n = 1968)	B7 (n = 359)	B8 (n = 182)	B9 (n = 122)	B (7-9)[c] (n = 666)	C (>9) (n = 74)
AEs (all grades)	1653 (84)	313 (87)	166 (91)	109 (89)	590 (89)	68 (92)
Drug-related AEs (all grades)	1349 (69)	240 (67)	114 (63)	74 (61)	429 (64)	29 (39)
Serious AEs[d]	708 (36)	192 (54)	126 (69)	82 (67)	402 (60)	52 (70)
Drug-related serious AEs	174 (9)	48 (13)	28 (15)	18 (15)	94 (14)	2 (3)
All grade 3 or 4 AEs	638 (33)	109 (30)	57 (31)	44 (36)	210 (32)	13 (18)
Drug-related grade 3 or 4 AEs	503 (26)	79 (22)	41 (23)	26 (21)	146 (22)	8 (11)
Deaths[e]	349 (18)	113 (31)	78 (43)	46 (38)	239 (36)	38 (51)

[a]Recorded at study entry (which is defined as start of therapy and is indicated by the initial visit); [b]Child-Pugh status missing for one patient; [c]three patients recorded as having Child-Pugh B but specific score not recorded; [d]any AE occurring at any dose that results in any of the following outcomes: death; life-threatening; hospitalization or prolongation of existing hospitalization; persistent or significant disability/incapacity; congenital anomaly/birth defect; medically important event; [e]treatment-emergent deaths occurring up to 30 days after last sorafenib dose.

Child-Pugh A and BCLC stage C had longer overall survival compared with patients with Child-Pugh B and BCLC stage C (11.2 months *vs.* 3.8 months) (Supplementary Fig. 1).

Of the individual components of Child-Pugh score, albumin level, ascites, and bilirubin level all appeared to be prognostically valuable for overall survival, as did encephalopathy to a lesser degree (Supplementary Fig. 2). However, it should be noted that ascites could be evaluated clinically or radiologically by the treating physician, and no allowance for possible treatment with diuretics was made when assessing ascites. In addition, the patient numbers in the moderate and severe groups for encephalopathy were extremely low, meaning these data should be interpreted with caution. International normalized ratio did not appear to be predictive of survival (Supplementary Fig. 2). These findings are also supported by a univariate Cox regression analysis in which the hazard ratio (95% confidence interval) for survival was 1.708 (1.573–1.855) for bilirubin and 1.755 (1.629–1.892) for albumin (Supplementary Table 9).

Discussion

The final analysis of the GIDEON registry provides insight into patients with HCC treated with sorafenib in real-life practice, thereby allowing evaluation across clinically relevant subgroups. In particular, the safety of sorafenib in HCC patients with poorer liver function remains an unanswered question, as pivotal phase III trials of sorafenib excluded Child-Pugh B patients.

In the GIDEON registry, the safety profile of sorafenib observed was similar between Child-Pugh A and Child-Pugh B patients, and was in line with the known safety profile of sorafenib [6,7]. The rate of the most common AEs was also broadly comparable between Child-Pugh groups, suggesting that the similar incidences observed were not due to the shorter duration of treatment in Child-Pugh B patients. These findings in this large international registry study support those from several smaller studies [13–17], suggesting that sorafenib tolerability is not remarkably different between Child-Pugh A and Child-Pugh B patients.

The greatest number of AEs occurred during the first 4 weeks of treatment irrespective of Child-Pugh score, which likely explains the high rate of discontinuation seen in this period across Child-Pugh subgroups. Notably, in the SHARP phase III trial, discontinuation due to AEs was comparable between the placebo and sorafenib groups (30% and 29%) [6], indicating that discontinuation due to AEs may be related to the underlying disease in some cases. A large proportion of patients were able to continue sorafenib treatment beyond 28 weeks, including 21% of Child-Pugh B patients, suggesting that patients who are able to continue treatment beyond the initial period are able to subsequently continue for long periods, and highlighting the importance of AE management in the first weeks of treatment [18]. Discontinuation due to AEs was higher in Child-Pugh B patients compared with Child-Pugh A, while discontinuation due to drug-related AEs was comparable. Similarly, discontinuation due to AEs, but not drug-related AEs, was higher in patients with baseline bilirubin greater than 3.0 mg/dl than in those with lower bilirubin levels. This suggests that in some cases physicians may be more likely to discontinue treatment in patients with advanced cirrhosis, and indicates that patients with a stable degree of liver dysfunction are able to continue sorafenib.

Previous studies have reported differences in AE incidence between Child-Pugh subgroups; however, it could not be determined if such differences were drug-related or due to disease progression [19]. A further report found that sorafenib was associated with dose-limiting toxicity in HCC patients with baseline bilirubin less than 1.5 times the upper limit of normal, with the main dose-limiting toxicity reported being elevated bilirubin [20]. However, in GIDEON, the safety profile of sorafenib was similar in patients with bilirubin levels less than 2.0 mg/dl and 2.0–3.0 mg/dl.

Table 4. Incidence of adverse events and drug-related adverse events occurring in ⩾10% of patients by Child-Pugh score.

n (%)	Child-Pugh score[a,b]											
	A (<7) (n = 1968)		B7 (n = 359)		B8 (n = 182)		B9 (n = 122)		B (7-9)[c] (n = 666)		C (>9) (n = 74)	
	AE	Drug-related AE	AE	Drug-related AE	AE	Drug-related AE	AE	Drug-related AE	AE	Drug-related AE	AE	Drug-related AE
Diarrhea	616 (31)	556 (28)	112 (31)	98 (27)	52 (29)	48 (26)	31 (25)	23 (19)	196 (29)	170 (26)	13 (18)	8 (11)
Hand-foot skin reaction	636 (32)	626 (32)	70 (20)	70 (20)	29 (16)	29 (16)	14 (11)	14 (11)	116 (17)	113 (17)	4 (5)	4 (5)
Fatigue	440 (22)	311 (16)	98 (27)	56 (16)	43 (24)	22 (12)	30 (25)	17 (14)	171 (26)	95 (14)	15 (20)	10 (14)
Anorexia	285 (15)	209 (11)	57 (16)	30 (8)	29 (16)	11 (6)	14 (11)	8 (7)	100 (15)	49 (7)	10 (14)	5 (7)
Abdomen pain	224 (11)	62 (3)	63 (18)	26 (7)	31 (17)	8 (4)	23 (19)	6 (5)	118 (18)	24 (4)	13 (18)	4 (5)
Liver dysfunction[d]	203 (10)	36 (2)	46 (13)	10 (3)	43 (24)	7 (4)	30 (25)	2 (2)	120 (18)	19 (3)	16 (22)	0
Rash/desquamation	258 (13)	238 (12)	41 (11)	35 (10)	17 (9)	15 (8)	8 (7)	7 (6)	66 (10)	57 (9)	4 (5)	3 (4)
Nausea	167 (8)	106 (5)	42 (12)	28 (8)	19 (10)	8 (4)	9 (7)	5 (4)	70 (11)	41 (6)	9 (12)	7 (9)
Hypertension	243 (12)	215 (11)	21 (6)	18 (5)	7 (4)	7 (4)	3 (2)	3 (2)	31 (5)	28 (4)	0	0

[a]Recorded at study entry (which is defined as start of therapy and is indicated by the initial visit); [b]Child-Pugh status missing for one patient; [c]three patients recorded as having Child-Pugh B but specific score not recorded; [d]liver dysfunction as an adverse event was based on physicians' selection on case report forms.

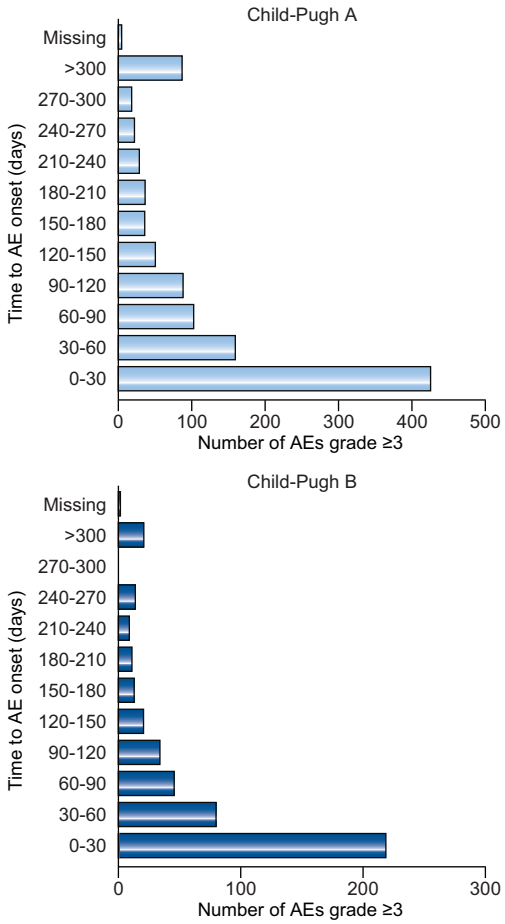

Fig. 2. Onset time of adverse events grade ⩾3 in Child-Pugh A and Child-Pugh B patients.

The data suggest that physicians' approaches to sorafenib dosing in clinical practice do not differ based on liver dysfunction, and are in accordance with the approved prescribing information in most cases. The initial sorafenib dose, median daily dose, and proportion of patients receiving a dose increase or reduction were broadly similar irrespective of the degree of liver dysfunction.

Together, the combined findings from GIDEON therefore suggest that dose modification is not required based solely on the degree of baseline liver dysfunction. This is supported by pharmacokinetic studies which have demonstrated there is no difference in the pharmacokinetic profile of sorafenib in Child-Pugh A and Child-Pugh B patients [14,19,21,22] and is reflected in the prescribing information [23]. However, because of the heterogeneous nature of patients categorized as Child-Pugh B, detailed assessment is required when deciding the most appropriate treatment option.

In line with previous studies, median overall survival was shorter in Child-Pugh B patients compared with Child-Pugh A patients [14,24]. The poorer outcomes observed in Child-Pugh B patients were as expected and likely relate to the natural progression of cirrhosis in these patients with more advanced disease [19,25]. However, because of the observational nature of the GIDEON study and lack of a control, the efficacy of sorafenib in Child-Pugh B patients cannot be assessed. Previous reports suggest that while Child-Pugh B patients have poorer outcomes compared with Child-Pugh A, sorafenib may offer clinical benefit in carefully selected Child-Pugh B patients [24,26,27].

Median overall survival and univariate Cox regression analysis highlighted that baseline bilirubin and albumin levels strongly influenced prognosis. Interestingly, higher albumin and lower bilirubin levels appeared to be associated with longer sorafenib treatment. These data therefore suggest that albumin and bilirubin levels may be of particular importance when considering the use of sorafenib therapy in patients with liver dysfunction. This is supported by the recent description of the albumin-bilirubin grade system, which stratifies HCC patients into three risk categories based on serum bilirubin and albumin levels only, and has shown to predict survival equally as well as the Child-Pugh system [28].

As GIDEON is an observational registry study, it is inherently limited by the lack of a randomized, controlled population and the potential for selection bias. The descriptive statistics employed do not allow for conclusive analysis of outcomes. In addition, no measure of compliance was collected. That said,

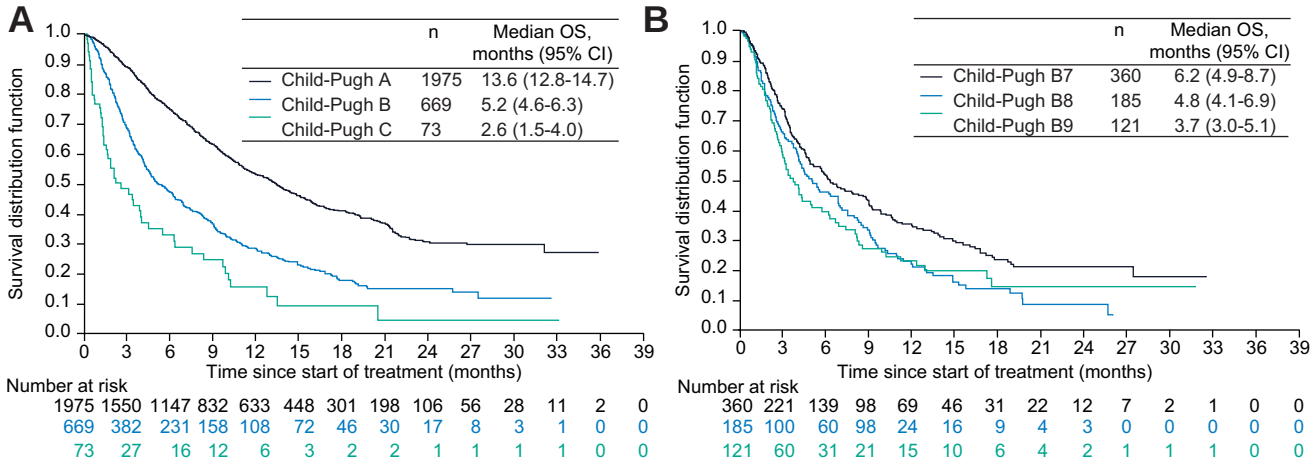

Fig. 3. Median overall survival across Child-Pugh subgroups. Kaplan-Meier analysis of median overall survival: (A) Child-Pugh subgroups; (B) Child-Pugh B subgroups. CI, confidence interval.

real-life observational studies such as GIDEON provide an opportunity to assess treatment patterns in clinical practice, and allow for the assessment of a wider patient population than in randomized clinical trials.

It has been reported that certain AEs, such as skin toxicity [29–31] or diarrhea [32], may act as biomarkers for sorafenib efficacy. In GIDEON, no obvious correlation between any AE and response was seen; however, because of the observational nature of the study, formal analysis of outcomes based on post-baseline factors was not considered appropriate. Further robust data are required to validate if any AE is a reliable pharmacodynamic biomarker for sorafenib efficacy.

Interestingly, a large number of patients enrolled did not have all of the required elements for Child-Pugh classification, particularly in the USA. International normalized ratio and albumin were the most common omissions, suggesting that many physicians may not routinely score Child-Pugh in clinical practice (even when data are being collected by a sponsor) or may assess liver disease based on other parameters.

In summary, these findings from the final analysis of GIDEON confirm that sorafenib is used clinically across a broad spectrum of HCC patients, including those with liver dysfunction. In this cohort, the safety profile of sorafenib was generally consistent in Child-Pugh A and Child-Pugh B patients. Despite a similar safety profile, a higher rate of treatment discontinuation was observed in patients with Child-Pugh B status, who have a poorer general condition. The data show that Child-Pugh B patients are heterogeneous, and highlight that certain factors may be especially important in the assessment of patients with liver dysfunction, emphasizing the need for careful assessment when making treatment decisions in these patients. Together, the data indicate the use of the recommended sorafenib dose with subsequent monitoring as an appropriate treatment option in HCC patients with more advanced liver dysfunction.

Financial support

GIDEON was sponsored by Bayer HealthCare Pharmaceuticals, Inc. and Onyx Pharmaceuticals, an Amgen subsidiary.

Conflict of interest

Professor Marrero has received honoraria for advisory arrangements from Bayer HealthCare Pharmaceuticals, Inc. and Onyx Pharmaceuticals, an Amgen subsidiary. Professors Furuse and Geschwind have received honoraria for advisory arrangements and research grant support from Bayer HealthCare Pharmaceuticals, Inc. Professor Venook has received honoraria for advisory arrangements and research grant support from Bayer HealthCare Pharmaceuticals, Inc. and Onyx Pharmaceuticals, an Amgen subsidiary. Professors Lencioni and Bronowicki have received honoraria for advisory arrangements from Bayer HealthCare Pharmaceuticals, Inc. Professor Papandreou has received research grant support from Bayer HealthCare Pharmaceuticals, Inc. Dr Nakajima, Mr Lehr, and Ms Heldner are employees of Bayer HealthCare Pharmaceuticals, Inc. Dr Nakajima has stock ownership with Bayer HealthCare Pharmaceuticals, Inc. Drs Kudo, Chen, Dagher, Ladrón de Guevara, Sanyal, Takayama, Yoon, and Ye have no relevant disclosures to report.

Authors' contributions

JAM, RL, MK, S-LY, and APV are members of the Global Steering and Publication Committee for the GIDEON study and were involved in the development of the GIDEON protocol, and in data review and interpretation. JAM, RL, MK, S-LY, APV, J-PB, X-PC, LD, JF, JFG, LL de G, CP, AJS, TT, and SKY were all responsible for the provision of patients and data acquisition. KN is the sponsor study physician and contributed to data analysis and interpretation. RLehr is the study statistician and contributed to statistical analysis. SH was responsible for the study supervision. All authors provided critical review of the manuscript for intellectual content, and approved the final version for publication.

Acknowledgments

The authors would like to thank all participating clinical sites that contributed to the GIDEON study. All data management-related activities for GIDEON were coordinated and overseen by Anja Laske at Bayer HealthCare Pharmaceuticals, Inc. The contract

research organization Kantar Health GmbH (Munich, Germany) is responsible for the data management system, data capture, quality review, statistical analysis, and report writing. Kieran Davey, PhD, at Complete HealthVizion provided assistance in the preparation and revision of the draft manuscript, funded by Bayer HealthCare AG. The authors take full responsibility for the scope, direction, and content of the manuscript. GIDEON is funded by Bayer HealthCare AG and Onyx Pharmaceuticals, an Amgen subsidiary.

Supplementary data

Supplementary data associated with this article can be found, in the online version, at http://dx.doi.org/10.1016/j.jhep.2016.07.020.

References

[1] Torre LA, Bray F, Siegel RL, Ferlay J, Lortet-Tieulent J, Jemal A. Global cancer statistics, 2012. CA Cancer J Clin 2015;65:87–108.
[2] Monsour Jr HP, Asham E, McFadden RS, Victor III DW, Muthuswamy B, Zaheer I. Hepatocellular carcinoma: the rising tide from east to west—review of epidemiology, screening and tumor markers. Transl Cancer Res 2013;2:492–506.
[3] Singal AG, El-Serag HB. Hepatocellular carcinoma from epidemiology to prevention: translating knowledge into practice. Clin Gastroenterol Hepatol 2015;13:2140–2151.
[4] Samuel M, Chow PKH, Chan Shih-Yen E, Machin D, Soo KC. Neoadjuvant and adjuvant therapy for surgical resection of hepatocellular carcinoma. Cochrane Database Syst Rev 2009, [Art. No.: CD001199].
[5] Schlachterman A, Craft Jr WW, Hilgenfeldt E, Mitra A, Cabrera R. Current and future treatments for hepatocellular carcinoma. World J Gastroenterol 2015;21:8478–8491.
[6] Llovet JM, Ricci S, Mazzaferro V, Hilgard P, Gane E, Blanc JF, et al. Sorafenib in advanced hepatocellular carcinoma. N Engl J Med 2008;359:378–390.
[7] Cheng AL, Kang YK, Chen Z, Tsao CJ, Qin S, Kim JS, et al. Efficacy and safety of sorafenib in patients in the Asia-Pacific region with advanced hepatocellular carcinoma: a phase III randomised, double-blind, placebo-controlled trial. Lancet Oncol 2009;10:25–34.
[8] Bruix J, Sherman M. Management of hepatocellular carcinoma: an update. Hepatology 2011;53:1020–1022.
[9] Peck-Radosavljevic M, Greten TF, Lammer J, Rosmorduc O, Sangro B, Santoro A, et al. Consensus on the current use of sorafenib for the treatment of hepatocellular carcinoma. Eur J Gastroenterol Hepatol 2010;22:391–398.
[10] Lencioni R, Marrero J, Venook A, Ye SL, Kudo M. Design and rationale for the non-interventional Global Investigation of therapeutic DEcisions in hepatocellular carcinoma and Of its treatment with sorafeNib (GIDEON) study. Int J Clin Pract 2010;64:1034–1041.
[11] European Medicines Agency. EUDRALEX: The rules governing medicinal products in the European Union. Available from: http://ec.europa.eu/enterprise/newsroom/cf/itemdetail.cfm?&item_id=897. Accessed 5 November 2015.
[12] Pugh RN, Murray-Lyon IM, Dawson JL, Pietroni MC, Williams R. Transection of the oesophagus for bleeding oesophageal varices. Br J Surg 1973;60:646–649.
[13] Ozenne V, Paradis V, Pernot S, Castelnau C, Vullierme MP, Bouattour M, et al. Tolerance and outcome of patients with unresectable hepatocellular carcinoma treated with sorafenib. Eur J Gastroenterol Hepatol 2010;22:1106–1110.
[14] Hollebecque A, Cattan S, Romano O, Sergent G, Mourad A, Louvet A, et al. Safety and efficacy of sorafenib in hepatocellular carcinoma: the impact of the Child-Pugh score. Aliment Pharmacol Ther 2011;34:1193–1201.
[15] Kim JE, Ryoo BY, Ryu MH, Chang HM, Suh DJ, Lee HC, et al. Sorafenib for hepatocellular carcinoma according to Child-Pugh class of liver function. Cancer Chemother Pharmacol 2011;68:1285–1290.
[16] Al-Rajabi R, Patel S, Ketchum NS, Jaime NA, Lu TW, Pollock BH, et al. Comparative dosing and efficacy of sorafenib in hepatocellular cancer patients with varying liver dysfunction. J Gastrointest Oncol 2015;6:259–267.
[17] da Fonseca LG, Barroso-Sousa R, Bento AD, Blanco B,P, Valente GL, Pfiffer TE, et al. Safety and efficacy of sorafenib in patients with Child-Pugh B advanced hepatocellular carcinoma. Mol Clin Oncol 2015;3:793–796.
[18] Brose MS, Frenette CT, Keefe SM, Stein SM. Management of sorafenib-related adverse events: a clinician's perspective. Semin Oncol 2014;41:S1–S16.
[19] Abou-Alfa GK, Amadori D, Santoro A, Figer A, De Greve J, Lathia C, et al. Safety and efficacy of sorafenib in patients with hepatocellular carcinoma (HCC) and Child-Pugh A *vs.* B cirrhosis. Gastrointest Cancer Res 2011;4:40–44.
[20] Miller AA, Murry DJ, Owzar K, Hollis DR, Kennedy EB, Abou-Alfa G, et al. Phase I and pharmacokinetic study of sorafenib in patients with hepatic or renal dysfunction: CALGB 60301. J Clin Oncol 2009;27:1800–1805.
[21] Lettieri JT, Mazzu AL, Huang L, Lathia CD. Effect of hepatic impairment on sorafenib pharmacokinetics: results of a multicenter, open-label, single-dose, phase I trial. J Clin Oncol 2011;29:abs2580.
[22] Mitchell DY, Prins K, Ploeger B, Grevel J, Lettieri J, Meinhardt G, et al. Impact of Child-Pugh status (A, B, or C) and duration of treatment on sorafenib exposure in patients with advanced hepatocellular carcinoma in the Phase IV HATT trial: a population pharmacokinetic analysis (abstract O-030). International Liver Cancer Association, Kyoto, Japan, 5–7 September, 2014.
[23] Bayer Pharma AG. Nexavar® (sorafenib). Summary of product characteristics. Available from: http://www.nexavar.com/scripts/pages/en/home//pdf/Nexavar_SmPC_June_2014.pdf. Accessed 5 November 2015.
[24] Pressiani T, Boni C, Rimassa L, Labianca R, Fagiuoli S, Salvagni S, et al. Sorafenib in patients with Child-Pugh class A and B advanced hepatocellular carcinoma: a prospective feasibility analysis. Ann Oncol 2013;24:406–411.
[25] Di Marco V, De Vita F, Koskinas J, Semela D, Toniutto P, Verslype C. Sorafenib: from literature to clinical practice. Ann Oncol 2013;24:ii30–ii37.
[26] Chiu J, Tang YF, Yao TJ, Wong A, Wong H, Leung RC, et al. The use of single-agent sorafenib in the treatment of patients with advanced hepatocellular carcinoma with underlying Child-Pugh B liver cirrhosis. J Clin Oncol 2011;29:abs4083.
[27] Ji YX, Zhang ZF, Lan KT, Nie KK, Geng CX, Liu SC, et al. Sorafenib in liver function impaired advanced hepatocellular carcinoma. Chin Med Sci J 2014;29:7–14.
[28] Johnson PJ, Berhane S, Kagebayashi C, Satomura S, Teng M, Reeves HL, et al. Assessment of liver function in patients with hepatocellular carcinoma: a new evidence-based approach – the ALBI grade. J Clin Oncol 2015;33:550–558.
[29] Otsuka T, Eguchi Y, Kawazoe S, Yanagita K, Ario K, Kitahara K, et al. Skin toxicities and survival in advanced hepatocellular carcinoma patients treated with sorafenib. Hepatol Res 2012;42:879–886.
[30] Shin SY, Lee YJ. Correlation of skin toxicity and hypertension with clinical benefit in advanced hepatocellular carcinoma patients treated with sorafenib. Int J Clin Pharmacol Ther 2013;51:837–846.
[31] Shomura M, Kagawa T, Shiraishi K, Hirose S, Arase Y, Koizumi J, et al. Skin toxicity predicts efficacy to sorafenib in patients with advanced hepatocellular carcinoma. World J Hepatol 2014;6:670–676.
[32] Bettinger D, Schultheiß M, Knüppel E, Thimme R, Blum HE, Spangenberg HC. Diarrhea predicts a positive response to sorafenib in patients with advanced hepatocellular carcinoma. Hepatology 2012;56:789.

Clinical Research Paper

Combined sequential use of HAP and ART scores to predict survival outcome and treatment failure following chemoembolization in hepatocellular carcinoma: a multi-center comparative study

David J. Pinato[1], Tadaaki Arizumi[2], Jeong Won Jang[3], Elias Allara[4,5], Puvan I. Suppiah[1], Carlo Smirne[4], Paul Tait[6], Madhava Pai[7], Glenda Grossi[4], Young Woon Kim[3], Mario Pirisi[4,8], Masatoshi Kudo[2], Rohini Sharma[1]

[1]Department of Surgery and Cancer, Imperial College London, Hammersmith Hospital, London, UK

[2]Department of Gastroenterology and Hepatology, Kinki University School of Medicine, Osaka-Sayama, Osaka, Japan

[3]Department of Internal Medicine, The Catholic University of Korea Incheon St. Mary's Hospital, Seoul, Republic of Korea

[4]Department of Translational Medicine, Università degli Studi del Piemonte Orientale "A. Avogadro", Novara, Italy

[5]School of Public Health, Università degli Studi di Torino, Torino, Italy

[6]Department of Radiology, Imperial College NHS Trust, Hammersmith Hospital, London, UK

[7]Department of Surgery, Imperial College NHS Trust, Hammersmith Hospital, London, UK

[8]Interdisciplinary Research Center of Autoimmune Diseases, Università degli Studi del Piemonte Orientale "A. Avogadro", Novara, Italy

Correspondence to: *David James Pinato,* ***email:*** *david.pinato@imperial.ac.uk*

Keywords: *prognosis, hepatocellular carcinoma, TACE, ART score, HAP score*

Received: *February 22, 2016* ***Accepted:*** *April 26, 2016* ***Published:*** *May 26, 2016*

ABSTRACT

Background: The prognosis of patients with hepatocellular carcinoma (HCC) undergoing transarterial chemoembolization (TACE) is variable, despite a myriad of prognostic markers. We compared and integrated the established prognostic models, HAP and ART scores, for their accuracy of overall survival (OS) prediction.

Results: In both training and validation sets, HAP and ART scores emerged as independent predictors of OS ($p<0.01$) with HAP achieving better prognostic accuracy (c-index: 0.68) over ART (0.57). We tested both scores in combination to evaluate their combined ability to predict OS. Subgroup analysis of BCLC-C patients revealed favorable HAP stage ($p<0.001$) and radiological response after initial TACE ($p<0.001$) as positive prognostic factors.

Patients and Methods: Prognostic scores were studied using multivariable Cox regression and c-index analysis in 83 subjects with Barcelona Clinic Liver Cancer (BCLC) A/B stage from UK and Italy (training set), and 660 from Korea and Japan (validation set), all treated with conventional TACE. Scores were further validated in an separate analysis of patients with BCLC-C stage disease (n=63) receiving initial TACE.

Conclusion: ART and HAP scores are validated indices in patients with intermediate stage HCC undergoing TACE. The HAP score is best suited for screening patients prior to initial TACE, whilst sequential ART assessment improves early detection of chemoembolization failure. BCLC-C patients with low HAP stage may be a subgroup where TACE should be explored in clinical studies.

INTRODUCTION

Patients presenting with liver-confined hepatocellular carcinoma (HCC), preserved liver function and performance status cluster into "intermediate stage" or Barcelona Clinic Liver Cancer (BCLC) B category [1]. In this patient subgroup where overall survival (OS) often extends beyond 2 years [2], guidelines recommend trans-arterial chemoembolization (TACE) with the intent of prolonging OS by achieving local disease control [3].

TACE is also indicated in early HCC when surgery or radiofrequency ablation is contraindicated [4]. In parallel, whilst not supported by randomized controlled trials (RCT), a growing number of single-center studies indicate that embolization is safe and effective also in patients with segmental portal vein invasion or systemic metastases [5]. Because of the evolving experience in the administration of TACE, achieving consensus regarding optimal selection criteria and best re-treatment strategy is critical in improving and maintaining clinical outcomes [6].

However, due to the heterogeneity in the prognosis of BCLC-B HCC, where predicted OS ranges from 11 to 45 months, treatment decisions in the individual patient are partially subjective, being influenced by the local expertise within each institution [7]. Previous studies have identified a number of individual adverse prognostic traits in patients undergoing TACE [8]. These have been variously combined to derive coherent prognostic models aiming to standardize the prognostic assessment across institutions [7, 9–12]. Based on these scores, subjects with shorter survival expectancy might be offered systemic treatment or best supportive care, avoiding exposure to the adverse effects of TACE.

Of the prognostic scores, the hepatoma arterial-embolization prognostic (HAP) score is a model constructed on baseline pre-TACE hypoalbuminemia <35 g/L, bilirubin >17 mmol/L, AFP >400 ng/ml and tumor size >7 cm designed to guide initial TACE treatment [11]. A second, recently qualified prognostic model, the ART score, is based on the deterioration of liver biochemistry following initial TACE and the presence of radiological response to treatment [12], and can be used to identify patients who may benefit from sequential retreatment [13] (Table 1).

Whilst scientifically interesting, the relationship between these scores and patient's overall survival has been questioned following validation in independent cohorts, casting doubt upon their clinical utility [14, 15]. As a result, the use of either score is not advocated within the current management guidelines for HCC. In addition, there are no available data to suggest which score is best in predicting patient prognosis, or how best to combine both scores in the clinical setting.

We designed this multi-institutional study aiming to validate the accuracy of HAP and ART score in predicting patients' survival after initial TACE. We employed independent cohorts of unselected, consecutive patients with HCC presenting within intermediate stage criteria from Europe and Asia to ensure ample generalizability of the results, evaluating both scores individually and in combination. Secondarily, we intended to investigate whether the proposed scores preserved prognostic prediction in a subgroup of patients exceeding BCLC-B criteria treated with TACE in a post-hoc analysis.

RESULTS

Demographics

The clinicopathologic features of both datasets are illustrated in Table 2. In the training set, median age was 72 years, 50% of the patients were staged as intermediate stage HCC according the BCLC algorithm, with preserved liver function (CTP A, 75%). Minimum follow-up time was 4 months or until date of death. At the time of analysis 37% of patients had died. Median OS was 26 months (4-162 months).

Survival analysis

On univariable analyses, intrahepatic spread ($p<0.007$), tumor size >5cm ($p<0.001$), AFP>400 ng/ml ($p<0.001$), CTP class ($p=0.008$), radiologic response post-TACE ($p=0.002$), CLIP ($p<0.001$), HAP ($p<0.001$) and ART score ($p=0.002$) emerged as significant predictors of OS in the training set (Table 3). Based on ART score, the median OS for patients of good prognosis (ART score <2.5) was 55 months, reducing to 22 months in patients with a poor score (Figure 1A). In patients with HAP stage A disease, median OS was not reached at the end of observation. Patients within HAP stage B or C had a median OS of 55 and 46 months respectively, deteriorating to 9 months in stage D disease (Figure 1B).

A multivariable regression model was constructed including HAP, ART score, mRECIST and CLIP score (categorized as 0-1 versus ≥2) with other significant univariable predictors being excluded from analysis to avoid collinearity. Cox regression analysis confirmed HAP and ART scores (Supplementary Table 1) together with mRECIST (Hazard Ratio [HR] 1.5 95%CI 1.0-2.3, $p=0.04$) as independent predictors of patients' OS.

Validation of prognostic models

The prognostic accuracy of the ART and HAP scores was further tested in a larger, independent validation dataset. As shown in Table 2, there was homogeneity across both datasets in terms of age, gender distribution, liver functional reserve (CTP A, 75%), stage (BCLC-B, 60%) and median OS which in the validation set, 23 months (range 1-115 months).

Table 1: The hepatoma arterial-embolisation prognostic (HAP) score and the assessment for re-treatment with TACE (ART) score

Prognostic Model	Variables	Prognostic Stratification
HAP Score	Albumin <35 g/L AFP >400 ng/dL Tumor diameter >7cm Bilirubin >17mmol/L	HAP A HAP B HAP C HAP D
ART Score	Child Pugh increase following TACE (+1, +2 points) AST >25% from baseline Lack of radiologic response	High risk (>2.5) Low risk (<2.5)

Table 2: Demographic and clinical characteristics of patients with HCC treated with TACE (training and validation set)

Baseline characteristic	n=83, (%) or median, (range)	n=660, (%) or median, (range)
Age, years	72 (47-84)	73 (42-89)
Gender		
Male	64 (77)	465 (70)
Female	19 (23)	195 (30)
Aetiology of Chronic Liver Disease		
Viral	49 (60)	533 (80)
Non Viral	31 (37)	127 (20)
Not characterized	3 (3)	
Child Turcotte Pugh Class		
A5	37 (45)	332 (49)
A6	25 (30)	168 (26)
B7	14 (17)	94 (14)
B8	5 (6)	43 (7)
B9	2 (2)	23 (4)
Maximum tumour diameter		
≤ 5 cm	26 (40)	565 (86)
> 5 cm	38 (60)	95 (14)
Number of nodules		
1	28 (34)	110 (17)
2	22 (26)	120 (18)
3	16 (20)	97 (15)
>3	17 (20)	248 (38)
Missing	-	85 (12)
AFP		
<400 ng/mL	77 (93)	534 (81)
≥400 ng/mL	6 (7)	126 (19)
Albumin, g/L	37 (23-49)	37 (20-50)
Total bilirubin, umol/L	19 (7-55)	14 (3-70)
ALT, IU/L	48 (13-177)	37 (4-277)
AST, IU/L	56 (16-188)	48 (6-303)

(*Continued*)

Baseline characteristic	n=83, (%) or median, (range)	n=660, (%) or median, (range)
ALP, IU/L	255 (113-529)	336 (108-1212)
INR	1.2 (1.0-1.6)	1.0 (1.0-2.0)
Platelet Count, x 10^9/L	115 (26-269)	115 (14-453)
BCLC Stage		
A	42 (50)	270 (40)
B	41 (50)	390 (60)
CLIP Score		
0-1	61 (73)	N.A.
≥2	22 (27)	
Number of TACE procedures		
1	42 (50)	171 (26)
2	16 (20)	139 (21)
≥3	25 (30)	274 (42)
Missing	-	76 (11)
Prior Treatments		
First line TACE	50 (60)	322 (48)
Resection	6 (7)	77 (12)
Transplantation	1 (1)	0 (0)
Radiofrequency ablation	22 (27)	243 (36)
Systemic treatment	4 (3)	18 (4)
Modified RECIST response following TACE		
Complete Response	22 (26)	268 (40)
Partial Response	40 (48)	110 (17)
Stable Disease	12 (15)	91 (14)
Progressive Disease	9 (11)	191 (29)
HAP Score		
A	23 (28)	274 (41)
B	32 (39)	209 (32)
C	24 (30)	137 (21)
D	3 (3)	40 (6)
ART Score		
<2.5	55 (66)	423 (64)
>2.5	28 (44)	237 (36)

Both ART and HAP score remained significant on univariate (*p<0.001*) and multivariate (*p<0.001*) analysis of OS with adjusted hazard ratios shown in Supplementary Table 2. Patients with an ART score >2.5 after initial TACE had an OS of 29 months (range 23-34) compared to those with an ART score <2.5 whose median OS was 45 months (range 40-50, *p<0.001*) (Figure 1C). Patients within HAP stage A or B had median OS of 52 (95%CI 45-58) and 37 (30-44) months compared with stage C or D with median OS of 19 (14-25) and 9 (8-10) months, respectively (p<0.001) (Figure 1D). Radiologic response to treatment emerged as additional multivariable predictor of OS (HR 1.7 95%CI 1.6-1.8 *p<0.001*).

We assessed the accuracy of the HAP and ART score in predicting early mortality using ROC curve analysis based on 1 and 2-year survival rates. In the training set, both scores had acceptable accuracy in estimating mortality after initial TACE, with AUROC values of 0.67 (95%CI 0.50-0-85) for the ART score and 0.75 (95%CI 0.62-0.89) for the HAP score at 1 year, and 0.75 (95%CI 0.63-0.86) for the ART score and 0.73 (95%CI 0.62-0-85) for the HAP score at 2 years (*p<0.05*) (Supplementary Figure 1A-B). In the validation set, the HAP score was a more accurate predictor of 1-year mortality with AUROC values of 0.70 (95%CI 0.66-0.75) compared to the ART score 0.57 (95%CI 0.52-0.62, *p<0.05*). Similarly, 2-year

Table 3: Univariate analysis of prognostic factors of overall survival (training set)

		UNIVARIATE ANALYSIS		
Variable	**N=83**	**Median OS (95% CI)**	**Hazard Ratio (95% CI)**	**P-value**
Age				
<65	32	-	-	0.45
>65	51			
Etiology				
Viral	31	-	-	0.91
Non-viral	49			
Intrahepatic spread				
Uninodular <50%	27	104 (12-196)	2.6 (1.3 – 5.2)	0.007*
Multinodular <50%	51	50 (40-59)		
Massive ≥50%	8	19 (5-35)		
Maximum tumour diameter				
<5 cm	67	55 (20-90)	3.9 (1.7-8.7)	<0.001*
≥5 cm	20	21 (16-27)		
AFP, ng/ml				
<400	78	55 (17-93)	8.2 (3.3 – 20.8)	<0.001*
≥400	8	14 (7-21)		
CLIP Score*				
0-1	61	104 (32-176)	2.3 (1.5-2.5)	0.001*
≥2	22	22 (18-25)		
BCLC				
A	42	-	-	0.22
B	41			
Child Turcotte Pugh Class				
A	62	104 (33-175)	2.9 (1.3-6.5)	0.008*
B	21	46 (10-83)		
Tumour Response (mRECIST)				
CR	22	NR	1.9 (1.2-2.9)	0.002*
PR	40	55 (36-73)		
SD	12	52 (26-79)		
PD	9	21 (7-37)		
HAP Score				
A	23	NR	3.1 (1.8-5.3)	<0.001*
B	32	55 (34-75)		
C	24	46 (18-82)		
D	3	9 (43-63)		
ART Score				
<2.5	55	104 (30-160)	3.1 (1.5-6.7)	0.002*
>2.5	28	22 (10-47)		

NR: Not reached.

mortality was more accurately predicted by the HAP score (0.67, 95%CI 0.63-0.71) than the ART score (0.53, 95%CI 0.50-0.58, *p<0.05*) (Supplementary Figure 1C-D).

The discriminatory capacity of each prognostic system was compared by means of Harrell's concordance index [22]. The HAP score displayed an overall better discriminatory ability in predicting OS with a c-score of 0.68 (95%CI 0.64-0.70) compared to the ART score (c-score 0.57, 95%CI 0.53- 0.60). The combination of

HAP and ART score yielded a pooled c-score of 0.69 (95% CI 0.65-0.72).

We further confirmed the prognostic validity of both HAP and ART score in a pooled analysis of patients belonging to both training and validation sets (n=746). As shown in Supplementary Figure 2, this confirmed the prognostic value of both scores in the entire study population (Log rank p<0.001 for both HAP and ART scores). Given the independent prognostic role observed for the HAP and ART scores we evaluated the accuracy of their combined sequential use in the entire study population. As shown in Supplementary Table 3, the ART score was able to detect a significant survival difference of 15 months in HAP B (p<0.001), 17.1 months in HAP C (p=0.001) and 1 month in HAP D (p=0.02) patients, with no effect on survival seen for patients clustering in HAP A stage (p=0.96) (Supplementary Figure 3).

Evaluation of prognostic models in patients exceeding *BCLC-B* criteria

We performed a separate survival analysis on 63 patients derived from the validation set who had been offered TACE despite exceeding BCLC-B staging criteria

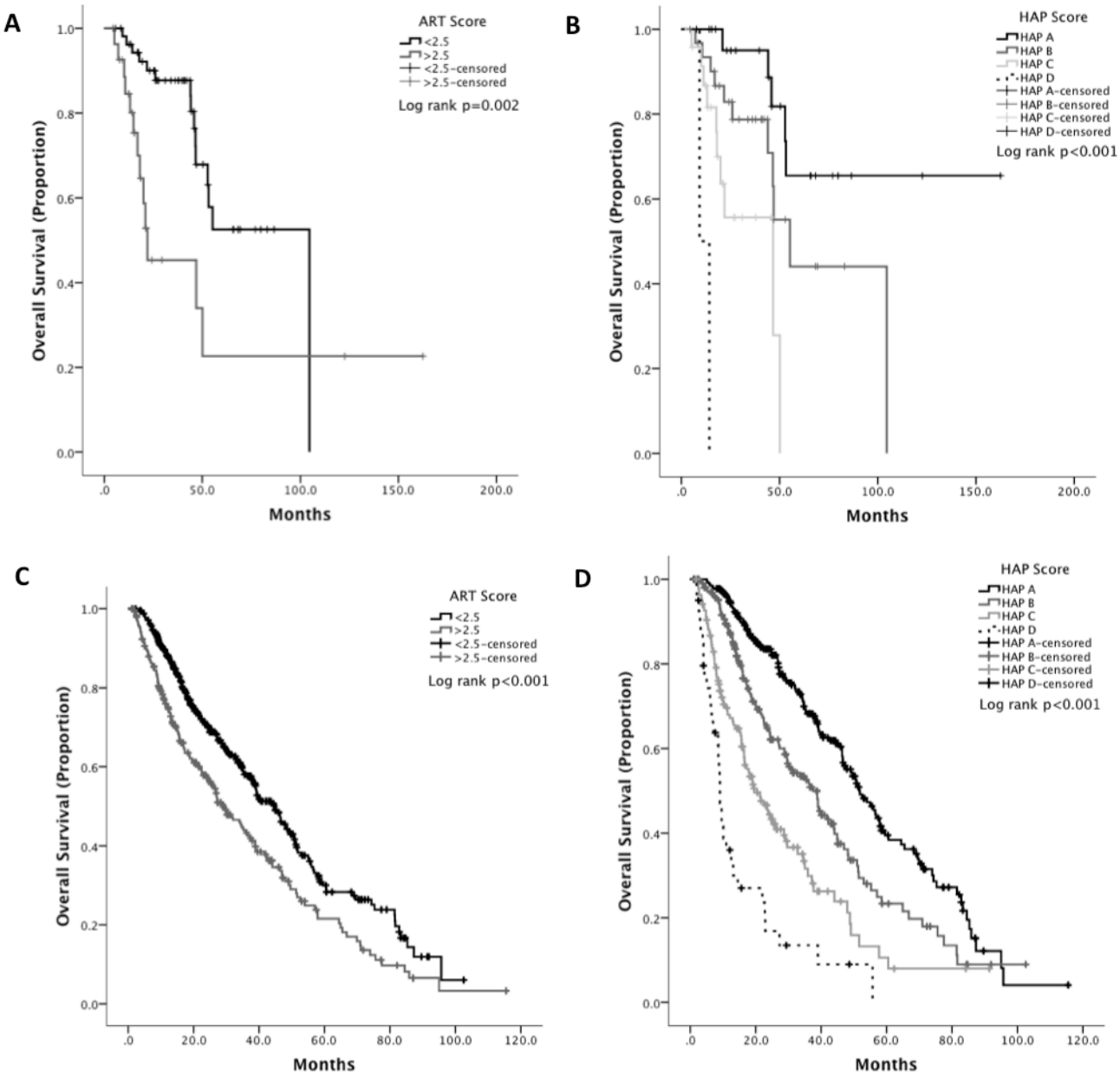

Figure 1: Kaplan Meier curve analysis showing the effect of ART and HAP score as predictors of overall survival in HCC in the training **(A, B)** and in the validation set **(C, D)**.

due to visceral metastatic spread (*n=29*, 46%), segmental portal vein involvement (*n=34*, 54%) or Child C cirrhosis (*n=1*, 1%). These patients had been excluded from the principal analysis (Figure 2). The median survival of this patient subgroup was 11.8 months (range 1.4-59 months) with a total of 45 deaths (71%) at the time of data analysis. Full clinicopathologic characterization is provided in Table 4.

Survival analysis revealed that response to TACE (HR 2.0 1.4-2.8, *p<0.001*) and the HAP (*p=0.02*) but not the ART score (*p=0.39*) predict OS after initial TACE. Median OS was 25.9 (range 8.6-43.1) in HAP A stage, 23.3 months (range 19.0-27.6) in HAP stage B, 11.8 months (5.4-11.8) in stage C and 10 months (6.5-13.4) in stage D (HR 1.5, 95%CI 1.1-2.2, *p=0.02*). However, in patients with BCLC-C, OS was not significantly different across HAP stages A and B (*p=0.75*), nor across C and D (*p=0.06*). The accuracy of OS estimation was optimized by dichotomizing the HAP score into stages A+B (median OS 23 months, range 12-34 months) against C+D (median OS 10 months, range 5-14 months, HR 2.6 95%CI 1.4-4.9 *p=0.002*). According to mRECIST criteria, median OS was 8 months (range 6-11 months) in patients with progressive disease, 16 months (range 8-25 months) with stable disease and 26 months with complete and partial response (range 6-45 months, *p<0.001*)(Figure 3).

DISCUSSION

The use of TACE in unresectable HCC as a palliative measure to improve survival whilst maintaining quality of life is supported by level I evidence from 2 primary RCTs and 3 meta-analyses [3]. However, significant heterogeneity in median OS has been reported in patients receiving TACE, varying from 16-40 months in early stage disease to 15-27 months in intermediate [23] and 4-15 months in advanced disease [5]. The wide range in OS figures observed within each stage stems from inter-institution variability in patient selection, diverse re-treatment criteria, and the evolving technique in delivering TACE.

Given the palliative intent of TACE it is important that patient selection is not only driven by the technical feasibility of the procedure, but also guided by careful consideration of the potential survival benefit against the risk of post-procedural adverse events. For this reason, the

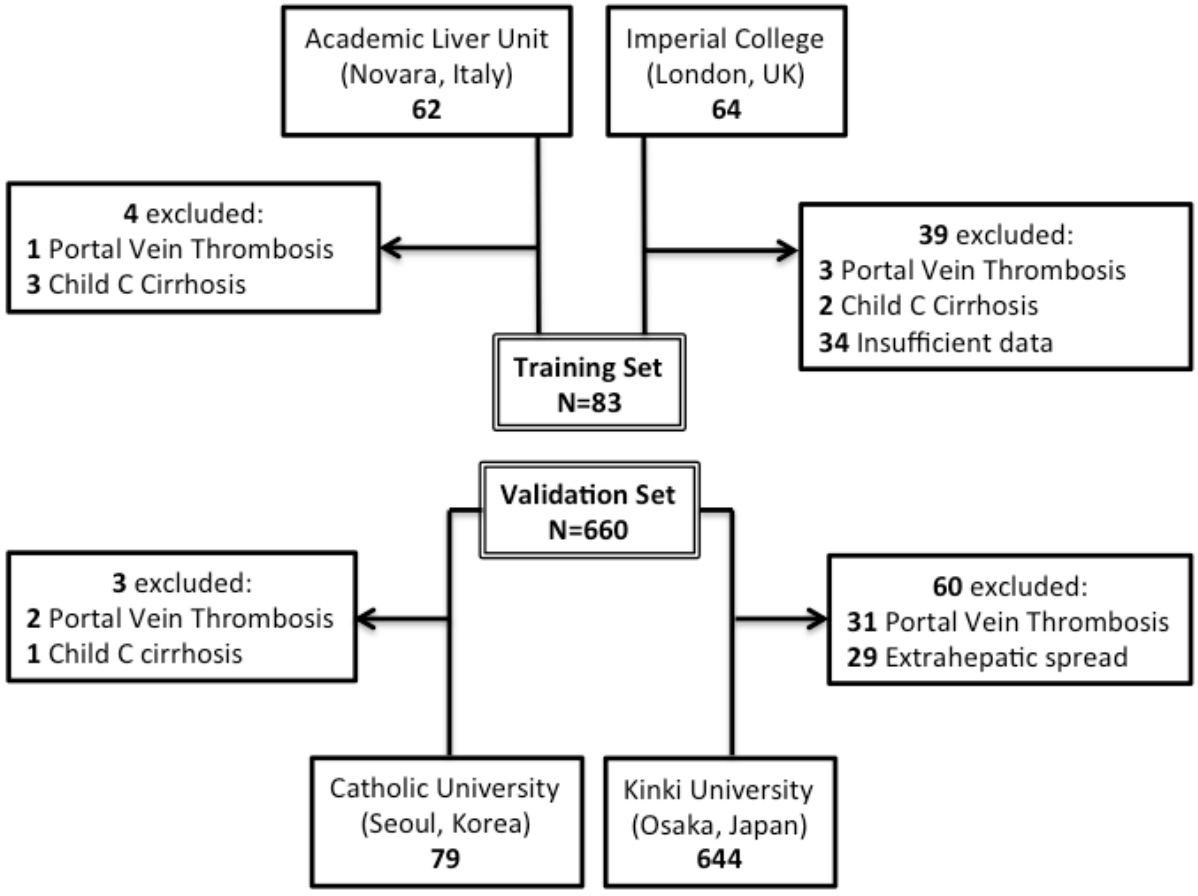

Figure 2: Study flow diagram illustrating patient inclusion in the training and validation set.

Table 4: Clinicopathologic characteristics of patients exceeding BCLC-B criteria

Baseline characteristic	n=63, (%) or median, (range)
Age, years	53 (34-87)
Gender	
Male	48 (76)
Female	15 (24)
Aetiology of Chronic Liver Disease	
Viral	48 (76)
Non Viral	15 (24)
Child Turcotte Pugh Class	
A	51 (80)
B	11 (19)
C	1 (1)
Maximum tumour diameter	
≤ 5 cm	33 (52)
> 5 cm	30 (48)
Number of nodules	
1	5 (8)
2	15 (24)
≥3	43 (68)
Extrahepatic Metastasis	
Absent	34 (54)
Present	29 (46)
Portal Vein Involvement (segmental)	
Absent	29 (46)
Present	34 (54)
AFP	
<400 ng/mL	43 (68)
≥400 ng/mL	20 (32)
Albumin, g/L	37 (21-46)
Total bilirubin, umol/L	13 (3-53)
ALT, IU/L	44 (10-122)
AST, IU/L	56 (14-138)
ALP, IU/L	220 (120-1901)
INR	1.1 (1.0-1.6)
Platelet Count, x 10^9/L	121 (14-1653)
Number of TACE procedures	
1	31 (50)
2	17 (20)
≥3	15 (30)
Modified RECIST response following TACE	
Complete Response	3 (5)
Partial Response	21 (32)
Stable Disease	11 (18)
Progressive Disease	28 (45)
HAP Score	
A	12 (19)
B	20 (32)
C	22 (35)
D	9 (14)
ART Score	
<2.5	32 (51)
>2.5	31 (49)

development of biomarkers to allow for a more objective selection of TACE candidates based on the likelihood to benefit from treatment has been at the focus of intense research efforts.

In our multi-institutional retrospective study of prognostic factors, the largest to our knowledge, we validated for the first time the significance of two recently qualified models, the HAP and the ART score in both Western and Asian patient populations, where survival outcomes can significantly differ as a result of the diverse disease etiology, screening policy and subsequent clinical management [24]. These scores have been proposed as objective and mutually exclusive strategies to select patients for initial as well as subsequent loco-regional therapies based on their capacity to predict long-term survival following TACE. Their prognostic potential, however, has never been compared, a point of major consequence given the emergence of discrepancies from their independent evaluation in separate studies, which has lead to uncertainties in terms of which strategy should be prioritized for clinical use [14, 15].

Whilst meant to inform treatment decisions in intermediate stage HCC, the original study that qualified the HAP score included only 31% of the patients with BCLC-B stage, with lack of complete staging data in the validation set. In addition, 36% of the patients exceeded BCLC-B criteria, though variables including portal vein involvement, PS or extra-hepatic disease were not

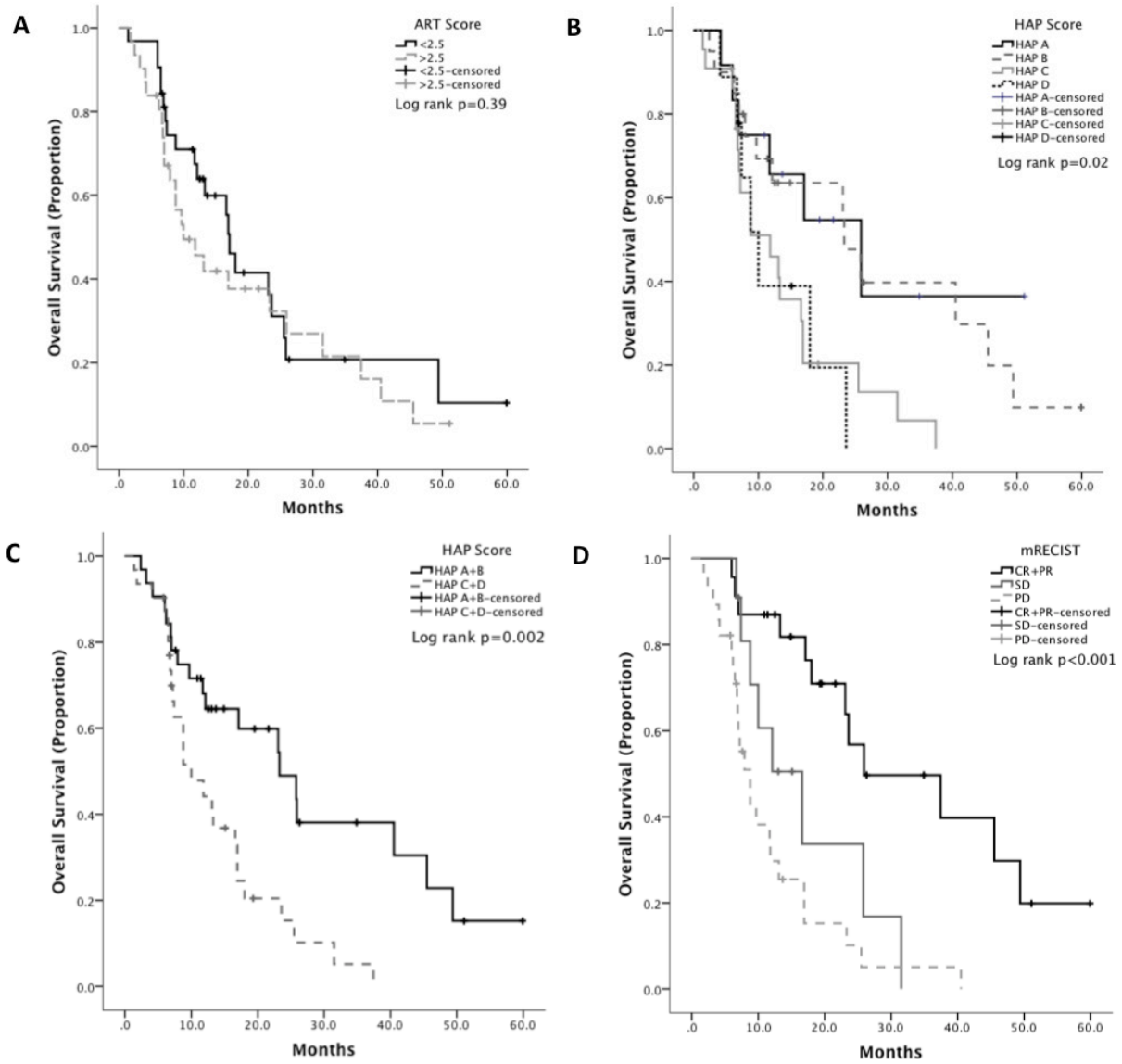

Figure 3: Kaplan Meier curve analysis showing the effect of different prognostic models on the overall survival of a subgroup of patients exceeding intermediate HCC staging criteria: ART score **(A)**, HAP score **(B, C)** mRECIST based radiologic response **(D)**.

(*Continued*)

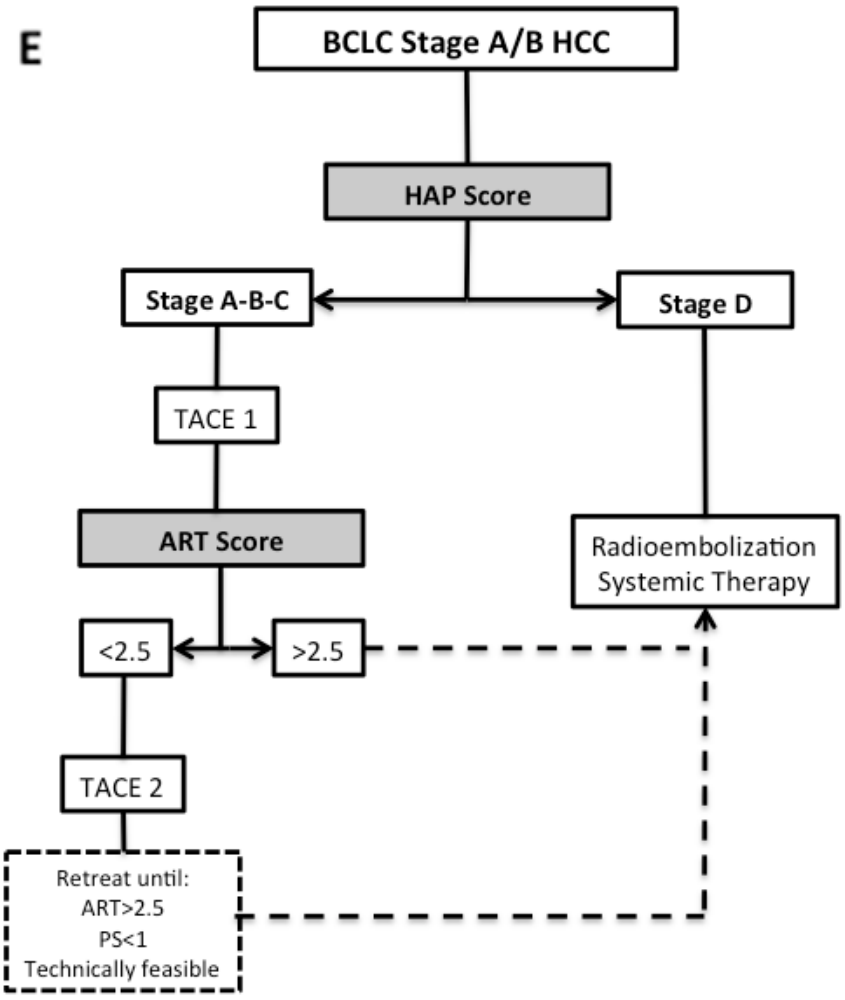

Figure 3(*Continued*): Panel **E** illustrates a proposed algorithm for the sequential use of the HAP and ART score in BCLC-A/B stage patients.

documented in the analysis, potentially causing a greater heterogeneity in survival [11].

Similar pitfalls may influence the validity of the ART score, where recent retrospective studies have in fact demonstrated that only 10-15% of the patients were eligible for ART score testing [14, 15] based on the original eligibility criteria, which excluded patients <2 TACE within 90 days [12], suggesting a reduced applicability of the model in the general population.

Unlike other studies, we included TACE candidates consecutively and in an unselected manner apart from BCLC stage, therefore allowing for the prognostic scores to predict for outcome after initial TACE more closely to a "real life" clinical practice scenario. In our study, both scores emerged as highly significant predictors of OS (Figure 1), preserving an independent effect when tested on a multivariable Cox regression model (Supplementary Tables 1, 2). Our data show that the HAP score displayed better accuracy in estimating short-term mortality at 1 and 2 years following TACE (Supplementary Figure 1), a finding that was confirmed by c-index analysis indicating a superior predictive accuracy of the HAP over the ART score in estimating long term OS.

Interestingly, whilst the predicted survival for each HAP stage in this study was similar to that of previously published data [11], wider OS differences were observed in the poor prognostic group according to the ART score (22 and 29 months in our study; 6.6 and 8.1 months in the study by Sieghart et al. [12]). There are several reasons that may account for the survival differences observed. Firstly, our study includes a significantly higher proportion of BCLC-A in both datasets. The ART score was derived from dynamic changes in biochemical and radiological parameters following initial TACE, and patients with <2 TACE within 90 days and those achieving complete response after initial treatment were excluded in the original study. Equally, survival times were calculated from the day of the second TACE, and reassessment of liver function was carried out one day prior to second TACE [12]. The different purpose of

our study, however, required a standardized comparison in homogenous populations unselected for clinico-pathologic features other than BCLC stage. This is a key point in the prognostic evaluation of the ART score, whose prognostic ability has been questioned in a previous analysis published by Kudo et al. which included patients from the same cohort included in this study [14]. The different selection criteria used for the two studies, however, are important in explaining the difference in our results. In the analysis by Kudo and in a subsequent, more comprehensive evaluation of the ART score in a cohort of 988 patients [25], only 12% of the patients underwent ≥2 TACE sessions within 90 days. In these patients the ART score failed to predict prognosis.

In our study, we obtained repeat blood tests and concurrent imaging reassessment 6-8 weeks after initial TACE, when patients presented for consideration of retreatment, a setting that – we believe – replicates a more appropriate time point for the clinical application of the ART score, rather than a pre-planned second TACE [12]. We also did not apply the 90-days interval criteria, considering the prognostic performance of the score in the whole patient population. Whilst the inherent differences in study design may account, in our opinion, for the heterogeneity in survival observed in ART score strata across studies, it should be emphasized that our study better approximates a routine clinical practice scenario where changes in the ART score could prompt changes in the management of unselected patients assessed following initial TACE. Whilst holding the undoubted advantage to be used sequentially to guide retreatment beyond initial TACE [10], based on our data, the ART score calculated after first TACE holds inferior accuracy in predicting short and long term prognosis compared to the HAP score.

However, given that both scores maintained a strong and independent prognostic value in our study, we were interested in testing their integrated effect in predicting OS in a large pooled cohort of 746 cases satisfying intermediate stage criteria. As shown in Supplementary Table 3, whilst the addition of the ART score is minimally or not significant at the extreme stages of the HAP prognostic algorithm, we surprisingly demonstrate the highest levels significance in the integration of the ART score in patients who belong to HAP stages B and C, suggesting that the dynamic changes in liver function and radiologic progression which compose the ART score may aid clinicians to reduce disease and treatment-related heterogeneity in survival outcomes, allowing to identify patients who are at higher risk of early mortality.

We propose an integrated algorithm with sequential use of both indices that may further refine prognostic prediction, with the HAP score being used as a screening tool to identify optimal candidates for initial TACE and the ART being sequentially used to identify early chemoembolization failure (Figure 3E). Whilst provocative, these conclusions should be further explored in adequately powered prospective studies.

As a secondary aim, we explored the prognostic in a separate analysis of a subgroup of patients with BCLC-C HCC, a patient subpopulation where TACE has been delivered with smaller but yet significant survival benefit in a number of retrospective case series [5]. Whilst the decision to treat was not supported by current BCLC guidelines, these patients received TACE at the discretion of the treating multidiscipilnary team, who felt, following case-by-case review, that TACE could have resulted in higher chances to achieve tumor control compared to other available therapies. We have shown that patients in the lower risk HAP stages, and those responding to initial TACE, achieve significant long-term benefit from treatment, albeit less than that in stage BCLC A/B. Interestingly, the ART score was not prognostic. Whilst the provision of TACE outside BCLC B stage should not be encouraged due to the lack of level I evidence, our findings are provocative in suggesting that a subset of patients with BCLC-C and HAP stage A+B, may benefit from TACE, a finding that may instigate further research.

The retrospective design and the relatively limited size of the training cohort stand as noteworthy limitations to our study. Perhaps unsurprisingly, the two cohorts demonstrated significant clinical heterogeneity, with Asian patients displaying lower tumor burden compared to Europeans, as a likely result of differing adherence to screening policies [14]. However, the process of independent validation in a large, independent cohort, the largest to have been utilized so far for the evaluation of prognostic models in intermediate-stage HCC, in conjunction with the levels of statistical significance achieved, confirms the validity, accuracy and generalizability of our results.

Additionally, we have analyzed objective and routinely collected data, which are likely to provide very low recall bias. The proportion of BCLC-A patients in both cohorts, who were offered TACE following multidisciplinary discussion confirming patient unsuitability for radical treatments, may account for the better survival figures observed here compared to other studies. Their inclusion is important in testing prognostic models in unselected TACE candidates. However, the significantly wider survival of this patient subgroup [26] warrants further validation studies focusing specifically on BCLC-A stage disease.

It is interesting to note that ROC curve analysis revealed AUROC values <0.75 in the prediction of landmark survival endpoints at 1 and 2 years, a finding that highlights the need to research into other factors other than those considered in the tested prognostic models as determinants of patients' survival after initial TACE. Similar considerations stem from the appraisal of the combined predictive ability of the combination of HAP

and ART score, where Harrel's c index analysis produced an overall score of 0.69.

In summary, we have demonstrated the HAP score as an accurate predictor of short and long-term mortality, advocating a better-suited role in the initial screening of TACE candidates. We propose the use of the ART score, a more effective model for sequential risk-assessment, to assess suitability of patients prior to retreatment following initial TACE. We showed the potential for both scores to integrate in a uniform, objective and readily applicable selection strategy to optimize the provision of TACE in patients within intermediate-stage criteria, highlighting limitations within BCLC-A and C stage tumours.

Our study provides preliminary but stimulating evidence regarding the use of TACE in advanced disease, suggesting a potential benefit in a subgroup of patients with good HAP stage. Whilst thought provoking, our findings stem from a limited sample size, predominantly from a single-institution, and warrant verification in independent, adequately powered studies, especially given the role of the provision of further anticancer therapies post-TACE refractoriness in influencing patients' survival. Equally, the exclusion of patients with incomplete data might have lead to selection bias, an issue that further strengthens the need for prospective validation of our findings.

As the number of prognostic models is increasing rapidly based on retrospective evidence [27–30], further prospective clinical trials should be instigated to confirm the clinical utility of the proposed prognostic biomarkers in the management of intermediate stage HCC.

PATIENTS AND METHODS

Patient characteristics

Our training set population was retrospectively collected and consisted of a total of 83 subjects including 58 consecutive patients treated with TACE between 2004 and 2013 at the academic Liver Unit in Novara (Italy), and patients eligible for the assessment of the ART score ($n=25$) obtained from a larger database of 64 consecutive patients treated at the Hammersmith Hospital, Imperial College London (UK) between 2001 and 2012. Patients exceeding BCLC-B criteria, i.e. with segmental portal vein thrombosis ($n=4$) or Child C cirrhosis ($n=5$) were excluded from the primary analysis (Figure 2).

The diagnosis of HCC was made according to the American Association for the Study of the Liver criteria [16]. Patients demographics, full blood count, liver function tests, AFP, tumor staging, Child-Turcotte-Pugh (CTP) class, Barcelona Clinic Liver Cancer (BCLC) [1] and Cancer of the Liver Italian Program (CLIP) [17] scores were collected prior to treatment. All patients had a performance status of zero. OS was calculated from the time of the first TACE to the time of death or last clinical follow up. Calculation of the HAP score followed the criteria published by Kadalayil et al [11]. Calculation of the ART score followed previously published criteria [12]: both biochemical and radiologic parameters were obtained 6-8 weeks following initial TACE. Multiphase contrast-enhanced computed tomography (CT) images were reported by a senior radiologist blinded to survival data in accordance with modified Response Evaluation in Solid Tumors (mRECIST) criteria [18]. At both institutions TACE protocol was planned following multidisciplinary review of clinical data and staging CT and confirmed on pre-treatment hepatic arterial angiogram. Depending on tumour burden and vascular anatomy, TACE was administered selectively or super-selectively using a 2.7-2.8 Fr microcatheter, which served for intraarterial infusion of doxorubicin emulsified in lipiodol followed by embolization with gelatin sponge particles: in total. TACE was super-selective in a total of 49 patients (59%), selective in 28 (34%) whereas 6 patients (7%) had lobar TACE. Following TACE-refractoriness a total of 28 patients received sorafenib after TACE refractoriness (34%), whilst 6 had radiofrequency ablation of the residual disease (7%) and 2 had surgical resection (2%). All the remaining patients received best supportive care only.

For the purpose of this study we defined TACE refractoriness as a pattern of disease progression that would prevent safe and effective treatment with repeat TACE. This included the emergence of extrahepatic disease progression, multifocal intrahepatic disease progression no longer amenable to TACE or loss of adequate arterial vascular access feeding the residual viable disease.

Validation of prognostic scores

The validation dataset was constructed as shown in Figure 2. This included a prospective series of 79 cases of HCC diagnosed at St. Mary's Hospital, Catholic University of Korea (Seoul, Republic of Korea) between June 2011 and July 2012 and a second retrospectively collected dataset of 644 consecutive patients with unresectable HCC treated with TACE at the Kinki University Faculty of Medicine (Osaka, Japan) between January 2004 and August 2013. In the Japanese subgroup chemoembolization was performed using 20-50 mg of epirubicin or 50-100 mg of cisplatin emulsified with lipiodol and gelatin sponge particles, for the Korean patients the TACE protocol consisted in the infusion of doxorubicin (50 mg) or combined epirubicin (50 mg) and cisplatin (60 mg) in a mixture of lipiodol followed by gelatin sponge embolization. Patients received intra-arterial treatment as appropriate for tumour burden, similarly to the training set. In total 572 patients (80%) had selective TACE, whilst the remaining 151 (20%) had lobar TACE. Response to treatment by mRECIST criteria

was assessed 6-8 weeks after TACE, reported by a senior radiologist blinded to survival data.

Treatment data post-TACE refractoriness was collected. In the Korean sub-cohort, patients were accrued prior to the clinical availability of sorafenib and were treated with hepatic intra-arterial chemotherapy (HAIC) with epirubicin (50 mg) and cisplatin (60 mg) as previously described [19]. In the Japanese group, HAIC or systemic treatment with sorafenib or TS-1 were offered in patients displaying progressive disease no longer amenable to TACE. In total, 145 patients (20%) receive HAIC, whilst 148 (20%) were offered sorafenib and 33 (5%) received TS-1, whilst the remaining patients received best supportive care only. The study was approved by the local Research Ethics Committees and conducted in accordance to the principles of the Declaration of Helsinki. All institutions used a "treatment on demand" TACE schedule and no TACE was delivered in the presence of complete radiologic response.

Statistical analysis

Kaplan-Meier statistics and Log-rank test were used to study the impact of the different clinical factors associated with OS on univariable analysis, with significant variables ($p<0.05$) being further tested on a multivariable stepwise backward Cox regression model. We used Harrell's rms packages to identify a subset of predictors by backward elimination [20], estimating the confidence intervals of the c-index statistics via bootstrapping (150 iterations). The proportional hazards assumption was tested by including the variable of interest and the product of the time varying variable constructed from the variable of interest in the Cox regression model. A resulting $p>0.05$ confirmed that the proportional hazards assumption over time was satisfied. The receiver operating characteristic (ROC) curve method was used to compare the discriminative ability of candidate variables in predicting 1 and 2-year mortality, with the area under the ROC curve (AUROC) being used to rank the prognostic models based on their predictive accuracy. Statistical analyses were performed using SPSS package version 11.5 5 (SPSS Inc., Chicago, IL, USA). R statistical package was used for c-index analysis [21].

ACKNOWLEDGMENTS

This work was presented orally at EASL 2015 International Liver Meeting and awarded a Young Investigator Award to DJP.

FUNDING

No specific funding was obtained to support the conduction of this study.

CONFLICTS OF INTEREST

The authors have no conflicts of interest to disclose.

Authors contribution

Study concept and design: DJP, RS.
Acquisition of data: DJP, TA, PIS, JWJ, CS, GG, YWK, MK, MP, MP, PT.
Analysis and interpretation of data: DJP, EA, MP, RS.
Drafting of the manuscript: DJP, EA, RS.
Critical revision of the manuscript for important intellectual content: DJP, TA, EA, JWJ, CS, YWK, MK, PIS, MP, RS.
Statistical analysis: DJP, EA, MP.
Administrative, technical, or material support: MP, MK, JWJ.
Study supervision: DJP, JWJ, MK, MP, RS.

REFERENCES

1. Llovet JM, Bru C, Bruix J. Prognosis of hepatocellular carcinoma: the BCLC staging classification. Semin Liver Dis. 1999; 19:329-338.
2. Farinati F, Vanin V, Giacomin A, Pozzan C, Cillo U, Vitale A, Nolfo AM, Poggio PD, Benvegnu L, Rapaccini G, Zoli M, Borzio F, Giannini EG, Caturelli E, Trevisani F and The Italian Liver Cancer g. BCLC-B hepatocellular carcinoma and transcatheter arterial chemoembolization: a 20-year survey by the Italian Liver Cancer group. Liver Int. 2015; 35:223-231.
3. Forner A, Gilabert M, Bruix J, Raoul JL. Treatment of intermediate-stage hepatocellular carcinoma. Nat Rev Clin Oncol. 2014; 11:525-535.
4. Guo Z, Zhong JH, Jiang JH, Zhang J, Xiang BD, Li LQ. Comparison of Survival of Patients with BCLC Stage A Hepatocellular Carcinoma After Hepatic Resection or Transarterial Chemoembolization: A Propensity Score-Based Analysis. Ann Surg Oncol. 2014; 21:3069-3076.
5. Zhao Y, Cai G, Zhou L, Liu L, Qi X, Bai M, Li Y, Fan D, Han G. Transarterial chemoembolization in hepatocellular carcinoma with vascular invasion or extrahepatic metastasis: A systematic review. Asia Pac J Clin Oncol. 2013; 9:357-364.
6. Dufour JF, Bargellini I, De Maria N, De Simone P, Goulis I, Marinho RT. Intermediate hepatocellular carcinoma: current treatments and future perspectives. Ann Oncol. 2013; 24 Suppl 2:ii24-29.
7. Bolondi L, Burroughs A, Dufour JF, Galle PR, Mazzaferro V, Piscaglia F, Raoul JL, Sangro B. Heterogeneity of patients with intermediate (BCLC B) Hepatocellular Carcinoma: proposal for a subclassification to facilitate treatment decisions. Semin Liver Dis. 2012; 32:348-359.
8. Heng-Jun G, Yao-Jun Z, Min-Shan C, Mei-Xian C, Jun-Ting H, Li X, Lau WY. Rationality and effectiveness of

transarterial chemoembolization as an initial treatment for BCLC B stage HBV-related hepatocellular carcinoma. Liver Int. 2014; 34:612-620.

9. Pinato DJ, Sharma R. An inflammation-based prognostic index predicts survival advantage after transarterial chemoembolization in hepatocellular carcinoma. Transl Res. 2012; 160:146-152.
10. Hucke F, Sieghart W, Pinter M, Graziadei I, Vogel W, Muller C, Heinzl H, Waneck F, Trauner M, Peck-Radosavljevic M. The ART-strategy: Sequential assessment of the ART score predicts outcome of patients with hepatocellular carcinoma re-treated with TACE. J Hepatol. 2014; 60:118-126.
11. Kadalayil L, Benini R, Pallan L, O'Beirne J, Marelli L, Yu D, Hackshaw A, Fox R, Johnson P, Burroughs AK, Palmer DH, Meyer T. A simple prognostic scoring system for patients receiving transarterial embolisation for hepatocellular cancer. Ann Oncol. 2013; 24:2565-2570.
12. Sieghart W, Hucke F, Pinter M, Graziadei I, Vogel W, Muller C, Heinzl H, Trauner M, Peck-Radosavljevic M. The ART of decision making: retreatment with transarterial chemoembolization in patients with hepatocellular carcinoma. Hepatology. 2013; 57:2261-2273.
13. Hucke F, Sieghart W, Pinter M, Graziadei I, Vogel W, Muller C, Heinzl H, Waneck F, Trauner M, Peck-Radosavljevic M. The ART-strategy: sequential assessment of the ART score predicts outcome of patients with hepatocellular carcinoma re-treated with TACE. J Hepatol. 2014; 60:118-126.
14. Kudo M, Arizumi T, Ueshima K. Assessment for retreatment (ART) score for repeated transarterial chemoembolization in patients with hepatocellular carcinoma. Hepatology. 2014; 59:2424-2425.
15. Terzi E, Terenzi L, Venerandi L, Croci L, Renzulli M, Mosconi C, Allegretti G, Granito A, Golfieri R, Bolondi L, Piscaglia F. The ART score is not effective to select patients for transarterial chemoembolization retreatment in an Italian series. Digestive diseases. 2014; 32:711-716.
16. Leoni S, Piscaglia F, Golfieri R, Camaggi V, Vidili G, Pini P, Bolondi L. The impact of vascular and nonvascular findings on the noninvasive diagnosis of small hepatocellular carcinoma based on the EASL and AASLD criteria. Am J Gastroenterol. 2010; 105:599-609.
17. A new prognostic system for hepatocellular carcinoma: a retrospective study of 435 patients: the Cancer of the Liver Italian Program (CLIP) investigators. Hepatology. 1998; 28:751-755.
18. Lencioni R, Llovet JM. Modified RECIST (mRECIST) assessment for hepatocellular carcinoma. Semin Liver Dis. 2010; 30:52-60.
19. Jang JW, Kwon JH, You CR, Kim JD, Woo HY, Bae SH, Choi JY, Yoon SK, Chung KW. Risk of HBV reactivation according to viral status and treatment intensity in patients with hepatocellular carcinoma. Antivir Ther. 2011; 16:969-977.
20. Harrell FE. (2010). rms: Regression Modeling Strategies.
21. Team RC. (2013). R: A language and environment for statistical computing. (Vienna, Austria: R Foundation for Statistical Computing).
22. Pinato DJ, Stebbing J, Ishizuka M, Khan SA, Wasan HS, North BV, Kubota K, Sharma R. A novel and validated prognostic index in hepatocellular carcinoma: the inflammation based index (IBI). J Hepatol. 2012; 57:1013-1020.
23. Sangro B. [Survival benefit with intraarterial techniques in hepatocellular carcinoma]. Gastroenterol Hepatol. 2014; 37 Suppl 2:95-101.
24. Hsu C, Shen YC, Cheng CC, Hu FC, Cheng AL. Geographic difference in survival outcome for advanced hepatocellular carcinoma: implications on future clinical trial design. Contemp Clin Trials. 2010; 31:55-61.
25. Arizumi T, Ueshima K, Iwanishi M, Minami T, Chishina H, Kono M, Takita M, Kitai S, Inoue T, Yada N, Hagiwara S, Ida H, Minami Y, Sakurai T, Nishida N, Kitano M, et al. Evaluation of ART Scores for Repeated Transarterial Chemoembolization in Japanese Patients with Hepatocellular Carcinoma. Oncology. 2015; 89 Suppl 2:4-10.
26. Yang HJ, Lee JH, Lee DH, Yu SJ, Kim YJ, Yoon JH, Kim HC, Lee JM, Chung JW, Yi NJ, Lee KW, Suh KS, Lee HS. Small single-nodule hepatocellular carcinoma: comparison of transarterial chemoembolization, radiofrequency ablation, and hepatic resection by using inverse probability weighting. Radiology. 2014; 271:909-918.
27. Adhoute X, Penaranda G, Naude S, Raoul JL, Perrier H, Bayle O, Monnet O, Beaurain P, Bazin C, Pol B, Folgoc GL, Castellani P, Bronowicki JP, Bourliere M. Retreatment with TACE: The ABCR SCORE, an aid to the decision-making process. J Hepatol. 2015; 62:855-862.
28. Kudo M, Matsui O, Izumi N, Kadoya M, Okusaka T, Miyayama S, Yamakado K, Tsuchiya K, Ueshima K, Hiraoka A, Ikeda M, Ogasawara S, Yamashita T, Minami T. Transarterial Chemoembolization Failure/Refractoriness: JSH-LCSGJ Criteria 2014 Update. Oncology. 2014; 87 Suppl 1:22-31.
29. Pinato DJ, Arizumi T, Allara E, Jang JW, Smirne C, Kim YW, Kudo M, Pirisi M, Sharma R. Validation of the Hepatoma Arterial Embolization Prognostic Score in European and Asian Populations and Proposed Modification. Clin Gastroenterol Hepatol. 2015; 13:1204-1208.e2.
30. Takayasu K, Arii S, Kudo M, Ichida T, Matsui O, Izumi N, Matsuyama Y, Sakamoto M, Nakashima O, Ku Y, Kokudo N, Makuuchi M. Superselective transarterial chemoembolization for hepatocellular carcinoma. Validation of treatment algorithm proposed by Japanese guidelines. J Hepatol. 2012; 56:886-892.

Factors predicting through-the-scope gastroduodenal stenting outcomes in patients with gastric outlet obstruction: a large multicenter retrospective study in West Japan

Kentaro Yamao, MD,[1] Masayuki Kitano, MD, PhD,[1] Takahisa Kayahara, MD, PhD,[2] Etsuji Ishida, MD,[2] Hiroshi Yamamoto, MD, PhD,[2] Kosuke Minaga, MD,[3] Yukitaka Yamashita, MD, PhD,[3] Jun Nakajima, MD,[4] Masanori Asada, MD, PhD,[4] Yoshihiro Okabe, MD,[4] Yukio Osaki, MD, PhD,[4] Yasutaka Chiba, PhD,[5] Hajime Imai, MD,[1] Masatoshi Kudo, MD, PhD[1]

Osaka-sayama, Kurashiki, Wakayama, Osaka, Japan

Background and Aims: Endoscopic gastroduodenal stenting for malignant gastric outlet obstruction recently has become more effective, but the factors that predict gastroduodenal stenting outcomes are poorly defined. This multicenter retrospective cohort study evaluated the clinical outcomes of gastroduodenal stenting in malignant gastroduodenal obstruction and identified factors predicting clinical ineffectiveness, stent dysfunction, and adverse events.

Methods: All consecutive patients with malignant gastroduodenal obstruction who underwent through-the-scope gastroduodenal stenting from 2009 to 2014 at 4 tertiary-care medical centers were identified. Clinically ineffective stenting was defined as symptom recurrence and a gastric outlet obstruction scoring system (GOOSS) score <2.

Results: Of the 278 patients (mean age ± standard deviation [SD] 71.7 ± 11.4 years), 121 (43.5%) and 87 (31.3%) had pancreatic and gastric cancer, respectively. Technical success was achieved in 277 patients (99.6%). GOOSS scores rose from 0.5 ± 0.6 to 2.6 ± 0.8. Stenting was ineffective in 32 patients (12.6%). Stent dysfunction that caused symptom recurrence during follow-up developed in 46 patients (16.6%). Adverse events occurred in 49 patients (17.7%). Three or more stenosis sites (odds ratio [OR] = 6.11; $P < .01$) and Karnofsky performance scores ≤50 (OR = 6.63; $P < .01$) predicted clinical ineffectiveness. Karnofsky performance scores ≤50 predicted stent dysfunction (hazard ratio [HR] = 3.63; $P < .01$). Bile duct stenosis (HR = 9.55; $P = .02$) and liver metastasis (HR = 9.42; $P < .01$) predicted stent overgrowth. Covered stent predicted stent migration (HR = 12.63; $P < .01$). Deployment of 2 stents predicted perforation (HR = 854.88; $P < .01$).

Conclusions: Through-the-scope gastroduodenal stenting tended to be ineffective in patients with poor performance status and long stenosis sites. Stent dysfunction occurred more frequently in patients with poorer performance status. Deployment of 2 stents was a risk factor for perforation. Identification of these risk variables may help yield better gastroduodenal stenting outcomes. (Gastrointest Endosc 2016;84:757-63.)

Patients with gastric or pancreatobiliary cancer sometimes develop gastric outlet obstruction (GOO) because of gastric or duodenal stenosis. Considering this systemic condition and its poor prognosis, it is better to treat unresectable cases of GOO with minimally invasive methods. In the past, the standard minimally invasive treatment for malignant duodenal obstruction was gastrojejunostomy (GJ). However, endoscopic gastroduodenal stenting for

Abbreviations: CI, confidence interval; GJ, gastrojejunostomy; GOO, gastric outlet obstruction; GOOSS, Gastric Outlet Obstruction Scoring System; HR, hazard ratio; KPS, Karnofsky performance status; OR, odds ratios.

DISCLOSURE: *The present study was supported by grants from the Japan Society for the Promotion of Science. All authors disclosed no financial relationships relevant to this article.*

0016-5107/$36.00
http://dx.doi.org/10.1016/j.gie.2016.03.1498

Received August 25, 2015. Accepted March 26, 2016.

Current affiliations: Department of Gastroenterology and Hepatology, Kinki University School of Medicine, Osaka-sayama (1), Department of Gastroenterology and Hepatology, Kurashiki Central Hospital, Okayama (2), Department of Gastroenterology, Japanese Red Cross Wakayama Medical Center, Wakayama (3), Department of Gastroenterology and Hepatology, Osaka Red Cross Hospital, Osaka (4), Clinical Research Center, Kinki University Hospital, Osaka-sayama, Japan (5).

Reprint requests: Masayuki Kitano, MD, PhD, Department of Gastroenterology and Hepatology, Kinki University School of Medicine, 377-2 Ohnohigashi, Osaka-sayama, 589-8511 Japan.

malignant GOO recently has become more effective, safer, and less expensive than GJ; it also has better short-term outcomes than GJ, particularly a shorter hospital stay and a more rapid return to oral intake.[1-4] The technical and clinical success rates of endoscopic gastroduodenal stenting by using the recently developed through-the-scope stent have been reported to be 95.5% to 100% and 82.3% to 91.0%, respectively.[5-8] However, through-the-scope gastroduodenal stenting is still ineffective in some patients, and stent dysfunction and adverse events can occur for various reasons.

Despite the many studies on the clinical efficacy of through-the-scope gastroduodenal stenting, the factors that predict poor stent efficacy, stent dysfunction, and adverse events are relatively poorly understood.[9-14] The purpose of the present retrospective multicenter cohort study was to evaluate the clinical outcomes of through-the-scope gastroduodenal stenting in malignant gastroduodenal obstruction and to identify factors that predict clinical ineffectiveness, stent dysfunction, and adverse events.

MATERIALS AND METHODS

This multicenter, retrospective clinical study was approved by the institutional ethics committees of the 4 hospitals, and all patients gave written informed consent.

Patients

All consecutive patients who underwent through-the-scope gastroduodenal stenting for malignant GOO between March 2009 and March 2014 at 4 tertiary-care medical centers (Kinki University, Kurashiki Central Hospital, Japanese Red Cross Wakayama Medical Center, and Osaka Red Cross Hospital) were identified by searching the medical databases of the 4 centers. Patients were included in the study if (1) they had undergone endoscopic gastroduodenal stenting with through-the-scope stents, (2) they had documented, unresectable malignant cancers, and (3) they had obstruction of the stomach or duodenum or jejunum that was causing nausea, vomiting, dysphagia, and oral intake difficulties. Patients were excluded if (1) there was clinical evidence of perforation or peritonitis, (2) intestinal roentgenography with contrast medium revealed multiple small bowel obstructions, and (3) the patient had undergone upper GI reconstruction surgery.

Equipment and procedure

Three through-the-scope self-expandable metal stent models ranging from 18 to 22 mm in diameter and from 6 to 12 cm in length were used: the Wall-Flex duodenal stent, uncovered type (Boston Scientific Japan, Tokyo, Japan), the Niti-S ComVi pyloric stent, covered type, and the Niti-S D pyloric and/or duodenal stent, uncovered type (both from Taewoong Medical, Seoul, South Korea). All stents were deployed under endoscopic and fluoroscopic guidance. Patients were sedated with intravenous midazolam and/or propofol.

For gastroduodenal stenting, a therapeutic endoscope with a 3.7-mm or 4.2-mm channel caliber that was either forward-viewing or side-viewing (GIF 1T-240, 2T-240, TJF 240, 260; Olympus Medical Systems, Tokyo, Japan) was used to place the through-the-scope stents. An ERCP catheter with a biliary guidewire was used. Thus, the endoscope was first allowed to come close to the gastric or duodenal stenosis site, after which a guidewire equipped with a catheter was passed through the stenosis site. It was then passed through the digestive tract as far as possible away from the site of stenosis. The distal or proximal lumen of the stenosis site was captured, and after confirming the position and length of the stenosis site, we determined the appropriate length and position of the stent. Thereafter, while we considered the shortening of the stent after extension, the duodenal stent was placed under endoscopic and fluoroscopic guidance.

Follow-up

If the duodenal stent was placed without any immediate adverse events, the patient could start clear fluid intake 1 to 5 days after stenting. An abdominal radiograph was performed 1 to 3 days after intervention to check the expansion and location of the stent. If, after receiving clear fluids, the patient showed no GOO symptoms, no stent dislocation, and sufficient stent expansion, the patient could start a semi-solid diet. Recurrence of GOO was diagnosed if the patient presented with appetite loss, nausea, and vomiting and if the stenosis was confirmed by imaging with endoscopic, radiographic, and/or CT examinations.

Outcome measurements and definitions

The primary aim was to identify factors that predicted the following stenting outcomes: clinical ineffectiveness, stent dysfunction, and adverse events. The secondary aims were to evaluate the technical success, procedure time, oral intake status, patient survival time, and duration of stent patency. Technical success was defined as adequate placement of the self-expandable metal stent across the stenosis, as confirmed by a combination of endoscopy and fluoroscopy. The degree of dysphagia was assessed before and after stent placement by using an adaptation of the gastric outlet obstruction scoring system (GOOSS),[15] in which swallowing ability is divided into 4 categories: 0, no oral intake; 1, liquids only; 2, soft solids; and 3, low-residue or full diet. Stenting was deemed to be clinically effective if, 7 days after stenting, the patient achieved a GOOSS score of $\geq$2 and/or relief of gastric outlet obstruction symptoms. Stenting was deemed to be ineffective when the GOOSS scores were <2 and relief from gastric outlet obstruction symptoms was not observed 7 days after stenting. Stent patency was defined

as the period between initial stent placement and recurrence of obstructive symptoms due to stent dysfunction. In calculating stent patency, patients were censored if they did not exhibit cessation of stent patency during their lifetimes. A stent was deemed to be dysfunctional when the patient showed a return of GOO symptoms, and the stent was found by imaging to be ingrown, overgrown, kinked, collapsed, broken, dislocated, or food impacted. Early and late adverse events were defined as those occurring within 7 days and later than 7 days after stenting, respectively.

The following factors were evaluated for their ability to predict clinical ineffectiveness, stent dysfunction that caused recurrence of obstruction, and adverse events: age, sex, diagnosis (pancreatic cancer, gastric cancer, or intrinsic disease), main organ of obstruction (stomach or duodenum), number of stenosis sites, GOOSS score before stenting, Karnofsky performance status (KPS),[16] presence of bile duct stenosis, liver metastasis, ascites, use of a covered or uncovered stent, number of stents used to cover a stenosis at the first treatment, and use of chemotherapy after stenting. A stenosis was considered to be intrinsic when the diagnosis was gastric, duodenal, or ampullary cancer and to be extrinsic when the diagnosis was pancreatic, bile duct, or gallbladder cancer, or another cancer. The stenosis sites were divided into 8 sites: gastric body, angle, antrum, bulb, and second, third, and fourth portion of the duodenum and jejunum, and the number of sites to which stenosis extended was measured.

All patients were followed-up to assess symptom resolution until study termination (October 2014) or patient death. When patients could not be followed-up directly for specific reasons, such as a move to another area, their families or personal physicians were contacted by telephone.

Statistical analysis

Continuous variables were expressed as means ± standard deviation (SD). Categoric data were expressed as n (%). Cumulative stent patency and survival were evaluated by using Kaplan-Meier analysis. A logistic regression model was applied to explore factors that were associated independently with clinical ineffectiveness. Odds ratios (ORs) and 95% confidence intervals (CIs) were reported. A Cox proportional hazards model was applied to explore prognostic factors that were associated independently with time until obstruction recurrence caused by overall stent dysfunction or, specifically, stent ingrowth, stent overgrowth, or stent migration. A Cox proportional hazards model also was applied to explore predictive factors for time until overall adverse events or, specifically, jaundice, bleeding, or perforation. Hazard ratios (HRs) and the 95% CIs were reported. All statistical analyses were performed by using SPSS Statistics version 19 (SPSS, Chicago, Ill). P values $< .05$ were considered to indicate statistical significance.

RESULTS

In total, 304 patients who underwent through-the-scope gastroduodenal stenting for malignant gastroduodenal obstruction during the study period were identified. Of these, 26 were excluded because there was clinical evidence of perforation (n = 1), there was evidence of multiple small-bowel obstructions on intestinal roentgenography (n = 5), or the patient had undergone upper GI reconstruction surgery (n = 20). As a result, 278 patients formed the study cohort.

Patient characteristics

The demographic and clinical characteristics of the 278 patients are shown in Table 1. Their mean age (± SD) was 71.7 ± 11.4 years. The etiology of the gastroduodenal obstruction was pancreatic cancer (n = 121, 43.5%), gastric cancer (n = 87, 31.3%), bile duct cancer (n = 22, 8.0%), lymph node metastasis from another cancer site (n = 13, 4.7%), duodenal cancer (n = 12, 4.3%), and gallbladder cancer (n = 12, 4.3%). The preoperative GOOSS scores were 0, 1, and 2 in 156 (56.1%), 100 (36.0%), and 22 (7.9%) patients, respectively. The average GOOSS score was 0.5 ± 0.6. The KPS score was ≥60 and ≤50 in 220 (79.1%) and 58 (20.9%) patients, respectively.

Technical success and clinical effectiveness of stenting

The mean follow-up time was 124.1 ± 165.6 days. Technical success was achieved in 277 of the 278 patients (99.6%). The single case of technical failure occurred because the guidewire could not pass through the obstructed areas because of the severity of the stricture. Clinical effectiveness (GOOSS score ≥2 and/or relief of gastric outlet symptoms 7 days after stenting) was achieved in 242 of the 277 technically successful patients (87.4%). In the remaining 35 patients, stenting was ineffective in 32 (11.7%), and 3 patients (1.1%) died within 7 days of stenting. The mean procedure time was 23.1 ± 11.8 minutes. The mean times from stenting to resumption of oral fluids and resumption of solids were 2.8 ± 1.7 and 4.2 ± 2.9 days, respectively. The GOOSS scores improved from 0.5 ± 0.6 before stenting to 2.6 ± 0.8 (change in GOOSS scores: 2.0 ± 1.0). Median patient survival was 88 days. Median stent patency was 242 days. In total, 266 and 11 patients needed 1 and 2 stents, respectively, to cover the whole length of the stenosis in the same session.

Stent dysfunction and adverse event rates

Stent dysfunction and other adverse events are shown in Table 2. Stent dysfunction occurred in 46 patients (16.6%): of these, 16 (5.8%) had stent ingrowth,

TABLE 1. Preoperative patient demographics and clinical characteristics (n = 278)

Age, mean ± SD, y	71.7 ± 11.4
Sex, no. (%)	
Male	163 (58.6)
Female	115 (41.4)
Tumor diagnosis, no. (%)	
Pancreatic cancer	121 (43.5)
Gastric cancer	87 (31.3)
Bile duct cancer	22 (8.0)
Lymph node metastasis from a cancer at another site	13 (4.7)
Duodenal cancer	12 (4.3)
Gallbladder cancer	12 (4.3)
Ampullary cancer	5 (1.8)
Other	6 (2.2)
Main site of stenosis, no. (%)	
Stomach	89 (32.0)
Body	1 (0.4)
Angle	28 (10.1)
Antrum	60 (21.6)
Duodenum	189 (68.0)
D1 (bulb)	63 (22.7)
D2 (2nd portion)	76 (27.3)
D3 (3rd portion)	41 (14.7)
D4 (4th portion)	9 (3.2)
Jejunum	0 (0)
GOOSS, no. (%)	
0	156 (56.1)
1	100 (36.0)
2	22 (7.9)
GOOSS, mean ± SD	0.5 ± 0.6
Karnofsky performance score,[16] no. (%)	
≤50%	58 (20.9)
≥60%	220 (79.1)

SD, Standard deviation; *D,* duodenum; *GOOSS,* Gastric Outlet Obstruction Scoring System.

11 (4.0%) had stent overgrowth, 11 (4.0%) had stent migration, and the remaining 8 (2.8%) had food impaction, stent kinking, collapse, or breakage. Forty-nine patients had adverse events that did not relate to stent dysfunction. Of these, 28 and 21 had early and late adverse events, respectively. The early adverse events consisted largely of jaundice (n = 17, 6.1%). The remaining early adverse events were hyperamylasemia (n = 3, 1.1%), aspiration pneumonia (n = 3, 1.1%), pancreatitis (n = 2, 0.7%), bleeding (n = 2, 0.7%), and perforation (n = 1, 0.4%). The late adverse events all consisted of bleeding (n = 9, 3.2%), jaundice (n = 7, 2.5%), and perforation (n = 5, 1.8%).

Predictive factors for clinical ineffectiveness

The 274 patients in whom stent placement was technically successful, and who survived past the first 7 days of stenting, were divided into 2 groups according to clinical efficacy. Thus, there were 242 and 32 patients in the clinically effective and ineffective groups, respectively. A multiple logistic regression model was applied to explore factors that predicted clinical ineffectiveness (Table 3). Three or more stenosis sites (OR 6.11; 95% CI, 2.16-17.30; $P < .01$) and KPS ≤50 (OR 6.63; 95% CI, 2.89-15.20; $P < .01$) predicted clinical ineffectiveness significantly.

Predictive factors for stent dysfunction that caused obstruction recurrence

The 277 patients in whom stent placement was technically successful were divided according to whether stent dysfunction caused a recurrence of obstruction (Supplemental Table 1, available online at www.giejournal.org). A Cox proportional hazards model revealed that KPS ≤50 (HR 3.63; 95% CI, 1.55-8.50; $P < .01$) was the only significant predictive factor for time until stent dysfunction. The same model was then applied to explore predictive factors for time until obstruction recurrence due to specific types of stent dysfunction, namely, stent ingrowth, overgrowth, and migration (Supplemental Tables 2 to 4, available online at www.giejournal.org). Predictive factors for stent ingrowth were not found. However, bile duct stenosis (HR 9.55; 95% CI, 1.46-62.68; $P = .02$) and liver metastases (HR 9.42; 95% CI, 2.11-41.95; $P < .01$) were predictive of time until stent overgrowth. Covered stent (HR 12.63; 95% CI, 2.35-67.80; $P < .01$) was the only significant predictive factor for time until stent migration.

Predictive factors for adverse events

The 277 patients in whom stent placement was technically successful were divided according to whether they developed an adverse event (n = 49) or not (n = 228). A Cox proportional hazards model revealed that use of uncovered stents (HR for covered stents = 0.27; 95% CI, 0.10-0.69; $P < .01$) and lack of chemotherapy after stenting (HR for chemotherapy after stenting = 0.42; 95% CI, 0.19-0.95; $P = .04$) predicted adverse events (Supplemental Table 5, available online at www.giejournal.org). A similar analysis searching for predictive factors for specific adverse events, namely, perforation, bleeding, and jaundice, revealed that deployment of 2 stents in the same session (HR 854.88; 95% CI, 11.36-64356.6; $P < .01$) was predictive of perforation (Supplemental Table 6, available online at www.giejournal.org). There were no significant predictive factors for bleeding and jaundice (data not shown).

DISCUSSION

This multicenter retrospective study was performed to identify factors that predicted the clinical outcomes of

TABLE 2. Stent dysfunction and other adverse events (n = 277)

Stent adverse event	Early period* no. (%)	Late period† no. (%)	Total no. (%)
Stent dysfunction	5 (1.8)	41 (14.8)	46 (16.6)
Stent ingrowth	1 (0.4)	15 (5.4)	16 (5.8)
Stent overgrowth	0 (0)	11 (4.0)	11 (4.0)
Stent migration	2 (0.7)	9 (3.2)	11 (4.0)
Food impaction	0 (0)	3 (1.1)	3 (1.1)
Kinking	1 (0.4)	1 (0.4)	2 (0.7)
Stent collapse	1 (0.4)	1 (0.4)	2 (0.7)
Stent breakage	0 (0)	1 (0.4)	1 (0.4)
Other adverse event	28 (10.1)	21 (7.6)	49 (17.7)
Jaundice	17 (6.1)	7 (2.5)	24 (8.7)
Bleeding	2 (0.7)	9 (3.2)	11 (4.0)
Perforation	1 (0.4)	5 (1.8)	6 (2.2)
Hyperamylasemia	3 (1.1)	0 (0)	3 (1.1)
Aspiration pneumonia	3 (1.1)	0 (0)	3 (1.1)
Pancreatitis	2 (0.7)	0 (0)	2 (0.7)

*Within 1 week after stenting.
†Later than 1 week after stenting.

through-the-scope gastroduodenal stenting for malignant gastroduodenal obstruction. The rate of clinical ineffectiveness after stenting was 11.7% (32/274), and the predictive factors for clinical ineffectiveness were KPS ≤50 ($P < .01$) and 3 or more stenosis sites ($P < .01$). The rate of stent dysfunction during follow-up was 16.6% (46/277), and stent dysfunction was predicted by KPS ≤50 ($P < .01$). The adverse event rate was 17.7% (49/277), and the use of an uncovered stent ($P < .01$) and lack of chemotherapy ($P = .04$) predicted adverse events.

The factors that predict the clinical ineffectiveness of through-the-scope gastroduodenal stenting are relatively poorly understood. Sato et al[12] proposed that KPS ≤50, peritoneal dissemination, and ascites were significant predictive factors of clinical ineffectiveness. Sasaki et al[11] also found that KPS ≤50 and ascites were risk factors for restricted solid oral intake. We found that KPS ≤50, but not ascites, predicted clinical ineffectiveness. Note that Mendelsohn et al[5] argued that ascites should not be a contraindication to duodenal stenting, because the clinical success of this procedure in patients with carcinomatosis was 81%. The apparent discrepancy between our study and those of Sato et al[12] and Sasaki et al[11] in terms of the predictive value of ascites probably reflects the different indications for gastroduodenal stenting. The previous studies did not confirm stenosis at the anal side of the small intestine by imaging with intestinal roentgenography with contrast medium. By contrast, in our study, we used intestinal roentgenography before stenting to confirm passage through the small intestine. If the contrast medium collected in the small intestine, we did not perform gastroduodenal stenting. In the case of peritonitis carcinomatosis, clinical ineffectiveness may result from not only ascites, but from poor motility or stenosis of the small intestine.

The present study is the first to show that a large number of stenosis sites (which indicates a long invasive area) significantly predicted the clinical ineffectiveness of gastroduodenal stenting. This result suggests that poor motility of the stomach and/or duodenum, caused by a long invasive area, may worsen GOO.[17,18]

The present study showed that the rate of overall stent dysfunction during follow-up was 16.6% (46/277). A closer examination of the causes of stent dysfunction revealed that the rates of stent ingrowth, overgrowth, and migration were 5.8% (16/277), 4.0% (11/277), and 4.0% (11/277), respectively.

Uncovered stents did not predict stent ingrowth, but covered stents did predict stent migration ($P < .01$). Several recent studies compared the clinical outcomes of covered and uncovered duodenal stents for the palliation of GOO.[6-9,14,19,20] A prospective randomized study comparing uncovered and covered stents showed that the uncovered group had more frequent stent ingrowth (18.0% vs 3.4%; $P = .02$), equally frequent stent overgrowth (3.4% vs 3.3%; $P = .99$), and less frequent stent migration (0% vs 13.6%; $P < .01$).[21] A similar prospective randomized study also showed that the uncovered group had more frequent tumor ingrowth (25.0% vs 0%; $P < .01$) and less frequent stent migration within 8 weeks (25.8% vs 2.8%; $P < .01$).[19] Similarly, the retrospective cohort study of Waidmann et al showed that the uncovered and covered groups were similar in terms of stent overgrowth rates (19% vs 13%; $P = .73$) and that all stent migrations were observed in the covered group (0% vs 56%; $P < .01$).[22] However, they did not detect any tumor ingrowth in either group (0% vs 0%). Thus, in all reports, including ours, stent migration occurred more frequently with covered stents than with uncovered stents; however, whether stent ingrowth relates to the use of uncovered stents remains unclear. Discrepancies between the studies on this issue may reflect differences in terms of stent materials or patient selection. Further large multicenter prospective studies that compare uncovered and covered self-expandable metal stents are warranted.

The present study also showed that bile duct stenosis and liver metastases predicted stent overgrowth in the present study. This reflects the close correlation between tumor progression and these 2 factors.

The present study also showed that the rate of perforation after stenting was 2.2% (6/277) and that the single predictive factor for perforation was deployment of 2 stents in the same session ($P < .01$). Little is known about perforation associated with gastroduodenal stenting. However, 2 studies reported the risk factors for perforation after colon stenting: the meta-analysis of Van Halsema et al[23] suggested that colon perforation can be predicted by the use

TABLE 3. Multivariable analysis of factors associated with clinical ineffectiveness (n = 274)*

	Effective (n = 242)	Ineffective (n = 32)	*P* value	OR	95% CI
Age, ≥71, y	154	15	.37	0.69	0.30-1.55
Sex, no.					
Male	146	20	.33	1.54	0.65-3.64
Female	96	12			
Diagnosis, no.					
Pancreatic cancer	112	7	.08	0.38	0.13-1.11
Gastric cancer	71	15	.82	1.12	0.44-2.86
Intrinsic disease†	88	15	.15	1.84	0.80-4.24
Main organ of obstruction, no.					
Stomach	74	13	.76	1.18	0.41-3.43
Duodenum	168	19			
≥3 stenosis sites, no.	20	11	< .01	6.11	2.16-17.30
GOOSS score of 0, no.	134	20	.35	1.47	0.66-3.26
KPS ≤50, no.	38	17	< .01	6.63	2.89-15.20
Bile duct stenosis, no.	111	18	.16	1.86	0.78-4.46
Liver metastasis, no.	70	9	.98	1.01	0.43-2.38
Ascites, no.	77	12	.46	1.34	0.61-2.93
Covered stent, no.	67	10	.74	1.15	0.51-2.59
Deployment of 2 stents, no.	6	4	.05	3.84	0.99-14.95
Chemotherapy after stenting, no.	79	0	.12	0.01	0.01-5.12

OR, Odds ratio; *CI,* confidence interval; *GOOSS,* Gastric Outlet Obstructive Scoring System; *KPS,* Karnofsky performance status[16].
*Excluding the 3 patients who died within 1 week of stenting.
†Gastric cancer, duodenal cancer, and ampullary cancer.

of stents with high axial force, a benign etiology, and bevacizumab treatment, whereas the subsequent retrospective cohort analysis of Boyle et al[24] reported that longer stenosis predicts colon perforation. The possibility that perforation is more likely to occur when the stent has high axial force and the stenosis is long is supported by our study on gastroduodenal stents, which showed deployment of 2 stents increased the risk of perforation. Deployment of 2 stents may increase the axial force of the stent compared with when just 1 stent is placed: the force is likely to be particularly strengthened by overlapped placement. In addition, 2 stents are needed in cases of long stenosis. Thus, regardless of the GI organ undergoing stenting, these observations together suggest that higher axial force and longer stenosis may promote perforation. This in turn suggests that deploying 2 stents should be avoided.

A major concern of patients with advanced digestive cancer is the maintenance of oral intake, because it is important for quality of life. GJ also is indicated in cases of stenosis at anal sites from the antrum because anastomosis is created at the gastric body. Oral intake improves more rapidly after gastroduodenal stent placement than after GJ, and stenting is less invasive; therefore, gastroduodenal stenting is increasingly becoming the first choice for GOO. This preference is bolstered by the fact that the 2 procedures do not differ in terms of technical and clinical success or the incidence of early adverse events. However, compared with GJ, gastroduodenal stenting is associated with a shorter time to late adverse events, recurrent obstructive symptoms, and reintervention.[2] The current study is consistent with the other studies that show duodenal stenting is safe (namely, it has a low incidence of major adverse events), there is a rapid progression of diet, and the hospital stay is relatively short.[3,4,25,26] However, given that we found that longer stenosis promotes the risk of gastroduodenal stenting ineffectiveness, GJ may be more suitable for cases with longer stenosis, particularly at anal sites from the antrum.

This study has 2 limitations. First, our study had a nonrandomized and retrospective design, which inherently decreases the statistical power of the study. Second, several different types of stents were used. To best identify the factors that predict gastroduodenal stent efficacy, dysfunction, and adverse events, a large, prospective, randomized controlled study on the same stent is needed.

In conclusion, we showed that several factors influence the clinical outcomes of gastroduodenal stenting. In particular, gastroduodenal stenting tended to be ineffective in patients with poor performance status and long stenosis sites, stent dysfunction occurred more frequently in patients with poorer performance status, and deployment

of 2 stents was a risk factor for perforation. The identification of these predictive factors may help to generate better gastroduodenal stenting outcomes.

REFERENCES

1. Jeurnink SM, Steyerberg EW, van Hooft JE, et al. Surgical gastrojejunostomy or endoscopic stent placement for the palliation of malignant gastric outlet obstruction (SUSTENT study): a multicenter randomized trial. Gastrointest Endosc 2010;71:490-9.
2. Jeurnink SM, Steyerberg EW, Hof G, et al. Gastrojejunostomy versus stent placement in patients with malignant gastric outlet obstruction: a comparison in 95 patients. J Surg Oncol 2007;96:389-96.
3. Chandrasegaram MD, Eslick GD, Mansfield CO, et al. Endoscopic stenting versus operative gastrojejunostomy for malignant gastric outlet obstruction. Surg Endosc 2012;26:323-9.
4. Mehta S, Hindmarsh A, Cheong E, et al. Prospective randomized trial of laparoscopic gastrojejunostomy versus duodenal stenting for malignant gastric outflow obstruction. Surg Endosc 2006;20:239-42.
5. Mendelsohn RB, Gerdes H, Markowitz AJ, et al. Carcinomatosis is not a contraindication to enteral stenting in selected patients with malignant gastric outlet obstruction. Gastrointest Endosc 2011;73:1135-40.
6. Costamagna G, Tringali A, Spicak J, et al. Treatment of malignant gastroduodenal obstruction with a nitinol self-expanding metal stent: an international prospective multicentre registry. Dig Liver Dis 2012;44:37-43.
7. Isayama H, Sasaki T, Nakai Y, et al. Management of malignant gastric outlet obstruction with a modified triple-layer covered metal stent. Gastrointest Endosc 2012;75:757-63.
8. Maetani I, Mizumoto Y, Shigoka H, et al. Placement of a triple-layered covered versus uncovered metallic stent for palliation of malignant gastric outlet obstruction: a multicenter randomized trial. Dig Endosc 2014;26:192-9.
9. Jang JK, Song HY, Kim JH, et al. Tumor overgrowth after expandable metallic stent placement: experience in 583 patients with malignant gastroduodenal obstruction. AJR Am J Roentgenol 2011;196:W831-6.
10. Cho YK, Kim SW, Hur WH, et al. Clinical outcomes of self-expandable metal stent and prognostic factors for stent patency in gastric outlet obstruction caused by gastric cancer. Dig Dis Sci 2010;55:668-74.
11. Sasaki T, Isayama H, Nakai Y, et al. Predictive factors of solid food intake in patients with malignant gastric outlet obstruction receiving self-expandable metallic stents for palliation. Dig Endosc 2012;24:226-30.
12. Sato T, Hara K, Mizuno N, et al. Gastroduodenal stenting with Niti-S stent: Long-term benefits and additional stent intervention. Dig Endosc 2015;27:121-9.
13. Canena JM, Lagos AC, Marques IN, et al. Oral intake throughout the patients' lives after palliative metallic stent placement for malignant gastroduodenal obstruction: a retrospective multicentre study. Eur J Gastroenterol Hepatol 2012;24:747-55.
14. Kim JH, Song HY, Shin JH, et al. Metallic stent placement in the palliative treatment of malignant gastroduodenal obstructions: prospective evaluation of results and factors influencing outcome in 213 patients. Gastrointest Endosc 2007;66:256-64.
15. Adler DG, Baron TH. Endoscopic palliation of malignant gastric outlet obstruction using self-expanding metal stents: experience in 36 patients. Am J Gastroenterol 2002;97:72-8.
16. Karnofsky DA, Burchenal JH. The clinical evaluation of chemotherapeutic agents in cancer. Evaluation of chemotherapeutic agents. New York, NY: Columbia University Press; 1949. p. 191-205.
17. Wilmer A, Andrioli A, Coremans G, et al. Ambulatory small intestional manometry. Detailed compalison of duodenal and jejunal motor activity in healty man. Dig Dis Sci 1997;42:1618-27.
18. Bortolotti M, Annese A, Coccia G. Twenty-four hour ambulatory antroduodenal manometry in normal subjects (co-operative study). Neurogastroenterol Motil 2000;12:231-8.
19. Kim CG, Choi IJ, Lee JY, et al. Covered versus uncovered self-expandable metallic stents for palliation of malignant pyloric obstruction in gastric cancer patients: a randomized, prospective study. Gastrointest Endosc 2010;72:25-32.
20. Seo EH, Jung MK, Park MJ, et al. Covered expandable nitinol stents for malignant gastroduodenal obstructions. J Gastroenterol Hepatol 2008;23:1056-62.
21. Lim SG, Kim JH, Lee KM, et al. Conformable covered versus uncovered self-expandable metallic stents for palliation of malignant gastroduodenal obstruction: a randomized prospective study. Dig Liver Dis 2014;46:603-8.
22. Waidmann O, Trojan J, Friedrich-Rust M, et al. SEMS vs cSEMS in duodenal and small bowel obstruction: high risk of migration in the covered stent group. World J Gastroenterol 2013;19:6199-206.
23. van Halsema EE, van Hooft JE, Small AJ, et al. Perforation in colorectal stenting: a meta-analysis and a search for risk factors. Gastrointest Endosc 2014;79:970-82.e7; quiz 83.e2, 83.e5.
24. Boyle DJ, Thorn C, Saini A, et al. Predictive factors for successful colonic stenting in acute large-bowel obstruction: a 15-year cohort analysis. Dis Colon Rectum 2015;58:358-62.
25. Maetani I, Akatsuka S, Ikeda M, et al. Self-expandable metallic stent placement for palliation in gastric outlet obstructions caused by gastric cancer: a comparison with surgical gastrojejunostomy. J Gastroenterol 2005;40:932-7.
26. Rudolph HU, Post S, Schluter M, et al. Malignant gastroduodenal obstruction: retrospective comparison of endoscopic and surgical palliative therapy. Scand J Gastroenterol 2011;46:583-90.

SUPPLEMENTAL TABLE 1. Multivariable analysis of factors associated with stent dysfunction (n = 277)

	No dysfunction (n = 231)	Stent dysfunction (n = 46)	*P* value	HR	95% CI
Age, y, ≥71, no.	120	18	.10	0.56	0.28-1.12
Sex					
Male	136	32	.24	1.52	0.76-3.04
Female	95	14			
Diagnosis					
Pancreatic cancer	101	19	.55	0.76	0.31-1.86
Gastric cancer	72	15	.48	0.49	0.07-3.55
Intrinsic disease*	85	19	.68	1.30	0.37-4.54
Main organ of obstruction					
Stomach	72	16	.33	2.45	0.41-14.69
Duodenum	159	30			
≥3 stenosis sites	27	4	.39	0.60	0.19-1.89
GOOSS score of 0	126	30	.59	1.20	0.62-2.31
KPS ≤50	48	10	< .01	3.63	1.55-8.50
Bile duct stenosis	110	21	.44	1.34	0.64-2.81
Liver metastasis	66	14	.73	1.13	0.57-2.25
Ascites	79	11	.49	0.78	0.39-1.57
Covered stent	62	16	.20	1.54	0.80-2.95
Deployment of 2 stents	11	0	> .99	<0.01	N/A
Chemotherapy after stenting	57	22	.66	1.18	0.56-2.46

HR, Hazard ratio; *CI,* confidence interval; *GOOSS,* Gastric Outlet Obstructive Scoring System; *KPS,* Karnofsky performance status[16].
*Gastric cancer, duodenal cancer, and ampullary cancer.

SUPPLEMENTAL TABLE 2. Multivariable analysis of factors associated with stent ingrowth (n = 277)

	No ingrowth (n = 261)	Ingrowth (n = 16)	*P* value	HR	95% CI
Age, y, ≥71, no.	132	6	.33	0.54	0.15-1.87
Sex					
Male	161	7	.15	0.45	0.15-1.33
Female	100	9			
Diagnosis					
Pancreatic cancer	115	5	.71	0.72	0.12-4.21
Gastric cancer	80	7	.85	1.32	0.08-22.41
Intrinsic disease*	95	9	.56	1.90	0.22-16.45
Main organ of obstruction					
Stomach	81	7	.60	0.47	0.03-7.46
Duodenum	180	9			
≥3 stenosis sites	29	2	.79	1.27	0.22-7.24
GOOSS score of 0	146	10	.63	0.76	0.26-2.29
KPS ≤50	54	4	.09	3.45	0.83-14.41
Bile duct stenosis	127	4	.43	0.57	0.14-2.35
Liver metastasis	77	3	.93	0.94	0.24-3.68
Ascites	87	3	.86	0.89	0.23-3.37
Covered stent	77	1	.06	0.13	0.02-1.05
Deployment of 2 stents	11	0	> .99	<0.01	N/A
Chemotherapy after stenting	72	7	.89	1.10	0.30-3.99

HR, Hazard ratio; *CI,* confidence interval; *GOOSS,* Gastric Outlet Obstructive Scoring System; *KPS,* Karnofsky performance status[16].
*Gastric cancer, duodenal cancer, and ampullary cancer.

SUPPLEMENTAL TABLE 3. Multivariable analysis of factors associated with stent overgrowth (n = 277)

	No overgrowth (n = 266)	Overgrowth (n = 11)	*P* value	HR	95% CI
Age, y, ≥71, no.	134	4	.69	0.76	0.19-3.03
Sex					
Male	159	9	.30	2.51	0.43-14.58
Female	107	2			
Diagnosis					
Pancreatic cancer	116	4	.09	0.14	0.01-1.34
Gastric cancer	83	4	.84	1.68	0.01-247.90
Intrinsic disease*	99	5	.83	1.33	0.10-18.64
Main organ of obstruction					
Stomach	84	4	.66	3.67	0.01-1198.04
Duodenum	182	7			
≥3 stenosis sites	29	2	.81	1.28	0.16-10.13
GOOSS score of 0	147	9	.30	2.54	0.44-14.76
KPS ≤50	56	2	.22	3.58	0.74-26.95
Bile duct stenosis	124	7	.02	9.55	1.46-62.68
Liver metastasis	73	7	< .01	9.42	2.11-41.95
Ascites	86	4	.38	1.88	0.46-7.74
Covered stent	74	4	.49	1.63	0.41-6.48
Deployment of 2 stents	11	0	> .99	<0.01	N/A
Chemotherapy after stenting	74	5	.72	1.36	0.26-7.11

HR, Hazard ratio; *CI,* confidence interval; *GOOSS,* Gastric Outlet Obstructive Scoring System; *KPS,* Karnofsky performance status[16].
*Gastric cancer, duodenal cancer, and ampullary cancer.

SUPPLEMENTAL TABLE 4. Multivariable analysis of factors associated with stent migration (n = 277)

	No migration (n = 266)	Migration (n = 11)	*P* value	HR	95% CI
Age, y, ≥71, no.	133	5	.78	1.26	0.25-6.26
Sex					
Male	159	9	.24	2.90	0.49-17.16
Female	107	2			
Diagnosis					
Pancreatic cancer	113	7	.44	2.54	0.24-26.76
Gastric cancer	85	2	.70	3.35	0.01-1586.32
Intrinsic disease*	101	3	.95	1.10	0.05-22.62
Main organ of obstruction					
Stomach	86	2	.88	1.63	0.01-763.35
Duodenum	180	9			
≥3 stenosis sites	31	0	> .99	<0.01	N/A
GOOSS score of 0	151	5	.80	0.82	0.18-3.83
KPS ≤50	56	2	.89	0.86	0.10-7.33
Bile duct stenosis	125	6	.92	0.92	0.16-5.42
Liver metastasis	77	3	.22	0.36	0.07-1.86
Ascites	88	2	.31	0.41	0.08-2.26
Covered stent	69	9	< .01	12.63	2.35-67.80
Deployment of 2 stents	11	0	> .99	<0.01	N/A
Chemotherapy after stenting	73	6	.81	1.24	0.23-6.69

HR, Hazard ratio; *CI,* confidence interval; *GOOSS,* Gastric Outlet Obstructive Scoring System; *KPS,* Karnofsky performance status[16].
*Gastric cancer, duodenal cancer, and ampullary cancer.

SUPPLEMENTAL TABLE 5. Multivariable analysis of factors associated with adverse events (n = 277)

	No adverse events (n = 228)	Adverse event (n = 49)	*P* value	HR	95% CI
Age, y, ≥71, no.	109	29	.54	1.21	0.65-2.25
Sex					
Male	136	32	.14	1.60	0.86-3.01
Female	92	17			
Diagnosis					
Pancreatic cancer	94	26	.47	1.35	0.59-3.10
Gastric cancer	78	9	.48	0.50	0.07-3.49
Intrinsic disease*	91	13	> .99	0.99	0.28-3.46
Main organ of obstruction					
Stomach	78	10	.82	0.82	0.15-4.38
Duodenum	150	39			
≥3 stenosis sites	24	7	.21	1.88	0.70-5.09
GOOSS score of 0	133	23	.29	0.72	0.39-1.33
KPS ≤50	47	11	.49	1.31	0.61-2.77
Bile duct stenosis	105	26	.71	0.88	0.46-1.70
Liver metastasis	68	12	.90	1.05	0.51-2.13
Ascites	73	17	.63	1.16	0.63-2.15
Covered stent	72	6	< .01	0.27	0.10-0.69
Deployment of 2 stents	7	4	.28	2.03	0.57-7.28
Chemotherapy after stenting	70	9	.04	0.42	0.19-0.95

HR, Hazard ratio; *CI,* confidence interval; *GOOSS,* Gastric Outlet Obstructive Scoring System; *KPS,* Karnofsky performance status[16].
*Gastric cancer, duodenal cancer, and ampullary cancer.

SUPPLEMENTAL TABLE 6. Multivariable analysis of factors associated with perforation (n = 277)

	No perforation (n = 271)	Perforation (n = 6)	*P* value	HR	95% CI
Age, y, ≥71, no.	135	3	.53	2.41	0.16-37.57
Sex					
Male	165	3	> .99	1.00	0.14-7.93
Female	106	3			
Diagnosis					
Pancreatic cancer	116	4	.23	5.91	0.32-109.14
Gastric cancer	86	1	.99	3837361.00	N/A
Intrinsic disease*	103	1	.99	<0.01	N/A
Main organ of obstruction					
Stomach	87	1	.42	0.01	0-482.86
Duodenum	184	5			
≥3 stenosis sites	30	1	.55	5.43	0.02-2.92
GOOSS score of 0	154	2	.12	0.11	0.01-1.86
KPS ≤50	56	2	.08	18.87	0.68-520.31
Bile duct stenosis	129	2	.05	0.03	0.01-1.08
Liver metastasis	78	2	.05	17.74	0.92-341.32
Ascites	88	2	.98	1.04	0.09-11.95
Covered stent	76	2	.35	0.25	0.01-4.58
Deployment of 2 stents	9	2	< .01	854.88	11.36-64356.6
Chemotherapy after stenting	77	2	.82	1.39	0.08-23.74

HR, Hazard ratio; *CI,* confidence interval; *GOOSS,* Gastric Outlet Obstructive Scoring System; *KPS,* Karnofsky performance status[16].
*Gastric cancer, duodenal cancer, and ampullary cancer.

Research Paper

Second-line ramucirumab therapy for advanced hepatocellular carcinoma (REACH): an East Asian and non-East Asian subgroup analysis

Joon Oh Park[1], Baek-Yeol Ryoo[2], Chia-Jui Yen[3], Masatoshi Kudo[4], Ling Yang[5], Paolo B. Abada[6], Rebecca Cheng[7], Mauro Orlando[8], Andrew X. Zhu[9], Takuji Okusaka[10]

[1]Samsung Medical Center, Sungkyunkwan University School of Medicine, Seoul, Republic of Korea

[2]Asan Medical Center, University of Ulsan College of Medicine, Seoul, Republic of Korea

[3]National Cheng Kung University Hospital, Tainan City, Taiwan

[4]Kinki University School of Medicine, Osaka-Sayama City, Osaka, Japan

[5]Eli Lilly and Company, Bridgewater, NJ, USA

[6]Eli Lilly and Company, Indianapolis, IN, USA

[7]Eli Lilly and Company, Taipei, Taiwan

[8]Eli Lilly and Company, Buenos Aires, Argentina

[9]Massachusetts General Hospital Cancer Center, Harvard Medical School, Boston, MA, USA

[10]National Cancer Center Hospital, Tokyo, Japan

Correspondence to: Joon Oh Park, **email:** oncopark@skku.edu

Keywords: *Asians, alpha-fetoprotein, clinical trial, liver neoplasms, vascular endothelial growth factor receptor-2*

Received: *May 23, 2016* ***Accepted:*** *October 10, 2016* ***Published:*** *October 20, 2016*

ABSTRACT

Purpose: REACH investigated second-line ramucirumab therapy for advanced hepatocellular carcinoma.

Results: Median overall survival was 8.2 months for ramucirumab and 6.9 months for placebo (HR, 0.835; 95% CI, 0.634–1.100; *p* = 0.2046) for East Asians, and 10.1 months for ramucirumab and 8.0 months for placebo (HR, 0.895; 95% CI, 0.690–1.161; *p* = 0.4023) for non-East Asians. Median overall survival in patients with baseline alpha-fetoprotein ≥ 400 ng/mL was 7.8 months for ramucirumab and 4.2 months for placebo (HR, 0.749; 95% CI, 0.519–1.082; *p* = 0.1213) for East Asians (*n* = 139), and 8.2 months for ramucirumab and 4.5 months for placebo (HR, 0.579; 95% CI, 0.371–0.904; *p* = 0.0149) for non-East Asians (*n* = 111). The most common grade ≥ 3 treatment-emergent adverse events in East Asians and non-East Asians included hypertension and malignant neoplasm progression.

Materials and methods: A post-hoc analysis of East Asians (*N* = 252) and non-East Asians (*N* = 313) in the intent-to-treat population was performed.

Conclusions: In East Asians and non-East Asians, ramucirumab did not significantly prolong overall survival. In patients with baseline alpha-fetoprotein ≥ 400 ng/mL, a potentially larger survival benefit was observed in both subgroups. Safety for East Asians was similar to non-East Asians.

INTRODUCTION

Among cancer deaths, liver cancer is the second most common cause [1]. Hepatocellular carcinoma represents approximately 70% to 90% of primary liver cancers [1, 2]. The incidence rates of liver cancer are highest in East Asian (EA) countries [1]. Intermediate rates occur in Southern Europe and Northern America, and the lowest rates occur in Northern Europe [1]. In general, EA patients have a poorer prognosis than non-EA patients. In the Asia-Pacific study of sorafenib versus placebo in EA patients, median overall survival (OS) in both treatment arms was shorter than the median OS in either arm of the SHARP study of sorafenib versus placebo in a global

cohort of patients [3, 4]. Nonetheless, the relative hazard ratios for survival benefits were similar [3, 4]. Survival was also shorter for EA patients compared to non-EA patients in the GIDEON non-interventional study [5]. The reasons for the shorter survivals in EA patients remain unclear, but may include differences in tumor-related factors or patient characteristics. The most common cause of liver cancer in EA patients is hepatitis B virus infection, which is prevalent in this region, whereas hepatitis C virus or alcohol use are the most common causes of liver cancer in non-EA patients [6]. Disease management can also vary across regions [7], and EA patients are more likely to present at a more advanced stage of the disease [8, 9].

Vascular endothelial growth factor (VEGF) and VEGF receptor-2 (VEGFR-2)-mediated signaling are important in the proliferation of hepatocellular carcinoma tumors [10–13]. Ramucirumab, a recombinant human IgG1 monoclonal antibody, binds with high affinity and specificity to the extracellular domain of VEGFR-2, preventing angiogenesis via VEGF- and VEGFR-2-mediated signaling [14]. Ramucirumab in patients with advanced hepatocellular carcinoma as a second-line treatment following first-line therapy with sorafenib did not demonstrate a significant OS improvement over best supportive care (primary endpoint) in the phase III REACH trial [15]. However, improvements in progression-free survival (PFS) and response rate were observed [15]. In a pre-specified subgroup analysis of patients with a baseline alpha-fetoprotein (AFP) ≥ 400 ng/mL, ramucirumab treated patients had improved OS compared to placebo-treated patients [15].

A post-hoc subgroup analysis of the REACH trial was performed in advanced hepatocellular carcinoma EA and non-EA patients following first-line therapy with sorafenib to explore safety and efficacy of ramucirumab treatment in these patient populations.

RESULTS

Patients

Figure 1 shows the CONSORT diagram for EA and non-EA patients. A total of 252 EA patients were randomized to receive ramucirumab (N = 126) or placebo (N = 126); 313 non-EA patients were randomized to receive ramucirumab (N = 157) or placebo (N = 156).

Baseline patient and disease characteristics for EA and non-EA patients were generally well balanced between treatment arms (Table 1). Differences between EA and non-EA patients were observed for age, Eastern Cooperative Oncology Group performance status (ECOG PS), etiology of liver disease, primary tumor present, presence of extra-hepatic spread, Barcelona Clinic Liver Cancer stage, baseline AFP, prior systemic therapy, and reasons for discontinuation of prior sorafenib therapy. Most differences were consistent with EA patients having a worse prognosis compared to non-EA patients.

Efficacy

In EA patients, median OS for ramucirumab-treated patients was 8.2 months and 6.9 months for placebo-treated patients (stratified HR, 0.835; 95% CI, 0.634–1.100; p = 0.2046) (Figure 2). Median PFS was 2.2 months for the ramucirumab arm and 1.5 months for the placebo arm (stratified HR, 0.721; 95% CI, 0.555–0.937; p = 0.0141) (Figure 2). The objective response rate (ORR) was 5.6% (95% CI, 2.7–11.0) for the ramucirumab arm and 0.8% (95% CI, 0.1–4.4) for placebo arm (p = 0.0298) (Table 2). The disease control rate (DCR) was 47.6% for the ramucirumab arm and 42.1% for the placebo arm (p = 0.3568).

In non-EA patients, median OS for ramucirumab-treated patients was 10.1 months and 8.0 months for placebo-treated patients (stratified HR, 0.895; 95% CI, 0.690–1.161; p = 0.4023) (Figure 2). Median PFS was 4.5 months for the ramucirumab arm and 2.7 months for the placebo arm (stratified HR, 0.549; 95% CI, 0.427–0.706; p < 0.0001) (Figure 2). The ORR was 8.3% (95% CI, 4.9–13.7) for the ramucirumab arm and 0.6% (95% CI, 0.1–3.5) for the placebo arm (p = 0.0012) (Table 2). The DCR was 63.1% for the ramucirumab arm and 48.7% for the placebo arm (p = 0.0096) (Table 2).

In EA patients with AFP ≥400 ng/mL (n = 139), median OS for the ramucirumab arm (n = 66) was 7.8 months and 4.2 months for the placebo arm (n = 73) (HR, 0.749; 95% CI, 0.519–1.082; p = 0.1213) (Figure 3). In non-EA patients with AFP ≥ 400 ng/mL (n = 111), median OS for ramucirumab-treated patients was 8.2 months (n = 53) and 4.5 months for placebo-treated patients (n = 58) (stratified HR, 0.579; 95% CI, 0.371–0.904; p = 0.0149) (Figure 3).

In EA patients with AFP < 400 ng/mL (n = 113), median OS for the ramucirumab arm (n = 60) was 9.0 months and 12.4 months for the placebo arm (n = 53) (HR, 1.083; 95% CI, 0.701–1.672; p = 0.7091) (Figure 3). In non-EA patients with AFP < 400 ng/mL (n = 197), median OS for ramucirumab–treated patients was 11.4 months (n = 100) and 11.6 months for placebo-treated patients (n = 97) (stratified HR, 1.099; 95% CI, 0.783–1.543; p = 0.5804) (Figure 3).

Post-discontinuation systemic anti-cancer therapies (PDT) were similar for ramucirumab and placebo-treated patients in both EA and non-EA subgroups; however, a higher percentage of EA patients received PDT than non-EA patients (EA: 37.3% for the ramucirumab arm vs. 38.1% for the placebo arm; non-EA: 20.4% for the ramucirumab arm vs. 26.9% for the placebo arm).

Safety

The EA safety population consisted of 123 patients in the ramucirumab arm and 123 patients in the placebo arm. The non-EA safety population consisted of 154 patients in the ramucirumab arm and 153 patients in the

Table 1: Baseline characteristics

	East Asian		Non-East Asian	
	Ramucirumab (*N* = 126)	Placebo (*N* = 126)	Ramucirumab (*N* = 157)	Placebo (*N* = 156)
Age, years				
Median (range)	61 (34–85)	59 (25–83)	66 (28–87)	64 (30–85)
< 65	80 (63.5)	83 (65.9)	70 (44.6)	79 (50.6)
≥ 65	46 (36.5)	43 (34.1)	87 (55.4)	77 (49.4)
Male	107 (84.9)	112 (88.9)	129 (82.2)	130 (83.3)
ECOG PS[a]				
0	63 (50.0)	63 (50.0)	96 (61.1)	90 (57.7)
1	63 (50.0)	63 (50.0)	61 (38.9)	66 (42.3)
Etiology of liver disease				
Hepatitis B	79 (62.7)	76 (60.3)	30 (19.1)	31 (19.9)
Hepatitis C	31 (24.6)	28 (22.2)	52 (33.1)	49 (31.4)
Significant alcohol use	10 (7.9)	13 (10.3)	49 (31.2)	50 (32.1)
Steatohepatitis (fatty liver)	3 (2.4)	4 (3.2)	16 (10.2)	16 (10.3)
Other	3 (2.4)	3 (2.4)	3 (1.9)	7 (4.5)
Unknown	10 (7.9)	8 (6.3)	30 (19.1)	26 (16.7)
Baseline Child-Pugh Class A	125 (99.2)	125 (99.2)	152 (96.8)	151 (96.8)
Primary tumor present	107 (84.9)	106 (84.1)	150 (95.5)	146 (93.6)
Macrovascular invasion present	40 (31.7)	37 (29.4)	42 (26.8)	42 (26.9)
Extrahepatic spread present	98 (77.8)	102 (81.0)	109 (69.4)	98 (62.8)
Baseline BCLC Stage				
Stage B	10 (7.9)	13 (10.3)	23 (14.6)	21 (13.5)
Stage C	116 (92.1)	113 (89.7)	134 (85.4)	135 (86.5)
Prior sorafenib therapy				
Sorafenib only	99 (78.6)	102 (81.0)	145 (92.4)	151 (96.8)
Sorafenib and other systemic therapy	27 (21.4)	24 (19.0)	12 (7.6)	5 (3.2)
Reason for discontinuation of sorafenib				
Progressive disease	116 (92.1)	112 (88.9)	130 (82.8)	127 (81.4)
Toxicity	10 (7.9)	14 (11.1)	27 (17.2)	29 (18.6)
Alpha fetoprotein				
< 400 ng/mL	60 (47.6)	53 (42.1)	100 (63.7)	97 (62.2)
≥ 400 ng/mL	66 (52.4)	73 (57.9)	53 (33.8)	58 (37.2)
Missing	0	0	4 (2.5)	1 (0.6)

Data are n (%) unless otherwise indicated. [a]Performance status evaluated according to guidelines of the Eastern Cooperative Oncology Group (ECOG), with a performance status (PS) of 0 indicating asymptomatic, 1 restricted in strenuous activity but ambulatory and able to do light work, or 2 ambulatory and capable of all self-care but unable to work. Abbreviations: BCLC = Barcelona Clinic Liver Cancer staging system; ECOG PS = Eastern Cooperative Oncology Group performance status.

placebo arm. The incidences of grade ≥ 3 treatment-emergent adverse events (TEAEs) were higher in the ramucirumab arm than the placebo arm for EA and non-EA patients (Tables 3 and 4). Any grade TEAEs occurring in at least 15% of patients and at a higher rate (at least 10% difference) in the ramucirumab arm than the placebo arm were peripheral edema, diarrhea, headache, thrombocytopenia, proteinuria, hypertension, hypoalbuminemia, and epistaxis for EA patients (Table 3), and peripheral edema, ascites, asthenia, hypertension, headache, and thrombocytopenia for non-EA patients (Table 4). Grade ≥ 3 TEAEs that occurred in at least 5%

Table 2: Best overall response

	East Asian		Non-East Asian	
	Ramucirumab (*N* = 126)	Placebo (*N* = 126)	Ramucirumab (*N* = 157)	Placebo (*N* = 156)
Best overall response				
Complete response	0	0	1 (0.6)	0
Partial response	7 (5.6)	1 (0.8)	12 (7.6)	1 (0.6)
Stable disease	53 (42.1)	52 (41.3)	86 (54.8)	75 (48.1)
Progressive disease	57 (45.2)	62 (49.2)	40 (25.5)	67 (42.9)
Not evaluable or assessed	9 (7.1)	11 (8.7)	18 (11.5)	13 (8.3)
Objective response rate	7 (5.6)	1 (0.8)	13 (8.3)	1 (0.6)
95% CI	2.7–11.0	0.1–4.4	4.9–13.7	0.1–3.5
p-value	0.0298		0.0012	
Disease control rate[a]	60 (47.6)	53 (42.1)	99 (63.1)	76 (48.7)
95% CI	39.1–56.3	33.8–50.8	55.3–70.2	41.0–56.5
p-value	0.3568		0.0096	

Data are *n* (%) unless otherwise indicated. [a]Denotes best response for complete response, partial response, or stable disease. Abbreviation: CI = confidence interval.

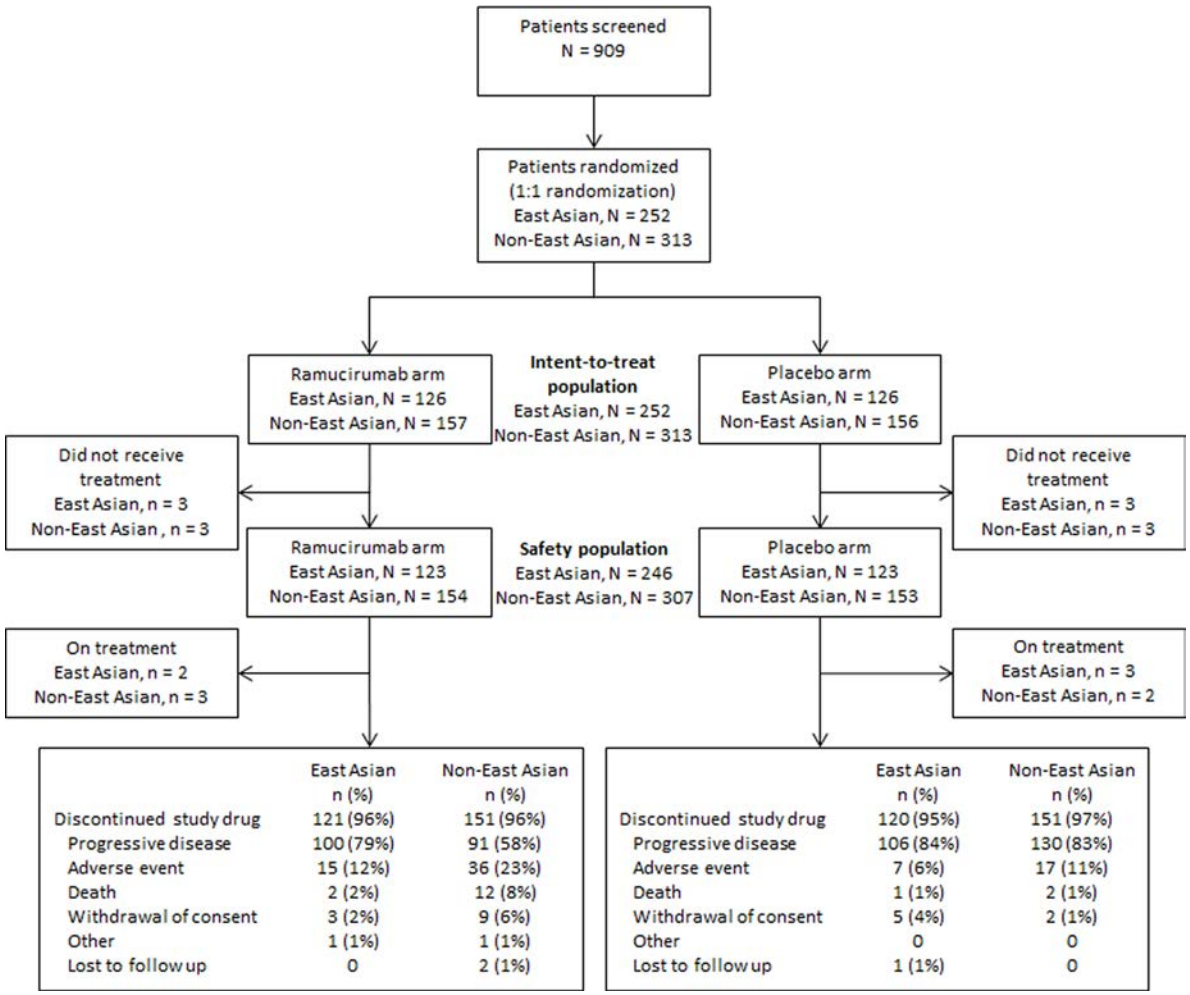

Figure 1: Trial profile for East Asian and non-East Asian patients.

Table 3: Adverse events in East Asian patients

	East Asian			
	Ramucirumab (*N* = 123)		Placebo (*N* = 123)	
	Any Grade	Grade ≥ 3	Any Grade	Grade ≥ 3
Treatment-emergent adverse events				
Any	119 (96.7)	64 (52.0)	110 (89.4)	48 (39.0)
Peripheral edema	41 (33.3)	0	15 (12.2)	0
Fatigue	28 (22.8)	2 (1.6)	20 (16.3)	4 (3.3)
Decreased appetite	26 (21.1)	2 (1.6)	26 (21.1)	0
Diarrhea	26 (21.1)	0	7 (5.7)	0
Headache	25 (20.3)	1 (0.8)	3 (2.4)	0
Ascites	24 (19.5)	4 (3.3)	14 (11.4)	4 (3.3)
Thrombocytopenia	24 (19.5)	5 (4.1)	6 (4.9)	0
Proteinuria	23 (18.7)	4 (3.3)	11 (8.9)	0
Pyrexia	22 (17.9)	0	14 (11.4)	0
Hypertension	21 (17.1)	8 (6.5)	8 (6.5)	1 (0.8)
Hypoalbuminemia	19 (15.4)	2 (1.6)	6 (4.9)	0
AAT increase	18 (14.6)	8 (6.5)	20 (16.3)	15 (12.2)
Epistaxis	18 (14.6)	0	5 (4.1)	0
Adverse events of special interest				
Liver injury/failure[a]	59 (48.0)	23 (18.7)	38 (30.9)	24 (19.5)
Bleeding/hemorrhage[a]	38 (30.9)	6 (4.9)	17 (13.8)	8 (6.5)
Gastrointestinal hemorrhage[b]	10 (8.1)	4 (3.3)	7 (5.7)	5 (4.1)
Pulmonary hemorrhage[b]	4 (3.3)	0	2 (1.6)	1 (0.8)
Hepatic hemorrhage[b]	1 (0.8)	1 (0.8)	2 (1.6)	2 (1.6)
Proteinuria[a]	24 (19.5)	4 (3.3)	11 (8.9)	0
Hypertension[a]	22 (17.9)	9 (7.3)	8 (6.5)	1 (0.8)
Renal failure[a]	10 (8.1)	2 (1.6)	6 (4.9)	0
Infusion-related reaction[a]	4 (3.3)	0	1 (0.8)	0
Arterial thromboembolic events[a]	1 (0.8)	0	2 (1.6)	1 (0.8)
Venous thromboembolic events[a]	1 (0.8)	0	1 (0.8)	1 (0.8)

Data are *n* (%). Only treatment-emergent adverse events in ≥ 15% of patients in the ramucirumab arm in East Asian patients are reported. A patient was only counted once for each category. Missing grades are counted in 'Any Grade'. Adverse events were coded using MedDRA version 16.1. [a]Pooled adverse event terms. [b]Pooled adverse event category comprising synonymous MedDRA preferred terms. Abbreviation: AAT = aspartate aminotransferase.

of patients and at a higher rate in the ramucirumab arm than the placebo arm were hypertension and malignant neoplasm progression for EA patients (Table 3; data not shown for malignant neoplasm progression), and hypertension, asthenia, ascites, general physical health deterioration, thrombocytopenia, and malignant neoplasm progression for non-EA patients (Table 4; data not shown for general physical health deterioration and malignant neoplasm progression).

The incidences of adverse events of special interest (AESIs) are shown in Tables 3 and 4 for EA and non-EA patients, respectively. Any grade AESIs that were more common (at least 10% difference) in the ramucirumab arm than the placebo arm were liver injury/failure, bleeding/hemorrhage, proteinuria, and hypertension for EA patients (Table 3), and liver injury/failure, hypertension, and proteinuria for non-EA patients (Table 4). Grade ≥ 3 AESIs that occurred at a higher rate in the ramucirumab arm than the placebo arm were hypertension, proteinuria, and renal failure for EA patients (Table 3), and hypertension, renal failure, infusion-related reaction, and proteinuria for non-EA patients (Table 4).

Table 4: Adverse events in non-East Asian patients

	Non-East Asian			
	Ramucirumab (*N* = 154)		Placebo (*N* = 153)	
	Any Grade	Grade ≥ 3	Any Grade	Grade ≥ 3
Treatment-emergent adverse events				
Any	151 (98.1)	108 (70.1)	150 (98.0)	84 (54.9)
Peripheral edema	60 (39.0)	1 (0.6)	35 (22.9)	1 (0.7)
Ascites	50 (32.5)	9 (5.8)	26 (17.0)	7 (4.6)
Asthenia	48 (31.2)	13 (8.4)	33 (21.6)	4 (2.6)
Fatigue	36 (23.4)	4 (2.6)	38 (24.8)	4 (2.6)
Nausea	36 (23.4)	0	31 (20.3)	0
Decreased appetite	35 (22.7)	3 (1.9)	24 (15.7)	2 (1.3)
Hypertension	34 (22.1)	26 (16.9)	12 (7.8)	9 (5.9)
Abdominal pain	32 (20.8)	4 (2.6)	42 (27.5)	10 (6.5)
Headache	28 (18.2)	1 (0.6)	12 (7.8)	0
Cough	27 (17.5)	1 (0.6)	14 (9.2)	0
Diarrhea	25 (16.2)	3 (1.9)	31 (20.3)	1 (0.7)
Pyrexia	24 (15.6)	1 (0.6)	12 (7.8)	1 (0.7)
Thrombocytopenia	24 (15.6)	8 (5.2)	6 (3.9)	1 (0.7)
Constipation	23 (14.9)	0	26 (17.0)	0
Adverse events of special interest				
Liver injury/failure[a]	81 (52.6)	35 (22.7)	65 (42.5)	41 (26.8)
Bleeding/hemorrhage[a]	52 (33.8)	11 (7.1)	38 (24.8)	13 (8.5)
Gastrointestinal hemorrhage[b]	15 (9.7)	7 (4.5)	16 (10.5)	12 (7.8)
Pulmonary hemorrhage[b]	5 (3.2)	1 (0.6)	2 (1.3)	1 (0.7)
Hepatic hemorrhage[b]	1 (0.6)	1 (0.6)	0	0
Hypertension[a]	34 (22.1)	26 (16.9)	12 (7.8)	9 (5.9)
Proteinuria[a]	24 (15.6)	2 (1.3)	2 (1.3)	0
Infusion-related reaction[a]	16 (10.4)	3 (1.9)	1 (0.7)	0
Renal failure[a]	10 (6.5)	4 (2.6)	12 (7.8)	3 (2.0)
Venous thromboembolic events[a]	5 (3.3)	2 (1.3)	3 (2.0)	3 (2.0)
Arterial thromboembolic events[a]	1 (0.6)	0	2 (1.3)	0
Congestive heart failure[a]	0	0	2 (1.3)	1 (0.7)
Healing complication[a]	0	0	1 (0.7)	0

Data are *n* (%). Only treatment-emergent adverse events in ≥ 15% of patients in the ramucirumab arm in non-East Asian patients are reported. A patient was only counted once for each category. Missing grades are counted in 'Any Grade'. Adverse events were coded using MedDRA version 16.1. [a]Pooled adverse event terms. [b]Pooled adverse event category comprising synonymous MedDRA preferred terms. Abbreviation: AAT = aspartate aminotransferase.

DISCUSSION

This subgroup analysis of REACH indicates that, while no significant OS benefit was shown in EA patients, there were improvements in PFS and ORR. Similar findings were noted in non-EA patients. Patients with AFP ≥400 ng/mL appeared to have a more favorable OS benefit in both the EA and non-EA groups, consistent with the findings in the overall intent-to-treat (ITT) population with AFP ≥ 400 ng/mL.

Overall, the survival benefit of ramucirumab was comparable in EA patients and non-EA patients, although EA patients had a shorter median OS compared with non-EA patients. A shorter median OS for EA patients versus non-EA patients was also observed in the SHARP and Asia-Pacific studies of sorafenib in hepatocellular

carcinoma [3, 4]. The shorter median OS for EA patients in REACH may partly be due to a higher prevalence of baseline characteristics associated with poor prognosis in EA patients compared to non-EA patients. For instance, EA patients in REACH had a higher incidence of hepatitis B infection, macrovascular invasion, extrahepatic spread, Barcelona Clinic Liver Cancer stage C, increased concentration of AFP, and poorer ECOG PS than non-EA patients. In addition, more EA patients were aged less than 65 years compared with non-EA patients. Notably, patients in the Asia-Pacific study were also reported to have a higher incidence of hepatitis B, extrahepatic spread, Barcelona Clinic Liver Cancer stage C, poorer ECOG PS, and younger age compared to patients enrolled in the SHARP study [3,4]. Post-discontinuation systemic anti-cancer therapy in REACH is unlikely to have contributed to the shorter OS in EA patients compared with non-EA patients given that a higher percentage of EA patients (38%) received PDT compared with non-EA patients (24%). Furthermore, no treatment has demonstrated a survival benefit to date in hepatocellular carcinoma after sorafenib treatment [15–18]. The improvement in PFS in EA patients was consistent with the improvement in non-EA patients, although PFS was shorter and the DCR was lower for EA patients than non-EA patients. The shorter PFS and DCR for EA patients may reflect the poorer prognosis and more rapidly progressive disease in the EA population. Despite known regional differences in the etiology and prognosis of hepatocellular carcinoma, ramucirumab demonstrated comparable survival efficacy in both EA and non-EA patients. These efficacy findings were similar to the overall REACH ITT population [15].

In patients with a baseline AFP ≥ 400 ng/mL, an improvement in OS was observed in both EA and non-EA patients treated with ramucirumab compared to placebo. This did not reach significance in the EA subgroup, likely due to the limitations of small sample size. Nonetheless, the difference in median OS was similar in the EA and non-EA subgroups and is generally consistent with the survival benefit observed in the overall ITT population with a baseline AFP ≥ 400 ng/mL in REACH [15]. This benefit was observed despite the overall poorer prognosis associated with EA patients compared to non-EA patients. We note that in the patients with baseline AFP ≥400 ng/mL, both EA and non-EA patients share a similar median OS in the placebo arm, which suggests that selection of

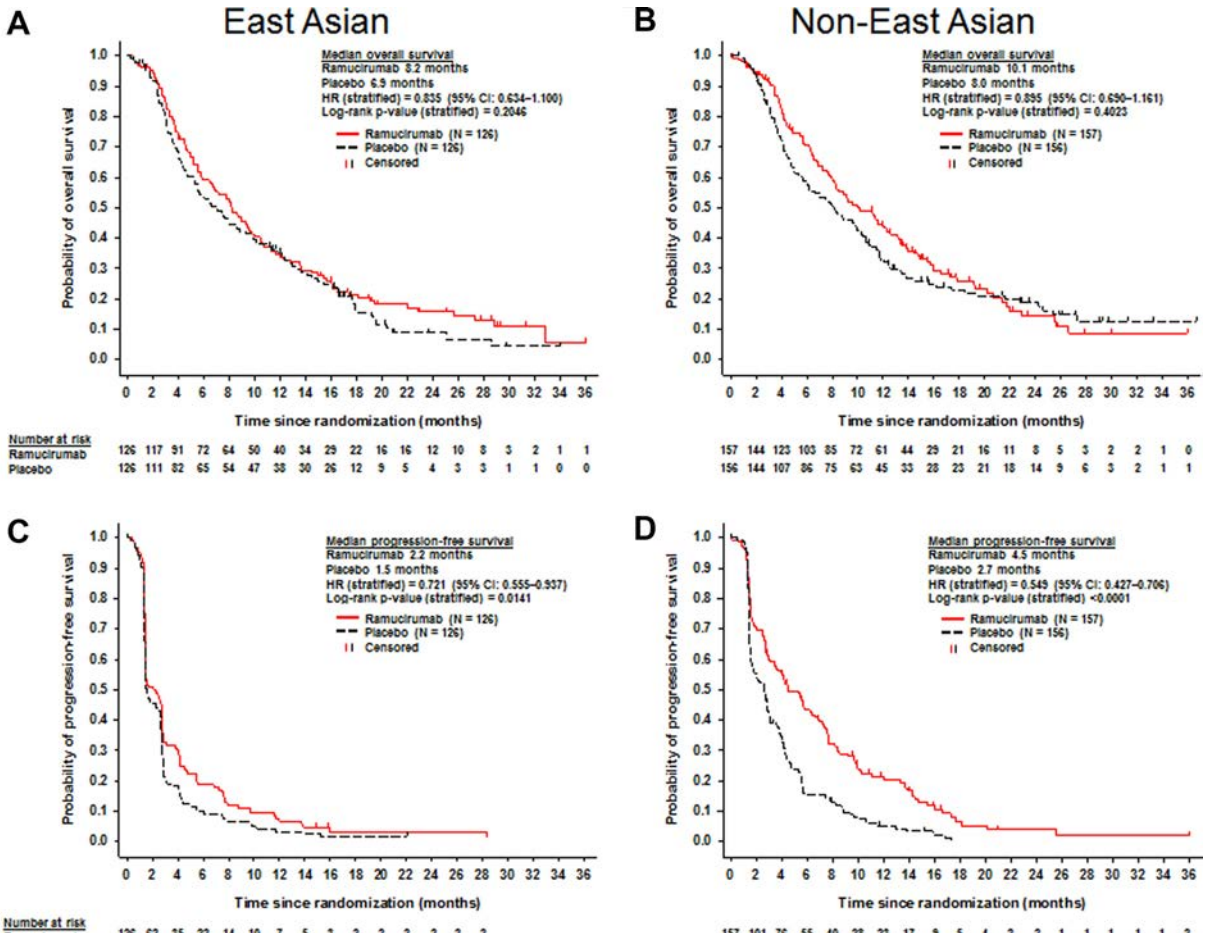

Figure 2: Kaplan-Meier plots of overall survival (A and B) and progression-free survival (C and D) for East Asian (A and C) and non-East Asian patients (B and D).

this subset of patients may normalize any differences in prognosis between regions. Consistent with the overall ITT population with baseline AFP < 400 ng/mL [15], no OS benefit was observed in EA or non-EA patients with ramucirumab treatment. The OS results from these subgroup analyses demonstrate that a baseline AFP ≥ 400 ng/mL may identify patients who are most likely to benefit from ramucirumab treatment, regardless of whether they are from EA or non-EA regions.

The efficacy benefits for EA and non-EA patients were achieved with an acceptable safety profile. The majority of AESIs were grade 1–2, and the grade ≥ 3 AESIs were generally comparable between EA and non-EA patients. The observed safety profiles for EA and non-EA patients were consistent with the underlying disease state and the overall ITT populations in trials of ramucirumab [15, 19, 20]. Liver injury and bleeding are of particular concern in patients with advanced hepatocellular carcinoma, who often have underlying cirrhosis. In both EA and non-EA patients, increases in the low grade AESIs of liver injury/failure and bleeding/hemorrhage were observed in the ramucirumab arms compared with the placebo arms, but an increase in higher grade events was not observed. Notably, no increased rate of high grade AESIs was observed in EA patients compared to non-EA patients, despite the prevalence of poor prognostic characteristics in the EA subgroup that might have put these patients at higher risk with ramucirumab treatment.

This subgroup analysis has a number of limitations including the fact that the study was not designed or powered to show significance in the EA and non-EA subgroups, which makes it difficult to make accurate inferences. Furthermore, this analysis was post-hoc and caution should be used when interpreting the results. Despite these limitations, the efficacy observations in the subgroups defined by an AFP < or ≥ 400 ng/mL have been very consistent, and therefore seem unlikely to be due to chance.

In this subgroup analysis of the REACH trial, ramucirumab generally demonstrated consistent efficacy across EA and non-EA regions. The data indicate that patients with baseline AFP ≥ 400 ng/mL may be deriving the majority of the benefit observed in both EA and non-EA patients. Ramucirumab was well tolerated in both EA and non-EA patients. Further evaluation of ramucirumab in patients with advanced hepatocellular

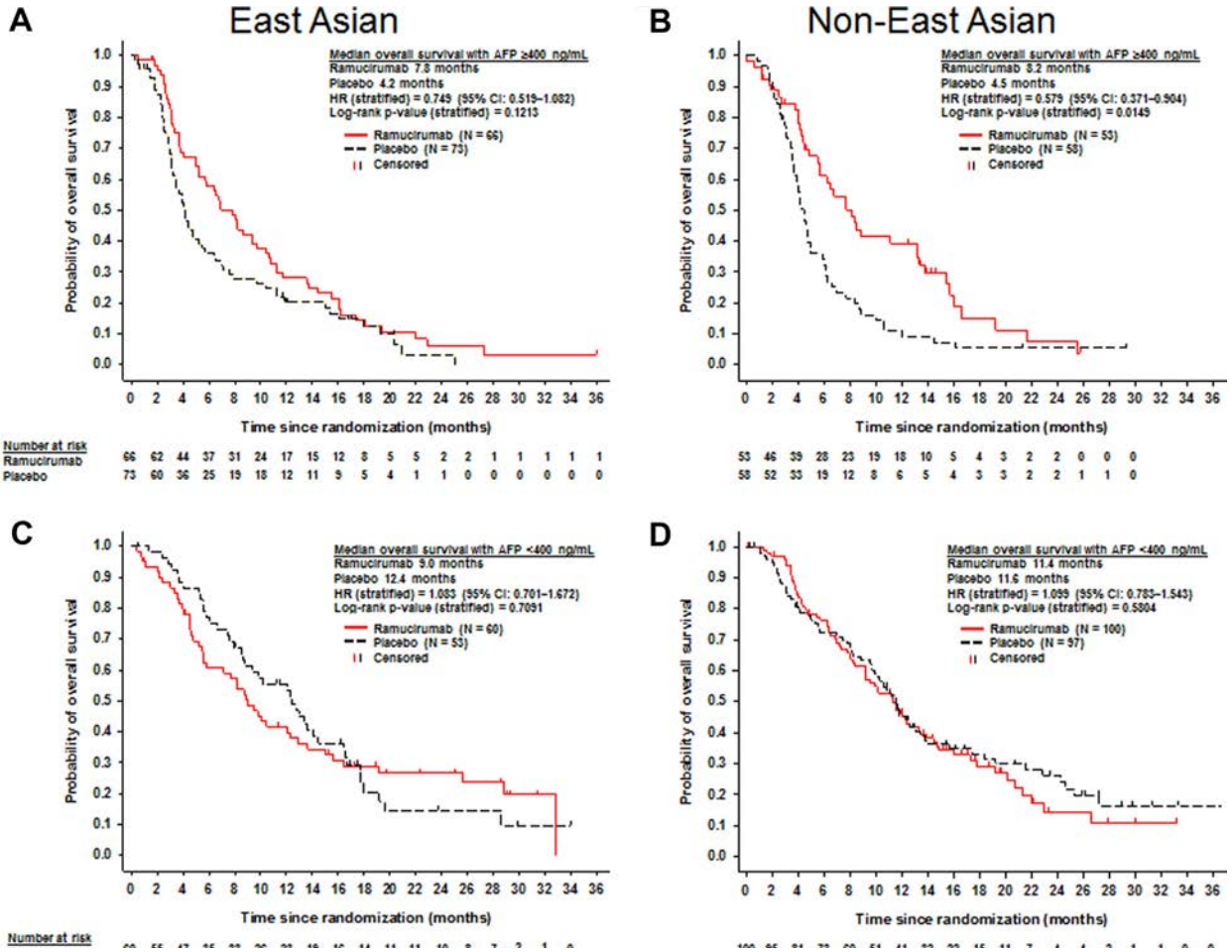

Figure 3: Kaplan-Meier plots of overall survival in patients with baseline alpha-fetoprotein ≥ 400 ng/mL (A and B) and alpha-fetoprotein < 400 ng/mL (C and D) for East Asian (A and C) and non-East Asian patients (B and D).

carcinoma is warranted. The REACH-2 trial will evaluate the efficacy and safety of ramucirumab in a global cohort of participants with hepatocellular carcinoma and elevated baseline AFP (ClinicalTrials.gov Identifier: NCT02435433).

MATERIALS AND METHODS

Study design and patients

The study design and demographic information for patients in REACH have been published previously [15]. Each center's institutional review board or independent ethics committee approved this study. The study followed the guiding principles of the Declaration of Helsinki and the Good Clinical Practice Guidelines of the International Conference on Harmonization. All patients provided written informed consent before enrollment. This study is registered with ClinicalTrials.gov, number NCT01140347.

Randomization and procedures

Randomization and procedures have been published previously [15]. Patients were randomly assigned in a 1:1 ratio to receive either ramucirumab 8 mg/kg or placebo intravenously every two weeks until disease progression, unacceptable toxicity, or withdrawal of consent. All patients received best supportive care. Predefined dose modifications were allowed to manage treatment-related toxicity. Randomization was stratified by geographic region (region 1 [n = 65]: Brazil, Canada, and the United States vs. region 2 [n = 248]: Australia, Europe, and Israel vs. region 3 [n = 252]: East Asia) and etiology of liver disease (hepatitis B vs. hepatitis C vs. other etiologies). Region 1 consisted of Brazil (n = 27), Canada (n = 1), and the United States (n = 37); region 2 consisted of Australia (n = 11), Austria (n = 8), Belgium (n = 8), Bulgaria (n = 6), the Czech Republic (n = 20), Finland (n = 3), France (n = 59), Germany (n = 40), Hungary (n = 1), Israel (n = 2), Italy (n = 51), the Netherlands (n = 3), Norway (n = 2), Portugal (n = 2), Romania (n = 7), Spain (n = 21), Sweden (n = 2), and Switzerland (n = 2); and region 3 consisted of Hong Kong (n = 24), Japan (n = 93), Philippines (n = 1), South Korea (n = 70), Taiwan (n = 58), and Thailand (n = 6).

Statistical analysis

Statistical methodology was the same as published previously [15]. The EA and non-EA subgroups were separately analyzed. The EA patient population was defined and analyzed as patients enrolled at study sites in region 3. The non-EA patient population was defined and analyzed as patients enrolled at study sites in regions 1 and 2 combined.

ACKNOWLEDGMENTS

We thank the patients, their families, the study sites, and the study personnel who participated in this clinical trial. This study was sponsored by Eli Lilly and Company. Medical writing support was provided by Marissa Philpott and Andrew Sakko, and editorial support was provided by Noelle Gasco, of inVentiv Health Clinical and funded by Eli Lilly and Company.

CONFLICTS OF INTEREST

Paolo B. Abada, Rebecca Cheng, Mauro Orlando, and Ling Yang are employees of Eli Lilly and Company. Andrew X. Zhu has acted in a consulting or advisory role for Amgen, Exelixis, and Sanofi, received research funding from Bayer and Onyx Pharmaceutical, and received grants from Eli Lilly and Company during the conduct of the study. All remaining authors have declared no conflicts of interest.

FINANCIAL SUPPORT

This study was sponsored by Eli Lilly and Company.

Authors' contributions

Paolo B. Abada, Rebecca Cheng, Mauro Orlando, and Ling Yang conceived and designed the study. Masatoshi Kudo, Takuji Okusaka, Joon Oh Park, Baek-Yeol Ryoo, Chia-Jui Yen, and Andrew X. Zhu collected the data. All authors analyzed and interpreted the data. All authors were involved in the drafting, review, and approval of the manuscript and the decision to submit for publication.

REFERENCES

1. Ferlay J, Soerjomataram I, Ervik M, Dikshit R, Eser S, Mathers C, Rebelo M, Parkin DM, Forman D, Bray F. GLOBOCAN 2012 v1.0, Cancer Incidence and Mortality Worldwide: IARC CancerBase No. 11. Lyon, France: International Agency for Research on Cancer; 2013 [cited 2016 Feb 12]. Available from: http://globocan.iarc.fr.
2. Torre LA, Bray F, Siegel RL, Ferlay J, Lortet-Tieulent J, Jemal A. Global cancer statistics, 2012. CA Cancer J Clin. 2015; 65:87–108.
3. Cheng AL, Kang YK, Chen Z, Tsao CJ, Qin S, Kim JS, Luo R, Feng J, Ye S, Yang TS, Xu J, Sun Y, Liang H, et al. Efficacy and safety of sorafenib in patients in the Asia-Pacific region with advanced hepatocellular carcinoma: a phase III randomised, double-blind, placebo-controlled trial. Lancet Oncol. 2009; 10:25–34.

4. Llovet JM, Ricci S, Mazzaferro V, Hilgard P, Gane E, Blanc JF, de Oliveira AC, Santoro A, Raoul JL, Forner A, Schwartz M, Porta C, Zeuzem S, et al. SHARP Investigators Study Group. Sorafenib in advanced hepatocellular carcinoma. N Engl J Med. 2008; 359:378–390.

5. Kudo M, Lencioni R, Ye SL, Bronowicki JP, Chen XP, Dagher L, Furuse J, Geschwind JF, Ladrón de Guevara L, Papandreou C, Sanyal AJ, Takayama T, Yoon SK, et al. Regional differences in treatment history, practices, and outcomes: final analysis of Gideon (Global Investigation of Therapeutic Decisions in Hepatocellular Carcinoma and of its Treatment with Sorafenib). Seventh International Liver Cancer Association Annual Conference, Washington, D.C., September 13–15, 2013 Final Programme & Book of Abstracts, pgs 11–12 [abstract O-011]. Available from: http://www.ilca2013.org/be-bruga/ilca2013/files/ILCAProvisionalProgramme2013_Final.pdf. Cited 2016 February 12.

6. El-Serag HB. Hepatocellular carcinoma. N Engl J Med. 2011; 365:1118–1127.

7. Fong ZV, Tanabe KK. The clinical management of hepatocellular carcinoma in the United States, Europe, and Asia: a comprehensive and evidence-based comparison and review. Cancer. 2014; 120:2824–2838.

8. Llovet JM. Updated treatment approach to hepatocellular carcinoma. J Gastroenterol. 2005; 40:225–235.

9. Llovet JM, Burroughs A, Bruix J. Hepatocellular carcinoma. Lancet. 2003; 362:1907–1917.

10. Sullivan LA, Brekken RA. The VEGF family in cancer and antibody-based strategies for their inhibition. MAbs. 2010; 2:165–175.

11. Tugues S, Koch S, Gualandi L, Li X, Claesson-Welsh L. Vascular endothelial growth factors and receptors: anti-angiogenic therapy in the treatment of cancer. Mol Aspects Med. 2011; 32:88–111.

12. Amini A, Masoumi MS, Morris DL, Pourgholami MH. The critical role of vascular endothelial growth factor in tumor angiogenesis. Curr Cancer Drug Targets. 2012; 12:23–43.

13. Zhu AX, Duda DG, Sahani DV, Jain RK. HCC and angiogenesis: possible targets and future directions. Nat Rev Clin Oncol. 2011; 8:292–301.

14. Spratlin JL, Cohen RB, Eadens M, Gore L, Camidge DR, Diab S, Leong S, O'Bryant C, Chow LQ, Serkova NJ, Meropol NJ, Lewis NL, Chiorean EG, et al. Phase I pharmacologic and biologic study of ramucirumab (IMC-1121B), a fully human immunoglobulin G1 monoclonal antibody targeting the vascular endothelial growth factor receptor-2. J Clin Oncol. 2010; 28:780–787.

15. Zhu AX, Park JO, Ryoo BY, Yen CJ, Poon R, Pastorelli D, Blanc JF, Chung HC, Baron AD, Pfiffer TE, Okusaka T, Kubackova K, Trojan J, et al. REACH Trial Investigators. Ramucirumab versus placebo as second-line treatment in patients with advanced hepatocellular carcinoma following first-line therapy with sorafenib (REACH): a randomised, double-blind, multicentre, phase 3 trial. Lancet Oncol. 2015; 16:859–870.

16. Llovet JM, Decaens T, Raoul JL, Boucher E, Kudo M, Chang C, Kang YK, Assenat E, Lim HY, Boige V, Mathurin P, Fartoux L, Lin DY, et al. Brivanib in patients with advanced hepatocellular carcinoma who were intolerant to sorafenib or for whom sorafenib failed: results from the randomized phase III BRISK-PS study. J Clin Oncol. 2013; 31:3509–3516.

17. Johnson PJ, Qin S, Park JW, Poon RT, Raoul JL, Philip PA, Hsu CH, Hu TH, Heo J, Xu J, Lu L, Chao Y, Boucher E, et al. Brivanib versus sorafenib as first-line therapy in patients with unresectable, advanced hepatocellular carcinoma: results from the randomized phase III BRISK-FL study. J Clin Oncol. 2013; 31:3517–3524.

18. Zhu AX, Kudo M, Assenat E, Cattan S, Kang YK, Lim HY, Poon RT, Blanc JF, Vogel A, Chen CL, Dorval E, Peck-Radosavljevic M, Santoro A, et al. Effect of everolimus on survival in advanced hepatocellular carcinoma after failure of sorafenib: the EVOLVE-1 randomized clinical trial. JAMA. 2014; 312:57–67.

19. Fuchs CS, Tomasek J, Yong CJ, Dumitru F, Passalacqua R, Goswami C, Safran H, dos Santos LV, Aprile G, Ferry DR, Melichar B, Tehfe M, Topuzov E, et al. REGARD Trial Investigators. Ramucirumab monotherapy for previously treated advanced gastric or gastro-oesophageal junction adenocarcinoma (REGARD): an international, randomised, multicentre, placebo-controlled, phase 3 trial. Lancet. 2014; 383:31–39.

20. Wilke H, Muro K, Van Cutsem E, Oh SC, Bodoky G, Shimada Y, Hironaka S, Sugimoto N, Lipatov O, Kim TY, Cunningham D, Rougier P, Komatsu Y, et al. RAINBOW Study Group. Ramucirumab plus paclitaxel versus placebo plus paclitaxel in patients with previously treated advanced gastric or gastro-oesophageal junction adenocarcinoma (RAINBOW): a double-blind, randomised phase 3 trial. Lancet Oncol. 2014; 15:1224–1235.

Liver Cancer

Liver Cancer 2017;6:16–26
DOI: 10.1159/000449343
Published online: November 29, 2016

EWALT 2015 Conference Proceedings: Review

Hepatocellular Carcinoma: Therapeutic Guidelines and Medical Treatment

Masatoshi Kudo[a] Franco Trevisani[b] Ghassan K. Abou-Alfa[c,d]
Lorenza Rimassa[e]

[a]Department of Gastroenterology and Hepatology, Kindai University Faculty of Medicine, Osaka-Sayama, Japan, [b]Semeiotic Unit, Department of Medical and Surgical Sciences, Alma Mater Studiorum – University of Bologna, Bologna, Italy, [c]Memorial Sloan Kettering Cancer Center, [d]Weill Cornell Medical College, N.Y., USA, [e]Medical Oncology and Hematology Unit, Humanitas Cancer Center, Humanitas Clinical and Research Center, Milan, Italy

Key Words
Hepatocellular carcinoma · Practice guideline · Treatment · Treatment algorithm

Abstract
Western and Eastern perspectives on therapeutic guidelines for hepatocellular carcinoma (HCC) have many commonalities but may also differ in certain aspects, as described in this article. In view of the limited therapeutic options for advanced HCC, evidence-based therapies are few, and thus there is a dependence on consensus-based guidelines. This article focuses on the Italian Association for the Study of the Liver guidelines and the Japanese approaches to therapy, while drawing attention to certain controversies from other academic bodies where applicable and appropriate.

Therapeutic Guidelines: The Western Perspective

In recent years several Western scientific associations have released and/or updated guidelines for the management of hepatocellular carcinoma (HCC) [1–3]. Refinements based on updated evidence and actual clinical practice have also been proposed [4]. The key points of Western guidelines are:

1. Surveillance. Six-monthly liver ultrasound examinations should be performed by experienced personnel. The measurement of alpha-fetoprotein combined with ultrasound is not

Masatoshi Kudo, MD, PhD
Department of Gastroenterology and Hepatology,
Kindai University Faculty of Medicine
377-2 Ohno-Higashi, Osaka-Sayama, 589-8511 (Japan)
Tel.+81 72 366 0221 (ext. 3149), E-Mail m-kudo@med.kindai.ac.jp

indicated because it barely (6–8%) increases the sensitivity, but significantly reduces the cost-effectiveness of surveillance. The target group comprises Child A/B cirrhotic patients, Child C patients listed for transplantation, non-cirrhotic hepatitis B surface antigen (HbsAg) carriers with active disease (or a family history of HCC), and hepatitis C virus (HCV)-infected patients with advanced fibrosis. There are different opinions regarding the use of alpha-fetoprotein, and the guidelines still lack recommendations or are unclear with respect to patients with non-alcoholic fatty liver disease, the population that has experienced the highest increase in HCC incidence in the Western Hemisphere.

2. Diagnosis. When a new nodule is detected by ultrasound in a cirrhotic liver, the recall policy is driven by the nodule size: for nodules <1 cm, 3-monthly ultrasound surveillance is recommended; for nodules >1 cm, HCC diagnosis requires detection of the typical vascular hallmarks (wash-in in the arterial phase and wash-out in the portal/delayed phases) by one radiological technique (computed tomography [CT] or magnetic resonance imaging [MRI]) at specialist centers [1–3] or by two radiological techniques at non-specialist centers [2]. The Italian Association for the Study of the Liver (AISF) also includes contrast-enhanced ultrasound among the diagnostic tools that are able to characterize nodules [4]. A "panoramic" imaging technique (CT or MRI) remains mandatory to assess the global tumoral burden for all guidelines. MRI has the highest sensitivity for detecting the typical vascular pattern in HCC <2 cm and is superior for the detection of hypovascular HCC when hepatocyte-specific contrast agents and post-vascular phase assessments are used. A biopsy is required if atypical features are evident on imaging and in noncirrhotic patients. A negative biopsy does not rule out malignancy, and 3-monthly ultrasound examinations are recommended. It is important to note that these diagnostic guidelines and tools are limited in scope to the screening population described herein.

3. Staging. All Western hepatology guidelines have endorsed the Balcelona Clinic Liver Cancer (BCLC) staging system for classification of patients into five prognostic strata according to their cancer burden, liver function, and performance status (PS). This system also proposes, in an evidence-based way, the standard of care treatment for each stage. However, because PS 1 does not preclude access to any available treatments for HCC, the Italian AISF has modified the BCLC therapeutic algorithm, and does not consider PS 1 a condition *per se* sufficient to up-grade a patient from earlier stages to advanced stages, for which only systemic therapy with sorafenib is recommended (AISF-BCLC staging system). Oncology experts differ in their opinions regarding the BCLC staging system, and some of them favor more precise systems [e.g., the Cancer of the Liver Italian Program, among others] for assessing advanced disease [5].

4. Treatment. Despite the BCLC indications, most associations (including AISF) have endorsed a more patient-tailored approach that is based on the multidisciplinary evaluation of each case and includes alternative first-line options [4]. Some key recommendations are (a) the presence of portal hypertension, hyperbilirubinemia, and multinodularity do not preclude hepatic resection, although this option must be accurately weighed against the risk of post-operative decompensation; (b) according to "transplant benefit" policy, liver transplantation may be considered even in patients slightly exceeding the Milan criteria as part of "expanded criteria" or "down-staging" protocols; (c) transarterial chemoembolization (TACE) should be adopted as the first-line therapy for intermediate (BCLC stage B) patients if they are not amenable to curative treatments (surgery or ablation); (d) the presence of segmental portal invasion is not a contraindication to TACE, although systemic therapy has shown possible benefits for these patients as a part of controlled studies; (e) the absence of an objective (complete or partial) response in treated lesions after two courses of TACE is considered a treatment failure, and sorafenib should be started (fig. 1); (f) combined loco-regional therapies (TACE plus ablation) offer maximum flexibility, allowing a nodule-by-nodule tailored

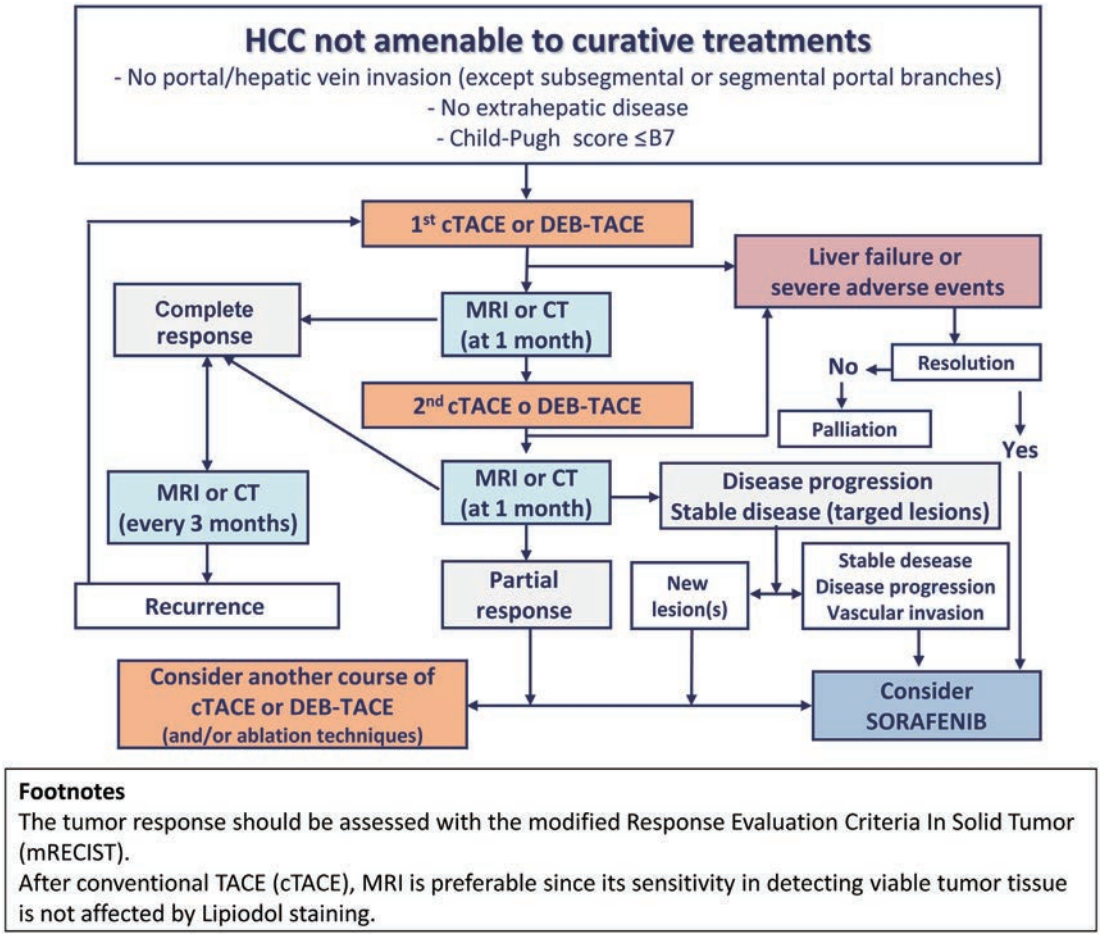

Fig. 1. Treatment algorithm for patients undergoing TACE, according to the recommendation of AISF. The flowchart is valid for any session of TACE. For conventional TACE (cTACE), MRI is preferable since lipiodol uptake causes beam hardening artifacts on CT that mask residual tumor tissue. The response to treatment is assessed by the modified Response Evaluation Criteria in Solid Tumor (mRECIST). Reproduced with permission from Bolondi N, et al. [4]

approach. Therefore, in non-surgical cases, a combined/sequential treatment should be considered for multinodular disease treated with TACE and for nodules >3 cm undergoing ablation. It is important to note that other guidelines, e.g., those of the National Comprehensive Cancer Network, are more cautious in these regards: they continue to limit transplantation to patients meeting published criteria and refrain from recommending combined local and systemic therapies, citing a lack of supporting data.

Therapeutic Guidelines: The Eastern Perspective

1. Evidence-Based Treatment Algorithm

The original Japan Society of Hepatology (JSH) HCC guidelines and all later updates contain an evidence-based treatment algorithm that is simple and easy to memorize. The algorithm includes three factors: (i) the degree of liver damage, (ii) the number of tumors, and (iii) the tumor diameter (fig. 2). The recommended treatment options can be narrowed down

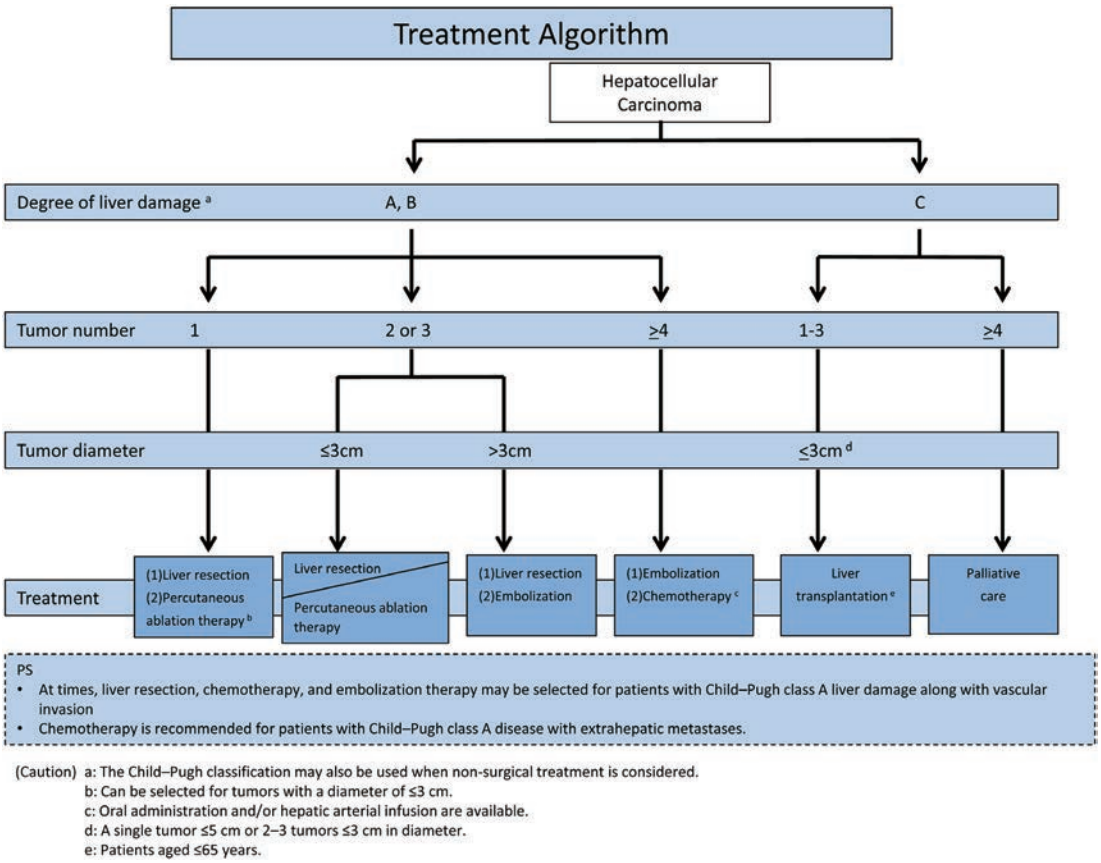

Fig. 2. JSH Evidence-based Treatment Algorithm. Modified with permission from Kokudo N, et al. [40]

to one or two by referring to this algorithm. The most recent version of the evidence-based treatment algorithm can be summarized as follows:

1. The order of the recommendations for surgical resection and percutaneous radiofrequency ablation (RFA) has been clarified. Based on the results of large nationwide cohort studies conducted by the Liver Cancer Study Group of Japan (LCSGJ) [6, 7], surgical resection is set as the first therapeutic choice for HCC patients with a single tumor with liver damage of grade A or B. If the tumor is smaller than 3 cm in cases meeting the above conditions, RFA is recommended as the second choice. During the target period for the current revision (2007–2011), there were three randomized controlled trials (RCTs) comparing surgery and RFA [8–10]. However, the results of these RCTs were not reflected in the treatment algorithm because the trials had several problems, as described elsewhere [11]. For a patient with liver damage of grade A or B and two or three tumors smaller than 3 cm, either surgical resection or RFA is recommended with no priority, based on a Japanese cohort study [6, 7].
2. Based on the results of the phase III clinical trial of sorafenib versus placebo in patients with advanced HCC (the SHARP study) [12], the multi-tyrosine kinase inhibitor sorafenib is suggested in the third version of the treatment algorithm. In patients with liver damage of grade A or B and four or more tumors confined to the liver, systemic chemotherapy, including molecular-targeted agents and hepatic arterial infusion chemotherapy (HAIC), is the second recommended treatment after TACE.
3. Since the first JSH-HCC guidelines, the assessment of liver damage covered five factors, including the indocyanine green (ICG) test, and has been used as an indicator of liver func-

tion. Although the ICG test is considered indispensable for surgical decision making in Japan, it is not routinely performed before non-surgical treatments such as RFA and TACE in current daily practice in Japan. The Child–Pugh classification serves as a substitute liver function grading system only before non-surgical treatments.

2. Consensus-Based Treatment Algorithm

Although sorafenib is recommended for patients with segmental portal vein invasion or portal invasion at the first portal branch (Vp1–3), the JSH-LCSGJ algorithm reflects the consensus that it is not recommended for patients with portal invasion at the main portal branch (Vp4) because of the risk of hepatic failure. However, HAIC is still recommended for patients with Vp4, and therefore recommendations regarding HAIC were left unchanged [13]. Moreover, because locoregional therapy for Child–Pugh C patients is now widely used, and many studies have reported its survival benefits, it is now described as a "well accepted treatment" rather than an "experimental treatment" in the revised algorithm (fig. 3) [14].

3. Definition of TACE Failure/Refractoriness

In the 2010 version of the JSH consensus-based treatment algorithm [15], TACE failure/refractoriness was defined assuming the use of superselective lipiodol TACE—which has been widely used worldwide, and particularly in Japan—and areas with lipiodol deposition were considered to be necrotic. However, this concept is not well accepted internationally [16]. Furthermore, following the approval in Japan in February 2014 of embolic drug-eluting beads (DEBs) that do not use lipiodol, the phrase needed to be changed from "lipiodol deposition" to "necrotic lesion or viable lesion." Accordingly, the section was revised to define TACE failure as an ineffective response after two or more consecutive TACE procedures as evaluated by CT or MRI after 1–3 months, even after chemotherapeutic agents have been changed and/or the feeding artery reanalyzed. Moreover, the appearance of new lesions in the liver in addition to those lesions recorded at the previous TACE procedure (other than the nodule being treated) was added to the definition of TACE failure/refractoriness. Following discussion of other issues related to continuous elevation of tumor markers, vascular invasion, and extrahepatic spread, descriptions similar to those in the previous version were approved (table 1). The revisions to these TACE failure definitions were approved by more than 85% of HCC experts.

Controversies Regarding Medical Treatment

The advent of sorafenib as a standard of care for advanced HCC [12] settled the basic question of how to treat that condition, but raised many other questions, the most contemporary of which concern the use of sorafenib in more cirrhotic settings and the influence, if any, of the etiology of HCC on outcomes.

Sorafenib was first approved by the United States Food and Drug Administration without any reference to the degree of cirrhosis [17] because of the "paucity of treatment options and variability in CP Scoring" [18]. In the phase II trial evaluating sorafenib in patients with advanced HCC, of 137 patients, 38 had Child–Pugh B cirrhosis [19]. In a retrospective analysis, it was found that the median duration of therapy was 4 months for Child–Pugh A patients and 1.8 months for Child–Pugh B patients, with a median overall survival (OS) of 9.5 months versus 3.2 months, respectively [20]. However, the fact that similar pharmacokinetics were evident in the two groups adds to the controversy. On the other hand, a phase I study evaluating sorafenib in 150 patients with organ dysfunction (including 17 patients with HCC) indicated that treatment with sorafenib was associated with dose-limiting elevations in serum biliru-

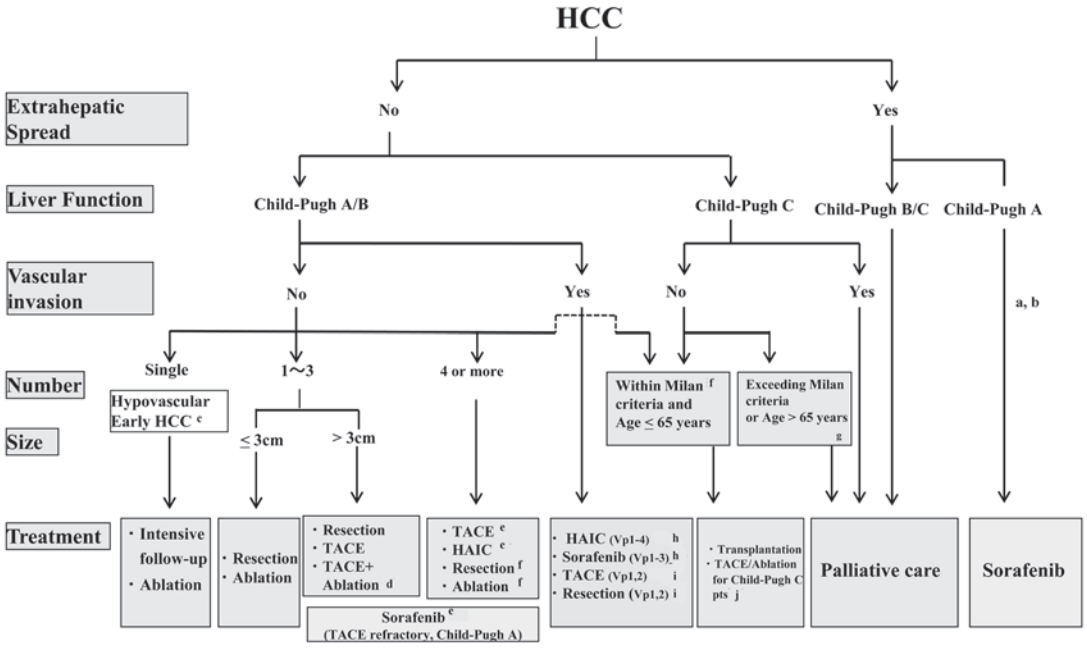

Fig. 3. JSH-LCSGJ Consensus-based Treatment Algorithm for HCC as revised in 2014. Reproduced with permission from Kudo M, et al. [14]

[a]Treatment should be performed as if extrahepatic spread is negative, when extrahepatic spread is not regarded as a prognostic factor. [b]Sorafenib is the first choice of treatment in this setting as a standard of care. [c]Intensive follow-up observation is recommended for hypovascular nodules by the Japanese Evidence-Based Clinical Practice Guidelines. However, local ablation therapy is frequently performed in the following cases: (1) when the nodule is diagnosed pathologically as early HCC, (2) when the nodules show decreased uptake on hepatocyte phase Gd-EOB-MRI, (3) when the nodules show decreased portal flow by CTAP or (4) decreased uptake is shown on the Kupffer phase of Sonazoid-enhanced US, since these nodules are known to frequently progress to typical hypervascular HCC. [d]Even for HCC nodules exceeding 3cm in diameter, combination therapy of TACE and ablation is frequently performed when resection is not indicated. [e]Transcatheter arterial chemoembolization (TACE) is the first choice of treatment in this setting. Hepatic arterial infusion chemotherapy (HAIC) using an implanted port is also recommended for TACE-refractory patients. The regimen for this treatment is usually low-dose FP (5FU+CDDP) or intraarterial 5FU infusion combined with systemic interferon therapy. Sorafenib is also a treatment of choice for TACE-refractory patients with Child-Pugh A liver function. [f]Resection is sometimes performed even when more than 4 nodules are present. Furthermore, ablation is sometimes performed in combination with TACE. [g]Milan criteria: Tumor size ≤3cm and tumor number ≤3; or solitary tumor ≤5cm. Even when liver function is good (Child-Pugh A/B), transplantation is sometimes considered for frequently recurring HCC patients. [h]Sorafenib and HAIC are recommended for HCC patients with Vp1,2 (minor portal vein invasion) or Vp3 (portal invasion at the 1st portal branch). Sorafenib is not recommended for HCC patients with Vp4 (portal invasion at the main portal branch), whereas HAIC is recommended for such patients with tumor thrombus in the main portal branch. [i]Resection and TACE is frequently performed when portal invasion is minimal, such as Vp1 (portal invasion at the 3rd or more peripheral portal branch) or Vp2 (portal invasion at the 2nd portal branch). [j]Local ablation therapy or subsegmental TACE is performed even for Child-Pugh C patients when transplantation is not indicated and there is no hepatic encephalopathy, no uncontrollable ascites, and a low bilirubin level (<3.0mg/dl). Although it is a well-accepted treatment in the routine clinical setting, there is no evidence of a survival benefit in Child-Pugh C patients. A prospective study is necessary to clarify this issue. Even in Child-Pugh A/B patients, transplantation is sometimes performed for relatively young patients with frequently or early recurring HCC after curative treatments.

bin concentration in patients with more advanced Child–Pugh scores [21]. Based on these observations, the authors recommended a dosing schedule for sorafenib based on bilirubin

Table 1. Definition of TACE failure/refractoriness (LCSGJ)

1. Intrahepatic lesion
I. Two or more consecutive ineffective responses within the treated tumors (viable lesion >50%) even after changing the chemotherapeutic agents and/or reanalysis of the feeding artery. The ineffective responses are determined by response evaluation CT/MRI images taken 1–3 months following adequately performed selective TACE
II. Two or more consecutive progressions in the liver (tumor numbers even increase compared to the tumor numbers before the previous TACE procedure) even after changing the chemotherapeutic agents and/or reanalysis of the feeding artery. The progressions are detected on response evaluation CT/MRI images taken 1–3 months following adequately performed selective TACE
2. Tumor marker
Continuous elevation of tumor markers right after TACE even though transient minor reduction is observed.
3. Appearance of ***vascular invasion***
4. Appearance of ***extrahepatic spread***

levels. This concept remains controversial, with a post-marketing study showing similar overall safety profiles and dosing strategies in the different Child–Pugh groups [22].

Multiple studies have shown that patients with Hepatitis B Virus (HBV)-related HCC who were treated with sorafenib had a modest prolongation in median OSin contrast to HCV-related HCC patients who had a substantial improvement in survival almost double that of the former group [23–25]. Within the limitations of the retrospective nature of most of these data, an etiology-dependent genomic difference in HCC was theorized. *CTNNB1* mutations are more commonly observed in HCV-related HCC than in HBV-related HCC and are associated with a specific WNT gene expression profile [26]. Sorafenib has been shown to interfere with WNT signaling output, leading to HCC growth suppression in preclinical models. Another explanation is the induction of sorafenib target CRAF by HCV core protein [27]. Although more exploration is certainly required, it should be emphasized that the utility of sorafenib is not undermined by this observation, and sorafenib remains an effective and life-prolonging therapy for HCC, irrespective of etiologic factors. Nonetheless the advent of next-generation sequencing of the somatic mutations in HCC will add to the controversy and may guide the next wave of clinical trials as the genetic heterogeneity and complexity of HCC become more evident and increasingly recognized.

Is It Time for a Second-Line Systemic Treatment?

Sorafenib is the only approved systemic agent for the treatment of advanced HCC and there is a great unmet need for new, effective therapies for this condition. Although the clinical and molecular diversity of HCC poses a challenge for drug developers, several novel targets are undergoing evaluation, most notably hepatocyte growth factor receptor (MET).

Table 2 shows the recently published multicenter, double-blind, randomized, placebo-controlled phase III trials of potential second-line HCC treatments [28–30]. These trials evaluated two small molecules, brivanib and everolimus, and a monoclonal antibody, ramucirumab, and all failed to reach their endpoints. Interestingly, the REACH trial identified a pre-defined subpopulation, i.e., patients with high baseline alpha-fetoprotein values, who benefited from treatment with ramucirumab [31].

However, some important lessons were learned from these trials, and our understanding of liver cancer is evolving. Until recently, it was not clear how long patients well enough

Table 2. Second-line phase III trials in advanced HCC

Trial	Principle target of experimental drug	No. of patients	Median OS
Brivanib versus placebo (BRISK-PS)[28]	VEGFR, FGFR	395	9.4 versus 8.2 months HR 0.89 (0.69–1.15), p=0.33
Everolimus versus placebo (EVOLVE-1)[29]	mTOR	546	7.6 versus 7.3 months HR 1.05 (0.86–1.27), p=0.68
Ramucirumab versus placebo (REACH)[30]	VEGFR2	565	9.2 versus 7.6 months HR 0.87 (0.72–1.05), p=0.14

VEGFR=vascular endothelial growth factor receptor; FGFR=fibroblast growth factor receptor; HR=hazard ratio; mTOR=mechanistic target of rapamycin.

to participate in subsequent clinical trials survived after progression on sorafenib, making it difficult to interpret single-arm phase II trials. Now, it has been shown that, compared with patients ineligible for second-line trials, potentially eligible patients have a longer OS (median: 7.8–8.6 months), and this sets a new potential benchmark for assessing single-arm phase II studies [32]. Moreover, the high failure rate of HCC phase III trials results from the peculiar characteristics of this disease, such as the high rate of toxicity related to the underlying liver dysfunction, the challenges of discerning signals of efficacy from nonrandomized phase II data (because of uninformative surrogate endpoints and prognostic heterogeneity within clinical and biologic subsets), the imbalances in disease (liver-only versus metastatic spread), and patient characteristics (Child–Pugh class, cause of cirrhosis, ethnicity).

Taking a step back to early-phase trials, the development of the oral MET-inhibitor tivantinib may be taken as an informative example. First, two phase Ib studies in HCC [33, 34] and then a randomized placebo-controlled phase II study with extensive biomarker analysis were conducted [35, 36]. This phase II study defined MET expression as a prognostic factor for second-line treatment. The study reached its primary endpoint of time-to-progression in the overall population and reached the predefined secondary efficacy endpoints in MET-high patients, showing that high MET-expression identifies a group of patients who benefit most. This strategy for patient selection is being applied in the ongoing METIV-HCC phase III trial [37].

Metabolomics as single agent did not fare any better. In a randomized phase III study of ADI-PEG 20 arginine deaminase versus placebo, there was no difference in survival in-between the two arms [38]. Future ADI-PEG 20 therapies will be based on combinatorial studies that would help enhance the activity of the drug.

Despite the discouraging outocmes of most recent studies, the latest have shown a more promising outcome. In a phase III trial, patients with advanced HCC who progressed on soarfenib were randomized to regorafenib, a similar mutli-tyrosine kinase versus placebo. The study showed an improvement in survival to 10.6 months versus 7.9 in favor of regorafenib. Further dissection of this positive outcome may be required considering the rather unrestrictive short use of prior sorafenib, the requirement of prior sorafenib tolerance, and the randomization up to 10 weeks after sorafenib failure which all may suggest a selection bias for the population [39].

In conclusion, to develop an effective second-line systemic treatment for advanced HCC, we need to better understand the clinical and biologic factors that affect prognosis and response so as to facilitate stratification and biomarker enrichment strategies. Additionally, we need to change our approach to the development of systemic therapies. In fact, we can no longer proceed with phase III trials of experimental drugs unless they show statistically significantly advantages in randomized phase II trials or clinically meaningful benefits in

nonrandomized phase II studies with an adequate number of homogeneous patients. Furthermore, the collection of biologic samples should become part of routine clinical practice to help identify and validate prognostic and predictive biomarkers (e.g., MET).

Disclosure Statement

Masatoshi Kudo
Lecturer: Bayer, Kowa, Taiho
Grants: Chugai, Otsuka, Takeda, Taiho, Sumitomo Dainippon, Daiichi Sankyo, MSD, Eisai
Franco Trevisani
Lectures, grants and advisory role: Bayer
Ghassan K. Abou-Alfa
Research: Abbott Laboratories, Amgen, Bayer, CASI, Celgene, Eli Lilly and Company/Imclone, Exelixis, Genentech, Immunomedics, Incyte, Momenta Pharmaceuticals, Myriad Genetics, Novartis, OncoMed Pharmaceuticals, Polaris Pharmaceuticals, Roche, and Vicus Therapeutics
Consulting: Aduro Biotech, Array, Astellas Pharma US, BioAlliance, Boston Scientific, Boston Therapeutics, BMS, CASI, Celgene, Cipla, Eli Lilly and Company, EMD Sorono, Gilead, IntegraGen, Medergy, MedImmune, Merrimack, Momenta, Novartis, Onxeo, Pharmacyclics, Sanofi-aventis, Silenseed, Sillajen, and Vicus Therapeutics.
Lorenza Rimassa
Consulting or advisory role: Lilly, Merck Serono, Bayer
Travel grants: ArQule
Other (Educational meeting speaker): Amgen

References

1 Bruix J, Sherman M, American Association for the Study of Liver Diseases: Management of hepatocellular carcinoma: an update. Hepatology 2011;53:1020–1022.
2 Llovet JM, Ducreux M, et al, European Association for the Study of the Liver, European Organisation for Research and Treatment of Cancer: EASL-EORTC clinical practice guidelines: management of hepatocellular carcinoma. J Hepatol 2012;56:908–943.
3 Verslype C, Rosmorduc O, Rougier P, ESMO Guidelines Working Group: Hepatocellular carcinoma: ESMO-ESDO Clinical Practice Guidelines for diagnosis, treatment and follow-up. Ann Oncol 2012;23(Suppl 7):vii41–vii48.
4 Bolondi L, Cillo U, Colombo M, Craxì A, Farinati F, Giannini EG, Golfieri R, Levrero M, Pinna AD, Piscaglia F, Raimondo G, Trevisani F, Bruno R, Caraceni P, Ciancio A, Coco B, Fraquelli M, Rendina M, Squadrito G, Toniutto P, Italian Association for the Study of the Liver (AISF), AISF Expert Panel, AISF Coordinating Committee: Position paper of the Italian Association for the Study of the Liver (AISF): the multidisciplinary clinical approach to hepatocellular carcinoma. Dig Liver Dis 2013;45:712–723.
5 Huitzil-Melendez FD, Capanu M, O'Reilly EM, Duffy A, Gansukh B, Saltz LL, Abou-Alfa GK: Advanced hepatocellular carcinoma: which staging systems best predict prognosis? J Clin Oncol 2010;28:2889–2895.
6 Hasegawa K, Makuuchi M, Takayama T, Kokudo N, Arii S, Okazaki M, Okita K, Omata M, Kudo M, Kojiro M, Nakanuma Y, Takayasu K, Monden M, Matsuyama Y, Ikai I: Surgical resection vs. percutaneous ablation for hepatocellular carcinoma: a preliminary report of the Japanese nationwide survey. J Hepatol 2008;49:589–594.
7 Hasegawa K, Kokudo N, Makuuchi M, Izumi N, Ichida T, Kudo M, Ku Y, Sakamoto M, Nakashima O, Matsui O, Matsuyama Y: Comparison of resection and ablation for hepatocellular carcinoma: a cohort study based on a Japanese nationwide survey. J Hepatol 2013;58:724–729.
8 Huang GT, Lee PH, Tsang YM, Lai MY, Yang PM, Hu RH, Chen PJ, Kao JH, Sheu JC, Lee CZ, Chen DS: Percutaneous ethanol injection versus surgical resection for the treatment of small hepatocellular carcinoma: a prospective study. Ann Surg 2005;242:36–42.
9 Chen MS, Li JQ, Zheng Y, Guo RP, Liang HH, Zhang YQ, Lin XJ, Lau WY: A prospective randomized trial comparing percutaneous local ablative therapy and partial hepatectomy for small hepatocellular carcinoma. Ann Surg 2006;243:321–328.
10 Huang J, Yan L, Cheng Z, Wu H, Du L, Wang J, Xu Y, Zeng Y: A randomized trial comparing radiofrequency ablation and surgical resection for HCC conforming to the Milan criteria. Ann Surg 2010;252:903–912.
11 Hasegawa K, Kokudo N, Makuuchi M: Surgery or ablation for hepatocellular carcinoma? Ann Surg 2008;247:557–558.

12 Llovet JM, Ricci S, Mazzaferro V, Hilgard P, Gane E, Blanc JF, de Oliveira AC, Santoro A, Raoul JL, Forner A, Schwartz M, Porta C, Zeuzem S, Bolondi L, Greten TF, Galle PR, Seitz JF, Borbath I, Häussinger D, Giannaris T, Shan M, Moscovici M, Voliotis D, Bruix J, SHARP Investigators Study Group: Sorafenib in advanced hepatocellular carcinoma. N Engl J Med 2008;359:378–390.
13 Kudo M: Treatment of advanced hepatocellular carcinoma with emphasis on hepatic arterial infusion chemotherapy and molecular targeted therapy. Liver Cancer 2012;1:62–70.
14 Kudo M, Matsui O, Izumi N, Iijima H, Kadoya M, Imai Y, Okusaka T, Miyayama S, Tsuchiya K, Ueshima K, Hiraoka A, Ikeda M, Ogasawara S, Yamashita T, Minami T, Yamakado K, Liver Cancer Study Group of Japan: JSH consensus-based clinical practice guidelines for the management of hepatocellular carcinoma: 2014 update by the Liver Cancer Study Group of Japan. Liver Cancer 2014;3:458–468.
15 Kudo M, Izumi N, Kokudo N, Matsui O, Sakamoto M, Nakashima O, Kojiro M, Makuuchi M, HCC Expert Panel of Japan Society of Hepatology: Management of hepatocellular carcinoma in Japan: Consensus-Based Clinical Practice Guidelines proposed by the Japan Society of Hepatology (JSH) 2010 updated version. Dig Dis 2011;29:339–364.
16 Raoul JL, Gilabert M, Piana G: How to define transarterial chemoembolization failure or refractoriness: a European perspective. Liver Cancer 2014;3:119–124.
17 U.S. Food and Drug Administration. FDA approves sorafenib (nexavar) for the treatment of unresectable hepatocellular carcinoma. Available at: http://www.fda.gov/cder/Offices/OODP/whatsnew/sorafenib.htm. Accessed October 3, 2015.
18 Kane RC, Farrell AT, Madabushi R, Booth B, Chattopadhyay S, Sridhara R, Justice R, Pazdur R: Sorafenib for the treatment of unresectable hepatocellular carcinoma. Oncologist 2009;14:95–100.
19 Abou-Alfa GK, Schwartz L, Ricci S, Amadori D, Santoro A, Figer A, De Greve J, Douillard JY, Lathia C, Schwartz B, Taylor I, Moscovici M, Saltz LB: Phase II study of sorafenib in patients with advanced hepatocellular carcinoma. J Clin Oncol 2006;24:4293–4300.
20 Abou-Alfa GK, Amadori D, Santoro A, Figer A, De Greve J, Lathia C, Voliotis D, Anderson S, Moscovici M, Ricci S: Safety and efficacy of sorafenib in patients with hepatocellular carcinoma (HCC) and Child-Pugh A versus B cirrhosis. Gastrointest Cancer Res 2011;4:40–44.
21 Miller AA, Murry DJ, Owzar K, Hollis DR, Kennedy EB, Abou-Alfa G, Desai A, Hwang J, Villalona-Calero MA, Dees EC, Lewis LD, Fakih MG, Edelman MJ, Millard F, Frank RC, Hohl RJ, Ratain MJ: Phase I and pharmacokinetic study of sorafenib in patients with hepatic or renal dysfunction: CALGB 60301. J Clin Oncol 2009;27:1800–1805.
22 Lencioni R, Kudo M, Ye SL, Bronowicki JP, Chen XP, Dagher L, Furuse J, Geschwind JF, de Guevara LL, Papandreou C, Takayama T, Yoon SK, Nakajima K, Lehr R, Heldner S, Sanyal AJ: GIDEON (Global Investigation of therapeutic DEcisions in hepatocellular carcinoma and Of its treatment with sorafeNib): second interim analysis. Int J Clin Pract 2014;68:609–617.
23 Bruix J, Raoul JL, Sherman M, Mazzaferro V, Bolondi L, Craxi A, Galle PR, Santoro A, Beaugrand M, Sangiovanni A, Porta C, Gerken G, Marrero JA, Nadel A, Shan M, Moscovici M, Voliotis D, Llovet JM: Efficacy and safety of sorafenib in patients with advanced hepatocellular carcinoma: subanalyses of a phase III trial. J Hepatol 2012;57:821–829.
24 Cheng AL, Kang YK, Lin DY, Park JW, Kudo M, Qin S, Chung HC, Song X, Xu J, Poggi G, Omata M, Pitman Lowenthal S, Lanzalone S, Yang L, Lechuga MJ, Raymond E: Sunitinib versus sorafenib in advanced hepatocellular cancer: results of a randomized phase III trial. J Clin Oncol 2013;31:4067–4075.
25 Abou-Alfa GK: Selection of patients with hepatocellular carcinoma for sorafenib. J Natl Compr Canc Netw 2009;7:397–403.
26 Lachenmayer A, Alsinet C, Savic R, Cabellos L, Toffanin S, Hoshida Y, Villanueva A, Minguez B, Newell P, Tsai HW, Barretina J, Thung S, Ward SC, Bruix J, Mazzaferro V, Schwartz M, Friedman SL, Llovet JM: Wnt-pathway activation in two molecular classes of hepatocellular carcinoma and experimental modulation by sorafenib. Clin Cancer Res 2012;18:4997–5007.
27 Giambartolomei S, Covone F, Levrero M, Balsano C: Sustained activation of the Raf/MEK/Erk pathway in response to EGF in stable cell lines expressing the hepatitis C virus (HCV) core protein. Oncogene 2001;20:2606–2610.
28 Llovet JM, Decaens T, Raoul JL, Boucher E, Kudo M, Chang C, Kang YK, Assenat E, Lim HY, Boige V, Mathurin P, Fartoux L, Lin DY, Bruix J, Poon RT, Sherman M, Blanc JF, Finn RS, Tak WY, Chao Y, Ezzeddine R, Liu D, Walters I, Park JW: Brivanib in patients with advanced hepatocellular carcinoma who were intolerant to sorafenib or for whom sorafenib failed: results from the randomized phase III BRISK-PS study. J Clin Oncol 2013;31:3509–3516.
29 Zhu AX, Kudo M, Assenat E, Cattan S, Kang YK, Lim HY, Poon RT, Blanc JF, Vogel A, Chen CL, Dorval E, Peck-Radosavljevic M, Santoro A, Daniele B, Furuse J, Jappe A, Perraud K, Anak O, Sellami DB, Chen LT: Effect of everolimus on survival in advanced hepatocellular carcinoma after failure of sorafenib: the EVOLVE-1 randomized clinical trial. JAMA 2014;312:57–67.
30 Zhu AX, Park JO, Ryoo BY, Yen CJ, Poon R, Pastorelli D, Blanc JF, Chung HC, Baron AD, Pfiffer TE, Okusaka T, Kubackova K, Trojan J, Sastre J, Chau I, Chang SC, Abada PB, Yang L, Schwartz JD, Kudo M, REACH Trial Investigators: Ramucirumab versus placebo as second-line treatment in patients with advanced hepatocellular carcinoma following first-line therapy with sorafenib (REACH): a randomised, double-blind, multicentre, phase 3 trial. Lancet Oncol 2015;16:859–870.
31 Zhu AX, Ryoo BY, Yen CJ, et al.: Ramucirumab (RAM) as second-line treatment in patients (pts) with advanced hepatocellular carcinoma (HCC): Analysis of patients with elevated α-fetoprotein (AFP) from the randomized phase III reach study. J Clin Oncol 33, 2015 (suppl 3; abstr 232).

32 Shao YY, Wu CH, Lu LC, Chan SY, Ma YY, Yen FC, Hsu CH, Cheng AL: Prognosis of patients with advanced hepatocellular carcinoma who failed first-line systemic therapy. J Hepatol 2014;60:313–318.
33 Santoro A, Simonelli M, Rodriguez-Lope C, Zucali P, Camacho LH, Granito A, Senzer N, Rimassa L, Abbadessa G, Schwartz B, Lamar M, Savage RE, Bruix J: A Phase-1b study of tivantinib (ARQ 197) in adult patients with hepatocellular carcinoma and cirrhosis. Br J Cancer 2013;108:21–24.
34 Puzanov I, Sosman J, Santoro A, Saif MW, Goff L, Dy GK, Zucali P, Means-Powell JA, Ma WW, Simonelli M, Martell R, Chai F, Lamar M, Savage RE, Schwartz B, Adjei AA: Phase 1 trial of tivantinib in combination with sorafenib in adult patients with advanced solid tumors. Invest New Drugs 2015;33:159–168.
35 Santoro A, Rimassa L, Borbath I, Daniele B, Salvagni S, Van Laethem JL, Van Vlierberghe H, Trojan J, Kolligs FT, Weiss A, Miles S, Gasbarrini A, Lencioni M, Cicalese L, Sherman M, Gridelli C, Buggisch P, Gerken G, Schmid RM, Boni C, Personeni N, Hassoun Z, Abbadessa G, Schwartz B, Von Roemeling R, Lamar ME, Chen Y, Porta C: Tivantinib for second-line treatment of advanced hepatocellular carcinoma: a randomised, placebo-controlled phase 2 study. Lancet Oncol 2013;14:55–63.
36 Rimassa L, Abbadessa G, Personeni N, Porta C, Borbath I, Daniele B, Van Laethem JL, Van Vlierberghe H, Trojan J, De Toni E, Peck-Radosavljevic M, Finn RS, Raoul JL, He AR, Lamar M, Wang Y, Von Roemeling RW, Schwartz BE, Bruix J, Santoro A: Tumor and plasma biomarker analysis from the randomized controlled phase II trial (RCT) of tivantinib in second-line hepatocellular carcinoma (HCC). 2016 Gastrointestinal Cancers Symposium. (San Francisco, January 21–23, 2016). J Clin Oncol 34, 2016 (suppl 4S; abstr 197).
37 Rimassa L, Porta C, Borbath I, Daniele B, Finn RS, Raoul JL, Schwartz LH, He AR, Trojan J, Radosavljevic MP, Abbadessa G, Goldberg T, Santoro A, Bruix J: Tivantinib in MET-high hepatocellular carcinoma patients and the ongoing phase III clinical trial. Hepat Oncol 2014;1:181–188.
38 Abou-Alfa, GK, et al. Phase III randomized study of second line ADI-peg 20 (A) plus best supportive care versus placebo (P) plus best supportive care in patients (pts) with advanced hepatocellular carcinoma (HCC). J Clin Oncol 2016;34 (suppl; abstr 4017).
39 Bruix, J. et al, World GI Oncology Congress, Barcelona 2016.
40 Kokudo N, Hasegawa K, Akahane M, Igaki H, Isumi N, Ichida T, Umemoto S, Kaneko S, Kawasaki S, Ku Y, Kudo M, Kubo S, Takayama T, Tateishi R, Fukuda T, Matsui O, Matsuyama Y, Murakami T, Arii S, Okazaki M, Makuuchi M: Evidence-based clinical practice guidelines for hepatocellular carcinoma: the Japan Society of Hepatology 2013 update (3rd JSH-HCC Guidelines). Hepatol Res 2015 (in press).

Dig Dis Sci (2016) 61:303–308
DOI 10.1007/s10620-015-3841-3

ORIGINAL ARTICLE

Clinical Outcome of Endoscopic Ultrasound-Guided Liver Abscess Drainage Using Self-Expandable Covered Metallic Stent (with Video)

Takeshi Ogura[1] · Daisuke Masuda[1] · Onda Saori[1] · Takagi Wataru[1] · Tatsushi Sano[1] · Atsushi Okuda[1] · Akira Miyano[1] · Masayuki Kitano[2] · Usama M. Abdel-aal[3] · Toshihisa Takeuchi[1] · Shinya Fukunishi[1] · Kazuhide Higuchi[1]

Received: 21 June 2015 / Accepted: 1 August 2015 / Published online: 9 August 2015

Abstract
Background Percutaneous drainage (PCD) is now the first-line drainage method for liver abscess because of its minimal invasiveness and high technical success rate. However, this procedure has several disadvantages, such as extra-drainage and self-tube removal. Recently, EUS-guided liver abscess drainage (EUS-AD) has been developed. However, only a few reports of EUS-AD have been reported. In addition, the clinical benefits of PCD and EUS-AD have not been reported.
Aims In the present study, the safety and feasibility of EUS-AD using fully covered SEMS (FCSEMS) and the clinical outcomes of EUS-AD and PCD were examined retrospectively.
Methods Twenty-seven consecutive patients who underwent PCD or EUS-AD between April 2012 and April 2015 were included in this study. EUS-AD was performed using FCSEMS. In addition, to prevent stent migration, 7-Fr pig tail plastic stent was placed within FCSEMS.
Results Technical success was achieved in all patients of both groups. Clinical success was 100 % in the EUS-AD group although it was 89 % in PCD group ($P = 034$). Three adverse events were seen in the PCD group (self-tube removal $n = 1$, tube migration $n = 2$), but no adverse events were seen in the EUS-AD group. The median hospital stay was significantly shorter in the EUS-AD group than in the PCD group (21 vs 41 days, $P = 0.03$).
Conclusion Because of the short hospital stay, the high clinical success rate, and the low adverse event rate compared to PCD, EUS-AD has potential as a first-line treatment for liver abscess.

Keywords Liver abscess · Endoscopic ultrasound-guided liver abscess drainage · Endoscopic ultrasound-guided fine-needle aspiration · Endoscopic ultrasound-guided drainage · Interventional EUS · Endoscopic ultrasound

Introduction

Liver abscesses sometimes require not only antibiotic agent treatment, but also drainage, such as percutaneous drainage (PCD) or aspiration [1, 2] or surgical drainage [3]. Surgical drainage is indicated for multiple abscesses or failed PCD, but this procedure is invasive and has relatively high mortality and morbidity rates [4, 5]. On the other hand, PCD is now the first-line drainage method for liver abscess because of its minimal invasiveness and high technical success rate [1, 2]. However, this procedure has several disadvantages, such as extra-drainage and self-tube removal.

Recently, interventional treatment using endoscopic ultrasound (EUS), such as biliary drainage [6] or pancreatic duct drainage [7], has been developed. In the same manner, EUS-guided liver abscess drainage (EUS-AD) has been developed [8]. This procedure may have several advantages, such as internal drainage and indicated in ascites patients,

Electronic supplementary material The online version of this article (doi:10.1007/s10620-015-3841-3) contains supplementary material, which is available to authorized users.

✉ Takeshi Ogura
oguratakeshi0411@yahoo.co.jp

[1] 2nd Department of Internal Medicine, Osaka Medical College, 1-1 Daigakuchou, Takatsukishi, Osaka 464-8681, Japan

[2] Department of Gastroenterology and Hepatology, Kinki University Faculty of Medicine, Osaka-sayama, Japan

[3] Division of Gastroenterology, Department of Internal Medicine, Sohag University, Sohag, Egypt

compared with PCD. However, only a few case reports or case series of EUS-AD have been reported [8–16]. In addition, the clinical benefits of PCD and EUS-AD have not been reported. Moreover, few cases of EUS-AD using self-expandable metallic stents (SEMSs) have been reported [13–16].

In the present study, the safety and feasibility of EUS-AD using fully covered SEMS (FCSEMS) and the outcomes of EUS-AD and PCD were examined retrospectively.

Materials and Methods

Patients

Consecutive patients with a liver abscess that needed drainage at Osaka Medical College between April 2012 and April 2015 were enrolled. Liver abscess was diagnosed by typical imaging, clinical symptoms such as abdominal pain and fever, and elevated markers of inflammation on blood examination.

In our institute, the first-line drainage method for liver abscess was PCD. Indications for EUS-AD were: (1) presence of ascites; (2) possibility of self-tube removal due to dementia; or (3) absence of a safe puncture route for the PCD procedure. All patients were given antibiotics before undergoing any procedures, and all patients underwent computed tomography (CT) the day after EUS-AD. Patients provided their written informed consent for all procedures associated with the study.

Technical Tips for Percutaneous Liver Abscess Drainage

PCD was performed by one experienced physician (D.M.) who was trained in percutaneous biliary drainage (PTCD). Liver abscesses were detected at a frequency of 5.0 MHz using a convex transducer under ultrasonographic guidance. The liver abscess was then punctured using an 18-G FNA needle, and necrotic material was aspirated. The contrast medium was injected, and a 0.035-inch guidewire was inserted into the cavity of the liver abscess. Finally, an 8-Fr pig tail drainage tube was placed within the liver abscess. If the clinical effect was insufficient, the drainage tube size was increased up to 10 Fr.

Technical Tips for EUS Drainage of Liver Abscess (Video)

EUS-AD was performed by one therapeutic endoscopist (T.O.) who was trained and experienced in both EUS and endoscopic retrograde cholangiopancreatography (ERCP). The liver abscess was visualized at a frequency of 7.5 MHz using a convex echoendoscope (GF-UGT260; Olympus Optical, Tokyo, Japan) connected to an ultrasound device (SSD5500; Aloka, Tokyo, Japan). If the liver abscess was located in the left lobe, puncture was performed mainly from the stomach. If the liver abscess was located in the right liver lobe, EUS-AD was performed from the duodenum. After the liver abscess was identified, it was punctured using a 19-G FNA needle (Sono Tip Pro Control 19G; Medi-Globe GmbH, Rosenheim, Germany or Medico's Hirata, Osaka, Japan) using Doppler ultrasonography to avoid any intervening vessels (Fig. 1a). Necrotic material was aspirated, and a small amount of the contrast medium was injected (Fig. 1b). Then, the 0.025-inch guidewire (VisiGlide; Olympus Medical Systems, Tokyo, Japan) was coiled within the liver abscess (Fig. 1c). Next, the ERCP cannula was exchanged to dilate the fistula. If SEMS insertion into the liver abscess was difficult, dilation was performed using a 4-mm balloon catheter (ZARA®, EPBD balloon catheter, Century Medical, Inc., Japan). The metallic stent delivery system was inserted into the liver abscess, and an FCSEMS (BONA stent, Standard Sci Tech Inc, Seoul, Korea, 10 mm × 6, 8 cm, or Niti-S Covered Metallic stent 10 mm × 12 cm, TaeWoong Medical, Seoul, Korea) was placed from the liver abscess to the stomach or duodenum (Fig. 1d, e). Finally, we inserted 7-Fr pig tail plastic stent within FCSEMS to prevent stent migration. If the clinical effect was insufficient, aspiration of necrotic material was performed under endoscopic guidance. Figure 2 showed CT imaging of pre- and post EUS-AD.

Definitions

The maximum size of the liver abscess was measured by CT imaging. Technical success was defined as successful placement of the PCD tube or EUS-AD stent. Clinical success was also defined as complete resolution of clinical symptoms, such as abdominal pain and fever, or decreased inflammation on blood examination within 14 days after each procedure. Recurrence of liver abscess after each procedure was defined as the typical symptoms with imaging findings. The follow-up period was measured from the day of performing PCD or EUS-AD to the final observation. Hospital stay was calculated from the day of each procedure to the day of each patient's discharge. Adverse events were defined according to the American Society for Gastrointestinal Endoscopy lexicon's severity grading system [17].

Results

Patients' Characteristics

In this study, 27 patients with a liver abscess were enrolled. Table 1 shows the patients' characteristics. PCD was

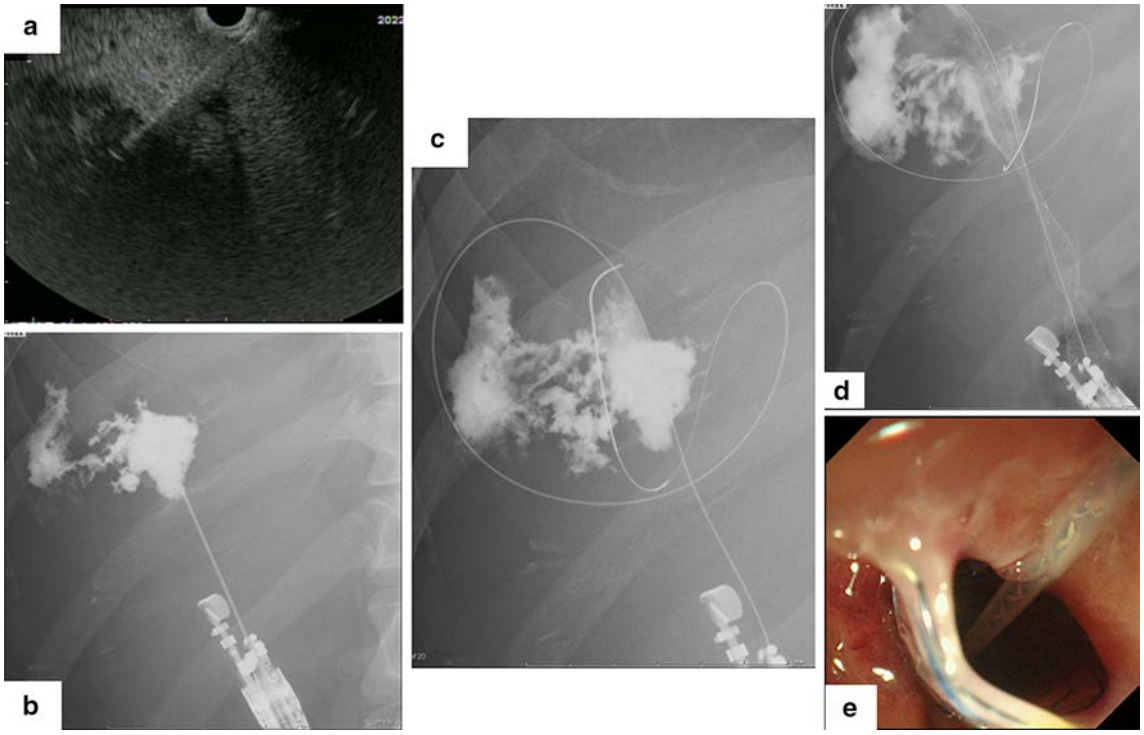

Fig. 1 **a** Liver abscess was punctured using 19G FNA needle. **b** The contrast medium was injected through FNA needle. **c** 0.025-inch guidewire was inserted into liver abscess cavity. **d** Fully covered self-expandable metallic stent was placed from liver abscess to the duodenum. **e** Endoscopic image of EUS-AD

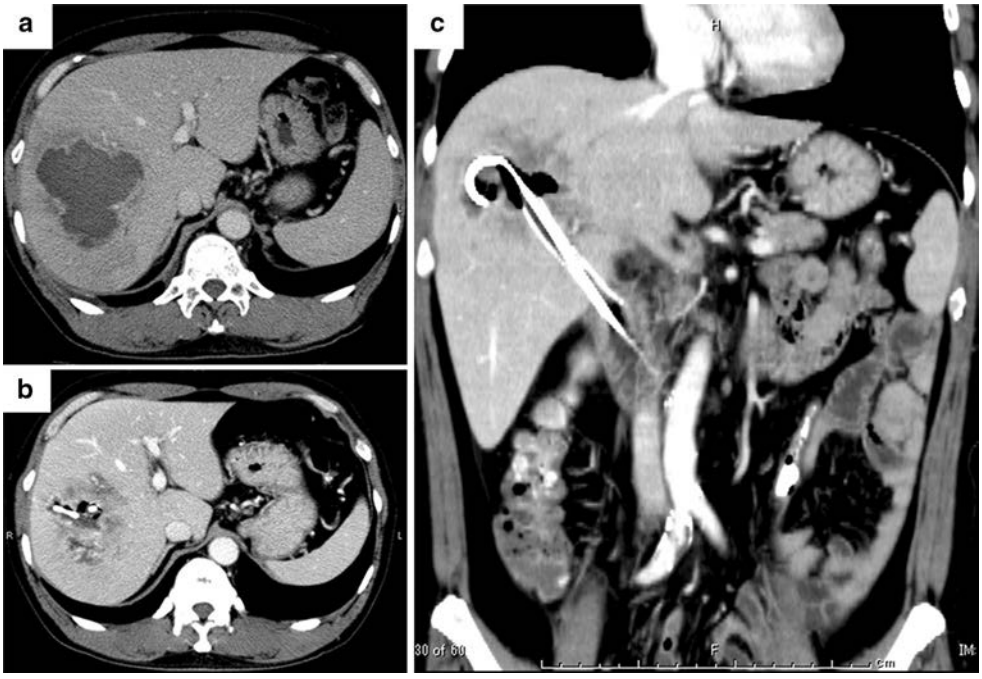

Fig. 2 **a** Huge liver abscess was seen in *right lobe*. **b** Size of liver abscess was decreased after 1 week from EUS-AD. **c** Fully covered self-expandable metallic stent and pig tail plastic stent were placed

performed for 19 consecutive patients (median age 66.0 years, range 46–85 years; 16 males, three females), and EUS-AD was performed for eight patients (median age 66.5 years, range 31–84 years; four males, three females). The location of the liver abscess was left in 12 and right in seven in the PCD group, and left in six and right in two in the EUS-AD group ($P = 0.56$). Median abscess size was not significantly different between PCD and EUS-AD (73.7 vs 74.6 mm, $P = 0.59$). On blood examination, the mean white blood cell (WBC) count was 14371.4/μl, and the mean C-reactive protein (CRP) was 16.3 mg/dl in the PCD group, and the mean WBC count was 13229.0/μl and the mean CRP was 10.4 mg/dl in the EUS-AD group, with no significant differences. Relatively long-term follow-up (PCD median 268 days, EUS-AD 218 days; $P = 0.09$) was performed.

The indications for EUS-AD were: (1) risk of self-tube removal, $n = 5$; (2) ascites, $n = 2$; and (3) recurrence of liver abscess after PCD tube removal, $n = 1$. The source of the infections was: *Klebsiella pneumonia* ($n = 9$), unknown ($n = 12$), *Escherichia coli* ($n = 4$), *Salmonella* (n = 1), and *Amebiasis* (n = 1).

Overall Outcomes of Percutaneous and EUS-Guided Liver Abscess Drainage

Table 2 shows the overall outcomes of percutaneous and EUS-guided liver abscess drainage. Technical success was achieved in all patients of both groups. Clinical success was obtained in all patients in the EUS-AD group. However, in the PDC group, effective drainage could not be obtained in two patients. One patient had a huge liver abscess (99.28 mm, caused by salmonella) and sepsis, and 25 days after the PCD procedure, this patient died. Another patient had advanced malignant cancer, and effective drainage could not be obtained. The median number of procedures was not significantly different between the two groups. On the other hand, three adverse events were seen in the PCD group (self-tube removal $n = 1$, tube migration $n = 2$), but no adverse events were seen in the EUS-AD group.

Table 1 Patients' characteristics

	PCD $n = 19$	EUS-AD $n = 8$	*P* value
Median age (range), year	66 (46–85)	66.5 (31–84)	0.40
Sex (male/female)	16:3	4:3	0.15
Location			
Left lobe	12	6	0.56
Right lobe	7	2	
Median abscess size (mm, range)	73.7 (32.8–144.4)	74.6 (61.9–99.3)	0.59
Mean WBC count (μl)	14371.4	13229.0	0.15
Mean CRP (mg/dl)	16.3	10.4	0.84
Median observation period, days (range)	268 (17–1081)	218 (17–396)	0.09

Table 2 Overall outcomes of PCD and EUS-AD

	PCD $n = 19$	EUS-AD $n = 8$	*P* value
Technical success % (*n*)	100 (19/19)	100 (8/8)	–
Clinical success % (*n*)	89 (17/19)	100 (8/8)	0.34
Median number of procedures (range)	1 (1–4)	1.5 (1–2)	0.35
Mean post-WBC count (μl)	9716.2	8822.5	
Mean post-CRP (mg/dl)	7.82	7.12	
Adverse event			
Total number	3	0	0.30
Adverse events			
Self-tube removal	1		
Stent migration	2		
Median hospital stay, days (range)	41 (17–187)	21 (11–200)	0.03
Recurrence of liver abscess (*n*)	1	0	0.60

Table 3 Summary of EUS-guided liver abscess drainage

References	Number	Location (*n*)	Approach route (*n*)	Stent	Technical success (%)	Clinical success (%)	Adverse events
Seewald et al. [8]	1	Left lobe	Gastric	7-Fr ENCD	100 (1/1)	100 (1/1)	None
Ang et al. [9]	1	Left lobe	Gastric	8-, 10-Fr pig tail PS	100 (1/1)	100 (1/1)	None
Noh et al. [10]	3	Caudate lobe (2)	Gastric (2)	7-Fr pig tail PS	100 (3/3)	100 (3/3)	None
		Left lobe (1)	Duodenal (1)	7-Fr ENCD			
Itoi et al. [11]	2	Caudate lobe (1)	Gastric (1)	7-Fr straight and pig tail PS	100 (2/2)	100 (2/2)	None
		Left lobe (1)	Duodenal (1)	5-Fr ENCD			
Keohane et al. [12]	2	Caudate lobe (2)	Gastric (2)	7-Fr pig tail PS	100 (2/2)	100 (2/2)	None
				10-Fr pig tail PS			
Medrado et al. [13]	1	Left lobe	Gastric	10 mm × 6 cm, FCSEMS	100 (1/1)	100 (1/1)	Stent migration
Alcaide et al. [14]	1	Left lobe	Gastric	LASEMS	100 (1/1)	100 (1/1)	None
Kawakami et al. [15]	1	Left lobe	Gastric	LASEMS	100 (1/1)	100 (1/1)	None
Tonozuka et al. [16]	7	Left lobe (6)	Gastric (6)	LASEMS (2)	100 (7/7)	71.4 (5/7)	None
		Right lobe (1)	Duodenal (1)	FCSEMS (5)			

ENCD endoscopic nasocystic drainage, *PS* plastic stent, *FCSEMS* fully covered self-expandable metallic stent, *LASEMS* lumen apposing self-expanding metallic stent

The median hospital stay was significantly shorter in the EUS-AD group than in the PCD group (21 vs 41 days, $P = 0.03$).

During follow-up, recurrence of the liver abscess was seen in one patient. This patient underwent PCD, and effective drainage was obtained. However, 6 months after tube removal, recurrence of the liver abscess was seen, and EUS-AD was performed. This patient underwent clinical follow-up for 6 months, with no recurrence of the liver abscess.

Discussion

The gold-standard treatment for liver abscess is PCD, and the technical success rate of this procedure has been reported to range from 85 to 95 % [18, 19]. However, the disadvantages of this procedure are extra-drainage and self-tube removal, and these adverse events may lead to patient discomfort. On the other hand, EUS-AD, a novel drainage procedure, has been reported. In the present study, the technical and functional success rates of EUS-AD were extremely high, and the rate of adverse events was low compared with PCD. In addition, the hospital stay was shorter in the EUS-AD group than in the PCD group. Compared with PCD, EUS-AD has several advantages, including initial internal drainage, so that the risk of self-tube removal is not present. In addition, the patient's quality of life is maintained. In addition, clear visualization of the internal vessels can be obtained by color Doppler ultrasound [11], and transcutaneous infection can be avoided. If the stent of EUS-AD is present without removal, it is difficult for a liver abscess to occur, although this should be confirmed by long-term follow-up.

However, in EUS-guided transluminal drainage, use of a metallic stent is one of the important points. First, if a plastic stent is used in EUS-guided transluminal drainage, the contents of the drainage area may leak into the abdominal cavity. Since a plastic stent is thin compared with a metallic stent, the contents of the drainage area may flow through the stent and drainage area or through the abscess wall [6]. On the other hand, SEMSs are expandable and have a large diameter, resulting in impaction between the stent and the surrounding drainage area or abscess wall. Second, a metallic stent has a large diameter ($\sim$ >30 Fr) that is clinically useful because it can provide an excellent drainage effect compared with a PCD tube.

Table 3 shows previous reports of EUS-AD using metallic stents. To date, only a few case reports or case series of EUS-AD have been reported [8–16]. In addition, only ten cases of EUS-AD using an SEMS have been reported [13–16]. According to these reports, technical success was obtained in all patients, and clinical success rates of EUS-AD ranged from 71.4 to 100 %. The approach route was from the stomach in 16 and the duodenum in three. Liver abscesses are usually located in the left or caudate lobe. Indeed, EUS-guided transluminal drainage for the right hepatic bile duct [20] or the right lobe is technically difficult. With EUS-AD, only one case of a right liver abscess has been reported [16]. On the other hand, in the present study, two cases of right liver abscess were included. To visualize the right lobe, the echoendoscope was introduced into the duodenum. First, the

common bile duct was identified, and then, the hepatic hilum was identified using counterclockwise rotation. Next, using the echoendoscope's right–left angle, echo-imaging, and radiographic guidance, the right hepatic lobe was identified. In this procedure, EUS was moved extremely slowly and softly to avoid duodenal perforation. However, this technique cannot be usually performed; therefore, it is one of the limitations of EUS-AD for right hepatic lobe.

Among the reports of EUS-AD using an SEMS, stent migration was seen as an adverse event. This fact suggested that if EUS-AD was performed from the stomach, especially the upper stomach, there is a possibility of stent migration as in EUS-guided hepaticogastrostomy (EUS-HGS). To prevent this adverse event, the tips of the EUS-AD should be as for EUS-HGS and a long SEMS should be selected [21, 22]. Recently, a novel SEMS with anti-migration properties and a large diameter has become available [14–16]. This SEMS has a definite clinical impact, but also several limitations. First, stent migration cannot be completely prevented. Indeed, stent migration occurred in a case of pancreatic fluid collection drainage [23]. Therefore, in cases with a possibility of stent migration, the stent in stent method (pig tail stent within SEMS) may be useful. Second, if the distance between the liver abscess and the intestinal wall which was punctured was far, this stent could not be used. For these reasons, we selected long FCSEMSs.

In the light of these previous reports, although our study was retrospective with a single operator, the present study was important because of the relatively large case series, and it is the first to compare the clinical outcomes between EUS-AD and PCD.

In conclusion, because of the short hospital stay, the high clinical success rate, and the low adverse event rate compared to PCD, EUS-AD has potential as a first-line treatment for liver abscess, although a prospective, randomized, controlled study is needed.

Compliance with ethical standards

Conflict of interest None.

References

1. Yu CHS, Ho SMS, Lau WY, et al. Treatment of pyogenic liver abscess: prospective randomized comparison of catheter drainage and needle aspiration. *Hepatology*. 2004;4:932–938.
2. Zerem E, Hadzic A. Sonographically guided percutaneous catheter drainage versus needle aspiration in the management of pyogenic liver abscess. *AJR. Am J Roentegnol*. 2007;3:W138–W142.
3. Tan YM, Chung YFA, Chow KHP, et al. An appraisal of surgical and percutaneous drainage for pyogenic liver abscesses lager than 5cm. *Ann Surg*. 2005;3:485–490.
4. Huang CJ, Pitt HA, Lipsett PA, et al. Pyogenic hepatic abscess. Changing trends over 42 years. *Ann Surg*. 1996;223:600–609.
5. Rahimian J, Wilson T, Orman V, et al. Pyogenic liver abscess: recent trends in etiology and mortality. *Clin Infect Dis*. 2004; 11:1654–1659.
6. Ogura T, Higuchi K. Dose endoscopic ultrasound-guided biliary drainage really have clinical impact? *World J Gastroenterol*. 2015;28:1049–1052.
7. Itoi T, Yasud I, Kurihara T, et al. Technique of endoscopic ulrasonography-guided pancreatic duct intervention (with videos). *J Hepatobiliary Pancreat Sci*. 2014;21:E4–E9.
8. Seewald S, Imazu H, Omar S, et al. EUS-guided drainage of hepatic abscess. *Gastrointest Endosc*. 2005;61:495–498.
9. Ang TL, Seewald S, Teo EK, et al. EUS-guided drainage of ruptured liver abscesses. *Endoscopy*. 2009;41:E21–E22.
10. Noh SH, Park do H, Kim YR, et al. EUS-guided drainage of hepatic abscesses not accessible to percutaneous drainage (with videos). *Gastrointest Endosc*. 2010;71:1314–1319.
11. Itoi T, Ang T, Seewald S, et al. Endoscopic ultrasonography guided drainage for tuberculous liver abscess drainage. *Dig Endosc*. 2011;23:158–161.
12. Keohane J, DiMaio CJ, Schattner MA, et al. EUS guided transgastric drainage of caudate lobe liver abscess. *J Interv Gastroenterol*. 2011;1:139–141.
13. Medrado BF, Carneiro FO, Vilaça TG, et al. Ensoscopic ultrasound-guided drainage of giant liver abscess associated with transgastric migration of self-expandable metallic stent. *Endoscopu*. 2013;45:E331–E332.
14. Alcaide N, Vargas-Garcia AL, de la Serna-Higuera C, et al. EUS-guided drainage of liver abscess by using a lumen-apposing metal stent (with video). *Gastrointest Endosc*. 2013;78:941–942. **(discussion 942)**.
15. Kawakami H, Kawakubo K, Kuwatani M, et al. Endoscopic ultrasound-guided liver abscess drainage using a dedicated, wide, fully covered self-expandable metallic stent with flared-ends. *Endoscopy*. 2014;46:E982–E983.
16. Tonozuka R, Itoi T, Tsuchiya T, et al. EUS-guided drainage of hepatic abscess and infected biloma using short and long metal stent (with videos). Gastrointest Endosc. Epub. 04/02/2015.
17. Cotton PB, Eisen GM, Aabakken L, et al. A lexicon for endoscopic adverse event: report of an ASGE workshop. *Gastrointest Endosc*. 2010;71:446–454.
18. Onder A, Kapan M, Böyük A, et al. Surgical management of pyogenic liver abscess. *Eur Rev Med Pharmacol Sci*. 2011;15: 1182–1186.
19. Ferraioli G, Garlaschelli A, Zanaboni D, et al. Percutaneous and surgical treatment of pyogenic liver abscesses: observation over a 21-year period in 148 patients. *Dig Liver Dis*. 2008;40:690–696.
20. Ogura T, Sano S, Onda S, et al. Endoscopic ultrasound-guided biliary drainage for right hepatic bile duct obstruction: novel technical tips. *Endoscopy*. 2015;47:72–75.
21. Ogura T, Masuda D, Imoto A, et al. Novel method of endoscopic ultrasound-guided hepacticogastrostomy to prevent for stent migration. *J Gastroenterol Hepatol*. 2014;29:1815–1821.
22. Itoi T, Isayama H, Sofuni A, et al. Stent selection and tips on placement technique of EUS-guided biliary drainage: transduodenal and transgastric stenting. *J Hepatobiliary Pancreat Sci*. 2011;18:664–672.
23. Bapaye A, Itoi T, Kongkam P, et al. New fully covered large-bore wide-flare removable metal stent for drainage of pancreatic fluid collections: results of a multicenter study. *Dig Endosc*. 2015; 27:499–504.

Comparison of the clinical impact of endoscopic ultrasound-guided choledochoduodenostomy and hepaticogastrostomy for bile duct obstruction with duodenal obstruction

Authors Takeshi Ogura[1], Yasutaka Chiba[2], Daisuke Masuda[1], Masayuki Kitano[3], Tatsushi Sano[1], Onda Saori[1], Kazuhiro Yamamoto[4], Hiroshi Imaoka[5], Akira Imoto[1], Toshihisa Takeuchi[1], Shinya Fukunishi[1], Kazuhide Higuchi[1]

Institutions Institutions are listed at end of article.

submitted 4. October 2014
accepted after revision 6. July 2015

Bibliography
DOI http://dx.doi.org/10.1055/s-0034-1392859
Published online: 18.9.2015
Endoscopy 2016; 48: 156–163

ISSN 0013-726X

Corresponding author
Takeshi Ogura, MD, PhD
2nd Department of Internal Medicine
Osaka Medical College
1-1 Daigakuchou
Takatsukishi
Osaka 569-8686
Japan
Fax: +81-52-7635233
oguratakeshi0411@yahoo.co.jp

Background and study aim: To date, only a few reports with small numbers of patients have described double stenting (biliary and duodenal), in particular endoscopic ultrasound (EUS)-guided biliary drainage, for patients with obstructive jaundice. In addition, no reports have sought to determine which EUS-guided biliary drainage route has better outcomes. The aim of the current study was to investigate adverse events and stent patency in patients who underwent EUS-guided biliary drainage and duodenal stenting.

Patients and methods: Patients who were admitted to the Osaka Medical College with obstructive jaundice caused by lower biliary obstruction and duodenal obstruction due to malignant tumor between June 2012 and April 2014 were retrospectively enrolled in the study.

Results: A total of 39 patients were enrolled in the study; 13 underwent EUS-guided choledochoduodenostomy (EUS-CDS), and 26 underwent EUS-guided hepaticogastrostomy (EUS-HGS). Adjusted analyses for covariates using propensity scores showed that the EUS-HGS group had significantly longer stent patency than the EUS-CDS group (duodenal stent patency: median 113 vs. 34 days; hazard ratio [HR] 0.415, 95 % confidence interval [CI] 0.175 – 0.984; $P=0.046$; biliary stent patency: median 133 vs. 37 days; HR 0.391, 95 % CI 0.156 – 0.981; $P=0.045$). On logistic regression analysis, only EUS-CDS was associated with adverse events, in particular reflux cholangitis (OR 10.285, 95 %CI 1.686 – 62.733; $P=0.012$).

Conclusion: In cases of obstructive jaundice with duodenal obstruction, EUS-HGS may be better than EUS-CDS, with longer stent patency and fewer adverse events.

Introduction

Obstructive jaundice is a major adverse effect of pancreatic or biliary carcinoma. Endoscopic biliary drainage is the gold standard method of treatment for obstructive jaundice [1, 2]. However, some patients with obstructive jaundice related to pancreatic or biliary carcinoma also have duodenal obstruction due to tumor invasion, making it difficult to reach the ampulla of Vater. Recently, endoscopic ultrasound (EUS)-guided biliary drainage and duodenal stenting have been developed for treatment in such cases.

The technique of EUS-guided biliary drainage depends on the approach route [3 – 9]. EUS-guided hepaticogastrostomy (EUS-HGS) involves the puncture of an intrahepatic bile duct (usually segment 3; B3) via the stomach, and subsequent stent placement. EUS-guided choledochoduodenostomy (EUS-CDS) entails puncture of the extrahepatic bile duct from the duodenum followed by stent placement. Both methods have been reported to have high rates of technical and functional success compared with endoscopic retrograde cholangiopancreatography (ERCP) [5 – 9]. Although relatively high rates of adverse events have also been reported [5 – 8], these methods have clinical impact in failed ERCP cases.

Insertion of a duodenal metal stent to resolve the duodenal stenosis is necessary as an add-on for both techniques [10]. To date, only a few small reports have described the combination of duodenal stenting and EUS-guided biliary drainage [11 – 19], and no reports have determined which of the two EUS routes is associated with better outcomes. The aim of the present study, therefore, was to compare adverse events and stent patency in EUS-guided biliary drainage techniques with duodenal stenting for malignant obstruction.

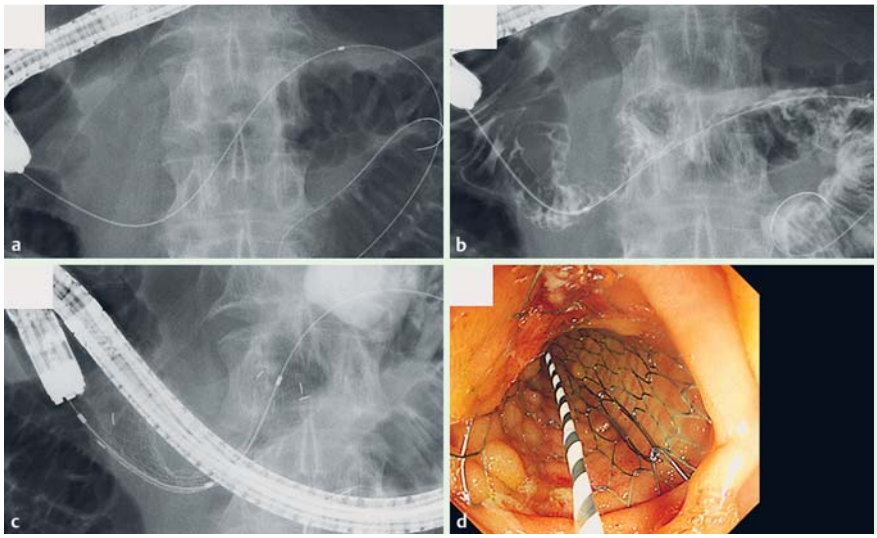

Fig. 1 Duodenal stent placement. **a** A 0.035-inch stiff guidewire was advanced through the duodenal stenosis using an endoscopic retrograde cholangiopancreatography catheter. **b** Contrast medium was injected, and the diameter of the stenosis was measured. **c,d** The duodenal metallic stent was successfully placed.

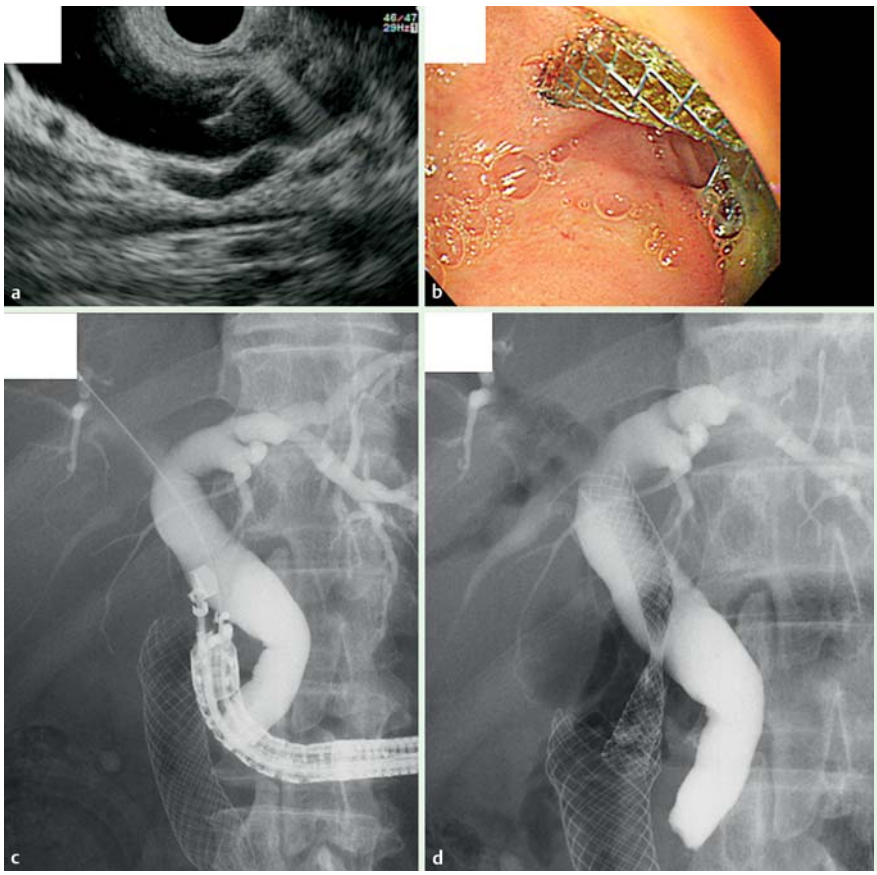

Fig. 2 Endoscopic ultrasound-guided choledochoduodenostomy. **a** The common bile duct was punctured using a 19-G needle. **b** Contrast medium was injected, and a 0.035-inch guidewire was inserted. **c,d** A metallic stent was inserted from the common bile duct to the duodenum.

Patients and methods

Patients

Consecutive patients who were admitted to the Osaka Medical College between 1 June 2012 and 1 April 2014 with obstructive jaundice and duodenal obstruction due to malignant tumor were retrospectively enrolled in the study. Patients were admitted with symptoms of vomiting and/or jaundice.

Patient records were retrospectively reviewed and the following data were recorded: patient characteristics, size of primary tumor, site and length of duodenal stenosis, type of EUS-guided biliary drainage performed, adverse events associated with duodenal stent placement or EUS-guided biliary drainage, stent patency, and overall survival. Technical and functional success rates of the procedures were also recorded.

Patients provided written, informed consent for all procedures associated with the study. The study was approved by the hospital's Institutional Review Board for human research.

Technical aspects of duodenal stent placement and EUS-guided biliary drainage

Duodenal stent placement was performed about 1 week before EUS-guided biliary drainage. All procedures were performed by one endoscopist (T.O.) who was trained and experienced in ther-

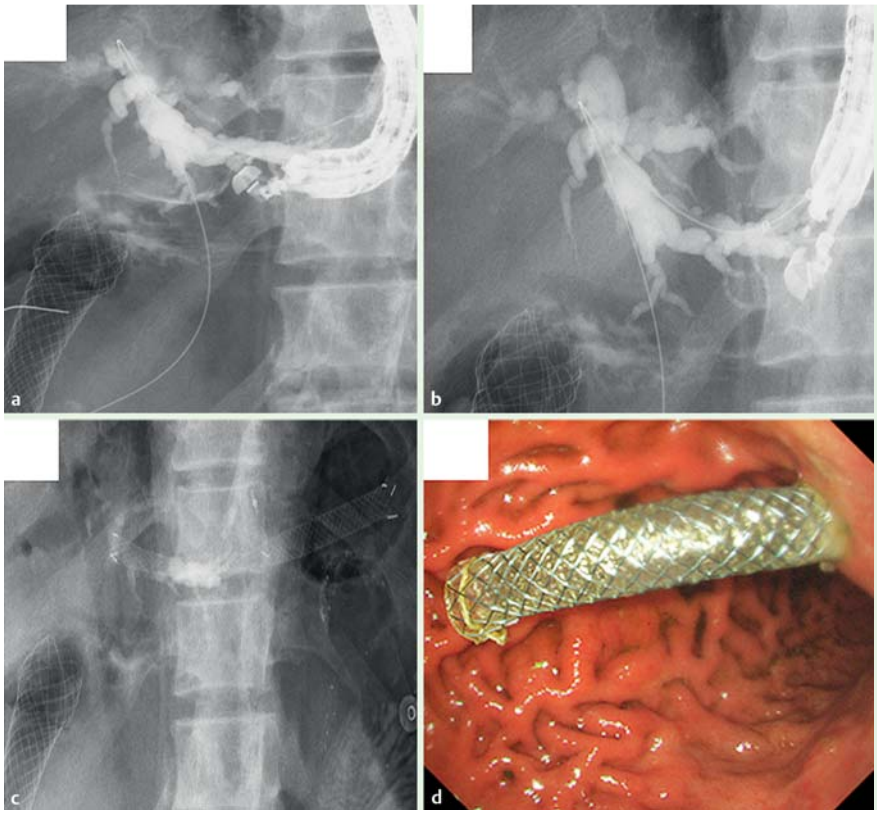

Fig. 3 Endoscopic ultrasound-guided hepaticogastrostomy. **a** A 0.025-inch guidewire was inserted into common bile duct. **b** A 4-mm balloon dilator was used to dilate the fistula. **c, d** A metallic stent was placed from the intrahepatic bile duct to the stomach.

apeutic endoscopy, EUS, and ERCP. Both EUS and ERCP were essential for EUS-guided biliary drainage: puncture of the bile duct required EUS and stent placement for biliary drainage required ERCP. All patients were given antibiotics before undergoing any procedure, and all patients underwent computed tomography (CT) scan the day after both duodenal stent placement and EUS-guided biliary drainage.

Duodenal stent placement (Fig. 1)

All procedures were performed using a colonoscope (CF260AZI; Olympus Optical Co. Ltd., Tokyo, Japan). The colonoscope was advanced to the obstructed site of the duodenum, and a 0.035-inch stiff guidewire (Easy Pass – Medi-Globe GmbH, Rosenheim, Germany) or a 0.025-inch guidewire was advanced through the duodenal stenosis using an ERCP catheter (MTW Endoskopie, Düsseldorf, Germany) (Fig. 1a). Contrast medium was injected, and the length of the stenosis was measured (Fig. 1b). A duodenal metallic stent was then inserted (Niti-S Duodenal Uncovered Metallic Stent – TaeWoong Medical, Seoul, Korea; Century Medical Inc., Tokyo, Japan) (Fig. 1c, d).

EUS-CDS (Fig. 2)

An echoendoscope (GF-UCT260; Olympus Optical Co. Ltd.) connected to an ultrasound device (SSD5500; Aloka, Tokyo, Japan) was introduced into the duodenal bulb (proximal to the stenosis), and the extrahepatic bile duct was identified to avoid puncturing the cystic duct. The extrahepatic bile duct was punctured using a 19-G needle (Sono Tip Pro Control 19G – Medi-Globe GmbH; Medico's Hirata Inc.) (Fig. 2a). Next, contrast medium was injected, and a 0.035-inch guidewire (Easy Pass) was inserted. To dilate the fistula, an ERCP catheter (MTW Endoskopie) was inserted (Fig. 2b). If the stent delivery system could not be inserted, the fistula was dilated using a 4-mm balloon catheter. Finally, a metallic stent (10 mm × 6 cm, Wallstent – Boston Scientific Japan, Tokyo, Japan; Bona stent – Sewoon Medical Co., Ltd., Seoul, Korea; Medico's Hirata Inc.) was inserted from the extrahepatic bile duct to the duodenum (Fig. 2c, d).

EUS-HGS (Fig. 3)

An echoendoscope was advanced into the stomach, and the intrahepatic bile duct (segment 3; B3) was identified. B3 was punctured using a 19-G fine-needle aspiration needle, and contrast medium was injected. A 0.025-inch guidewire was then inserted into the right intrahepatic or common bile duct (Fig. 3a). Next, if it was difficult to pass the delivery system for the metallic stent through the stomach and bile duct wall, a 4-mm balloon dilator (Hurricane balloon dilator; Boston Scientific Japan) was used to dilate the fistula (Fig. 3b). Finally, a metallic stent was placed from B3 to the stomach (10 mm × 10 cm, End-bare type, Niti-S Biliary Cover Stent – TaeWoong Medical; Century Medical Inc., Tokyo, Japan) (Fig. 3c, d).

Definitions

The type of duodenal stenosis was classified according to the location of the stenosis in relation to the ampulla of Vater (type I, proximal to and no involvement of the ampulla of Vater; type II, affecting the second part of the duodenum and the ampulla of Vater; and type III, affecting the third part of the duodenum without involvement of the ampulla of Vater) [20].

The patency of stents used for duodenal and EUS-guided biliary drainage was measured from the day of stent placement to stent dysfunction, patient death, or last follow-up. Stent dysfunction included stent obstruction, stent migration, and cholangitis.

Recurrence of obstructive jaundice on laboratory examination and biliary dilation on imaging such as CT was considered to be due to stent obstruction. Stent migration was examined by CT.

Cholangitis was defined as liver enzyme elevation and typical symptom such as fever.

Technical success of EUS-guided biliary drainage or duodenal stenting was defined as complete stent placement. Functional success of EUS-guided biliary drainage was defined as a decrease in bilirubin to < 75 % of pre-drainage levels within 30 days [9]. Adverse events were classified as early (up to and including 14 days after EUS-guided biliary drainage) or late (at any time from 14 days after the procedure).

Statistical analysis

Results are presented as mean (SD). Patient characteristics were compared by Student's *t* test for continuous variables and Fisher's exact test for categorical variables.

Overall survival was measured from the day that EUS-guided biliary drainage was performed to the time of death or last follow-up examination. Survival curves for overall survival, duodenal stent patency, and biliary stent patency were estimated using the Kaplan – Meier method. The log-rank test was used to compare survival curves, and censored data were taken into account.

The method using propensity scores was performed for survival curves adjusted for covariates [21]. Covariates were selected by judging whether the following two conditions could be ruled out clinically: the factor was related to the drainage procedure (EUS-CDS or EUS-HGS), and the factor was related to stent patency or adverse events. When these two relationships could not be ruled out, the factor was included as a covariate. This is because over-adjustment bias may be generated if a factor, for which at least one of these two relationships can be ruled out, is a covariate [22]. Even if neither of these two relationships could be ruled out, factors that were regarded as intermediate variables, which could generate collider stratification bias, were excluded [23]. The propensity score for each patient was calculated using the logistic regression model, with drainage procedure as the response variable and covariates as the explanatory variables, and the adjusted survival curves were created by weighting the calculated propensity score for each patient.

Logistic regression was used to estimate the odds ratio (OR) and the 95 % confidence interval (CI) of various factors associated with increasing frequency of adverse events.

Differences with a *P* value of less than 0.05 were considered to be significant. All analyses were performed using SAS version 9.1.3 software (SAS Institute, Inc., Cary, North Carolina, USA).

Results

Patient characteristics

A total of 39 patients were enrolled in the study; 13 underwent EUS-CDS (age 71 years [SD 10.7]; male:female, 62 %:38 %), and 26 underwent EUS-HGS (age 70 years [SD 8.1]; male:female, 50 %:50 %) (**Table 1**). The EUS-CDS group comprised 11 pancreaticobiliary cancers and 2 others, and the EUS-HGS group included 21 pancreaticobiliary cancers and 5 others. The site of the duodenal stenosis was not significantly different between the groups ($P = 0.08$).

Early adverse events were not seen in any patients. Late adverse events were seen in eight patients, with six cases (46 %) of nonocclusion cholangitis (without metallic stent obstruction) in the EUS-CDS group, and two cases (8 %) of stent occlusion due to sludge in the EUS-HGS group. The six EUS-CDS patients underwent conversion to EUS-HGS from EUS-CDS, and no further cholangitis occurred until patient death. Late adverse events occurred significantly more often in the EUS-CDS group ($P = 0.005$).

Comparison of EUS-CDS and EUS-HGS

Fig. 4 shows the Kaplan – Meier curve of overall survival by type of EUS-guided biliary drainage. There was no significant difference between the groups (EUS-CDS median 98 days, EUS-HGS median 133 days; hazard ratio (HR) 0.648, 95 %CI 0.309 – 1.359; $P = 0.247$).

Fig. 5 shows the Kaplan – Meier curve of duodenal stent patency by type of EUS-guided biliary drainage. Again, no significant difference was observed between the groups (EUS-CDS median 42 days, EUS-HGS median 113 days; HR 0.557, 95 %CI 0.335 – 1.467; $P = 0.343$).

Fig. 6 shows the Kaplan – Meier curves of biliary stent patency by type of EUS-guided biliary biliary drainage. The log-rank test showed that biliary stent patency was significantly longer in the EUS-HGS group than in the EUS-CDS group (EUS-CDS median 43 days, EUS-HGS median 133 days; HR 0.492, 95 %CI 0.239 – 1.013; $P = 0.0497$).

Fig. 7, **Fig. 8**, and **Fig. 9** show the adjusted Kaplan – Meier curves of overall survival, duodenal stent patency, and biliary stent patency, respectively, where the following six factors were selected as covariates: age (≥ 75 or < 75 years), sex (male/female), pancreaticobiliary carcinoma, type of duodenal stenosis (Type I or other), length of duodenal stenosis (≥ 3 cm or < 3 cm), and size of tumor (≥ 3 cm or < 3 cm). For overall survival, no significant difference was observed between the groups (EUS-CDS median 95

Table 1 Patient characteristics.

	EUS-CDS (n = 13)	EUS-HGS (n = 26)	P-value
Age, mean (SD), years	71 (10.7)	70 (8.1)	0.62
Sex, male:female, n	8:5	13:13	0.50
Total serum bilirubin, mean (SD), mg/dL	11.5 (9.5)	7.2 (5.9)	0.25
Tumor size, mean (SD), cm	3.66 (1.46)	3.60 (2.10)	0.42
Length of stenosis, mean (SD), cm	4.28 (2.4)	4.10 (3.25)	0.54
Type of duodenal stenosis, n (%)			0.08
I	7 (54)	21 (81)	
II	6 (46)	5 (19)	
III	0	0	
Chemotherapy, n (%)	3 (23)	9 (35)	0.42
Adverse events	6	2	0.005
Final diagnosis, n (%)			0.78
Pancreaticobiliary cancer	11 (85)	21 (81)	
Others	2 (15)	5 (19)	

EUS, endoscopic ultrasound; CDS, choledochoduodenostomy; HGS, hepaticogastrostomy.

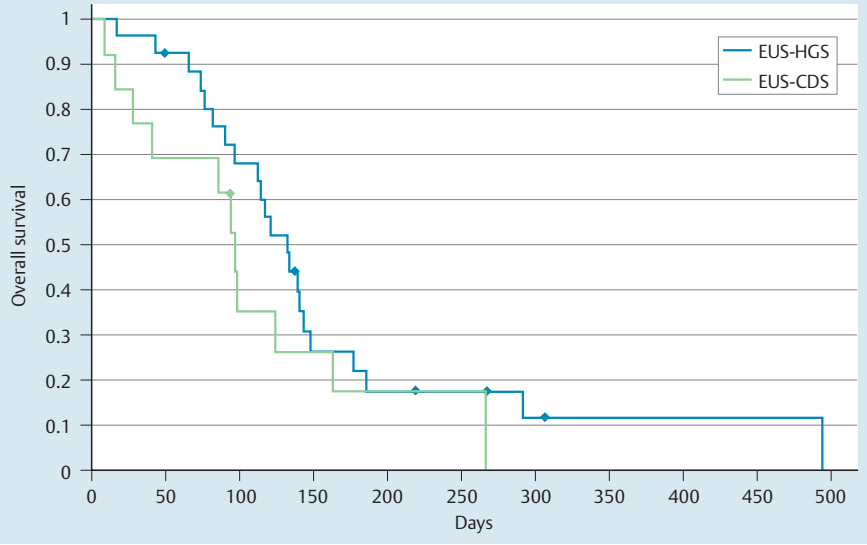

Fig. 4 The Kaplan – Meier curve of overall survival by type of endoscopic ultrasound (EUS)-guided biliary drainage. No statistically significant difference was observed between the groups (EUS-CDS median 98 days, EUS-HGS median 133 days; hazard ratio 0.648, 95 % confidence interval 0.309 – 1.359; $P = 0.247$). CDS, choledochoduodenostomy; HGS, hepaticogastrostomy.

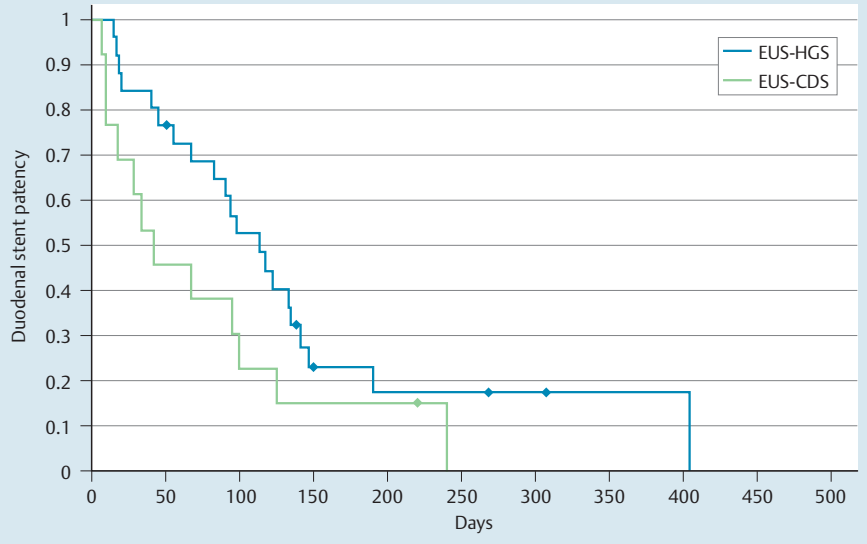

Fig. 5 The Kaplan – Meier curve of duodenal stent patency by type of endoscopic ultrasound (EUS)-guided biliary drainage. No statistically significant difference was observed between the groups (EUS-CDS median 42 days, EUS-HGS median 113 days; hazard ratio 0.557, 95 % confidence interval 0.335 – 1.467; $P = 0.343$). CDS, choledochoduodenostomy; HGS, hepaticogastrostomy.

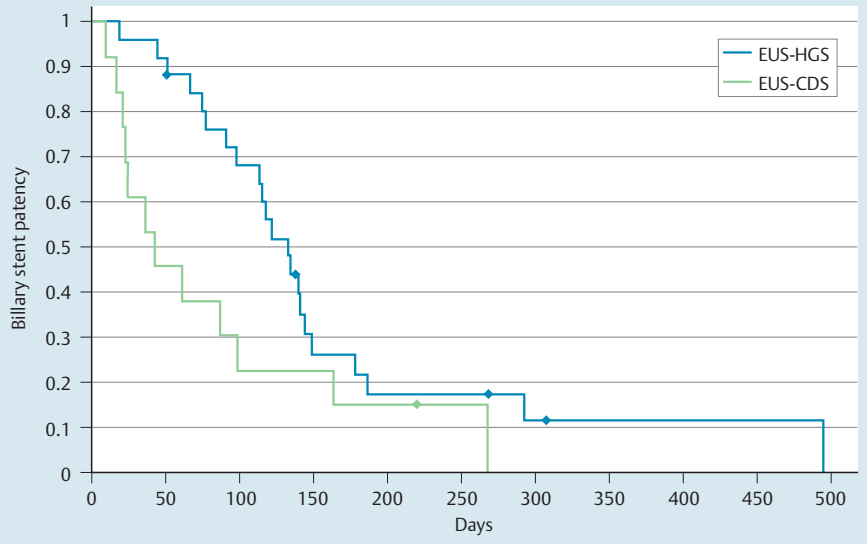

Fig. 6 The Kaplan – Meier curve of biliary stent patency by type of endoscopic ultrasound (EUS)-guided biliary drainage. The log-rank test showed that biliary stent patency was significantly longer in the EUS-HGS group than in the EUS-CDS group (EUS-CDS median 43 days, EUS-HGS median 133 days; hazard ratio 0.492, 95 % confidence interval 0.239 – 1.013; $P = 0.0497$). CDS, choledochoduodenostomy; HGS, hepaticogastrostomy.

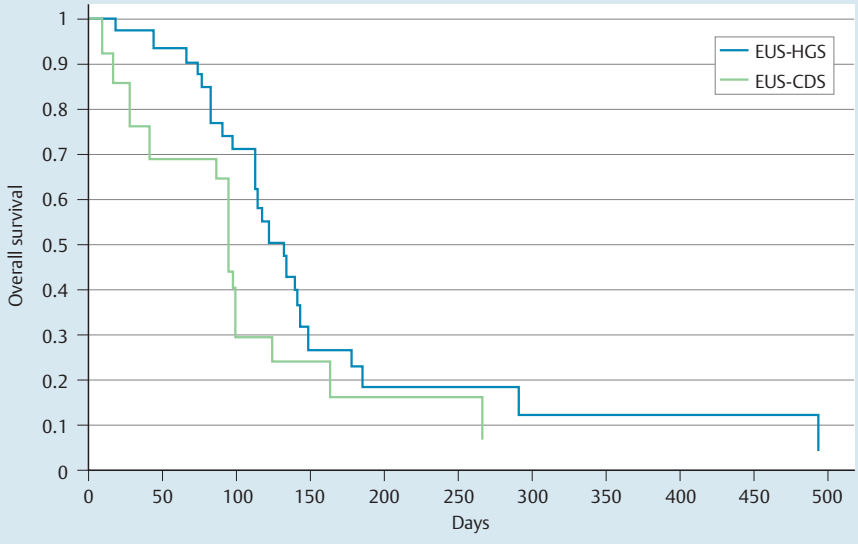

Fig. 7 The adjusted Kaplan–Meier curve of overall survival by type of endoscopic ultrasound (EUS)-guided biliary drainage. No statistically significant difference was observed between the groups (EUS-CDS median 95 days, EUS-HGS median 133 days; hazard ratio 0.531, 95 % confidence interval 0.237 – 1.193; $P = 0.123$). CDS, choledochoduodenostomy; HGS, hepaticogastrostomy.

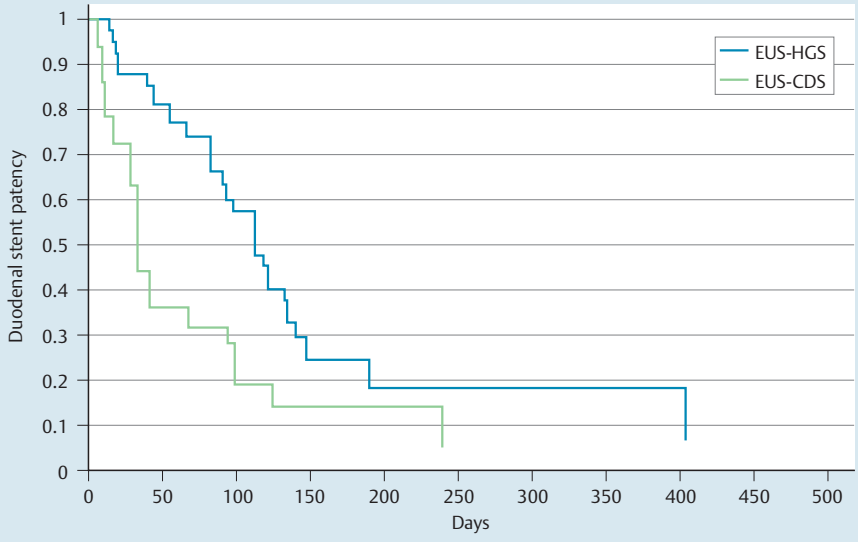

Fig. 8 The adjusted Kaplan – Meier curve of duodenal stent patency by type of endoscopic ultrasound (EUS)-guided biliary drainage. Stent patency was significantly longer in the EUS-HGS group than in the EUS-CDS group (EUS-CDS median 34 days, EUS-HGS median 113 days; hazard ratio 0.415, 95 % confidence interval 0.175 – 0.984; $P = 0.046$). CDS, choledochoduodenostomy; HGS, hepaticogastrostomy.

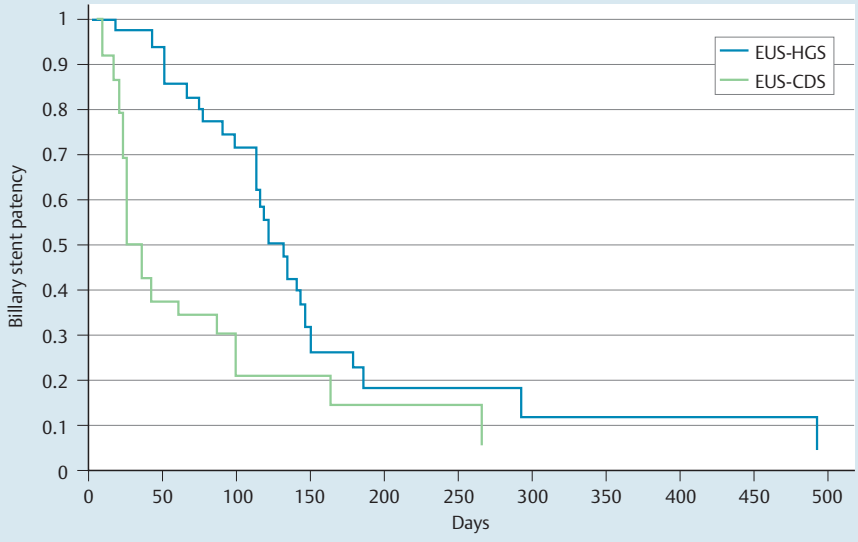

Fig. 9 The adjusted Kaplan – Meier curve of biliary stent patency by type of endoscopic ultrasound (EUS)-guided biliary drainage. Stent patency was significantly longer in the EUS-HGS group than in the EUS-CDS group (EUS-CDS median 37 days, EUS-HGS median 133 days; hazard ratio 0.391, 95 % confidence interval 0.156 – 0.981; $P = 0.045$). CDS, choledochoduodenostomy; HGS, hepaticogastrostomy.

days, EUS-HGS median 133 days; HR 0.531, 95 %CI 0.237 – 1.193; *P* = 0.123). However, duodenal stent patency and biliary stent patency were significantly longer in the EUS-HGS group than in the EUS-CDS group (duodenal stent patency: EUS-CDS median 34 days, EUS-HGS median 113 days; HR 0.415, 95 %CI 0.175 – 0.984; *P* = 0.046; biliary stent patency: EUS-CDS median 37 days, EUS-HGS median 133 days; HR 0.391, 95 %CI 0.156 – 0.981; *P* = 0.045).

Risk factors for adverse events

Risk factors associated with adverse events of EUS-guided biliary drainage were identified using logistic regression analysis. Age (OR 2.308, 95 %CI 0.466 – 11.422; *P* = 0.305), sex (OR 0.938, 95 %CI 0.198 – 4.438; *P* = 0.935), length of stenosis (OR 2.308, 95 %CI 0.466 – 11.442; *P* = 0.305), site of stenosis (OR 3.00, 95 %CI 0.032 – 2.780; *P* = 0.289), and size of tumor (OR 0.462, 95 %CI 0.080 – 2.662; *P* = 0.387) were not associated with adverse events. Only EUS-guided biliary drainage technique (EUS-CDS/EUS-HGS) was associated with adverse events (OR 10.285, 95 %CI 1.686 – 62.733; *P* = 0.012).

Discussion

Cholangitis, which is one of the adverse events of stent placement under ERCP, may reduce patient quality of life, and the rates of this adverse event have been reported to be between 6.5 % and 22 % [24 – 27]. One of the causes of cholangitis may be duodenobiliary reflux, with metallic stent placement across the ampulla of Vater being a predisposing factor. In addition, duodenobiliary reflux often results in metallic stent occlusion or ascending cholangitis [28, 29]. The rate of cholangitis may be higher in cases of obstructive jaundice with duodenal obstruction than in cases without duodenal obstruction [30, 31]. In addition, duodenal metallic stent placement has been shown to be a significant risk factor for biliary metallic stent dysfunction [30, 31].

EUS-guided biliary drainage has a clinical impact for patients with obstructive jaundice complicated by duodenal obstruction and an inaccessible papilla. EUS-guided biliary drainage also has the advantage over stent placement under ERCP guidance in that acute pancreatitis is unlikely. Although EUS-guided biliary drainage is associated with a risk of bile peritonitis and stent migration, technical and functional success rates are high, and several efforts to prevent adverse events have also been reported [6 – 8]. There have been only a few reports of EUS-guided biliary drainage for patients with obstructive jaundice and duodenal obstruction [11 – 19]. Among previous reports, as shown in **Table e2** (available online), only seven have described EUS-guided biliary drainage for patients with duodenal stents. In these reports, as in the present study, the main disease was pancreatic cancer, and technical and functional success rates were high. Stent patency was also similar in the reported cases and the present study. However, a lack of data on late adverse events, including cholangitis, makes it difficult to compare these previous studies with the present results.

Hamada et al. [19] reported that transmural biliary drainage can be an alternative to transpapillary drainage in patients with an indwelling duodenal metallic stent. Among 21 patients (7 EUS-BD and 14 transpapillary drainage), the stent patency rate was higher in EUS-guided biliary drainage patients than in transpapillary patients (100 % vs. 71 % at 1 month, and 83 % vs. 29 % at 3 months) [19]. In addition, the rate of stent dysfunction also tended to be lower in EUS-guided biliary drainage patients than in transpapillary patients (14 % vs. 54 %; *P* = 0.157). Although the results need to be validated by a randomized, controlled trial, EUS-guided biliary drainage may be superior to ERCP-guided drainage for obstructive jaundice patients with duodenal obstruction.

No reports have determined which EUS-guided biliary drainage technique has the best outcomes. In the present study, although overall survival was not different between the EUS-HGS group and the EUS-CDS group, stent patency of the biliary metallic stent was significantly longer in the EUS-HGS group than in the EUS-CDS group. Furthermore, the only risk factor for adverse events such as cholangitis was the EUS-guided biliary drainage technique performed. The reasons for this were examined, and the following are offered as possible explanations. Because the duodenal lumen that is invaded by tumor is narrow compared with the stomach, duodenobiliary reflux may occur easily and directly. Indeed, in the present study, nonoccluded cholangitis due to duodenobiliary reflux was not seen in the EUS-HGS group. Environmental differences in the bacteria between the stomach and the duodenum may play an important role in the development of cholangitis; *Helicobacter pylori* may not be present in the stomach compared with the duodenum. Indeed, the EUD-CDS patients who developed cholangitis did not have a recurrence of cholangitis after conversion to EUS-HGS.

The present study has several limitations, including patient selection bias and the retrospective study design. Patient selection bias is the biggest limitation because type I duodenal obstruction was rare in the EUS-CDS group. However, the statistical power of the study is relatively high because of the large number of patients included compared with previous studies. In addition, there are no previous published studies that compared EUS-CDS with EUS-HGS for patients with obstructive jaundice and duodenal obstruction. Therefore, the present study may be the first of its kind, although the results need to be validated by a prospective, randomized, controlled trial.

In conclusion, EUS-HGS may be better than EUS-CDS in cases of obstructive jaundice with duodenal obstruction, with longer stent patency and fewer adverse events.

Competing interests: None

Institutions

[1] 2nd Department of Internal Medicine, Osaka Medical College, Osaka, Japan
[2] Clinical Research Center, Kinki University Hospital, Osaka-Sayama, Japan
[3] Department of Gastroenterology and Hepatology, Kinki University Faculty of Medicine, Osaka-Sayama, Japan
[4] Department of Radiology, Osaka Medical College, Osaka, Japan
[5] Department of Gastroenterology, Aichi Cancer Center Hospital, Nagoya, Japan

References

1 *Fogel EL, Sherman S, Devereaux BM* et al. Therapeutic biliary endoscopy. Endoscopy 2001; 33: 31 – 38
2 *Willams EJ, Taylor S, Fairclough P* et al. Are we meeting the standards set for endoscopy? Results of a large-scale prospective survey of endoscopic retrograde cholangio-pancreatograph practice Gut 2007; 56: 821 – 829
3 *Bories E, Pesenti C, Caillo F* et al. Transgastric endoscopic ultrasonography-guided biliary drainage: results of a pilot study. Endoscopy 2007; 39: 287 – 291
4 *Giovannini M, Dotti M, Bories E* et al. Hepaticogastrostomy by echo-endoscopy as a palliative treatment in a patient with metastatic biliary obstruction. Endoscopy 2003; 35: 1076 – 1078
5 *Park doH, Jang JW, Lee SS* et al. EUS-guided biliary drainage with transluminal stenting after failed ERCP: predictors of adverse events and long-term results. Gastrointest Endosc 2011; 74: 1276 – 1284

6 *Ogura T*, *Kurisu Y*, *Masuda D* et al. Novel method of endoscopic ultrasound-guided hepaticogastrostomy to prevent stent dysfunction. J Gastroenterol Hepatol 2014; 29: 1815 – 1821
7 *Park doH*, *Jeong SU*, *Lee BU* et al. Prospective evaluation of treatment algorithm with enhanced guidewire manipulation protocol for EUS-guided biliary drainage after failed ERCP (with video). Gastrointest Endosc 2013; 78: 91 – 101
8 *Hara K*, *Yamao K*, *Hijioka S* et al. Prospective clinical study of endoscopic ultrasound-guided choledochoduodenostomy with direct metallic stent placement using a forward-viewing echoendoscope. Endoscopy 2013; 45: 392 – 396
9 *Itoi T*, *Isayama H*, *Sofuni A* et al. Stent selection and tips on placement technique of EUS-guided biliary drainage: transduodenal and transgastric stenting. J Hepatobiliary Pancreat Sci 2011; 18: 664 – 672
10 *Baron TH*. Expandable metal stents for the treatment of cancerous obstruction of the gastrointestinal tract. N Engl J Med 2001; 344: 1681 – 1687
11 *Horaguchi J*, *Fujita N*, *Noda Y* et al. Endosonography-guided biliary drainage in cases with difficult transpapillary endoscopic biliary drainage. Dig Endosc 2009; 21: 239 – 244
12 *Belletrutti PJ*, *Gerdes H*, *Schattner MA*. Successful endoscopic ultrasound-guided transduodenal biliary drainage through a pre-existing duodenal stent. JOP 2010; 11: 234 – 236
13 *Iwamuro M*, *Kawamoto H*, *Harada R* et al. Combined duodenal stent placement and endoscopic ultrasonography-guided biliary drainage for malignant duodenal obstruction with biliary stricture. Dig Endosc 2012; 22: 236 – 240
14 *Belletrutti PJ*, *DiMaio CJ*, *Gerdes H* et al. Endoscopic ultrasound guided biliary drainage in patients with unapproachable ampullae due to malignant duodenal obstruction. J Gastrointest Cancer 2011; 42: 137 – 142
15 *Kawakubo K*, *Isayama H*, *Nakai Y* et al. Simultaneous duodenal metal stent placement and EUS-guided choledochoduodenostomy for unresectable pancreatic cancer. Gut Liver 2012; 6: 399 – 402
16 *Khashab MA*, *Fujii LL*, *Baron TH* et al. EUS-guided biliary drainage for patients with malignant biliary obstruction with an indwelling duodenal stent (with videos). Gastrointest Endosc 2012; 76: 209 – 231
17 *Tonozuka R*, *Itoi T*, *Sofuni A* et al. Endoscopic double stenting for the treatment of malignant biliary and duodenal obstruction due to pancreatic cancer. Dig Endosc 2013; 25: 100 – 108
18 *Artifon EL*, *Frazão MS*, *Wodak S* et al. Endoscopic ultrasound-guided choledochoduodenostomy and duodenal stenting in patients with unresectable periampullary cancer: one-step procedure by using linear echoendoscope. Scand J Gastroenterol 2013; 48: 374 – 379
19 *Hamada T*, *Isayama H*, *Nakai Y* et al. Transmural biliary drainage can be an alternative to transpapillary drainage in patients with indwelling duodenal stent. Dig Dis Sci 2014; 59: 1931 – 1938
20 *Utignani M*, *Tringail A*, *Shah SG* et al. Combined endoscopic stent insertion in malignant biliary and duodenal obstruction. Endoscopy 2007; 27: 1243 – 1248
21 *Cole SR*, *Hernan MA*. Adjusted survival curves with inverse probability weights. Comput Methods Programs Biomed 2004; 75: 45 – 49
22 *Schisterman EF*, *Cole SR*, *Platt RW*. Overadjustment bias and unnecessary adjustment in epidemiological studies. Epidemiology 2009; 20: 488 – 495
23 *Cole SR*, *Platt RW*, *Schisterman EF* et al. Illustrating bias due to conditioning on a collider. Int J Epidemiol 2010; 39: 417 – 420
24 *Adler DG*, *Baron TH*, *Davila RE* et al. ASGE guideline: the role of ERCP in diseases of the biliary tract and the pancreas. Gastrointest Endosc 2005; 6: 1 – 8
25 *Dumonceau JM*, *Tringali A*, *Blero D* et al. Biliary stenting: indications, choice of stents and results. Endoscopy 2012; 44: 277 – 298
26 *Cheng JL*, *Bruno MJ*, *Bergman JJ* et al. Endoscopic palliation of patients with biliary obstruction caused by nonresectable hilar cholangiocarcinoma: efficacy of self-expandable metallic Wallstents. Gastrointest Endosc 2002; 56: 33 – 39
27 *Wasan SM*, *Ross WA*, *Staerkel GA* et al. Use of expandable metallic biliary stents in resectable pancreatic cancer. Am J Gastroenterol 2009; 70: 284 – 289
28 *Misra S*, *Dwivedi M*. Reflux of duodenal contents and cholangitis in patients undergoing self-expanding metal stent placement. Gastrointest Endosc 2009; 70: 317 – 321
29 *Okamoto T*, *Fujioka S*, *Yanagisawa S* et al. Placement of a metallic stent across the main duodenal papilla may predispose to cholangitis. Gastrointest Endosc 2006; 63: 792 – 796
30 *Hamada T*, *Isayama H*, *Nakai Y* et al. Duodenal invasion is a risk factor for the early dysfunction of biliary metal stents in unresectable cancer. Gastrointest Endosc 2011; 74: 317 – 321
31 *Hamada T*, *Nakai Y*, *Isayama H* et al. Duodenal metal stent placement is a risk factor for biliary metal stent dysfunction: an analysis using a time-dependent covariate. Surg Endosc 2013; 27: 1243 – 1248

Correction

Ogura T, Chiba Y, Masuda D et al. Comparison of the clinical impact of endoscopic ultrasound-guided choledochoduodenostomy and hepaticogastrostomy for bile duct obstruction with duodenal obstruction. Endoscopy 2015 DOI 10.1055/s-0034-1392859

The name of the co-author Kazuhide Higuchi was misspelt in the authors' list. The name should read "Kazuhide Higuchi".

We apologize to the authors for this error.

Table e2

online content viewable at:
http://dx.doi.org/10.1055/s-0034-1392859

ORIGINAL ARTICLE

Pathogenicity of IgG in patients with IgG4-related disease

Masahiro Shiokawa,[1] Yuzo Kodama,[1] Katsutoshi Kuriyama,[1] Kenichi Yoshimura,[2] Teruko Tomono,[1] Toshihiro Morita,[1] Nobuyuki Kakiuchi,[1] Tomoaki Matsumori,[1] Atsushi Mima,[1] Yoshihiro Nishikawa,[1] Tatsuki Ueda,[1] Motoyuki Tsuda,[1] Yuki Yamauchi,[1] Ryuki Minami,[1] Yojiro Sakuma,[1] Yuji Ota,[1] Takahisa Maruno,[1] Akira Kurita,[1] Yugo Sawai,[1] Yoshihisa Tsuji,[1] Norimitsu Uza,[1] Kazuyoshi Matsumura,[3] Tomohiro Watanabe,[1] Kenji Notohara,[4] Tatsuaki Tsuruyama,[5] Hiroshi Seno,[1] Tsutomu Chiba[1]

▶ Additional material is published online only. To view please visit the journal online (http://dx.doi.org/10.1136/gutjnl-2015-310336).

For numbered affiliations see end of article.

Correspondence to
Dr Yuzo Kodama Department of Gastroenterology and Hepatology, Kyoto University Graduate School of Medicine, 54 Shogoin-kawahara-cho, Sakyo-ku, Kyoto 606-8507, Japan;
kodamayu@kuhp.kyoto-u.ac.jp

Received 13 July 2015
Revised 29 January 2016
Accepted 18 February 2016
Published Online First
10 March 2016

ABSTRACT

Objective IgG4-related disease (IgG4-RD) is a systemic disease characterised by elevated serum IgG4 and IgG4-positive lymphoplasmacytic infiltration in the affected tissues. The pathogenic role of IgGs, including IgG4, in patients with IgG4-RD, however, is unknown.

Design We examined the pathogenic activity of circulating IgGs in patients with IgG4-RD by injecting their IgGs into neonatal male Balb/c mice. Binding of patient IgGs to pancreatic tissue was also analysed in an ex vivo mouse organ culture model and in tissue samples from patients with autoimmune pancreatitis (AIP).

Results Subcutaneous injection of patient IgG, but not control IgG, resulted in pancreatic and salivary gland injuries. Pancreatic injury was also induced by injecting patient IgG1 or IgG4, with more destructive changes induced by IgG1 than by IgG4. The potent pathogenic activity of patient IgG1 was significantly inhibited by simultaneous injection of patient IgG4. Binding of patient IgG, especially IgG1 and IgG4, to pancreatic tissue was confirmed in both the mouse model and AIP tissue samples.

Conclusions IgG1 and IgG4 from patients with IgG4-RD have pathogenic activities through binding affected tissues in neonatal mice.

Significance of this study

What is already known on this subject?

- IgG4-related disease (IgG4-RD) is considered an autoimmune disease due to its favourable response to steroid treatment. The pathophysiology of IgG4-RD, however, remains largely unknown.
- Dramatic responses to treatment with rituximab, an anti-CD20 antibody, in patients with IgG4-RD suggest that elevated serum IgG and/or IgG4 in patients with IgG4-RD have pathogenic roles.
- In pemphigus vulgaris (PV), the pathogenicity of autoantibodies was established by inducing pemphigus in neonatal mice after passive transfer of immunoglobulins from patients with PV.

What are the new findings?

- Subcutaneous injection of patient IgG, but not control IgG, resulted in neonatal mouse pancreatic and salivary gland injuries.
- IgG1 and IgG4 in patients with IgG4-RD have pathogenic effects on neonatal mouse pancreas and salivary gland.
- This antibody in patients with IgG4-RD might recognise molecules in the extracellular matrix of neonatal mouse tissues.

How might it impact on clinical practice in the foreseeable future?

- If the pathogenic effects of IgG in patients with IgG4-RD observed in this study are involved in the pathophysiology of human autoimmune pancreatitis, our data in neonatal mice might provide clues to the discovery of an autoantigen in patients with IgG4-RD.
- An ELISA system detecting the autoantibodies for this antigen may be a useful tool for diagnosis and disease activity monitoring of IgG4-RD.

INTRODUCTION

IgG4-related disease (IgG4-RD) is a novel immune-mediated disorder characterised by elevated serum IgG4 levels and IgG4-positive lymphoplasmacytic infiltration in the involved organs in association with tumour-like swelling and variable degrees of tissue injury and fibrosis.[1] These distinctive clinical and pathological features were first identified in patients with autoimmune pancreatitis (AIP), now referred as type 1 AIP, a unique form of chronic pancreatitis.[2 3] Since then, simultaneous or metachronous lesions with pathological features similar to those in the pancreas have been observed in other organs,[4 5] leading to the concept of a new systemic disease named IgG4-RD.[6 7] Along with

Linked

▶ http://dx.doi.org/10.1136/gutjnl-2016-311678

CrossMark

To cite: Shiokawa M, Kodama Y, Kuriyama K, *et al*. *Gut* 2016;**65**:1322–1332.

increased recognition of the concept of IgG4-RD, the number of the patients diagnosed with IgG4-RD is rapidly increasing. The pathophysiology of IgG4-RD, however, remains largely unknown.

Previous reports revealed the presence of several autoantibodies in the serum from patients with IgG4-RD.[8–13] Moreover, it is well recognised that steroid treatment is generally very effective in patients with IgG4-RD. These facts suggest that the disease has an autoimmune nature. Recent studies demonstrated dramatic clinical responses in patients with IgG4-RD to the anti-CD20 antibody rituximab, along with significant depletion of B cells and plasmablasts.[14] These findings suggest that elevated IgG and/or IgG4 levels in patients with IgG4-RD may have pathogenic roles.

IgG4 is considered a non-inflammatory, or rather anti-inflammatory, immunoglobulin because of its distinctive biological characteristics, such as the ability to exchange Fab arms,[15] inability to fix complement and low affinity for Fc receptors.[16] In some diseases, however, IgG4 antibodies act as tissue-destructive autoantibodies, as observed in pemphigus vulgaris (PV),[17] idiopathic membranous glomerulonephritis[18] and muscle-specific kinase myasthenia gravis.[19] In a previous study of PV, the pathogenicity of autoantibodies was first established by inducing pemphigus in neonatal mice after passive transfer of immunoglobulins from patients with PV.[17] Subsequently, IgG4 autoantibodies against intercellular adhesion molecules, desmoglein 1 and 3, were identified in patient sera as the pathogenic antibodies.[20] Humans have most of the mouse genes and important domains are conserved. If human IgG has pathological effects on mice, it may have similar activities in humans.

In the present study, therefore, we injected patient IgGs into neonatal Balb/c mice and investigated the histopathological changes in the affected organs to examine the pathogenic activities of IgG and IgG subtypes derived from patients with IgG4-RD.

MATERIALS AND METHODS

Patients

Serum samples were obtained from 10 consecutive patients who met the comprehensive diagnostic criteria for IgG4-RD 2011,[7] the diagnostic criteria of AIP[21] or IgG4-related kidney disease.[22] In 3 of 10 patients, additional blood samples were collected after 8 weeks treatment with prednisolone. Serum samples were also obtained from five healthy controls and five disease controls (three patients with histologically proven pancreatic cancer and two patients who met the Mayo criteria for primary sclerosing cholangitis[23]). Controls were age-matched (±5 years) and sex-matched with patients with IgG4-RD. An overview of the clinical characteristics of the patients and controls is provided in online supplementary table S1.

Preparation of human IgG

Human IgG injected into mice was prepared from human serum samples by Ab-Rapid PuRe EX (P-015, Prote Nova, Japan) according to the manufacturer's instructions. The IgG was dialysed with phosphate-buffered saline (PBS, pH 7.2), concentrated by ultrafiltration using Amicon Ultra (UFC805024, Millipore, Germany), and stored at −20°C. Concentration of purified IgG was measured using the Human IgG EIA Kit (MK136, Takara, Japan). The IgG fraction purity was confirmed by testing for IgA, IgM, IgE and protein contamination using the Human IgA ELISA Kit (E88-102, Bethyl Laboratories, USA), Human IgM ELISA Kit (E88-100, Bethyl Laboratories), Human IgE ELISA Kit (E88-108, Bethyl Laboratories) and Coomassie Brilliant Blue staining, respectively.

Preparation of human IgG subclasses

IgG1 and IgG4 were purified from human serum samples by Capture Select IgG1 (Hu) affinity matrix (191303005, Invitrogen, USA) and Capture Select IgG4 (Hu) affinity matrix (290005, Invitrogen), respectively, according to the manufacturer's instructions. Briefly, human serum was loaded onto the column and washed with PBS. The IgG subclass fraction (IgG1 or IgG4) was eluted with 0.1 M glycine (pH 2.8) and neutralised with 1.5 M Tris (pH 7.5). The eluted IgG subclass fractions were concentrated by ultrafiltration using Amicon Ultra (UFC805024, Millipore) under extensive washing with PBS (pH 7.2). Concentrations of purified IgG subclasses were quantitated by Human IgG1 Platinum ELISA (BMS2092, eBioscience, USA), Human IgG2 Platinum ELISA (BMS2093, eBioscience), Human IgG3 Platinum ELISA (BMS2094, eBioscience) and Human IgG4 Platinum ELISA (BMS2095, eBioscience), according to the manufacturer's instructions. Subclass purity was confirmed by testing for IgA, IgM, IgE, the other IgG subclasses, and protein contamination using the protocol described above.

Concentrations of human IgGs or IgG subclasses in human and mouse sera

Concentrations of human IgG, IgG1, IgG2, IgG3 and IgG4 in human and mouse sera were measured by the methods described above.

Animal model

See online supplementary methods.

Ex vivo mouse pancreatic organ culture assay

Ex vivo pancreatic organ culture assay was performed by following the method of the ex vivo PV assay.[24] Briefly, anaesthetised 8-week-old mice (SLC, Japan) were perfused with intravenous administration of PBS. The pancreas was removed and trimmed by removing fat tissue and cut in half. Purified IgG (50 µL, 1 mg/mL) was injected into the pancreas using a 27-gauge needle. The pancreatic tissue was placed into a 24-well cell culture plate (662160, Greiner Bio-one, Germany) with 400 µL PBS containing the purified IgG (1 mg/mL) and maintained in a humidified incubator with 5% CO_2 at 37°C. After 1 h culture, the pancreatic tissue was rinsed with PBS three times for 20 min each, placed into OCT compound, and frozen at −30°C.

Histological evaluation

See online supplementary methods.

Immunohistochemical study

The immunohistochemical study was performed according to standard methods for mouse and human tissue sections. The primary antibodies used were CD3 1:100 (ab16669, Abcam, England), CD45R 1:100 (ab64100, Abcam), F4/80 1:100 (ab6640, Abcam), amylase 1:100 (ab21156, Abcam), human IgG 1:100 (ab109489, Abcam) and Gr1 1:100 (14-5931-82, eBioscience), following antigen retrieval with 10 mM citrate buffer pH 6.0; and IgG4 1:100 (418051, NICHIREI, Japan), collagen IV 1:100 (ab6586, Abcam), following antigen retrieval with proteinase K. Sections were incubated with primary antibodies at room temperature for 60 min. For detection, Universal Dako LSAB+ Kit (Dako, Denmark) was used according to the

manufacturer's instructions. Detection times were equally standardised for all the sections.

Immunofluorescence study

The immunofluorescence study was performed with a standard method for mouse and human tissue sections and mouse organ culture sections. For direct immunofluorescence, fluorescein isothiocyanate-conjugated rabbit antibodies specific to human IgG 1:50 (F0185, Dako), IgG1 1:50 (AF006, The Binding Site, USA), IgG2 1:50 (HP6014, Sigma-Aldrich), IgG3 1:50 (HP6050, Sigma-Aldrich) and IgG4 1:50 (HP6025, Sigma-Aldrich) were used. For indirect immunofluorescence, C1q 1:100 (ab11861, Abcam) and the same primary antibodies described in the Immunohistochemical study section were used

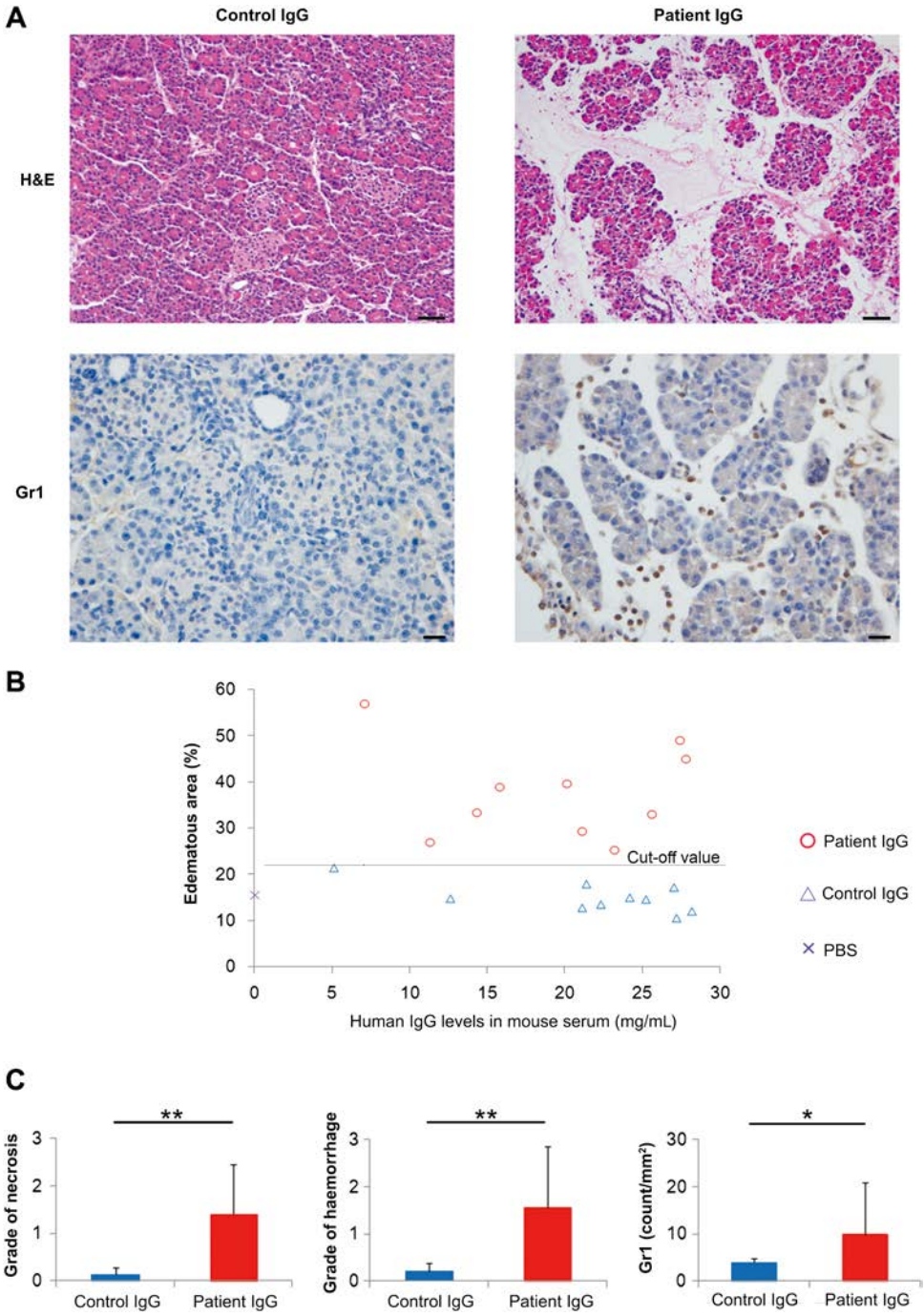

Figure 1 Induction of pancreatic injury in mice by subcutaneous injection of IgG from patients with IgG4-RD. Pancreatic injury 12 h after subcutaneous injection of control IgG (n=10) or patient IgG (n=10) with IgG4-RD. (A) H&E staining and immunohistochemical staining for Gr1 in pancreatic tissue sections. Scale bars: 50 μm (upper panels), 20 μm (lower panels). (B) Oedema (separation) development by IgG injection. The cut-off value of the oedematous area was defined as the mean +2 SD in mice given control IgG or PBS, 21.1%. (C) Histologic grade of necrosis, haemorrhage and Gr1-positive cell count. Data are shown as mean±SEM. *p<0.05 and **p<0.005 by paired Student's t test. (D) Dose-dependent induction of pancreatic injury in mice by injection of IgG from patients with IgG4-RD. Oedematous area, histologic grade of necrosis and haemorrhage in pancreatic tissues were assessed in mice given two different doses of IgG from the same patients (patients 1, 2, 9 and 10) or mice given several different doses of control IgG (control 1) and purchased IgG. (E) Time course of the effect of patient IgG (patients 1 and 9) or control IgG (control 2) and purchased IgG on mouse pancreas. IgG4-RD, IgG4-related disease; PBS, phosphate-buffered saline.

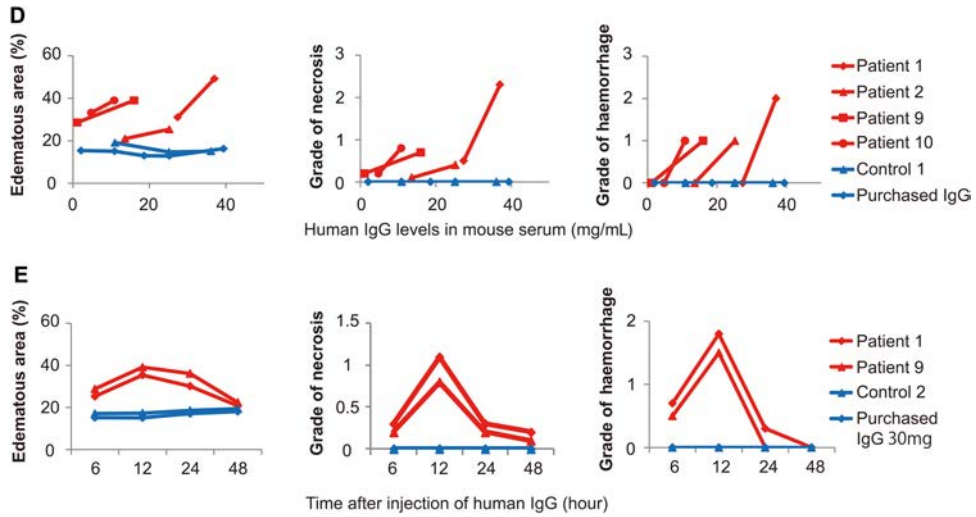

Figure 1 Continued

and as secondary antibodies Alexa Fluor 488 antimouse IgG 1:100 (A-21202, Life Technologies, USA), Alexa Fluor 488 anti-rabbit IgG 1:100 (A-21206, Life Technologies), Alexa Fluor 594 antimouse IgG 1:100 (A-21203, Life Technologies) and Alexa Fluor 594 antirabbit IgG 1:100 (A-21207, Life Technologies) were used.

Immunoelectron microscopy study

See online supplementary methods.

Statistics

Differences were assessed using Student's t test for continuous data and the χ^2 test and the Fisher's exact test for categorical data. Statistical analysis was performed using the Statistical Package for Social Sciences (SPSS V.17.0). All statistical tests were two-sided. A p value of <0.05 was considered statistically significant.

Study approval

Studies involving animals were performed with the approval of the institutional animal ethics committee. Human studies were performed according to the Declaration of Helsinki, and were approved by the Institutional Review Board of Kyoto University Hospital. All patients and controls provided written informed consent prior to inclusion in the study.

RESULTS

Induction of pancreatic injury in mice by subcutaneous injection of IgG from patients with IgG4-RD

Subcutaneous injection of control IgG yielded a dose-dependent increase in the human IgG concentration in neonatal mouse serum (see online supplementary figure S1). Based on these data, the injection dose of patient IgG or each IgG subclass was determined to obtain the actual patient serum concentration in the mouse serum. The dose of the control IgG or IgG subclasses administered to mice was adjusted to that of each corresponding age-matched and sex-matched patient. As a result, serum human IgG concentrations in mice given patient IgG and mice given control IgG were statistically equivalent (19.4 vs 21.4 mg/mL, p=0.53). Under these conditions, subcutaneous injection of patient IgG into neonatal mice induced pancreatic injury (figure 1A) with a maximum change observed 12 h after the injection, whereas control IgG had no effect. Histologically, oedematous changes in the intralobular and interlobular spaces and around the pancreatic duct, acini necrosis, haemorrhage and infiltration of Gr1-positive polymorphonuclear leucocytes were observed in the mouse pancreas injected with patient IgG (figure 1A and see online supplementary figure S2A). No fibrous changes were detected. Quantification of the oedematous area revealed the development of oedema in all of the mice injected with patient IgG, but in none of the mice injected with control IgG (figure 1B). The levels of necrosis, haemorrhage and Gr1-positive cell infiltration were significantly greater in mice injected with patient IgG than in mice injected with control IgG (figure 1C). On the other hand, infiltration of macrophages (F4/80 positive), T cells (CD3 positive) and B cells (CD20 positive) was scarcely induced by injection with patient IgG (data not shown). Pancreatic injuries were induced by injection of patient IgG in a dose-dependent manner (figure 1D). Serum amylase levels were also significantly higher in mice given patient IgG than in mice given control IgG (1652 vs 1307 IU/L, p=0.021). The pathogenic effect of patient IgG on mice was significantly reduced when we used patient IgG obtained 8 weeks after the initiation of steroid treatment (see online supplementary figure S3). The dose of injected patient IgG obtained before and after steroid treatment was equal. These findings clearly demonstrated that IgG in the sera from patients with IgG4-RD had pathogenic effects on mouse pancreas.

Induction of injuries to other organs in mice following subcutaneous injection of IgG from patients with IgG4-RD

In addition to the pancreas, we analysed salivary gland, kidney, prostate, lung, heart, liver and intestine tissue of the mice 12 h after injecting patient or control IgG. Among these organs, the salivary gland exhibited oedematous changes similar to that in the pancreas in all mice injected with patient IgG, but control IgG had no effect (see online supplementary figure S4). Unlike in the pancreas, acini necrosis, haemorrhage and infiltration of Gr1-positive polymorphonuclear leucocytes were not apparent in the salivary glands. The pathogenic activity of patient IgG on the salivary gland was also diminished when we used patient IgG obtained 8 weeks after the initiation of steroid treatment (data not shown). No pathological changes were observed in kidney, prostate, lung, heart, liver or intestine, except for oedematous changes around the lower bile duct.

Deposition of IgG and IgG subclasses from patients with IgG4-RD in mouse tissues

We conducted tissue-staining studies to assess whether the pathogenic activity of patient IgG is mediated by direct binding to pancreatic tissues. Immunohistochemistry detected human IgG and IgG4 deposition at the base of the acini, interlobular space (figure 2A) and around the pancreatic duct (see online supplementary figure S2B) in all mice injected with patient IgG, but not in mice injected with control IgG. IgG1 was weakly detected in 6 of 10 mice given patient IgG, but not in any mice given control IgG (figure 2A). We could not examine the deposition of IgG2 or IgG3 as antibodies for formaldehyde-fixed tissue were not available. Direct immunofluorescence also detected human IgG in pancreatic tissues in mice injected with patient IgG (figure 2B). Dual immunofluorescence studies revealed that the administered patient IgG did not colocalise with pancreatic acini expressing amylase. Most patient IgG colocalised with collagen IV expression in the basement membrane or extracellular matrix (ECM; figure 2B). The immunoelectron microscopy study revealed human IgG, IgG1 and IgG4 deposition at the base of the acini in all mice injected with patient IgG, but not in mice injected with control IgG (see online supplementary figure S5). Consistent with these results, patient IgG4 was easily visualised in the salivary glands of mice injected with patient IgG, but not in mice injected with control IgG (see online supplementary figure S6). To study the formation of

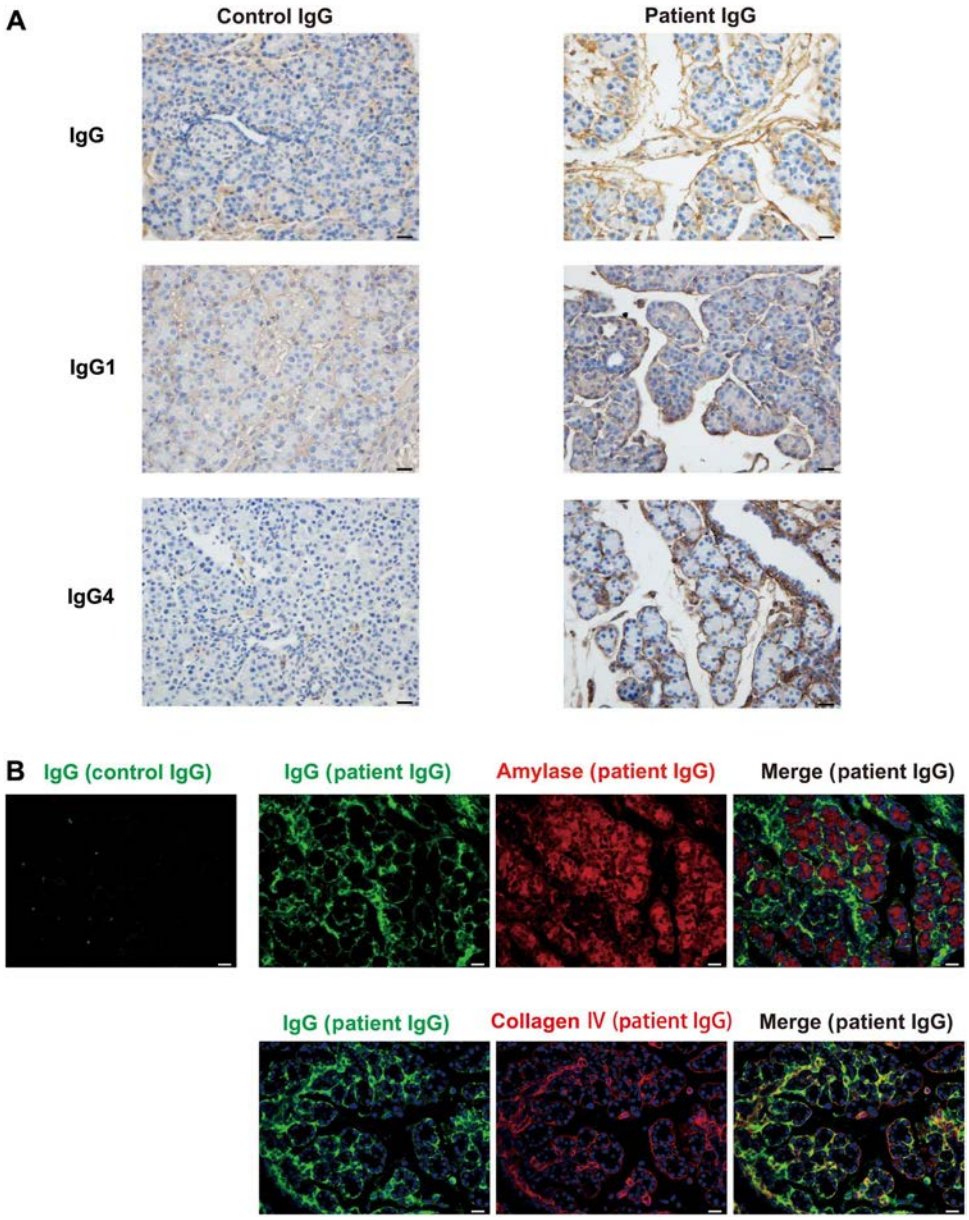

Figure 2 Binding of patient IgG, IgG1 and/or IgG4 to pancreatic tissues in mice injected with IgG from patients with IgG4-RD. Immunohistochemical and immunofluorescence studies 12 h after subcutaneous injection of control IgG or IgG from patients with IgG4-RD. (A) Immunohistochemical staining for IgG, IgG1 and IgG4 of mouse pancreatic tissue sections. Note that IgG and IgG4 were detected at the base of the acini and the interlobular space of pancreatic tissues in all the mice given patient IgG, but not in mice given control IgG. Scale bars: 20 μm. (B) Immunofluorescence staining of mouse pancreas. Upper panels show staining for IgG (green), amylase (red) and a merged image. Lower panels show staining for IgG (green), collagen IV (red) and a merged image. IgG was detected in collagen IV-expressing basement membrane or extracellular matrix. Scale bars: 20 μm. Representative photos are shown. IgG4-RD, IgG4-related disease.

immunocomplexes, we performed an immunofluorescence study to evaluate the pancreatic deposition of C1q in neonatal mice injected with patient or control IgG. Similar to human IgG deposition, C1q was stained at the base of the acini and the interlobular space in mice injected with patient IgG, but not in mice injected with control IgG (see online supplementary figure S7).

To further analyse the binding activity of patient IgG and its subclasses to mouse pancreatic tissue, we performed an ex vivo organ culture assay using the method applied for the ex vivo PV assay.[25] Patient IgG or control IgG was directly injected into pancreatic organ culture, and binding of human IgG or each IgG subclass was analysed by immunofluorescence. Similar to the in vivo study, human IgG was detected in the intralobular and interlobular spaces (figure 3A), and around the pancreatic duct (see online supplementary figure S2C), in the pancreas of mice injected with patient IgG, but not in mice injected with control IgG. Consistent with the in vivo study, as shown in figure 2B, immunofluorescence analysis in the organ culture assay also detected colocalisation of IgG with collagen IV expression, but not with amylase (figure 3B). With regard to IgG subclasses, IgG1 was detected in 6 of 10, and IgG4 in 10 of 10 pancreatic organ culture samples, whereas IgG2 and IgG3 were not or were only faintly detected (figure 3C). These data indicate that IgG, especially IgG1 and IgG4, from patients with IgG4-RD bind to mouse pancreatic tissue.

Distinctive pathogenicity of IgG1 and IgG4 from patients with IgG4-RD

Based on the results of the mouse pancreas binding studies of each human IgG subclass (figure 3C), we next analysed the pathogenic activity of IgG1 or IgG4 from patients with

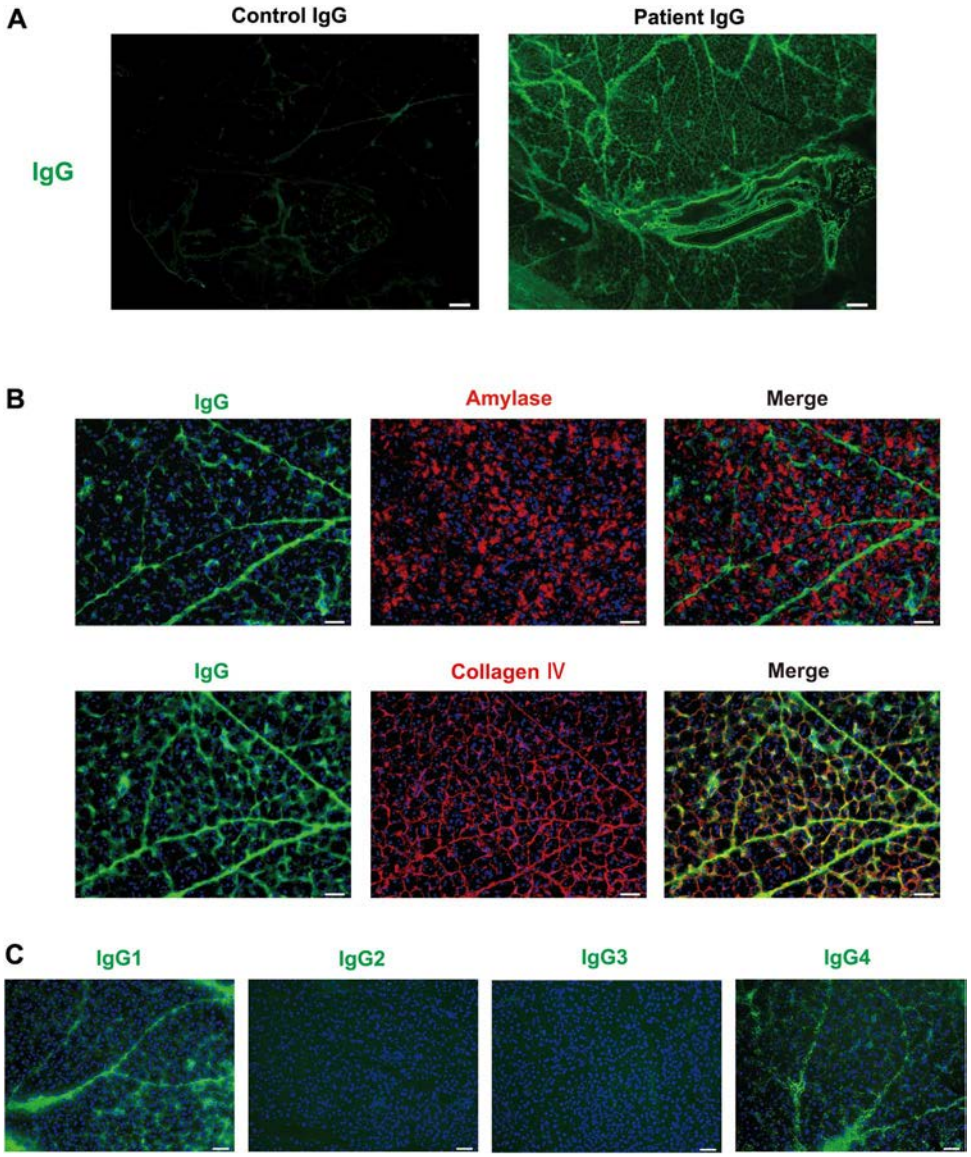

Figure 3 Binding of patient IgG and IgG subclasses to mice pancreatic tissues in ex vivo organ culture assay. Binding of human IgG and IgG subclasses to pancreatic tissues was assessed by immunofluorescence studies in ex vivo mice pancreatic organ cultures. (A) Immunofluorescence staining for IgG. IgG was detected in intralobular and interlobular spaces, and around the pancreatic duct in pancreatic tissues injected with patient IgG, but not in tissues injected with control IgG. Scale bars: 200 μm. (B) Upper panels show staining for IgG (green), amylase (red) and a merged image. Lower panels show staining for IgG (green), collagen IV (red) and a merged image. IgG was detected in collagen IV-expressing basement membrane or extracellular matrix. Scale bars: 20 μm. (C) Immunofluorescence staining for IgG1, IgG2, IgG3 and IgG4. IgG1 and IgG4 were detected, whereas IgG2 and IgG3 were not. Scale bars: 50 μm. Representative photos are shown.

IgG4-RD. IgG1 and IgG4 were prepared from patients 1, 2 and 9 and controls 1 and 2, from whom sufficient serum samples were obtained. IgG1, IgG4 alone or IgG1 + IgG4 was subcutaneously injected into neonatal mice and pancreatic injury was evaluated (figure 4). The injection dose of a patient and control IgG subclass was determined by the same method as IgG injection. Oedematous changes, acini necrosis, haemorrhage and infiltration of Gr1-positive polymorphonuclear leucocytes were induced in the pancreas of mice given patient IgG1 or IgG4, but not in mice given control IgG1 or IgG4 (figure 4A,B). Both IgG1 and IgG4 had pathogenic activity, but IgG1 had more prominent pathogenic activity than IgG4 (figure 4B). Notably, the potent pathogenic effect of patient IgG1 was significantly attenuated by simultaneous injection of patient IgG4, suggesting an inhibitory effect of IgG4 on the pathogenic activity of IgG1 (figure 4B). Indeed, immunohistochemical studies revealed stronger IgG1 staining in mice given only IgG1 than in mice given IgG1 + IgG4 (figure 4C). By contrast, the intensity of IgG4 staining in mice given only IgG4 was equal to that in mice given IgG1 + IgG4 (figure 4C). These findings suggest that

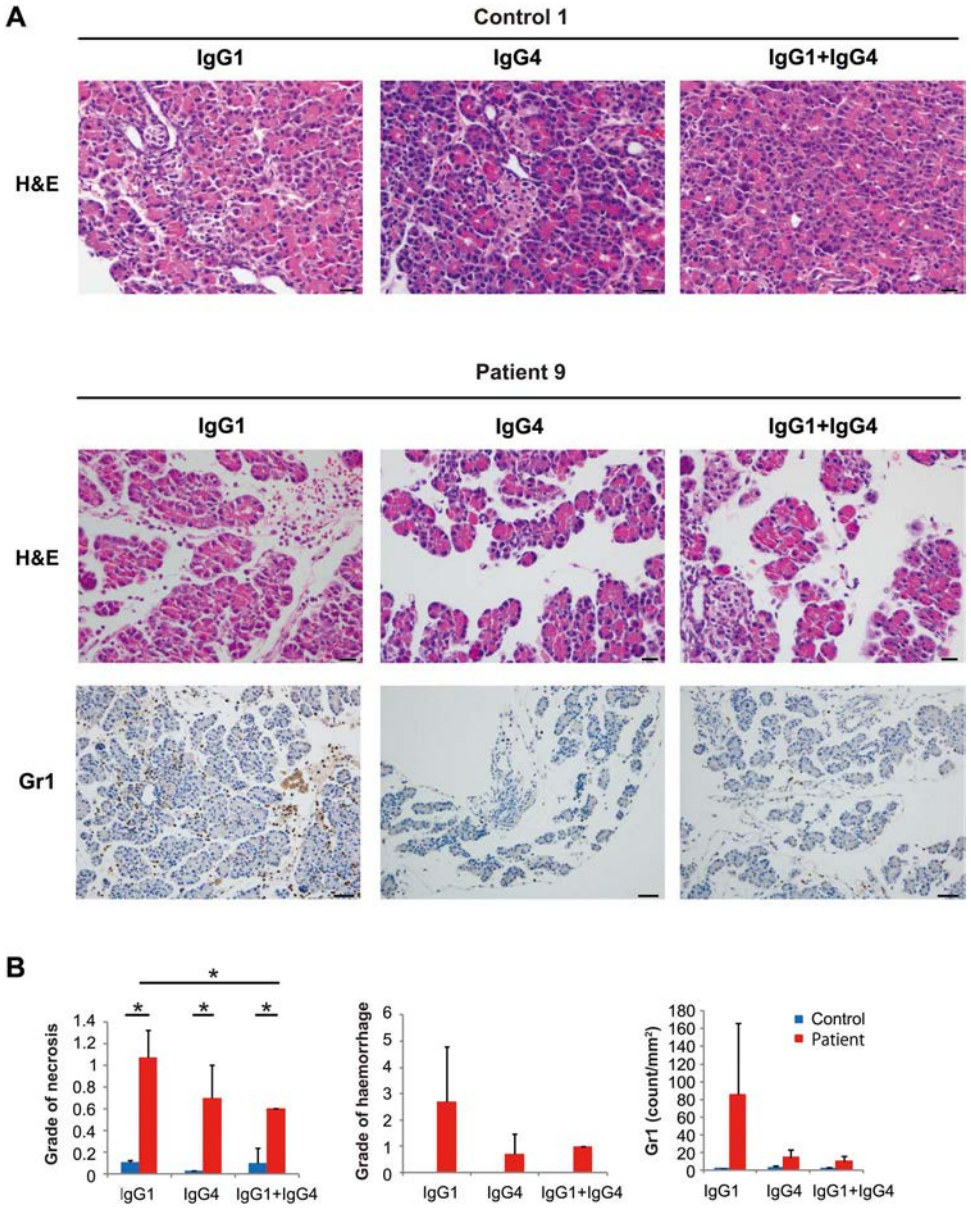

Figure 4 Pathogenic activities of IgG1 and IgG4 from patients with IgG4-RD on mouse pancreas. Pancreatic injury was evaluated in neonatal mice 12 h after subcutaneous injection of IgG1 or IgG4 alone, or IgG1 + IgG4. (A) Upper panels show H&E staining of pancreatic tissue sections of mice injected with IgG subclasses prepared from control 1. Middle panels and lower panels show H&E staining and immunohistochemical staining for Gr1, respectively, of pancreatic tissue sections in mice injected with IgG subclasses prepared from patient 9. Scale bars: 20 μm. (B) Histologic grade of necrosis, haemorrhage and Gr1-positive cell count were assessed. Data are shown as mean±SEM. *p<0.05 by paired Student's t test. Note that both IgG1 and IgG4 from patients had pathogenic activities, but IgG1 had a more pronounced effect than IgG4. This potent pathogenic activity of IgG1 was significantly diminished by simultaneous injection of the patient IgG4. (C) Immunohistochemical staining for human IgG1 and IgG4 in mouse pancreatic tissue sections injected by patient IgG1 or IgG4 or IgG1 + IgG4. Note that the intensity of IgG1 staining in mice given patient IgG1 + IgG4 was less than that in mice given only IgG1 (upper panels). In contrast, the intensity of IgG4 staining in mice given patient IgG1 + IgG4 was similar to that in mice given only IgG4 (lower panels). Scale bars: 20 μm. Similar data were obtained in all the mouse pancreatic tissue sections examined, and representative photos are shown. IgG4-RD, IgG4-related disease.

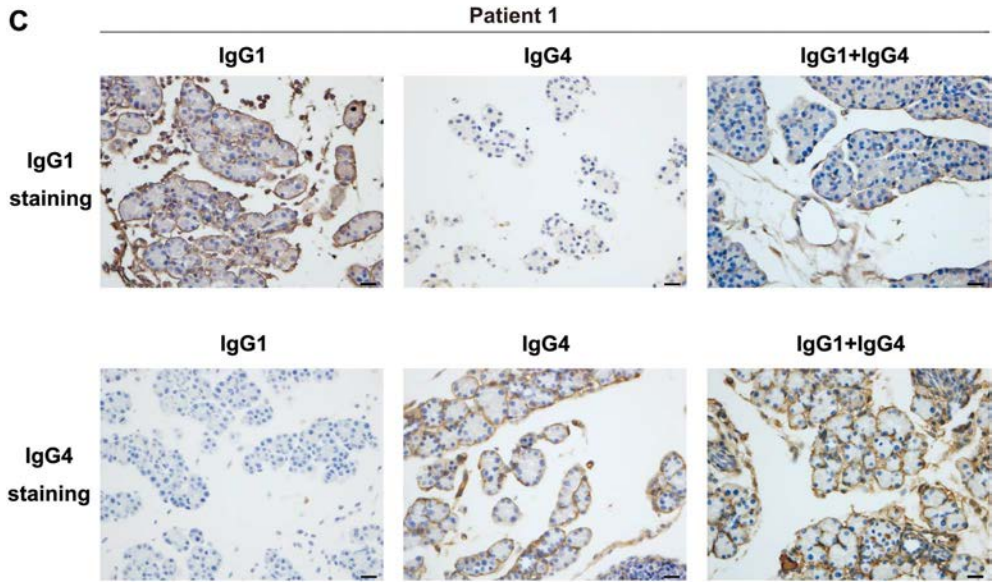

Figure 4 Continued

IgG4 competes with IgG1 to bind to the pancreas tissue and that IgG4 has higher binding affinity than IgG1.

Deposition of IgG4 in the pancreatic tissue from patients with AIP

The results of the mouse studies suggested that the IgG1 and IgG4 from patients with IgG4-RD bound to the pancreatic tissue and also had some pathogenic activity (figure 4). Thus, we next performed tissue-staining studies to evaluate whether IgG1 or IgG4 was deposited in the pancreas of patients with AIP. In addition to typical infiltration of IgG4-positive plasma cells, immunohistochemistry revealed linear staining of IgG4 at the base of the acini, the interlobular space (figure 5A) and around the duct of all the patients examined (see online supplementary figure S2D). IgG1 was faintly stained in two of five patient tissues (data not shown). Immunofluorescence study also detected IgG4 in the affected areas of AIP (figure 5B,C). Similar to the results from mouse pancreas, colocalisation of IgG4 with collagen IV, but not amylase, was observed in the pancreas from patients with AIP (figure 5B), suggesting the binding of IgG4 to the basement membrane or ECM in the intralobular lesions. In the interlobular lesions, IgG4 fluorescence overlapped with collagen IV expression in the ECM (figure 5C). In contrast, normal pancreas and chronic pancreatitis tissues showed no IgG4 staining (data not shown). Immunoelectron microscopy also detected IgG and IgG1 deposition at the base of the acini in the pancreas of patients with AIP (see online supplementary figure S8), although IgG4 was not detected, probably due to technical problems.

DISCUSSION

In this study, by passively transferring patient IgG, we demonstrated the pathogenic effects of IgGs, including IgG4, obtained from patients with IgG4-RD on neonatal mouse pancreas. To our knowledge, this is the first report showing the pathogenicity of IgGs from patients with IgG4-RD.

According to the reported model for PV in which IgG pathogenicity was confirmed,[17 20] we assessed the pathogenic effects of immunoglobulins from patients with IgG4-RD by injecting patient IgG into neonatal mice. Surprisingly, subcutaneous injection of patient IgG induced pancreatic lesions, whereas control IgG had no effect. Pancreatic enlargement and interlobular dissociation are the part of imaging and histopathological features of AIP, respectively.[2 25] The oedematous lesions observed in this study may be reflected by these imaging and histological abnormalities found in patients with AIP. The haemorrhage and infiltration of polymorphonuclear cells observed in the mice are not typical findings of AIP. It should be noted, however, that polymorphonuclear cell infiltration is also detected in an animal model of PV produced by injecting mice with pathogenic IgG obtained from patients with PV, although polymorphonuclear cell infiltration is not observed in patients with PV.[17] In our model, we observed no fibrotic changes, which are found in AIP, especially type 1 AIP. The reason for the absence of fibrotic changes in our mouse model is unknown at present, but a longer observation period may be required to detect the development of fibrosis. Alternatively, previous reports suggest the involvement of Foxp3 (+) T cells in the development of fibrosis in AIP.[26] Indeed, we analysed neonatal mice repeatedly injected with patient or control IgG for 2 weeks after birth as a chronic model. Induction of B cell/T cell infiltration and fibrosis, however, were minimal (data not shown). In general, tissue-resident plasma cells and T cells are considered to derive from tissue-specific antigen-primed B cells and T cells.[27 28] At this point, our model appears to lack the antigen sensitisation step for B cells and T cells, and only recapitulates the effect of the antibody on a specific tissue. This may partly explain why our model exhibited only acinar cell injury, and not the B cell/T cell responses and subsequent development of fibrosis observed in human AIP. Taken together, we speculate that the IgG in patients with IgG4-RD includes pathogenic autoantibodies against specific molecules present in the neonatal pancreas. Interestingly, Maillette de Buy Wenniger *et al*[29] reported highly specific and dominant B cell receptor clones in the sera from patients with IgG4-RD that completely disappeared after steroid treatment. Given our findings of reduced pathogenicity of patient IgG after steroid therapy, such dominant B cell receptor clones might be responsible for the autoantibody production.

To clarify whether the pathogenic activity of the injected IgG was exerted through its direct effects on affected tissues, we assessed the binding of the injected IgG to the injured organs by immunohistochemical and immunofluorescence studies. Patient

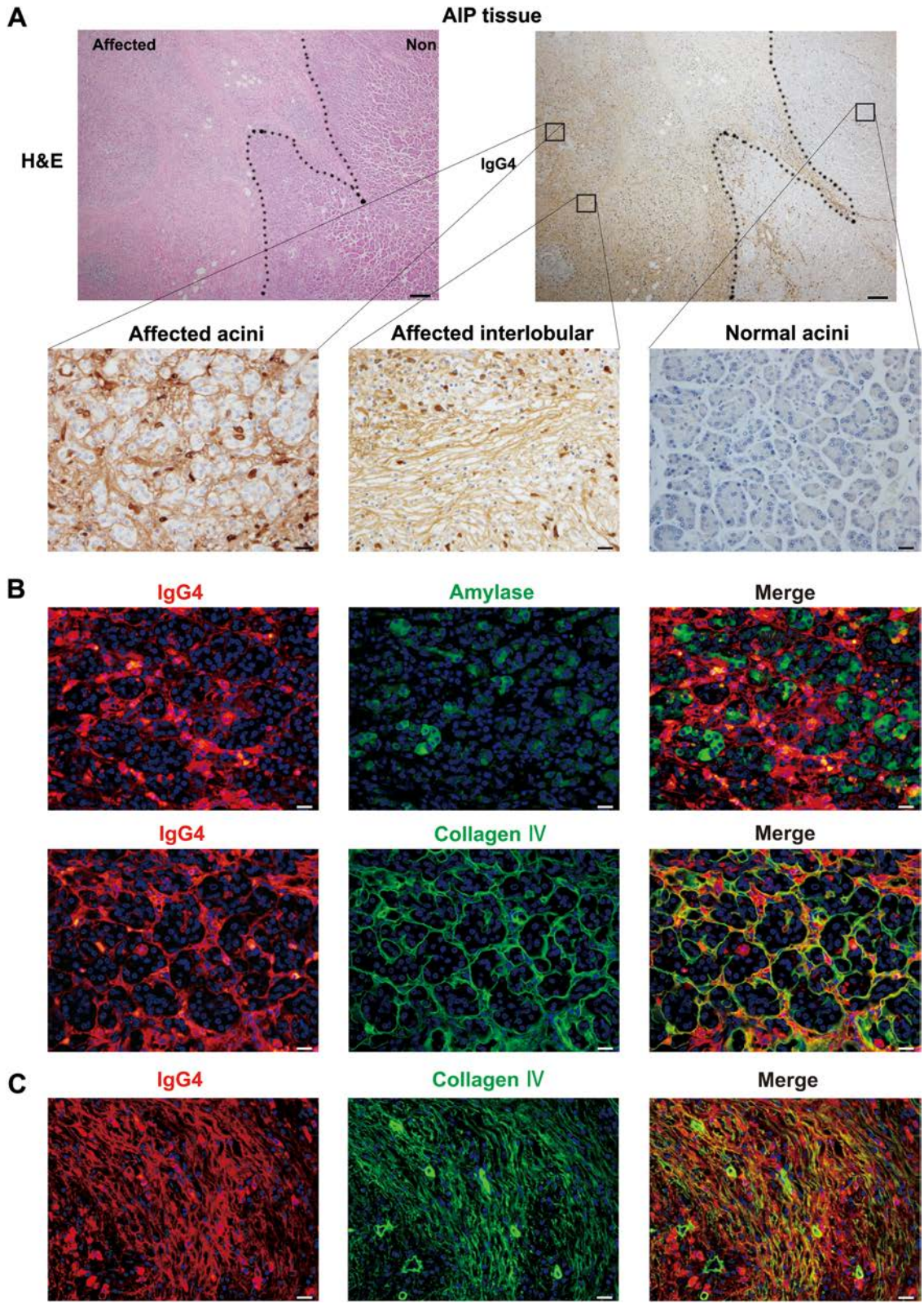

Figure 5 Deposition of IgG4 to pancreatic tissue in patients with autoimmune pancreatitis (AIP). Immunohistochemical and immunofluorescence studies for pancreatic tissues in patients with AIP. (A) Upper panels show H&E staining and immunohistochemical staining for IgG4 in tissue sections from the boundary between affected (left) and non-affected (right) AIP lesions. Scale bars: 200 μm. Lower panels show high-power magnification of immunohistochemical staining for IgG4 in the areas with affected acini and interlobular space, and non-affected acini. Note that in addition to the typical staining of IgG4-positive plasma cells, linear staining of IgG4 was observed at the base of the acini and the interlobular space of the affected areas, but not in non-affected areas. Scale bars: 20 μm. (B) Immunofluorescence staining of affected acini in AIP. Upper panels show staining for IgG4 (red), amylase (green) and a merged image. Lower panels show staining for IgG4 (red), collagen IV (green) and a merged image. Note that IgG4 was bound to collagen IV-expressing basal side of the acini, merging as yellow. Scale bars: 20 μm. (C) Immunofluorescence staining of interlobular lesions in AIP showing IgG4 (red), collagen IV (green) and a merged image. IgG4 was bound to collagen IV-expressing extracellular matrix, merging as yellow. Scale bars: 20 μm. Similar data were obtained in all the patients examined, and representative photos are shown.

IgG, but not control IgG, was stained in the mouse pancreatic tissues. To confirm our in vivo data, we also performed ex vivo organ culture studies, as performed in the study for PV.[24] Similar to the in vivo study, we found direct binding of the patient IgG to neonatal mouse pancreatic tissues. Importantly, the immunofluorescence staining of patient IgG occurred on both the basal side of the acini and the interlobular space, and overlapped with that of collagen IV, but not with amylase or cytokeratin in mouse pancreas. These results are compatible with our human data as well as with previous data presented by others showing the deposition of IgG and IgG4 at the basement membrane of the pancreatic acini and around the pancreatic duct in patients with AIP.[30 31] Taken together, these findings suggest that the autoantibodies in patient serum may recognise molecules involved in cell–ECM adhesion. Various molecules are involved in cell–ECM adhesion in each organ. The presence of IgG autoantibodies directed at these molecules with resulting cell adhesion disruption is a common feature of several autoimmune diseases; for example, anti-BP180 antibodies in bullous pemphigoid[32] and anti-BP180, laminin-332, α6 integrin or β4 integrin antibodies in mucous membrane pemphigoid.[33] Notably, the predominant IgG subclasses of the autoantibodies in these diseases are IgG1 and IgG4 antibodies.

To identify the autoantigen, antigen screening was performed using mouse pancreatic tissue extracts or mouse pancreatic stellate cell extracts expressing pancreatic ECM by both immunoprecipitation experiments and western blot analysis using patient IgG and control IgG as antibodies. Some candidate proteins specific for patient IgG were identified by subsequent mass spectrometry analysis. No antibody among these candidates, including collagen IV, however, was detected by ELISA in the serum samples obtained from patients with IgG4-RD (data not shown). One possible reason for this finding is that the autoantigen was denatured or degraded by our experimental preparations or procedures. For example, the autoantigens of idiopathic membranous nephropathy (PLA2R) and Goodpasture's syndrome (type IV collagen α3) are detected in a configuration-dependent manner. Further efforts are necessary to identify the true antigen by adjusting the experimental conditions.

In the present study, we attempted to define the pathogenicity of IgG subclasses obtained from patients with IgG4-RD by passively transferring each IgG subclass into neonatal mice. Among the IgG subclasses, both IgG1 and IgG4 had binding and pathogenic activity in mouse pancreatic tissue. IgG1 was more pathogenic than IgG4 in terms of neutrophil infiltration, haemorrhage and acinar cell necrosis. Because the ability to fix complement is much weaker in IgG4 than in IgG1,[16] it is reasonable to consider that the IgG1 subclass exerts direct cytotoxic activity on pancreatic tissue through the generation of immunocomplexes. Indeed, our immunofluorescence study of C1q staining strongly suggests the formation of immunocomplexes in the pancreatic tissue of mice injected with patient IgG. Consistent with this notion, decreased complement levels are often observed in patients with IgG4-RD, suggesting the involvement of complement and IgG1 immunocomplexes in the pathophysiology of IgG4-RD.[34] On the other hand, in our model, we observed no significant difference in the levels of apoptosis or autophagy between the mice injected with patient IgG and those injected with control IgG (data not shown). Another important observation in this study is that patient IgG4 has dual functions. IgG4 isolated from patients with IgG4-RD induced pancreatic injury when this IgG subtype alone was injected. In contrast, IgG4 inhibited pancreatic injury induced by IgG1 from the same patients. Thus, circulating IgG4 from patients with IgG4-RD may have both pathogenic and protective roles. Importantly, the intensity of IgG1 staining in the extracellular space of the pancreas was markedly decreased when IgG1 was administered together with IgG4. In contrast, the intensity of IgG4 staining remained unchanged in the presence or absence of IgG1. Based on these data, we speculate that IgG4 recognising autoantigens in the extracellular space competes with IgG1 recognising the same antigen, and that binding of pathogenic IgG1 to the extracellular space was inhibited due to the higher binding activity of IgG4 to the extracellular space. Interestingly, a similar antagonistic function of IgG4 antibodies against pathogenic IgG1 autoantibodies was demonstrated in an experimental model of autoimmune myasthenia gravis.[15]

In summary, we provide new evidence of pathogenic activity of IgGs obtained from patients with IgG4-RD on neonatal mice. Whether the pathogenic effects of IgG from patients with IgG4-RD observed in this study are involved in the pathophysiology of human AIP needs to be clarified in future studies.

Author affiliations
[1]Department of Gastroenterology and Hepatology, Kyoto University Graduate School of Medicine, Kyoto, Japan
[2]Translational Research Center, Kyoto University Hospital, Kyoto, Japan
[3]Department of Gastroenterology and Hepatology, Shiga Medical Center for Adults, Shiga, Japan
[4]Department of Anatomic Pathology, Kurashiki Central Hospital, Kurashiki, Okayama, Japan
[5]Department of Diagnostic Pathology, Kyoto University Hospital, Kyoto, Japan

Contributors Study concept, design, acquisition of data, analysis and interpretation of data and drafting of the manuscript: MS, YK, TW and TC. Study supervision: TC. Statistical analysis: KY. Acquisition of data, and administrative, technical or material support: MS, TT, TMo, NK, TMa, AM, YN, TU, MT, YY, RM, YS, YO, TM AK, YS, YT, NU, KM, KN and TT. Pathological evaluation: KN and TT.

Funding This work was supported by JSPS KAKENHI 21229009, 24229005 and 24659363; the research programme of the Project for Development of Innovative Research on Cancer Therapeutics (P-Direct) from the Ministry of Education, Culture, Sports, Science and Technology of Japan; Health and Labour Sciences Research Grants for Research on Intractable Diseases from the Ministry of Health, Labour and Welfare, Japan and Practical Research Project for Rare/Intractable Diseases Grant in Japan Agency for Medical Research and Development (AMED).

Competing interests None declared.

Patient consent Obtained.

Ethics approval Institutional Review Board of Kyoto University Hospital.

Provenance and peer review Not commissioned; externally peer reviewed.

REFERENCES

1 Stone JH, Zen Y, Deshpande V. IgG4-related disease. *N Engl J Med* 2012;366:539–51.
2 Finkelberg DL, Sahani D, Deshpande V, *et al*. Autoimmune pancreatitis. *N Engl J Med* 2006;355:2670–6.
3 Hamano H, Kawa S, Horiuchi A, *et al*. High serum IgG4 concentrations in patients with sclerosing pancreatitis. *N Engl J Med* 2001;344:732–8.
4 Chiba T. Are immunoglobulin G4-positive multiorgan lymphoproliferative syndrome and autoimmune pancreatitis different manifestations of a common clinicopathologic entity? *Gastroenterology* 2010;138:781–4.
5 Yamamoto M, Ohara M, Suzuki C, *et al*. Elevated IgG4 concentrations in serum of patients with Mikulicz's disease. *Scand J Rheumatol* 2004;33:432–3.
6 Kamisawa T, Funata N, Hayashi Y, *et al*. A new clinicopathological entity of IgG4-related autoimmune disease. *J Gastroenterol* 2003;38:982–4.
7 Umehara H, Okazaki K, Masaki Y, *et al*. Comprehensive diagnostic criteria for IgG4-related disease (IgG4-RD), 2011. *Mod Rheumatol* 2012;22:21–30.
8 Aparisi L, Farre A, Gomez-Cambronero L, *et al*. Antibodies to carbonic anhydrase and IgG4 levels in idiopathic chronic pancreatitis: relevance for diagnosis of autoimmune pancreatitis. *Gut* 2005;54:703–9.
9 Nishi H, Tojo A, Onozato ML, *et al*. Anti-carbonic anhydrase II antibody in autoimmune pancreatitis and tubulointerstitial nephritis. *Nephrol Dial Transplant* 2007;22:1273–5.
10 Nishimori I, Miyaji E, Morimoto K, *et al*. Serum antibodies to carbonic anhydrase IV in patients with autoimmune pancreatitis. *Gut* 2005;54:274–81.

11 Asada M, Nishio A, Uchida K, *et al*. Identification of a novel autoantibody against pancreatic secretory trypsin inhibitor in patients with autoimmune pancreatitis. *Pancreas* 2006;33:20–6.
12 Endo T, Takizawa S, Tanaka S, *et al*. Amylase alpha-2A autoantibodies novel marker of autoimmune pancreatitis and fulminant type 1 diabetes. *Diabetes* 2009;58:732–7.
13 Frulloni L, Lunardi C, Simone R, *et al*. Identification of a novel antibody associated with autoimmune pancreatitis. *N Engl J Med* 2009;361:2135–42.
14 Hart PA, Topazian MD, Witzig TE, *et al*. Treatment of relapsing autoimmune pancreatitis with immunomodulators and rituximab: the Mayo Clinic experience. *Gut* 2013;62:1607–15.
15 van der Neut Kolfschoten M, Schuurman J, Losen M, *et al*. Anti-inflammatory activity of human IgG4 antibodies by dynamic Fab arm exchange. *Science* 2007;317:1554–7.
16 Vidarsson G, Dekkers G, Rispens T. IgG subclasses and allotypes: from structure to effector functions. *Front Immunol* 2014;5:520.
17 Anhalt GJ, Labib RS, Voorhees JJ, *et al*. Induction of pemphigus in neonatal mice by passive transfer of IgG from patients with the disease. *N Engl J Med* 1982;306:1189–96.
18 Beck LH Jr, Salant DJ. Membranous nephropathy: recent travels and new roads ahead. *Kidney Int* 2010;77:765–70.
19 Plomp JJ, Huijbers MG, van der Maarel SM, *et al*. Pathogenic IgG4 subclass autoantibodies in MuSK myasthenia gravis. *Ann N Y Acad Sci* 2012;1275:114–22.
20 Sitaru C, Mihai S, Zillikens D. The relevance of the IgG subclass of autoantibodies for blister induction in autoimmune bullous skin diseases. *Arch Dermatol Res* 2007;299:1–8.
21 Shimosegawa T, Chari ST, Frulloni L, *et al*. International consensus diagnostic criteria for autoimmune pancreatitis: guidelines of the International Association of Pancreatology. *Pancreas* 2011;40:352–8.
22 Kawano M, Saeki T, Nakashima H, *et al*. Proposal for diagnostic criteria for IgG4-related kidney disease. *Clin Exp Nephrol* 2011;15:615–26.
23 Burak KW, Angulo P, Lindor KD. Is there a role for liver biopsy in primary sclerosing cholangitis? *Am J Gastroenterol* 2003;98:1155–8.
24 Ishii K, Amagai M. In vitro pathogenicity assay for anti-desmoglein autoantibodies in pemphigus. *Methods Mol Biol* 2013;961:219–25.
25 Masaru T, Koichi S. Clinical diagnostic criteria of autoimmune pancreatitis; revised proposal, 2006, Pathohistological findings of the pancreas. *Suizo* 2007;22:646–50.
26 Zen Y, Fujii T, Harada K, *et al*. Th2 and regulatory immune reactions are increased in immunoglobulin G4-related sclerosing pancreatitis and cholangitis. *Hepatology* 2007;45:1538–46.
27 Kunkel EJ, Butcher EC. Plasma-cell homing. *Nat Rev Immunol.* 2003;3:822–9.
28 Islam SA, Luster AD. T cell homing to epithelial barriers in allergic disease. *Nat Med* 2012;18:705–15.
29 Maillette de Buy Wenniger LJ, Doorenspleet ME, Klarenbeek PL, *et al*. Immunoglobulin G4+ clones identified by next-generation sequencing dominate the B cell receptor repertoire in immunoglobulin G4 associated cholangitis. *Hepatology* 2013;57:2390–8.
30 Deshpande V, Chicano S, Finkelberg D, *et al*. Autoimmune pancreatitis: a systemic immune complex mediated disease. *Am J Surg Pathol* 2006;30:1537–45.
31 Detlefsen S, Bräsen JH, Zamboni G, *et al*. Deposition of complement C3c, immunoglobulin (Ig)G4 and IgG at the basement membrane of pancreatic ducts and acini in autoimmune pancreatitis. *Histopathology* 2010;57:825–35.
32 Zillikens D. Acquired skin disease of hemidesmosomes. *J Dermatol Sci* 1999;20:134–54.
33 Sitaru C, Zillikens D. Mechanisms of blister induction by autoantibodies. *Exp Dermatol* 2005;14:861–75.
34 Muraki T, Hamano H, Ochi Y, *et al*. Autoimmune pancreatitis and complement activation system. *Pancreas* 2006;32:16–21.

GUT

Pathogenicity of IgG in patients with IgG4-related disease

Masahiro Shiokawa, Yuzo Kodama, Katsutoshi Kuriyama, Kenichi Yoshimura, Teruko Tomono, Toshihiro Morita, Nobuyuki Kakiuchi, Tomoaki Matsumori, Atsushi Mima, Yoshihiro Nishikawa, Tatsuki Ueda, Motoyuki Tsuda, Yuki Yamauchi, Ryuki Minami, Yojiro Sakuma, Yuji Ota, Takahisa Maruno, Akira Kurita, Yugo Sawai, Yoshihisa Tsuji, Norimitsu Uza, Kazuyoshi Matsumura, Tomohiro Watanabe, Kenji Notohara, Tatsuaki Tsuruyama, Hiroshi Seno and Tsutomu Chiba

Gut 2016 65: 1322-1332 originally published online March 10, 2016
doi: 10.1136/gutjnl-2015-310336

Published in final edited form as:
Cancer Res. 2016 March 1; 76(5): 1135–1145. doi:10.1158/0008-5472.CAN-15-2272.

Cdx2 Expression and Intestinal Metaplasia Induced by *H. pylori* Infection of Gastric Cells Is Regulated by NOD1-Mediated Innate Immune Responses

Naoki Asano[1,2], **Akira Imatani**[1], **Tomohiro Watanabe**[2,3], **Jun Fushiya**[1], **Yutaka Kondo**[1], **Xiaoyi Jin**[1], **Nobuyuki Ara**[1], **Kaname Uno**[1], **Katsunori Iijima**[1], **Tomoyuki Koike**[1], **Warren Strober**[2], and **Tooru Shimosegawa**[1]

[1]Division of Gastroenterology, Tohoku University Graduate School of Medicine, Sendai, Miyagi, Japan [2]Mucosal Immunity Section, Laboratory of Host Defenses, National Institute of Allergy and Infectious Diseases, Bethesda, Maryland [3]Center for Innovation in Immunoregulative Technology and Therapeutics, Graduate School of Medicine, Kyoto University, Sakyo-ku, Kyoto, Japan

Abstract

Chronic infection with the bacterial *Helicobacter pylori* is a major cause of gastric and duodenal ulcer disease, gastric mucosal atrophy, and cancer. *H. pylori*–induced expression of the intestinal epithelial–specific transcription factor caudal-related homeobox 2 (Cdx2) contributes to intestinal metaplasia, a precursor event to gastric cancer. Given a role for the bacterial pattern recognition molecule nucleotide-binding oligomerization domain 1 (NOD1) in the innate immune response to bacterial infection, we investigated mechanisms used by NOD1 to regulate *H. pylori* infection and its propensity towards the development of intestinal metaplasia. We found that Cdx2 was induced by *H. pylori* infection in both normal and neoplastic gastric epithelial cells in a manner that was inversely related to NOD1 signaling. Mechanistic investigations revealed that Cdx2 induction relied upon activation of NF-κB but was suppressed by NOD1-mediated activation of TRAF3, a negative regulator of NF-κB. *In vivo*, prolonged infection of NOD1-deficient mice with *H. pylori* led to increased Cdx2 expression and intestinal metaplasia. Furthermore, gastric epithelial cells from these mice exhibited increased nuclear expression of the NF-κB p65 subunit and decreased

Corresponding Author: Naoki Asano, Tohoku University Graduate School of Medicine, 1-1 Seiryo-machi, Aoba-ku, Sendai, Miyagi 980-8574, Japan. Phone: 812-2717-7171; Fax: 812-2717-7177; asanon@med.tohoku.ac.jp.

Disclosure of Potential Confiicts of Interest
No potential confiicts of interest were disclosed.

Note: Supplementary data for this article are available at Cancer Research Online (http://cancerres.aacrjournals.org/).

Authors' Contributions
Conception and design: N. Asano, W. Strober, T. Shimosegawa
Development of methodology: N. Asano, A. Imatani
Acquisition of data (provided animals, acquired and managed patients, provided facilities, etc.): N. Asano, A. Imatani, T. Watanabe, J. Fushiya, Y. Kondo, N. Ara, K. Uno
Analysis and interpretation of data (e.g., statistical analysis, biostatistics, computational analysis): N. Asano, A. Imatani, T. Watanabe, T. Koike, W. Strober
Writing, review, and/or revision of the manuscript: N. Asano, T. Watanabe, W. Strober
Administrative, technical, or material support (i.e., reporting or organizing data, constructing databases): Y. Kondo, X. Jin, K. Iijima, T. Koike
Study supervision: W. Strober, T. Shimosegawa

expression of TRAF3. Overall, our findings illuminated a role for NOD1 signaling in attenuating *H. pylori*–induced Cdx2 expression in gastric epithelial cells, suggesting a rationale to augment NOD1 signaling in *H. pylori*–infected patients to limit their risks of accumulating precancerous gastric lesions.

Introduction

Chronic gastric infection with *Helicobacter pylori* (*H. pylori*) can cause intestinal metaplasia, a pathologic change that is frequently a precursor of gastric cancer (1). Intestinal metaplasia is, at least in part, caused by *H. pylori*–induced expression of caudal-related homeobox 2 (Cdx2), a protein involved in the normal differentiation of the intestinal epithelium, which in this context causes aberrant intestinalization of the gastric epithelium (2–4). Although Cdx2 acts as a tumor suppressor in the small and large intestine, its aberrant expression in the gastric mucosa is considered to be pro-oncogenic. This is supported by recent studies showing that Cdx2 provides “lineage-specific” survival for already deregulated cancer cells via its capacity to activate the Wnt/catenin signaling pathway (5).

Nucleotide-binding oligomerization domain 1 (NOD1) is an intracellular component of the innate immune system, which is highly expressed in epithelial cells and is activated by a peptide derived from peptidoglycan (PGN), a component of the bacterial wall injected into the *H. pylori*–infected cell by type IV secretion system (6). It has been demonstrated in studies of *H. pylori* infection in NOD1-deficient mice that absence of NOD1 results in greatly enhanced bacterial burden (7, 8), and polymorphisms in the *NOD1* gene correlate with *H. pylori* infection–related diseases (9, 10). However, the role of NOD1 in the regulation of *H. pylori*–induced gastric intestinal metaplasia is unknown.

Materials and Methods

Animals

NOD1-deficient mice were obtained as previously described (8). C57BL/6 (NOD1-intact) mice were purchased from CLEA Japan. Both NOD1-deficient and NOD1-intact mice were reared in the same animal facility in Tohoku University (Sendai, Miyagi, Japan). Mice were handled according to the Regulations for Animal Experiments and Related Activities at Tohoku University.

Cell lines

Human gastric cancer–derived epithelial cell lines AGS and KATOIII were purchased from ATCC, where the cell lines had been authenticated by short tandem repeat profiling. Human cancer–derived epithelial cell lines GCIY and NUGC-4 were obtained from Tohoku University Cell Bank, where the cell lines had been authenticated by short tandem repeat analysis. The normal murine gastric epithelial cell line GSM06 was obtained from Riken Cell Bank, where the cell line had been authenticated by simple sequence length polymorphism analysis. Cells were maintained according to the manufacturers’ protocols, and the cell lines were carefully checked for morphologic consistency by microscope. In

addition, cultures of the cell lines were checked for mycoplasma contamination using Cycleave PCR Mycoplasma Detection Kit (TaKaRa).

In vitro H. pylori infection experiments

GCIY, AGS, and GSM06 were infected with 5×10^7 CFU/mL cytotoxin-associated gene pathogenicity island (*cag*PAI)-positive *H. pylori* (strain 43504, ATCC), which corresponds to 50 multiplicity of infection (MOI). In the indicated experiment, GCIY cells were infected with 50 MOI *cag*PAI$^-$ *H. pylori* (Microbiological Research Institute, Tokushima, Japan). Total RNA was collected using TRIzol reagent (Invitrogen) and subjected to RT-PCR using Super Script III First-Strand Synthesis System (Invitrogen). The synthesized cDNA was subjected to semiquantitative PCR for Cdx2, MUC2, and GAPDH as previously described (11). Similarly, total protein was collected from the infected and noninfected cells and was subjected to Western blotting as previously described (8). In the indicated experiments, the cells were treated with NF-κB inhibitor BAY11-7082 (Calbiochem) or were transfected with NOD1-siRNA (Dharmacon) or TRAF3-expressing plasmid (InvivoGen) or incubated with 100 ng/mL iE-DAP (Invivo-Gen) prior to infection.

Luciferase assay

Transcription factor–binding site in the 5′-promoter region of human Cdx2 was analyzed using MatInspector software (Genomatix). Next, the 5′-promoter region of Cdx2 was obtained by PCR and ligated into Luciferase Reporter Vector-pGL3 (Pro-mega) using DNA Ligation Kit (Takara). The latter was transfected into GCIY cells together with pRL-TK plasmid (Promega) using Trans-IT-LT1 Transfection Reagent (Mirus). Transfected cells were infected with *H. pylori*, and the relative luciferase activity was measured using Dual-Luciferase Reporter Assay System (Pro-mega). In the indicated experiments, pNF-κB-Luc reporter plas-mid (Clontech) was transfected into the cells with TRAF3-expressing plasmid (InvivoGen).

Electrophoretic mobility shift assay

Nuclear extracts were obtained from *H. pylori*–infected and uninfected GCIY cells and incubated with appropriate oligonucleotides representing the NF-κB–binding site in the Cdx2 promoter. Electrophoretic mobility shift assay (EMSA) was performed using Gel-Shift Kit from Panomics.

Establishment of NOD1 knockdown stable cell line

GSM06 cells were transfected with mouse NOD1-shRNA vector (OriGene), using a 4D-Nucleofector System (Lonza). A stable NOD1-deficient clone was established by selection with puromycin (Thermo Scientific). Vector with noneffective scrambled shRNA (OriGene) was used as control.

qPCR

Total RNA was extracted from gastric epithelial cells and murine gastric mucosa, and the synthesized cDNA was subjected to qPCR (StepOnePlus, Applied Biosystems) for NOD1, Cdx2, MUC2, trefoil factor 2 (TFF2), TFF3, TRAF3, TNFα, and β-actin. The relative

amount of gene expression was normalized using β-actin mRNA and shown in arbitrary units. Each sample was performed in triplicate.

In vivo H. pylori infection

Five 8-week-old male NOD1-intact and NOD1-deficient mice were anesthetized and orally infected with 2.5×10^8 CFU *cag*PAI$^+$ *H. pylori* (strain 43504, ATCC: previously reported to colonize mice; refs. 12–14) on days 0, 2, and 4 as described previously (8). Five NOD1-intact and five NOD1-deficient mice without oral *H. pylori* infection were also used as uninfected controls. After confirming the colonization of *H. pylori* in the stomach by quantitative culture on Columbia HP agar plates (Becton Dickinson) at 5 weeks, the infected mice were maintained under normal housing conditions until sacrifice at 12 months after oral *H. pylori* administration. At that point, the chronic infection of mice was confirmed by quantitative culture, and their gastric mucosae were processed for hematoxylin–eosin (H&E) staining to detect inflammatory cell infiltration and histologic changes associated with intestinal metaplasia. Two NOD1-deficient and two NOD1-intact mice were sacrificed at 8 months after infection to evaluate the histologic changes in their stomachs at an earlier time point. Inflammation was scored using the criteria developed by Rogers and colleagues (15). Intestinal metaplasia was evaluated by the ratio of metaplastic glands to total glands. In addition, *H. pylori* colonization was evaluated by quantitative culture as previously described (8). Immunohistochemical examination of gastric tissues was evaluated using antibodies to detect Cdx2 (BioGenex) and NF-κB subunit (p65; Cell Signaling Technology), while total RNA was extracted for qPCR analysis as described above. The *in vivo* infection experiment was repeated five times.

Statistical analysis

Student *t* test was used to evaluate the significance of the differences between two groups. In the case where multiple samples were compared, Dunnett test was performed to evaluate the significance of the differences. A value of $P < 0.05$ was considered as statistically significant.

Results

H. pylori infection of gastric epithelial cell lines induces/ enhances Cdx2 expression

The occurrence of gastric intestinal metaplasia during *H. pylori* infection has been reported to be dependent on induction of Cdx2 expression in gastric epithelial cells (3). Thus, in initial studies, we evaluated Cdx2 expression and other epithelial cell differentiation markers in human gastric cancer cell lines before and after infection with *H. pylori.* Among the evaluated cell lines, uninfected GCIY cells expressed gastric-type mucins, mucin 1 (MUC1) and MUC5AC, but not an intestinal-type mucin MUC2; more importantly, they expressed very low level of Cdx2 (Supplementary Fig. S1). This expression pattern indicated that, with respect to intestinal metaplasia, uninfected GCIY cells are similar to epithelial cells of the gastric mucosa not infected by *H. pylori* (3, 16). In contrast, AGS, NUGC-4, and KATOIII cells expressed Cdx2 and MUC2 prior to infection with *H. pylori*.

With this information in hand, we next addressed whether *H. pylori* infection induces increased Cdx2 expression in cell lines with and without baseline Cdx2 expression. Accordingly, the induction of Cdx2 was evaluated both in cultures of GCIY and AGS cells infected with *cag*PAI^{+} *H. pylori*. The expression of Cdx2 mRNA (as well as MUC2 mRNA) was induced in GCIY cells at 3 hours after *H. pylori* infection (Fig. 1A); in addition, Cdx2 protein was expressed at this time point and then increased progressively over 24 hours (Fig. 1B). In parallel studies, the preexisting level of Cdx2 present in AGS cells increased progressively during 24 hours of infection (Supplementary Fig. S2). In studies of both cell lines, visual assessments of Cdx2 increases were confirmed by densitometry. These results indicated that *in vitro H. pylori* infection results in the increased expression of Cdx2 in epithelial cell lines, regardless of preexistent Cdx2 expression levels.

*cag*PAI is an important *H. pylori* virulence factor that, in epidemiologic studies, has been shown to confer a higher risk for the occurrence of infection-associated gastric carcinoma (17, 18). Furthermore, its injection into gastric epithelial cells via a type IV secretion system results in the entry of cytotoxin-associated gene A (CagA) and PGN, the source of NOD1 ligand, and thus, the activation of signaling pathways relevant to Cdx2 expression (19).

We therefore investigated whether Cdx2 induction by *H. pylori* infection requires bacteria expressing *cag*PAI. Although *cag*PAI^{-} *H. pylori*, heat-killed *H. pylori*, and culture supernatants of infected cells induced Cdx2 expression to some extent, optimal induction of Cdx2 expression required live *cag*PAI^{+} *H. pylori* (Fig. 1C). These results, thus, show that intracellular entry of *H. pylori* components are necessary for maximal *H. pylori* induction of Cdx2 expression in an epithelial cell line.

H. pylori infection–induced Cdx2 expression is dependent on NF-κB

H. pylori infection of epithelial cells has been shown to result in NF-κB activation, and the analysis of the 5′-promoter region of Cdx2 showed that it contains an NF-κB–binding site (20, 21). We therefore investigated if *H. pylori* induction of Cdx2 expression is dependent on NF-κB signaling. In initial studies, we transfected GCIY cells with a Cdx2 promoter–reporter plasmid (Supplementary Fig. S3), containing a promoter construct with an intact NF-κB–binding site (cdx2-luc) or a construct not containing this binding site (cdx2-N0-luc) and then subjected the cells to *H. pylori* infection. Cells expressing cdx2-luc, but not cdx2-N0-luc, exhibited enhanced promoter activity upon infection with *H. pylori* (Fig. 2A and B). These data thus provide initial evidence that NF-κB activation is involved in the induction of Cdx2 expression upon *H. pylori* infection.

In further studies, we sought to confirm the role of NF-κB activation in Cdx2 induction. First, we subjected nuclear extracts of cells obtained from *H. pylori*–infected or uninfected GCIY cell cultures to EMSA using ^{32}P-labeled oligonucleotides that contain either NF-κB consensus–binding sequences or the NF-κB–binding sequence present in the Cdx2 promoter. Enhanced binding of nuclear extracts to NF-κB–binding sequences in the Cdx2 promoter was seen in cells derived from *H. pylori*–infected cultures, but not in those derived from uninfected cultures (Fig. 2C). Second, we assessed the effect of BAY11-7082, an NF-κB inhibitor on Cdx2 expression, in *H. pylori*–infected cells. BAY11-7082 inhibited Cdx2 induction in cells from such cultures in a dose-dependent manner (Fig. 2D) that paralleled its

ability to inhibit NF-κB expression in *H. pylori*–infected cells (Supplementary Fig. S4). Together, these studies buttress the idea that Cdx2 expression induced by *H. pylori* infection does in fact depend, at least in part, on NF-κB activation.

NOD1 signaling has an inhibitory effect on Cdx2 induction by *H. pylori*

Activation of NOD1 plays an important host defense role in acute gastric infection with *H. pylori* by inducing the expression of bactericidal mediators (7, 8, 22). It was therefore possible that NOD1 signaling also regulates *H. pylori* induction of Cdx2. To examine this question, we conducted a series of studies addressing the role of NOD1 signaling on *H. pylori* induction of Cdx2 mainly in AGS cells, i.e., cells that had previously been shown to support a full range of NOD1 signaling effects (8).

In initial studies, we evaluated Cdx2 expression in *H. pylori*–infected AGS cells transfected with NOD1-specific siRNA, previously evaluated for its capacity to substantially inhibit NOD1 expression (Supplementary Fig. S5). We found that AGS cells transfected with NOD1-siRNA exhibited greatly enhanced *H. pylori*–induced Cdx2 expression compared with cells transfected with control siRNA (Fig. 3A). In addition, NOD1-siRNA significantly enhanced *H. pylori*–induced Cdx2 promoter activity (Fig. 3B). These results suggested that NOD1 has an inhibitory effect on *H. pylori*–induced Cdx2 expression.

In complementary studies, we determined whether the above findings obtained with AGS cells (a human gastric cancer cell line) were also observed with GSM06 cells, a normal murine gastric epithelial cell line, which expresses neither MUC2 nor Cdx2 prior to *H. pylori* infection (Supplementary Fig. S6). In preliminary studies, we established that GSM06 cells, stably expressing NOD1-shRNA, exhibit an 88% reduction in NOD1 mRNA expression compared with GSM06 cells expressing control shRNA (Fig. 3C). We then infected the shRNA-transfected cells with *H. pylori* and assessed their expression of Cdx2. GSM06 cells exhibited rapid upregulation of Cdx2 upon infection with *H.pylori*, indicating that such upregulation occurs in normal epithelial cells as well as gastric cancer cell lines (Fig. 3D). In addition, GSM06 cells expressing NOD1-shRNA exhibited significantly higher expression of Cdx2 compared with the cell line expressing control shRNA. This result showed that NOD1 inhibition of Cdx2 upregulation during *H. pylori* infection is also observed in normal gastric epithelial cells and thus reinforced our findings obtained with gastric cancer cell lines.

The above results, showing that the downregulation of NOD1 signaling enhances *H. pylori* induction of Cdx2, suggested that the stimulation of cells with NOD1 ligand during *H. pylori* infection might downregulate Cdx2 expression induced by *H. pylori* infection. In studies designed to address this possibility, we assessed the effect of NOD1 ligand stimulation on Cdx2 expression induced in cultures of *H. pylori*–infected gastric epithelial cells. Preincubation of GCIY cells with NOD1 ligand (iE-DAP) led to greatly reduced Cdx2 expression in *H. pylori*–infected cells (Fig. 3E). Similarly, preincubation of AGS cells with iE-DAP exhibited a lesser but, nevertheless, significant reduction in *H. pylori*–induced Cdx2 expression (Supplementary Fig. S7). In studies of either type of cells, stimulation with iE-DAP alone had no effect on Cdx2 expression (Supplementary Fig. S8). These studies thus

reinforce the idea that NOD1 signaling has a negative effect on *H. pylori*–induced Cdx2 expression.

TRAF3, a downstream signaling molecule induced by NOD1, downregulates Cdx2

In previous studies, we showed that in epithelial cells, RICK, activated by NOD1 stimulation, binds to TRAF3 and thus sets in motion a signaling pathway that leads to the production of type I IFN (8). In addition, we showed that downregulation of TRAF3 in NOD1 ligand–stimulated cells leads to enhanced NF-κB reporter activity. Thus, as had been noted previously in other experimental systems (23), increased TRAF3 expression suppresses the NF-κB signaling pathway. Since, as shown above, Cdx2 expression is under the control of NF-κB, these previous studies suggested that NOD1 might be regulating Cdx2 via its effect on TRAF3. To examine this possibility, we first determined the effect of TRAF3 regulation on NF-κB reporter activity in cultures of AGS cells infected with *H. pylori*. Cotransfection of an NF-κB reporter plasmid with a TRAF3 expression plasmid led to a significant reduction in reporter activation, whereas, in contrast, cotransfection of the same reporter plasmid with TRAF3-siRNA led to enhanced reporter activation (Fig. 4A). Thus, TRAF3 expression does indeed downregulate NF-κB activation in *H. pylori*–infected cells. We next determined the effect of TRAF3 overexpression on the induction of Cdx2 in cultures of AGS cells infected with *H. pylori*. The level of Cdx2 mRNA was upregulated by *H. pylori* infection, as noted previously, and such enhancement was accompanied by low-level expression of TRAF3 (Fig. 4B). However, Cdx2 expression was greatly downregulated in cells transfected with a TRAF3-expressing plasmid. Interestingly, such downregulation was particularly evident in *H. pylori*–infected cells, possibly reflecting the fact that in such cells, the transfected TRAF3 was being more efficiently activated by the increased NOD1 signaling resulting from *H. pylori* infection. In any case, these results suggested that TRAF3, a downstream signaling molecule of NOD1, could negatively regulate Cdx2 expression induced by *H. pylori*.

Effect of NOD1 signaling on the occurrence of intestinal metaplasia and the expression of Cdx2 during *in vivo H. pylori* infection

In a final series of studies, we determined whether the NOD1-mediated negative regulation of Cdx2 expression, observed in the above *in vitro* studies, was also manifested in physiologic gastric epithelial cells *in vivo*. To this end, we orally infected NOD1-intact and NOD1-deficient mice with *cag*PAI^{+} *H. pylori* and then, 8 or 12 months after infection, i.e., after prolonged *H. pylori* infection, determined the occurrence of intestinal metaplasia and the expression of Cdx2 in the gastric epithelium.

As indicated previously by Goldenring and Nomura, intestinal metaplasia in mice is best identified by both morphologic criteria, i.e., the presence of goblet cells (containing mucus that can be stained by Alcian blue) in the gastric mucosa and the presence of various markers previously shown to be associated with this morphologic change (24). Accordingly, we first determined goblet cell frequencies in the gastric tissues obtained from mice infected with *H. pylori* for 12 months. We found that goblet cells were more frequently seen in tissue from NOD1-deficient mice than in that of NOD1-intact mice, as assessed by H&E-stained

tissue and by Alcian blue–stained tissue (Fig. 5A and B). Similar histologic changes were observed in mice infected with *H. pylori* for 8 months (data not shown).

Also pursuing the Goldenring/Nomura criteria for the identification of intestinal metaplasia, we next assessed Cdx2 expression in tissues derived from mice after 12 months of *H. pylori* infection. Both immunohistologic analysis and qPCR studies disclosed that NOD1-deficient tissue exhibited higher levels of Cdx2 than NOD1-intact tissue (Fig. 5A and C). In addition, mRNA levels of MUC2 and TFF3 [other epithelial cell markers of intestinal metaplasia (25)] were significantly higher in gastric tissues from NOD1-deficient mice as compared with NOD1-intact mice. In contrast to these findings in infected mice, Cdx2 expression evaluated by immunohistologic analysis was barely seen in tissues from either NOD1-intact or NOD1-deficient mice without *H. pylori* infection (data not shown).

The above morphologic and marker studies showed that prolonged *H. pylori* infection is associated with a greater level of intestinal metaplasia in NOD1-deficient mice than in NOD1-intact mice. Two additional observations relating to this conclusion suggest that these differences were not simply due to the severity of the *H. pylori* infection in these mice. First, the lamina propria of NOD1-deficient mice and NOD1-intact mice with prolonged *H. pylori* infection displayed equal levels of inflammation, suggesting that increased intestinal metaplasia expression and higher Cdx2 levels in NOD1-deficient mice were not due to the possibility that these mice have a more severe chronic gastric inflammation (Supplementary Fig. S9). This was supported by the fact that *H. pylori*–infected NOD1-intact and NOD1-deficient mice expressed equally increased levels of TNFα compared with the uninfected mice (Supplementary Fig. S10). Second, quantification of bacteria in gastric tissues disclosed that after prolonged *H. pylori* infection, NOD1-deficient mice displayed a substantially lower *H. pylori* bacterial load than NOD1-intact mice with prolonged infection (Fig. 5D). This observation is consistent with previous studies that have shown that gastric tissue that displays extensive intestinal metaplasia is less able to support *H. pylori* colonization (26). Taken together, these observations support the notion that the more severe intestinal metaplasia and increased Cdx2 in NOD1-deficient mice were not simply due to more intense chronic infection and inflammation.

Signaling pathway activation in NOD1-intact and NOD1-deficient tissue from mice with prolonged *H. pylori* infection

The above *in vitro* studies showed that epithelial cells with reduced NOD1 levels exhibit increased NF-κB activation, and this accounts, at least in part, for the increased expression of Cdx2. To determine if a similar phenomenon occurs *in vivo*, we immunostained the gastric tissue obtained from mice after prolonged *H. pylori* infection for NF-κB. Immunostaining of NF-κB p65 disclosed strikingly increased staining in epithelial cell nuclei of NOD1-deficient tissue as compared with NOD1-intact tissue (Fig. 5E), indicating that during *H. pylori* infection, NOD1 inhibits NF-κB expression *in vivo* as well as *in vitro*.

In parallel studies, we determined tissue expression of TRAF3, the NOD1 signaling component shown above, to inhibit NF-κB activation and to downregulate Cdx2 in overexpression studies. TRAF3 mRNA levels were more than 3-fold higher in the tissue of NOD1-intact mice as compared with that of NOD1-deficient (Fig. 5F).

These findings are compatible with the results of *in vitro* studies of epithelial cells discussed above in that they suggest that NOD1 signaling results in downregulation of Cdx2 via TRAF3 inhibition of NF-κB (Fig. 6).

As such, they support the notion that the mechanism of NOD1 downregulation of Cdx2 derived from the study of epithelial cell lines also obtains in physiologic epithelial cells.

Discussion

Previous studies addressing the role of NOD1 in *H. pylori* infection of the gastric mucosa clearly showed that this innate immune receptor is an important part of the mucosal host defense program (7, 8). These studies, however, did not consider the possibility that NOD1 activation may also play a role during established infection that addresses *H. pylori* induction of Cdx2 and IM, a feature of chronic *H. pylori* infection that is considered a precursor to gastric cancer (1). In this study, we fill this gap with studies showing that NOD1 activation inhibits infection-induced Cdx2 expression both *in vitro* and *in vivo*. In addition, we show in extensive *in vivo* studies that the absence of NOD1 leads to enhanced intestinal metaplasia in mice with prolonged *H. pylori* infection and thus that NOD1 inhibits this precancerous change.

In our initial studies, we found that *H. pylori* infection of both cancer cell line cells and nonneoplastic cell line led to prompt and robust expression of Cdx2. In addition, we showed that such induction was greatly enhanced by *H. pylori* expression of the *cag*PAI virulence factor possibly because CagA induces activation of NF-κB (27). This *in vitro* Cdx2 induction system allowed us to probe the effect of NOD1 signaling on *H. pylori* Cdx2 induction and, subsequently, to conduct studies that defined the mechanism of such effects. Our basic observation was that downregulation of NOD1 signaling led to increased *H. pylori*–induced Cdx2 expression, and upregulation had the opposite effect. These *in vitro* studies thus clearly established that NOD1 signaling has a regulatory function with respect to *H. pylori* induction of Cdx2.

In further studies focused on the nature of the NOD1 signaling mechanism responsible for downregulating Cdx2 induction, we showed initially that increased Cdx2 expression in gastric cancer cells lines by *H. pylori* infection depends on NF-κB activation. This finding is consistent with previous reports showing that *H. pylori* infection causes the activation of NF-κB (28) and that the activation of this transcription factor is involved in the induction of Cdx2 expression (20, 21). We then showed that NF-κB activation is negatively regulated by NOD1 signaling probably because such signaling activates TRAF3 (8, 29). This possibility was in fact supported by *in vitro* studies in which we showed that transfection of an epithelial cell line with a TRAF3 expression vector down-regulated *H. pylori*–induced NF-κB activity, whereas TRAF3-siRNA upregulated such activity; in addition, overexpression of TRAF3 greatly inhibited Cdx2 expression especially in *H. pylori*–infected cells in which NOD1 signaling (and presumably TRAF3 activation) was enhanced. Finally, the idea that NOD1 signaling inhibits *H. pylori*–induced Cdx2 expression by negative regulation of NF-κB was supported by *in vivo* studies in which we showed that prolonged infection with *H. pylori* in NOD1-deficient mice as compared with that in NOD1-intact mice was

accompanied by greatly increased nuclear expression of NF-κB p65 associated with greatly decreased expression of TRAF3.

Our observation that NOD1 signaling regulates *H. pylori*–induced Cdx2 expression in epithelial cells infected by *H. pylori in vitro* was fully corroborated by *in vivo* studies in which we showed that NOD1-deficient mice manifest greatly increased intestinal metaplasia both 8 and 12 months after infection. Moreover, the gastric mucosa of NOD1-deficient mice expressed increased levels of Cdx2 and other markers of intestinal metaplasia. Finally, as already mentioned, the gastric mucosa of NOD1-deficient mice displayed molecular changes in NF-κB and TRAF3, indicative of increased Cdx2 expression. These studies thus supported the notion that NOD1 signaling regulates Cdx2 in physiologic epithelial cells as well as in epithelial cell lines.

One important difference between *H. pylori*–induced Cdx2 expression *in vitro* and *in vivo* is that *in vitro*, such induction is immediate, whereas, *in vivo*, it is delayed and evident only after months of infection. This delayed appearance of Cdx2 (and accompanying intestinal metaplasia) may be due to the presence of cytokines in the *in vivo* environment that have an inhibitory effect on infection-induced Cdx2 expression. For instance, IFNγ, an inflammatory cytokine induced by *H. pylori* infection *in vivo* has been shown to cause dephosphorylation of STAT3 (30), another factor that is activated by CagA (31) that can induce Cdx2 expression (32). Whatever the explanation, the difference in the *in vitro* versus *in vivo* time course of *H. pylori*–induced Cdx2 expression by no means invalidates the NOD1-regulatory effect; on the contrary, it indicates that the latter is operating at a level not affected by secondary effects of the infection.

Recent studies have suggested that *Helicobacter* infection of the gastric mucosa can induce another type of precancerous change known as spasmolytic polypeptide–expressing metaplasia (SPEM; refs. 18, 33), which is characterized by parietal cell atrophy and the expression of TFF2 (24). As in the case of a recent study of mice infected with *Helicobacter felis* (18), we did find some evidence that SPEM was also induced in our chronic *H. pylori* infection model in that TFF2 levels in the infected mice were increased compared with the uninfected mice. However, this TFF2 increase was not as high as that of TFF3 and did not differ between NOD1-deficient and NOD1-intact mice (data not shown). Thus, it seems likely that TFF2-associated SPEM in *H. pylori* infection is not regulated by NOD1; nevertheless, further studies are warranted.

In previous studies, chronic infection or excessive responses to commensal organisms has been linked to the development of neoplasia in several gastrointestinal or even nongastrointestinal organs (34–36). The mechanism proposed to explain these associations involved activation of Toll-like receptor (TLR) signaling and its subsequent effects on cell survival and activation. It should be noted, however, that in a recent report, Banerjee and colleagues showed that although there was no difference in inflammation scores, mice lacking MyD88, an adaptor molecule involved in TLR signaling, exhibited early and rapid advancement to gastric dysplasia in response to *H. felis* infection compared with their littermate controls (37). Thus, the relation of innate signaling to neoplasia is not necessarily proneoplastic. This is supported, to some extent, by the studies reported here, which show

that a deficiency in innate immune signaling, in this case NOD1 deficiency, can in fact, lead to the appearance of factors such as Cdx2 and the promotion of precancerous lesions via abrogation of the regulation of NF-κB signaling.

The relation of gastric NOD1 responses to *H. pylori* infection and induction of gastric cancer is complex because on one hand, such responses can protect against the initiation of infection and, on the other hand, can intensify inflammation once infection has been established. The protective effect has been demonstrated in studies showing that type I interferon responses induced by NOD1 stimulation reduce the level of *H. pylori* infection (8) and that β-defensin production induced by NOD1 exerts a negative influence on *H. pylori* survival (38). The reciprocal proinflammatory effect has been shown in studies showing that NOD1 signaling enhances epithelial chemokine responses and that an *H. pylori* organism bearing a mutation in its NOD1-stimulating peptidoglycan induces decreased inflammation and malignant transformation *in vivo* (39). These negative and positive effects on *H. pylori*–induced inflammation, however, are probably independent from the effects of NOD1 on Cdx2 expression reported here, as the latter influences malignant transformation in gastric tissue harboring a chronic and stable infection. That such an antimalignant NOD1 effect does, in fact, operate in human populations with chronic *H. pylori* infection and thus alters the latter's outcome is suggested by a recent study showing that a certain NOD1 polymorphism in a large Chinese population confers a decreased risk of intestinal metaplasia; this finding thus opens the door to the possibilities that subtle molecular differences in NOD1 structure leading to increased NOD1 responses may downregulate Cdx2 expression (40); in addition, it has been shown that in humans, NOD1 expression is decreased in cancerous gastric tissue, but not noncancerous tissue (39).

In conclusion, we show here that *H. pylori* infection leads to increased expression of Cdx2 and that insufficiency of the innate immunity–related molecule NOD1 enhanced such expression and was associated with increased appearance of precancerous intestinal metaplasia in the gastric mucosa. Thus, our findings suggest that augmentation of NOD1 signaling in patients with *H. pylori* infection may inhibit not only gastric colonization of this organism but the capacity of this infection, once established, to induce tumor development.

Supplementary Material

Refer to Web version on PubMed Central for supplementary material.

Acknowledgments

The authors thank Ms. Kiiko Ogashiwa for her help in histology.

Grant Support

This work was supported by JSPS KAKENHI 25460925.

References

1. Rokkas T, Filipe MI, Sladen GE. Detection of an increased incidence of early gastric cancer in patients with intestinal metaplasia type III who are closely followed up. Gut. 1991; 32:1110–3. [PubMed: 1955163]

2. Silberg DG, Sullivan J, Kang E, Swain GP, Moffett J, Sund NJ, et al. Cdx2 ectopic expression induces gastric intestinal metaplasia in transgenic mice. Gastroenterology. 2002; 122:689–96. [PubMed: 11875002]
3. Barros R, Camilo V, Pereira B, Freund JN, David L, Almeida R. Pathophysiology of intestinal metaplasia of the stomach: emphasis on CDX2 regulation. Biochem Soc Trans. 2010; 38:358–63. [PubMed: 20298183]
4. Mutoh H, Hakamata Y, Sato K, Eda A, Yanaka I, Honda S, et al. Conversion of gastric mucosa to intestinal metaplasia in Cdx2-expressing transgenic mice. Biochem Biophys Res Commun. 2002; 294:470–9. [PubMed: 12051735]
5. Salari K, Spulak ME, Cuff J, Forster AD, Giacomini CP, Huang S, et al. CDX2 is an amplified lineage-survival oncogene in colorectal cancer. Proc Natl Acad Sci U S A. 2012; 109:E3196–205. [PubMed: 23112155]
6. Hatakeyama M. *Helicobacter pylori* and gastric carcinogenesis. J Gastroenterol. 2009; 44:239–48. [PubMed: 19271114]
7. Viala J, Chaput C, Boneca IG, Cardona A, Girardin SE, Moran AP, et al. Nod1 responds to peptidoglycan delivered by the *Helicobacter pylori* cag pathogenicity island. Nat Immunol. 2004; 5:1166–74. [PubMed: 15489856]
8. Watanabe T, Asano N, Fichtner-Feigl S, Gorelick PL, Tsuji Y, Matsumoto Y, et al. NOD1 contributes to mouse host defense against *Helicobacter pylori* via induction of type I IFN and activation of the ISGF3 signaling pathway. J Clin Invest. 2010; 120:1645–62. [PubMed: 20389019]
9. Oikawa T, Asano N, Imatani A, Ohyauchi M, Fushiya J, Kondo Y, et al. Gene polymorphisms of NOD1 and interleukin-8 influence the susceptibility to erosive esophagitis in *Helicobacter pylori* infected Japanese population. Hum Immunol. 2012; 73:1184–9. [PubMed: 22902391]
10. Rosenstiel P, Hellmig S, Hampe J, Ott S, Till A, Fischbach W, et al. Influence of polymorphisms in the NOD1/CARD4 and NOD2/CARD15 genes on the clinical outcome of *Helicobacter pylori* infection. Cell Microbiol. 2006; 8:1188–98. [PubMed: 16819970]
11. Ohyauchi M, Imatani A, Yonechi M, Asano N, Miura A, Iijima K, et al. The polymorphism interleukin 8 -251 A/T influences the susceptibility of *Helicobacter pylori* related gastric diseases in the Japanese population. Gut. 2005; 54:330–5. [PubMed: 15710978]
12. Sawai N, Kita M, Kodama T, Tanahashi T, Yamaoka Y, Tagawa Y, et al. Role of gamma interferon in *Helicobacter pylori*-induced gastric inflammatory responses in a mouse model. Infect Immun. 1999; 67:279–85. [PubMed: 9864227]
13. Hahm KB, Lee KM, Kim YB, Hong WS, Lee WH, Han SU, et al. Conditional loss of TGF-beta signalling leads to increased susceptibility to gastrointestinal carcinogenesis in mice. Aliment Pharmacol Ther. 2002; 16(Suppl 2):115–27. [PubMed: 11966532]
14. Olczak AA, Seyler RW Jr, Olson JW, Maier RJ. Association of *Helicobacter pylori* antioxidant activities with host colonization proficiency. Infect Immun. 2003; 71:580–3. [PubMed: 12496216]
15. Rogers AB, Taylor NS, Whary MT, Stefanich ED, Wang TC, Fox JG. *Helicobacter pylori* but not high salt induces gastric intraepithelial neoplasia in B6129 mice. Cancer Res. 2005; 65:10709–15. [PubMed: 16322215]
16. Silva E, Teixeira A, David L, Carneiro F, Reis CA, Sobrinho-Simoes J, et al. Mucins as key molecules for the classification of intestinal metaplasia of the stomach. Virchows Arch. 2002; 440:311–7. [PubMed: 11889603]
17. Atherton JC. The pathogenesis of *Helicobacter pylori*-induced gastro-duodenal diseases. Annu Rev Pathol. 2006; 1:63–96. [PubMed: 18039108]
18. Nomura S, Baxter T, Yamaguchi H, Leys C, Vartapetian AB, Fox JG, et al. Spasmolytic polypeptide expressing metaplasia to preneoplasia in *H. felis*-infected mice. Gastroenterology. 2004; 127:582–94. [PubMed: 15300590]
19. Chamaillard M, Hashimoto M, Horie Y, Masumoto J, Qiu S, Saab L, et al. An essential role for NOD1 in host recognition of bacterial peptidoglycan containing diaminopimelic acid. Nat Immunol. 2003; 4:702–7. [PubMed: 12796777]
20. Huo X, Zhang HY, Zhang XI, Lynch JP, Strauch ED, Wang JY, et al. Acid and bile salt-induced CDX2 expression differs in esophageal squamous cells from patients with and without Barrett's esophagus. Gastroenterology. 2010; 139:194–203. [PubMed: 20303354]

21. Kim S, Domon-Dell C, Wang Q, Chung DH, Di Cristofano A, Pandolfi PP, et al. PTEN and TNF-alpha regulation of the intestinal-specific Cdx-2 homeobox gene through a PI3K, PKB/Akt, and NF-kappaB-dependent pathway. Gastroenterology. 2002; 123:1163–78. [PubMed: 12360479]
22. Hirata Y, Ohmae T, Shibata W, Maeda S, Ogura K, Yoshida H, et al. MyD88 and TNF receptor-associated factor 6 are critical signal transducers in *Helicobacter pylori*-infected human epithelial cells. J Immunol. 2006; 176:3796–803. [PubMed: 16517750]
23. He JQ, Oganesyan G, Saha SK, Zarnegar B, Cheng G. TRAF3 and its biological function. Adv Exp Med Biol. 2007; 597:48–59. [PubMed: 17633016]
24. Goldenring JR, Nomura S. Differentiation of the gastric mucosa III. Animal models of oxyntic atrophy and metaplasia. Am J Physiol Gastrointest Liver Physiol. 2006; 291:G999–1004. [PubMed: 17090722]
25. Winn B, Tavares R, Fanion J, Noble L, Gao J, Sabo E, et al. Differentiating the undifferentiated: immunohistochemical profile of medullary carcinoma of the colon with an emphasis on intestinal differentiation. Hum Pathol. 2009; 40:398–404. [PubMed: 18992917]
26. Yabuki N, Sasano H, Tobita M, Imatani A, Hoshi T, Kato K, et al. Analysis of cell damage and proliferation in *Helicobacter pylori*-infected human gastric mucosa from patients with gastric adenocarcinoma. Am J Pathol. 1997; 151:821–9. [PubMed: 9284831]
27. Lamb A, Yang XD, Tsang YH, Li JD, Higashi H, Hatakeyama M, et al. *Helicobacter pylori* CagA activates NF-kappaB by targeting TAK1 for TRAF6-mediated Lys 63 ubiquitination. EMBO Rep. 2009; 10:1242–9. [PubMed: 19820695]
28. Keates S, Hitti YS, Upton M, Kelly CP. *Helicobacter pylori* infection activates NF-kappa B in gastric epithelial cells. Gastroenterology. 1997; 113:1099–109. [PubMed: 9322504]
29. Zarnegar B, Yamazaki S, He JQ, Cheng G. Control of canonical NF-kappaB activation through the NIK-IKK complex pathway. Proc Natl Acad Sci U S A. 2008; 105:3503–8. [PubMed: 18292232]
30. Fang P, Hwa V, Rosenfeld RG. Interferon-gamma-induced dephosphorylation of STAT3 and apoptosis are dependent on the mTOR pathway. Exp Cell Res. 2006; 312:1229–39. [PubMed: 16427044]
31. Bronte-Tinkew DM, Terebiznik M, Franco A, Ang M, Ahn D, Mimuro H, et al. *Helicobacter pylori* cytotoxin-associated gene A activates the signal transducer and activator of transcription 3 pathway *in vitro* and *in vivo*. Cancer Res. 2009; 69:632–9. [PubMed: 19147578]
32. Cobler L, Pera M, Garrido M, Iglesias M, de Bolos C. CDX2 can be regulated through the signalling pathways activated by IL-6 in gastric cells. Biochim Biophys Acta. 2014; 1839:785–92. [PubMed: 24953186]
33. Schmidt PH, Lee JR, Joshi V, Playford RJ, Poulsom R, Wright NA, et al. Identification of a metaplastic cell lineage associated with human gastric adenocarcinoma. Lab Invest. 1999; 79:639–46. [PubMed: 10378506]
34. Datta A, Sinha-Datta U, Dhillon NK, Buch S, Nicot C. The HTLV-I p30 interferes with TLR4 signaling and modulates the release of pro- and anti-inflammatory cytokines from human macrophages. J Biol Chem. 2006; 281:23414–24. [PubMed: 16785240]
35. Kelly MG, Alvero AB, Chen R, Silasi DA, Abrahams VM, Chan S, et al. TLR-4 signaling promotes tumor growth and paclitaxel chemoresistance in ovarian cancer. Cancer Res. 2006; 66:3859–68. [PubMed: 16585214]
36. Aravalli RN. Role of innate immunity in the development of hepatocellular carcinoma. World J Gastroenterol. 2013; 19:7500–14. [PubMed: 24282342]
37. Banerjee A, Thamphiwatana S, Carmona EM, Rickman B, Doran KS, Obonyo M. Deficiency of the myeloid differentiation primary response molecule MyD88 leads to an early and rapid development of helicobacter-induced gastric malignancy. Infect Immun. 2014; 82:356–63. [PubMed: 24166959]
38. Grubman A, Kaparakis M, Viala J, Allison C, Badea L, Karrar A, et al. The innate immune molecule, NOD1, regulates direct killing of *Helicobacter pylori* by antimicrobial peptides. Cell Microbiol. 2010; 12:626–39. [PubMed: 20039881]
39. Suarez G, Romero-Gallo J, Piazuelo MB, Wang G, Maier RJ, Forsberg LS, et al. Modification of *Helicobacter pylori* peptidoglycan enhances NOD1 activation and promotes cancer of the stomach. Cancer Res. 2015; 75:1749–59. [PubMed: 25732381]

40. Li ZX, Wang YM, Tang FB, Zhang L, Zhang Y, Ma JL, et al. NOD1 and NOD2 genetic variants in association with risk of gastric cancer and its precursors in a Chinese population. PLoS One. 2015; 10:e0124949. [PubMed: 25933107]

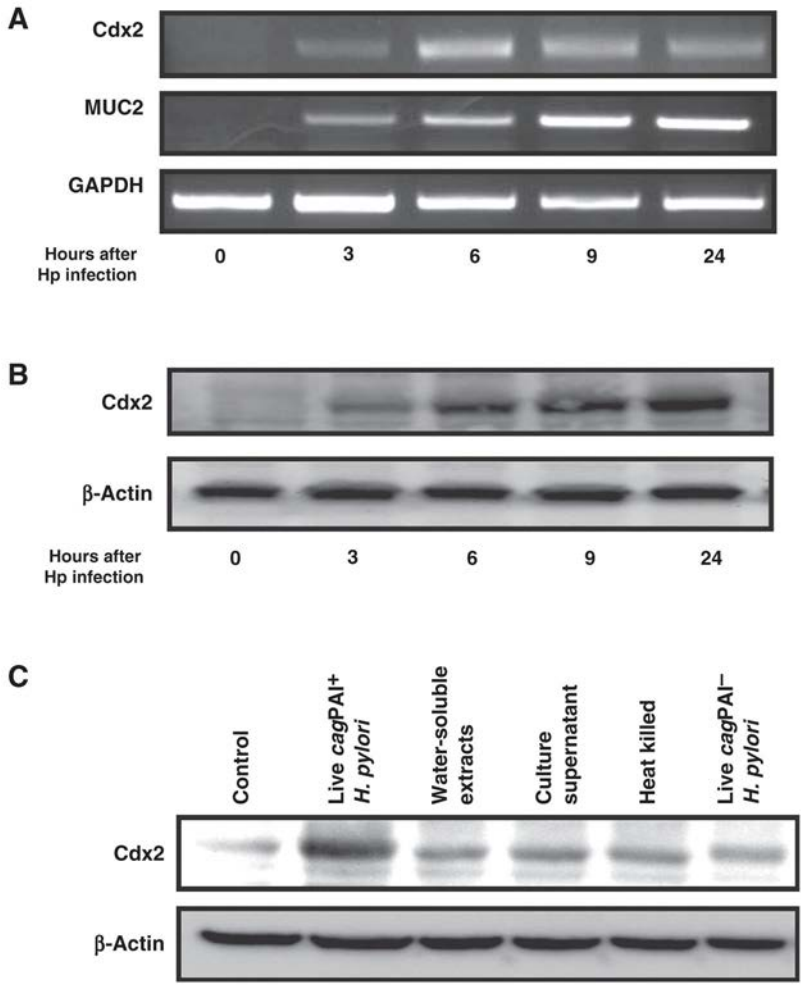

Figure 1.

*cag*PAI$^+$ *H. pylori* induces Cdx2 in human gastric epithelial cells. A, total RNA extracted from GCIY cells infected with 5×10^7 CFU/mL *cag*PAI$^+$ *H. pylori* (Hp) were subjected to RT-PCR. B and C, cell lysates were extracted from H. *pylori* (Hp)-infected GCIY cells (B) and GCIY cells stimulated with the indicated *H. pylori*-related products (C), and were subjected to Western blotting.

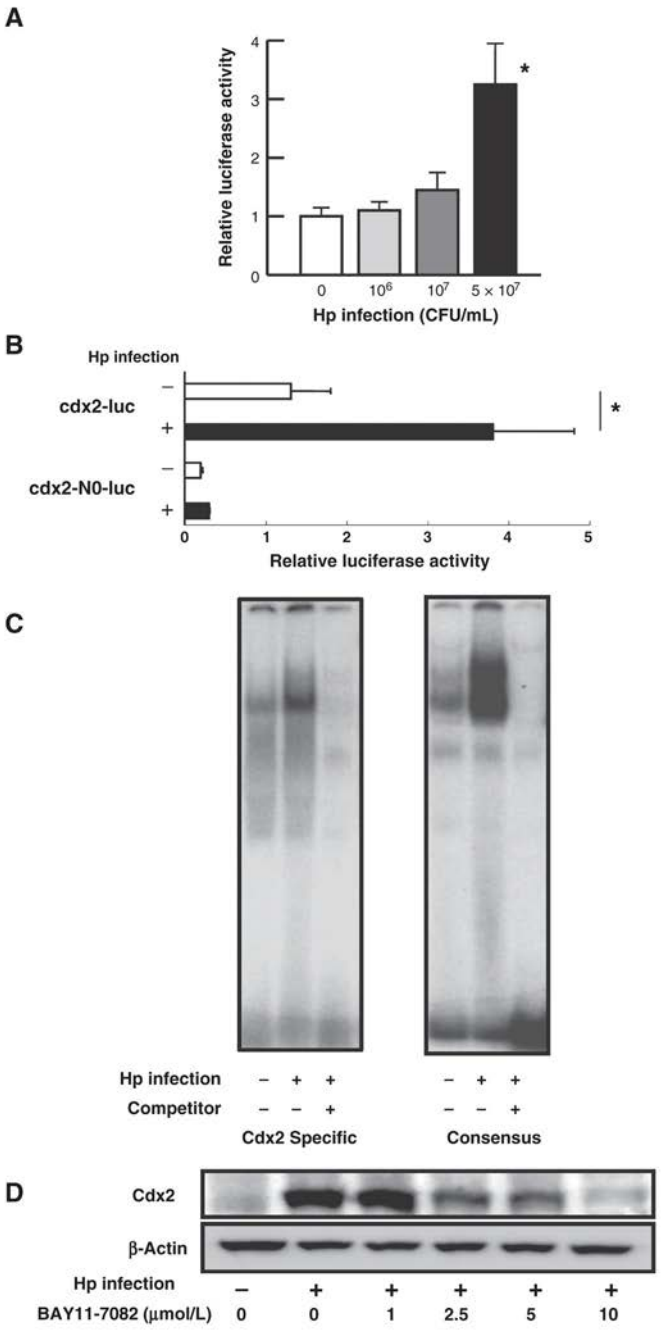

Figure 2.

H. pylori (Hp) induction of Cdx2 is dependent on NF-κB. A and B, GCIY cells transfected with cdx2-luc or cdx2-N0-luc plasmids with control pRL-TK plasmid were infected with the indicated amount (or 5 ×10^7 CFU/mL in B) of *H. pylori*; cell lysates were assessed for luciferase activity. C, nuclear extracts of *H. pylori*–infected GCIY cells were subjected to EMSA. D, GCIY cells were infected with 5 × 10^7 CFU/mL *H. pylori* in the absence or presence of BAY11-7082; cell lysates were subjected to Western blotting. Results shown in A and B indicate means ± SD. *, $P < 0.05$ as compared with uninfected cells.

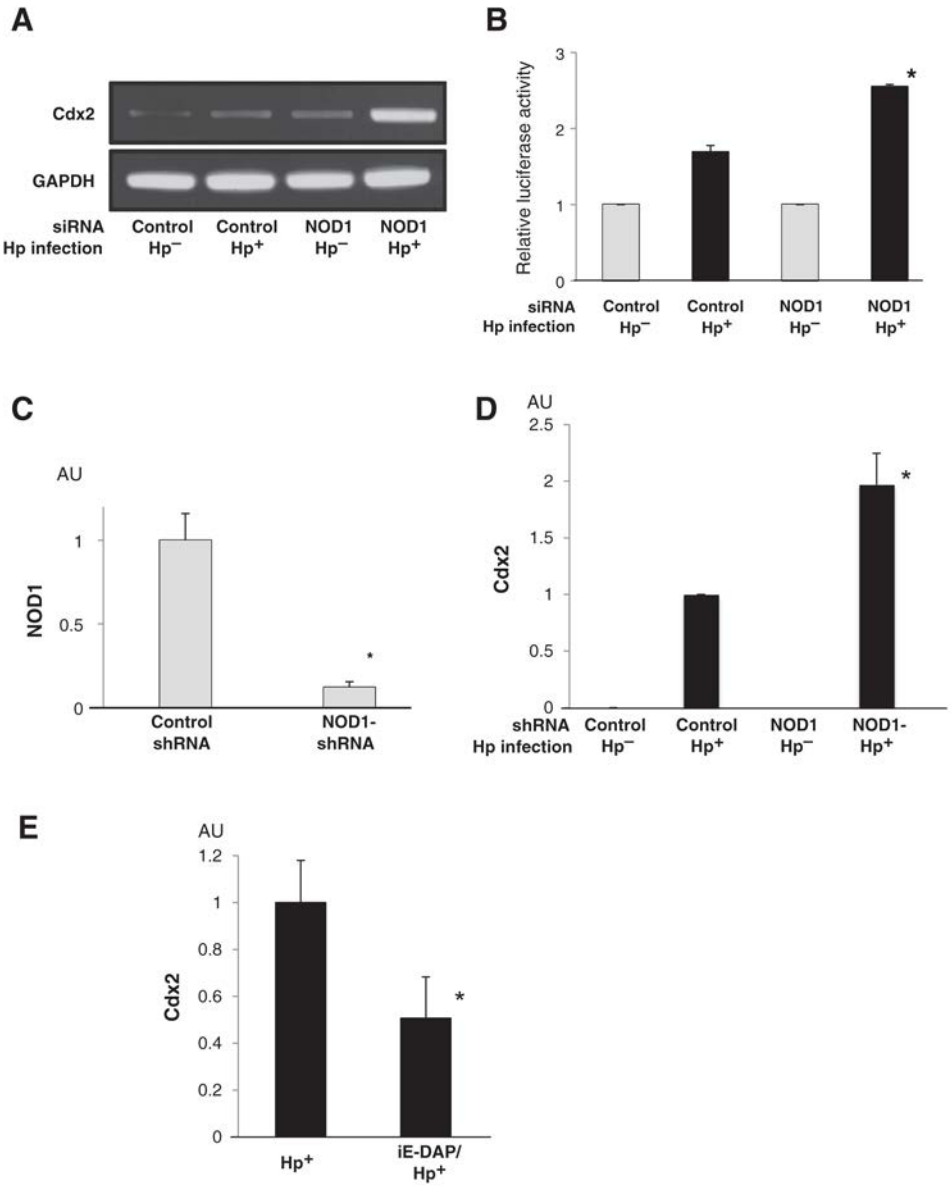

Figure 3.

NOD1 suppresses Cdx2 expression induced by *H. pylori* (Hp) infection. A, total RNA extracted from AGS cells transfected with the indicated siRNA and infected with *H. pylori* was subjected to RT-PCR. B, AGS cells were cotransfected with the indicated siRNA, cdx2-luc reporter vector, and pRL-TK plasmid; cell lysates were subjected to luciferase assay. C, total RNA extracted from GSM06 cell stably expressing either control shRNA or NOD1-shRNA was subjected to qPCR. D, GSM06 cells stably expressing NOD1-shRNA were infected with 5×10^7 CFU/mL *H. pylori*. Total RNA was extracted and subjected to qPCR. E, GCIY cells were infected with *H. pylori* with or without preincubation with iE-DAP. Total RNA was extracted and subjected to qPCR. Results shown in B–E indicated as means ± SD. *, $P < 0.05$ as compared with *H. pylori*-infected cells transfected with control siRNA

(B), control shRNA transfected cells (C and D), and non-pretreated cells (E). AU, arbitrary units.

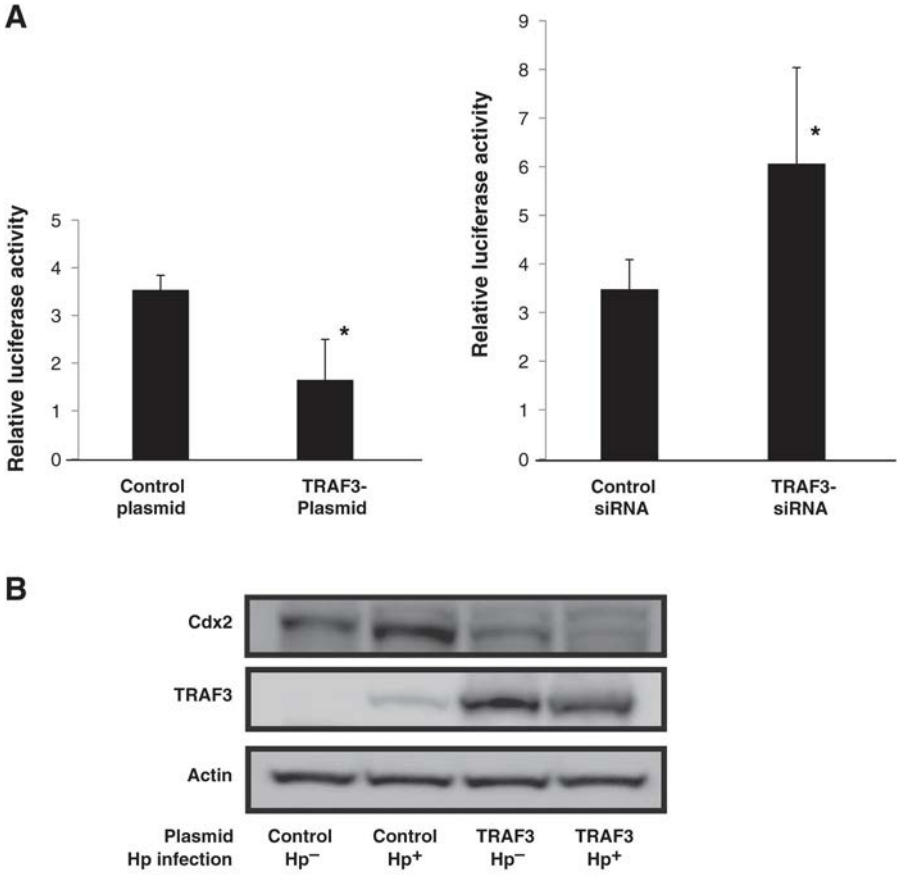

Figure 4.

TRAF3 suppresses NF-κB activation and Cdx2 expression. A, AGS cells transfected with an NF-κB reporter plasmid together with pRL-TK plasmid and cotransfected with either a TRAF3 expression plasmid or TRAF3-siRNA were infected with *H. pylori* (Hp), and relative luciferase activity was measured. Results, means ± SD. *, $P < 0.05$ as compared with control plasmid or control siRNA–transfected cells. B, AGS cells transfected with either a control plasmid or a TRAF3 expression plasmid were cultured in either *H. pylori*–infected or uninfected media. After 24 hours, cell lysates were obtained and subjected to Western blotting.

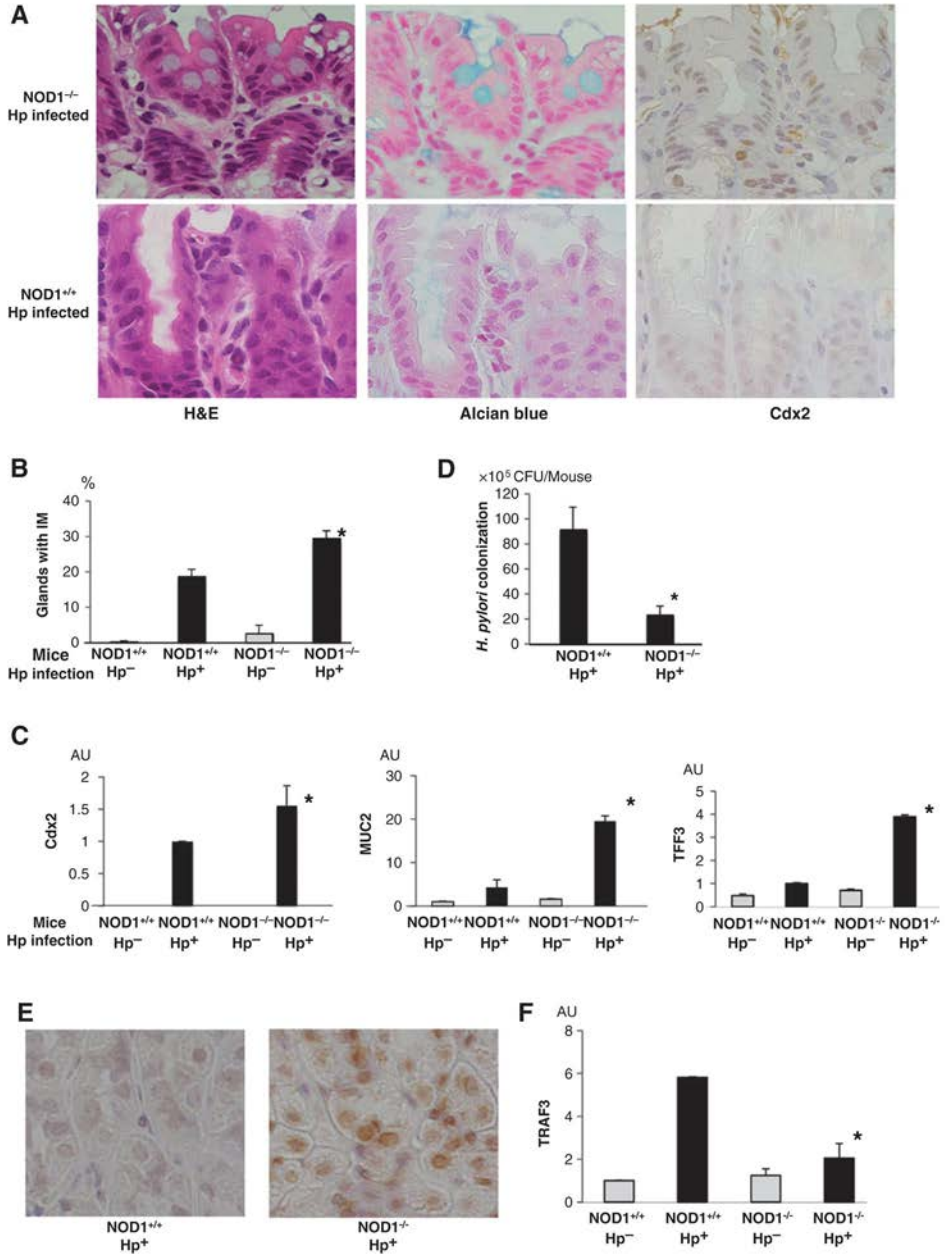

Figure 5.

NOD1 deficiency enhances the formation of gastric intestinal metaplasia during *in vivo H. pylori* (Hp) infection. A, H&E staining, Alcian blue staining, and immunohistochemistry for Cdx2 of gastric mucosa removed from *H. pylori*–infected NOD1-deficient and NOD1-intact mice. B, percentage of glands exhibiting intestinal metaplasia (IM) in the stomachs of NOD1-intact and NOD1-deficient mice. C, total RNA extracted from the stomachs of these mice was subjected to qPCR. D, loads of *H. pylori* in the stomachs of NOD1-intact and NOD1-deficient mice 12 months after initiation of *H. pylori* infection. E, gastric expression of NF-κB p65 in the stomach of NOD1-intact and NOD1-deficient mice. F, total RNA extracted from the stomachs of chronically infected mice was subjected to qPCR. Results

shown in B, C, D, and F indicate means ± SD.*, $P < 0.05$ as compared with *H. pylori*–infected NOD1-intact mice. AU, arbitrary units.

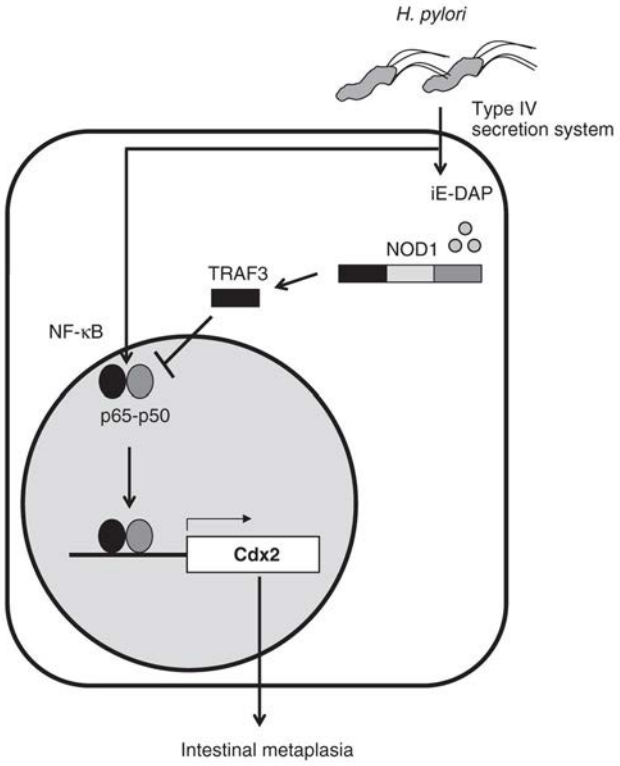

Figure 6.
Schematic view of the suppressive role of NOD1 on *H. pylori* infection–induced Cdx2 induction.

Through-the-scope enteral metal stent placement using a short-type single-balloon enteroscope for malignant surgically reconstructed jejunal stenosis (with video)

Self-expandable metal stent (SEMS) placement in surgically reconstructed intestine is technically challenging, and only a few reports have been published.[1,2] Here, we describe a case of successful SEMS placement for surgically reconstructed jejunal stenosis using a newly developed short-type single-balloon enteroscope (sSBE). A 70-year-old man presented to our hospital with fever and jaundice. Six months earlier, he had undergone subtotal stomach-preserving pancreatoduodenectomy with PD-II reconstruction for duodenal cancer. Computed tomography revealed a dilated intrahepatic bile duct as a result of stenosis in the surgically reconstructed jejunal loop caused by cancer recurrence (Fig. 1a). We could reach the stenosis using a sSBE (SIF-H290S; channel diameter, 3.2 mm; Olympus, Tokyo, Japan); however, it was impossible to pass beyond the stenosis (Fig. 1b). Because of the advanced stage of cancer, palliative through-the-scope (TTS) SEMS placement was attempted. A 0.035-inch guidewire was advanced beyond the stenosis, and an uncovered SEMS (18-mm wide, 80-mm long; Niti-S Enteral Colonic Stent; Taewoong Medical, Gimpo, Korea) was deployed (Fig. 2, Video S1). The postoperative period was uneventful. Jaundice and cholangitis resolved in a few days. Abdominal X-ray revealed that the stent was well expanded. The sSBE is compatible with the use of various interventional devices through its large working channel. To date, there is only one report on TTS SEMS placement, but it used a short-type double-balloon enteroscope (DBE).[3] In comparison with DBE, SBE was assumed to be more disadvantageous in carrying out deep insertion.[4] Having been equipped with a passive bending part, the sSBE has an increased endoscope flexibility. A recent article using sSBE showed its success rate of insertion to the blind end to be 92%.[5] Although the safety of SEMS placement in the jejunum is yet to be established, TTS SEMS placement using sSBE could be an effective, minimally invasive treatment option for patients with advanced cancer.

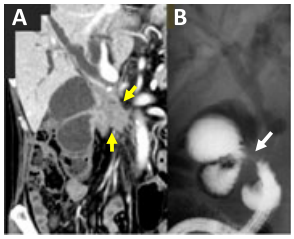

Figure 1 (A) Contrast-enhanced computed tomography showing a dilated intrahepatic bile duct and a jejunal stenosis (arrows). (B) Fluoroscopic image showing a jejunal stenosis (arrow) located near the choledochojejunostomy site.

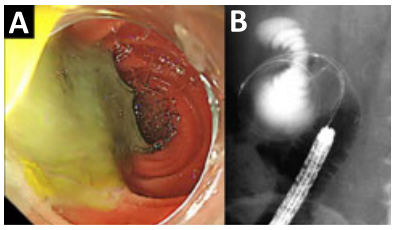

Figure 2 Uncovered enteral self-expandable metal stent was deployed across the stenotic lesion. (A) Endoscopic view; (B) fluoroscopic view.

Authors declare no conflicts of interest for this article.

Kosuke Minaga[1], Masayuki Kitano[1] and Mamoru Takenaka[1]
[1]*Department of Gastroenterology and Hepatology, Kindai University Faculty of Medicine, Osaka-Sayama, Japan*
doi: 10.1111/den.12702

REFERENCES

1 Nakahara K, Okuse C, Matsumoto N et al. Enteral metallic stenting by balloon enteroscopy for obstruction of surgically reconstructed intestine. *World J. Gastroenterol.* 2015; **21**: 7589–7593.
2 Kida A, Matsuda K, Noda Y. Endoscopic metallic stenting by double-balloon enteroscopy and its overtube for malignant gastrointestinal obstruction as palliative treatment. *Dig. Endosc.* 2013; **25**: 552–553.
3 Shimatani M, Takaoka M, Tokuhara M et al. Through-the-scope self-expandable metal stent placement using newly developed short double-balloon endoscope for the effective management of malignant afferent-loop obstruction. *Endoscopy* 2016; **48**: E6–E7.
4 Shah RJ, Smolkin M, Yen R et al. A multicenter, U.S. experience of single-balloon, double-balloon, and rotational overtube-assisted enteroscopy ERCP in patients with surgically altered pancreaticobiliary anatomy (with video). *Gastrointest. Endosc.* 2013; **77**: 593–600.
5 Shimatani M, Takaoka M, Ikeura T et al. Evaluation of endoscopic retrograde cholangiopancreatography using a newly developed short-type single-balloon endoscope in patients with altered gastrointestinal anatomy. *Dig. Endosc.* 2014; **26** (Suppl 2): 147–155.

SUPPORTING INFORMATION

ADDITIONAL SUPPORTING INFORMATION may be found in the online version of this article at the publisher's website:

Video S1. Through-the-scope enteral metal stent placement using a short-type single-balloon enteroscope for malignant surgically reconstructed jejunal stenosis.

Diagnosis of autoimmune pancreatitis by EUS-guided FNA using a 22-gauge needle: a prospective multicenter study CME

Atsushi Kanno, MD, PhD,[1] Atsushi Masamune, MD, PhD,[1] Fumiyoshi Fujishima, MD, PhD,[2] Takuji Iwashita, MD, PhD,[3] Yuzo Kodama, MD, PhD,[4] Akio Katanuma, MD,[5] Hirotaka Ohara, MD, PhD,[6] Masayuki Kitano, MD, PhD,[7] Hiroyuki Inoue, MD, PhD,[8] Takao Itoi, MD, PhD,[9] Nobumasa Mizuno, MD, PhD,[10] Hiroyuki Miyakawa, MD, PhD,[11] Rintaro Mikata, MD, PhD,[12] Atsushi Irisawa, MD, PhD,[13] Satoko Sato, MD, PhD,[2] Kenji Notohara, MD, PhD,[14] Tooru Shimosegawa, MD, PhD[1]

Sendai, Gifu, Kyoto, Sapporo, Nagoya, Osaka, Tsu, Tokyo, Chiba, Aizu-wakamatsu, Kurashiki, Japan

Background and Aims: Histopathologic examination is critical for diagnosing autoimmune pancreatitis (AIP). However, specimens obtained using EUS-guided FNA (EUS-FNA) are not recommended for histopathologic diagnosis because of inadequate sample size volume. We evaluated EUS-FNA efficacy for AIP diagnosis using a 22G needle.

Methods: Seventy-eight patients exhibiting the imaging characteristics indicative of AIP in the pancreatic parenchyma and pancreatic duct underwent EUS-FNA with a 22G needle at 12 institutions between February 2013 and March 2014. Samples were evaluated for tissue sampling conditions, CD38- and IgG4-positive plasma cell counts, storiform fibrosis (SF), and obliterative phlebitis (OP).

Results: Tissue specimens containing >10, 5 to 10, and 1 to 4 high-power fields (HPFs) were obtained from 29 (37.2%), 18 (23.1%), and 15 (19.2%) of 78 patients, respectively. The mean ± standard deviation (SD) CD38- and IgG4-positive plasma cell counts were 23.2 ± 18.8/HPF and 5.1 ± 6.7/HPF, respectively. SF was detected in 49 of 78 patients (62.8%) and OP in 38 of 78 patients (48.7%). According to the International Consensus Diagnostic Criteria (ICDC), histopathologic levels corresponded to level 1 in 32, level 2 in 13, and unclassifiable in 17 patients. Hence, 45 of 78 patients (57.7%) could be diagnosed with lymphoplasmacytic sclerosing pancreatitis according to ICDC.

Conclusions: Pancreatic tissues with at least 1 HPF were obtained by EUS-FNA from approximately 80% of patients, and nearly 60% of patients were diagnosed with ICDC level 2 or higher. Our findings indicate that EUS-FNA with a 22G needle may be useful for the histopathologic diagnosis of AIP. (Clinical trial registration number: UMIN000010097.) (Gastrointest Endosc 2016;84:797-804.)

Abbreviations: AIP, autoimmune pancreatitis; HPF, high-power field; ICDC, International Consensus Diagnostic Criteria; IgG, immunoglobulin G; LPSP, lymphoplasmacytic sclerosing pancreatitis; OP, obliterative phlebitis; SF, storiform fibrosis; SD, standard deviation.

DISCLOSURE: *The following author received research support for this study from a Grant-in-Aid from the Japan Society for the Promotion of Science (no. 25461020): A. Kanno. All authors disclosed no financial relationships relevant to this publication. The following authors received research support from the Ministry of Health, Labor, and Welfare of Japan (Principal Investigators: Tsutomu Chiba, Tsuneyo Mimori, and Yoshifumi Takeyama): A. Masamune, H. Obara, M. Kitano, T. Itoi, A. Irisawa, K. Notohara, and T. Shimosegawa.*

See CME section; p. 833.

0016-5107/$36.00
http://dx.doi.org/10.1016/j.gie.2016.03.1511

Received August 16, 2015. Accepted March 30, 2016.

Current affiliations: Division of Gastroenterology (1), Department of Pathology (2), Tohoku University Graduate School of Medicine, Sendai, Japan; First Department of Internal Medicine, Gifu University Hospital, Gifu, Japan (3), Department of Gastroenterology and Hepatology, Kyoto University Graduate School of Medicine, Kyoto, Japan (4), Center for Gastroenterology, Teine-Keijinkai Hospital, Sapporo, Japan (5), Department of Gastroenterology and Metabolism, Nagoya City University Graduate School of Medical Sciences, Nagoya, Japan (6), Department of Gastroenterology and Hepatology, Kinki University Faculty of Medicine, Osaka, Japan (7), Department of Gastroenterology and Hepatology, Mie University School of Medicine, Tsu, Japan (8), Department of Gastroenterology and Hepatology, Tokyo Medical University, Tokyo, Japan (9), Department of Gastroenterology, Aichi Cancer Center Hospital, Nagoya, Japan (10), Department of Gastroenterology, Sapporo Kosei Hospital, Sapporo, Japan (11), Department of Gastroenterology and Nephrology, Chiba University Graduate School of Medicine, Chiba, Japan (12), Department of Gastroenterology, Fukushima Medical University Aizu Medical Center, Aizu-wakamatsu, Japan (13), Department of Anatomic Pathology, Kurashiki Central Hospital, Kurashiki, Japan (14).

Reprint requests: Atsushi Kanno, MD, PhD, Division of Gastroenterology, Tohoku University Graduate School of Medicine, 1-1 Seiryo-machi, Aoba-ku, Sendai, Miyagi 980-8574, Japan.

Autoimmune pancreatitis (AIP) is a rare type of pancreatitis with a hypothesized autoimmune mechanism and distinctive clinical characteristics. AIP is currently regarded as a pancreatic manifestation of systemic immunoglobulin G (IgG)4-related disease[1] and has several distinct clinical, serologic, and morphologic characteristics. Histologically, lymphoplasmacytic sclerosing pancreatitis (LPSP) is a characteristic feature of type 1 AIP,[2] whereas idiopathic duct-centric chronic pancreatitis and granulocytic epithelial lesions are of type 2 AIP.[3-5] Compared with Western countries, type 2 AIP is extremely rare in Japan.[6-8] The world's first clinical diagnostic criteria for AIP were released by the Japan Pancreas Society in 2002.[9] Subsequently, diagnostic criteria for AIP have been proposed in several other countries.[10-14] To standardize the diagnostic criteria of AIP, the International Consensus Diagnostic Criteria (ICDC) were proposed in 2011.[15] EUS-guided FNA (EUS-FNA) is not included in ICDC as a method for histopathologic diagnosis of AIP because of the difficulty in obtaining adequate specimens for histopathologic analysis. However, several reports have suggested that EUS-FNA is useful for the diagnosis of AIP.[16-18] Therefore, we conducted a prospective multicenter study to investigate whether EUS-FNA is useful for the histopathologic diagnosis of AIP.

METHODS

This multicenter study was prospectively conducted between February 2013 and March 2014 at 12 tertiary care referral centers. The inclusion criteria included patients exhibiting the imaging characteristics, such as diffuse or segmental/focal enlargement with delayed enhancement and diffuse or segmental/focal or multiple irregular narrowing of the main pancreatic duct without marked upstream dilatation, indicative of AIP in the pancreatic parenchyma and pancreatic duct according to the ICDC. These findings were detected by cross-sectional images via CT and/or magnetic resonance imaging techniques. Exclusion criteria were as follows: (1) patients less than 20 years old, (2) patients in whom EUS-FNA is difficult (eg, cases with surgically altered anatomy), (3) patients with a performance status > 2 as defined by the Eastern Cooperative Oncology Group, (4) patients with malignant tumors, and (5) patients who declined to participate. Patients with surgically altered anatomy were excluded because it was difficult to acquire clear EUS images from the stomach or duodenum in such cases. All patients who participated in this study provided written informed consent. The study was approved by the institutional review board at all participating institutions and was registered on February 22, 2013 at the University Hospitals Medical Information Network (UMIN000010097).

A linear echoendoscope with an Expect 22G needle (Boston Scientific Japan, Tokyo, Japan) was used to perform EUS-FNA. EUS-FNA processing of histologic samples and immunostaining were performed as previously described.[18] Endosonographers punctured the enlarged region in segmental or focal type AIP. In patients with a diffusely enlarged pancreas, the endosonographer determined the puncture site. Endosonographers did not change the pancreatic region for puncture in each session of EUS-FNA. After the puncture, a needle was moved up and down 10 to 20 times within the enlarged pancreas by pulling the needle stylet slowly and steadily (slow-pull method) or by aspiration under 20 mL of negative pressure (aspiration method). The endosonographer at each institution decided whether to use the slow-pull or aspiration method.

The number of punctures was 3.4 ± 1.3 (mean ± standard deviation [SD]; range, 1-7). Tissue samples were fixed in formalin and embedded in paraffin, and several thin serial sections were prepared at each institution. The sliced sections were subsequently sent to the Tohoku University Hospital for histologic examination. Hematoxylin and eosin, Masson's trichrome, and Elastica-Masson staining were performed on each section. Immunohistochemical staining was performed using antibodies against IgG4 (Invitrogen, Gaithersburg, Md) and CD38 (Novocastra, Newcastle upon Tyne, UK).

An expert pathologist (F.F.), who was blinded to all clinical information, reviewed the histopathologic specimens. An average of >10 IgG4- and CD38-positive plasma cells per high-power field (HPF, 400×) was defined as IgG4-positive and lymphocyte-plasma cell infiltration, respectively. Tissue samples were also examined for the presence of storiform fibrosis (SF), obliterative phlebitis (OP), and granulocytic epithelial lesions. OP was diagnosed by Elastica-Masson staining. Because the arteries and veins are usually found next to each other in the pancreas, OP unaccompanied by arteries was judged to be a suspected diagnosis.

Statistics

Statistical analysis was performed using SPSS, version 20.0 (SPSS Inc., Chicago, Ill). A P value < .05 was considered to be statistically significant.

RESULTS

Clinical findings

Eighty-one patients were assessed for eligibility, and 3 patients were excluded because of pancreatic cancer (n = 1) or surgically altered anatomy (n = 2). Table 1 summarizes the clinical characteristics of the 78 enrolled patients. A male-to-female ratio of 60:18 and a mean ± SD age of 65.8 ± 11.1 years were observed. Seventy-seven of the 78 patients (98.7%) showed pancreatic enlargement; 39.7% (31/78), 33.3% (26/78), and 25.6% (20/78) had diffuse, segmental, and focal enlargement, respectively. Only 1 patient did not exhibit pancreatic enlargement. In this patient the endosonographer

TABLE 1. Clinical profiles of the enrolled patients

Characteristics	Values
Sex, male-to-female	60:18
Age, y (mean ± SD)	65.8 ± 11.1
Pancreatic imaging	
Enlargement	77/78 (98.7%)
Diffuse enlargement	31/77 (40.3%)
Segmental enlargement	26/77 (33.8%)
Focal enlargement	20/77 (26.0%)
MPD narrowing	70/78 (89.7%)
Diffuse (≥2/3)	24/70 (34.3%)
Segmental (1/3-2/3)	21/70 (30.0%)
Focal (<1/3)	24/70 (34.3%)
Serology	
IgG4 ± SD, mg/dL	421.0 ± 351.2
IgG4, ≥135 mg/dL	63/78 (80.8%)
Level 1, ≥270 mg/dL	43/78 (55.1%)
Level 2, ≥135 mg/dL <270 mg/dL	20/78 (25.6%)
OOI (including overlapping cases)	44/78 (56.4%)
Level 1	
Sclerosing cholangitis (hilar)	5
Sclerosing cholangitis (intrapancreatic lesion)	15
Retroperitoneal fibrosis	2
Level 2	
Sialadenitis, dacryoadenitis	28
Interstitial nephritis	3
OOI for type 2	
Inflammatory bowel disease (ulcerative colitis)	2
Others	7
Treatment	
Steroid administration	52/78 (66.7%)
Effective cases	52/52 (100%)

MPD, Main pancreatic duct; *IgG*, immunoglobulin G; *OOI*, other organ involvement.

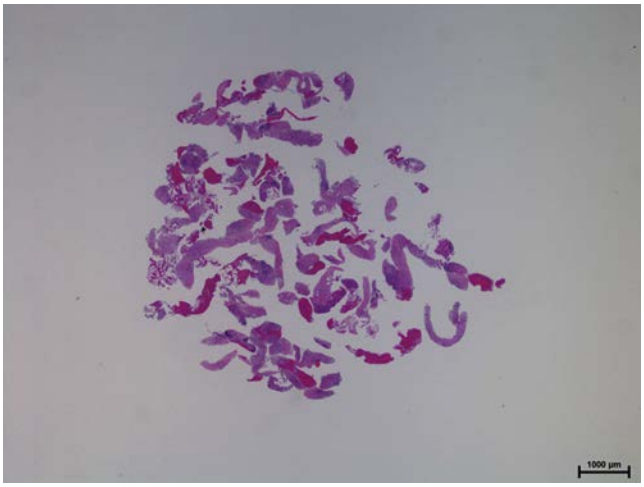

Figure 1. Macroscopic findings of the specimens obtained by EUS-FNA with a 22G needle demonstrated adequate specimens for histopathologic diagnosis (H&E, orig. mag. ×10).

TABLE 2. Tissue acquisition of the enrolled AIP patients

0	1-4 HPFs	5-10 HPFs	≥10 HPFs
16 (20.5%)	15 (19.2%)	18 (23.1%)	29 (37.2%)

AIP, Autoimmune pancreatitis; *HPFs*, high-power fields.

TABLE 3. Histopathologic findings of the enrolled AIP patients

Findings	Per-protocol
IgG4-positive plasma cells (mean ± SD)	5.1 ± 6.7/HPFs
IgG4 (≥10/HPFs)	19/78 (24.4%)
CD38-positive plasma cells (mean ± SD)	23.2 ± 18.8/HPFs
CD38 (≥10/HPFs)	43/78 (55.1%)
Storiform fibrosis	49/78 (62.8%)
Obliterative phlebitis	38/78 (48.7%)

AIP, Autoimmune pancreatitis; *IgG*, Immunoglobulin G; *HPFs*, high-power fields; *CD*, cluster of differentiation.

punctured the pancreatic body where the main pancreatic duct was irregularly narrowed.

Main pancreatic duct narrowing was observed in 70 patients (89.7%). Among them, approximately two thirds of the patients presented with segmental main pancreatic duct narrowing. Serum IgG4 was increased to ≥135 mg/dL (upper limit of normal range in Japan) in 63 of 78 patients (80.8%). The number of patients with levels 1 (IgG4 >270 mg/dL) and 2 (IgG4 ≥ 135 and <270 mg/dL) in the serologic criteria were 43 and 20, respectively. The involvement of other organs was detected in 44 of 78 patients (56.4%).

No patients had a history of steroid treatment, and steroids were administered to 52 patients (66.7%) after EUS-FNA. No patients had been treated with immunomodulating drugs.

Histopathologic examination

Tissue acquisition. The numbers of patients whose tissue specimens contained >10, 5 to 10, and 1 to 4 HPFs were 29 (37.2%), 18 (23.1%), and 15 (19.2%), respectively (Fig. 1, Tables 2 and 3). Pancreatic tissue specimens from 16 patients (20.5%) contained no HPFs. The following results are presented per protocol (n = 78).

IgG4-positive plasma cells. Abundant lymphoplasmacytic infiltration was observed in these specimens (Fig. 2). The mean ± SD IgG4-positive plasma cell count was 5.1 ± 6.7 per HPF (Fig. 3). Specimens from 19 patients (24.4%) contained >10 IgG4-positive plasma cells per HPF on an average.

CD38-positive plasma cells. The mean ± SD CD38-positive plasma cell count was 23.2 ± 18.8 per HPF

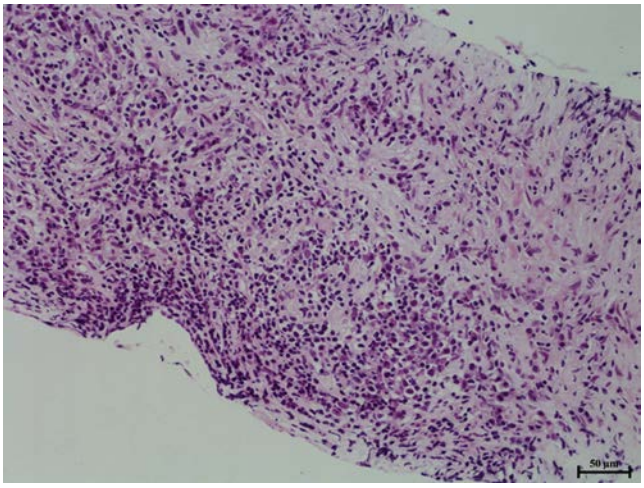

Figure 2. The findings in high-power fields (H&E, orig. mag. ×400) reveal abundant lymphoplasmacytic infiltration.

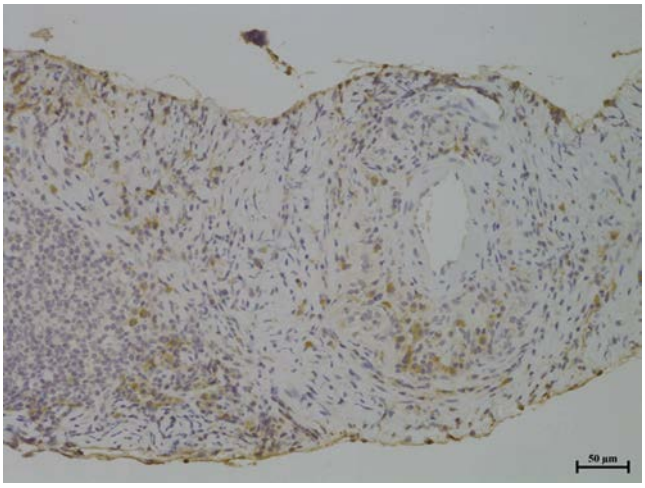

Figure 4. Immunohistochemical staining of CD38. Abundant CD38-positive plasma cells were found in the high-power field (orig. mag. ×400).

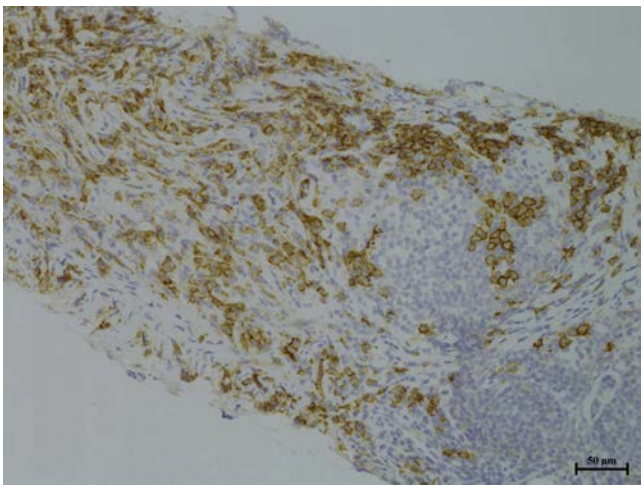

Figure 3. IgG4 immunostaining in the specimens obtained by EUS-FNA shows markedly increased numbers of IgG4-positive plasma cells (orig. mag. ×400).

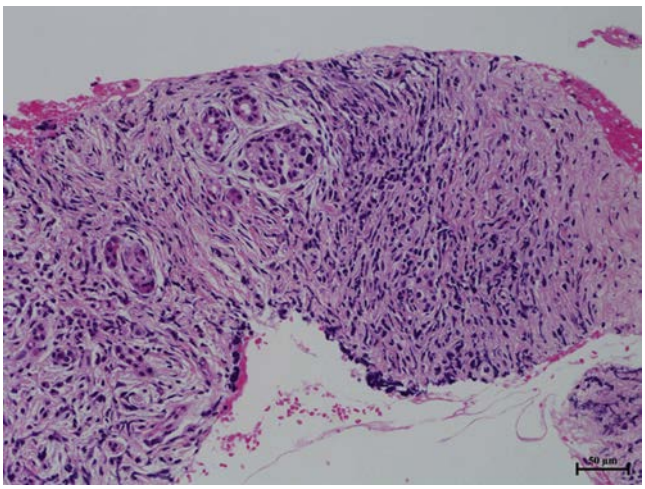

Figure 5. A specimen showing storiform fibrosis in high-power fields (H&E, orig. mag. ×400).

(Fig. 4). Specimens from 43 patients (55.1%) contained >10 CD38-positive plasma cells per HPF on average.

SF, OP, and granulocytic epithelial lesions. The presence of SF was observed in 49 patients (62.8%) (Fig. 5) and of OP in 38 patients (48.7%) (Fig. 6). Granulocytic epithelial lesions were not observed in any of the patients.

Histopathologic diagnosis according to the ICDC

Of the 62 patients whose specimens contained at least 1 HPF, 3 or 4 items were positively identified as level 1 in 32 patients and 2 items were positively identified as level 2 in 13 patients, indicating that 45 of 62 patients (70.5%) had LPSP according to the ICDC. Therefore, 45 of 78 patients (57.7%) undergoing EUS-FNA had LPSP according to the ICDC. Table 4 summarizes the histopathologic findings stratified by the number of HPFs acquired by EUS-FNA. The number of patients diagnosed as having LPSP were significantly higher in specimens containing >10 HPFs than in those containing ≤10 HPFs (28/29 vs 17/33; $P < .01$).

There were no patients with type 2 AIP in this study. This result was not unexpected because cases of type 2 AIP are extremely rare in Japan.[3] Our previous study demonstrated that type 2 AIP could be accurately diagnosed by EUS-FNA.[18]

Adverse events

There were no adverse events (eg, pancreatitis) during or after EUS-FNA in any of the 78 enrolled patients.

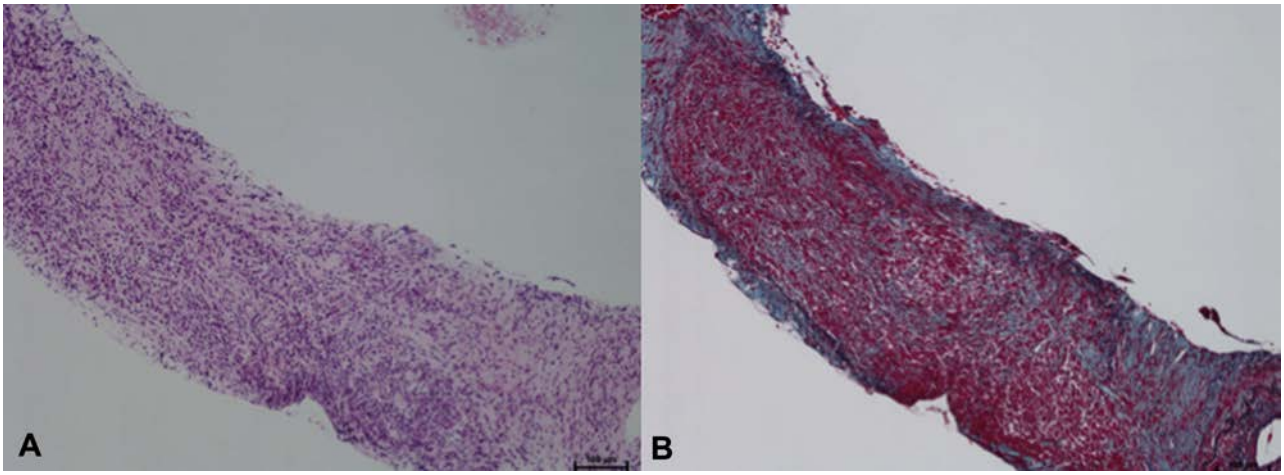

Figure 6. Obstructive phlebitis revealed by (**A**) H&E and (**B**) Elastica-Masson staining (orig. mag. ×200) shows that the infiltration of inflammatory cells obstructed the vein.

TABLE 4. Summary of the histopathologic findings according to the number of HPFs obtained via EUS-FNA

	No. of HPFs obtained by EUS-FNA			
	0	**1–4**	**5–10**	**>10**
No. of patients	16	15	18	29
IgG4 (≥10/HPFs)	—	0 (0%)	4 (22.2%)	15 (51.7%)
CD38 (≥10/HPFs)	—	3 (20.0%)	12 (66.7%)	28 (96.6%)
Storiform fibrosis	—	9 (60.0%)	15 (83.3%)	25 (86.2%)
Obliterative phlebitis	—	4 (26.7%)	7 (38.9%)	27 (93.1%)
No. of patients diagnosed as LPSP according to ICDC	—	7 (46.7%)	10 (55.6%)	28 (96.6%)

HPFs, High-power fields; *IgG*, immunoglobulin G; *LPSP*, lymphoplasmacytic sclerosing pancreatitis; *ICDC*, International consensus diagnostic criteria; —, not acquired data.

Contribution of histologic findings to the diagnosis of AIP according to the ICDC

According to the ICDC,[15] 25 patients could be diagnosed as having definitive type 1 AIP in the absence of histologic findings based on pancreatic imaging, serum IgG4, and other organ involvement (Fig. 7). Of these 25 patients, 9, 5, and 11 patients had histologic findings of level 1, level 2, and undiagnosed AIP in the specimens obtained by EUS-FNA, respectively. In contrast, 53 patients could not be diagnosed with definitive type 1 AIP based on pancreatic imaging, serum IgG4, and other organ involvement. Of these 53 patients, 23, 8, and 22 patients had histologic findings of level 1, level 2, and undiagnosed AIP, respectively. These 23 level 1 patients could be diagnosed as definitive type 1 AIP solely based on the histologic findings of EUS-FNA specimens (Fig. 7).

DISCUSSION

Histologic examination is important for the diagnosis of AIP. According to the ICDC, if 3 of 4 cardinal histopathologic findings are present (ie, LPSP), type 1 AIP can be definitively diagnosed without the need for any additional findings. The ICDC currently requires histologic specimens to be acquired by EUS-trucut biopsy sampling or operation but not EUS-FNA.[15,19-21] However, the needles for EUS-trucut biopsy sampling are not commercially available in several countries. EUS-trucut biopsy sampling or EUS-FNA using a large-gauge needle poses a risk of adverse events (eg, bleeding or perforation), and it is difficult to handle an endoscope with tight angulation.[22] We have previously reported that the histologic diagnosis of AIP according to the ICDC could be made in 20 of 25 patients (80%) using EUS-FNA with a 22G needle.[18] A 22G aspiration needle has been widely used in clinical examinations in Japan. To extend this finding, we conducted a multicenter, prospective study. In agreement with our previous study, pancreatic tissues with at least 1 HPF were obtained from approximately 80% of patients by EUS-FNA with a 22G needle. Nearly 60% of patients were diagnosed with ICDC level 2 or higher, supporting the notion that EUS-FNA with a 22G needle is useful for the histopathologic diagnosis of AIP. In line with this finding, studies, including a nationwide epidemiologic survey, showed that EUS-FNA has become the most widely used modality for obtaining pancreatic tissue specimens for the diagnosis of AIP.[16-18,23]

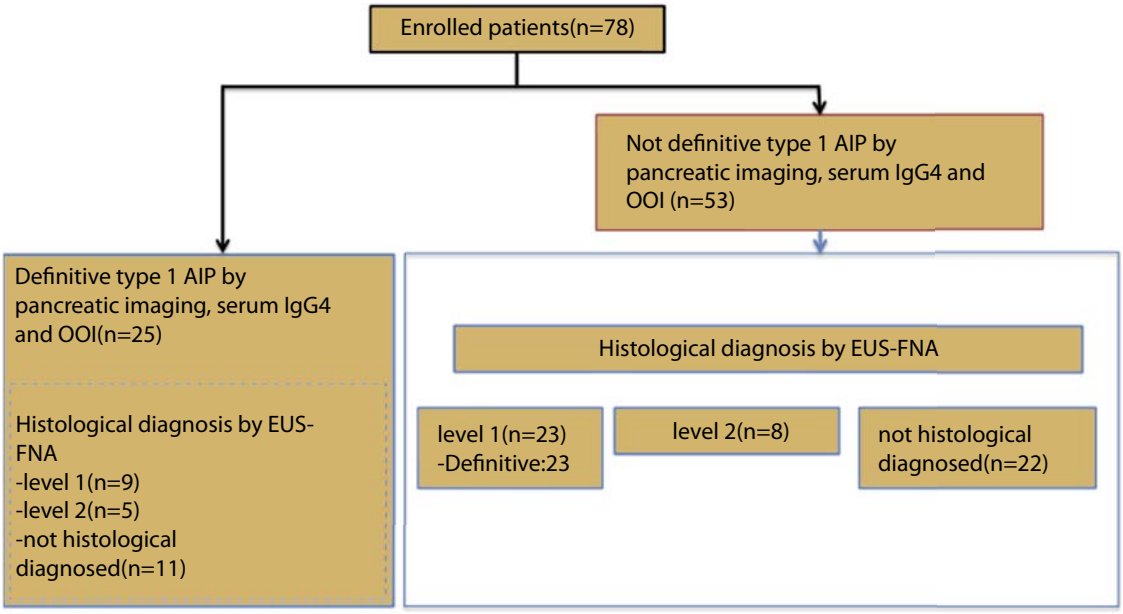

Figure 7. Flowchart illustrating the summary of this study focusing on the diagnosis according to the ICDC. *AIP,* autoimmune pancreatitis; *OOI,* other organ involvement; *ICDC,* International consensus diagnostic criteria.

TABLE 5. Comparison between the 2 groups of patients whose histologic samples were or were not obtained by EUS-FNA

	Sample obtained (n = 62)	Sample not obtained (n = 16)	*P* value
Sex (male/female)	48/14	12/4	.99
Age, y (mean ± SD)	65.6 ± 11.4	60.0 ± 10.2	.90
No. of punctures	3.5 ± 1.3	3.1 ± 1.1	.26
Region punctured (head/body/tail)	22/35/5	6/7/3	.40
Range of pancreatic enlargement (diffuse/other)	24/38	7/8	.57
MPD findings (narrowing/not narrowing)	55/7	15/1	.99

MPD, Main pancreatic duct.

In this study adequate tissue sampling was unsuccessful in 16 of 78 patients (20.5%). We compared the clinical features between patients whose tissue specimens contained at least 1 HPF (n = 62) and those with no HPF (n = 16). As shown in Table 5, there were no significantly different factors between the 2 groups. Our ability to obtain a sufficient histologic sample via EUS-FNA in each examination could be influenced by several factors (eg, individual technique of the endosonographer, hardness of the pancreas, and specific devices selected for EUS-FNA). Consequently, it is very difficult to clarify the optimal conditions for obtaining good-quality histologic samples by EUS-FNA. There are several important tips to optimize histopathologic sampling by EUS-FNA. We have emphasized the importance of quick movement of the FNA needle and selection of whitish pancreatic tissue from tubifex-like pieces.[18] We can collect many pancreatic tissue samples on 1 glass slide by trimming the aspirated specimens using a disposable 18G needle. Several studies have suggested that adequate processing of EUS-FNA specimens is important to obtain specimens suitable for histologic diagnosis.[18,24] However, it is difficult to standardize the processing of EUS-FNA specimens because the involvement of pathologic departments varied among the institutions. Iwashita et al[25] reported that macroscopic on-site quality assessment increases the diagnostic yield of EUS-FNA. Moreover, the presence of OP suggests AIP. OP was identified or suspected in 38 patients (48.7%). The diagnostic rate of OP in this study was excellent compared with that of OP in previous studies.[16,17,26] Elastica-Masson staining was useful to detect elastic fibers, which is also critical for diagnosing OP. On the other hand, the rate of IgG4-positive plasma cells was relatively low, in agreement with a previous study.[18] In this study some patients had serum IgG4 levels below 135 mg/dL. These results suggest that the existence of IgG4-positive plasma cells in histopathologic samples varies depending on the AIP activity. In the future, EUS-FNA may provide useful information regarding the function and behavior of IgG4-positive plasma cells in AIP.

There were no observed adverse events (eg, pancreatitis) during or after EUS-FNA in any of the 78 enrolled patients. In a systematic review by Wang et al,[27] of the 8246 patients undergoing EUS-FNA for pancreatic lesions, 36 (.44%) developed pancreatitis, which was mild to moderate in most cases. This rate is significantly lower than that after ERCP; in which a higher incidence of pancreatitis (3.5%) and pancreatitis-related mortality (3.1%) has been reported in a systematic review.[28]

Seventeen cases could not be diagnosed as LPSP, and in this study 28 of 29 patients whose specimen contained >10 HPFs could be diagnosed as LPSP. The number of patients diagnosed as LPSP were significantly higher in specimens containing >10 HPFs than in those containing ≤10 HPFs ($P < .01$). Therefore, most of these undiagnosed patients might have been diagnosed as LPSP if adequate sample material containing more HPFs was obtained. The development of specific needles for safe and adequate sampling for histopathologic analysis is urgently needed.

The ICDC uses the following 4 items for the histopathologic diagnosis of type 1 AIP: (1) infiltration of lymphocyte-plasma cells, (2) >10 IgG4-positive plasma cells in HPF, (3) SF, and (4) OP.[15] In this study, 13 patients satisfied all 4 items and 19 and 13 patients satisfied 3 and 2 items, respectively. Therefore, 32 patients were diagnosed as having level 1 and 13 patients as having level 2 in the histologic criteria according to the ICDC. In the ICDC, the diagnosis of definitive type 1 AIP could be made solely on the basis of a level 1 histologic finding (ie, LPSP). In these cases, ductal imaging on ERCP is not essential for the diagnosis of AIP and might be avoided. In addition, 53 patients could not be diagnosed as definitive AIP on the basis of pancreatic imaging, serology, and other organ involvement. Twenty-three of these 53 patients had level 1 histologic findings in EUS-FNA samples and could be diagnosed as definitive type 1 AIP without the aid of pancreatic imaging, serology, other organ involvement, and response to steroids. Therefore, further studies are required to clarify whether EUS-FNA should be included in the future diagnostic criteria of AIP as a method to obtain pancreatic samples for histologic evaluation.

ACKNOWLEDGMENTS

We express our deepest appreciation for the members of this study group: A. Kanno, A. Masamune (Senior Author), K. Kume, S. Hamada, K. Kikuta, S. Miura, T. Takikawa, E. Nakano, S. Hongo, N. Yoshida, M. Hirota, and T. Shimosegawa from Tohoku University Graduate School of Medicine (Division of Gastroenterology); F. Fujishima and S. Sato from Tohoku University Graduate School of Medicine (Department of Pathology); T. Iwashita and I. Yasuda from Gifu University Hospital (First Department of Internal Medicine); Y. Kodama and A. Kurita from Kyoto University Graduate School of Medicine (Department of Gastroenterology and Hepatology); H. Maguchi, A. Katanuma, K. Yane, K. Matsumoto, and R. Takagi from Teine-Keijinkai Hospital (Center for Gastroenterology); H. Ohara and I. Naito from Nagoya City University Graduate School of Medical Sciences (Department of Gastroenterology and Metabolism); M. Kitano, K. Kadosaka, S. Oomoto, and T. Miyata from Kinki University Faculty of Medicine (Department of Gastroenterology and Hepatology); H. Inoue and R. Yamada from Mie University School of Medicine (Department of Gastroenterology and Hepatology); T. Itoi and N. Ikeuchi from Tokyo Medical University (Department of Gastroenterology and Hepatology); N. Mizuno from Aichi Cancer Center Hospital (Department of Gastroenterology); H. Miyakawa from Sapporo Kosei Hospital (Department of Gastroenterology); R. Mikata from Chiba University Graduate School of Medicine (Department of Gastroenterology and Nephrology); A. Irisawa, A. Yamabe, and G. Shibukawa from Fukushima Medical University Aizu Medical Center (Department of Gastroenterology); and K. Notohara from Kurashiki Central Hospital (Department of Anatomic Pathology).

REFERENCES

1. Umehara H, Okazaki K, Masaki Y, et al. Comprehensive diagnostic criteria for IgG4-related disease (IgG4-RD), 2011. Mod Rheumatol 2012;22:21-30.
2. Kawaguchi K, Koike M, Tsuruta K, et al. Lymphoplasmacytic sclerosing pancreatitis with cholangitis: a variant of primary sclerosing cholangitis extensively involving pancreas. Hum Pathol 1991;22:387-95.
3. Notohara K, Burgart LJ, Yadav D, et al. Idiopathic chronic pancreatitis with periductal lymphoplasmacytic infiltration: clinicopathologic features of 35 cases. Am J Surg Pathol 2003;27:1119-27.
4. Zamboni G, Luttges J, Capelli P, et al. Histopathological features of diagnostic and clinical relevance in autoimmune pancreatitis: a study on 53 resection specimens and 9 biopsy specimens. Virchows Arch 2004;445:552-63.
5. Sugumar A, Kloppel G, Chari ST. Autoimmune pancreatitis: pathologic subtypes and their implications for its diagnosis. Am J Gastroenterol 2009;104:2308-10.
6. Kawa S, Okazaki K, Notohara K, et al. Autoimmune pancreatitis complicated with inflammatory bowel disease and comparative study of type 1 and type 2 autoimmune pancreatitis. J Gastroenterol 2015;50:805-15.
7. Hart PA, Kamisawa T, Brugge WR, et al. Long-term outcomes of autoimmune pancreatitis: a multicentre, international analysis. Gut 2013;62:1771-6.
8. Kamisawa T, Notohara K, Shimosegawa T. Two clinicopathologic subtypes of autoimmune pancreatitis: LPSP and IDCP. Gastroenterology 2010;139:22-5.
9. Members of the Criteria Committee for Autoimmune Pancreatitis of the Japan Pancreas Society. Diagnostic criteria for autoimmune pancreatitis by the Japan Pancreas Society (2002) [Japanese with English abstract]. Suizo 2002;17:585-7.
10. Kim KP, Kim MH, Kim JC, et al. Diagnostic criteria for autoimmune chronic pancreatitis revisited. World J Gastroenterol 2006;12:2487-96.
11. Chari ST, Smyrk TC, Levy MJ, et al. Diagnosis of autoimmune pancreatitis: the Mayo Clinic experience. Clin Gastroenterol Hepatol 2006;4:1010-6; quiz 934.
12. Chari ST, Takahashi N, Levy MJ, et al. A diagnostic strategy to distinguish autoimmune pancreatitis from pancreatic cancer. Clin Gastroenterol Hepatol 2009;7:1097-103.

13. Schneider AL, Löhr JM, Singer MV. The M-ANNHEIM classification of chronic pancreatitis: introduction of a unifying classification system based on a review of previous classification of the disease. J Gastroenterol 2007;42:101-19.
14. Pearson RK, Longnecker DS, Chari ST, et al. Controversies in clinical pancreatology: autoimmune pancreatitis: does it exist? Pancreas 2003;27:1-13.
15. Shimosegawa T, Chari ST, Frulloni L, et al. International consensus diagnostic criteria for autoimmune pancreatitis: guidelines of the International Association of Pancreatology. Pancreas 2011;40:352-8.
16. Iwashita T, Yasuda I, Doi S, et al. Use of samples from endoscopic ultrasound-guided 19-gauge fine-needle aspiration in diagnosis of autoimmune pancreatitis. Clin Gastroenterol Hepatol 2012;10:316-22.
17. Ishikawa T, Itoh A, Kawashima H, et al. Usefulness of EUS combined with contrast-enhancement in the differential diagnosis of malignant versus benign and preoperative localization of pancreatic endocrine tumors. Gastrointest Endosc 2010;71:951-9.
18. Kanno A, Ishida K, Hamada S, et al. Diagnosis of autoimmune pancreatitis by EUS-FNA by using a 22-gauge needle based on the International Consensus Diagnostic Criteria. Gastrointest Endosc 2012;76:594-602.
19. Levy MJ, Reddy RP, Wiersema MJ, et al. EUS-guided trucut biopsy in establishing autoimmune pancreatitis as the cause of obstructive jaundice. Gastrointest Endosc 2005;61:467-72.
20. Levy MJ, Smyrk TC, Takahashi N, et al. Idiopathic duct-centric pancreatitis: disease description and endoscopic ultrasonography-guided trucut biopsy diagnosis. Pancreatology 2011;11:76-80.
21. Mizuno N, Bhatia V, Hosoda W, et al. Histological diagnosis of autoimmune pancreatitis using EUS-guided trucut biopsy: a comparison study with EUS-FNA. J Gastroenterol 2009;44:742-50.
22. Itoi T, Itokawa F, Kurihara T, et al. Experimental endoscopy: objective evaluation of EUS needles. Gastrointest Endosc 2009;69:509-16.
23. Kanno A, Masamune A, Okazaki K, et al. Nationwide epidemiological survey of autoimmune pancreatitis in Japan in 2011. Pancreas 2015;44:535-9.
24. Unno J, Kanno A, Masamune A, et al. The usefulness of endoscopic ultrasound-guided fine-needle aspiration for the diagnosis of pancreatic neuroendocrine tumors based on the World Health Organization classification. Scand J Gastroenterol 2014;49:1367-74.
25. Iwashita T, Yasuda I, Mukai T, et al. Macroscopic on-site quality evaluation of biopsy specimens to improve the diagnostic accuracy during EUS-guided FNA using a 19-gauge needle for solid lesions: a single-center prospective pilot study (MOSE study). Gastrointest Endosc 2015;81:177-85.
26. Imai K, Matsubayashi H, Fukutomi A, et al. Endoscopic ultrasonography-guided fine needle aspiration biopsy using 22-gauge needle in diagnosis of autoimmune pancreatitis. Dig Liver Dis 2011;43:869-74.
27. Wang KX, Ben QW, Jin ZD, et al. Assessment of morbidity and mortality associated with EUS-guided FNA: a systematic review. Gastrointest Endosc 2011;73:283-90.
28. Andriulli A, Loperfido S, Napolitano G, et al. Incidence rates of post-ERCP complications: a systematic survey of prospective studies. Am J Gastroenterol 2007;102:1781-8.

APPENDIX

This study group consists of A. Kanno, A. Masamune, K. Kume, S. Hamada, K. Kikuta, S. Miura, T. Takikawa, E. Nakano, S. Hongo, N. Yoshida, M. Hirota, T. Shimosegawa, Tohoku University Graduate School of Medicine (Division of Gastroenterology); F. Fujishima, S. Sato, Tohoku University Graduate School of Medicine (Department of Pathology); T. Iwashita, I Yasuda, Gifu University Hospital (First Department of Internal Medicine); Y. Kodama, A. Kurita, Kyoto University Graduate School of Medicine (Department of Gastroenterology and Hepatology); H. Maguchi, A. Katanuma, K. Yane, K. Matsumoto, R. Takagi, Teine-Keijinkai Hospital (Center for Gastroenterology); H. Ohara, I. Naito, Nagoya City University Graduate School of Medical Sciences (Department of Gastroenterology and Metabolism); M. Kitano, K. Kadosaka, S. Oomoto, T. Miyata, Kinki University Faculty of Medicine (Department of Gastroenterology and Hepatology); H. Inoue, R. Yamada, Mie University School of Medicine (Department of Gastroenterology and Hepatology); T. Itoi, N. Ikeuchi, Tokyo Medical University (Department of Gastroenterology and Hepatology); N. Mizuno, Aichi Cancer Center Hospital (Department of Gastroenterology); H. Miyakawa, Sapporo Kosei Hospital (Department of Gastroenterology); R. Mikata, Chiba University Graduate School of Medicine (Department of Gastroenterology and Nephrology); A. Irisawa, A. Yamabe, G. Shibukawa, Fukushima Medical University Aizu Medical Center (Department of Gastroenterology); K. Notohara, Kurashiki Central Hospital (Department of Anatomic Pathology).

JGH Journal of Gastroenterology and Hepatology

JGHF

doi:10.1111/jgh.13394

REVIEW ARTICLE

Asian consensus statements on endoscopic management of walled-off necrosis Part 1: Epidemiology, diagnosis, and treatment

Hiroyuki Isayama,* Yousuke Nakai,* Rungsun Rerknimitr,† Christopher Khor,‡ James Lau,§ Hsiu-Po Wang,¶ Dong Wan Seo,** Thawee Ratanachu-ek,†† Sundeep Lakhtakia,‡‡ Tiing Leong Ang,§§ Shomei Ryozawa,¶¶ Tsuyoshi Hayashi,*** Hiroshi Kawakami,††† Natusyo Yamamoto,* Takuji Iwashita,‡‡‡ Fumihide Itokawa,§§§ Masaki Kuwatani,¶¶¶ Masayuki Kitano,**** Keiji Hanada,†††† Hirofumi Kogure,* Tsuyoshi Hamada,* Ryan Ponnudurai,‡‡‡‡ Jong Ho Moon,§§§§ Takao Itoi,§§§ Ichiro Yasuda,¶¶¶¶ Atsushi Irisawa,***** and Iruru Maetani,†††††

*Department of Gastroenterology, Graduate School of Medicine, The University of Tokyo, †††††Division of Gastroenterology and Hepatology, Department of Internal Medicine, Toho University Ohashi Medical Center and, §§§Department of Gastroenterology and Hepatology, Tokyo Medical University, Tokyo, ***Department of Gastroenterology, Hokkaido Cancer Center, †††Department of Gastroenterology and Hepatology and, ¶¶¶Division of Endoscopy, Hokkaido University Hospital, Sapporo, Department of Gastroenterology, ¶¶Saitama Medical University International Medical Center, Saitama, ††††Onomichi General Hospital, Onomichi, ¶¶¶¶Teikyo University Mizonokuchi Hospital, Kanagawa, *****Aizu Medical Center, Fukushima Medical University, Aizuwakamatsu, ‡‡‡First Department of Internal Medicine, Gifu University Hospital, Gifu, ****Department of Gastroenterology and Hepatology, Kinki University Faculty of Medicine, Osaka-sayama, Japan; †Division of Gastroenterology, Department of Medicine, Chulalongkorn University and, ††Department of Surgery, Rajavithi Hospital, Bangkok, Thailand; Department of Gastroenterology and Hepatology, ‡Singapore General Hospital and, §§Changi General Hospital, Singapore, Singapore; Department of Internal Medicine, §§§§Soon Chun Hyang University School of Medicine, Digestive Disease Center and Research Institute, Bucheon and **Asan Medical Center, University of Ulsan College of Medicine, Seoul, Korea; §Department of Surgery, Endoscopic Center, Prince of Wales Hospital, The Chinese University of Hong Kong, Hong Kong, China; ¶Endoscopic Division, National Taiwan University Hospital, National Taiwan University, Taipei, Taiwan; ‡‡Asian Institute of Gastroenterology, Hyderabad, India; and ‡‡‡‡Prince Court Medical Center, Kuala Lumpur, Malaysia

Key words
acute necrotizing pancreatitis, endoscopic necrosectomy, endoscopy, endosonography, walled-off necrosis.

Accepted for publication 22 March 2016.

Correspondence
Dr. Hiroyuki Isayama, Department of Gastroenterology, Graduate School of Medicine, The University of Tokyo, 7-3-1 Hongo Bunkyo-ku, Tokyo 113-8655, Japan.
Email: isayama-tky@umin.ac.jp

Author contributions: HI was involved with study conception, study design, creation of the preliminary statements list and the allocated statement, drafting of the manuscript, critical revision of the manuscript, obtaining funding, face-to-face meetings, and voting.
YN, NY, RR, and CK were involved with creation of the preliminary statements list and the allocated statement, drafting of the manuscript, critical revision of the manuscript, face-to-face meetings, and voting.
All authors were involved with creation of the allocated statement, drafting of the manuscript, critical revision of the manuscript, obtaining funding, face-to-face meetings, and voting.
Funding: An unrestricted education grant was provided by Century Medical Inc., FujiFilm Medical Corp., and Hitachi Medical Company.

Abstract

Walled-off necrosis (WON) is a relatively new term for encapsulated necrotic tissue after severe acute pancreatitis. Various terminologies such as pseudocyst, necroma, pancreatic abscess, and infected necrosis were previously used in the literature, resulting in confusion. The current and past terminologies must be reconciled to meaningfully interpret past data. Recently, endoscopic necrosectomy was introduced as a treatment option and is now preferred over surgical necrosectomy when the expertise is available. However, high-quality evidence is still lacking, and there is no standard management strategy for WON. The consensus meeting aimed to clarify the diagnostic criteria for WON and the role of endoscopic interventions in its management. In the Consensus Conference, 27 experts from eight Asian countries took an active role and examined key clinical aspects of WON diagnosis and endoscopic management. Statements were crafted based on literature review and expert opinion, employing the modified Delphi method. All statements were substantiated by the level of evidence and the strength of the recommendation. We created 27 consensus statements for WON diagnosis and management, including details of endoscopic procedures. When there was not enough solid evidence to support the statements, this was clearly acknowledged to facilitate future research. Proposed management strategies were formulated and are illustrated using flow charts. These recommendations, which are based on the best current scientific evidence and expert opinion, will be useful for guiding endoscopic management of WON. Part 1 of this statement focused on the epidemiology, diagnosis, and timing of intervention.

These sponsors did not participate in the literature search, consensus discussion, voting, lecture preparation, or manuscript preparation.

History of presentation: These consensus statements were presented at the Tokyo Conference of Asian Pancreato-biliary Interventional Endoscopy (T-CAP) 2014 in Tokyo, Japan and Asian Pacific Digestive Week (APDW) 2014 in Bali, Indonesia.

Introduction

Severe acute pancreatitis is a challenging disease for gastroenterologists. Severe acute pancreatitis with necrosis in the pancreatic parenchyma or surrounding fat tissue may lead to the formation of encapsulated fluid collections. Sometimes, this condition can be confused with pseudocyst or retention of pancreatic secretions due to disruption of the pancreatic duct. In the revised Atlanta classification of acute pancreatitis,[1] encapsulated necrotic tissues were defined as "walled-off necrosis (WON)." However, endoscopic management of WON has not yet been well established, and different conditions were described in previous publications. In addition, few studies have focused specifically on the management of WON.

Treatment strategies for infected WON can be challenging. While WON may be improved by drainage alone, most cases require necrosectomy because of the underlying infected solid necrotic tissue. Open surgical necrosectomy was the standard treatment for infected WON, but the procedure was associated with high morbidity and mortality. Endoscopic necrosectomy, which was first reported by Seifert *et al.* in 2000,[2] initially involves endoscopic transmural drainage (currently achieved mainly through endoscopic ultrasound [EUS] guidance, followed by direct insertion of the endoscope into the cavity for removal of necrotic tissue by irrigation, suction, and the use of endoscopic accessories). Since the first report by Seifert,[2] several larger series have been published with good outcomes. However, the exact role of endoscopic necrosectomy among other options in the management of WON remains to be clearly established.

Given the lack of high-level evidence regarding the endoscopic management of WON, a consensus group was convened to formulate recommendations for the management of WON. Specifically, these recommendations were formulated by combining a formal literature review of the diagnostic criteria and role of endoscopic management of WON with expert opinions from Asian endoscopists.

Methods

A modified Delphi process was employed to establish this consensus statement. The statement was established based on a literature review and a consensus among the panelists. A principal planning group created lists of statements that were distributed to all the members. Statements were made for clinical questions, and each clinical question was allocated to one or two of the members.

A comprehensive literature search was performed in the MEDLINE and EMBASE databases as well as the Cochrane Trials Register in human subjects. The key words used for searching were "Walled-off necrosis," "Walled-off pancreatic necrosis," "Severe acute pancreatitis," "Necrotizing pancreatitis," "Organized pancreatic necrosis," "Pseudocyst," "Endoscopic necrosectomy," and "Necrosectomy." The doctors allocated to each statement then carefully reviewed and selected the appropriate literature.

Faculty of the Tokyo Conference of Asian Pancreato-biliary Interventional Endoscopy (T-CAP; http://www.t-cap.jp/) formed the working group for this consensus statement. The members of this working group were from eight Asian countries: 17 from Japan; 2 each from Thailand, Singapore, and Korea; and 1 each from Taiwan, Hong Kong, Malaysia, and India. All T-CAP faculty members were pancreaticobiliary endoscopists, and all were gastroenterologists apart from two surgeons (TR and JL). The 17 Japanese members were able to utilize the interventional radiology approach for treatment of WON when needed. Planning group members (HI, YN, NY, CK, and RR) created lists of statements and allocated them to the members. A face-to-face meeting was held in February 2014 in Tokyo. Each member made a presentation focusing on background, a summary of the scientific literature, the level of evidence, their proposed statement, and unanswered questions. Attendees discussed each statement, and amendments were made if needed. Thereafter, the statements were voted on by all attendees. Voting recommendations are shown in Table 1. The discussion was continued until an agreement of greater 80% for the A and B level of recommendations (accept completely and accept with some reservations) was reached. After the face-to-face meeting, each statement was corrected and presented again at the T-CAP annual meeting on June 27, 2014 in Tokyo and at Asian Pacific Digestive Week on October 24, 2014 in Bali for open discussion. Finally, the corrected statements were discussed among the faculty members via the Internet.

Consensus statements

1. Epidemiology

CQ1-1 What is the incidence of WON after acute pancreatitis?

Answer: The proportion of patients with necrotizing pancreatitis in a large series was 20–40%, and the proportion of WON cases treated with necrosectomy was 2–4%. We concluded that the incidence of WON should be between these figures.

Quality of evidence: III
Classification of recommendation: C
Level of agreement: a-100%, b-0%, c-0%, d-0%, e-0%

None of the studies analyzed cases with all types of WON (sterile or infected); rather, the studies analyzed cases of acute necrotizing pancreatitis (overestimation) or patients undergoing necrosectomy (underestimation). Because of the relatively recent introduction of the term "WON" in 2005, some studies referred to "infected necrotizing pancreatitis" or "infected pancreatic necrosis" and thus might include cases that were not WON. Previously, WON has also been described as "organized pancreatic necrosis," "necroma," "pancreatic sequestration," "pseudocyst associated with necrosis," and "subacute pancreatic necrosis."

Patients with necrotizing pancreatitis develop necrosis of the pancreatic parenchyma, the peripancreatic tissue, or both, and some of these patients subsequently develop WON. To date, the incidence of WON has remained unknown because we only have data regarding the incidence of necrotizing pancreatitis and treated WON. Table 2 presents a literature review, and the incidence of necrotizing pancreatitis in large series studies was reported to be 22.9% (359 of 1568 cases),[3] 29.7% (203 of 683),[4] and 39.5% (121 of 306).[5] The largest study, which included 9421 patients from China, reported that necrosectomy was performed in 412 patients (4.4%).[6] Based on our review of the literature, the incidence of necrotizing pancreatitis in a large series was 20–40%; however, this figure overestimates the incidence of WON because patients with necrotizing pancreatitis do not necessarily develop WON. The incidence of WON in patients treated with necrosectomy was 2–4%, which is likely an underestimation of the overall incidence of WON. Therefore, we concluded that the overall incidence

Table 1 Quality of evidence, classification of recommendations, and voting schema of the modified Canadian Task Force on the Periodic Health Examination

Category and grade	Description
Quality of evidence	
I	Evidence obtained from at least 1 RCT.
II-1	Evidence obtained from well-designed control trials without randomization.
II-2	Evidence obtained from a well-designed cohort or case–control study.
II-3	Evidence obtained from comparisons between times and places with or without intervention.
III	Opinion of respected authorities based on clinical experience and expert committees
Classification of the recommendation	
A	There is good evidence to support the statement.
B	There is fair evidence to support the statement.
C	There is poor evidence to support the statement, but the recommendation was made on other grounds.
D	There is fair evidence to refute the statement.
E	There is good evidence to refute the statement.
Voting on the recommendation	
A	Accept completely
B	Accept with some reservations
C	Accept with major reservations
D	Reject with reservations
E	Reject completely

Table 2 Incidence of walled-off necrosis (WON)

Author	Year	Country	No. of patients	WON; number (%)
Hartwig[5]	2002	Germany	306	121 (39.5)
Beger[3]	2003	Germany	1568	359 (22.9)
Lee[70]	2006	Singapore	373	14 (3.8)
Mofidi[71]	2007	UK	1248	233 (18.9)
Babu[20]	2010	UK	1535	28 (1.8)
Garg[4]	2010	India	683	203 (29.7)
De Rai [72]	2010	Italy	1173	29 (2.5)
Beenen[24]	2011	New Zealand	577	25 (4.3)
Guo [6]	2013	China	9421	412 (4.4)

of WON should be between these figures. All the attending physicians agreed that the literature was too limited to estimate the true incidence of WON and concluded that prospective data collection from a large number of outpatients/inpatients is required to clarify the true incidence of WON and the cause of WON.

Unanswered question: Due to the absence of an article evaluating the incidence of all types of WON, the incidence of WON is currently unknown.

CQ1-2 Are there any etiological factors that predispose a patient to develop WON?

Answer: While the most common causes of acute pancreatitis resulting in necrotizing pancreatitis or WON are biliary factors and alcohol consumption, no etiological factors have been identified that predispose a patient to develop necrotizing pancreatitis or WON.

Quality of evidence: III
Classification of recommendation: C
Level of agreement: a-90%, b-10%, c-0%, d-0%, e-0%

A considerably wide range of etiologies have been reported for acute pancreatitis, which can potentially cause WON. However, the distribution of the etiologies for WON has not been clarified. The largest study, which included 639 patients from the Netherlands, reported that the predominant cause of necrotizing pancreatitis was biliary factors (48%), followed by alcohol consumption (24%), and unknown factors (19%).[7] Based on our review of the literature, the leading causes of acute pancreatitis resulting in WON were biliary factors (median 40%, range 14–81%), alcohol consumption (median 27%, range 2–70%), and idiopathic factors (median 14%, range 4–45%).[6–38]"In addition to these etiologies, underlying obesity can affect the clinical course of acute pancreatitis. Obesity, especially visceral fat,[39,40] is a known risk factor for severe acute pancreatitis and was reported to cause more local complications including necrosis. Therefore, it is likely that obesity can be a risk factor for WON, although there were no high level clinical evidences."

We reviewed the literature to estimate the proportions of etiologies leading to the development of WON; however, we acknowledge several biases. First, because most studies did not analyze all consecutive cases of WON, and only patients with WON who were undergoing necrosectomy were evaluated, the true underlying etiologies of all WON cases were unclear. Second, the lack of uniformity in terminology, as described in CQ 1-1, prevented an optimal estimation. Collection of prospective registry data from multiple centers based on the uniform definition of WON is necessary.

Unanswered question: The incidence of acute pancreatitis leading to WON with a rare etiology (e.g. pancreas divisum or drug-induced pancreatitis) is unknown. The natural courses and outcomes of WON have not been fully evaluated according to each etiology.

2. Diagnosis of WON

CQ.2. How can we make a diagnosis of WON?

Answer: WON is defined as a mature, encapsulated collection of necrotic pancreatic and/or peripancreatic tissue that develops ≥4 weeks after the onset of acute pancreatitis. Contrast-enhanced computed tomography (CE-CT) is commonly used as a standard technique to diagnose WON. Magnetic resonance imaging (MRI), transabdominal ultrasound (US), or EUS may be used as a complementary modality to better define the presence of a solid component.

Quality of evidence: II-3
Classification of recommendation: C
Level of agreement: a-95%, b-5%, c-0%, d-0%, e-0%

Walled-off necrosis is a relatively new clinical entity. The differential diagnosis of WON from pseudocyst is important because the treatment procedure for each disease is different, and these two entities are sometimes misdiagnosed.

To make the correct diagnosis, both imaging findings and clinical course are important. There are two types of acute pancreatitis defined in the Revised Atlanta Classification (2012): interstitial edematous pancreatitis and necrotizing pancreatitis. Four weeks after the onset of acute pancreatitis, acute peripancreatic fluid that collects and becomes encapsulated with a well-defined inflammatory wall is referred to as a "pseudocyst." Pseudocysts contain mostly liquid components. On the other hand, necrotizing pancreatitis with acute necrotic collection develops into WON at 4 weeks after onset. WON is also a well-defined, encapsulated inflammatory collection similar to a pseudocyst, but solid components are present. The detection of solid components is important for distinguishing WON from pseudocyst using imaging modalities.

Contrast-enhanced computed tomography depicts "WON" as heterogeneous with liquid and non-liquid density with varying degrees of loculations (some may appear homogeneous).[1,41] However, CE-CT may not readily distinguish solid content from liquid content in some cases (Fig. 1). MRI,[1,42,43] transabdominal US[1,42], or EUS[1,42] may be required for this distinction. MRI and US are also recommended especially for pregnant patients and for patients with renal insufficiency or allergy to iodine.[42,44] US-guided or EUS-guided fine needle aspiration (FNA) might be available for a diagnosis of infected WON.[1,42,45] We reviewed the reported literature in Table 3.

Unanswered question: What are the diagnostic yields of MRI and EUS for the detection of WON with solid components in fluid collections?

3. Diagnosis of infection

CQ3-1. What are the symptoms and imaging findings of infected WON?

Answer: Persistent sepsis or progressive clinical deterioration is indicative of infected WON. The presence of gas bubbles within the WON on computed tomography (CT) is suggestive of infection.

Quality of evidence: III
Classification of recommendation: C
Level of agreement: a-94%, b-6%, c-0%, d-0%, e-0%

A definitive diagnosis of infected WON is mandatory because the treatment strategy obviously differs from that utilized for sterile WON. However, optimal diagnostic methods that make use of imaging modalities and clinical findings have not yet been established. Therefore, signs of infection should be monitored carefully based on assessments of clinical manifestations as well as performance of blood tests, blood cultures, and CT scans, especially in the late phase of acute pancreatitis.

There have been no studies examining the diagnostic accuracy of imaging findings of infected WON. High-quality guidelines, which were evaluated by Loveday *et al.*,[46] described that "the presence of gas bubbles within pancreatic/peripancreatic necrosis" on CT was as an important indication of infection.[47–49] Gas within the fluid collection sometimes suggests an underlying fistula to the gastrointestinal lumen, and the risk of infection can be higher in patients with fistula to the colon than to the duodenum. Therefore, when gas is seen within the fluid collection on the cross-sectional images, the presence of fistula and subsequent infection should be carefully evaluated. In addition to gas within the fluid collection, shrinkage of the cavity, bleeding within the cavity, and abdominal pain can be the signs of fistula formation to the gastrointestinal lumen. There were no significant differences in common clinical signs (e.g. elevated white blood cell counts or fever) between sterile and infected pancreatic/peripancreatic necrosis.[50] The relationship between the occurrence of infected pancreatic/peripancreatic necrosis and the severity of pancreatitis (extent of necrosis, occurrence of organ failure, and pulmonary, renal, and cardiocirculatory insufficiency) was well investigated; however, groups at high risk for developing infected WON were not clearly identified.[51,52] Although definitive criteria do not exist, high-quality guidelines developed in the past decade stated that deterioration of the clinical course (e.g. systemic toxicity, organ

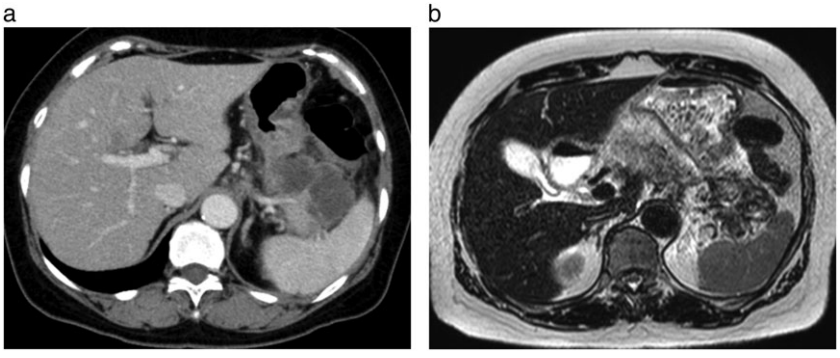

Figure 1 Detection of solid components in a cavity of walled-off necrosis (WON). (1a) Contrast-enhanced computed tomography did not reveal solid components in WON cavities. (1b) Magnetic resonance imaging showed solid components in WON cavities.

Table 3 Clinical studies examining the diagnosis of pancreatic necrosis or WON

Author	Year	No. of patients	Disease	Modality	Timing of imaging	Design	Pro/retro	Result
Mainwarning [73]	1989	40 (PNec 18)	PFC	CECT	During the 2 weeks preceding surgery	Observational/cross-sectional	Retrospective	CT grading (C, D, R): differentiation of PCt and PNec
Morgan [43]	1997	19 (18 patients)	PFC	MR/CECT/US	3–20 weeks (average 8 weeks)	Interventional/sequential comparison	Prospective	Solid debris: MR (89) = US > CT (22%)
Lecesne [74]	1999	30 (PNec?)	AP	MR/CECT	23 patients ≤ 1 week, 2 patients between 1 and 2 weeks, 5 patients ≥ 2 weeks	Observational comparison	Retrospective	PNec: MR = CECT
Hirota [75]	2002	21 (PNec 8)	PNec	MR/CECT	Acute phase	Observational/comparison	Prospective	MRI can discriminate (1) necrotic area, (2) perinecrotic fluid collection, (3) hemorrhagic foci
Arvanitakis [76]	2004	39 (PNec 6)	AP	MR/CECT	Days ≤3, 7, 30	Interventional/sequential comparison	Prospective	Staging AP severity: MR = CECT
Viremouneix [77]	2007	90 (PNec 12–19)	AP	MR/CECT	≤ 6 days	Interventional/sequential comparison	Prospective	Staging AP severity: MR > CECT
Takahashi [41]	2008	78 (WOPN 45, PCt 28, Abscess 5)	PFC	CECT	During the week prior to endoscopic treatment	Observational/cross-sectional		CT can differentiate WOPN from PCt (79.5–83.6%)
Ocampo [78]	2009	129	PNec	CECT	Average 8.3 days	Observational/cross-sectional	Retrospective	Patients with peri-PNec: higher rates of infected PNec and mortality
Jurgensen [30]	2012	31	PNec	EUS	ND	Observational/cross-sectional	Retrospective	PNec with high liquid content: A high risk of complications

PFC, pancreatic fluid collection; PCt, pseudocyst; PNec, pancreatic necrosis; AP, acute pancreatitis; WON, walled-off necrosis; .WOPN, walled-off pancreatic necrosis; CECT, contrast-enhanced computed tomography; MR, magnetic resonance; EUS, endoscopic ultrasound; US, transabdominal ultrasound; CT, computed tomography.

failure, or sepsis) indicates the occurrence of infected pancreatic/peripancreatic necrosis, especially in the late phase of acute pancreatitis (3 or more weeks after the onset of acute pancreatitis). [47–49]

Unanswered question: What is the diagnostic accuracy of imaging findings of infected WON?

CQ3-2. Is image-guided FNA necessary for the diagnosis of infection?

Answer: Image-guided FNA is accurate tool for distinguishing sterile from infected WON. However, it is not always needed to establish a diagnosis of infection.

Quality of evidence: III
Classification of recommendation: C
Level of agreement: a-94%, b-6%, c-0%, d-0%, e-0%

A definitive diagnosis of infected WON can be made by positive culture of fluid in the WON cavity, which can be readily obtained by image-guided FNA (CT, US, or EUS). However, the indication for FNA and its impact on the management of WON have not been well established.

Several clinical studies have shown the safety and diagnostic validity of Gram's stain and culture of specimens obtained by percutaneous FNA from the necrotic area.[8,50,52–56] High-quality guidelines in the past decade recommended that patients with suspected infected necrosis should undergo FNA to prove infection prior to (surgical) necrosectomy.[47–49] The false-negative rate was reported to be 0–17% (median, 4%), even in studies in which repeat FNA was performed.[50,52–55] Recent randomized controlled trials (RCTs) determined that patients without positive Gram's stain or culture were eligible for minimally invasive step-up intervention (i.e. percutaneous catheter drainage or endoscopic transluminal drainage) depending either on the deterioration of the clinical course (e.g. systemic toxicity, organ failure, or sepsis) or on the presence of gas bubbles within pancreatic/peripancreatic necrosis on CT.[27,57]

The attendees disagreed that image-guided FNA (e.g. US-guided, EUS-guided, and CT-guided FNA) is indispensable for the diagnosis of infection. This procedure appears to be omitted in many hospitals because sonographers, radiologists, and endosonographers may not be routinely available. In addition, conservative treatments such as antimicrobial agents or minimally invasive interventions have been accepted as initial treatments, even in cases of suspected infected WON. Thus, the need for image-guided FNA seems to be limited in patients for whom highly invasive intervention is scheduled only if the presence of a bacterial infection is proven.

Unanswered question: Is FNA truly an indispensable modality for infected WON? When should we perform FNA for the diagnosis of WON?

4. Indication for treatment

CQ4-1. Is there a role for medical treatment of WON?

Answer: Yes. Medical treatment is the first step in the management of patients with WON.

Quality of evidence: II-2
Classification of recommendation: B
Level of agreement: a-100%, b-0%, c-0%, d-0%, e-0%

Medical treatment is the first step in the management of patients with WON. Patients will require supportive therapy, which includes systemic antibiotics, nutritional support, and other organ support such as mechanical ventilation and inotropic support as required.

Nutrition: A meta-analysis of RCTs has shown that in severe acute pancreatitis, including acute pancreatitis associated with WON, enteral nutrition decreased systemic infections, multi-organ failure, the need for surgical intervention, and mortality compared with parenteral nutrition.[58] Parenteral nutrition should be avoided unless enteral nutrition is not available, not tolerated, or not meeting the caloric needs of the patient.

Antibiotics: A meta-analysis of RCTs has shown that antibiotics do not prevent secondary infection of necrosis.[59] Hence, their role is only in the treatment of an active or suspected infection. Some reports have indicated that antibiotics alone may suffice for the treatment of infected WON in patients in good clinical condition. Thus, based on data from large case series, it is acknowledged that selected clinically stable patients with infected necrosis who are minimally symptomatic can be treated with antibiotics alone but require intervention if clinical deterioration occurs.[56–59]

Drugs that suppress the secretion of pancreatic juice: Octreotide and somatostatin analogues are not recommended because they did not show significant effectiveness in the treatment of severe acute pancreatitis.[60]

Protease inhibitors: Protease inhibitors lack a definite clinical benefit based on meta-analyses.[61,62] The routine use of protease inhibitors is not recommended by current guidelines, and a recent review of a Japanese administrative dataset also did not show any benefits.[63]

Antacid drugs: Histamine H2-receptor antagonist also failed to show any benefits for patients with acute pancreatitis. This was acknowledged in the 2006 Japanese guidelines.[64] A pilot RCT from Korea also showed no benefits of proton pump inhibitor therapy.[65]

Unanswered question: Which medical treatments are effective during the necrosectomy procedure?

CQ4-2. What are the indications for drainage in WON?

Answer: Drainage (with or without necrosectomy) is recommended for symptomatic WON.

Quality of evidence: II-2
Classification of recommendation: C
Level of agreement: a-80%, b-15%, c-5%, d-0%, e-0%

A drainage procedure (with or without necrosectomy) is indicated for patients with symptomatic WON who are unresponsive to medical treatment. The modalities include an endoscopic approach, a percutaneous approach, and surgical necrosectomy. A recent RCT demonstrated that a minimally invasive step-up approach reduces mortality and major

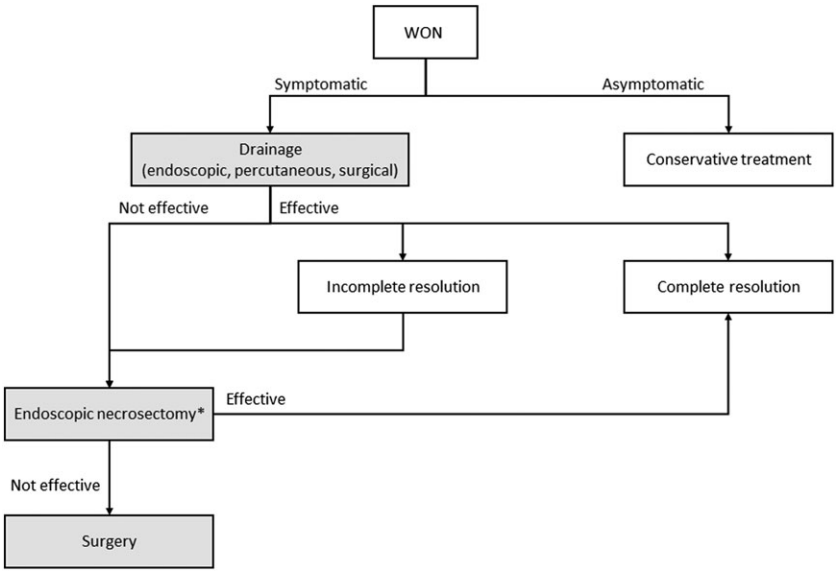

Figure 2 Flow chart illustrating the proposed management of walled-off necrosis (WON). *If endoscopic procedure is impossible, surgical or percutaneous necrosectomy will be performed.

complications from 69% to 40% compared with primary open necrosectomy.[22]

Unanswered question: For patients with WON, when should we proceed directly to drainage without waiting for medical treatment failure?

5. Timing of necrosectomy

CQ5. Should we perform necrosectomy immediately after the diagnosis of WON?

Answer: The initial step for the treatment of symptomatic WON is either percutaneous or endoscopic drainage. Necrosectomy should then be considered if the drainage procedure is not effective.

Quality of evidence: II-2
Classification of recommendation: B
Level of agreement: a-68%, b-32%, c-0%, d-0%, e-0%

There are no clear criteria regarding when to proceed to necrosectomy. There are two types of treatment strategies for necrosectomy: necrosectomy during the initial drainage session (direct necrosectomy) and necrosectomy after a failed response to drainage (step-up approach). Based on the literature review, 35–55% of patients with infected WON can be treated successfully with percutaneous or endoscopic drainage alone.[21,66,67] Mouli *et al*. pooled eight retrospective observational studies ($n = 324$) on conservative treatment for patients with infected pancreatic necrosis and found that only 26% of them needed subsequent necrosectomy. In four observational studies ($n = 157$) on drainage alone for infected pancreatic necrosis, 38% of patients underwent necrosectomy.[68] Although endoscopic necrosectomy is effective and requires a relatively short treatment period, it can cause serious complications including death. The morbidity and mortality rates in previous large-scale studies were reported to be 14–33% and 5.8–11%.[17,26,36] Therefore, endoscopic necrosectomy should be considered only after the failure of the step-up approach.[7,22,69]

Figure 2 presents a flowchart illustrating the WON management strategy proposed by this working group. Endoscopic management for infected WON should be considered if the patient fails to improve after the initial medical treatment and drainage. Surgical procedures should be considered when endoscopic necrosectomy is ineffective (See CQ 6 in Part 2).

Unanswered question: How can we predict which patients will require necrosectomy?

Summary

In summary, WON is a new term, and various terminologies were previously used in the literature, resulting in confusion. In addition, high-level evidence is still lacking regarding the endoscopic management of WON. We tried to make the consensus statements through a formal literature review in combination with expert opinions from Asian endoscopists. Part 1 of the Asian consensus statements regarding endoscopic management of WON in severe acute pancreatitis focused on the epidemiology, diagnosis, and timing of intervention. Part 2 of the Asian consensus statements highlight endoscopic management of WON and its adjunctive treatment.

References

1 Banks PA, Bollen TL, Dervenis C *et al.* Classification of acute pancreatitis—2012: revision of the Atlanta classification and definitions by international consensus. *Gut* 2013; **62**: 102–11.
2 Seifert H, Wehrmann T, Schmitt T, Zeuzem S, Caspary WF. Retroperitoneal endoscopic debridement for infected peripancreatic necrosis. *Lancet* 2000; **356**: 653–5.
3 Beger HG, Rau B, Isenmann R. Natural history of necrotizing pancreatitis. *Pancreatology* 2003; **3**: 93–101.
4 Garg PK, Sharma M, Madan K, Sahni P, Banerjee D, Goyal R. Primary conservative treatment results in mortality comparable to surgery in patients with infected pancreatic necrosis. *Clin. Gastroenterol. Hepatol.* 2010; **8**: 1089–94 e2.

5 Hartwig W, Werner J, Muller CA, Uhl W, Buchler MW. Surgical management of severe pancreatitis including sterile necrosis. *J. Hepatobiliary Pancreat. Surg.* 2002; **9**: 429–35.
6 Guo Q, Lu H, Hu W, Zhang Z. A retroperitoneal approach for infected pancreatic necrosis. *Scand. J. Gastroenterol.* 2013; **48**: 225–30.
7 van Santvoort HC, Bakker OJ, Bollen TL *et al.* A conservative and minimally invasive approach to necrotizing pancreatitis improves outcome. *Gastroenterology* 2011; **141**: 1254–63.
8 Rodriguez JR, Razo AO, Targarona J *et al.* Debridement and closed packing for sterile or infected necrotizing pancreatitis: insights into indications and outcomes in 167 patients. *Ann. Surg.* 2008; **247**: 294–9.
9 Tzovaras G, Parks RW, Diamond T, Rowlands BJ. Early and long-term results of surgery for severe necrotising pancreatitis. *Dig. Surg.* 2004; **21**: 41–6; discussion 6-7.
10 Wig JD, Mettu SR, Jindal R, Gupta R, Yadav TD. Closed lesser sac lavage in the management of pancreatic necrosis. *J. Gastroenterol. Hepatol.* 2004; **19**: 1010–5.
11 Connor S, Alexakis N, Raraty MG *et al.* Early and late complications after pancreatic necrosectomy. *Surgery* 2005; **137**: 499–505.
12 Reddy M, Jindal R, Gupta R, Yadav TD, Wig JD. Outcome after pancreatic necrosectomy: trends over 12 years at an Indian centre. *ANZ J. Surg.* 2006; **76**: 704–9.
13 Farkas G, Marton J, Mandi Y, Leindler L. Surgical management and complex treatment of infected pancreatic necrosis: 18-year experience at a single center. *J. Gastrointest. Surg.* 2006; **10**: 278–85.
14 Voermans RP, Veldkamp MC, Rauws EA, Bruno MJ, Fockens P. Endoscopic transmural debridement of symptomatic organized pancreatic necrosis (with videos). *Gastrointest. Endosc.* 2007; **66**: 909–16.
15 Papachristou GI, Takahashi N, Chahal P, Sarr MG, Baron TH. Peroral endoscopic drainage/debridement of walled-off pancreatic necrosis. *Ann. Surg.* 2007; **245**: 943–51.
16 Gardner TB, Chahal P, Papachristou GI *et al.* A comparison of direct endoscopic necrosectomy with transmural endoscopic drainage for the treatment of walled-off pancreatic necrosis. *Gastrointest. Endosc.* 2009; **69**: 1085–94.
17 Seifert H, Biermer M, Schmitt W *et al.* Transluminal endoscopic necrosectomy after acute pancreatitis: a multicentre study with long-term follow-up (the GEPARD Study). *Gut* 2009; **58**: 1260–6.
18 Parikh PY, Pitt HA, Kilbane M *et al.* Pancreatic necrosectomy: North American mortality is much lower than expected. *J. Am. Coll. Surg.* 2009; **209**: 712–9.
19 Cheung MT, Li WH, Kwok PC, Hong JK. Surgical management of pancreatic necrosis: towards lesser and later. *J. Hepatobiliary Pancreat. Sci.* 2010; **17**: 338–44.
20 Babu BI, Sheen AJ, Lee SH, O'Shea S, Eddleston JM, Siriwardena AK. Open pancreatic necrosectomy in the multidisciplinary management of postinflammatory necrosis. *Ann. Surg.* 2010; **251**: 783–6.
21 Horvath K, Freeny P, Escallon J *et al.* Safety and efficacy of video-assisted retroperitoneal debridement for infected pancreatic collections: a multicenter, prospective, single-arm phase 2 study. *Arch. Surg.* 2010; **145**: 817–25.
22 van Santvoort HC, Besselink MG, Bakker OJ *et al.* A step-up approach or open necrosectomy for necrotizing pancreatitis. *N. Engl. J. Med.* 2010; **362**: 1491–502.
23 Raraty MG, Halloran CM, Dodd S *et al.* Minimal access retroperitoneal pancreatic necrosectomy: improvement in morbidity and mortality with a less invasive approach. *Ann. Surg.* 2010; **251**: 787–93.
24 Beenen E, Brown L, Connor S. A comparison of the hospital costs of open vs. minimally invasive surgical management of necrotizing pancreatitis. *HPB* 2011; **13**: 178–84.
25 Varadarajulu S, Phadnis MA, Christein JD, Wilcox CM. Multiple transluminal gateway technique for EUS-guided drainage of symptomatic walled-off pancreatic necrosis. *Gastrointest. Endosc.* 2011; **74**: 74–80.
26 Gardner TB, Coelho-Prabhu N, Gordon SR *et al.* Direct endoscopic necrosectomy for the treatment of walled-off pancreatic necrosis: results from a multicenter U.S. series. *Gastrointest. Endosc.* 2011; **73**: 718–26.
27 Bakker OJ, van Santvoort HC, van Brunschot S *et al.* Endoscopic transgastric vs surgical necrosectomy for infected necrotizing pancreatitis: a randomized trial. *JAMA* 2012; **307**: 1053–61.
28 Senthil Kumar P, Ravichandran P, Jeswanth S. Case matched comparison study of the necrosectomy by retroperitoneal approach with transperitoneal approach for necrotizing pancreatitis in patients with CT severity score of 7 and above. *Int. J. Surg.* 2012; **10**: 587–92.
29 Tong Z, Li W, Yu W *et al.* Percutaneous catheter drainage for infective pancreatic necrosis: is it always the first choice for all patients? *Pancreas* 2012; **41**: 302–5.
30 Jurgensen C, Neser F, Boese-Landgraf J, Schuppan D, Stolzel U, Fritscher-Ravens A. Endoscopic ultrasound-guided endoscopic necrosectomy of the pancreas: is irrigation necessary? *Surg. Endosc.* 2012; **26**: 1359–63.
31 Bausch D, Wellner U, Kahl S *et al.* Minimally invasive operations for acute necrotizing pancreatitis: comparison of minimally invasive retroperitoneal necrosectomy with endoscopic transgastric necrosectomy. *Surgery* 2012; **152**: S128–34.
32 Tan J, Tan H, Hu B *et al.* Short-term outcomes from a multicenter retrospective study in China comparing laparoscopic and open surgery for the treatment of infected pancreatic necrosis. *J. Laparoendosc. Adv. Surg. Tech. A* 2012; **22**: 27–33.
33 Gluck M, Ross A, Irani S *et al.* Dual modality drainage for symptomatic walled-off pancreatic necrosis reduces length of hospitalization, radiological procedures, and number of endoscopies compared to standard percutaneous drainage. *J. Gastrointest. Surg.* 2012; **16**: 248–56; discussion 56-7.
34 Ulagendra Perumal S, Pillai SA, Perumal S, Sathyanesan J, Palaniappan R. Outcome of video-assisted translumbar retroperitoneal necrosectomy and closed lavage for severe necrotizing pancreatitis. *ANZ J. Surg.* 2014; **84**: 270–4.
35 Rana SS, Bhasin DK, Rao C, Gupta R, Singh K. Non-fluoroscopic endoscopic ultrasound-guided transmural drainage of symptomatic non-bulging walled-off pancreatic necrosis. *Dig. Endosc.* 2013; **25**: 47–52.
36 Yasuda I, Nakashima M, Iwai T *et al.* Japanese multicenter experience of endoscopic necrosectomy for infected walled-off pancreatic necrosis: The JENIPaN study. *Endoscopy* 2013; **45**: 627–34.
37 Bang JY, Wilcox CM, Trevino J *et al.* Factors impacting treatment outcomes in the endoscopic management of walled-off pancreatic necrosis. *J. Gastroenterol. Hepatol.* 2013; **28**: 1725–32.
38 Gou S, Xiong J, Wu H *et al.* Five-year cohort study of open pancreatic necrosectomy for necotizing pancreatitis suggests it is a safe and effective operation. *J. Gastrointest. Surg.* 2013; **17**: 1634–42.
39 Premkumar R, Phillips AR, Petrov MS, Windsor JA. The clinical relevance of obesity in acute pancreatitis: targeted systematic reviews. *Pancreatology* 2015; **15**: 25–33.
40 Yashima Y, Isayama H, Tsujino T *et al.* A large volume of visceral adipose tissue leads to severe acute pancreatitis. *J. Gastroenterol.* 2011; **46**: 1213–8.
41 Takahashi N, Papachristou GI, Schmit GD *et al.* CT findings of walled-off pancreatic necrosis (WOPN): differentiation from pseudocyst and prediction of outcome after endoscopic therapy. *Eur. Radiol.* 2008; **18**: 2522–9.
42 Thoeni RF. The revised Atlanta classification of acute pancreatitis: its importance for the radiologist and its effect on treatment. *Radiology* 2012; **262**: 751–64.
43 Morgan DE, Baron TH, Smith JK, Robbin ML, Kenney PJ. Pancreatic fluid collections prior to intervention: evaluation with MR imaging compared with CT and US. *Radiology* 1997; **203**: 773–8.

44 Zaheer A, Singh VK, Qureshi RO, Fishman EK. The revised Atlanta classification for acute pancreatitis: updates in imaging terminology and guidelines. *Abdom. Imaging* 2013; **38**: 125–36.
45 da Costa DW, Boerma D, van Santvoort HC *et al.* Staged multidisciplinary step-up management for necrotizing pancreatitis. *Br. J. Surg.* 2014; **101**: e65–79.
46 Loveday BP, Srinivasa S, Vather R *et al.* High quantity and variable quality of guidelines for acute pancreatitis: a systematic review. *Am. J. Gastroenterol.* 2010; **105**: 1466–76.
47 Working Party of the British Society of Gastroenterology; Association of Surgeons of Great Britain and Ireland; Pancreatic Society of Great Britain and Ireland; Association of Upper GI Surgeons of Great Britain and Ireland. UK guidelines for the management of acute pancreatitis. *Gut* 2005; **54** (Suppl 3): iii1–9.
48 Banks PA, Freeman ML. Practice guidelines in acute pancreatitis. *Am. J. Gastroenterol.* 2006; **101**: 2379–400.
49 Amano H, Takada T, Isaji S *et al.* Therapeutic intervention and surgery of acute pancreatitis. *J. Hepatobiliary Pancreat. Sci.* 2010; **17**: 53–9.
50 Gerzof SG, Banks PA, Robbins AH *et al.* Early diagnosis of pancreatic infection by computed tomography-guided aspiration. *Gastroenterology* 1987; **93**: 1315–20.
51 Perez A, Whang EE, Brooks DC *et al.* Is severity of necrotizing pancreatitis increased in extended necrosis and infected necrosis? *Pancreas* 2002; **25**: 229–33.
52 Buchler MW, Gloor B, Muller CA, Friess H, Seiler CA, Uhl W. Acute necrotizing pancreatitis: treatment strategy according to the status of infection. *Ann. Surg.* 2000; **232**: 619–26.
53 Banks PA, Gerzof SG, Langevin RE, Silverman SG, Sica GT, Hughes MD. CT-guided aspiration of suspected pancreatic infection: bacteriology and clinical outcome. *Int. J. Pancreatol.* 1995; **18**: 265–70.
54 Rau B, Pralle U, Mayer JM, Beger HG. Role of ultrasonographically guided fine-needle aspiration cytology in the diagnosis of infected pancreatic necrosis. *Br. J. Surg.* 1998; **85**: 179–84.
55 Ashley SW, Perez A, Pierce EA *et al.* Necrotizing pancreatitis: contemporary analysis of 99 consecutive cases. *Ann. Surg.* 2001; **234**: 572–9; discussion 9-80.
56 Lee JK, Kwak KK, Park JK *et al.* The efficacy of nonsurgical treatment of infected pancreatic necrosis. *Pancreas* 2007; **34**: 399–404.
57 van Brunschot S, van Grinsven J, Voermans RP *et al.* Transluminal endoscopic step-up approach versus minimally invasive surgical step-up approach in patients with infected necrotising pancreatitis (TENSION trial): design and rationale of a randomised controlled multicenter trial [ISRCTN09186711]. *BMC Gastroenterol.* 2013; **13**: 161.
58 Al-Omran M, Albalawi ZH, Tashkandi MF, Al-Ansary LA. Enteral versus parenteral nutrition for acute pancreatitis. *Cochrane Database Syst. Rev.* 2010; **20**(1): CD002837.
59 Wittau M, Mayer B, Scheele J, Henne-Bruns D, Dellinger EP, Isenmann R. Systematic review and meta-analysis of antibiotic prophylaxis in severe acute pancreatitis. *Scand. J. Gastroenterol.* 2011; **46**: 261–70.
60 Uhl W, Buchler MW, Malfertheiner P, Beger HG, Adler G, Gaus W. A randomised, double blind, multicentre trial of octreotide in moderate to severe acute pancreatitis. *Gut* 1999; **45**: 97–104.
61 Seta T, Noguchi Y, Shimada T, Shikata S, Fukui T. Treatment of acute pancreatitis with protease inhibitors: a meta-analysis. *Eur. J. Gastroenterol. Hepatol.* 2004; **16**: 1287–93.
62 Singh VP, Chari ST. Protease inhibitors in acute pancreatitis: lessons from the bench and failed clinical trials. *Gastroenterology* 2005; **128**: 2172–4.
63 Yasunaga H, Horiguchi H, Hashimoto H, Matsuda S, Fushimi K. Effect and cost of treatment for acute pancreatitis with or without gabexate mesylate: a propensity score analysis using a nationwide administrative database. *Pancreas* 2013; **42**: 260–4.
64 Takeda K, Takada T, Kawarada Y *et al.* JPN guidelines for the management of acute pancreatitis: medical management of acute pancreatitis. *J. Hepatobiliary Pancreat. Surg.* 2006; **13**: 42–7.
65 Yoo JH, Kwon CI, Yoo KH *et al.* Effect of proton pump inhibitor in patients with acute pancreatitis—pilot study. *Korean J Gastroenterol* 2012; **60**: 362–7.
66 van Baal MC, van Santvoort HC, Bollen TL, Bakker OJ, Besselink MG, Gooszen HG. Systematic review of percutaneous catheter drainage as primary treatment for necrotizing pancreatitis. *Br. J. Surg.* 2011; **98**: 18–27.
67 van Brunschot S, Bakker OJ, Besselink MG *et al.* Treatment of necrotizing pancreatitis. *Clin. Gastroenterol. Hepatol.* 2012; **10**: 1190–201.
68 Mouli VP, Sreenivas V, Garg PK. Efficacy of conservative treatment, without necrosectomy, for infected pancreatic necrosis: a systematic review and meta-analysis. *Gastroenterology* 2013; **144**: 333–40.e2.
69 Besselink MG, Verwer TJ, Schoenmaeckers EJ *et al.* Timing of surgical intervention in necrotizing pancreatitis. *Arch. Surg.* 2007; **142**: 1194–201.
70 Lee VT, Chung AY, Chow PK *et al.* Infected pancreatic necrosis—an evaluation of the timing and technique of necrosectomy in a Southeast Asian population. *Ann. Acad. Med. Singapore* 2006; **35**: 523–30.
71 Mofidi R, Lee AC, Madhavan KK, Garden OJ, Parks RW. Prognostic factors in patients undergoing surgery for severe necrotizing pancreatitis. *World J. Surg.* 2007; **31**: 2002–7.
72 De Rai P, Zerbi A, Castoldi L *et al.* Surgical management of acute pancreatitis in Italy: lessons from a prospective multicentre study. *HPB* 2010; **12**: 597–604.
73 Mainwaring R, Kern J, Schenk WG 3rd, Rudolf LE. Differentiating pancreatic pseudocyst and pancreatic necrosis using computerized tomography. *Ann. Surg.* 1989; **209**: 562–7; discussion 7-8.
74 Lecesne R, Taourel P, Bret PM, Atri M, Reinhold C. Acute pancreatitis: interobserver agreement and correlation of CT and MR cholangiopancreatography with outcome. *Radiology* 1999; **211**: 727–35.
75 Hirota M, Kimura Y, Ishiko T, Beppu T, Yamashita Y, Ogawa M. Visualization of the heterogeneous internal structure of so-called pancreatic necrosis by magnetic resonance imaging in acute necrotizing pancreatitis. *Pancreas* 2002; **25**: 63–7.
76 Arvanitakis M, Delhaye M, De Maertelaere V *et al.* Computed tomography and magnetic resonance imaging in the assessment of acute pancreatitis. *Gastroenterology* 2004; **126**: 715–23.
77 Viremouneix L, Monneuse O, Gautier G *et al.* Prospective evaluation of nonenhanced MR imaging in acute pancreatitis. *J. Magn. Reson. Imaging* 2007; **26**: 331–8.
78 Ocampo C, Zandalazini H, Kohan G, Silva W, Szelagowsky C, Oria A. Computed tomographic prognostic factors for predicting local complications in patients with pancreatic necrosis. *Pancreas* 2009; **38**: 137–42.

JGH Journal of Gastroenterology and Hepatology

JGHF

doi:10.1111/jgh.13398

REVIEW ARTICLE

Asian consensus statements on endoscopic management of walled-off necrosis. Part 2: Endoscopic management

Hiroyuki Isayama,* Yousuke Nakai,* Rungsun Rerknimitr,† Christopher Khor,‡ James Lau,§ Hsiu-Po Wang,¶ Dong Wan Seo,** Thawee Ratanachu-ek,†† Sundeep Lakhtakia,‡‡ Tiing Leong Ang,§§ Shomei Ryozawa,¶¶ Tsuyoshi Hayashi,*** Hiroshi Kawakami,††† Natusyo Yamamoto,* Takuji Iwashita,‡‡‡ Fumihide Itokawa,§§§ Masaki Kuwatani,¶¶¶ Masayuki Kitano,**** Keiji Hanada,*,†† Hirofumi Kogure,* Tsuyoshi Hamada,* Ryan Ponnudurai,*,‡‡ Jong Ho Moon,*,§§ Takao Itoi,§§§ Ichiro Yasuda,† Atsushi Irisawa*,† and Iruru Maetani††

*Department of Gastroenterology, Graduate School of Medicine, The University of Tokyo, §§§Department of Gastroenterology and Hepatology, Tokyo Medical University, ††Division of Gastroenterology and Hepatology, Department of Internal Medicine, Toho University Ohashi Medical Center, Tokyo, ¶¶Department of Gastroenterology, Saitama Medical University International Medical Center, Saitama, ***Department of Gastroenterology, Hokkaido Cancer Center, †††Department of Gastroenterology and Hepatology and ¶¶¶Division of Endoscopy, Hokkaido University Hospital, Sapporo, ‡‡‡First Department of Internal Medicine, Gifu University Hospital, Gifu, ****Department of Gastroenterology and Hepatology, Kinki University Faculty of Medicine, Osaka-sayama, *††Department of Gastroenterology, Onomichi General Hospital, Onomichi, †Department of Gastroenterology, Teikyo University Mizonokuchi Hospital, Kanagawa, †*Department of Gastroenterology, Fukushima Medical University, Aizu Medical Center, Aizuwakamatsu, Japan, †Division of Gastroenterology, Department of Medicine, Chulalongkorn University, ††Department of Surgery, Rajavithi Hospital, Bangkok, Thailand, ‡Department of Gastroenterology and Hepatology, Singapore General Hospital, §§Department of Gastroenterology and Hepatology, Changi General Hospital, Singapore, Singapore, §Department of Surgery, Endoscopic Center, Prince of Wales Hospital, The Chinese University of Hong Kong, Hong Kong, China, ¶Endoscopic Division, National Taiwan University Hospital, National Taiwan University, Taipei, Taiwan, **Department of Internal Medicine, University of Ulsan College of Medicine, Asan Medical Center, Seoul, *§§Digestive Disease Center and Research Institute, Department of Internal Medicine, Soon Chun Hyang University School of Medicine, Bucheon/Seoul, Korea, ‡‡Asian Institute of Gastroenterology, Hyderabad, India, *‡‡Prince Court Medical Center, Kuala Lumpur, Malaysia

Key words
acute necrotizing pancreatitis, endoscopic necrosectomy, endoscopy, endosonography, walled-off necrosis.

Accepted for publication 22 March 2016.

Correspondence
Hiroyuki Isayama, Department of Gastroenterology, Graduate School of Medicine, The University of Tokyo, 7-3-1 Hongo Bunkyo-ku, Tokyo, 113-8655, Japan.
Email: isayama-tky@umin.ac.jp

Author contributions: H. I. was involved with the study conception, study design, creation of the preliminary statements list and the allocated statement, drafting of the manuscript, critical revision of the manuscript, obtaining funding, face-to-face meetings, and voting. Y. N., N. Y., R. R., and C. K. were involved with the creation of the preliminary statements list and the allocated statement, drafting of the manuscript, critical revision of the manuscript, face-to-face meetings, and voting. All authors were involved with the creation of the allocated statement, drafting of the manuscript, critical revision of the manuscript, obtaining funding, face-to-face meetings, and voting.
Funding: An unrestricted education grant was provided by Century Medical Inc., FujiFilm Medical Corp., and Hitachi Medical Company. These sponsors did not participate in the literature search, consensus discussion, voting, lecture preparation, or manuscript preparation.

Abstract

Walled-off necrosis (WON) is a new term for encapsulated necrotic tissue after severe acute pancreatitis. Various terminologies such as pseudocyst, necroma, pancreatic abscess, and infected necrosis were previously used in the literature, resulting in confusion. The current and past terminologies must be reconciled to meaningfully interpret past data. Recently, endoscopic necrosectomy was introduced as a treatment option and is now preferred over surgical necrosectomy when the expertise is available. However, high-quality evidence is still lacking, and there is no standard management strategy for WON. The consensus meeting aimed to clarify the diagnostic criteria for WON and the role of endoscopic interventions in its management. In the Consensus Conference, 27 experts from eight Asian countries took an active role and examined key clinical aspects of WON diagnosis and endoscopic management. Statements were crafted based on literature review and expert opinion, employing the modified Delphi method. All statements were substantiated by the level of evidence and the strength of the recommendation. We created 27 consensus statements for WON diagnosis and management, including details of endoscopic procedures. When there was not enough solid evidence to support the statements, this was clearly acknowledged to facilitate future research. Proposed management strategies were formulated and are illustrated using flow charts. These recommendations, which are based on the best current scientific evidence and expert opinion, will be useful for guiding endoscopic management of WON. Part 2 of this statement focused on the endoscopic management of WON.

History of presentation: These consensus statements were presented at the Tokyo Conference of Asian Pancreato-biliary Interventional Endoscopy (T-CAP) 2014 in Tokyo, Japan and Asian Pacific Digestive Week 2014 in Bali, Indonesia.

Introduction

Part 2 of the Asian consensus statements regarding endoscopic management of walled-off necrosis (WON) focuses on endoscopic treatment and simultaneous managements. As with Part 1, given the lack of high-level evidence, statements were formulated by combining a formal literature review of the diagnostic criteria and role of endoscopic management of WON with expert opinions from Asian endoscopists, employing the same modified Delphi process (Table 1).

Results

6. Treatment option. CQ6. What are the best interventions for necrosectomy? Should we utilize a surgical, transmural, transpapillary, or percutaneous approach?

Answer: An endoscopic (transgastric/retroperitoneal) approach with or without necrosectomy is associated with lower morbidity when compared with open surgery.

Table 1 Quality of evidence, classification of recommendations, and voting schema of the modified Canadian Task Force on the Periodic Health Examination

Category and grade	Description
Quality of evidence	
I	Evidence obtained from at least 1 RCT
II-1	Evidence obtained from well-designed control trials without randomization
II-2	Evidence obtained from a well-designed cohort or case–control study
II-3	Evidence obtained from comparisons between times or places with or without intervention
III	Opinion of respected authorities based on clinical experience and expert committees
Classification of the recommendation	
A	There is good evidence to support the statement
B	There is fair evidence to support the statement
C	There is poor evidence to support the statement, but the recommendation was made on other grounds
D	There is fair evidence to refute the statement
E	There is good evidence to refute the statement
Voting on the recommendation	
A	Accept completely
B	Accept with some reservations
C	Accept with major reservations
D	Reject with reservations
E	Reject completely

Quality of evidence: I
Classification of recommendation: A
Level of agreement: a-100%, b-0%, c-0%, d-0%, e-0%

We performed a systematic review of both surgical and endoscopic necrosectomy. The methods were selected from articles obtained from the PubMed and Medline databases, the Cochrane Controlled Trials Registry, and references in primary source materials with the following keywords: infected pancreatic necrosis and pancreatitis necrosis. Human studies in the English literature published between 1990 and 2013 were considered. We employed a comparative study of endoscopic/retroperitoneal necrosectomy with open surgery. A total of seven studies were identified[1–7] that compared open with endoscopic necrosectomy (five observational studies and two randomized controlled trials [RCTs]; Fig. 1). In the observational studies, patients who underwent open necrosectomy were sicker. Most patients experienced more than one organ failure before surgery. When we pooled results from these studies, surgical debridement was associated with more early (new-onset organ failure, bleeding, enterocutaneous fistula, bowel perforation, and pancreatic fistula) and late complications (incisional hernia, exocrine, and endocrine pancreatic insufficiencies) [47.3% *vs* 71.7%; $P < 0.001$; relative risk [RR], 95% confidence interval [CI]: 0.62, 0.48–0.81]. Open surgery was associated with a higher rate of postoperative multi-organ failure (20 *vs* 59%; RR, 95%CI: 0.31, 0.23–0.42) and death (16.5 *vs* 36.6%; $P = 0.003$; RR, 95%CI: 0.42, 0.24–0.75). When RCTs and observational studies were separately analyzed, differences in new-onset organ failure persisted in favor of endoscopic approaches in both RCTs and observational studies. Differences in complications and mortality were noted only in observational studies. The results from the original systematic review are shown in Figure 2a, b and c.

Unanswered question: Which is better; the endoscopic transgastric approach or the minimally invasive surgical retroperitoneal approach?

7. Technical issues in endoscopic necrosectomy. CQ7-1. Endoscope for puncture: is esophagogastroduodenoscope (EGD) or endoscopic ultrasound (EUS) preferable?

Answer: EUS is recommended for transmural drainage, given its higher technical success rate.

Quality of evidence: I
Classification of recommendation: A
Level of agreement: a-100%, b-0%, c-0%, d-0%, e-0%

Puncture and entry into the WON cavity is a first step in endoscopic necrosectomy. EUS-guided puncture was becoming first choice instead of puncture at a bulging lesion with an EGD or duodenoscope. This procedure has been conventionally performed but EUS has the advantage of allowing visualization of both the window of entry and intervening vessels, especially when the window of cyst entry is small on CT or when extrinsic compression is less obvious on endoscopy. No RCTs have been published comparing EGD and EUS in endoscopic necrosectomy, although two RCTs[8,9] in patients with pancreatic pseudocyst showed a higher technical success rate with EUS (100% *vs* 33%[8] and 94% *vs* 72%[9]). EUS can theoretically visualize intervening vessels and therefore avoid bleeding, but no significant differences were noted in the complication rates (0% *vs* 13.3%[8] and 7% *vs* 10%[9]) because of

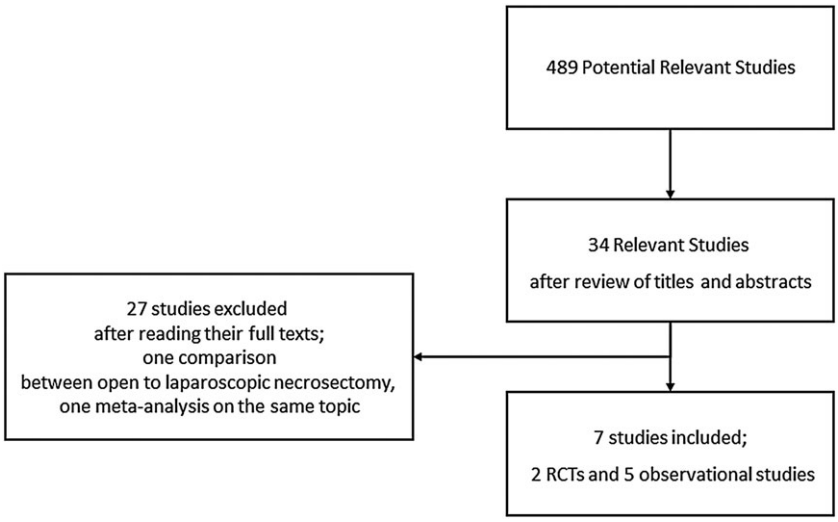

Figure 1 Flow diagram illustrating the study selection protocol for the comparison of treatments for walled-off necrosis (WON). RCT, randomized controlled trial.

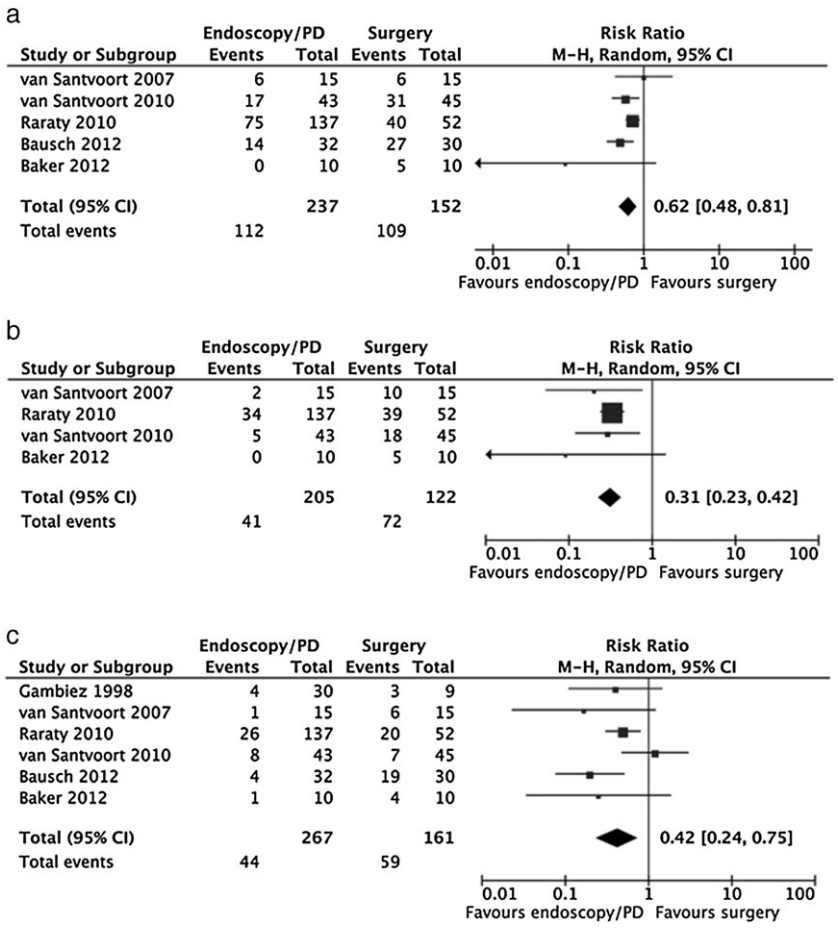

Figure 2 Comparison of endoscopy/percutaneous treatment strategies and surgery. (a) Complications: The endoscopic and percutaneous approaches are associated with fewer complications when compared with open surgery (47.3% *vs* 71.7%, $P < 0.001$). (b) New-onset organ failure: The endoscopic and percutaneous approaches are associated with less post-procedure new-onset organ failure (20 *vs* 59%, $P < 0.001$). (c) Mortality: The endoscopic and percutaneous approaches are associated with a lower rate of mortality when compared with surgery (16.5 *vs* 36.6%, $P = 0.003$). CI, confidence interval; PD, pancreatic duct.

the small sample sizes. Although the EGD approach can achieve a high success rate when performed by experts even in cases without extrinsic compression,[10–12] one prospective study[13] showed that the EGD approach failed in 43% of cases, mostly because of the lack of extrinsic compression, which was successfully rescued by EUS. Therefore, given its higher technical success rate, puncture under EUS guidance is recommended when available. However, in clinical practice, the utilization of EUS in endoscopic necrosectomy differs significantly (45–96%),[14–16] likely depending on the availability of EUS or endoscopists' preferences.

Unanswered question: Do we still need EUS guidance in patients with bulging WON?

CQ7-2. Puncture: Fine needle aspiration (FNA) needle or needle knife?

Answer: Puncture can be performed using cautery or non-cautery devices, but there is no evidence to support a preference for one modality over the other.

Quality of evidence: III
Classification of recommendation: C
Level of agreement: a-100%, b-0%, c-0%, d-0%, e-0%

A cautery or non-cautery device is employed at the initial puncture. Either an FNA needle or a needle knife is commonly used as an initial puncture device. The choice of puncture device is largely based on endoscopists' preferences. While a non-cautery FNA needle was used in 96% of cases in a Japanese multicenter retrospective study,[15] a needle knife, which is a cautery device, was used in 53% of pancreatic pseudocyst cases in an international ASGE survey.[14] The risk of bleeding might increase when cautery devices are used because of the possibility of burning through the fistula. Although initial entry with a cautery or non-cautery device is highly successful, an over-the-wire device might be safer. A needle knife is the most commonly used cautery device, but it can be non-coaxial to the guidewire even when used in an over-the-wire manner. In some countries, an over-the-wire coaxial cautery device (CystoGastro set, EndoFlex GmbH, Germany) is available and preferred over a needle knife. Because no RCTs have been conducted, we cannot draw a conclusion.

Unanswered question: Are cauterized or non-cauterized punctures a better choice?

CQ7-3. Which is preferable: CO_2 or air insufflation?

Answer: CO_2 insufflation is preferred over air insufflation.

Quality of evidence: III
Classification of recommendation: C
Level of agreement: a-53%, b-47%, c-0%, d-0%, e-0%

Gas embolism can occur and be fatal during endoscopic necrosectomy when there is direct communication between the cavity and the bloodstream. Recently, CO_2 insufflation has been preferred in many endoscopic procedures because of its rapid absorption. It is believed that CO_2 insufflation has a smaller risk of gas embolism than air insufflation because a small amount of CO_2 is readily absorbed. Air embolism during endoscopic necrosectomy was anecdotally reported.[15–18] Recently, one case of fatal CO_2 embolism was also reported,[19] showing that even CO_2 insufflation can sometimes be associated with embolism. We should be aware of this rare but serious complication of endoscopic necrosectomy.

Unanswered question: How can we predict and prevent gas embolism during endoscopic necrosectomy?

CQ7-4. Fistula dilation: What is the recommended modality for achieving fistula dilation (electric cautery, bougie, balloon, or a combination of these modalities)?

Answer: Cautery, bougie, balloon, or a combination of techniques may be used.

Quality of evidence: III
Classification of recommendation: C
Level of agreement: a-100%, b-0%, c-0%, d-0%, e-0%

Various techniques and devices (i.e. bougie, balloon, or cautery) are used for fistula dilation.[20,21] A combination of these techniques/devices is often utilized to obtain fistula dilation adequate for stent placement or endoscopic necrosectomy, and no comparative studies have been conducted. The extent of fistula dilation depends on the size and number of stents or the size of endoscope for necrosectomy. In the transgastric approach, balloon dilation up to 15 mm is considered to be safe (expert opinion).[21] The recent development of large-bore self-expandable metal stents[22–24] that allow scope insertion can reduce the size of the fistula dilation (i.e. balloon dilation of 4–6 mm is adequate). Spontaneous fistula to gastrointestinal lumen is sometimes observed in WON. If the spontaneous fistula can be endoscopically identified and approached, this should be used as the route for drainage rather than to create a new fistula for prevention of unnecessary adverse events.

Unanswered question: The dilation method for endoscopic necrosectomy has not been adequately studied and is not standardized.

CQ7-5. Drainage methods: Is additional nasocystic drainage necessary for the necrosectomy procedure?

Answer: Additional nasocystic drainage has not been demonstrated to be helpful.

Quality of evidence: II-3
Classification of recommendation: C
Level of agreement: a-44%, b-56%, c-0%, d-0%, e-0%

Some endoscopists utilize additional external nasocystic drainage during endoscopic necrosectomy sessions.[15,16] External drainage can be used for monitoring adequate drainage and for irrigation. However, no studies have demonstrated the efficacy of external drainage.[25] Given the discomfort associated with a nasocystic tube, routine use cannot be recommended. Multiple gateway[26] or dual modality[27] (combined percutaneous and endoscopic drainage) techniques may be viable alternatives. The role of additional external drainage (and irrigation) might also differ between plastic stents and large-bore metal stents.

Unanswered question: In which cases is external drainage useful?

CQ7-6. Stent selection in endoscopic necrosectomy: Which stents are suitable?

Answer: Double pigtail stents are commonly used in drainage and endoscopic necrosectomy. Multiple stents are usually required to maintain adequate tract diameter. Fully covered metal stents hold promise for use in endoscopic necrosectomy therapy.

Quality of evidence: III
Classification of recommendation: C
Level of agreement: a-83.3%, b-16.7%, c-0%, d-0%, e-0%

To maintain an adequate tract for endoscopic necrosectomy, multiple plastic stents, especially double pigtail stents, are most commonly used in clinical practice. Recently, the use of large-bore metal stents has been increasingly reported.[23,28–32] Although promising results with metal stents have been reported, there are no comparative studies regarding the types or numbers of stents used in endoscopic necrosectomy. A large-bore metal stent can provide better drainage and easy access to the necrosectomy without stent exchange, which might decrease the number of sessions or the total cost.

Unanswered question: Is plastic stenting for endoscopic necrosectomy safer and more cost-effective than metal stenting, or *vice versa*?

CQ7-7. Approach route of endoscopic necrosectomy: Are multiple-site punctures necessary in endoscopic necrosectomy?

Answer: Multiple-site drainage may be an alternative to single-site endoscopic necrosectomy.

Quality of evidence: II-2
Classification of recommendation: B
Level of agreement: a-94%, b-6%, c-0%, d-0%, e-0%

Drainage or endoscopic necrosectomy for WON is commonly performed from a single site. Recently, multiple-site drainage using a transluminal, percutaneous route, or a combination route was introduced. For patients with WON, multiple-site drainage was shown to improve the success rate, reduce complications, and shorten hospital stay in some retrospective studies.[26,27,33–35] One comparative study[26] concluded that a multiple transluminal gateway technique might reduce the need for endoscopic necrosectomy or surgery. The safety and efficacy of and the indications for multiple *versus* conventional single gateway techniques should be compared in RCTs.

Unanswered question: Which cases require multiple-site puncture?

CQ7-8. Debridement methods and devices: What are the appropriate devices and endoscopes?

Answer: The use of various endoscopes and devices has been reported. Hydrogen peroxide irrigation during necrosectomy may be a helpful adjunct.

Quality of evidence: III
Classification of recommendation: C
Level of agreement: a-61%, b-39%, c-0%, d-0%, e-0%

A regular endoscope is used for endoscopic necrosectomy; however, the use of water-jet, pediatric, or ultrathin endoscopes has been reported. In addition, various devices for therapeutic endoscopy can be utilized for endoscopic necrosectomy, but few devices are dedicated for this procedure. No studies have compared different endoscopes and devices. An ultrathin endoscope can provide easy access to WON, but devices for the removal of necrotic tissue are limited because of the small working channel. A water-jet endoscope with a large working channel allows irrigation during necrosectomy as well as insertion of various devices such as a basket catheter, a snare, biopsy forceps, alligator forceps, a Roth net retriever, and a tripod/pentapod retriever. For irrigation during necrosectomy, two retrospective non-comparative studies reported that the use of hydrogen peroxide was effective for reducing the number of sessions and the need for external irrigation.[36,37]

Unanswered question: What is the role of hydrogen peroxide in WON treatment?

CQ7-9. Medications during endoscopic necrosectomy: Are antibiotics needed?

Answer: Antibiotics should routinely be administered when performing endoscopic necrosectomy.

Quality of evidence: III
Classification of recommendation: C
Level of agreement: a-94.4%, b-5.6%, c-0%, d-0%, e-0%

Medical treatment is recognized as the first-line treatment for WON, but the necessity of medical treatment, including antibiotic treatment, during endoscopic necrosectomy has not been adequately discussed. Prophylactic antibiotics are not recommended for patients with acute pancreatitis to prevent infection of pancreatic necrosis or reduce mortality.[38] The use of antibiotics is recommended in patients with infected WON, but the duration of antibiotics administration has not been clarified. Transmural interventions for sterile WON can introduce contamination or infection, and prophylactic antibiotics should be given prior to endoscopic interventions. In addition, some endoscopists prefer the use of antacids during necrosectomy to prevent peptic ulcer, while others do not to prevent infection in the necrotic cavity. The use of cimetidine[39] or PPI[40] in acute pancreatitis patients has not been shown to be beneficial, but no studies have evaluated the use of antacids in endoscopic necrosectomy.

Unanswered question: The appropriate classes of antibiotics or its duration for endoscopic treatment of WON should be clarified. The role of antacids during endoscopic necrosectomy should also be investigated.

CQ7-10. Irrigation between sessions: Is irrigation necessary between necrosectomy sessions?

Answer: Irrigation between necrosectomy sessions may be unnecessary.

Quality of evidence: II-2
Classification of recommendation: B
Level of agreement: a-100%, b-0%, c-0%, d-0%, e-0%

Irrigation between sessions is performed with the aim of avoiding infection and reducing the amount of necrotic tissue in the cavity. Prevention of infectious complications and a decrease in the procedure time or the number of sessions are expected by adding irrigation. Although based on our literature review, we could not determine the advantages of irrigation between endoscopic necrosectomy sessions, most attending endoscopists perform this technique, and further investigations are warranted both in cases treated by drainage alone and drainage in combination with necrosectomy. Another issue is the usefulness of irrigation with peroxide. Using peroxide may reduce the volume of necrotic tissue, which leads to fewer necrosectomy sessions or a shorter procedure.

Unanswered question: Which patients require irrigation, if any? What is the role of hydrogen peroxide in the irrigation procedure?

8. Complications of endoscopic necrosectomy.

CQ8-1. What are the potential risks of endoscopic necrosectomy?

Answer: Endoscopic necrosectomy is associated with definite risks of morbidity (bleeding, perforation, air embolism, etc.) and mortality.

Quality of evidence: II-2
Classification of recommendation: A
Level of agreement: a-100%, b-0%, c-0%, d-0%, e-0%

We reviewed studies of endoscopic necrosectomy,[7,15–17,19,23,28,29,31,36,41–79] including case reports, case series, and previous review articles.[41,46,50,53,57,58,61,72,73] Data on complications were collected retrospectively. Finally, we analyzed a total of 37

articles[7,15–17,19,23,28,29,31,42–45,48,49,51,52,54–56,59,60,62–71,74,75,78–80] and 633 patients after excluding unclear data on complication rates. The rates of morbidity and mortality associated with endoscopic necrosectomy were 27.3% (173/633) and 4.4% (28/633), respectively. The most common complication associated with endoscopic necrosectomy was bleeding (12.6%; 80/633), which may occur during both balloon dilation of the gastrointestinal tract fistula and necrosectomy. Bleeding should be classified as immediate or delayed for detailed analyses. The severity of 80 bleeding cases was classified on the basis of the ASGE workshop[80] as follows: mild/moderate/severe/unspecified: 67/2/9/2. Perforation (4.4%; 28/633) was the second most frequent complication after bleeding. Air embolism is a potentially lethal complication that was observed in five patients (0.8%; 5/633).

On the other hand, the success rate of endoscopic necrosectomy is not well known because of the lack of a standard definition of treatment success. We reviewed 38 published articles that reported treatment success, and a total of 697 patients treated with endoscopic necrosectomy were analyzed.[7,15–17,19,23,28,29,31,36,42,43,45,47–49,51,52,54–56,59,60,63–71,74–79] When we define the resolution of the WON cavity as "treatment success," the success rate was 82.6% (576/697). In addition, the recurrence rate after endoscopic necrosectomy was retrospectively studied. Six articles evaluated the recurrence of WON and reported a recurrence rate of 24.4% (84/344).[16,17,54,64,66,69]

Unanswered question: How can we reduce the complications associated with endoscopic necrosectomy?

CQ8-2. How can we manage the complications of endoscopic necrosectomy?

Answer: Most bleeding can be controlled endoscopically or radiologically. The majority of perforations can be managed conservatively.

Quality of evidence: III
Classification of recommendation: C
Level of agreement: a-75%, b-25%, c-0%, d-0%, e-0%

Fortunately, the majority of complications was of mild severity and resolved with conservative therapy. Most bleeding (88.8%, 71/80) could be controlled by direct endoscopic coagulation, epinephrine injection, or clips. A multidisciplinary approach involving skilled interventional endoscopists, radiologists, and surgeons is necessary to manage cases of severe bleeding. However, we should rule out pseudoaneurysm between sessions. The majority of perforations (71.4%, 20/28) could be treated conservatively. Although air embolism is a very rare complication, it is potentially severe and even lethal. Fatal gas embolism after endoscopic necrosectomy was reported despite the use of carbon dioxide insufflation.[19] Gas embolism should be considered promptly if cardiovascular and/or respiratory symptoms develop abruptly during endoscopic necrosectomy, and protocols should be available to manage these critical situations. Caution should be undertaken in the event that this rare and dangerous gas embolism occurs during endoscopic necrosectomy using carbon dioxide insufflation. Further studies aimed at identifying the risk factors of gas embolisms are necessary to allow optimal treatment for endoscopic necrosectomy.

Unanswered question: How can we monitor gas embolism during endoscopic necrosectomy?

9. Nutrition during necrosectomy.

CQ9. What is the recommended method for providing nutrition during endoscopic necrosectomy?

Answer: Oral feeding or enteral nutrition should be the primary method for providing nutrition.

Quality of evidence: III
Classification of recommendation: C
Level of agreement: a-67%, b-33%, c-0%, d-0%, e-0%

Discussion. No studies have assessed recommended methods for providing nutrition during endoscopic necrosectomy for WON. Four meta-analyses[81–84] comparing total parenteral nutrition with total enteral nutrition (TEN) in patients with SAP showed that TEN is significantly superior when considering mortality and infectious complications. Thus, we recommended TEN rather than total parenteral nutrition during necrosectomy for WON. However, further prospective studies on methods for providing nutrition (enteral *vs* parenteral) during endoscopic necrosectomy are still warranted.

Unanswered question: The optimal method for providing nutrition during necrosectomy is still unknown.

10. Endpoints of endoscopic necrosectomy.

CQ10-1. What is the endpoint of endoscopic necrosectomy (after clinical resolution)?

Answer: The endpoint of endoscopic debridement is achieved when the pink granulation tissue lining the wall is uncovered. This may require near complete removal of the necrotic tissue.

Quality of evidence: III
Classification of recommendation: B
Level of agreement: a-73%, b-27%, c-0%, d-0%, e-0%

The endpoints of endoscopic necrosectomy are not well defined. They can be complete removal of necrotic tissue, disappearance of the cavity, improvement of the clinical conditions, or a combination of these. All endpoints are arbitrary and subjected to experts' individual definitions.[27,45,51,64,79]

Many experts have used imaging findings, the number of endotherapy sessions, direct visualization of the cavity appearance, and duration of treatment as means to follow-up.[27,45,51,64,79] The ultimate goal of endoscopic necrosectomy is the control of infection without further need for antibiotic treatment, which is eventually indicated by clinical resolution. Many parameters are associated with successful endoscopic necrosectomy as described in the literature, including a decrease in the size of the cavity, the development of pink granulation tissue in the cavity, and the amount of necrotic tissue removed. However, the individual endoscopic center determines the specifics of each of these parameters. For instance, optimum cavity reduction may be defined as "at least a 40% decrease compared to the original size" at one center,[79] whereas other centers may require a reduction of close to 100%.[64] In addition, certain centers require at least three sessions of endotherapy in 1 month during the entire duration of treatment.[45] Data are also lacking about the appropriate interval between necrosectomy sessions. In clinical practice, endoscopic necrosectomy is often performed two to three times a week, depending on the patients' condition, but when clinical symptoms

do not improve after necrosectomy because of infection in the undrained area, aggressive necrosectomy with a shorter interval is sometimes needed.

CT is commonly selected as the imaging modality of choice[27,64] for the evaluation of cavity reduction. There are no data about how often we should check CT between sessions of necrosectomy, but CT is usually performed every 1–2 weeks. Contrast-enhanced CT is recommended in case of bleeding within the cavity to check pseudoaneurysm. If direct endoscopic visualization of the cavity is allowed, the amount of residual necrosis can be assessed, which could reduce the number of CT scans needed between necrosectomy sessions. It is possible that CT may only be required during the final evaluation to ensure that the endpoint of treatment is achieved.

Unanswered question: To date, the smallest percentage of cavity reduction needed to ensure the success of endotherapy has not been assessed in a prospective trial. Another question is whether an endoscopic evaluation of the cavity alone, without the addition of a CT scan, is adequate for evaluating treatment success.

CQ10-2. How long should we keep stents in place? Is stent exchange necessary?

Answer: In patients with disruption of the main pancreatic duct, long-term transmural stent placement may be necessary to prevent recurrence. Transpapillary bridging of the main pancreatic duct is recommended before removal of the transmural stent.

Quality of evidence: II-3
Classification of recommendation: B
Level of agreement: a-73%, b-27%, c-0%, d-0%, e-0%

Discussion. No data regarding the timing of transmural stent removal after necrosectomy are available. The conventional strategy following successful endoscopic transmural drainage of WON has been to remove the transmural stents 6–8 weeks after the resolution of fluid collection has been confirmed during follow-up cross-sectional imaging. Many experts have suggested that the transmural stent can be left in place permanently; however, this suggestion is only based on the results of a study with an intermediate follow-up duration of less than 5 years. More data on long-term transmural stenting are required to ensure its safety and durability. Transmural stents can be successfully removed in most cases after endoscopic necrosectomy, but recurrence sometimes occurs, especially in cases with main pancreatic duct disruption.[33,85–87] Pancreatogram with pancreatic duct drainage has been reported to be useful in those cases. The initial outcome of endoscopic transmural drainage for WON with disconnected pancreatic duct syndrome is excellent. However, because of continuous leakage of enzyme-rich pancreatic secretions from the viable disconnected upstream pancreatic parenchyma, this strategy is associated with higher rates of pancreatic fluid collection (PFC) recurrence in patients with disconnected pancreatic duct syndrome. These recurrences following transmural stent removal usually occur within 1 year. One of the strategies used to prevent recurrences is placement of long-term transmural stents, and several studies demonstrated that this practice is associated with a decreased frequency of recurrence.[87] Recurrence of PFC was significantly decreased in patients with indwelling transmural stents than in patients in whom the stents were removed (0 *vs* 20.8%; $P = 0.02$).[33] In an RCT of 46 patients who had successful transmural drainage of PFC, stent retrieval was associated with higher recurrence rates, especially in patients with rupture of the main pancreatic duct.[87] The lower rates of recurrence may occur because the transmural stents keep the fistula open, thereby preventing recurrence.

Unanswered question: How can we select patients whose transmural stent can be safely removed without recurrence?

11. Prognostic factors of endoscopic necrosectomy.

CQ11. What are the predictive factors for clinical success of endoscopic necrosectomy?

Answer: Good medical health (ASA I and II) and normal body mass index are predictive factors for clinical success of endoscopic necrosectomy. Central necrotic collections are almost always accessible by endoscopic necrosectomy, but not flank or lower abdomen collections. Adjunctive percutaneous drainage may be needed in these situations.

Quality of evidence: II-3
Classification of recommendation: B
Level of agreement: a-94%, b-6%, c-0%, d-0%, e-0%

Discussion. Endoscopic necrosectomy is less successful in patients with obesity and/or poor medical health (ASA classification ≥3). In the JENIPaN study,[15] patients in poor medical health (ASA classification ≥3) were more likely to experience unsuccessful endoscopic necrosectomy. In addition, a US multicenter study[16] showed that body mass index >32 was a risk factor for failed endoscopic necrosectomy. In cases of unsuccessful endoscopic necrosectomy, surgical interventions should be considered, although such patients are also likely to respond poorly to surgical intervention or may be too sick for surgery. Another point to consider is the location of the WON. Hypothetically, endoscopic necrosectomy could be easily performed on all WON located in the central peripancreatic area, but WON at the periphery may require an additional approach such as a surgical or percutaneous route. A Scandinavian group reported that 33% of patients with extensive WON reaching the lower abdomen needed subsequent surgery.[66] A retrospective study[64] showed that a history of diabetes prior to pancreatitis, size and extension of the WON, and collections in one or both paracolic gutters were predictive factors of further need for surgical interventions. WON extending to the paracolic gutter is a risk factor for failure of endoscopic necrosectomy because transmural endoscopic approach is difficult or impossible. However, it is not readily predictable whether WON in the paracolic gutter would be refractory to endoscopic approach or not. Therefore, additional percutaneous approach should be considered when follow-up CT scan after endoscopic necrosectomy showed a separated WON in the paracolic gutter (expert opinion).

Although patients with extensive WON sometimes required additional surgical necrosectomy, a combined endoscopic and percutaneous approach seemed to be useful, even for patients with extensive WON.[15,17] The Virginia Mason Clinic team reported that no patients required surgical necrosectomy if treated by dual-modality drainage (DMD), a combined endoscopic and percutaneous approach.[27] DMD demonstrated high resolution rate

with low mortality, avoiding both surgical necrosectomy and pancreaticocutaneous fistula. The group advocated that DMD reduced adverse events compared with direct endoscopic necrosectomy because necrosectomy is performed through percutaneous route, if necessary, and transmural route is only for drainage. Because expertise both in endoscopy and interventional radiology is necessary in DMD, the group admitted there is a concern about generalizability of this procedure. Therefore, a prospective study of aggressive necrosectomy methods, including the multiple gateway technique,[26] is warranted to evaluate whether this approach can obviate the need for the combined approach or even surgery.

Unanswered question: The question of whether an endoscopic, percutaneous or surgical approach should be the first-line approach for peripherally located WON is still unanswered. Some experts recommend the selection of a combined approach as a first-line approach, but we should clarify the clinical course of WON after these different approaches are applied to determine the appropriate approach for WON.

12. Role of endoscopic retrograde cholangiopancreatography (ERCP) in WON with pancreatic duct disruption (PDD) after endoscopic necrosectomy.

CQ-12-1. Is pancreatography required for optimal management of WON with suspected PDD (after endoscopic necrosectomy)?

Answer: The diagnosis and classification of PDD may be recommended for optimal management of patients with WON with suspected PDD (after endoscopic necrosectomy).

Quality of evidence: III
Classification of recommendation: C
Level of agreement: a-93%, b-7%, c-0%, d-0%, e-0%

Discussion. WON is sometimes complicated by PDD. In the presence of pancreatic juice leakage, complete resolution of the complications of pancreatitis cannot be achieved, and recurrence may occur even after complete resolution of WON. In studies of PDD in patients with acute pancreatitis, the incidence determined by many imaging modalities including ERCP, magnetic resonance imaging, and secretin magnetic resonance cholangiopancreatography (MRCP)[88–91] ranged from 10% to 50%. Gluck *et al.* reported that PDD occurred in up to 50% of all patients with WON.[88] Among ERCP, magnetic resonance imaging, and secretin MRCP, the latter seems to be the best choice for PDD detection. In a prospective study by Gillams *et al.*, secretin MRCP detected 50% more leaks.[92] To date, no published studies have explored the role of pancreatography in the management of PDD under the definition of WON. Most of the studies included a mixture of patients with severe pancreatitis and patients with chronic pancreatitis. Our consensus was that PDD treatment in a patient with WON should be similar to PDD treatment in a patient with fluid collection because of acute pancreatitis. In two studies examining endoscopic treatment for PDD, the types of PDD (complete *vs* partial leakage) and successful bridging of the leakage by stent insertion were the predictors of successful treatment.[93,94] Despite the lack of studies exploring PDD in patients with WON, our group agreed that the diagnosis and classification of PDD is optimal and recommended in patients with WON and suspected PDD (Fig. 3).

Unanswered question: More information about the incidence and treatment outcome of PDD in WON is needed, particularly the outcome of endoscopic treatment in patients with WON and PDD. The timing of ERCP with stent placement (before, concurrently, or after endoscopic necrosectomy) should also be clarified.

CQ-12-2. Is ERP the modality of choice for treatment of PDD in WON?

Answer: ERP with pancreatic stenting might be efficacious in managing PDD, but it should be performed by a skilled endoscopist.

Quality of evidence: III
Classification of recommendation: C
Level of agreement: a-93%, b-7%, c-0%, d-0%, e-0%

Endoscopic pancreatic stenting may be a promising treatment for PDD. However, no studies have focused on stenting as a treatment for WON. Previous studies on the management of severe pancreatitis with fluid collection described endoscopic pancreatic stenting for treatment of PDD.[89,93,95] ERP-related complications, especially the infection of necrotic tissue, might be theoretically more severe than the infection of fluid collections alone. A retrospective study of ERP in 105 patients with pancreatitis demonstrated that 12.5% (2/16) of patients with severe pancreatitis developed sepsis after ERP.[89] Shrode *et al.* conducted a

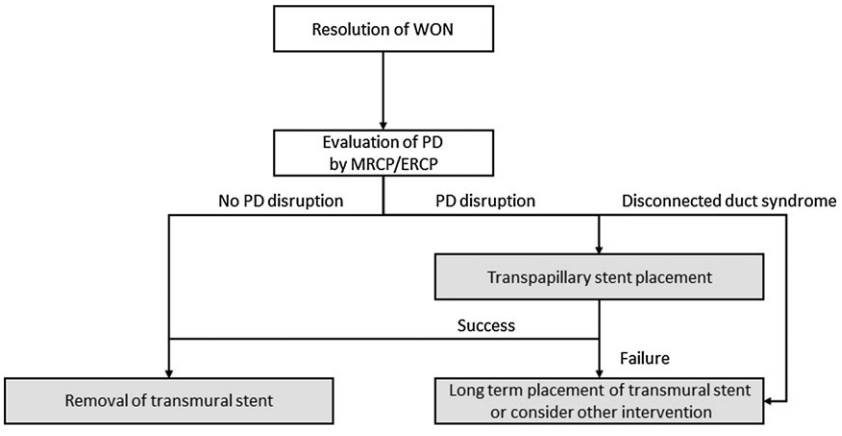

Figure 3 Flowchart illustrating strategies for removing stents after improvement of walled-off necrosis (WON). ERCP, endoscopic retrograde cholangiopancreatography; MRCP, magnetic resonance cholangiopancreatography; PD, pancreatic duct.

retrospective study of endoscopic treatment of PDD with stenting and pseudocyst drainage.[95] ERCP-related complications occurred in up to 26.5% of the 113 patients with PDD who underwent ERCP with tentative stenting.[2] Two studies focusing on pancreatic stenting were conducted retrospectively. Telford *et al.* reported a success rate of 68% for endoscopic pancreatic stenting for PDD in 43 patients after acute pancreatitis,[93] but four of these patients (9%) experienced a deterioration in clinical status after stent placement, including one fatality. Another study by Varadarajulu *et al.* included 97 patients with PDD, and stent insertion was successful in 52 patients (55%).[94] These authors found that a partially disrupted duct with successful stent bridging correlated well with clinical success.

In conclusion, ERP with endoscopic pancreatic stenting is efficacious for managing PDD; however, it should be cautiously performed because of the high rate of post-procedural complications. The group suggests that ERP with endoscopic pancreatic stenting should be performed by a skilled endoscopist with prompt back-up assistance from interventionists and surgeons.

Unanswered question: The role of routine ERCP after endoscopic necrosectomy is debatable because only patients with PDD will benefit from this procedure. It is likely that we need to learn more about the incidence of PDD in patients with WON because the number of ERCPs required will determine the cost-effectiveness of routine ERP after endoscopic necrosectomy.

Conclusions

A working group comprising 27 members from eight Asian countries created 27 statements regarding the endoscopic management of WON. While recent changes in the definition and terminology of acute pancreatitis have led to simplification and standardization, these changes also caused some confusion when we reviewed the past literature. We hope that our statements will be helpful for understanding the current status and future perspectives regarding the management of WON. Due to the limited evidence available in this field, we were not able to provide answers to all of our clinical questions. To overcome this limitation, a total of 27 Asian experts including 2 surgeons and 17 interventional radiologists contributed to our statements, and we employed the Delphi method, which reflects expert opinions objectively. Finally, we hope that by including unanswered questions, we can encourage clinicians, including endoscopists, surgeons, and interventional radiologists, to conduct carefully designed studies exploring the management of WON in the future.

References

1 Gambiez LP, Denimal FA, Porte HL, Saudemont A, Chambon JP, Quandalle PA. Retroperitoneal approach and endoscopic management of peripancreatic necrosis collections. *Arch. Surg.* 1998; **133**: 66–72.
2 Connor S, Alexakis N, Raraty MG *et al.* Early and late complications after pancreatic necrosectomy. *Surgery* 2005; **137**: 499–505.
3 van Santvoort HC, Besselink MG, Bollen TL, Buskens E, van Ramshorst B, Gooszen HG. Case-matched comparison of the retroperitoneal approach with laparotomy for necrotizing pancreatitis. *World J. Surg.* 2007; **31**: 1635–42.
4 Raraty MG, Halloran CM, Dodd S *et al.* Minimal access retroperitoneal pancreatic necrosectomy: improvement in morbidity and mortality with a less invasive approach. *Ann. Surg.* 2010; **251**: 787–93.
5 van Santvoort HC, Besselink MG, Bakker OJ *et al.* A step-up approach or open necrosectomy for necrotizing pancreatitis. *N. Engl. J. Med.* 2010; **362**: 1491–502.
6 Bakker OJ, van Santvoort HC, van Brunschot S *et al.* Endoscopic transgastric vs surgical necrosectomy for infected necrotizing pancreatitis: a randomized trial. *JAMA* 2012; **307**: 1053–61.
7 Bausch D, Wellner U, Kahl S *et al.* Minimally invasive operations for acute necrotizing pancreatitis: comparison of minimally invasive retroperitoneal necrosectomy with endoscopic transgastric necrosectomy. *Surgery* 2012; **152**: S128–34.
8 Varadarajulu S, Christein JD, Tamhane A, Drelichman ER, Wilcox CM. Prospective randomized trial comparing EUS and EGD for transmural drainage of pancreatic pseudocysts (with videos). *Gastrointest. Endosc.* 2008; **68**: 1102–11.
9 Park DH, Lee SS, Moon SH *et al.* Endoscopic ultrasound-guided versus conventional transmural drainage for pancreatic pseudocysts: a prospective randomized trial. *Endoscopy* 2009; **41**: 842–8.
10 Monkemuller KE, Baron TH, Morgan DE. Transmural drainage of pancreatic fluid collections without electrocautery using the Seldinger technique. *Gastrointest. Endosc.* 1998; **48**: 195–200.
11 Baron TH. Drainage of pancreatic fluid collections: is EUS really necessary? *Gastrointest. Endosc.* 2007; **66**: 1123–5.
12 Chahal P, Papachristou GI, Baron TH. Endoscopic transmural entry into pancreatic fluid collections using a dedicated aspiration needle without endoscopic ultrasound guidance: success and complication rates. *Surg. Endosc.* 2007; **21**: 1726–32.
13 Varadarajulu S, Wilcox CM, Tamhane A, Eloubeidi MA, Blakely J, Canon CL. Role of EUS in drainage of peripancreatic fluid collections not amenable for endoscopic transmural drainage. *Gastrointest. Endosc.* 2007; **66**: 1107–19.
14 Yusuf TE, Baron TH. Endoscopic transmural drainage of pancreatic pseudocysts: results of a national and an international survey of ASGE members. *Gastrointest. Endosc.* 2006; **63**: 223–7.
15 Yasuda I, Nakashima M, Iwai T *et al.* Japanese multicenter experience of endoscopic necrosectomy for infected walled-off pancreatic necrosis: The JENIPaN study. *Endoscopy* 2013; **45**: 627–34.
16 Gardner TB, Coelho-Prabhu N, Gordon SR *et al.* Direct endoscopic necrosectomy for the treatment of walled-off pancreatic necrosis: results from a multicenter U.S. series. *Gastrointest. Endosc.* 2011; **73**: 718–26.
17 Seifert H, Biermer M, Schmitt W *et al.* Transluminal endoscopic necrosectomy after acute pancreatitis: a multicentre study with long-term follow-up (the GEPARD Study). *Gut* 2009; **58**: 1260–6.
18 Jow AZ, Wan D. Complication of cardiac air embolism during ERCP and EUS-assisted cyst-gastrostomy for pancreatic pseudocyst. *Gastrointest. Endosc.* 2012; **75**: 220–1.
19 Bonnot B, Nion-Larmurier I, Desaint B *et al.* Fatal gas embolism after endoscopic transgastric necrosectomy for infected necrotizing pancreatitis. *Am. J. Gastroenterol.* 2014; **109**: 607–8.
20 Varadarajulu S, Tamhane A, Blakely J. Graded dilation technique for EUS-guided drainage of peripancreatic fluid collections: an assessment of outcomes and complications and technical proficiency (with video). *Gastrointest. Endosc.* 2008; **68**: 656–66.
21 Prasad GA, Varadarajulu S. Endoscopic ultrasound-guided abscess drainage. *Gastrointest. Endosc. Clin. N. Am.* 2012; **22**: 281–90 ix.
22 Itoi T, Binmoeller KF, Shah J *et al.* Clinical evaluation of a novel lumen-apposing metal stent for endosonography-guided pancreatic pseudocyst and gallbladder drainage (with videos). *Gastrointest. Endosc.* 2012; **75**: 870–6.
23 Yamamoto N, Isayama H, Kawakami H *et al.* Preliminary report on a new, fully covered, metal stent designed for the treatment of pancreatic fluid collections. *Gastrointest. Endosc.* 2013; **77**: 809–14.

24 Chandran S, Efthymiou M, Kaffes A *et al.* Management of pancreatic collections with a novel endoscopically placed fully covered self-expandable metal stent: a national experience (with videos). *Gastrointest. Endosc.* 2015; **81**: 127–35.
25 Jurgensen C, Neser F, Boese-Landgraf J, Schuppan D, Stolzel U, Fritscher-Ravens A. Endoscopic ultrasound-guided endoscopic necrosectomy of the pancreas: is irrigation necessary? *Surg. Endosc.* 2012; **26**: 1359–63.
26 Varadarajulu S, Phadnis MA, Christein JD, Wilcox CM. Multiple transluminal gateway technique for EUS-guided drainage of symptomatic walled-off pancreatic necrosis. *Gastrointest. Endosc.* 2011; **74**: 74–80.
27 Ross AS, Irani S, Gan SI *et al.* Dual-modality drainage of infected and symptomatic walled-off pancreatic necrosis: long-term clinical outcomes. *Gastrointest. Endosc.* 2014; **79**: 929–35.
28 Antillon MR, Bechtold ML, Bartalos CR, Marshall JB. Transgastric endoscopic necrosectomy with temporary metallic esophageal stent placement for the treatment of infected pancreatic necrosis (with video). *Gastrointest. Endosc.* 2009; **69**: 178–80.
29 Tarantino I, Traina M, Barresi L, Volpes R, Gridelli B. Transgastric plus transduodenal necrosectomy with temporary metal stents placement for treatment of large pancreatic necrosis. *Pancreas* 2010; **39**: 269–70.
30 Krishnan A, Ramakrishnan R. EUS-guided endoscopic necrosectomy and temporary cystogastrostomy for infected pancreatic necrosis with self-expanding metallic stents. *Surg. Laparosc. Endosc. Percutan. Tech.* 2012; **22**: e319–21.
31 Sarkaria S, Sethi A, Rondon C *et al.* Pancreatic necrosectomy using covered esophageal stents: a novel approach. *J. Clin. Gastroenterol.* 2014; **48**: 145–52.
32 Senthil Kumar P, Ravichandran P, Jeswanth S. Case matched comparison study of the necrosectomy by retroperitoneal approach with transperitoneal approach for necrotizing pancreatitis in patients with CT severity score of 7 and above. *Int. J. Surg.* 2012; **10**: 587–92.
33 Bang JY, Wilcox CM, Trevino J *et al.* Factors impacting treatment outcomes in the endoscopic management of walled-off pancreatic necrosis. *J. Gastroenterol. Hepatol.* 2013; **28**: 1725–32.
34 Mukai S, Itoi T, Sofuni A *et al.* Novel single transluminal gateway transcystic multiple drainages after EUS-guided drainage for complicated multilocular walled-off necrosis (with videos). *Gastrointest. Endosc.* 2014; **79**: 531–5.
35 Gluck M, Ross A, Irani S *et al.* Dual modality drainage for symptomatic walled-off pancreatic necrosis reduces length of hospitalization, radiological procedures, and number of endoscopies compared to standard percutaneous drainage. *J. Gastrointest. Surg.* 2012; **16**: 248–56 discussion 56-7.
36 Siddiqui AA, Easler J, Strongin A *et al.* Hydrogen peroxide-assisted endoscopic necrosectomy for walled-off pancreatic necrosis: a dual center pilot experience. *Dig. Dis. Sci.* 2014; **59**: 687–90.
37 Abdelhafez M, Elnegouly M, Hasab Allah MS, Elshazli M, Mikhail HM, Yosry A. Transluminal retroperitoneal endoscopic necrosectomy with the use of hydrogen peroxide and without external irrigation: a novel approach for the treatment of walled-off pancreatic necrosis. *Surg. Endosc.* 2013; **27**: 3911–20.
38 Villatoro E, Mulla M, Larvin M. Antibiotic therapy for prophylaxis against infection of pancreatic necrosis in acute pancreatitis. *Cochr. Database Systemat. Rev.* 2010 Cd002941.
39 Morimoto T, Noguchi Y, Sakai T, Shimbo T, Fukui T. Acute pancreatitis and the role of histamine-2 receptor antagonists: a meta-analysis of randomized controlled trials of cimetidine. *Eur. J. Gastroenterol. Hepatol.* 2002; **14**: 679–86.
40 Yoo JH, Kwon CI, Yoo KH *et al.* [Effect of proton pump inhibitor in patients with acute pancreatitis — pilot study]. *Korean J. Gastroenterol. = Taehan Sohwagi Hakhoe chi.* 2012; **60**: 362–7.
41 Alvarez-Sanchez MV, Jenssen C, Faiss S, Napoleon B. Interventional endoscopic ultrasonography: an overview of safety and complications. *Surg. Endosc.* 2014; **28**: 712–34.
42 Ang TL, Kwek AB, Tan SS, Ibrahim S, Fock KM, Teo EK. Direct endoscopic necrosectomy: a minimally invasive endoscopic technique for the treatment of infected walled-off pancreatic necrosis and infected pseudocysts with solid debris. *Singapore Med. J.* 2013; **54**: 206–11.
43 Ang TL, Teo EK, Fock KM. Endoscopic drainage and endoscopic necrosectomy in the management of symptomatic pancreatic collections. *J. Dig. Dis.* 2009; **10**: 213–24.
44 Bakker OJ, van Santvoort HC, van Brunschot S *et al.* Endoscopic transgastric vs surgical necrosectomy for infected necrotizing pancreatitis: a randomized trial. *Jama.* 2012; **307**: 1053–61.
45 Belle S, Collet P, Post S, Kaehler G. Temporary cystogastrostomy with self-expanding metallic stents for pancreatic necrosis. *Endoscopy* 2010; **42**: 493–5.
46 Bello B, Matthews JB. Minimally invasive treatment of pancreatic necrosis. *World J. Gastroenterol.* 2012; **18**: 6829–35.
47 Coelho D, Ardengh JC, Eulalio JM, Manso JE, Monkemuller K, Coelho JF. Management of infected and sterile pancreatic necrosis by programmed endoscopic necrosectomy. *Dig. Dis.* 2008; **26**: 364–9.
48 Escourrou J, Shehab H, Buscail L *et al.* Peroral transgastric/transduodenal necrosectomy: success in the treatment of infected pancreatic necrosis. *Ann. Surg.* 2008; **248**: 1074–80.
49 Fischer A, Schrag HJ, Keck T, Hopt UT, Utzolino S. Debridement and drainage of walled-off pancreatic necrosis by a novel laparoendoscopic rendezvous maneuver: experience with 6 cases. *Gastrointest. Endosc.* 2008; **67**: 871–8.
50 Freeman ML, Werner J, van Santvoort HC *et al.* Interventions for necrotizing pancreatitis: summary of a multidisciplinary consensus conference. *Pancreas* 2012; **41**: 1176–94.
51 Gardner TB, Chahal P, Papachristou GI *et al.* A comparison of direct endoscopic necrosectomy with transmural endoscopic drainage for the treatment of walled-off pancreatic necrosis. *Gastrointest. Endosc.* 2009; **69**: 1085–94.
52 Gutierrez JP, Wilcox CM, Monkemuller K. New technique to carry out endoscopic necrosectomy lavage using a pump. *Dig. Endosc.* 2014; **26**: 117–8.
53 Haghshenasskashani A, Laurence JM, Kwan V *et al.* Endoscopic necrosectomy of pancreatic necrosis: a systematic review. *Surg. Endosc.* 2011; **25**: 3724–30.
54 Hookey LC, Debroux S, Delhaye M, Arvanitakis M, Le Moine O, Deviere J. Endoscopic drainage of pancreatic-fluid collections in 116 patients: a comparison of etiologies, drainage techniques, and outcomes. *Gastrointest. Endosc.* 2006; **63**: 635–43.
55 Hritz I, Fejes R, Szekely A *et al.* Endoscopic transluminal pancreatic necrosectomy using a self-expanding metal stent and high-flow water-jet system. *World J. Gastroenterol.* 2013; **19**: 3685–92.
56 Itoi T, Nageshwar Reddy D, Yasuda I. New fully-covered self-expandable metal stent for endoscopic ultrasonography-guided intervention in infectious walled-off pancreatic necrosis (with video). *J. Hepatobiliary Pancreat. Sci.* 2013; **20**: 403–6.
57 Kahaleh M. Endoscopic necrosectomy for walled-off pancreatic necrosis. *Clin. Endosc.* 2012; **45**: 313–5.
58 Kawakami H, Itoi T, Sakamoto N. Endoscopic ultrasound-guided transluminal drainage for peripancreatic fluid collections: where are we now? *Gut Liver.* 2014; **8**: 341–55.
59 Koo JE, Park do H, Oh J *et al.* EUS-guided multitransgastric endoscopic necrosectomy for infected pancreatic necrosis with noncontagious retroperitoneal and peritoneal extension. *Gut Liver.* 2010; **4**: 140–5.
60 Mathew A, Biswas A, Meitz KP. Endoscopic necrosectomy as primary treatment for infected peripancreatic fluid collections (with video). *Gastrointest. Endosc.* 2008; **68**: 776–82.

61 Navaneethan U, Vege SS, Chari ST, Baron TH. Minimally invasive techniques in pancreatic necrosis. *Pancreas* 2009; **38**: 867–75.
62 Navaneethan UMM, Schmulewitz N *et al.* Endoscopic necrosectomy in the management of symptomatic walled off pancreatic necrosis. *Am. J. Gastroenterol.* 2008; **103**: S514–5.
63 Okabe Y, Kaji R, Ishida Y *et al.* Trans-gastric endoscopic drainage using a large balloon for pancreatic necrosis and abscess — two case reports. *Dig. Endosc.* 2009; **21** (Suppl 1): S71–4.
64 Papachristou GI, Takahashi N, Chahal P, Sarr MG, Baron TH. Peroral endoscopic drainage/debridement of walled-off pancreatic necrosis. *Ann. Surg.* 2007; **245**: 943–51.
65 Raczynski S, Teich N, Borte G, Wittenburg H, Mossner J, Caca K. Percutaneous transgastric irrigation drainage in combination with endoscopic necrosectomy in necrotizing pancreatitis (with videos). *Gastrointest. Endosc.* 2006; **64**: 420–4.
66 Rische S, Riecken B, Degenkolb J, Kayser T, Caca K. Transmural endoscopic necrosectomy of infected pancreatic necroses and drainage of infected pseudocysts: a tailored approach. *Scand. J. Gastroenterol.* 2013; **48**: 231–40.
67 Rodrigues RA, Correia LP, Rohr MR *et al.* Endoscopic resolution of pseudocyst infection and necrosis as a complication of endoscopic pseudocyst drainage. A case report. *Jop* 2008; **9**: 499–503.
68 Sadik R, Kalaitzakis E, Thune A, Hansen J, Jonson C. EUS-guided drainage is more successful in pancreatic pseudocysts compared with abscesses. *World J. Gastroenterol.* 2011; **17**: 499–505.
69 Seewald S, Ang TL, Richter H *et al.* Long-term results after endoscopic drainage and necrosectomy of symptomatic pancreatic fluid collections. *Dig. Endosc.* 2012; **24**: 36–41.
70 Seewald S, Groth S, Omar S *et al.* Aggressive endoscopic therapy for pancreatic necrosis and pancreatic abscess: a new safe and effective treatment algorithm (videos). *Gastrointest. Endosc.* 2005; **62**: 92–100.
71 Seifert H, Wehrmann T, Schmitt T, Zeuzem S, Caspary WF. Retroperitoneal endoscopic debridement for infected peripancreatic necrosis. *Lancet* 2000; **356**: 653–5.
72 van Brunschot S, Bakker OJ, Besselink MG *et al.* Treatment of necrotizing pancreatitis. *Clin. Gastroenterol. Hepatol.* 2012; **10**: 1190–201.
73 van Brunschot S, Fockens P, Bakker OJ *et al.* Endoscopic transluminal necrosectomy in necrotising pancreatitis: a systematic review. *Surg. Endosc.* 2014; **28**: 1425–38.
74 Voermans RP, Veldkamp MC, Rauws EA, Bruno MJ, Fockens P. Endoscopic transmural debridement of symptomatic organized pancreatic necrosis (with videos). *Gastrointest. Endosc.* 2007; **66**: 909–16.
75 Will U, Wanzar I, Meyer F. Endoscopic necrosectomy—a feasible and safe alternative treatment option for infected pancreatic necroses in severe acute pancreatitis: preliminary results of 18 patients in an ongoing single-center prospective observational study. *Pancreas* 2012; **41**: 652–5.
76 Will U, Wegener C, Graf KI, Wanzar I, Manger T, Meyer F. Differential treatment and early outcome in the interventional endoscopic management of pancreatic pseudocysts in 27 patients. *World J. Gastroenterol.* 2006; **12**: 4175–8.
77 Charnley RM, Lochan R, Gray H, O'Sullivan CB, Scott J, Oppong KE. Endoscopic necrosectomy as primary therapy in the management of infected pancreatic necrosis. *Endoscopy* 2006; **38**: 925–8.
78 Aso A, Igarashi H, Matsui N *et al.* Large area of walled-off pancreatic necrosis successfully treated by endoscopic necrosectomy using a grasping-type scissors forceps. *Dig. Endosc.* 2014; **26**: 474–7.
79 Gornals JB, De la Serna-Higuera C, Sanchez-Yague A, Loras C, Sanchez-Cantos AM, Perez-Miranda M. Endosonography-guided drainage of pancreatic fluid collections with a novel lumen-apposing stent. *Surg. Endosc.* 2013; **27**: 1428–34.
80 Cotton PB, Eisen GM, Aabakken L *et al.* A lexicon for endoscopic adverse events: report of an ASGE workshop. *Gastrointest. Endosc.* 2010; **71**: 446–54.
81 Petrov MS, van Santvoort HC, Besselink MG, van der Heijden GJ, Windsor JA, Gooszen HG. Enteral nutrition and the risk of mortality and infectious complications in patients with severe acute pancreatitis: a meta-analysis of randomized trials. *Arch. Surg.* 2008; **143**: 1111–7.
82 Cao Y, Xu Y, Lu T, Gao F, Mo Z. Meta-analysis of enteral nutrition versus total parenteral nutrition in patients with severe acute pancreatitis. *Ann. Nutr. Metab.* 2008; **53**: 268–75.
83 Petrov MS, Whelan K. Comparison of complications attributable to enteral and parenteral nutrition in predicted severe acute pancreatitis: a systematic review and meta-analysis. *Br. J. Nutr.* 2010; **103**: 1287–95.
84 Yi F, Ge L, Zhao J *et al.* Meta-analysis: total parenteral nutrition versus total enteral nutrition in predicted severe acute pancreatitis. *Intern. Med.* 2012; **51**: 523–30.
85 Varadarajulu S, Wilcox CM. Endoscopic placement of permanent indwelling transmural stents in disconnected pancreatic duct syndrome: does benefit outweigh the risks? *Gastrointest. Endosc.* 2011; **74**: 1408–12.
86 Rana SS, Bhasin DK, Rao C, Sharma R, Gupta R. Consequences of long term indwelling transmural stents in patients with walled off pancreatic necrosis & disconnected pancreatic duct syndrome. *Pancreatology* 2013; **13**: 486–90.
87 Arvanitakis M, Delhaye M, Bali MA *et al.* Pancreatic-fluid collections: a randomized controlled trial regarding stent removal after endoscopic transmural drainage. *Gastrointest. Endosc.* 2007; **65**: 609–19.
88 Gluck M, Ross A, Irani S *et al.* Endoscopic and percutaneous drainage of symptomatic walled-off pancreatic necrosis reduces hospital stay and radiographic resources. *Clin. Gastroenterol. Hepatol.* 2010; **8**: 1083–8.
89 Neoptolemos JP, London NJ, Carr-Locke DL. Assessment of main pancreatic duct integrity by endoscopic retrograde pancreatography in patients with acute pancreatitis. *Br. J. Surg.* 1993; **80**: 94–9.
90 Uomo G, Molino D, Visconti M, Ragozzino A, Manes G, Rabitti PG. The incidence of main pancreatic duct disruption in severe biliary pancreatitis. *Am. J. Surg.* 1998; **176**: 49–52.
91 Peng R, Zhang XM, Ji YF *et al.* Pancreatic duct patterns in acute pancreatitis: a MRI study. *PLoS One* 2013; **8** e72792.
92 Gillams AR, Kurzawinski T, Lees WR. Diagnosis of duct disruption and assessment of pancreatic leak with dynamic secretin-stimulated MR cholangiopancreatography. *AJR Am. J. Roentgenol.* 2006; **186**: 499–506.
93 Telford JJ, Farrell JJ, Saltzman JR *et al.* Pancreatic stent placement for duct disruption. *Gastrointest. Endosc.* 2002; **56**: 18–24.
94 Varadarajulu S, Noone TC, Tutuian R, Hawes RH, Cotton PB. Predictors of outcome in pancreatic duct disruption managed by endoscopic transpapillary stent placement. *Gastrointest. Endosc.* 2005; **61**: 568–75.
95 Shrode CW, Macdonough P, Gaidhane M *et al.* Multimodality endoscopic treatment of pancreatic duct disruption with stenting and pseudocyst drainage: how efficacious is it? *Digest. Liver Dis.: Off. J. Ital. Soc. Gastroenterol. Ital. Assoc. Study Liver.* 2013; **45**: 129–33.

SYSTEMATIC REVIEW AND META-ANALYSIS

The clinical impact of ultrasound contrast agents in EUS: a systematic review according to the levels of evidence

Pietro Fusaroli, MD,[1] Bertrand Napoleon, MD,[2] Rodica Gincul, MD,[2] Christine Lefort, MD,[2] Laurent Palazzo, MD,[3] Maxime Palazzo, MD,[3] Masayuki Kitano, MD,[4] Kosuke Minaga, MD,[4] Giancarlo Caletti, MD,[1] Andrea Lisotti, MD[1]

Bologna, Italy; Lyon, Paris, France; Osaka-Sayama, Japan

Background and Aims: The use of contrast-harmonic EUS (CH-EUS) in routine clinical practice is increasing rapidly but is not yet standardized. We present the levels of evidence (LEs) found in the literature to put its clinical outcomes in the appropriate perspective.

Methods: We conducted a systematic review of the available English-language articles. The LEs were stratified according to the Oxford Centre for Evidence-Based Medicine guidelines.

Results: Overall, 210 articles were included and presented according to different pathologic conditions. For pancreatic solid neoplasms, the pooled sensitivity and specificity in the diagnosis of pancreatic carcinoma were very high (LE 1); quantitative analysis and guidance of FNA were reported as investigational research (LE 2-3). For pancreatic cystic lesions, the identification of neoplastic solid components as hyperenhanced lesions represented a promising application of CH-EUS (LE 2). For lymph nodes, CH-EUS increased the diagnostic yield of B-mode EUS for the detection of malignancy (LE 2). For submucosal tumors, CH-EUS seemed useful for differential diagnosis and risk stratification (LE 2-3). For other applications, differential diagnosis of gallbladder and vascular abnormalities by CH-EUS were reported (LE 2-3).

Conclusions: The LEs of CH-EUS in the literature have evolved from the initial descriptive studies to multicenter and prospective trials, and even meta-analyses. The differential diagnosis between benign and malignant lesions is the main field of application of CH-EUS. With regard to pancreatic solid neoplasms, the concomitant use of both CH-EUS and EUS-FNA may have additive value in increasing the overall accuracy by overcoming the false-negative results associated with each individual technique. Other applications are promising but still investigational. (Gastrointest Endosc 2016;84:587-96.)

INTRODUCTION

In transabdominal ultrasonography, ultrasound contrast agents (UCAs) are essential along with B-mode imaging for the investigation of several abnormalities, in particular for the differential diagnosis of solid liver lesions.[1,2] It has been established that a biopsy is no longer indicated for the diagnosis of liver lesions showing characteristic enhancement in the background of a specific disease, such as hepatocellular carcinoma arising in liver cirrhosis. Similarly, the use of UCAs has become widespread in EUS to enhance its diagnostic accuracy, mainly in pancreaticobiliary diseases.[3]

Initially, color and/or power Doppler imaging were used with first-generation UCAs to perform contrast-enhanced EUS (CE-EUS). Subsequently, after the first feasibility study with a prototype echoendoscope,[4] second-generation UCAs were used with a dedicated contrast harmonic in EUS (CH-EUS) and quickly became established thanks to their safety and favorable interobserver agreement (IOA).[5] CH-EUS was used in the investigation of pancreatic lesions, gallbladder abnormalities, submucosal tumors (SMTs), lymph nodes, and other abnormal conditions. However, despite its popularity, consensus is still lacking about the exact role of CH-EUS in the diagnostic workup of GI lesions.

Abbreviations: CE-EUS, contrast-enhanced-EUS; CH-EUS, contrast-harmonic EUS; CP, chronic pancreatitis; GIST, gastrointestinal stromal tumor; IOA, interobserver agreement; IPMN, intraductal papillary mucinous neoplasm; LE, level of evidence; NET, neuroendocrine tumor; NPV, negative predictive value; PC, pancreatic cancer; PCL, pancreatic cystic lesion; SMT, submucosal tumor; UCA, ultrasound contrast agent.

DISCLOSURE: *All authors disclosed no financial relationships relevant to this publication.*

0016-5107/$36.00
http://dx.doi.org/10.1016/j.gie.2016.06.006

(footnotes continued on last page of article)

We present the results of the work of a group of experts who reviewed the literature and their own experience of UCAs in EUS. All the GI pathologic conditions that are amenable to investigation by CE-EUS and/or CH-EUS were scrutinized. The findings and statements reported in this article were endowed with their own level of evidence (LE), which is currently the only reliable indicator of scientific quality. Moreover, we put the technical aspects and outcomes of CH-EUS into a clinical perspective.

MATERIALS AND METHODS

We conducted a systematic review of the available English-language literature up to the end of 2015 through MEDLINE using the PubMed and Google Scholar interfaces. The following search terms were used: contrast (title or abstract) OR contrast-enhanced (title or abstract) OR contrast-enhanced harmonic (title or abstract) OR CE-EUS (title or abstract) OR CH-EUS (title or abstract) OR CEH-EUS (title or abstract) AND endoscopic ultrasound (title or abstract) OR EUS (title or abstract) OR endosonography (title or abstract or MeSH terms) OR endoscopic ultrasonography (title or abstract). Moreover, the references of selected articles were analyzed to obtain any other article that eluded the primary search.

We looked for all research articles including randomized controlled trials, prospective and retrospective studies, meta-analyses, systematic reviews, and surveys pertinent to CH-EUS. Studies enrolling up to 10 patients were categorized as case series. We also included letters and case reports describing recent, innovative, or original applications of CH-EUS. Commentaries, non-English-language articles, congress proceedings and abstracts, and articles in which EUS was not the principal subject matter were excluded from the analysis.

LEs were stratified according to the Centre for Evidence-Based Medicine, University of Oxford, 2011 edition:[6] LE 1, systematic review of cross-sectional studies with consistently applied reference standard and blinding; LE 2, individual cross-sectional studies with consistently applied reference standard and blinding; LE 3, non-consecutive studies or studies without consistently applied reference standards; LE 4, case-control studies, or poor or non-independent reference standard; LE 5, mechanism-based reasoning.

The technical aspects of CH-EUS were not the focus of this research; a detailed description regarding how to perform CH-EUS can be found elsewhere.[3,7]

RESULTS

After exclusion of non-pertinent articles, 210 manuscripts were finally included for the purpose of this systematic review. The published research focused primarily on solid pancreatic (n = 82) and pancreatic cystic neoplasms (n = 28); other studies assessed the diagnostic performance of CH-EUS on gallbladder lesions (n = 12), vascular abnormalities (n = 12), SMTs (n = 7), lymph nodes (n = 6), and gastric neoplasms (n = 5). A detailed classification of the studies included according to the indications and the corresponding LE is presented in Table 1.

Overall, we identified a predominance of review articles (LE 5) and a fair number of articles with LE 1 to 2. In particular, 2 meta-analyses on the diagnostic performance of CH-EUS for the differential diagnosis of pancreatic adenocarcinoma were found.[8,9] A large number (n = 45) of expert reviews focused on technical issues in multiple indications.[3,7,10-13]

We present a schematic description of the results of our systematic review according to the LE. We also provide a detailed analysis of each article included in this systematic review (meta-analysis, prospective studies, retrospective studies, case series and case reports) in Supplementary Tables 1 to 5 (available online at www.giejournal.org).

Interobserver agreement in CH-EUS

Four studies evaluated IOA for the assessment of pancreatic solid neoplasms.[5,14-16] In the series with 5 senior and 2 junior observers focusing on the diagnosis of pancreatic cancer (PC), IOA was good (kappa = 0.66) for all operators. IOA was good for the junior (kappa = 0.76) and excellent for the senior (κ = 0.90) observers.[14] We believe that the good results for the beginners indicate that the learning curve for CH-EUS might be relatively short. Another recent multicentric study[16] confirmed that experienced operators in both EUS and CH-EUS showed better IOA than other operators; however, overall IOA for CH-EUS (κ = 0.32) was fair. Fusaroli et al[5] evaluated the IOA for CH-EUS of SMTs and showed that IOA was substantial for the uptake (κ = 0.64), slight for the pattern of distribution (κ = 0.18), and fair for the washout of UCA (κ = 0.39). Xia et al[17] reported

TABLE 1. Summary of levels of evidence according to the study subject

Levels of evidence	1	2	3	4	5	Total
Interobserver agreement	–	–	2	–	–	2
Pancreas						
Solid neoplasms	2	24	7	14	35	82
Cystic neoplasms	–	9	1	3	15	28
Lymph nodes	–	5	–	–	1	6
Submucosal tumors	–	3	–	3	1	7
Gallbladder lesions	–	3	2	2	5	12
Vascular abnormalities	–	–	4	5	3	12
Gastric neoplasms	–	1	1	1	2	5
Other indications	–	2	–	9	45*	56
Total	2	47	17	37	107	210

*Includes review on technical issues and on multiple indications.

very good IOA between 2 experts (κ = 0.953) for undetermined intra-abdominal lesions. Finally, substantial IOA (κ = 0.77) for CH-EUS in the assessment of gallbladder wall thickening was reported (LE 2).[18]

Pancreatic solid neoplasms

PC represents more than 90% of all pancreatic solid neoplasms and 55% to 73% of all pancreatic solid masses.[14,15,19-24] The specificity and accuracy of EUS for the diagnosis of PC range from 53% to 69% and 72% to 83%, respectively.[25,26] In a recent meta-analysis, EUS-guided FNA showed high sensitivity (86.8%) and specificity (95.8%) for diagnosing PC.[27] However, the negative predictive value (NPV) of EUS-FNA was low (30%-70%), and was thus insufficient to reliably rule out the diagnosis of PC (LE 1).[23]

CE-EUS for the differential diagnosis of pancreatic solid neoplasms. CE-EUS using first-generation UCAs with color and/or power Doppler with a high mechanical index provided promising results in terms of differential diagnosis. Although PC most often demonstrated a hypoenhancing appearance due to the presence of desmoplastic changes, mass-forming chronic pancreatitis (CP) had similar enhancement to that of normal pancreatic parenchyma (depending on the degree of inflammation and fibrosis). Neuroendocrine tumors (NETs) were usually hyperenhancing (LE 2).[28-33]

The addition of contrast enhancement to conventional color and/or power Doppler imaging improved the sensitivity from 73.2% to 91.1% and the specificity from 83.3% to 93.3% for the diagnosis of PC. CE-EUS also provided greater diagnostic sensitivity (83.3%) for differentiating small PCs (≤2 cm) from other tumors when compared with power Doppler EUS (11%) and contrast-enhanced CT (50%) (LE 2).[32]

Performance of CH-EUS for the differential diagnosis of pancreatic solid neoplasms. After some early reports,[4,34] several studies confirmed the usefulness of CH-EUS for the diagnosis of PC.[14,15,21,23] These studies confirmed the typical heterogeneous hypoenhancement pattern of PC demonstrating high sensitivity (89%-96%) and specificity (64%-94%) versus the hyperenhanced pattern that was strongly suggestive for lesions other than adenocarcinoma (positive predictive value [PPV] 88%-94%). Two studies even reported a slightly better performance of CH-EUS compared with EUS-FNA for diagnosing PC. The sensitivity and NPV were 89% to 96% and 88% to 91% for CH-EUS and 72% to 93% and 77% to 86% for EUS-FNA, respectively (Table 2) (LE 2).[14,23]

One meta-analysis by Gong et al[9] assessed data from 12 studies, 5 evaluating CE-EUS and 7 evaluating CH-EUS, involving 1139 patients. The pooled sensitivity and specificity for the diagnosis of PC were 94% and 89%, respectively; the area under the curve was 0.97, thereby confirming high diagnostic accuracy of the technique (LE 1).

Kitano et al[15] also demonstrated the superiority of CH-EUS over other imaging modalities for diagnosing small PCs (<2 cm), with sensitivity and specificity of 91.2% and 94.4% for CH-EUS and 70.6% and 91.9% for CT, respectively (LE 2).

On the other hand, hyper- or isoenhancement is a strong negative predictor of PC. Kitano et al[15] observed that hyperenhanced lesions were diagnosed as NETs with a sensitivity of 79% and specificity of 99%; this finding could be partly explained according to the relatively high prevalence of NETs in their study population. It should also be emphasized that hyperenhancement per se is not specific for the diagnosis of NETs because it may be seen in mass-forming pancreatitis, pseudo-solid serous cystadenoma, lymphoma, and certain types of pancreatic metastases (LE 3).[35] As far as mass-forming pancreatitis is concerned, studies showed an iso- or hyperenhanced pattern in most cases.[14,15,23,28-33] Nevertheless, 22% of the patients with mass-forming CP in the largest series reported (n = 46) showed a hypoenhanced CH-EUS pattern, probably due to fibrosis with decreased vascularization (LE 2).[15]

Quantitative CH-EUS for the differential diagnosis of pancreatic solid neoplasms. Some authors have used computer-assisted quantitative analysis of CH-EUS enhancement in an attempt to further improve the accuracy of the differential diagnosis of pancreatic solid tumors.[36-40]

Seicean et al[37] used quantitative analysis of the contrast uptake ratio after administration of UCAs. Based on histograms obtained from the CH-EUS video recordings, they showed that the index of contrast uptake ratio was significantly lower in PC than in mass-forming pancreatitis. Another software analyzing time-intensity curves of CH-EUS was evaluated in 3 studies.[38-40] Matsubara et al[39] found that the rate of echo intensity reduction from the peak at 1 minute was greatest in PC, followed by mass-forming CP, autoimmune pancreatitis, and NETs (LE 2).

More recently, Săftoiu et al[36] evaluated the time-intensity curve of patients with pancreatic solid neoplasms and observed that quantitative CH-EUS was able to differentiate between PC and CP with very good sensitivity and specificity (87.5% and 92.7%, respectively). In addition, they described increased diagnostic accuracy when an artificial neural network evaluated the time-intensity curves (sensitivity 94.6% and specificity 94.4%) (LE 2).

Prediction of malignancy of pancreatic NETs. Pancreatic NETs are a heterogeneous group of malignancies with different biological characteristics. Tumor size, grading, and the Ki67 proliferation index are known predictors of malignancy. Histologically, microvessel density is inversely correlated with tumor grading.

The evaluation of microvascularization with CE-EUS was shown to have high diagnostic value to predict malignancy with a sensitivity, a specificity, and an accuracy of 90.5%, 90%, and 90.2%, respectively (LE 2).[41]

TABLE 2. CH-EUS and CE-EUS for the diagnosis of pancreatic adenocarcinoma

Reference	Design	Technique	UCA	Cases	Sensitivity (%)	Specificity (%)	Accuracy (%)
Săftoiu et al, 2015[36]	PS-M	qCH-EUS	SonoVue	167	88	93	NR
Gincul et al, 2014[14]	PS-M	CH-EUS	SonoVue	100	96	94	95
Park et al, 2014[76]	RS	CH-EUS	SonoVue	90	92	68	84
Lee et al, 2013[77]	PS	CH-EUS	SonoVue	37	93	86	92
Gheonea et al, 2013[40]	PS	qCH-EUS	SonoVue	51	94	89	NR
Figueiredo et al, 2012[78]	PS	CE-EUS+E	SonoVue	47	93	67	79
Hocke et al, 2012[79]	PS	CH-EUS*	SonoVue	58	92	90	NR
Imazu et al, 2010[38]	PS	qCH-EUS	Sonazoid	30	100	100	NR
Matsubara et al, 2011[39]	RS	qCH-EUS	Sonazoid	91	96	93	95
Kitano et al, 2012[15]	PS	CH-EUS	Sonazoid	277	95	89	91
Seicean et al, 2010[37]	PS	qCH-EUS	SonoVue	30	80	92	86
Săftoiu et al, 2010[80]	PS	CE-EUS+E	SonoVue	54	88	100	93
Fusaroli et al, 2010[21]	PS	CH-EUS	SonoVue	90	96	64	82
Napoleon et al, 2010[23]	PS	CH-EUS	SonoVue	35	89	88	89
Sakamoto et al, 2008[32]	PS	CE-EUS	Levovist	156	85	89	87
Dietrich et al, 2008[33]	PS	CE-EUS	Levovist	93	92	100	95
Hocke et al, 2007[31]	RS	CE-EUS	SonoVue	100	78	87	NR
Hocke et al, 2006[30]	PS	CE-EUS	SonoVue	86	91	93	NR
Becker et al, 2001[29]	PS	CE-EUS	Optison	23	94	100	NR
Total, median (range)		19 studies		1615	92 (78-100)	90 (64-100)	90 (79-95)

Sonazoid (GE Healthcare, Milwaukee, Wisc), Sonovue (BR1, Bracco, Italy), Levovist (Schering AG, Berlin, Germany), Optison (GE Healthcare, Milwaukee, Wis, USA).
CH-EUS, Contrast-enhanced harmonic endoscopic ultrasound; *CE-EUS*, contrast-enhanced endoscopic ultrasound; *UCA*, ultrasound contrast agent; *PS-M*, prospective multicenter study; *qCH-EUS*, quantitative CE-EUS; *NR*, not reported; *PS*, prospective study; *RS*, retrospective study; *E*, elastography.
*Hocke et al compared contrast-enhanced high mechanical index and low mechanical index.

The usefulness of CH-EUS in predicting malignancy of pancreatic NETs has been evaluated in a recent retrospective study. The authors included 92 patients with pancreatic NETs and observed that heterogeneous enhancement on CH-EUS was able to predict malignancy with a sensitivity, a specificity, PPV, and NPV of 93.3%, 93.5%, 87.5%, and 96.7%, respectively. A similar diagnostic yield was also shown in small (<2 cm) GI tumors (LE 3).[42]

CH-EUS-FNA. Three recent studies have evaluated the outcome of CH-EUS-FNA, based on the assumption that inserting the needle into necrotic areas that show no signs of vascularization on CH-EUS can be avoided. Sugimoto et al[43] required fewer needle passes to obtain adequate specimens in 40 consecutive patients (LE 2). Seicean et al[44] observed a tendency for increased accuracy in patients who underwent CH-EUS-FNA compared with EUS-FNA (86.5% vs 78.4%) (LE 2). In a large retrospective cohort, Hou et al[45] achieved adequate specimens in 96.6% of patients undergoing CH-EUS-FNA versus 86.7% in the EUS-FNA group (LE 3).

Key issues. The use of CH-EUS in the differential diagnosis of pancreatic solid neoplasms is established; in particular, the lack of hypoenhancement is a strong negative predictor of PC. Quantitative analysis and guidance of EUS-FNA still represent investigational applications of CH-EUS.

Pancreatic cystic lesions

Differential diagnosis among inflammatory pancreatic pseudocysts and the various types of true pancreatic cystic lesions (PCLs), which may be benign, borderline, or malignant, is crucial for selecting candidates for surgical treatment.

Cytopathologic analysis of EUS-FNA samples usually leads to a definitive diagnosis in only 50% of cases.[46] The presence of hyperenhanced solid components/mural nodule within cystic lesions[47] is considered the strongest predictor of malignancy; also in this setting, however, the accuracy of EUS-FNA is suboptimal due to a high false-negative rate.

Differential diagnosis of PCLs. Hirooka et al[28] reported the first description of the CE-EUS pattern of PCLs. Enhancement was observed in 3 of 3 cases of serous cystadenoma and 6 of 8 mucin-producing tumors, whereas no pseudocyst (n = 5) presented enhancement (LE 2).

Hocke et al[48] recently reported on CH-EUS in 125 undetermined PCLs. Enhancement of the cystic wall or of intracystic structures (septae, nodules) was present only in 6% of the pseudocysts or dysontogenetic cystic lesions but in 100% of the PCLs, including serous cystadenoma, mucinous cystadenoma, intraductal papillary mucinous neoplasm (IPMN), cystic NETs, and cystic pancreatic carcinoma (LE 2).[48]

TABLE 3. CH-EUS and CE-EUS for the differential diagnosis of benign and malignant lymph nodes

Reference	Design	Technique	UCA	Cases	Sensitivity (%)	Specificity (%)	Accuracy (%)
Miyata et al, 2016[61]	PS	CH-EUS	Sonazoid	143	83	91	88
Xia et al, 2010[17]	PS	CH-EUS	Sonazoid	34*	96	100	97
Hocke et al, 2008[60]	PS	CE-EUS	SonoVue	122	60	92	80
Kanamori et al, 2006[59]	PS-RS	CE-EUS	Levovist	71	100	85	92
Kojima et al, 2003[58]	PS	Echo-lymphography	Carbon dioxide microbubbles	55	96	90	93
Total, median (range)	5 studies			425	96 (60-100)	91 (85-100)	93 (80-97)

CH-EUS, Contrast-enhanced harmonic endoscopic ultrasound; *CE-EUS*, contrast-enhanced endoscopic ultrasound; *UCA*, ultrasound contrast agent; *PS*, prospective study; *PS-RS*, retrospective cohort with prospective validation.
*Xia et al enrolled 43 patients with undetermined intra-abdominal lesions; among them, 23 had malignant lymph nodes and 11 had benign lymph nodes; data were calculated accordingly.

Fusaroli et al[49] studied 76 patients with PCLs. The investigators reported that 86% of serous and 89% of mucinous cysts were hyperenhanced, whereas 90% of pseudocysts were hypoenhanced. The authors concluded that CH-EUS was not useful for discrimination between serous and mucinous cysts but was highly specific for the diagnosis of pseudocysts (LE 2).

In addition, Kamata et al[50] found that the accuracy of B-mode EUS and CH-EUS for the differential diagnosis of serous and mucinous cysts did not differ significantly (sensitivity 85 % vs 79 %; specificity 46 % vs 96 %; accuracy 73 % vs 84 %, respectively) (LE 2).

CH-EUS for the diagnosis of mural nodules and/or malignancy in IPMN. Yamashita et al[51] reported on 17 patients with IPMN who presented mural nodules with a median diameter of 10 mm. All patients were examined by CT, color Doppler EUS, and CH-EUS, which showed vascularization within the nodules in 41%, 0%, and 76% of cases, respectively. All but one case of vascularized mural nodules shown by CH-EUS were confirmed neoplastic at surgical histopathology. Sensitivity, specificity, and accuracy of CH-EUS for the detection of malignant mural nodules were 100%, 80%, and 94%, respectively (LE 2).[51]

Similar results were reported by Fusaroli et al,[49] who observed that neoplastic solid components within PCLs were always hyperenhanced (malignant IPMNs and cystic pancreatic NETs), whereas mucus clots and pseudocyst debris were non-enhanced (LE 2).

The superiority of CH-EUS versus CT and B-mode EUS in identifying neoplastic mural nodules was also shown by Harima et al[52] (the accuracy of CH-EUS was 98% compared with 92% for CT and 72% for EUS) (LE 2d) and by Kamata et al[50] (identification of mural nodules ≥4 mm by CH-EUS was strongly correlated to malignant PCLs, odds ratio = 56) (LE 2).

Yamamoto et al[53] compared the evidence from quantitative CH-EUS (time-intensity curve) with the pathologic specimens of 30 patients who underwent surgical resection for IPMN. High-grade dysplasia IPMN and invasive cancer showed significantly lower intensity change, lower rate of reduction in echo pattern, and lower nodule/parenchyma contrast ratio compared with low and intermediate grade dysplasia IPMN (accuracy 80%, 86.7%, and 93.3%, respectively) (LE 2).

Key issues. CH-EUS does not add to B-mode EUS in terms of differentiation between serous and mucinous PCLs. The identification of neoplastic solid components as hyperenhanced lesions inside PCLs represents the most promising application of CH-EUS in this setting.

Lymph nodes

The differential diagnosis of benign and malignant lymph nodes is critical for cancer staging and has a major impact on treatment options and patient survival. B-mode criteria based on topographic distribution, size, shape, borders, and echogenicity have suboptimal diagnostic accuracy.[54,55]

EUS-FNA has largely been used for the pathologic confirmation of enlarged lymph nodes. However, EUS-FNA presents limitations too, mainly represented by false-negative results (sensitivity ranging from 83% to 93%).[56,57]

CE-EUS for the determination of lymph node nature. An early report[58] described an ancestor technique of echo-lymphography consisting of EUS-guided intranodal injection of carbon dioxide microbubbles. In patients with lymph node enlargement (24 malignant, 31 benign), EUS evaluation after intranodal injection of UCA reached a sensitivity of 95.8%, specificity of 90.3%, and diagnostic accuracy of 92.7% (LE 2).

In 2 subsequent studies using CE-EUS in patients with visible lymph node swelling, Kanamori et al[59] found 100% sensitivity with 84.9% specificity and diagnostic accuracy of 92.2% in a group of 71 patients. In a larger population of 122 patients, Hocke et al[60] were not able to replicate such good results in terms of sensitivity (60.4%), although their specificity was still good (91.9%) (LE 2) (Table 3).

CH-EUS for the determination of lymph node nature. CH-EUS was used to investigate the microvascular architecture of intra-abdominal lesions of unknown origin. Xia et al[17] evaluated 34 patients with lymph node

enlargement (23 malignant/11 benign based on EUS-FNA) and reported very good results in terms of sensitivity (95.7%), specificity (100%), and diagnostic accuracy (97.0%). Subsequently, the same group[61] confirmed the optimal diagnostic accuracy of CH-EUS for the determination of lymph node nature in 109 patients (sensitivity 83%, specificity 91%, diagnostic accuracy 88%) (LE 2).

Key issues. In comparison with the well-established B-mode EUS criteria for the differential diagnosis of lymph nodes, the use of CH-EUS increases the diagnostic yield for the detection of malignancy.

Submucosal tumors

EUS is a powerful tool for the differential diagnosis of SMTs; however, the common finding of a hypoechoic mass arising from the third (submucosa) or the fourth (muscularis propria) layer of the gut wall does not allow discrimination between malignant SMTs such as gastrointestinal stromal tumors (GISTs) and benign entities such as leiomyoma and schwannoma.[62]

EUS-FNA can provide tissue specimens allowing tissue evaluation via histology and immunohistochemistry to confirm the nature of SMTs,[63,64] but its overall accuracy is not higher than 75%.

CH-EUS for the differential diagnosis of SMTs. CH-EUS was described in a small group of 17 SMTs of the upper GI tract. All hyperenhanced lesions were diagnosed as GISTs on the basis of EUS-FNA, whereas the hypoenhanced SMTs were confirmed to be benign (lipoma or leiomyoma). Although the data were very preliminary, it was shown that CH-EUS might help discriminate GISTs from benign SMTs with good accuracy (LE 2).[65]

CH-EUS for the estimation of malignant potential in GISTs. Two studies evaluated the diagnostic potential of CE-EUS or CH-EUS for estimating the grading of GISTs.[66,67]

Sakamoto et al[66] stratified 29 patients who underwent surgical resection of GISTs into low-grade and high-grade malignancy groups. The authors observed that CH-EUS was able to identify the presence of irregular microvascularization in the high-grade malignancy group with a sensitivity of 100%, a specificity of 63%, and an overall accuracy of 83%, as opposed to the low-grade malignancy group, which exhibited a regular microvascular pattern (LE 2).[66]

Key issues. Initial findings suggest that CH-EUS is promising in terms of differentiation between leiomyoma and GIST and for the risk stratification of GIST; however, further research in this field is warranted.

Other indications

Differential diagnosis of gallbladder lesions. The detection of gallbladder wall thickening or polyps by ultrasonography can raise suspicion of biliary neoplasia. However, the differential diagnosis between benign and malignant gallbladder lesions can be challenging, especially when small abnormalities are seen. Polyps >10 mm and concomitant primary sclerosing cholangitis are risk factors for malignancy; moreover, the presence of vascularization within the lesion or deep invasion into the gallbladder wall are strong suspicious findings.[68]

The first description in 1998 reported on the superiority of CE-EUS after sonicated albumin injection versus standard EUS for the differential diagnosis of gallbladder lesions and assessment of the depth of tumor invasion (LE 2).[28]

These findings were replicated in a cohort of 93 patients with gallbladder polyps larger than 10 mm; the detection of intratumoral irregular vascularization by CH-EUS had 93.5% sensitivity and 93.2% specificity for malignancy (LE 2).[69]

With regard to gallbladder wall thickening, CH-EUS showed significantly higher diagnostic accuracy for malignancy than standard EUS (94.4 vs 73.1%) (LE 2).[18]

Assessment of splanchnic vascular abnormalities. Recently, Paik et al[70] evaluated the usefulness of CH-EUS compared with CT scan for the assessment of morphologic and hemodynamic characteristics of visceral vascular diseases. In a small number of patients, the authors observed that CH-EUS accurately identified or ruled out visceral vascular lesions such as arterial dissection, stenosis, or occlusion (LE 3).

Assessment of esophageal varices. Three studies[71-73] evaluated CE-EUS after injection of first-generation galactose-based UCA for the assessment of esophageal varices. Overall, it was reported that CE-EUS improved the quality of the depiction of varices versus standard color Doppler in all cases. Moreover, the authors observed that CE-EUS demonstrated the presence of perforating veins in 75.9% of the patients with recurrent esophageal varices[72] and arterial flow in patients with high-risk esophageal varices (LE 3).[73]

Staging of gastric neoplasms. Nomura et al[74] reported their retrospective experience with CE-EUS using air-filled albumin in patients with upper GI diseases. The authors reported 30 cases with gastric carcinoma in which the accuracy for the assessment of the infiltration depth for CE-EUS was 90% compared with 77% for standard EUS (LE 3).

Iordache et al[75] evaluated the application of CE-EUS for the preoperative assessment of 20 patients with locally advanced gastric cancer. The authors found that CE-EUS assessment of cancer vascularization could be useful for the evaluation of pathologic characteristics (ie, microvascular density or vascular endothelial growth factor expression) (LE 2).

Key issues. In selected cases, CH-EUS may represent a useful tool to characterize gallbladder abnormalities that are difficult to classify with other techniques; in particular, hyperenhanced components are predictive of malignancy. Other investigational or anecdotal applications have been reported for CH-EUS in vascular lesions and gastric neoplasms.

CONCLUSIONS

The use of UCAs in EUS is established in several indications, including pancreaticobiliary tumors, SMTs, lymph nodes, and gallbladder lesions. The LEs in the CH-EUS literature have evolved from the initial descriptive studies to multicenter and prospective trials, and even meta-analysis.

The differential diagnosis between benign and malignant lesions appears to be the main field of application of CH-EUS. Moreover, the sensitivity for the detection of malignancy may be increased by CH-EUS in particular conditions such as PCLs and CP.

With regard to pancreatic solid neoplasms, the accuracy of CH-EUS has been shown to be comparable with that of EUS-FNA. Moreover, the concomitant use of both CH-EUS and EUS-FNA may prove to have additive value in increasing the overall accuracy by overcoming the false-negative results of each individual technique.

EUS-FNA is not going to be replaced by CH-EUS; however, CH-EUS may contribute to the selective use of EUS-FNA, for instance, by guiding the FNA needle into non-necrotic areas of tumors. In particular cases, EUS-FNA could even be spared when CH-EUS features and clinical presentation are strongly indicative of a specific condition, eg, hypoenhanced resectable pancreatic solid tumors in good surgical candidates, hyperenhanced pancreatic solid tumors in patients with recurrent hypoglycemia, or homogeneously hyperenhanced lymph nodes in patients with early stage GI cancer.

Future applications of CH-EUS include prediction of the biological properties of neoplasms such as the grade of malignancy of pancreatic NETs and GISTs and the response to chemotherapy of PC.

REFERENCES

1. Piscaglia F, Nolsøe C, Dietrich CF, et al. The EFSUMB Guidelines and Recommendations on the Clinical Practice of Contrast Enhanced Ultrasound (CEUS): update 2011 on non-hepatic applications. Ultraschall Med 2012;33:33-59.
2. Dietrich CF. Comments and illustrations regarding the guidelines and good clinical practice recommendations for contrast-enhanced ultrasound (CEUS)—update 2008. Ultraschall Med 2008;29(Suppl 4): S188-202.
3. Fusaroli P, Saftoiu A, Mancino MG, et al. Techniques of image enhancement in EUS (with videos). Gastrointest Endosc 2011;74: 645-55.
4. Kitano M, Sakamoto H, Matsui U, et al. A novel perfusion imaging technique of the pancreas: contrast-enhanced harmonic EUS (with video). Gastrointest Endosc 2008;67:141-50.
5. Fusaroli P, Kypraios D, Mancino MG, et al. Interobserver agreement in contrast harmonic endoscopic ultrasound. J Gastroenterol Hepatol 2012;27:1063-9.
6. OCEBM Levels of Evidence Working Group. The Oxford 2011 Levels of Evidence. Oxford Centre for Evidence Based Medicine. Available at: http://www.cebm.net/index.aspx?o=5653. Accessed May 4th, 2016.
7. Alvarez-Sánchez MV, Napoléon B. Contrast-enhanced harmonic endoscopic ultrasound imaging: basic principles, present situation and future perspectives. World J Gastroenterol 2014;20:15549-63.
8. D'Onofrio M, Biagioli E, Gerardi C, et al. Diagnostic performance of contrast-enhanced ultrasound (CEUS) and contrast-enhanced endoscopic ultrasound (ECEUS) for the differentiation of pancreatic lesions: a systematic review and meta-analysis. Ultraschall Med 2014;35: 515-21.
9. Gong TT, Hu DM, Zhu Q. Contrast-enhanced EUS for differential diagnosis of pancreatic mass lesions: a meta-analysis. Gastrointest Endosc 2012;76:301-9.
10. Fusaroli P, Kypraios D, Caletti G, et al. Pancreatico-biliary endoscopic ultrasound: a systematic review of the levels of evidence, performance and outcomes. World J Gastroenterol 2012;18:4243-56.
11. Săftoiu A, Dietrich CF, Vilmann P. Contrast-enhanced harmonic endoscopic ultrasound. Endoscopy 2012;44:612-7.
12. Giovannini M. Contrast-enhanced and 3-dimensional endoscopic ultrasonography. Gastroenterol Clin North Am 2010;39:845-58.
13. Kwek BE, Ang TL, Seo DW, et al. Contrast-enhanced harmonic endoscopic ultrasonography of solid pancreatic lesions. Endosc Ultrasound 2013;2:142-7.
14. Gincul R, Palazzo M, Pujol B, et al. Contrast-harmonic endoscopic ultrasound for the diagnosis of pancreatic adenocarcinoma: a prospective multicenter trial. Endoscopy 2014;46:373-9.
15. Kitano M, Kudo M, Yamao K, et al. Characterization of small solid tumors in the pancreas: the value of contrast-enhanced harmonic endoscopic ultrasonography. Am J Gastroenterol 2012;107:303-10.
16. Soares JB, Iglesias-Garcia J, Gonçalves B, et al. Interobserver agreement of contrast-enhanced harmonic endoscopic ultrasonography in the evaluation of solid pancreatic lesions. Endosc Int Open 2015;3:E205-9.
17. Xia Y, Kitano M, Kudo M, et al. Characterization of intra-abdominal lesions of undetermined origin by contrast-enhanced harmonic EUS (with videos). Gastrointest Endosc 2010;72:637-42.
18. Imazu H, Mori N, Kanazawa K, et al. Contrast-enhanced harmonic endoscopic ultrasonography in the differential diagnosis of gallbladder wall thickening. Dig Dis Sci 2014;59:1909-16.
19. Ryan DP, Hong TS, Bardeesy N. Pancreatic adenocarcinoma. N Engl J Med 2014;371:1039-49.
20. Kalra MK, Maher MM, Mueller PR, et al. State-of-the-art imaging of pancreatic neoplasms [Review]. Br J Radiol 2003;76:857-65.
21. Fusaroli P, Spada A, Mancino MG, et al. Contrast harmonic echo-endoscopic ultrasound improves accuracy in diagnosis of solid pancreatic masses. Clin Gastroenterol Hepatol 2010;8:629-34.e1-2.
22. Iglesias-Garcia J, Larino-Noia J, Abdulkader I, et al. Quantitative endoscopic ultrasound elastography: an accurate method for the differentiation of solid pancreatic masses. Gastroenterology 2010;139: 1172-80.
23. Napoleon B, Alvarez-Sanchez MV, Gincoul R, et al. Contrast-enhanced harmonic endoscopic ultrasound in solid lesions of the pancreas: results of a pilot study. Endoscopy 2010;42:564-70.
24. Krishna SG, Li F, Bhattacharya A, et al. Differentiation of pancreatic ductal adenocarcinoma from other neoplastic solid pancreatic lesions: a tertiary oncology center experience. Gastrointest Endosc 2015;81: 370-9.
25. Rösch T, Lorenz R, Braig C, et al. Endoscopic ultrasound in pancreatic tumor diagnosis. Gastrointest Endosc 1991;37:347-52.
26. Giovannini M, Thomas B, Erwan B, et al. Endoscopic ultrasound elastography for evaluation of lymph nodes and pancreatic masses: a multicenter study. World J Gastroenterol 2009;15:1587-93.
27. Puli SR, Bechtold ML, Buxbaum JL, et al. How good is endoscopic ultrasound-guided fine-needle aspiration in diagnosing the correct etiology for a solid pancreatic mass? A meta-analysis and systematic review. Pancreas 2013;42:20-6.
28. Hirooka Y, Goto H, Ito A, et al. Contrast-enhanced endoscopic ultrasonography in pancreatic diseases: a preliminary study. Am J Gastroenterol 1998;93:632-5.
29. Becker D, Strobel D, Bernatik T, et al. Echo-enhanced color- and power-Doppler EUS for the discrimination between focal pancreatitis and pancreatic carcinoma. Gastrointest Endosc 2001;53:784-9.

30. Hocke M, Schulze E, Gottschalk P, et al. Contrast-enhanced endoscopic ultrasound in discrimination between focal pancreatitis and pancreatic cancer. World J Gastroenterol 2006;12:246-50.
31. Hocke M, Ignee A, Topalidis T, et al. Contrast-enhanced endosonographic Doppler spectrum analysis is helpful in discrimination between focal chronic pancreatitis and pancreatic cancer. Pancreas 2007;35:286-8.
32. Sakamoto H, Kitano M, Suetomi Y, et al. Utility of contrast-enhanced endoscopic ultrasonography for diagnosis of small pancreatic carcinomas. Ultrasound Med Biol 2008;34:525-32.
33. Dietrich CF, Ignee A, Braden B, et al. Improved differentiation of pancreatic tumors using contrast-enhanced endoscopic ultrasound. Clin Gastroenterol Hepatol 2008;6:590-7.e1.
34. Dietrich CF, Ignee A, Frey H. Contrast-enhanced endoscopic ultrasound with low mechanical index: a new technique. Z Gastroenterol 2005;43:1219-23.
35. Fusaroli P, D'Ercole MC, De Giorgio R, et al. Contrast harmonic endoscopic ultrasonography in the characterization of pancreatic metastases (with video). Pancreas 2014;43:584-7.
36. Săftoiu A, Vilmann P, Dietrich CF, et al. Quantitative contrast-enhanced harmonic EUS in differential diagnosis of focal pancreatic masses (with videos). Gastrointest Endosc 2015;82:59-69.
37. Seicean A, Badea R, Stan-Iuga R, et al. Quantitative contrast-enhanced harmonic endoscopic ultrasonography for the discrimination of solid pancreatic masses. Ultraschall Med 2010;31:571-6.
38. Imazu H, Uchiyama Y, Matsunaga K, et al. Contrast-enhanced harmonic EUS with novel ultrasonographic contrast (Sonazoid) in the preoperative T-staging for pancreaticobiliary malignancies. Scand J Gastroenterol 2010;45:732-8.
39. Matsubara H, Itoh A, Kawashima H, et al. Dynamic quantitative evaluation of contrast-enhanced endoscopic ultrasonography in the diagnosis of pancreatic diseases. Pancreas 2011;40:1073-9.
40. Gheonea DI, Streba CT, Ciurea T, et al. Quantitative low mechanical index contrast-enhanced endoscopic ultrasound for the differential diagnosis of chronic pseudotumoral pancreatitis and pancreatic cancer. BMC Gastroenterol 2013;13:2.
41. Ishikawa T, Itoh A, Kawashima H, et al. Usefulness of EUS combined with contrast-enhancement in the differential diagnosis of malignant versus benign and preoperative localization of pancreatic endocrine tumors. Gastrointest Endosc 2010;71:951-9.
42. Palazzo M, Palazzo L, Aubert A, et al. Contrast harmonic endoscopic ultrasonography is able to predict aggressivity in pancreatic neuroendocrine tumors. Gastroenterology 2015;148:S-127.
43. Sugimoto M, Takagi T, Hikichi T, et al. Conventional versus contrast-enhanced harmonic endoscopic ultrasonography-guided fine-needle aspiration for diagnosis of solid pancreatic lesions: a prospective randomized trial. Pancreatology 2015;15:538-41.
44. Seicean A, Badea R, Moldovan-Pop A, et al. Harmonic contrast-enhanced endoscopic ultrasonography for the guidance of fine-needle aspiration in solid pancreatic masses. Ultraschall Med. Epub 2015 Aug 14. http://dx.doi.org/10.1055/s-0035-1553496.
45. Hou X, Jin Z, Xu C, et al. Contrast-enhanced harmonic endoscopic ultrasound-guided fine-needle aspiration in the diagnosis of solid pancreatic lesions: a retrospective study. PLoS One 2015;10:e0121236.
46. Thornton GD, McPhail MJ, Nayagam S, et al. Endoscopic ultrasound guided fine needle aspiration for the diagnosis of pancreatic cystic neoplasms: a meta-analysis. Pancreatology 2013;13:48-57.
47. Tanaka M, Fernández-del Castillo C, Adsay V, et al; International Association of Pancreatology. International consensus guidelines 2012 for the management of IPMN and MCN of the pancreas. Pancreatology 2012;12:183-97.
48. Hocke M, Cui XW, Domagk D, et al. Pancreatic cystic lesions: the value of contrast-enhanced endoscopic ultrasound to influence the clinical pathway. Endosc Ultrasound 2014;3:123-30.
49. Fusaroli P, Serrani M, De Giorgio R, et al. Contrast harmonic-endoscopic ultrasound is useful to identify neoplastic features of pancreatic cysts (with videos). Pancreas 2016;45:265-8.
50. Kamata K, Kitano M, Omoto S, et al. Contrast-enhanced harmonic endoscopic ultrasonography for differential diagnosis of pancreatic cysts. Endoscopy 2016;48:35-41.
51. Yamashita Y, Ueda K, Itonaga M, et al. Usefulness of contrast-enhanced endoscopic sonography for discriminating mural nodules from mucous clots in intraductal papillary mucinous neoplasms: a single-center prospective study. J Ultrasound Med 2013;32:61-8.
52. Harima H, Kaino S, Shinoda S, et al. Differential diagnosis of benign and malignant branch duct intraductal papillary mucinous neoplasm using contrast-enhanced endoscopic ultrasonography. World J Gastroenterol 2015;21:6252-60.
53. Yamamoto N, Kato H, Tomoda T, et al. Contrast-enhanced harmonic endoscopic ultrasonography with time-intensity curve analysis for intraductal papillary mucinous neoplasms of the pancreas. Endoscopy 2016;48:26-34.
54. Catalano MF, Sivak MV Jr, Rice T, et al. Endosonographic features predictive of lymph node metastasis. Gastrointest Endosc 1994;40:442-6.
55. Vassallo P, Edel G, Roos N, et al. In-vitro high-resolution ultrasonography of benign and malignant lymph nodes. A sonographic-pathologic correlation. Invest Radiol 1993;28:698-705.
56. Wiersema MJ, Vilmann P, Giovannini M, et al. Endosonography-guided fine-needle aspiration biopsy: diagnostic accuracy and complication assessment. Gastroenterology 1997;112:1087-95.
57. Wiersema MJ, Vazquez-Sequeiros E, Wiersema LM. Evaluation of mediastinal lymphadenopathy with endoscopic US-guided fine-needle aspiration biopsy. Radiology 2001;219:252-7.
58. Kojima S, Goto H, Hirooka Y, et al. Differentiation of benign and malignant lymph nodes with contrast-enhanced echolymphography using endoscopic ultrasound-guided puncture. Hepatogastroenterology 2003;50:1285-91.
59. Kanamori A, Hirooka Y, Itoh A, et al. Usefulness of contrast-enhanced endoscopic ultrasonography in the differentiation between malignant and benign lymphadenopathy. Am J Gastroenterol 2006;101:45-51.
60. Hocke M, Menges M, Topalidis T, et al. Contrast-enhanced endoscopic ultrasound in discrimination between benign and malignant mediastinal and abdominal lymph nodes. J Cancer Res Clin Oncol 2008;134:473-80.
61. Miyata T, Kitano M, Omoto S, et al. Contrast-enhanced harmonic endoscopic ultrasonography for assessment of lymph node metastases in pancreatobiliary carcinoma. World J Gastroenterol 2016;22:3381-91.
62. Davila RE, Faigel DO. GI stromal tumors. Gastrointest Endosc 2003;58:80-8.
63. Ando N, Goto H, Niwa Y, et al. The diagnosis of GI stromal tumors with EUS-guided fine needle aspiration with immunohistochemical analysis. Gastrointest Endosc 2002;55:37-43.
64. Chen VK, Eloubeidi MA. Endoscopic ultrasound-guided fine-needle aspiration of intramural and extraintestinal mass lesions: diagnostic accuracy, complication assessment, and impact on management. Endoscopy 2005;37:984-9.
65. Kannengiesser K, Mahlke R, Petersen F, et al. Contrast-enhanced harmonic endoscopic ultrasound is able to discriminate benign submucosal lesions from gastrointestinal stromal tumors. Scand J Gastroenterol 2012;47:1515-20.
66. Sakamoto H, Kitano M, Matsui S, et al. Estimation of malignant potential of GI stromal tumors by contrast-enhanced harmonic EUS (with videos). Gastrointest Endosc 2011;73:227-37.
67. Yamashita Y, Kato J, Ueda K, et al. Contrast-enhanced endoscopic ultrasonography can predict a higher malignant potential of gastrointestinal stromal tumors by visualizing large newly formed vessels. J Clin Ultrasound 2015;43:89-97.

68. Choi WB, Lee SK, Kim MH, et al. A new strategy to predict the neoplastic polyps of the gallbladder based on a scoring system using EUS. Gastrointest Endosc 2000;52:372-9.
69. Choi JH, Seo DW, Choi JH, et al. Utility of contrast-enhanced harmonic EUS in the diagnosis of malignant gallbladder polyps (with videos). Gastrointest Endosc 2013;78:484-93.
70. Paik WH, Choi JH, Seo DW, et al. Clinical usefulness with the combination of color Doppler and contrast-enhanced harmonic EUS for the assessment of visceral vascular diseases. J Clin Gastroenterol 2014;48:845-50.
71. Sato T, Yamazaki K, Toyota J, et al. Evaluation of hemodynamics in esophageal varices. Value of endoscopic color Doppler ultrasonography with a galactose-based contrast agent. Hepatol Res 2003;25:55-61.
72. Sato T, Yamazaki K, Toyota J, et al. Perforating veins in recurrent esophageal varices evaluated by endoscopic color Doppler ultrasonography with a galactose-based contrast agent. J Gastroenterol 2004;39:422-8.
73. Sato T, Yamazaki K, Toyota J, et al. Evaluation of arterial blood flow in esophageal varices via endoscopic color Doppler ultrasonography with a galactose-based contrast agent. J Gastroenterol 2005;40:64-9.
74. Nomura N, Goto H, Niwa Y, et al. Usefulness of contrast-enhanced EUS in the diagnosis of upper GI tract diseases. Gastrointest Endosc 1999;50:555-60.
75. Iordache S, Filip MM, Georgescu CV, et al. Contrast-enhanced power Doppler endosonography and pathological assessment of vascularization in advanced gastric carcinomas–a feasibility study. Med Ultrason 2012;14:101-7.
76. Park JS, Kim HK, Bang BW, et al. Effectiveness of contrast-enhanced harmonic endoscopic ultrasound for the evaluation of solid pancreatic masses. World J Gastroenterol 2014;20:518-24.
77. Lee TY, Cheon YK, Shim CS. Clinical role of contrast-enhanced harmonic endoscopic ultrasound in differentiating solid lesions of the pancreas: a single-center experience in Korea. Gut Liver 2013;7:599-604.
78. Figueiredo FA, da Silva PM, Monges G, et al. Yield of contrast-enhanced power doppler endoscopic ultrasonography and strain ratio obtained by EUS-elastography in the diagnosis of focal pancreatic solid lesions. Endosc Ultrasound 2012;1:143-9.
79. Hocke M, Ignee A, Dietrich CF. Advanced endosonographic diagnostic tools for discrimination of focal chronic pancreatitis and pancreatic carcinoma–elastography, contrast enhanced high mechanical index (CEHMI) and low mechanical index (CELMI) endosonography in direct comparison. Z Gastroenterol 2012;50:199-203.
80. Săftoiu A, Iordache SA, Gheonea DI, et al. Combined contrast-enhanced power Doppler and real-time sonoelastography performed during EUS, used in the differential diagnosis of focal pancreatic masses (with videos). Gastrointest Endosc 2010;72:739-47.
81. Yamashita Y, Ueda K, Itonaga M, et al. Tumor vessel depiction with contrast-enhanced endoscopic ultrasonography predicts efficacy of chemotherapy in pancreatic cancer. Pancreas 2013;42:990-5.
82. Ang TL, Teo EK, Ang D, et al. A pilot study of contrast harmonic endosonography using DEFINITY™ in the evaluation of suspected pancreatic and peri-ampullary malignancies. J Interv Gastroenterol 2011;1:160-5.
83. Sakamoto H, Kitano M, Suetomi Y, et al. Utility of contrast-enhanced endoscopic ultrasonography for diagnosis of small pancreatic carcinomas. Ultrasound Med Biol 2008;34:525-32.
84. Ray S, Das K, Mridha AR. Pancreatic and peripancreatic nodal tuberculosis in immunocompetent patients: report of three cases. JOP 2012;13:667-70.
85. Hyodo N, Hyodo T. Ultrasonographic evaluation in patients with autoimmune-related pancreatitis. J Gastroenterol 2003;38:1155-61.
86. Kanno A, Masamune A, Hamada S, et al. Sudden disappearance of the blood flow in a case of pancreatic acinar cell carcinoma. Intern Med 2014;53:2589-93.
87. Yamamoto K, Itoi T, Tsuchiya T, et al. Hemosuccus pancreaticus diagnosed by contrast-enhanced endoscopic ultrasonography (with video). J Hepatobiliary Pancreat Sci 2014;21:356-8.
88. Kim JW, Shin SS, Heo SH, et al. Imaging findings of localized lymphoid hyperplasia of the pancreas: a case report. Korean J Radiol 2011;12:510-4.
89. Rao RN, Vij M, Singla N, et al. Malignant pancreatic extra-gastrointestinal stromal tumor diagnosed by ultrasound guided fine needle aspiration cytology. A case report with a review of the literature. JOP 2011;12:283-6.
90. Hocke M, Ignee A, Dietrich CF. Three-dimensional contrast-enhanced endoscopic ultrasound for the diagnosis of autoimmune pancreatitis. Endoscopy 2011;43(suppl 2) UCTN: E381-2.
91. Kasono K, Hyodo T, Suminaga Y, et al. Contrast-enhanced endoscopic ultrasonography improves the preoperative localization of insulinomas. Endocr J 2002;49:517-22.
92. Fujii M, Yoshioka M, Niguma T, et al. A solid pseudopapillary neoplasm without cysts that occurred in a patient diagnosed by endoscopic ultrasound-guided fine-needle aspiration: a case report. J Med Case Rep 2014;8:243.
93. Singh A, Agarwal AA, Sonkar AA et al. Solid pseudopapillary tumour of pancreas. BMJ Case Rep. Epub 2014 Apr 17.
94. Nishi T, Kawabata Y, Hari Y, et al. A case of pancreatic neuroendocrine tumor in a patient with neurofibromatosis-1. World J Surg Oncol 2012;10:153.
95. Rodriguez A, Canto MI, Makary MA. Endoscopic localization and tattooing of a proinsulinoma for minimally invasive resection. Pancreas 2011;40:474-7.
96. Suzuki S, Kaji S, Koike N, et al. Pancreatic schwannoma: a case report and literature review with special reference to imaging features. JOP 2010;11:31-5.
97. Ueda K, Yamashita Y, Itonaga M. Real-time contrast-enhanced endoscopic ultrasonography-guided fine-needle aspiration (with video). Dig Endosc 2013;25:631.
98. Rana SS, Bhasin DK, Reddy YR, et al. Morphological features of fluid collections on endoscopic ultrasound in acute necrotizing pancreatitis: do they change over time? Ann Gastroenterol 2014;27:258-61.
99. Ohno E, Itoh A, Kawashima H, et al. Malignant transformation of branch duct-type intraductal papillary mucinous neoplasms of the pancreas based on contrast-enhanced endoscopic ultrasonography morphological changes: focus on malignant transformation of intraductal papillary mucinous neoplasm itself. Pancreas 2012;41:855-62.
100. Ohno E, Hirooka Y, Itoh A, et al. Intraductal papillary mucinous neoplasms of the pancreas: differentiation of malignant and benign tumors by endoscopic ultrasound findings of mural nodules. Ann Surg 2009;249:628-34.
101. Yamashita Y, Ueda K, Itonaga M, et al. Usefulness of contrast-enhanced endoscopic sonography for discriminating mural nodules from mucous clots in intraductal papillary mucinous neoplasms: a single-center prospective study. J Ultrasound Med 2013;32:61-8.
102. Salvia R, Malleo G, Marchegiani G, et al. Pancreatic resections for cystic neoplasms: from the surgeon's presumption to the pathologist's reality. Surgery 2012;152(3 Suppl 1):S135-42.
103. Konstantinidis IT, Kambadakone A, Catalano OA, et al. Lymphoepithelial cysts and cystic lymphangiomas: Under-recognized benign cystic lesions of the pancreas. World J Gastrointest Surg 2014;6:136-41.
104. Onishi I, Kitagawa H, Harada K, et al. Intraductal papillary neoplasm of the bile duct accompanying biliary mixed adenoneuroendocrine carcinoma. World J Gastroenterol 2013;19:3161-4.
105. Sakamoto H, Kitano M, Komaki T, et al. Small invasive ductal carcinoma of the pancreas distinct from branch duct intraductal papillary mucinous neoplasm. World J Gastroenterol 2009;15:5489-92.
106. Kang G, Park HJ, Kim JY, et al. Glomus tumor of the stomach: a clinicopathologic analysis of 10 cases and review of the literature. Gut Liver 2012;6:52-7.
107. Baek YH, Choi SR, Lee BE, et al. Gastric glomus tumor: analysis of endosonographic characteristics and computed tomographic findings. Dig Endosc 2013;25:80-3.

108. Guarise A, Faccioli N, Ferrari M, et al. Duodenal duplication cyst causing severe pancreatitis: imaging findings and pathological correlation. World J Gastroenterol 2006;12:1630-3.
109. Hirooka Y, Naitoh Y, Goto H, et al. Contrast-enhanced endoscopic ultrasonography in gallbladder diseases. Gastrointest Endosc 1998;48:406-10.
110. Park CH, Chung MJ, Oh TG, et al. Differential diagnosis between gallbladder adenomas and cholesterol polyps on contrast-enhanced harmonic endoscopic ultrasonography. Surg Endosc 2013;27:1414-21.
111. Inui K, Yoshino J, Miyoshi H. Diagnosis of gallbladder tumors. Intern Med 2011;50:1133-6.
112. Fan DS, Sorser SA, Gamarra RM. Secondary Sclerosing Cholangitis due to Gallbladder Adenocarcinoma. Case Rep Gastroenterol 2013;7:134-9.
113. Velosa M, Lopes S, Castro R, et al. Cholecystoduodenal fistula diagnosed with contrast-enhanced endoscopic ultrasound. Endoscopy 2013;45(suppl 2) UCTN: E18-9.
114. Dietrich CF. Contrast-enhanced low mechanical index endoscopic ultrasound (CELMI-EUS). Endoscopy 2009;41(suppl 2):E43-4.
115. Imori Y, Fujimoto H, Hanada S, et al. Idiopathic accessory hemiazygos vein aneurysm with an incidental mediastinal mass. Intern Med 2012;51:2347-9.
116. Ogura T, Masuda D, Kurisu Y, et al. Splenic artery aneurysm masquerading as a pancreatic tumor–diagnosis by contrast-enhanced endoscopic ultrasound. Endoscopy 2012;44(suppl 2) UCTN: E428-9.
117. Seicean A, Badea R, Stan-Iuga R, et al. Double splenic artery pseudoaneurysm associating splenic infarction in chronic pancreatitis. J Gastrointestin Liver Dis 2012;21:313-5.
118. Nagamatsu H, Takahashi K, Ueo T, et al. A case of splenic artery aneurysm simulating a pancreas tumor. Nihon Shokakibyo Gakkai Zasshi 2011;108:1420-7.
119. Moreno M, Gimeno-García AZ, Corriente MM, et al. EUS-FNA of a portal vein thrombosis in a patient with a hidden hepatocellular carcinoma: confirmation technique after contrast-enhanced ultrasound. Endoscopy 2014;46(suppl 1) UCTN: E590-1.
120. Kocaman O, Sentürk H, Danalıoğlu A, et al. Endosonography and elastography in the diagnosis of esophageal tuberculosis. Turk J Gastroenterol 2013;24:290-1.
121. Chaudhary V, Rana SS, Sharma V, et al. Esophageal duplication cyst in an adult masquerading as submucosal tumor. Endosc Ultrasound 2013;2:165-7.
122. Carrara S, Doglioni C, Arcidiacono PG, et al. Gastric metastasis from ovarian carcinoma diagnosed by EUS-FNA biopsy and elastography. Gastrointest Endosc 2011;74:223-5.
123. Romagnuolo J, Hoffman B, Vela S, et al. Accuracy of contrast-enhanced harmonic EUS with a second-generation perflutren lipid microsphere contrast agent (with video). Gastrointest Endosc 2011;73:52-63.
124. Hirooka Y, Naitoh Y, Goto H, et al. Usefulness of contrast-enhanced endoscopic ultrasonography with intravenous injection of sonicated serum albumin. Gastrointest Endosc 1997;46:166-9.
125. Pandey S, Shetty SA, Janarthanan K, et al. Pancreatico-pleural and bronchial fistulae and associated pseudocysts: case series. JOP 2014;15:478-84.
126. Kim EB, Lee TH, Kim JS, et al. Primary fallopian tube carcinoma diagnosed with endoscopic ultrasound elastography with fine needle biopsy. Clin Endosc 2014;47:464-8.
127. Wang G, Chen P, Zong L. Accessory spleen arising from the gastric fundus mimicking gastrointestinal stromal tumor following splenectomy: A case report. Exp Ther Med 2014;7:349-51.
128. Hijioka S, Sawaki A, Mizuno N, et al. Contrast-enhanced endoscopic ultrasonography (CE-EUS) findings in adrenal metastasis from renal cell carcinoma. J Med Ultrason (2001) 2011;38:89-92.

Received February 23, 2016. Accepted June 2, 2016.

Current affiliations: Gastroenterology Unit, Hospital of Imola, University of Bologna, Bologna, Italy (1); Department of Gastroenterology, Private Hospital Jean Mermoz, Lyon, France (2); Trocadero Clinic, Paris, France (3); Department of Gastroenterology and Hepatology, Kinki University Faculty of Medicine, Osaka-Sayama, Japan (4).

Reprint requests: Professor Pietro Fusaroli, MD, Gastroenterology Unit, Hospital of Imola, Department of Medical and Surgical Science, University of Bologna, Via Montericco 4, 40026 Imola (BO), Italy.

SUPPLEMENTARY TABLE 1. Diagnostic performance of CH-EUS for the evaluation of solid pancreatic neoplasms

Reference	Title	Main results	Study design, LE (population)
D'Onofrio et al, Ultraschall Med, 2014[8]	Diagnostic performance of contrast-enhanced ultrasound (CEUS) and contrast-enhanced endoscopic ultrasound (ECEUS) for the differentiation of pancreatic lesions: a systematic review and meta-analysis	Adenocarcinoma: CEUS and CH-EUS sensitivity 0.89 (0.85 - 0.92); specificity 0.84 (0.77 - 0.89); pooled DOR, was 61.12 (34.81 - 107.32). Neoplastic vs non-neoplastic: pooled sensitivity 0.95 (0.93 - 0.96); specificity 0.72 (0.58 - 0.83); pooled DOR 57.63 (33.62 - 98.78)	Meta-analysis, LE 1, (27 studies)
Gong et al, Gastrointest Endosc 2012[9]	Contrast-enhanced EUS for differential diagnosis of pancreatic mass lesions: a meta-analysis	Adenocarcinoma pooled sensitivity 94% (0.91-0.95); specificity 89% (0.85-0.92)	Meta-analysis, LE 1, (12 studies; 1139 patients)
Săftoiu et al, Gastrointest Endosc 2015[36]	Quantitative contrast-enhanced harmonic EUS in differential diagnosis of focal pancreatic masses (with videos)	The sensitivity of qCH-EUS was 87.5%, specificity 92.72%, PPV 96.07%, and NPV 78.46% Artificial neural network sensitivity was 94.6%, specificity 94.4%, PPV 97.2%, and NPV 89.5%	Prospective, LE 2, (167 patients)
Gincul et al, Endoscopy 2014[14]	Contrast-harmonic endoscopic ultrasound for the diagnosis of pancreatic adenocarcinoma: a prospective multicenter trial	Diagnosis of PC: CH- EUS accuracy 95%; sensitivity 96%; specificity 94%; PPV 97%; NPV 91%. No significant differences between CH-EUS and EUS-FNA Good interobserver agreement ($\kappa = 0.66$); excellent intraobserver agreement ($\kappa = 0.76$ for junior, 0.90 for senior)	Prospective multicentric, LE 2, (100 patients)
Gheonea et al, BMC Gastroenterol 2013[40]	Quantitative low mechanical index contrast-enhanced endoscopic ultrasound for the differential diagnosis of chronic pseudotumoral pancreatitis and pancreatic cancer	Sensitivity 93.8% (77.8%-98.9%); specificity 89.5% (65.5%-98.2%) Mass-forming pancreatitis showed hypervascular features in early arterial phase while adenocarcinomas were usually hypovascular, with low CE during all phases; significant differences in TIC analysis ($P < .001$)	Prospective, LE 2, (53 patients)
Lee et al, Gut Liver 2013[77]	Clinical role of contrast-enhanced harmonic endoscopic ultrasound in differentiating solid lesions of the pancreas: a single-center experience in Korea	28 of 30 pancreatic carcinomas (93%) had persistent hypovascular signals in the early and late phase; sensitivity 93%; diagnostic accuracy 92%	Prospective, LE 2, (37 patients)
Yamashita et al, Pancreas 2013[81]	Tumor vessel depiction with contrast-enhanced endoscopic ultrasonography predicts efficacy of chemotherapy in pancreatic cancer	Positive vessel sign in 20 patients. Progression-free survival ($P = .037$) and overall survival ($P = .027$) significantly longer in the positive vessel sign groups. Positive vessel sign independently related to longer overall survival (HR 0.22; 0.08-0.53)	Prospective, LE 2, (37 patients)
Imazu et al, Scand J Gastroenterol 2012[38]	Novel quantitative perfusion analysis with contrast-enhanced harmonic EUS for differentiation of autoimmune pancreatitis from pancreatic carcinoma	Peak intensity and MIG evaluated by TIC were significantly higher in AIP vs PC. ROC curve identified a MIG cutoff value of 12.5 for diagnosis of PC	Prospective, LE 2, (30 patients)
Kitano et al, Am J Gastroenterol 2012[15]	Characterization of small solid tumors in the pancreas: the value of contrast-enhanced harmonic endoscopic ultrasonography	CH-EUS interobserver agreement test $\kappa = 0.94$ ($P < .001$). Hypoenhancement for ductal carcinomas: sensitivity 95.1% (92.7%-96.7%); specificity 89.0% (83.0%-93.1%). Small carcinomas, CH-EUS sensitivity 91.2% (82.5%-95.1%), specificity 94.4% (86.2%-98.1%). Hypervascular enhancement for NETs: sensitivity 78.9% (61.4%-89.7%), specificity 98.7% (96.7%-98.8%) CH-EUS superior to MDCT in diagnosing small ($\leq$2 cm) carcinomas ($P < .05$). Combined CH-EUS and FNA, sensitivity of EUS-FNA increased from 92.2% to 100%	Prospective, LE 2, (277 patients)
Ang et al, J Intervent Gastroenterol 2012[82]	A pilot study of contrast harmonic endosonography using DEFINITY™ in the evaluation of suspected pancreatic and peri-ampullary malignancies	Malignant masses had inhomogeneous hypoechoic pattern with abnormal vessels; focal pancreatitis or fat-sparing masses had diffuse enhancement ($P < .001$). CH-EUS detected vascular invasion missed by EUS in 2 of 16 PC	Prospective, LE 2, (29 patients)

(*continued on the next page*)

SUPPLEMENTARY TABLE 1. Continued

Reference	Title	Main results	Study design, LE (population)
Fusaroli et al, Clin Gastroenterol Hepatol 2010[21]	Contrast harmonic echo-endoscopic ultrasound improves accuracy in diagnosis of solid pancreatic masses	Hypoenhancing mass with an inhomogeneous pattern: sensitivity (96%); diagnostic accuracy (82%) for adenocarcinomas Hyperenhancement specifically excluded adenocarcinoma (98%) 11 of 13 NETs were non-hypoenhancing	Prospective, LE 2, (90 patients)
Imazu et al, Scand J Gastroenterol 2010[38]	Contrast-enhanced harmonic EUS with novel ultrasonographic contrast (Sonazoid) in the preoperative T-staging for pancreaticobiliary malignancies	Harmonic EUS accuracy for T-staging 69.2%; CH-EUS accuracy for T-staging 92.4% ($P < .05$)	Prospective, LE 2, (26 patients)
Ishikawa et al, Gastrointest Endosc 2010[41]	Usefulness of EUS combined with contrast-enhancement in the differential diagnosis of malignant versus benign and preoperative localization of pancreatic endocrine tumors	Pancreatic NET: EUS sensitivity 95.1%, MDCT 80.6%; US 45.2% Heterogeneous texture independent factor for malignancy (OR = 53.33; 95% CI, 10.79-263.58) Heterogeneous hypoechoic areas and anechoic areas (filling defects at CH-EUS) corresponded to hemorrhage or necrosis on pathologic examination	Prospective, LE 2, (41 patients)
Napoleon et al, Endoscopy 2010[23]	Contrast-enhanced harmonic endoscopic ultrasound in solid lesions of the pancreas: results of a pilot study	16 of 18 hypointense lesions on CH-EUS were adenocarcinomas; sensitivity 89%; specificity 88%; NPV 88%; PPV 89%; accuracy 88.5%. EUS-FNA sensitivity 72%; specificity 100%; NPV 77%; PPV 100%; accuracy 86% Among 5 false-negative EUS-FNA, 4 were correctly diagnosed by CH-EUS	Prospective, LE 2, (35 patients)
Seicean et al, Ultraschall Med 2010[37]	Quantitative contrast-enhanced harmonic endoscopic ultrasonography for the discrimination of solid pancreatic masses	Contrast uptake index was significantly lower in PC vs mass-forming pancreatitis. Cutoff value of 0.17 for diagnosing PC corresponded to an AUC of 0.86 (0.67-1.00); sensitivity 80%; specificity 91.7%; PPV 92.8%; NPV 78%	Prospective, LE 2, (30 patients)
Dietrich et al, Clin Gastroenterol Hepatol 2008[33]	Improved differentiation of pancreatic tumors using contrast-enhanced endoscopic ultrasound	57 of 62 ductal adenocarcinomas presented hypovascular pattern Hypovascularity for diagnosis of malignancy: sensitivity 92% (82%-97%); specificity 100% (89%-100%)	Prospective, LE 2, (93 patients)
Kitano et al, Gastrointest Endosc 2008[4]	A novel perfusion imaging technique of the pancreas: contrast-enhanced harmonic EUS (with video)	Optimal mechanical index (0.4) was identified for adequate visualization Apparent perfusion and vessel images were observed in pancreato-biliary carcinomas, GISTs, lymph nodes, and metastases	Prospective, LE 2, (104 patients)
Sakamoto et al, Ultrasound Med Biol 2008[83]	Utility of contrast-enhanced endoscopic ultrasonography for diagnosis of small pancreatic carcinomas	EUS sensitivity for small (< 2 cm) adenocarcinomas, 94.4% Differential diagnosis ductal adenocarcinomas vs other tumors, sensitivity: MDCT 50.0%; power Doppler-EUS 11.0%; CH-EUS 83.3%	Prospective, LE 2, (156 patients)
Hocke et al, Pancreas 2007[31]	Contrast-enhanced endosonographic Doppler spectrum analysis is helpful in discrimination between focal chronic pancreatitis and pancreatic cancer	Resistance index 0.59 $\pm$ 0.12 mass-forming pancreatitis and 0.77 $\pm$ 0.12 in ductal adenocarcinomas ($P < .0001$). Cutoff value 0.70: sensitivity 78%; specificity 87%; PPV 87%; NPV 77%	Prospective, LE 2, (100 patients)
Hocke et al, World J Gastroenterol 2006[30]	Contrast-enhanced endoscopic ultrasound in discrimination between focal pancreatitis and pancreatic cancer	EUS sensitivity 73.2% and specificity 83.3% for PC CH-EUS sensitivity 91.1% and specificity 93.3% for PC	Prospective, LE 2, (86 patients)
Becker et al, Gastrointest Endosc 2001[29]	Echo-enhanced color- and power-Doppler EUS for the discrimination between focal pancreatitis and pancreatic carcinoma	All (15 of 15) patients with hypoperfused lesions had PC. 1 of 8 patients with hyperperfused mass had PC; 7 focal pancreatitis CH-EUS sensitivity 94%; specificity 100%	Prospective, LE 2, (23 patients)

(*continued on the next page*)

SUPPLEMENTARY TABLE 1. Continued

Reference	Title	Main results	Study design, LE (population)
Hirooka et al, Am J Gastroenterol 1998[28]	Contrast-enhanced endoscopic ultrasonography in pancreatic diseases: a preliminary study	All islet cell tumor (3/3) and serous cystoadenoma (4/4) presented enhancement; 8 of 10 mucin-producing tumors, 3 of 4 with chronic pancreatitis presented enhancement No enhancement was observed in ductal cell carcinomas or in pseudocyst	Prospective, LE 2, (37 patients)
Fusaroli et al, Pancreas 2014[35]	Contrast harmonic endoscopic ultrasonography in the characterization of pancreatic metastases (with video)	All pancreatic metastases appeared hypoechoic CH-EUS: 6 hypoenhancing (colon cancer, sarcoma, and breast and ovarian cancer); 4 hyperenhancing (renal cancer and lymphoma); 1 isoenhancing (melanoma)	Retrospective, LE 3, (11 patients)
Iordache et al, Endosc Ultrasound 2012[75]	Power Doppler endoscopic ultrasound for the assessment of pancreatic neuroendocrine tumors	14 pancreatic NETs; 117 adenocarcinomas Power Doppler vascular index sensitivity for NET, 71.4%. CH-EUS sensitivity 100%; specificity 79.5%; accuracy 81.7%	Retrospective, LE 3, (131 patients)
Matsubara et al, Pancreas 2011[39]	Dynamic quantitative evaluation of contrast-enhanced endoscopic ultrasonography in the diagnosis of pancreatic diseases	Accuracy: CH-EUS 84.0%; TIC 88.0% CH-EUS with TIC, sensitivity 95.8%; specificity 92.6%; accuracy 94.7%	Retrospective, LE 3, (71 patients)
Park et al, World J Gastroenterol 2014[76]	Effectiveness of contrast-enhanced harmonic endoscopic ultrasound for the evaluation of solid pancreatic masses	CH-EUS sensitivity 92%; specificity 68%; accuracy 82%; AUC 0.799	Retrospective, LE 3, (90 patients)
Hocke et al, Pancreas 2007[31]	Contrast-enhanced endosonographic Doppler spectrum analysis is helpful in discrimination between focal chronic pancreatitis and pancreatic cancer	EUS sensitivity 73%; specificity 83%; CH-(power Doppler)-EUS sensitivity 91%; specificity 93% Resistance index was 0.59 $\pm$ 0.12 in focal pancreatitis; 0.77 $\pm$ 0.12 in ductal adenocarcinomas ($P < .0001$)	Retrospective (Letter to the editor), LE 3, (126 patients)
Figueiredo et al, Endosc Ultrasound 2012[78]	Yield of contrast-enhanced power Doppler endoscopic ultrasonography and strain ratio obtained by EUS-elastography in the diagnosis of focal pancreatic solid lesions	Malignant lesions had higher strain ratio on EUS-E (31 $\pm$ 32 vs 8 $\pm$ 9, $P = .001$) and more hypovascular pattern (93% vs 33%, $P < .001$). SR cutoff value of 8: AUC 0.91 (0.47-0.98) for prediction of malignancy. Hypovascularity (OR = 2.6; 1.5-130) was independently predictive of malignancy. EUS-FNA: sensitivity 79%; specificity 85%. EUS-E: sensitivity 90%; specificity 75%. CH-EUS sensitivity 93%; specificity 67%	Prospective, LE 2, (47 patients), Combined CH-EUS and EUS-E*
Hocke et al, Z Gastroenterol 2012[79]	Advanced endosonographic diagnostic tools for discrimination of focal chronic pancreatitis and pancreatic carcinoma–elastography, contrast enhanced high mechanical index (CEHMI) and low mechanical index (CELMI) endosonography in direct comparison	EUS B-mode sensitivity 61.5%; specificity 73.7%. EUS-E sensitivity 33.4%; specificity 94.7%. CH-EUS (low MI) sensitivity 76.9%; specificity 84.2%. CH-EUS (high MI) sensitivity 92.3%; specificity 89.5%. The combination of 3 methods did not improve accuracy of CH-EUS (high MI) alone	Prospective, LE 3, (58 patients), Combined CH-EUS and EUS-E*
Săftoiu et al, Gastrointest Endosc 2010[80]	Combined contrast-enhanced power Doppler and real-time sonoelastography performed during EUS, used in the differential diagnosis of focal pancreatic masses (with videos)	CH-EUS combined to EUS-E (hypovascular and hard masses): sensitivity 75.8%; specificity 95.2%; accuracy 83.3%; PPV 96.2%; NPV 71.4% for PC	Prospective, LE 2, (54 patients), Combined CH-EUS and EUS-E*
Ray et al, JOP 2012[84]	Pancreatic and peripancreatic nodal tuberculosis in immunocompetent patients: report of 3 cases	Description of pancreatic tuberculosis	Case series, LE 4, (3 patients)
Hyodo et al, J Gastroenterol 2003[85]	Ultrasonographic evaluation in patients with autoimmune-related pancreatitis	Description of IgG-4 related AIP	Case series, LE 4, (5 patients)
Kanno et al, Intern Med. 2014[86]	Sudden disappearance of the blood flow in a case of pancreatic acinar cell carcinoma	Pancreatic acinar cell carcinoma	Case report, LE 4
Yamamoto et al, J Hepatobiliary Pancreat Sci 2014[87]	Hemosuccus pancreaticus diagnosed by contrast-enhanced endoscopic ultrasonography (with video)	Hemosuccus pancreaticus	Case report, LE 4

(*continued on the next page*)

SUPPLEMENTARY TABLE 1. Continued

Reference	Title	Main results	Study design, LE (population)
Kim et al, Korean J Radiol 2011[88]	Imaging findings of localized lymphoid hyperplasia of the pancreas: a case report	Pancreatic lymphoid hyperplasia	Case report, LE 4
Rao et al, JOP 2011[89]	Malignant pancreatic extra-gastrointestinal stromal tumor diagnosed by ultrasound guided fine needle aspiration cytology. A case report with a review of the literature	Malignant pancreatic extra-gastrointestinal stromal tumor	Case report, LE 4
Hocke et al, Endoscopy 2011[90]	Three-dimensional contrast-enhanced endoscopic ultrasound for the diagnosis of autoimmune pancreatitis	AIP (3D CH-EUS)	Case report, LE 4
Kasono et al, Endocr J 2002[91]	Contrast-enhanced endoscopic ultrasonography improves the preoperative localization of insulinomas	Small insulinoma	Case report, LE 4
Fujii et al, J Med Case Rep 2014[92]	A solid pseudopapillary neoplasm without cysts that occurred in a patient diagnosed by endoscopic ultrasound-guided fine-needle aspiration: a case report	Pseudopapillary tumor	Case report, LE 4
Singh et al, BMJ Case Rep 2014[93]	Solid pseudopapillary tumour of pancreas	Pseudopapillary tumor	Case report, LE 4
Nishi et al, World J Surg Oncol 2012[94]	A case of pancreatic neuroendocrine tumor in a patient with neurofibromatosis-1	P-NET in neurofibromatosis-1	Case report, LE 4
Rodriguez et al, Pancreas 2011[95]	Endoscopic localization and tattooing of a proinsulinoma for minimally invasive resection	EUS tattooing	Case report, LE 4
Suzuki et al, JOP 2010[96]	Pancreatic schwannoma: a case report and literature review with special reference to imaging features	Pancreatic schwannoma	Case report, LE 4
CH-EUS-guided FNA			
Sugimoto et al, Pancreatology 2015[43]	Conventional versus contrast-enhanced harmonic endoscopic ultrasonography-guided fine-needle aspiration for diagnosis of solid pancreatic lesions: A prospective randomized trial	Fewer needle passes were required to obtain samples from solid pancreatic lesions using CH-EUS-guided FNA than those required using conventional EUS-FNA	Prospective, LE 2, (40 patients)
Seicean et al, Ultraschall Med 2015[44]	Harmonic contrast-enhanced endoscopic ultrasonography for guidance of fine-needle aspiration in solid pancreatic masses	Core cytology accuracy 78.4%; CH-EUS-guided FNA accuracy 86.5%	Prospective, LE 2, (51 patients)
Hou et al, PLoS One 2015[45]	Contrast-enhanced harmonic endoscopic ultrasound-guided fine-needle aspiration in the diagnosis of solid pancreatic lesions: a retrospective study	Adequate specimens in CH-EUS-guided FNA 96.6%; EUS-FNA 86.7% CH-EUS-guided FNA: sensitivity 81.6%; specificity 100%; PPV 100%; NPV 71.4%; accuracy 87.9%	Retrospective, LE 3, (163 patients)
Ueda et al, Dig Endosc. 2013[97]	Real-time contrast-enhanced endoscopic ultrasonography-guided fine-needle aspiration (with video)	CH-EUS-guided FNA description	Case report, LE 4, (2 patients)

CH-EUS, Contrast-harmonic EUS; *LE*, level of evidence; *CEUS*, contrast-enhanced ultrasound; *DOR*, diagnostic odds ratio; *qCH-EUS*, quantitative CH-EUS; *PPV*, positive predictive value; *NPV*, negative predictive value; *CE*, contrast enhancement; *TIC*, time-intensity curve; *HR*, hazard ratio; *MIG*, minimum intensity gain; *AIP*, autoimmune pancreatitis; *PC*, pancreatic cancer; *ROC*, receiver operating characteristic; *NET*, neuro-endocrine tumor; *MDCT*, multi-detector computed tomography; *OR*, odds ratio; *CI*, confidence interval; *AUC*, area under the curve; *GIST*, gastrointestinal stromal tumor; *SR*, strain ratio; *MI*, mechanical index.
*Article describing combined techniques (ie, CH-EUS and EUS-E) are reported duplicated in both tables.

SUPPLEMENTARY TABLE 2. Diagnostic performance of CH-EUS for the evaluation of pancreatic cystic neoplasms

Reference	Title	Main results	Study design, LE (population)
Kamata et al, Endoscopy 2016[50]	Contrast-enhanced harmonic endoscopic ultrasonography for differential diagnosis of pancreatic cysts	CH-EUS was significantly more accurate for the identification of mural nodule (sensitivity 97% vs 97%; specificity 75% vs 40%; accuracy 84% vs 64%). Diagnosis of malignancy: CH-EUS AUROC 0.93; EUS AUROC 0.84 ($P = .028$). CH-EUS identification of mural nodule $\geq$ 4 mm had an odds ratio of 56.0 for the diagnosis of malignancy	Prospective, LE 2 (70 patients)
Yamamoto et al, Endoscopy 2016[53]	Contrast-enhanced harmonic endoscopic ultrasonography with time-intensity curve analysis for intraductal papillary mucinous neoplasms of the pancreas	IPMN with high-grade dysplasia and invasive cancer showed significantly lower intensity change, lower reduction rate in echo pattern and lower nodule/parenchyma contrast ratio (accuracy 80%, 86.7%, and 93.3%, respectively). Strong linear correlation between echo intensity change and microvessel density was found	Prospective, LE 2 (30 patients)
Fusaroli et al, Pancreas 2016[49]	Contrast enhanced-endoscopic ultrasound is useful to identify neoplastic features of pancreatic cysts (with videos)	>85% of mucinous and serous cysts were hyperenhanced while 90% of pseudocysts were hypoenhanced. CH-EUS allows discrimination between pseudocysts and mucinous and serous cysts. Presence of hyperenhanced solid component represents neoplastic features (malignant IPMN and cystic P-NET) while mucus clots and pseudocyst debris were non-enhanced	Prospective, LE 2 (76 patients)
Harima et al, World J Gastroenterol 2015[52]	Differential diagnosis of benign and malignant branch duct intraductal papillary mucinous neoplasm using contrast-enhanced endoscopic ultrasonography	Among 50 patients with pancreatic cystic lesions, 15 presented mural nodules. The diagnostic accuracy of CH-EUS for the detection of mural nodules was 98%, compared with 92% for MDCT and 72% for EUS	Prospective, LE 2 (50 patients)
Hocke et al, Endoscopic Ultrasound 2014[48]	Pancreatic cystic lesions: The value of contrast-enhanced endoscopic ultrasound to influence the clinical pathway	All cystic neoplasia presented CE (n = 56); sensitivity 100% 4 of 69 non-neoplastic cystic lesions (pseudocyst or dysontogenetic cystic) presented CE; specificity 94.5%	Prospective, LE 2 (125 patients)
Rana et al, Ann Gastroenterol 2014[98]	Morphological features of fluid collections on endoscopic ultrasound in acute necrotizing pancreatitis: do they change over time?	After acute necrotizing pancreatitis, 87% patients had fluid collection with solid debris. Follow-up EUS at 3 and 6 months revealed progressively decreasing solid content in PFCs	Prospective, LE 2 (47 patients)
Ohno et al, Pancreas 2012[99]	Malignant transformation of branch duct-type intraductal papillary mucinous neoplasms of the pancreas based on contrast-enhanced endoscopic ultrasonography morphological changes: focus on malignant transformation of intraductal papillary mucinous neoplasm itself	Follow-up: 42.5 months (12–105). 30 patients underwent surgery; malignant transformation in 9 cases (6.3%). 5-year MT rate was 10.7%. Invasive ductal carcinoma in 5 patients Presence of mural nodules at initial diagnosis and involvement of main pancreatic duct were significant predictors of transformation	Prospective, LE 2 (142 patients)
Ohno et al, Ann Surg 2009[100]	Intraductal papillary mucinous neoplasms of the pancreas: differentiation of malignant and benign tumors by endoscopic ultrasound findings of mural nodules	Type III-IV (papillary or invasive) mural nodule (OR, 10.8; 2.8-56.1) and symptomatic IMPNs (OR, 4.3; 1.4-14.7) were independently related to malignancies Presence of type III-IV nodule: sensitivity 60%; specificity 92.9%; accuracy 75.9% for diagnosis of malignancies	Prospective, LE 2 (87 patients)
Yamashita et al, J Ultrasound Med 2013[101]	Usefulness of contrast-enhanced endoscopic sonography for discriminating mural nodules from mucous clots in intraductal papillary mucinous neoplasms: a single-center prospective study	12 mural nodules; 5 mucous clots CH-EUS sensitivity 100%; specificity 80%; PPV 92%; NPV 100%; accuracy 94%	Prospective LE 2 (17 patients)
Salvia et al, Surgery 2012[102]	Pancreatic resections for cystic neoplasms: from the surgeon's presumption to the pathologist's reality	The use of a routine radiologic workup (MDCT and MRI) was associated with a favorably correct characterization of the cystic lesion while EUS did not seem to improve diagnostic accuracy	Retrospective, LE 3 (476 patients)

(*continued on the next page*)

SUPPLEMENTARY TABLE 2. Continued

Reference	Title	Main results	Study design, LE (population)
Konstantinidis et al, World J Gastrointest Surg 2014[103]	Lymphoepithelial cysts and cystic lymphangiomas: Under-recognized benign cystic lesions of the pancreas	Description of lymphoepithelial cysts and cystic lymphangiomas	Case series, LE 4 (12 patients)
Onishi et al, World J Gastroenterol 2013[104]	Intraductal papillary neoplasm of the bile duct accompanying biliary mixed adenoneuroendocrine carcinoma	Intraductal papillary neoplasm	Case report, LE 4
Sakamoto et al, World J Gastroenterol 2009[105]	Small invasive ductal carcinoma of the pancreas distinct from branch duct intraductal papillary mucinous neoplasm	Ductal carcinoma	Case report, LE 4

CH-EUS, Contrast-harmonic EUS; *LE*, level of evidence; *AUROC*, area under the receiver operating characteristic; *IPMN*, intraductal papillary mucinous neoplasia; *P-NET*, pancreatic neuroendocrine tumor; *MDCT*, multi-detector computed tomography; *CE*, contrast enhancement; *PFC*, pancreatic fluid collection; *MT*, malignant transformation; *OR*, odds ratio; *PPV*, positive predictive value; *NPV*, negative predictive value; *MRI*, magnetic resonance imaging.

SUPPLEMENTARY TABLE 3. Original studies evaluating the diagnostic performance of CH-EUS and CE-EUS for the differential diagnosis between benign and malignant lymph nodes

Reference	Title	Main results	Study design, LE (population)
Miyata et al, World J Gastroenterol 2016[61]	Contrast-enhanced harmonic endoscopic ultrasonography for assessment of lymph node metastases in pancreatobiliary carcinoma	109 consecutive patients (143 lymph nodes) with pancreaticobiliary carcinoma were enrolled Heterogeneous CH-EUS pattern for the differential diagnosis of benign vs malignant LNs: sensitivity 83%; specificity 91%; accuracy 88%. CH-EUS was more accurate than standard and color Doppler EUS	Prospective, LE: 2 (109 patients)
Xia et al, Gastrointest Endosc 2010[17]	Characterization of intra-abdominal lesions of undetermined origin by contrast-enhanced harmonic EUS (with videos)	CH-EUS for diagnosis malignant vs benign: sensitivity 96.3%; specificity 100%; PPV 100%; NPV 94.1%; accuracy 97.6% Differential diagnosis benign vs malignant LNs (extrapolated from text): sensitivity 95.7%; specificity 100%; accuracy 97.0%	Prospective, LE: 2 (34 patients with LNs)
Hocke et al, J Cancer Res Clin Oncol 2008[60]	Contrast-enhanced endoscopic ultrasound in discrimination between benign and malignant mediastinal and abdominal lymph nodes	EUS B-mode specificity 86% for benign LNs; sensitivity 68% for malignant LNs CE-EUS specificity 91% for benign LNs; sensitivity for malignant LNs 60% (increased sensitivity, 73%, after exclusion of malignant lymphoma)	Prospective, LE: 2 (122 patients)
Kanamori et al, Am J Gastroenterol 2006[59]	Usefulness of contrast-enhanced endoscopic ultrasonography in the differentiation between malignant and benign lymphadenopathy	CE-EUS (retrospective) sensitivity 100%; specificity 86.4%; accuracy 92.3% CE-EUS (prospective) sensitivity 100%; specificity 81.8%; accuracy 92.0%	Retrospective + prospective validation, LE: 2 (71 patients)
Kojima et al, Hepatogastroenterology 2003[58]	Differentiation of benign and malignant lymph nodes with contrast-enhanced echolymphography using endoscopic ultrasound-guided puncture	CE-echo-lymphography: sensitivity 95.8%; specificity 90.3%; PPV 88.5%; NPV 96.6%; accuracy 92.7%	Prospective, LE: 2 (55 patients)

CH-EUS, Contrast-harmonic EUS; *CE-EUS*, contrast-enhanced EUS; *LE*, level of evidence; *LN*, lymph node; *PPV*, positive predictive value; *NPV*, negative predictive value; *CE*, contrast enhancement.

SUPPLEMENTARY TABLE 4. Original studies evaluating the diagnostic performance of CH-EUS and CE-EUS for the assessment of submucosal tumors

Reference	Title	Main results	Study design, LE (population)
Yamashita et al, J Clin Ultrasound 2015[67]	Contrast-enhanced endoscopic ultrasonography can predict a higher malignant potential of gastrointestinal stromal tumors by visualizing large newly formed vessels	CH-EUS presence of intra-tumoral vessels significantly correlated to higher risk of GIST ($P = .005$)	Prospective, LE 2 (13 patients)
Kannengiesser et al, Scand J Gastroenterol 2012[65]	Contrast-enhanced harmonic endoscopic ultrasound is able to discriminate benign submucosal lesions from gastrointestinal stromal tumors	CH-EUS, 9 lesions hypoenhanced: 4 lipomas and 5 leiomyomas 8 of 8 hyperenhanced SMTs are GISTs	Prospective, LE 2 (17 patients)
Sakamoto et al, Gastrointest Endosc 2011[66]	Estimation of malignant potential of GI stromal tumors by contrast-enhanced harmonic EUS (with videos)	CH-EUS prediction of GIST malignancies (irregular vessels): sensitivity 100%; specificity 63%; accuracy 83% EUS-FNA sensitivity 63%; specificity 92%; accuracy 81% CH-EUS significantly more accurate than MDCT and power Doppler-EUS ($P < .05$)	Prospective, LE 2 (29 patients)
Kang et al, Gut Liver 2012[106]	Glomus tumor of the stomach: a clinicopathologic analysis of 10 cases and review of the literature	Description of glomic tumors	Case series, LE 4 (10 patients)
Baek et al, Dig Endosc 2013[107]	Gastric glomus tumor: analysis of endosonographic characteristics and computed tomographic findings	Description of glomic tumors	Case series, LE 4 (7 patients)
Guarise et al, World J Gastroenterol 2006[108]	Duodenal duplication cyst causing severe pancreatitis: imaging findings and pathological correlation	Duodenal SMT	Case report, LE 4

CH-EUS, Contrast-harmonic EUS; *CE-EUS*, contrast-enhanced EUS; *LE*, level of evidence; *GIST*, gastrointestinal stromal tumor; *SMT*, submucosal tumor; *MDCT*, multi-detector computer tomography.

SUPPLEMENTARY TABLE 5. Original articles evaluating the diagnostic performance of CH-EUS and CE-EUS in other indications (gallbladder abnormalities, focal liver lesions, vascular abnormalities, gastric neoplasms, etc.)

Reference	Title	Main results	Study design, LE (population)
Gallbladder abnormalities			
Imazu et al, Dig Dis Sci 2014[18]	Contrast-enhanced harmonic endoscopic ultrasonography in the differential diagnosis of gallbladder wall thickening	Harmonic EUS for GB malignancies: sensitivity 83.3%; specificity 65%; accuracy 73.1% CH-EUS for GB malignancies: sensitivity 89.6%; specificity 98%; accuracy 94.4% ($P < .001$ vs EUS)	Prospective, LE 2 (36 patients)
Choi et al, Gastrointest Endosc 2013[69]	Utility of contrast-enhanced harmonic EUS in the diagnosis of malignant gallbladder polyps (with videos)	CH-EUS (irregular vessel pattern) for diagnosis of malignant GB polyp: sensitivity 90.3%; specificity 96.6% CH-EUS (perfusion defects) for diagnosis of malignant GB polyp: sensitivity 90.3%; specificity 94.9% CH-EUS (final diagnosis): sensitivity 93.5%; specificity 90.0%	Prospective, LE 2 (93 patients)
Hirooka et al, Gastrointest Endosc 1998[109]	Contrast-enhanced endoscopic ultrasonography in gallbladder diseases	EUS B-mode vs CH-EUS for depth of tumor invasion: accuracy 78.6% vs 92.9%	Prospective, LE 2 (38 patients)
Park et al, Surg Endosc 2013[110]	Differential diagnosis between gallbladder adenomas and cholesterol polyps on contrast-enhanced harmonic endoscopic ultrasonography	CH-EUS for diagnosis of adenomas vs cholesterol polyps: sensitivity 75.0%; specificity 66.6%	Retrospective, LE 3 (87 patients)
Inui et al, Intern Med 2011[111]	Diagnosis of gallbladder tumors	Description of CH-EUS appearance in GB cancer	Retrospective, LE 3 (48 patients)
Fan et al, Case Rep Gastroenterol 2013[112]	Secondary sclerosing cholangitis due to gallbladder adenocarcinoma	GB adenocarcinomas	Case report, LE 4
Velosa et al, Endoscopy 2013[113]	Cholecystoduodenal fistula diagnosed with contrast-enhanced endoscopic ultrasound	GB fistula	Case report, LE 4
Focal liver lesions			
Dietrich. Endoscopy 2009[114]	Contrast-enhanced low mechanical index endoscopic ultrasound (CELMI-EUS)	P-NET metastasis	Case report, LE 4
Vascular abnormalities			
Paik et al, J Clin Gastroenterol 2014[70]	Clinical usefulness with the combination of color Doppler and contrast-enhanced harmonic EUS for the assessment of visceral vascular diseases	EUS B-mode, color Doppler and CH-EUS accurately identified visceral vascular lesions in 11 of 11 patients, and confirmed 1 suspected SMA dissection	Prospective, LE 3 (12 patients)
Sato et al, J Gastroenterol 2005[73]	Evaluation of arterial blood flow in esophageal varices via endoscopic color Doppler ultrasonography with a galactose-based contrast agent	CE-EUS showed presence of arterial flow in high-risk esophageal varices	Prospective, LE 3 (110 patients)
Sato et al, J Gastroenterol 2004[72]	Perforating veins in recurrent esophageal varices evaluated by endoscopic color Doppler ultrasonography with a galactose-based contrast agent	CE-EUS showed images of perforating veins in 22 of 29 (75.9%) patients with recurrent esophageal varices	Prospective, LE 3 (29 patients)
Sato et al, Hepatol Res 2003[71]	Evaluation of hemodynamics in esophageal varices. Value of endoscopic color Doppler ultrasonography with a galactose-based contrast agent	Perforating veins Type 1: in-flow from the paraesophageal veins Type 2 showed out-flow to the paraesophageal veins Type 3 mixed type both in-flow and out-flow. CE-EUS improved color Doppler images (60 of 62 patients, 96.8%)	Prospective, LE 3 (62 patients)

(*continued on the next page*)

SUPPLEMENTARY TABLE 5. Continued

Reference	Title	Main results	Study design, LE (population)
Imori et al, Intern Med 2012[115]	Idiopathic accessory hemiazygos vein aneurysm with an incidental mediastinal mass	Hemiazygos aneurysm	Case report, LE 4
Ogura et al, Endoscopy 2012[116]	Splenic artery aneurysm masquerading as a pancreatic tumor–diagnosis by contrast-enhanced endoscopic ultrasound	Splenic artery aneurysm	Case report, LE 4
Seicean et al, J Gastrointestin Liver Dis 2012[117]	Double splenic artery pseudoaneurysm associating splenic infarction in chronic pancreatitis	Splenic artery aneurysm	Case report, LE 4
Nagamatsu et al, Nihon Shokakibyo Gakkai Zasshi 2011[118]	A case of splenic artery aneurysm simulating a pancreas tumor	Splenic artery aneurysm	Case report, LE 4
Moreno et al, Endoscopy 2014[119]	EUS-FNA of a portal vein thrombosis in a patient with a hidden hepatocellular carcinoma: confirmation technique after contrast-enhanced ultrasound	Portal vein thrombosis	Case report, LE 4
Esophageal tumors			
Kocaman et al, Turk J Gastroenterol 2013[120]	Endosonography and elastography in the diagnosis of esophageal tuberculosis	Esophageal tuberculosis	Case report, LE 4
Chaudhary et al, Endosc Ultrasound 2013[121]	Esophageal duplication cyst in an adult masquerading as submucosal tumor	Duplication cyst	Case report, LE 4
Gastric neoplasms			
Iordache et al, Med Ultrason 2012[75]	Contrast-enhanced power Doppler endosonography and pathological assessment of vascularization in advanced gastric carcinomas–a feasibility study	Correlation between CH-EUS vascularity and pathological parameters of angiogenesis (MVD and VEGF)	Prospective, LE 2 (20 patients)
Nomura et al, Gastrointest Endosc 1999[74]	Usefulness of contrast-enhanced EUS in the diagnosis of upper GI tract diseases	Description of CH-EUS pattern in upper GI neoplasia (esophageal, gastric cancer, and SMLs)	Retrospect., LE 3 (30 patients)
Carrara et al, Gastrointest Endosc 2011[122]	Gastric metastasis from ovarian carcinoma diagnosed by EUS-FNA biopsy and elastography	Ovarian cancer metastasis	Case report, LE 4
Other indications			
Fusaroli et al, World J Gastroenterol 2012[10]	Pancreatico-biliary endoscopic ultrasound: a systematic review of the levels of evidence, performance and outcomes	Systematic review	Systematic review, LE 5
Romagnuolo et al, Gastrointest Endosc 2011[123]	Accuracy of contrast-enhanced harmonic EUS with a second-generation perflutren lipid microsphere contrast agent (with video)	Comparison of EUS B-mode vs CH-EUS accuracy in pancreatic and non-pancreatic lesions Accuracy 79.2% vs 83.3% (*P* not significant)	Prospective, LE 2 (21 patients)
Xia et al, Gastrointest Endosc 2010[17]	Characterization of intra-abdominal lesions of undetermined origin by contrast-enhanced harmonic EUS (with videos)	CH-EUS for diagnosis malignant vs benign: sensitivity 96.3%; specificity 100%; PPV 100%; NPV 94.1%; accuracy 97.6%	Prospective, LE 2 (43 patients)
Dietrich et al, Z Gastroenterol 2005[34]	Contrast-enhanced endoscopic ultrasound with low mechanical index: a new technique	Description	Case series, LE 4 (6 patients)
Hirooka et al, Gastrointest Endosc 1997[124]	Usefulness of contrast-enhanced endoscopic ultrasonography with intravenous injection of sonicated serum albumin	Description	Case series, LE 4 (33 patients)

(*continued on the next page*)

SUPPLEMENTARY TABLE 5. Continued

Reference	Title	Main results	Study design, LE (population)
Pandey et al, JOP 2014[125]	Pancreatico-pleural and bronchial fistulae and associated pseudocysts: case series	Description of fistulae	Case series, LE 4 (5 patients)
Kim et al, Clin Endosc 2014[126]	Primary fallopian tube carcinoma diagnosed with endoscopic ultrasound elastography with fine needle biopsy	Primary ovarian carcinoma	Case report, LE 4
Wang et al, Exp Ther Med 2014[127]	Accessory spleen arising from the gastric fundus mimicking gastrointestinal stromal tumor following splenectomy: A case report	Accessory spleen	Case report, LE 4
Hijioka et al, J Med Ultrason 2011[128]	Contrast-enhanced endoscopic ultrasonography (CE-EUS) findings in adrenal metastasis from renal cell carcinoma	Adrenal metastasis	Case report, LE 4

CH-EUS, Contrast-harmonic EUS; *CE-EUS*, contrast-enhanced EUS; *LE*, level of evidence; *GB*, gallbladder; *P-NET*, pancreatic neuroendocrine tumor; *SMA*, superior mesenteric artery; *MVD*, microvascular density; *VEGF*, vascular endothelial growth factor; *SML*, submucosal lesion; *PPV*, positive predictive value; *NPV*, negative predictive value.

医局員名簿

近畿大学医学部　消化器内科学教室　同門会名簿

（平成29年12月時点）

平成11年入局

氏名	出身大学（卒業年）	勤務先	勤務先住所	電話番号
工藤　正俊	京都大学（昭和53年）	近畿大学医学部 消化器内科	〒589-8511 大阪狭山市大野東377-2	072-366-0221
汐見　幹夫	近畿大学（昭和55年）	関空国際空港クリニック	〒549-0001 泉佐野市泉州空港北１	072-456-7185
上硲 俊法	近畿大学（昭和60年）	近畿大学医学部 臨床検査医学	〒589-8511 大阪狭山市大野東377-2	072-366-0221
由谷　逸郎	近畿大学（昭和62年）	富田林病院	〒584-0082 富田林市向陽台1-3-36	0721-29-1121
松井　繁長	近畿大学（平成3年）	近畿大学医学部 消化器内科	〒589-8511 大阪狭山市大野東377-2	072-366-0221
谷池　聡子	近畿大学（平成7年）	（非常勤） 近畿大学医学部　堺病院		
亀山　千晴	近畿大学（平成7年）	しあわせクリニック	〒544-0024 大阪市生野区生野西2-5-14 寺田町田中ビル1F	06-6711-2525
遠田　弘一	近畿大学（平成7年）	慈温堂遠田医院	〒589-0011 大阪狭山市半田1-624-3	072-367-4772
中岡　良介	近畿大学（平成8年）	山本病院	〒648-0072 橋本市東家6-7-26	0736-32-8899
末冨　洋一郎	近畿大学（平成8年）	末冨放射線科医院	〒759-0212 山口県宇部市際波1445-3	0836-41-1231
小川　力	近畿大学（平成11年）	高松赤十字病院	〒760-0017 高松市番町4-1-3	087-831-7101
井上　達夫	近畿大学（平成11年）	井上医院	〒593-8312 堺市西区草部181	072-271-0022
梅原　泰	近畿大学（平成11年）	辻健太郎クリニック	〒543-0027 大阪市天王寺区筆ケ崎町5-52	06-6772-3939
加藤　玲明	近畿大学（平成11年）	かとう内科眼科クリニック	〒665-0877 宝塚市中山桜台2-2-1 2F	0797-69-6456
坂口　康浩	近畿大学（平成11年）	熊取坂口クリニック	〒590-0451 泉南郡熊取町野田3-353-4	072-493-8855
辻　　直子（近大堺）	京都府立医科大学（昭和60年）	近畿大学医学部　堺病院 消化器内科	〒590-0132 堺市南区原山台2-7-1	072-299-1120
南野　達夫（近大奈良）	近畿大学（昭和55年）	なんの医院	〒573-1171 枚方市三栗1-14-12	072-856-0107

平成12年入局

北野　雅之	鳥取大学（平成2年）	和歌山県立医科大学 第二内科	〒641-8509 和歌山市紀三井寺811-1	073-447-2300

氏名	出身大学 （卒業年）	勤務先	勤務先住所	電話番号
川崎　俊彦	京都大学 （昭和58年）	近畿大学医学部　奈良病院 消化器内科	〒630-0293 生駒市乙田町1248-1	0743-77-0880
鄭　　浩柄	東京慈恵会 医科大学 （平成8年）	神戸市立医療センター中央 市民病院	〒650-0047 神戸市中央区港島南町2-1-1	078-302-4321
南　　康範	近畿大学 （平成9年）	近畿大学医学部 消化器内科	〒589-8511 大阪狭山市大野東377-2	072-366-0221
黒木　恵美 （旧姓：石川）	近畿大学 （平成11年）	（非常勤） PL病院・りんくう総合医 療センター・近畿大学医学 附属病院		
山口　美樹 （旧姓：永島）	近畿大学 （平成12年）	みきクリニック	〒543-0018 大阪市天王寺区空清町5-18	06-6711-0761
梅原　康湖 （旧姓：小村）	近畿大学 （平成12年）	（非常勤） 近畿大学医学部　堺病院		
乾　　可苗	近畿大学 （平成12年）			
坂本　洋城	近畿大学 （平成12年）	葛城病院	〒596-0825 岸和田市土生町2-33-1	072-422-9909
福永　豊和 （近大奈良）	京都大学 （平成4年）	北野病院	〒530-8480 大阪市北区扇町2-4-20	06-6312-1221

平成13年入局

萩原　智	近畿大学 （平成10年）	近畿大学医学部 消化器内科	〒589-8511 大阪狭山市大野東377-2	072-366-0221
福田　信宏	近畿大学 （平成10年）	福田内科医院	〒501-0236 瑞穂市本田1017-1	058-327-0721
市川　勉	近畿大学 （平成12年）	内海町いちかわ診療所	〒722-2632 広島県福山市内海町ロ355-1	084-980-9099
岡田　無文	近畿大学 （平成13年）	咲花病院	〒594-1105 和泉市のぞみ野1-3-30	0725-55-1919
畑中　絹世 （旧姓：乾）	川崎医科大学 （平成13年）	（非常勤） りんくう総合医療センター		
清水　昌子 （旧姓：豊澤）	近畿大学 （平成13年）			
宮本　容子 （旧姓：北口）	近畿大学 （平成12年）			

平成14年入局

秋山　智之	近畿大学 （平成14年）	平成立石病院	〒124-0012 東京都葛飾区立石5-1-9	03-3692-2121
朝隈　豊	近畿大学 （平成14年）	朝隈医院		
北井　聡	近畿大学 （平成14年）	きたいクリニック	〒575-0023 四条畷市楠公2-8-10	072-879-2540

氏名	出身大学 （卒業年）	勤務先	勤務先住所	電話番号
高橋　俊介	近畿大学 （平成14年）	堺市立総合医療センター	〒593-8304 堺市西区家原寺町1-1-1	072-272-1199
冨田　崇文	近畿大学 （平成14年）	富田病院	〒649-6253 和歌山県岩出市紀泉台2	0736-62-1522
齋藤　佳寿 （旧姓：野田）	近畿大学 （平成14年）			
西尾　健	近畿大学 （平成14年）	咲花病院	〒594-1105 和泉市のぞみ野1-3-30	0725-55-1919
宮部　欽生	近畿大学 （平成14年）	尾道市立市民病院	〒722-0055 広島県尾道市新高山3-1170-177	0848-47-1155
水野　成人 （近大奈良）	京都府立 （昭和61年）	近畿大学医学部　奈良病院 消化器内科	〒630-0293 生駒市乙田町1248-1	0743-77-0880

平成15年入局

仲谷　達也	近畿大学 （平成3年）			
田北　雅弘	近畿大学 （平成15年）	近畿大学医学部 消化器内科	〒589-8511 大阪狭山市大野東377-2	072-366-0221
大久保　充	近畿大学 （平成15年）	東京医科大学　八王子医療 センター	〒193-0944 八王子市館町1163	042-665-5611
川崎　正憲	近畿大学 （平成15年）	近畿大学医学部　奈良病院 消化器内科	〒630-0293 生駒市乙田町1248-1	0743-77-0880
坂本　康明	近畿大学 （平成15年）	坂本内科クリニック	〒596-0045 岸和田市別所町1-14-28 2F	072-433-1120
柴田　千栄 （旧姓：辰巳）	近畿大学 （平成15年）	（非常勤） 新生会病院		
上田　泰輔	近畿大学 （平成15年）	上田内科	〒572-0042 寝屋川市東大利町14-32	072-826-0045

平成17年入局

上嶋　一臣	神戸大学 （平成7年）	近畿大学医学部 消化器内科	〒589-8511 大阪狭山市大野東377-2	072-366-0221

平成18年入局

小牧　孝充	近畿大学 （平成7年）	富田林病院　消化器内科	〒584-0082 富田林市向陽台1-3-36	0721-29-1121
永井　知行	近畿大学 （平成16年）	近畿大学医学部 消化器内科	〒589-8511 大阪狭山市大野東377-2	072-366-0221
永田　嘉昭	近畿大学 （平成16年）	永田消化器内科クリニック	〒755-0023 山口県宇部市恩田町4-2-17	0836-21-2311

平成19年入局

今井　元	近畿大学 （平成17年）	近畿大学医学部 消化器内科	〒589-8511 大阪狭山市大野東377-2	072-366-0221

氏名	出身大学 （卒業年）	勤務先	勤務先住所	電話番号
鍋島　紀滋 （近大奈良）	京都大学 （昭和61年）	三菱京都病院	〒615-8087 京都市西京区桂御所町1番地	075-381-2111
茂山　朋広 （近大奈良）	近畿大学 （平成17年）	しげやまクリニック	〒663-8111 兵庫県西宮市二見町13-21	0798-65-9292

平成20年入局

早石　宗右	近畿大学 （平成18年）	早石病院	〒543-0027 大阪市天王寺区筆ケ崎町2-75	06-6771-1227
矢田　典久	滋賀医科大学 （平成11年）	やだ消化器内視鏡クリニック	〒608-8080 京都府京都市山科区竹鼻竹ノ街道町33-1	075-582-0080

平成21年入局

有住　忠晃	近畿大学 （平成19年）	くしもと町立病院	〒649-3510 和歌山県東牟婁郡串本町サンゴ台691-7	0735-62-7111
鎌田　研	近畿大学 （平成19年）	近畿大学医学部 消化器内科	〒589-8511 大阪狭山市大野東377-2	072-366-0221
高山　政樹	近畿大学 （平成19年）	近畿大学医学部　奈良病院 消化器内科	〒630-0293 奈良県生駒市乙田町1248-1	0743-77-0880
峯　　宏昌	近畿大学 （平成19年）	山本病院	〒648-0072 橋本市東家6-7-26	0736-32-8899
宮田　剛	近畿大学 （平成19年）	近畿大学医学部 消化器内科	〒589-8511 大阪狭山市大野東377-2	072-366-0221
奥田　英之 （近大奈良）	近畿大学 （平成19年）	近畿大学医学部　奈良病院 消化器内科	〒630-0293 生駒市乙田町1248-1	0743-77-0880
奥村　直巳 （近大堺）	近畿大学 （平成19年）	うえだ奥村クリニック	〒547-0021 大阪市平野区喜連東2-11-21	06-6703-1315
山本　典雄 （近大堺）	近畿大学 （平成19年）	大阪市立大学医学部 呼吸器内科	〒545-8585 大阪市阿倍野区旭町1-4-3	06-6645-3611

平成22年入局

樫田　博史	京都大学 （昭和58年）	近畿大学医学部 消化器内科	〒589-8511 大阪狭山市大野東377-2	072-366-0221
櫻井　俊治	京都大学 （平成7年）	近畿大学医学部 消化器内科	〒589-8511 大阪狭山市大野東377-2	072-366-0221
高場　雄久 （近大堺）	近畿大学 （平成20年）	永山病院	〒590-0406 泉南郡熊取町大久保東1-1-10	072-453-1122

平成23年入局

西田　直生志	大阪医科大学 （昭和60年）	近畿大学医学部 消化器内科	〒589-8511 大阪狭山市大野東377-2	072-366-0221
大本　俊介	近畿大学 （平成21年）	近畿大学医学部 消化器内科	〒589-8511 大阪狭山市大野東377-2	072-366-0221

氏名	出身大学 （卒業年）	勤務先	勤務先住所	電話番号
足立　哲平	近畿大学 （平成21年）	（非常勤） はりま病院		
門阪　薫平	近畿大学 （平成21年）	（非常勤） 串本病院		
木下　大輔 （近大奈良）	近畿大学 （平成20年）	近畿大学医学部　奈良病院 消化器内科	〒630-0293 生駒市乙田町1248-1	0743-77-0880
秦　　康倫 （近大奈良）	近畿大学 （平成21年）	近畿大学医学部　奈良病院 消化器内科	〒630-0293 生駒市乙田町1248-1	0743-77-0880
松本　望 （近大堺）	近畿大学 （平成21年）	尾道総合病院	〒722-8508 広島県尾道市平原1-10-23	0848-22-8111

平成24年入局

千品　寛和	近畿大学 （平成22年）	近畿大学医学部 消化器内科	〒589-8511 大阪狭山市大野東377-2	072-366-0221
山田　光成	近畿大学 （平成18年）	近畿大学医学部 消化器内科	〒589-8511 大阪狭山市大野東377-2	072-366-0221
水内　梨絵 （旧姓：田中）	近畿大学 （平成22年）	北九州市小倉医師会健診センター	〒802-0076 福岡県北九州市小倉北区中島1-19-17	093-551-3185
河野　匡志 （近大堺）	近畿大学 （平成22年）	近畿大学医学部 消化器内科	〒589-8511 大阪狭山市大野東377-2	072-366-0221
丸山　康典 （近大堺）	近畿大学 （平成22年）	近畿大学医学部　堺病院 糖尿病・代謝内科	〒590-0132 堺市南区原山台2-7-1	072-299-1120

平成25年入局

山雄　健太郎	東京医科大学 （平成18年）	近畿大学医学部 消化器内科	〒589-8511 大阪狭山市大野東377-2	072-366-0221
岡元　寿樹	近畿大学 （平成23年）	近畿大学医学部 消化器内科	〒589-8511 大阪狭山市大野東377-2	072-366-0221
南　　知宏	近畿大学 （平成23年）	近畿大学医学部 消化器内科	〒589-8511 大阪狭山市大野東377-2	072-366-0221
尾﨑　信人 （近大堺）	近畿大学 （平成23年）	京都市立病院 消化器内科	〒604-8845 京都府京都市中京区壬生東高田町1-2	075-311-5311

平成26年入局

米田　頼晃	北里大学 （平成13年）	近畿大学医学部 消化器内科	〒589-8511 大阪狭山市大野東377-2	072-366-0221
岡崎　能久	大阪大学 （平成13年）			

平成27年入局

依田　広	京都大学 （平成8年）	近畿大学医学部 消化器内科	〒589-8511 大阪狭山市大野東377-2	072-366-0221

氏名	出身大学 （卒業年）	勤務先	勤務先住所	電話番号
三長　孝輔	京都大学 （平成19年）	近畿大学医学部 消化器内科	〒589-8511 大阪狭山市大野東377-2	072-366-0221
松田　友彦	弘前大学 （平成19年）	みみはら高砂クリニック	〒590-0820 堺市堺区高砂町4-109-2	072-241-4990
岩西　美奈	近畿大学 （平成25年）			

平成28年入局

渡邉　智裕	京都大学 （平成5年）	近畿大学医学部 消化器内科	〒589-8511 大阪狭山市大野東377-2	072-366-0221
竹中　完	近畿大学 （平成13年）	近畿大学医学部 消化器内科	〒589-8511 大阪狭山市大野東377-2	072-366-0221
橋本　有人	近畿大学 （平成26年）	富田林病院	〒584-0082 富田林市向陽台1-3-36	0721-29-1121
岡本　彩那	兵庫医科大学 （平成23年）	近畿大学医学部 消化器内科	〒589-8511 大阪狭山市大野東377-2	072-366-0221

平成29年入局

中井　敦史	徳島大学 （平成22年）	近畿大学医学部 消化器内科	〒589-8511 大阪狭山市大野東377-2	072-366-0221
石川　嶺	近畿大学 （平成24年）	近畿大学医学部 消化器内科	〒589-8511 大阪狭山市大野東377-2	072-366-0221
河野　辰哉	近畿大学 （平成27年）	近畿大学医学部 消化器内科	〒589-8511 大阪狭山市大野東377-2	072-366-0221
高島　耕太	近畿大学 （平成27年）	近畿大学医学部 消化器内科	〒589-8511 大阪狭山市大野東377-2	072-366-0221
髙田　隆太郎	近畿大学 （平成27年）	近畿大学医学部 消化器内科	〒589-8511 大阪狭山市大野東377-2	072-366-0221
田中　秀和	近畿大学 （平成27年）	近畿大学医学部 消化器内科	〒589-8511 大阪狭山市大野東377-2	072-366-0221
半田　康平	近畿大学 （平成27年）	近畿大学医学部 消化器内科	〒589-8511 大阪狭山市大野東377-2	072-366-0221
福永　朋洋	近畿大学 （平成27年）	近畿大学医学部 消化器内科	〒589-8511 大阪狭山市大野東377-2	072-366-0221
吉田　晃浩	近畿大学 （平成27年）	近畿大学医学部 消化器内科	〒589-8511 大阪狭山市大野東377-2	072-366-0221

近畿大学消化器内科　同門会役員

会長　　工藤正俊

幹事　　松井繁長

会計　　上嶋一臣

庶務　　西田直生志

同門会実行委員

南　康範（委員長)、永井知行、千品寛和、宮田　剛

同門会担当秘書

浦田亜樹

近畿大学医学部消化器内科教室同門会会則

第一条 名称

本会は近畿大学医学部消化器内科教室同門会と称する。

第二条 目的

本会は会員相互の親睦及び教室の隆盛を図ることを目的とする。

第三条 会員

会員は消化器内科教室出身者、教室員及び同教室の発展に寄与するものをもって構成される。

第四条 役員

１．本会の運営を円滑にするために幹事会を設ける。幹事会は代表幹事を長とし、代表幹事が指名する教室員をもって構成する。尚、幹事会は代表幹事が随時召集するものとする。その他、会計をおく。

２．会長

① 会長は現職主任教授より選出される。

② 会長退任後は名誉会長となる。また、名誉会長は主任教授経験者からも選出できる。

３．顧問

本会の発展に寄与したもので、幹事会が推戴する。

４．役員の選出

① 幹事は役員より選出する。

② 代表幹事は医局長が兼任する。

５．幹事の任期は２年とする。但し再任を妨げない。

第五条 会議

１．総会は年１回の開催とする。

２．幹事会において仮決議された条件の最終決定権は総会に委ねられる。

３．決議は総会出席者の多数決により成立する。

第六条 会計

１．本会の経費は会費をもって充てる。

２．本会の会費は年額壱萬円とする。

３.会計年度は４月１日から翌年３月31までとし､会計担当者は年1回会計報告を行う。

第七条

事務局は近畿大学医学部消化器内科教室内に置く。

第八条　会則の改正

会則の改正は幹事会の仮決議を経て総会で議決されるものとする。

附則　除名規定

本会の名誉を毀損したものや、その他本会に不適当と考えられるものは
幹事会の動議により総会にて除名が議決される。